近畿大学医学部消化器内科学教室
平成 24 年度　年報

Kinki University School of Medicine

Department of Gastroenterology and Hepatology

Annual Report-2012-

近畿大学医学部　消化器内科学
近畿大学医学部附属病院　光学治療センター
近畿大学医学部附属病院　中央超音波診断・治療室
近畿大学医学部堺病院　消化器内科
近畿大学医学部奈良病院　消化器・内分泌内科

年報 Annual Report 2012

近畿大学医学部消化器内科学教室

医局員集合写真

第7回 Kinki GUT Club 平成25年1月20日

目　　次

2012 年 Annual Report の発刊にあたって

近畿大学消化器内科学教室主任教授　工藤正俊

1.はじめに

　　2012 年の教育、研究、診療の実績をお届けします。近畿大学医学部に消化器内科学教室が新設されたのは平成 11 年 4 月であります。従って平成 25 年 3 月でやっと丸 14 年が経過したことになります。開設当初は医局のスペースも 2 部屋のみでスタッフ 8 名、研修医 6 名、計 14 名での出発でありました。現在では狭山の本院に籍を置くスタッフは約 40 名、また堺病院や奈良病院もそれなりに人材・設備共に整いつつあります。

　　しかしながら、新設私立医大の宿命かもしれませんが、2004 年より始まった新臨床研修医制度の余波をまともに受けて消化器内科も毎年 5〜6 人から 12〜13 人入局していた入局者数が最近では激減し、また次第に開業あるいは結婚退職、郷里への U ターンなどの退職者も増え、現在はなお厳しい状況に置かれているというのが現状です。ただし、ここ数年は 2-4 人の入局がコンスタントに続いており、良い傾向が見え始めました。今後の更なる消化器内科学教室の発展のために医局員一同が一致団結して診療、研究、教育活動に専念していかなければならない重要な時期であると考えております。

2.診療活動

　　別添えの資料をご覧頂ければ一目瞭然でありますが、消化器内科の年間の入院及び外来収入、及びそれを合計した総収入は平成 11 年の開設初年度は約 8 億程度でありましたが、平成 24 年には 31 億円を超える収入となっており、病院経営にも多大の貢献をしております。平成 24 年度は病院全体も約 19 億の黒字決算となりました。消化器内科の貢献も大きいと考えております。また一日平均入院患者数も年間を通して 80 人前後、平均在院日数も 8 日を切っており極めて多忙な診療活動を行っていることがおわかり頂けると思います。腹部超音波検査の件数も確実に右肩上がりであり、内視鏡の件数も総件数が平成 24 年度は 22,123 例と着実に上昇を示しております。また、肝癌に対するラジオ波治療（RFA）の総件数も多く、日経新聞や朝日新聞、読売新聞、週刊朝日等にも度々取り上げられ、総件数としては連続 7 年以上、日本国内の 2 位（内科と外

科の件数、及び転移性肝癌を含めて）に位置づけられるという実績を残しております。ラジオ波は平成 11 年 6 月より開始し、平成 23 年 12 月末の時点で総件数 4,000 例に達しており、5 年生存率は 70%強であり、手術とほぼ同等の治療成績が得られております。現在、C 型肝炎治療を積極的に行っており、大阪南部から C 型肝炎・肝癌を根絶したいと願っています。

　　　平成 15 年度に導入した早期胃癌に対する内視鏡的粘膜下層切開剥離術（ESD）も確実に症例数が増え、今後も益々増え続けていくものと考えております。もちろん、ESD 関連の研究論文も少しずつ増えていっております。また、高度先進医療としての大腸 ESD も平成 22 年より開始され、症例も増加しています。また従来より行っていた胆膵グループによる超音波内視鏡検査の件数も増加しています。平成23年度には内視鏡室が光学治療センターに格上げとなり、スペースも拡充されました。平成 23 年 11 月 27 日に第 1 回目を行った関西消化器内視鏡ライブコースも第 2 回目が平成 24 年 11 月 25 日に行われ、約 300 人の参加者を得て成功裏に終わりました。

　　　御承知のように大和川以南は一般に「南大阪」と呼ばれておりますが、その南大阪の人口は約 260 万にも達しております。その 260 万人の医療圏の中で大学医学部は近畿大学のみであります。その意味でこの 260 万人の方々の健康を守るのが我々に課せられた使命であります。

3.教育活動

　　　教育は当然のことながら大学医学部の役割の極めて根幹を占める重要な部分であります。消化器内科学は消化器コースの内の肝臓の責任科であり、肝臓のユニットを 1 週間担当している他、上部消化管、下部消化管、胆膵のユニットや臨床腫瘍コースならびに画像診断のコースでも講義を担当しております。更には病因・病態のコースの 3 週間のうち 1 週間の責任科として大変多忙な教育活動を行っております。5 年生 6 年生のクリニカルクラークシップも例年 6 年生を常時 6 人程度受け入れており、講義や総括など充実した bed side 教育となるよう全力を尽くしております。

　　　平成 20 年 10 月から病院長に任ぜられ、今期で 3 期目となりましたのでその公務のために教育活動の多くの部分を北野准教授、松井講師はじめ多くの講師の先生方にご負担をおかけすることになってしまい、申し訳なく思っております。消化器コース及び病因・病態コースあるいは日々のクリニカルクラー

クシップ等の教育活動では決して手を抜かず積極的に行っていくつもりですので何卒ご容赦下さい。この紙面をお借りして感謝とお詫びを申し上げたいと思います。

3．研究活動
（1）論文業績
　　　英文論文の発表は 1999 年消化器内科の設立当初は一桁台でありましたが、年と共に確実に増加し、3 年目からは平均 20 編以上の英文論文がコンスタントに出るようになりました。2010 年の英文論文数は 51 編に達しました。残念ながら 2011 年は 48 編、2012 年は 44 編にとどまりました。しかしながら何とか毎年 50 編の大台を超えたいと祈念しております。また 14 年間の総インパクトファクターは 1380.583 点であり英文総論文数は 438 編ですので、近畿大学消化器内科のような小さな所帯の教室としてはまずまずの結果を残せているのではないかと思っております。来年以降も最低、英文原著論文は 50 編以上を目標に頑張っていきたいと考えておりますので教室員の皆様の自覚と更なる奮闘を期待致しております。

（2）厚生労働省科学研究費補助金事業研究班の活動
平成 22 年度に採択された厚労科研（がん臨床部門）**「進行・再発肝細胞癌に対する動注化学療法と分子標的薬併用による新規治療法の確立を目指した臨床試験（Phase III）ならびに効果を予測する biomarker の探索研究」**（工藤班）の主任研究者として日本発のエビデンスを創出すべく、努力しています。また平成 23 年度には厚労科研（難病・がん等の疾患分野の医療の実用化部門）**「慢性ウイルス性肝疾患の非侵襲的線化評価法の開発と臨床的有用性の確立」**（工藤班）の主任研究者としても採択され、多くの大学との協同研究を開始しています。またその他にも下記の厚労科研の分担研究者として教室の先生方に実務を担当して頂いております。この場をお借りして感謝申し上げます。

① 「血小板低値例へのインターフェロン治療法の確立を目指した基礎および臨床的研究」（西口班）（厚労科研）
② 「抗悪性腫瘍薬による肝炎ウイルス再活性化の調査とその対応に関する研究」（池田班）（国立がん研究センターがん研究補助金）

③ 「初発肝細胞癌に対する肝切除とラジオ波焼灼両方の有効性に関する多施設共同研究」（國土班）（厚労科研）

④ 「肝がんの新規治療法に関する研究」（本多班）（厚労科研）

⑤ 「多発肝のう胞症に対する治療ガイドライン作成と試料バンクの構築」（大河内班）（厚労科研）

⑥ 「進行肝胆膵がんの治療法の開発に関する研究」（奥坂班）（国立がん研究センターがん研究補助金）

⑦ 「Ｃ型肝炎ウイルス（ＨＣＶ）陽性進行肝臓がん症例に対するテーラーメイドがんペプチドワクチンの第Ⅱ相単盲検無作為割付群間比較臨床試験」（文科省知的クラスター事業）

（3）今後の研究の方向性

　　　今年の消化器内科の論文も一覧するとやはりまだまだ Impact factor の高い雑誌に掲載されているのは少ないようです。やはり Impact factor 15 点以上の雑誌を目指すには prospective な比較試験など中・長期的な視野に立った研究計画を組んで質の高い臨床研究を進めて行くことが現時点での我々に課せられた最も大きな課題と考えております。臨床試験については 2008 年 9 月 11 日に大阪府より認証を受けた NPO 法人「日本肝がん臨床研究機構（JLOG）」を中心に現在 7 つの prospective study が走っております。そのうち 3 つが厚労科研に採択されたため現在では 4 つの前向き試験を行っております。なかでもSELECTED study は H24 年 10 月に終了し、ポジティブな結果が得られたためH25 の AASLD で oral 発表すると共に、NEJM にも投稿予定です。来年中には SILIUS 試験の結果も出る予定です。これからも世界へ向けて発信できるような成果を出して行くつもりでおります。もちろん、retrospective な解析研究で新しいデータを publish していくという努力も今後も続けていかなければなりません。

　　　また基礎研究の分野でも西田直生志准教授、櫻井俊治講師、萩原智講師を中心に積極的に研究を進めて頂いており、今後の publication を期待しております。

　　　もう一つの重要な点は私が常日頃申し上げておりますように症例観察の重要性であります。臨床においては一例一例がたとえ同じ病名であったとしても一例として同じ症例はありません。同じ病気でも一つとして全く同一である

ということはなく、何か異なるメッセージを発信しているのです。そのことを的確にキャッチすることにこそ意味があるという目で一例一例の患者さんを注意深く診療し観察していくことこそが最も大事であると考えています。そのような注意深い観察から新しい臨床的な発見も生まれてきますし、また逆にそのような観察眼が生まれる素地としては臨床家として真面目に臨床と向き合って最高の level に到達している必要があります。そのような点で日々の臨床の現場には"clinical pearl"とでも言うべきものがあちこちに転がっている、まさに宝の山であります。そのような理由で症例観察に基づいたケースレポートを書くということも極めて、その本人の勉強になることはもちろんのこと、今後の新しい疾患概念の確立、新しい治療法の着想などに結びつき得る重要な姿勢であると思われます。残念ながら、ケースレポートは最近の Impact factor 重視主義の多くの Journal から採用されない傾向にはありますが、それでも short report や Letter to the Editor などとしては採用されますので業績をあげるという目的ではなく、症例をキチンと観察・整理して document していくという姿勢に立つことは重要であります。すなわち症例の観察研究を報告することは我々、アカデミアに籍を置く者に課せられた使命であると自覚すべきと考えております。

　　　ここまで読まれた方は最初に私が述べたような大規模な前向きな比較試験を行うべきということと症例の観察研究とでは全く正反対の次元の違うことを述べているように思われるかもしれません。しかしこの 2 つは臨床を知り尽くし、かつ、臨床をじっくり真面目にやっている医師にしかできないことであるという点で共通していることであります。基礎研究あるいは臨床に結びつくかもしれない基礎研究までは MD ではなくとも PhD でも実行可能なことであり、その field ではしばしば PhD の方が quality の高い研究成果を上げ得るかも知れません。しかしながら、臨床の疑問点にもとづいた基礎研究もしくは本当に臨床に直結するような基礎研究や症例の観察研究、および大規模臨床試験などはその価値を知り得る MD にしかできないことであることは間違いありませんし、それらを遂行し得るのは患者さんと日々正面から向き合っている最高水準の医師にしかできない研究であります。そのような点でこの二つは決して矛盾するものではありませんし、両方ともに臨床家こそがやるべき研究であります。

　　　以上、述べた 2 つの異なったアプローチは、我々の教室の研究の方向性として今後も積極的に実行して行きたいと思っております。繰り返しになりますが、臨床的な発想に基づく、あるいは臨床に本当に必要な基礎的データを抑

えるという研究は、大変重要ですのでそれらは引き続き継続していかなくては
なりません。

　2009 年に私が立ち上げた日本肝がん分子標的治療研究会（第 1 回研究会:
2010 年 1 月 16 日、参加者 450 人）は年 2 回開かれております。肝癌はこれか
らは分子標的治療の時代ですのでゲノム生物学教室（西尾和人教授）との共同
研究は今後も継続していきたいと思っています。特許も出願することが出来ま
したし、Impact Factor が 7 以上の雑誌にもこの分野で 2-3 編通りました。臨床
的ニーズに基づいた基礎研究で成果を上げることほどエキサイティングなこと
はありません。是非とも近畿大学から肝がんに関して臨床に貢献できる基礎的
エビデンスを次々と発信して行きたいと心から願っています。

(3) Research Conference
　現在消化器内科では定期の各グループの臨床カンファレンスに加え、毎
週火曜日の早朝の 1 時間みっちりと Research Conference を行っております。
このカンファレンスでは全て英語で Presentation から Discussion までを行って
おります。ほとんど 1 年を通じて海外からの留学生がおりますし、特筆すべき
点としてこれまではアジアの留学生が中心でしたが平成 22 年はイタリア人の
Dr. Lorenzo が apply してできたことです。これも日本における肝細胞癌研究の
leading center としてヨーロッパの国からも認知され始めている証拠であると
思いますので大変喜ばしいと思っております。平成 23 年には世界で最も古い歴
史のあるイタリアボローニャ大学の Prof. Bolondi の教室から Dr. Alberto がや
ってきて 3 か月の研修を終えて帰りました。そのような留学生にも配慮して
Research Conference は英語で行っておりますが、やはりこの English
Research Conference というのが消化器内科が行っているカンファレンスの中
でも最も重要であると考えております。もちろん、このカンファレンスへの出
席は本人の自発的意欲に基づくものではありますが、毎週多くの教室員に参加
して頂いております。以下にこの数年の出席率を示しますが、出席率の高い医
局員ほどやはり研究に対する activity が高い傾向にあると感じておりますので
今後も引き続き積極的に参加して頂きたいと思っております。
　副次的な効果としてこのカンファレンスを通じて海外で英語で
Discussion できる英語力や自信も自然と磨かれるものと確信しております。

English Reseach Conference 出席状況

教室員	2008		2009		2010		2011		2012	
	出席回数	出席率	出席回数	出席率	出席回数	出席率	出席回数	出席率	出席回数	出席率
工藤	27/27	100	20/20	100	29/29	100	23/23	100	32/32	100
樫田	－	－	－	－	12/19	63	20/23	87	27/32	84
西田	－	－	－	－	－	－	5/5	100	24/32	75
北野	25/27	93	16/20	80	21/29	72	21/23	91	25/32	78
松井	22/27	81	18/20	90	23/29	79	23/23	100	30/32	94
上嶋	6/27	22	3/20	15	12/29	41	7/23	30	9/32	28
櫻井	－	－	－	－	17/19	89	20/23	87	25/32	78
南	19/24	79	1/2	50	－	－	13/14	93	31/32	97
井上	17/25	68	16/20	80	25/29	86	21/23	91	23/32	72
萩原	11/24	46	5/20	25	9/29	31	11/23	48	10/32	31
矢田	7/11	64	14/19	74	26/29	90	14/23	61	9/32	28
北井	15/27	56	8/20	40	15/29	52	13/23	57	20/32	63
朝隈	16/27	59	12/20	60	11/29	38	15/23	65	15/32	47
坂本	19/27	70	1/2	50	12/19	63	11/23	48	20/32	6
永井	18/19	95	17/20	85	14/29	48	12.5/23	54	23/32	72
川崎	23/27	85	6/20	30	4/29	14	6/23	26	4/32	13
田北	1/2	50	13/20	65	15/29	52	7/23	30	9/23	39
早石	10/19	53	9/19	47	5/29	17	8/23	35	9/23	39
田中	－	－	－	－	－	－	－	－	24/27	89
千品	－	－	－	－	－	－	－	－	29/32	91
山田	－	－	－	－	－	－	－	－	23/25	92
今井	－	－	9/15	60	18/29	62	10/23	43	13/32	41
永田	－	－	13/15	87	16/29	55	12/23	52	11/32	34
有住	－	－	7/15	47	15/29	52	17/23	74	26/32	81
鎌田	－	－	11/15	73	15/29	52	10/23	43	16/32	50
高山	－	－	4/7	57	－	－	13/14	93	16/32	50
宮田	－	－	9/15	60	16/29	55	14.5/23	63	22/32	69

峯	–	–	9/15	60	17/29	59	17/23	74	19/32	59
足立	–	–	–	–	–	–	8/14	57	22/32	69
大本	–	–	–	–	–	–	12/14	86	29/32	91
門阪	–	–	–	–	–	–	12/14	86	22/32	69
南（知）	–	–	–	–	–	–	–	–	4/4	100

4.学会活動および海外における活動

　　　2012 年における国内の学会発表については 118 演題、国際学会の発表については 54 演題、海外特別講演は 35、国内特別講演は 60 でありました。私自身の海外出張は 2012 年は 19 回とこれも例年通りでありました。

　2012 年
　　1. 1 月 22 日-24 日　　　Advisory Board Meeting に出席
　　　　　　　　　　　　　　（San Francisco, USA）

　　2. 2 月 16 日-19 日　　　APASL 2012 にて講演 3 つとインベスティゲー
　　　　　　　　　　　　　　ターミーティング 2 つ
　　　　　　　　　　　　　　（Taipei, Taiwan）

　　3. 2 月 23 日-27 日　　　世界超音波医学会（WFUMB）理事会に理事長と
　　　　　　　　　　　　　　して出席
　　　　　　　　　　　　　　（Dubai, UAE）

　　4. 2 月 24 日-25 日　　　台湾消化器病学会にて特別講演
　　　　　　　　　　　　　　（Taipei, Taiwan）

　　5. 4 月 6 日-8 日　　　　韓国 Yonsei 大学および、HCC Expert
　　　　　　　　　　　　　　Symposium on Tumor Therapy にて講演
　　　　　　　　　　　　　　（Seoul, Korea）

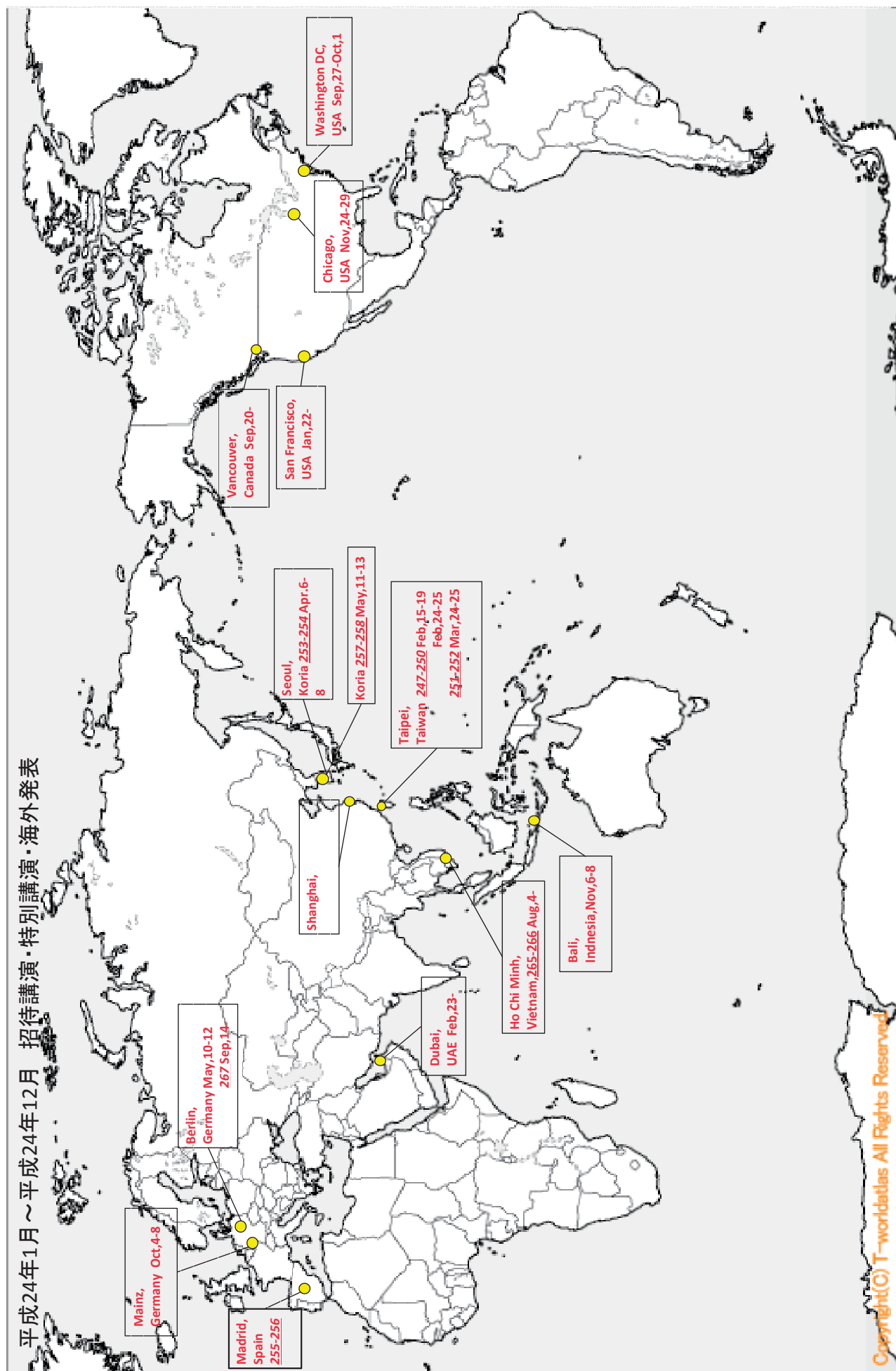　　6. 4 月 21 日-24 日　　　ヨーロッパ超音波医学会（Euroson）にて
　　　　　　　　　　　　　　2 つの特別講演

（Madrid,Spain）

7. 5 月 10 日-12 日　　　ヨーロッパ超音波医学会（Euroson）教育講演会
　　　　　　　　　　　　（Euroson school)にて招待講演
　　　　　　　　　　　　（Berlin,Germany）

8. 5 月 12 日-14 日　　　第 4 回アジア超音波造影イメージング
　　　　　　　　　　　　（Asian Conference on Ultrasound Contrast
　　　　　　　　　　　　Imaging)にて 2 つの講演
　　　　　　　　　　　　（Seoul, Korea）

9. 6 月 13 日-15 日　　　10th International Conference of the Asian
　　　　　　　　　　　　Clinical Oncology Society(ACOS)
　　　　　　　　　　　　にて特別講演
　　　　　　　　　　　　（Seoul, Korea）

10. 7 月 5 日-8 日　　　The 3rd Asia Pacific Primary Liver Cancer
　　　　　　　　　　　　Expert Meeting(APPLE)を co-chairman として
　　　　　　　　　　　　主催、3 つの講演と 1 つの司会
　　　　　　　　　　　　（Shanghai,China）

11. 8 月 3 日-5 日　　　BESTT Meeting にて講演
　　　　　　　　　　　　（Ho Chi Minh,Vietnum）

12. 9 月 13 日-18 日　　　国際肝癌学会（International Liver Cancer
　　　　　　　　　　　　Association）にて 3 つの講演と 1 つの司会
　　　　　　　　　　　　（Berlin,Germany）

13. 9 月 20 日-23 日　　　International Liver Forum で講演
　　　　　　　　　　　　（Vancouver,Canada）

14. 9 月 27 日-10 月 1 日　世界超音波医学会（WFUMB）理事会に理事長と

して出席
(Washington DC,USA)
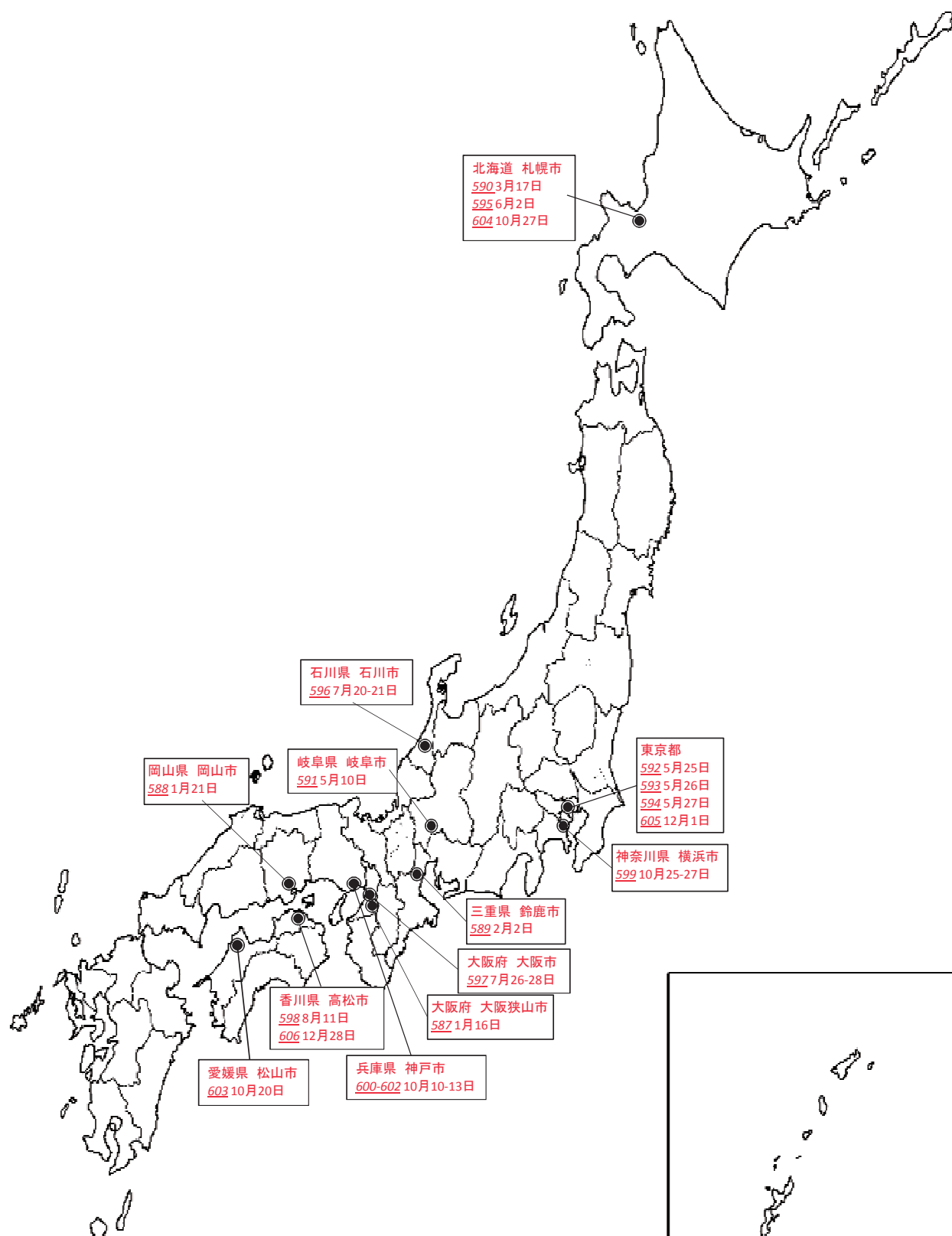
15. 10 月 4 日-8 日　　　　FALK Symposium にて講演
　　　　　　　　　　　　(Mainz,Germany)

16. 11 月 3 日-4 日　　　　Asia Pacific Virtual Meeting にて講演
　　　　　　　　　　　　（アジア 7 ヶ国を中継講演）
　　　　　　　　　　　　(Taipei,Taiwan)

17. 11 月 6 日-8 日　　　　AFSUMB 2012（アジア超音波医学会）にて 4 つ
　　　　　　　　　　　　の講演、および理事会 2 つ総会 1 つに出席
　　　　　　　　　　　　(Bali,Indonesia)

18. 11 月 11 日-13 日　　　米国肝臓学会(AASLD)へ出席(Boston,USA)

19. 11 月 24 日-29 日　　　米国放射線学会(RSNA)へ出席
　　　　　　　　　　　　AFSUMB 理事会、WFUMB Consensus on
　　　　　　　　　　　　Elastography の打ち合わせ、WFUMB-RSNA の
　　　　　　　　　　　　President 同士の会合に出席
　　　　　　　　　　　　(Chicago,USA)

平成24年1月～平成24年12月　招待講演・特別講演・海外発表

Washington DC,
USA Sep,27-Oct,1

Chicago,
USA Nov,24-29

Vancouver,
Canada Sep,20-

San Francisco,
USA Jan,22-

Seoul,
Koria 253-254 Apr.6-
8

Koria 257-258 May,11-13

Taipei,
Taiwan 247-250 Feb,15-19
Feb,24-25
251-252 Mar,24-25

Shanghai,

Ho Chi Minh,
Vietnam,265-266 Aug,4-

Bali,
Indnesia,Nov,6-8

Dubai,
UAE Feb,23-

Berlin,
Germany May,10-12
267 Sep,14

Mainz,
Germany Oct,4-8

Madrid,
Spain
255-256

平成24年1月～平成24年12月　招待講演・特別講演

北海道　札幌市
590 3月17日
595 6月2日
604 10月27日

石川県　石川市
596 7月20-21日

東京都
592 5月25日
593 5月26日
594 5月27日
605 12月1日

岐阜県　岐阜市
591 5月10日

岡山県　岡山市
588 1月21日

神奈川県　横浜市
599 10月25-27日

三重県　鈴鹿市
589 2月2日

大阪府　大阪市
597 7月26-28日

香川県　高松市
598 8月11日
606 12月28日

大阪府　大阪狭山市
587 1月16日

愛媛県　松山市
603 10月20日

兵庫県　神戸市
600-602 10月10-13日

5. 留学生受け入れ

　　留学生の受け入れですが、1999 年から 2000 年にかけて中国上海から Ding Hong 先生（丁　紅）（上海医科大学）、2001 年には中国広州から Wen YL 先生（文　艶玲）（中山医科大学）、2002 年には中国広州から Zheng RQ 先生（鄭栄琴）（中山医科大学）、2003 年には中国重慶より Zhou Pei（周　佩）（人民解放軍重慶病院）、2004 年にはカンボジアより Ly Sokhey 先生、2005 年にはタイから Worawan Chinamnan 先生、同じく 2005 年に若干時期を違えてインドから Kaushal Madan 先生（All India Institute of Medical Science: AIIMS）、2007 年 Kunal Das 先生を受け入れました。2008 年 Yu Xia（北京、中国）、2009 年 Md. Nadiruzzaman（バングラディシュ）、2010 年 Lorenzo Andreana（イタリア）が来ていました。またエジプトから Alshimaa 先生も来られました。2011 年にはマレーシアから Hadzri 先生が来られましたし、またイタリア　ボローニャ大学からも Alberto 先生が来られました。2012 年 7 月‐9 月には中国から Dr.Zhang Shuo も受け入れました。このように毎年、留学生が日中友好協会、笹川財団や日本消化器病学会、日本超音波医学会のフェローシップ留学生あるいは自国での fund をもって私どもの教室を希望して頂き、受け入れてきました。また来年度以降も先生方にはご迷惑をお掛けするかと思いますが、これも国際交流、アジアや世界への日本の貢献、各々の英語力に磨きをかけるという意味で有益と思いますので何卒御理解・御協力のほどお願い申し上げます。

6. 人事について

　　冒頭でも述べましたが、2003 年までの入局者は毎年 5、6 名〜12、13 名と大学内でも最も多くの入局者がおりましたが、2004 年に新臨床研修医制度が開始されてからの入局者、すなわち 2006 年の入局者は 2 名に留まり、2007 年の入局者も 1 名に留まりました。2008 年には 8 名もの入局者が入って来られました。2011 年は 3 名の研修医が入局し、2012 年にも 3 名が入局しました。反面、2-3 人の方が医局を離れました。従いまして依然、医局としての体制は大変厳しい状況にあります。このような状況の中で南大阪では大阪大学や大阪市大、和医大、奈良医大などがそれぞれの大学に人を引き上げているという状況のため、消化器内科医が激減し、南大阪の多くの公的病院では消化器内科医がほとんどゼロの状態が続いております。そのあおりで近医からの紹介患者や外来患者数は激増し、消化器内科の診療にも大きな負担がかかっております。しばら

くはこのような状況が続くものと思われるますので、本学ならびに分院の奈良病院、堺病院ともに結束して一人でも多くの人に入局して頂き、教育・研究・診療を円滑に行っていきたいと考えております。

7. NPO 法人「日本肝がん臨床研究機構（Japan Liver Oncology Group）」の活動

1. **JLOG 0801 trial**「肝癌早期診断のための多施設共同無作為化比較試験（Sonazoid-Enhanced LivEr Cancer Trial for Early Detection（SELECTED Study））」

→2012 年 10 月終了、現在データ解析中、学会および論文発表予定

2. **JLOG 0901 trial** 「進行・再発肝細胞癌に対する動注化学療法と分子標的薬併用による新規治療法の確立を目指した臨床試験（Phase III）ならびに効果を予測する biomarker の探索研究（Randomized Controlled Trial Comparing Efficacy of Sorafenib versus Sorafenib In combination with Low dose cisplatin/fluorouracil hepatic arterial InfUSion chemotherapy in Patients with Advanced Hepatocellular Carcinoma And Explolatory Study of Biomarker Predicting Its Efficacy (SILIUS Phase III trial))」

→**2010 年より厚労科研に移行**（厚生労働省科学研究費補助金 厚生労働省科学研究費補助金事業研究班（がん臨床部門）平成 23 年度「進行・再発肝細胞癌に対する動注化学療法と分子標的薬併用による新規治療法の確立を目指した臨床試験（Phase III）ならびに効果を予測する biomarker の探索研究」（工藤班））→2013 年で終了

3. **JLOG 0902 trial**「早期肝癌診断における EOB-MRI の有用性に関する多施設共同研究（Diagnosis of Early LIver Cancer Through EOB-MRI(DELICATE Study))」

4. **JLOG 1001 trial** 「切除不能肝細胞癌に対する肝動脈化学塞栓療法（TACE）とソラフェニブの併用療法第 II 相臨床試験（Phase II study: Transcatheter Arterial Chemoembolization Therapy In Combination with Sorafenib (TACTICS Study))」

5. **JLOG 1002 trial**「慢性肝疾患における非侵襲的弾性検査法を用いた肝線維化評価予測に関する研究(Assessment of Liver FIBROsis by Real-time Tissue ELASTography in Chronic Liver Disease (FIBROELAST Study))」

→**2011 年より厚労科研に移行**（厚生労働省科学研究費補助金事業研究班（難病・がん等の疾患分野の医療の実用化部門）平成 23 年度「慢性ウイルス性肝疾患の非侵襲的線化評価法の開発と臨床的有用性の確立」（工藤班））

6. **JLOG 1003 trial**「非侵襲的弾性検査法を用いた肝線維化度評価によるウイルス性肝炎患者における肝発癌・門脈圧亢進症の発現予測（<u>P</u>rediction of Incidence of Liver <u>C</u>ancer or por<u>T</u>al Hypertension in Patients with Viral Hepatitis by <u>U</u>se of <u>R</u>eal-time Tissue <u>E</u>lastography（PICTURE Study））」

→**2011 年より厚労科研に移行**（厚生労働省科学研究費補助金事業研究班（難病・がん等の疾患分野の医療の実用化部門）平成 23 年度「慢性ウイルス性肝疾患の非侵襲的線化評価法の開発と臨床的有用性の確立」（工藤班））

7. **JLOG 1004 trial**「インスリン抵抗性を合併する C 型代償性肝硬変患者を対象とした BCAA 顆粒製剤の肝細胞癌抑制効果に関する第 III 相臨床試験（<u>BCAA</u> Granule for patients with Hepatitis C-related <u>L</u>iver Cirrhosis and Insulin Resistance <u>O</u>n the Effect of Reduction of <u>C</u>arcinogenic Ris<u>K</u> in the Liver(Phase III study)(BLOCK Study))」

8. おわりに

　　この年報を作成にあたりましては例年の如く、教授秘書、医局秘書の秘書連合軍の 13 名の皆様に全面的に編集をして頂き大変感謝を致しております。また、医局員の皆様にも大変この一年お世話になりました。この一年間も大変なハードワークではありましたが、無事皆様の頑張りにより乗り切ることができました。この場をお借りして深く感謝申し上げます。2010 年には念願の一病棟まるまる消化器内科が占めるという状態が実現しましたし、腹部超音波室も拡充されました。2013 年には救急災害棟も完成いたします。光学治療センターの拡充も終了しましたので何卒昨年以上にモチベーションを上げて頂いて日本一、あるいは世界一の消化器内科学教室へ育つようにご尽力頂きたいと思います。2013 年も教育・診療・研究において、特に英文論文、新しい研究の立ち上げということについては 2012 年以上に積極的に取り組んでいきたいと考えておりますので医局員全員が共通の価値観と消化器内科の将来の方向性に対するベクトルを共有し、心を一つにして邁進して頂きたいと祈念・期待しております。

<div align="right">2013 年 9 月　大阪狭山にて</div>

2012 年度表彰式一覧

➢ Highest Impact Factor Award 2012(最高インパクトファクター賞)

    1 位　西田直生志　11.665（Hepatology）
    2 位　櫻井俊治　　7.856（Cancer Res）

        ※　3 位　北野雅之　7.282（Am J Gastroenterol）
        ※　工藤正俊　4.327（Curr Cancer Drug Tar）

➢ Most Numbers of Paper Award 2012 （最多英文論文発表賞）

    1 位　萩原　智　4 本（Brit J Cancer, Hepatol Res, Digest Dis×2）
    2 位　南　康範　3 本（Eur J Radiol, Digest Dis, J Med Ultrason）

        ※　工藤正俊　10 本

➢ Total Highest Impact Factor Award 2012 （累積最高インパクトファクター賞）

    1 位　西田直生志　14.038（2 本）
    2 位　萩原　智　　11.987（4 本）

        ※　3 位　櫻井俊治　9.050（2 本）
        ※　工藤正俊　15.188（10 本）

➢ 最多入院受持患者賞

    1 位　矢田典久　250 人
    2 位　宮田　剛　231 人

        ※　3 位　今井　元　212 人

➢ 最多緊急内視鏡賞

    1 位　川崎正憲　20 件
    1 位　足立哲平　20 件

        ※　3 位　峯　宏昌　17 人

➢ 最多外来患者診療賞

    1 位　萩原　智　1,665 人
    2 位　矢田典久　1,286 人

        ※ 3 位　松井繁長　1,115 人
        ※　工藤正俊　1,117 人

工藤正俊（くどうまさとし）

昭和 29 年	愛媛県西条市生まれ	
昭和 53 年	京都大学医学部 卒業	
同	京都大学医学部附属病院 勤務（研修医）	
昭和 54 年	神戸市立中央市民病院内科 勤務（研修医）	
昭和 55 年	同 消化器内科 医員	
昭和 60 年	同 消化器内科 副医長	
昭和 62 年	カリフォルニア大学留学（デービスメデイカルセンター）	
平成元年	神戸市立中央市民病院消化器内科 副医長 復職	
平成 4 年	同 消化器内科 医長	
平成 9 年	近畿大学医学部第 2 内科学 助教授	
平成 11 年	近畿大学医学部消化器内科学 教授 現在に至る	
（現在の併任）	近畿大学医学部附属病院病院長（平成 20 年 10 月～現在）	
	近畿大学医学部中央臨床検査部長（平成 20 年 10 月～現在）	
	近畿大学医学部光学治療センター長（平成 20 年 10 月～現在）	
	近畿大学医学部高度先端医療センター長（平成 20 年 10 月～現在）	
	近畿大学医学部 NICU 部長（平成 22 年 10 月～現在）	
	近畿大学医学部附属病院救急災害センター長（平成 25 年 9 月 1 日～現在）	
	近畿大学医学部奈良病院消化器内科 教授（兼務）	
	近畿大学医学部堺病院消化器科 教授（兼務）	
	神戸市立中央市民病院消化器内科 顧問（兼務）	

主な所属学会

日本消化器病学会（財団評議員・指導医・専門医）、日本肝臓学会（理事・指導医・専門医・治験支援委員会委員長・生涯教育委員会副委員長）、日本消化器内視鏡学会（評議員・指導医・専門医）、日本超音波医学会（理事・指導医・専門医・国際交流委員会委員長）、日本内科学会(評議員・認定内科医)、日本高齢消化器病学会（理事），日本核医学会(評議員・専門医)、日本肝癌研究会（常任幹事・追跡調査委員長・取扱規約委員長・肝癌治療効果判定基準作成委員会委員長・事務局代表）、日本肝移植研究会（世話人）、肝血流動態イメージ研究会（幹事）、日本腹部造影エコー・ドプラ診断研究会（事務局・代表世話人）、肝癌治療シミュレーション研究会（副代表幹事・企画委員）、超音波治療研究会（常任世話人）、日本肝がん分子標的治療研究会（代表世話人・事務局代表）、日本消化器内視鏡財団（評議員）、日本臨床腫瘍学会（評議員・保険委員会委員（2013 年 4 月－現在））、日本癌学会（評議員）、米国肝臓学会（AASLD）（肝癌部門企画運営委員：Steering Committee of hepatobiliary malignancy）、米国消化器病学会（AGA）、世界肝臓学会 （IASL）、欧州肝臓学会（EASL）、米国消化器内視鏡学会（ASGE）など。

委員・資格など

- 世界超音波医学会（WFUMB），President（理事長）
- アジア超音波医学会（AFSUMB）Secretary（庶務担当理事）
- 国際肝癌学会（ILCA）理事（Founding Board Member, Governing Board Council Member）
- 米国肝臓学会（AASLD）肝癌部門運営委員会委員（Steering Committee Member）

- 日本肝がん臨床研究機構（JLOG）（理事長）
- 世界保健機構（WHO）Blue Book「Classification of the Tumor」改訂委員（平成 21 年 5 月 1 日）
- ウイルス肝炎研究財団　日米医学協力研究会肝炎専門部会研究員
- International Liver Thought Leadership Study（ILCS），Council member
- アジア太平洋肝癌専門家会議（APPLE）理事長（President）
- Editor-in-Chief: Liver Cancer（Karger, Basel）

受賞
- 米国核医学会 Berson-Yalow Award 受賞（平成元年 6 月）
- 日本対がん協会がん研究助成奨励賞 受賞（平成 4 年 3 月）
- 日本消化器病学会奨励賞 受賞（平成 4 年 4 月）
- 日本核医学会賞 受賞（平成 5 年 10 月）
- 米国超音波医学会（AIUM）学会賞受賞（平成 15 年 6 月 4 日）
- ボローニャ大学医学部医学会名誉会員賞（平成 18 年 9 月 15 日）
- フィリピン超音波医学会名誉会員（Honorary Member of PSUCMI）（平成 20 年 3 月 19 日）
- アジア太平洋消化器病学会（APDW）OKUDA Award 受賞（平成 20 年 9 月 13 日）
- 北米放射線学会 Certificate of Merit 受賞（平成 20 年）
- インド肝臓学会 Madangopalan Award 受賞（平成 21 年 3 月 28 日）
- 北米放射線学会 Cum Laude 賞受賞（平成 21 年 12 月）（7000 編の論文中上位 10 編に採択）
- 日本肝臓学会「日本肝臓学会機関誌 Highest Citation 賞」受賞（平成 22 年 6 月）
- JISAN Lecture Award Presented by Korean Society of Ultrasound in Medicine（平成 22 年 5 月）
- 米国超音波医学会名誉会員賞（AIUM Honorary Member Award）受賞（平成 23 年 4 月）
- 韓国超音波医学会名誉会員賞（KSUM honorary Award）受賞（平成 23 年 5 月）
- 日本肝臓学会「日本肝臓学会機関誌 Highest Citation 賞」受賞（平成 23 年 6 月）（2 回目）
- Romanian Society of Ultrasound in Medicine and Biology（SRUMB）Honorary Award 受賞（平成 23 年 6 月）
- 北米放射線学会 Certificate of Merit 受賞（平成 23 年 11 月）（2 回目）
- USE 論文賞（応用物理学会論文賞）」受賞（平成 24 年 11 月）

著書（単著）
- Contrast Harmonic Imaging in the Diagnosis and Treatment of Liver Tumors（Springer-Verlag　2003）
- 肝腫瘍における造影ハーモニックイメージング（医学書院　2001）

編集
- 松井　修，**工藤正俊**，編集：消化器疾患の造影エコー Up Date．南江堂，東京，2003.
- **工藤正俊**，編集：肝細胞癌治療の最近の進歩，消化器病セミナー97，へるす出版，東京，2004.
- 河田純男，白鳥康史，**工藤正俊**，榎本信幸，編集，小俣政男，監修：肝疾患 Review 2004，日本メディカルセンター，東京，2004.
- 河田純男，白鳥康史，**工藤正俊**，榎本信幸，編集，小俣政男，監修：肝疾患 Review 2006-2007，日本メディカルセンター，東京，2006.
- 河田純男，横須賀收，**工藤正俊**，榎本信幸，編集，小俣政男，監修：肝疾患 Review 2008-2009，日本メディカルセンター，東京，2008.
- 河田純男，横須賀收，**工藤正俊**，榎本信幸，編集，小俣政男，監修：肝疾患 Review 2010-2011，日本メディカルセンター，東京，2010.
- 幕内雅敏，菅野健太郎，**工藤正俊**，編集：今日の消化器疾患治療指針　第 3 版，医学書院，東京，2010.
- **工藤正俊**，泉　並木，編集：症例から学ぶ　ウイルス肝炎の治療戦略．（株）診断と治療社，東京，2010.
- **工藤正俊**，編集：肝細胞癌の分子標的治療，アークメディア，東京，2010.
- 山雄健次，**工藤正俊**，編集：見逃し，誤りを防ぐ！肝・胆・膵癌画像診断アトラス，羊土社，東京，2010.
- **工藤正俊**，編集：医学のあゆみ「肝癌の分子標的治療」，医歯薬出版株式会社，東京，2011.
- **工藤正俊**，編集：「肝細胞がん診療の進歩：Up-To-Data」，最新医学社，大阪，2011.
- **工藤正俊**，編集：朝倉内科学，矢崎義雄，「総編集」，朝倉書店，東京，2013.
- **工藤正俊**，國分茂博，編集：EOB-MRI/ソナゾイド造影超音波による肝癌の診断と治療，医学書院，東京，2013

SIENTIFIC PAPER PUBLICATION:

特別講演・招待講演・教育講演:

学術論文　　　　　英文論文: 455 (IF: 1525.015)
　　　　　　　　　和文論文:942
教科書（単著）　　英文: 3　　　　和文: 8
分担執筆　　　　　英文: 21　　　和文: 224

国際学会: 273
国内学会: 608

科学研究費等外部資金の獲得状況

・　文部科学省科学研究費補助金　　　　基盤研究(A)　　　2件（総額 1,100 万円）
　　　　　　　　　　　　　　　　　　基盤研究(B)　　　6件（総額 2,311 万円）
　　　　　　　　　　　　　　　　　　基盤研究(C)　　12件（総額 1,240 万円）
　　　　　　　　　　　　　　　　　　挑戦的萌芽研究　3件（総額　　310 万円）
　　　（主任研究者）　　　　　　　　　　　　　　　　　　　（　　　260 万円）
　　　「肝細胞癌の発癌・進展の分子機序: 造影超音波クッパー相と遺伝子発現を用いた融合解析」
　　　（分担研究者）　　　　　　　　　　　　　　　　　　　（　　　　50 万円）
　　　「肝細胞癌のソラフェニブ著効例における感受性規定遺伝子変異の探索」（主任研究者　西尾和人）
・　知的クラスター創生事業（がんペプチドワクチン）　　1件（総額　　10 万円）
・　車両財団がん研究助成金　　　　　　　　　　　　　　1件（総額　100 万円）
・　学会奨励研究補助金　　　　　　　　　　　　　　　　6件（総額　530 万円）
・　医師会・民間医学振興財団等研究補助金　　　　　　32件（総額 2,089 万 5 千円）
・　国立がん研究センターがん研究開発費（分担研究者）　　（　　　245 万円）
　　　「抗悪性腫瘍薬による肝炎ウイルス再活性化の調査とその対応に関する研究」（班長　池田公史）
・　国立がん研究センターがん研究開発費（分担研究者）　　（　　　　12 万円）
　　　「進行肝胆膵がんの治療法の開発に関する研究」（班長　奥坂拓志）

・　厚生労働省省科学研究費　　　　　**主任研究者**　　5件（総額 2 億 2,375 万円）
　　1.（がん臨床研究事業）
　　　「進行・再発肝細胞癌に対する動注化学療法と分子標的薬併用による新規治療法の確立を目指した臨床試験（Phase III）ならびに効果を予測する biomarker の探索研究」
　　2.（難病・がん等の疾患分野の医療の実用化研究事業）
　　　「慢性ウイルス性肝疾患の非侵襲的線化評価法の開発と臨床的有用性の確立」

・　厚生労働省科学研究費　　　　　　**分担研究者**　　29件（総額 3,325 万円）
　　1.（肝炎等克服緊急対策研究事業）
　　　「血小板低値例へのインターフェロン治療法の確立を目指した基礎および臨床的研究」（班長　西口修平）

2．（がん臨床研究事業）
「初発肝細胞癌に対する肝切除とラジオ波焼灼両方の有効性に関する多施設共同研究」（班長　國土典宏）
3．（肝炎等克服緊急対策研究事業）
「肝がんの新規治療法に関する研究」（班長　本多政夫）
4．（難治性疾患克服研究事業）
「多発肝のう胞症に対する治療ガイドライン作成と試料バンクの構築」（班長　大河内信弘）
5．（難病・がん等の疾患分野の医療の実用化研究事業）
「慢性ウイルス性肝疾患患者の情報収集の在り方等に関する研究」（班長　相崎英樹）

ガイドライン策定委員会委員

- 「科学的根拠に基づく肝癌診療ガイドライン」（日本肝臓学会編），金原出版
- 「「慢性肝炎の治療ガイドライン」（日本肝臓学会編），文光堂
- 「肝癌診療マニュアル」（日本肝臓学会編），医学書院
- 「肝癌治療効果判定基準」（日本肝癌研究会取扱い規約委員会編），肝臓
- 臨床病理「肝癌取り扱い規約」（日本肝癌研究会編）
- Clinical Practice Guidelines for Hepatocellular Carcinoma, Japan Society of Hepatology, Hepatology Research
- General Rules for the Clinical and Pathological Study of Primary Liver Cancer, 3rd English Version, Liver Cancer Study Group of Japan, Kanehara, Tokyo, 2010
- Response Evaluation criteria in the Cancer of the Liver (RECICL), Liver Cancer Study Group of Japan, Hepatology Research
- 「多発肝のう胞症に対する治療ガイドライン」

特許取得

発明の名称：　ソラフェニブの効果予測方法
出願番号：　特願 2011-104275
出願日：　2011 年 5 月 9 日
発明者：　荒尾徳三、松本和子、西尾和人、工藤正俊
出願人：　学校法人近畿大学

発明の名称：　N 型糖鎖を利用した膵臓癌の診断方法
公開番号：　特許公開 2009-270996
公開日：　2009 年 11 月 19 日
発明者：　荒尾徳三、松本和子、西尾和人、坂本洋城、北野雅之、工藤正俊
出願人：　住友ベークライト株式会社

全国規模の学会・研究会事務局

- 日本肝癌研究会（**事務局・追跡調査委員長・常任幹事**）
- 日本腹部造影エコー・ドプラ診断研究会（**代表世話人・事務局**）
- NPO 法人日本肝がん臨床研究機構（**理事長・事務局**）
- 日本肝がん分子標的治療研究会（**代表世話人・事務局**）

全国規模の研究会世話人・役員

平成 6 年 4 月−8 年 3 月　　日本超音波医学会腹部造影エコー研究部会幹事
平成 7 年 11 月−現在　　　肝血流動態イメージ研究会世話人
平成 8 年 4 月−現在　　　日本腹部造影エコー・ドプラ造影研究会世話人（事務局兼務）（平成 25 年より**代表世話人**）
平成 9 年 7 月−現在　　　肝動脈塞栓療法研究会世話人
平成 10 年−現在　　　　　国際造影超音波研究会（現、Asia Contrast Ultrasound Imaging Society）世話人
平成 11 年 10 月−現在　　臨床消化器病研究会世話人
平成 11 年 7 月−現在　　　西日本肝臓研究会世話人
平成 13 年 5 月−現在　　　肝疾患フォーラム世話人
平成 14 年 4 月―現在　　　犬山シンポジウム会員
平成 14 年 9 月−現在　　　日本消化器画像診断研究会世話人
平成 16 年−現在　　　　　Liver Forum in Kyoto 世話人
平成 18 年−現在　　　　　肝癌治療シミュレーション研究会副代表幹事

平成 19 年 11 月-現在　　　日本超音波治療研究会常任世話人
平成 20 年-現在　　　　　　日本肝がん分子標的治療研究会（**代表世話人**）

関西地区研究会代表世話人
・平成 11 年-平成 19 年　関西造影超音波研究会（**代表世話人**）
・平成 13 年-現在　　　　関西 B 型肝炎研究会（**代表世話人**）
・平成 14 年-現在　　　　肝癌局所治療研究会（**代表世話人**）
・平成 14 年-現在　　　　大阪消化器化学療法懇話会（**代表世話人**）
・平成 15 年-現在　　　　臨床消化器病フォーラム（**代表世話人**）
・平成 18 年-平成 22 年　Bay Area Gut Club（**代表世話人**）
・平成 18 年-平成 22 年　South Osaka Liver Club（**代表世話人**）
・平成 19 年-現在　　　　関西肝血流動態イメージ研究会（**代表世話人**）
・平成 20 年-現在　　　　Kinki Liver Club（**代表世話人**）
・平成 21 年-現在　　　　南大阪肝疾患研究会（**代表世話人**）
・平成 21 年-現在　　　　南大阪肝胆膵疾患研究会（**代表世話人**）

関西地区研究会世話人
・平成　2 年-現在　　　　大阪肝穿刺生検治療研究会世話人
・平成　6 年-現在　　　　兵庫インターベンショナルラディオロジー研究会世話人
・平成　8 年-現在　　　　肝胆膵治療フォーラム・神戸世話人
・平成　9 年-現在　　　　京都肝疾患懇話会世話人
・平成　9 年-現在　　　　肝臓分子生物学研究会
・平成 11 年-平成 18 年　肝代謝コロキウム世話人
・平成 11 年-現在　　　　大阪肝胆膵懇話会世話人
・平成 11 年-現在　　　　南大阪肝胆膵疾患研究会世話人
・平成 11 年-現在　　　　南大阪消化器病懇話会世話人
・平成 11 年-現在　　　　南大阪肝疾患研究会世話人
・平成 11 年-平成 24 年　消化器ラウンドテーブルディスカッション世話人
・平成 11 年-平成 18 年　泉州肝臓病研究会世話人
・平成 11 年-平成 18 年　大阪肝炎ミーティング世話人
・平成 12 年-現在　　　　大阪肝臓病談話会世話人
・平成 12 年-現在　　　　関西経皮内視鏡的胃瘻造設術研究会世話人
・平成 12 年-現在　　　　肝疾患座談会 in Kyoto 世話人
・平成 12 年-現在　　　　近畿肝癌談話会常任幹事
・平成 13 年-現在　　　　関西肝血流動態イメージ研究会世話人
・平成 16 年-平成 23 年　あおい肝臓研究会世話人
・平成 18 年-現在　　　　大阪肝臓ミーティング世話人
・平成 19 年-現在　　　　近畿・超音波内視鏡研究会顧問

全国規模の国内研究会主催
・1997 年 2 月　　第 3 回肝血流動態イメージ研究会（神戸）
・1996 年 10 月　第 1 回日本造影エコードプラ診断研究会（神戸）
・2005 年 2 月　　第 11 回肝血流動態イメージ研究会（横浜）
・2007 年 9 月　　第 2 回肝癌治療シミュレーション研究会（大阪）
・2008 年 8 月　　日本消化器画像診断研究会（大阪）
・2010 年 1 月　　第 1 回日本肝癌分子標的治療研究会（神戸）
・2014 年 2 月　　第 20 回肝血流動態・機能イメージ研究会（大阪）（予定）

国内学会主催
・第 45 回日本肝臓学会総会（2009 年 6 月），神戸
・第 83 回日本超音波医学会学術集会（2010 年 5 月），京都
・第 50 回日本肝癌研究会（2014 年 6 月），京都（予定）
・日本超音波医学会第 89 回学術集会（2016 年 5 月），京都（予定）

近畿地区学会主催
・消化器地方会
・消化器内視鏡地方会

国際学会主催

・SH Single Topic Conference on HCC（2005 年）, Awaji-shima
・The 3rd International Kobe Liver Cancer Symposium on HCC（IKLS）（2009 年 6 月）, Kobe
・The 2nd Asia Pacific Primary Liver Cancer Expert Meeting（APPLE）（2011 年 7 月）, Osaka
・The 14th WFUMB 2013（世界超音波医学会）（2013 年 5 月）, Sao Paulo
・The 4th International Kyoto Liver Cancer Symposium(IKLS)（2014 年 6 月),Kyoto（予定）
・The 6th Asia Pacific Primary Liver Cancer Expert Meeting（APPLE）（2015 年 7 月),Kobe(予定）
・AFSUMB 2016（アジア超音波医学会）（2016 年 5 月）,Kyoto（予定）

消化器内科学教室業績抜粋

	1999	2000	2001	2002	2003	2004	2005	2006	2007	2008	2009	2010	2011	2012	2013	計
英文論文 (著書・分担執筆を含む) (Impact Factor)	8 44.626	12 38.663	27 62.069	13 19.776	22 53.353	21 73.701	25 63.245	15 39.819	31 96.273	45 146.061	26 98.7	51 124.732	48 146.139	46 170.726	73 292.37	463 1470.257
英文論文 (著書・分担執筆)	1	1	4	0	1	1	0	0	0	2	0	1	0	2		13
和文論文 (著書・分担執筆を含む)	37	41	43	34	31	54	45	39	46	73	81	130	65	54		443
海外学会発表	2	9	4	6	24	23	14	14	17	26	20	35	66	52		139
国内学会発表	46	59	71	114	107	81	70	52	77	89	64	96	102	62		766
海外特別講演	0	11	4	11	8	18	16	25	18	36	34	43	35	35		147
国内特別講演	37	40	40	52	37	38	39	27	38	40	64	93	75	60		388
単著教科書			1		1 (英文)											2

消化器内科年度別診療実績

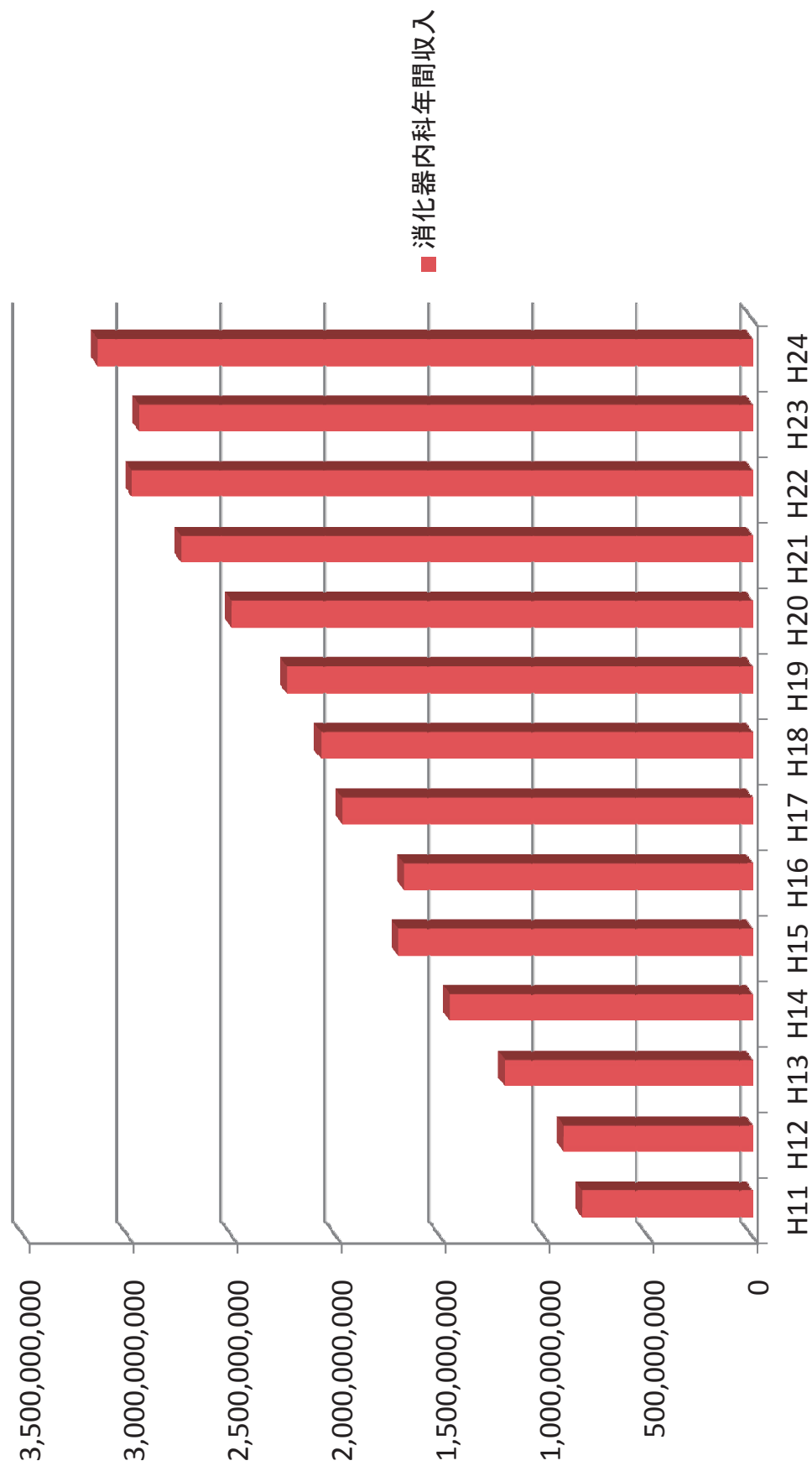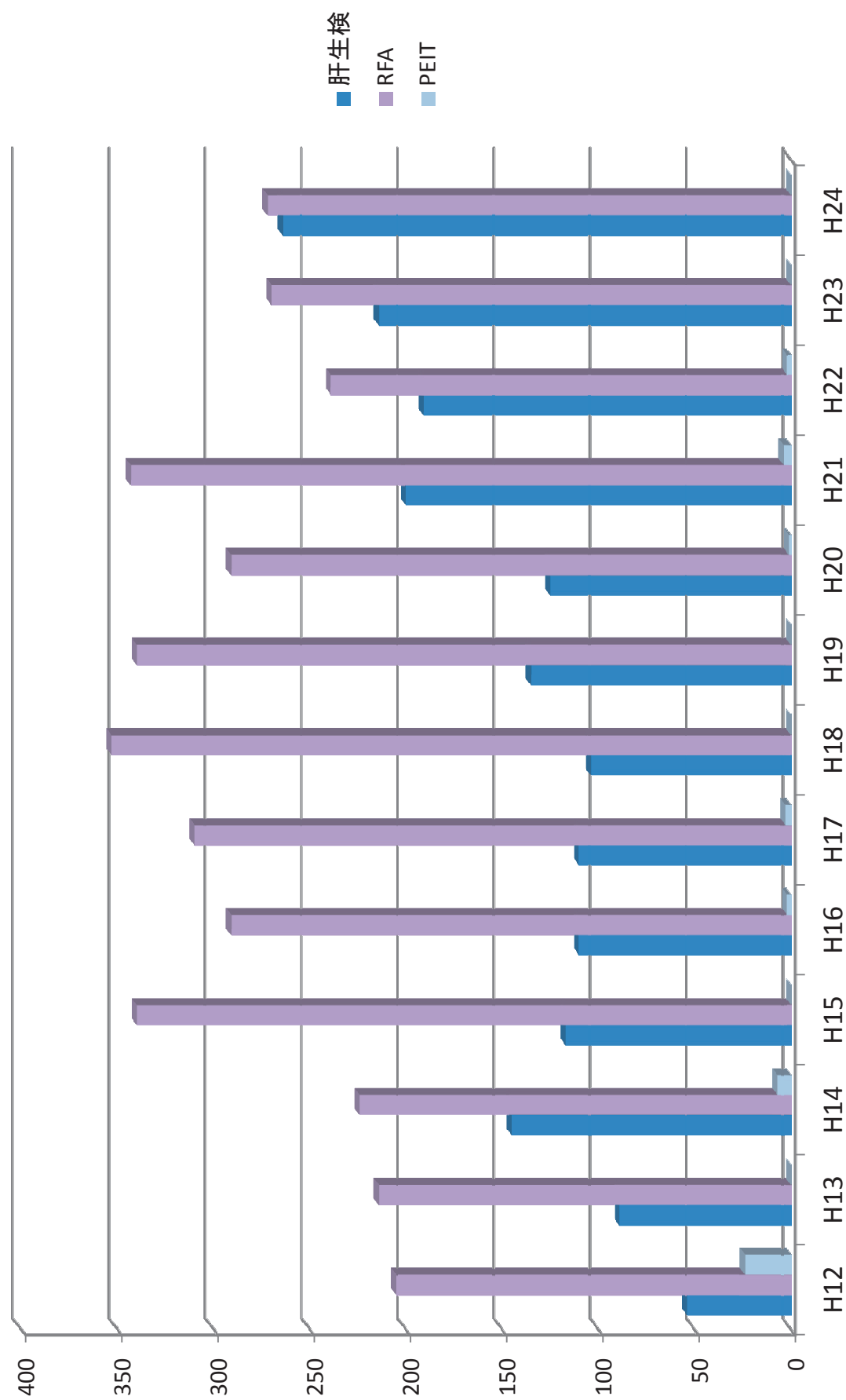|	H11	H12	H13	H14	H15	H16	H17	H18	H19	H20	H21	H22	H23	H24
稼働床	40	44	44	44	60	78	78	77	76	73	85	84	84	84
稼働率	107.2%	98.5%	126.7%	148.2%	121.0%	89.5%	95.3%	89.2%	94.7%	96.3%	91.8%	89.9%	85.8%	89.0%
日平均入院患者数	40.0	43.3	55.8	65.2	72.6	69.8	74.4	68.7	72.0	70.3	70.3	76.1	72.0	74.7
平均在院日数	31.1	25.6	21.4	18.6	15.4	14.7	12.8	10.7	10.5	9.6	9	8.6	7.9	7.2
年間入院収入	501,570,188	570,616,464	801,199,124	923,171,333	1,065,481,449	1,023,271,279	1,152,778,111	1,106,484,453	1,224,122,968	1,244,806,271	1,312,812,506	1,516,925,835	1,417,104,402	1,535,069,456
年間外来収入	314,641,639	334,517,979	386,084,329	530,035,297	635,562,806	649,876,475	818,049,485	966,247,389	1,013,910,559	1,257,804,553	1,432,350,698	1,464,645,183	1,529,385,181	1,610,826,432
消化器内科年間収入	816,211,827	905,134,443	1,187,283,453	1,453,206,630	1,701,044,255	1,673,147,754	1,970,827,596	2,072,731,842	2,238,033,527	2,502,610,824	2,745,163,204	2,981,571,018	2,946,489,583	3,145,895,888

消化器内科年間入院収入

年間入院収入

消化器内科入院診療実績

凡例:
- 日平均入院患者数
- 平均在院日数

消化器内科年間外来収入

年間外来収入

H11 H12 H13 H14 H15 H16 H17 H18 H19 H20 H21 H22 H23 H24

消化器内科年間総収入

消化器内科年間収入

経皮的局所治療・肝生検総件数

凡例: 肝生検 / RFA / PEIT

横軸: H12　H13　H14　H15　H16　H17　H18　H19　H20　H21　H22　H23　H24

縦軸: 0　50　100　150　200　250　300　350　400

腹部造影エコー検査

凡例: レポビスト（薄い青）、ソナゾイド（濃い青）
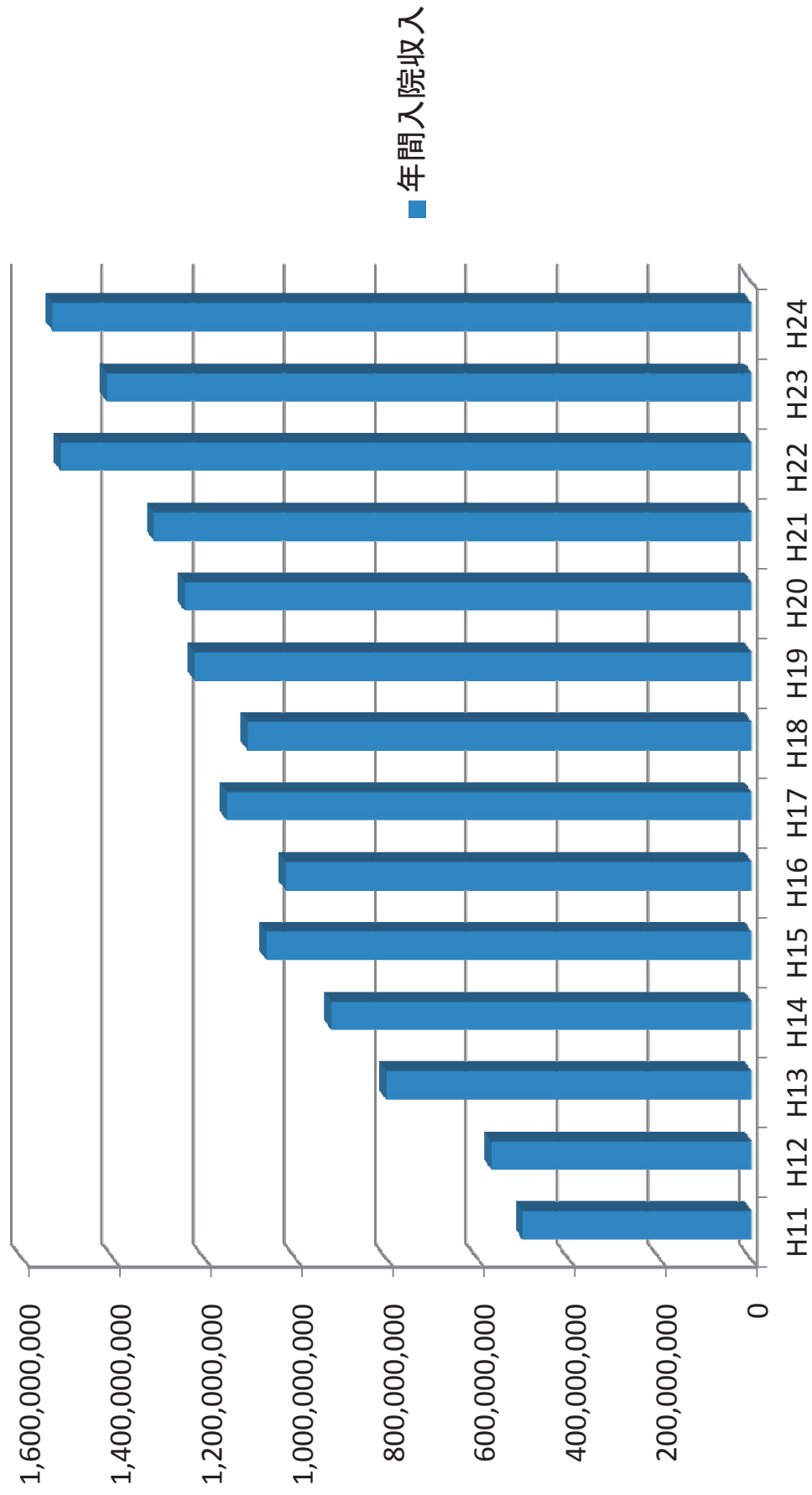
	H11	H12	H13	H14	H15	H16	H17	H18	H19	H20	H21	H22	H23	H24
縦軸	0	100	200	300	400	500	600	700						
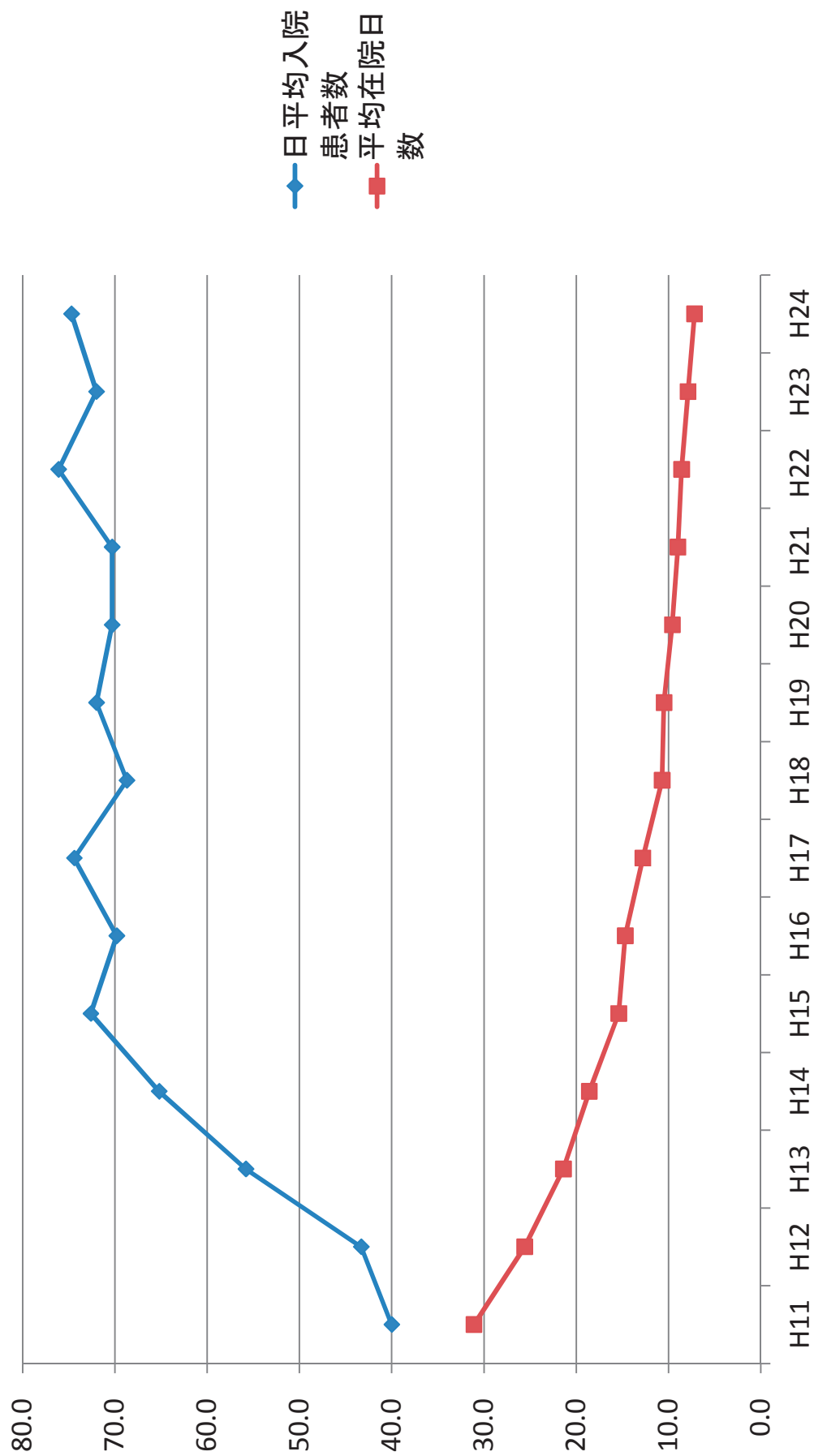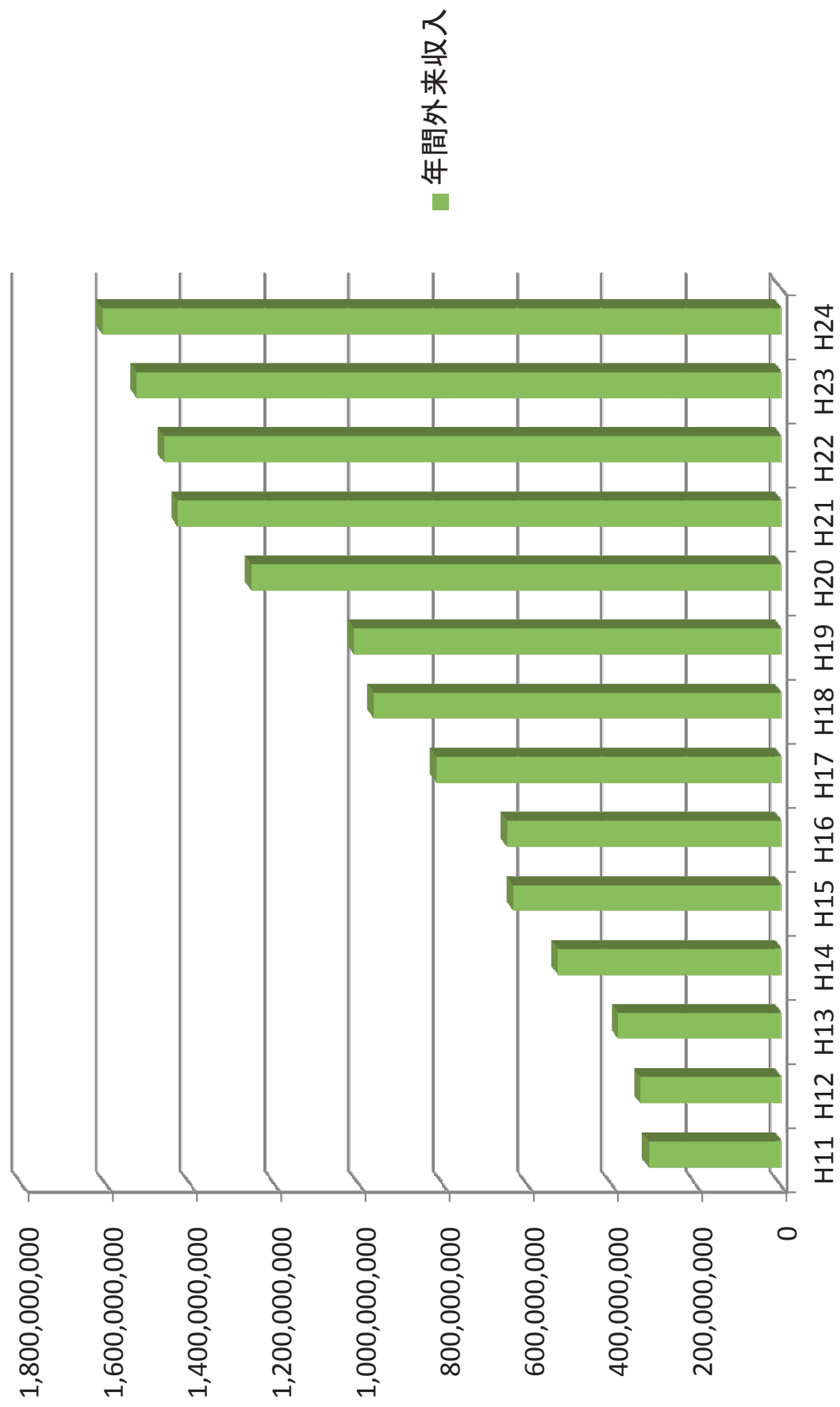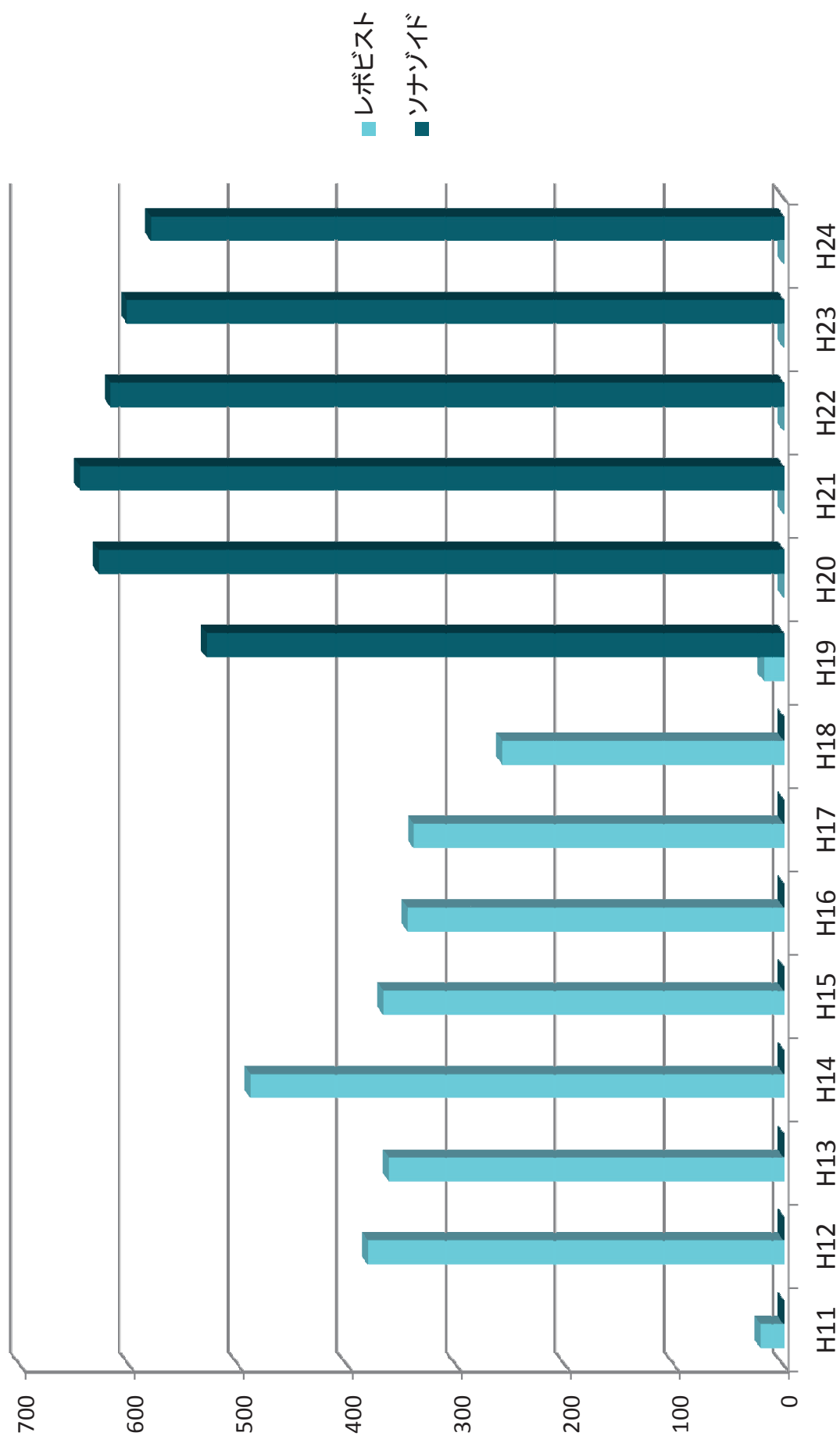
内視鏡部年報

検査	H11	H12	H13	H14	H15	H16	H17	H18	H19	H20	H21	H22	H23	H24
胃・十二指腸ファイバー球部	4032	4318	4434	4780	4926	5208	5453	5934	6534	6588	6742	7215	7640	8205
乳頭部・肛側	165	160	187	181	263	254	327	316	373	365	482	520	441	462
大腸ファイバースコピー	1537	1479	1433	1648	1883	1947	2175	2548	2796	2904	2754	2934	3047	3320
気管支ファイバースコピー	420	412	376	429	428	434	445	417	426	450	475	558	561	537
小腸ファイバースコピー	1	0	3	3	0	0	4	0	37	75	62	63	81	110
計（スクリーニング）	6155	6369	6433	7041	7500	7843	8404	9215	10166	10382	10515	11290	11770	12634
胃生検	1509	1650	1851	1908	2005	2101	2473	2533	2412	2261	2175	2134	2095	2066
大腸生検	1028	970	831	829	861	869	952	1143	1088	987	932	1001	946	1027
気管支生検	245	222	227	265	260	296	281	314	302	314	345	393	371	338
小腸生検	1	0	0	2	0	0	1	0	11	8	12	18	17	27
計	2783	2842	2909	3004	3126	3266	3707	3990	3813	3570	3464	3546	3429	3458
胆道ドレナージ	43	43	60	66	121	96	151	122	141	142	234	225	169	167
乳頭切開	15	19	14	11	44	44	46	44	48	46	74	132	102	102
乳頭バルーン拡張術	0	6	8	2	1	0	9	11	13	5	5	9	4	0
結石除去	16	24	15	17	38	49	55	51	62	65	86	130	87	95
食道静脈瘤結紮術	72	79	51	62	97	100	75	58	81	83	62	69	78	68
硬化療法	2	9	13	13	23	12	7	4	5	12	11	7	14	11
EISL	-	22	52	56	47	54	40	27	22	11	26	31	36	21
食道ブジー	116	137	124	152	210	308	252	246	234	308	284	269	256	213
APC	6	8	22	23	25	32	24	52	72	65	68	32	33	31
異物除去	6	2	3	11	14	17	14	11	18	21	14	20	22	21
胃ポリペクトミー	12	18	18	16	7	12	9	1	2	0	1	2	4	2
大腸ポリペクトミー	257	300	296	344	397	111	89	66	41	20	22	42	37	74
EMR（胃・食道）	27	24	64	73	70	73	90	100	52	127	52	39	143	208
ESD(胃・食道)	-	-	-	-	36	32	52	51	71	82	98	109	110	167
EMR(大腸)	-	-	-	-	-	290	373	470	443	458	467	484	476	556
緊急内視鏡検査	84	114	135	291	425	485	487	337	265	192	272	308	330	232
凝固止血バイポーラ	35	48	50	91	91	68	89	52	51	32	63	63	81	117
色素撒布法	216	291	459	724	1194	1470	1582	1909	1753	1731	1891	1937	2013	2171
トロンビン被覆療法	81	88	113	193	198	236	294	369	387	319	326	282	332	335
アルト被覆療法	41	41	52	97	91	96	180	161	190	144	182	130	133	178
経皮内視鏡的胃瘻造設術	-	14	18	10	15	23	33	28	54	33	69	74	87	74
超音波内視鏡(胃)	48	77	181	170	205	249	293	379	505	523	622	895	989	1346
超音波内視鏡(大腸)	-	17	28	6	8	5	5	0	1	0	1	0	4	9
計	1077	1381	1776	2428	3357	3836	4203	4498	4511	4419	4930	5289	5430	6031

消化管内視鏡検査件数年次推移

凡例:
- 胃・十二指腸ファイバー球部
- 乳頭部・肛側
- 大腸ファイバースコピー
- 気管支ファイバースコピー
- 小腸ファイバースコピー
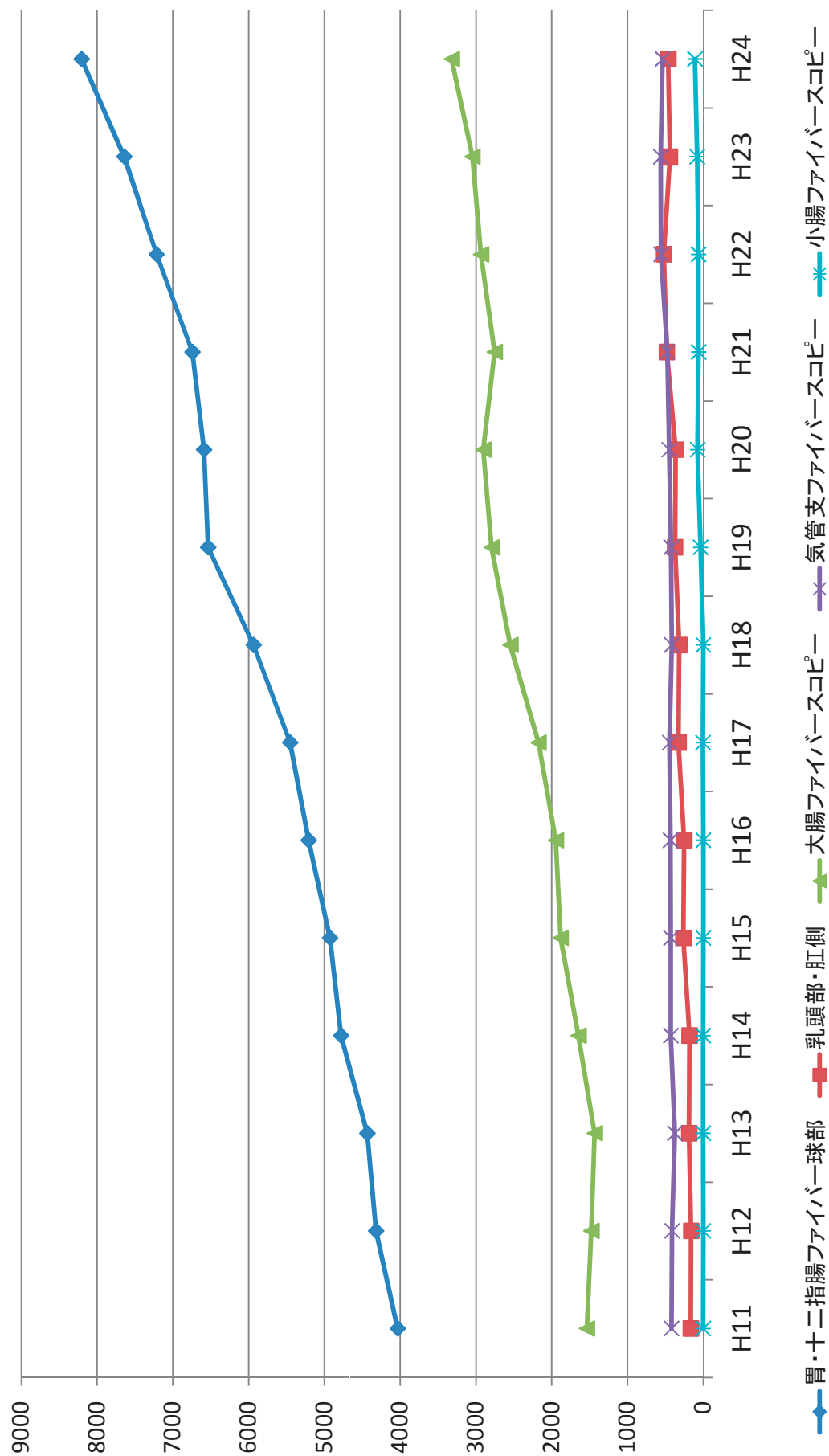
緊急内視鏡検査
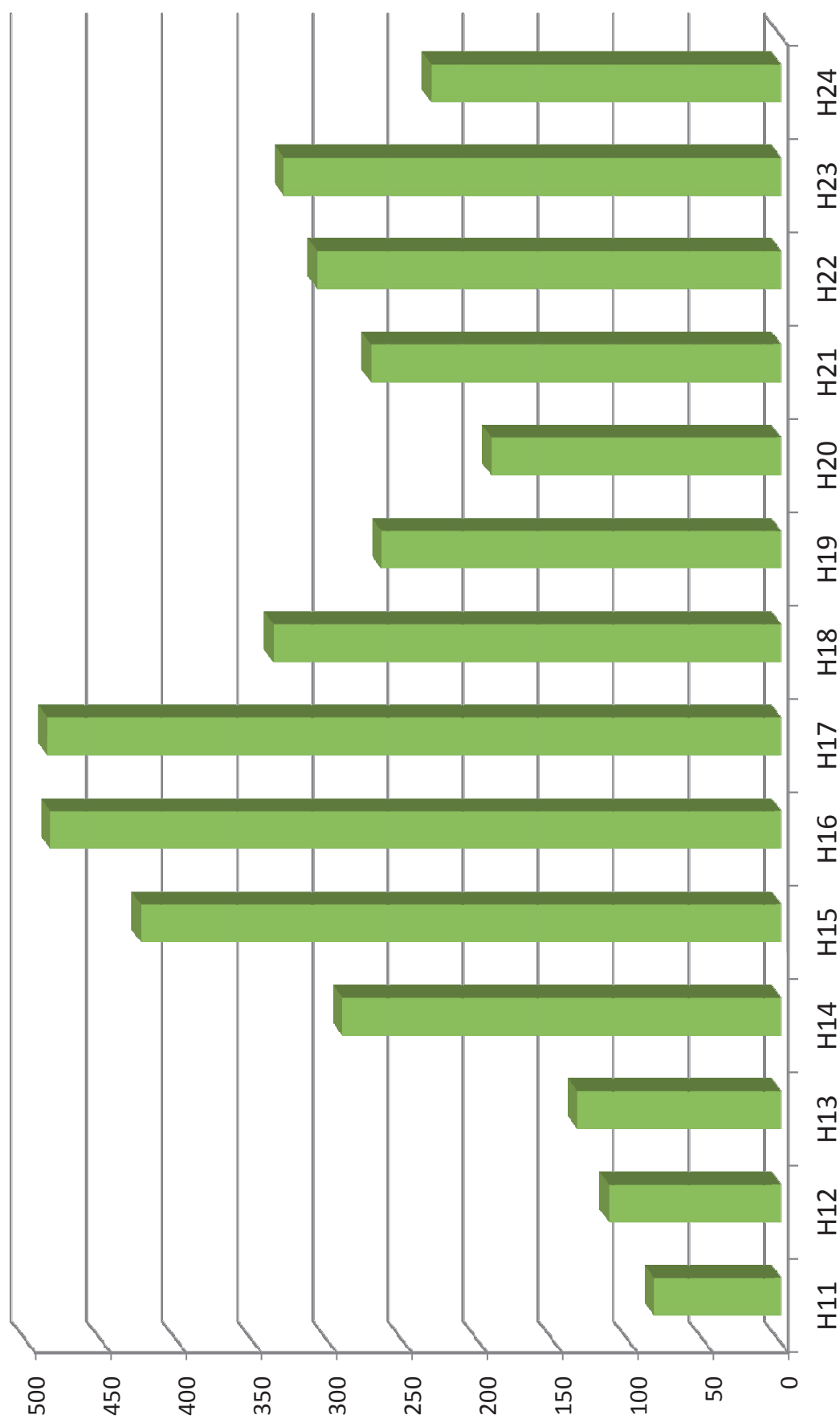
内視鏡下生検総件数
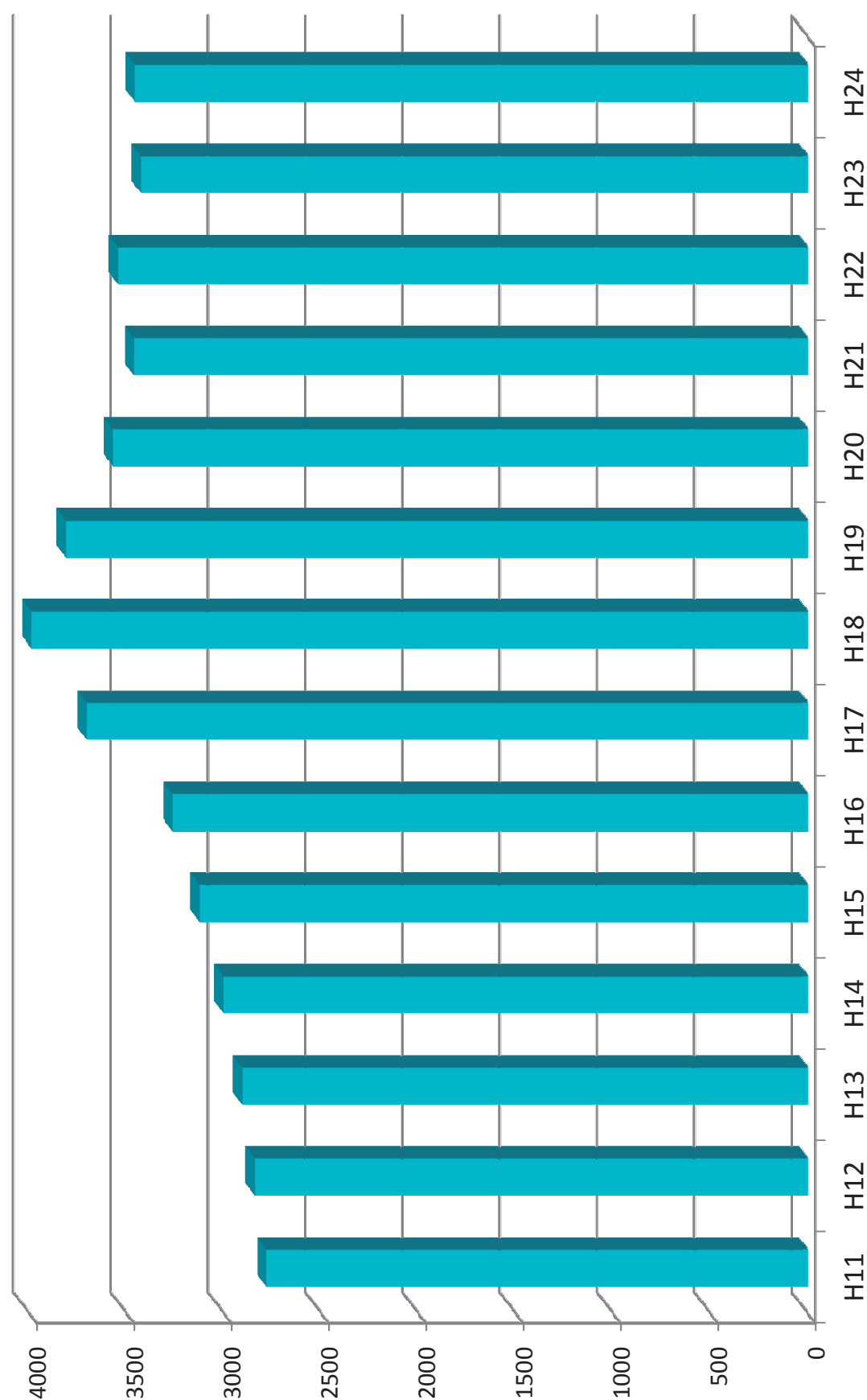
早期癌に対する内視鏡的粘膜下層切開剥離術
ESD(胃・食道)
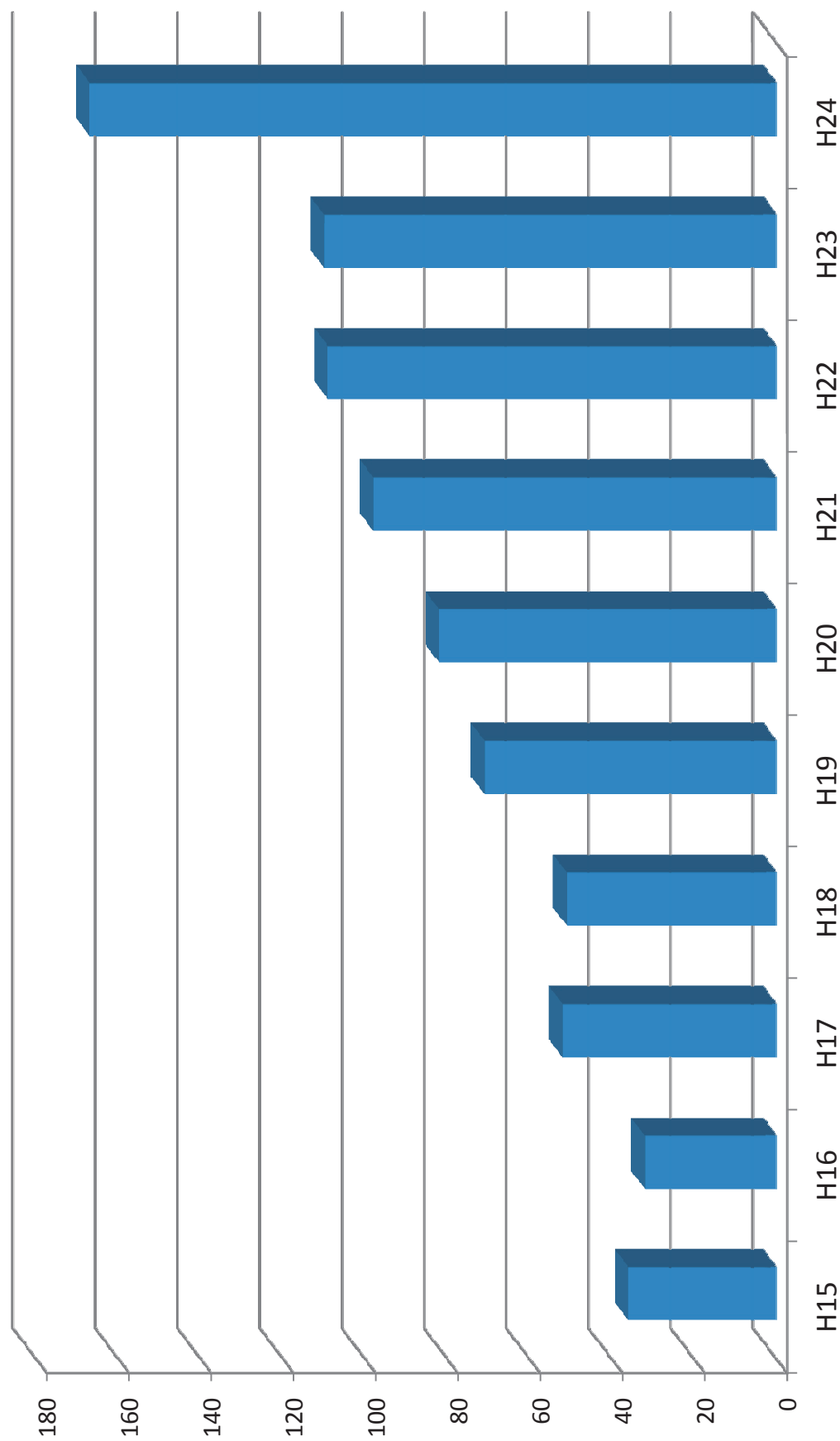
内視鏡検査（スクリーニング）数
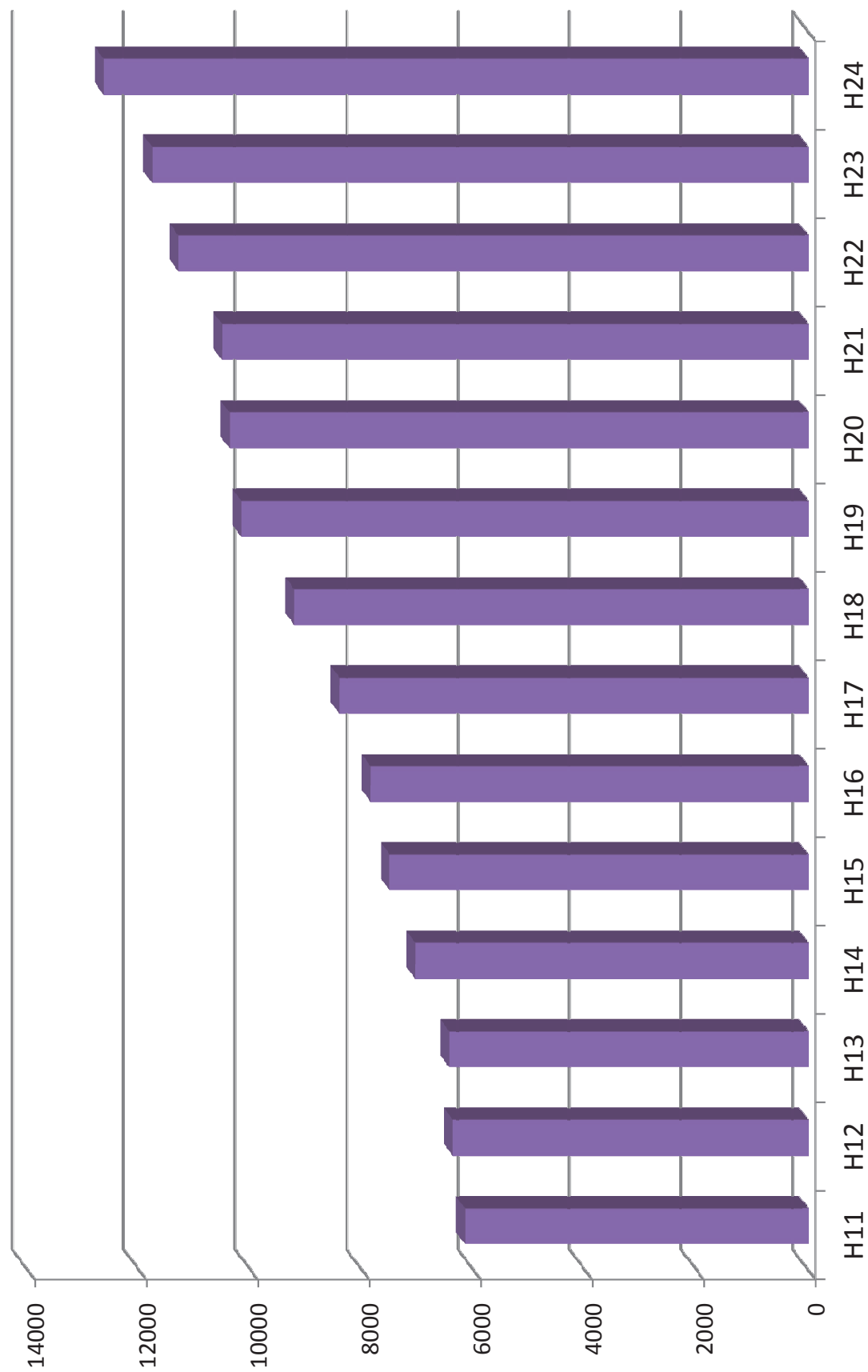
近畿大学　消化器内科学教室医局員

主任教授	工藤正俊	S53	肝臓・消化器・肝癌の診断と治療
教授（内視鏡部）	樫田博史	S58	下部消化管
准教授	汐見幹夫	S55	上部・胆膵内視鏡（関空クリニック所長・教授兼務）
	西田直生志	S60	肝臓病学・肝癌の分子生物学
	北野雅之	H2	消化管全般・胆膵疾患
講師	松井繁長	H3	食道静脈瘤止血・上部消化管
	(医局長)		
医学部講師	上嶋一臣	H7	慢性肝炎・肝癌の治療
	(病棟医長)		
	櫻井俊治	H7	上部消化管・分子生物学
	(外来医長)		
	南　康範	H9	肝疾患・消化器一般
	萩原　智	H10	肝疾患・消化器一般
	井上達夫	H11	肝疾患・消化器一般
	矢田典久	H11	肝疾患・消化器一般
	坂本洋城	H12	胆膵疾患・消化器一般
	朝隈　豊	H14	上部消化管・消化器一般
	北井　聡	H14	肝疾患・消化器一般
助教	川崎正憲	H15	消化器内視鏡・消化器一般
	田北雅弘	H15	肝疾患・消化器一般
	永井知行	H16	ゲノム生物学
	永田嘉昭	H16	消化器一般
	今井　元	H17	胆膵疾患・消化器一般
	山雄健太郎	H18	胆膵疾患・消化器一般
	山田光成	H18	消化器一般
	有住忠晃	H19	肝疾患・消化器一般
	鎌田　研	H19	胆膵疾患・消化器一般
	峯　宏昌	H19	消化器一般
	宮田　剛	H19	胆膵疾患・消化器一般
	高山政樹	H19	消化器一般

	足立哲平	H20	肝疾患・消化器一般
	大本俊介	H20	消化器一般
	門阪薫平	H20	胆膵疾患・消化器一般
	田中梨絵	H22	消化器一般
	千品寛和	H22	消化器一般
	南　知宏	H23	消化器一般
	岡元寿樹	H23	消化器一般

非常勤	仲谷達也	H3	仲谷クリニック
	中岡良介	H8	山本病院内科
	福田信宏	H10	朝日大学附属村上病院　消化器内科
	市川　勉	H13	内海町いちかわ診療所
	黒木恵美	H12	肝疾患・消化器一般
	柴田千栄	H15	肝疾患・消化器一般
	上田泰輔	H15	肝疾患・消化器一般

大学院4年	峯　宏昌	H19	消化器一般
大学院3年	足立哲平	H20	肝疾患・消化器一般
	大本俊介	H20	消化器一般
	門阪薫平	H20	胆膵疾患・消化器一般
大学院1年	南　知宏	H23	消化器一般
	千品寛和	H22	消化器一般

| **実験助手** | 鏡　郁子 |
| | 垣井麻莉 |

データマネージャー（CRC業務）

児玉美由紀

臨床研究補助	弓削公子
教授秘書	田中真紀
	村橋亜季
	上田由未子
	本廣佳香
日本肝癌研究会	田村利恵
	前原なつみ

医局秘書　　　　胡桃由佳

　　　　　　　　　朝隈　智

　　　　　　　　　林　直子

分院勤務

堺病院	辻　直子	S60	近畿大学堺病院　准教授・科長
	谷池聡子	H7	近畿大学堺病院　診療講師
	奥村直巳	H21	近畿大学堺病院　臨床助教
	高場雄久		近畿大学堺病院　臨床助教
	松本　望		近畿大学堺病院　臨床助教
	丸山康典		近畿大学堺病院　臨床助教
	河野　匡志		近畿大学堺病院　臨床助教
	尾崎　信人		近畿大学堺病院　臨床助教

奈良病院	川崎俊彦	S58	近畿大学奈良病院消化器内分泌内科　准教授
	岸谷　譲	S62	近畿大学奈良病院消化器内分泌内科　講師
	宮部欽生	H14	近畿大学奈良病院消化器内分泌内科　診療講師
	清水昌子	H12	近畿大学奈良病院消化器内分泌内科　診療助教
	茂山朋広	H17	近畿大学奈良病院消化器内分泌内科　診療助教
	奥田英之	H19	近畿大学奈良病院消化器内分泌内科　診療助教
	木下大輔	H20	近畿大学奈良病院消化器内分泌内科　臨床助教
	秦　康倫	H21	近畿大学奈良病院消化器内分泌内科　臨床助教

他病院勤務	山本健二		岡本クリニック
	林　道友		医療法人恵和会　林内科クリニック　院長
	中里　勝		上ヶ原病院
	南野達夫	S55	なんの医院
	水野成人	S61	神戸薬科大学　医療薬学研究室
			近畿大学奈良病院消化器内分泌内科　非常勤医師
	鍋島紀滋	S61	三菱京都病院消化器内科
	由谷逸朗	S62	高石藤井病院
	川端一史	H元年	川端内科クリニック
	米田　円	H元年	米田内科胃腸科
	渡邉和彦	H3	結核予防会大阪府支部相談診療所
	森村正嗣	H3	森村医院
	仲谷達也	H3	仲谷クリニック
	福永豊和	H4	北野病院消化器内科
	遠田弘一	H7	慈温堂遠田医院　院長
	遠田由紀		

亀山千晴	H7	しあわせクリニック
小牧孝充	H7	富田林病院消化器内科
鄭　浩柄	H8	神戸市医療センター中央市民病院
中岡良介	H8	山本病院内科
末冨洋一郎	H8	末冨放射線科医院
福田信宏	H10	朝日大学歯学部附属村上記念病院　消化器内科
小川　力	H11	高松赤十字病院　消化器内科
坂口康浩	H11	河崎内科病院
梅原　泰	H11	辻　腎太郎クリニック
加藤玲明	H11	宝塚市立病院消化器内科
		近畿大学奈良病院消化器内分泌内科　非常勤医師
宮本容子	H12	近畿大学奈良病院消化器内分泌内科　非常勤医師
梅原康湖	H12	JR 大阪鉄道病院　非常勤医師
永島美樹	H12	桃坂クリニック
市川　勉	H13	内海町いちかわ診療所
冨田崇文	H14	冨田病院
齊藤佳寿	H14	介護老人保健施設　徳田山
高橋俊介	H14	市立堺病院
西尾　健	H14	南堺病院
坂本康明	H15	（医）坂本クリニック
早石宗右	H18	医療法人早石会　早石病院
山本典雄	H19	医療法人山紀会　内科

医局員の略歴
および近況

2013 年の抱負

　昨年不十分であった対外的な活動を積極的に行いたい。

　手始めに1月に経鼻内視鏡研究会と消化器内視鏡学会地方会セミナー座長を務めました。12 月には次回セミナーを会長として開催させていただきます。樫田・北野先生はじめ皆様のご協力・ご支援をこの場をお借りしてお願いします。

　また、3月の消化器病学会総会、5月の内視鏡学会総会でも座長を務めます。座長だけでなく、6月の胃瘻の研究会ではアンケートを実施・発表の予定です。

汐見　幹夫

樫田　博史

略　歴
1959 年 1 月　京都市に生まれる
1983 年 3 月　京都大学医学部卒業
同年　　6 月　神戸市立中央市民病院　　内科研修医
1985 年 6 月　　　　　同　　　　　　消化器内科専攻医
1988 年 6 月　　　　　同　　　　　　消化器内科医員
1990 年 4 月　　　　　同　　　　　　消化器内科副医長
1997 年 4 月　　　　　同　　　　　　消化器内科医長
2001 年 8 月　昭和大学横浜市北部病院　消化器センター助（2007 年より准）
教授
2010 年 4 月　近畿大学教授　医学部内科学教室（消化器内科部門）
2010 年 10 月　光学治療センター消化器内視鏡部長
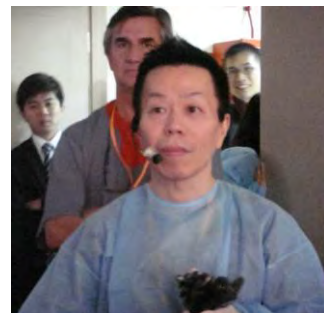
　2012 年は、長年待たれていた光学治療センターの拡張工事が、漸く 3 月末に
始まり、5 月中には完成してブースが 2 部屋増えたのが大きな出来事でした。
工事中も内視鏡を休むことなく継続したため、年間の内視鏡件数が 2 年前の約
1.5 倍に増加しました。
　2011 年秋から開始した内視鏡ライブも 11 月 25 日に 2 回目を迎え、装いも新
たに「関西消化器内視鏡ライブコース」として開催されました。運悪く大阪マ
ラソンと日程が重なり、ホテルの予約が取れないために参加を断念された方も
おられたにも関わらず、前年を上回る 350 名超の参加者を得て、大盛況でした。
ロシアから参加された聴衆にも感動してもらえました。
　それに先立ち 4 月には新入局員を対象にコロンモデルを用いた大腸内視鏡挿
入ハンズオンを行い、6 月には前年同様、周辺地域の若手の先生方を集めて、
動物摘出臓器を用いた、EMR/ESD ハンズオン・トレーニングを開催させて頂
きました。
　消化管グループからは、欧米の学会を含め、数多くの学会・研究会に演題を
発表しましたが、学位論文を除くと原著論文の数がやや少なかったのが心残り
です。私自身は大腸内視鏡挿入法の本の出版にこぎつけました、また、マレー
シア、台湾、韓国などに招いて頂いて、講演やライブをさせて頂きました。た
またま去年はアジア出張が多かったのですが、日本以外のアジア諸国も発展め
ざましいこと、英語はむしろ日本人よりずっと流暢であることを目の当たりに
し、うかうかしていられないな、と感じました。

今年は、５月末に内視鏡レンタルの更新時期を迎えるため、昨秋発売された
オリンパスの新しいシステムが当院にも入ってきます。病診連携やライブなど
を通じて紹介患者を一層増やし、最先端の診断・治療技術で以てどんどん患者
を救っていければ、と願っています。また、アジアのみならず欧米の施設とも
交流を深めていきたいと思います。

　患者や検査・治療件数が増えると臨床に没頭しがちですが、その合間にもプ
ロスペクティブにスタディを組んで、学会シンポジウム発表や原著論文として
形に残して頂きたいと希望しています。また、昨年の工事にも関わらずもはや
手狭になってしまった光学治療センターですが、近い将来何とかしたいと模索
している今日このごろです。

まつい　しげなが
松井　　繁長
平成３年　　　近畿大学医学部卒業
平成３年　　　近畿大学第２内科入局
平成１１年　近畿大学消化器内科助手
平成１４年　近畿大学消化器内科講師
平成１８年　近畿大学消化器内科医局長
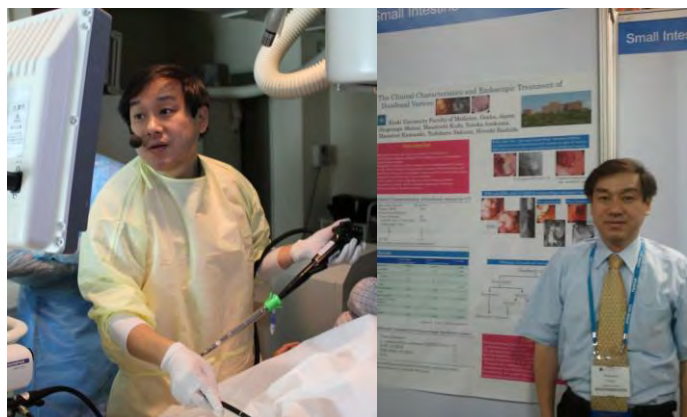
専門領域
消化器病、消化器内視鏡、門脈圧亢進症、食道、胃静脈瘤
早期胃癌の内視鏡診断・治療

所属学会
日本内科学会、日本消化器病学会、日本消化器内視鏡学会
日本門脈圧亢進症学会、日本消化管学会
資格
日本内科学会認定医
日本消化器病学会（専門医、学会評議員、近畿支部評議員）
日本消化器内視鏡学会（指導医、学術評議員、近畿支部評議員）
日本門脈圧亢進症学会評議員
近畿大学医学博士

去年も相変わらず、忙しくあっという間に終わった１年であった。臨床面では
食道・胃の ESD が年 200 件以上になり、紹介例も順調に増えてきている。
また、ESD 症例が増えたことにより若手のトレーニングも充実してきており、
消化管グループ全員のさらなる ESD 手技の向上を目指していきたい。
次に、学外活動としては第２回内視鏡ライブを開催し、参加者がさらに増えて
盛会に終了した。今後も近畿大学の内視鏡をアピールできる会として特色の

ある企画運営が必要であろうし、さらに意義のある場にしていきたい。

また、近隣の医療機関との連携も重要視し、勉強会、研究会、アニマルモデルのハンズオンセミナーなどを開催したり、特別講演なども数多く行い、近畿大学との交流を深めるように活動を行った。

研究面では、上部消化管では「食道・胃 ESD の偶発症対策」、「ESD 後潰瘍治癒における防御因子増強薬の有用性」「ヘリコバクターピロリ除菌治療」、「十二指腸静脈瘤の病態と治療」、「薬剤性消化管粘膜傷害」、「GERD の実態調査」などをテーマにして、DDW、UEGW、APDW などの国際学会や総会シンポジウムなどで発表をおこなった。

しかし、反省しなければならないのは、研究内容を英文論文にほとんどできていないことである。今年は現状の活動をさらにアップさせながら、忙しさ（医局長業務を含む）にかまけずに論文作成にがんばっていきたいです。

北野　雅之

平成　2 年 3 月	鳥取大学医学部医学科卒業
平成 2 年 4 月―平成 6 年 3 月	鳥取大学大学院医学研究科博士課程
平成 6 年 4 月―平成 8 年 7 月	鳥取大学医学部附属病院第二内科医員
平成 8 年 8 月―平成 10 年 11 月	Sweden Lund 大学　客員研究員
平成 10 年 12 月―平成 12 年 3 月	鳥取大学医学部臨床薬理学講座助手
平成 12 年 4 月―平成 13 年 3 月	近畿大学医学部消化器内科助手
平成 13 年 4 月―平成 19 年 3 月	同　　　　講師
平成 19 年 4 月―現在	同　　　　准教授

2012 年度を振り返って

　2012 年度は、田中先生、山田先生、千品先生の三名の先生方に入局頂き、消化器内科は一段と盛り上がってきています。忙しい科でありますが、3 人とも前向きに頑張って、着実に診療の知識・技術を向上させているのを見て、嬉しく思っております。

　診療では、工藤教授のリーダーシップで、地域における中核病院としてのますますの役割を担うこととなってきています。また、他府県からの紹介も増え、最先端医療を行う病院としての知名度も増してきました。工藤教授は病院長というご多忙の責務があるにもかかわらず、消化器内科の診療レベル向上にご尽力されているのを見て、私自身もついていかなければと思い、微力ながら頑張ってきました。EUS 検査・治療も定着し、毎日一日中 EUS 診療を行うようになり、総件数は 1500 件近くまで到達しました。また、それぞれの担当医も年間何百件も行っているため、専門医に相当する技術、あるいはそれ以上の技術を習得しているのを確信しております。EUS ガイド下治療は、総件数で 300 件を超すようになり、おそらく全国でも 1, 2 位の数になっていると考えております。ERCP についても、関西の主要病院で行われた多施設共同研究で、近大が最も症例登録数が多く、地域における需要度が高いことを再認識しております。また、国内外からの見学者も多数お越しになって頂き、そのおかげで、教室の先生方が丁寧に手技を説明できるようになってきました。

　研究では、前述の関西地方の研究成果で、「膵癌による閉塞性黄疸に対するカバー付金属ステントの有用性」を、関西胆膵内視鏡医を代表して米国 DDW で Oral presentation させて頂きました。この発表は日本の膵癌診療ガイドラインに取り入れられることとなりました。また、膵腫瘍性病変診断における造影ハーモニック EUS の有用性を American Journal of Gastroenterology で発表しました。2000 年より動物実験から開始した造影 EUS プロジェクトも現在は世界的に認識されるようになり、工藤教授をはじめ、サポート頂いた先生

方に深謝いたします。また、2012 年は、共同研究者の目覚ましい活躍が印象に残る年でした。今井先生が、当院における EUS 下胆道ドレナージ術の成績を、UEGW で Oral presentation しました。私が 20 万回練習するようにと言ったようですが、本番では原稿なしでスラスラと自信を持って発表したのは、誇らしかったです。門阪先生は、慢性膵炎の EUS 像について、研究を行っております。症例数が多く説得力のある結果であるためか、多数の依頼原稿を執筆しています。さらに、門阪先生はこの研究により日本消化器病学会近畿支部で Young Investigator Award を受賞しました。門阪先生の努力により、2013 年夏に膵臓学会と共同開催される国際膵臓研究シンポジウムで私が講演する機会を頂くこととなりました。鎌田先生は、IPMN の経過観察に EUS が有用であることを国際膵癌学会で Oral presentation を行い、同時に Young Investigator Award を受賞しました。卒後 6 年目ですが、何十回と全国学会の主題演題で発表を行い、百戦錬磨であるため、私は安心して同時期に韓国で行われた消化器インターベンション学会の講演へ出向することができました。この内容は Endoscopy に投稿中で、来年に公表できるよう頑張っていきたいと考えております。宮田先生は、2012 年に初めて全国総会での主題演題で発表する機会がありましたが、初めてではないかのような落ち着きで分かり易く発表しました。現在行っている研究成果は、2013 年の米国 DDW に採択され、20 万回の練習の後、原稿なしで発表してくれるものと思われます。論文では、坂本先生が、世界で初めて十二指腸乳頭括約筋切開を行わない胆道内視鏡観察法について、Gastrointestinal Endoscopy に報告しました。この内容を私が中国で講演する機会があり、大反響がありました。坂本先生は、全国の研究会で講演を多数しており、大阪弁でハキハキと分かり易く説明するため、聴衆に好評です。大本先生は、上述の 6 名に追いつけるよう必死になって、研究活動を行っております。造影 EUS の多施設共同研究の打ち合わせ会では、重要なポイントを指摘し、プロトコール作成に貢献しております。2013 年にさらに活躍することが期待されます。

　最後に、工藤教授をはじめとする熱心な指導者・同僚・共同研究者に恵まれたことに感謝し、私自身も 2013 年に向けて成長を続けていきたいと思います。

佐藤錦・ナポレオン・紅きらり
南　康範

　以前に野田先生が地元のお土産で医局に持ってきてくれた「サクランボ」を食べてからすっかりその味の虜です。それ以来、毎年山形の農家からサクランボをお取り寄せしています。そして、その「サクランボ好き」が高じて、家の庭でたわわに実るサクランボを夢みるようになり、とうとう昨年末にサクランボの苗木を 4 本購入しちゃいました。購入時では棒苗のため「単なる棒」と揶揄されましたが、この春に芽吹いて少しばかりですが白い花を咲かせてうれしいかぎりですし、4 月上旬のある朝 6 時に起きて綿棒を使って受粉作業するほどサクランボに真剣です！サクランボ栽培についてもかなり勉強しました（医学論文を書くのは後回しにして）。

　サクランボと言えば「山形」なので寒い地域でしか栽培できないと思われやすいですが、（確かに冬期における低温要求時間があるものの）大阪でもたぶん栽培できそうです。また、なぜ 4 本も購入したのかと言うと、サクランボは自家受粉しません、つまり 1 本の木では実を付けず収穫するには異種のサクランボが複数本必要となります。受粉確立を上げる作戦で、佐藤錦 2 本、ナポレオン、1 本、紅きらり 1 本の計 4 本を購入したのです（佐藤錦はナポレオンと紅きらりと相性が良い）。

　「狭い庭で木が大きくなったらどうするか!?」については大きくなってから考えることにして、数年後にはいっぱいサクランボが収穫できて医局のみんなに振る舞うことができることでしょう。楽しみにして下さい。

略歴：
平成 9 年 3 月　近畿大学医学部卒業
平成 9 年 4 月　近畿大学医学部旧第 1 外科入局
平成 10 年 7 月　八尾徳洲会病院外科
平成 11 年 4 月　近畿大学医学部大学院（外科学）入学
平成 12 年 7 月　旧第 1 外科から消化器内科へ出向
平成 15 年 3 月　近畿大学医学部大学院（外科学）卒業
平成 15 年 4 月　近畿大学医学部消化器内科助手
平成 18 年 5 月　近畿大学医学部消化器内科講師
平成 20 年 12 月－平成 21 年 3 月　University California, San Diego (UCSD)

の Department of Radiology に Visiting fellow として短期留学

平成 21 年 4 月　近畿大学医学部堺病院

平成 23 年 4 月　近畿大学医学部消化器内科

資格：外科専門医、肝臓専門医、消化器病専門医、消化器内視鏡専門医
　　　超音波専門医・指導医

役職：*World Journal of Radiology,* an Editorial Board Member (2009-2013)

２０１２年度を振り返って

近畿大学　医学部附属病院　消化器内科　　永井　知行

　２０１２年度はいろいろと環境が変わり、刺激の多い１年でした。
まず私事ですが、大阪市内に住居を変えることになり、おかげで通勤時間が長くなって不便な点もありましたが、家の周りに大川や桜宮公園、大阪城などの緑と水に囲まれた環境はすばらしく、また、店やレストランも多く非常に楽しい生活を送ることができて、大阪市内に早く住んでおけばよかったと思うほどでした。
あいにく１３年１月からの３ヶ月間をくしもと町立病院に赴任することになりその生活はしばらくお預けとなりましたが、串本は交通の便は不便ではあるものの、串本海中公園や潮岬などの観光スポットも多く、くしもと町立病院の他科の先生達と飲みにいったりして快適に過ごさせて頂きました。
（春から夏にかけて串本は観光シーズンで、ダイビングやサーフィン、釣りなどをされる方は非常に充実した生活を送ることができると思います。）

くしもと町立病院では消化器疾患だけでなく、高血圧や糖尿病などの生活習慣病などとともに救急では外傷患者も診察することが必要です。大学病院の外来では高血圧や糖尿病などの治療・followは他科にして頂いており、特に抗血小板薬や抗凝固薬などは中止する立場でしたが、初めて処方する立場にたつことにもなりました。おかげで高血圧や糖尿病の診療・治療スキルを身につけることができ非常に有益な経験ができました。やはり、仕事としてプレッシャーの中で追い詰められながら、実際の現場で経験をしていかないと本当のスキルは身につかないとつくづく実感しました。

１２年度は新しいことにチャレンジできた年度だと思いますが、１３年度も新たなチャレンジをしていきたいと思います。

追伸）
串本でこのエッセイを書いています。4月から大学に復帰するとともに大阪市内の生活に戻ることも楽しみにしています。

略歴）
04 年　　　　　　　　近畿大学医学部　卒業
04 年〜 06 年　　　　神戸労災病院　臨床研修医
06 年〜 08 年　　　　市立岸和田市民病院　消化器内科
08 年〜現在　　　　　近畿大学医学部附属病院　消化器内科
所属学会）
日本内科学会、日本消化器病学会、日本消化器内視鏡学会、日本肝臓学会
日本癌学会、日本臨床腫瘍学会、日本分子標的学会、米国癌学会
専門医・学位）
日本内科学会認定医、日本消化器病学会専門医、日本内視鏡学会専門医
医学博士（平成２３年度）

田北　雅弘

略歴）

H15　近畿大学医学部卒

H15　近畿大学医学部　消化器内科

H17　天理よろづ相談所病院　消化器内科

H24　近畿大学　医学博士

H24　近畿大学　医学部　助手

H24　10-12 月串本町立病院　内科

H25　近畿大学　医学部　助手

山行歴：2012 3 月　金剛山、5 月　燕岳、　9 月大和葛城山

目標：肝臓専門医、今年こそもっと山登りを！ジャグリングも！

有住忠晃　徳島出身

略歴
昭和 57 年 2 月 6 日：出生
昭和 60 年 4 月：鳴門聖母幼稚園入園
昭和 63 年 4 月：北島町立北島北小学校入学
平成 6 年 4 月：北島町立北島中学校入学
平成 9 年 4 月：徳島県立徳島北高校入学
平成 12 年 4 月：代々木ゼミナール原宿校入学
平成 13 年 4 月：近畿大学医学部医学科入学
平成 19 年 4 月：近畿大学医学部付属病院研修医
平成 21 年 4 月：近畿大学医学部付属病院　消化器内科　入局
平成 21 年 4 月：近畿大学医学部大学院内科学系　入学
現在に至る

2013 年の目標
日常診療・研究・学会発表・論文を頑張ります。

峯　宏昌
平成 19 年 3 月：近畿大学医学部卒業
平成 19 年 4 月：近畿大学医学部付属病院　研修医
平成 21 年 4 月：近畿大学医学部消化器内科　助教
平成 22 年 4 月：近畿大学医学部大学院内科学系　入学

　子供ができると人は成長すると思っていましたが、子供も 1 歳 6 か月を迎え、そろそろ
2 人目もと考えるほどですが、親になっても簡単に人間は変わることがないようで、いま
だに色々失敗し、色々な方に支えられ、日々過ごしています。
　気が付けば医師になり 7 年目、消化器内科にお世話になり 5 年目になりました。
研修医時代には 7 年目の先生はだいぶ上で、頼れる存在に感じたものですが、今自分が研
修医の方々に同じように感じてもらえているかどうか・・・
　この 1 年で近大病院での IBD 教室の立ち上げや近畿中部地区 CD 勉強会での講演、NST
関連の研究会の世話人などと、様々なことを経験させていただきました。
次の 1 年でも、色々な人と出会い、刺激され、また次の step に行けるよう、そして後輩や
研修医にあの時自分が感じたような頼りになる先輩になれるよう、日々精進していきたい
と思います。
　もう 7 年目、まだ 7 年目な私ですが、今後ともどうぞご指導のほどよろしくお願いしま
す。

門阪　薫平
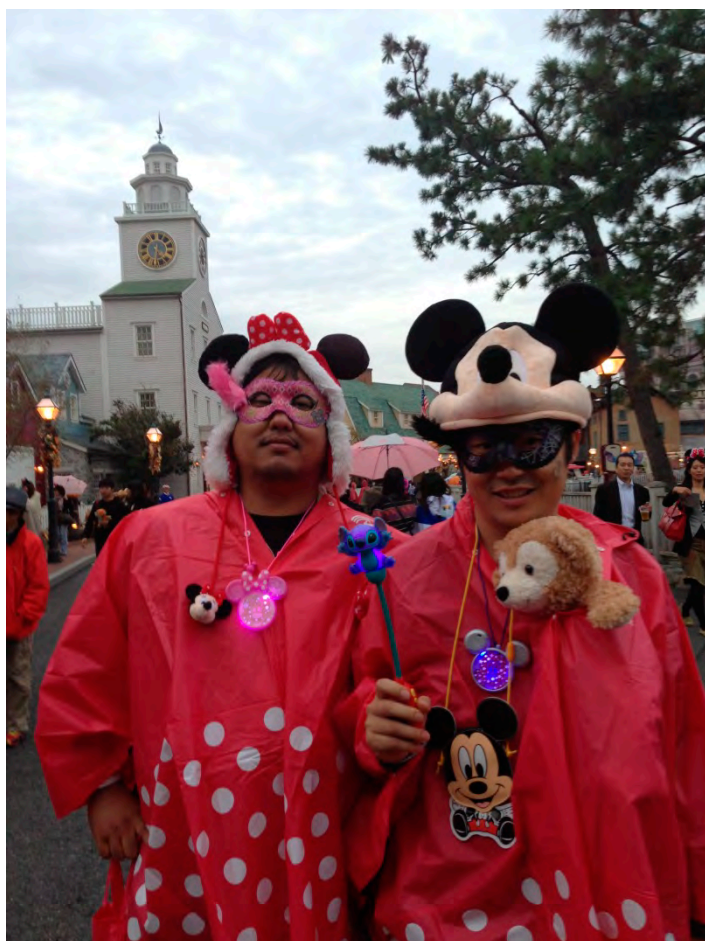
| 平成 21 年 3 月 | 近畿大学医学部医学科卒業 |
| 平成 21 年 4 月 | 近畿大学医学部消化器内科助手 |

2012 年度を振り返って

　2012 年度は、工藤教授　北野准教授、坂本先生、今井先生、鎌田先生、宮田先生のご指導のもと、消化器病学会、内視鏡学会、超音波学会、膵臓学会、JDDW にて主演題で発表させていただきました。また日本消化器病学会近畿支部会で Young Investigator Award を受賞し、ますますやる気に満ちています。今年は論文を必ず 2 本は書く意気込みで、頑張っていきたいと考えております。

山田　光成

略歴）

平成 18 年　　　　　近畿大学医学部卒業

平成 22 年〜24 年　育和会記念病院　研修医

平成 24 年〜　　　　近畿大学医学部　消化器内科

近畿大学病院　消化器内科にお世話になり　もう一年が経ちました。ネガティブな性格を一気にポジティブにすると、地に足がつかない気がしてしまいますので難しいですが。昨年より更に前向きな部分を増やして成長しようと考えておりますので、皆様よろしくお願いします。

近畿大学医学部奈良病院　消化器・内分泌内科　2012 年年報（1～12 月）

１．スタッフ
　　　准教授　　　　　　　川崎俊彦（昭和 58 年卒）
　　　講師　　　　　　　　岸谷　譲（昭和 62 年卒）
　　　診療講師　　　　　　清水昌子（平成 12 年卒）
　　　診療講師　　　　　　宮部欽生（平成 14 年卒）
　　　診療助教　　　　　　茂山朋広（平成 17 年卒）
　　　診療助教　　　　　　奥田英之（平成 19 年卒）
　　　診療助教　　　　　　木下大輔（平成 20 年卒）
　　　診療助教　　　　　　秦　康倫（平成 21 年卒）

　　　非常勤医師　　　　　水野成人

２．臨床業績
　　　１日平均外来患者　　　92.7 人
　　　１日平均在院患者　　　28.3 人
　　　平均在院日数　　　　　10.9 日

　　　上部内視鏡検査　　　　3244 件（含 ESD 71 件）
　　　下部内視鏡検査　　　　1785 件（含 EMR 325 件+ESD9 件）
　　　ERCP　　　　　　　　　196 件
　　　腹部超音波　　　　　　2548 件
　　　腹部血管造影　　　　　124 件
　　　ラジオ波治療　　　　　55 件

３．学会業績（総会）
（１）JDDW 2012「上部消化管スクリーニング内視鏡検査において消化管運動抑
　　　制剤の投与は必須ではない」
（２）JDDW 2012
　　　　「腸管重複症に対して SB ナイフ Jr を用いて内視鏡的隔壁切除を施行し
　　　た１例」
（３）JDDW 2012「ランソプラゾールによる collagenous colitis の４症例」

４．学会業績（地方会）
（１）第 96 回日本消化器病学会近畿支部例会「虫垂粘液嚢胞腺腫の 1 例」
（２）第 96 回日本消化器病学会近畿支部例会
　　　「微小膵癌との鑑別を要した自己免疫性膵炎の 1 例」
（３）第 88 回日本消化器内視鏡学会近畿支部例会「Lemmel 症候群の 1 例」
（４）第 88 回日本消化器内視鏡学会近畿支部例会
　　　「貧血を契機に発見された腸間膜静脈硬化症の 1 例」
（５）第 97 回日本消化器病学会近畿支部例会
　　　「上腹部痛で発見された低分化型肝癌の 1 例」
（６）第 97 回日本消化器病学会近畿支部例会「無症候性膵内分泌腫瘍の 1 例」
（７）日本超音波医学会第 39 回関西地方会学術集会
　　　「C 造影超音波動脈優位相下 RFA が有用であった肝癌の 1 例」
（８）日本超音波医学会第 39 回関西地方会学術集会「造影エコー検査にて診断
　　　可能であった，限局性結節性過形成（FNH）の 1 例」
（９）第 89 回日本消化器内視鏡学会近畿支部例会
　　　「Inflammatory fibroid polyp の 1 例」
（10）第 49 回日本糖尿病学会近畿地方会「インスリンアスパルト混合製剤
　　　(70Mix)でのみ局所インスリンアレルギーを生じた 1 例」

５．学会業績（研究会）
（１）第 12 回 R24 肝臓カンファレンス
　　　「ペグインターフェロンα-2A の投与が有効であった C 型肝硬変症の 1 例」
（２）第 13 回奈良肝臓ミーティング
　　　「当院の C 型慢性肝炎に対する 3 剤併用療法の治療経験」
（３）第 58 回奈良県消化器内視鏡研究会
　　　「EUS-FNA で術前診断が可能であった神経性腫瘍の 1 例」

６．論文業績
（１）「特発性腸間膜静脈硬化症」
　　　（近畿大学医学部奈良病院消化器・内分泌内科）
　　　川崎俊彦、奥田英之，宮部欽生
　　　消化器の臨床　１５（５）：５５３−５５４，２０１２

川崎俊彦

略歴
昭和 58 年　　　　　京都大学医学部医学科専門課程卒業
昭和 58 年　　　　　京都大学医学部附属病院（研修医）
昭和 59 年　　　　　大阪府済生会野江病院（内科医員）
昭和 61 年　　　　　京都大学医学部附属病院（第一内科医員）
平成 2 年　　　　　　京都桂病院（内科医員）
平成 5 年　　　　　　Diagnostic Radiology, Yale University School of Medicine,
　　　　　　　　　　（Visiting Scientist）
平成 6 年　　　　　　神戸中央市民病院（内科副医長）
平成 6 年　　　　　　西神戸医療センター（内科副医長）
平成 9 年　　　　　　西神戸医療センター（内科医長）に昇進
平成 12 年　　　　　近畿大学医学部附属病院（講師）
平成 16 年　　　　　大阪北逓信病院第 1 内科（部長）
平成 22 年　　　　　近畿大学医学部奈良病院消化器・内分泌内科（准教授）

2012 年の反省と 2013 年の抱負。
　2012 年は 8 人の固定メンバーでほぼ満足が行く活動ができたのではないかと
思います。その反面，今まで非常勤でお手伝いして頂いた，加藤先生，宮本先
生，林先生が辞められることになったのは残念でした。
　学会活動は、総会 3 題，地方会 10 題，研究会 3 題の発表ができ、このクラス
の病院としては十分な業績ではないかと思います。
　時間内の救急もかなり受け入れ可能な体制となったのですが、やはり吐血な
どの消化器内科の救急患者は伸び悩んでおり、今後も地道に実績を積み重ねて
良く必要があると思います。
　大腸 ESD，造影超音波も本格導入され，一流の病院も仲間入りができてきたの
ではないかと思います。
　2013 年は更に次のステップへ進みたいところだったのですが，主要メンバー
が 2 人，家庭の事情で退職することがほぼ内定しており，現状を維持するのが
精一杯ではないかと思います。

消化器内科学業績一覧(2012 年)

Ⅰ. 英文論文（著書・分担執筆）

1. 2012 Kitano M, Sakamoto H, **Kudo M**: Endoscopic ultrasound: contrast enhancement. In "Interventional Endoscopic Ultrasound", Gastrointestinal Endoscopy Clinics of North America, Chang KJ, Lightdale CJ, ed, 2012, pp349-358.

2. 2012 **Kudo M**: Better anti-proliferative and angiogenic drugs: how and when? Clinical Dilemmas In Hepatocellular Carcinoma, Wiley-Blackwell, Hoboken, USA, 2012 (Book Chapter)

II．英文論文

過去の年報への記載漏れ分

1. 2009 Kim SR, Imoto S, Nakajima T, Ando K, Mita K, Fukuda K, Nishikawa R, Koma Y, Matsuoka T, **Kudo M**, Hayashi Y: Utility of Gd-EOB-DTPA-enhanced MRI in diagnosing small hepatocellular carcinoma. **Case Report Gastroenterol** 3: 187-192, 2009.

2012 年

1. 2012 Minami Y, Okumura N, Yamamoto N, Tsuji N, Kono Y, **Kudo M***: Quantification of tumor vascularity with contrast-enhanced ultrasound for early response of transcatheter arterial chemoembolization for hepatocellular carcinoma: a report of three cases. **J Med Ultrason** 28: 15-19, 2012. **(IF=0.635)**

2. 2012 Kitano M, **Kudo M**, Yamao K, Takagi T, Sakamoto H, Komaki T, Kamata K, Imai H, Chiba Y, Okada M, Murakami T, Takeyama Y: Characterization of small solid tumors in the pancreas: The value of contrast-enhanced harmonic endoscopic ultrasonography. **Am J Gastroenterol** 107, 303-310, 2012. **(IF=7.553)**

3. 2012 Sakamoto H, Kimura H, Sekijima M, Matsumoto K, Arao T, Chikugo T, Yamada Y, Kitano M, Ito A, Takeyama Y, **Kudo M**, Nishio K: Plasma concentrations of angiogenesis-related molecules in patients with pancreatic cancer. **Jpn J Clin Oncol** 42: 105-112, 2012. **(IF=1.898)**

4. 2012 Clavien PA, Lesurtel M, Bossuyt PM, Gores GJ, Langer B, Perrier A, Abecassis M, Balabaud C, Barritt GJ, Belghiti J, Bhoori S, Bossuyt P, Breitenstein S, Broelsch C, Bruix J, Burra P, Burroughs A, Busuttil R, Charlton M, Cherqui D, Colombo ML, d'Albuquerque C, D'Alessandro A, de Santibanez EJ, Dufour F, Durand F, Dutkowski P, Duvoux C, El-Serag H, Fan ST, Finn RS, Fisher R, Forner A, Freeman R, Fung J, Geier

A, Germani G, Gores G, Gouw AS, Grant D, Greig P, Gurusamy
K, Hanto D, Heaton N, Heim M, Hemming A, Hippen B, Hisham A,
Hubscher S, Ichida T, Kahn D, Kew M, Kita Y, Kiuchi T,
Klintmalm GB, Kneteman N, Kojiro M, **Kudo M**, Langer B, Lee JM,
Lee SG, Lencioni R, Lerut J, Lesurtel M, Livraghi T, Llovet
JM, Lo CM, Lodge P, MacCaughan G, Madoff D, Majno P, Marcellin
P, Marrero J, Mazzaferro V, Mergental H, Merle P, Miksad R,
Mornex F, Mullhaupt B, Olthoff K, Paradis V, Perrier A,
Pestalozzi B, Pomfret E, Poon R, Porte R, Greig P, Prasad KR,
Raptis D, Roskams T, Rossi M, Samuel D, Schlitt H, Schwartz
M, Sexton Dobby AM, Shaked A, Sherman M, Siegler M, Suh KS,
Todo S, Toso C, Trevisani F, Trotter JJ, Veldecasas GJ,
Vauthey N, Vilgrain V, Villamil F, Vonlanthen R, Wald C, Weber
A, Wiesner R, Wright L, Yao F, Zheng SS, Zucman-Rossi J:
Recommendations for liver transplantation for
hepatocellular carcinoma: an international consensus
conference report. **Lancet Oncol** 13: e11-22, 2012. **(IF=25.117)**

5. 2012   Minami Y, Kitai S, **Kudo M**[*]: Treatment response assessment of
radiofrequency ablation for hepatocellular carcinoma:
Usefulness of virtual CT sonography with magnetic navigation.
Eur J Radiol 81: e277-280, 2012. **(IF=2.512)**

6. 2012   Watanabe T, Yamashita K, Fujikawa S, Sakurai T, **Kudo M**,
Shiokawa M, Kodama Y, Uchida K, Okazaki K, Chiba T:
Involvement activation of toll-like receptors and
nucleotide-binding oligomerization domain-like receptors in
enhanced IgG4 responses in autoimmune pancreatitis.
Arthritis Rheum 64: 914-924, 2012. **(IF=7.477)**

7. 2012   Takayasu K, Arii S, **Kudo M**, Ichida T, Matsui O, Izumi N,
Matsuyama Y, Sakamoto M, Nakashima O, Ku Y, Kokudo N, Makuuchi
M: Superselective transarterial chemoembolization for
hepatocellular carcinoma. Validation of treatment algorithm
proposed by Japanese guidelines. **J Hepatol** 56: 886-892,
2012. **(IF=9.858)**

8. 2012 <u>Kudo M</u>*, Tateishi R, Yamashita T, Ikeda M, Furuse J, Ikeda K, Kokudo N, Izumi N, Matsui O: Current status of hepatocellular carcinoma treatment in Japan: Case study and discussion-voting system. **Clin Drug Invest** 32;suppl.2:37-51, 2012. **(IF=1.915)**

9. 2012 <u>Kudo M</u>*: Closing remarks. **Clin Drug Invest** 32;suppl.2:52, 2012. **(IF=1.915)**

10. 2012 Saito J, Kim SR, <u>Kuod M</u>, Imoto S, Ando K, Nakajima T, Fukuda K, Otono Y, Kim SK, Komaki T, Yano H, Nakashima O, Sugimoto K, Matsuoka T: Well-differentiated hepatocellular carcinoma detected as hypovascularity by only CT during hepatic arteriography. **Intern Med** 51:885-890, 2012. **(IF=0.973)**

11. 2012 Lencioni R, <u>Kudo M</u>, Ye SL, Bronowicki JP, Chen XP, Dagher L, Furuse J, Geschwind JF, Guevara LL, Papandreou C, Sanyal AJ, Takayama T, Yoon SK, Nakajima K, Cihon F, Heldner S, Marrero JA: First interim analysis of the GIDEON (Global Investigation of therapeutic DEcisions in hepatocellular carcinoma and Of its treatment with sorafeNib) non-interventional study. **Int J Clin Pract** 66:675-683, 2012. **(IF=2.427)**

12. 2012 Okada M, Ishii K, Numata K, Hyodo T, Kumano S, Kitano M, <u>**Kudo M**</u>, Murakami T: Can the biliary enhancement of Gd-EOB-DTPA predict the degree of liver function？ **Hepatob Pancreatic Dis Int** 11:307-313, 2012. **(IF=1.259)**

13. 2012 <u>Kudo M</u>*: Welcome to the first issue of Liver Cancer. **Liver Cancer** 1(1):1, 2012. **(IF=0.000)**

14. 2012 Hagiwara S, <u>Kudo M</u>, Nagai T, Inoue T, Ueshima K, Nishida N, Watanabe T, Sakurai T: Activation of JNK and high expression level of CD133 predict a poor response to Sorafenib in hepatocellular carcinoma. **Brit J Cancer** 106:1997-2003, 2012. **(IF=5.082)**

15. 2012 Shiina T, Maki T, Yamakawa M, Mitake T, **Kudo M**, Fujimoto K: Mechanical model analysis for quantitative evaluation of liver fibrosis based on ultrasound tissue elasticity imaging. **Jpn J Appl Phys** 51:07GF11-1-8, 2012. **(IF=1.067)**

16. 2012 Tsuji Y, Watanabe T, **Kudo M**, Arai H, Strober W, Chiba T: Sensing of commensal organisms by the intracellular sensor NOD1 Mediates experimental pancreatitis. **Immunity** 37:326-338, 2012. **(IF=19.795)**

17. 2012 Sakamoto H, Kitano M, Kamata K, Miyata T, Kadosaka K, Imai H, Takeyama Y, **Kudo M**: Transcatheter endoscopy for pancreaticobiliary duct diseases (with videos). **Gastrointest Endosc** 76:892-899, 2012. **(IF=5.210)**

18. 2012 Takahashi K, Kashida H, **Kudo M**: Hepatic nodules associated with an inferior mesentric arteriovenous malformation. **Internal Med** 51:2753-2755, 2012. **(IF=0.973)**

19. 2012 **Kudo M***: Why does every hepatocellular carcinoma clinical trial using molecular targeted agents fail? **Liver Cancer** 1(2):59-60, 2012. **(IF=0.000)**

20. 2012 **Kudo M***: Treatment of advanced hepatocellular carcinoma with emphasis on hepatic arterial infusion chemotherapy and molecular targeted therapy. **Liver Cancer** 1(2):62-70, 2012. **(IF=0.000)**

21. 2012 Park AM, **Kudo M**, Hagiwara S, Tabuchi M, Watanabe T, Munakata H, Sakurai T: p38MAPK suppresses chronic pancreatitis by regulating HSP27 and BAD expression. **Free Radical Bio Med** 52:2284-2291, 2012. **(IF=5.271)**

22. 2012 Sakurai T, Kashida H, **Kudo M**: Case of Peutz-Jeghers syndrome with depressed-type early duodenal carcinoma. **Digest Endosc** 24:489, 2012. **(IF=1.610)**

23. 2012 **Kudo M***: Preface. **Digest Dis** 30:539-540, 2012. **(IF=2.725)**

24. 2012   Hagiwara S, Sakurai T, Nishina S, Tanaka K, Ikeda M, Ueshima K, Minami Y, Inoue T, Yada N, Kitai S, Takita M, Nagai T, Hayaishi S, Arizumi T, Park AM, Munakata H, Nishida N, **Kudo M**: Characteristic pattern of reactivation of hepatitis B virus during chemotherapy for solid cancers. **Digest Dis** 30:541-546, 2012. **(IF= 2.725)**

25. 2012   Nishida N, Arizumi T, Hayaishi S, Takita M, Kitai S, Yada N, Hagiwara S, Inoue T, Minami Y, Ueshima K, Sakurai T, Ikai I, **Kudo M**: Gender differences in the livers of patients with hepatocellular carcinoma and chronic hepatitis C infection. **Digest Dis** 30:547-553, 2012. **(IF= 2.725)**

26. 2012   Ueda T, Tsuchiya K, Hashimoto S, Inoue T, Inao M, Tanaka A, Kaito M, Imazaki F, Nishiguchi S, Mochida S, Yokosuka O, Yatsuhashi H, Izumi N, **Kudo M**, for RETRY study group: Retreatment with peginterferon alfa-2a plus ribavirin in patients who failed previous peginterferon alfa-2b plus ribavirin combination therapy. **Digest Dis** 30:554-560, 2012. **(IF= 2.725)**

27. 2012   Hagiwara S, Sakurai T, Takita M, Ueshima K, Minami Y, Inoue T, Yada N, Kitai S, Nagai T, Hayaishi S, Arizumi T, Nishida N, **Kudo M**: Risk of HCC development in cases of hepatitis C treated by long-term, low-dose PEG-IFNα2a. **Digest Dis**, 30:561-567, 2012. **(IF= 2.725)**

28. 2012   Kobayashi S, Kim SR, Imoto S, Ando K, Hirakawa M, Saito J, Fukuda K, Otono Y, Sakaki M, Tsuchida S, Kim SK, Hayashi Y, Nakano M, **Kudo M**: Histopathological diagnosis of early HCC through biopsy -efficacy of victoria blue and cytokeratin 7 staining-. **Digest Dis** 30:574-579, 2012. **(IF= 2.725)**

29. 2012   Tsuchida S, Fukumoto T, Toyokawa A, Awazu M, Kusunoki N, Kido M, Takahashi M, Tanaka M, Kuramitsu K, Kim SR, **Kudo M**, Ku Y: Novel non-trocar technique for laparoscopic radiofrequency ablation. **Digest Dis** 30:588-591, 2012. **(IF= 2.725)**

30. 2012   Minami Y, <u>Kudo M</u>*: Hepatocellular carcinoma with obstructive jaundice: endoscopic and percutaneous biliary drainage. **Digest Dis** 30:592-597, 2012. **(IF=2.725)**

31. 2012   <u>Kudo M</u>*, Ueshima K, Arizumi T: Real-life clinical practice with sorafenib in advanced hepatocellular carcinoma: a aingle center experience. **Digest Dis** 30:609-616, 2012. **(IF= 2.725)**

32. 2012   Katsube T, Okada M, Kumano S, Imaoka I, Kagawa Y, Hori M, Ishii K, Tanigawa N, Imai Y, <u>Kudo M</u>, Murakami T: Estimation of liver function using T2* mapping on gadolinium ethoxybenzyl diethylenetriamine pentaacetic acid enhanced magnetic resonance imaging. **Eur J Radiol** 81:1460-1464, 2012. **(IF= 2.512)**

33. 2012   Nishida N, <u>Kudo M</u>, Nagasaka T, Ikai I, Goel A: Characteristic patterns of altered DNA methylation predict emergence of human hepatocellular carcinoma. **Hepatology** 56:994-1003, 2012. **(IF=12.003)**

34. 2012   Kitano M, Sakamoto H, <u>Kudo M</u>: Endoscopic ultrasound: contrast enhancement. **Gastrointest Endosc Clin N Am** 22:349-358, 2012. **(IF=0.000)**

35. 2012   <u>Kudo M</u>: Signaling pathway/molecular targets and new targeted agents under development in hepatocellular carcinoma. **World J Gastroenterol** 18:6005-6017, 2012. **(IF=2.547)**

36. 2012   Inoue T, Kitai S, Hayaishi S, <u>Kudo M</u>: Septicemia due to vibrio cholerae serogroup non-01/non-0139 strain in a cirrhotic patient. **Clin J Gastroenterol** 5:383-387, 2012. **(IF=0.000)**

37. 2012   <u>Kudo M</u>: Japan's successful model of nationwide hepatocellular carcinoma surveillance highlighting the urgent need for global surveillance. **Liver Cancer** 1(3):141-143, 2012. **(IF=0.000)**

38. 2012   Okusaka T, Kasugai H, Ishii H, **Kudo M**, Sata M, Tanaka K, Shioyama Y, Chayama K, Kumada H, Yoshikawa M, Seki T, Saito H, Hayashi N, Shiratori K, Okita K, Sakaida I, Honda M, Kusumoto Y, Tsutsumi T, Sakata K: A randomized phase II trial of intra-arterial chemotherapy using SM-11355 (Miriplatin) for hepatocellular carcinoma.   **Invest New Drug** 30: 2015-2025, 2012. (IF=3.498)

39. 2012   Hagiwara S, **Kudo M**, Chung H, Ueshima K, Inoue T, Haji S, Watanabe T, Park AM, Munakata H, Sakurai T: Activation of c-Jun N-terminal kinase in non-cancerous liver tissue predicts a high risk of recurrence after hepatic resection for hepatocellular carcinoma.   **Hepatol Res** 42: 394-400, 2012. (IF=2.072)

40. 2012   Sakurai T, **Kudo M**, Umemura A, He G, Elsharkawy AM, Seki E, Karin M: p38 α inhibits liver fibrogenesis and consequent hepatocarcinogenesis by curtailing accumulation of reactive oxygen species. **Cancer Res** 73:215-224, 2012. (IF=8.650)

41. 2012   **Kudo M**[*]: Targeted therapy for liver cancer: updated review in 2012.   **Curr Cancer Drug Tar** 12: 1062-1072, 2012. (IF=4.000)

42. 2012   Kaneko S, Furuse J, **Kudo M**, Ikeda K, Honda M, Nakamoto Y, Onchi M, Shiota G, Yokosuka O, Sakaida I, Takehara T, Ueno Y, Hiroishi K, Nishiguchi S, Moriwaki H, Yamamoto K, Sata M, Obi S, Miyayama S, Imai Y: Guideline on the use of new anticancer drugs for the treatment of hepatocellular carcinoma 2010 update.   **Hepatol Res** 42: 523-542, 2012. (IF=2.072)

43. 2012   Inoue T, **Kudo M**[*], Komuta M, Hayaishi S, Ueda T, Takita M, Kitai S, Hatanaka K, Yada N, Hagiwara S, Chung H, Sakurai T, Ueshima K, Sakamoto M, Maenishi O, Hyodo T, Okada M, Kumano S, Murakami T: Assessment of Gd-EOB-DTPA-enhanced MRI for HCC and Dysplastic nodule and comparison of detection sensitivity versus MDCT.   **J Gastroenterol** 47: 1036-1047, 2012. (IF=3.788)

44. 2012 D'Onofrio M, Barbi E, Dietrich CF, Kitano M, Numata K, Sofuni A, Principe F, Gallotti A, Zamboni GA, Mucell RP: Pancreatic multicenter ultrasound study (PAMUS). **Eur J Radiol**, 81: 630-638, 2012. **(IF=2.512)**

Ⅲ．和文論文（著書・分担執筆）

1. 2012　上嶋一臣，<u>工藤正俊</u>：肝細胞癌に対する分子標的治療―治療成績と新規分子標的薬の開発の動向―．第1部 Overview 肝癌の診断・治療，肝疾患 Review 2012〜2013, 日本メディカルセンター，東京，p54-63，2012（分担執筆）

2. 2012　<u>工藤正俊</u>：肝細胞癌の病型分類（肝癌取扱い規約）と予後予測（JIS スコア）．臨床に役立つ消化器疾患の診断基準・病型分類・重症度の用い方 改訂第2版　編集 田尻久雄，五十嵐正広，小池和彦，杉山政則，日本メディカルセンター，東京，p215-223，2012．（分担執筆）

3. 2012　<u>工藤正俊</u>：発刊に寄せて．第6回日本肝がん分子標的治療研究会記録　「SORAFENIB PRACTICE BOOK-Sorafenib 治療の実践!! 多数症例の使用経験を踏まえた治療の実践と問題点の解決を示す-」監・編集 市田隆文，アークメディア，東京，p2，2012．（分担執筆）

4. 2012　上嶋一臣，有住忠晃，早石宗右，田北雅弘，北井　聡，矢田典久，井上達夫，萩原　智，南　康範，櫻井俊治，西田直生志，<u>工藤正俊</u>：当院における肝細胞癌分子標的治療の現状．第6回日本肝がん分子標的治療研究会 記録「SORAFENIB PRACTICE BOOK-Sorafenib 治療の実践!! 多数症例の使用経験を踏まえた治療の実践と問題点の解決を示す-」監・編集 市田隆文，アークメディア，東京，p25-30，2012．（分担執筆）

5. 2012　<u>工藤正俊</u>：Medical Practice コラム "One Point Advice",文光堂，東京，2012（分担執筆）（印刷中）

6. 2012　<u>工藤正俊</u>：慢性肝炎の治療ガイド 2010．文光堂，東京，2012（分担執筆）

7. 2012　<u>工藤正俊</u>：肝細胞癌のスクリーニングと診断．慢性肝炎の治療ガイド 2010，日本肝臓学会編集，文光堂，東京，2012（分担執筆）（印刷中）

8.　2012　　　井上達夫，<u>工藤正俊</u>：肝機能障害治療中に生じた下肢浮腫例．浮腫の診療指針，文光堂，東京，2012（分担執筆）（印刷中）

9.　2012　　　北野雅之：Interventional EUS の極意「EUS-PD のコツ」．胆膵内視鏡治療-手技の極意とトラブルシューティング，羊土社，東京，pp143-147，2012（分担執筆）．

10.　2012　北野雅之：Interventional EUS の極意「EUS-GBD のコツ」．胆膵内視鏡治療-手技の極意とトラブルシューティング，羊土社，東京，pp148-151，2012（分担執筆）．

11.　2012　北野雅之，伊佐山浩通，山雄健次：12）超音波内視鏡 ②超音波内視鏡ガイド下穿刺術．消化器内視鏡ハンドブック，日本メディカルセンター，東京，pp111-122，2012（分担執筆）．

IV．和文論文

1. 2012 犬塚　義，大﨑往夫，松田史博，坂本　梓，幡丸景一，邉見慎一郎，石川哲朗，齋藤澄夫，西川浩樹，喜多竜一，岡部純弘，木村　達，若狭朋子，萩原　智，工藤正俊：エンテカビル・ペグインターフェロンα-2b 併用 48 週治療にて HBs 抗原が消失した B 型慢性肝炎の 1 例．　肝臓 53: 42-47, 2012.

2. 2012 南　康範，工藤正俊：肝細胞癌のリスク因子とサーベイランスの影響．　"Factors that affect risk for hepatocellular carcinoma effects of surveillance"，Review of Gastroenterology & Clinical Gastroenterology and Hepatology 6: 64-67, 2012.

3. 2012 松井繁長，樫田博史，朝隈　豊，川崎正憲，櫻井俊治，工藤正俊：異所性静脈瘤に対する内視鏡治療．　臨牀消化器内科 27: 181-189, 2012.

4. 2012 工藤正俊：わが国の肝炎・肝癌対策について．　Workshop「肝炎・肝癌対策との比較で胃炎・胃癌対策を考える」，The GI FOREFRONT 7: 103-106, 2012.

5. 2012 大本俊介，松井繁長，櫻井俊治，朝隈　豊，川崎正憲，樫田博史，工藤正俊：プロトンポンプ阻害薬投与患者における GerdQ 問診票を使用した治療実態の検討．　Pharma Medica 30: 77-81, 2012.

6. 2012 坂本洋城，北野雅之，今井　元，宮田　剛，鎌田　研，門阪薫平，工藤正俊：消化器癌の見逃しを防ぐ-早期発見・適切な治療のための診断の実際 胆道癌・膵臓癌．　見逃してはいけない消化器疾患-消化器緊急疾患・消化器癌を中心に-，消化器の臨床 15: 82-88, 2012.

7. 2012 上嶋一臣，工藤正俊：肝癌に対する抗血管新生療法．　特集：「癌の抗血管新生療法」，血管医学-Vascular Biology & Medicine- 13: 51-57, 2012.

8.　　2012　　鎌田　研，北野雅之，坂本洋城，今井　元，宮田　剛，門阪薫平，工藤正俊：内視鏡的胆嚢ドレナージ術．　特集：「胆道・膵のドレナージとステント」，臨牀消化器内科 27: 445-452, 2012.

9.　　2012　　上嶋一臣，工藤正俊：Brivanib.　肝胆膵 64: 669-675, 2012.

10.　　2012　　上嶋一臣，工藤正俊：Ramucirumab.　肝胆膵 64: 697-700, 2012.

11.　　2012　　門阪薫平，北野雅之，鎌田　研，宮田　剛，今井　元，坂本洋城，樫田博史，工藤正俊：EUS 下胆嚢ドレナージ．特集「内視鏡的胆膵管ドレナージのすべて」，消化器内視鏡 24: 351-355, 2012.

12.　　2012　　南　康範，工藤正俊：RFA のための術前画像診断．　肝胆膵画像 14: 221-224, 2012.

13.　　2012　　工藤正俊：肝細胞癌診療の新しいパラダイム．　岐阜県医師会医雑誌 25: 33-41, 2012.

14.　　2012　　有住忠晃，上嶋一臣，竹田治彦，大﨑往夫，萩原　智，井上達夫，北井　聡，矢田典久，櫻井俊治，西田直生志，工藤正俊：進行肝細胞患者に対する分子標的薬（ソラフェニブ）投与における治療効果判定基準の比較．　肝臓 53: 344-347, 2012.

15.　　2012　　有住忠晃，上嶋一臣，早石宗右，田北雅弘，北井　聡，井上達夫，矢田典久，萩原　智，南　康範，櫻井俊治，西田直生志，工藤正俊：進行肝細胞癌に対するソラフェニブ投与例における SD の持続期間と生存期間の検討．　肝臓 53: 348-350, 2012.

16.　　2012　　矢田典久，工藤正俊：腹部エコー検査と新たな画像診断．medicina 49: 1150-1154, 2012.

17.　　2012　　工藤正俊：序説 早期肝細胞癌の画像診断 update．　肝胆膵画像 14: 285-288, 2012.

18.　　2012　　上嶋一臣，工藤正俊：肝癌制圧への治療の開発状況．　ウイルス

肝炎・肝癌制圧の分子基盤の各論，BIO Clinica　27: 38-41, 2012.

19.　2012　<u>工藤正俊</u>，井上達夫：序説・肝細胞癌と鑑別を要する多血性腫瘤．肝胆膵画像 14: 382-385, 2012.

20.　2012　上嶋一臣，<u>工藤正俊</u>：わが国での肝細胞癌治療の現状と問題点．特集「肝細胞癌治療の現状と画像診断」．画像診断 32: 874-880, 2012.

21.　2012　上嶋一臣，<u>工藤正俊</u>：肝細胞癌の分子標的治療．特集「肝細胞癌治療の現状と画像診断」．画像診断 32: 930-937, 2012.

22.　2012　<u>工藤正俊</u>：進行肝癌の治療．日本消化器病学会雑誌 109:1327-1334, 2012.

23.　2012　泉　並木，西口修平，<u>工藤正俊</u>，金子周一，佐田通夫，小俣政男：C型代償性肝硬変に対するペグインターフェロンα-2a（40KD）とリバビリン併用療法におけるALTおよびAFPに対する効果―臨床第Ⅱ/Ⅲ相試験サブ解析―．「新薬と臨床」61: 1559-1568, 2012.

24.　2012　上嶋一臣，<u>工藤正俊</u>：肝がん 1)肝がん化学療法-レジメン選択の基本．別冊 臨床腫瘍プラクティスⅡ「消化器がん化学療法レジメン」98-99, 2012.

25.　2012　上嶋一臣，<u>工藤正俊</u>：肝がん 2)肝がん化学療法に用いられるレジメン，①シスプラチン（CDDP）単独療法．別冊 臨床腫瘍プラクティスⅡ「消化器がん化学療法レジメン」100-101, 2012.

26.　2012　上嶋一臣，<u>工藤正俊</u>：肝がん 2)肝がん化学療法に用いられるレジメン，②ミリプラチン単独療法．別冊 臨床腫瘍プラクティスⅡ　「消化器がん化学療法レジメン」102-103, 2012.

27.　2012　上嶋一臣，<u>工藤正俊</u>：肝がん 2)肝がん化学療法に用いられるレジメン，③ソラフェニブ単独療法．別冊 臨床腫瘍プラクティスⅡ　「消化器がん化学療法レジメン」104-105, 2012.

28. 2012 上嶋一臣，工藤正俊: 各臓器別の最新治療と新薬の動向「肝細胞がん」．「抗がん剤治療の最前線：分子標的薬剤の使用による進歩（後篇）最新医学」67: 2220-2229, 2012.

29. 2012 工藤正俊: 肝腫瘍の診断・治療に挑む－次世代へのメッセージ．特集「肝胆膵疾患に挑む－次世代へのメッセージ」，肝胆膵画像 14: 578-583, 2012.

30. 2012 松井繁長，樫田博史，工藤正俊: 胃潰瘍・十二指腸潰瘍．特集「消化管疾患の病態と診断・治療（Ⅰ）」，医学と薬学 68: 625-630, 2012.

31. 2012 矢田典久，工藤正俊: 超音波エラストグラフィによる肝線維化評価．特集「びまん性肝疾患の画像診断：Update2012」，臨床画像 28: 1470-1477, 2012.

32. 2012 井上達夫，工藤正俊: 腹部超音波検査．Ⅲ.消化管疾患の検査法，日本医師会雑誌「消化器疾患診断のすべて」 141: 90-93, 2012.

33. 2012 櫻井俊治，工藤正俊: 機能的ゲノム解析から分子診断・分子標的治療へ ②シグナル伝達異常とバイオマーカー探索．The Liver Cancer Journal 4: 35-39, 2012.

34. 2012 工藤正俊: 巻頭言．特集「肝細胞癌のすべて 2012」，肝胆膵 65: 931-934, 2012.

35. 2012 北井　聡，工藤正俊: 肝細胞癌のステージングシステム．特集「肝細胞癌のすべて 2012」，肝胆膵 65: 1158-1163, 2012.

36. 2012 上嶋一臣，工藤正俊: Everolimus（RAD001）．特集「肝細胞癌のすべて 2012」，肝胆膵 65: 1302-1306, 2012.

37. 2012 上嶋一臣，工藤正俊: Axitinib．特集「肝細胞癌のすべて 2012」，肝胆膵 65: 1307-1310, 2012.

38. 2012 有住忠晃，工藤正俊: 分子標的治療．特集「肝細胞癌のすべて 2012」，肝胆膵 65: 1370-1374, 2012.

39. 2012 工藤正俊: 編集後記. 特集「肝細胞癌のすべて 2012」, 肝胆膵 65:1384, 2012.

40. 2012 宮田　央, 宮田　学, 工藤正俊: PEG-IFNα2a+リバビリン療法施行中にＢ型慢性肝炎の急性増悪を起こしたＢ型Ｃ型重複感染の一例. 肝臓 53: 846-852, 2012.

41. 2012 樫田博史, 川崎正憲, 筑後孝章, 前西　修, 所　忠男: 転移性小腸腫瘍の診断.　臨牀消化器内科 27: 503-510, 2012.

42. 2012 矢田典久: Real-time tissue elastography による肝線維化診断. 特集「肝細胞癌のすべて 2012」, 肝胆膵 65:1043-1048, 2012.

43. 2012 井上達夫: コンセンサスに基づく肝癌診療ガイドライン. 特集「肝細胞癌のすべて 2012」, 肝胆膵 65:1194-1198, 2012.

Ⅴ．招待講演・特別講演（海外）

1. <u>**Kudo M**</u>: Special Lecture "CEUS, EOB-MRI, targeted theerapy and Japanese HCC guideline." "Cancer Genomics: a way to personalized medicine", Taipei, Taiwan, February 15, 2012.

2. <u>**Kudo M**</u>: Special Lecture "Evolving strategies on the treatment of HCC: Physician's perspective." "HCC and other liver tumors", The 22nd conference of the Asian Pacific Association for the Study of the Liver (APASL 2012), Taipei, Taiwan, February 16-19, 2012.

3. <u>**Kudo M**</u>: Special Lecture "Hepatocellular carcinoma." "APASL-AASLD symposium-When east meets west: Management of the complications of cirrhosis", The 22nd conference of the Asian Pacific Association for the Study of the Liver (APASL 2012), Taipei, Taiwan, February 16-19, 2012.

4. <u>**Kudo M**</u>: Special Lecture "Real life experience with Sorafenib: GIDEON, the largest prospective global study in HCC." "Satellite symposium Advances in HCC management : from diagnosis to treatment", The 22nd conference of the Asian Pacific Association for the Study of the Liver (APASL 2012), Taipei, Taiwan, February 16-19, 2012.

5. <u>**Kudo M**</u>: Special Lecture "From JSH treatment guideline to combination therapy." "HCC Expert Meeting -New Advances in HCC Management", Taipei, Taiwan, March 24, 2012.

6. <u>**Kudo M**</u>: Special Lecture "Management of hepatocellular carcinoma: Recent progress." The 42nd Annual Meeting of the Gastroenterological Society of Taiwan (GEST) and The 21st Annual Meeting of the Digestive Endoscopy Society of Taiwan (DEST), Taipei, Taiwan, March 25, 2012.

7. <u>**Kudo M**</u>: Invited Lecture "Management of hepatocellular carcinoma." Yonsei University, Korea, April 6, 2012.

8. <u>**Kudo M**</u>: Invited Lecture "The role of TACE & Nexavar in HCC treatment." HCC Expert Symposium on Tumor Therapy, Seoul, Korea, April 7-8, 2012.

9. **Kudo M**: Opening Lectures "WFUMB Lecture Contrast enhanced EUS of pancreatic tumors." EFSUMB Annual Meeting EUROSON 2012, Madrid, Spain, April 22, 2012.

10. **Kudo M**: Invited Lecture "Endoscopic ultrasound in the differential diagnosis of cystic pancreatic lesions: do we always need it?" EFSUMB Annual Meeting EUROSON 2012, Madrid, Spain, April 22, 2012.

11. **Kudo M**: Invited Lecture "CEUS as a screening tool of HCC in cirrhotic liver.", ACUCI 2012, The 4th Asian Conference on Ultrasound Contrast Imaging, Korea, May 11-13, 2012.

12. **Kudo M**: Invited Lecture "CEUS in the pancreatobiliary intervention.", ACUCI 2012, The 4th Asian Conference on Ultrasound Contrast Imaging, Korea, May 11-13, 2012.

13. **Kudo M**: Educational Lecture "Intravascular treatment (TACE, HAIC)", 10th International Conference ofthe Asian Clinical Oncology Society (ACOS), Seoul, Korea, June 13-15, 2012.

14. **Kudo M**: Invited Lecture "Observations of hepatocellular carcinoma (HCC) management patterns from the global HCC BRIDGE study: an analysis of the Asian cohort." Evening Symposium "Recent observation in the management of HCC", The 3rd Asia-Pacific Primary Liver Cancer Expert Meeting (APPLE),Shanghai, China, July 6-8, 2012.

15. **Kudo M**: Invited Lecture "Japanese treatment algorithm. " Session XII " Algorithm Consensus Discussion", The 3rd Asia-Pacific Primary Liver Cancer Expert Meeting (APPLE),Shanghai, China, July 6-8, 2012.

16. **Kudo M**: Invited Lecture "Management of TACE failure: Difinition on TACE failure/refractoriness", Expert Panel Opinion on Interventions In Hepatocellular Carcinoma (EPOIHCC), Shanghai, China, July 8, 2012.

17. **Kudo M**: Invited Lecture "Review of the evidence suppporting combination therapy in intermediate HCC: GIDEON", Expert Panel Opinion on Interventions In Hepatocellular Carcinoma (EPOIHCC),

Shanghai, China, July 8, 2012.

18. **Kudo M**: Invited Lecture "Diagnosis by Imaging: Eastern approach", Program for the Advancement of Therapy in Hepatocellular Carcinoma (PATH), Shanghai, China, July 9-10, 2012.

19. **Kudo M**: Invited Lecture "Real life experience with Nexavar: GIDEON 2nd IA" "Advanced HCC: rich evidence for Nexavar", Advances in HCC management in Asia, Ho Chi Minh , Vietnam, August 4-5, 2012.

20. **Kudo M**: Invited Lecture "Controversies on the role of TACE" "Intermediate HCC", Advances in HCC management in Asia, Ho Chi Minh , Vietnam, August 4-5, 2012.

21. **Kudo M**: Invited Lecture "Liver biopsy: Is it useful for staging?", Sixth Annual Conference International Liver Cancer Association(ILCA), Berlin, Germany, September 14-16, 2012.

22. **Kudo M**: Invited Lecture "HCC challenges: Definition on TACE failure and refractoriness.", HCC Expert Meeting and Asia Pacific Virtual Meeting -Expert discussion on HCC management-, Taipei, Taiwan, November 3, 2012.

23. Kitano M: Harmonic imaging: Is the expense worth it? Interventional EUS 2012, March 24-25, 2012, Mumbai, India.

24. Kitano M: EUS guided pancreatic duct interventions: Curiosity or clinical practice? Interventional EUS 2012, March 24-25, 2012, Mumbai, India.

25. Kitano M: EUS-guided biliary drainage. BONASTENT SUMMIT 2012, March 31-April 1, 2012, Jeju-do, Korea.

26. Kitano M: The treatment for pancreatic cancer by endoscopy. 9th Beijing International Digestive Disease Forum, June 8-10, 2012, Beijing, China.

27. Kitano M: Invited Lecture "Better imaging, better diagnosis?" 18th International Symposium on Endoscopic Ultrasonography (EUS2012),

September 6-8, 2012, Corinthia Hotel, Saint Petersburg, Russia.

28. Kitano M: Invited Lecture "Contrast enhanced EUS & elastography" The 6th Meeting of the Society of Gastrointestinal Intervention (SGI2012), October 5-6, 2012, Sheraton Grande Walkerhill, Seoul, Korea.

29. Kitano M: Invited Lecture "Contrast Enhanced Harmonic EUS" 5th Nottingham Masterclass in Advanced Imaging and EndoTherapy, October 26, 2012, Nottingham University Hospital, Nottingham, United Kingdom.

30. Kitano M: Invited Lecture "Recent advances in diagnosis and treatmenet for biliary obstraction" 2012 Nanjing International Digestion and Digestive Endoscopy Forum, November 2-4, 2012, Nanjing Drum Tower hospital, Jiangsu, China.

31. Kitano M: Invited Lecture "EUS-guided biliary interventions" Tokyo Conference of Asian Pancreato-biliary interventional Endoscopist, 2012, November 2-4, 2012, Garden City, Shinagawa, Tokyo.

32. Kitano M: Invited Lecture "EUS Anatomy of Bilio-pancreatic System (Linear)" 4th EUS Phantom Workshop, November 17, 2012, National Taiwan University Hospital Endoscopic Optical Diagnosis and Treatment Center, Hsinchu, Taiwan.

33. Yeh HZ, Sun MS, Yasuda K, Kitano M, Ch eng TY: Invited Lecture "Hands-on EUS simulator practice" 4th EUS Phantom Workshop, November 17, 2012, National Taiwan University Hospital Endoscopic Optical Diagnosis and Treatment Center, Hsinchu, Taiwan.

34. Kitano M: Invited Lecture "To increase the diagnostic yield of EUS -contrast enhancement or elastography" 15th EUS and 12th Early Gl Cancer Conference of Taiwan, November 18, 2012, Classroom 501, National Taiwan University, College of Medicine, Taipei, Taiwan.

35. Kashida K: Invited Lecture "Large colon neoplasm-how to decide the treatment method and how to do it" 15th EUS and 12th Early Gl Cancer Conference of Taiwan, November 18, 2012, Classroom 501, National Taiwan University, College of Medicine, Taipei, Taiwan.

VI. 招待講演・特別講演（国内）

1. <u>工藤正俊</u>: 講演「肝臓がんの内科的治療」，近畿大学医学部附属病院がんセンター第 35 回ともに生きる会，平成 24 年 1 月 16 日，近畿大学医学部附属病院 PET 棟 3 階　大会議室，大阪.

2. <u>工藤正俊</u>: 特別講演「肝細胞癌診療の新しいパラダイム」，第 3 回中四国肝臓病研究会，平成 24 年 1 月 21 日，ホテルグランヴィア岡山，岡山.

3. <u>工藤正俊</u>: 特別講演「Sonazoid は肝癌診療をどう変えたか？」，第 17 回鈴鹿肝胆膵画像研究会，平成 24 年 2 月 2 日，ホテルグリーンパーク鈴鹿，三重.

4. <u>工藤正俊</u>: 特別講演「肝硬変・肝癌の治療のガイドラインと発癌抑制」，リーバクト配合顆粒発売 15 周年記念講演会，平成 24 年 3 月 17 日，ホテルオークラ札幌，北海道.

5. <u>工藤正俊</u>: 特別講演「肝癌診療の最新の進歩」，第 13 回岐阜肝臓外科研究会，平成 24 年 5 月 10 日，じゅうろくプラザ，岐阜.

6. <u>工藤正俊</u>: ランチョンセミナー2 特別講演「ソナゾイド発売 5 年」，日本超音波医学会第 85 回学術集会，平成 24 年 5 月 25 日，グランドプリンスホテル新高輪，東京.

7. <u>工藤正俊</u>: 特別講演「肝細胞癌診療の新しいパラダイム」，第 9 回城北消化器病研究会，平成 24 年 5 月 26 日，ホテルメトロポリタン池袋，東京.

8. <u>工藤正俊</u>: ランチョンセミナー12「肝疾患に対する超音波診断の新展開 -Real-time Tissue Elastography を用いて-」，日本超音波医学会第 85 回学術集会，平成 24 年 5 月 27 日，グランドプリンスホテル新高輪，東京.

9. <u>工藤正俊</u>: ランチョンセミナーIII　「組織弾性法の領域別臨床応用」，第 37 回日本超音波検査学会，平成 24 年 6 月 2 日，札幌コンベンションセンター，北海道.

10. <u>工藤正俊</u>: ワークショップ 1 基調講演「肝癌のバイオマーカー（分子・血液・画像）による悪性度診断・治療効果判定」，第 48 回日本肝癌研究会，平

成 24 年 7 月 20-21 日，石川県立音楽堂，石川．

11. <u>工藤正俊</u>: ワークショップ 1 総括発言 肝細胞癌に対する新しい治療戦略，「肝癌治療のアルゴリズムを含めて」，第 10 回日本臨床腫瘍学会学術集会，平成 24 年 7 月 26-28 日，大阪国際会議場， 大阪．

12. <u>工藤正俊</u>: 特別講演「肝疾患診療の最近の話題」， 東四国ベアネットカンファレンス， 平成 24 年 8 月 11 日，JR ホテルクレメント高松，香川．

13. <u>工藤正俊</u>: 肝がんディベートセッション 2 特別講演 ラジオ波の適応と優位性「原発性肝がんに対する治療方針 外科 vs RF 治療」，第 50 回日本癌治療学会学術集会，パシフィコ横浜，神奈川．

14. <u>工藤正俊</u>: シンポジウム 1 基調講演「分子標的治療の限界を超える新しい肝癌治療法の開発」，第 54 回日本消化器病学会大会，平成 24 年 10 月 10-13 日，神戸国際展示場，兵庫．

15. <u>工藤正俊</u>: シンポジウム 1 特別発言「分子標的治療の限界を超える新しい肝癌治療法の開発」，第 54 回日本消化器病学会大会，平成 24 年 10 月 10-13 日，神戸国際展示場，兵庫．

16. <u>工藤正俊</u>:サテライトシンポジウム10 特別発言，第16回日本肝臓学会大会，平成 24 年 10 月 10-13 日，ポートピアホテル，兵庫．

17. <u>工藤正俊</u>: 特別講演「肝胆膵疾患の造影超音波診断」， 日本超音波医学会第 22 回四国地方会学術集会，平成 24 年 10 月 20 日，松山市総合コミュニティーセンター，愛媛．

18. <u>工藤正俊</u>: ランチョンセミナー「肝胆膵疾患における造影超音波の役割」，超音波分科会（日本超音波医学会第 42 回北海道地方会学術集会），平成 24 年 10 月 27 日，札幌医科大学臨床教育研究棟講堂記念ホール，札幌．

19. <u>工藤正俊</u>: 特別講演「肝細胞がん診療の新しいパラダイム」，第 7 回JULIET，平成 24 年 12 月 1 日，野村コンファレンスプラザ日本橋,東京．

20. <u>工藤正俊</u>: 特別講演「What we learned from the Negative studies.」TACE Refractory Focus Expert Meeting, 平成 24 年 12 月 28 日，JR クレメントホテル高松，高松．

21. 櫻井俊治: Session 「当院における免疫調整剤の使用について」, 南近畿 UC フォーラム, 平成 24 年 1 月 11 日, スイスホテル南海大阪, 大阪.

22. 朝隈　豊: 「早期食道・胃がんの内視鏡診断と治療」, 消化器病市民公開講座　最新の消化器の病気のお話, 平成 24 年 1 月 22 日, 泉佐野泉の森ホール, 大阪.

23. 樫田博史: 「小腸・大腸の内視鏡診断と治療」, 消化器病市民公開講座　最新の消化器の病気のお話, 平成 24 年 1 月 22 日, 泉佐野泉の森ホール, 大阪.

24. 坂本洋城: 「胆・膵がんの内視鏡診断と治療」, 消化器病市民公開講座　最新の消化器の病気のお話, 平成 24 年 1 月 22 日, 泉佐野泉の森ホール, 大阪.

25. 萩原　智: 「肝炎の診断と治療」, 消化器病市民公開講座　最新の消化器の病気のお話, 平成 24 年 1 月 22 日, 泉佐野泉の森ホール, 大阪.

26. 井上達夫: 「肝がんの診断と治療」, 消化器病市民公開講座　最新の消化器の病気のお話, 平成 24 年 1 月 22 日, 泉佐野泉の森ホール, 大阪.

27. 朝隈　豊: 「PPI が必要な酸関連疾患」, 布施地区消化器フォーラム, 平成 24 年 1 月 28 日, シェラトン都ホテル大阪, 大阪.

28. 松井繁長: 「GERD と NSAIDs 潰瘍の現状と今後の展望」, Next Lecture Meeting, 平成 24 年 1 月 28 日, SAYAKA ホール, 大阪.

29. 北野雅之: 特別講演「EUS による胆膵疾患の診断と治療」, 第 41 回岐阜県消化器内視鏡フォーラム, 平成 24 年 2 月 9 日, 長良川国際会議場, 岐阜.

30. 北野雅之: 基調講演「膵癌診療における最近の Topics」, 第 1 回びわこ膵がんフォーラム, 平成 24 年 2 月 17 日, クサツエストピアホテル, 滋賀.

31. 松井繁長: ショートレクチャー「NSAID 潰瘍の現状とリスクマネジメント」, 河内長野病診連携の会, 平成 24 年 2 月 25 日, ノバティホール南館, 大阪.

32. 坂本洋城: 特別講演「EUS up to date 〜造影 EUS・Interventional EUS〜」,

第 3 回大分胆膵スキルアップセミナー，平成 24 年 2 月 25 日．

33. 北野雅之：「超音波内視鏡の基礎から応用まで」，超音波内視鏡勉強会，平成 24 年 3 月 5 日，鳥取県厚生病院，鳥取．

34. 上嶋一臣：特別講演「肝癌診療における分子標的薬の役割」，東京西部肝癌セミナー， 平成 24 年 3 月 15 日，吉祥寺東急イン，東京．

35. 南　康範：講演「肝細胞癌分子標的治療の Up to Date」，第 8 回 Kinki Liver Club，スイスホテル南海大阪，大阪．

36. 松井繁長：特別講演「NSAIDs 潰瘍の現状と今後の展望」，八尾消化器セミナー，平成 24 年 3 月 24 日，八尾商工会議所，大阪．

37. 松井繁長：特別講演「Helicobacter pylori 感染と除菌の最近の話題」，Next Lecture Meeting in 天理，平成 24 年 4 月 19 日，ウェルカムハウス，奈良．

38. 北野雅之：超音波内視鏡による胆膵疾患の診断と治療．大阪 NEXT シンポジウム，平成 24 年 5 月 26 日，大阪国際会議場，大阪．

39. 松井繁長：特別講演「GERD と NSAIDs 潰瘍の現状と今後の展望」，ケーエスケー消化管セミナー，平成 24 年 6 月 7 日，第一三共株式会社和歌山営業所，和歌山．

40. 上嶋一臣：ランチョンセミナー18「肝がん分子標的治療の現状と効果判定における PIVKA-II の有用性」，第 48 回日本肝臓学会総会，平成 24 年 6 月 7-8 日，ホテル日航金沢，金沢．

41. 北野雅之：特別講演「胆道ドレナージ術〜基礎から応用まで〜」，第 4 回三重胆膵内視鏡スキルアップセミナー，平成 24 年 6 月 15 日，ホテルグリーンパーク津，三重．

42. 坂本洋城：明日から使える EUS の標準的描出法，第 3 回関西 FNA Club のご案内，平成 24 年 6 月 16 日，TKP 新大阪，大阪．

43. 萩原　智：化学療法施行後に B 型肝炎ウイルス再活性化を認めた 2 例．第 14 回関西 B 型肝炎研究会，平成 24 年 6 月 23 日，ガーデンシティクラブ大

阪，大阪．

44. 北野雅之：特別講演「造影ハーモニック超音波内視鏡」，第 13 回東海腹部造影エコー研究会，平成 24 年 6 月 30 日，愛知産業労働センターウインクあいち，名古屋．

45. 松井繁長：教育講演「食道静脈瘤に対する内視鏡治療（EIS/EVL）」，第 21 回近畿食道・胃静脈瘤研究会，平成 24 年 6 月 30 日，大阪薬業年金会館，大阪

46. 松井繁長：特別講演「H. pylori 感染と除菌治療の最近の話題」，KSK NEXT Meetinng，平成 24 年 7 月 12 日，関西エアポートワシントンホテル，大阪．

47. 松井繁長：特別講演「NSAIDs 潰瘍の現状とリスクマネジメント」，スズケン NEXT Meeting，平成 24 年 7 月 28 日，スズケン岸和田支店，大阪．

48. 北野雅之：特別講演「最新 EMS レポート」，第 9 回大阪胆膵内視鏡ワークショップ，平成 24 年 8 月 3 日，ホテルグランヴィア大阪，大阪．

49. 北野雅之：特別講演「膵嚢胞性疾患に対する診断と治療の問題点：診断」，日本消化器内視鏡学会臨時セミナー，平成 24 年 8 月 18-19 日，神戸ポートピアホテル，兵庫．

50. 松井繁長：特別講演「GERD と NSAIDs 潰瘍の現状と今後の展望」，Nexium Lecture Meeting，平成 24 年 8 月 25 日，（株）スズケン藤井寺支店，大阪．

51. 北野雅之：特別講演「日常診療で見落としやすい膵疾患」，日常診療における膵疾患を考える会，平成 24 年 8 月 30 日，リーガロイヤルホテル堺，大阪．

52. 北野雅之：講義「消化器領域の超音波診療」，第 2 回超音波判読教室，平成 24 年 9 月 19 日，大阪府医師会館，大阪．

53. 松井繁長：症例提供施設，早期胃癌研究会 9 月度例会，平成 24 年 9 月 19 日，笹川記念会館，東京．

54. 松井繁長：特別講演「ヘリコバクターピロリ感染における最近の話題」，Next Lecture Meeting，平成 24 年 9 月 29 日，香芝市ふたかみ文化センタ

一，奈良．

55. 松井繁長：特別講演「酸関連疾患における薬物治療現状～GERD から H. pylori 感染まで～」，Next Lecture Meeting，平成 24 年 10 月 13 日，LIC はびきの，大阪．

56. 北野雅之：胆膵領域の抽出法 - 基本とコツ、教えます-．ランチョンセミナー22「コンベックス EUS を使いこなす！-描出法から治療の応用まで-．第 20 回日本消化器関連学会週間 JDDW2012（第 16 回日本肝臓学会大会・第 54 回日本消化器病学会大会・第 84 回日本消化器内視鏡学会総会・第 10 回日本消化器外科学会大会・第 50 回日本消化器がん検診学会大会・第 43 回日本消化器吸収学会総会合同），平成 24 年 10 月 10 日-13 日，神戸国際会議場，兵庫．

57. 松井繁長：特別講演「食道疾患の現状と診断/治療～GERD/他疾患も含めて」，河内長野市医師会学術講演会，平成 24 年 10 月 20 日，河内長野医師会館，大阪．

58. 松井繁長：特別講演「NSAIDs 潰瘍の現状とリスクマネジメント」，KSK NEXT Meetinng，平成 24 年 10 月 25 日，和泉図書館，大阪．

59. 北野雅之：特別講演「EUS 診療の全て FNA から造影エコーまで」．第 5 回胆膵セミナー in 広島，平成 24 年 11 月 10 日，三井ガーデンホテル広島，広島．

60. 北野雅之：特別講演「切除不能膵がんに対する超音波内視鏡下腹腔神経叢ブロック術による疼痛の緩和」．第 23 回がん患者の QOL 推進事業講習会，平成 24 年 12 月 1 日，明治安田生命ホール，東京．

Ⅶ．学会発表（海外シンポジウム）

1. 2012　Sakamoto H, Kitano M, <u>**Kudo M**</u>: A prospective study feasibility combination of EUS guided broad plexus-neuro lysis and celiac ganglion neurolysis. International Symposium "EUS-FNA: Current status and new developments", The 83rd Congress of the Japan Gastroenterological Endoscopy Society, Tokyo, Japan, May 12-14, 2012.

2. 2012　Kitano M, Sakamoto H, <u>**Kudo M**</u>: EUS-guided drainage for biliary obstruction after unsuccessful ERCP. International Symposium "EUS-FNA: Current status and new developments", The 83rd Congress of the Japan Gastroenterological Endoscopy Society, Tokyo, Japan, May 12-14, 2012.

Ⅷ．学会発表（海外一般演題）

1. 2012 Venook A, Lencioni R, Marrero J, **Kudo M**, Nakajima K, Ye SL, Cihon F: Second interim analysis of GIDEON (Global Investigation of therapeutic DEcisions in unresectable hepatocellular carcinoma and Of its treatment with sorafeNib): differences in adverse-event reporting across physician specialties. 2012 Gastrointeritinal Cancers Symposium (ASCO-GI 2012), San Francisco, USA, January 19-21.

2. 2012 Geschwind JF, Lencioni R, Marrero J, Venook A, Ye SL, Nakajima K, Cihon F, **Kudo M**: Worldwide trends in locoregional therapy for hepatocellular carcinoma (HCC): second interim analysis of the GIDEON (Global Investigation of therapeutic DEcisions in HCC and Of its treatment with sorafeNib) study. 2012 Gastrointeritinal Cancers Symposium (ASCO-GI 2012), San Francisco, USA, January 19-21, 2012.

3. 2012 Tsuji N, Okumura N, Yamamoto N, Takaba T, Matsumoto N, **Kudo M**: Percutaneous endoscopic gastrostomy with gastropexy greatly reduces the risk of peristomal infection. Clinical Nutrition Week 2012, Florida, USA, January 21-24, 2012.

4. 2012 Furuse J, Ye SL, Marrero J, Lencioni R, Venook A, Nakajima K, **Kudo M**: GIDEON (Global Investigation of therapeutic DEcisions in hepatocellular carcinoma and Of its Treatment with sorafeNib) second interim analysis (IA): subgroup analysis by race. Asian Pacific Association for the Study of the Liver (APASL) 2012, Taipei, Taiwan, February 16-19, 2012.

5. 2012 Chen PJ, Park JW, Chen M, Sherman M, Johnson P, Colombo M, **Kudo M**, Roberts L, Huang B, Wagner S: Observations of hepatocellular carcinoma (HCC) management ptterns from the

Global HCC BRIDGE Study: An interim analysis of the Asia-Pacific (AP) Cohort. Asian Pacific Association for the Study of the Liver (APASL) 2012, Taipei, Taiwan, February 16-19, 2012.

6.   2012   Geschwind JF, Lencioni R, Marrero J, Venook A, Ye SL, Nakajima K, <u>Kudo M</u>: Worldwide trends in locoregional therapy (LRT) for hepatocellular carcinoma (HCC): 2nd interim analysis [1500 patients] of the GIDEON (Global Investigation of therapeutic DEcisions in HCC and Of its treatment with sorafeNib) study. SIR 2012, San Francisco, USA, March 24-29, 2012.

7.   2012   Nagai T, Arao T, Matsumoto K, Fujita Y, Hayashi H, Kimura H, Hagiwara S, Sakurai T, Ueshima K, Haji S, <u>Kudo M</u>, Nishio K: Prognostic impact of EMT-related genes on post-operative prognosis in hepatocellular carcinoma. AACR 103rd Annual Meeting 2011, Chicago, USA, March 31- April 4, 2012.

8.   2012   Bronowicki JP, Ye SL, <u>Kudo M</u>, Marrero J, Dagher, Furuse J, Geschwind JF, Guevara LLd, Papandreou C, Sanyal AJ, Takayama T, Yoon SK, Nakajima K, Lencioni R: GIDEON (Global Investigation of therapeutic decisions in hepatocellular carcinoma and of its treatment with Soraenib) Second interim analysis: Clinical findings in Child-pugh B score subgourps. 47th Annual Meeting of the European Association for the Sudy of the Liver (EASL) , Barcelona, Spain, April 18-22, 2012.

9.   2012   Colombo M, Roberts L, Schwartz M, Degos F, Sherman M, Chen PJ, Chen M, Park JW, <u>Kudo M</u>, Johnson P, Huang B, Wagner S, Orsini L: Observed patterns of systemic therapy use in hepatocellular carcinoma (HCC) patients from the multinational HCC BRIDGE Study: Results of a second interim analysis. 47th Annual Meeting of the European Association for the Sudy of the Liver (EASL) , Barcelona, Spain, April 18-22, 2012.

10. 2012 Miyata T, Kitano M, Sakamoto H, Imai H, Kamata K, Kadosaka K, <u>Kudo M</u>: Role of contrast-enhanced harmonic EUS in differentiating malignant from benigh lymphadenopathy. The 83rd Congress of the Japan Gastroenterological Endoscopy Society, Tokyo, Japan, May 12-14, 2012.

11. 2012 Kadosaka K, Kitano M, Sakamoto H, Imai H, Kamata K, Miyata T, <u>Kudo M</u>: Estination of EUS features of chronic pancreatitis in comparison with clinical symptoms. The 83rd Congress of the Japan Gastroenterological Endoscopy Society, Tokyo, Japan, May 12-14, 2012.

12. 2012 Nishida N, <u>Kudo M</u>, Arizumi T, Hayaishi S, Takita M, Kitai S, Yada N, Inoue T, Hagiwara S, Minami Y, Ueshima K, Sakurai T, Nagasaka T, Goel A: Novel association between global DNA hypomethylation and chromosomal instability phenotype in human hepatocellular carcinoma. Digestive Disease Week(DDW) 2012, San Diego, USA, May 19-22.

13. 2012 Kamata K, Kitano M, <u>Kudo M</u>, Imai H, Sakamoto H: Detection of small concomitant carcinomas distinct from intraductal papillary mucinous neoplasms under surveillance of the whole pancreas using EUS. Digestive Disease Week(DDW) 2012, San Diego, USA, May 19-22.

14. 2012 Okumura N, Tsuji N, Yamamoto N, <u>Kudo M</u>: Percutaneous endoscopic gastrostomy with gastropexy greatly reduces the risk of peristomal infection and eases pain after the operation. Digestive Disease Week(DDW) 2012, San Diego, USA, May 19-22.

15. 2012 Sakurai T, Hagiwara S, Inoue T, Ueshima K, Matsui S, Nishida N, Kashida H, <u>Kudo M</u>: Activation of JNK in the Non-cancerous liver tissue predicts a high risk of recurrence after hepatic resection for hepatocellular carcinoma. Digestive Disease Week(DDW) 2012, San Diego, USA, May 19-22.

16. 2012 Arizumi T, Ueshima K, <u>Kudo M</u>: The decrease of blood flow

after administration of sorafenib may improve overall survival in patients with advanced hepatocellular carcinoma. Digestive Disease Week(DDW) 2012, San Diego, USA, May 19-22.

17.　2012　Minami Y, Hatanaka K, Arizumi T, Hayaishi S, Takita M, Kitai S, Yada N, Inoue T, Hagiwara S, Ueshima K, Nishida N, <u>Kudo M</u>: The gross classification of hepatocellular carcinoma: usefulness of contrast-enhanced sonography using perfluorocarbon microbubbles (sonazoid). Digestive Disease Week(DDW) 2012, San Diego, USA, May 19-22.

18.　2012　Inoue T, Arizumi T, Kitai S, Yada N, Hagiwara S, Minami Y, Sakurai T, Ueshima K, Nishida N, <u>Kudo M</u>: Usefulness of contrast-enhanced ultrasonography to evaluate a post treatment effect of radiofrequentry ablation about hepatocellular carcinoma: comparison with contrast-enhanced CT. Digestive Disease Week(DDW) 2012, San Diego, USA, May 19-22.

19.　2012　Sakamoto H, Kitano M, <u>Kudo M</u>: A prospective feasibility study on EUS guided broad plexus in combination of celiac ganglion neurolysis in pancreatic cancer pain. Digestive Disease Week(DDW) 2012, San Diego, USA, May 19-22.

20.　2012　Matsui S, <u>Kudo M</u>, Kashida H, Asakuma Y, Sakurai T, Kawasaki M: Effect of rebamipide for endoscopic submucosal dissection (ESD)-induced ulcer in early gastric cancer: a randomized controlled trial. Digestive Disease Week(DDW) 2012, San Diego, USA, May 19-22.

21.　2012　Cheng AL, Kang YK, Ryoo BY, Yen CJ, Lim HY, Oh DY, Austin TS, Wang Q, Greenberg J, Beckman RA, <u>Kudo M</u>: Phase 1b dose-escalation study of a phase 2 randomized trial to assess the safety and tolerability of tigatuzumab (CS-1008) in combination with sorafenib in patients (pts) with advanced hepatocellular carcinoma (HCC). ASCO 2012 Annual Meeting, Chicago, USA, June 1-5, 2012.

22.　　2012　　Park JW, Sherman M, Colombo M, Roberts L, Schwartz M, Degos F, Chen PJ, Chen M, <u>Kudo M</u>, Johnson P, Therneau T, Huang B, Orsini LS: Observations of hepatocellular carcinoma (HCC) management patterns from the Global HCC BRIDGE Study: First characterization of the full study population.　ASCO 2012 Annual Meeting, Chicago, USA, June 1-5, 2012.

23.　　2012　　Orsini LS, Park JW, <u>Kudo M</u>, Chen PJ, Chen M: Observations of hepatocellular carcinoma (HCC) management patterns from the global HCC BRIDGE Study: An interim analysis of HCC burden of illness in the Asia-Pacific (AP) cohort. International Society for Pharmacoeconomics and Outsomes Research (ISPOR) 5th Asia-Pacific Conference, Taipei, Taiwan, September 2-4, 2012.

24.　　2012　　Llovet JM, Decaens T, Raoul JL, Boucher E, <u>Kudo M</u>, Chang C, Kang YK, Assenat E, Lim HY, Boige V, Mathurin P, Fartoux, L, Lin DY, Bruix J, Poon RT, Sherman M, Blanc JF, Finn RS, Tak WY, Chao Y, Ezzeddine R, Liu D, Walters I, Park JW: Brivanib versus placebo in patients with advanced hepatocellular carcinoma (HCC) who failed or were intolerant to sorafenib: results from the phase III Brisk-Ps Study. Sixth Annual Conference International Liver Cancer Association(ILCA), Berlin, Germany, September 14-16, 2012.

25.　　2012　　Arizumi T, Ueshima K, <u>Kudo M</u>: The decrease of blood flow after administration of sorafenib may improve overall survival in patients with advanced hepatocellular carcinoma. Sixth Annual Conference International Liver Cancer Association(ILCA), Berlin, Germany, September 14-16, 2012.

26.　　2012　　Raoul JL, Decaens T, Boucher E, <u>Kudo M</u>, Chang C, Kang YK, Assenat E, Lim HY, Boige V, Mathurin P, Fartoux L, Lin DY, Poon RT, Sherman M, Blanc JF, Finn RS, Tak WY, Chao Y, Liu D, Walters I, Park JW, Llovet JM: Brivanib versus placebo

in patients with advanced hepatocellular carcinoma who failed or were intolerant to sorafenib: assessment of baseline and on-treatment alpha-fetoprotein levels in the phase III Brisk-Ps study. Sixth Annual Conference International Liver Cancer Association(ILCA), Berlin, Germany, September 14-16, 2012.

27. 2012   Sherman M, Colombo M, Roberts L, Schwartz M, Degos F, Chen PJ, Chen M, Park JW, **Kudo M**, Johnson P, Huang B, Wagner S, Orsini LS: Observations of hepatocellular carcinoma (HCC) management patterns from the global HCC BRIDGE study: global comprison of outcomes by staging system. Sixth Annual Conference International Liver Cancer Association(ILCA), Berlin, Germany, September 14-16, 2012.

28. 2012   Kaneko S, Unaba Y, Kanai F, Aramaki T, Yamamoto T, Tanaka K , Yamakado K, **Kudo M**, Imanaka K, Arai Y: Final results of a randomized Phase II study of TSU-68 after transarterial chemoembolisation in Japanese patients with unresectable hepatocellular carcinoma. Chemoembolization. ESMO 2012, Vienna, Austria, September 28-October 2, 2012.

29. 2012   Bronowicki JP, Ye SL, **Kudo M**, Marrero J, Venook A, Nakajima K, Lencioni R: GIDEON (Global Investigation of therapeutic DEcisions in hepatocellular carcinoma and of its treatment with soraeNib) second interim analysis: subgoup analysis by disease aetiology. ESMO 2012, Vienna, Austria, September 28-October 2, 2012.

30. 2012   Ikeda K, Kumada H, **Kudo M**, Kawazoe S, Osaki Y, Ikeda M, Okusaka T, Suzuki T, O'Brien JP, Okita K: Phase I/II trial of lenvatinib (E7080), a multi-targeted tyrosine kinase inhibitor, in patients with advanced hepatocellular carcinoma (HCC). ESMO 2012, Vienna, Austria, September 28-October 2, 2012.

31. 2012   Takayama M, Matsui S, Kawasaki M, Asakuma Y, Sakurai T, Kashida H, **Kudo M**: Usefulness of rebamipide for endoscopic

submucosal dissection (ESD) -induces ulcer in early gastric cancer: prospective randomized study. 20th United European Gastroenterology Week (UEGW), Amsterdam, The Netherlands, October 20-24, 2012.

32. 2012 Adachi T, Takayama M, Mine H, Nagai T, Nagata Y, Kawasaki M, Asakuma Y, Sakurai T, Matsui S, Kashida H, **Kudo M**: Comparison of four different proton pump inhibitors in helicobacter pylori eradication treatment. 20th United European Gastroenterology Week (UEGW), Amsterdam, The Netherlands, October 20-24, 2012.

33. 2012 Roayaie S, Jibara G, Tabrizian P, Park JW, Chen M, **Kudo M**, Yan L, Guohong H, Yang J, Blanc JF, Johnson P, Sherman M, Roberts L, Schwartz M: Role of hepatic resection for hepatocellular carcinoma: analysis of the HCC BRIDGE study. The 63th Annual Meeting of the American Association for the Study of Liver Disease (AASLD), Boston, USA, November 9-13, 2012.

34. 2012 Arai K, Kaneko S, Yamashita T, Ikeda K, Furuse J, **Kudo M**: Efficacy and safety of miriplatin for hepatocellular carcinoma: a multi-center retrospective study in Japan. The 63th Annual Meeting of the American Association for the Study of Liver Disease (AASLD), Boston, USA, November 9-13, 2012.

35. 2012 Sunagozaka H, Kaneko S, Ikeda K, Furuse J, **Kudo M**: Sorafenib deteriorates liver function in patients with advanced hepatocellular carcinoma: a multi-center retrospective study in Japan. The 63th Annual Meeting of the American Association for the Study of Liver Disease (AASLD), Boston, USA, November 9-13, 2012.

36. 2012 Yamashita T, Kaneko S, Furuse J, **Kudo M**, Ikeda K: Predicting the treatment efficacy of sorafenib in patients for hepatocellular carcinoma: a multi-center retrospective study in Japan. The 63th Annual Meeting of the American

Association for the Study of Liver Disease (AASLD), Boston, USA, November 9-13, 2012.

37.   2012   Hasegawa K, Makuuchi M, Kokudo N, Izumi N, Ichida T, **Kudo M**, Ku Y, Sakamoto M, Nakashima O, Matsui O, Matsuyama Y: Surgical resection for lymph node metastasis from hepatocellular carcinoma: a report of the Japanese nationwide survey. The 63th Annual Meeting of the American Association for the Study of Liver Disease (AASLD), Boston, USA, November 9-13, 2012.

38.   2012   Schwartz M, Sherman M, Colombo M, Roberts L, Degos F, Chen PJ, Chen M, Park JW, **Kudo M**, Johnson P, Huang B, Orsini LS: Observations of hepatocellular carcinoma(HCC) management patterns from the global HCC BRIDGE study: global comparison of outcomes by locoregional therapy. The 63th Annual Meeting of the American Association for the Study of Liver Disease (AASLD), Boston, USA, November 9-13, 2012.

39.   2012   Bronowicki JP, Ye SL, **Kudo M**, Marrero J, Venook A, Nakajima K, Lencioni R: GIDEON (Global Investigation of therapeutic DEcisions in hepatocellular carcinoma and Of its treatment with SoraeNib) second interim analysis: subgoup analysis by disease aetiology. The 63th Annual Meeting of the American Association for the Study of Liver Disease (AASLD), Boston, USA, November 9-13, 2012.

40.   2012   Sasaki K, **Kudo M**, Sengupta S, Murakami T: Feasibility study of iron density quantification in liver with single source dual energy CT with first kVp switching. 98th Scientific Assembly and Annual Meeting (RSNA 2012), Chicago, USA, November 25-30, 2012.

41.   2012   **Kudo M**, Hyodo T, Yamada K, Sengupta S, Murakami T: Can virtual monochromatic image with dual-energy CT correct beam hardening effect and reduce contrast agent? Phantom experiment. 98th Scientific Assembly and Annual Meeting (RSNA 2012), Chicago, USA, November 25-30, 2012.

42. 2012 Okada M, Murakami T, Numata K, <u>Kudo M</u>, Zech CJ, Nakano M: How to use liver imaging reporting and data system(LI-RADS) in patients with hepatocellular carcinoma(HCC). 98th Scientific Assembly and Annual Meeting (RSNA 2012), Chicago, USA, November 25-30, 2012.

43. 2012 Imai H, Kitano M, Kadosaka K, Kamata K, Miyata T, Sakamoto H, <u>Kudo M</u>: Utility of EUS-guided gallbladder drainage for rescue treatment of malignant biliary obstruction. Asian Pacific Digestive Week (APDW) 2012, Bangkok, Thailand, December 5-8, 2012.

44. 2012 Sakamoto H, Kitano M, Imai H, Kamata K, Miyata T, Kadosaka K, <u>Kudo M</u>: Diffrential diagnosis of SMT and evaluation of malignant potentioal gists by contrast enhanced harmonic EUS. Asian Pacific Digestive Week (APDW) 2012, Bangkok, Thailand, December 5-8, 2012.

45. 2012 Sakamoto H, Kitano M, Imai H, Kamata K, Miyata T, Kadosaka K, <u>Kudo M</u>: A prospective feasibility study on EUS guided broad plexus neurolysis in combination with celiac ganglion neurolysis. Asian Pacific Digestive Week (APDW) 2012, Bangkok, Thailand, December 5-8, 2012.

46. 2012 Sakamoto H, Kitano M, Imai H, Miyata T, Kamata K, Kadosaka K, <u>Kudo M</u>: Trans-catheter endoscopy for pancreaticobiliary duct diseases. Asian Pacific Digestive Week (APDW) 2012, Bangkok, Thailand, December 5-8, 2012.

47. 2012 Kashida H, Sakurai T, Asakuma Y, Kawasaki M, Nagata Y, Nagai T, Takayama M, Mine H, Adachi T, Matsui S, <u>Kudo M</u>: Endoscopic submucosal dissection for the colorectum: usefulness and feasibility. Asian Pacific Digestive Week (APDW) 2012, Bangkok, Thailand, December 5-8, 2012.

48. 2012 Nagai N, Ueshima K, Hayaishi S, Takita M, Kitai S, Yada N, Inoue T, Hagiwara S, Minami Y, Nishida N, <u>Kudo M</u>: The retrospective study of novel anticancer agent, miriplatin

in TACE and TAI for unresectable hepatocellular carcinoma in Japan. Asian Pacific Digestive Week (APDW) 2012, Bangkok, Thailand, December 5-8, 2012.

49.　2012　Matsui S, Kashida H, Kawasaki M, Asakuma Y, Sakurai T, **Kudo M**: The clinical characteristics and endscopic treatment of duodenal varices. Asian Pacific Digestive Week (APDW) 2012, Bangkok, Thailand, December 5-8, 2012.

50.　2012　Nagai T, Adachi T, Takayama M, Mine H, Nagata Y, Kawasaki M, Asakuma Y, Sakurai T, Matsui S, Shiomi M, Kashida H, **Kudo M**: Albumin levels can be a predictive factor for the short-term complications after percutaneous endoscopic gastrostomy in retrospective study. Asian Pacific Digestive Week (APDW) 2012, Bangkok, Thailand, December 5-8, 2012.

51.　2012　Takayama M, Matsui S, Kawasaki M, Asakuma Y, Kashida H, **Kudo M**: A prospective randomized controlled study of a rebamipid monotherapy in the treatment of endoscopic submucosal dissection (ESD)-induced ulcers. Asian Pacific Digestive Week (APDW) 2012, Bangkok, Thailand, December 5-8, 2012.

52.　2012　Adachi T, Matsui S, Takayama M, Kawasaki M, Asakuma Y, Sakurai T, Kashida H, **Kudo M**: Comparison of different proton pump inhibitors (PPI)in helicobacter pylori eradication. Asian Pacific Digestive Week (APDW) 2012, Bangkok, Thailand, December 5-8, 2012.

IX．学会発表

（国内シンポジウム・パネルディスカッション・ワークショップ）

1. 2012 犬塚　義，木村　達，大﨑往夫，<u>工藤正俊</u>：ペグインターフェロンα-2b・エンテカビル 48 週間併用療法の治療成績．　ワークショップ「ウイルス肝炎治療の新たな展開」，日本消化器病学会近畿支部第 96 回例会，平成 24 年 1 月 28 日，大阪国際交流センター，大阪．

2. 2012 津田泰宏，樋口和秀，西口修平，<u>工藤正俊</u>：PEG-IFN α2a/RBV 併用療法における Response-Guided Therapy と IL28B 多型との関連性の検討：ReGIT-J study．　ワークショップ「ウイルス肝炎治療の新たな展開」，日本消化器病学会近畿支部第 96 回例会，平成 24 年 1 月 28 日，大阪国際交流センター，大阪．

3. 2012 大本俊介，松井繁長，足立哲平，川崎正憲，高山政樹，峯　宏昌，永井知行，永田嘉昭，朝隈　豊，櫻井俊治，樫田博史，<u>工藤正俊</u>：プロトンポンプ阻害薬内服中 GERD 患者における GerdQ の有用性．　Young Investigator Session「食道」，日本消化器病学会近畿支部第 96 回例会，平成 24 年 1 月 28 日，大阪国際交流センター，大阪．

4. 2012 今井　元，北野雅之，<u>工藤正俊</u>：当院における悪性胃十二指腸狭窄に対する消化管ステントの成績．　シンポジウム「手術不能進行癌に対する集学的治療の現況と新たな展開（消化管）」，日本消化器病学会近畿支部第 96 回例会，平成 24 年 1 月 28 日，大阪国際交流センター，大阪．

5. 2012 谷浦允厚，安達　融，河野匡志，松本　望，高場雄久，奥村直己，山本典雄，冨田崇文，梅原康湖，森村正嗣，米田　円，山田哲，辻　直子，亀井敬子，北野義徳，田中　晃，落合　健，前倉俊治，南　康範，<u>工藤正俊</u>：成人腸重積で発症した盲腸癌の 1 例．Freshman Session「消化管」，日本消化器病学会近畿支部第 96 回例会，平成 24 年 1 月 28 日，大阪国際交流センター，大阪．

6. 2012 　　　玉田博之，秦　康倫，木下大輔，奥田英之，茂山朋広，宮部欽生，豊澤昌子，岸谷　譲，川崎俊彦，工藤正俊，佐藤克明，木谷光太郎，井上雅智，太田善夫：虫垂粘液嚢胞腺腫の１例．Freshman Session「消化管」，日本消化器病学会近畿支部第96回例会，平成24年1月28日，大阪国際交流センター，大阪．

7. 2012 　　　和田翔太，宮部欽生，木下大輔，秦　康倫，奥田英之，茂山朋広，豊澤昌子，岸谷　譲，川崎俊彦，工藤正俊：微小膵癌との鑑別を要した自己免疫性膵炎の１例．Freshman Session「肝胆膵」，日本消化器病学会近畿支部第96回例会，平成24年1月28日，大阪国際交流センター，大阪．

8. 2012 　　　安達　融，谷浦允厚，河野匡志，松本　望，高場雄久，奥村直己，山本典雄，冨田崇文，梅原康湖，森村正嗣，米田　円，山田哲，辻　直子，野口周也，大野恭裕，落合　健，前倉俊治，南康範，工藤正俊：糖尿病に対しインスリン導入後早期に発症した腫瘤形成性膵炎の１例．Freshman Session「肝胆膵」，日本消化器病学会近畿支部第96回例会，平成24年1月28日，大阪国際交流センター，大阪．

9. 2012 　平木洋子，早石宗右，川崎正憲，朝隈　豊，南　康範，松井繁長，工藤正俊：脾仮性動脈瘤の胃内穿破に対してIVRによる止血が有用であった一例．Freshman Session「肝胆膵」，日本消化器病学会近畿支部第96回例会，平成24年1月28日，大阪国際交流センター，大阪．

10. 2012 　櫻井俊治，松井繁長，工藤正俊：内視鏡治療における高齢者の特殊性．シンポジウム「高齢者における内視鏡治療の適応と限界（消化管）」，第88回日本消化器内視鏡学会近畿地方会，平成24年3月17日，大阪国際交流センター，大阪．

11. 2012 　門阪薫平，北野雅之，工藤正俊：当院におけるEUS下複合神経叢溶解術の適応と限界．ワークショップ「EUSによる消化器疾患の診断と治療の進歩」，第88回日本消化器内視鏡学会近畿地方会，平成24年3月17日，大阪国際交流センター，大阪．

12. 2012 　高場雄久，松本　望，奥村直己，山本典雄，冨田崇文，梅原康湖，森村正嗣，米田　円，山田　哲，辻　直子，南　康範，工藤正俊：

リセドロネートによると考えられた十二指腸潰瘍の一例．Fresh Endoscopist Session，第 88 回日本消化器内視鏡学会近畿地方会，平成 24 年 3 月 17 日，大阪国際交流センター，大阪．

13. 2012 一木美穂，奥田英之，宮部欽生，茂山朋広，豊澤昌子，秦　康倫，木下大輔，川崎俊彦，太田善夫，工藤正俊：貧血を契機に発見された腸間膜静脈硬化症の一例．Fresh Endoscopist Session，第 88 回日本消化器内視鏡学会近畿地方会，平成 24 年 3 月 17 日，大阪国際交流センター，大阪．

14. 2012 　田中梨絵，峯　宏昌，大本俊介，足立哲平，高山政樹，永田嘉昭，永井知行，川崎正憲，朝隈　豊，櫻井俊治，松井繁長，樫田博史，工藤正俊：難治性潰瘍性大腸炎に対して IFX が奏功した症例．Fresh Endoscopist Session，第 88 回日本消化器内視鏡学会近畿地方会，平成 24 年 3 月 17 日，大阪国際交流センター，大阪．

15. 2012 　大本俊介，足立哲平，高山政樹，峯　宏昌，永田嘉昭，永井知行，川崎正憲，朝隈　豊，櫻井俊治，松井繁長，樫田博史，工藤正俊：シングルバルーン小腸内視鏡検査（SBE）にて診断された小腸血管性病変の検討．Young Endoscopist Session，第 88 回日本消化器内視鏡学会近畿地方会，平成 24 年 3 月 17 日，大阪国際交流センター，大阪．

16. 2012 　木下大輔，秦　康倫，奥田英之，茂山朋広，宮部欽生，豊澤昌子，岸谷　譲，川崎俊彦，工藤正俊：Lemmel 症候群の 1 例．Young Endoscopist Session，第 88 回日本消化器内視鏡学会近畿地方会，平成 24 年 3 月 17 日，大阪国際交流センター，大阪．

17. 2012 宮田　剛，北野雅之，工藤正俊：当院における Stage I 膵癌の特徴．シンポジウム 5「膵胆道癌の早期診断」，第 98 回日本消化器病学会総会，京王プラザ，平成 24 年 4 月 19 日-21 日．

18. 2012 矢田典久，萩原　智，工藤正俊：超音波エラストグラフィーによる非アルコール性脂肪性肝炎診断．シンポジウム 8「臓器線維化（肝・膵を中心）研究・診療の最前線」，第 98 回日本消化器病学会総会，京王プラザ，平成 24 年 4 月 19 日-21 日．

19. 2012 門阪薫平，北野雅之，工藤正俊：EUS による早期慢性膵炎の各画像

所見と臨床症状の検討．ワークショップ5「生活習慣と肝・胆・膵疾患」，第98回日本消化器病学会総会，京王プラザ，平成24年4月19日-21日．

20. 2012 鎌田　研，北野雅之，<u>工藤正俊</u>：限局性腫瘤を形成した自己免疫性膵炎におけるEUS所見の検討．ワークショップ10「IgG4関連肝胆膵疾患の診断と治療−非典型例へのアプローチ」，第98回日本消化器病学会総会，京王プラザ，平成24年4月19日-21日．

21. 2012 坂本洋城，北野雅之，<u>工藤正俊</u>：造影ハーモニックEUSによるSMTの鑑別診断およびGISTの悪性度評価．　ワークショップ6「上部消化管粘膜下腫瘍の内視鏡による診断と治療」，第83回日本消化器内視鏡学会総会，平成24年5月12日-14日，グランドプリンスホテル新高輪，東京．

22. 2012 坂本洋城，北野雅之，<u>工藤正俊</u>：当院におけるEUS下複合神経叢融解術の適応と限界．シンポジウム4「EUSガイド下治療の適応と限界」，第83回日本消化器内視鏡学会総会，平成24年5月12日-14日，グランドプリンスホテル新高輪，東京．

23. 2012 鎌田　研，北野雅之，<u>工藤正俊</u>：胆石性膵炎の診断・治療におけるEUSの役割．シンポジウム1「胆・膵疾患の救急医療の現状と治療戦略」，第83回日本消化器内視鏡学会総会，平成24年5月12日-14日，グランドプリンスホテル新高輪，東京．

24. 2012 松井繁長，朝隈　豊，<u>工藤正俊</u>：噴門部静脈瘤合併巨大型食道静脈瘤の内視鏡的治療の工夫．シンポジウム11「危ない静脈瘤出血の病態と治療」，第83回日本消化器内視鏡学会総会，平成24年5月12日-14日，グランドプリンスホテル新高輪，東京．

25. 2012 宮田　剛，北野雅之，<u>工藤正俊</u>：EUSガイド下治療におけるトラブルシューティング．VTRシンポジウム1「内視鏡治療に伴う偶発症の対処法−胆膵病変−」，第83回日本消化器内視鏡学会総会，平成24年5月12日-14日，グランドプリンスホテル新高輪，東京．

26. 2012 今井　元，北野雅之，<u>工藤正俊</u>：当院でのEUS下胆管ドレナージ術の安全性の検討．VTRシンポジウム6「安全かつ効果的な胆道Stentingを求めて」，第83回日本消化器内視鏡学会総会，平成24

年 5 月 12 日-14 日，グランドプリンスホテル新高輪，東京.

27. 2012 門阪薫平，北野雅之，工藤正俊：EUS による早期慢性膵炎の画像
所見と臨床症状との関連性の検討．パネルディスカッション 5「慢
性膵炎の内視鏡診断と治療」，第 83 回日本消化器内視鏡学会総会，
平成 24 年 5 月 12 日-14 日，グランドプリンスホテル新高輪，東京.

28. 2012 松井繁長，川崎正憲，工藤正俊：十二指腸静脈瘤の臨床的特徴と
治療指針．ワークショップ 3「異所性静脈瘤の病態と治療指針」，
第 83 回日本消化器内視鏡学会総会，平成 24 年 5 月 12 日-14 日，グ
ランドプリンスホテル新高輪，東京.

29. 2012 鎌田　研，北野雅之，工藤正俊：IPMN の診断・フォローアップに
おける EUS の役割．ワークショップ 9「IPMN の診断・治療における
内視鏡の役割」，第 83 回日本消化器内視鏡学会総会，平成 24 年 5
月 12 日-14 日，グランドプリンスホテル新高輪，東京.

30. 2012 工藤正俊：シンポジウム「今後の超音波医学の発展のために」，パ
ネリスト；工藤正俊，椎名　毅，竹中　克，日本超音波医学会第
85 回学術集会，平成 24 年 5 月 25 日-27 日，グランドプリンスホテ
ル新高輪，東京.

31. 2012 矢田典久，工藤正俊：肝領域における組織弾性評価法：「硬さ」と
「粗さ」の違い．シンポジウム 6「組織弾性評価の手法と用語の標
準化に向けて」，第 83 回日本消化器内視鏡学会総会，日本超音波
医学会第 85 回学術集会，平成 24 年 5 月 25 日-27 日，グランドプ
リンスホテル新高輪，東京.

32. 2012 小谷敦志，久保田義則，谷口京子，河野ふみえ，前川　清，中江
健市，保田知生，工藤正俊：下肢静脈超音波検査における仰臥位
での下腿深部静脈血栓症診断の検討．ワークショップ 14「静脈エ
コーで何処まで観るか？：目的別にみた検査法の工夫」，日本超音
波医学会第 85 回学術集会，平成 24 年 5 月 25 日-27 日，グランド
プリンスホテル新高輪，東京.

33. 2012 宮田　剛，北野雅之，工藤正俊：造影ハーモニック EUS（CH-EUS）
を用いた腹部リンパ節の良悪性診断の試み．ワークショップ 1「超
音波内視鏡の進歩-診断と治療への応用-」，日本超音波医学会第

85回学術集会，平成24年5月25日-27日，グランドプリンスホテル新高輪，東京．

34. 2012 矢田典久，工藤正俊：超音波エラストグラフィーによる非アルコール性脂肪性肝炎診断．ワークショップ6「消化器疾患診療における超音波Elastographyの有用性」，日本超音波医学会第85回学術集会，平成24年5月25日-27日，グランドプリンスホテル新高輪，東京．

35. 2012 工藤正俊：肝細胞癌の化学療法．シンポジウム3「肝細胞癌の治療戦略」，第48回日本肝臓学会総会，平成24年6月7-8日，石川県立音楽堂，金沢．

36. 2012 早石宗右，南　康範，工藤正俊：造影エコーによる肝癌肉眼分類の有用性について．パネルディスカッション「肝細胞癌画像診断の進歩」，第48回日本肝臓学会総会，平成24年6月7-8日，石川県立音楽堂，金沢．

37. 2012 矢田典久，工藤正俊：Real-time Tissue Elastographyによる非アルコール性脂肪性肝炎の囲い込み．ワークショップ2「肝疾患における画像診断の課題と新たな展開」，第48回日本肝臓学会総会，平成24年6月7-8日，石川県立音楽堂，金沢．

38. 2012 上嶋一臣，南　康範，工藤正俊：肝癌診療ガイドラインにおける治療アルゴリズムの妥当性〜実臨床への展開とその問題点〜．ワークショップ12「肝癌診療ガイドラインの活用と改訂への提案」，第48回日本肝臓学会総会，平成24年6月7-8日，ANAクラウンプラザホテル金沢，金沢．

39. 2012 奥坂拓志，工藤正俊，池田公史，高山忠利，沼田和司，泉　並木，國土典宏，古瀬　純司，角谷眞澄，木村丹香子：国際共同非介入試験GEDEON第2回中間解析における日本人集団解析結果ならびに投与開始時AFP値での層別解析の検討．ワークショップ13「肝細胞癌に対する分子標的薬開発の基礎から臨床」，第48回日本肝臓学会総会，平成24年6月7-8日，ANAクラウンプラザホテル金沢，金沢．

40. 2012 萩原　智，工藤正俊，大﨑往夫：Drug freeを目指したエンテカビ

ルと PEG-IFNα2b 48 週併用療法の効果について．ワークショップ
22「B 型慢性肝炎に対する抗ウイルス療法の継続と終了をめぐっ
て」，第 48 回日本肝臓学会総会，平成 24 年 6 月 7-8 日，ポルテ金
沢，金沢．

41. 2012　上嶋一臣，有住忠晃，早石宗右，田北雅弘，北井　聡，矢田典久，
井上達夫，萩原　智，南　康範，櫻井俊治，西田直生志，工藤正
俊：当院における肝細胞癌分子標的治療の現状．パネルディスカ
ッション「ソラフェニブ治療の実践－多数症例の使用経験を踏まえ
た治療の実践と問題点の解決を示す―」，平成 24 年 6 月 16 日，第
6 回日本肝がん分子標的治療研究会，ザ・プリンス箱根，神奈川．

42. 2012　宮田　剛，北野雅之，竹山宜典，工藤正俊：膵切除後合併症に対
する EUS ガイド下治療の有用性．シンポジウム 5「膵切除の合併症
とその対処法」，第 43 回日本膵臓学会大会，平成 24 年 6 月 28-29
日，ホテルメトロポリタン山形，山形．

43. 2012　坂本洋城，北野雅之，竹山宜典，安田武生，中居卓也，工藤正俊：
膵上皮内癌と StageⅠ膵癌の臨床的および病理学的特徴．シンポ
ジウム 6「膵癌の早期診断と病理」，第 43 回日本膵臓学会大会，平
成 24 年 6 月 28-29 日，ホテルメトロポリタン山形，山形．

44. 2012　今井康陽，兵頭朋子，岡田真広，小来田幸世，工藤正俊，村上卓
道：High risk nodule の自然経過と多血化因子．シンポジウム 1
「肝癌診療における Gd-EOB-DTPA 造影 MRI の役割」，第 48 回日本
肝癌研究会，平成 24 年 7 月 20-21 日，石川県立音楽堂，石川．

45. 2012　高山忠利，池田公史，沼田和司，泉　並木，國土典宏，古瀬純司，
奥坂拓志，角谷眞澄，伊藤雄一郎，工藤正俊：Sorafenib 国際試験
GIDEON の中間析:TACE 施行歴による層別解析．パネルディスカッ
ション 4「肝細胞癌分子標的治療：現状と問題点」，第 48 回日本
肝癌研究会，平成 24 年 7 月 20-21 日，石川県立音楽堂，石川．

46. 2012　喜多竜一，那須章洋，木村　達，大﨑往夫，依田　広，恵荘裕嗣，
千葉　勉，西田直生志，工藤正俊：多発性の限局性結節性過形成
（FNH）および FNH 様結節に関する検討．ワークショップ 2「肝癌
類似病変診断の新しい展開：肝細胞腺腫と FNH を中心に」，第 48
回日本肝癌研究会，平成 24 年 7 月 20-21 日，ANA クラウンプラザ

ホテル金沢，石川.

47. 2012 宮田　剛，北野雅之，工藤正俊：当院における進行膵癌の癌性疼痛に対する治療戦略．シンポジウム 2「進行膵癌に対する治療戦略の現状と展望」，日本消化器病学会近畿支部第 97 回例会，平成 24 年 9 月 1 日，京都テルサ，京都.

48. 2012 鎌田　研，北野雅之，工藤正俊：EUS 下胆道ドレナージ術の工夫．ビデオワークショップ「胆道疾患内視鏡治療困難例に対する手技の工夫」，第 48 回日本胆道学会学術集会，平成 24 年 9 月 20-21 日，京王プラザホテル，東京.

49. 2012 坂本洋城，北野雅之，工藤正俊：癌性疼痛に対する EUS 下腹腔内神経叢/節ブロック術のストラテジー．シンポジウム 16「胆膵疾患に対する therapeutic EUS の現状（EUS-FNA を除く）」，第 20 回日本消化器関連学会週間 JDDW2012（第 16 回日本肝臓学会大会・第 54 回日本消化器病学会大会・第 84 回日本消化器内視鏡学会総会・第 10 回日本消化器外科学会大会・第 50 回日本消化器がん検診学会大会・第 43 回日本消化器吸収学会総会合同），平成 24 年 10 月 10 日-13 日，神戸国際会議場，兵庫.

50. 2012 鎌田　研，北野雅之，工藤正俊：膵癌診断ストラテジーと各画像検査の比較検討．パネルディスカッション 2「超音波検査発見胆膵病変の精密検査のストラテジー」，第 20 回日本消化器関連学会週間 JDDW2012（第 16 回日本肝臓学会大会・第 54 回日本消化器病学会大会・第 84 回日本消化器内視鏡学会総会・第 10 回日本消化器外科学会大会・第 50 回日本消化器がん検診学会大会・第 43 回日本消化器吸収学会総会合同），平成 24 年 10 月 10 日-13 日，神戸国際展示場，兵庫.

51. 2012 宮田　剛，北野雅之，工藤正俊：Stage0/I 膵癌の臨床的特徴．パネルディスカッション 4「膵癌早期発見に向けた取組み」，第 20 回日本消化器関連学会週間 JDDW2012（第 16 回日本肝臓学会大会・第 54 回日本消化器病学会大会・第 84 回日本消化器内視鏡学会総会・第 10 回日本消化器外科学会大会・第 50 回日本消化器がん検診学会大会・第 43 回日本消化器吸収学会総会合同），平成 24 年 10 月 10 日-13 日，ポートピアホテル南館，兵庫.

52. 2012 西田直生志，工藤正俊：肝発癌における酸化ストレスとエピゲノム変異．パネルディスカッション 5「消化器癌と酸化ストレス」，第 20 回日本消化器関連学会週間 JDDW2012（第 16 回日本肝臓学会大会・第 54 回日本消化器病学会大会・第 84 回日本消化器内視鏡学会総会・第 10 回日本消化器外科学会大会・第 50 回日本消化器がん検診学会大会・第 43 回日本消化器吸収学会総会合同），平成 24 年 10 月 10 日-13 日，ポートピアホテル，兵庫．

53. 2012 門阪薫平，北野雅之，工藤正俊：ADL 不良の急性胆嚢炎および胆管炎例に対する EUS ドレナージ術．パネルディスカッション 26「75 歳以上における腹腔鏡下胆嚢摘出術の安全性の検討」，第 20 回日本消化器関連学会週間 JDDW2012（第 16 回日本肝臓学会大会・第 54 回日本消化器病学会大会・第 84 回日本消化器内視鏡学会総会・第 10 回日本消化器外科学会大会・第 50 回日本消化器がん検診学会大会・第 43 回日本消化器吸収学会総会合同），平成 24 年 10 月 10 日-13 日，神戸国際会議場，兵庫．

54. 2012 西田直生志，工藤正俊：肝癌の遺伝子変化および背景肝組織の男女差に関する検討．ワークショップ 7「消化器疾患と性差」，第 20 回日本消化器関連学会週間 JDDW2012（第 16 回日本肝臓学会大会・第 54 回日本消化器病学会大会・第 84 回日本消化器内視鏡学会総会・第 10 回日本消化器外科学会大会・第 50 回日本消化器がん検診学会大会・第 43 回日本消化器吸収学会総会合同），平成 24 年 10 月 10 日-13 日，神戸国際会議場，兵庫．

55. 2012 矢田典久，藤本研治，工藤正俊：Support Vector Machine を用いた Real-time Tissue Elastograhy による F Stage 推定値．ワークショップ 11「低侵襲な肝疾患診断法の進歩」，第 20 回日本消化器関連学会週間 JDDW2012（第 16 回日本肝臓学会大会・第 54 回日本消化器病学会大会・第 84 回日本消化器内視鏡学会総会・第 10 回日本消化器外科学会大会・第 50 回日本消化器がん検診学会大会・第 43 回日本消化器吸収学会総会合同），平成 24 年 10 月 10 日-13 日，ポートピアホテル，兵庫．

56. 2012 永井知行，樫田博史，工藤正俊：当院での EMR の工夫．ビデオワークショップ 2「下部消化管：大腸内視鏡挿入法と EMR の基本と工夫」，日本消化器内視鏡学会近畿支部第 89 回支部例会，平成 24 年 11 月 10 日，大阪国際交流センター，大阪．

X．学会発表（国内一般演題）

1. 2012 早石宗右，南　康範，畑中絹世，有住忠晃，田北雅弘，北井聡，矢田典久，井上達夫，萩原　智，西田直生志，<u>工藤正俊</u>：造影エコーによる肝癌肉眼分類の有用性について．　日本消化器病学会近畿支部第 96 回例会，平成 24 年 1 月 28 日，大阪国際交流センター，大阪．

2. 2012 南　康範，有住忠晃，早石宗右，田北雅弘，北井　聡，矢田典久，井上達夫，萩原　智，上嶋一臣，<u>工藤正俊</u>，柳生行伸，村上卓道：Interventional radiology における新しい支援画像「FlightPlan」の初期臨床経験．　第 18 回肝血流動態イメージ研究会，平成 24 年 1 月 28 日－29 日，神戸ポートピアホテル，兵庫．

3. 2012 早石宗右，南　康範，畑中絹世，有住忠晃，田北雅弘，北井聡，矢田典久，井上達夫，萩原　智，上嶋一臣，西田直生志，<u>工藤正俊</u>：造影エコーによる肝癌肉眼分類の有用性について．第 18 回肝血流動態イメージ研究会，平成 24 年 1 月 28 日－29 日，神戸ポートピアホテル，兵庫．

4. 2012 矢田典久，萩原　智，<u>工藤正俊</u>：超音波エラストグラフィーによる非アルコール性脂肪性肝炎診断．　第 18 回肝血流動態イメージ研究会，平成 24 年 1 月 28 日－29 日，神戸ポートピアホテル，兵庫．

5. 2012 有住忠晃，上嶋一臣，竹田治彦，大﨑往夫，早石宗右，田北雅弘，北井　聡，矢田典久，井上達夫，萩原　智，南　康範，櫻井俊治，西田直生志，<u>工藤正俊</u>：進行肝細胞癌患者に対する分子標的薬（ソラフェニブ）投与における治療効果判定基準の比較．　第 18 回肝血流動態イメージ研究会，平成 24 年 1 月 28 日－29 日，神戸ポートピアホテル，兵庫．

6. 2012 小川　力，大原芳章，宮本由貴子，柴峠光成，山岡竜也，廣瀬哲朗，西平友彦，嶋田俊秀，荻野哲朗，河合直之，<u>工藤正俊</u>：CE-US、CT-Angio、EOB-MRI と病理の比較～術前診断が 2cm 以下の肝切除症例～．　第 18 回肝血流動態イメージ研究会，平成 24

年 1 月 28 日－29 日，神戸ポートピアホテル，兵庫．

7.　　2012　　高山政樹，川崎正憲，峯　宏昌，永田嘉昭，永井知行，朝隈
　　　　　　　　豊，櫻井俊治，松井繁長，樫田博史，<u>工藤正俊</u>：シングルバル
　　　　　　　　ーン小腸内視鏡検査にて診断された小腸血管性病変の検討．
　　　　　　　　第 8 回日本消化管学会総会学術集会，平成 24 年 2 月 10 日-11
　　　　　　　　日，仙台国際センター，宮城．

8.　　2012　　大本俊介，松井繁長，足立哲平，峯　宏昌，高山政樹，永井知
　　　　　　　　行，永田嘉昭，川崎正憲，櫻井俊治，樫田博史，<u>工藤正俊</u>：プ
　　　　　　　　ロトンポンプ阻害薬（PPI）内服中 GERD 患者に対する GerdQ に
　　　　　　　　よる治療効果の評価．第 98 回日本消化器病学会総会，京王プラ
　　　　　　　　ザ，平成 24 年 4 月 19 日-21 日．

9.　　2012　　足立哲平，有住忠晃，早石宗右，田北雅弘，北井　聡，矢田典
　　　　　　　　久，井上達夫，萩原　智，南　康範，櫻井俊治，上嶋一臣，西
　　　　　　　　田直生志，<u>工藤正俊</u>：非上皮性肝悪性腫瘍の 3 例．第 98 回日本
　　　　　　　　消化器病学会総会，京王プラザ，平成 24 年 4 月 19 日-21 日．

10.　　2012　　早石宗右，南　康範，足立哲平，有住忠晃，田北雅弘，北井
　　　　　　　　聡，矢田典久，井上達夫，萩原　智，上嶋一臣，<u>工藤正俊</u>，鄭
　　　　　　　　浩柄：経皮的ラジオ波焼灼術後の後出血予防における穿刺経路
　　　　　　　　焼灼の有効性の検討．第 98 回日本消化器病学会総会，京王プラ
　　　　　　　　ザ，平成 24 年 4 月 19 日-21 日．

11.　　2012　　朝隈　豊，松井繁長，足立哲平，大本俊介，高山政樹，永田嘉
　　　　　　　　昭，川崎正憲，櫻井俊治，樫田博史，<u>工藤正俊</u>：当院における
　　　　　　　　表在型パレット食道腺癌に対する内視鏡的診断と治療の検討．
　　　　　　　　第 83 回日本消化器内視鏡学会総会，平成 24 年 5 月 12 日-14 日，
　　　　　　　　グランドプリンスホテル新高輪，東京．

12.　　2012　　門阪薫平，北野雅之，<u>工藤正俊</u>：早期慢性膵炎における EUS 画
　　　　　　　　像の臨床的意義．日本超音波医学会第 85 回学術集会，平成 24
　　　　　　　　年 5 月 25 日-27 日，グランドプリンスホテル新高輪，東京．

13.　　2012　　今井　元，北野雅之，<u>工藤正俊</u>：当院における EUS 下胆道ドレ
　　　　　　　　ナージ術の有用性．日本超音波医学会第 85 回学術集会，平成
　　　　　　　　24 年 5 月 25 日-27 日，グランドプリンスホテル新高輪，東京．

14. 2012 前野知子，横川美加，辻　裕美子，塩見香織，前川　清，井上達夫，南　康範，工藤正俊: ソナゾイド造影超音波による肝血管腫の診断についての検討．日本超音波医学会第85回学術集会，平成24年5月25日-27日，グランドプリンスホテル新高輪，東京．

15. 2012 前川　清，横川美加，辻　裕美子，前野知子，塩見香織，井上達夫，南　康範，工藤正俊: ソナゾイド造影超音波における AP Shunt の診断について．日本超音波医学会第85回学術集会，平成24年5月25日-27日，グランドプリンスホテル新高輪，東京．

16. 2012 有住忠晃，上嶋一臣，工藤正俊: 進行肝細胞癌に対するソラフェニブ投与における投与後の腫瘍濃染の低下の有無と生存期間の検討．第48回日本肝臓学会総会，平成24年6月7-8日，石川県立音楽堂，金沢．

17. 2012 早石宗右，南　康範，工藤正俊: 経皮的ラジオ波焼灼術後の後出血予防における穿刺経路焼灼の有効性の検討．第48回日本肝臓学会総会，平成24年6月7-8日，石川県立音楽堂，金沢．

18. 2012 小川　力，紫峠光成，工藤正俊: 外科切除標本からの 2cm 以下の HCC に対する CE-US，動注 CT，EOB-MRI の術前診断の比較，検討．第48回日本肝臓学会総会，平成24年6月7-8日，JR 金沢駅前もてなしドーム，金沢．

19. 2012 南　康範，工藤正俊: Interventional radiology における新しい支援画像「FlightPlan」の有用性．第48回日本肝臓学会総会，平成24年6月7-8日，JR 金沢駅前もてなしドーム，金沢．

20. 2012 田北雅弘，萩原　智，有住忠晃，早石宗右，上田泰輔，北井聡，矢田典久，井上達夫，南　康範，鄭　浩柄，上嶋一臣，櫻井俊治，西田直生志，工藤正俊: IL28B と PEG-IFN/RBV 併用療法をうけた HCV ジェノタイプ 1 型高ウイルス量患者の効果との関連について．48回日本肝臓学会総会，平成24年6月7-8日，JR 金沢駅前もてなしドーム，金沢．

21.　2012　門阪薫平，北野雅之，竹山宜典，工藤正俊：早期慢性膵炎の EUS 画像と臨床所見の比較検討．第 43 回日本膵臓学会大会，平成 24 年 6 月 28-29 日，ホテルメトロポリタン山形，山形．

22.　2012　今井　元，北野雅之，工藤正俊，門阪薫平，宮田　剛，鎌田　研，坂本洋城，安田武生，竹山宜典：膵神経内分泌腫瘍診断における EUS の有用性．第 43 回日本膵臓学会大会，平成 24 年 6 月 28-29 日，ホテルメトロポリタン山形，山形．

23.　2012　兵藤朋子，岡田真広，香川祐毅，任　星雲，柏木伸夫，柳生行伸，今岡いずみ，松木　充，足利竜一郎，石井一成，村上卓道，矢田典久，工藤正俊，前西　修：Dual energy CT を用いた肝脂肪の定量評価-ファントム実験と初期臨床経験．第 71 回近畿大学医学会学術講演会，平成 24 年 7 月 14 日，近畿大学医学部大講堂，大阪狭山．

24.　2012　長谷川　潔，國土典宏，幕内雅敏，泉　並木，市田隆文，工藤正俊，具　英成，坂本亨宇，中島　收，松井　修，松山　裕：肝細胞癌に対する肝切除と経皮的局所法の長期成績：全国データに基づく比較検討．第 48 回日本肝癌研究会，平成 24 年 7 月 20-21 日，石川県立音楽堂，石川．

25.　2012　井上達夫，有住忠晃，早石宗右，北井　聡，矢田典久，萩原　智，南　康範，上嶋一臣，西田直生志，工藤正俊：肝細胞癌に対するラジオ波焼灼療法の治療効果判定における造影超音波検査の有用性〜造影 CT との比較〜．第 48 回日本肝癌研究会，平成 24 年 7 月 20-21 日，石川県立音楽堂，石川．

26.　2012　有住忠晃，上嶋一臣，早石宗右，田北雅弘，北井　聡，井上達夫，矢田典久，萩原　智，南　康範，櫻井俊治，西田直生志，工藤正俊：進行肝細胞癌に対するソラフェニブ投与における投与後の腫瘍濃染の低下の有無と生存期間の検討．第 48 回日本肝癌研究会，平成 24 年 7 月 20-21 日，石川県立音楽堂，石川．

27.　2012　兵頭明子，岡田真広，香川祐毅，日高正二朗，任　誠雲，柳生行伸，上嶋一臣，矢田典久，工藤正幸，石井一成，工藤正俊，村上卓道：肝血行動態解析によるソラフェニブ治療効果の早期予測-CT perfusion を用いて．第 48 回日本肝癌研究会，平成 24

年7月20-21日, 石川県立音楽堂, 石川.

28. 2012 小川　力, 森岡弓子, 野田晃世, 上田祐也, 宮本由貴子,　野上明子, 吉岡正博, 石川哲朗, 松中寿浩, 玉置敬之, 芝峠光成, 工藤正俊: ソナゾイド US による nodule in nodule pattern の HCC の診断. 第48回日本肝癌研究会, 平成24年7月20-21日, 石川県立音楽堂, 石川.

29. 2012 南　康範, 有住忠晃, 早石宗右, 田北雅弘, 北井　聡, 矢田典久, 井上達夫, 萩原　智, 上嶋一臣, 西田直生志, 工藤正俊: 転移性肝癌に対する肝動脈塞栓術とラジオ波焼灼術の併用療法の有用性. 第48回日本肝癌研究会, 平成24年7月20-21日, 石川県立音楽堂, 石川.

30. 2012 永井知行, 木村英晴, 荒尾徳三, 松本和子, 藤田至彦, 吉田修平, 林　秀敏, 工藤正俊, 西尾和人: ソラフェニブの上皮間葉移行阻害効果. 第10回日本臨床腫瘍学会学術集会, 平成24年7月26-28日, 大阪国際会議場, 大阪.

31. 2012 高橋一肇, 奥田英之, 秦　康倫, 木下大輔, 茂山朋広, 宮部欽生, 清水昌子, 岸谷　譲, 川崎俊彦, 太田善夫, 工藤正俊: 上腹部痛で発見された低分化型肝癌の一例. 日本消化器病学会近畿支部第97回例会, 平成24年9月1日, 京都テルサ, 京都.

32. 2012 山田光成, 北野雅之, 宮田　剛, 坂本洋城, 門阪薫平, 鎌田研, 今井　元, 工藤正俊: 胆管胆汁細胞診にて診断し得た胆嚢癌の1例. 日本消化器病学会近畿支部第97回例会, 平成24年9月1日, 京都テルサ, 京都.

33. 2012 足立哲平, 高山政樹, 峯　宏昌, 永井知行, 永田嘉昭, 川崎正憲, 朝隈　豊, 櫻井俊治, 松井繁長, 樫田博史, 工藤正俊: 当院における PPI 別ヘリコバクターピロリ菌除菌治療成績の検討. 日本消化器病学会近畿支部第97回例会, 平成24年9月1日, 京都テルサ, 京都.

34. 2012 門阪薫平, 北野雅之, 山田光成, 大本俊介, 鎌田　研, 宮田剛, 今井　元, 坂本洋城, 工藤正俊: 早期慢性膵炎の EUS 所見とその臨床所見について. 日本消化器病学会近畿支部第97回例

会，平成 24 年 9 月 1 日，京都テルサ，京都．

35.　2012　大本俊介，北野雅之，山田光成，　門阪薫平，宮田　剛，鎌田
研，今井　元，坂本洋城，工藤正俊：造影ハーモニック EUS
（CH-EUS）によってのみ存在診断および境界診断が可能であっ
た膵癌の 2 例．日本消化器病学会近畿支部第 97 回例会，平成 24
年 9 月 1 日，京都テルサ，京都．

36.　2012　秦　康倫，木下大輔，奥田英之，茂山朋広，宮部欽生，清水昌
子，岸谷　譲，川崎俊彦，辻江正徳，井上雅智，太田善夫，工
藤正俊：無症候性膵内分泌腫瘍の 1 例．日本消化器病学会近畿
支部第 97 回例会，平成 24 年 9 月 1 日，京都テルサ，京都．

37.　2012　河野匡志，丸山康典，松本　望，高場雄久，奥村直己，冨田崇
文，梅原康湖，谷池聡子，森村正嗣，辻　直子，米田　円，山
田　哲，亀井敬子，田中　晃，落合　健，前倉俊治，南　康範，
工藤正俊：1 年以上の下痢、下血で受診した腸重積合併 1 型 S
状結腸癌による成人型腸重積の 1 例．日本消化器病学会近畿支
部第 97 回例会，平成 24 年 9 月 1 日，京都テルサ，京都．

38.　2012　南　知宏，松井繁長，足立哲平，高山政樹，峯　宏昌，永田嘉
昭，永井知行，川崎正憲，朝隈　豊，櫻井俊治，樫田博史，工
藤正俊：著明な蛋白漏出性胃腸症を呈し、ステロイドが奏効し
た Cronkhite-Canada 症候群の一例．日本消化器病学会近畿支部
第 97 回例会，平成 24 年 9 月 1 日，京都テルサ，京都．

39.　2012　田中寛樹，北野雅之，坂本洋城，今井　元，鎌田　研，宮田
剛，門阪薫平，工藤正俊：上部胆管癌との鑑別を要した IgG4 関
連胆管炎．日本消化器病学会近畿支部第 97 回例会，平成 24 年 9
月 1 日，京都テルサ，京都．

40.　2012　宮内正晴，北野雅之，坂本洋城，今井　元，鎌田　研，　宮田
剛，門阪薫平，工藤正俊：巨大胆石が十二指腸球部に穿通し胆
石イレウスを起こした一例．日本消化器病学会近畿支部第 97 回
例会，平成 24 年 9 月 1 日，京都テルサ，京都．

41.　2012　宮田　剛，大本俊介，門阪薫平，鎌田　研，今井　元，坂本洋
城，北野雅之，工藤正俊：当院における Stage1 膵癌の特徴．第

61 回近畿膵疾患談話会，平成 24 年 9 月 29 日，エーザイ株式会社大阪コミュニケーションオフィス，大阪．

42.　2012　今井　元，北野雅之，<u>工藤正俊</u>: EUS 下胆管ドレナージ術の穿刺ルートおよびステント留置法の使い分けと成績．第 20 回日本消化器関連学会週間 JDDW2012（第 16 回日本肝臓学会大会・第 54 回日本消化器病学会大会・第 84 回日本消化器内視鏡学会総会・第 10 回日本消化器外科学会大会・第 50 回日本消化器がん検診学会大会・第 43 回日本消化器吸収学会総会合同），平成 24 年 10 月 10 日-13 日，神戸国際展示場，兵庫．

43.　2012　大本俊介，松井繁長，足立哲平，峯　宏昌，高山政樹，永井知行，永田嘉昭，川崎正憲，朝隈　豊，櫻井俊治，樫田博史，<u>工藤正俊</u>: プロトンポンプ阻害薬（PPI）内服中 GERD 患者に対する GerdQ による治療実態の検討．第 20 回日本消化器関連学会週間 JDDW2012（第 16 回日本肝臓学会大会・第 54 回日本消化器病学会大会・第 84 回日本消化器内視鏡学会総会・第 10 回日本消化器外科学会大会・第 50 回日本消化器がん検診学会大会・第 43 回日本消化器吸収学会総会合同），平成 24 年 10 月 10 日-13 日，神戸国際展示場，兵庫．

44.　2012　奥村　直己，辻　直子，<u>工藤正俊</u>，山本典雄，高場雄久，松本望，冨田崇文，森村正嗣，山田　哲，米田 円，南　康範，丸山康典，河野匡志，梅原康湖: Helicobacter pylori 除菌前後の内視鏡所見の比較検討．第 20 回日本消化器関連学会週間 JDDW2012（第 16 回日本肝臓学会大会・第 54 回日本消化器病学会大会・第 84 回日本消化器内視鏡学会総会・第 10 回日本消化器外科学会大会・第 50 回日本消化器がん検診学会大会・第 43 回日本消化器吸収学会総会合同），平成 24 年 10 月 10 日-13 日，神戸国際展示場，兵庫．

45.　2012　河野匡志，辻　直子，丸山康典，松本　望，高場雄久，奥村直己，山本典雄，冨田崇文，梅原康湖，森村正嗣，米田 円，山田　哲，落合　健，本庶　元，南　康範，<u>工藤正俊</u>: 当院における H. pylori CAM 耐性の年次変化（2001 年～2010 年）．第 20 回日本消化器関連学会週間 JDDW2012（第 16 回日本肝臓学会大会・第 54 回日本消化器病学会大会・第 84 回日本消化器内視鏡学会総会・第 10 回日本消化器外科学会大会・第 50 回日本消

化器がん検診学会大会・第 43 回日本消化器吸収学会総会合同），
平成 24 年 10 月 10 日-13 日，神戸国際展示場，兵庫.

46.　2012　丸山康典，辻　直子，河野匡志，松本　望，高場雄久，奥村直
己，山本典雄，冨田崇文，梅原康湖，森村正嗣，米田　円，山
田　哲，落合　健，本庶　元，南　康範，工藤正俊：当院にお
ける H. pylori 除菌の年次変化（2001 年〜2010 年）．第 20 回日
本消化器関連学会週間 JDDW2012（第 16 回日本肝臓学会大会・第
54 回日本消化器病学会大会・第 84 回日本消化器内視鏡学会総
会・第 10 回日本消化器外科学会大会・第 50 回日本消化器がん
検診学会大会・第 43 回日本消化器吸収学会総会合同），平成 24
年 10 月 10 日-13 日，神戸国際展示場，兵庫.

47.　2012　永田嘉昭，松井繁長，足立哲平，大本俊介，峯　宏昌，　高山
政樹，永井知行，川崎正憲，朝隈　豊，櫻井俊治，樫田博史，
工藤正俊：高齢者に対する早期胃癌 ESD についての検討．第 20
回日本消化器関連学会週間 JDDW2012（第 16 回日本肝臓学会大
会・第 54 回日本消化器病学会大会・第 84 回日本消化器内視鏡
学会総会・第 10 回日本消化器外科学会大会・第 50 回日本消化
器がん検診学会大会・第 43 回日本消化器吸収学会総会合同），平
成 24 年 10 月 10 日-13 日，神戸国際展示場，兵庫.

48.　2012　朝隈　豊，松井繁長，足立哲平，大本俊介，高山政樹，峯　宏
昌，永井知行，永田嘉昭，川崎正憲，櫻井俊治，樫田博史，工
藤正俊：当院における胃 ESD 症例での多発例の検討．第 20 回日
本消化器関連学会週間 JDDW2012（第 16 回日本肝臓学会大会・第
54 回日本消化器病学会大会・第 84 回日本消化器内視鏡学会総
会・第 10 回日本消化器外科学会大会・第 50 回日本消化器がん
検診学会大会・第 43 回日本消化器吸収学会総会合同），平成 24
年 10 月 10 日-13 日，神戸国際展示場，兵庫.

49.　2012　永井知行，大本俊介，高山政樹，峯　宏昌，永田嘉昭，川崎正
憲，朝隈　豊，　櫻井俊治，松井繁長，汐見幹夫，樫田博史，
工藤正俊：経皮内視鏡的胃瘻造設術（PEG）の患者背景と早期合
併症．第 20 回日本消化器関連学会週間 JDDW2012（第 16 回日本
肝臓学会大会・第 54 回日本消化器病学会大会・第 84 回日本消
化器内視鏡学会総会・第 10 回日本消化器外科学会大会・第 50
回日本消化器がん検診学会大会・第 43 回日本消化器吸収学会総

会合同），平成 24 年 10 月 10 日-13 日，神戸国際展示場，兵庫．

50.　　2012　足立哲平，樫田博史，大本俊介，高山政樹，峯　宏昌，永井
知行，　永田嘉昭，川崎正憲，朝隈　豊，　櫻井俊治，松井繁長，
工藤正俊：大腸 ESD 導入時の治療成績に関する検討．第 20 回日
本消化器関連学会週間 JDDW2012（第 16 回日本肝臓学会大会・第
54 回日本消化器病学会大会・第 84 回日本消化器内視鏡学会総
会・第 10 回日本消化器外科学会大会・第 50 回日本消化器がん
検診学会大会・第 43 回日本消化器吸収学会総会合同），平成 24
年 10 月 10 日-13 日，神戸国際展示場，兵庫．

51.　　2012　宮部欽生，木下大輔，秦　康倫，奥田英之，茂山朋広，　清水
昌子，岸谷譲，川崎俊彦，米倉竹夫，工藤正俊：腸管重複症に
対し SB ナイフ Jr を用いて内視鏡的隔壁切除を施行した 1 例．第
20 回日本消化器関連学会週間 JDDW2012（第 16 回日本肝臓学会
大会・第 54 回日本消化器病学会大会・第 84 回日本消化器内視
鏡学会総会・第 10 回日本消化器外科学会大会・第 50 回日本消
化器がん検診学会大会・第 43 回日本消化器吸収学会総会合同），
平成 24 年 10 月 10 日-13 日，神戸国際展示場，兵庫．

52.　　2012　高山政樹，樫田博史，足立哲平，峯　宏昌，永田嘉昭，永井知
行，川崎正憲，朝隈　豊，　櫻井俊治，松井繁長，工藤正俊，
竹山宜典，筑後孝章：シングルバルーン小腸内視鏡検査（SBE）
にて診断し得た小腸癌について．第 20 回日本消化器関連学会週
間 JDDW2012（第 16 回日本肝臓学会大会・第 54 回日本消化器病
学会大会・第 84 回日本消化器内視鏡学会総会・第 10 回日本消
化器外科学会大会・第 50 回日本消化器がん検診学会大会・第 43
回日本消化器吸収学会総会合同），平成 24 年 10 月 10 日-13 日，
神戸国際展示場，兵庫．

53.　　2012　秦　康倫，木下大輔，奥田英之，茂山朋広，宮部欽生，清水昌
子，岸谷　譲，川崎俊彦，太田善夫，工藤正俊：ランソプラゾ
ールによる collagenous colitis の 4 症例．第 20 回日本消化器
関連学会週間 JDDW2012（第 16 回日本肝臓学会大会・第 54 回日
本消化器病学会大会・第 84 回日本消化器内視鏡学会総会・第 10
回日本消化器外科学会大会・第 50 回日本消化器がん検診学会大
会・第 43 回日本消化器吸収学会総会合同），平成 24 年 10 月 10
日-13 日，神戸国際展示場，兵庫．

54.   2012   田北雅弘，井上達夫，有住忠晃，早石宗右，北井　聡，矢田典久，萩原　智，南　康範，上嶋一臣，西田直生志，工藤正俊：肝嚢胞に対するオレイン酸モノエタノールアミン注入療法の検討．第 20 回日本消化器関連学会週間 JDDW2012（第 16 回日本肝臓学会大会・第 54 回日本消化器病学会大会・第 84 回日本消化器内視鏡学会総会・第 10 回日本消化器外科学会大会・第 50 回日本消化器がん検診学会大会・第 43 回日本消化器吸収学会総会合同），平成 24 年 10 月 10 日-13 日，神戸国際展示場，兵庫．

55.   2012   井上達夫，有住忠晃，早石宗右，田北雅弘，北井　聡，矢田典久，萩原　智，南　康範，上嶋一臣，西田直生志，工藤正俊：肝細胞癌に対するラジオ波焼灼療法の治療効果判定における造影超音波検査の有用性の検討〜造影 CT との比較〜．第 20 回日本消化器関連学会週間 JDDW2012（第 16 回日本肝臓学会大会・第 54 回日本消化器病学会大会・第 84 回日本消化器内視鏡学会総会・第 10 回日本消化器外科学会大会・第 50 回日本消化器がん検診学会大会・第 43 回日本消化器吸収学会総会合同），平成 24 年 10 月 10 日-13 日，神戸国際展示場，兵庫．

56.   2012   大本俊介，北野雅之，工藤正俊：診断確定に造影ハーモニック EUS が有用であった膵腫瘍の検討．日本消化器内視鏡学会近畿支部第 89 回支部例会，平成 24 年 11 月 10 日，大阪国際交流センター，大阪．

57.   2012   丸山康典，河野匡志，松本　望，高場雄久，奥村直己，山本典雄，富田崇文，梅原康湖，谷池聡子，森村正嗣，山田　哲，辻　直子，落合　健，前倉俊治，南　康範，工藤正俊：生検で消失したバレット腺癌の一例．日本消化器内視鏡学会近畿支部第 89 回支部例会，平成 24 年 11 月 10 日，大阪国際交流センター，大阪．

58.   2012   足立哲平，松井繁長，高山政樹，峯　宏昌，永井知行，永田嘉昭，川崎正憲，朝隈　豊，櫻井俊治，樫田博史，工藤正俊，大東弘治，上田和毅，　奥野清隆：腸重積で発見された炎症性線維性ポリープの 1 例．日本消化器内視鏡学会近畿支部第 89 回支部例会，平成 24 年 11 月 10 日，大阪国際交流センター，大阪．

59.　　2012　　千品寛和，松井繁長，田北雅弘，川崎正憲，朝隈　豊，櫻井俊治，樫田博史，工藤正俊：慢性腎不全合併十二指腸静脈瘤に対して内視鏡的硬化療法治療が奏効した一例．日本消化器内視鏡学会近畿支部第 89 回支部例会，平成 24 年 11 月 10 日，大阪国際交流センター，大阪.

60.　　2012　　峯　宏昌，朝隈　豊，足立哲平，高山政樹，永田嘉昭，永井知行，川崎正憲，櫻井俊治，松井範長，樫田博史，工藤正俊：リンパ管侵襲を伴う胃粘膜内癌の一例．日本消化器内視鏡学会近畿支部第 89 回支部例会，平成 24 年 11 月 10 日，大阪国際交流センター，大阪.

61.　　2012　　木下大輔，秦　康倫，奥田英之，茂山朋広，宮部欽生，清水昌子，岸谷　譲，川崎俊彦，太田善夫，工藤正俊：Inflammatory fibroid polyp の一例．日本消化器内視鏡学会近畿支部第 89 回支部例会，平成24年11月10日，大阪国際交流センター，大阪.

62.　　2012　　南　知宏，朝隈　豊，足立哲平，高山政樹，峯　宏昌，永田嘉昭，永井知行，川崎正憲，櫻井俊治，松井繁長，樫田博史，工藤正俊：吐血を契機に発見した妊婦の特発性食道粘膜下血腫の一例．日本消化器内視鏡学会近畿支部第 89 回支部例会，平成 24 年 11 月 10 日，大阪国際交流センター，大阪.

写真で綴る消化器内科
2012年

第48回　日本肝癌研究会

第29回　犬山シンポジウム

1.17 新年会
堺東にて

超音波医学会理事会
2月　ドバイ
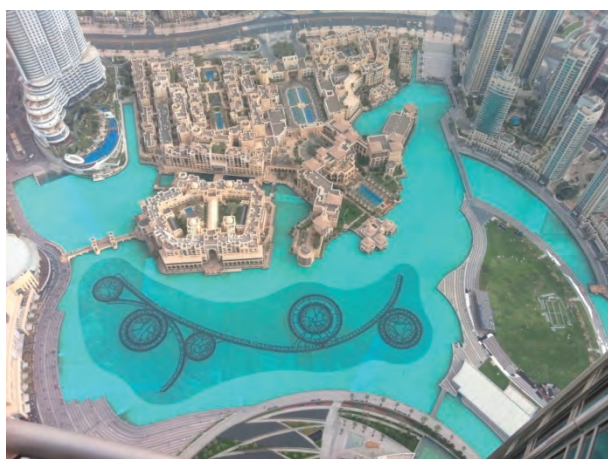
**台湾消化器病学会
特別講演**

陳教授と

Pei Jer chen教授
（真ん中）と

Yun Fan Liaw教授と

Dinn-shin chen教授（右）と

ヨンセイ大学で
特別講演

ヨンセイ大学
Young Nyn Park副学長と

ソウル肝臓研究会
特別講演
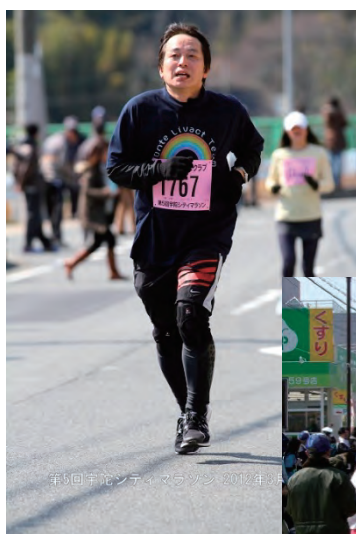
3.11
宇陀シティマラソン

4.29
堺シティマラソン

6.10
OTTY マラソン

医局員と
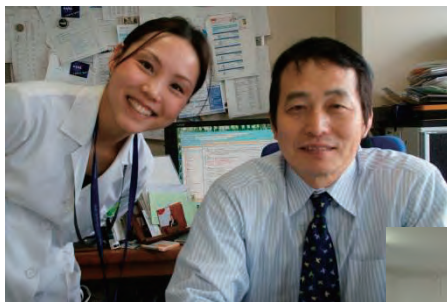
まゆみさん送別会

4.10
歓送迎会 *堺東にて*

4.16
3学年講義
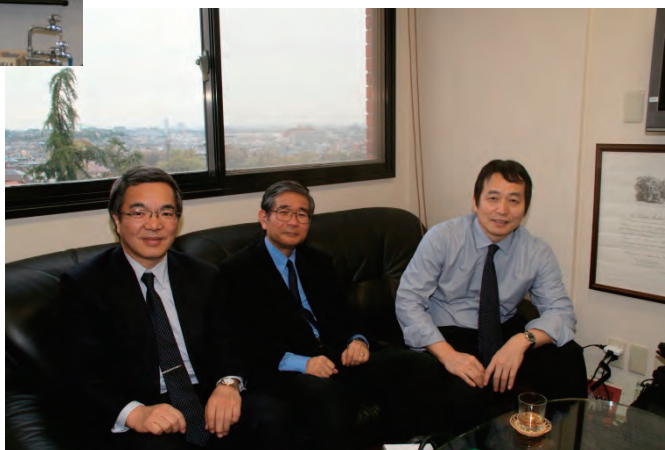
ヨーロッパ超音波医学会
特別講演

韓国超音波医学会講演
5月

アジア造影超音波
医学会講演（ソウル）
5月
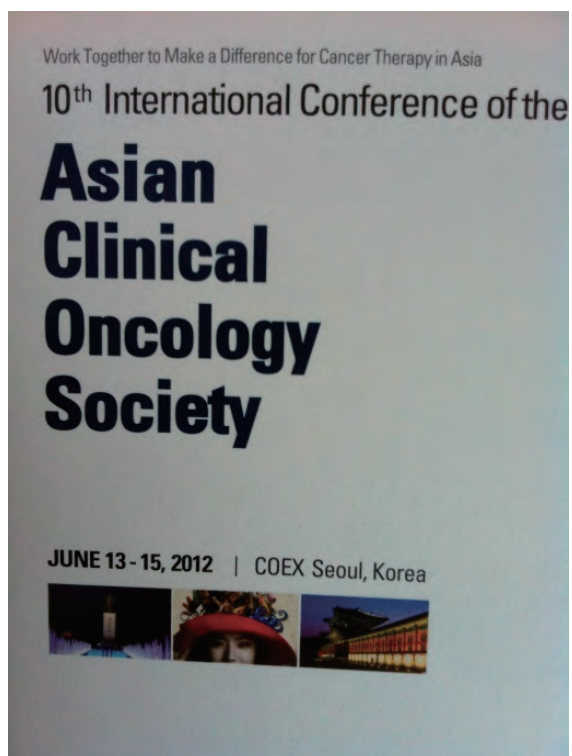
アジア臨床腫瘍学会講演
（ソウル）6月

沖縄肝臓研究会講演
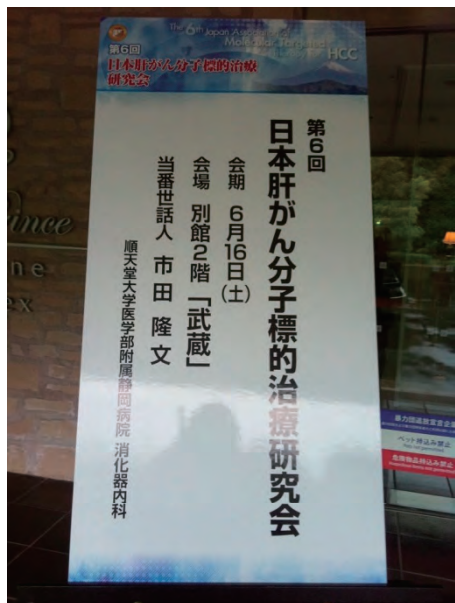
新しいJournal
Liver Cancer 発刊

Editor-in-chief
に就任
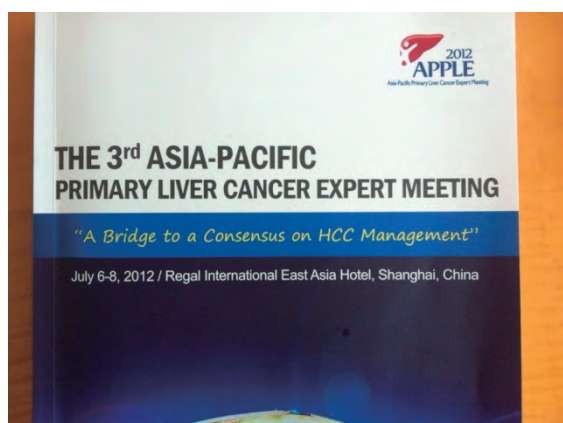
第3回アジア太平洋肝癌専門家会議(APPLE)
(上海)7月

中国東方肝胆外科大学で特別講演
Bruix,Llovet,Shermanらと

APPLEで近大への
過去の留学生と懇談
7月

世界超音波医学会
（理事長　工藤正俊）
京都　7月

日本肝癌研究会
（金沢）
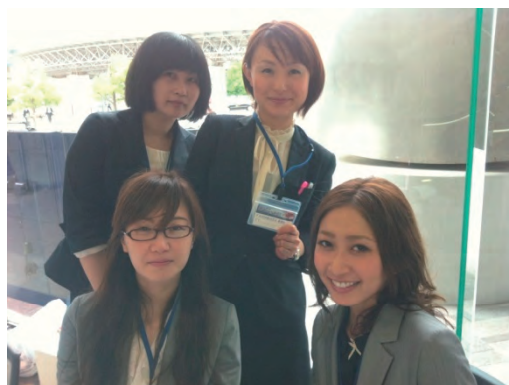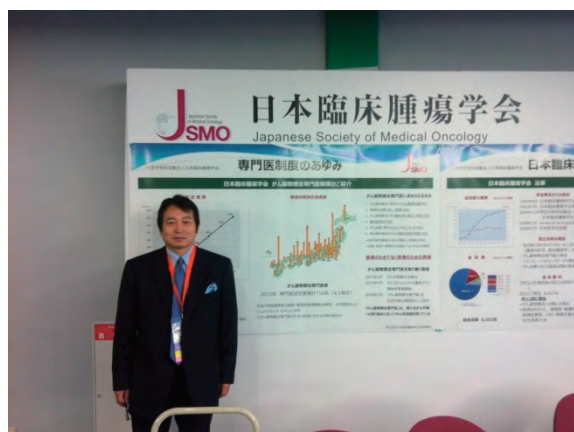
アジア肝癌研究会講演
（ホーチミン）
（アジア7か国を衛星中継）

留学生受け入れ
**Dr.Zhang Shuo
(China)
（3か月間）**
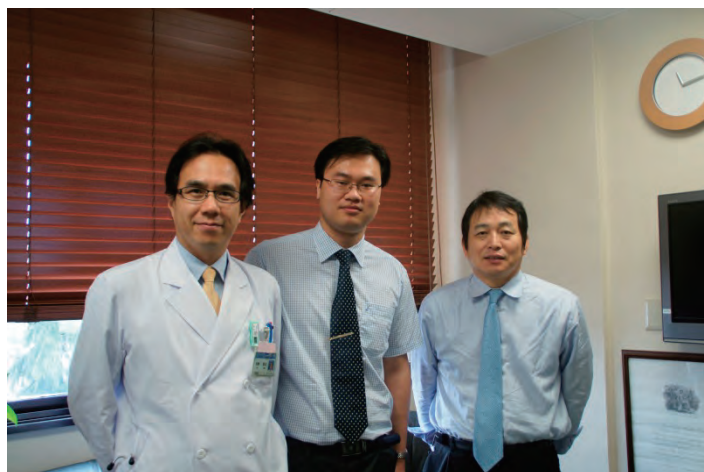
8.20　Dr. Vera 特別講演 (UCSD)

中央臨床検査部（中央臨床検査部長として）

クリクラ学生特別講義

4.17
(新井・岩西・植木・富田・山﨑)

4.26
(新子・近都・眞鍋・慶元・外山・
松廣）

5.9
(緒方・橋本）

5.15
(加納・倉光・西原・西本・森）

5.28
(皆良田・鮫島・吉岡・加藤・
都築）

6.4
(石田・伊藤・小川・村田・
山田・吉田)
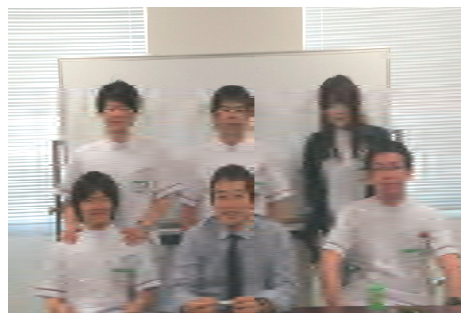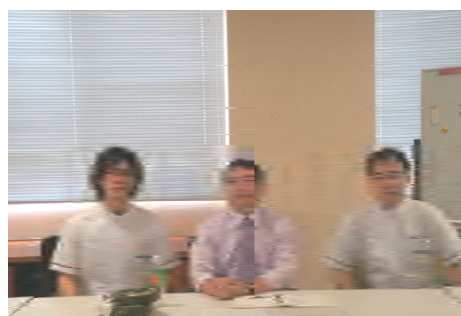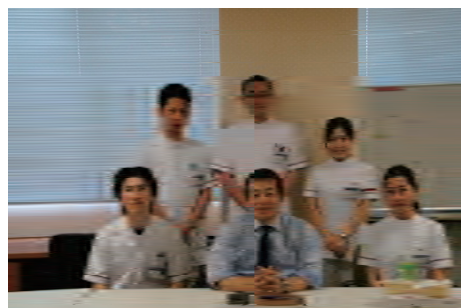
6.16
(石原・丹正・横山・大埼・葉山・
藤元)
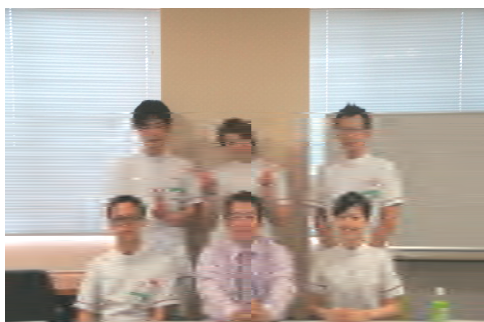
6.26
(古藤・谷・津保・峠・西村）

7.3
(田中・渡部・岡田・宮田）

8.21
(赤松・瀬戸・藤元・伊賀・水野・
龍神）

9.4
(飯田・近藤・冨田・勝瀬・菊池・
増田）

9.18
（平・松尾・八木・奥村・鈴木・
幕谷）

9.25
(岡田・齋藤・松澤・鬼頭・楠本・
松田）

10.15
(板野・田島・堀江・川口・玉井・
山本）

10.29
(川崎・島・前田・有馬・河野・
山本）

9.13-18 国際肝癌学会 (ILCA) で講演
（ベルリン）

ILCA（ベルリン）にて
井上、有住、東Drと

世界超音波医学会(WFUSUMB)
理事会（ワシントン）7月
（理事長　工藤正俊）

世界超音波医学会
（理事長　工藤正俊）
理事会
7月（ワシントンD.C）

FALK Symposiumにて講演
（マインツ、ドイツ）10月

アジア超音波医学会
（インドネシア）11月

関西消化器内視鏡ライブコース
11月25日　近畿大学円形講堂および光学治療センター

肝癌撲滅運動　12月　大阪狭山市にて
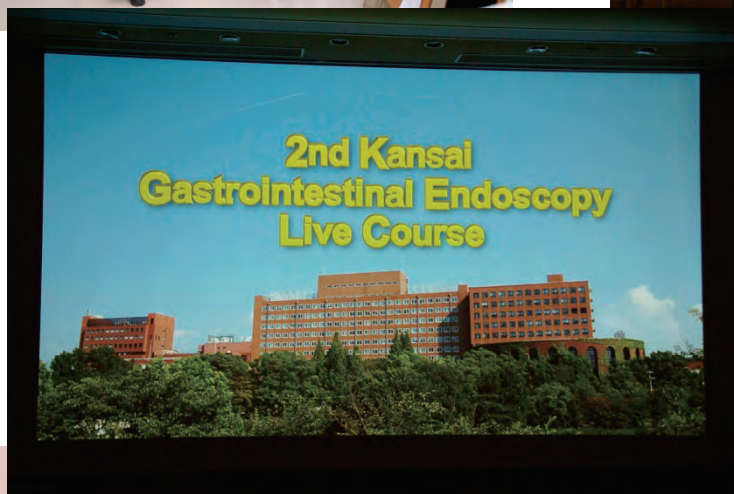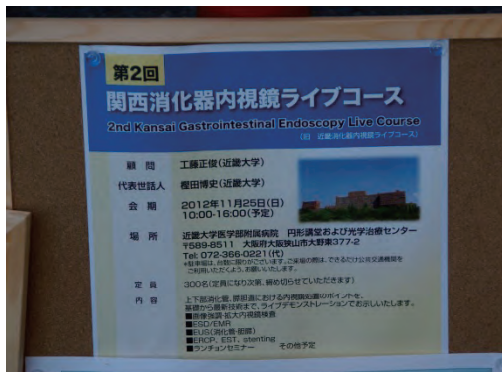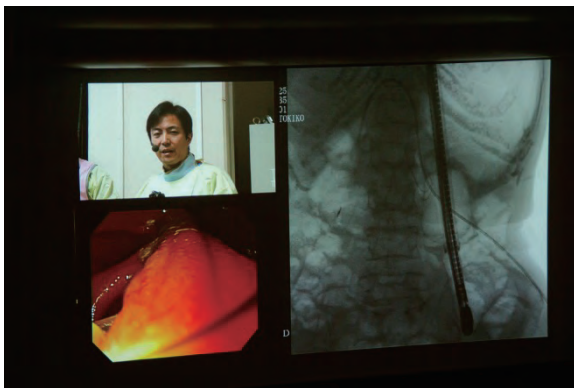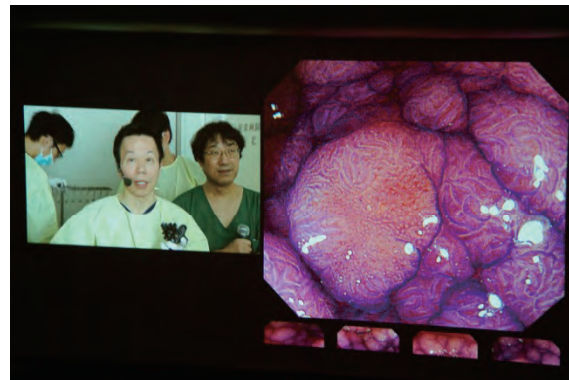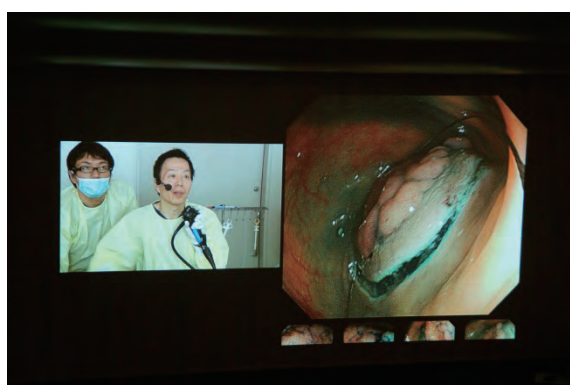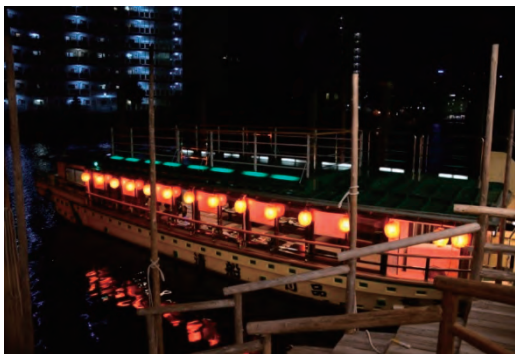
10月27-28　医局旅行
東京・品川　船清（屋形船）
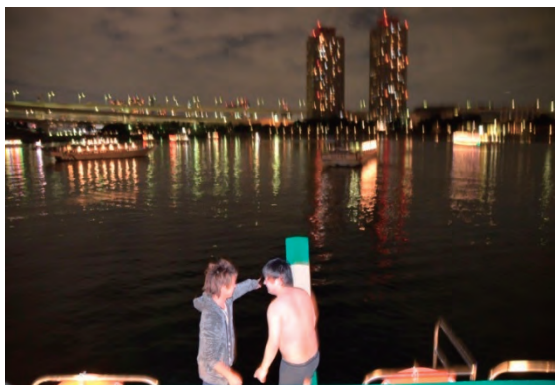
別刷
新聞・雑誌・報道等

Utility of Gd-EOB-DTPA-Enhanced MRI in Diagnosing Small Hepatocellular Carcinoma

Soo Ryang Kim[a]   Susumu Imoto[a]   Taisuke Nakajima[a]

Kenji Ando[a]   Keiji Mita[a]   Katsumi Fukuda[a]   Ryo Nishikawa[a]

Yu-ichiro Koma[a]   Toshiyuki Matsuoka[b]   Masatoshi Kudo[c]

Yoshitake Hayashi[d]

[a]Department of Gastroenterology, Kobe Asahi Hospital, Kobe, [b]Department of Radiology, Osaka City University Medical School, Osaka, [c]Department of Gastroenterology and Hepatology, Kinki University School of Medicine, Osakasayama, and [d]Division of Molecular Medicine and Medical Genetics, International Center for Medical Research and Treatment (ICMRT), Kobe University Graduate School of Medicine, Kobe, Japan

Abstract

We describe an 8-mm hepatocellular carcinoma (HCC) with hepatitis C virus-related cirrhosis in a 74-year-old woman. Ultrasound (US) revealed an 8-mm hyperechoic nodule in segment 6 of the liver. Contrast-enhanced computed tomography (CT) and US revealed no hypervascularity in the early phase and no washout in the late phase and the Kupffer phase, respectively. CT during arteriography revealed no hypervascularity and CT during arterial portography disclosed no perfusion defect. Gadolinium-ethoxybenzyl-diethylenetriamine pentaacetic acid (Gd-EOB-DTPA)-enhanced magnetic resonance imaging (MRI) revealed no hypervascularity in the early phase, but disclosed a defect in the hepatobiliary phase. Histologically, the nodule was diagnosed as well-differentiated HCC characterized by more than two-fold the cellularity of the non-tumorous area, with a high nuclear:cytoplasmic ratio, increased cytoplasmic eosinophilia, fatty change, and slight cell atypia with an irregular thin trabecular pattern. Our case demonstrates the utility of Gd-EOB-DTPA-enhanced MRI in the diagnosis of small HCC.

Soo Ryang Kim, MD

Department of Gastroenterology, Kobe Asahi Hospital
3-5-25 Bououji-cho, Nagata-ku
Kobe 653-0801 (Japan)
Tel. +81 78 612 5151, Fax +81 78 612 5152, E-Mail asahi-hp@arion.ocn.ne.jp

Introduction

Gadolinium-ethoxybenzyl-diethylenetriamine pentaacetic acid (Gd-EOB-DTPA) is a new liver-specific contrast agent used in magnetic resonance imaging (MRI). A bolus injection of Gd-EOB-DTPA allows the evaluation of tumor vascularity in a manner similar to evaluation with gadolinium-triamine pentaacetic acid (Gd-DTPA) [1]. Moreover, it begins to accumulate in normally functioning hepatocytes in the hepatobiliary phase [1, 2] 20 min after injection, thereby enhancing the liver parenchyma. On the other hand, tumors appear like hypointense lesions because they lack normally functioning hepatocytes [2, 3].

Here, we describe an 8-mm well-differentiated hepatocellular carcinoma (HCC) detected in the hepatobiliary phase (20 min after injection), whereas contrast-enhanced ultrasound (US) and computed tomography (CT) did not reveal hypervascularity in the early phase and washout in the late phase; also, CT during arteriography (CTA) and CT during arterial portography (CTAP) did not reveal hypervascularity and perfusion defect, respectively.

Case Report

A 74-year-old woman with hepatitis C virus (HCV)-related cirrhosis was admitted to Kobe Asahi Hospital in April 2008 for further examination of an 8-mm hyperechoic nodule in segment 6. HCV antibody and HCV RNA were positive, hepatitis B surface antigen and hepatitis B virus DNA were negative, and laboratory data on admission disclosed the following values: platelets $7.2 \times 10^4/\mu l$ (normal 13.0–36.9), aspartate aminotransferase 26 IU/l (10–40), alanine aminotransferase 20 IU/l (5–40), thymol turbidity 18.5 U/l (0–4), zinc surface turbidity 13.7 U/l (2–12), indocyanine green retention rate at 15 min 7% (0–10), and γ-globulin 23.3% (10.6–20.5). The levels of tumor markers revealed the following: α-fetoprotein 7.1 ng/ml (0–9.9), protein induced by vitamin K absence II 42 mAU/ml (0–40). US disclosed an 8-mm hyperechoic nodule in segment 6 (**fig. 1**). Contrast-enhanced CT revealed no hypervascularity in the early phase and no washout in the late phase. Contrast-enhanced US revealed no hypervascularity in the early vascular phase and no defect in the Kupffer phase. CTA revealed no hypervascularity and CTAP revealed no perfusion defect. Superparamagnetic iron oxide (SPIO)-MRI revealed isointensity in both T1 and T2 sequences. Gd-EOB-DTPA-enhanced MRI revealed no hypervascularity in the early phase, but disclosed a defect in the hepatobiliary phase (**fig. 2**). Histologically, the nodule was diagnosed as well-differentiated HCC characterized by more than two-fold the cellularity of the non-tumorous area, with a high nuclear:cytoplasmic ratio, increased cytoplasmic eosinophilia, fatty change, and slight cell atypia with an irregular thin trabecular pattern (**fig. 3**). The HCC was treated with radiofrequency ablation, and the ablated HCC was confirmed by Gd-EOB-DTPA-enhanced MRI. Complete necrosis of the tumor was revealed by US-guided biopsy.

Discussion

HCC is known to arise multicentrically in cases of virally induced liver cirrhosis, developing from dysplastic nodules into HCC [4, 5]. When considering the most appropriate therapeutic approach, it is important to distinguish between dysplastic nodules and HCC. Although the usefulness of detecting hypervascular HCCs has been reported [1], neither hypovascular lesions nor lesions with weakly increased arterial flow have been evaluated to date. These latter nodules are difficult to evaluate in dynamic studies with Gd-DTPA. No significant quantitative difference is observed between HCCs and dysplastic nodules in terms of the enhancement ratios and the contrast-to-noise ratio [6]. A combination of CTA and CTAP, as well as SPIO-enhanced MRI, has been conducted to distinguish between these two entities [7, 8]. It is known that SPIO accumulates in some HCCs [8]. SPIO-enhanced MRI, however, is of limited use in the

evaluation of HCCs, being by itself insufficient for determining the therapeutic strategy for the treatment of HCCs. When a combination of CTA and CTAP is used [7], the blood supply is very informative in evaluating the malignancy of liver lesions. CTA and CTAP are too invasive, however, for routine application.

In our case, imaging studies by modalities such as contrast-enhanced US and CT revealed no hypervascularity in the early phase and no washout in the Kupffer phase and the late phase. CTA did not reveal hypervascularity, and CTAP did not reveal perfusion defect. We have emphasized the superiority of CT arterioportal angiography to contrast-enhanced CT and MRI in the diagnosis of HCC in nodules smaller than 20 mm [9]. We have also detected a 10-mm well-differentiated HCC showing perfusion defect at CTAP, when contrast-enhanced US, CT, and MRI revealed no hypervascularity in the early phase or washout in the late phase, and CTA showed no hypervascular stain [9]. In this study, however, even with CT arterioportal angiography, we were not able to detect the 8-mm HCC. Although the data remain preclinical, specific enhancement with Gd-EOB-DTPA has been reported for the differentiation of HCC [10]. Gd-EOB-DTPA-enhanced MRI provides additional diagnostic clues – the level of hepatocyte function and excretion [11]. We detected an 8-mm HCC with Gd-EOB-DTPA-enhanced MRI, showing a defect in the hepatobiliary phase (20 min after injection). Our case demonstrates the utility of Gd-EOB-DTPA-enhanced MRI in the diagnosis of small HCC, even of an 8-mm nodule, although all nodules recognized as hypointense in the hepatobiliary phase and diagnosed as HCCs are associated with potential misdiagnosis. In our case the well-differentiated HCC was confirmed histologically.

Further study is needed to compare the utility of Gd-EOB-DTPA-enhanced MRI with contrast-enhanced US, CT, and CT arterioportal angiography in the diagnosis of HCC in nodules smaller than 20 mm.

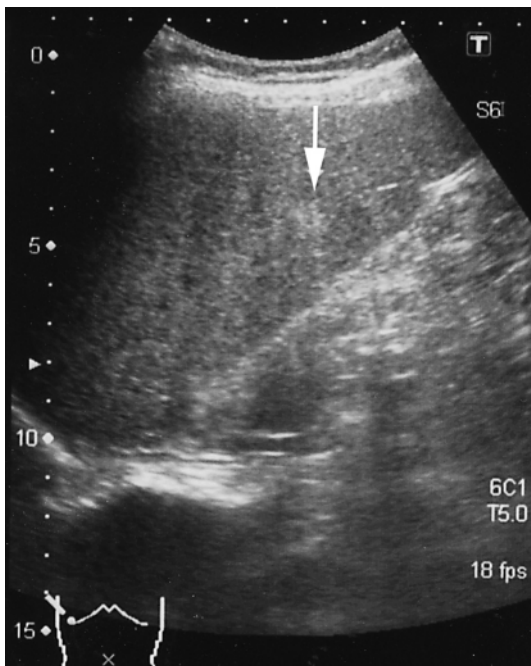**Fig. 1.** US disclosed an 8-mm hyperechoic nodule in segment 6.

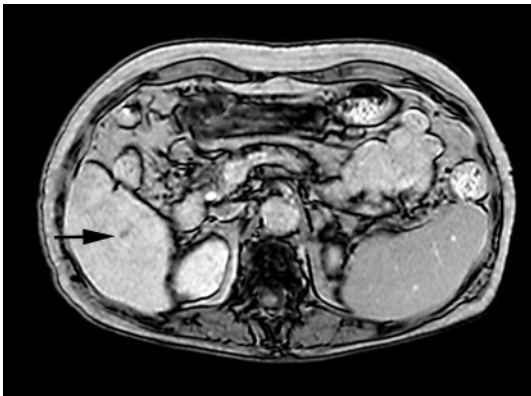**Fig. 2.** Gd-EOB-DTPA-enhanced MRI disclosed a defect in the hepatobiliary phase.

Fig. 3. Histologically, the nodule was diagnosed as well-differentiated HCC characterized by more than two-fold the cellularity of the non-tumorous area, with a high N/C ratio, increased cytoplasmic eosinophilia, fatty change, and slight cell atypia with an irregular thin trabecular pattern.
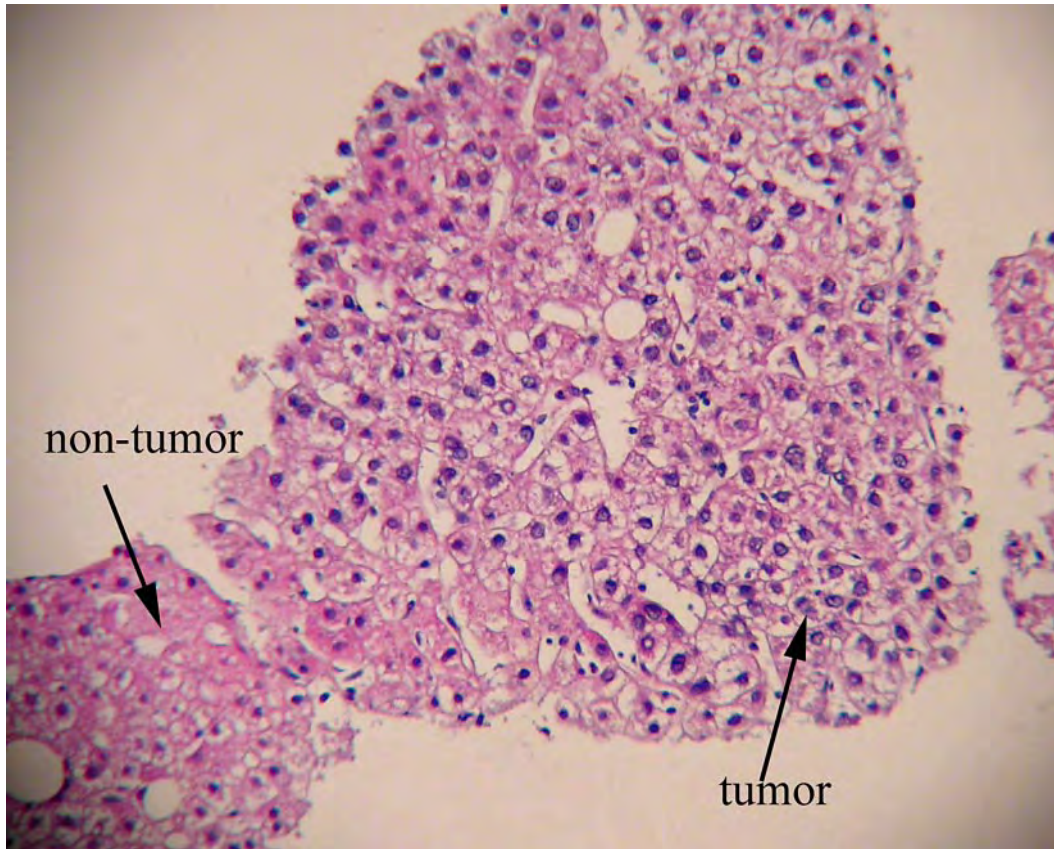
References

1 Vogl TJ, Kummel S, Hammerstingl R, Schellenbeck M, Schumacher G, Balzer T, Schwarz W, Müller PK, Bechstein WO, Mack MG, Söllner O, Felix R: Liver tumors: comparison of MR imaging with Gd-EOB-DTPA and Gd-DTPA. Radiology 1996;200:59–67.

2 Reimer P, Rummeny EJ, Shamsi K, Balzer T, Daldrup HE, Tombach B, Hesse T, Berns T, Peters PE: Phase II clinical evaluation of Gd-EOB-DTPA: dose, safety aspects, and pulse sequence. Radiology 1996;199:177–183.

3 Hamm B, Staks T, Muhler A, Bollow M, Taupitz M, Frenzel T, Wolf KJ, Weinmann HJ, Lange L: Phase I clinical evaluation of Gd-EOB-DTPA as a hepatobiliary MR contrast agent: safety, pharmacokinetics, and MR imaging. Radiology 1995;195:785–792.

4 Nakamura Y, Terada T, Terasaki S, Ueda K, Nonomura A, Kawahara E, Matsui O: Atypical adenomatous hyperplasia in liver cirrhosis: low-grade hepatocellular carcinoma or borderline lesion? Histopathology 1990;17:27–35.

5 Sakamoto M, Hirohashi S, Shimosato Y: Early stages of multistep hepatocarcinogenesis: adenomatous hyperplasia and early hepatocellular carcinoma. Hum Pathol 1991;22:172–178.

6 Saito K, Kotake F, Ito N, Ozuki T, Mikami R, Abe K, Shimazaki Y: Gd-EOB-DTPA enhanced MRI for hepatocellular carcinoma: quantitative evaluation of tumor enhancement in hepatobiliary phase. Magn Reson Med Sci 2005;4:1–9.

7 Hayashi M, Matsui O, Ueda K, Kawamori Y, Kadoya M, Yoshikawa J, Gabata T, Takashima T, Nonomura A, Nakanuma Y: Correlation between the blood supply and grade of malignancy of hepatocellular nodules associated with liver cirrhosis: evaluation by CT during intraarterial injection of contrast medium. AJR Am J Roentgenol 1999;172:969–976.

8 Imai Y, Murakami T, Yoshida S, Nishikawa M, Ohsawa M, Tokunaga K, Murata M, Shibata K, Zushi S, Kurokawa M, Yonezawa T, Kawata S, Takamura M, Nagano H, Sakon M, Monden M, Wakasa K, Nakamura H: Superparamagnetic iron oxide-enhanced magnetic resonance images of hepatocellular carcinoma: correlation with histological grading. Hepatology 2000;32:205–212.

9 Kim SR, Ando K, Mita K, Fuki S, Ikawa H, Kanbara Y, Imoto S, Matsuoka T, Hayashi Y, Kudo M: Superiority of CT arterioportal angiography to contrast-enhanced CT and MRI in the diagnosis of hepatocellular carcinoma in nodules smaller than 2 cm. Oncology 2007;72(suppl 1):58–66.

10 Ni Y, Marchal G, Yu J, Mühler A, Lukito G, Baert AL: Prolonged positive contrast enhancement with Gd-EOB-DTPA in experimental liver tumors; potential value in tissue characterization. J Magn Reson Imaging 1994;4:355–363.

11 Schuhmann-Giampieri G, Schmitt-Willichi H, Press WR, Negishi C, Weinmann HJ, Speck U: Preclinical evaluation of Gd-EOB-DTPA as a contrast agent in MR imaging of the hepatobiliary system. Radiology 1992;183:59–64.

CASE REPORT

Quantification of tumor vascularity with contrast-enhanced ultrasound for early response of transcatheter arterial chemoembolization for hepatocellular carcinoma: a report of three cases

**Yasunori Minami · Naoya Okumura ·
Norio Yamamoto · Naoko Tsuji · Yuko Kono ·
Masatoshi Kudo**

Abstract Many contrast-enhanced ultrasound (CE-US) studies have been conducted by qualitative analysis of blood flow, such as classification of enhancement pattern. We evaluated early response of transcatheter arterial chemoembolization (TACE) for hepatocellular carcinoma (HCC) by quantitative analysis of intratumoral vascularity with CE-US in three patients. Three patients (one man, two women) with HCCs were treated in July 2009. CE-US with perfluorocarbon microbubbles (Sonazoid) and CT were performed serially before and 5 days after TACE. Post-processing enhancement intensity on US was analyzed to determine mean transit time (s), time to peak (s), enhancement peak intensity (dB), and "A" (scaling factor) by ultrasound quantification software after the data were fitted to a gamma variate curve. Mean transit time was prolonged by TACE in all three patients. Mean transit time rates on CE-US were 64.3, 33.8, and 65.6%, respectively, whereas the avascular rates on CT were 59.07, 31.71, and 62.25%, respectively. Mean transit time rates on CE-US approximated avascular rates on CT. Mean transit time rate may quantitatively indicate the early response of HCC to TACE.

Keywords Hepatocellular carcinoma · Transcatheter arterial chemoembolization · Contrast-enhanced ultrasound · Perfluorocarbon microbubbles

Introduction

Doppler ultrasound has been used to estimate blood flow, as the mean velocity multiplied by the vessel area, but using this to evaluate intratumoral vascularity accurately can be difficult because of its faint signals [1]. Microbubbles, developed as contrast agents for ultrasound, are considered useful for increasing the intensity of echoes [2–4]. Thus, contrast-enhanced ultrasound (CE-US) can depict intratumoral vascularity sensitively and accurately, and is considered useful for diagnosing hepatic tumors and assessing the therapeutic response in hepatocellular carcinoma (HCC) [5–10]. However, the pattern classification of tumor enhancement generally done in these CE-US studies is a qualitative analysis of blood flow for the evaluation of therapeutic response.

This preliminary trial assessed the early response of HCC to transcatheter arterial chemoembolization (TACE) by quantitative analysis of intratumoral vascularity on CE-US in three patients.

Materials and methods

The Ethics Committee of our institution approved the study protocol. Written informed consent was obtained from each patient at enrollment.

Y. Minami (✉) · M. Kudo
Department of Gastroenterology and Hepatology,
Kinki University Faculty of Medicine, 377-2 Ohono-Higashi,
Osaka-Sayama, Osaka 589-8511, Japan
e-mail: minkun@med.kindai.ac.jp

Y. Minami · N. Okumura · N. Yamamoto · N. Tsuji
Department of Gastroenterology and Hepatology, Sakai Hospital
Kinki University Faculty of Medicine, 2-7-1 Harayamadai,
Minami, Sakai, Osaka 590-0132, Japan

Y. Kono
Department of Medicine, Division of Gastroenterology
and Hepatology, University of California, San Diego (UCSD),
200 W. Arbor Dr. MC 8756, San Diego, CA 92103, USA

🖄 Springer

Three patients (one man, two women; 65, 82, and 85 years old) with multiple HCCs were treated by TACE in July 2009. The primary tumor size in each patient was 7.3, 13, and 6.5 cm in diameter, respectively.

Hepatic angiography was performed before TACE. An emulsion of iodized oil (Lipiodol Ultra-Fluide; Laboratoires Guerbet, Aulnay-sous-Bois, France) and a chemotherapeutic agent, epirubicin (Kyowa Hakko Co., Tokyo, Japan) (20–40 mg), was then injected, followed by the injection of a gelatin sponge via a catheter. The tip of the catheter was placed selectively into the segmental arteries feeding the tumors; otherwise, it was placed into the right or left branch of the hepatic artery. The volume of injected emulsion was determined by tumor size (maximum: 10 ml).

CE-US and contrast-enhanced computerized tomography (CE-CT) were performed serially before and 5 days after TACE. Areas demonstrating iodized oil accumulation in the tumor after TACE were regarded as the avascular area. Persistent low-density areas on both plain and arterial phase dynamic CT scans were also regarded as necrotic. Enhancing areas on arterial phase dynamic CT were regarded as viable, and supplied by feeding arteries.

Use of CE-US to assess effectiveness

The contrast agent used was Sonazoid (Daiichi-Sankyo, Tokyo, Japan), which consists of a phospholipid shell containing perfluorocarbon microbubbles. The recommended clinical dose for imaging of liver lesions is 0.010 ml of encapsulated gas per kilogram of body weight.

B-mode sonographic scans were obtained using a Philips iU22 unit (Philips Medical Systems, Seattle, WA, USA) with a C5-1 curvilinear transducer. Vascular findings were obtained in the vascular phase (from 10 s to the last 5–7 min after injection of the contrast agent). Acquisitions were obtained for about 30 s at a low mechanical index (MI = 0.1) setting at a rate of seven frames per second with the patient holding his/her breath. CE-US image data were saved in the ultrasound hard-disk system, and then transferred to a PC for further quantitative analyses with advanced ultrasound quantification software (QLAB 8.1; Philips Medical Systems). In the region of interest (ROI) delineating each tumor, the computer-assisted program calculated acquisition of time (s)/signal intensity (dB) curves [11]. Thereafter, we fitted the data to a gamma variate curve using raw data. The mean transit time (s), defined as the width at half the maximum height (full width at half maximum), time to peak intensity (s), peak intensity (dB), and "A" (scaling factor) were obtained by QLAB software from the gamma variate curves using the formula shown below.

$$Y(t) = A \times t \times \exp(-\text{alpha} \times t) + C$$

$Y(t)(dB)$, enhancement intensity at time t; $t(s)$, time after injection

The gamma variate is a mathematical function that can be used to describe tracer dilution curves, and the relations between flow, circulation times, and volumes were established according to kinetic principles (Fig. 1).

Results

Parameters of mean transit time and time to peak intensity are related to the time, whereas parameters of peak intensity and "A" are related to the brightness on US. Table 1 shows parameters of time–intensity curves on contrast-enhanced US before and after TACE for HCC (Fig. 2). TACE prolonged mean transit time in all three patients.

Fig. 1 The time–intensity curve fitted by gamma variate analysis. Intratumoral vascularity changed because vascular resistance could increase due to transcatheter arterial chemoembolization (TACE). We hypothesized that mean transit time and time to peak would be prolonged and peak intensity and parameter A would decrease following TACE
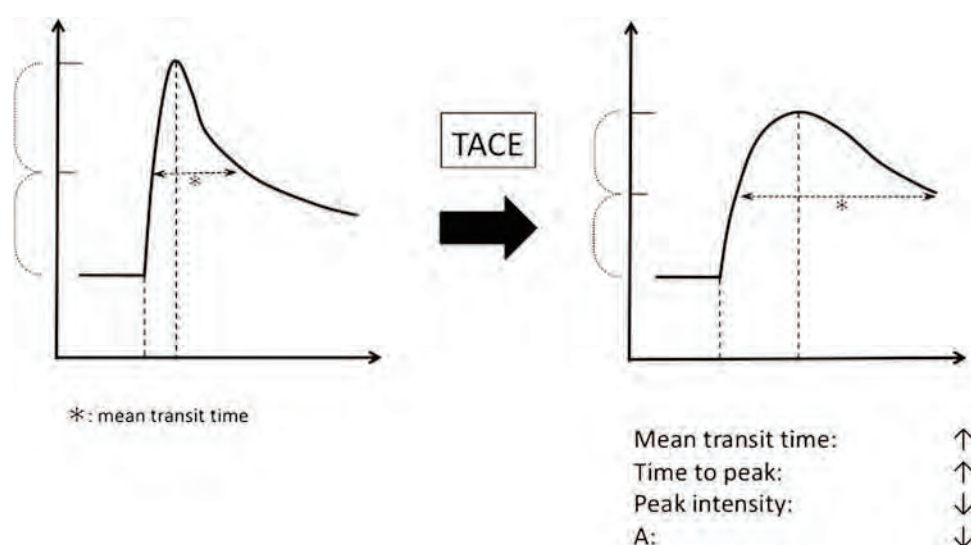
*: mean transit time

Mean transit time: ↑
Time to peak: ↑
Peak intensity: ↓
A: ↓

Table 1 Parameters of time–intensity curves on contrast-enhanced US before and after TACE for HCC

Case	Parameter	Before TACE	After TACE
Case 1	Mean transit time (s)	4.98	7.75
	Time to peak (s)	7.35	6.77
	Peak intensity (dB)	11.01	12.09
	A	1.21	1.46
Case 2	Mean transit time (s)	12.31	36.45
	Time to peak (s)	16.61	23.19
	Peak intensity (dB)	13.64	13.07
	A	1.41	6.64
Case 3	Mean transit time (s)	15.44	23.53
	Time to peak (s)	13.6	12.64
	Peak intensity (dB)	18.78	11.68
	A	3.79	13.49

HCC hepatocellular carcinoma, *TACE* transcatheter arterial chemo-embolization, *US* ultrasound

Time to peak was prolonged in case 2 and slightly shortened in the other patients. Peak intensity declined in case 3, but not in the other cases. Parameter *A* was markedly elevated in two patients, and slightly elevated in one patient.

To calculate the intratumoral avascular rate of TACE on CT, unenhanced and iodized oil-retaining areas were measured for density on the slice level with the maximum tumor size. The avascular rate was calculated with the following formula: avascular rate = (nonenhancing area + area of iodized oil retention)/(total area of tumor) × 100. The avascular rates in these three patients were 59.07, 31.71, and 62.25%, respectively (Table 2). However, mean transit time rate was calculated with the following formula: mean transit time rate = (mean transit time before TACE)/(mean transit time after TACE) × 100. Mean transit time rates in these three patients were 64.3, 33.8, and 65.6%, respectively (Table 2).

There were no serious side effects or procedure-related complications (e.g., hemorrhage, infection, hepatic failure, or death). Low grade fever occurred in all patients after TACE and then resolved with administration of nonsteroidal anti-inflammatory drugs.

Discussion

We did not directly calculate the real blood flow volume or velocity in the tumor. Some parameters of the time–intensity curve that could be related to the blood flow were compared before and after TACE in this preliminary trial. Following TACE, intratumoral vascularity declines because of increased vascular resistance. Therefore, we presumed that time parameters would be prolonged, whereas intensity parameters such as peak intensity and parameter A would decrease.

In all three patients, mean transit time was prolonged by TACE; however, time to peak intensity was not significantly prolonged. In case 3, the prolongation of contrast washout time in the tumor was induced by increased resistance to the intratumoral blood flow, but persistent vascularity in viable HCC might not seriously affect time to peak. Despite differences in cross-sectional images between US and CT, Table 2 shows approximate values between avascular rates on CT and mean transit time rates on US. Mean transit time rate might estimate treatment response of HCC to TACE. Of course, further prospective studies with a larger number of patients must be performed before definitive conclusions can be drawn. If our hypothesis is confirmed, mean transit time rate could be useful for providing an early quantitative assessment of treatment response to TACE.

After TACE, peak intensity and parameter A did not always change as predicted. One reason could be that the intratumoral intensity was strongly influenced by thick vessels in which blood flowed abundantly in the tumor. A second reason could be that the intensity fluctuated with the depth of the ROI. Fundamentally, we tried to keep the same image on CE-US before and after TACE. However, slight differences in cross-sectional images can be assumed to cause major changes in intensity value on CE-US, although we could not recognize these intensity differences on US.

CE-US is a useful tool for predicting the early efficacy not only of TACE but also of molecularly targeted drugs such as imatinib, sunitinib, sorafenib, and bevacizumab [12–16]. Lassau et al. [16] reported that CE-US might be useful for detecting and quantifying dynamic early changes in tumor vascularity after initiation of bevacizumab therapy in patients with HCC. These early parameter changes in tumor perfusion may be predictive of tumor response, progression-free survival, and overall survival, and could become surrogate measures of the effectiveness of molecularly targeted drugs in patients with HCC.

The principal premise of this method is that fitting of the time–intensity curve is needed to demonstrate persistent intratumoral vascularity after TACE. The data for the gamma variate curve would not fit accurately in patients showing complete response to TACE. There is a problem that needs to be resolved, i.e., how much blood flow needs to remain in order to assess the vascularity accurately. In this trial, the observation time was approximate 30 s on early vascular images because static US images were obtained while the patient held his/her breath. However, Lassau et al. [12–16] obtained the time–intensity curve for a 3-min observation on US without breath-holding. It remains controversial whether one static US image with a
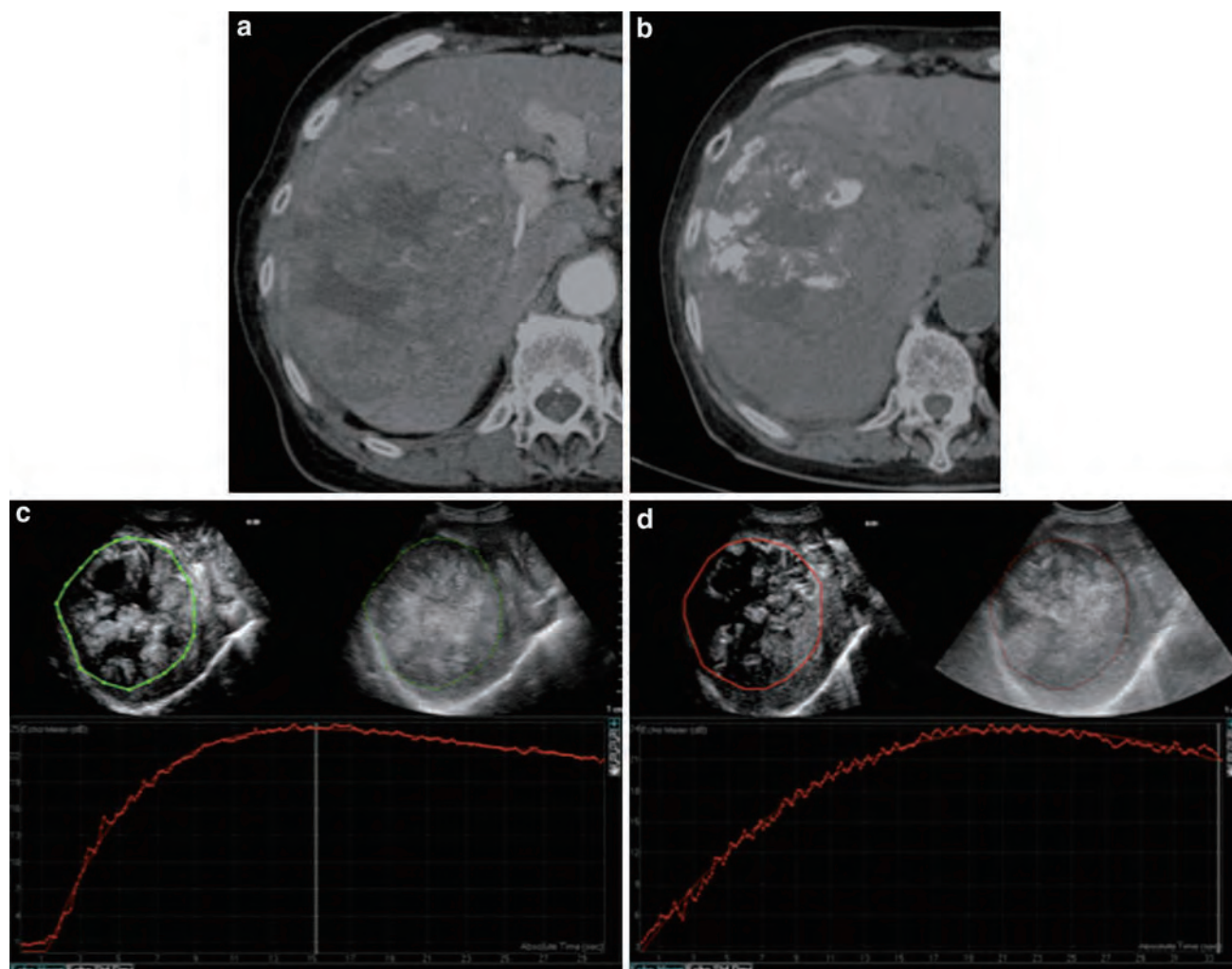
Fig. 2 An 85-year-old woman with hepatocellular carcinoma (HCC) measuring 10 cm in diameter (case 3). **a** Early-phase dynamic CT scan showed a huge HCC as an enhanced lesion in the right hepatic lobe before transcatheter arterial chemoembolization (TACE). **b** After TACE, an area of iodized oil accumulation was depicted in the tumor on plain CT. **c** Contrast-enhanced US (CE-US) showed an enhanced HCC nodule before TACE. *Left top*: the region of interest was set over the whole tumor. *Right top*: B-mode US showed the same cross-sectional image as CE-US. *Bottom: notched curve* indicates time–intensity. *Smooth solid curve* was obtained by gamma variate curve fitting. **d** *Left top*: non-vascular area was partially expanded in the tumor by TACE. However, fully intratumoral vascularity was still depicted. *Bottom*: The slope of the wash-in and washout of the gamma variate curve became gentler. Mean transit time and time to peak were prolonged after TACE in this case

Table 2 Comparison of treatment response rate on CT and mean transit time rate on contrast-enhanced US after TACE

	CT Avascular rate (%)	US Mean transit time rate (%)
Case 1	59.07	64.25
Case 2	31.71	33.77
Case 3	62.25	65.61

HCC hepatocellular carcinoma, *TACE* transcatheter arterial chemo-embolization, *US* ultrasound

short observation or cross-sectional US images with a long observation would be more useful. In our patients, the time holding their breath varied, and we could not evaluate the parameter AUC (area under the curve) under the same condition in all our patients. Therefore, we did not investigate AUC in our trial.

In the present study, mean transit time was prolonged by TACE in three patients. Mean transit time rate on CE-US could be useful for quantitative assessment of early treatment response of HCC to TACE.

References

1. Cosgrove D, Eckersley R, Blomley M, Harvey C. Quantification of blood flow. Eur Radiol. 2001;11(8):1338–44.
2. Solbiati L, Tonolini M, Cova L, Goldberg SN. The role of contrast-enhanced ultrasound in the detection of focal liver lesions. Eur Radiol. 2001;11:E15–26.
3. Konopke R, Bunk A, Kersting S. The role of contrast-enhanced ultrasound for focal liver lesion detection: an overview. Ultrasound Med Biol. 2007;33(10):1515–26.
4. Kudo M. New sonographic techniques for the diagnosis and treatment of hepatocellular carcinoma. Hepatol Res. 2007;37:S193–9.
5. Cioni D, Lencioni R, Bartolozzi C. Therapeutic effect of transcatheter arterial chemoembolization on hepatocellular carcinoma: evaluation with contrast-enhanced harmonic power Doppler ultrasound. Eur Radiol. 2000;10(10):1570–5.
6. Minami Y, Kudo M, Kawasaki T, Kitano M, Chung H, Maekawa K, Shiozaki H. Transcatheter arterial chemoembolization of hepatocellular carcinoma: usefulness of coded phase-inversion harmonic sonography. AJR Am J Roentgenol. 2003;180:703–8.
7. Kono Y, Lucidarme O, Choi SH, Rose SC, Hassanein TI, Alpert E, Mattrey RF. Contrast-enhanced ultrasound as a predictor of treatment efficacy within 2 weeks after transarterial chemobolization of hepatocellular carcinoma. J Vasc Interv Radiol. 2007;18:57–65.
8. Xia Y, Kudo M, Minami Y, Hatanaka K, Ueshima K, Chung H, Hagiwara S, Inoue T, Ishikawa E, Kitai S, Takahashi S, Tatsumi C, Ueda T, Hayaishi S, Maekawa K. Response evaluation of transcatheter arterial chemoembolizaion in hepatocellular carcinomas: the usefulness of sonazoid-enhanced harmonic sonography. Oncology. 2008;75:S99–105.
9. Hunt SJ, Yu W, Weintraub J, Prince MR, Kothary N. Radiologic monitoring of hepatocellular carcinoma tumor viability after transhepatic arterial chemoembolization: estimating the accuracy of contrast-enhanced cross-sectional imaging with histopathologic correlation. J Vasc Interv Radiol. 2009;20:30–8.
10. Patel S, Saito A, Yoneda Y, Hayano T, Shiratori K. Comparing enhancement and washout patterns of hepatic lesions between sonazoid-enhanced ultrasound and contrast-enhanced computed tomography. J Med Ultrasonics. 2010;37:167–73.
11. Gauthier TP, Averkiou MA, Leen ELS. Perfusion quantification using dynamic contrast-enhanced ultrasound: the impact of dynamic range and gain on time-intensity curves. Ultrasonics. 2010;51:102–6.
12. Lassau N, Koscielny S, Albiges L, Chami L, Benatsou B, Chebil M, Roche A, Escudier BJ. Metastatic renal cell carcinoma treated with sunitinib: early evaluation of treatment response using dynamic contrast-enhanced ultrasonography. Clin Cancer Res. 2010;16(4):1216–25.
13. Lassau N, Lamuraglia M, Chami L, Leclère J, Bonvalot S, Terrier P, Roche A, Le Cesne A. Gastrointestinal stromal tumors treated with imatinib: monitoring response with contrast-enhanced sonography. AJR Am J Roentgenol. 2006;187(5):1267–73.
14. Lassau N, Chami L, Benatsou B, Peronneau P, Roche A. Dynamic contrast-enhanced ultrasonography (DCE-US) with quantification of tumor perfusion: a new diagnostic tool to evaluate the early effects of antiangiogenic treatment. Eur Radiol. 2007;17:F89–98.
15. Lassau N, Chebil M, Chami L, Bidault S, Girard E, Roche A. Dynamic contrast-enhanced ultrasonography (DCE-US): a new tool for the early evaluation of antiangiogenic treatment. Target Oncol. 2010;5(1):53–8.
16. Lassau N, Koscielny S, Chami L, Chebil M, Benatsou B, Roche A, Ducreux M, Malka D, Boige V. Advanced hepatocellular carcinoma: early evaluation of response to bevacizumab therapy at dynamic contrast-enhanced US with quantification—preliminary results. Radiology. 2011;258(1):291–300.

PANCREAS AND BILIARY TRACT

Characterization of Small Solid Tumors in the Pancreas: The Value of Contrast-Enhanced Harmonic Endoscopic Ultrasonography

Masayuki Kitano, MD, PhD[1], Masatoshi Kudo, MD, PhD[1], Kenji Yamao, MD, PhD[2], Tadayuki Takagi, MD, PhD[2], Hiroki Sakamoto, MD, PhD[1], Takamitsu Komaki, MD, PhD[1], Ken Kamata, MD[1], Hajime Imai, MD[1], Yasutaka Chiba, PhD[3], Masahiro Okada, MD, PhD[4], Takamichi Murakami, MD, PhD[4] and Yoshifumi Takeyama, MD, PhD[5]

OBJECTIVES: **Contrast-enhanced harmonic endoscopic ultrasonography (CH-EUS), a novel technology, visualizes parenchymal perfusion in the pancreas. This study prospectively evaluated how accurately CH-EUS characterizes pancreatic lesions and compared its diagnostic ability with that of contrast-enhanced multidetector-row computed tomography (MDCT) and endoscopic ultrasonography-guided fine needle aspiration (EUS-FNA).**

METHODS: **A total of 277 consecutive patients with pancreatic solid lesions that were detected by conventional EUS underwent CH-EUS for evaluation of vascularity. After infusing an ultrasound contrast, CH-EUS was performed by using an echoendoscope and a specific mode for contrast harmonic imaging. On the basis of the intensity of enhancement, the lesions were categorized into four patterns: nonenhancement, hypoenhancement, isoenhancement, and hyperenhancement. For comparison, all patients underwent MDCT. The ability of CH-EUS to differentiate ductal carcinomas from the other solid tumors, particularly small lesions (≤2 cm in diameter) was assessed, and compared with the differentiating abilities of MDCT and EUS-FNA.**

RESULTS: **In terms of reading the CH-EUS images, the κ-coefficient of the interobserver agreement test was 0.94 ($P<0.001$). CH-EUS-depicted hypoenhancement diagnosed ductal carcinomas with a sensitivity and specificity of 95.1% (95% confidence interval (CI) 92.7–96.7%) and 89.0% (95% CI 83.0–93.1%), respectively. For diagnosing small carcinomas by CH-EUS, the sensitivity and specificity were 91.2 % (95% CI 82.5–95.1%) and 94.4% (95% CI 86.2–98.1%), respectively. CH-EUS-depicted hypervascular enhancement diagnosed neuroendocrine tumors with a sensitivity and specificity of 78.9% (95% CI 61.4–89.7%) and 98.7% (95% CI 96.7–98.8%), respectively. Although CH-EUS and MDCT did not differ significantly in diagnostic ability with regard to all lesions, CH-EUS was superior to MDCT in diagnosing small (≤2 cm) carcinomas ($P<0.05$). In 12 neoplasms that MDCT failed to detect, 7 ductal carcinomas and 2 neuroendocrine tumors had hypoenhancement and hyperenhancement on CH-EUS, respectively. When CH-EUS was combined with EUS-FNA, the sensitivity of EUS-FNA increased from 92.2 to 100%.**

CONCLUSIONS: **CH-EUS is useful for characterizing conventional EUS-detected solid pancreatic lesions. EUS equipped with contrast harmonic imaging may play an important role in the characterization of small tumors that other imaging methods fail to depict and may improve the diagnostic yield of EUS-FNA.**

SUPPLEMENTARY MATERIAL is linked to the online version of the paper at http://www.nature.com/ajg

[1]Department of Gastroenterology and Hepatology, Kinki University School of Medicine, Osaka-sayama, Japan; [2]Department of Gastroenterology, Aichi Cancer Center, Nagoya, Japan; [3]Division of Biostatistics, Clinical Research Center, Kinki University School of Medicine, Osaka-sayama, Japan; [4]Department of Radiology, Kinki University School of Medicine, Osaka-sayama, Japan; [5]Department of Surgery, Kinki University School of Medicine, Osaka-sayama, Japan. **Correspondence:** Masayuki Kitano, MD, PhD, Department of Gastroenterology and Hepatology, Kinki University School of Medicine, 377-2 Ohno-higashi, Osaka-sayama 589-8511, Japan. E-mail: m-kitano@med.kindai.ac.jp
Received 26 March 2011; accepted 10 September 2011

The American Journal of GASTROENTEROLOGY

INTRODUCTION

Endoscopic ultrasonography (EUS) is widely used to diagnose pancreatic diseases because its spatial resolution is superior to that of other modalities (1–8). Doppler EUS with and without contrast enhancement allows characterization of pancreatic tumors on the basis of their vascularity (9–14). The hypovascularity is a typical feature of ductal carcinoma on Doppler EUS. However, Doppler EUS is limited in dynamic perfusion imaging with contrast agents. Doppler mode cannot depict very slowly flowing microscopic vessels and parenchymal perfusion (9,15,16). Moreover, Doppler used with ultrasound contrast agents is prone to artifacts such as blooming, which makes the visualized blood vessels wider than when conventional B mode imaging is performed (9,15,16).

Contrast-enhanced harmonic technology allows real-time perfusion imaging without Doppler-related artifacts (15,16), and has improved the depiction and characterization of digestive diseases by transabdominal ultrasonography (US) (17–20). In the first report on contrast harmonic imaging by EUS, large vessels were identified after infusion of the ultrasound contrast, and parenchymal enhancement was observed in the liver of some patients (21). Recently, we found that contrast-enhanced harmonic imaging could be generated by using an echoendoscope with a wide-band transducer (22,23). This EUS system can detect harmonic signals emitted by the contrast agent, and can filter out signals that originate from the tissue. Consequently, contrast-enhanced harmonic EUS (CH-EUS) technology visualizes not only parenchymal perfusion but also the microvasculature in digestive organs (22–26). The aims of the present study were (i) to determine whether solid lesions in the pancreas that are depicted by conventional EUS can be characterized by CH-EUS, (ii) to compare the abilities of CH-EUS and multidetector-row computed tomography (MDCT) in diagnosing pancreatic neoplasms, and (iii) to assess whether CH-EUS can improve the diagnostic yield of EUS-guided fine needle aspiration (EUS-FNA).

METHODS

Patients

Between March 2007 and May 2009, 277 consecutive patients with solid lesions detected by conventional EUS underwent CH-EUS at the Kinki University School of Medicine or the Aichi Cancer Center. For comparison, all enrolled patients also underwent MDCT. None of these 277 patients have been included in previous publications (22–25). Patients who had previously undergone surgical resection of the stomach, had an allergy to the contrast agent, or had severe cardiopulmonary dysfunction were excluded from this study. This study was performed with the approval of the ethics committee of the Kinki University School of Medicine and the Aichi Cancer Center, and written informed consent was obtained from each patient before enrollment.

EUS and CH-EUS

Observation of the pancreas by conventional EUS and CH-EUS was performed by two endosonographers (M.K. and T.T.). The endosonographers used the same protocol and were unaware of the results of the US, CT (previous surveillance), MRCP, endoscopic retrograde cholangiopancreatography, or MDCT investigations. Both endosonographers were experienced in EUS, having performed >3,000 of this procedure. An echoendoscope developed for CH-EUS (GF-UCT260, Olympus Medical Systems, Tokyo, Japan) was used at each institute. Ultrasound images were analyzed using an ALOKA ProSound SSD α-10 (ALOKA, Tokyo, Japan).

The patient was sedated with midazolam and propofol, after which the echoendoscope was inserted into the gastroduodenal lumen. The whole pancreas was first observed by conventional EUS. When conventional EUS revealed a solid lesion (a hypoechoic nodule or heterogeneous region), images of the ideal scanning plane were displayed to portray the whole area of the lesion. Thereafter, the imaging mode was changed to the extended pure harmonic detection (ExPHD) mode. This mode synthesizes the filtered second-harmonic components with signals obtained from the phase shift, which is used for contrast-enhanced harmonic imaging (22,23). The transmitting frequency and mechanical index were 4.7 MHz and 0.3, respectively.

The ultrasound contrast agent, Sonazoid (Daiichi-Sankyo, Tokyo, Japan; GE Healthcare Milwaukee, WI), was used for CH-EUS. This agent consists of microbubbles of perfluorobutane surrounded by a lipid membrane. Immediately before CH-EUS, the contrast agent was reconstituted with 2 ml of sterile water for injection, and a dose of 15 μl/kg body weight was prepared in a 2 ml syringe. A bolus injection of the ultrasound contrast agent was administered at a speed of 1 ml/s through a 22-gauge cannula placed in the antecubital vein. This was followed by a 10-ml saline solution flush to ensure that all contrast was administered into the circulation. After infusion, the pancreas was imaged in a real-time fashion at least for 90 s.

All CH-EUS data were stored in a recording system and reviewed by two readers (M.K. and K.Y.) who were absent during the examination and unaware of the US, CT (previous surveillance), MRCP, or MDCT results. The CH-EUS images were evaluated in a blinded fashion. The interobserver variability of CH-EUS-determined vascular patterns was assessed by calculating the κ-coefficient after the two blinded readers had made their individual independent reading. Thereafter, the two readers reassessed the images of that yielded discrepant findings together to reach an agreement.

EUS-guided fine needle aspiration

After completing the observation of the pancreatic lesion, EUS-FNA was carried out with a 22- or 25-gauge aspiration needle (Cook, Winston-Salem, NC). A cytopathologist was present in the endoscopy room for on-site sample evaluation. If the sample was inadequate, punctures were repeated until adequacy of the sample was ensured with a maximum of five passes. Thereafter, samples were processed and evaluated in the pathology department by using Papanicolaou staining for cytology and hematoxylin–eosin and immunohistochemical staining for histology.

Contrast-enhanced MDCT

All patients were also imaged by contrast-enhanced 64-row MDCT (LightSpeed VCT, General Electric Medical Systems,

Milwaukee, WI). The MDCT was started 30 and 70 s after 2 ml/kg of contrast media (Iopamilon, Bayer Yakuhin, Osaka, Japan) was injected into the antecubital vein. The images were evaluated in a blinded fashion by two radiologists (T.M. and M.O.) with 24 and 16 years of experience in gastrointestinal imaging, respectively, who were completely unaware of the results of the other imaging modalities. The interobserver variability of MDCT-determined vascular patterns was assessed after the two blinded readers had made their individual independent reading ($\kappa = 0.92$). Thereafter, the two readers reassessed the images of that yielded discrepant findings together to reach an agreement.

Diagnosis of pancreatic tumors

Final diagnoses were based on the histology of the resected tumors. For patients who did not undergo surgical resection, final diagnoses were based on the histology or cytology of samples obtained by EUS-FNA. In cases where pancreatic malignancy was excluded on the basis of EUS-FNA, the final diagnosis was confirmed by following the patient for at least 12 months.

Study design

This study was a prospective observational cohort study that had three aims. The first was to determine whether CH-EUS can aid the differential diagnosis of pancreatic solid lesions detected by conventional EUS. The second aim was to compare the abilities of CH-EUS and MDCT in diagnosing pancreatic carcinomas. The third aim was to assess whether CH-EUS improved the diagnostic yield obtained by EUS-FNA.

The solid lesions were classified into four categories: non-enhancement, hypoenhancement, isoenhancement, and hyper-enhancement lesions according to the classification of our previous report on contrast-enhanced harmonic imaging by transabdominal US, which was based on the intensity of enhancement relative to the surrounding tissue (17). Ductal carcinomas were defined as lesions with hypoenhancement, and the sensitivity and specificity of CH-EUS in diagnosing ductal carcinomas in all the lesions, and in the small (≤ 2 cm in diameter) lesions only, were assessed. These CH-EUS sensitivities and specificities were then compared with those of MDCT. Similarly, neuroendocrine tumors were defined as lesions with hyperenhancement, and the sensitivity and specificity with which CH-EUS diagnosed the neuroendocrine tumors in all the lesions, and in the small (≤ 2 cm in diameter) lesions only, were calculated. These CH-EUS sensitivities and specificities were compared with those of MDCT. In addition, when the ductal carcinomas were categorized as a solid lesion on the basis of a positive EUS-FNA and/or hypoenhancement on CH-EUS, the sensitivity and specificity with which the combination of EUS-FNA and CH-EUS diagnosed the ductal carcinomas in surgically resected lesions were calculated. The sensitivity and specificity values in diagnosing ductal carcinomas were compared between EUS-FNA, CH-EUS, and EUS-FNA in combination with CH-EUS.

Statistical analysis

All analyses were performed using the statistical software SAS 9.1.3 (SAS Institute, Cary, NC). A κ-coefficient with >0.8 relat-

ing to the CH-EUS-determined vascular patterns was considered to indicate very good interobserver agreement. Receiver operating characteristic analyses were performed for CH-EUS, MDCT, EUS-FNA, and the combination of EUS-FNA and CH-EUS to examine the diagnostic accuracy as a series of pairs of sensitivity and specificity. The McNemar test was applied to evaluate the difference between CH-EUS and MDCT in terms of differentiating ductal carcinomas from other solid tumors on the basis of vascularity and differentiating neuroendocrine tumors from other solid tumors. The McNemar test was also used to evaluate the differences between CH-EUS alone, EUS-FNA alone, and EUS-FNA combined with CH-EUS in terms of diagnosing ductal carcinomas among solid lesions. When the P value was < 0.05, the difference was regarded as significant.

RESULTS

None of the 277 patients who underwent CH-EUS exhibited any apparent side effects that related to the ultrasound contrast agent. The ExPHD mode for contrast harmonic imaging could not depict the pancreas very clearly before infusion of the ultrasound contrast (**Figure 1a**). After the contrast agent infusion was commenced, echo signals from the ultrasound contrast peaked ~20 s later and parenchymal perfusion images throughout the pancreas could be observed for at least 90 s (**Figure 1b**). In contrast, the conventional EUS images did not change after infusing the contrast (**Figure 1a,b**).

Table 1 shows the final diagnoses of the 277 lesions. The pathological diagnoses of the 277 lesions revealed there were 204, 19, 46, 6, and 2 cases of ductal carcinoma, neuroendocrine tumor, inflammatory pseudotumor, metastasis, and solid pseudopapillary neoplasm, respectively. EUS-FNA was performed in all but one of the 277 patients: the one exception took anticoagulation drugs to prevent the recurrence of acute myocardial infarction that had occurred 1 month previously. For 92 patients, the final diagnoses were made on the basis of surgical resection followed by histology. Diagnoses of the remaining 185 lesions were based on the histology or cytology of samples taken by EUS-FNA and follow-up. In particular, malignancy was excluded in 43 of these 185 patients after pathological diagnosis of EUS-FNA samples and a follow-up period for >12 months.

Based on the intensity of enhancement in the lesions, as shown by CH-EUS, the 277 solid lesions were classified into the following four categories (**Table 2**): nonenhancement ($n = 7$), hypoenhancement ($n = 203$), isoenhancement ($n = 47$), and hyperenhancement ($n = 20$). Nonenhancement lesions are characterized by a lack of enhancement (**Figure 1**). Hypoenhancement lesions are characterized by a heterogeneous distribution and a lower intensity of enhancement relative to the surrounding pancreatic tissue (**Figure 2**). Isoenhancement lesions are characterized by a homogeneous distribution and a similar intensity of enhancement relative to the surrounding pancreatic tissue without any margins (**Figure 3**). Hyperenhancement lesions are characterized by a higher intensity of enhancement relative to the surrounding pancreatic tissue (**Figure 4**). Interobserver agreement testing
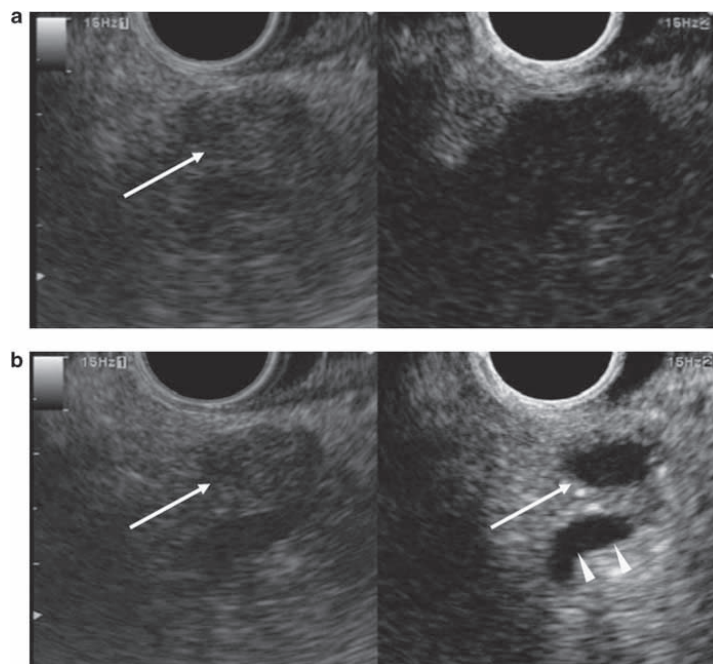
PANCREAS AND BILIARY TRACT

Figure 1. A typical example of a solid lesion with nonenhancement (in this case, an inflammatory pseudotumor). (**a**) Images before infusion of the ultrasound contrast. Conventional endoscopic ultrasonography (EUS; left) reveals a slightly hypoechoic area (arrow) at the pancreas head whereas the specific mode for contrast harmonic imaging (right) cannot depict either the pancreatic parenchyma or the area very clearly. (**b**) Images 30 s after infusion of the ultrasound contrast. Although the conventional EUS images (left) do not change over time, contrast-enhanced harmonic endoscopic ultrasonography (CH-EUS; right) shows parenchymal perfusion imaging in the pancreas, and indicates that this area (arrow) has nonenhancement and a clear margin relative to the surrounding tissue. CH-EUS also shows the pancreatic duct as an avascular structure (arrowheads).

Table 1. Patient characteristics

Age (mean±s.d.)	64.3±11.0
Sex, male/female	173/104
Maximum tumor diameter (mm, mean±s.d.)	32.4±14.9
Pathological diagnosis	n, *Total* (n, *surgically resected*)
Ductal carcinoma	204 (67)
Neuroendocrine tumor	19 (19)
Inflammatory pseudotumor	46 (3)
Metastasis	6 (1)
Solid pseudopapillary neoplasm	2 (2)

revealed that the κ-coefficient for the four vascular patterns was 0.94 ($P < 0.001$). Of the 204 ductal carcinomas, 194 had a hypoenhancement pattern (**Table 2** and **Figure 2;** see **Supplementary Video S1** online), whereas 15 of the 19 neuroendocrine tumors had a hyperenhancement pattern (**Table 2** and **Figure 4;** see

Supplementary Video S2 online) and 42 of the 46 inflammatory pseudotumors had either a nonenhancement or isoenhancement pattern (**Table 2** and **Figures 1** and **3**).

A hypoenhancement pattern, determined by CH-EUS, was calculated to diagnose ductal carcinomas with a sensitivity and specificity of 95.1% and 89.0%, respectively (**Table 3**). The area under the receiver operating characteristic curve (AUC) was 0.91 (see **Supplementary Figure S1** online). Although the AUC of CH-EUS was greater than that of MDCT (0.88), the two imaging methods did not differ significantly in terms of the accuracy with which they diagnosed ductal carcinomas ($P = 0.206$). For small lesions (≤2 cm in diameter), the sensitivity, specificity, and AUC (see **Supplementary Figure S2** online) were 91.2%, 94.4%, and 0.93, respectively (**Table 3**). When only small lesions (≤2 cm in diameter) were considered, CH-EUS was superior to MDCT in diagnosing pancreatic carcinomas ($P = 0.034$). A CH-EUS-determined hyperenhancement pattern could diagnose neuroendocrine tumors with a sensitivity and specificity of 78.9% and 98.0%, respectively. The AUC of the receiver operating characteristic analysis was 0.94. Even for small lesions, a hyperenhancement pattern achieved a sensitivity, specificity, and AUC of 83.0%, 100%, and 0.92, respec-

Table 2. CH-EUS-determined vascular patterns of each solid pancreatic disease

	Vascular pattern (*n*)				
	Nonenhancement	Hypoenhancement	Isoenhancement	Hyperenhancement	Total
Ductal carcinoma	0	194	7	3	204
Neuroendocrine tumor	0	1	3	15	19
Inflammatory pseudotumor	6	4	36	0	46
Metastasis	0	3	1	2	6
SPN	1	1	0	0	2
Total	7	203	47	20	277

CH-EUS, contrast-enhanced harmonic endoscopic ultrasonography; SPN, solid pseudopapillary neoplasm.
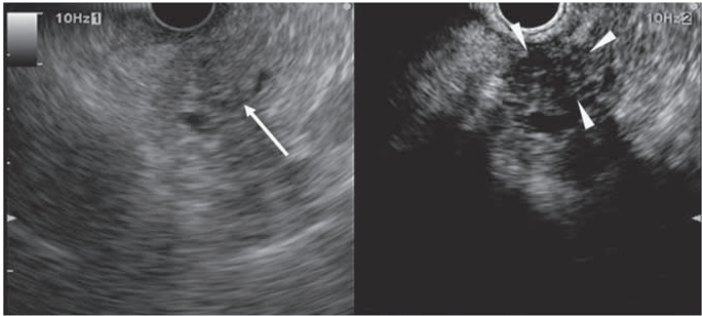
Figure 2. A typical example of a solid lesion with hypoenhancement (in this case, a ductal carcinoma of 15 mm in maximum diameter; see **Supplementary Video S1** online). Conventional endoscopic ultrasonography (EUS; left) shows a heterogeneous area (arrow) without a clear margin at the pancreas head. Contrast-enhanced harmonic endoscopic ultrasonography (CH-EUS; right) indicates that the area is hypovascular (arrowheads) compared with the surrounding tissue.
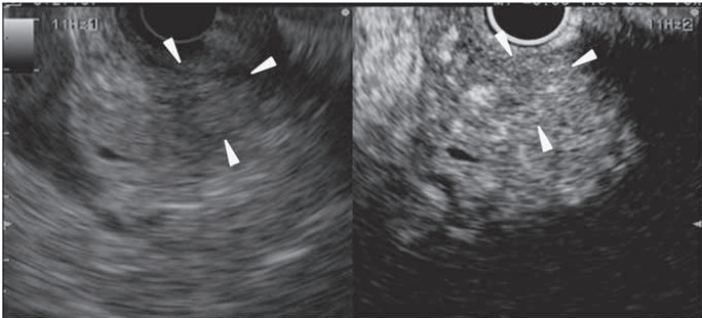
Figure 3. A typical example of a solid lesion with isoenhancement (in this case, an inflammatory pseudotumor). Conventional endoscopic ultrasonography (EUS; left) shows a hypoechoic area (arrowheads) at the pancreas head. Contrast-enhanced harmonic endoscopic ultrasonography (CH-EUS; right) indicates enhancement in this area similar to the surrounding tissue; a margin is not observed.

tively. These values did not differ significantly from those of MDCT (*P* = 0.16 and *P* = 0.5 for all and small lesions, respectively).

Conventional EUS depicted six ductal carcinomas as heterogeneous regions without clear margin. Subsequent CH-EUS showed these six lesions to be hypovascular nodules, and detected their rims (**Figure 2**). MDCT did not depict 12 neoplasms (10 ductal carcinomas and 2 neuroendocrine tumors). All the 12 lesions were <2 cm. CH-EUS depicted 7 of the 10 carcinomas as lesions with hypoenhancement (**Figure 2**). CH-EUS also demonstrated that the two neuroendocrine tumors had hyperenhancement (**Figure 4**).
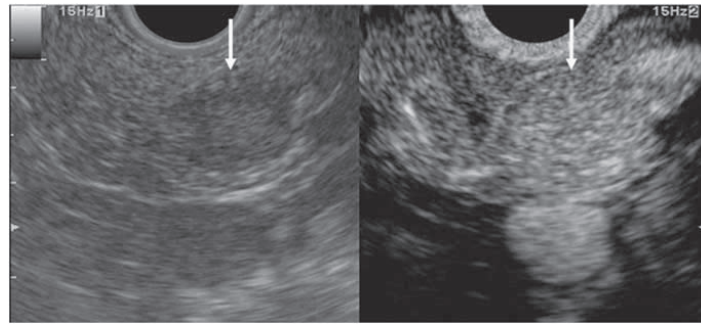
Figure 4. A typical example of a solid lesion with hyperenhancement (in this case, a neuroendocrine tumor of 10 mm in maximum diameter; see **Supplementary Video S2** online). Conventional endoscopic ultrasonography (EUS; left) shows a hypoechoic mass (arrow) at the pancreas body. Contrast-enhanced harmonic endoscopic ultrasonography (CH-EUS; right) indicates that enhancement in the mass is higher than in the surrounding tissue.

Table 3. The sensitivity and specificity of CH-EUS and MDCT in depicting ductal carcinomas as a solid lesion with hypoenhancement

	Sensitivity (95% CI)	Specificity (95% CI)	AUC (s.e.)
Total (n=277)			
CH-EUS	95.1% (92.7−96.7)	89.0% (83.0−93.1)	0.91 (0.02)
MDCT	91.7% (88.9−93.7)	84.2% (76.9−89.7)	0.88 (0.02)
Lesions that are <2 cm (n=67)			
CH-EUS	91.2% (82.5−95.1)	94.4% (86.2−98.1)	0.93 (0.03)
MDCT	70.6% (60.3−76.1)	91.9% (86.2−98.4)	0.81 (0.05)

AUC, area under receiver operating characteristic curve; CH-EUS, contrast-enhanced harmonic endoscopic ultrasonography; 95% CI, 95% confidence interval; MDCT, multidetector-row computed tomography.

Table 4. The sensitivity and specificity of CH-EUS, EUS-FNA, and a combination of EUS-FNA and CH-EUS in diagnosing ductal carcinomas in patients who underwent surgical resection of the tumor (*n*=91)

	Sensitivity (95% CI)	Specificity (95% CI)	AUC (s.e.)
CH-EUS	90.6% (85.5−97.8)	92.6% (80.5−97.8)	0.92 (0.03)
EUS-FNA	92.2% (88.2−92.2)	100% (90.5−100)	0.96 (0.02)
EUS-FNA+CH-EUS[a]	100% (96.4−100)	92.6% (84.1−92.6)	0.96 (0.03)

AUC, area under receiver operating characteristic curve; CH-EUS, contrast-enhanced harmonic endoscopic ultrasonography; 95% CI, 95% confidence interval; EUS-FNA, endoscopic ultrasonography-guided fine needle aspiration; MDCT, multidetector-row computed tomography.
[a]A solid lesion with hypoenhancement on CH-EUS and/or a positive EUS-FNA finding is categorized as a ductal carcinoma.

Table 4 shows the sensitivities, specificities, and AUCs for CH-EUS, EUS-FNA, and EUS-FNA combined with CH-EUS in terms of diagnosing ductal carcinomas in 91 patients who underwent surgical resection of the tumor. The sensitivity, specificity, and AUC (see **Supplementary Figure S3** online) with which EUS-FNA diagnosed ductal carcinomas were 92.2%, 100%, and 0.96, respectively (**Table 4**). EUS-FNA and CH-EUS did not differ significantly in terms of the diagnostic accuracy ($P=0.58$). However, the specificity of EUS-FNA (100%) was higher than CH-EUS (92.6%) (**Table 4**). In contrast, there were five cases with false-negative EUS-FNA findings, whereas CH-EUS revealed that those five tumors had hypoenhancement. When the ductal carcinomas were regarded as a tumor with hypoenhancement on CH-EUS and/or a positive EUS-FNA, the sensitivity, specificity, and AUC with which ductal carcinomas were diagnosed was 100%, 92.6%, and 0.96, respectively (**Table 4**). Combining CH-EUS with EUS-FNA increased the sensitivity of EUS-FNA from 92.2 to 100%.

DISCUSSION

Ultrasound contrast agents composed of microbubbles produce stronger second harmonic signals as well as a greater phase shift than does the tissue by resonance (23). The ExPHD mode employed for CH-EUS selectively detects signals from microbubbles and filters those from the tissue by combining the phase-shift signals with the second harmonic signals (23). Although this processing cannot depict pancreatic tissue very clearly before infusion of an ultrasound contrast, imaging of the signals of microbubbles located in the pancreatic vasculature can be achieved after infusion. In contrast, remarkable changes are not observed in conventional EUS images of the pancreas after contrast agent infusion because conventional EUS depicts signals from tissue rather than

from microbubbles. Thus, images of parenchymal perfusion in the pancreas can only be obtained when contrast agents are combined with the use of the ExPHD mode, a specific mode for contrast harmonic imaging. This novel imaging technology in the field of EUS allows the characterization of a pancreatic solid lesion by estimating its vascularity, which is difficult by conventional EUS. EUS mostly depicts ductal carcinomas, neuroendocrine tumors, and inflammatory pseudotumors as solid hypoechoic masses, and it is sometimes difficult to differentiate benign from malignant pancreatic masses (27). In the present study, CH-EUS enabled us to categorize pancreatic lesions that are depicted by conventional EUS into four vascular patterns: nonenhancement, hypoenhancement, isoenhancement, and hyperenhancement lesions. The κ-coefficient for the four vascular patterns was 0.94, indicating good reproducibility.

The vast majority of the diagnosed pancreatic carcinomas were found to have a hypoenhancement pattern, namely a heterogeneous distribution and a lower intensity of enhancement relative to the surrounding pancreatic tissue. Recently, two different groups reported that CH-EUS with the ultrasound contrast agent SonoVue (Bracco Imaging, Milan, Italy) could be used to diagnose pancreatic carcinomas with high sensitivity (89% and 96% positive identification in 35 and 90 patients, respectively) (28,29). The present study used a different ultrasound contrast agent (Sonazoid) to diagnose pancreatic carcinomas in a large number of patients with a similar high sensitivity (95%), and the specificity (89%) was equal to or even higher than those of the previous two reports (88% and 64%, respectively). CH-EUS with Sonazoid depicted neuroendocrine tumors as hypervascular lesions with a sensitivity of 79%, which is again higher than those in the previous two reports (67% and 69%, respectively). Our experiences with CH-EUS using Sonazoid and SonoVue indicate that the two ultrasound contrast agents differ in terms of intensities and durations of signaling after infusion. CH-EUS images obtained with SonoVue disappear within 60 s, which limits the duration of observation (22). In contrast, after infusion of Sonazoid, parenchymal perfusion can be observed throughout the pancreas for at least 90 s (the present study). Thus, the longer-lasting effect of Sonazoid improves the observation of the pancreas by CH-EUS. The differences in the diagnostic accuracy for the pancreatic tumors by the two ultrasound contrast agents would appear to be related to differences in their signaling intensities and durations.

Most carcinomas exhibit a hypoenhancement pattern on MDCT, which is frequently employed for the detection and characterization of pancreatic ductal carcinomas (30,31). In the present study, the AUCs of CH-EUS for diagnosis of ductal carcinomas were greater than those of MDCT. When all lesions were considered, CH-EUS and MDCT did not differ significantly in terms of the diagnostic accuracy for ductal carcinomas. However, when small lesions (≤2 cm in diameter) were considered, CH-EUS was significantly more accurate than MDCT in diagnosing carcinomas ($P = 0.034$). This result may be related to the superior spatial resolution that is obtained with EUS (1–8). Indeed, EUS detected, as solid lesions, 10 carcinomas and 2 neuroendocrine tumors that MDCT did not detect. The 12 lesions were <2 cm. Subsequent CH-EUS revealed that 7 of the 10 carcinomas and the 2 neuro-

endocrine tumors displayed hypoenhancement and hyperenhancement, respectively. Thus, when EUS detects a small solid lesion not detected by MDCT, CH-EUS could be helpful in characterizing the lesion by depicting its vasculature.

EUS-FNA is also a useful tool for characterizing a solid mass detected by conventional EUS (27). If the EUS-FNA diagnosis is a malignant tumor, patients should be recommended to undergo surgery because EUS-FNA is highly specific for the identification of pancreatic carcinomas. However, deciding between surgery and follow-up in patients whose EUS-FNA findings are negative is sometimes difficult, because false-negative EUS-FNA results cannot be excluded. When Napoleon et al. (29) compared CH-EUS and EUS-FNA for the identification of pancreatic carcinomas, the sensitivity of CH-EUS for carcinoma identification was higher than that of EUS-FNA, and four of the five carcinomas with false-negative EUS-FNA findings had hypoenhancement. In the present study, CH-EUS was not superior to EUS-FNA for identification of pancreatic carcinomas. However, CH-EUS found that all ductal carcinomas with false-negative EUS-FNA findings had hypoenhancement. When the ductal carcinomas were regarded as a tumor with a positive EUS-FNA and/or a hypoenhancement on CH-EUS, combining CH-EUS with EUS-FNA improved the sensitivity with which EUS-FNA identified ductal carcinomas from 92.2 to 100%. Therefore, CH-EUS before EUS-FNA complements EUS-FNA in identifying ductal carcinomas and helps making decisions about the next treatment approach. Thus, when CH-EUS reveals a hypovascular pattern in a pancreatic tumor, even if the EUS-FNA findings are negative, surgical resection or pathological re-evaluation by EUS-FNA of the tumor should be recommended.

Interestingly, CH-EUS is better than conventional EUS in clearly depicting the outline of six pancreatic carcinomas. Fusaroli et al. (28) also reported that CH-EUS allowed the detection of small lesions in seven patients who had uncertain standard EUS findings because of biliary stents or chronic pancreatitis. These results suggest that contrast harmonic imaging might be useful for the identification of some lesions that were not clearly defined by conventional EUS. In addition, it is likely that CH-EUS facilitates EUS-FNA of lesions by helping to identify the target for EUS-FNA. To prove the real utility of contrast harmonic enhancement for increasing the diagnostic yield of EUS-FNA, a study comparing the diagnostic accuracy of CH-EUS-guided FNA with that of conventional EUS-guided FNA should be performed.

We conclude that CH-EUS is useful for characterizing solid lesions identified in the pancreas by conventional EUS, particularly small ones that other imaging methods cannot identify. CH-EUS also complements EUS-FNA by improving its sensitivity.

CONFLICT OF INTEREST
Guarantor of the article: Masayuki Kitano, MD, PhD.
Specific author contributions: M. Kitano: writing of the manuscript, drafting conception and design, and performing EUS;

Study Highlights

WHAT IS CURRENT KNOWLEDGE

✔ Pancreatic carcinoma has a particularly poor prognosis, because it is difficult to diagnose at an early stage.

✔ Endoscopic ultrasonography (EUS) is a highly sensitive method for detecting pancreatic lesions, especially small tumors.

✔ Contrast-enhanced harmonic EUS (CH-EUS) technology visualizes not only the parenchymal perfusion, but also the microvasculature in the pancreas.

WHAT IS NEW HERE

✔ CH-EUS effectively characterizes solid lesions that are detected in the pancreas by conventional EUS.

✔ CH-EUS-determined hypoenhancement pattern diagnosed ductal carcinoma with high sensitivity and specificity.

✔ CH-EUS is superior to multidetector-row computed tomography (MDCT) in distinguishing small ductal carcinomas from other tumors, and plays an important role in the characterization of small tumors that MDCT cannot detect.

✔ Combining CH-EUS with endoscopic ultrasonography-guided fine needle aspiration (EUS-FNA) improves the sensitivity with which EUS-FNA identifies ductal carcinomas.

REFERENCES

1. Rösch T, Lorenz R, Braig C *et al.* Endoscopic ultrasound in pancreatic tumor diagnosis. Gastrointest Endosc 1991;37:347–52.
2. Yasuda K, Mukai H, Nakajima M *et al.* Staging of pancreatic carcinoma by endoscopic ultrasonography. Endoscopy 1993;25:151–5.
3. Gress FG, Hawes RH, Savides TJ *et al.* Role of EUS in the preoperative staging of pancreatic cancer: a large single-center experience. Gastrointest Endosc 1999;50:786–91.
4. DeWitt J, Devereaux B, Chriswell M *et al.* Comparison of endoscopic ultrasonography and multidetector computed tomography for detecting and staging pancreatic cancer. Ann Internal Med 2004;141:753–63.
5. Ngamruengphong S, Zhou Y, Chak A *et al.* EUS and survival in patients with pancreatic cancer: a population-based study. Gastrointes Endosc 2010;72:78–83.
6. Rösch T, Lightdale CJ, Botet JF *et al.* Localization of pancreatic endocrine tumors by endoscopic ultrasonography. N Eng J Med 1992;326:1721–6.
7. Khashab MA, Yong E, Lennon AM *et al.* EUS is still superior to multidetector computed tomography for detection of pancreatic neuroendocrine tumors. Gastrointest Endosc 2011;73:691–6.
8. Ishikawa T, Itoh A, Kawashima H *et al.* Usefulness of EUS combined with contrast-enhancement in the differential diagnosis of malignant versus benign and preoperative localization of pancreatic endocrine tumors. Gastrointes Endosc 2010;71:951–9.
9. Sakamoto H, Kitano M, Suetomi Y *et al.* Utility of contrast-enhanced endoscopic ultrasonography for diagnosis of small pancreatic carcinomas. Ultrasound Med Biol 2008;34:525–32.
10. Becker D, Strobel D, Bernatik T *et al.* Echo-enhanced color- and power-Doppler EUS for the discrimination between focal pancreatitis and pancreatic carcinoma. Gastrointest Endosc 2001;53:784–9.
11. Săftoiu A, Popescu C, Cazacu S *et al.* Power Doppler endoscopic ultrasonography for the differential diagnosis between pancreatic cancer and pseudotumoral chronic pancreatitis. J Ultrasound Med 2006;25:363–72.
12. Hocke M, Schulze E, Gottschalk P *et al.* Contrast-enhanced endoscopic ultrasound in discrimination between focal pancreatitis and pancreatic cancer. World J Gastroenterol 2006;12:246–50.
13. Dietrich CF, Ignee A, Braden B *et al.* Improved differentiation of pancreatic tumors using contrast-enhanced endoscopic ultrasound. Clin Gastroenterol Hepatol 2008;6:590–7.
14. Săftoiu A, Iordache SA, Gheonea DI *et al.* Combined contrast-enhanced power Doppler and real-time sonoelastography performed during EUS, used in the differential diagnosis of focal pancreatic masses (with videos). Gastrointest Endosc 2010;72:739–47.
15. Kudo M. Various contrast-enhanced imaging modes after administration of Levovist. In Kudo M (ed). Contrast Harmonic Imaging in the Diagnosis and Treatment of Hepatic Tumors. Springer: Tokyo, 2003, pp. 22–30.
16. Whittingham TA. Contrast-specific imaging techniques; technical perspective. In Quaia E (ed). Contrast Media in Ultrasonography. Basic Principles and Clinical Applications. Springer: Berlin, 2005, pp. 43–84.
17. Kitano M, Kudo M, Maekawa K *et al.* Dynamic imaging of pancreatic diseases by contrast enhanced coded phase inversion harmonic ultrasonography. Gut 2004;53:854–9.
18. Inoue T, Kitano M, Kudo M *et al.* Diagnosis of gallbladder diseases by contrast-enhanced phase-inversion harmonic ultrasonography. Ultrasound Med Biol 2007;33:353–61.
19. Fukuta N, Kitano M, Maekawa K *et al.* Estimation of the malignant potential of gastrointestinal stromal tumors: the value of contrast-enhanced coded phase-inversion harmonic US. J Gastroenterol 2005;40:247–55.
20. Kersting S, Konopke R, Kersting F *et al.* Quantitative perfusion analysis of transabdominal contrast-enhanced ultrasonography of pancreatic masses and carcinomas. Gastroenterology 2009;137:1903–11.
21. Dietrich CF, Ignee A, Frey H. Contrast-enhanced endoscopic ultrasound with low mechanical index: a new technique. Z Gastroenterol 2005;43:1219–3.
22. Kitano M, Sakamoto H, Matsui U *et al.* A novel perfusion imaging technique of the pancreas: contrast-enhanced harmonic EUS (with video). Gastrointest Endosc 2008;67:141–50.
23. Kitano M, Kudo M, Sakamoto H *et al.* Preliminary study of contrast-enhanced harmonic endosonography with second-generation contrast agents. J Med Ultrasonics 2008;35:11–8.
24. Xia Y, Kitano M, Kudo M *et al.* Characterization of intra-abdominal lesions of undetermined origin by contrast-enhanced harmonic EUS (with video). Gastrointest Endosc 2010;72:637–42.
25. Sakamoto H, Kitano M, Matsui S *et al.* Estimation of malignant potential of GI stromal tumors by contrast-enhanced harmonic EUS (with videos). Gastrointest Endosc 2011;73:227–37.
26. Romagnuolo J, Hoffman B, Vela S *et al.* Accuracy of contrast-enhanced harmonic EUS with a second-generation perflutren lipid microsphere contrast agent (with video). Gastrointest Endosc 2011;73:52–63.
27. DeWitt J. EUS in pancreatic neoplasms. In: Hawes RH, Fockens P (eds). Endosonography. Saunders Elsevier: Philadelphia, 2006, pp. 177–203.
28. Fusaroli P, Spada A, Mancino MG *et al.* Contrast harmonic echo-endoscopic ultrasound improves accuracy in diagnosis of solid pancreatic masses. Clin Gastroenterol Hepatol 2010;8:629–34.
29. Napoleon B, Alvarez-Sanchez MV, Gincoul R *et al.* Contrast-enhanced harmonic endoscopic ultrasound in solid lesions of the pancreas: results of a pilot study. Endoscopy 2010;42:564–70.
30. Boland GW, O'Malley ME, Saez M *et al.* Pancreatic-phase versus portal vein-phase helical CT of the pancreas: optimal temporal window for evaluation of pancreatic adenocarcinoma. Am J Roentgenol 1999;172:605–8.
31. Imbriaco M, Megibow AJ, Ragozzino A *et al.* Value of the single-phase technique in MDCT assessment of pancreatic tumors. Am J Roentgenol 2005;184:1111–7.

Plasma Concentrations of Angiogenesis-related Molecules in Patients with Pancreatic Cancer

Hiroki Sakamoto[1], Hideharu Kimura[2], Masaru Sekijima[3], Kazuko Matsumoto[2], Tokuzo Arao[2,*], Takaaki Chikugo[4], Yasuhide Yamada[5], Masayuki Kitano[1], Akihiko Ito[4], Yoshifumi Takeyama[6], Masatoshi Kudo[1] and Kazuto Nishio[2,*]

[1]Department of Gastroenterology and Hepatology, Kinki University School of Medicine, 377-2 Ohno-higashi, Osaka-Sayama, Osaka 589-8511, [2]Department of Genome Biology, Kinki University School of Medicine, 377-2 Ohno-higashi, Osaka-Sayama, Osaka 589-8511, [3]Advanced Medical Science Research Center, Mitsubishi Chemical Medience Corporation, 14 Sunayama, Kamisu, Ibaraki 314-0255, [4]Department of Pathology, Kinki University School of Medicine, 377-2 Ohno-higashi, Osaka-Sayama, Osaka 589-8511, [5]Department of Medical Oncology, National Cancer Center Hospital, Tsukiji 5-1-1, Chuo-ku, Tokyo 104-0045 and [6]Department of Surgery, Kinki University School of Medicine, 377-2 Ohno-higashi, Osaka-Sayama, Osaka 589-8511, Japan

*For reprints and all correspondence: Tokuzo Arao and Kazuto Nishio, Department of Genome Biology, Kinki University School of Medicine, 377-2 Ohno-higashi, Osaka-Sayama, Osaka 589-8511, Japan. E-mail: arao@med.kindai.ac.jp; knishio@med.kindai.ac.jp

Background: Anti-angiogenic agents are now being clinically evaluated for the treatment of pancreatic cancer and a detailed investigation of the angiogenic profile of pancreatic cancer is needed. The aim of this study was to evaluate the plasma concentrations of angiogenesis-related molecules in patients with pancreatic cancer, compared with those with other diseases.
Methods: Plasma samples obtained from 45 patients with pancreatic cancer were analyzed and compared with those from 9 patients with pancreatitis, 16 patients with benign hepatobiliary diseases and 58 patients with colorectal cancers. The plasma levels of angiogenesis-related molecules including angiopoietin-2, follistatin, granulocyte-colony stimulating factor, hepatocyte growth factor, interleukin-8, leptin, platelet-derived growth factor beta polypeptide, platelet endothelial cell adhesion molecule-1 and vascular endothelial growth factor were determined using an antibody suspension bead arrays system.
Results: The plasma levels of all the angiogenesis-related molecules were not increased in patients with pancreatic cancer, compared with those with pancreatitis and benign hepatobiliary diseases, whereas the levels of those with colorectal cancer were markedly increased. The plasma interleukin-8 concentration was significantly elevated in patients with distant metastases and was associated with a poor treatment outcome of chemotherapy in patients with pancreatic cancer.
Conclusions: The plasma levels of angiogenesis-related molecules were not elevated in patients with pancreatic cancer, compared with those with benign diseases or colorectal cancer. The plasma interleukin-8 level may be a novel biomarker for the response to chemotherapy in patients with pancreatic cancer and warrants further prospective study.

Key words: pancreatic cancer − angiogenesis − plasma − IL-8

INTRODUCTION

Pancreatic cancer (PC) is a highly metastatic and biological-ly aggressive malignancy that is the fourth leading cause of death from cancer, with an overall 5-year survival rate of 6% and a median survival period of <6 months (1). The only potential cure is surgery. However, since the diagnosis of PC is often established at an advanced stage, <20% of patients diagnosed with this disease are suitable candidates for surgi-cal resection.

Tumor angiogenesis, the process of new blood vessel for-mation, is considered to be an important mechanism for solid tumors to proliferate and metastasize beyond the limits of passive diffusion ($\sim$2–3 mm^3) in the setting of tumor growth (2). The balance between pro- and anti-angiogenic factors is shifted to enable the sustained production of pro-angiogenic factors, leading to the production of new blood vessels that support the tumor. Angiogenesis is crucial for the proliferation and metastasis of solid tumors, including PC (3). To date, anti-angiogenic agents are widely used for standard treatment in colorectal cancer (CC), renal cell car-cinoma and hepatocellular carcinoma and are now consid-ered to be well-validated targets for cancer treatment (4). Especially, vascular endothelial growth factor (VEGF)-tar-geted therapy has become important for the systemic treatment of several solid tumors. Therefore, anti-angiogenic agents are currently under extensive investigation as novel approaches to the management of PC. Although a monoclo-nal antibody to VEGF and axitinib, a small-molecule tyrosine-kinase inhibitor, have yielded promising response rates in some phase II studies, they have not been shown to prolong survival when added to chemotherapy in any rando-mized phase III trials for patients with PC (5–8). Angiogenesis-targeted therapy is now under clinical evalu-ation in patients with PC; therefore, a detailed investigation of the angiogenic profile of PC is needed.

The imaging findings of PC are commonly believed to reveal hypo-vascular tumors; however, several studies have shown an association between elevated VEGF expression and the intra-tumoral microvessel density (9,10), an increased size and the enhanced local spreading of the tumor (9), the presence of liver metastases and a poor prognosis in patients with PC (11–13). Meanwhile, plasma or serum angiogenesis-related molecules, including both pro- and anti-angiogenic factors, are expected to be biomarkers of tumor-related angio-genesis. Some studies have shown that a high level of circu-lating VEGF can be used as a prognostic factor in patients with PC (14,15). To date, however, no data on angiogenesis-related molecules in patients with PC compared with those in patients with other cancers or benign pancreatic disease or the simultaneous measurement of multiplex factors have been reported. Thus, the angiogenic profile remains unclear in patients with PC, and such data may be useful for introducing anti-angiogenic therapy for the treatment of PC. We previous-ly showed that the antibody suspension bead arrays system was a powerful tool for screening biomarkers in a clinical

setting (16) In this study, we measured the plasma levels of angiogenesis-related factors in patients with PC and then evaluated the correlations between these levels and the clinic-al characteristics of patients with PC.

PATIENTS AND METHODS

PATIENTS

A total of 45 patients diagnosed as having PC at the Kinki University Hospital, Osaka, Japan, between April 2007 and March 2009 were enrolled. The patients' characteristics are shown in Table 1. The diagnosis of PC was confirmed by histopathological examination of a resected tumor, biopsy or cytology specimen. The staging of the PC was determined according to the TNM classification. The clinical features of the patients, including age, sex, tumor location and size, TNM staging, presence of distant metastasis, performance status (PS), CRP, carcinoembryonic antigen (CEA), carbohy-drate antigen 19-9 (CA19-9) and treatment were recorded. Among the 23 patients who received chemotherapy (10 with gemcitabine alone, 5 with TS-1 alone and 8 with a combin-ation of gemcitabine and TS-1), the response to chemother-apy, the progression-free survival time and the overall survival time were recorded. The tumor response was evalu-ated at a month after the start of therapy and every 2 months thereafter using computerized tomography according to the

Table 1. Patient characteristics

	PC		CC (n = 58)	P (n = 9)	HD (n = 16)
	All (n = 45)	Chemotherapy (n = 23)			
Age (years)					
Median	69	68	58	65	67
Range	39–81	39–80	31–79	43–78	50–84
Gender					
Male	16	6	37	9	11
Female	29	17	21	0	5
TNM stage					
I, II	7	0	9	—	—
III, IV	38	23	49	—	—
Lymph node metastasis					
Negative	23	9	11	—	—
Positive	22	14	47	—	—
Distant metastasis					
Negative	31	14	54	—	—
Positive	41	9	4	—	—

PC, pancreatic cancer; CC, colorectal cancer; P, pancreatitis; HD, hepatobiliary disease.

response evaluation criteria in solid tumors; the response was then classified as a complete response, a partial response, stable disease or progressive disease. The patients with PC ($n = 45$), pancreatitis (P, $n = 9$) or benign hepatobiliary disease (HD, $n = 16$) were treated at the Kinki University Hospital and the 58 patients with CC were treated at the National Cancer Center Hospital, Tokyo, Japan (16). All nine patients in the pancreatitis group had chronic pancreatitis and the patients in the benign hepatobiliary disease group consisted of 12 patients with stones in the bile duct or gallbladder and 4 patients with acute cholangitis. Informed consent was obtained from all the subjects, and the study was approved by the institutional review board at Kinki University Hospital and National Cancer Center Hospital.

BLOOD SAMPLE COLLECTION AND PREPARATION OF PLASMA SAMPLE

Blood samples were collected before the initial treatments. Four milliliters of peripheral venous blood was drawn into a tube containing ethylenediaminetetraacetic acid (EDTA) and immediately prepared by centrifugation at $\times 1200\,g$ for 10 min. Plasma samples were removed and stored at $-80°C$ until use.

MEASUREMENT OF ANGIOGENESIS-RELATED FACTORS IN PLASMA

The plasma concentrations of angiogenesis-related factors were measured using an antibody suspension bead array, Bio-Plex Pro™ Assays and Human Angiogenesis 9-Plex Panel (Bio-Rad Laboratories, Hercules, CA). The molecules used in this panel were as follows: angiopoietin-2, follistatin, granulocyte-colony stimulating factor (G-CSF), hepatocyte growth factor (HGF), interleukin-8 (IL-8), leptin, platelet-derived growth factor beta polypeptide (PDGF-BB), platelet endothelial cell adhesion molecule-1 (PECAM-1) and VEGF. Data were obtained using a Bio-Plex suspension array system® (Bio-Rad Laboratories, Hercules, CA). The assay was performed according to the manufacturer's instructions and a previously described method (16,17). Plasma samples were diluted 1 in 4 with the appropriate diluents prior to assay. The samples were tested in duplicate and the averages were used for analysis.

STATISTICAL ANALYSIS

The plasma levels of each angiogenesis-related molecule were summarized as the mean and standard deviation and then compared between the group of patients with PC and the group with CC, pancreatitis or benign hepatobiliary disease using the Mann–Whitney test. In a group of patients with PC, the plasma levels were compared across subgroups of patients on the basis of age (≤ 60 years vs. >60 years), sex, tumor location (head vs. body or tail), tumor size (≤ 20 mm vs. >20 mm), TNM stage (I, II vs. III, IV), lymph node metastasis status and distant metastasis status

using the Mann–Whitney test. The analyses for survival time [progression-free survival (PFS) and overall survival (OS)] were performed in the group of patients who received chemotherapy. In terms of the analysis for survival time, clinical factors including age (≤ 60 years vs. >60 years), sex, tumor size (≤ 20 mm vs. >20 mm), TNM stage (I, II vs. III, IV), lymph node metastasis status, distant metastasis status, PS, CRP, CEA, CA19-9 and the plasma levels of each angiogenesis-related factor were examined using the Cox proportional hazards model. The survival distributions for PFS and OS were estimated using the Kaplan–Meier method. The differences between two groups were compared using the log-rank test. A P value <0.05 was considered statistically significant. Data analyses were performed using IBM® SPSS® Statistics 19 software (IBM Corporation, Somers, NY).

RESULTS

PATIENT CHARACTERISTICS

A total of 45 patients with PC, 9 patients with pancreatitis, 16 patients with benign hepatobiliary diseases and 58 patients with TNM stage-matched CCs were enrolled in this study (Table 1). The patients with PC ranged in age from 39 to 81 years, with a median of 69 years and the male:female ratio was 16:29. The TNM stages of the patients with PC were as follows: stage I, 5; stage II, 2; stage III, 22 and stage IV, 16. Among the patients with PC, 10 patients received surgery, 4 received best supportive care and 31 received chemotherapy. The clinical data for 8 patients who received chemotherapy was missing, so 23 patients receiving chemotherapy were analyzed.

PLASMA CONCENTRATIONS OF ANGIOGENESIS-RELATED MOLECULES AMONG PATIENTS WITH PC COMPARED WITH THOSE WITH CC, PANCREATITIS OR BENIGN HEPATOBILIARY DISEASE

The plasma concentrations of angiogenesis-related molecules are shown in Fig. 1. The plasma concentrations of all the molecules could be determined in all the samples except for two samples in which the leptin concentrations were below the detectable limit. The levels of G-CSF, HGF, IL-8, leptin, PECAM-1 and VEGF in the patients with PC were significantly lower than those in the patients with colon cancer. The plasma concentration of follistatin in patients with PC was significantly higher than that in patients with colon cancer. Compared with the patients with benign diseases, the concentrations of follistatin, HGF and VEGF in the patients with PC were significantly lower than those in the patients with either pancreatitis or benign hepatobiliary disease, while the leptin level was lower than that in patients with benign hepatobiliary disease. These results clearly indicated that the concentrations of most angiogenesis-related molecules were not elevated in patients with PC but were elevated in patients with CC.
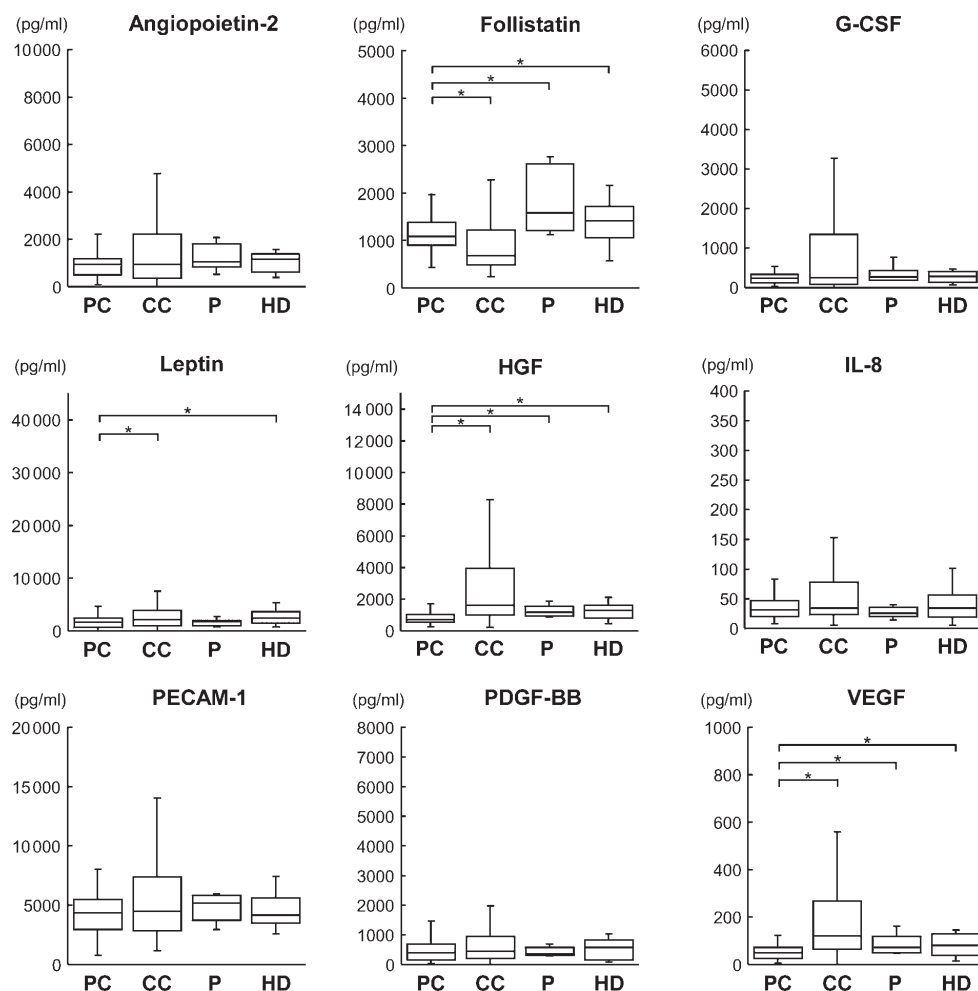
Figure 1. Plasma concentrations of angiogenesis-related molecules in patients with pancreatic cancer, colon cancer, pancreatitis or hepatobiliary disease. The differences in the follistatin, hepatocyte growth factor (HGF), leptin and vascular endothelial growth factor (VEGF) levels between the pancreatic cancer group and the other groups were statistically significant (*$P < 0.05$). The top and bottom quartiles and the median values are depicted as box plots.

CORRELATION BETWEEN ANGIOGENESIS-RELATED MOLECULES AND THE CLINICAL FEATURES OF ALL THE PC PATIENTS

Next, we evaluated the correlation between the plasma concentrations of angiogenesis-related molecules and clinical features including age, sex, tumor location, tumor size, TNM stage, lymph node metastasis and distant metastasis in all the patients with PC (Table 2). Although the reason remains unknown, the plasma concentrations of HGF and PECAM were significantly elevated in the older age group. Regarding distant metastasis, the plasma IL-8 level was significantly higher in the metastasis-positive group than in the metastasis-negative group ($P = 0.024$, Fig. 2, Table 2). The

HGF and angiopoietin-2 levels tended to be higher in the metastasis-positive group, but the differences were not significant ($P = 0.073$ and $P = 0.073$).

UNIVARIATE ANALYSIS OF CLINICAL BIOMARKERS FOR PFS AND OS

To find biomarkers for the response to chemotherapy among patients with PC, clinical molecular factors were evaluated according to treatment outcome among chemotherapy-treated patients with PC (Table 3). The CRP, CEA and CA19-9 levels were significantly associated with PFS ($P = 0.026$, 0.015 and 0.017, respectively), and the CEA and CA19-9

Table 2. Correlation between plasma angiogenic molecules and patient characteristics in pancreatic cancer

	n	Angiopoietin-2	Follistatin	G-CSF	HGF	IL-8	Leptin	PDGF-BB	PECAM	VEGF
Age (years)										
≤60	10	805.9 ± 447.5	1059.5 ± 317.9	223.7 ± 156.9	604.7 ± 316.2	26.6 ± 11.2*	1121.9 ± 964.4	373.2 ± 350.4	3336.9 ± 1709.6	44.3 ± 35.0*
>60	35	1107.1 ± 858.9	1216.0 ± 530.2	294.4 ± 301.7	956.9 ± 518.9	45.2 ± 34.3	2004.0 ± 1599.3	623.8 ± 670.7	4657.8 ± 1733.7	61.9 ± 48.6
Gender										
Male	16	1218.7 ± 1041.2	1285.2 ± 569.0	338.2 ± 411.9	1010.2 ± 573.2	45.3 ± 30.1	1679.6 ± 2021.3	541.8 ± 529.2	4817.5 ± 2095.5	64.9 ± 57.5
Female	29	941.7 ± 613.3	1123.8 ± 444.5	245.8 ± 163.8	806.1 ± 449.7	38.7 ± 32.2	1878.8 ± 1190.7	582.7 ± 672.7	4114.1 ± 1593.6	54.1 ± 39.2
Tumor location										
Head	25	883.3 ± 541.7	1195.6 ± 487.7	244.9 ± 182.0	808.0 ± 392.2	41.9 ± 34.8	1635.9 ± 1159.1	551.6 ± 707.2	4166.9 ± 1718.1	54.0 ± 43.5
Body tail	20	1236.3 ± 1004.2	1163.2 ± 509.8	321.0 ± 364.5	966.8 ± 609.1	40.1 ± 27.8	2023.1 ± 1884.0	588.73 ± 506.2	4610.9 ± 1906.2	62.9 ± 50.0
Tumor size										
≤20 mm	8	840.2 ± 434.8	1075.4 ± 388.5	241.5 ± 159.8	637.7 ± 384.9	26.2 ± 12.7	1542.5 ± 1039.5	572.1 ± 486.3	4314.0 ± 2230.0	50.1 ± 37.9
>20 mm	37	1083.5 ± 847.8	1204.1 ± 513.5	286.8 ± 297.8	930.7 ± 511.5	44.3 ± 33.5	1865.4 ± 1608.5	567.3 ± 650.5	4375.1 ± 1700.1	59.7 ± 48.1
TNM stage										
I, II	7	1006.9 ± 611.0	1183.4 ± 320.5	318.1 ± 260.2	660.2 ± 297.1	32.1 ± 18.6	2088.6 ± 1625.6	541.1 ± 483.8	4613.7 ± 2452.5	60.9 ± 44.5
III, IV	38	1046.3 ± 827.6	1180.8 ± 520.9	271.5 ± 283.1	918.9 ± 522.3	42.7 ± 33.3	1756.3 ± 1514.6	573.1 ± 646.8	4318.3 ± 1688.3	57.4 ± 47.0
Lymph node metastasis										
Absence	23	1017.6 ± 787.8	1312.3 ± 574.9	309.1 ± 352.0	822.8 ± 466.2	39.9 ± 36.2	1910.1 ± 1866.0	654.6 ± 770.5	4523.6 ± 2115.9	62.7 ± 55.0
Presence	22	1063.8 ± 813.9	1044.2 ± 350.4	247.0 ± 171.0	937.0 ± 538.6	42.3 ± 26.6	1701.2 ± 1075.7	477.7 ± 406.8	4197.7 ± 1420.6	52.9 ± 35.2
Distant metastasis										
Absence	31	942.1 ± 761.8	1218.9 ± 539.7	288.7 ± 326.1	789.5 ± 426.4	37.7 ± 33.9	1943.6 ± 1714.2*	585.0 ± 708.7	4313.4 ± 2022.2	58.1 ± 52.3
Presence	14	1257.4 ± 842.1	1097.7 ± 369.8	256.7 ± 119.3	1075.9 ± 606.0	48.7 ± 24.8	1507.6 ± 936.7	530.8 ± 371.1	4476.7 ± 1213.1	57.6 ± 30.2

*$P < 0.05$ using the Mann–Whitney Test compared with the other group. Data indicates the mean and standard deviation (pg/ml).
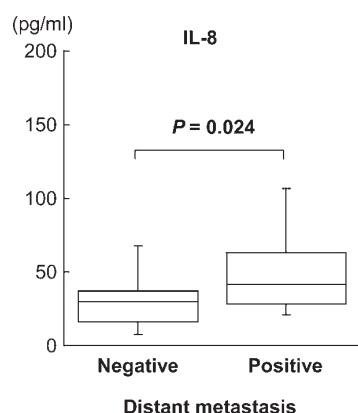
Figure 2. The plasma interleukin-8 (IL-8) was significantly higher among patients with metastasis than those without metastasis in patients with pancreatic cancer. The median IL-8 levels in patients with metastasis and without metastasis were 41.6 pg/ml (range, 21.2–106.5 pg/ml) and 26.8 pg/ml (range, 7.9–171.6 pg/ml), respectively. The top and bottom quartiles and the median values are depicted as box-plots.

levels were significantly associated with OS ($P = 0.003$ and 0.012, respectively). The TNM stages tended to be a poor prognostic factor, but the relation was not significant ($P = 0.065$ and $P = 0.177$), presumably because of the small number of samples. Of note, the plasma IL-8 level was significantly associated with the PFS and OS ($P = 0.039$ and $P = 0.01$).

Figure 3 shows the Kaplan–Meier estimates for PFS and OS with regard to the concentrations of plasma IL-8. Although the determination of an optimal cutoff value was beyond the scope of this study, all the patients were divided into two groups according to the median value (29.0 pg/ml). The median PFS of the high IL-8 group was 240 days (95% CI: not reached −504.3) and that of the low IL-8 group was 331 days (95% CI: 176.5–485.5), showing a significantly shorter PFS for the patients in the high IL-8 group ($P = 0.025$, log-rank test). The median OS of the high IL-8 group was 481 days (95% CI: not reached −971.9) and that of the low IL-8 group was 542 days (95% CI: 482.6–601.4), showing a tendency toward a shorter OS for the high IL-8

Table 3. Univariate analysis of clinical features and plasma angiogenesis-related factor levels for progression-free survival and overall survival

	Progression-free survival			Overall survival		
	HR	95% CI	*P* value	HR	95%CI	*P* value
Clinical features						
Age (years) (≤60 vs. >60)	1.641	(0.542–4.970)	0.381	2.032	(0.585–7.066)	0.265
Gender (male vs. female)	1.008	(0.388–2.621)	0.986	0.985	(0.357–2.723)	0.977
Tumor location (head vs. body tail)	0.637	(0.266–1.528)	0.313	0.698	(0.286–1.706)	0.431
Tumor size (mm) (≤20 vs. >20)	0.770	(0.222–2.668)	0.680	0.766	(0.212–2.768)	0.684
TNM stage (III vs. IV)	2.483	(0.945–6.520)	0.065	2.141	(0.845–5.427)	0.109
LN metastases (absence vs. presence)	1.098	(0.451–2.675)	0.836	1.380	(0.559–3.407)	0.485
Distant metastases (absence vs. presence)	2.425	(0.946–6.217)	0.065	1.878	(0.752–4.691)	0.177
PS (0 vs. 1)	1.805	(0.645–5.052)	0.261	1.350	(0.448–4.075)	0.594
CRP (<0.3 vs. ≥0.3)	3.434	(1.160–10.171)	0.026	2.315	(0.810–6.619)	0.117
CEA	1.088	(1.016–1.165)	0.015	1.125	(1.040–1.218)	0.003
CA19-9	1.000	(1.000–1.000)	0.017	1.000	(1.000–1.000)	0.012
Angiogenesis-related factors						
Angiopoietin-2	1.000	(1.000–1.000)	0.653	1.000	(1.000–1.001)	0.444
Follistatin	1.000	(1.000–1.001)	0.237	1.000	(1.000–1.001)	0.140
G-CSF	1.000	(0.999–1.001)	0.849	1.000	(0.999–1.001)	0.810
HGF	1.000	(1.000–1.001)	0.200	1.001	(1.000–1.002)	0.118
IL-8	1.012	(1.001–1.023)	0.039	1.016	(1.004–1.029)	0.010
Leptin	1.000	(0.999–1.000)	0.137	1.000	(1.000–1.000)	0.468
PDGF-BB	1.000	(0.999–1.001)	0.927	1.000	(1.000–1.001)	0.394
PECAM-1	1.000	(1.000–1.000)	0.542	1.000	(1.000–1.000)	0.443
VEGF	1.001	(0.994–1.008)	0.878	1.002	(0.994–1.010)	0.626

HR, hazard ratio; CI, confidence interval; LN, lymph node; meta, metastasis; PS, performance status.
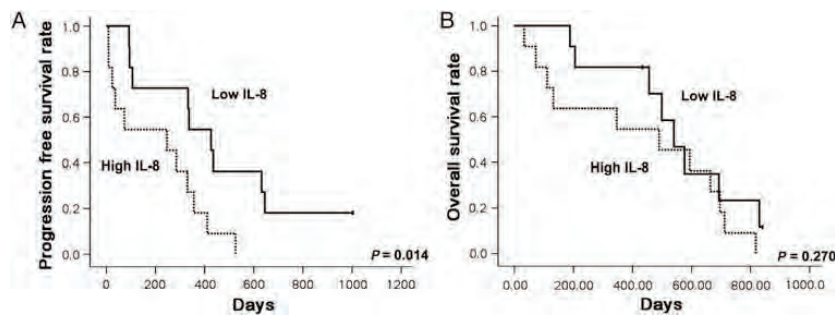
Figure 3. Kaplan–Meier curves for progression-free survival (A) and overall survival (B) according to the plasma IL-8 level in pancreatic cancer patients who received chemotherapy. The median value was used as the cut-off value. High IL-8, pancreatic cancer patients whose plasma IL-8 level was >29.0 pg/ml. Low IL-8, those whose plasma IL-8 level was <29.0 pg/ml. The difference was evaluated using the log-rank test.

group, although the trend was not significant ($P = 0.108$, log-rank test) (Fig. 3B). These results indicate that a high plasma IL-8 level is associated with a poor treatment outcome among patients with PC who were treated with chemotherapy.

DISCUSSION

We analyzed the plasma levels of multiple angiogenesis-related molecules in patients with PC using the antibody suspension bead arrays system. All the molecules were simultaneously measured using a 15-μl volume of sample plasma. Since biopsies for PC are usually invasive, our approach is to find plasma biomarkers that can be safely and repeatedly used.

Some studies have shown that the plasma concentrations of HGF, IL-8 and VEGF are significantly higher among PC patients than among healthy controls (18–20). Unexpectedly, we found that the plasma levels of angiogenesis-related molecules were not increased in patients with PC but were increased in patients with CC. Although we did not have any data on healthy controls, we directly compared the plasma levels of angiogenesis-related molecules in patients with PC and those with benign diseases or CC; the results suggested that the involvement of angiogenesis is smaller in PC than it is in CC. In CCs, the VEGF monoclonal antibody bevacizumab has been shown to provide a significant clinical benefit when added to chemotherapy, and this agent is already widely used for standard therapy. On the other hand, no active anti-angiogenic agents have been established for the treatment of PC. These clinical differences in anti-angiogenic agents may be explained by the absence of increased angiogenesis-related molecules in PC and the increased presence of these molecules in CC. However, the levels of VEGF and HGF were clearly increased in a partial subpopulation of patients with PC, but not in all patients (Fig. 1), suggesting that patient selection using effective biomarkers for anti-angiogenic therapy may be useful and necessary for the introduction of anti-angiogenic therapy to the treatment of PC.

IL-8, a member of the CXC chemokine family, is one of the major mediators of the inflammatory response (21). In cancer cells, secretion of IL-8 from cancer cells can enhance the proliferation and survival of cancer cells through autocrine signaling pathways (22). In addition, tumor-derived IL-8 will activate endothelial cells in the tumor vasculature to promote angiogenesis and induce a chemotactic infiltration of neutrophil into the tumor site (22). We examined the protein expression levels of IL-8 against a pair of sample-available primary and metastatic PC tumor tissues using immunohistochemistry. Immunohistochemical studies showed that cytoplasmic IL-8 expression was observed in a part of primary and metastatic tumor cells. IL-8 expressing cell numbers are likely to be increased in metastatic tumor, although further analysis is necessary (Supplementary data, Fig. S1). In PC, IL-8 is linked to tumor progression through its regulation of angiogenesis and the expression level of IL-8 appears to be correlated with the tumorigenic and metastatic potential (21,23). These oncogenic properties of IL-8 are consistent with our result. Our findings raised the possibility that IL-8 may be a useful biomarker for the response to chemotherapy in patients with PC, although the sample size in the present study was relatively small. To date, no predictive biomarker for the response to chemotherapy in patients with PC exists; therefore, a prospective study is needed. Meanwhile, plasma IL-8 levels in CC patients without and with metastasis were 56.0 ± 38.6 and 108.3 ± 90.1 pg/ml, respectively, and the mean level with metastasis was higher than that without metastasis. However, the correlation did not achieve statistical significance ($P = 0.297$), because the sample size of patients with metastasis was too small (four cases) to conclude.

In conclusion, we evaluated the plasma levels of angiogenesis-related molecules using the antibody suspension bead arrays system and found that the levels of these molecules basically were not increased in PC patients, compared with patients with CC or benign diseases. Our results raised the possibility that the IL-8 level may be a biomarker for the response to chemotherapy in PC patients.

Supplementary data

Supplementary data are available at http://www.jjco.oxfordjournals.org.

Acknowledgements

Funding

Conflict of interest statement

None declared.

References

1. Jemal A, Siegel R, Xu J, Ward E. Cancer Statistics, 2010. *CA Cancer J Clin* 2010;60:277−300.
2. Folkman J. Addressing tumor blood vessels. *Nat Biotechnol* 1997;15:510−1.
3. Folkman J. Angiogenesis in cancer, vascular, rheumatoid and other disease. *Nat Med* 1995;1:27−31.
4. Ma WW, Adjei AA. Novel agents on the horizon for cancer therapy. *CA Cancer J Clin* 2009;59:111−37.
5. Kindler HL, Friberg G, Singh DA, Locker G, Nattam S, Kozloff M, et al. Phase II trial of bevacizumab plus gemcitabine in patients with advanced pancreatic cancer. *J Clin Oncol* 2005;23:8033−40.
6. Kindler HL, Niedzwiecki D, Hollis D, Sutherland S, Schrag D, Hurwitz H, et al. Gemcitabine plus bevacizumab compared with gemcitabine plus placebo in patients with advanced pancreatic cancer: phase III trial of the Cancer and Leukemia Group B (CALGB 80303). *J Clin Oncol* 2010;28:3617−22.
7. Van Cutsem E, Vervenne WL, Bennouna J, Humblet Y, Gill S, Van Laethem JL, et al. Phase III trial of bevacizumab in combination with gemcitabine and erlotinib in patients with metastatic pancreatic cancer. *J Clin Oncol* 2009;27:2231−7.
8. Spano J-P, Chodkiewicz C, Maurel J, Wong R, Wasan H, Barone C, et al. Efficacy of gemcitabine plus axitinib compared with gemcitabine alone in patients with advanced pancreatic cancer: an open-label randomised phase II study. *Lancet* 2008;371:2101−8.
9. Itakura J, Ishiwata T, Friess H, Fujii H, Matsumoto Y, Büchler MW, et al. Enhanced expression of vascular endothelial growth factor in human pancreatic cancer correlates with local disease progression. *Clin Cancer Res* 1997;3:1309−16.
10. Fujimoto K, Hosotani R, Wada M, Lee JU, Koshida T, Miyamoto Y, et al. Expression of two angiogenic factors, vascular endothelial growth factor and platelet-derived endothelial cell growth factor in human pancreatic cancer, and its relationship to angiogenesis. *Eur J Cancer* 1998;34:1439−47.
11. Seo Y, Baba H, Fukuda T, Takashima M, Sugimachi K. High expression of vascular endothelial growth factor is associated with liver metastasis and a poor prognosis for patients with ductal pancreatic adenocarcinoma. *Cancer* 2000;88:2239−45.
12. Ikeda N, Adachi M, Taki T, Huang C, Hashida H, Takabayashi A, et al. Prognostic significance of angiogenesis in human pancreatic cancer. *Br J Cancer* 1999;79:1553−63.
13. Niedergethmann M, Hildenbrand R, Wostbrock B, Hartel M, Sturm JW, Richter A, et al. High expression of vascular endothelial growth factor predicts early recurrence and poor prognosis after curative resection for ductal adenocarcinoma of the pancreas. *Pancreas* 2002;25:122−9.
14. Kobayashi A, Yamaguchi T, Ishihara T, Ohshima T, Baba T, Shirai Y, et al. Usefulness of plasma vascular endothelial growth factor in the diagnosis of pancreatic carcinoma. *Pancreas* 2005;31:74−8.
15. Karayiannakis AJ, Bolanaki H, Syrigos KN, Asimakopoulos B, Polychronidis A, Anagnostoulis S, et al. Serum vascular endothelial growth factor levels in pancreatic cancer patients correlate with advanced and metastatic disease and poor prognosis. *Cancer Lett* 2003;194:119−24.
16. Yamada Y, Arao T, Matsumoto K, Gupta V, Tan W, Fedynyshyn J, et al. Plasma concentrations of VCAM-1 and PAI-1: a predictive biomarker for post-operative recurrence in colorectal cancer. *Cancer Sci* 2010;101:1886−90.
17. Kimura H, Kasahara K, Sekijima M, Tamura T, Nishio K. Plasma MIP-1beta levels and skin toxicity in Japanese non-small cell lung cancer patients treated with the EGFR-targeted tyrosine kinase inhibitor, gefitinib. *Lung Cancer* 2005;50:393−9.
18. Kemik O, Purisa S, Kemik AS, Tuzun S. Increase in the circulating level of hepatocyte growth factor in pancreatic cancer patients. *Bratisl Lek Listy* 2009;110:627−9.
19. Ebrahimi B, Tucker SL, Li D, Abbruzzese JL, Kurzrock R. Cytokines in pancreatic carcinoma. *Cancer* 2004;101:2727−36.
20. Chang YT, Chang MC, Wei SC, Tien YW, Hsu C, Liang PC, et al. Serum vascular endothelial growth factor/soluble vascular endothelial growth factor receptor 1 ratio is an independent prognostic marker in pancreatic cancer. *Pancreas* 2008;37:145−50.
21. Xie K. Interleukin-8 and human cancer biology. *Cytokine Growth Factor Rev* 2001;12:375−91.
22. Waugh DJ, Wilson C. The interleukin-8 pathway in cancer. *Clin Cancer Res* 2008;14:6735−41.
23. Shi Q, Abbruzzese JL, Huang S, Fidler IJ, Xiong Q, Xie K. Constitutive and inducible interleukin 8 expression by hypoxia and acidosis renders human pancreatic cancer cells more tumorigenic and metastatic. *Clin Cancer Res* 1999;5:3711−21.

Recommendations for liver transplantation for hepatocellular carcinoma: an international consensus conference report

Pierre-Alain Clavien, MD,
Department of Surgery, Swiss HPB and Transplant Centers, University Hospital Zurich, Zurich, Switzerland

Mickael Lesurtel, MD,
Department of Surgery, Swiss HPB and Transplant Centers, University Hospital Zurich, Zurich, Switzerland

Patrick M M Bossuyt, PhD,
Department of Clinical Epidemiology and Biostatistics, Academic Medical Center, Amsterdam, Netherlands

Gregory J Gores, MD,
Division of Gastroenterology and Hepatology, Mayo Clinic, Rochester, MN, USA

Bernard Langer, MD, and
Department of Surgery, University of Toronto, Toronto, ON, Canada

Arnaud Perrier, MD on behalf of the OLT for HCC Consensus Group
Department of Internal Medicine, University Hospital of Geneva, Geneva, Switzerland

Abstract

Although liver transplantation is a widely accepted treatment for hepatocellular carcinoma (HCC), much controversy remains and there is no generally accepted set of guidelines. An international consensus conference was held on Dec 2–4, 2010, in Zurich, Switzerland, with the aim of reviewing current practice regarding liver transplantation in patients with HCC and to develop internationally accepted statements and guidelines. The format of the conference was based on the Danish model. 19 working groups of experts prepared evidence-based reviews according to the Oxford classification, and drafted recommendations answering 19 specific questions. An independent jury of nine members was appointed to review these submissions and make final recommendations, after debates with the experts and audience at the conference. This report presents the final 37 statements and recommendations, covering assessment of candidates for liver transplantation, criteria for listing in cirrhotic and non-cirrhotic patients, role of tumour downstaging, management of patients on the waiting list, role of living donation, and post-transplant management.

Correspondence to: Prof Pierre-Alain Clavien, Department of Surgery, University Hospital Zurich, Raemistrasse 100, CH-8091, Zurich, Switzerland, clavien@access.uzh.ch.
P-AC and ML contributed equally to this work.

Introduction

Although liver transplantation was first done in human beings by Tom Starzl in 1963, the procedure did not begin to gain wide acceptance until the mid-1980s, when effective immunosuppression with ciclosporin became available. Currently, overall 1-year and 5-year survival after liver transplantation exceeds 85% and 70%, respectively, in most centres.[1,2]

Hepatocellular carcinoma (HCC) is a major health problem worldwide, which continues to increase because of the association of HCC with hepatitis B and C viruses. HCC was one of the first indications for liver transplantation, because it was postulated that this approach would eliminate the tumour and cure the underlying liver disease. However, it soon became apparent that the success of liver transplantation depends on the tumour load; patients with extensive disease had very poor outcomes, whereas most patients with small tumours could be cured. This led to many controversies around the use of liver transplantation in patients with HCC, such as the selection of patients in the context of worldwide organ shortage, control of the tumour load while patients wait for a graft, use of living donors, and the choice of immunosuppression or adjuvant therapies.

The goal of liver transplantation, regardless of the underlying disease, is providing liver recipients with the maximum benefit possible from the limited resource of deceased and living donor organs, in a fair, ethical, and cost-effective manner. Thus, indications for the procedure and allocation of donor organs are closely scrutinised by all stakeholders in liver transplantation. With the endorsement of most international societies concerned with liver transplantation or HCC, we organised a conference that aimed to reach wide consensus throughout the medical and non-medical population on various aspects of the use of liver transplantation for patients with HCC, based on the best available evidence.

Methods

An international consensus conference on liver transplantation for HCC was held on Dec 2–4, 2010, in Zurich, Switzerland, under the auspices of ten international societies focused on liver diseases or transplantation, with the aim of establishing a consensus regarding indications for liver transplantation in patients with HCC and to provide internationally accepted statements and guidelines for the conduct of liver transplantation programmes. For this purpose, we developed a novel format based on the Danish model (figure).[3] The organising committee identified key topics and appointed 19 working groups composed of four to six experts from various areas of medicine, selected on the basis of their scientific and clinical records, to prepare reviews of the evidence and draft recommendations. Working groups were asked to follow the Oxford classification of levels of evidence.[4] The material prepared by the various panels is available as a supplement of *Liver Transplantation*.[5–24] Each working group did an English language literature search of Pubmed, Embase, and Scopus databases, and the Cochrane central register of controlled trials. Text, keywords, and medical subject heading terms were used for titles and abstracts. Manual cross-referencing was also used to find further relevant articles. Search terms and dates varied according to topic (webappendix). A jury of nine members, who were selected from various clinical and academic areas and who were not actively involved in liver transplantation, was appointed to review and comment on the submitted papers and to finalise and grade the final recommendations.

Around 300 participants from five continents attended the meeting in Zurich. Each of the 19 working groups, assisted by members of the jury, prepared statements associated with a level of evidence from their review of the literature. The chair of each working group gave a 15-min presentation covering specific questions, followed by questions from the jury and the

audience. The prepared statements could be modified in real time according to the debates during the conference. Then, a poll of the audience was obtained through an anonymous electronic voting system to inform the jury of the strength of consensus.

The jury met independently after the conference to produce the final recommendations, based on the expert reports, debates, and attendee voting. The jury concluded by voting to assign a level of evidence for each recommendation, according to the Oxford classification, with respect to diagnosis, prognosis, or therapy. They also determined the strength of each recommendation according to the grading of recommendations assessment, development, and evaluation system (GRADE).[25] From the initial statements and recommendations proposed by the panels of experts, 27 were dropped or merged with other statements or recommendations, ten were left unchanged, and another 27 were reworded. Among the definitive 37 statements and recommendations, the level of evidence proposed by the experts was modified in three cases by the jury after discussion with the statistician (PMMB).

The present review was prepared by a writing committee, which included the president (AP), vice president (BL), and statistician (PMMB) of the jury, along with three members of the organising committee (ML, GJG, P-AC). The manuscript was circulated among the working groups for confirmation of accuracy of the data with no possibility to alter the recommendations. The final version was approved by each member of the jury. The recommendations are presented in table 1.

Assessment of candidates with HCC for liver transplantation

The purpose of cancer staging is to accurately predict prognosis and to link tumour stage with specific therapeutic interventions. The ideal staging system for HCC should take into account tumour stage, liver function, and functional status of the patient. Several staging systems have been developed over the past three decades, although none has gained worldwide acceptance (table 2).[26–34] The Barcelona Clinic Liver Cancer (BCLC) and Cancer of the Liver Italian Program (CLIP) staging systems have been the most popular in Europe and the USA, and the Japan Integrated Staging Score (JIS) in Japan. The BCLC is the only system that links prognosis with treatment recommendations, and thereby was selected in several major trials of HCC therapy. For example, the role of portal hypertension in selecting patients for major liver resection versus liver transplantation has been validated in Japan[35] and the USA.[36]

Pathological features in the explanted liver that have prognostic value for staging HCC include tumour size and number of nodules, satellite lesions, vascular invasion (macroscopic or microscopic), and lymph-node metastases. However, staging systems to guide therapy before liver transplantation are necessary and are mainly based on imaging information. Preoperative and post-transplant liver staging systems can be used in assessing outcome. This led to recommendations 1 and 2: (1) when considering treatment options for patients with HCC, the BCLC staging system is the preferred staging system to assess the prognosis of patients with HCC; (2) the TNM system (7th edn), including pathological examination of the liver, should be used for determining the prognosis after transplantation with the addition of the assessment of microvascular invasion.

Despite incremental technological advances in cross-sectional imaging techniques (ultrasonography, CT, and MRI), standard imaging methods can underestimate or overestimate the extent of HCC in up to 25% of cases, compared with pathological findings of the explanted liver.[18] Recent reports suggest that either dynamic CT or MRI, including unenhanced, arterial, portal venous, and delayed phases, provide improved sensitivity and specificity compared with standard techniques of the past. Currently, there is no data showing the superiority of either MRI or CT. Conclusive imaging features rely on the

presence of arterial enhancement followed by washout on portal venous or delayed imaging.[37] Such examinations should follow established protocols, which define the amount and rate of contrast given, the precise individualised timing of image acquisition, and image reconstruction with minimum slice thickness. Dynamic ultrasonography has improved the accuracy of ultra sonography, but is less useful than CT or MRI because of the inability to reliably acquire images of the entire liver during a particular contrast phase. Bone scintigraphy has been used for evaluating bone metastases; however, the technique is poor in terms of cost-effectiveness when used routinely. There is insufficient data to propose ^{18}F-fluorodeoxyglucose (FDG)-PET for staging HCC before liver transplantation. These finding are summarised in recommendations 3 and 4: (3) either dynamic CT or dynamic MRI with the presence of arterial enhancement followed by washout on portal venous or delayed imaging is the best non-invasive test to make a diagnosis in cirrhotic patients suspected of having HCC and for preoperative staging; (4) extrahepatic staging should include CT of the chest, and CT or MRI of the abdomen and pelvis.

Because of improvements in the accuracy of non-invasive imaging, the need for liver biopsy in the work-up of cirrhotic patients with HCC being considered for liver transplantation has changed in recent years. The specificity of liver biopsy is close to 100%, but sensitivity varies depending on location of the tumour, needle size (86–90% with an 18 gauge cutting needle, 67% with 21–22 gauge needle), and tumour size (>90% for nodules >1 cm vs 83% for nodules <1 cm). A positive tumour biopsy is clinically relevant to rule in a diagnosis of HCC, but a negative biopsy is less useful. There is also the risk of tumour seeding after liver biopsy, which has been reported to be 2·7% (95% CI 1·8–4·0) with a median time interval between biopsy and seeding of 17 months (IQR 7–48).[38]

The American Association for the Study of Liver Disease (AASLD) has proposed an algorithm for diagnosis of HCC based on availability of state-of-the-art CT or MRI.[39] These data are summarised as recommendations 5 and 6: (5) tumour biopsy is not required in cirrhotic patients considered for liver transplantation who have high-quality dynamic CT or MRI findings typical for HCC and a lesion larger than 1 cm according to current AASLD guidelines; (6) for patients with lesions smaller or equal to 10 mm or atypical findings, non-invasive imaging does not allow an accurate diagnosis, and should not be used to make a decision for or against transplantation.

Criteria for listing candidates with HCC in cirrhotic livers for deceased-donor liver transplantation

In the context of shortage of available grafts, decisions have to take into account the collective benefit of all potential liver recipients, in addition to the benefit for the individual patient. Liver transplantation achieves excellent results in patients with limited tumour load. Patients with solitary HCC of less than 5 cm or with up to three nodules of less than 3 cm (the Milan criteria[40]) have a 5-year survival of 70% after liver transplantation, with recurrence in less than 10%. This survival matches post-transplant survival of most other indications for liver transplantation.[1,2]

In the context of organ shortage for liver transplantation, an extension of the boundaries of transplantation for HCC must take into account the benefit for individual HCC patients as well as the consequences for all potential liver recipients. Whether, and to what extent, post-transplant survival could be lowered, because of expansion of the HCC receiver pool, while remaining acceptable, depends on the effect on mortality for non-HCC patients awaiting transplantation. Even though a survival opportunity considerably lower than that achieved in non-HCC patients might be considered worth the risk of surgery for some patients with HCC, the negative effects on others on the donor list must be taken into consideration. This

led to recommendation 7: liver transplantation should be reserved for HCC patients who have a predicted 5-year survival comparable to non-HCC patients.

Among criteria used for listing patients with HCC, gross features of tumours are important. Burroughs and colleagues[41] did a meta-analysis of 101 studies assessing the effect of HCC staging in terms of size and number of nodules on post-transplant recurrence and survival. 74 of the studies, comprising 22 432 patients, were used for quantitative analysis. There was variability in the reporting of tumour characteristics, with information missing for time on the waiting list, immunosuppression, and bridging therapy. Two-thirds of the studies were based on explant findings, and few compared pretransplant imaging with explant data. If multiple versus single nodules were considered, the definition of multiple was poorly reported. Burroughs and colleagues[41] concluded that assessment of the diameter of the largest nodule or total diameter of nodules was the best predictor of outcome, and that total tumour size (sum of diameters) of 10 cm or larger (vs <10 cm) was associated with a four-times increased risk of death or recurrence. Measurement of volume might be a better way to assess tumour burden, but the data to support this are not yet available.[42] A study using the Organ Procurement and Transplant Network (OPTN) database suggested that a total tumour volume cutoff at 115 cm^3 and α-fetoprotein concentration higher than 400 ng/mL could discriminate between patients with acceptable outcome and those with poor outcome.[43] There is insufficient evidence regarding the effect of number of nodules on outcome of liver transplantation.

This led to recommendation 8: preoperative assessment of the size of the largest tumour or total diameter of tumours should be the main consideration in selecting HCC patients for liver transplantation. In 1996, after a period of unrestricted indications for liver transplantation, associated with overall 5-year survival below 50%, the Milan criteria were introduced. These criteria set restrictive limits for size and number of tumours in candidates for liver transplantation.[40] Mazzaferro and colleagues[44] did a systematic review that included 90 studies, comprising 17 780 patients over 15 years (1612 patients in level 1b studies, 16 043 in level 2 studies, and 125 in level 4 studies). Their review showed that the Milan criteria are an independent prognostic factor for outcome after liver transplantation. Application of the Milan criteria for patients with HCC with chronic hepatitis and cirrhosis achieves similar post-transplant survival to that in non-HCC indications. In the European Liver Transplant Registry (ELTR), Organ Procurement and Transplantation Network (OPTN), and Australia and New Zealand Liver Transplant Registry (ANZLTR), 5-year survival for non-HCC was 65–87%.[1,2,45] The jury concluded with recommendation 9: the Milan criteria are currently the benchmark for selection of HCC patients for liver transplantation, and the basis for comparison with other suggested criteria.

As evidence accumulated of good outcomes in some patients outside the Milan criteria, there was a drive to identify expanded criteria and to increase the number of eligible candidates for liver transplantation. Among the many proposals, only the University of California San Francisco (UCSF) criteria (one tumour ≤6·5 cm, three nodules at most with the largest ≤4·5 cm, and total tumour diameter ≤8 cm) have been prospectively validated by the proponent group, with outcome data comparable to those from other retrospective studies.[46,47] This is summarised in recommendation 10: a modest expansion of the number of potential candidates may be considered on the basis of several studies showing comparable survival for patients outside the Milan criteria.

It is essential to consider how expansion of criteria beyond the Milan criteria might affect the survival of candidates for liver transplantation who do not have HCC. According to studies based on Markov models[48] using data from the USA, patients outside the Milan criteria would need to achieve 5-year survival of 60% or higher to prevent a substantial

decrement to the life-years available to the entire population of candidates for liver transplantation. The effect on non-HCC patients could vary widely, depending on the composition of the population on the waiting list and the scarcity of available donor livers in a transplant region and in individual centres. Any decision by a centre to expand criteria should take into account the current mortality on the waiting list, and should only be done if a low mortality will not be substantially increased by additional expanded-criteria cases. For example, a centre with very low or no mortality on the waiting list might expand their criteria for patients with HCC with lower post-transplant survival than that expected for non-HCC candidates, whereas such strategy would not be acceptable in another centre with a high death rate on the waiting list. Thus, the jury proposed recommendation 11: patients with a worse prognosis may be considered for liver transplantation outside the Milan criteria if the dynamics on the waiting list allow it without undue prejudice to other recipients with a better prognosis.

Since gross features of tumours are unable to define subclasses of patients with better biology and outcome, several biomarkers have been studied—eg, G3, EpCAM, miR26, and poor-survival gene signatures. However, these biomarkers have not been studied in the setting of liver transplantation.[49] Several studies highlighted the value of preoperative α-fetoprotein concentrations in predicting outcome after liver transplantation,[43,50,51] but there is no agreement on the cutoff values to consider, which ranged from 200 to 1000 ng/mL. A recent study using the Scientific Registry of Transplant Recipients (SRTR) data suggested adding α-fetoprotein concentration to total tumour volume as a predictor of outcome after liver transplantation.[43] In several studies, α-fetoprotein concentration lower than 400 ng/mL has been used in selecting patients for liver transplantation after downstaging protocols, in addition to criteria based on tumour size and number.[52] Another group found that dynamic changes in α-fetoprotein concentrations higher than 15 ng/mL are the most relevant preoperative predictor of recurrence and overall survival after orthotopic liver transplantation.[50] Recommendations 12 and 13 summarise this topic: (12) α-fetoprotein concentrations add prognostic information in HCC patients and may be used for making decisions regarding transplantation in combination with imaging criteria; (13) biomarkers other than α-fetoprotein cannot yet be used for clinical decision making regarding liver transplantation for HCC.

HCC often involves branches of portal or hepatic veins (or both), causing a tumour thrombus. Vascular invasion of HCC affects prognosis after liver transplantation.[53–55] Macrovascular invasion involves branches of portal or hepatic veins, or both. It can be detected using high-quality imaging and in a pathological specimen, and is generally considered an absolute contraindication for liver transplantation. Micro vascular invasion, which is identified only by microscopic observation, is associated with poorer outcome or increased recurrence rates after liver transplantation. Although it correlates with larger tumour size (>3 cm), multiple nodules, histological grade (moderately *vs* poor differentiated), and gross features such as confluent multinodular type,[56] microvascular invasion cannot be reliably detected before transplantation and is therefore not useful for clinical decision making.

Conventional imaging modalities are ineffective for preoperative detection of microvascular invasion. Only one study suggested a value for PET in predicting microvascular invasion.[57] Several studies from Japan suggested that serum concentrations of des-gamma-carboxyprothrombin (also known as protein induced by vitamin K absence [PIVKA]) correlate well with microvascular invasion.[58,59] Positive and negative correlations of α-fetoprotein with microvascular invasion have been reported. The available data led to recommendation 14: indication for liver trans plantation in HCC should not rely on microvascular invasion because it cannot be reliably detected prior to transplantation.

Criteria for HCC candidates with non-cirrhotic livers

Although most HCC occurs in patients with liver cirrhosis, about 10% of cases arise in absence of cirrhosis. In such patients, diagnosis is often made at an advanced stage. Resection is currently the preferred therapeutic option, when feasible, since patients with good liver reserve have high tolerance for extensive liver resection.[60] However, as in cirrhotic patients, the risk of local recurrence is high, ranging from 30 to 73%, and affects 5-year overall survival (25–81%) and disease-free survival (24–54%).[61,62] Several pathological features are associated with poor prognosis, such as the presence of satellite or multiple nodules, microvascular and macrovascular invasion, and R1 resection. The subtype of fibrolamellar HCC seems to have similar outcomes.[63]

Data from the ELTR suggest that liver transplantation might be appropriate in some non-cirrhotic patients with recurrent HCC after resection, with long-term survival approaching 60% at 5 years.[64] In this study, the absence of cirrhosis or fibrosis, and seronegativity for hepatitis C and hepatitis B virus was confirmed in all patients. Macrovascular and lymph-node invasion, and early recurrence (<1 year) after resection were significant risk factors for poor outcome. Tumour diameter and Milan criteria of the initial HCC were unrelated to outcome.

There are few reports of cases of primary liver transplantation in non-cirrhotic patients with HCC.[64,65] The data available suggest that the risk factors for poor outcomes after liver transplantation are the same as those identified for recurrent disease after resection. Patients without these risk factors had a 5-year survival of 67%, even though most had tumours outside the Milan criteria. This information led to recommendations 15 and 16: (15) the Milan criteria and its modifications are not applicable to patients with HCC developing in a non-cirrhotic liver. Such patients with non-resectable HCC and absence of macrovascular invasion and extrahepatic spread may be considered as appropriate candidates for liver transplantation; (16) patients with HCC in a non-cirrhotic liver, who were treated by resection and have intrahepatic recurrence of HCC and no evidence of macrovascular invasion or extrahepatic spread, may be considered for salvage transplantation.

Role of downstaging of HCC

The goal of downstaging using locoregional therapy—eg, alcohol injection, radiofrequency ablation (RFA), transarterial chemoembolisation (TACE), transarterial radioembolisation (TARE), or liver resection—is to decrease the tumour size and number in patients initially presenting with tumours that do not meet locally acceptable criteria for liver transplantation.

Success in downstaging has been reported in many studies, although most of these are uncontrolled observational studies with no method emerging as superior and each carrying some risk. The largest experience is with TACE and RFA.[66] Two prospective studies showed that survival after liver transplantation in patients with large tumour burden successfully treated by downstaging was similar to survival in patients who initially met the criteria for transplantation.[52,67] These issues are addressed in recommendations 17 and 18: (17) transplantation may be considered after successful downstaging; (18) liver transplantation after successful downstaging should achieve a 5-year survival comparable to that of HCC patients who meet the criteria for liver transplantation without requiring downstaging.

There is debate about how best to assess successful downstaging. European Association for the Study of the Liver (EASL) guidelines suggest that such assessment should be exclusively based on the amount of viable tumour, as differentiated from necrosis by contrast CT or MRI.[68] Most available reports have used the Milan criteria to define

successful downstaging.[52,67,69] There is currently no well defined upper limit for size and number of lesions as eligibility criteria for downstaging, although the presence of vascular invasion and extrahepatic disease are generally considered absolute con train dications. Some groups add serum α-fetoprotein concentrations for assessment of downstaging; however, there is no agreement on a threshold. Recommendations 19 and 20 address downstaging: (19) criteria for successful downstaging should include tumour size and number of viable tumours; (20) α-fetoprotein concentrations before and after downstaging may add additional information.

Once a tumour has been successfully downstaged to within acceptable criteria, a minimum observation period of 3 months is often recommended before considering liver transplantation. It is crucial to define criteria for failure of downstaging, which may include, before listing: failure to achieve listing criteria, tumour progression with development of vascular invasion, extrahepatic spread, or tumour size and number remaining beyond inclusion criteria; and, after listing: tumour progression requiring delisting and recurrence of HCC after liver transplantation. This consideration led to statement 21: based on existing evidence, no recommendation can be made for preferring a specific locoregional therapy for downstaging over others.

Managing patients on the waiting list

With increases in waiting times for liver transplantation in many centres, it has become common practice to monitor patients with HCC to ensure that they remain within the acceptability criteria for liver transplantation. Strategies have also been developed to treat patients whose HCC is at risk or shows signs of progression while waiting for a graft. There is no agreement about specific timing or optimum imaging methods to use for these patients, although a 3-month interval is common.

Recommendations are based on the known capabilities of the imaging methods used for diagnosis and staging of HCC (see recommendations 3 and 12). There are also reports showing that a rise in α-fetoprotein concentration is associated with poorer outcome after liver transplantation, and of reduction in that risk by successful locoregional therapy. This information is reflected in recommendation 22: periodic waiting-list monitoring should be performed by imaging (dynamic CT, dynamic MRI, or contrast-enhanced ultrasonography) and serum α-fetoprotein measurements.

Dropout of HCC patients on the waiting list is common because of cancer progression or other medical reasons. Locoregional therapy as a bridging strategy for patients on the waiting list aims to decrease tumour-related dropout rates and reduce the incidence of recurrent diseases after liver transplantation. Several cohort studies and a preliminary analysis of large registries suggest that bridging strategies with locoregional therapy are likely to be beneficial for patients having to wait 6 months or longer.[70] There is, however, no evidence that bridging strategies are of any benefit in patients with United Network for Organ Sharing (UNOS) T1 tumours (<2 cm). Bridging strategies might be appropriate for patients with UNOS T2 lesions (one nodule 2–5 cm or three or fewer nodules each ≤3 cm) who are likely to wait 6 months or longer. The presence of larger tumours and high α-fetoprotein concentrations seem to predict a higher risk for dropout.

Although the most popular bridging strategy is TACE, pathological studies show a marginal advantage for RFA in terms of tumour necrosis.[71,72] Liver resection before transplantation in patients with well preserved liver function, and newer strategies such as a combination of TACE with RFA and use of [90]yttrium radioembolisation or targeted therapies, have shown some benefits in preliminary studies. This topic is summarised by the following three statements from the jury: (23) based on current absence of evidence, no recommendation

can be made on bridging therapy in patients with UNOS T1 (≤2 cm) HCC; (24) in patients with UNOS T2 (one nodule 2–5 cm or three or fewer nodules each ≤3 cm) HCC (Milan criteria) and a likely waiting time of longer than 6 months, locoregional therapy may be appropriate; (25) no recommendation can be made for preferring one type of locoregional therapy to others. The topic also generated two additional recommendations: (26) patients found to have progressed beyond criteria acceptable for listing for liver transplantation should be placed on hold and considered for downstaging; (27) patients with progressive disease, in whom locoregional therapy intervention is not considered appropriate or is ineffective, should be removed from the waiting list.

Role of living-donor liver transplantation for HCC

Living-donor liver transplantation (LDLT) using the right or left hemiliver of a healthy donor is the only option for liver transplantation in some countries, particularly in Asia, where there is limited or no availability of deceased-donor organs. LDLT has also been used in other countries with well established programmes for organ donation from brain dead or non-heart-beating donors, because of organ shortage, long waiting times associated with deaths on the waiting list, drop-out due to medical reasons, or progression of tumours beyond acceptable criteria.

The main issue in LDLT is donor safety, because of the risk of complications or death, even if small. The concept of double equipoise was proposed to describe the balance between the recipient's survival benefit with LDLT and the risk of a complication or death of a healthy donor.[73] The risks and benefits need to be openly discussed and understood by all parties involved in such cases, and meet the test of equipoise.

Some studies have suggested a higher risk of tumour recurrence with the use of partial grafts from living relatives versus whole grafts from deceased donors. Six studies compared deceased-donor liver transplantation (DDLT) and LDLT for HCC, including a report from a multicentre US consortium of LDLT centres.[74–79] No convincing difference in outcome could be identified according to type of graft, although a higher risk of recurrence was noted in fast-tracked patients, since a short delay between diagnosis and liver transplantation might not allow enough time for the biological behaviour of the tumour to manifest. Therefore, it might be important to consider a period of observation (eg, 3 months) when offering LDLT in recipients with HCC. This topic is covered in recommendations 28 and 29: (28) LDLT is acceptable for HCC patients who have an expected 5-year survival similar to comparably staged patients receiving a deceased-donor liver. In LDLT, careful attention should be given to psychosocial considerations regarding both donor and recipient; (29) LDLT must be restricted to centres of excellence in liver surgery and liver transplantation to minimise donor risk and maximise recipient outcome.

Should LDLT be offered to patients with tumour stages beyond the accepted criteria for listing for deceased donation? This might seem to be ethically acceptable, since unlike deceased-donor donation, other listed patients are not adversely affected by this process. However, the question raises ethical concerns regarding the double equipoise principle, since the risk to the donor might not be acceptable below a certain expected survival threshold for the recipient. There was considerable disagreement among the experts at the conference on what that threshold might be. Those who set a priority on donor protection would not consider offering LDLT to patients with a tumour beyond criteria for DDLT, whereas others supported the procedure even for patients with a very dismal prognosis, to maximise individual patient benefit and patients' choice.

The jury recognised that there are differences in current practice and suggested that any institution using LDLT should take a clear position, make it known to the public, and, when

endorsing criteria beyond those accepted for deceased donation, provide rigorous safeguards to guarantee full disclosure to donor and recipients and to prevent donor coercion and increased risk-taking by the surgical team.

The use of deceased-donor organs is usually justified for graft failure after LDLT.[80] The panel of experts supported use of deceased-donor graft for failed LDLT, even if extended criteria were used. Rates of retrans plantation because of graft failure after LDLT are typically low, and when needed, outcomes are excellent. The jury agreed with the use of retransplantation in recipients who received a living graft within the accepted criteria for liver transplantation. However, based on utility, justice, and equity, they did not support retransplantation for patients who were beyond these criteria, because these patients would not have qualified for DDLT in the first place, and their acceptance of LDLT did not benefit patients on the DDLT waiting list. The vote of the audience at the conference was in line with this re com mendation (46% strongly disagreed and 25% disagreed with the use of retransplantation in patients beyond the accepted criteria). This discussion led the jury to formulate recommendations 30 and 31: (30) in patients following LDLT for HCC within the accepted regional criteria for DDLT, retransplantation for graft failure is justified; (31) in patients following LDLT for HCC outside the accepted regional criteria for DDLT, retransplantation for graft failure using a deceased-donor organ is not recommended.

Post-transplant management

The main concern after liver transplantation for HCC is the risk of tumour recurrence, which occurs in 8–20% of recipients.[81] HCC recurrence is usually seen within the first 2 years after liver transplantation, and is associated with a median survival of less than 1 year (IQR 7–18 months) from the time of diagnosis.[82] The adoption of routine imaging and α-fetoprotein monitoring has led to the detection of early recurrence, with a possibility of cure with ablation therapies in up to a third of cases.[83] However, studies addressing the issue of protocols for monitoring are scarce. A limitation for the use of routine imaging examination (CT or MRI) is the high cost or poor cost-effectiveness to detect HCC recurrence, and most centres have limited their application to every 6 months or yearly intervals for the first 3–5 years after liver transplantation or in the presence of abnormal α-fetoprotein concentrations, leading to recommendation 32: post-transplant monitoring may include 6–12-monthly contrast-enhanced CT or MRI imaging and α-fetoprotein measurements.

There is debate about how to adjust the immunosuppression in HCC patients after liver transplantation. Immunosuppressive drugs are associated with oncogenic properties in experimental models, and most programmes are careful to balance the inherent risks of rejection and tumour recurrence.[84] However, there are no randomised controlled trials (RCTs) that have shown that lowering immunosuppression reduces the risk of HCC recurrence after liver transplantation.

One class of immunosuppressive drugs, the mTOR inhibitors, might be of particular relevance for patients with HCC who receive a liver transplantation, since experimental studies have shown that this drug has strong immunosuppressive effects with concomitant anti-neoplastic properties.[85] Uncontrolled pilot trials and retrospective analyses have suggested that sirolimus, an mTOR inhibitor, was associated with lower tumour recurrence and improved survival after liver transplantation;[86–88] however, these results have not been confirmed in an RCT. This topic is covered in statements 33 and 34: (33) there is currently insufficient evidence from clinical trials to base a recommendation for choosing the type or dose of immunosuppression therapy to influence the incidence of HCC recurrence or its prognosis; (34) based on current evidence, no recommendation can be made on the use of mTOR inhibitors to reduce the risk of HCC recurrence outside clinical trials.

To assess whether adjuvant therapies are effective to decrease post-transplantation tumour recurrence and improve overall survival, the experts identified eight uncontrolled studies (226 patients)[89–96] and four RCTs (213 patients).[96–100] Difficulties in interpreting these studies include variability in the drugs tested (doxorubicin, cisplatin, fluorouracil, gemcitabine, or mithoxanthrone) and in the inclusion criteria and endpoints selected, and small sample sizes. Single-arm, retrospective studies suggest a benefit for using adjuvant therapy, but their level of evidence is too low (level 4) to support recommendations. Controlled studies have also provided inconsistent results.

Two compounds show some early promise: sorafenib and licartin. Sorafenib, a multitargeted tyrosine-kinase inhibitor, has been shown to have an antitumour effect in patients with advanced HCC,[101] and is currently being studied as adjuvant therapy after resection or ablation of HCC in a multicentre phase 3 trial (STORM trial). Licartin, a ^{131}I-radiolabelled murine monoclonal antibody that specifically binds HCC cells, was shown to have a positive effect on prevention of tumour recurrence and on survival, in a small, placebo-controlled, randomised, double-blind study.[97] This led to recommendation 35: current evidence does not justify the routine use of adjuvant antitumour therapy after liver transplantation for HCC outside of a controlled clinical trial.

There is considerable debate about how to treat HCC recurrence after liver transplantation. Most recurrences are associated with systemic tumour dissemination, thus retransplantation is not indicated. A distinction must be made for de-novo HCC, which typically occurs at a later stage and most often in the setting of recurrent hepatitis C and advancing fibrosis. Such cases should probably be treated as having new tumours and retransplantation might be justified;[102] however, the data to support this approach are limited.

Locoregional therapy for HCC recurrence, including liver resection, radiofrequency ablation, or TACE, has been successfully used in selected patients with limited disease, and might be considered when technically feasible.[103] Sorafenib has been used with limited side-effects after liver transplantation, sometimes in conjunction with mTOR inhibitors, and might be considered when systemic treatment is warranted.[104] This topic is summarised in the last two recommendations: (36) HCC recurrence after liver transplantation may be treated by surgery for resectable lesions or by locoregional therapy or systemic therapy (including sorafenib) for unresectable lesions; (37) liver retransplantation is not appropriate treatment for recurrent HCC.

Conclusion

The 37 recommendations and statements presented here cover the most controversial topics surrounding liver transplantation for HCC, and may guide transplantation programmes around the world to improve management of their HCC patients. The phrasing of many recommendations permits adjustment according to variations in programme and regional circumstances, among which might be team experience and the availability of donor organs or living donation. Although the conference was not designed to address future areas of research, the existence of weak recommendations or absence of recommendation in a controversial area might serve as the basis to identify key questions that urgently require convincing answers.

Acknowledgments

OLT for HCC consensus group

Organising committee—J Belghiti (France); J Bruix (Spain); P-A Clavien (Switzerland); G Gores, D W Hanto, G Klintmalm, M Charlton (USA); C-M Lo (China); R J Porte (Netherlands).

Jury—A Perrier (president; Switzerland); B Langer (vice-president; Canada); G Barritt, (Australia); P Bossuyt (Netherlands); R Finn, B Hippen (USA); A Hisham (Malaysia); P Marcellin (France); A Sexton Dobby (Switzerland).

Chairs of the expert panels—A K Burroughs (UK); C Duvoux, D Samuel (France); A S H Gouw (Netherlands); D Grant, P Greig, N Kneteman (Canada); J M Lee (Korea); J Lerut (Belgium); J Llovet (Spain); V Mazzaferro (Italy); P Majno, B Müllhaupt (Switzerland); R Freeman, K Olthoff, E Pomfret, M Schwartz, J Trotter, F Yao (USA).

Details of members of the expert panels, local organising committee, and writing committee can be found in the webappendix p1.

References

1. European Liver Transplant Registry. [accessed Jan 1, 2011] Results. 2011. www.eltr.org/spip.php?rubrique37.

2. Organ Procurement and Transplantation Network. [accessed Jan 1, 2011] OPTN/SRTR Annual Report. www.ustransplant.org/annual_reports.

3. Grundahl, J. The Danish consensus conference model. In: Joss, S.; Durant, J., editors. Public participation in science: the role of consensus conferences in Europe. London: Science Museum; 1995.

4. Oxford Centre for Evidence-based Medicine. Levels of evidence. 2009 Mar. http://www.cebm.net/index.aspx?o=1025.

5. Lesurtel M, Clavien PA. 2010 international consensus conference on liver transplantation for hepatocellular carcinoma: texts of experts. Liver Transpl. 2011; 17(suppl 2):S1–S5. [PubMed: 21656651]

6. Samuel D, Colombo M, El-Serag H, Sobesky R, Heaton N. Toward optimizing the indications for orthotopic liver transplantation in hepatocellular carcinoma. Liver Transpl. 2011; 17(suppl 2):S6–S13. [PubMed: 21858912]

7. Müllhaupt B, Durand F, Roskams T, Dutkowski P, Heim M. Is tumor biopsy necessary? Liver Transpl. 2011; 17(suppl 2):S14–S25. [PubMed: 21744470]

8. Olthoff KM, Forner A, Hübscher S, Fung J. What is the best staging system for hepatocellular carcinoma in the setting of liver transplantation? Liver Transpl. 2011; 17(suppl 2):S26–S33. [PubMed: 21656653]

9. Lee JM, Trevisani F, Vilgrain V, Wald C. Imaging diagnosis and staging of hepatocellular carcinoma. Liver Transpl. 2011; 17(suppl 2):S34–S43. [PubMed: 21739567]

10. Mazzaferro V, Bhoori S, Sposito C, et al. Milan criteria in liver transplantation for hepatocellular carcinoma: an evidence-based analysis of 15 years of experience. Liver Transpl. 2011; 17(suppl 2):S44–S57. [PubMed: 21695773]

11. Germani G, Gurusamy K, Garcovich M, et al. Which matters most: Number of tumors, size of the largest tumor, or total tumor volume? Liver Transpl. 2011; 17(suppl 2):S58–S66. [PubMed: 21584928]

12. Llovet JM, Paradis V, Kudo M, Zucman-Rossi J. Tissue biomarkers as predictors of outcome and selection of transplant candidates with hepatocellular carcinoma. Liver Transpl. 2011; 17(suppl 2):S67–S71. [PubMed: 21594967]

13. Gouw AS, Balabaud C, Kusano H, Todo S, Ichida T, Kojiro M. Markers for microvascular invasion in hepatocellular carcinoma: where do we stand? Liver Transpl. 2011; 17(suppl 2):S72–S80. [PubMed: 21714066]

14. Prasad KR, Young RS, Burra P, et al. Summary of candidate selection and expanded criteria for liver transplantation for hepatocellular carcinoma: a review and consensus statement. Liver Transpl. 2011; 17(suppl 2):S81–S89. [PubMed: 21748847]

15. Lerut J, Mergental H, Kahn D, et al. Place of liver transplantation in the treatment of hepatocellular carcinoma in the normal liver. Liver Transpl. 2011; 17(suppl 2):S90–S97. [PubMed: 21796760]

16. Majno P, Lencioni R, Mornex F, Girard N, Poon RT, Cherqui D. Is the treatment of hepatocellular carcinoma on the waiting list necessary? Liver Transpl. 2011; 17(suppl 2):S98–S108. [PubMed: 21954097]

17. Yao FY, Breitenstein S, Broelsch CE, Dufour JF, Sherman M. Does a patient qualify for liver transplantation after the down-staging of hepatocellular carcinoma? Liver Transpl. 2011; 17(suppl 2):S109–S116. [PubMed: 21584927]

18. Kneteman N, Livraghi T, Madoff D, de Santibañez E, Kew M. Tools for monitoring patients with hepatocellular carcinoma on the waiting list and after liver transplantation. Liver Transpl. 2011; 17(suppl 2):S117–S127. [PubMed: 21584926]

19. Pomfret EA, Lodge JP, Villamil FG, Siegler M. Should we use living donor grafts for patients with hepatocellular carcinoma? Ethical considerations. Liver Transpl. 2011; 17(suppl 2):S128–S132. [PubMed: 21656657]

20. Grant D, Fisher RA, Abecassis M, McCaughan G, Wright L, Fan ST. Should the liver transplant criteria for hepatocellular carcinoma be different for deceased donation and living donation? Liver Transpl. 2011; 17(suppl 2):S133–S138. [PubMed: 21634006]

21. Greig PD, Geier A, D'Alessandro AM, Campbell M, Wright L. Should we perform deceased donor liver transplantation after living donor liver transplantation has failed? Liver Transpl. 2011; 17(suppl 2):S139–S146. [PubMed: 21563294]

22. Duvoux C, Kiuchi T, Pestalozzi B, Busuttil R, Miksad R. What is the role of adjuvant therapy after liver transplantation for hepatocellular carcinoma? Liver Transpl. 2011; 17(suppl 2):S147–S158. [PubMed: 21714065]

23. Schlitt HJ, Mornex F, Shaked A, Trotter JF. Immunosuppression and hepatocellular carcinoma. Liver Transpl. 2011; 17(suppl 2):S159–S161. [PubMed: 21506251]

24. Davis E, Wiesner R, Valdecasas J, Kita Y, Rossi M, Schwartz M. Treatment of recurrent hepatocellular carcinoma after liver transplantation. Liver Transpl. 2011; 17(suppl 2):S162–S166. [PubMed: 21688382]

25. Schunemann HJ, Oxman AD, Brozek J, et al. Grading quality of evidence and strength of recommendations for diagnostic tests and strategies. BMJ. 2008; 336:1106–1110. [PubMed: 18483053]

26. Chevret S, Trinchet JC, Mathieu D, et al. A new prognostic classification for predicting survival in patients with hepatocellular carcinoma. Groupe d'Etude et de Traitement du Carcinome Hepatocellulaire. J Hepatol. 1999; 31:133–141. [PubMed: 10424293]

27. Kudo M, Chung H, Osaki Y. Prognostic staging system for hepatocellular carcinoma (CLIP score): its value and limitations, and a proposal for a new staging system, the Japan Integrated Staging Score (JIS score). J Gastroenterol. 2003; 38:207–215. [PubMed: 12673442]

28. Leung TW, Tang AM, Zee B, et al. Construction of the Chinese University Prognostic Index for hepatocellular carcinoma and comparison with the TNM staging system, the Okuda staging system, and the Cancer of the Liver Italian Program staging system: a study based on 926 patients. Cancer. 2002; 94:1760–1769. [PubMed: 11920539]

29. Llovet JM, Bru C, Bruix J. Prognosis of hepatocellular carcinoma: the BCLC staging classification. Semin Liver Dis. 1999; 19:329–338. [PubMed: 10518312]

30. Okuda K, Ohtsuki T, Obata H, et al. Natural history of hepatocellular carcinoma and prognosis in relation to treatment. Study of 850 patients. Cancer. 1985; 56:918–928. [PubMed: 2990661]

31. Omagari K, Honda S, Kadokawa Y, et al. Preliminary analysis of a newly proposed prognostic scoring system (SLiDe score) for hepatocellular carcinoma. J Gastroenterol Hepatol. 2004; 19:805–811. [PubMed: 15209629]

32. Tateishi R, Yoshida H, Shiina S, et al. Proposal of a new prognostic model for hepatocellular carcinoma: an analysis of 403 patients. Gut. 2005; 54:419–425. [PubMed: 15710994]

33. A new prognostic system for hepatocellular carcinoma: a retrospective study of 435 patients: the Cancer of the Liver Italian Program (CLIP) investigators. Hepatology. 1998; 28:751–755. [PubMed: 9731568]

34. Wildi S, Pestalozzi BC, McCormack L, et al. Critical evaluation of the different staging systems for hepatocellular carcinoma. Br J Surg. 2004; 91:400–408. [PubMed: 15048738]

35. Makuuchi M, Sano K. The surgical approach to HCC: our progress and results in Japan. Liver Transpl. 2004; 10(suppl 1):46–52.

36. Bilimoria MM, Lauwers GY, Doherty DA, et al. Underlying liver disease, not tumor factors, predicts long-term survival after resection of hepatocellular carcinoma. Arch Surg. 2001; 136:528–535. [PubMed: 11343543]

37. Freeman RB, Mithoefer A, Ruthazer R, et al. Optimizing staging for hepatocellular carcinoma before liver transplantation: a retrospective analysis of the UNOS/OPTN database. Liver Transpl. 2006; 12:1504–1511. [PubMed: 16952174]

38. Silva MA, Hegab B, Hyde C, et al. Needle track seeding following biopsy of liver lesions in the diagnosis of hepatocellular cancer: a systematic review and meta-analysis. Gut. 2008; 57:1592–1596. [PubMed: 18669577]

39. Bruix J, Sherman M. Management of hepatocellular carcinoma. Hepatology. 2005; 42:1208–1236. [PubMed: 16250051]

40. Mazzaferro V, Regalia E, Doci R, et al. Liver transplantation for the treatment of small hepatocellular carcinomas in patients with cirrhosis. N Engl J Med. 1996; 334:693–699. [PubMed: 8594428]

41. Germani G, Gurusamy K, Garcovich M, et al. What matters: number of tumours, size of largest tumour, or total volume of tumour? Liver Transpl. 2011 published online May 16.

42. Toso C, Trotter J, Wei A, et al. Total tumor volume predicts risk of recurrence following liver transplantation in patients with hepatocellular carcinoma. Liver Transpl. 2008; 14:1107–1115. [PubMed: 18668667]

43. Toso C, Asthana S, Bigam DL, et al. Reassessing selection criteria prior to liver transplantation for hepatocellular carcinoma utilizing the Scientific Registry of Transplant Recipients database. Hepatology. 2009; 49:832–838. [PubMed: 19152426]

44. Mazzaferro V, Bhoori S, Sposito C, et al. Milan Criteria in liver transplantation for HCC: an evidence-based analysis on 15 years of experience. Liver Transpl. 2011 published online June 21.

45. [accessed Nov 1, 2010] Australia and New Zeland Liver Transplant Registry. 21st report. http://www.anzltr.org/thisYear

46. Yao FY, Ferrell L, Bass NM, et al. Liver transplantation for hepatocellular carcinoma: expansion of the tumor size limits does not adversely impact survival. Hepatology. 2001; 33:1394–1403. [PubMed: 11391528]

47. Yao FY, Xiao L, Bass NM, et al. Liver transplantation for hepatocellular carcinoma: validation of the UCSF-expanded criteria based on preoperative imaging. Am J Transplant. 2007; 7:2587–2596. [PubMed: 17868066]

48. Volk ML, Vijan S, Marrero JA. A novel model measuring the harm of transplanting hepatocellular carcinoma exceeding Milan criteria. Am J Transplant. 2008; 8:839–846. [PubMed: 18318783]

49. Villanueva A, Hoshida Y, Toffanin S, et al. New strategies in hepatocellular carcinoma: genomic prognostic markers. Clin Cancer Res. 2010; 16:4688–4694. [PubMed: 20713493]

50. Vibert E, Azoulay D, Hoti E, et al. Progression of alphafetoprotein before liver transplantation for hepatocellular carcinoma in cirrhotic patients: a critical factor. Am J Transplant. 2010; 10:129–137. [PubMed: 20070666]

51. Zheng SS, Xu X, Wu J, et al. Liver transplantation for hepatocellular carcinoma: Hangzhou experiences. Transplantation. 2008; 85:1726–1732. [PubMed: 18580463]

52. Ravaioli M, Grazi GL, Piscaglia F, et al. Liver transplantation for hepatocellular carcinoma: results of down-staging in patients initially outside the Milan selection criteria. Am J Transplant. 2008; 8:2547–2557. [PubMed: 19032223]

53. Lohe F, Angele MK, Rentsch M, et al. Multifocal manifestation does not affect vascular invasion of hepatocellular carcinoma: implications for patient selection in liver transplantation. Clin Transplant. 2007; 21:696–701. [PubMed: 17988261]

54. Parfitt JR, Marotta P, Alghamdi M, et al. Recurrent hepatocellular carcinoma after transplantation: use of a pathological score on explanted livers to predict recurrence. Liver Transpl. 2007; 13:543–551. [PubMed: 17394152]

55. Shah SA, Tan JC, McGilvray ID, et al. Does microvascular invasion affect outcomes after liver transplantation for HCC? A histopathological analysis of 155 consecutive explants. J Gastrointest Surg. 2007; 11:464–471. [PubMed: 17436131]

56. Liver Cancer Study Group of Japan. General rules for the clinical and pathological study of primary liver cancer. Tokyo: Kanehara Co; 1997.

57. Kornberg A, Freesmeyer M, Barthel E, et al. 18F-FDG-uptake of hepatocellular carcinoma on PET predicts microvascular tumor invasion in liver transplant patients. Am J Transplant. 2009; 9:592–600. [PubMed: 19191771]

58. Fujiki M, Takada Y, Ogura Y, et al. Significance of des-gamma-carboxy prothrombin in selection criteria for living donor liver transplantation for hepatocellular carcinoma. Am J Transplant. 2009; 9:2362–2371. [PubMed: 19656125]

59. Shirabe K, Itoh S, Yoshizumi T, et al. The predictors of microvascular invasion in candidates for liver transplantation with hepatocellular carcinoma—with special reference to the serum levels of des-gamma-carboxy prothrombin. J Surg Oncol. 2007; 95:235–240. [PubMed: 17323337]

60. Clavien PA, Petrowsky H, DeOliveira ML, et al. Strategies for safer liver surgery and partial liver transplantation. N Engl J Med. 2007; 356:1545–1559. [PubMed: 17429086]

61. Chang CH, Chau GY, Lui WY, et al. Long-term results of hepatic resection for hepatocellular carcinoma originating from the noncirrhotic liver. Arch Surg. 2004; 139:320–325. [PubMed: 15006892]

62. Lang H, Sotiropoulos GC, Domland M, et al. Liver resection for hepatocellular carcinoma in non-cirrhotic liver without underlying viral hepatitis. Br J Surg. 2005; 92:198–202. [PubMed: 15609381]

63. Liu S, Chan KW, Wang B, et al. Fibrolamellar hepatocellular carcinoma. Am J Gastroenterol. 2009; 104:2617–2624. [PubMed: 19638962]

64. Mergental H, Porte RJ. Liver transplantation for unresectable hepatocellular carcinoma in patients without liver cirrhosis. Transpl Int. 2010; 23:662–667. [PubMed: 20345561]

65. Houben KW, McCall JL. Liver transplantation for hepatocellular carcinoma in patients without underlying liver disease: a systematic review. Liver Transpl Surg. 1999; 5:91–95. [PubMed: 10071346]

66. Lesurtel M, Mullhaupt B, Pestalozzi BC, et al. Transarterial chemoembolization as a bridge to liver transplantation for hepatocellular carcinoma: an evidence-based analysis. Am J Transplant. 2006; 6:2644–2650. [PubMed: 16939518]

67. Yao FY, Kerlan RK, Hirose R, et al. Excellent outcome following down-staging of hepatocellular carcinoma prior to liver transplantation: an intention-to-treat analysis. Hepatology. 2008; 48:819–827. [PubMed: 18688876]

68. Bruix J, Sherman M, Llovet JM, et al. Clinical management of hepatocellular carcinoma. Conclusions of the Barcelona-2000 EASL conference. J Hepatol. 2001; 35:421–430. [PubMed: 11592607]

69. Lewandowski RJ, Kulik LM, Riaz A, et al. A comparative analysis of transarterial downstaging for hepatocellular carcinoma: chemoembolization versus radioembolization. Am J Transplant. 2009; 9:1920–1928. [PubMed: 19552767]

70. Majno PE, Lencioni R, Mornex F, et al. Is treatment of HCC on the waiting list necessary? Liver Transpl. 2011; 17(suppl 2):S98–S108. [PubMed: 21954097]

71. Martin AP, Goldstein RM, Dempster J, et al. Radiofrequency thermal ablation of hepatocellular carcinoma before liver transplantation—a clinical and histological examination. Clin Transplant. 2006; 20:695–705. [PubMed: 17100718]

72. Pompili M, Mirante VG, Rondinara G, et al. Percutaneous ablation procedures in cirrhotic patients with hepatocellular carcinoma submitted to liver transplantation: assessment of efficacy at explant analysis and of safety for tumor recurrence. Liver Transpl. 2005; 11:1117–1126. [PubMed: 16123960]

73. Cronin DC, Millis JM. Living donor liver transplantation: the ethics and the practice. Hepatology. 2008; 47:11–13. [PubMed: 18161704]

74. Di Sandro S, Slim AO, Giacomoni A, et al. Living donor liver transplantation for hepatocellular carcinoma: long-term results compared with deceased donor liver transplantation. Transplant Proc. 2009; 41:1283–1285. [PubMed: 19460539]

75. Fisher RA, Kulik LM, Freise CE, et al. Hepatocellular carcinoma recurrence and death following living and deceased donor liver transplantation. Am J Transplant. 2007; 7:1601–1608. [PubMed: 17511683]

76. Hwang S, Lee SG, Joh JW, et al. Liver transplantation for adult patients with hepatocellular carcinoma in Korea: comparison between cadaveric donor and living donor liver transplantations. Liver Transpl. 2005; 11:1265–1272. [PubMed: 16184545]

77. Kulik L, Abecassis M. Living donor liver transplantation for hepatocellular carcinoma. Gastroenterology. 2004; 127(suppl 1):277–282.

78. Lo CM, Fan ST, Liu CL, et al. Living donor versus deceased donor liver transplantation for early irresectable hepatocellular carcinoma. Br J Surg. 2007; 94:78–86. [PubMed: 17016793]

79. Vakili K, Pomposelli JJ, Cheah YL, et al. Living donor liver transplantation for hepatocellular carcinoma: increased recurrence but improved survival. Liver Transpl. 2009; 15:1861–1866. [PubMed: 19938113]

80. Olthoff KM, Merion RM, Ghobrial RM, et al. Outcomes of 385 adult-to-adult living donor liver transplant recipients: a report from the A2ALL Consortium. Ann Surg. 2005; 242:314–323. [PubMed: 16135918]

81. Zimmerman MA, Ghobrial RM, Tong MJ, et al. Recurrence of hepatocellular carcinoma following liver transplantation: a review of preoperative and postoperative prognostic indicators. Arch Surg. 2008; 143:182–188. [PubMed: 18283144]

82. Hollebecque A, Decaens T, Boleslawski E, et al. Natural history and therapeutic management of recurrent hepatocellular carcinoma after liver transplantation. Gastroenterol Clin Biol. 2009; 33:361–369. [PubMed: 19398289]

83. Roberts JP. Tumor surveillance-what can and should be done? Screening for recurrence of hepatocellular carcinoma after liver transplantation. Liver Transpl. 2005; 11(suppl 2):45–46.

84. Hojo M, Morimoto T, Maluccio M, et al. Cyclosporine induces cancer progression by a cell-autonomous mechanism. Nature. 1999; 397:530–534. [PubMed: 10028970]

85. Soll C, Clavien PA. Inhibition of mammalian target of rapamycin: two goals with one shot? J Hepatol. 2011; 54:182–183. [PubMed: 20952085]

86. Chinnakotla S, Davis GL, Vasani S, et al. Impact of sirolimus on the recurrence of hepatocellular carcinoma after liver transplantation. Liver Transpl. 2009; 15:1834–1842. [PubMed: 19938137]

87. Toso C, Meeberg GA, Bigam DL, et al. De novo sirolimus-based immunosuppression after liver transplantation for hepatocellular carcinoma: long-term outcomes and side effects. Transplantation. 2007; 83:1162–1168. [PubMed: 17496530]

88. Toso C, Merani S, Bigam DL, et al. Sirolimus-based immunosuppression is associated with increased survival after liver transplantation for hepatocellular carcinoma. Hepatology. 2010; 51:1237–1243. [PubMed: 20187107]

89. Stone MJ, Klintmalm GB, Polter D, et al. Neoadjuvant chemotherapy and liver transplantation for hepatocellular carcinoma: a pilot study in 20 patients. Gastroenterology. 1993; 104:196–202. [PubMed: 8380393]

90. Cherqui D, Piedbois P, Pierga JY, et al. Multimodal adjuvant treatment and liver transplantation for advanced hepatocellular carcinoma. A pilot study. Cancer. 1994; 73:2721–2726. [PubMed: 8194012]

91. Roayaie S, Frischer JS, Emre SH, et al. Long-term results with multimodal adjuvant therapy and liver transplantation for the treatment of hepatocellular carcinomas larger than 5 centimeters. Ann Surg. 2002; 235:533–539. [PubMed: 11923610]

92. Hsieh CB, Chou SJ, Shih ML, et al. Preliminary experience with gemcitabine and cisplatin adjuvant chemotherapy after liver transplantation for hepatocellular carcinoma. Eur J Surg Oncol. 2008; 34:906–910. [PubMed: 18166289]

93. Olthoff KM, Rosove MH, Shackleton CR, et al. Adjuvant chemotherapy improves survival after liver transplantation for hepatocellular carcinoma. Ann Surg. 1995; 221:734–741. [PubMed: 7794077]

94. Zhang ZH, Ma LW, Song SB, et al. Adjuvant chemotherapy after orthotopic liver transplantation for advanced hepatocellular carcinoma. Zhonghua Zhong Liu Za Zhi. 2005; 27:45–47. (in Chinese). [PubMed: 15771799]

95. Chen GH, Lu MQ, Cai CJ, et al. Clinical study of adjuvant individualized chemotherapy for hepatocellular carcinoma after liver transplantation. Zhonghua Wai Ke Za Zhi. 2004; 42:1040–1043. (in Chinese). [PubMed: 15498315]

96. Sun J, Hou BH, Jian ZX, et al. Value of perioperative adjuvant therapy in liver transplantation for advanced hepatocellular carcinoma. Nan Fang Yi Ke Da Xue Xue Bao. 2007; 27:471–473. (in Chinese). [PubMed: 17545034]

97. Xu J, Shen ZY, Chen XG, et al. A randomized controlled trial of Licartin for preventing hepatoma recurrence after liver transplantation. Hepatology. 2007; 45:269–276. [PubMed: 17256759]

98. Soderdahl G, Backman L, Isoniemi H, et al. A prospective, randomized, multi-centre trial of systemic adjuvant chemotherapy versus no additional treatment in liver transplantation for hepatocellular carcinoma. Transpl Int. 2006; 19:288–294. [PubMed: 16573544]

99. Pokorny H, Gnant M, Rasoul-Rockenschaub S, et al. Does additional doxorubicin chemotherapy improve outcome in patients with hepatocellular carcinoma treated by liver transplantation? Am J Transplant. 2005; 5:788–794. [PubMed: 15760403]

100. Li N, Zhou J, Weng D, et al. Adjuvant adenovirus-mediated delivery of herpes simplex virus thymidine kinase administration improves outcome of liver transplantation in patients with advanced hepatocellular carcinoma. Clin Cancer Res. 2007; 13:5847–5854. [PubMed: 17908978]

101. Llovet JM, Ricci S, Mazzaferro V, et al. Sorafenib in advanced hepatocellular carcinoma. N Engl J Med. 2008; 359:378–390. [PubMed: 18650514]

102. Kita Y, Klintmalm G, Kobayashi S, et al. Retransplantation for de novo hepatocellular carcinoma in a liver allograft with recurrent hepatitis B cirrhosis 14 years after primary liver transplantation. Dig Dis Sci. 2007; 52:392–393.

103. Taketomi A, Fukuhara T, Morita K, et al. Improved results of a surgical resection for the recurrence of hepatocellular carcinoma after living donor liver transplantation. Ann Surg Oncol. 2010; 17:2283–2289. [PubMed: 20204531]

104. Yoon DH, Ryoo BY, Ryu MH, et al. Sorafenib for recurrent hepatocellular carcinoma after liver transplantation. Jpn J Clin Oncol. 2010; 40:768–773. [PubMed: 20494947]
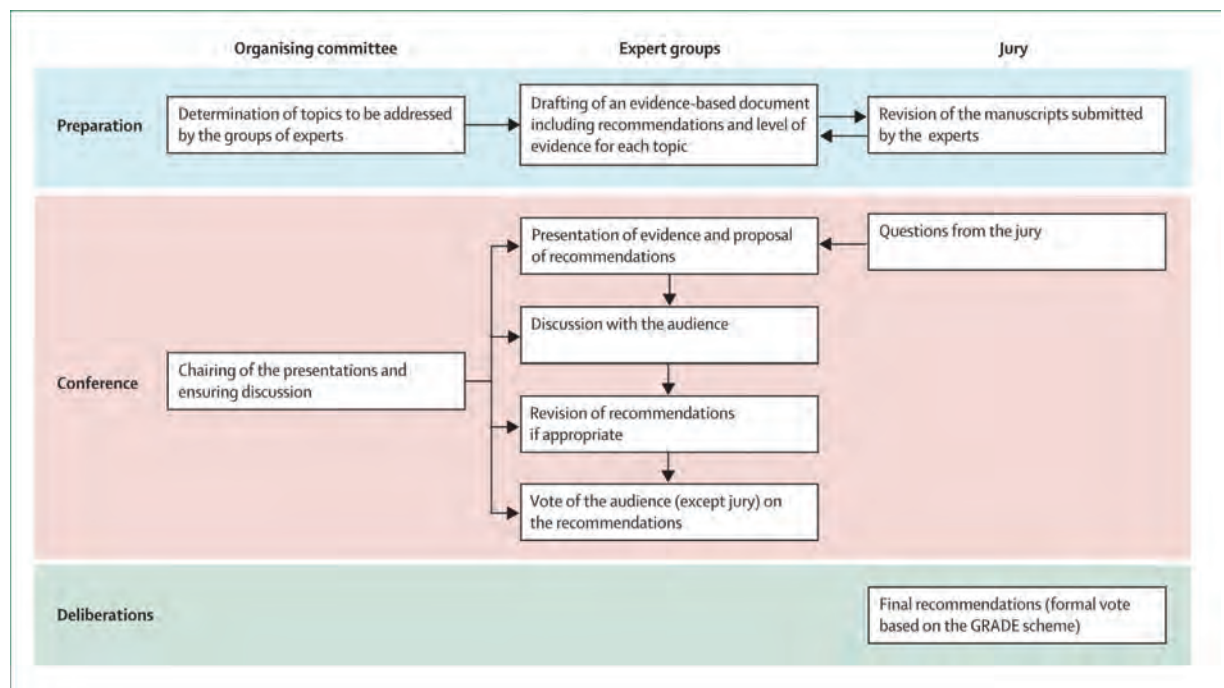
Figure 1. Format of the HCC consensus conference
The role of the organising committee, expert groups, and jury at each step of the conference.
HCC=hepatocellular carcinoma. GRADE=grading of recommendations assessment,
development, and evaluation.

Table 1

Summary of recommendations and statements

	Level of evidence	Strength of recommendation
Assessment of candidates with HCC for liver transplantation		
1. When considering treatment options for patients with HCC, the BCLC staging system is the preferred staging system to assess the prognosis of patients with HCC	2b (P)	Strong
2. The TNM system (7th edn) including pathological examination of the explanted liver, should be used for determining prognosis after transplantation with the addition of assessment of microvascular invasion	2b (P)	Strong
3. Either dynamic CT or dynamic MRI with the presence of arterial enhancement followed by washout on portal venous or delayed imaging is the best non-invasive test to make a diagnosis in cirrhotic patients suspected of having HCC and for preoperative staging	1b (D)	Strong
4. Extrahepatic staging should include CT of the chest, and CT or MRI of the abdomen and pelvis	3b (D)	Strong
5. Tumour biopsy is not required in cirrhotic patients considered for liver transplantation who have high-quality dynamic CT or MRI findings typical for HCC and a lesion larger than 1 cm according to current AASLD guidelines	1b (D)	Weak
6. For patients with lesions smaller or equal to 10 mm, non-invasive imaging does not allow an accurate diagnosis and should not be used to make a decision for or against transplantation	1b (D)	Strong
Criteria for listing candidates with HCC in cirrhotic livers for DDLT		
7. Liver transplantation should be reserved for HCC patients who have a predicted 5-year survival comparable to non-HCC patients	NA	Weak
8. Preoperative assessment of the size of the largest tumour or total diameter of tumours should be the main consideration in selecting patients with HCC for liver transplantation	2a (P)	Strong`
9. The Milan criteria are currently the benchmark for the selection of HCC patients for liver transplantation, and the basis for comparison with other suggested criteria	2a (P)	Strong
10. A modest expansion of the number of potential candidates may be considered on the basis of several studies showing comparable survival for patients outside the Milan criteria	3b (P)	Weak
11. Patients with worse prognosis may be considered for liver transplantation outside the Milan criteria if the dynamics of the waiting list allow it without undue prejudice to other recipients with a better prognosis	NA	Weak
12. α-fetoprotein concentrations add prognostic information in HCC patients and may be used for making decisions regarding transplantation in combination with imaging criteria	2b (P)	Weak
13. Biomarkers other than α-fetoprotein cannot yet be used for clinical decision making regarding liver transplantation for HCC	2b (P)	Strong
14. Indication for liver transplantation in HCC should not rely on microvascular invasion because it cannot be reliably detected prior to transplantation	2b (P)	Strong
Criteria for HCC candidates with non-cirrhotic livers		
15. The Milan criteria and its modifications are not applicable to patients with HCC developing in a non-cirrhotic liver. Such patients with non-resectable HCC and absence of macrovascular invasion and extrahepatic spread may be considered as appropriate candidates for liver transplantation	4 (P)	Weak
16. Patients with HCC in non-cirrhotic liver who were treated by resection, and have intrahepatic recurrence of HCC and no evidence of lymph node or macrovascular invasion, may be considered for salvage transplantation	4 (P)	Weak
Role of downstaging		
17. Transplantation may be considered after successful downstaging	5 (P)	Weak
18. Liver transplantation after successful downstaging should achieve a 5-year survival comparable to that of HCC patients who meet the criteria for liver transplantation without requiring downstaging	5 (P)	Strong
19. Criteria for successful downstaging should include tumour size and number of viable tumours	4 (P)	Strong
20. α-fetoprotein concentrations before and after downstaging may add additional information	4 (P)	Weak

	Level of evidence	Strength of recommendation
21. Based on existing evidence, no recommendation can be made for preferring a specific locoregional therapy for downstaging over others	NA	None
Managing patients on the waiting list		
22. Periodic waiting-list monitoring should be performed by imaging (dynamic CT, dynamic MRI, or contrast-enhanced ultrasonography) and α-fetoprotein measurements	5 (P)	Strong
23. Based on current absence of evidence, no recommendation can be made on bridging therapy in patients with UNOS T1 (≤2 cm) HCC	NA	None
24. In patients with UNOS T2 (one nodule 2–5 cm or three or more nodules each ≤3 cm) HCC (Milan criteria) and a likely waiting time longer than 6 months, locoregional therapy may be appropriate	4 (P)	Weak
25. No recommendation can be made for preferring any type of locoregional therapy to others	NA	None
26. Patients found to have progressed beyond criteria acceptable for listing for liver transplantation should be placed on hold and considered for downstaging	5 (P)	Strong
27. Patients with progressive disease in whom locoregional intervention is not considered appropriate, or is ineffective, should be removed from the waiting list	5 (P)	Strong
Role of LDLT		
28. LDLT is acceptable for HCC patients who have an expected 5-year survival similar to comparably staged patients receiving a deceased donor liver. In LDLT, careful attention should be given to psychosocial considerations regarding both donor and recipient	NA	Weak
29. LDLT must be restricted to centres of excellence in liver surgery and liver transplantation to minimise donor risk and maximise recipient outcome	NA	Strong
30. In patients following LDLT for HCC within the accepted regional criteria for DDLT, retransplantation for graft failure is justified	5 (P)	Weak
31. In patients following LDLT for HCC outside the accepted regional criteria for DDLT, retransplantation for graft failure using a deceased donor organ is not recommended	5 (P)	Strong
Post-transplant management		
32. Post-transplant monitoring may include 6–12 monthly contrast-enhanced CT or MRI imaging and α-fetoprotein measurements	5 (P)	Weak
33. There is currently insufficient evidence from clinical trials to base a recommendation for choosing the type or dose of immunosuppression therapy to influence the incidence of HCC recurrence or its prognosis	NA	None
34. Based on current evidence, no recommendation can be made on the use of mTOR inhibitors solely to reduce the risk of HCC recurrence outside clinical trials	NA	None
35. The current evidence does not justify the routine use of adjuvant antitumour therapy after liver transplantation for HCC outside of a controlled clinical trial	NA	Weak
36. HCC recurrence after liver transplantation may be treated by surgery for resectable lesions or by locoregional therapy or systemic therapy (including sorafenib) for unresectable lesions	4 (P)	Weak
37. Liver retransplantation is not appropriate treatment for recurrent HCC	NA	Strong

Level of evidence for each recommendation refers to the Oxford classification.[4] HCC=hepatocellular carcinoma. BCLC=Barcelona Clinic Liver Cancer. TNM=tumour, node, metastasis. P=prognosis. D=diagnosis. AASLD=American Association for the Study of Liver Diseases. NA=not applicable. OLT=orthotopic liver transplantation. UNOS=United Network for Organ Sharing. LDLT=living donor liver transplantation. DDLT=deceased donor liver transplantation.

Lancet Oncol. Author manuscript; available in PMC 2012 August 13.

— 200 —

Table 2

Staging systems for stratification of patients with hepatocellular carcinoma

	TNM (7th ed)	Okuda	CLIP	BCLC	JIS	GRETCH	CUPI	Tokyo
Year introduced	2010	1985	1998	1999	2003	1999	2002	2005
Liver function	No	Bilirubin, albumin, ascites	CTP class	CTP class, portal hypertension	CTP class	Bilirubin, alkaline phosphatase	Bilirubin, alkaline phosphatase, ascites	Bilirubin, albumin
Performance status	No	No	No	Yes, ECOG status	No	Yes, Karnofsky	No	No
Tumour burden	Number of nodules, tumour size, PV invasion, metastasis	Tumour > or <50% of liver	Tumour > or <50% of liver, PV invasion, metastasis	Number of nodules, tumour size, PV invasion, metastasis	TNM stage, define by LCSGJ	PV thrombosis	TNM stage	Number of nodules, tumour size
α-fetoprotein concentration	No	No	Yes, cutoff 400 ng/ mL	No	No	Yes, cutoff 25 ng/mL	Yes, cutoff 500 ng/ mL	No
Staging categories	I, II, III, IV	Score 0–4; stage I, II, III	0–6	0, A, B, C, D	0–5	Score 0–3 risk groups	Score 0–12; three risk groups	0–8
Other parameters							+/– symptom disease	

The Up-to-7 criteria system was not selected since it does not include clinical performance, liver function, or tumour markers. Furthermore, since the system is dependent on microvascular invasion, it is not clinically applicable. TNM=tumour, node, metastasis. CLIP=Cancer of the Liver Italian Program. BCLC=Barcelona Clinic Liver Cancer. JIS=Japan Integrated Scoring. GRETCH=Groupe d'Etude et de Traitement du Carcinoma Hepatocellulaire. CUPI=Chinese University Prognostic Index. CTP=Child-Pugh-Turcotte. ECOG=Eastern Cooperative Oncology Group. PV=portal vein. LCSGJ=Liver cancer study group of Japan.

Treatment response assessment of radiofrequency ablation for hepatocellular carcinoma: Usefulness of virtual CT sonography with magnetic navigation

Yasunori Minami *, Satoshi Kitai, Masatoshi Kudo

Division of Gastroenterology and Hepatology, Department of Internal Medicine, Kinki University School of Medicine, 377-2 Ohno-Higashi, Osaka-Sayama 589-8511, Japan

ARTICLE INFO

ABSTRACT

Purpose: Virtual CT sonography using magnetic navigation provides cross sectional images of CT volume data corresponding to the angle of the transducer in the magnetic field in real-time. The purpose of this study was to clarify the value of this virtual CT sonography for treatment response of radiofrequency ablation for hepatocellular carcinoma.

Patients and methods: Sixty-one patients with 88 HCCs measuring 0.5–1.3 cm (mean $\pm$ SD, 1.0 ± 0.3 cm) were treated by radiofrequency ablation. For early treatment response, dynamic CT was performed 1–5 days (median, 2 days). We compared early treatment response between axial CT images and multi-angle CT images using virtual CT sonography.

Results: Residual tumor stains on axial CT images and multi-angle CT images were detected in 11.4% (10/88) and 13.6% (12/88) after the first session of RFA, respectively ($P = 0.65$). Two patients were diagnosed as showing hyperemia enhancement after the initial radiofrequency ablation on axial CT images and showed local tumor progression shortly because of unnoticed residual tumors. Only virtual CT sonography with magnetic navigation retrospectively showed the residual tumor as circular enhancement. In safety margin analysis, 10 patients were excluded because of residual tumors. The safety margin more than 5 mm by virtual CT sonographic images and transverse CT images were determined in 71.8% (56/78) and 82.1% (64/78), respectively ($P = 0.13$). The safety margin should be overestimated on axial CT images in 8 nodules.

Conclusion: Virtual CT sonography with magnetic navigation was useful in evaluating the treatment response of radiofrequency ablation therapy for hepatocellular carcinoma.

© 2011 Elsevier Ireland Ltd. All rights reserved.

1. Introduction

Recently, a virtual CT sonographic visualization system with magnetic navigation was introduced to the clinical practice of Hepatology [1–6]. Virtual CT sonography using magnetic navigation can show any cross sectional images of CT volume data in real-time corresponding to the angle of the transducer attached to the sensor in the magnetic field. Therefore, real-time virtual CT sonography can indicate the 3-dimensional relationship between liver vasculature and tumors. It has been reported that the safety and feasibility of virtual CT sonography with magnetic navigation guidance of percutaneous radiofrequency ablation (RFA) in patients with hepatocellular carcinoma (HCC), even though the nodules are poorly defined on B-mode sonography [2,3]. However, there are no reports of virtual CT sonography for therapeutic evaluation.

In this study, we evaluated the value of this virtual CT sonography with magnetic navigation for treatment response of RFA for HCC.

2. Materials and methods

The Ethics Committee of our institution approved the study protocol. Written informed consent was obtained from each patient or a family member at enrollment.

Between January 2006 and June 2006, all 61 patients (43 men, 18 women; age range, 55–84 years; mean age $\pm$ SD, 69.7 years $\pm$ 6.9) with 88 HCCs were treated by percutaneous RFA (Table 1). We usually evaluate the treatment response of RFA by only axial CT images. In this study, treatment response using virtual CT sonography was retrospectively assessed based on not only the axial images but also all cross sectional images. We compared early treatment response between axial CT images and multi-angle CT images using virtual CT sonography.

HCCs were diagnosed based on three-phase contrast-enhanced CT findings such as positive enhancement in the arterial phase and wash-out in the equilibrium phase in patients with chronic liver

* Corresponding author at: Department of Gastroenterology and Hepatology, Kinki University School of Medicine, 377-2 Ohno-Higashi, Osaka-Sayama 589-8511, Japan. Tel.: +81 72 366 0221x3149; fax: +81 72 367 2880.

E-mail address: minkun@med.kindai.ac.jp (Y. Minami).

Table 1
Baseline clinical characteristics of patients.

Age (years)	
Mean ± SD (range)	69.7 ± 6.9 (55–84)
Sex	
Male/female	43/18
Etiology of liver chronic disease	
HBV/HCV/HBV + HCV/none	7/52/2/0
Child–Pugh classification A/B/C	39/22/0
Diameter of entire hepatic malignancies (cm)	
Mean ± SD (range)	1.6 ± 0.5 (0.5–3.5)
Previous treatments	
None/TACE	44/17

Note. Data are presented as mean ± standard deviation unless otherwise indicated. HCC: hepatocellular carcinoma, TACE: transcatheter arterial chemoembolization.

disease. All patients met the following criteria for treatment with RFA: presence of viable HCCs with a maximum diameter not greater than 4.0 cm, percutaneous accessibility of the tumors, absence of portal tumor thrombus and extrahepatic metastasis, prothrombin time ratio greater than 50%, total bilirubin less than 3.0 mg/dl, and platelet count greater than 50,000/μL.

2.1. Equipment and techniques

B-mode sonographic scans were obtained by EUB 8500 unit (HITACHI Medico, Tokyo, Japan) with a 3.5 MHz curved-array transducer. The virtual CT sonography system (Real-time Virtual Sonography; HITACHI Medico, Tokyo, Japan) was composed of EUB 8500 unit, magnetic location detector unit, a magnetic field generator and a magnetic sensor attached to the ultrasonic transducer [2,3]. This generator produced an interacting magnetic field yielding an approximately spherical 70 cm uniform magnetic field of

0.03 T. A smooth image of virtual CT sonography was provided by a display of 10 frames per a second display as 256 by 256 pixel images.

A multidetector CT (LightSpeed VCT, GE Medical Systems, Milwaukee, WI) was used for diagnosis. Triple-phase contrast-enhanced CT scans were performed with a 5.0-mm slice thickness at 40, 70 and 180 s after initiating the injection of contrast media to obtain late hepatic arterial, portal venous and equilibrium phase images, respectively.

Patients were treated by RFA (Cooled-tip RF ablation system; Radionics, Burlington, MA). A 200-W, 480-kHz monopolar RF generator regulated by impedance (CC-1, Radionics) was used as the energy source.

2.2. Virtual CT sonography using magnetic navigation

The magnetic generator was set up on a bed without the patient. The magnetic sensor was attached to the ultrasonic transducer connected to the magnetic location detector unit of EUB 8500. After starting the Real-time Virtual Sonography software, CT volume data of the late arterial phase after the RFA procedure was installed in the EUB 8500 unit as digital imaging and communication in medicine (DICOM) standard via the local area network in our hospital. We selected a CT image at the caudal level of the xiphoid, and took the transducer lengthwise in a position about 20 cm above the bed in front of the magnetic generator, that is, we set the transducer in the air. Thereafter, we could set a common point as the position of the transducer at the xiphoid level CT image. Virtual CT sonography could start to show the image on the monitor of EUB 8500 corresponding to the movement of the transducer in the magnetic field although the patient was not on the bed (Fig. 1).
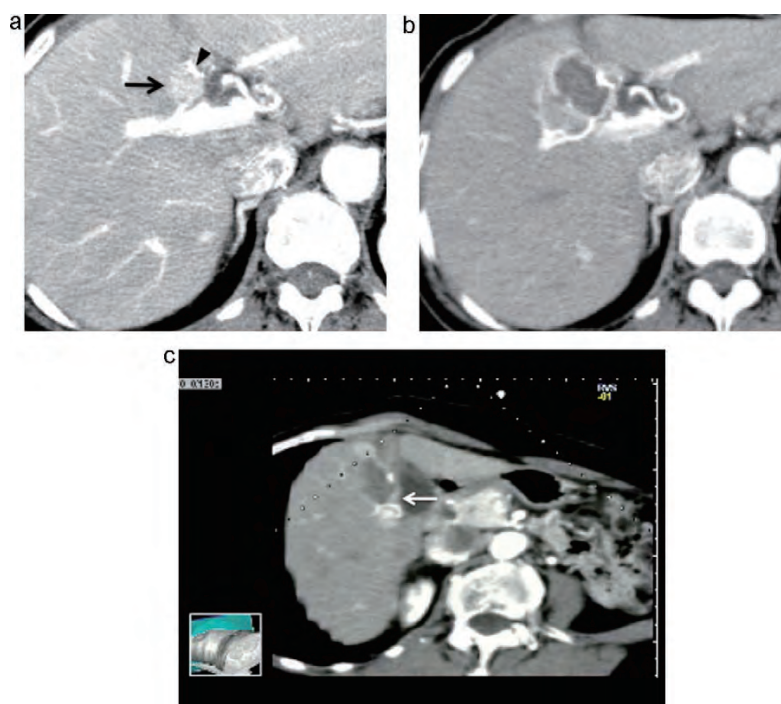

Fig. 1. A 70-year-old man with 1.5 cm local tumor progression of hepatocellular carcinoma after transcatheter arterial chemoembolization about 1 year ago. (A) Early phase dynamic CT scan shows local tumor progression of hepatocellular carcinoma as enhanced lesion (arrow) in segment 4 of liver. Iodized oil accumulated spot was depicted in touch with viable hepatocellular carcinoma (arrowhead). (B) Axial CT scan of early phase obtained two days after radiofrequency ablation therapy shows that thin enhancement around the ablated area could be caused by hyperemia. (C) Virtual CT sonography obtained from the same CT volume data of Fig. 1B shows a circular enhancement portion (arrow) by oblique dimensional assessment. Left bottom: plane against the body trunk shows the transducer angle.

Table 2
Residual hepatic malignancies after radiofrequency ablation between virtual CT sonographic images and axial CT images.

	Virtual CT sonographic images		
	Negative	Positive	Total
Axial CT images			
Negative	76	2	78
Positive	0	10	10
Total	76	12	88

Table 3
Safety margin after radiofrequency ablation between virtual CT sonographic images and axial CT images.

	Virtual CT sonographic images		
	5 mm<	5 mm>	Total
Axial CT images			
5 mm<	56	8	64
5 mm>	0	14	14
Total	56	22	78

2.3. Assessment of treatment response and follow-up

For early treatment response, dynamic CT was performed 1–5 days (median, 2 days). A tumor was considered to have been successfully ablated when there were no longer any enhanced regions either within the entire tumor during the arterial phase and at least a 0.5 cm margin of apparently normal hepatic tissue surrounding the tumor during the portal phase [7,8]. Part of the tumor was diagnosed as remaining viable when images of the ablated area showed nodular peripheral enhancement. The residual portion was treated with additional RFA the following week.

If 1-month follow-up CT images showed successful ablation and no new tumors, three-phase contrast-enhanced CT scans were repeated at 3-month intervals. The follow-up time ranged from 4 to 18 months (mean ± SD, 8.9 ± 2.4 months).

2.4. Statistical analysis

Data are expressed as mean ± SD. We compared early treatment response between axial CT images and multi-angle CT images using virtual CT sonography. Differences between the two groups were evaluated by Chi-square test. A P value less than 0.05 was considered significant.

3. Results

Residual tumor stains on axial CT images and multi-angle CT images were detected in 11.4% (10/88) and 13.6% (12/88) after the first session of RFA, respectively ($P = 0.65$, Chi square test) (Table 2). There are no false positive cases by axial CT diagnosed complete ablation by virtual CT sonography. After first ablation therapy, the maximal diameter of the residual tumors ranged from 0.5 to 1.3 cm (mean ± SD, 1.0 ± 0.3 cm) on axial CT. Tumors showing residual enhancement underwent additional radiofrequency procedures on next week. However, two patients showed local tumor progression of HCC a few months after the initial ablation because of unnoticed residual tumors by axial CT assessment. These two patients were diagnosed as showing hyperemia enhancement after RFA on axial CT images. However, only virtual CT sonography with magnetic navigation retrospectively showed the residual tumor as circular enhancement in these two patients (Fig. 1).

In safety margin analysis, 10 patients were excluded because of residual tumors. The safety margin more than 5 mm by virtual CT sonographic images and axial CT images were determined in 71.8% (56/78) and 82.1% (64/78), respectively ($P = 0.13$, Chi square test) (Table 3). In 56 HCC nodules, the findings of both modalities could detect the safety margin more than 5 mm. Moreover, the safety margin less than 5 mm was shown in 14 HCCs on both modalities. For 70 of the 78 nodules, findings visualized on virtual CT sonography of safety margin agreed with findings seen on axial dynamic CT. However, in remaining 8 nodules, the findings of safety margin showed discrepant on between virtual CT sonographic images and axial CT images. We could mention that the safety margin was overestimated on axial CT images. On the other hand, there are

no patients with the safety margin more than 5 mm by axial CT diagnosed insufficient by virtual CT sonography.

4. Discussion

Axial CT images are mainly used in the evaluation of the therapeutic response of HCCs after RFA [7–9]. In this study, two patients with two HCC nodules showed local tumor progression a few months after first ablation because of residual tumors that were unnoticed on axial CT images. The shape of enhanced lesion can help to diagnose small residual HCC or hyperemia. However, it is often difficult to distinguish between small residual HCC and hyperemia lesion because of each showing enhancement on arterial CT images. By one-sectional CT images, small HCC could not be necessarily depicted as circular enhancement. Findings indicated that even though differences did not quite reach significance, however, multi-angle CT images could show the residual HCC in these two patients. Moreover, we found that virtual CT sonography was highly sensitive in patients with 8 HCC nodules for assessing the 5 mm safety margin around the whole tumor. Assessment of RFA with 3-dimensional information must have higher accuracy than with 2-dimension's. Local tumor progression after RFA could be related to poor accuracy of the treatment response evaluation.

Magnetic navigation has two features for clinical application as treatment response of RFA therapy. The first is a bodily sensation. Usual virtual CT sonography system runs on a PC [10–12]; thereby, virtual images used to provide only visual information. On the other hand, this virtual CT sonography with magnetic navigation system can show any cross-section of MPR imaging corresponding to the movement of the transducer. By magnetic navigation, we can also feel any cross-section of MPR images from the angle of the transducer. Because of RFA procedure guided by sonography, we might be able to make the use of this bodily sensation to the second RFA sessions. The second is its swift response. With powerful operating computer, virtual CT sonography with magnetic navigation can display smoothly for each movement of the transducer in the magnetic field in real-time.

Contrast harmonic sonography with an intravenous contrast agent has demonstrated an intratumoral micro flow sensitively and accurately [1,13]. Small residual HCCs after RFA could be depicted on contrast harmonic sonography. However, even on B-mode sonography, as well as on contrast harmonic sonography, it is almost impossible to identify the safety margin because of the difficulty in identifying the edge between the necrotic tumor and the ablated peritumoral liver tissue. Therefore, contrast harmonic sonography can only reveal whether residual tumor is present; it cannot be used to identify whether the safety margin is large enough [14–17]. On the other hand, virtual CT sonography could evaluate the safety margin easily in comparison with CT images after/before RFA without sonographic dead-zones.

The principal limitation of this study was the retrospective, which inherently decreases the statistical strength. Another limitation is the preliminary nature of this study with the relatively small number of patients and short follow-up time. Further prospective

studies of this technique with a larger number of patients are warranted.

In conclusion, real-time virtual CT sonography with magnetic navigation could show multi-cross sections of MPR images, which provided 3-dimensional information in the liver easily. In addition, we can also feel any cross-sections of MPR images from the angle of the transducer by magnetic navigation. Virtual CT sonography can be useful in evaluating the treatment response of RFA therapy for HCC.

References

[1] Kudo M. New sonographic techniques for the diagnosis and treatment of hepatocellular carcinoma. Hepatol Res 2007;37:S193–9.
[2] Minami Y, Kudo M, Chung H, et al. Percutaneous radiofrequency ablation of sonographically unidentifiable liver tumors. Feasibility and usefulness of a novel guiding technique with an integrated system of computed tomography and sonographic images. Oncology 2007;72:111–6.
[3] Minami Y, Chung H, Kudo M, et al. Radiofrequency ablation of hepatocellular carcinoma: value of virtual CT sonography with magnetic navigation. AJR 2008;190:W335–41.
[4] Sandulescu L, Saftoiu A, Dumitrescu D, Ciuree T. The role of real-time virtual sonography in the assessment of malignant liver lesions. J Gastrointestin Liver Dis 2009;18:103–8.
[5] Okamoto E, Sato S, Sanchez-Siles AA, et al. Evaluation of virtual CT sonography for enhanced detection of small hepatic nodules: a prospective pilot study. AJR 2010;194:1272–8.
[6] Kisaka Y, Hirooka M, Koizumi Y, et al. Contrast-enhanced sonography with abdominal virtual sonography in monitoring radiofrequency ablation of hepatocellular carcinoma. J Clin Ultrasound 2010;38(3):138–44.
[7] Livraghi T, Meloni F, Stasi MD, et al. Sustained complete response and complications rate of radiofrequency ablation of very early hepatocellular carcinoma in cirrhosis: is resection still the treatment choice. Hepatology 2008;47:82–9.
[8] Oriando A, Leandro G, Olivo M, Andriulli A, Cottone M. Radiofrequency thermal ablation vs. percutaneous ethanol injection for small hepatocellular carcinoma in cirrhosis: meta-analysis of randomized controlled trials. Am J Gastroenterol 2009;104:514–24.
[9] Kei SK, Rhim H, Choi D, Lee WJ, Lim HK, Kim YS. Local tumor progression after radiofrequency ablation of liver tumors: analysis of morphologic pattern and site of recurrence. AJR 2008;190:1544–51.
[10] Hirooka M, Iuchi H, Kurose K, Kumagi T, Horiike N, Onji M. Abdominal virtual ultrasonographic images reconstructed by multi-detector row helical computed tomography. Eur J Radiol 2005;53:312–7.
[11] Hirooka M, Iuchi H, Kumagi T, et al. Virtual sonographic radiofrequency ablation of hepatocellular carcinoma visualized on CT but not on conventional sonography. AJR 2006;186:S255–60.
[12] Kudo K, Moriyasu F, Mine Y, et al. Preoperative RFA simulation for liver cancer using a CT virtual ultrasound system. Eur J Radiol 2007;61(2):324–31.
[13] Omata M, Lesmana LA, Tateishi R, et al. Asian pacific association for the study of the liver consensus recommendations on hepatocellular carcinoma. Hepatol Int 2010;4:439–74.
[14] Wen YL, Kudo M, Zheng RQ, et al. Radiofrequency ablation of hepatocellular carcinoma: therapeutic response using contrast-enhanced coded phase-inversion harmonic sonography. AJR 2003;181:57–63.
[15] Bartolotta TV, Taibbi A, Midiri M, De Maria M. Hepatocellular cancer response to radiofrequency tumor ablation: contrast-enhanced ultrasound. Abdom Imaging 2008;33(5):501–11.
[16] Luo W, Numata K, Morimoto M, et al. Role of sonazoid-enhanced three-dimensional ultrasonography in the evaluation of percutaneous radiofrequency ablation of hepatocellular carcinoma. Eur J Radiol 2010;75(1):91–7.
[17] Gervais DA, Kalva S, Thabet A. Percutaneous image-guided therapy of intraabdominal malignancy: imaging evaluation of treatment response. Abdom Imaging 2009;34(5):593–609.

Involvement of Activation of Toll-like Receptors and Nucleotide-Binding Oligomerization Domain–like Receptors in Enhanced IgG4 Responses in Autoimmune Pancreatitis

Tomohiro Watanabe,[1] Kouhei Yamashita,[1] Saori Fujikawa,[1] Toshiharu Sakurai,[2]
Masatoshi Kudo,[2] Masahiro Shiokawa,[1] Yuzo Kodama,[1] Kazushige Uchida,[3]
Kazuichi Okazaki,[3] and Tsutomu Chiba[1]

Objective. IgG4-related disease is a recently recognized entity affecting multiple organs, including the pancreas, biliary tracts, and salivary glands. Although IgG4-related disease is characterized by systemic IgG4 antibody responses and by infiltration of IgG4-expressing plasma cells, the innate immune responses leading to adaptive IgG4 antibody responses are poorly understood. The aim of this study was to clarify the innate immune responses leading to IgG4 antibody production.

Methods. IgG4 and cytokine responses to various nucleotide-binding oligomerization domain (NOD)–like receptor (NLR) and Toll-like receptor (TLR) ligands were examined using peripheral blood mononuclear cells (PBMCs) from healthy control subjects and patients with IgG4-related autoimmune pancreatitis.

Results. Activation of NOD-2 in monocytes from healthy control subjects induced IgG4 production by B cells in a BAFF-dependent and T cell–independent manner. In addition, PBMCs from patients with IgG4-related disease produced a large amount of IgG4 upon stimulation with NLR and TLR ligands; this enhanced IgG4 production was associated with the induction of BAFF by NLR and TLR ligands. Monocytes from patients with IgG4-related disease induced IgG4 production by B cells from healthy control subjects upon stimulation with NLR and TLR ligands.

Conclusion. The results of these studies suggest that abnormal innate immune responses against microbial antigens may underlie the immunopathogenesis of IgG4-related disease.

Autoimmune pancreatitis is a unique form of chronic pancreatitis, and autoimmune reactions are considered to be involved in its pathogenesis (1,2). Currently, the diagnosis of autoimmune pancreatitis is based on characteristic clinical findings such as hypergammaglobulinemia, irregular narrowing of the main pancreatic duct, and lymphoplasmacytic infiltration of the pancreas associated with fibrosis (3). Another important feature of autoimmune pancreatitis is the variety of extrapancreatic manifestations (4). Sclerosing cholangitis, sialoadenitis, and retroperitoneal fibrosis are sometimes seen in patients with autoimmune pancreatitis. In addition to the clinicopathologic findings described above, most patients with autoimmune pancreatitis have elevated serum levels of IgG4 (5). Moreover, abundant infiltration of IgG4-expressing plasmacytes is observed in both pancreatic and extrapancreatic lesions (4,6). Based on these recent findings, it is generally accepted that an enhanced systemic IgG4 response is one of the most important immunologic features in autoimmune

pancreatitis, and that autoimmune pancreatitis is considered to be a pancreatic manifestation of systemic IgG4-related disease (3,4) and IgG4-positive multiorgan lymphoproliferative syndrome (7).

Our present understanding of the immunopathogenesis of autoimmune pancreatitis is limited. Although the presence of autoantibodies against carbonic anhydrase and lactoferrin in the serum of patients with autoimmune pancreatitis suggests the involvement of excessive autoimmune responses (1,2), pathogenic antigens have not been identified. In addition, it remains unknown whether an enhanced IgG4 response is responsible for the development of autoimmune pancreatitis, or whether it is an epiphenomenon associated with inflammatory reactions. Given the fact that a significant population of patients with autoimmune pancreatitis have a diagnosis of inflammatory bowel disease, the development of which requires excessive immune reactions to intestinal microflora (8–10), it is possible that enhanced immune responses toward microbial antigens underlie the immunopathogenesis of autoimmune pancreatitis. Consistent with this idea, an accumulation of plasma cells expressing IgG4 was observed in the gastrointestinal tract of patients with autoimmune pancreatitis (11). Moreover, our group recently reported 2 cases of autoimmune pancreatitis in patients whose peripheral blood mononuclear cells (PBMCs) exhibited enhanced Th2 cytokine responses upon stimulation with microbial antigens (12,13).

Antigens derived from the intestinal microflora activate the host innate immune system via pattern recognition receptors such as Toll-like receptors (TLRs) and nucleotide-binding oligomerization (NOD)–like receptors (NLRs) (10,14). Antigen-presenting cells (APCs) interact with B cells to induce IgG and IgA production (14). Interestingly, the activation of TLRs and NLRs in APCs, including dendritic cells, monocytes, and macrophages, leads to immunoglobulin class switching through production of BAFF and APRIL (15,16). However, the roles played by APCs expressing TLRs and NLRs in IgG4 responses are poorly defined.

In this study, we sought to determine how the activation of TLRs and NLRs in APCs enhances IgG4 responses linked to autoimmune pancreatitis. NOD-2 is an intracellular NLR for small peptides derived from the bacterial cell wall component peptidoglycan (PGN) (10). Here, we provide evidence that NOD-2 activation in monocytes enhances production of IgG4 from B cells via secretion of BAFF in a T cell–independent manner, in healthy control subjects. Moreover, we report that PBMCs from patients with autoimmune pancreatitis

exhibited enhanced production of IgG4 upon stimulation with NLR and TLR ligands. Thus, we propose that excessive innate immune responses to microbial antigens may underlie the immunopathogenesis of IgG4-related autoimmune pancreatitis.

PATIENTS AND METHODS

Stimulation of cells with a broad range of microbial antigens. PBMCs (2×10^6/ml) from healthy control subjects were stimulated with FK-156 (20 μg/ml; Astellas Pharma), muramyldipeptide (MDP) (20 μg/ml; InvivoGen), PGN (10 μg/ml; Sigma-Aldrich), palmitoyl-3-cysteine-serine-lysine-4 (Pam$_3$CSK$_4$) (1 μg/ml; InvivoGen), double-stranded RNA (dsRNA) (25 μg/ml; InvivoGen), lipopolysaccharide (LPS) (1 μg/ml; Sigma-Aldrich), flagellin (1 μg/ml; InvivoGen), and R837 (50 μg/ml; InvivoGen) for 14 days in complete RPMI medium, as previously described (17,18). In some experiments, CD3+ T cells, CD14+ monocytes, and CD19+ B cells (1×10^6/ml) were isolated from PBMCs by positive selection using anti-human CD3, CD14, and CD19 microbeads, respectively (Miltenyi Biotech) (19). Depletion of CD14+ monocytes was performed by negative selection, using anti-CD14 microbeads. The isolated cell populations were cultured with the indicated doses of a neutralizing anti-BAFF monoclonal antibody (R&D Systems) or a mouse IgG control antibody (eBioscience). CD14+ monocytes were incubated with 10 μM SB203580 (p38 and RICK inhibitor), PD98059 (ERK inhibitor), SP600125 (JNK inhibitor), or BAY 11-7082 (NF-κB inhibitor) (all from InvivoGen) for 1 hour, followed by overnight stimulation with MDP (20 μg/ml). Culture supernatants were collected at the indicated time points.

Enzyme-linked immunosorbent assays (ELISAs). Culture supernatants were assayed for the measurement of interleukin-6 (IL-6), IL-8, IL-12p40, IL-17, tumor necrosis factor (TNF), interferon-γ (IFNγ), APRIL, and BAFF, using ELISA kits (PharMingen and eBioscience). The production of IgG1 and IgG4 was determined by ELISAs. Anti-human IgG1 and IgG4 antibodies (PharMingen) were used as capture antibodies, and horseradish peroxidase (HRP)–labeled anti-human IgG antibody (PharMingen) was used for detection. The production of IgA and IgE was determined using an ELISA (Bethyl Laboratories).

Fluorescence-activated cell sorter analysis. PBMCs were preincubated with Fc-blocking solution (Miltenyi Biotech), stained with fluorescein isothiocyanate–conjugated anti-human CD14 or CD19 antibody (both from eBioscience) and phycoerythrin-labeled anti-human BAFF (R&D Systems), APRIL (BioLegend), B cell maturation antigen (BCMA; R&D Systems), HLA–DR, CD40, CD80, CD86 (all from eBioscience), inducible costimulator (ICOS) ligand (eBioscience), CD163 (BioLegend), BAFF receptor (BAFF-R; BioLegend), and TACI (BioLegend). An intracellular staining kit (PharMingen) was used for intracellular staining of BAFF and APRIL. Stained cells were analyzed on an Accuri C6 cytometer (Accuri Cytometers).

Immunoblotting. CD14+ monocytes from healthy control subjects were stimulated with MDP (20 μg/ml). At the indicated time points, protein extracts were isolated and

subjected to immunoblotting as described previously (18). The primary antibodies used in this study were as follows: actin (Santa Cruz Biotechnology), phospho-p38, total p38, phospho-ERK, total ERK, phospho-JNK, total JNK, and total IκBα (Cell Signaling Technology). To detect NOD-2 expression, cells were first immunoprecipitated with monoclonal NOD-2 antibody (eBioscience) followed by immunoblotting with polyclonal NOD-2 antibody (Santa Cruz Biotechnology).

Small interfering RNA (siRNA) study. MonoMac6 cells (1×10^6/ml), a human monocytic cell line, were transfected with control siRNA or NOD-2–specific siRNA (25 nM; Santa Cruz Biotechnology), using TransIT-TKO transfection reagent (Mirus). Cells were stimulated with MDP (20 μg/ml) for 36 hours after transfection and then incubated for an additional 24 hours.

NF-κB activation assay. Nuclear extracts were prepared using an extraction kit (Clontech), and the binding activity of nuclear extract to NF-κB p50, p65, c-Rel, p52, and RelB was measured using a TransAM NF-κB kit (Active Motif). Nuclear extracts (10 μg) isolated from monocytes stimulated with MDP (20 μg/ml) for 30 minutes were applied to each well coated with NF-κB consensus oligonucleotides and then incubated with rabbit anti-p50, anti-p65, anti–c-Rel, anti-p52, and anti-RelB antibodies followed by HRP-labeled anti-rabbit IgG.

Studies using peripheral blood cells from patients with autoimmune pancreatitis. Ethics permission for this study was granted by the review board of Kyoto University. Healthy control subjects (n = 24) and treatment-naive patients with IgG4-related autoimmune pancreatitis (n = 8) were enrolled in this study after informed consent was obtained. PBMCs, CD14+ monocytes, and CD19+ B cells were isolated from the patients and stimulated with a broad range of microbial antigens, as described above.

Statistical analysis. Student's t-test was used to evaluate statistical significance. Statistical analysis was performed with the StatView version 4.5 program (Abacus Concepts). P values less than 0.05 were considered significant.

RESULTS

NOD-2–induced IgG4 production by PBMCs from healthy controls. Although an enhanced IgG4 response is one of the most important immunologic features in patients with autoimmune pancreatitis (4,5), the molecular mechanisms accounting for increased production of this IgG subtype in patients with autoimmune pancreatitis are poorly understood. To address the role of microbial antigens in the production of IgG4, PBMCs from healthy control subjects were stimulated with a broad range of TLR and NLR ligands (FK-156 [NOD-1 ligand], MDP [NOD-2 ligand], Pam3CSK4 [TLR-1/2 ligand], PGN [TLR-2/6 ligand], dsRNA [TLR-3 ligand], LPS [TLR-4 ligand], flagellin [TLR-5 ligand], and R837 [TLR-7 ligand]) for 14 days.

Activation of NOD-2 by MDP induced the production of IgG4, but not IgG1, by PBMCs from healthy control subjects (Figure 1). In contrast, activation of
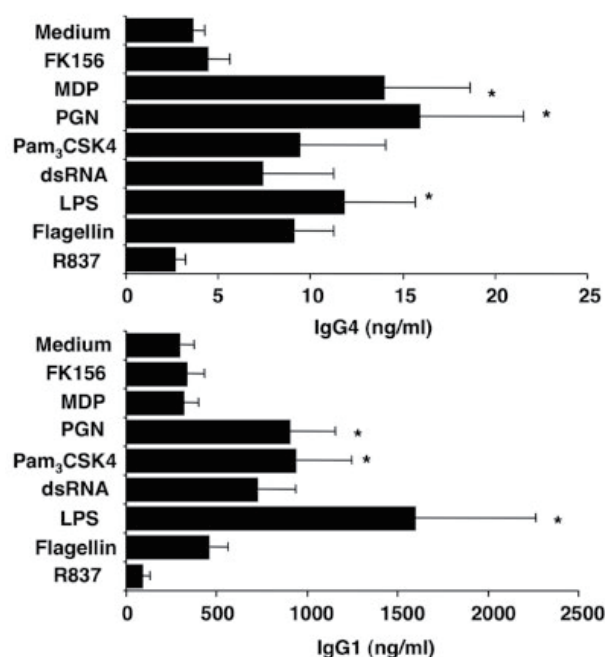

Figure 1. Muramyldipeptide (MDP)–induced activation of nucleotide-binding oligomerization domain 2 (NOD-2) enhances IgG4 production by peripheral blood mononuclear cells (PBMCs) from healthy control subjects. PBMCs (2×10^6/ml) from healthy control subjects (n = 14) were stimulated with a broad range of NOD-like receptor (NLR) and Toll-like receptor (TLR) ligands (FK-156, 20 μg/ml; MDP, 20 μg/ml; peptidoglycan [PGN], 10 μg/ml; palmitoyl-3-cysteine-serine-lysine-4 [Pam3CSK4], 1 μg/ml; double-stranded RNA [dsRNA], 25 μg/ml; lipopolysaccharide [LPS], 1 μg/ml; flagellin, 1 μg/ml; R837, 50 μg/ml) for 14 days. Production of IgG4 and IgG1 in the culture supernatants was determined by enzyme-linked immunosorbent assay. Bars show the mean ± SEM. * = $P < 0.05$ versus medium.

TLR-2 and TLR-4 induced the production of both IgG1 and IgG4. Thus, these data suggest that activation of NOD-2 enhances the IgG4 response rather than the IgG1 response. Because the regulation of IgG4 production is dependent on Th2 cytokines (20), we evaluated the profiles of cytokines induced by MDP. Stimulation with MDP did not induce production of Th1-associated cytokines such as IFNγ and IL-12p40, Th2-associated cytokines such as IL-4 and IL-13, or Th17-associated cytokines such as IL-6 and IL-17 (data not shown). These results suggested that IgG4 production by MDP is not associated with typical Th1, Th2, or Th17 cell responses. Significant production of IL-10 was induced in PBMCs stimulated with MDP. All of the TLR and NLR ligands enhanced IL-8 production, which suggests that the doses of microbial antigens used in this study were sufficient to cause innate immune responses.

T cell–independent IgG4 production by NOD-2.
We next determined the types of cells that are involved in enhanced IgG4 production through NOD-2 activation. Initially, we isolated CD3+ T cells, CD19+ B cells, and CD14+ monocytes and then examined the types of cells expressing NOD-2 at the protein level. Immunoprecipitation followed by immunoblotting with anti–NOD-2 antibody revealed that NOD-2 expression was limited to CD14+ monocytes (Figure 2A). Consistent with this NOD-2 expression in monocytes, the depletion of CD14+ cells from PBMCs reduced IgG4 production stimulated by MDP-induced activation of NOD-2 (data not shown). These results suggested that activation of monocytes expressing NOD-2 is responsible for MDP-induced IgG4 production.

To confirm these results, we assessed IgG4 production by CD19+ B cells cocultured with CD14+ monocytes or CD3+ T cells. MDP-induced IgG4 production was observed in the coculture containing both B cells and monocytes (Figure 2B). In contrast, the addition of CD3+ T cells to the culture reduced MDP-induced IgG4 production. These results showed that the presence of monocytes and B cells is sufficient for MDP-induced IgG4 production, and that NOD-2 activation induces IgG4 production in a T cell–independent manner. The production of IgG1, IgA, and IL-10 was comparable in the coculture containing monocytes and B cells, regardless of whether cells were activated with MDP. Furthermore, the optimal induction of IL-10 by MDP required B cells, T cells, and monocytes, suggesting that T cells are the main producers of this cytokine. Taken together, these data suggested that stimulation of MDP activates NOD-2 in monocytes and then induces IgG4 production by B cells in a T cell–independent manner.

We examined regulation of the expression of surface markers in monocytes stimulated with MDP. MDP-induced activation of NOD-2 enhanced cell surface expression of HLA–DR and costimulatory molecules such as CD40, CD80, and CD86, whereas no significant change was observed in the cell surface expression of CD163 or ICOS ligand (data not shown).

IgG4 production by NOD-2 activation of BAFF signaling pathways. We next examined the effects of NOD-2 activation in monocytes on the survival of B cells. The percentage of annexin V–positive apoptotic B cells was significantly reduced in PBMCs stimulated with MDP (Figure 3A). These results suggested that MDP-induced activation of NOD-2 in monocytes enhances the survival of CD19+ B cells by inhibiting apoptotic cell death.
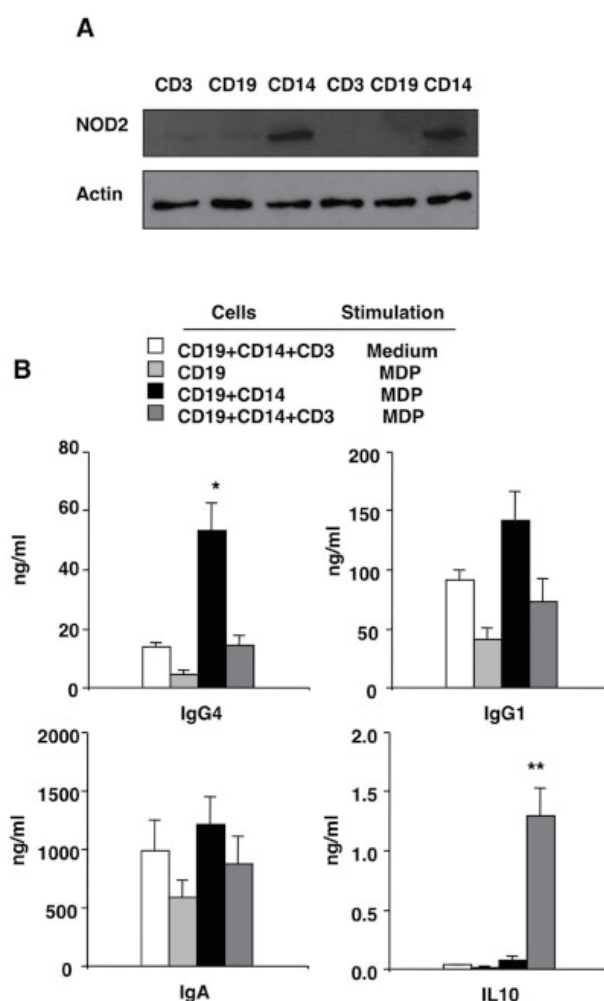
The TNF family members BAFF and APRIL are

Figure 2. MDP-induced activation of NOD-2 in monocytes induces IgG4 production by B cells in a T cell–independent manner. **A,** CD3+ T cells, CD14+ monocytes, and CD19+ B cells were purified from the PBMCs of healthy control subjects. Protein extracts were isolated from CD3+ T cells, CD19+ B cells, and CD14+ monocytes and then subjected to immunoprecipitation with anti–NOD-2 antibody, followed by immunoblotting with anti–NOD-2 antibody. Expression of NOD-2 by immunoblotting using 2 healthy controls is shown. **B,** CD19+ B cells (1×10^6/ml) from healthy control subjects (n = 6) were cocultured with CD14+ monocytes (1×10^6/ml) and/or CD3+ T cells (1×10^6/ml) in the presence of MDP (20 μg/ml) for 14 days. Culture supernatants were analyzed for the production of IgG4, IgG1, IgA, and interleukin-10 (IL-10). Bars show the mean ± SEM. * = $P < 0.05$; ** = $P < 0.01$ versus the 3 other coculture conditions. See Figure 1 for other definitions.

crucial survival factors for peripheral B cells (21,22). Innate immune cells such as APCs and epithelial cells produce BAFF and APRIL to cause T cell–independent immunoglobulin responses (15,16). Therefore, we ad-
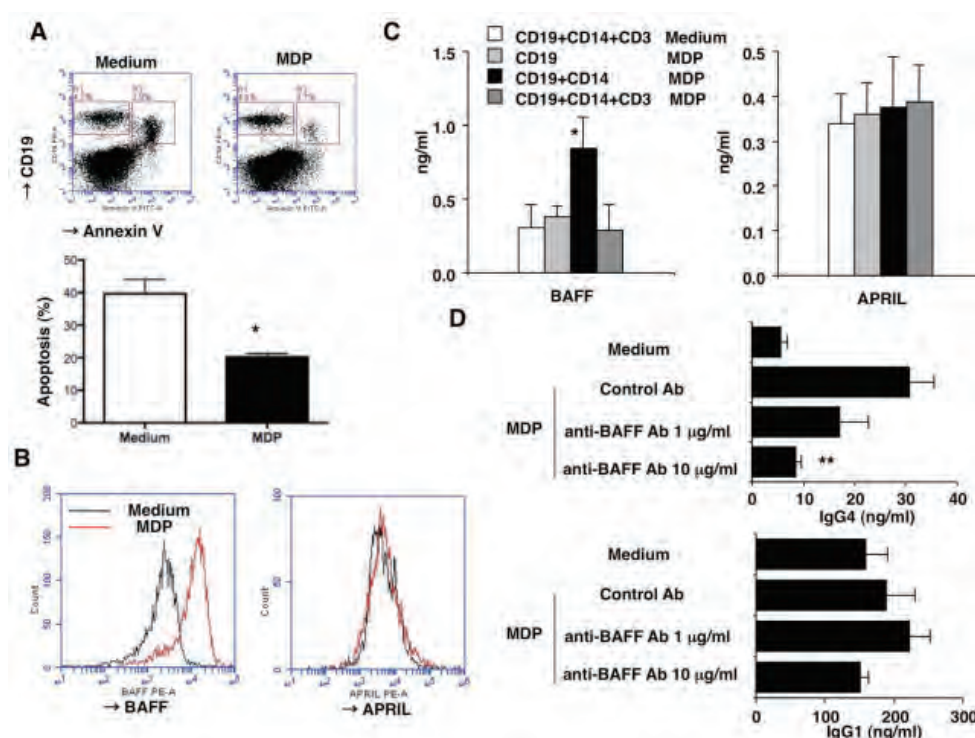
Figure 3. MDP-induced activation of NOD-2 in monocytes induces IgG4 production in a BAFF-dependent manner. **A,** PBMCs from healthy control subjects were stimulated with MDP for 24 hours and then stained with phycoerythrin (PE)–conjugated anti-CD19 antibody (Ab) and fluorescein isothiocyanate (FITC)–conjugated annexin V. The percentage of apoptotic annexin V–positive CD19+ B cells was decreased by stimulation with MDP. ∗ = P < 0.05 versus medium. **B,** CD14+ monocytes from healthy control subjects were stimulated with MDP for 24 hours, and intracellular expression of BAFF and APRIL was determined by flow cytometry. **C,** CD19+ B cells from healthy control subjects (n = 6) were cocultured with CD14+ monocytes and/or CD3+ T cells in the presence of MDP for 24 hours. Culture supernatants were analyzed for the production of BAFF and APRIL. ∗ = P < 0.05 versus other coculture conditions. **D,** CD19+ B cells from healthy control subjects (n = 6) were cocultured with CD14+ monocytes in the presence of neutralizing anti-BAFF antibody or control antibody for 14 days. Culture supernatants were analyzed for the production of IgG4 and IgG1. ∗∗ = P < 0.01 versus control. Bars in **A, C,** and **D** show the mean ± SEM. See Figure 1 for other definitions.

dressed whether MDP-induced activation of NOD-2 stimulates production of BAFF and/or APRIL and thereby enhances IgG4 production. Intracellular staining revealed a marked increase in BAFF, but not APRIL, expression in monocytes stimulated with MDP (Figure 3B). We next determined whether MDP-mediated BAFF production depends on NOD-2 activation. For this purpose, we used MonoMac6 cells, a human monocytic cell line, because of the very low efficiency of gene transfection in primary monocytes. MDP-mediated BAFF production was reduced in MonoMac6 cells transfected with NOD-2–specific siRNA, which suggested NOD-2–dependent BAFF production upon stimulation with MDP (data not shown).

The production of BAFF in the coculture con-taining B cells and monocytes was enhanced upon stimulation with MDP (Figure 3C). More importantly, abrogation of BAFF signaling by its neutralizing anti-body inhibited the production of IgG4 in a dose-dependent manner (Figure 3D). BAFF binds to the receptors BCMA, TACI, and BAFF-R, which are expressed on the cell surface of B cells (21,22). Stimulation of PBMCs with MDP enhanced cell surface expression of TACI on B cells (data not shown), suggesting that the interaction between TACI and BAFF is involved in enhanced IgG4 production mediated by NOD-2 activation. Consistent with these data, the addition of BAFF alone led to a marked increase in IgG4 production by CD19+ B cells (data not shown). These results suggested a novel mechanism of IgG4 production mediated by NOD-2 activation: monocytes produce BAFF upon
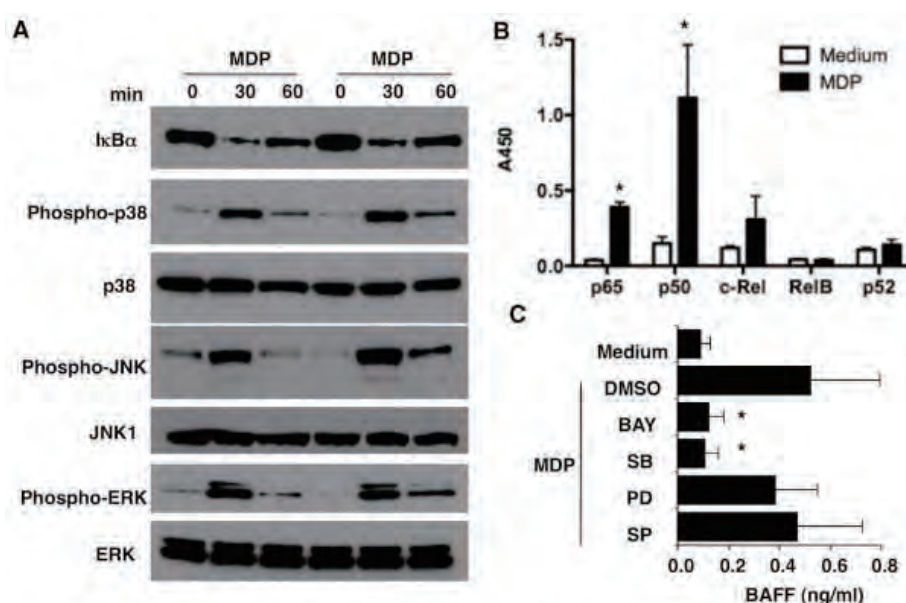
Figure 4. MDP-induced activation of NOD-2 in monocytes stimulates BAFF production via NF-κB activation. **A,** CD14+ monocytes from 2 healthy control subjects were stimulated with MDP, and protein extracts were isolated at the indicated time points. Whole extracts were subjected to immunoblotting with anti-IκBα, phospho-p38, p38, phospho-JNK, JNK-1, phospho-ERK, and ERK antibodies. **B,** Nuclear extracts were isolated from monocytes stimulated with MDP (20 μg/ml) for 30 minutes. The activation of NF-κB subunits in the nuclear extracts was determined. ∗ = $P <$ 0.05 versus medium. **C,** CD14+ monocytes (1×10^6/ml) from healthy control subjects (n = 4) were preincubated with 10 μM BAY 11-7082 (BAY, NF-κB inhibitor), SB203580 (SB; p38 and RICK inhibitor), PD98059 (PD; ERK inhibitor), or SP600125 (SP; JNK inhibitor) for 1 hour, followed by overnight stimulation with MDP (20 μg/ml). Culture supernatants were analyzed for production of BAFF. ∗ = $P <$ 0.05 versus DMSO. Bars in **B** and **C** show the mean ± SEM. See Figure 1 for other definitions.

NOD-2 activation by MDP, and BAFF induce IgG4 production via interaction between BAFF and TACI.

NF-κB–dependent BAFF production by NOD-2. We next examined the signaling pathway involved in NOD-2–induced BAFF production in monocytes. Previous studies have established that NOD-2 activation results in interactions between the CARD domain of the NOD molecule and the CARD domain of a downstream effector molecule, the serine/threonine kinase RICK; activated RICK generated in this manner activates NF-κB and MAP kinases (MAPKs) (10). Stimulation of monocytes with MDP led to degradation of IκBα and enhanced expression of the phosphorylated forms of p38, JNK, and ERK (Figure 4A). In addition, the binding of NF-κB subunits p65 and p50 to consensus sequences was markedly enhanced in nuclear extracts isolated from monocytes upon stimulation with MDP (Figure 4B). In contrast, there was no significant difference in the binding of c-Rel, RelB, or p52 in the nuclear extracts either with or without MDP stimulation. These results suggested that MDP-induced activation of

NOD-2 results in the activation of NF-κB and MAPK in monocytes.

In subsequent studies to determine which of the previously established components of NOD-2 signaling were relevant to BAFF production, monocytes were preincubated with various inhibitors specific to these pathways, including PD98059 (ERK inhibitor), SB203580 (p38 and RICK inhibitor), SP600125 (JNK inhibitor), and BAY 11-7082 (NF-κB inhibitor) and then stimulated with MDP. The addition of BAY 11-7082 or SB203580 to cultures led to reduced BAFF production by monocytes (Figure 4C). In contrast, the addition of PD98059 or SP600125 had no inhibitory effects on BAFF production. To exclude toxic effects of these inhibitors, we performed a gene-silencing study. Transfection of p65 siRNA into MonoMac6 cells led to a substantial reduction in BAFF production upon stimulation with MDP as compared with cells transfected with control siRNA (data not shown). Taken together, these results suggested that BAFF production by MDP is induced by the activation of NF-κB through RICK.
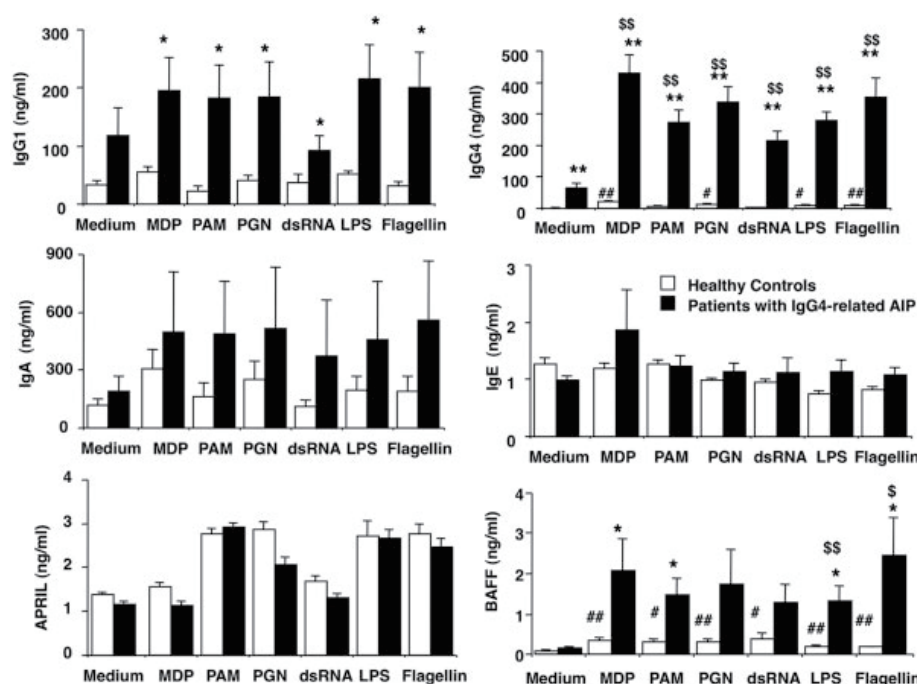
Figure 5. Nucleotide-binding oligomerization domain–like receptor (NLR) and Toll-like receptor (TLR) ligands induce production of BAFF and IgG4 by peripheral blood mononuclear cells (PBMCs) from patients with IgG4-related autoimmune pancreatitis (AIP). PBMCs (1×10^6/ml) from healthy control subjects (n = 10) and patients with IgG4-related autoimmune pancreatitis (n = 8) were stimulated with a broad range of NLR and TLR ligands for 14 days, as described in Figure 1. Culture supernatants obtained at 14 days were assayed for the presence of IgG1, IgG4, IgA, and IgE. Culture supernatants obtained at 2 days were assayed for the presence of APRIL and BAFF. Bars show the mean ± SEM. ∗ = $P < 0.05$ and ∗∗ = $P < 0.01$ versus healthy controls; # = $P < 0.05$ and ## = $P < 0.01$ versus medium; \$ = $P < 0.05$ and \$\$ = $P < 0.01$ versus medium. MDP = muramyldipeptide; PAM = palmitoyl-3-cysteine-serine-lysine-4; PGN = peptidoglycan; dsRNA = double-stranded RNA; LPS = lipopolysaccharide.

IgG4 production by PBMCs from patients with IgG4-related autoimmune pancreatitis via activation of NLRs and TLRs. As mentioned above, we identified a novel pathway of NOD-2–mediated IgG4 production by using PBMCs from healthy control subjects. To establish the significance of this finding in the immunopathogenesis of IgG4-related disease, we compared the immune responses of PBMCs from patients with IgG4-related autoimmune pancreatitis with those of PBMCs from healthy controls. Patients enrolled in this study met the criteria for the diagnosis of autoimmune pancreatitis (23,24) and were diagnosed as having lymphoplasmacytic sclerosing pancreatitis. The mean ± SD serum levels of IgG4 and IgG1 in patients enrolled in this study were 665 ± 232 mg/dl (normal range 4.8–105) and 1,050 ± 567 mg/dl (normal range 320–748), respectively. PBMCs from healthy control subjects and patients were stimulated with NLR and TLR ligands to measure the production of immunoglobulins and cytokines.

Basal production of IgG4 by PBMCs was markedly elevated in patients compared with controls, and this enhanced IgG4 production by patient PBMCs was augmented in the presence of a broad range of NLR and TLR ligands (Figure 5, top). Although the activation of NOD-2 preferentially induces IgG4 production in healthy PBMCs, not only NOD-2 ligands (MDP) but also TLR ligands (Pam$_3$CSK$_4$ and PGN [TLR-2 ligands], dsRNA [TLR-3 ligand], LPS [TLR-4 ligand], and flagellin [TLR-5 ligand]) efficiently induced IgG4 production by PBMCs from patients. Similar results were observed for IgG1, although the difference between control subjects and patients was much smaller than the differences observed for IgG4 (Figure 5, top).

PBMCs from patients and control subjects produced comparable levels of IgA and IgE upon stimulation with NLR and TLR ligands (Figure 5, middle). Interestingly, BAFF production by PBMCs from patients was much higher than that by PBMCs from

control subjects upon stimulation with NOD-2 and TLR ligands (Figure 5, bottom). In contrast, stimulation of PBMCs with NLR and TLR ligands induced comparable levels of APRIL in control subjects and patients (Figure 5, bottom). These results suggested that PBMCs from patients with IgG4-related autoimmune pancreatitis produce a large amount of IgG4 upon stimulation with NLR and TLR ligands, and that such enhancement of IgG4 production is associated with BAFF induced by NLR and TLR ligands.

Defective Th1 cell responses in patients with IgG4-related autoimmune pancreatitis. We next evaluated the profiles of cytokines induced by NLR and TLR ligands in patients with IgG4-related autoimmune pancreatitis. In patients compared with controls, IFNγ production by PBMCs was markedly reduced upon stimulation with TLR-2, TLR-3, TLR-4, and TLR-5 ligands (for PAM, mean $\pm$ SEM 229 $\pm$ 61 pg/ml versus 1,184 $\pm$ 290 pg/ml; for dsDNA, 260 $\pm$ 82 pg/ml versus

3,810 $\pm$ 1,400 pg/ml; for LPS, 1,690 $\pm$ 974 pg/ml versus 4,530 $\pm$ 929 pg/ml; for flagellin, 872 $\pm$ 530 pg/ml versus 4,110 $\pm$ 960 pg/ml). Stimulation with MDP induced comparable levels of IFNγ production by PBMCs from controls and those from patients (data not shown). Given the fact that IFNγ is a prototypical Th1 cytokine, these results suggested that PBMCs from patients with IgG4-related autoimmune pancreatitis show defective Th1 cell responses to TLR ligands. Consistent with this reduced IFNγ production, the production of IL-12p40, which is associated with Th1 cell responses, was significantly reduced in patients compared with controls upon stimulation with TLR-2 or TLR-4 ligand (for PAM, mean $\pm$ SEM 130 $\pm$ 18 pg/ml versus 456 $\pm$ 91 pg/ml; for LPS, 344 $\pm$ 58 pg/ml versus 670 $\pm$ 128 pg/ml). In addition, IL-6 production by TLR-2 and TLR-5 ligands was reduced in PBMCs from patients compared with controls (for PAM, mean $\pm$ SEM 3,491 $\pm$ 554 pg/ml versus 7,664 $\pm$ 848 pg/ml; for
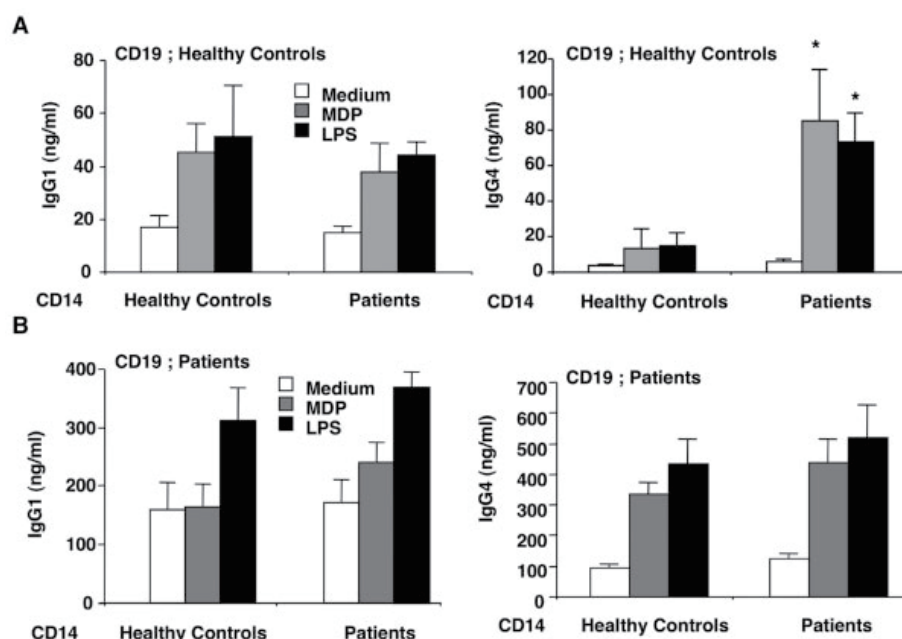

Figure 6. Monocytes isolated from patients with IgG4-related autoimmune pancreatitis induce IgG4 production by B cells from healthy controls upon stimulation with MDP and LPS. **A,** CD19+ B cells (1 $\times$ 10^6/ml) from healthy control subjects (n = 4) were cocultured with CD14+ monocytes (1 $\times$ 10^6/ml) from control subjects (n = 4) or patients with IgG4-related autoimmune pancreatitis (n = 4) in the presence of MDP (20 μg/ml) or LPS (1 μg/ml) for 14 days. **B,** CD19+ B cells (1 $\times$ 10^6/ml) from patients with IgG4-related autoimmune pancreatitis (n = 4) were cocultured with CD14+ monocytes (1 $\times$ 10^6/ml) from control subjects (n = 4) or patients (n = 4) in the presence of MDP (20 μg/ml) or LPS (1 μg/ml) for 14 days. Culture supernatants obtained at 14 days were assayed for the presence of IgG1 and IgG4. Bars show the mean $\pm$ SEM. $*$ = $P < 0.05$ versus the respective controls. See Figure 5 for definitions.

flagellin, 4,403 ± 345 pg/ml versus 7,207 ± 750 pg/ml). In contrast, no significant difference between patients and control subjects was observed in the production of IL-17 or IL-10 by PBMCs stimulated with NLR and TLR ligands (data not shown). Thus, these studies clearly showed that defective Th1 cell responses to TLR ligands, but not NLR ligands, are associated with enhanced IgG4 production by PBMCs from patients with IgG4-related autoimmune pancreatitis.

Induction of IgG4 responses by monocytes from patients with IgG4-related autoimmune pancreatitis. In a final series of experiments, we determined the type of cells that play a critical role in the generation of IgG4 responses in patients with IgG4-related autoimmune pancreatitis. Because PBMCs from patients with autoimmune pancreatitis produced a large amount of BAFF upon stimulation with TLR and NLR ligands, we hypothesized that monocyte-induced activation of TLRs and NLRs is responsible for enhanced IgG4 production in patients with IgG4-related autoimmune pancreatitis. To this end, we conducted coculture experiments in which CD19+ B cells and CD14+ monocytes isolated from the PBMCs of healthy control subjects and patients were stimulated with MDP or LPS in various combinations.

First, we set up a coculture system in which CD19+ B cells from healthy control subjects were incubated with monocytes from healthy control subjects or patients. Monocytes isolated from patients, but not control subjects, induced production of IgG4 by healthy B cells upon stimulation with MDP or LPS (Figure 6A). In contrast, no differences were observed between patients and control subjects in IgG1 production upon stimulation with MDP or LPS (Figure 6A). Enhanced IgG4 production by monocytes from patients was significantly reduced by IFNγ (data not shown), suggesting that impaired Th1 cell responses are involved in enhanced IgG4 responses in patients with IgG4-related disease.

Next, we set up a coculture system in which CD19+ B cells from patients were incubated with monocytes from healthy control subjects or patients. B cells from patients produced comparable levels of IgG1 and IgG4 regardless of whether these cells were cocultured with monocytes from healthy controls or patients (Figure 6B). These data suggested that activation of NOD-2 or TLR-4 in the monocytes of patients triggers IgG4 production by healthy CD19+ B cells, and that monocyte activation of TLRs and NLRs underlies the immunopathogenesis of enhanced IgG4 production in IgG4-related disease.

DISCUSSION

Although autoimmune pancreatitis is characterized by systemic IgG4 antibody responses and is considered to be a pancreatic manifestation of IgG4-related disease and IgG4-positive multiorgan lymphoproliferative syndrome, the innate immune responses leading to adaptive IgG4 antibody responses are poorly understood. In the current study, we examined the innate immune responses inducing IgG4 antibody production. In our initial studies, we used healthy PBMCs to show that B cells produce a large amount of IgG4 in a T cell–independent manner when B cells are cocultured with monocytes stimulated with MDP, a NOD-2 ligand. Furthermore, we showed that BAFF produced by MDP-activated monocytes induces IgG4 production by B cells. Thus, we characterized T cell–independent IgG4 production induced by NOD-2 signaling, which operates in monocytes. With respect to the role of NOD-2 in IgG4-related autoimmune pancreatitis, we showed that NOD-2 activation enhances the production of BAFF and IgG4 by PBMCs from patients with autoimmune pancreatitis. More importantly, we showed that MDP-stimulated monocytes isolated from patients with autoimmune pancreatitis induce production of IgG4 by B cells from healthy controls. Therefore, these data suggest that NOD-2–dependent BAFF production in monocytes plays an important role in the generation of an IgG4 response in autoimmune pancreatitis.

NOD-2–mediated BAFF production by monocytes is an indispensable step for T cell–independent IgG4 production, as shown in this study. We showed enhanced activation of NF-κB and MAPKs in monocytes upon stimulation with MDP. Moreover, BAFF production mediated by MDP was markedly decreased by the addition of pharmacologic inhibitors for NF-κB and RICK, which strongly suggests that MDP-induced activation of NOD-2 elicits BAFF production by monocytes via NF-κB activation. Compatible with this idea, the BAFF gene promoter contains many NF-κB binding sites (25). In this study, however, the molecular mechanisms by which NOD-2–mediated BAFF production enhances IgG4 production remain unknown. BAFF is a crucial survival factor for peripheral B cells (21,22). In fact, the percentage of apoptotic B cells was reduced in the presence of monocytes stimulated with MDP, which suggests an expansion of B cells due to BAFF production induced by NOD-2 activation. Thus, one possible mechanism for BAFF-dependent IgG4 production may be promotion of the activation or expansion of B cells that are already committed to IgG4 production. In this

regard, the survival of B cells committed to IgG4 production is enhanced in the presence of IL-21 (26). Therefore, it is possible that BAFF, in concert with IL-21 and/or other unidentified factors, enhances IgG4 production via promoting the expansion of IgG4-committed B cells. Alternatively, BAFF may directly induce IgG4 class-switch DNA recombination. Although Litinskiy et al reported that BAFF induces IgG4 class-switch DNA recombination in the presence of IL-4 (15), we failed to detect IL-4 in cells stimulated with MDP.

Although the activation of NOD-2, but not TLRs, preferentially induces IgG4 production by PBMCs from healthy control subjects, not only MDP but also many TLR ligands induce IgG4 production by PBMCs from patients with IgG4-related autoimmune pancreatitis. This enhanced IgG4 production by TLR ligands is associated with the reduced production of proinflammatory Th1 cytokines and with the enhanced production of BAFF. Thus, in contrast to NOD-2–induced IgG4 production, which is dependent on BAFF production by monocytes, the reduced production of Th1 cytokines may also be involved in enhanced TLR-induced IgG4 production in autoimmune pancreatitis. Consistent with this idea, IgG4 production by healthy B cells upon coculture with monocytes from patients with IgG4-related disease is reduced in the presence of IFNγ. Therefore, it seems likely that not only NOD-2–mediated BAFF production but also TLR-mediated production of BAFF and reduced production of Th1 cytokines are involved in the generation of systemic IgG4 responses in patients with autoimmune pancreatitis. In addition, our preliminary data show that basophils isolated from patients with autoimmune pancreatitis, but not those from healthy control subjects, induce production of a large amount of IgG4 by B cells upon stimulation with TLR-2 and TLR-4 ligands (Watanabe T, et al: unpublished observation). Further phenotypic analysis of basophils from patients with autoimmune pancreatitis and healthy control subjects may provide the mechanisms accounting for differences in TLR and NLR ligands that drive the production of this immunoglobulin subclass. In any case, these data suggest that activation of both NLRs and TLRs is involved in the development of enhanced IgG4 production in patients with autoimmune pancreatitis.

TLR activation enhances the production of BAFF rather than APRIL in patients with IgG4-related autoimmune pancreatitis. Thus, BAFF plays an important role in T cell–independent IgG4 production. Similarly, Alsaleh et al observed that TLR activation in synovial fibroblasts from patients with rheumatoid ar-

thritis cause T cell–independent IgG secretion via BAFF-mediated but not APRIL-mediated signaling pathways (27). Thus, the immunopathogenesis of rheumatoid arthritis and autoimmune pancreatitis may be similar, in that T cell–independent and BAFF-dependent immunoglobulin secretion is seen in both diseases. Although BAFF binds to the receptors BCMA, TACI, and BAFF-R expressed on the cell surface of B cells (21,22), TACI delivers innate immunoglobulin-inducing signals to B cells (28). In the current study, TACI expression in B cells was up-regulated in PBMCs stimulated with MDP. Therefore, the interaction between TACI and BAFF may be involved in T cell–independent IgG4 production. Blockade of TACI-specific signaling pathways may provide new insights into the immunopathogenesis of IgG4-related disease.

The role of an IgG4 antibody response in the immunopathogenesis of IgG4-related disease is poorly understood. Several lines of evidence suggest an anti-inflammatory rather than an inflammatory role of this immunoglobulin subclass. First, the interaction between IgG4 and the Fcγ receptor or C1q is weaker than that of other IgG subclasses (20). Second, IgG4 antibodies can exchange Fab arms by swapping a heavy chain and an attached light chain (half-molecule) with a heavy–light chain pair from another molecule, which results in bispecific antibodies (29). This bispecific property of IgG4 antibodies protects against the autoimmune disease myasthenia gravis by competing pathogenic IgG1 antibodies against acetylcholine receptor (29). Third, elevated IgG4 levels are considered to be a marker of tolerance induction in IgE-related allergic disorders (20,30). These unique properties of IgG4 prompt us to speculate that enhanced IgG4 antibody responses may be an epiphenomenon associated with inflammatory reactions. In this study, we identified BAFF as a critical player in IgG4 production. Thus, it is an interesting question whether or not BAFF inhibition influences the clinical course of IgG4-related disease and IgG4-positive multiorgan lymphoproliferative syndrome.

Our findings have certain implications with respect to possible mechanisms of IgG4-related autoimmune pancreatitis. Activation of NOD-2 and TLR ligands enhances IgG4 responses by PBMCs from patients with IgG4-related autoimmune pancreatitis, which suggests the possible involvement of abnormal innate immune responses against intestinal microflora in the development of IgG4-related autoimmune pancreatitis. Alternatively, microbial infections trigger the development of IgG4-related autoimmune pancreatitis. In conclusion, abnormal innate immune responses via NLRs

and TLRs may underlie the immunopathogenesis of IgG4-related disease and IgG4-positive multiorgan lymphoproliferative syndrome.

AUTHOR CONTRIBUTIONS

All authors were involved in drafting the article or revising it critically for important intellectual content, and all authors approved the final version to be published. Dr. Watanabe had full access to all of the data in the study and takes responsibility for the integrity of the data and the accuracy of the data analysis.

Study conception and design. Watanabe, Yamashita.
Acquisition of data. Watanabe, Yamashita, Fujikawa, Sakurai, Kudo, Shiokawa, Kodama, Uchida, Okazaki, Chiba.
Analysis and interpretation of data. Watanabe, Yamashita, Fujikawa, Sakurai, Kudo, Shiokawa, Kodama, Uchida, Okazaki, Chiba.

REFERENCES

 1. Finkelberg DL, Sahani D, Deshpande V, Brugge WR. Autoimmune pancreatitis. N Engl J Med 2006;355:2670–6.
 2. Okazaki K, Chiba T. Autoimmune related pancreatitis. Gut 2002; 51:1–4.
 3. Okazaki K, Uchida K, Fukui T. Recent advances in autoimmune pancreatitis: concept, diagnosis, and pathogenesis. J Gastroenterol 2008;43:409–18.
 4. Kamisawa T, Okamoto A. Autoimmune pancreatitis: proposal of IgG4-related sclerosing disease. J Gastroenterol 2006;41:613–25.
 5. Hamano H, Kawa S, Horiuchi A, Unno H, Furuya N, Akamatsu T, et al. High serum IgG4 concentrations in patients with sclerosing pancreatitis. N Engl J Med 2001;344:732–8.
 6. Khosroshahi A, Stone JH. A clinical overview of IgG4-related systemic disease. Curr Opin Rheumatol 2010;23:57–66.
 7. Masaki Y, Dong L, Kurose N, Kitagawa K, Morikawa Y, Yamamoto M, et al. Proposal for a new clinical entity, IgG4-positive multiorgan lymphoproliferative syndrome: analysis of 64 cases of IgG4-related disorders. Ann Rheum Dis 2009;68:1310–5.
 8. Ravi K, Chari ST, Vege SS, Sandborn WJ, Smyrk TC, Loftus EV Jr. Inflammatory bowel disease in the setting of autoimmune pancreatitis. Inflamm Bowel Dis 2009;15:1326–30.
 9. Zamboni G, Luttges J, Capelli P, Frulloni L, Cavallini G, Pederzoli P, et al. Histopathological features of diagnostic and clinical relevance in autoimmune pancreatitis: a study on 53 resection specimens and 9 biopsy specimens. Virchows Arch 2004;445: 552–63.
10. Strober W, Murray PJ, Kitani A, Watanabe T. Signalling pathways and molecular interactions of NOD1 and NOD2. Nat Rev Immunol 2006;6:9–20.
11. Deheragoda MG, Church NI, Rodriguez-Justo M, Munson P, Sandanayake N, Seward EW, et al. The use of immunoglobulin G4 immunostaining in diagnosing pancreatic and extrapancreatic involvement in autoimmune pancreatitis. Clin Gastroenterol Hepatol 2007;5:1229–34.
12. Akitake R, Watanabe T, Zaima C, Uza N, Ida H, Tada S, et al. Possible involvement of T helper type 2 responses to Toll-like receptor ligands in IgG4-related sclerosing disease. Gut 2010;59: 542–5.
13. Ueno K, Watanabe T, Kawata Y, Gotoh T, Tsuji Y, Ida H, et al.

14. Akira S, Takeda K. Toll-like receptor signalling. Nat Rev Immunol 2004;4:499–511.
15. Litinskiy MB, Nardelli B, Hilbert DM, He B, Schaffer A, Casali P, et al. DCs induce CD40-independent immunoglobulin class switching through BLyS and APRIL. Nat Immunol 2002;3:822–9.
16. He B, Qiao X, Cerutti A. CpG DNA induces IgG class switch DNA recombination by activating human B cells through an innate pathway that requires TLR9 and cooperates with IL-10. J Immunol 2004;173:4479–91.
17. Watanabe T, Asano N, Murray PJ, Ozato K, Tailor P, Fuss IJ, et al. Muramyl dipeptide activation of nucleotide-binding oligomerization domain 2 protects mice from experimental colitis. J Clin Invest 2008;118:545–59.
18. Watanabe T, Asano N, Fichtner-Feigl S, Gorelick PL, Tsuji Y, Matsumoto Y, et al. NOD1 contributes to mouse host defense against Helicobacter pylori via induction of type I IFN and activation of the ISGF3 signaling pathway. J Clin Invest 2010;120: 1645–62.
19. Chung H, Watanabe T, Kudo M, Chiba T. Hepatitis C virus core protein induces homotolerance and cross-tolerance to Toll-like receptor ligands by activation of Toll-like receptor 2. J Infect Dis 2010;202:853–61.
20. Aalberse RC, Stapel SO, Schuurman J, Rispens T. Immunoglobulin G4: an odd antibody. Clin Exp Allergy 2009;39:469–77.
21. Mackay F, Schneider P. Cracking the BAFF code. Nat Rev Immunol 2009;9:491–502.
22. Mackay F, Silveira PA, Brink R. B cells and the BAFF/APRIL axis: fast-forward on autoimmunity and signaling. Curr Opin Immunol 2007;19:327–36.
23. Okazaki K, Kawa S, Kamisawa T, Ito T, Inui K, Irie H, et al. Japanese clinical guidelines for autoimmune pancreatitis. Pancreas 2009;38:849–66.
24. Okazaki K, Kawa S, Kamisawa T, Shimosegawa T, Tanaka M, Research Committee for Intractable Pancreatic Disease and Japan Pancreas Society. Japanese consensus guidelines for management of autoimmune pancreatitis: I. Concept and diagnosis of autoimmune pancreatitis. J Gastroenterol 2010;45:249–65.
25. He B, Raab-Traub N, Casali P, Cerutti A. EBV-encoded latent membrane protein 1 cooperates with BAFF/BLyS and APRIL to induce T cell-independent Ig heavy chain class switching. J Immunol 2003;171:5215–24.
26. Wood N, Bourque K, Donaldson DD, Collins M, Vercelli D, Goldman SJ, et al. IL-21 effects on human IgE production in response to IL-4 or IL-13. Cell Immunol 2004;231:133–45.
27. Alsaleh G, Francois A, Knapp AM, Schickel JN, Sibilia J, Pasquali JL, et al. Synovial fibroblasts promote immunoglobulin class switching by a mechanism involving BAFF. Eur J Immunol 2011;41:2113–22.
28. Cerutti A, Puga I, Cols M. Innate control of B cell responses. Trends Immunol 2011;32:202–11.
29. Van der Neut Kolfschoten M, Schuurman J, Losen M, Bleeker WK, Martinez-Martinez P, Vermeulen E, et al. Anti-inflammatory activity of human IgG4 antibodies by dynamic Fab arm exchange. Science 2007;317:1554–7.
30. Savilahti EM, Rantanen V, Lin JS, Karinen S, Saarinen KM, Goldis M, et al. Early recovery from cow's milk allergy is associated with decreasing IgE and increasing IgG4 binding to cow's milk epitopes. J Allergy Clin Immunol 2010;125:1315–21.

IgG4-related autoimmune pancreatitis involving the colonic mucosa. Eur J Gastroenterol Hepatol 2008;20:1118–21.

Superselective transarterial chemoembolization for hepatocellular carcinoma. Validation of treatment algorithm proposed by Japanese guidelines

Kenichi Takayasu[1,*,†], Shigeki Arii[2,†], Masatoshi Kudo[3,†], Takafumi Ichida[4,†], Osamu Matsui[5,†], Namiki Izumi[6,†], Yutaka Matsuyama[7,†], Michiie Sakamoto[8,†], Osamu Nakashima[9,†], Yonson Ku[10,†], Norihiro Kokudo[11,†], Masatoshi Makuuchi[12,†]

[1]Diagnostic Radiology, National Cancer Center Hospital, Tokyo, Japan; [2]Hepato-Biliary-Pancreatic Surgery, Tokyo Medical and Dental University Graduate School of Medicine, Tokyo, Japan; [3]Department of Gastroenterology and Hepatology, Kinki University School of Medicine, Sayama, Japan; [4]Department of Hepatology and Gastroenterology, Juntendo Shizuoka Hospital, Izunokuni, Japan; [5]Department of Radiology, Kanazawa University Graduate School of Medical Science, Kanazawa, Japan; [6]Department of Gastroenterology and Hepatology, Musashino Red Cross Hospital, Musashino, Japan; [7]Department of Biostatistics, School of Public Health, University of Tokyo, Tokyo, Japan; [8]Department of Pathology, Keio University School of Medicine, Tokyo, Japan; [9]Department of Clinical Laboratory Medicine, Kurume University Hospital, Kurume, Japan; [10]Department of Surgery, Kobe University Graduate School of Medicine, Kobe, Japan; [11]Hepato-Biliary-Pancreatic Surgery Division, Artificial Organ and Transplantation Division, Department of Surgery, Graduate School of Medicine, University of Tokyo, Tokyo, Japan; [12]Surgery, Japanese Red Cross Medical Center, Tokyo, Japan

Background & Aims: Transcatheter arterial chemoembolization with lipiodol (TACE) is widely performed in patients with hepatocellular carcinoma (HCC) unsuitable for curative treatment. It has recently been recommended for patients with 2 or 3 tumors >3 cm or ⩾4 tumors in a treatment algorithm proposed by Japanese guidelines. However, the best indication and appropriateness of the algorithm for TACE are still unclear.

Methods: In 4966 HCC patients who underwent TACE, survival was evaluated based on tumor number, size and liver function; and the adequacy of the algorithm for TACE was validated. Exclusion criteria were: vascular invasion, extrahepatic metastasis, and prior treatment. The mean follow up period was 1.6 years.

Results: The overall median and 5-year survivals were 3.3 years and 34%, respectively. Multivariate analysis revealed that Child–Pugh class, tumor number, size, alpha-fetoprotein, and des-gamma carboxy-prothrombin were independent predictors. The survival rate decreased as the tumor number ($p = 0.0001$) and size increased ($p = 0.04$ to $p = 0.0001$) in all but one subgroup in both Child–Pugh-A and -B. The stratification of these patients to four treatments in the algorithm showed potential ability to discriminate survivals of the resection and ablation (non-TACE) groups from those of the TACE group in Child–Pugh-B and partially in A.

Conclusions: TACE showed higher survival rates in patients with fewer tumor numbers, smaller tumor size, and better liver function. The treatment algorithm proposed by the Japanese guidelines might be appropriate to discriminate the survival of patients with non-TACE from TACE therapy.

Introduction

Hepatocellular carcinoma (HCC) is the sixth most common cancer worldwide with 626,000 new cases every year, and is the third most common cause of death from cancer [1]. The frequency of curative treatment, such as resection, local ablation, and/or liver transplantation is low (only 30%) due to advanced cancer stage and associated liver cirrhosis at the time of diagnosis [2]. Among several treatments, transcatheter arterial chemoembolization with lipiodol (TACE) is widely performed in patients with unresectable HCC at an initial and recurrent time, which accounts for 32% and 58% of all treatment modalities, respectively, in Japan [3]. Superselective TACE is indispensable to maximize the effect in targeted tumors and to minimize liver injury [4].

Recently, two treatment algorithms for HCC were proposed: the Barcelona Clinic Liver Cancer (BCLC) classification, in 2001 [5] and the Japanese guidelines, in 2005 [6]. The first one recommends TACE in patients with multi-nodular HCC in Child–Pugh A or B in the intermediate stage, while the second recommends TACE in patients with 2 or 3 tumors, >3 cm in diameter or ⩾4 tumors in liver damage A or B. In both guidelines, vascular invasion and/or extrahepatic spread are excluded. However, the survival rate of TACE-stratified to recommended treatment of the Japanese guidelines algorithm and its appropriateness have not

been yet determined. Thus, we conducted this research with a large scale of samples.

Patients and methods

During 6 years, from January 2000 to December 2005, a total of 60,773 patients with primary liver cancer were prospectively registered bi-annually by the Liver Cancer Study Group of Japan (LCSGJ) throughout 800 medical institutions using a registration/questionnaire sheet with more than 180 questions. Among them, 53,008 patients were clinically diagnosed with HCC with multiple imaging modalities, tumor markers, and/or needle biopsy. Four thousand nine hundred sixty-six patients were selected in the current cohort study. Inclusion criteria were the following: TACE was performed in naïve patients as an initial treatment and any other therapy such as resection and local ablation was not performed during the first investigation period within at least 2 years. Exclusion criteria were: vascular invasion of the portal and hepatic veins, invasion of the biliary duct, extrahepatic spread and history of previous treatment for HCC.

HCC was diagnosed using ultrasonography (US), dynamic computed tomography (CT), magnetic resonance imaging (MRI), and/or pathologically by biopsy specimens (3.2%). Abnormal elevation of tumor markers was also referred: alpha-fetoprotein (AFP) >400 ng/ml (normal, <20) and des-gamma carboxyl prothrombin (DCP) >100 mAU/ml (normal, <40). Typical HCC was depicted as hyper-attenuation in arterial phase and hypo-attenuation or wash-out in delayed phase (around 3 min after the beginning of contrast injection) of dynamic CT and on dynamic MRI. If the tumor showed an atypical profile and was larger than 2 cm in diameter, further examination was recommended as follows: angiography, combination of CT and angiography, MRI with super-paramagnetic iron oxide, CE-US with micro-bubble (Levovist, Bayer Schering Pharma, Germany), and/or needle biopsy. If the tumor was less than 2 cm, a follow up study with US was recommended [6]. The extrahepatic metastases were routinely examined by CT, US, and chest X-ray.

The distribution of background factors of patients with TACE is shown in Table 1. The study population predominantly consisted of patients older than 60 years [n = 4205 (85%)] and among them 3369 were male patients (68%). The proportion of Child–Pugh A/B/C was 69% (n = 3229 patients), 28% (n = 1296), and 4% (n = 167), respectively. 3479 patients (73%) were positive for hepatitis C virus antibody and 449 were positive for hepatitis B virus surface antigen. The maximum tumor size was ⩽2 cm in diameter for 32% and ⩽3 cm for 56% of tumors. The mean diameter was 3.8 ± 3.5 (standard deviation, SD) cm. The tumor number was one in 2252 patients (46%), two in 1003, three in 565, and more than four in 1092. 1868 patients (40%) had a normal AFP value and 900 had more than 401 ng/ml. 2128 patients (52%) had a DCP value ⩽100 mAU/ml.

According to the TNM stage revised by the LCSGJ in 2000 [7], 836 patients were in stage I, 2070 (43%) in stage II, and 1887 in stage III. The embolization area was less than one segment in 1589 patients (33%), equal to or more than one segment to less than one lobe in 2134 (44%), and the whole liver in only 247 patients (5%). Hypervascular HCC accounted for 98% (n = 4787 patients) and non-hypervascular HCC for 2% (n = 100). Mean bilirubin value was 1.1 ± 0.9 mg/dl (SD). Performance status (PS) according to Eastern Cooperative Oncology Group scale was PS0 in 1485 (80%) patients, PS1 in 298, PS2 in 48, PS3 in 23, and PS4 in 2 out of 1856 patients, namely 99% of patients, which were available during the last two years (January, 2004 to December, 2005) of the present study, were in PS0–2.

In most patients, the catheter tip was advanced at the nearest site of the feeding artery as possible. The emulsion of the anticancer agent and lipiodol followed by gelatin sponge particles was injected under X-ray monitoring. The dose of emulsion and particles of embolic materials was determined mainly based on the tumor size and extension. The anticancer agent used was epirubicin hydrochloride in 1490 patients (74%), doxorubicin hydrochloride in 191 patients, mitomycin C in 190 patients, and cisplatin and zinostatin stimalamer (SMANCS) in 72 patients each, for a total of 2015 patients with a mean dose of lipiodol of 4.8 ± 3.0 ml (SD), which data were available during the last two years (January, 2004 to December, 2005). The patients underwent dynamic CT or MRI with AFP and DCP measurement every three to four months, and repeated TACE was determined when local recurrence, intrahepatic metastases and/or de novo HCC was found.

To analyze the survival rate, all patients in Child–Pugh A or B were divided in four groups depending on tumor number (single, two, three, and more than four lesions). Each group was subsequently subdivided in four subgroups based on tumor size; ⩽2, 2.1 to 3.0, 3.1 to 5.0, and ⩾5.1 cm in diameter. Patients in Child–Pugh C were excluded from this analysis due to their small number (n = 167). The survival rate was calculated from the date of TACE to December 31, 2005. Patient's death was the endpoint irrespective of the cause of death. The mean follow up period was 1.6 ± 1.3 years (SD). TACE-related death was designated as death within 30 days after the initial TACE.

Treatment algorithm proposed by Japanese guidelines

The treatment algorithm proposed by Japanese guidelines [6] has six treatments determined by three factors: degree of liver damage [7], number of tumors, and tumor diameter (Fig. 1). For patients with liver damage A or B, four treatments are recommended: resection for single tumor or local ablation for single tumor ⩽2 cm and liver damage B; resection or ablation for 2 or 3 tumors ⩽3 cm; resection or TACE for 2 or 3 tumors >3 cm; TACE or hepatic arterial infusion chemotherapy for more than 4 tumors. For patients with liver damage C, liver transplantation for 1 to 3 tumors ⩽3 cm or single tumor ⩽5 cm as indicated by the Milan criteria [8], and palliative care for ⩾4 tumors are recommended. In the present study, Child–Pugh class was adopted instead of degree of liver damage because the former is widely used to evaluate liver function, especially for candidates to TACE.

The executing rate of TACE was calculated with the following formula: number of patients stratified to TACE in treatment algorithm divided by a total number of patients who actually received TACE × 100 (%). The adequacy of treatment algorithm for TACE was validated when the survivals of patients stratified to TACE group (for 2 or 3 lesions >3 cm or more than 4 lesions) and those of patients stratified to non-TACE group (such as resection and ablation for single lesion or 2 or 3 lesions ⩽3 cm) could be discriminated.

Statistical analysis

The survival rate was obtained by the Kaplan–Meier method and compared by the log-rank test in Tables 1, 2A and B, and 3. The multivariate analysis was performed with the Cox's proportional hazard model. All variables, except for one of the embolization area of the liver due to the factor obtained following TACE therapy, with *p* value less than 0.05 on univariate analysis, were subjected to multivariate analysis. All significance tests were two-tailed, and *p* value less than 0.05 was considered statistically significant. All statistical analyses were carried out with the Statistical Analysis System (SAS) version 8.02 (SAS Inc., Cary, NC).

Results

Survival rates

For overall survival of the 4966 patients who underwent TACE, the median, and 1-, 2-, 3-, 4- and 5-year survival rates were 3.3 years (40 months) and 87%, 70%, 55%, 42% and 34%, respectively (Fig. 2). The 3- and 5-year survival in Child–Pugh A, B, and C was 61% and 40%; 43% and 22%; 23% and 0%, respectively (Table 1).

Patient characteristics analyzed by univariate and multivariate analyses

The univariate analysis revealed that there was a significant difference between the following seven variables (*p* = 0.0001); Child–Pugh class, maximum tumor size, number of lesions, AFP, DCP, TNM stage, and extent of embolization area (Table 1).

The multivariate analysis showed that the following five variables were independent predictors in trial 1; Child–Pugh class, tumor size, number of lesions, AFP, and DCP (Supplementary Table 1). In trial 2, where tumor size and number of lesions in trial 1 were replaced by TNM stage, four variables were independent predictors: Child–Pugh class, TNM stage, AFP, and DCP.

Survival rates of patients stratified to four groups divided by lesion number and to four subgroups subdivided by lesion size

In Child–Pugh A patients (n = 3194), the overall median and 3-year survival rate in four groups divided by tumor number: single, two, three, and more than 4 lesions, were 5.4 years and 73%, 3.8 years and 59%, 3.1 years and 52%, and 2.8 years and

Research Article

Table 1. Distribution of background factors and results of the univariate analysis in 4966 patients with hepatocellular carcinoma who underwent transcatheter arterial chemoembolization with lipiodol.

| Background factors	No. of patients	Proportion (%)	Survivals (%)				p	Hazard ratio (95% CI)
			1-yr	3-yr	4-yr	5-yr		
Age, yr							0.88	
<60	756	15	85	56	43	39		Ref.
≥60	4205	85	87	55	42	33		1.01 (0.88, 1.16)
Gender							0.40	
M	3369	68	86	54	42	35		1.05 (0.93, 1.18)
F	1597	32	89	56	42	33		Ref.
Child-Pugh classification							0.0001	
A	3229	69	90	61	49	40		Ref.
B	1296	28	82	43	27	22		1.81 (1.62, 2.04)
C	167	4	69	23	12	-		3.05 (2.44, 3.81)
HBV and HCV							0.50	
HCV Ab positive	3479	73	87	55	41	34		1.01 (0.87, 1.18)
HBs Ag positive	449	9	84	53	37	35		1.11 (0.90, 1.38)
Both positive	89	2	89	58	54	43		0.83 (0.56, 1.25)
Both negative	768	16	86	56	44	32		Ref.
Maximum tumor size (cm)							0.0001	
≤2	1549	32	93	65	50	42		Ref.
2.1-3	1178	24	89	53	42	35		1.38 (1.19, 1.60)
3.1-5	1291	27	85	52	37	29		1.62 (1.41, 1.87)
≥5.1	811	17	77	44	34	23		2.19 (1.88, 2.56)
No. of lesions							0.0001	
1	2252	46	91	66	53	45		Ref.
2	1003	20	88	55	42	34		1.35 (1.17, 1.56)
3	565	12	86	45	27	20		1.77 (1.50, 2.08)
≥4	1092	22	79	39	30	20		2.18 (1.91, 2.48)
Alpha-fetoprotein (ng/ml)							0.0001	
≤20	1868	40	92	64	50	44		Ref.
21-200	1613	34	89	55	40	30		1.38 (1.21, 1.57)
201-400	311	7	82	45	33	29		1.73 (1.40, 2.14)
401-1000	309	7	81	43	32	21		2.07 (1.68, 2.55)
≥1001	591	13	72	38	32	23		2.49 (2.13, 2.92)
Des-gamma carboxy-prothrombin (mAU/ml)							0.0001	
≤100	2128	52	92	65	52	40		Ref.
101-299	599	15	88	52	41	32		1.50 (1.26, 1.78)
300-499	245	6	84	49	27	24		1.93 (1.54, 2.42)
500-999	294	7	82	50	33	20		1.89 (1.51, 2.36)
≥1000	794	20	76	38	26	18		2.52 (2.18, 2.91)
TNM stage							0.0001	
I (T1N0M0)	836	17	93	72	59	51		Ref.
II (T2N0M0)	2070	43	90	60	46	37		1.51 (1.27, 1.80)
III (T3N0M0)	1887	39	81	42	30	22		2.60 (2.19, 3.09)
Extent of embolization							0.0001	
<one segment	1589	33	90	64	51	44		Ref.
1 seg. ≤ to <1 lobe	2134	44	87	55	41	32		1.33 (1.17, 1.51)
1 lobe ≤ to <whole liver	873	18	85	47	32	23		1.67 (1.43, 1.94)
Whole liver	247	5	74	37	29	-		2.27 (1.85, 2.80)

Cancer
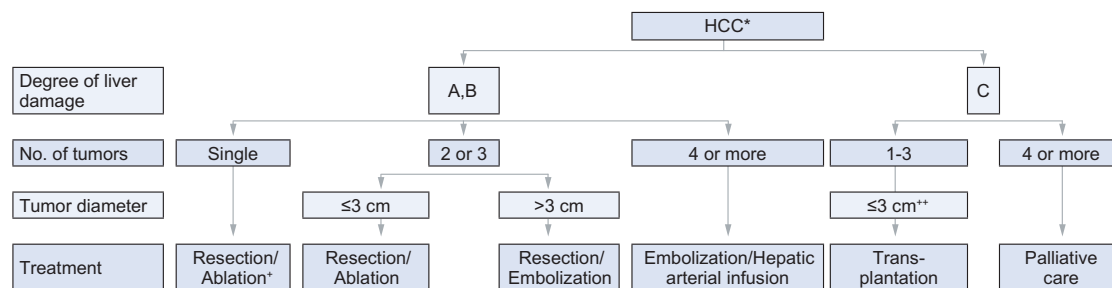
Fig. 1. Treatment algorithm for HCC proposed by Japanese guidelines. (+) shows local ablation for single lesion ⩽2 cm in patients with liver damage B. (++) means liver transplantation for no more than 3 lesions ⩽3 cm or single lesion ⩽5 cm. The asterisk shows that for patients with vascular invasion and liver damage A, hepatectomy, TACE or hepatic arterial infusion chemotherapy may be recommended, while chemotherapy is an option for patients with extrahepatic metastasis.

46%, respectively (p = 0.0001, Table 2A). The survival rate of four subgroups subdivided by tumor size from ⩽2 cm to ⩾5.1 cm decreased as the lesion size increased in all (p = 0.04 to p = 0.0001) but one group with 3 lesions (p = 0.07). The highest 3-year survival was 80% in patients with single lesion ⩽2 cm, and the lowest 3-year survival was 30% in patients with more than 4 lesions ⩾5.1 cm.

In Child–Pugh B (n = 1284), the overall median and 3-year survival rate of four groups were 3.1 years and 53%, 2.8 years and 49%, 2.0 years and 24%, and 1.9 years and 22%, respectively (p = 0.0001, Table 2B). The survival rate of four subgroups divided by tumor size in each group decreased as the lesion size increased in all (p = 0.01 to p = 0.0004) but one group with single lesion (p = 0.49). The highest 3-year survival was 65%, found in patients with 2 lesions ⩽2 cm, and the lowest was 0% in patients with three lesions ⩾5.1 cm.

Validation of the treatment algorithm proposed by the Japanese guidelines

Of 3168 patients with TACE in Child–Pugh A, 1475 were stratified to resection or ablation therapy for single lesion in the treatment algorithm (Fig. 1), 506 to resection or ablation for 2 or 3 lesions ⩽3 cm, 463 to resection or TACE for 2 or 3 lesions >3 cm, and 724 to TACE or hepatic arterial infusion chemotherapy for ⩾4 lesions (Table 3). The median and 3-year survival rates of the corresponding four treatments were 5.4 years and 73%, 3.5 years and 59%, 3.4 years and 55%, and 2.8 years and 46%, respectively, with a significant difference (p = 0.0001). The comparisons of the survival curves between two treatment groups showed a significant difference in all (p = 0.013 to p = 0.0001) but one comparison between treatments for 2 or 3 lesions ⩽3 cm and for 2 or 3 lesions >3 cm (p = 0.06) (Fig. 3). Namely, survival discrimination was feasible between one of two TACE treatments for >4 lesions and non-TACE therapies such as resection or ablation.

Similarly, 1274 patients with Child–Pugh B were stratified to four treatment categories (Table 3). The median and 3-year survivals of these treatments from single to ⩾4 lesions were 3.1 years and 53%, 2.8 years and 49%, 1.7 years and 30%, and 1.9 years and 22%, respectively, with a significant difference (p = 0.0001). The comparisons of survival curves between two treatment groups showed a significant difference in all (p = 0.0001) but two comparisons; single lesion *vs.* 2 or 3 lesions ⩽3 cm (p = 0.79) and 2 or 3 lesions >3 cm *vs.* ⩾4 lesions (p = 0.84)

(Fig. 4). Namely, survival discrimination was feasible between two TACE therapy groups, i.e., 2 or 3 lesions >3 cm and ⩾4 lesions and two non-TACE groups.

The executing rate of TACE was 37% in both Child–Pugh A (1187/3168 patients) and B (467/1274).

TACE-related mortality rate

After the initial TACE, treatment-related death occurred in 19 (0.38%) out of 4966 patients. The breakdown of the cause of death was cancer in 5 patients (26%), hepatic failure in 3 (16%), rupture of esophago-gastric varices in one patient, intra-peritoneal rupture of HCC in another patient, and other causes in 9 patients. Ten patients were in Child–Pugh A, 8 were in class B and one was in class C.

Discussion

The present study demonstrates that the overall median and 3-, and 5-year survival rates of TACE were 3.3 years (40 months), 55%, and 34%, respectively, and were better than those previously reported by the LCSGJ (34 months, 47%, and 26% [9]), mainly due to exclusion criteria of vascular invasion in the current study. The multivariate analysis revealed that five variables were independent predictors in trial 1: Child–Pugh class, tumor size, tumor number, AFP, and DCP; and four variables in trial 2, where tumor size and tumor number were replaced by TNM stage. These results are similar to those of a previous study [9] other than Child–Pugh class instead of degree of liver damage and DCP value were newly adopted.

There was an inverse correlation between tumor number and overall survival of patients with TACE therapy (p = 0.0001) in both Child–Pugh A and B (Tables 2A and B) as well as between tumor diameter and survival in all but one group, each in Child–Pugh A and B. Namely, the fewer the tumor number and the smaller the tumor size, the better the survival rates. The best 3-year survival was found in patients with a single HCC ⩽2 cm in Child–Pugh A, and the worst 3-year survival (0%) in patients with three lesions ⩾5.1 cm in class B. However, in clinical practice, the best survivor with TACE is not recommended to TACE but to resection or local ablation due to relatively higher 3-year survival rates, 90% and 85%, respectively [3]. The current study has revealed a wide range of survival rates for patients with

Research Article

Table 2. The overall survivals of four groups divided by tumor number and survivals of four subgroups divided by tumor size in patients who underwent TACE. (A) Child–Pugh A (n = 3194 patients). (B) Child–Pugh B (n = 1284).

A

Group/subgroup	No. of patients	Survival (%) 1-yr	3-yr	4-yr	5-yr	Median (yr)	p	Hazard ratio (95% CI)
Single lesion								
Overall*	1475	93	73	62	52	5.4		
≤2 cm	546	97	80	73	65	-	0.0001	Ref.
2.1-3.0	353	92	71	56	36	4.5		1.88 (1.36, 2.62)
3.1-5.0	328	92	66	53	46	4.6		1.97 (1.42, 2.75)
≥5.1	219	86	66	48	-	4.2		2.38 (1.64, 3.46)
Two lesions								
Overall*	634	91	59	47	40	3.8		
≤2 cm	178	97	64	49	42	3.9	0.04	Ref.
2.1-3.0	144	91	50	39	-	2.8		1.57 (1.01, 2.44)
3.1-5.0	190	90	66	47	39	4.0		1.23 (0.80, 1.90)
≥5.1	104	84	53	45	38	4.1		1.94 (1.19, 3.15)
Three lesions								
Overall*	361	90	52	33	24	3.1		
≤2 cm	102	92	65	30	-	3.6	0.07	Ref.
2.1-3.0	82	95	51	32	-	3.1		1.16 (0.68, 1.99)
3.1-5.0	111	94	48	38	-	3.0		1.30 (0.80, 2.10)
≥5.1	58	73	35	-	-	2.2		2.02 (1.19, 3.45)
More than 4 lesions								
Overall*	724	82	46	37	25	2.8		
≤2 cm	168	92	59	54	44	4.4	0.0001	Ref.
2.1-3.0	137	83	54	51	32	4.0		1.47 (0.97, 2.25)
3.1-5.0	207	82	43	25	16	2.5		2.00 (1.38, 2.90)
≥5.1	190	74	30	18	-	1.7		2.89 (2.01, 4.17)

B

Group/subgroup	No. of patients	Survival (%) 1-yr	3-yr	4-yr	5-yr	Median (yr)	p	Hazard ratio (95% CI)
Single lesion								
Overall*	568	87	53	34	30	3.1		
≤2 cm	213	89	56	33	24	3.3	0.49	Ref.
2.1-3.0	169	88	50	44	39	2.9		1.00 (0.69, 1.44)
3.1-5.0	132	87	54	20	-	3.1		1.24 (0.83, 1.86)
≥5.1	47	78	49	-	-	2.5		1.40 (0.80, 2.47)
Two lesions								
Overall*	276	83	49	34	-	2.8		
≤2 cm	86	93	65	48	-	4.0	0.0004	Ref.
2.1-3.0	70	93	43	21	-	2.3		1.86 (1.04, 3.34)
3.1-5.0	82	69	41	27	-	2.1		2.49 (1.47, 4.21)
≥5.1	31	58	-	-	-	1.5		3.66 (1.83, 7.32)
Three lesions								
Overall*	150	77	24	14	-	2.0		
≤2 cm	40	89	28	19	-	2.0	0.005	Ref.
2.1-3.0	43	76	30	-	-	2.3		1.09 (0.50, 2.35)
3.1-5.0	41	73	34	17	-	1.8		1.31 (0.65, 2.64)
≥5.1	23	62	-	-	-	1.4		3.16 (1.49, 6.72)
More than 4 lesions								
Overall*	290	72	22	10	-	1.9		
≤2 cm	57	90	32	24	-	2.0	0.01	Ref.
2.1-3.0	68	75	17	8	-	2.1		1.53 (0.85, 2.76)
3.1-5.0	89	73	25	-	-	2.0		1.54 (0.88, 2.69)
≥5.1	65	54	-	-	-	1.2		2.55 (1.43, 4.56)

*A significant difference was demonstrated in overall survival among four groups (p = 0.0001).

TACE, mainly because of the heterogeneity of the population, therefore it would be helpful for candidates to determine chemoembolization as tailor-made treatment of choice; this is particularly suitable for patients averse to curative therapy and with severely associated diseases, or elderly patients.

The executing rate of patients who actually had undergone TACE and were stratified to TACE in the treatment algorithm was 37% in both Child–Pugh A and B. Namely, the remaining 63% of patients satisfied the criteria of resection or local ablation (non-TACE therapy), which could suggest the possible increase of survival in these patients, if they underwent resection or local ablation. The reason for the lower executing rate might be the less publicity in which the guideline was published one year after the completion of this 6-year study.

The discrimination of patients' survival was feasible in this treatment algorithm between TACE and non-TACE therapies in Child–Pugh B and in part in class A. Further studies are needed to validate the suitability of these guidelines using patients who underwent resection or local ablation and are stratified to four treatments like in the TACE study.

To our knowledge, the present study is the first report to clarify the median and 3- and 4-year survivals of patients treated by TACE and stratified in the four treatments recommended by the Japanese guidelines in Child–Pugh A and B, separately. Interestingly, Llovet et al. [10] stated that chemoembolization improved median survival up to 19–20 months in intermediate stage of BCLC classification, which is similar to our results; 1.7 years (20 months) in patients with TACE for 2 or 3 lesions >3 cm and

Cancer

Table 3. Survival rates of patients treated with TACE stratified to four treatment categories recommended by Japanese guidelines in Child–Pugh A and B.

Criteria of treatment	No. of patients	Survival (%)				Median	p	Hazard ratio (95% CI)
		1-yr	3-yr	4-yr	5-yr	(yr)		
Child-Pugh A	3168							
Single lesion	1475	93	73	62	52	5.4	0.0001	Ref.
2-3 lesions, ≤3 cm	506	94	59	40	36	3.5		1.45 (1.18, 1.78)
2-3 lesions, >3 cm	463	87	55	44	31	3.4		1.82 (1.48, 2.25)
≥4 lesions	724	82	46	37	25	2.8		2.39 (2.01, 2.84)
Child-Pugh B	1274							
Single lesion	568	87	53	34	30	3.1	0.0001	Ref.
2-3 lesions, ≤3 cm	239	90	49	33	-	2.8		1.04 (0.79, 1.36)
2-3 lesions, >3 cm	177	68	30	19	-	1.7		2.11 (1.62, 2.75)
≥4 lesions	290	72	22	10	-	1.9		2.17 (1.72, 2.74)

No. of at risk   4966   2876   1478   786   335   120
patients
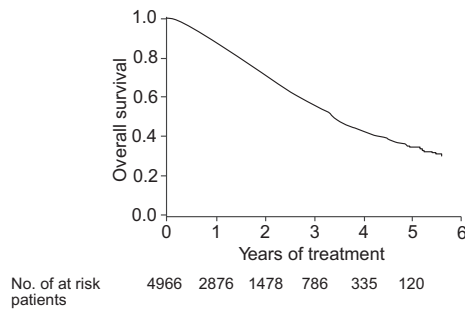
Fig. 2. Overall survival rate of 4966 HCC patients who underwent TACE.
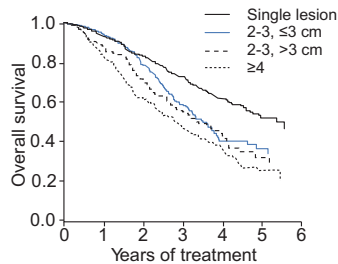
Fig. 3. The survival curves of 3168 patients in Child–Pugh A stratified to four treatment groups according to Japanese guidelines. Overall, there was a significant difference ($p = 0.0001$). There was also a significant difference between two treatment groups except for one; 2 or 3 lesions ⩽3 cm vs. 2 or 3 lesions >3 cm ($p = 0.06$).

1.9 years (23 months) in those for ⩾4 lesions in Child–Pugh B (Table 3). If the criteria for TACE are similar in the intermediate stage of the BCLC staging system [5] and in the treatment algorithm of the Japanese guidelines: equal to or more than 4 lesions and/or 2 or 3 lesions >3 cm [11], the current data will be useful to compare the survival outcomes of TACE in the East and West. The survival rates of our study will be also used as reference data
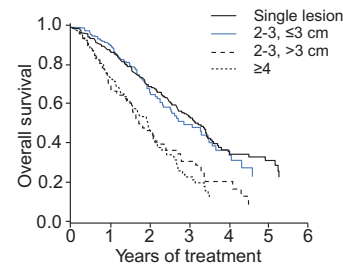
Fig. 4. The survival curves of 1274 patients in Child–Pugh B stratified to four treatment groups. Overall, a significant difference was seen ($p = 0.0001$). A significant difference was observed between two groups except for two; single lesion vs. 2 or 3 lesions ⩽3 cm, and 2 or 3 lesions >3 cm vs. ⩾4 lesions.

when clinical trials of TACE with or without anti-angiogenic drugs are newly designed [12,13].

The treatment-related mortality rate was 0.38%, which was slightly improved compared to that of our previous study of 0.5% [9], and much better than that of 2.4% reported by a systematic review [14]. The improvement is mainly attributable to the exclusion criteria of vascular or biliary duct invasion and the decreased proportion of Child–Pugh C patients, from 10% [9] to 4%.

As a limitation of this study, the session numbers of TACE per patient and dosage of anticancer agent used at initial TACE were not available due to lack of inclusion in the questionnaire sheet. Our patients received different TACE protocols for anticancer agent. Given that the large majority of patients were treated with epirubicin or doxorubicin, it could be worth limiting the analysis to these patient cohorts.

In conclusion, the overall median and 3- and 5-year survival of TACE were 3.3 years, 55% and 34% in 4966 HCC patients without vascular invasion and extrahepatic spread. The tumor number, size, liver function, AFP, and DCP were independent predictors. These results will be helpful for physicians to select chemoembolization as optimal therapy for their patients, especially when curative treatment is contraindicated due to severely associated disease and/or aging. The treatment algorithm of the Japanese guidelines might be appropriate to discriminate patient survival

Cancer

— 222 —

Research Article

with non-TACE from TACE therapy in Child–Pugh B and in part in A. The survival rates of patients stratified to TACE in these guidelines will be useful for comparing the outcome of TACE in the East and West, and for designing new clinical trials for TACE with and without a novel molecular targeted agent as reference data.

Conflict of interest

The authors who have taken part in this study declared that they do not have anything to disclose regarding funding or conflict of interest with respect to this manuscript.

Supplementary data

Supplementary data associated with this article can be found, in the online version, at doi:10.1016/j.jhep.2011.10.021.

References

[1] Parkin DM, Bray F, Ferlay J, Pisani P. Global cancer statistics, 2002. CA Cancer J Clin 2005;55:74–108.
[2] Bruix J, Llovet JM. Prognostic prediction and treatment strategy in hepatocellular carcinoma. Hepatology 2002;35:519–524.
[3] Ikai I, Kudo M, Arii S, Omata M, Kojiro M, Sakamoto M, et al. Report of the 18th follow up survey of primary liver cancer in Japan. Hepatol Res 2010;40:1043–1059.
[4] Matsui O, Kadoya M, Yoshikawa J, Gabata T, Arai K, Demachi H, et al. Small hepatocellular carcinoma: treatment with subsegmental transcatheter arterial embolization. Radiology 1993;188:79–83.
[5] Bruix J, Sherman M, Llovet JM, Beaugrand M, Lencioni R, Burroughs AK, et al. Clinical management of hepatocellular carcinoma. Conclusions of the Barcelona-2000 EASL conference. European Association for the Study of the Liver. J Hepatol 2001;35:421–430.
[6] Makuuchi M, Kokudo N, Arii S, Futagawa S, Kaneko S, Kawasaki S, et al. Development of evidence-based clinical guidelines for the diagnosis and treatment of hepatocellular carcinoma in Japan. Hepatol Res 2008;38:37–51.
[7] The Liver Cancer Study Group of Japan. The general rules for the clinical and pathological study of primary liver cancer. 2nd English ed. Tokyo, Japan: Kanehara & Co., Ltd.; 2003.
[8] Mazzaferro V, Regalia E, Doci R, Andreola S, Pulvirenti A, Bozzetti F, et al. Liver transplantation for the treatment of small hepatocellular carcinomas in patients with cirrhosis. N Engl J Med 1996;334:693–699.
[9] Takayasu K, Arii S, Ikai I, Omata M, Okita K, Ichida T, et al. Prospective cohort study of transarterial chemoembolization for unresectable hepatocellular carcinoma in 8510 patients. Gastroenterology 2006;131:461–469.
[10] Llovet JM, Di Bisceglie AM, Bruix J, Kramer BS, Lencioni R, Zhu AX, et al. Design and endpoints of clinical trials in hepatocellular carcinoma. J Natl Cancer Inst 2008;100:698–711.
[11] Takayama T. Hepatocellular carcinoma. In: Clavien PA, editor. Malignant liver tumors: current and emerging therapies. London: Wiley-Blackwell; 2010. p. 317–323.
[12] Sergio A, Cristofori C, Cardin R, Pivetta G, Ragazzi R, Baldan A, et al. Transcatheter arterial chemoembolization (TACE) in hepatocellular carcinoma (HCC): the role of angiogenesis and invasiveness. Am J Gastroenterol 2008;103:914–921.
[13] Lencioni R, Zou J, Leberre M, Meinhardt G, Voliotis D, Bruix J, et al. Sorafenib (SOR) or placebo (PL) in combination with transarterial chemoembolization (TACE) for intermediate–stage hepatocellular carcinoma (SPACE). ASCO Meeting Abstracts 2010;28:TPS178.
[14] Marelli L, Stigliano R, Triantos C, Senzolo M, Cholongitas E, Davies N, et al. Transarterial therapy for hepatocellular carcinoma: which technique is more effective? A systematic review of cohort and randomized studies. Cardiovasc Intervent Radiol 2007;30:6–25.

Cancer

Current Status of Hepatocellular Carcinoma Treatment in Japan
Case Study and Discussion-Voting System

Masatoshi Kudo,[1] *Ryosuke Tateishi,*[2] *Tatsuya Yamashita,*[3] *Masafumi Ikeda,*[4] *Junji Furuse,*[5] *Kenji Ikeda,*[6] *Norihiro Kokudo,*[7] *Namiki Izumi*[8] and *Osamu Matsui*[9]

1   Department of Gastroenterology and Hepatology, Kinki University School of Medicine, Osaka, Japan
2   Department of Gastroenterology, University of Tokyo Hospital, Tokyo, Japan
3   Department of Gastroenterology, Kanazawa University Hospital, Kanazawa, Japan
4   Division of Hepatobiliary and Pancreatic Oncology, National Cancer Center Hospital East, Kashiwa, Japan
5   Medical Oncology Division, Kyorin University School of Medicine, Mitaka, Japan
6   Department of Hepatology, Toranomon Hospital, Tokyo, Japan
7   Hepato-Biliary Pancreatic Surgery Division, Department of Surgery, Graduate School of Medicine, University of Tokyo, Tokyo, Japan
8   Department of Gastroenterology and Hepatology, Musashino Red Cross Hospital, Musashino, Japan
9   Department of Imaging Diagnosis and Interventional Radiology, Division of Cardiovascular Medicine, Kanazawa University Graduate School of Medical Science, Kanazawa, Japan

Abstract

The Toward Integrated Treatment of Advanced Hepatocellular Carcinoma with Nexavar (TiTAN) Symposium was held in August 2010 in Tokyo, Japan, during which the position of sorafenib (Nexavar®) in the treatment of HCC in Japan (for which it received approval in 2009) was discussed by a panel of eight expert hepatologists in a session chaired by Dr Kudo. The following article focuses on the discussion that went on during this session, including question and answer sessions regarding the experiences of the 350 conference attendees in treating patients with HCC, as well as some of the more challenging disease management issues.

Since 2008, when the phase III Sorafenib Hepatocellular Carcinoma Assessment Randomized Protocol (SHARP) trial demonstrated an increase in the median overall survival (OS) for patients with unresectable HCC treated with sorafenib compared with placebo, international and Japanese guidelines recommend sorafenib as a first-line option for patients with advanced HCC Child–Pugh liver function class A who have extrahepatic metastasis. Sorafenib is also recommended for patients unresponsive to transarterial chemoembolization (TACE) or hepatic arterial infusion chemotherapy (HAIC). Importantly, if HCC is judged to be unresponsive to TACE, treatment should be switched to sorafenib in a timely manner.

Almost half of the conference attendees said that they used both the Japan Society of Hepatology clinical practice guidelines and the clinical practice

guidelines for HCC when determining treatment strategies for individual HCC patients. Sorafenib should currently not be used as adjuvant therapy or in combination with TACE or HAIC until evidence from ongoing clinical trials shows that it is beneficial in these settings.

1. Introduction

Numerous patients with hepatocellular carcinoma (HCC) have been treated with sorafenib (Nexavar®, Bayer, Berlin, Germany) in clinical practice in Japan following its approval for this indication on 20 May 2009.[1]

The Toward Integrated Treatment of Advanced Hepatocellular Carcinoma with Nexavar (TiTAN) Symposium was held on 28 August 2010 in Tokyo, Japan, during which the position of sorafenib in the treatment of HCC in Japan was discussed by a panel of eight experts (Dr Ryosuke Tateishi, Dr Tatsuya Yamashita, Dr Masafumi Ikeda, Dr Junji Furuse, Dr Kenji Ikeda, Dr Norihiro Kokudo, Dr Namiki Izumi and Dr Osamu Matsui) in a session chaired by Dr Masatoshi Kudo. During this session, approximately 350 conference attendees were questioned regarding their experiences in treating patients with HCC, with answers given by means of a wireless voting system. Some of the more challenging issues in the management of HCC were also discussed. The following article focuses on the discussion that went on during this session, with particular emphasis on sorafenib.

2. Current Practice Guidelines for Hepatocellular Carcinoma

2.1 Asian-Pacific Association for the Study of the Liver Guidelines

The first meeting of the Asian-Pacific Association for the Study of the Liver (APASL) working committee was held in Bali, Indonesia, in December 2008 to develop consensus recommendations for the management of HCC; 21 experts from Japan, Hong Kong, Korea, Taiwan, China, Pakistan, Singapore, India and Indonesia attended the meeting.[2]

The APASL treatment algorithm for HCC (figure 1a) is similar to that proposed in the evidence-based Japan Society of Hepatology (JSH) clinical practice guidelines for HCC[3] (see figure 1b). In the APASL algorithm, sorafenib is a first-line option for the treatment of HCC with extrahepatic metastasis or extensive portal invasion (main portal vein tumour thrombus) in Child–Pugh class A or B patients. APASL has the following recommendations regarding systemic therapy:[2]

- As a systemic treatment, sorafenib is strongly recommended for the treatment of advanced-stage patients who are not suitable for loco-regional therapy and who have Child–Pugh liver function class A (quality of evidence level 1b, strength of recommendation grade A).
- Sorafenib 'may be used' with caution in patients with Child–Pugh liver function class B (4, C).
- Cytotoxic drugs are not routinely recommended but may be considered in highly selected patients whose general and hepatic conditions are adequate (3, C).

2.2 American Association for the Study of Liver Diseases Practice Guidelines 2010

The American Association for the Study of Liver Disease practice guidelines, which were updated in 2010,[5] have gained wide acceptance throughout the USA and Europe. The 2010 guideline update recommends sorafenib for stage C (advanced) HCC with portal invasion, tumour status N1, M2 or performance status test 1–2 according to the Barcelona Clinic liver cancer[6] staging system (see figure 1a in article 1 of this supplement). Similar to the 2005 version, sorafenib is recommended (based on grade 1 level of evidence) as a first-line option in patients who cannot benefit from resection, transplantation, ablation or transarterial chemoembolization (TACE), and still have preserved liver function.[5]
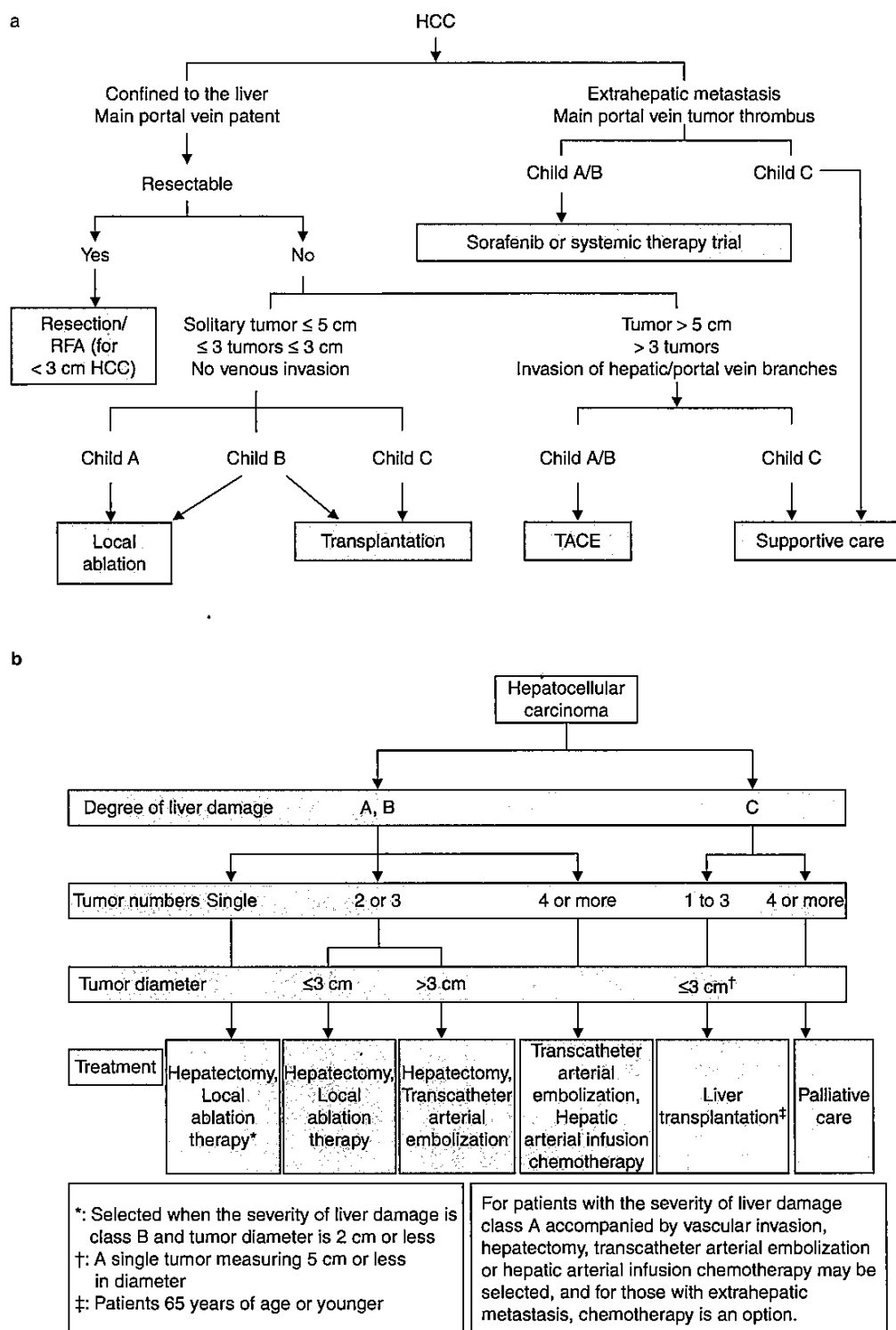
a

HCC

Confined to the liver
Main portal vein patent

Extrahepatic metastasis
Main portal vein tumor thrombus

Child A/B   Child C

Resectable

Sorafenib or systemic therapy trial

Yes   No

Resection/
RFA (for
< 3 cm HCC)

Solitary tumor ≤ 5 cm
≤ 3 tumors ≤ 3 cm
No venous invasion

Tumor > 5 cm
> 3 tumors
Invasion of hepatic/portal vein branches

Child A   Child B   Child C   Child A/B   Child C

Local ablation   Transplantation   TACE   Supportive care

b

Hepatocellular carcinoma

Degree of liver damage   A, B   C

Tumor numbers Single   2 or 3   4 or more   1 to 3   4 or more

Tumor diameter   ≤3 cm   >3 cm   ≤3 cm†

Treatment

| Hepatectomy, Local ablation therapy* | Hepatectomy, Local ablation therapy | Hepatectomy, Transcatheter arterial embolization | Transcatheter arterial embolization, Hepatic arterial infusion chemotherapy | Liver transplantation‡ | Palliative care |

*: Selected when the severity of liver damage is class B and tumor diameter is 2 cm or less
†: A single tumor measuring 5 cm or less in diameter
‡: Patients 65 years of age or younger

For patients with the severity of liver damage class A accompanied by vascular invasion, hepatectomy, transcatheter arterial embolization or hepatic arterial infusion chemotherapy may be selected, and for those with extrahepatic metastasis, chemotherapy is an option.

Fig. 1. Treatment algorithms for hepatocellular carcinoma (HCC) from (a) the Asian-Pacific Association for the Study of the Liver (reproduced with permission from Omata et al.),[2] (b) the evidence-based Japan Society of Hepatology (JSH) Clinical Practice Guidelines for HCC[3] and (c) the consensus-based JSH clinical practice guidelines for hepatocellular carcinoma 2010 update.[4] HAIC = hepatic arterial infusion chemotherapy; RFA = radiofrequency ablation; TACE = transarterial chemoembolization.

Treatment algorithm for hepatoma
based on JSH consensus (2010 update)
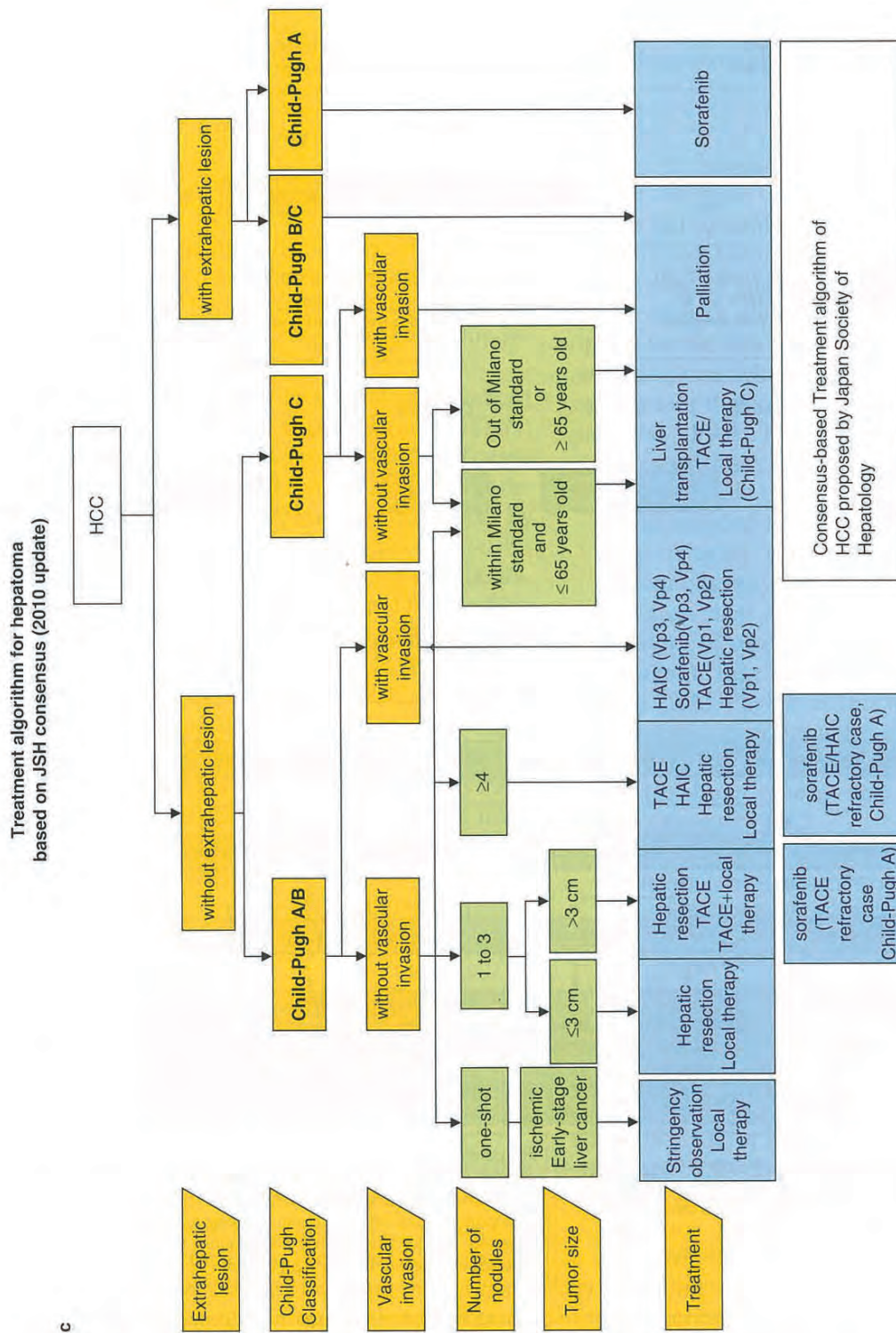
Fig. 1. Contd

2.3 Japanese Guidelines (Evidence and Consensus-Based Clinical Practice Guidelines for Hepatocellular Carcinoma)

The evidence-based JSH clinical practice guidelines for HCC 2009 update[3] (issued in November 2009) are based on data obtained up to mid-2007 and therefore do not reflect the results of the phase III Sorafenib Hepatocellular Carcinoma Assessment Randomized Protocol (SHARP)[7] trial published in 2008.

If updated, the JSH clinical practice guidelines for HCC would list sorafenib as an important treatment choice. In the current version, hepatic arterial infusion chemotherapy (HAIC) is recommended for the management of advanced HCC (see figure 1b in article 1 of this supplement);[3] sorafenib therapy is now a suitable option for the management of advanced HCC.

The consensus-based JSH clinical practice guidelines for HCC 2010 update,[4] which is based on both evidence and consensus, recommends sorafenib for the management of patients with HCC and Child–Pugh liver function class A in the following cases: patients without extrahepatic metastasis with or without vascular invasion who have either four of more nodules and are unresponsive to TACE/HAIC or who have one to three nodules and a tumour size of more than 3 cm and are unresponsive to TACE; and patients with extrahepatic metastasis (figure 1c).

When conference attendees were asked which guidelines they referred to when determining treatment strategies for individual HCC patients, 30% of the 319 respondents said that they used the JSH clinical practice guidelines for HCC,[3] 11% said the JSH consensus-based clinical practice guidelines for HCC[4] and 43% said both the JSH clinical practice guidelines and consensus-based clinical practice guidelines. None of the attendees used the Barcelona Clinic liver cancer staging and treatment strategy, while 14% used strategies devised at their institutions and 1% of attendees opted to use other guidelines.

3. Treatment of Hepatocellular Carcinoma with Extrahepatic Metastasis

Conference attendees were asked how they would treat HCC Child–Pugh class A patients

with extrahepatic metastasis. From the 326 attendees who responded, 85% said they would use oral sorafenib, 5% said an oral fluoropyrimidine (5-fluorouracil, uracil-tegafur or TS-1), 3% said interferon plus an oral fluoropyrimidine (5-fluorouracil, uracil-tegafur or TS-1), 4% said intravenous chemotherapy, 1% best supportive care and the remaining 3% said they would use another undefined method.

Dr Tateishi commented that although the presence of extrahepatic metastasis is a strong predictor of poor prognosis, extrahepatic metastasis itself rarely affects patient prognosis. It is still controversial whether we should concentrate on intrahepatic lesions in patients with extrahepatic metastasis when the vast majority of the tumour burden is located in the liver.

The SHARP trial was a placebo controlled phase III study of sorafenib in 602 previously untreated HCC patients in Europe, North/South America and Australia.[7] In a subset analysis of 421 patients with vascular invasion and/or extrahepatic metastasis, sorafenib significantly inhibited disease progression and prolonged OS compared with placebo; median time to disease progression was 4.1 months versus 2.7 months (hazard ratio [HR] = 0.64; 95% confidence interval [CI] 0.48, 0.84) and the median survival time was 8.9 months versus 6.7 months (HR = 0.77; 95% CI 0.60, 0.99).[8] This result supports the theory that sorafenib is a suitable first-line option for advanced HCC with vascular invasion and/or extrahepatic metastasis.

Dr Kudo commented that an excellent response to sorafenib has been reported in several cases of lung, lymph node and bone metastases of HCC,[9] thus systemic therapy with sorafenib could effectively control extrahepatic metastasis of HCC, perhaps not in all patients but at least in some.

Dr Furuse agreed that using sorafenib to control extrahepatic metastasis of HCC is reasonable, and highlighted that 85% of the respondents chose sorafenib when asked how they would treat HCC with extrahepatic metastasis. He also noted that some other options, including fluoropyrimidines such as S-1, have shown promising activity against metastatic lesions, but that no systemic therapy other than sorafenib has been shown to

improve the prognosis in patients with advanced HCC.[10] For these reasons, Dr Furuse concluded that he had no objection to the first-line use of sorafenib for the management of extrahepatic metastasis of HCC.

Dr Izumi presented data on the survival outcome of 42 patients with advanced HCC who had been treated with sorafenib (400 or 800 mg/day) at the Musashino Red-Cross Hospital between July 2009 and June 2010. All patients had experienced repeated recurrence while being treated with a variety of therapies available for HCC before the approval of sorafenib, 12 patients had extensive vascular invasion (VP3/4) and 12 had metastases in the bone (n = 6) or lungs (n = 6). Subgroup analyses (where p < 0.05 was considered statistically significant), performed to identify variables predicting survival benefits with sorafenib, showed that the survival time was longer in patients without extensive vascular invasion (n = 30) than in those with vascular invasion (n = 12) at baseline (p < 0.00001), and in patients with (n = 12) versus those without (n = 30) extrahepatic metastasis at baseline (p = 0.0043).

The improved prognosis of patients with extrahepatic metastasis after treatment with sorafenib contradicts findings from a subgroup analysis of the SHARP trial in which response to sorafenib was worse in patients with extrahepatic metastasis than in those without.[11] This apparent discrepancy may be due to differences in patient characteristics, because intrahepatic lesions had been controlled in the 42 patients with extrahepatic metastasis treated by Dr Izumi.

A case study was presented of a man aged 80 years with stage IVb HCV-related HCC whose extrahepatic metastasis, which had appeared in his ribs despite control of his intrahepatic lesions, had responded to treatment with sorafenib. After 8 months' treatment with sorafenib at 800 mg/day, the bone metastatic lesions were judged as stable disease (SD) suggesting that in patients without intrahepatic lesions, extrahepatic metastasis may show a sustained response to sorafenib.

In summary, sorafenib is the only drug shown to improve the survival of HCC patients with extrahepatic metastasis and well preserved liver function. At the TiTAN Symposium 2010, con-

sensus was reached as to the use of sorafenib as a first-line treatment of HCC with extrahepatic metastasis in Child–Pugh class A patients, as recommended in the current (2010 update) JSH clinical practice guidelines for HCC.[4]

4. Definition of Unresponsiveness to Transarterial Chemoembolization

The JSH clinical practice guidelines for HCC[4] define the following situations as being unsuitable for TACE: all vessels used for treatment have been devastated and no feeding vessels can be selectively catheterized; liver function has deteriorated to Child–Pugh class C during repeated cycles of TACE; extensive portal invasion (VP3/4) is present; or a large arterioportal shunt has formed.

As mentioned in article 3 in this supplement, 'unresponsiveness to TACE' is defined in the JSH clinical practice guidelines for HCC[4] (see also table I). An analysis of the prognosis of patients with HCC who became unresponsive to TACE or who required a further cycle of TACE to control a new lesion within 3 months showed that these patients were most likely to show worsening liver function. Furthermore, repeating TACE at intervals of 3 months or less predicted an increased risk of progression to Child–Pugh class B and a lower cumulative survival rate. Ninety-four patients with HCC, Child–Pugh class A and four of more nodules who underwent TACE as their initial treatment at Musashino Red-Cross Hospital had a cumulative survival rate of 86% at 1 year, 54% at 3 years and 30% at 5 years.[12] These rates are lower than the corresponding values observed in

Table I. Definition of unresponsive to TACE as defined in the Japan Society of Hepatology clinical practice guidelines for hepatocellular carcinoma[4]

Poor accumulation (<50%) of lipiodol in intrahepatic lesions as assessed by CT immediately (at least 1 month) after two consecutive cycles of TACE
New multiple intrahepatic lesions detected by CT immediately (minimum 1 month) after two successive cycles of TACE
Appearance of vascular invasion
Appearance of extrahepatic metastasis
A continuous increase of tumour marker level only with an initial decrease immediately after a cycle of TACE

CT = computed tomography; TACE = transarterial chemoembolization.

Table II. Conference attendee responses regarding TACE for the treatment of HCC

Question		No. of respondents	How attendees responded
QA4	How long do you wait to administer a cycle of TACE after the previous cycle?	318	1 month: 6% 3 months: 59% 6 months: 31% 9 months: 4% 12 months: 1%
QA5	How many cycles of TACE on average do you administer to a single HCC patient?	320	1–2 cycles: 2% 3–4 cycles: 53% 5–7 cycles: 43% ≥8 cycles: 3%
QA6	How do you treat HCC that has recurred at progressively decreasing intervals on TACE and seems to be unresponsive to TACE?	318	TACE repeated at shorter intervals: 8% TACE with another cytotoxic drug: 27% HAIC: 33% Sorafenib: 29% Systemic chemotherapy: 2% Others: 1%
QA7	Do you think that unresponsiveness to TACE should be defined?	328	Yes: 93% No: 7%
QA8	Do you think that the proposed definition of unresponsiveness to TACE is appropriate?	320	Appropriate: 60% Partly inappropriate: 39% Inappropriate: 1%
QA9a	Do you switch TACE to another treatment when judging the disease as unresponsive to TACE?	315	Yes: 98% No: 2%
QA9b	Which treatment do you choose for HCC unresponsive to TACE?	317	Sorafenib: 56% HAIC: 44% Others: 0%
QA10	Which treatment do you choose for HCC unsuitable for TACE?	322	Systemic chemotherapy – oral: 5% Systemic chemotherapy – intravenous: 3% Sorafenib: 79% BSC: 2% Others: 11%

BSC = best supportive care; **HAIC** = hepatic arterial infusion chemotherapy; **HCC** = hepatocellular carcinoma; **TACE** = transarterial chemoembolization.

similar patients receiving surgical resection or radiofrequency ablation[13] as their initial treatment. Forty patients died, including 34 (85%) from HCC, one (2.5%) from hepatic failure and five (12.5%) from an unrelated condition. Thirteen patients (14%) had extrahepatic metastasis in bone (n = 10) or lung (n = 3). The calculated cumulative probability of progression from Child–Pugh class A to class B was 18.6% at 1 year, 63.0% at 3 years and 88.1% at 5 years. TACE repeated at intervals of 3 months or less was significantly associated with a risk of progression to Child–Pugh class B (p = 0.023) and shorter survival after TACE (p = 0.016).

When conference delegates were questioned regarding their use of TACE for patients with HCC, the majority reported that they would ad-

minister between three and seven cycles of TACE with an interval of 3–6 months between cycles (table II QA4–5). For patients unresponsive to TACE, almost one-third of attendees said that they would continue to use TACE, either at shorter intervals or with a different cytotoxic drug (table II QA6).

These results show that, historically, TACE has been used repeatedly to treat HCC, even if it was unresponsive, as no other effective treatments were available. Now that sorafenib provides an alternative treatment option for patients with advanced HCC, it is imperative to define 'unresponsiveness to TACE' in order to permit timely switching of TACE to other treatments. Notably, 93% of conference delegates agreed that unresponsiveness to TACE should be defined, but

only 60% felt that the definition of 'unresponsiveness to TACE' proposed in the JSH clinical practice guidelines for HCC[4] was appropriate (table II QA7–8); the proposed definition of 'unresponsiveness to TACE' must be validated.

5. Treatment of Hepatocellular Carcinoma Unresponsive to or Unsuitable for Transarterial Chemoembolization

At least two cycles of TACE should be administered to patients with HCC before determining whether HCC is unresponsive to TACE for the following reasons: it is uncertain whether the lipiodol/embolizing agent enters and sufficiently embolizes the target vessel; any collateral circulation cannot be found before TACE;[14,15] and HCC unresponsive to TACE with one drug may respond to TACE with another drug.[16,17]

An early study, which reported response to serial cycles of TACE in 142 patients with HCC, showed that the complete response rate was significantly higher after more than three cycles of TACE compared with only one cycle (28% vs 12%; p < 0.001)[15] supporting that one cycle of TACE

is insufficient to determine whether HCC is unresponsive to TACE.

Dr K. Ikeda presented the following case studies of long-term HCC survivors who received repeated cycles of TACE:

- An 84-year-old man with liver cirrhosis and HCC concurrent with bladder cancer had received approximately two cycles of TACE per year since 1996. He was diagnosed with progressive disease during 1998 and died in 1999 (figure 2a). If an assessment of 'unresponsive to TACE' had been made at the time of diagnosis of progressive disease alternative treatments could have been considered. This case study suggests that although the decision to switch from TACE to another treatment should not be made before administering at least two cycles, this decision should not be left too late.
- A 61-year-old woman with liver cirrhosis and HCC had ascites and was in Child–Pugh class B. Her HCC was controlled by four cycles of TACE performed from 1998 to 1999 but began to grow rapidly in 2000 (figure 2b). The patient died without responding to the fifth cycle of TACE given over 6 months after the fourth.

Appearance of resistance to therapy during repeated TACE therapy
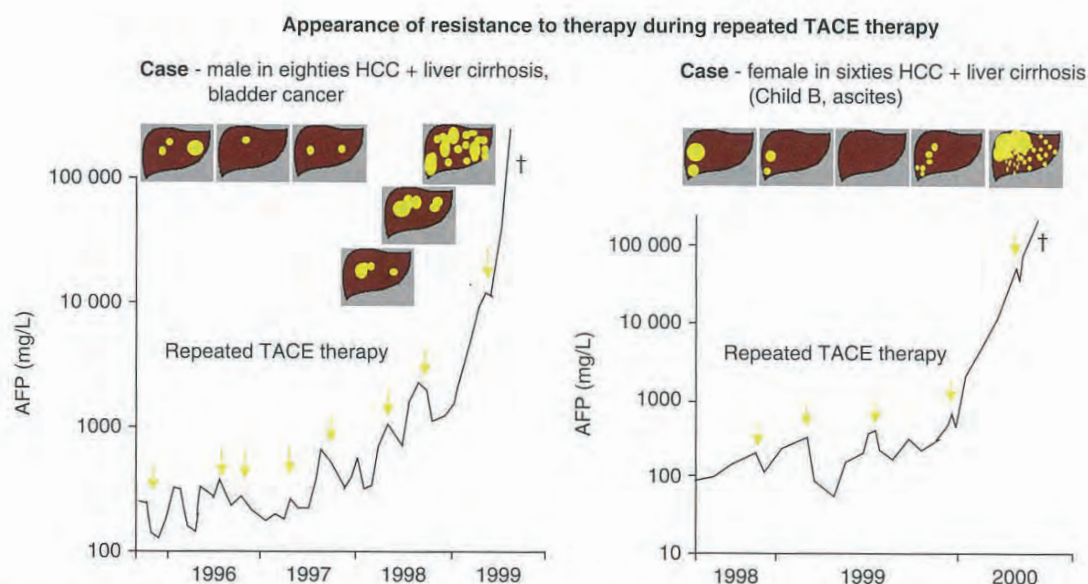
Fig. 2. Two case studies that represent long-term hepatocellular carcinoma (HCC) survivors who received repeated cycles of transarterial chemoembolization (TACE): (**a**) An 82-year-old man with liver cirrhosis and HCC concurrent with bladder cancer received approximately two cycles of TACE per year since 1996, his disease worsened during 1998 and he died in 1999. (**b**) A 61-year-old woman with liver cirrhosis and HCC with ascites and in Child–Pugh class B had her HCC controlled by four cycles of TACE performed from 1998 to 1999, but which began to grow rapidly in 2000 resulting in death. **AFP** = alpha fetoprotein. † Patient died.

The current provisional definition of 'unresponsiveness to TACE' suggests that the initial assessment of tumour response to each cycle of TACE may be performed 'a minimum of 1 month' after treatment. This case study illustrates that if response to TACE is assessed at 3–6 months after treatment, it may be too late for further treatment options.

Dr K. Ikeda concluded that it was appropriate that the current provisional definition of 'unresponsiveness to TACE' in the JSH clinical practice guidelines for HCC[4] requires 'two successive cycles of TACE' for observing 'poor lipiodol accumulation' and the 'appearance of a new lesion' and stated that as TACE is curative, we should try to repeat TACE for as long as possible.

The majority (98%) of conference attendees said that when judging HCC as unresponsive to TACE they would switch to another treatment, with 56% stating that they would choose sorafenib and 44% HAIC as the alternative treatment (table II QA9a–b).

In the SHARP trial, the subgroup of patients who had previously undergone TACE represents patients with HCC unresponsive to TACE. In these patients, the median time to progression (TTP) was significantly longer for the sorafenib arm (n = 86) than the placebo arm (n = 90) (HR = 0.57; 5.8 months vs 4.0 months), although the median survival time was similar between treatment groups (HR 0.75; 11.9 months vs 9.9 months).[18] The results of this subgroup analysis suggest that sorafenib may be effective for HCC unresponsive to TACE.

Dr Kudo presented two case studies of patients with HCC unresponsive to TACE who had received sorafenib for over 1 year, depicting the effectiveness of sorafenib for HCC unresponsive to TACE:

• A 79-year-old woman with stage III non-B, non-C type HCC in Child–Pugh class A had a large lesion that was unresponsive to TACE. In June 2009, sorafenib was started at 800 mg/day and then downtitrated to 400 mg/day. As of May 2010, the patient was still receiving sorafenib and was in good condition (Eastern Cooperative Oncology Group performance score was 0)

without experiencing any adverse reactions. The HCC was assessed as SD (Figure 3a).

• In June 2009, sorafenib was started at 800 mg/day in an 81-year-old man with stage III non-B, non-C type HCC judged unresponsive to TACE because of poor accumulation of lipiodol. In July 2009, dizziness occurred and some doses were omitted. Subsequently, sorafenib was restarted at the same dose. As of 10 May 2010, the patient was still receiving sorafenib and was assessed as having a performance score of 0 and SD (figure 3b).

Sorafenib may also be used in combination with TACE and several clinical studies assessing the efficacy and safety of this combination are ongoing. The SPACE study (ClinicalTrials.gov identifier NCT00855218) is a randomized, placebo controlled, phase II study investigating TACE with doxorubicin-loaded DC beads (currently unavailable in Japan), with or without sorafenib 400 mg twice a day, in patients (n = 300) with intermediate-stage (unresectable) HCC at 95 to 100 centres in the USA, Europe and Asia. The primary endpoint is progression-free survival. Secondary endpoints include OS, time to untreatable progression, vascular invasion, time to extrahepatic metastasis, patient's reported treatment outcome, biomarkers and safety. That study commenced in March 2009 and is scheduled for completion by March 2012.

The randomized, controlled, phase II JLOG0903 study (Transcatheter Arterial Chemoembolization Therapy in Combination with Sorafenib [TACTICS] trial, NCT01217034) is currently in progress at approximately 40 Japanese institutions. Eligibility criteria include unresectable HCC, Child–Pugh class A, one of fewer previous TACE cycles, tumour size 10 cm or less and 10 or fewer nodules. Exclusion criteria include vascular invasion and distant metastasis. The primary endpoint of the study is time to untreatable progression. Secondary endpoints include TTP, OS, objective response rate, tumour markers and safety. Among 228 subjects planned for enrolment, those allocated to the sorafenib group will receive alternating cycles of TACE and sorafenib (400 mg/day increasing to 400 mg twice a day) until progression. Study completion is expected in approximately September 2016.
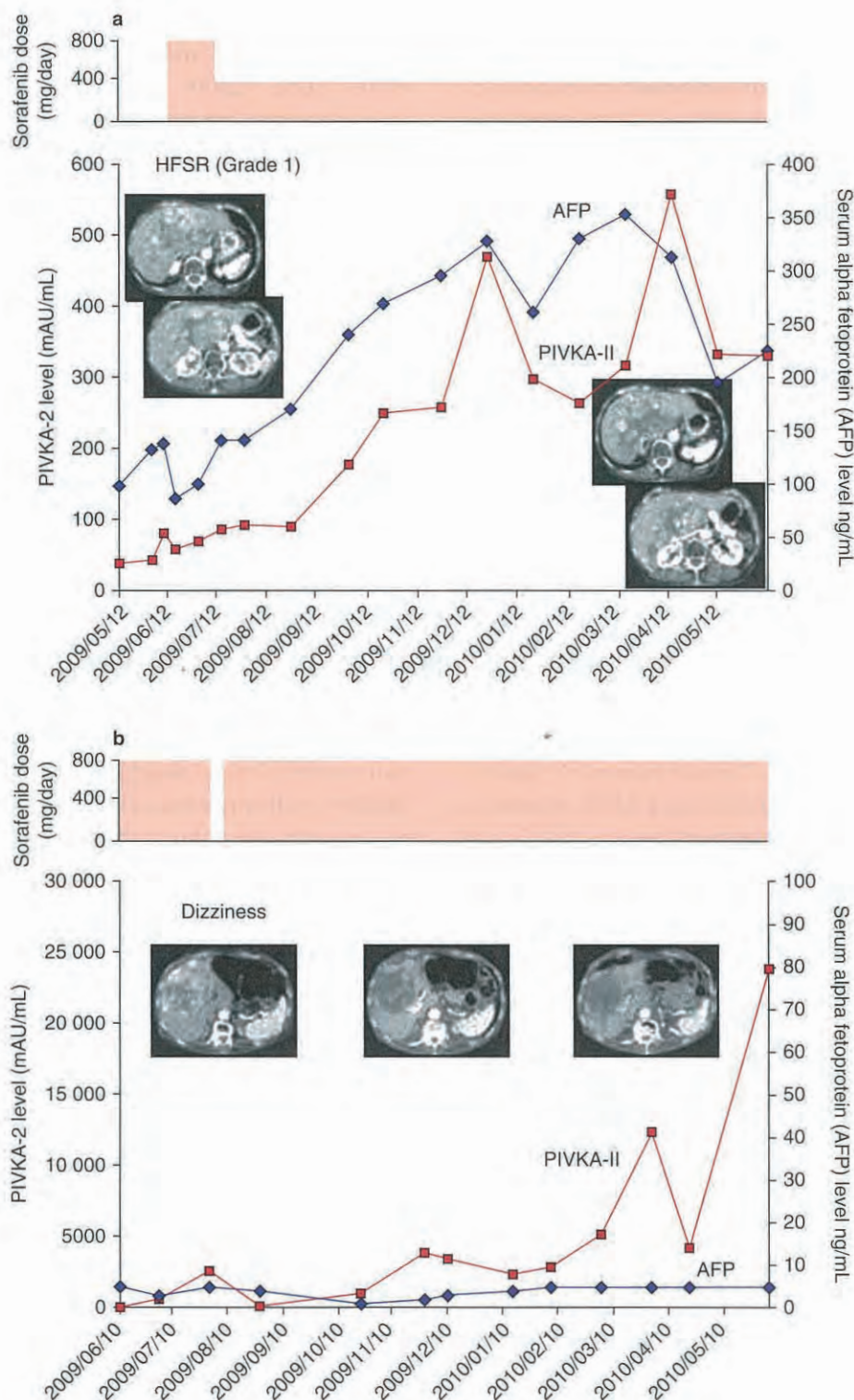
Fig. 3. Two case studies of patients with hepatocellular carcinoma (HCC) unresponsive to transarterial chemoembolization (TACE) who have received sorafenib for more than 1 year showing the effectiveness of sorafenib in this setting. (**a**) A 79-year-old woman with stage III non-B, non-C type (NBNC) HCC in Child–Pugh class A with a large lesion that was unresponsive to TACE. (**b**) An 81-year-old man, stage III NBNC HCC judged as unresponsive to TACE because of poor accumulation of lipiodol. **AFP** = alpha fetoprotein; **HFSR** = hand–foot skin reaction; **PIVKA-II** = protein induced by vitamin K absence II.

In summary, treatment strategies for HCC unresponsive to TACE are as follows:

- Before worsening of hepatic functional reserve, sorafenib is a treatment option for HCC unresponsive to TACE, which responds poorly to HAIC.
- Conventional treatments combined with sorafenib and other molecular targeted agents (e.g. the tyrosine kinase inhibitor of the epidermal growth factor receptor, erlotinib, a multitargeted tyrosine kinase inhibitor, sunitinib, and the humanized monoclonal antibody against the antivascular epidermal growth factor, bevacizumab) may also become treatment options in the future. Such combinations are still under investigation and will not come into use until their efficacy/safety have been confirmed in clinical trials.
- The proposed definition of 'unresponsiveness to TACE' needs further review and validation for practical use.

HCC that is unsuitable for TACE is also defined in the JSH clinical practice guidelines for HCC,[4] as described above. When delegates were questioned on which treatment option they would choose for HCC unsuitable for TACE, 79% said they would use sorafenib (table II QA10).

6. Treatment of Hepatocellular Carcinoma with Hepatic Arterial Infusion Chemotherapy and Sorafenib

HAIC is effective in terms of tumour response and survival for the management of HCC newly diagnosed with vascular invasion, but is much less effective against advanced HCC that has become unresponsive to TACE after repeated cycles.[19] Such cases may respond to sorafenib followed sequentially by HAIC.

As discussed in article 2 in this supplement, previous treatment with sorafenib followed sequentially by HAIC may be better than concurrent treatment with HAIC and sorafenib. It is thought that sorafenib enhances the cytotoxic effect of HAIC by inhibiting tumour vascularisation, or by normalizing anatomical vascular architecture; however, the benefit of previous treatment with sorafenib needs to be confirmed in a large clinical trial.

6.1 Differential Use of Hepatic Arterial Infusion Chemotherapy and Sorafenib

Combining sorafenib with HAIC appears promising but has not yet been approved. At present, the choice between using sorafenib or HAIC is a 'trial and error' approach because been no biomarkers have been identified that can predict response to either treatment. As response to HAIC differs among patients, a reasonable approach is to use HAIC initially and to assess response after approximately 4–6 weeks. If successful, HAIC may be continued; however, if there is no response, treatment may be switched to sorafenib.

When conference attendees were asked how they would treat HCC newly diagnosed with vascular invasion, the majority chose HAIC with (43%) or without (16%) an implanted reservoir (table III QA14). Notably, when asked how they would treat HCC with vascular invasion that had failed to respond to HAIC, 85% of respondents chose sorafenib (table III QA15).

When asked whether they would consider using sorafenib before HAIC to treat HCC newly diagnosed with portal invasion in a Child–Pugh class A patient, more hepatologists than expected chose to consider using sorafenib before HAIC (68%) (table III QA16). Interestingly, 84% of respondents said they would consider using the combination of HAIC with sorafenib, even though it has not yet been approved (table III QA17).

Dr Kudo concluded that Japanese hepatologists often use HAIC to manage HCC with vascular invasion, and many want to try it in combination with sorafenib. However, sorafenib cannot be used in combination with any cytotoxic drug at present, because the efficacy and safety of such a combination has not been established, as stated in the prescribing information.[20] In addition, as HAIC is used only in Japan, an international study cannot be expected to provide evidence for the combination of HAIC with sorafenib. Therefore, a well-designed prospective study should be conducted in Japan in order to establish the efficacy and safety of this combination, as described below.

Table III. Conference attendee responses regarding the use of HAIC for the treatment of HCC

Question		No. of respondents	How attendees responded
QA14	How will you treat HCC newly diagnosed with vascular invasion?	293	Surgical resection: 18% TACE: 6% HAIC without an indwelling catheter: 16% HAIC with an implanted reservoir: 43% Sorafenib: 13% Oral fluoropyrimidine (5FU, UFT or TS-1): 0% Interferon plus fluoropyrimidine (5FU, UFT or TS-1): 0% Intravenous chemotherapy: 0%; Others: 4%
QA15	How will you treat HCC with vascular invasion failing to respond to HAIC?	309	Sorafenib: 85% Surgical resection: 6% TACE: 1% HAIC without an indwelling catheter: 0% HAIC with an implanted reservoir: 2% Oral fluoropyrimidine (5FU, UFT or TS-1): 0% Interferon plus fluoropyrimidine (5FU, UFT or TS-1): 2% Intravenous chemotherapy: 0%; Others: 3%
QA16	Do you consider using sorafenib before HAIC to treat HCC newly diagnosed with portal invasion in a Child–Pugh class A patient?	310	Yes: 68% No: 32%
QA17	Do you want to consider combination use of HAIC with sorafenib, which has not been approved yet?	309	Yes: 84% No: 16%

5FU = 5-fluorouracil; HAIC = hepatic arterial infusion chemotherapy; HCC = hepatocellular carcinoma; TACE = transarterial chemoembolization; UFT = uracil-tegafur.

6.2 Ongoing Trials to Assess the Combination of Hepatic Arterial Infusion Chemotherapy and Sorafenib in Japan

Although there is widespread belief in Japan that HAIC is extremely effective for HCC with vascular invasion, there is no evidence to support this. Therefore, robust evidence for its efficacy must be derived from a domestic study. As current international guidelines recommend sorafenib as a first-line option for HCC with vascular invasion, a series of clinical trials have been established to evaluate the potential benefit of combining HAIC with sorafenib with the primary objective being to establish the efficacy of sorafenib plus HAIC with cisplatin in comparison with sorafenib alone. A small (n = 21) phase I study (UMIN Clinical Trials Registry identifier UMIN000001496), which has completed recruitment, will determine the recommended dosage regimen for sorafenib plus HAIC with cisplatin. After this study, randomized phase II and III studies will be conducted to evaluate the efficacy/safety and clinical benefit of this combination, compared with sorafenib alone.

The phase Ib/II Sorafenib in Combination with Low-dose FP Intra-arterial Infusion Chemotherapy (SILIUS) trial (JLOG0901; NCT00933816), which was completed in October 2010, assessed the combination of sorafenib and HAIC with low doses of 5-fluorouracil and cisplatin (FP). HAIC with low-dose FP is administered via an implanted reservoir. That study included patients with advanced HCC and assessed dose-limiting toxicities (phase Ib) and TTP (phase II) as primary outcome measures. The phase Ib part of the study was completed in August 2010.[21] As the TTP with sorafenib plus HAIC with low-dose FP was found to be much better than with low-dose FP alone, the data monitoring committee recommended progressing directly to a phase III study. The ongoing phase III SILIUS randomized controlled study, being conducted at 25 Japanese centres, is comparing sorafenib plus low-dose FP with sorafenib alone (ClinicalTrials.gov identifier NCT01214343; UMIN Clinical Trials Registry identifier UMIN000004315). The study has a planned completion date of September 2013. If this study successfully shows the superiority of sorafenib combined with low-

dose FP over sorafenib alone, the combination may be presented as a novel treatment option for HCC with vascular invasion.

The treatment of HCC with vascular invasion can be summarized as follows:

- For the management of HCC newly diagnosed with vascular invasion in Child–Pugh class A patients: HAIC may be used first, and if this fails, switch to sorafenib; previous treatment with sorafenib followed by HAIC may be a reasonable option depending on the patient's clinical profile.
- For the management of HCC with vascular invasion or with multifocal disease that has become unresponsive to TACE, sorafenib may be used first.

7. Optimum Dose of Sorafenib

The current recommended dose of sorafenib is 800 mg/day,[20] although excellent responses to 400 mg/day have recently been reported.[22] Some studies have suggested better efficacy and tolerability of sorafenib 400 mg/day in Japanese patients, while others have reported that 800 mg/day is well tolerated and maintains high dose intensity for prolonged periods.[22]

When asked what starting dose they would prescribe, 48% of attendees replied that they would initially prescribe sorafenib at 800 mg/day; however, the majority (80%) of attendees who would

start sorafenib at doses lower than 800 mg/day would uptitrate to 800 mg/day if tolerated (table IV QA18–QA19). Concern regarding unmanageable, potentially serious adverse reactions was the most frequent reason for using lower doses (table IV QA20).

Sorafenib is a first-line option for the treatment of patients with advanced HCC and extrahepatic metastasis in Child–Pugh liver function class A. As sorafenib has caused hepatic encephalopathy and hand–foot skin reaction more frequently in Japanese HCC patients,[23] Japanese hepatologists not experienced in using sorafenib may become concerned about its potential adverse effects at 800 mg/day. For some patient populations (e.g. elderly patients, those with low body weight or significant comorbidities), it may be prudent to start sorafenib at lower doses; however, as the drug has been shown to be effective at 800 mg/day (400 mg twice a day), if well tolerated, its dose should be uptitrated to 800 mg/day after several weeks.

8. Future Prospects

8.1 Sorafenib as Neoadjuvant or Adjuvant Chemotherapy

A promising strategy is neoadjuvant treatment with sorafenib followed by hepatic resection in

Table IV. Conference attendee responses regarding the optimum dose of sorafenib for the treatment of HCC

Question		No. of respondents	How attendees responded
QA18	At which dose do you currently start sorafenib?	300	800 mg/day: 48% 600 mg/day: 1% 400 mg/day: 33% 200 mg/day: 2% Individualized: 16%.
QA19	To those who start sorafenib at any other dose than 800 mg/day: how do you modify the dose after starting sorafenib?	175	Not modified: 20% Uptitrated to 800 mg/day if tolerated: 80%
QA20	To those who start sorafenib at any other dose than 800 mg/day: why do you start sorafenib at doses other than 800 m/day?	180	Adequate efficacy even at a reduced dose in Japanese patients, unlike in US/European patients: 6% Concern about unmanageable potentially serious adverse reactions at 800 mg/day: 61% Efficacy even at a reduced dose after sustained treatment: 14% Better compliance to treatment at a lower dose: 19%

HCC = hepatocellular carcinoma.

patients with advanced but resectable HCC or HCC with extrahepatic metastasis; however, well-designed clinical trials are needed to establish the benefit of sorafenib in this setting. Sorafenib may also be effective against HCC following non-curative resection (including HCC with extra-hepatic metastasis).

The benefit of sorafenib administered before or after hepatic transplantation is controversial. Although there has been a case report of successful downstaging of HCC by sorafenib administered before transplantation,[24] sorafenib is unlikely to cause downstaging in such cases because most responses to the drug reported to date are only SD. Furthermore, patients in Child–Pugh class B or C are not suitable for sorafenib therapy. Therefore, it is questionable whether sorafenib is effective for HCC patients with reduced liver function who are candidates for transplantation.

Sorafenib may be considered as neoadjuvant or adjuvant therapy to reduce the risk of recurrence after transplantation. Concerns regarding the use of sorafenib in this setting include sorafenib-induced hepatic damage and graft rejection, as well as interactions between sorafenib and immuno-suppressants.[25] After liver transplantation, HCC recurs at a rate of approximately 10%, and it is widely accepted that recurrent HCC after liver transplantation is incurable. There have been several reports of an excellent response to sorafenib in patients with recurrent HCC following liver transplantation.[25-27]

8.1.1 Sorafenib as Adjuvant Treatment in the Prevention of Recurrence of Hepatocellular Carcinoma Trial

The Sorafenib as Adjuvant Treatment in the Prevention of Recurrence of Hepatocellular Carcinoma (STORM) trial (NCT00692770) is designed to evaluate the benefit of sorafenib as postoperative adjuvant therapy. This phase III study has recruited 1065 intermediate to high-risk patients following hepatic resection, radiofrequency ablation, or percutaneous ethanol injection therapy, who will be allocated to receive oral treatment with sorafenib (400 mg twice a day) or placebo for up to 4 years. The primary endpoint is recurrence-free survival; secondary endpoints include

time to recurrence and OS. The estimated study completion date is October 2014.

9. Conclusions

Sorafenib is recommended as a first-line option for patients with HCC with extrahepatic metastasis in both international and Japanese guidelines. Its use should be restricted to patients in Child–Pugh class A. Sorafenib is also a first-line option for HCC unresponsive to TACE in Child–Pugh class A patients, because HCC unresponsive to TACE responds poorly to HAIC, and is also indicated for the treatment of HCC with four or more nodules or vascular invasion.

It is important to minimize the risk of treatment discontinuation with sorafenib due to adverse reactions. To avoid serious adverse events, dose reductions or interruptions may be useful. If HCC is judged as unresponsive to TACE, treatment should be switched to sorafenib in a timely manner. Sorafenib should not be used as adjuvant therapy or in combination with TACE or HAIC until evidence from clinical trials shows it is beneficial in these settings.

The SHARP trial demonstrated an increase in the median OS for patients with unresectable HCC treated with sorafenib compared with placebo. Clinical studies are currently planned or ongoing to evaluate the benefit of sorafenib as an adjunct to HAIC, TACE, or curative therapies. It is hoped that the combination of sorafenib with conventional therapies will prolong the survival of HCC patients. Planned and ongoing clinical studies will answer the question of whether sorafenib has survival benefit for patients with HCC at any stage.

Acknowledgements

References

1. Bayer Healthcare Pharmaceuticals. Nexavar approved in Japan for the treatment of advanced liver cancer. 2009 [cited; Available from: http://press.bayerhealthcare.com/en/press/auth/news-details-page.php/13182/2009-0239

2. Omata M, Lesmana LA, Tateishi R, et al. Asian Pacific Association for the Study of the Liver consensus recommendations on hepatocellular carcinoma. Hepatology International 2010; 4 (2): 439-74

3. The Japan Society of Hepatology. The Japanese HCC Clinical Practice Guideline. Treatment algorithm for hepatocellular carcinoma. Hepatology Research 2010; 40 (Suppl. 1): 8-9

4. Kudo M, Izumi N, Kokudo N, et al. Management of hepatocellular carcinoma in Japan: Consensus-Based Clinical Practice Guidelines proposed by the Japan Society of Hepatology (JSH) 2010 updated version. Dig Dis 2011; 29 (3): 339-64

5. Bruix J, Sherman M. AASLD Practice Guideline: Management of Hepatocellular Carcinoma: An Update. Available at http://www.aasld.org/practiceguidelines/Documents/Bookmarked%20Practice%20Guidelines/HCCUpdate2010.pdf (Accessed 14 Nov 2010). Hepatology 2010; July: 1-35

6. Llovet JM, Burroughs A, Bruix J. Hepatocellular carcinoma. Lancet 2003; 362 (9399): 1907-17

7. Llovet JM, Ricci S, Mazzaferro V, et al. Sorafenib in advanced hepatocellular carcinoma. N Engl J Med 2008; 359 (4): 378-90

8. Sherman M, Mazzaferro V, Amadori D, et al. Efficacy and safety of sorafenib in patients with advanced hepatocellular carcinoma and vascular invasion or extrahepatic spread: A subanalysis from the SHARP trial. J Clin Oncol 2008; 26 (May 20 suppl): abstract 4584

9. Kudo M, Ueshima K. Positioning of a molecular-targeted agent, sorafenib, in the treatment algorithm for hepatocellular carcinoma and implication of many complete remission cases in Japan. Oncology 2010 Jul; 78 (Suppl. 1): 154-66

10. Furuse J, Okusaka T, Kaneko S, et al. Phase I/II study of the pharmacokinetics, safety and efficacy of S-1 in patients with advanced hepatocellular carcinoma. Cancer Sci 2010; 101 (12): 2606-11

11. Llovet JM, Bruix J. Molecular targeted therapies in hepatocellular carcinoma. Hepatology 2008 Oct; 48 (4): 1312-27

12. Arii S, Yamaoka Y, Futagawa S, et al. Results of surgical and nonsurgical treatment for small-sized hepatocellular carcinomas: a retrospective and nationwide survey in Japan. The Liver Cancer Study Group of Japan. Hepatology 2000; 32 (6): 1224-9

13. Shiina S, Teratani T, Obi S, et al. A randomized controlled trial of radiofrequency ablation with ethanol injection for small hepatocellular carcinoma. Gastroenterology 2005; 129 (1): 122-30

14. Charnsangavej C, Chuang VP, Wallace S, et al. Angiographic classification of hepatic arterial collaterals. Radiology 1982; 144 (3): 485-94

15. Ikeda K, Kumada H, Saitoh S, et al. Effect of repeated transcatheter arterial embolization on the survival time in patients with hepatocellular carcinoma. An analysis by the Cox proportional hazard model. Cancer 1991; 68 (10): 2150-4

16. Kawamura Y, Ikeda K, Hirakawa M, et al. Efficacy of platinum analogue for advanced hepatocellular carcinoma unresponsive to transcatheter arterial chemoembolization with epirubicin. Hepatol Res 2009; 39 (4): 346-54

17. Maeda N, Osuga K, Higashihara H, et al. Transarterial chemoembolization with cisplatin as second-line treatment for hepatocellular carcinoma unresponsive to chemoembolization with epirubicin-lipiodol emulsion. Cardiovasc Intervent Radiol 2011 Feb; 35 (1): E82-9

18. Galle P, Blanc J, Van Laethem J-L, et al. Efficacy and safety of sorafenib in patients with hepatocellular carcinoma and prior anti-tumor therapy: a subanalysis from the SHARP trial. 43rd annual meeting of the European Association for the Study of the Liver (EASL 2008) Milan, Italy April 23-27, 2008 2008 [cited; Available from: http://www.ncbi.nlm.nih.gov/entrez/query.fcgi?cmd=Retrieve&db=PubMed&dopt=Citation&list_uids=18817997

19. Iwasa S, Ikeda M, Okusaka T, et al. Transcatheter arterial infusion chemotherapy with a fine-powder formulation of cisplatin for advanced hepatocellular carcinoma refractory to transcatheter arterial chemoembolization. Jpn J Clin Oncol 2011 Jun; 41 (6): 770-5

20. Bayer HealthCare Pharmaceuticals Inc. Sorafenib. Prescribing information. Available at http://www.nexavar.com/html/download/Nexavar_PI.pdf Accessed 2 December 2010. 2009:

21. Ueshima K, Kudo M, Tanaka M, et al. Session 11-05, Phase I study of sorafenib in combination with low-dose cisplatin and fluorouracil intra-arterail infusion chemotherapy. Osaka, Japan: The 2nd Asia-Pacific Primary Liver Cancer Expert Meeting-A Bridge to Consensus on HCC Management, 2011

22. Kudo M. Molecular Targeted Therapy of Hepatocellular Carcinoma. Tokyo: Arc Media, 2010

23. Kudo. M, Imanaka K, Chida N, et al. Phase III study of sorafenib after transarterial chemoembolisation in Japanese and Korean patients with unresectable hepatocellular carcinoma. Eur J Cancer 2011; (14): 2117-27

24. Vagefi PA, Hirose R. Downstaging of hepatocellular carcinoma prior to liver transplant: is there a role for adjuvant sorafenib in locoregional therapy? J Gastrointest Cancer 2010; 41 (4): 217-20

25. Saab S, McTigue M, Finn RS, et al. Sorafenib as adjuvant therapy for high-risk hepatocellular carcinoma in liver transplant recipients: feasibility and efficacy. Exp Clin Transplant 2010; 8 (4): 307-13

26. Yeganeh M, Finn RS, Saab S. Apparent remission of a solitary metastatic pulmonary lesion in a liver transplant recipient treated with sorafenib. Am J Transplant 2009; 9 (12): 2851-4

27. Bhoori S, Toffanin S, Sposito C, et al. Personalized molecular targeted therapy in advanced, recurrent hepatocellular carcinoma after liver transplantation: a proof of principle. J Hepatol 2010; 52 (5): 771-5

Correspondence: Dr *Masatoshi Kudo*, Department of Gastroenterology and Hepatology, Kinki University School of Medicine, 377-2, Ohno-Higashi, Osaka-Sayama, Osaka, 589-8511.

E-mail: m-kudo@med.kindai.ac.jp

Closing Remarks

Masatoshi Kudo

Department of Gastroenterology and Hepatology, Kinki University School of Medicine, Osaka-Sayama, Japan

In Japan, traditional treatment strategies for hepatocellular carcinoma (HCC), such as trans-arterial chemoembolization (TACE) and hepatic arterial infusion chemotherapy (HAIC), are common in clinical practice. However, these therapies have their limitations: TACE can cause damage to the surrounding liver and HAIC can be associated with systemic adverse events in addition to regional adverse events, including cholecystitis, ulcer, pancreatitis and liver failure in patients with advanced cirrhosis. Furthermore, less than 50% of patients who receive HAIC will experience a reduction in tumour size.

The management of HCC has greatly changed since the approval of sorafenib (Nexavar®), a multi-targeted oral kinase inhibitor, which was approved by the Japanese Ministry of Health, Labour and Welfare for the treatment of patients with non-resectable HCC in May 2009. Sorafenib is the first approved systemic treatment for HCC, and has been shown to prolong the lives of patients with this disease effectively. To achieve the best results with sorafenib, it is recommended that it be used at an early stage in patients who are unresponsive to or who do not qualify for conventional treatment. Sorafenib should be continued for a long period with good management (including monitoring and prevention strategies) of adverse events.

The position of sorafenib as an antineoplastic agent for HCC in Japan is currently being established. At present, data on the use of sorafenib in Japanese patients are limited and there is little information as to what patient population would benefit the most from sorafenib treatment. The use of sorafenib with traditionally used treatments is promising. The multitargeted action of sorafenib in combination with TACE is a plausible strategy for the treatment of HCC as sorafenib has the ability to target Braf, vascular endothelial growth factor receptors and platelet-derived growth factor receptors in turn inhibiting cell proliferation, angiogenesis and/or inducing apoptosis. Many clinical trials of sorafenib in combination with TACE are planned or are ongoing.

Further clinical investigation of sorafenib in Japan is warranted. In particular, analysis of the accumulating clinical experience will be able to determine the details of how sorafenib should be used in the Japanese patient population.

Acknowledgement and Disclosures

INTERNAL MEDICINE

Well-differentiated Hepatocellular Carcinoma Detected as Hypovascularity by Only CT during Hepatic Arteriography

Jun Saito[1], Soo Ryang Kim[1], Masatoshi Kudo[2], Susumu Imoto[1], Kenji Ando[1], Taisuke Nakajima[1], Katsumi Fukuda[1], Yumi Otono[1], Soo Ki Kim[3], Takamitsu Komaki[4], Hirohisa Yano[5], Osamu Nakashima[5], Kayo Sugimoto[6] and Toshiyuki Matsuoka[7]

Abstract

We describe a well-differentiated hepatocellular carcinoma (HCC) with alcohol-related liver cirrhosis in a 69-year-old man. Ultrasonography (US) disclosed a 10 mm hypoechoic nodule in segment 4; Sonazoid contrast-enhanced US and gadolinium-ethoxybenzyl-diethylenetriamine pentaacetic acid (Gd-EOB-DTPA)-enhanced magnetic resonance imaging (MRI) revealed no defect in either the Kupffer phase or the hepatobiliary phase. Computed tomography during hepatic arteriography (CTHA), however, revealed a hypovascular nodule, but CT during arterial portography showed no perfusion defect. Histological analysis indicated a well-differentiated HCC. Thus, our detection of well-differentiated HCC disclosed by only CTHA attested to the efficiency of this modality, suggesting that it is more sensitive than Gd-EOB-GTPA-enhanced MRI.

Key words: well-differentiated hepatocellular carcinoma, imaging studies, Gd-EOB-DTPA-enhanced MRI, CT during hepatic arteriography, hypovascular tumor, Sonazoid contrast-enhanced US

Introduction

The definitive diagnosis of nodular lesions detected by imaging techniques in the cirrhotic liver remains a critical challenge for clinicians. The issue is particularly complicated for small (1-2 cm) nodules, many of which may be preneoplastic with uncertain malignant potential (1), such as macroregenerative nodules, low-grade dysplastic nodules (LGDN), high-grade dysplastic nodules (HGDN), or more rarely, hemangiomas that are found in up to 42% of explanted livers (2-4).

Recently, clinicians have been able to conduct computed tomography (CT) scanning during angiography, CT during hepatic arteriography (CTHA) and CT during arterial portography (CTAP), thereby simultaneously acquiring data on lesions and intranodular blood flow (5, 6). Moreover, development of the newly introduced diagnostic imaging techniques, Sonazoid contrast-enhanced ultrasonography (US) (7) and gadolinium-ethoxybenzyl-diethylenetriamine pentaacetic acid (Gd-EOB-DTPA)-enhanced magnetic resonance imaging (MRI) (8), have provided higher degrees of detectability of small hepatocellular carcinoma (HCC).

Here, we describe a 10 mm well-differentiated HCC appearing as a hypovascular tumor, with alcohol-related liver cirrhosis, disclosed by only CTHA, whereas Sonazoid contrast-enhanced US and Gd-EOB-DTPA-enhanced MRI revealed no defect in either the Kupffer phase or the hepatobiliary phase; also, contrast-enhanced CT revealed no washout in the equilibrium phase.

Case Report

A 69-year-old man with alcohol-related liver cirrhosis was

[1]Department of Gastroenterology, Kobe Asahi Hospital, Japan, [2]Department of Gastroenterology and Hepatology, Kinki University School of Medicine, Japan, [3]Department of Gastroenterology and Hepatology, Kyoto University, Japan, [4]Department of Internal Medicine, Saiseikai-Tondabayashi Hospital, Japan, [5]Department of Pathology, Kurume University School of Medicine, Japan, [6]Department of Pharmacy, Kobe Asahi Hospital, Japan and [7]Department of Radiology, Osaka City University Medical School, Japan
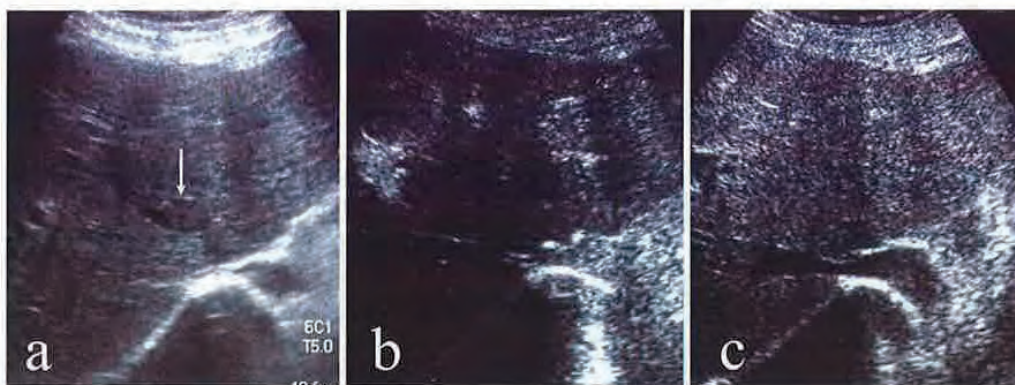
Figure 1. Imaging findings of US. (a) B-mode US reveals a 10 mm hypoechoic nodule in segment 4 (arrow). The hypovascular nodule is not visible in either (b) the early vascular phase (5 sec) or (c) the Kupffer phase (15 min) on Sonazoid contrast-enhanced US. Contrast-enhanced US imaging was performed with Xario SSA-660A, PVT-375BT probe (3.5 MHz) (Toshiba Medical Systems). PS-low; mechanical index: 0.2, frame rate: 15 fps, dynamic range: 45 dB, injection of Sonazoid: 0.0075 mL/ kg

admitted to Kobe Asahi Hospital in July 2010 for further examination of a 10 mm hypoechoic nodule in segment four (S4). His alcohol consumption over 40 years was 360 mL/ day. A physical examination on admission showed no remarkable abnormalities and no evidence of lymph adenopathy or splenomegaly. The serum was negative for hepatitis C virus antibody and hepatitis B surface antigen. Laboratory data disclosed the following values: platelets $10.2 \times 10^4/\mu L$ (normal, 13.1-36.2), total protein 7.0 g/dL (6.7-8.3), γ-glutamyl transpeptidase 281 IU/L (0-30), albumin 4.2 g/dL (4.0-5.0), total bilirubin 0.9 mg/dL (0.3-1.2), prothrombin time 82% without encephalopathy and ascites, classified as Child-Pugh classification A of cirrhosis. Alpha-fetoprotein (AFP), lens culinaris agglutinin A-reactive fraction of alpha fetoprotein (AFP L3) and protein-induced vitamin K absence (PIVKA II) were within normal ranges. A US-guided biopsy disclosed alcohol-related liver cirrhosis with pericellular fibrosis. B-mode US disclosed a 10 mm hypoechoic nodule in S4 (Fig. 1a). Sonazoid contrast-enhanced US revealed no hypervascular nodule in the early vascular phase (Fig. 1b) and no defect in the Kupffer phase (Fig. 1c). Plain CT showed no fatty liver or any nodule in the liver (Fig. 2a); contrast-enhanced CT revealed no enhanced nodule in the arterial phase (Fig. 2b) and no washout in the equilibrium phase (Fig. 2c); Gd-EOB-DTPA-enhanced MRI revealed no enhanced nodule in the arterial phase (Fig. 2d), and no defect in the hepatobiliary phase (Fig. 2e). CTHA, however, revealed a hypovascular nodule (Fig. 3a, b), but CTAP revealed no perfusion defect (Fig. 3c). A US-guided biopsy of the nodule was diagnosed as well-differentiated HCC characterized by more than two-fold the cellularity of the non-tumorous area, clear cell change and mild cell atypia (Fig. 4a, b). Immunohistochemical staining of CD34 in the nodule was positive in the sinusoidal blood space, implying capillarization compatible with well-differentiated

HCC (Fig. 4c, d). The organic anion transporter (OATP) 1B3 (9), being positive in both the nodule and the non-nodular lesion, was compatible with the absence of defect in the hepatobiliary phase as determined by Gd-EOB-DTPA-enhanced MRI (Fig. 5a, b).

Discussion

Confirmation of arterial hypervascularity by three imaging modalities (triphasic CT, triphasic MRI, and contrast-enhanced US), even in the absence of a significant (>400 ng/mL) rise in α-fetoprotein, is recommended by the European Association for the Study of the Liver as diagnostic criteria for HCC nodules larger than 2 cm in patients with cirrhosis (10). This recommendation for the management of HCC provides a rational approach to the problem but leaves some areas of uncertainty, particularly those concerning the interpretation of discordant vascularity, the use of imaging techniques in nodules smaller than 2 cm, the meaning of truly hypovascular nodules, and the management of those diagnosed as LGDN or HGDN at guided biopsy.

To resolve the areas of uncertainty, we previously evaluated the superiority of CT arterioportal angiography for nodules smaller than 2 cm, and concluded that the modality is superior to contrast-enhanced CT and contrast-enhanced MRI (11). Nonetheless, the status of imaging studies in the diagnosis of HCC smaller than 2 cm has changed with the introduction of new contrast agents for US and MRI. First, Sonazoid was exclusively approved in Japan in 2007 as a second-generation US contrast agent; second, Gd-EOB-DTPA, a new liver-specific contrast agent used in MRI, was approved in 2008. Taking these improvements into consideration, we evaluated the effectiveness of four imaging modalities (contrast-enhanced CT, Sonazoid contrast-enhanced US, Gd-EOB-DTPA-enhanced MRI, CT arterioportal angi-
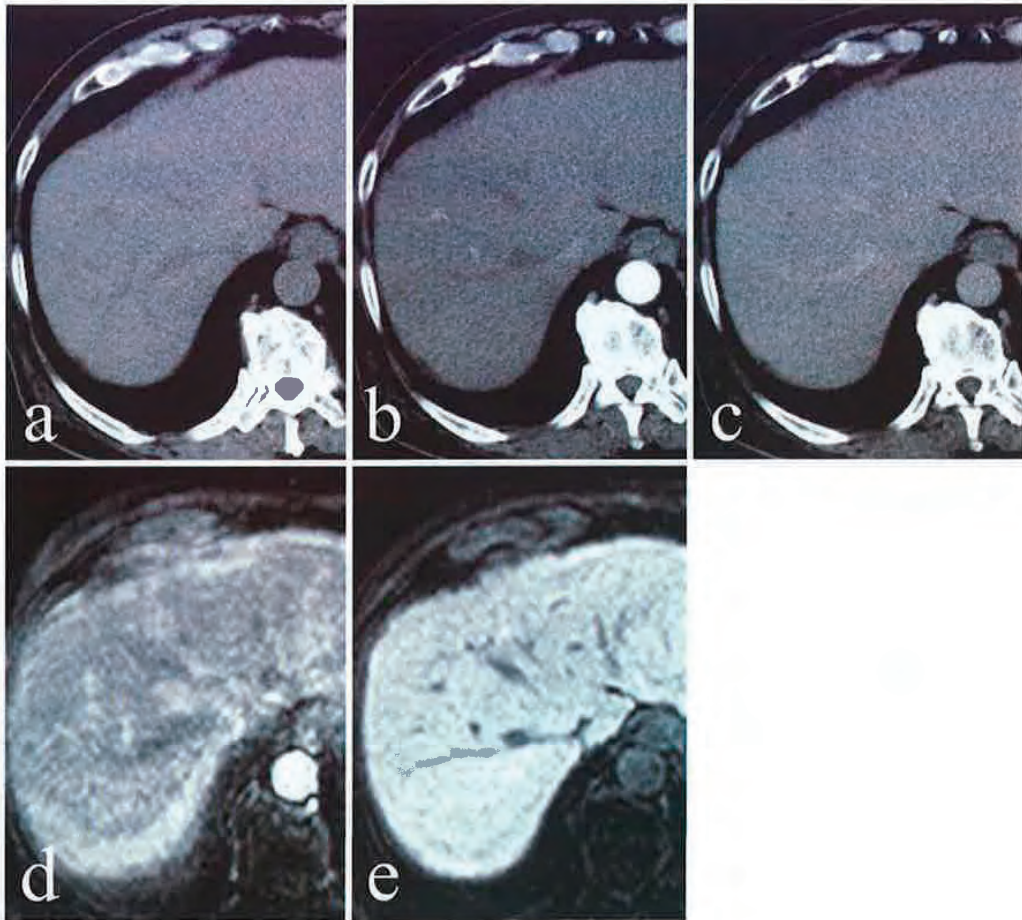
Figure 2. Imaging findings of CT and MRI. (a) Plain CT reveals no fatty liver or any nodule in the liver. (b) Contrast-enhanced CT reveals no enhanced nodule in the arterial phase and (c) no washout in the equilibrium phase. CT imaging was performed with Somatom Emotion 16-Slice configuration (Siemens Japan). (d) Gd-EOB-DTPA-enhanced MRI reveals no enhanced nodule in the arterial phase and (e) no defect in the hepatobiliary phase. MR imaging at the hepatobiliary phase was performed with Gyroscan 10T-NT (Philips Medical Systems), Intera 1.0T version 12.1. THRIVE; TR/TE: 5.4/2.8 msec, FA: 20°, SENSE factor: 2, slice thickness: 6 mm (gap -2.5 mm), slice number: 70, matrix: 160×512

ography) in the diagnosis of HCC smaller than 2 cm. Consequently, the following patterns disclosed by these imaging modalities were deemed to be a conclusive diagnosis of HCC: 1) hypervascularity in the arterial phase and washout in the equilibrium phase (by contrast-enhanced CT), 2) hypervascularity in the early vascular phase and defect in the Kupffer phase (by Sonazoid contrast-enhanced US), 3) hypervascularity in the arterial phase and/or defect in the hepatobiliary phase (by Gd-EOB-DTPA-enhanced MRI) and 4) hypervascularity by CTHA and/or perfusion defect by CTAP (by CT arterioportal angiography). The results showed that the diagnostic sensitivity of CT arterioportal angiography was 88.2% in all nodules and 95.8% in moderately-differentiated HCC, with a significant difference between contrast-enhanced CT and CT arterioportal angiography ($p < 0.05$). No difference was observed, however, among Sona-

zoid contrast-enhanced US, Gd-EOB-DTPA-enhanced MRI and CT arterioportal angiography. The combined sensitivity of Sonazoid contrast-enhanced US and Gd-EOB-DTPA-enhanced MRI in all nodules was 94.1% due to improvement in the diagnostic capabilities of each modality (12). For the diagnosis of nodules smaller than 2 cm, these two imaging modalities have provided higher sensitivity with Sonazoid CEUS and Gd-EOB-DTPA-enhanced MRI than with Sonovue contrast-enhanced US and contrast-enhanced CT (13), or with Sonovue contrast-enhanced US and gadolinium-enhanced MRI (14). Such sensitivity in the diagnosis of well-differentiated HCC was, however, not explicit with the use of those imaging modalities in the present study.

According to the classification by the International Working Party of the World Congress of Gastroenterology, he-
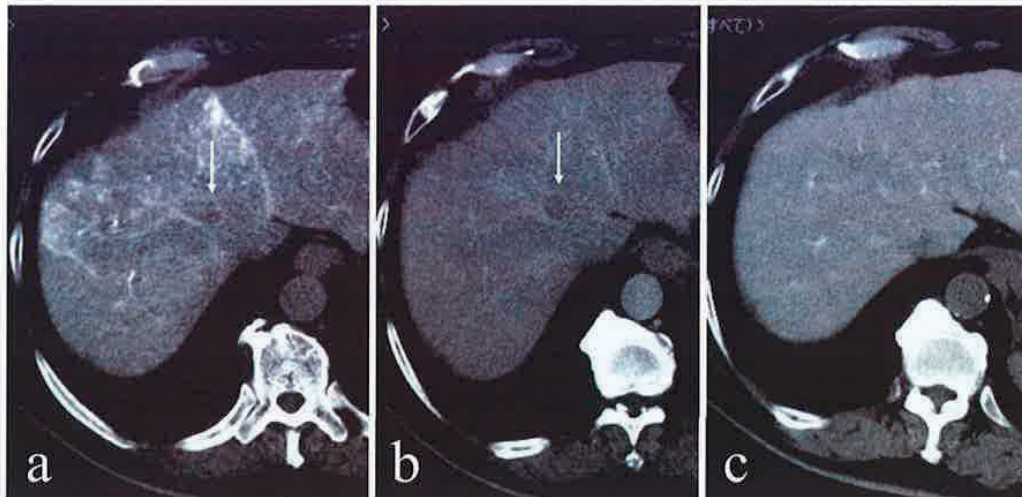
Figure 3. Imaging findings of CT arterioportal angiography. CTHA reveals a hypovascular nodule in both (a) the early phase (arrow) and (b) the late phase (arrow), (c) although CTAP does not reveal any perfusion defect. CTHA was performed using 40-60 mL of contrast medium at the rate of 2-3 mL/s into the common hepatic artery, scanned early phase (15 s) and late phase (60 s). CTAP was performed using 80-90 mL of contrast medium at the rate of 2-3 mL/s.
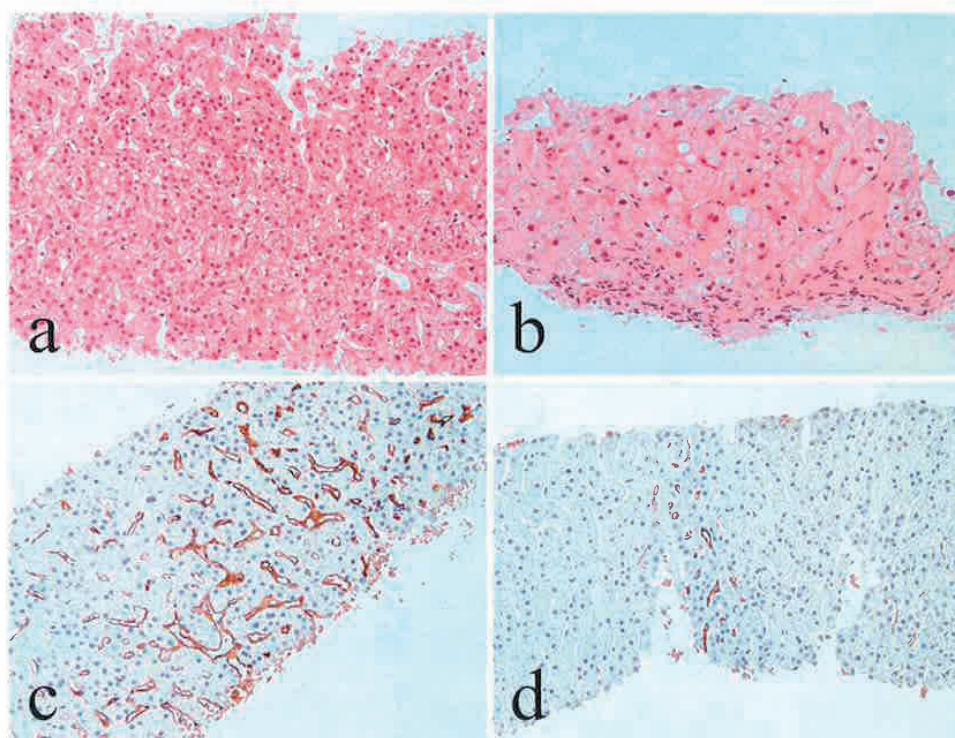
Figure 4. Histological findings of the US-guided biopsy specimens. (a) Well-differentiated HCC characterized by more than two-fold the cellularity of the non-tumorous area, clear cell change and mild cell atypia, and (b) non-nodular lesion (Hematoxylin and Eosin staining). (c) Capillarization is evident in the sinusoidal blood space, and (d) non-nodular lesion (immunohistochemical staining by CD34).

patic nodules in patients with chronic liver diseases are subdivided into regenerative nodules (mono acinus and multi acinus), LGDN, HGDN, well-differentiated HCC, moderately-differentiated HCC and poorly-differentiated
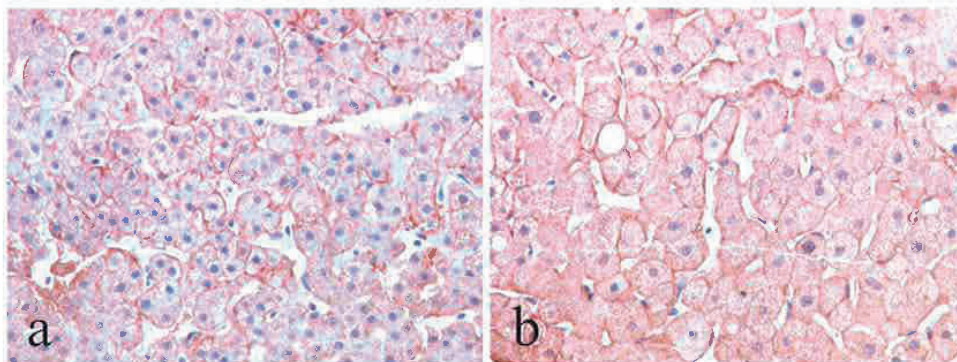
Figure 5. Expression of OATP 1B3 is observed in both (a) the nodular lesion and (b) the non-nodular lesion.

HCC, in ascending order of histologic grades, representing a sequence of multistep hepatocarcinogenesis (1). In a sequence of multistep carcinogenesis, the differentiation of HGDN from well-differentiated HCC is pivotal. From the viewpoint of histopathology, consensus on the criteria of well-differentiated HCC has been established (15). From the viewpoint of imaging studies on early HCC, there is controversy among hepatologists engaged in the diagnosis of well-differentiated HCC. Some insist that Gd-EOB-DTPA-enhanced MRI is most sensitive in disclosing defect in the hepatobiliary phase (16) and others insist that CTAP with CT arterioportal angiography is the most sensitive in disclosing perfusion defect (11). Although defect disclosed by CTHA, implying hypovascular HCC, has been reported to occur before perfusion defect disclosed by CTAP (6), the finding has not been verified in the clinical setting. We described a 10 mm well-differentiated HCC disclosed by only CTHA as a hypovascular tumor, whereas Sonazoid contrast-enhanced US, contrast-enhanced CT and Gd-EOB-DTPA-enhanced MRI revealed no defect in the Kupffer phase and no washout in the equilibrium phase and no defect in the hepatobiliary phase; also, CTAP revealed no perfusion defect.

Concerning OATP 1B3, there was no difference of OATP 1B3 expression in either the nodule or the non-nodular lesion in the present case of well-differentiated HCC. That is compatible with two reports, describing that OATP 1B3 was highly expressed in some of moderately-differentiated HCC, whereas it was hardly observed in well-differentiated HCC (9, 17). Concerning insufficient quality of the images, the unhomogeneous enhanced area depicted with CTHA and Sonazoid contrast-enhanced US might be explained by pericellular fibrosis due to alcohol-related liver cirrhosis.

The present results demonstrated that CTHA is more sensitive than Gd-EOB-GTPA-enhanced MRI in the diagnosis of well-differentiated HCC, although no clinical trials have been undertaken to evaluate the sensitivity of the two above modalities in the diagnosis of well-differentiated HCC. Further study is needed to clarify the sensitivity of imaging studies in the diagnosis of well-differentiated HCC smaller than 2 cm.

The authors state that they have no Conflict of Interest (COI).

Acknowledgement
We are indebted to Ms. Yoshiko Kawamura of Kobe Asahi Hospital for the preparation of the manuscript.

References

1. International Working Party. Terminology of nodular hepatocellular lesions. Hepatology **22**: 983-989, 1995.
2. Theise N, Schwartz M, Miller C, Thung S. Macroregenerative nodules and hepatocellular carcinoma in forty-four sequential adult liver explants with cirrhosis. Hepatology **16**: 949-955, 1992.
3. Mion F, Grozel L, Boillot O, Paliard P, Berger F. Adult cirrhotic liver explants: precancerous lesions and undetected small hepatocellular carcinomas. Gastroenterology **111**: 1587-1592, 1996.
4. Burrel M, Llovet J, Ayuso C, et al. MRI angiography is superior to helical CT for detection of HCC prior to liver transplantation: an explant correlation. Hepatology **38**: 1034-1042, 2003.
5. Hayashi M, Matsui O, Ueda K, Kawamori Y, Gabata T, Kadoya M. Progression to hypervascular hepatocellular carcinoma: correlation with intranodular blood supply evaluated with CT during intraarterial injection of contrast material. Radiology **225**: 143-149, 2002.
6. Tajima T, Honda H, Taguchi K, et al. Sequential hemodynamic change in hepatocellular carcinoma and dysplastic nodules: CT angiography and pathologic correlation. AJR Am J Roentgenol **178**: 885-897, 2002.
7. Inoue T, Kudo M, Hatanaka K, et al. Imaging of hepatocellular carcinoma: qualitative and quantitative analysis of postvascular phase contrast enhanced ultrasonography with sonazoid. Comparison with superparamagnetic iron oxide magnetic resonance images. Oncology **75**: 48S-54S, 2008.
8. Saito K, Kotake F, Ito N, et al. Gd-EOB-DTPA enhanced MRI for hepatocellular carcinoma: quantitative evaluation of tumor enhancement in hepatobiliary phase. Magn Reson Med Sci **4**: 1-9, 2005.
9. Narita M, Hatano E, Arizono S, et al. Expression of OATP1B3 determines uptake of Gd-EOB-DTPA in hepatocellular carcinoma. J Gastroenterol **44**: 793-798, 2009.
10. Bruix J, Sherman M, Llovet J, et al. Clinical management of hepatocellular carcinoma. Conclusions of the Barcelona-2000 EASL conference. J Hepatol **35**: 421-430, 2001.
11. Kim SR, Ando K, Mita K, et al. Superiority of CT arterioportal

angiography to contrast-enhanced CT and MRI in the diagnosis of hepatocellular carcinoma in nodules smaller than 2 cm. Oncology **72**: 58S-66S, 2007.

12. Mita K, Kim SR, Kudo M, et al. Diagnostic sensitivity of imaging modalities for hepatocellular carcinoma smaller than 2 cm. World J Gastroenterol **16**: 4187-4192, 2010.

13. Bolondi L, Gaiani S, Celli N, et al. Characterization of small nodules in cirrhosis by assessment of vascularity: the problem of hypovascular hepatocellular carcinoma. Hepatology **42**: 27-34, 2005.

14. Forner A, Vilana R, Ayuso C, et al. Diagnosis of hepatic nodules 20 mm or smaller in cirrhosis: prospective validation of the noninvasive diagnostic criteria for hepatocellular carcinoma. Hepatology **47**: 97-104, 2008.

15. International Consensus Group for Hepatocellular Neoplasia. Pathologic diagnosis of early hepatocellular carcinoma: a report of the International Consensus Group for Hepatocellular Neoplasia. Hepatology **49**: 658-664, 2009.

16. Motosugi U, Ichikawa T, Sou H, et al. Liver parenchymal enhancement of hepatocyte-phase images in Gd-EOB-DTPA-enhanced MR imaging: which biological markers of the liver function affect the enhancement? J Magn Reson Imaging **30**: 1042-1046, 2009.

17. Kitao A, Matsui O, Yoneda N, et al. The uptake transporter OATP8 expression decreases during multistep hepatocarcinogenesis: correlation with gadoxetic acid enhanced MR imaging. Eur Radiol **21**: 2056-2066, 2011.

THE INTERNATIONAL JOURNAL OF
CLINICAL PRACTICE

First interim analysis of the GIDEON (Global Investigation of therapeutic DEcisions in hepatocellular carcinoma and Of its treatment with sorafeNib) non-interventional study

R. Lencioni,[1] M. Kudo,[2] S.-L. Ye,[3] J.-P. Bronowicki,[4] X.-P. Chen,[5] L. Dagher,[6] J. Furuse,[7] J. F. Geschwind,[8] L. L. de Guevara,[9] C. Papandreou,[10] A. J. Sanyal,[11] T. Takayama,[12] S. K. Yoon,[13] K. Nakajima,[14] F. Cihon,[15] S. Heldner,[16] J. A. Marrero[17]

SUMMARY

Aims: Global Investigation of therapeutic DEcisions in hepatocellular carcinoma and Of its treatment with sorafeNib (GIDEON), a global, non-interventional, surveillance study, aims to evaluate the safety of sorafenib in all patients with unresectable hepatocellular carcinoma (uHCC) under real-life practice conditions, particularly Child-Pugh B patients, who were not well represented in clinical trials. **Methods:** Treatment decisions are determined by each physician according to local prescribing guidelines and clinical practice. Patients with uHCC who are candidates for systemic therapy, and for whom a decision has been made to treat with sorafenib, are eligible for inclusion. Demographic data and medical and disease history are recorded at entry. Sorafenib dosing and adverse events (AEs) are collected throughout the study. **Results:** From January 2009 to April 2011, >3000 patients from 39 countries were enrolled. The prespecified first interim analysis was conducted when the initial approximately 500 treated patients had been followed up for ≥4 months; 479 were valid for safety evaluation. Preplanned subgroup analyses indicate differences in patient characteristics, disease aetiology and previous treatments by region. Variation in sorafenib dosing by specialty are also observed; Child-Pugh status did not appear to influence the starting dose of sorafenib. The type and incidence of AEs was consistent with findings from previous clinical studies. AE profiles were comparable between Child-Pugh subgroups. **Discussion:** The GIDEON study is generating a large, robust database from a broad population of patients with uHCC. First interim analyses have shown global and regional differences in patient characteristics, disease aetiology and practice patterns. Subsequent planned analyses will allow further evaluation of early trends.

What's known

- Currently, there is no global consensus on the management of patients with uHCC. A worldwide study of regional uHCC treatment practices is therefore needed to advance the management of uHCC
- The oral multikinase inhibitor sorafenib is the only systemic therapy indicated for the treatment of uHCC, but data from Child-Pugh B patients are limited

What's new

- The non-interventional GIDEON study is evaluating sorafenib in uHCC under real-life clinical practice conditions and therefore includes a broader patient demographic than that represented in controlled clinical trials
- GIDEON allows global variations in uHCC management to be evaluated in a single robust study, and the prespecified first interim analysis results highlight differences in patient and disease characteristics, aetiology, and risk factors for uHCC, and sorafenib dosing, by region and physician specialty
- The type and incidence of AEs is as expected and appears to be similar in Child-Pugh A and B patients

[1]Division of Diagnostic Imaging and Intervention, Pisa University Hospital and School of Medicine, Pisa, Italy
[2]Department of Gastroenterology and Hepatology, Kinki University School of Medicine, Osaka, Japan
[3]Liver Cancer Institute and Zhongshan Hospital, Fudan University, Shanghai, China
[4]Department of Gastroenterology and Hepatology, INSERM U954, University Hospital of Nancy, University Henri Poincaré, Vandœuvre-lès-Nancy, France
[5]Hepatic Surgery Center, Tongji Hospital, Tongji Medical College, Huazhong University of Science and Technology, Wuhan, China
[6]Policlínica Metropolitana, Caracas, Venezuela
[7]Kyorin University, Mitaka, Tokyo, Japan
[8]Vascular and Interventional Radiology, Johns Hopkins University School of Medicine, Baltimore, MD, USA
[9]Hospital Angeles Clínica Londres, Mexico City, Mexico
[10]University Hospital of Larissa, Larissa, Greece
[11]Virginia Commonwealth University Medical Center, Richmond, VA, USA
[12]Department of Digestive Surgery, Nihon University School of Medicine, Tokyo, Japan
[13]The Catholic University of Korea, Seoul, Korea
[14]Global Medical Affairs, Bayer HealthCare Pharmaceuticals, Montville, NJ, USA
[15]Clinical Statistics, Bayer HealthCare Pharmaceuticals, Montville, NJ, USA
[16]Global Medical Affairs and Pharmacovigilance, Bayer HealthCare Pharmaceuticals, Berlin, Germany
[17]Department of Medicine, University of Michigan, Ann Arbor, MI, USA

Introduction

Liver cancer is the fifth most prevalent neoplasm worldwide but the second most common cause of cancer-related mortality in men (1). In women, it is the seventh most common cancer but the sixth leading cause of cancer-related death (1). This is in part because of the poor prognosis for many patients, more than 70% of whom present with advanced disease (2,3). The highest incidence of liver cancer is found in East and South-East Asia and in middle and West Africa (1). Although the incidence rate in more developed regions of the world is lower, including central Europe and the USA, liver cancer

incidence rates in the developed world are increasing (1). The global incidence of hepatocellular carcinoma (HCC) is predicted to continue to increase until a plateau is reached in 2015–2020 (2). Risk factors for the development of HCC include hepatitis B viral (HBV) and hepatitis C viral (HCV) infection, high alcohol intake, obesity and diabetes (1,4).

HCC treatments have developed rapidly over the last two decades in parallel with significant developments in diagnosis, surveillance, staging system and tumour assessment criteria. However, the majority of patients present with unresectable HCC (uHCC). Current non-surgical treatment options include loco-regional treatment (LRT), for example transarterial

675

Correspondence to:
Riccardo Lencioni,
Division of Diagnostic Imaging
and Intervention,
Pisa University Hospital and
School of Medicine,
Via Paradisa 2, Building No. 29,
IT-56124 Pisa, Italy
Tel.: +39 050 997 321
Fax: +39 050 997 320
Email: riccardo.lencioni@
med.unipi.it

chemoembolisation (TACE) and ablation therapy, although it is recognised that these have maximal effect for smaller tumours without vascular invasion (5–8).

Two placebo-controlled Phase III studies (SHARP and Asia-Pacific) have demonstrated that the oral multikinase inhibitor sorafenib (Nexavar®; Bayer HealthCare Pharmaceuticals, Berlin, Germany; Onyx Pharmaceuticals, San Francisco, CA) significantly improves overall survival in patients with uHCC (9,10). Sorafenib is the first systemic anticancer agent to be indicated for patients with uHCC and is currently recommended for selected patients with Child-Pugh A or B liver function and unresectable disease who are unsuitable for liver transplantation (5,8). Sorafenib is also indicated in patients with local disease unsuitable for surgery because of performance status or comorbidity, and for patients with metastatic disease (5).

The Global Investigation of therapeutic DEcisions in HCC and Of its treatment with sorafeNib (GIDEON) study is the largest prospective, non-interventional study undertaken in patients with uHCC. The study was initiated to fulfil the post-approval commitment to licensing agencies to gather more comprehensive data on the use of sorafenib in patients with Child-Pugh B liver function, who were excluded from the randomised clinical trials, resulting in limited data for patients with more severe liver dysfunction (11). The primary objective of GIDEON is to evaluate the safety of sorafenib in uHCC patients under real-life clinical practice conditions (12). Importantly, the GIDEON study is inclusive of the diverse HCC population from 39 countries, thus allowing both global and regional evaluation of prognostic and predictive factors.

The robust database provided by GIDEON on treatment patterns and outcomes for uHCC patients who are candidates for systemic therapy is a unique resource to further study multiple patient subgroups and physicians' practice patterns around the world. Thus, the GIDEON study can generate data that could better inform treatment choices and ultimately improve outcomes for patients with uHCC. Results from the first interim analysis are presented in this paper.

Methods

Study design and objectives
GIDEON is a global, non-interventional, surveillance study in which assignment to a particular therapy is not mandated by a study protocol but is decided by the participating physician, as previously described (13). The primary objective is to

evaluate the safety of sorafenib in patients with uHCC who are candidates for systemic therapy and in whom a decision to treat with sorafenib has been made in real-life practice conditions. The secondary objectives include efficacy and duration of therapy with sorafenib. Objectives will be evaluated in a variety of patient subsets, both globally and across regions.

The first patient entered the study in 2009 and the last patient was enrolled in April 2011, 20 months before the anticipated date. Two preplanned interim analyses were defined based on prespecified numbers of patients who are treated with sorafenib and followed for at least 4 months, the first interim at 500 patients and the second interim at 1500 patients. The final analysis is planned 12 months after enrolment of the 3000th treated patient (12).

The study is being conducted according to established regulations and recommendations relating to the conduct of a non-interventional study, according to Good Clinical Practice where applicable to a non-interventional study, and according to relevant local laws, regulations and organisations, with documented approval from appropriate ethics committee(s)/institutional review board as required (12).

Patients
Eligible patients must have histologically, cytologically or radiographically diagnosed uHCC and a life expectancy of >8 weeks. They must also have provided signed, informed consent, and the local physician must have decided to treat them with sorafenib. Radiographic diagnosis is based on findings from multidimensional dynamic computed tomography (CT), CT hepatic arteriography/CT arterial portography, or magnetic resonance imaging. Patient exclusion criteria are based on the approved local product information for sorafenib (12). Patients who received at least one dose of sorafenib and underwent at least one follow-up assessment after start of treatment are evaluable for safety.

Data collection
All data are collected using case report forms, as previously described (12). Dosage details and duration of sorafenib treatment are determined for each patient, and data for discontinuation are summarised. Adverse events (AEs) and serious AEs (SAEs) are graded according to the Common Terminology Criteria for Adverse Events version 3.0; other safety variables are summarised descriptively.

Statistical methods
Based on previously conducted large, global, multicentre sorafenib studies for HCC, overall incidence

rates of approximately 1–2% had been observed for AEs of interest for further safety monitoring. Approximately 3000 treated patients will provide an 84% chance of observing an AE, with a true incidence of 1% in at least 25 patients. An overall sample size of 3000 patients was therefore considered sufficient for evaluation of safety of both the overall population and specific subgroups (12). All baseline and safety data are summarised using descriptive statistics. Preplanned subgroup analyses of safety data were performed, stratified by region and physician specialty for multiple data points, such as patient demographics and treatment history.

Results

Patients

Per protocol, the first planned interim analysis was initiated when the initial approximately 500 treated patients had been followed for at least 4 months. Based on these criteria, the cut-off date used for the first interim analysis was 11 April 2010. A total of 511 patients have been enrolled from 140 sites. Patients have been enrolled from 39 countries across five regions: Europe, Latin America, the USA, Japan and Asia-Pacific (Figure 1). Of these, 479 were evaluable for safety analyses. Thirty-two patients were excluded from the safety analyses, as they did not receive sorafenib treatment or received sorafenib but had no post-baseline evaluation.

Patient characteristics at baseline

Demographics and baseline characteristics for patients evaluable for safety analyses are presented by region and by leading physician specialty in Table 1. Based on this first interim analysis, Asia-Pacific countries enrolled the most patients. The distribution of males/females was generally similar across geographic regions, except for Latin America. Patients in Asia-Pacific were relatively younger than those in other regions.

Primary physician specialty

Overall, hepatologists/gastroenterologists (Hep/GIs) were the most common treating physicians (52%) for patients with uHCC. Medical oncologists (Med Oncs) treated 35% of patients across all regions. Other treating specialties were less commonly reported: surgery (7%), traditional Chinese medicine (2%), radiology (1%) and anaesthesiology (1%). Baseline characteristics were generally similar between patients treated by Hep/GIs and those treated by Med Oncs.

Prior locoregional treatment

Overall, 55% of patients received prior LRT (Table 1). TACE was the most commonly received LRT, with 44% of all patients receiving prior TACE compared with only 15%, 5% and 3% of patients receiving prior radiofrequency ablation, hepatic arterial infusion and percutaneous ethanol injection, respectively.

Prior locoregional treatment by region

Wide regional variation was observed in the use of prior LRT. In Japan all patients received LRT prior to sorafenib treatment; however, in Asia-Pacific, the USA and Europe, 68%, 46% and 45% of patients received prior LRT, respectively. TACE was the most commonly received LRT in each region, although with considerable regional variation. Prior TACE treatment was more frequent in Japan (90%) and Asia-Pacific (62%) and less common in Europe (27%) and Latin America (22%).

Disease characteristics at study entry

Disease characteristics at study entry (defined as start of sorafenib therapy, indicated by the initial visit) are provided in Table 2. Patients were enrolled across all Barcelona Clinic Liver Cancer (BCLC) stages. The majority of patients (53%) had BCLC stage C; however, 19% of patients had BCLC stage B, and 10% and 6% had stage A and D, respectively. More
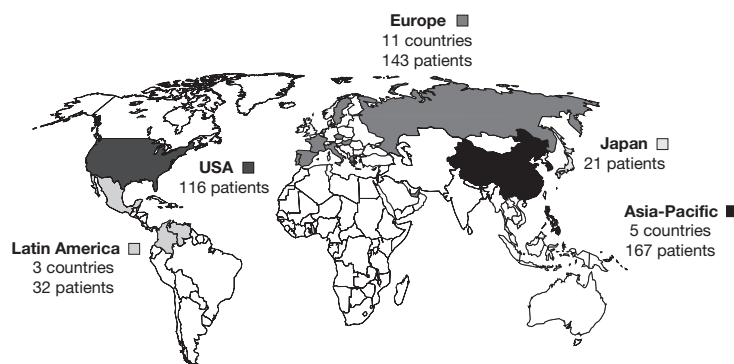

Figure 1 Distribution of patients included in the first interim analysis, by region

Table 1 Demographic and baseline characteristics

		Geographic regions					Specialty*	
	Total	Asia-Pacific	Europe	USA	Latin America	Japan	Hep/GI†	Med Onc
Patients, *n* (% of total)	479 (100)	167 (35)	143 (30)	116 (24)	32 (7)	21 (4)	248 (52)	168 (35)
Median age, years	62	54	68	62	65	70	60/67	61
Gender, *n* (%)								
Male	392 (82)	144 (86)	125 (87)	89 (77)	15 (47)	19 (90)	210 (85)	134 (80)
Female	87 (18)	23 (14)	18 (13)	27 (23)	17 (53)	2 (10)	38 (15)	34 (20)
ECOG PS, *n* (%)‡,§								
0	181 (38)	51 (31)	69 (48)	41 (35)	5 (16)	15 (71)	114 (46)	40 (24)
1	199 (42)	78 (47)	50 (35)	43 (37)	22 (69)	6 (29)	93 (38)	75 (45)
≥2	62 (13)	14 (8)	22 (15)	22 (19)	4 (12)	0	36 (15)	23 (14)
Prior LRT, *n* (%)¶	264 (55)	114 (68)	64 (45)	53 (46)	12 (38)	21 (100)	132 (53)	88 (52)
Prior TACE, *n* (%)	212 (44)	104 (62)	39 (27)	43 (37)	7 (22)	19 (90)	107 (43)	68 (40)
Prior RFA, *n* (%)	72 (15)	17 (10)	35 (25)	8 (7)	6 (19)	6 (29)	45 (18)	20 (12)
Prior HAI, *n* (%)	26 (5)	14 (8)	2 (1)	6 (5)	2 (6)	2 (10)	17 (7)	4 (2)
Prior PEI, *n* (%)	15 (3)	4 (2)	8 (6)	0	0	3 (14)	12 (5)	2 (1)

*Other specialties not tabulated included surgery (*n* = 35), radiology (*n* = 6), anaesthesiology (*n* = 4) and traditional Chinese medicine (*n* = 10); †Hep/GI population comprised 178 patients treated by hepatologists and 70 patients treated by gastroenterologists; ‡Recorded at study entry (which is defined as start of therapy and is indicated by the initial visit); §Data missing for 37 patients; ¶Data missing for one patient.
ECOG PS, Eastern Cooperative Oncology Group performance status; GI, gastroenterologist; HAI, hepatic arterial infusion; Hep, hepatologist; LRT, locoregional treatment; Med Onc, medical oncologist; PEI, percutaneous ethanol injection; RFA, radiofrequency ablation; TACE, transarterial chemoembolisation.

patients had tumour, node, metastasis (TNM) stage III and IV disease (37% and 35%, respectively) than stage I (6%) or II (14%).

As might be anticipated, the majority of patients in the overall population had Child-Pugh A status (*n* = 278; 58%) and there were fewer Child-Pugh B patients (*n* = 134; 28%). Subgroup analyses of disease characteristics at study entry suggest differences in many prognostic and predictive factors across regions and by treating-physician specialty (Table 2).

Disease characteristics by region

Some regional variation was observed: patients in Asia-Pacific tended to have more advanced HCC based on BCLC and TNM status at study entry than in other regions (Table 2). In Asia-Pacific, 74% of patients had BCLC stage C disease and 50% had TNM stage IV disease compared with 24–51% and 13–43%, respectively, across other regions. Extrahepatic spread was also observed within considerably more patients in Asia-Pacific (60%) than in other regions (16–34%).

There was some regional variation observed in Child-Pugh status (Table 2). A higher percentage of patients (60–76%) in Asia-Pacific, Europe and Japan had less advanced liver disease (i.e. Child-Pugh A) than in either the USA (41%) or Latin America (44%).

Differences in the aetiology of underlying liver disease were observed across regions (Table 2). The majority of patients in Asia-Pacific had HBV infection (84%), whereas HCV infection was more common in Europe (33%) and the USA (50%). A greater proportion of patients in Europe (42%) and the USA (34%) had alcoholic liver disease compared with other regions (16–19%). Thus, the major aetiologies for uHCC were HCV and alcoholic liver disease in Europe and the USA and HBV in Asia-Pacific.

Disease characteristics by physician specialty

Based on subgroup analyses by leading physician specialty, variations in disease characteristics were also seen between patients principally treated by Med Oncs and those treated by Hep/GIs (Table 2). Med Oncs tended to treat a greater number of patients with advanced HCC (64% of patients had BCLC stage C or D; 46% of patients had TNM stage IV) compared with Hep/GIs (59% of patients had BCLC stage C or D; 28% of patients had TNM stage IV). Hep/GIs treated more patients with Child-Pugh B status compared with Med Oncs (32% and 20%, respectively).

Sorafenib administration

Sorafenib administration data from the overall population are presented in Table 3. Overall, 76% of patients received the approved initial daily dose of

Table 2 Disease characteristics

		Geographic regions					Specialty	
	Total (n = 479)	Asia-Pacific (n = 167)	Europe (n = 143)	USA (n = 116)	Latin America (n = 32)	Japan (n = 21)	Hep/GI (n = 248)	Med Onc (n = 168)
BCLC staging*,†, n (%)								
Stage A	47 (10)	1 (1)	20 (14)	17 (15)	8 (25)	1 (5)	21 (8)	20 (12)
Stage B	92 (19)	19 (11)	32 (22)	21 (18)	11 (34)	9 (43)	55 (22)	25 (15)
Stage C	253 (53)	123 (74)	73 (51)	43 (37)	9 (28)	5 (24)	129 (52)	98 (58)
Stage D	29 (6)	7 (4)	7 (5)	11 (9)	3 (9)	1 (5)	17 (7)	10 (6)
TNM stage*,‡, n (%)								
Stage I	31 (6)	2 (1)	10 (7)	14 (12)	5 (16)	0	15 (6)	8 (5)
Stage II	69 (14)	13 (8)	17 (12)	18 (16)	11 (34)	10 (48)	41 (17)	16 (10)
Stage IIIa	121 (25)	44 (26)	39 (27)	30 (26)	7 (22)	1 (5)	69 (28)	37 (22)
Stage IIIb	15 (3)	3 (2)	4 (3)	7 (6)	0	1 (5)	8 (3)	7 (4)
Stage IIIc	40 (8)	14 (8)	16 (11)	8 (7)	2 (6)	0	20 (8)	15 (9)
Stage IV	167 (35)	83 (50)	40 (28)	31 (27)	4 (13)	9 (43)	69 (28)	78 (46)
Extrahepatic spread*, n (%)	193 (40)	101 (60)	49 (34)	32 (28)	5 (16)	6 (29)	88 (35)	84 (50)
Child-Pugh status§, n (%)								
A	278 (58)	101 (60)	100 (70)	47 (41)	14 (44)	16 (76)	149 (60)	91 (54)
B	134 (28)	44 (26)	30 (21)	41 (35)	15 (47)	4 (19)	80 (32)	34 (20)
C	11 (2)	1 (1)	2 (1)	8 (7)	0	0	5 (2)	5 (3)
CLIP score¶, n (%)								
0	30 (6)	5 (3)	11 (8)	7 (6)	6 (19)	1 (5)	16 (6)	10 (6)
1	93 (19)	19 (11)	39 (27)	19 (16)	7 (22)	9 (43)	53 (21)	26 (15)
2	99 (21)	30 (18)	33 (23)	20 (17)	8 (25)	8 (38)	60 (24)	23 (14)
3	75 (16)	27 (16)	20 (14)	22 (19)	4 (13)	2 (10)	48 (19)	20 (12)
4–6	68 (14)	34 (20)	15 (10)	15 (13)	3 (9)	1 (5)	46 (19)	16 (10)
Aetiology of underlying liver disease**, n (%)								
Hepatitis B	194 (41)	140 (84)	25 (17)	23 (20)	1 (3)	5 (24)	89 (36)	77 (46)
Hepatitis C	146 (30)	12 (7)	47 (33)	58 (50)	17 (53)	12 (57)	82 (33)	44 (26)
Alcohol	138 (29)	29 (17)	60 (42)	40 (34)	5 (16)	4 (19)	84 (34)	42 (25)
Liver cirrhosis††, n (%)								
Yes‡‡	327 (68)	111 (66)	104 (73)	78 (67)	20 (63)	14 (67)	197 (79)	86 (51)
No	107 (22)	42 (25)	27 (19)	25 (22)	10 (31)	3 (14)	34 (14)	62 (37)

*Recorded at study entry (which is defined as start of therapy and is indicated by the initial visit); †Data missing for six patients and not evaluable for 52 patients; ‡Data missing for six patients and not evaluable for 30 patients; §Data missing for five patients and not evaluable for 51 patients; ¶Data missing for seven patients and not evaluable for 107 patients; **Patients could have >1 underlying liver disease; other aetiologies included non-alcoholic steatohepatitis, metabolic factors and haematochromatosis; ††Data missing for one patient and unknown for 47 patients; ‡‡Includes clinical, histologic or radiologic diagnosis.
BCLC, Barcelona Clinic Liver Cancer; CLIP, Cancer of the Liver Italian Program; TNM, tumour, node, metastasis.

800 mg sorafenib, while 24% of patients received an initial daily dose of <800 mg. The majority of patients were treated for >4 weeks (75%). However, treatment duration data based on interim analyses are preliminary, as data will also reflect the point at which patients started the study relative to the timing of database cut-off.

Sorafenib administration by region
Based on these preliminary findings, regional variation in dosing was observed. In Asia-Pacific, 66% of patients received sorafenib for >4 weeks compared with 77–97% of patients in other regions. Therefore,

patients in Asia-Pacific tended to stop sorafenib therapy earlier than patients in other regions. The lowest median daily dose was given in Japan (521 mg) and the USA (564 mg). Patients in Asia-Pacific, Europe and Latin America tended to receive a much higher median daily dose (710–800 mg).

Sorafenib administration by physician specialty
Variations in sorafenib dosing patterns were seen across physician specialties (Table 3). A greater percentage of Hep/GIs initiated sorafenib therapy at 800 mg/day compared with Med Oncs (83% and 65%, respectively), and Hep/GIs gave a higher

Table 3 Summary of sorafenib administration stratified by region, specialty and Child-Pugh status

Sorafenib administration	Total (n = 479)	Geographic regions					Specialty		Child-Pugh status*,†	
		Asia-Pacific (n = 167)	Europe (n = 143)	USA (n = 116)	Latin America (n = 32)	Japan (n = 21)	Hep/GI (n = 248)	Med Onc (n = 168)	Child-Pugh A (n = 278)	Child-Pugh B (n = 134)
Duration of treatment, n (%)‡,§										
≤4 weeks	106 (22)	50 (30)	25 (17)	26 (22)	1 (3)	4 (19)	53 (21)	40 (24)	47 (17)	44 (33)
>4–8 weeks	87 (18)	32 (19)	23 (16)	22 (19)	5 (16)	5 (24)	44 (18)	28 (17)	45 (16)	29 (22)
>8–12 weeks	72 (15)	24 (14)	20 (14)	22 (19)	3 (9)	3 (14)	32 (13)	32 (19)	38 (14)	19 (14)
>12–16 weeks	53 (11)	14 (8)	19 (13)	10 (9)	5 (16)	5 (24)	35 (14)	15 (9)	34 (12)	10 (7)
>16–20 weeks	56 (12)	11 (7)	26 (18)	10 (9)	5 (16)	4 (19)	22 (9)	22 (13)	44 (16)	7 (5)
>20–24 weeks	30 (6)	9 (5)	8 (6)	9 (8)	4 (13)	0	16 (6)	12 (7)	20 (7)	8 (6)
>24–28 weeks	25 (5)	11 (7)	7 (5)	6 (5)	1 (3)	0	13 (5)	9 (5)	18 (6)	2 (1)
>28 weeks	38 (8)	10 (6)	10 (7)	10 (9)	8 (25)	0	24 (10)	7 (4)	27 (10)	10 (7)
Median daily dose¶,**, mg	692	710	779	564	800	521	774	570	624	800
Initial dose of 800 mg/day††, n (%)	363 (76)	133 (80)	114 (80)	69 (59)	31 (97)	16 (76)	206 (83)	109 (65)	221 (79)	100 (75)
Permanent discontinuation of sorafenib because of AEs, n (%)	133 (28)	49 (29)	36 (25)	37 (32)	2 (6)	9 (43)	81 (33)	34 (20)	69 (25)	53 (40)

*At start of therapy; †Data missing for five patients and not evaluable for 51 patients; ‡Time in weeks from initial visit to last dosing date (for ongoing patients to last visit date) +1; §Data missing for 12 patients; ¶Determined per patient based on actual days on study drug (interruptions excluded); **Based on 367 patients; †† 114 patients received ≤ 600 mg/day and data missing for two patients.

AE, adverse event; GI, gastroenterologist; Hep, hepatologist; Med Onc, medical oncologist.

median daily dose than Med Oncs (774 mg and 570 mg, respectively).

Sorafenib administration by Child-Pugh status

Sorafenib administration based on Child-Pugh classification was also assessed (Table 3). Duration of treatment was generally shorter in Child-Pugh A than in Child-Pugh B patients. A greater number of Child-Pugh A patients received treatment for >8 weeks compared with Child-Pugh B patients (65% vs. 42%). These preliminary data suggest that patients with advanced Child-Pugh status tended to stop sorafenib treatment earlier than patients with less advanced disease. However, a number of Child-Pugh B patients were treated for longer periods, and 7% and 10% of Child-Pugh B and Child-Pugh A patients, respectively, received >28 weeks of sorafenib therapy.

Child-Pugh score did not seem to influence the starting dose of sorafenib, and at least 75% of patients in both Child-Pugh A and Child-Pugh B groups received the recommended initial daily dose of 800 mg sorafenib (79% and 75%, respectively). Overall, the dosing strategy for Child-Pugh B patients did not appear to be different from that for Child-Pugh A patients.

Safety assessments

Safety data from this first interim analysis are preliminary; however, the overall safety profile of sorafenib in this first interim analysis was consistent with that reported in previous clinical studies and no unforeseen AEs were reported (Tables 4 and 5). A total of 87% of patients reported at least one AE. Drug-related AEs were experienced by 319 patients (67%): 41% with grade 1 or 2 events and 25% with grade 3 or 4 events. Overall, 42% of patients (n = 201) experienced SAEs and 11% experienced drug-related SAEs. Study drug was permanently discontinued as a result of AEs in 28% of patients. This was because of a variety of AEs, each with a relatively low incidence in the overall population. The most commonly reported AEs in the overall population included diarrhoea, hand-foot skin reaction, fatigue, rash/desquamation and anorexia (Table 5). Hand-foot skin reaction and fatigue were the most commonly reported grade 3 or 4 AEs within the study population.

AE profiles were comparable between subgroups of Child-Pugh status (Table 4). The overall incidence of treatment-emergent AEs was slightly higher in Child-Pugh B patients than in Child-Pugh A patients (91% vs. 84%, respectively); however, the incidence of drug-related AEs was similar in both Child-Pugh A

Table 4 Treatment-emergent adverse events by Child-Pugh status

Treatment-emergent adverse events, n (%)	Total (n = 479)	Child-Pugh status at start of therapy		
		Child-Pugh A (<7) (n = 278)	Child-Pugh B (7–9) (n = 134)	Child-Pugh C (>9) (n = 11)
AEs (all grades)	415 (87)	234 (84)	122 (91)	10 (91)
AEs (grade 3 or 4)	194 (41)/43 (9)	98 (35)/19 (7)	70 (52)/20 (15)	4 (36)/2 (18)
Drug-related AEs (all grades)	319 (67)	193 (69)	84 (63)	6 (55)
Drug-related AEs (grade 3 or 4)	110 (23)/12 (3)	66 (24)/7 (3)	31 (23)/5 (4)	3 (27)/0
SAEs* (all grades)	201 (42)	93 (33)	80 (60)	7 (64)
Drug-related SAEs* (all grades)	51 (11)	28 (10)	22 (16)	0
AEs resulting in permanent discontinuation of sorafenib†	133 (28)	69 (25)	53 (40)	5 (45)
Deaths‡	114 (24)	49 (18)	50 (37)	4 (36)

*An SAE is defined as any AE occurring at any dose that results in any of the following outcomes: death; life-threatening; hospitalisation or prolongation of existing hospitalisation; persistent or significant disability/incapacity; congenital anomaly/birth defect; medically important event; †Any AE; ‡Deaths while on treatment and up to 30 days after last dose of study drug.
AE, adverse event; SAE, serious adverse event.

Table 5 Treatment-emergent adverse events in ≥5% of the total study population

n (%)	Treatment-emergent adverse events (n = 479)		Treatment-emergent drug-related adverse events (n = 479)	
	All grades	Grade 3 or 4	All grades	Grade 3 or 4
Any adverse event	415 (87)	161 (34)	319 (67)	109 (23)
Diarrhoea	132 (28)	10 (2)	114 (24)	8 (2)
Hand-foot skin reaction	126 (26)	26 (5)	124 (26)	26 (5)
Fatigue	81 (17)	27 (6)	51 (11)	16 (3)
Rash/ desquamation	73 (15)	12 (3)	63 (13)	12 (3)
Anorexia	55 (11)	24 (5)	39 (8)	7 (1)
Abdominal pain	53 (11)	20 (4)	-	-
Liver dysfunction	42 (9)	11 (2)	-	-
Nausea	41 (9)	5 (1)	25 (5)	4 (1)
Ascites	39 (8)	24 (5)	-	-
Hyperbilirubinemia	38 (8)	22 (5)	-	-
Hypertension	36 (8)	12 (3)	29 (6)	9 (2)
Alopecia	29 (6)	0	28 (6)	0
Vomiting	29 (6)	3 (1)	-	-
Weight loss	28 (6)	4 (1)	-	-
Fever	25 (5)	2 (<1)	-	-
Encephalopathy	25 (5)	10 (2)	-	-

and B patients (69% vs. 63%, respectively). The incidence of grade 3 or 4 drug-related events was consistent, with 23–24% of grade 3 and 3–4% of grade 4 events experienced by patients in each of the Child-Pugh A and B subgroups. Drug-related SAEs occurred in 10% of Child-Pugh A and 16% of Child-Pugh B patients. The rate of discontinuation of sorafenib because of AEs, regardless of any causal relationship with sorafenib, was higher in patients with Child-Pugh B status (40%) than in patients with Child-Pugh A status (25%). The safety profile of Child-Pugh B patients was generally consistent with the overall safety profile.

Discussion

The GIDEON study is, to date, the largest, prospective, non-interventional global study to investigate the treatment of patients with uHCC in the real world and reflects participating physicians' current practice. Data have been collected from a wide uHCC population, and the study database allows analyses of global and regional differences in patient characteristics, disease aetiology, underlying liver disorders and practice patterns.

Demographic data for patients in the first interim analysis of this study were consistent with findings from previously reported epidemiological HCC studies (14,15). The first interim analyses of the GIDEON study highlight notable regional differences in patient and disease characteristics, aetiology and risk factors of uHCC. Global variations in the aetiology of HCC, in particular HBV and HCV, have been previously reported (2,16). TACE is the current standard of care for patients with multinodular, intermediate-stage uHCC (13,17) and this is reflected in the patterns of TACE used in this first interim analysis. Interestingly,

regional variations are observed with patients in Japan and Asia-Pacific receiving more prior TACE than in other regions. This is the first time that variations in the management of uHCC in real-life practice have been evaluated in a single robust study with consistent methodology.

In this interim analysis, dosing differences based on non-clinical factors such as region and specialty are observed; however, Child-Pugh status does not appear to be a factor for sorafenib dosing patterns. The sorafenib dosing findings in this study are preliminary. Sorafenib dosing will continue to be evaluated in the GIDEON study, with the aim of optimising sorafenib treatment. It will be important to further explore reasons for these differences in sorafenib usage (between Med Oncs and Hep/GIs, and across regions).

The safety profile reported in this first interim analysis is consistent with that previously published from randomised clinical trials, with no unexpected AEs (9,10). The most commonly reported drug-related AEs reflect the findings of previous clinical studies of sorafenib in patients with uHCC. In the SHARP and Asia-Pacific studies, diarrhoea, fatigue and hand-foot skin reactions were also the most commonly reported drug-related AEs (9,10).

The safety profile observed in the GIDEON first interim analysis is generally similar in both Child-Pugh A and B patients. Overall, Child-Pugh B score does not appear to be associated with an increased incidence of drug-related AEs, compared with Child-Pugh A. These interim safety results support published data from clinical studies of patients with HCC on the safety of sorafenib in Child-Pugh B patients, in which there was no major difference in the incidence/grade of AEs between Child-Pugh A and B patients (11,18–20).

The results from this first interim analysis are preliminary and should be interpreted accordingly. Observational studies have their limitations, principally in the lack of a control arm and randomised study population; nonetheless, results from the GIDEON study provide the opportunity to evaluate a wide range of data in uHCC patients and sorafenib use globally. Initial findings provide an interesting insight into real-life clinical practice. The study is ongoing with final analyses planned 12 months after enrolment of the 3000th treated patient (12). Future reports will provide further

evidence that may help inform treatment choices and contribute to the advancement of HCC management.

Author contributions

RL, MK, S-LY and JAM are members of the Global Steering and Publication Committee for the GIDEON study and have been involved in discussion and modification of the GIDEON protocol, and in data review and interpretation. RL was responsible for the conception and design of the manuscript. RL, MK, S-LY, JAM, J-PB, X-PC, LD, JF, JFG, LL de G, CP, AJS, TT and SKY were all responsible for the provision of patients/data acquisition. All authors provided critical review of the manuscript, and approved the final version for publication. KN is the sponsor study physician adviser and has contributed to data analysis and interpretation. FC is the study statistician and has contributed to statistical analysis. SH is responsible for the global study management and for the supervision of the set-up and conduct of the study.

References

1 Jemal A, Bray F, Center MM et al. Global cancer statistics. *CA Cancer J Clin* 2011; **61**: 69–90.
2 Venook AP, Papandreou C, Furuse J, de Guevara LL. The incidence and epidemiology of hepatocellu-

lar carcinoma: a global and regional perspective. *Oncologist* 2010; **15**(Suppl 4): 5–13.
3 Thomas MB, Jaffe D, Choti MM et al. Hepatocellular carcinoma: consensus recommendations of the National Cancer Institute Clinical Trials Planning Meeting. *J Clin Oncol* 2010; **28**: 3994–4005.

4 El-Serag HB, Rudolph KL. Hepatocellular carcinoma: epidemiology and molecular carcinogenesis. *Gastroenterology* 2007; **132**: 2557–76.
5 National Comprehensive Cancer Network. NCCN Clinical Practice Guidelines in Oncology: hepatobiliary cancers (Version 2.2012). http://

www.nccn.org/professionals/physician_gls/f_guidelines.asp, http://www.nccn.org/professionals/physician_gls/pdf/hepatobiliary.pdf. (accessed April 2011).

6 Lopez PM, Villanueva A, Llovet JM. Systematic review: evidence-based management of hepatocellular carcinoma – an updated analysis of randomized controlled trials. *Aliment Pharmacol Ther* 2006; **23**: 1535–47.

7 Gish RG, Marrero JA, Benson AB. A multidisciplinary approach to the management of hepatocellular carcinoma. *Gastroenterol Hepatol (N Y)* 2010; **6**(Suppl 3): 1–16.

8 Bruix J, Sherman M. Management of hepatocellular carcinoma: an update. *Hepatology* 2011; **53**: 1020–2.

9 Cheng AL, Kang YK, Chen Z et al. Efficacy and safety of sorafenib in patients in the Asia-Pacific region with advanced hepatocellular carcinoma: a phase III randomised, double-blind, placebo-controlled trial. *Lancet Oncol* 2009; **10**: 25–34.

10 Llovet JM, Ricci S, Mazzaferro V et al. Sorafenib in advanced hepatocellular carcinoma. *N Engl J Med* 2008; **359**: 378–90.

11 Ozenne V, Paradis V, Pernot S et al. Tolerance and outcome of patients with unresectable hepatocellular carcinoma treated with sorafenib. *Eur J Gastroenterol Hepatol* 2010; **22**: 1106–10.

12 Lencioni R, Marrero J, Venook A, Ye SY, Kudo M. Design and rationale for the non-interventional Global Investigation of therapeutic DEcisions in hepatocellular carcinoma and Of its treatment with sorafeNib (GIDEON) study. *Int J Clin Pract* 2010; **64**: 1034–41.

13 Lencioni R. Loco-regional treatment of hepatocellular carcinoma. *Hepatology* 2010; **52**: 762–73.

14 Farinati F, Rinaldi M, Gianni S, Naccarato R. How should patients with hepatocellular carcinoma be staged? Validation of a new prognostic system. *Cancer* 2000; **89**: 2266–73.

15 Tandon P, Garcia-Tsao G. Prognostic indicators in hepatocellular carcinoma: a systematic review of 72 studies. *Liver Int* 2009; **29**: 502–10.

16 Sanyal AJ, Yoon SK, Lencioni R. The etiology of hepatocellular carcinoma and consequences for treatment. *Oncologist* 2010; **15**(Suppl 4): 14–22.

17 Lord R, Suddle A, Ross PJ. Emerging strategies in the treatment of advanced hepatocellular carcinoma: the role of targeted therapies. *Int J Clin Pract* 2011; **65**: 182–8.

18 Abou-Alfa GK, Schwartz L, Ricci S et al. Phase II study of sorafenib in patients with advanced hepatocellular carcinoma. *J Clin Oncol* 2006; **24**: 4293–300.

19 Furuse J, Ishii H, Nakachi K et al. Phase I study of sorafenib in Japanese patients with hepatocellular carcinoma. *Cancer Sci* 2008; **99**: 159–65.

20 Yau T, Chan P, Ng KK et al. Phase 2 open-label study of single-agent sorafenib in treating advanced hepatocellular carcinoma in a hepatitis B-endemic Asian population: presence of lung metastasis predicts poor response. *Cancer* 2009; **115**: 428–36.

Can the biliary enhancement of Gd-EOB-DTPA predict the degree of liver function?

Masahiro Okada, Kazunari Ishii, Kazushi Numata, Tomoko Hyodo, Seishi Kumano, Masayuki Kitano, Masatoshi Kudo and Takamichi Murakami

Osaka, Japan

BACKGROUND: Excretion of gadolinium-ethoxybenzyl-diethyl-enetriamine pentaacetic acid (Gd-EOB-DTPA) in the bile may be related to liver function, because of elimination from the liver after preferential uptake by hepatocytes. The purpose of this study was to investigate the relation between liver and biliary enhancement in patients with or without liver dysfunction, and to compare the tumor-to-liver contrast in these patients.

METHODS: Forty patients [group 1: normal liver and Child-Pugh class A in 20 patients, group 2: Child-Pugh class B in 18 patients and Child-Pugh C in 2] were evaluated. All patients underwent MR imaging of the liver using a 1.5-Tesla system. T1-weighted 3D images were obtained at 5, 10, 15 and 20 minutes after Gd-EOB-DTPA injection. The relation between group 3 (total bilirubin <1.8 mg/dL) and group 4 (total bilirubin ≥1.8 mg/dL) was investigated at 20 minutes. Liver and biliary signals were measured, and compared between groups 1 and 2 or groups 3 and 4. Tumor-to-liver ratio was also evaluated between groups 1 and 2. Scheffé's *post-hoc* test after two-way repeated-measures ANOVA and Pearson's correlation test were used for statistical analysis.

RESULTS: Liver enhancement showed significant difference at all time points between groups 1 and 2. Biliary enhancement did not show a significant difference between groups 1 and 2 at 5 minutes, but did at 10, 15 and 20 minutes. At 20 minutes, significant differences between groups 3 and 4 were seen for liver and biliary enhancement. At all time points, liver enhancement correlated with biliary enhancement in both groups. At 5 minutes and 20 minutes, statistical differences between groups 1 and 2 were seen for tumor-to-liver ratio.

CONCLUSIONS: The degree of biliary enhancement has a close correlation to that of liver enhancement. It is especially important that insufficient liver enhancement causes lower tumor-to-liver contrast in the hepatobiliary phase of Gd-EOB-DTPA.

Introduction

Gadolinium-ethoxybenzyl-diethylenetriamine pentaacetic acid (Gd-EOB-DTPA, gadoxetic acid; Primovist®, Bayer Schering Pharma AG, Berlin, Germany) is a liver-specific contrast agent which facilitates lesion detection and characterization.[1-3] Gd-EOB-DTPA is now clinically available in many countries of the European, American and Asian continents.

Gd-EOB-DTPA is administered via bolus injection and is rapidly cleared from the intravascular space to the extracellular space, thus acting as both an extracellular and hepatocyte-specific contrast agent. Interestingly, Gd-EOB-DTPA is eliminated from the body through both the renal and hepatobiliary pathways.[4, 5] Hamm et al[2] stated that Gd-EOB-DTPA is eliminated dose-independently in almost equal proportions from the hepatobiliary system and the kidney in healthy volunteers, thus 50% of the Gd-EOB-DTPA is excreted in the human biliary system.

To the best of our knowledge, only limited data regarding the quality of biliary duct and liver visualization with Gd-EOB-DTPA between liver cirrhosis and normal liver parenchyma are currently available.[6-9] Tschirch et al[7] found that the biliary enhancement after Gd-EOB-DTPA injection in patients with liver cirrhosis resulted in a decreased or even non-visualization of the biliary system using a three-point scale to grade biliary visualization.

Author Affiliations: Department of Radiology (Okada M, Ishii K, Hyodo T, Kumano S and Murakami T) and Department of Gastroenterology and Hepatology (Kitano M and Kudo M), Kinki University Faculty of Medicine, Osaka-Sayama, Osaka 589-8511, Japan; Gastroenterological Center, Yokohama City University Medical Center, Yokohama, Japan (Numata K)

Corresponding Author: Masahiro Okada, MD, Department of Radiology, Kinki University Faculty of Medicine, 377-2 Ohno-Higashi, Osaka-Sayama, Osaka 589-8511, Japan (Tel: +81-72-366-0221; Fax: +81-72-367-1685; Email: mokada@gaia.eonet.ne.jp)

Excretion of Gd-EOB-DTPA in the bile may be related to liver function, because of elimination from the liver after preferential uptake by hepatocytes. Regarding the relation between liver and biliary enhancement in the hepatobiliary phase, many questions remain to be answered, although new studies have attempted to determine the transporters for the enhancement in Gd-EOB-DTPA-enhanced MR.[10, 11] Thus, we should appreciate the property of Gd-EOB-DTPA to provide liver and biliary enhancement as liver function. And we think it is especially important that insufficient liver enhancement causes a lower detection rate of hepatocellular carcinoma (HCC) as a critical issue in patients with liver cirrhosis compared with those without liver cirrhosis in the hepatobiliary phase of Gd-EOB-DTPA.

Hence, the purpose of our study was to investigate whether the degree of biliary enhancement can allow the image evaluation of liver enhancement, which is necessary for the detection of liver tumors.

Methods

Patients

Between February and March 2008, forty consecutive patients underwent Gd-EOB-DTPA-enhanced MRI to evaluate focal hepatic lesions (Table 1). Thirty-five patients had chronic hepatitis or liver cirrhosis (19 had HCC), and 5 had normal liver function (3 had a hepatic metastatic lesion from colorectal cancer without chronic hepatitis or cirrhosis). None had undergone transcatheter arterial chemoembolization or radiofrequency ablation at least one month before MRI examination. None had biliary stones and biliary obstruction.

Patients were divided into two groups. Group 1 consisted of 20 patients with normal liver function and Child-Pugh class A, and group 2 consisted of 18 patients with Child-Pugh class B and 2 with Child-Pugh class C.

Table 1. Baseline characteristics of the 40 patients

Variables	Data
Median age (range, yr)	66 (28-86)
Sex (male/female)	24/16
Child-Pugh classification (A/B/C)	15/18/2
Normal liver function	5
Etiology of underlying liver disease	
HCV	26
HBV	3
Alcoholic	3
Cryptogenic	6
Colorectal cancer	2
Median serum total bilirubin level (range, mg/mL)	1.3 (0.2-3.8)

In each group, 20 consecutive patients were analyzed.

In addition, from receiver-operating characteristics (ROC) analysis, 1.8 mg/dL of total bilirubin was adopted as the cut-off value of insufficient biliary enhancement at 20 minutes post-injection according to Tschirch et al.[7] When all patients were separated into two groups by cut-off value (group 3: total bilirubin <1.8 mg/dL and group 4: total bilirubin ≥1.8 mg/dL), liver and biliary enhancement effects were compared.

This study was conducted in accordance with the principles of the *Declaration of Helsinki*.[12] The Ethics Committee at our institution deemed that approval of this study was unnecessary due to the retrospective character of the evaluation.

MR imaging

All patients underwent magnetic resonance (MR) imaging of the liver using a 1.5-Tesla system (Gyroscan NOVA, Philips Healthcare, Best, The Netherlands). An eight-channel phased-array surface coil was used and covered the whole liver. Gd-EOB-DTPA was used as a routine clinical study for detecting liver tumors. All patients received 25 μmol/kg body weight Gd-EOB-DTPA, which was administered at 2 mL/sec though an IV line placed in the cubital vein and flushed with 30-36 mL of 0.9% saline at 2 mL/sec. A fat-suppressed T1-weighted gradient echo (GRE) sequence as 3D turbo field echo provided as a T1 high-resolution isotropic volume examination (THRIVE; TR/TR=2.13/4.31, flip angle 15°, field of view (FOV) 306×380 mm, matrix 512×512, thickness 5 mm, acquisition time 20 seconds) was obtained for each patient before and at 5, 10, 15, and 20 minutes after injection of Gd-EOB-DTPA. We obtained the arterial phase with the bolus tracking system to image optimal arterial enhancement of liver tumors. But this study was used for the investigation of liver and biliary enhancement, therefore the arterial phase of Gd-EOB-DTPA was not analyzed for this purpose, because no biliary enhancement was seen at this phase.

As other MR sequences in our routine clinical examination, T1-weighted images of dual echoes (in-phase and out-of-phase) were obtained before enhancement in a single breath hold. After injection of Gd-EOB-DTPA, T2-weighted images with fat suppression and diffusion weighted images were obtained at 3 to 10 minutes.

Imaging analysis

Liver enhancement

One observer (15 years of experience in abdominal radiology) measured the liver enhancement by evaluating the signal intensity (SI) change of hepatic enhancement

for all patients on a Dicom viewer (Synapse; FujiFilm Medical, Tokyo, Japan). Quantitative liver enhancement was calculated in the form of liver-to-muscle ratio (LMR). To evaluate the SI change of liver parenchyma of the T1-weighted GRE image (THRIVE), LMRs between the SI of liver parenchyma and the SI of erector spinae muscle were calculated at 5, 10, 15 and 20 minutes after injection of Gd-EOB-DTPA. The SI of liver parenchyma was calculated as the mean value of five regions of interest (ROIs; 50-100 pixels, 3 ROIs in the right lobe and 2 in the left lobe), which were taken in the liver parenchyma with exclusion of focal lesions, major branches of the portal and hepatic veins, and artifacts in the lateral segment affected by heart beat. A ROI was placed on a homogeneous area of liver parenchyma for each slice. The SI of erector spinae was calculated as the mean value of four ROIs, which were taken from 2 ROIs in the right erector spinae and two in the left with exclusion of ambient fat and artifact. Finally, liver enhancement by LMR was calculated as follows:

$$LMR = SI_{liver} / SI_{muscle}$$

All LMRs were plotted over time, and mean and standard deviation (SD) were recorded.

Biliary enhancement

One observer (15 years of experience in abdominal radiology) measured the visualization of the common hepatic duct by evaluating the SI change of biliary enhancement for all patients on a Dicom viewer. The SI of biliary enhancement also used small ROIs within common hepatic ducts. Finally, bile duct-to-muscle ratio (BMR) was calculated as follows:

$$BMR = SI_{bile\ duct} / SI_{muscle}$$

All BMRs were plotted over time, and mean and SD were recorded.

In addition, comparison between groups 3 (total bilirubin <1.8 mg/dL) and 4 (total bilirubin ≥1.8 mg/dL) was performed to investigate the difference of liver and biliary enhancement at 20 minutes post-Gd-EOB-DTPA injection.

Tumor-to-liver ratio (TLR)

One observer (15 years of experience in abdominal radiology) measured the tumor intensity by evaluating the SI for all HCCs on a Dicom viewer. The SI of liver enhancement surrounding the HCC also used ROIs. Twenty-five HCCs (10 in group 1, 15 in group 2; >1 cm) in 19 patients were measured. Finally, TLR was calculated as follows:

$$TLR = SI_{tumor} / SI_{liver}$$

All TLRs were plotted over time, and mean and SD were recorded.

Estimated glomerular filtration rate (eGFR)

eGFR was measured and compared between groups 1 and 2, or groups 3 and 4. The following equations were used:

For men, eGFR (mL/min/1.73 m^2)=194×Cr$^{-1.094}$× age$^{-0.287}$

For women, eGFR (mL/min/1.73 m^2)=194×Cr$^{-1.094}$× age$^{-0.287}$×0.739

Cr: serum creatinine.

Statistical analysis

Scheffé's method of *post-hoc* test after two-way repeated-measures ANOVA was used to compare differences between the two groups (group 1 versus group 2, and group 3 versus group 4) in liver and biliary enhancement. The correlation between liver and biliary enhancement was investigated using Pearson's correlation test. The Statistical Package for Social Science Programming (version 11.0; SPSS, Chicago, IL) was used for analysis. A P value <0.05 was considered statistically significant.

Results

Liver enhancement provided as LMR

Repeated-measures ANOVA showed a significant difference between groups 1 and 2 (between-groups: P=0.0005, F=14.23; time-line: P=0.0001, F=75.02; confounding factor: P=0.0001, F=14.38). The LMR showed significant differences at all time points after Gd-EOB-DTPA injection between groups 1 and 2, using Scheffé's method (Table 2). Compared with group 1, the increase in SI of the LMR over time was delayed in group 2 (Figs. 1 and 2).

Biliary enhancement provided as BMR

Patients showed almost no apparent biliary enhancement at 5 minutes post-injection of Gd-EOB-DTPA. Repeated-measures ANOVA showed a significant difference between groups 1 and 2 (between-groups: P=0.0013, F=12.09; time-line: P=0.0001, F=76.24; confounding factor: P=0.0001, F=9.82). The BMR of the common hepatic duct between the two groups did not show a significant difference at 5 minutes, but did

Table 2. Liver enhancement: LMR of groups 1 and 2

Groups	5 min	10 min	15 min	20 min
1	1.48±0.17*	1.65±0.23**	1.79±0.24#	1.86±0.27##
2	1.37±0.23	1.38±0.27	1.47±0.29	1.56±0.31

*: P<0.03, **: P<0.0002, #: P<0.003, ##: P<0.003, compared with group 2.
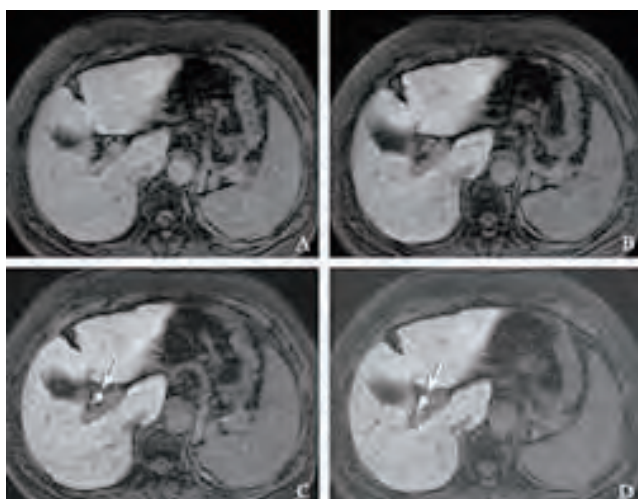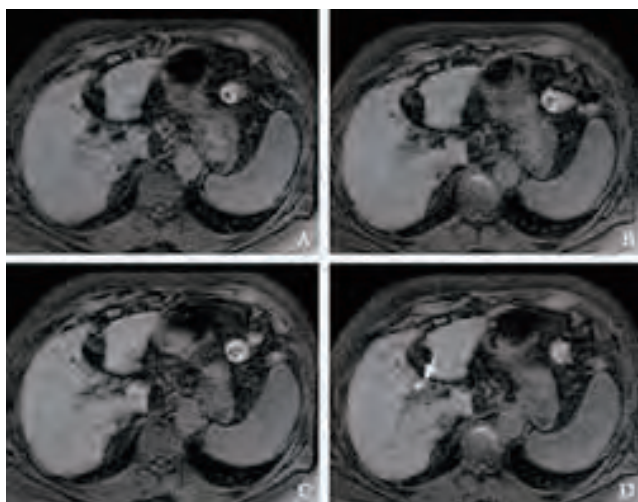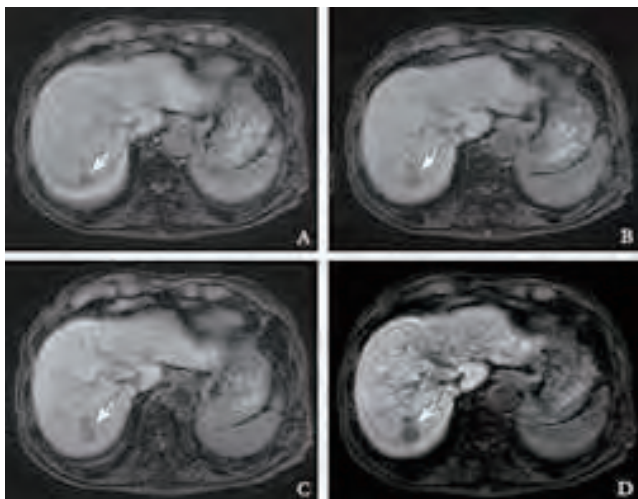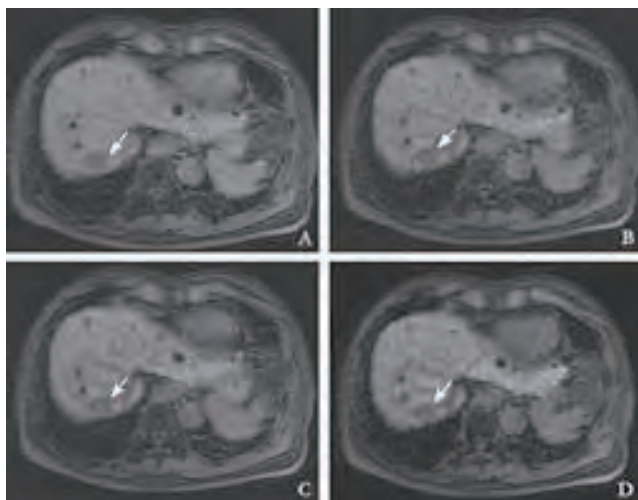
Fig. 1. Gd-EOB-DTPA-enhanced MRI from a 59-year-old woman (group 1) with hepatitis C liver cirrhosis (total bilirubin, 1.4 mg/dL). **A:** 5 minutes, **B:** 10 minutes, **C:** 15 minutes, **D:** 20 minutes post-Gd-EOB-DTPA injection. Fat-suppressed 3D T1-weighted GRE images in the transaxial plane demonstrating the liver and biliary enhancement over time. After 5 and 10 minutes (**A, B**), no biliary enhancement was seen. After 15 and 20 minutes (**C, D**), Gd-EOB-DTPA-enhanced MRI showed enhancement of the common hepatic duct (arrows; BMR: 5.67 at 15 minutes and 6.73 at 20 minutes). Liver enhancement LMR: 1.52 at 5 minutes, 1.67 at 10 minutes, 1.82 at 15 minutes and 1.95 at 20 minutes) gradually increased over time (**A-D**).

Fig. 2. Gd-EOB-DTPA enhanced MRI from a 75-year-old woman (group 2) with hepatitis C liver cirrhosis (total bilirubin, 3.6 mg/dL). **A:** 5 minutes, **B:** 10 minutes, **C:** 15 minutes, **D:** 20 minutes post-Gd-EOB-DTPA injection. Fat-suppressed 3D T1-weighted GRE images in the transaxial plane demonstrating the liver and biliary enhancement over time. After 5, 10 and 15 minutes (**A, B, C**), no biliary enhancement was seen. After 20 minutes (**D**), Gd-EOB-DTPA-enhanced MRI showed enhancement of the common hepatic duct (arrow; BMR: 3.38 at 20 minutes). Weak liver enhancement (LMR: 1.33 at 5 minutes, 1.39 at 10 minutes, 1.50 at 15 minutes and 1.54 at 20 minutes) was seen at each time point (**A-D**).

Table 3. Biliary enhancement: BMR of groups 1 and 2

Groups	5 min	10 min	15 min	20 min
1	1.10±0.52	3.26±2.17[*]	5.34±2.70[#]	6.38±2.18[##]
2	1.00±0.40	2.01±1.40	3.00±2.23	3.61±3.02

*: $P<0.02$, #: $P<0.002$, ##: $P<0.008$, compared with group 2.

Table 4. Liver and biliary enhancement: LMR and BMR of groups 3 and 4 at 20 minutes

Groups	LMR	BMR
3	1.92±0.29[*]	6.87±0.33[#]
4	1.44±0.26	3.25±0.31

*: $P<0.002$, #: $P<0.007$, compared with group 4.

Table 5. TLR of groups 1 and 2

Groups	5 min	10 min	15 min	20 min
1	0.69±0.04[*]	0.76±0.09	0.64±0.05	0.55±0.06[#]
2	0.83±0.02	0.83±0.03	0.79±0.02	0.74±0.03

*: $P<0.02$, #: $P<0.01$, compared with group 2.

show statistically significant differences at 10, 15 and 20 minutes by Scheffé's method (Table 3). Compared with group 1, the increase in SI of the BMR over time was delayed in group 2 (Figs. 1 and 2; Table 3).

Comparison between groups 3 and 4

At 20 minutes post-Gd-EOB-DTPA injection, significant differences between groups 3 and 4 were seen in both LMR and BMR (Table 4).

TLR

At 5 and 20 minutes post-Gd-EOB-DTPA injection, statistical differences between groups 1 and 2 were seen for TLR (Table 5). Figs. 3 and 4 show the comparison between groups 1 and 2.

Correlation between liver enhancement and biliary enhancement

At all time points, liver enhancement correlated with biliary enhancement in both groups by Pearson's correlation ($P<0.001$ at all time points, $r=0.94$ at 5 minutes, $r=0.73$ at 10 minutes, $r=0.61$ at 15 minutes and $r=0.63$ at 20 minutes).

eGFR

No significant difference was seen in the eGFRs of group 1 (78.9±15.1 mL/min/1.73 m^2) and group 2 (79.8± 22.2 mL/min/1.73 m^2). Moreover, groups 3 (79.2±18.2 mL/min/1.73 m^2) and 4 (79.4±23.5 mL/min/1.73 m^2) did not show significant difference.

Fig. 3. Gd-EOB-DTPA enhanced MRI from a 65-year-old woman (group 1) with cryptogenic liver disease (total bilirubin, 0.8 mg/dL). **A:** 5 minutes, **B:** 10 minutes, **C:** 15 minutes, **D:** 20 minutes post-Gd-EOB-DTPA injection. Fat-suppressed 3D T1-weighted GRE images in the transaxial plane demonstrating the HCC (arrows) and liver enhancement over time. Gd-EOB-DTPA-enhanced MRI showed the TLR gradually increased over time (**A-D**); 0.71 at 5 minutes, 0.73 at 10 minutes, 0.63 at 15 minutes and 0.52 at 20 minutes.

Fig. 4. Gd-EOB-DTPA-enhanced MRI from a 74-year-old woman (group 2) with hepatitis C liver cirrhosis (total bilirubin, 2.0 mg/dL). **A:** 5 minutes, **B:** 10 minutes, **C:** 15 minutes, **D:** 20 minutes post-Gd-EOB-DTPA injection. Fat-suppressed 3D T1-weighted GRE images in the transaxial plane demonstrating the HCC (arrows) and liver enhancement over time. Gd-EOB-DTPA-enhanced MRI showed the following TLR over time; 0.85 at 5 minutes, 0.83 at 10 minutes, 0.81 at 15 minutes and 0.81 at 20 minutes (**A-D**).

Discussion

Our results clearly revealed that the degree of biliary enhancement was related to that of liver enhancement in the hepatobiliary phase of Gd-EOB-DTPA-enhanced MRI. Therefore, strong enhancement of the bile duct substantially shows effective liver enhancement, which allows a higher detection rate of HCC in the normal or damaged liver. Both liver and biliary enhancement effects provide functional information about physiologic and pathologic biliary flow, and thus may be affected by liver function.

It is important to evaluate the liver enhancement, which is necessary for the detection of liver tumors on Gd-EOB-DTPA-enhanced MRI. We investigated the TLR between HCCs and liver parenchyma, and significant differences were observed at 5 and 20 minutes. Therefore, we believe unsatisfactory liver enhancement after Gd-EOB-DTPA injection leads to decreased detection of HCCs. However, the pathology of the HCCs was not obtained, because all were diagnosed by using the AASLD guidelines. Further analysis is recommended.

Liver and biliary enhancement at all time points post-Gd-EOB-DTPA injection had significant differences in SI between groups 1 and 2. This means the biliary enhancement may be closely correlated with liver enhancement in Gd-EOB-DTPA-enhanced MRI. At 5 minutes post-injection, a very close correlation ($r=0.94$) between liver and biliary enhancement was seen, and a relatively close correlation was observed at 10-20 minutes ($r=0.61$ to 0.73). In the hepatobiliary phase at 5 minutes, the uptake of Gd-EOB-DTPA by hepatocytes may be mixed with the extracellular distribution of this contrast agent. Therefore, in this phase at 5 minutes it is difficult to understand the mechanism of liver and biliary contrast enhancement. Whereas, the hepatobiliary phase between 10 and 20 minutes showed a relatively close correlation between liver and biliary enhancement. Thus biliary enhancement should be recognized as a biomarker of liver enhancement and as a useful method of clinical evaluation. The SI of the common hepatic duct became markedly elevated after the administration of Gd-EOB-DTPA in group 1 of our study, which was also reported by Carlos et al.[13] In addition, we found a difference between normal liver function and liver dysfunction in the elevated SI of the common hepatic duct at 15 and 20 minutes post-injection.

According to Tschirch et al,[7] only 40% of the cirrhosis group in the hepatobiliary phase was sufficient for anatomical visualization of the biliary tree after Gd-EOB-DTPA injection, although all subjects in the control group showed sufficient visualization. And they reported a significant difference between normal liver function and liver dysfunction at 10, 20 and 30 minutes for biliary enhancement. Their results motivated us

to undertake the quantitative investigation of not only biliary enhancement, but also liver enhancement. And our analysis demonstrated that biliary enhancement may be a biomarker of sufficient liver enhancement after Gd-EOB-DTPA injection. More importantly, impaired liver function can be suspected in patients with a reduced detection of liver tumor. Therefore, the grading of biliary enhancement may be a promising evaluation for insufficient liver enhancement, which may have a negative impact on detecting hepatic tumor. Visual evaluation of optimal liver enhancement is sometimes difficult in daily clinical MR practice. Thus, we suggest that the evaluation of biliary enhancement should be used as a biomarker of sufficient or insufficient liver enhancement.

Our result showed significant differences in biliary enhancement at 10, 15 and 20 minutes between groups 1 and 2, while Tschirch et al[7] reported a significant difference in biliary enhancement between normal liver function and liver dysfunction at 10, 20 and 30 minutes. Thus, our results are the same. Other researchers reported the relation between biliary enhancement in Gd-EOB-DTPA-enhanced MRI and liver function, whereas, to our knowledge, our study has quantitatively shown for the first time the close correlation between SI of the liver and the bile duct at each time point.

Patients with total bilirubin ≥1.8 mg/dL (group 4) showed poor visualization of the common bile duct in our study. This result (Table 4) was consistent with the comparison between groups 1 and 2 (Table 3) and compatible with previous reports.[7, 8] Multifactor evaluation of Child-Pugh classification includes a factor for total bilirubin, which may reflect the Child-Pugh class. Because total bilirubin is often used clinically due to the simple sampling, the judgement of effective contrast enhancement of the liver and the bile duct by total bilirubin may be reasonable.

It is known that Gd-EOB-DTPA is excreted in the biliary and renal systems. Because we investigated the effect of biliary enhancement compared to liver parenchymal enhancement, the difference of the renal excretion factor between groups could be excluded by measuring eGFR. In our study, no difference in renal function was observed between the groups.

In previous studies,[2, 13] biliary enhancement at 10-20 minutes post-injection of Gd-EOB-DTPA was enough in patients with a functionally unimpaired liver. In our study, group 1 showed a high enhancement effect on both liver and biliary enhancement, and a significant difference was seen between groups 1 and 2 at 10 minutes post-Gd-EOB-DTPA injection (Tables 2 and 3). The increase in SIs of LMR and BMR tended to be

delayed in group 2, as compared with group 1. Therefore, the changing rate of the SI over time is recognized as an important factor in time-intensity curve analysis for both liver and biliary enhancement on Gd-EOB-DTPA-enhanced MRI.

Our study has some limitations. First, the number of patients was relatively small. Second, we had no data from the indocyanine green (ICG) test, although the ICG retention rate at 15 minutes (ICG-R15) has been reported to be a significant predictor of the SI of the bile duct after Gd-EOB-DTPA injection.[8, 9] In our hospital, the ICG-R15 test is unusual to avoid the cumbersome procedure. Third, the hepatobiliary phase of the Gd-EOB-DTPA-enhanced MRI was only obtained up to 20 minutes, so the subsequent time-intensity courses of liver and biliary enhancement were not analyzed. However, we believe that 20 minutes post-Gd-EOB-DTPA injection is clinically standard and useful, because the liver-to-lesion contrast, such as in HCC detection, is best at 20 minutes as previously reported.[14]

In conclusion, patients with severe liver cirrhosis have a decreased visualization of the liver and bile duct during the hepatobiliary phase on Gd-EOB-DTPA-enhanced MRI. Thus, the degree of biliary enhancement has a close correlation to that of liver enhancement.

References

1 Ichikawa T, Saito K, Yoshioka N, Tanimoto A, Gokan T, Takehara Y, et al. Detection and characterization of focal liver lesions: a Japanese phase III, multicenter comparison between gadoxetic acid disodium-enhanced magnetic resonance imaging and contrast-enhanced computed tomography predominantly in patients with hepatocellular carcinoma and chronic liver disease. Invest Radiol 2010;45:133-141.

2 Hamm B, Staks T, Mühler A, Bollow M, Taupitz M, Frenzel T, et al. Phase I clinical evaluation of Gd-EOB-DTPA as a hepatobiliary MR contrast agent: safety, pharmacokinetics, and MR imaging. Radiology 1995;195:785-792.

3 Huppertz A, Balzer T, Blakeborough A, Breuer J, Giovagnoni A, Heinz-Peer G, et al. Improved detection of focal liver lesions at MR imaging: multicenter comparison of gadoxetic acid-enhanced MR images with intraoperative findings. Radiology 2004;230:266-275.

4 Mühler A, Heinzelmann I, Weinmann HJ. Elimination of gadolinium-ethoxybenzyl-DTPA in a rat model of

severely impaired liver and kidney excretory function. An experimental study in rats. Invest Radiol 1994;29:213-216.

5 Schuhmann-Giampieri G, Schmitt-Willich H, Press WR, Negishi C, Weinmann HJ, Speck U. Preclinical evaluation of Gd-EOB-DTPA as a contrast agent in MR imaging of the hepatobiliary system. Radiology 1992;183:59-64.

6 Ryeom HK, Kim SH, Kim JY, Kim HJ, Lee JM, Chang YM, et al. Quantitative evaluation of liver function with MRI Using Gd-EOB-DTPA. Korean J Radiol 2004;5:231-239.

7 Tschirch FT, Struwe A, Petrowsky H, Kakales I, Marincek B, Weishaupt D. Contrast-enhanced MR cholangiography with Gd-EOB-DTPA in patients with liver cirrhosis: visualization of the biliary ducts in comparison with patients with normal liver parenchyma. Eur Radiol 2008;18:1577-1586.

8 Takao H, Akai H, Tajima T, Kiryu S, Watanabe Y, Imamura H, et al. MR imaging of the biliary tract with Gd-EOB-DTPA: effect of liver function on signal intensity. Eur J Radiol 2011; 77:325-329.

9 Motosugi U, Ichikawa T, Sou H, Sano K, Tominaga L, Kitamura T, et al. Liver parenchymal enhancement of hepatocyte-phase images in Gd-EOB-DTPA-enhanced MR imaging: which biological markers of the liver function affect the enhancement? J Magn Reson Imaging 2009;30:1042-1046.

10 Tsuboyama T, Onishi H, Kim T, Akita H, Hori M, Tatsumi M, et al. Hepatocellular carcinoma: hepatocyte-selective enhancement at gadoxetic acid-enhanced MR imaging-- correlation with expression of sinusoidal and canalicular transporters and bile accumulation. Radiology 2010;255:824-833.

11 Narita M, Hatano E, Arizono S, Miyagawa-Hayashino A, Isoda H, Kitamura K, et al. Expression of OATP1B3 determines uptake of Gd-EOB-DTPA in hepatocellular carcinoma. J Gastroenterol 2009;44:793-798.

12 World Medical Association Declaration of Helsinki. Ethical principles for medical research involving human subjects. World Medical Association. Bull World Health Organ 2001; 79:373-374.

13 Carlos RC, Branam JD, Dong Q, Hussain HK, Francis IR. Biliary imaging with Gd-EOB-DTPA: is a 20-minute delay sufficient? Acad Radiol 2002;9:1322-1325.

14 Frericks BB, Loddenkemper C, Huppertz A, Valdeig S, Stroux A, Seja M, et al. Qualitative and quantitative evaluation of hepatocellular carcinoma and cirrhotic liver enhancement using Gd-EOB-DTPA. AJR Am J Roentgenol 2009;193:1053-1060.
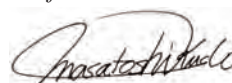
Editorial

Welcome to the First Issue of *Liver Cancer*

Prof. M. Kudo

Editor *Liver Cancer*

Hepatocellular carcinoma (HCC) is the sixth most common cancer and the third leading cause of cancer death worldwide. HCC is a peculiar malignant tumor that is completely different from other solid tumors because of its high recurrence rate after curative treatment (80% at 5 year). HCC arises in chronically damaged liver, i.e., in patients with chronic hepatitis or liver cirrhosis caused by viral hepatitis B or C or with nonalcoholic steatohepatitis-related cirrhosis. For HCC, therefore, it is easy to define the high-risk patient group. In Asia, approximately 80% of HCCs are related to infection with hepatitis B virus, which is endemic. The exception is Japan, where hepatitis C is more prevalent than hepatitis B. Japan is the only country that has experienced both hepatitis B-related HCC (around 30 years ago) and hepatitis C-related HCC (since the 1970s). The Liver Cancer Study Group of Japan (LCSGJ) was founded in 1965; in the 1980s, it started nationwide surveillance of HCC based on serum alpha-fetoprotein levels and ultrasound examinations.

There are many unresolved issues relating to HCC, including its pathogenesis, its molecular pathology, signal transduction during hepatocarcinogenesis, curative treatment (ablation, resection, or transplantation), palliative treatment (transarterial chemoembolization), hepatic arterial infusion chemotherapy, molecular targeted therapy, imaging diagnosis, early detection, and liver transplantation.

Sorafenib, which is an orally administered small-molecule tyrosine kinase inhibitor, targets vascular endothelial growth factor receptors, the platelet-derived growth factor receptor, and Raf kinase. Various other new molecular targeted agents and their combination with conventional therapies are currently under investigation.

Ongoing developments in diagnostic techniques and treatment strategies for HCC are reported in a wide range of journals, the fields of which depend on the medical backgrounds and areas of expertise of the authors (e.g., basic research, pathology, epidemiology, radiology, hepatology, surgery, and organ transplantation); a specific journal for reviews, updates, and discussion of research on HCC is lacking. *Liver Cancer* is the first international peer-reviewed journal of its kind to focus exclusively on basic and clinical research in the field of HCC, including the treatment and management of early, intermediate, and advanced HCC. *Liver Cancer* will start by publishing invited and submitted reviews quarterly. These will be followed by original articles addressing new issues in the field. Original articles describing basic and clinical research will be important resources for information exchange provided by this academic platform. This new journal will play an important role in generalizing and updating knowledge in the field of liver cancer.

You are invited to contribute articles to *Liver Cancer* describing your recent contributions to advances in the field.

npg

Activation of JNK and high expression level of CD133 predict a poor response to sorafenib in hepatocellular carcinoma

S Hagiwara[1], M Kudo[1], T Nagai[1], T Inoue[1], K Ueshima[1], N Nishida[1], T Watanabe[2] and T Sakurai*,[1]

[1]Department of Gastroenterology and Hepatology, Kinki University, 377-2, Osaka-Sayama, Osaka 589-8511, Japan; [2]Center for Innovation in Immunoregulative Technology and Therapeutics, Kyoto University Graduate School of Medicine, Kyoto, Japan

BACKGROUND: Hepatocellular carcinoma (HCC) ranks as the third leading cause of cancer deaths worldwide. While sorafenib, a multikinase inhibitor targeting the Raf/extracellular signal-regulated protein kinase (ERK) pathway, has been shown recently to provide a survival advantage to patients with advanced HCC, a predictive biomarker has not been developed. We studied whether c-Jun N-terminal kinase (JNK), which promotes liver carcinogenesis in mice, affects therapeutic response to sorafenib in HCC patients.
METHODS: We collected pathological specimens from 39 patients with advanced HCC before starting sorafenib treatment, and measured JNK activity in HCCs.
RESULTS: In patients treated with sorafenib, the expression of phospho-c-Jun in HCC, as a read out of JNK activity, was significantly higher ($P < 0.001$) in the non-responder group than in the responder group. c-Jun N-terminal kinase activation in HCC was associated with a decreased time to progression and a poor overall survival ($P = 0.0028$ and $P = 0.0008$, respectively).
CONCLUSION: In addition, JNK activity was significantly correlated with CD133 expression level. Correspondingly, high expression level of CD133 was linked to a poor response to sorafenib. Furthermore, D-JNKi, a specific JNK inhibitor, reduced the growth of xenografted CD133$^+$ cells in athymic mice. In conclusion, JNK activation was positively correlated with CD133 expression level and inversely correlated with the therapeutic response to sorafenib, suggesting that JNK activity may be considered as a new predictive biomarker for response to sorafenib treatment.
British Journal of Cancer (2012) **106,** 1997–2003. doi:10.1038/bjc.2012.145   www.bjcancer.com
Published online 17 May 2012
© 2012 Cancer Research UK

Molecular Diagnostics

Unlike most solid tumours, the incidence and mortality of hepatocellular carcinoma (HCC) have increased in the United States and Europe in the past decade. Most patients are diagnosed at advanced stages, so there is an urgent need for new systemic therapies. Studies in patients with lung, breast or colorectal cancers have indicated that the heterogeneity of cancer cells within a tumour affect its response to therapeutics designed to target-specific molecules. When tumour progression requires alterations in specific signalling pathways, drugs that selectively block them might slow tumour growth. Identification of molecules that mediate tumour progression, and trials that monitor them as biomarkers, might lead to personalised therapy; reagents that interfere with signalling pathways required for HCC progression might be used to treat selected populations, and thereby maximise the efficacy and cost benefit. However, no specific alterations are yet known to be implicated in HCC progression, so it is important to improve our understanding of its molecular pathogenesis.

Mitogen-activated protein kinases (MAPKs), serine/threonine-specific protein kinases, respond to extracellular stimuli and have a pivotal role in various cellular processes, such as gene expression, mitosis, differentiation, proliferation and cell survival/apoptosis (Chang and Karin, 2001; Dhillon et al, 2007). Mitogen-activated protein kinase comprises the extracellular

signal-regulated protein kinase (ERK), c-Jun N-terminal kinase (JNK) and p38MAPK. Accumulating evidence suggests that activation or inactivation of MAPK regulates inflammatory responses and provides a growth advantage to hepatocytes during malignant transformation and liver tumourigenesis (Sakurai et al, 2006, 2008; Hui et al, 2007; Whittaker et al, 2010). Abnormal activation of ERK is often observed in human HCC. It has been shown that systemic administration of sorafenib, a tyrosine kinase inhibitor targeting the Raf/ERK pathway, extended the survival of patients with advanced-stage HCC significantly in several clinical trials (Abou-Alfa et al, 2006; Llovet et al, 2008). Mouse cancer models have shown that the JNK pathway is implicated in regulating liver carcinogenesis. c-Jun N-terminal kinase activation contributes to hepatocyte proliferation and HCC development by regulating cyclin D and vascular endothelial growth factor (VEGF), a potent proangiogenic substance responsible for tumour neovascularisation (Schwabe et al, 2003; Sakurai et al, 2006; Sakurai and Kudo, 2011). c-Jun, a downstream target of JNK, promotes chemically induced liver cancer development through suppression of the p53 pathway (Eferl et al, 2003). Proliferation of HCC cells requires JNK-dependent downregulation of p21 (Hui et al, 2008). However, the extent of the involvement of JNK in the development of human liver cancers is unknown. Recently, we have reported that activation of JNK in non-cancerous liver tissue predicts a high risk of recurrence after hepatic resection for hepatocellular carcinoma, suggesting the importance of JNK in human HCC (Hagiwara et al, 2011).

A novel theory in the field of tumour biology postulates that the capacity to maintain tumour formation and growth is found in a small population of cells, called tumour-initiating cells or cancer stem cells. The stem cell-like characteristics of these cells are believed to render these cells resistant to conventional therapies and allow them to drive tumourigenesis. CD133, a transmembrane glycoprotein, is a valuable marker of cancer stem cell and is expressed in 1–5% of human HCC, while absent in normal liver cells (Ma *et al*, 2007). In addition to its role as a marker, CD133 has been reported to play a functional part in regulating tumourigenesis of liver cancer stem cells via regulating IL-8, CXCL1 and ERK signalling (Tang *et al*, 2011).

PATIENTS AND METHODS

Patients

From May 2009 to June 2010, 39 patients with refractory HCC, which could not be controlled by standard therapeutic modalities, received sorafenib (Nexavar; Bayer HealthCare Pharmaceuticals-Onyx Pharmaceuticals, Leverkusen, Germany) at Kinki University Hospital. All pathological specimens of HCC were taken by needle biopsy before sorafenib treatment.

The study protocols conformed to the ethical guidelines of the 1975 Declaration of Helsinki and were approved by the institutional review boards. Written informed consent was obtained from all patients for subsequent use of their collected tissues.

Eligibility criteria, treatment regimen and assessment of response to sorafenib

The eligibility criteria for sorafenib therapy were (1) advanced HCC, which was uncontrollable with standard treatments, or HCC with distant metastasis; (2) age <81 years; (3) an Eastern Cooperative Group performance status of 0 or 1; (4) Child-Pugh grade A; (5) encephalopathy degree 0; (6) leukocyte count >3000 cells mm^{-3}, haemoglobin level >10 g dl^{-1}, platelet count $>80\,000$ cells mm^{-3}; and (7) serum creatinine <1.5 mg dl^{-1}, serum aspartate aminotransferase <200 IU l^{-1}, serum alanine aminotransferase <200 IU l^{-1} and serum total bilirubin <3.0 mg dl^{-1}. These criteria were based on the susceptibility to adverse side effects. The diagnosis of HCC was made based on haematoxylin–eosin staining of histopathological specimens in all patients.

Sorafenib was given orally at a daily dose of 800 mg, divided into two equal doses. Treatment interruptions and up to two dose reductions (first to 400 mg once daily and then to 400 mg every 2 days) were permitted for drug-related adverse effects (National Cancer Institute-Common Terminology Criteria (NCI-CTC, version 3)). Treatment was continued until the occurrence of radiologic progression, as defined by the Response Evaluation Criteria in Solid Tumors (RECIST, Version 1.1).

Assessed by contrast enhanced computed tomography or magnetic resonance imaging every 4 weeks, therapeutic response to sorafenib was defined according to the criteria of RECIST (Version 1.1). A partial response (PR) was defined as at least 30% decrease in the sum of the longest diameter of target lesions with the baseline sum of the longest diameter of target lesions as the reference. Progressive disease (PD) was defined as at least 20% increase in the sum of the longest diameter of target lesions. Stable disease (SD) was defined as meeting neither PR nor PD criteria. When the response achieved for intrahepatic HCC differed from that for extrahepatic HCC, the worse response was determined as the achieved response. Assessment of response was introduced best overall response of RECIST.

Immunohistochemistry

Immunohistochemical analysis was performed on paraffin sections of human HCC and mouse tumours. Immunohistochemical staining was carried out with antibodies raised against phospho-c-Jun (Ser63; 1:100), phospho-JNK (1:100) and CD133 (1:100) from Cell Signaling Technology (Danvers, MA, USA) and visualised using Dako LSAB System-HRP (Dako, Carpinteria, CA, USA). Five fields of images per sample were taken and total and stain-positive nuclei were counted by Image J software (NIH, Bethesda, MD, USA).

Western blot analysis

To prepare tissue lysate, HCC tissue was homogenised with CelLytic-MT Mammalian Tissue Lysis/Extraction reagent (Sigma-Aldrich, St Louis, MO, USA) with protease inhibitor, Complete (Roche Diagnostics, Mannheim, Germany), and phosphatase inhibitor (Toyobo, Osaka, Japan) and centrifuged. Equal protein amounts of tissue lysates were electrophoresed through a reducing SDS polyacrylamide gel and electroblotted onto a PVDF membrane. The membrane was blocked and incubated with primary antibodies for CD133, phospho-c-Jun, c-Jun, phospho-ERK1/2, ERK1/2 from Cell Signaling Technology (Beverly, MA, USA) and β-actin (Sigma-Aldrich). The levels of each protein were detected with horseradish peroxidase-linked secondary antibodies and the ECL plus System (GE Healthcare, Piscataway, NJ, USA). To evaluate the signal intensity, obtained western blot image data were quantified using Image J software (NIH).

Inoculation of sorted CD133$^+$ HCC cells into nude mice

Human liver cancer cell line HepG2 and HuH7 obtained from the Riken Cell Bank (Tsukuba, Japan) were cultured in DMEM with 100 U ml^{-1} penicillin, 100 μg ml^{-1} streptomycin and 10% (FBS) at 37 °C under 5% CO$_2$/95% air. For isolating CD133-positive and -negative cells, cells were collected by trypsin treatment, washed twice with 1% BSA/PBS and labelled with anti-CD133-allophyco-cyanin antibody (Miltenyi Biotec, Bergisch Gladbach, Germany) for 20 min on ice, in the dark. Then, cells were washed once in ice-cold 1% BSA/PBS, and sorted on a FACS Vantage SE (BD, San Diego, CA, USA). CD133-positive and -negative cells were collected separately, washed with PBS and cultured under normal condition for 5 days. Cells were collected by trypsin treatment and suspended in mixture of DMEM and Matrigel (BD) (1:1), and injected. CD133$^+$ cells were subcutaneously inoculated into 6-week-old female BALB/c nude mice. From 1 week after subcutaneous inoculation, TAT control peptide and D-JNKi were administered at 25 nmol per mouse once a week and the mice were autopsied 4 weeks later. D-JNKi is an efficient inhibitor of the action of all three JNK isoforms and is made by linking the 20 amino-acid terminal JNK-inhibitory sequence (i.e., the JNK-binding domain of JIP-1/IB1) to a 10-amino acid HIV-TAT transporter sequence.

All animal procedures were performed according to approved protocols and in accordance with the recommendations for the proper care and use of laboratory animals. The Medical Ethics Committee of Kinki University School of Medicine approved the present study.

Statistical analysis

Relationships between the parameters of the patients treated with sorafenib were investigated using Student's *t*-test, the Mann–Whitney *U*-test and Fisher's exact test. Cumulative survival and time-to-progression (TTP) curves were constructed using the Kaplan–Meier method and compared using the log-rank test. The relationship between numeric data (e.g., number on PCNA-positive tumour cells) was determined using Student's *t*-test.

Molecular Diagnostics

— 264 —

All analyses were performed using the SPSS software (version 11.5; SPSS Inc., Chicago, IL, USA).

RESULTS

Association between JNK activation and poor therapeutic response to sorafenib

Among 39 patients treated, a complete response and PR was achieved in 0 (0%) and 5 (12.8%), respectively. The overall response rate was 12.8%. Stable disease was noted in 13 patients (33%), and the disease control rate (complete response + PR + SD) was 46.2%. Progressive disease was noted in 17 patients (43.6%). Four patients were excluded from the assessment of response because they died of rupture of HCC or of oesophageal varices after the start of treatment and computed tomography could not be performed. No significant difference was observed in any of nine parameters such as age, sex, the cause of disease, tumour grade or previous therapy, between the responder group and the non-responder group (Table 1). We evaluated the change in tumour blood flow by using CT scan to confirm how sorafenib worked. In 13 out of 18 responders (72%), arterial blood supply was decreased while in 8 out of 17 non-responders (47%) the arterial blood flow was decreased.

We investigated the association between the therapeutic response to sorafenib and JNK activation using HCC specimens collected before treatment. As shown in Figure 1, phospho-JNK/c-Jun expression in HCC cells was significantly higher in the non-responder group than in the responder group.

Association between JNK activation and poor prognosis in patients treated with sorafenib

The median TTP was 2.0 months (95% confidence interval: 0–7.9 months). The cumulative progression-free survival rates at 3, 6 and 12 months were 49%, 44% and 29%, respectively. All enrolled patients were also included in a survival assessment. Twenty-five patients were still alive at the end of the observation period (median: 6.0 months, range: 1.3–12.1 months), while 14 patients had died. The causes of death were tumour progression ($n = 10$) and rupture of HCC or oesophageal varices ($n = 4$). The median survival time was 12.1 months (95% confidence interval: 7.9–16.4 months). The cumulative survival rate at 3, 6 and 12 months were 81%, 75% and 56%, respectively.

We examined the impact of JNK activation in HCC cells on the prognosis of patients treated with sorafenib. Hepatocellular carcinoma specimens collected by needle biopsy before sorafenib treatment were stained with anti-phospho-c-Jun antibody and the data were quantified. Patients were divided into high and low p-c-Jun expression groups by setting the median level as the cutoff between the two groups. As shown in Figure 2A, a log-rank test using the Kaplan–Meier method showed significant TTP prolongation in the low p-c-Jun expression group, compared with the high expression group ($P = 0.0028$). We also found significant prolongation of overall survival (OS) in the low p-c-Jun expression group compared with the high expression group ($P = 0.0008$; Figure 2B). The duration of sorafenib treatment was 151 ± 116 days in the low p-c-Jun group and 80 ± 97 days in the high p-c-Jun group.

Table 1 Comparison of patient characteristics according to the anticancer effect

Variable	Responder (PR + SD) ($n = 18$)	Non-responder (PD) ($n = 17$)	P-value
Age – years	70.5 (54–78)	74 (35–80)	0.95
Sex – no. (%)			1
Male	13 (72)	12 (71)	
Female	5 (28)	5 (29)	
Cause of disease – no. (%)			0.82
Hepatitis B	3 (17)	4 (24)	
Hepatitis C	9 (50)	9 (53)	
Non-B, non-C	6 (33)	4 (24)	
ECOG performance status – no. (%)			0.49
0	18 (100)	16 (94)	
1	0 (0)	1 (6)	
BCLC stage – no. (%)			0.51
B (intermediate)	11 (61)	8 (47)	
C (advanced)	7 (39)	9 (53)	
Tumour grade – no. (%)			0.62
Well	2 (11)	0 (0)	
Moderate	11 (61)	12 (71)	
Poor	5 (28)	5 (29)	
AFP (ng ml^{-1}) – median (range)	276 (2–22 619)	89 (3–228 540)	0.56
DCP (mAU ml^{-1}) – median (range)	641 (5–26 624)	481.5 (9–61 180)	0.93
Previous therapy (last) – no. (%)			0.09
OP	1 (6)	5 (29)	
RFA	1 (6)	2 (12)	
TACE	11 (61)	10 (59)	
HAIC	3 (17)	0 (0)	
None	2 (11)	0 (0)	

Abbreviations: ECOG = Eastern Cooperative Oncology Group; BCLC = Barcelona Clinic Liver Cancer; AFP = α-fetoprotein; DCP = des-γ-carboxyprothrombin; OP = operation; RFA = radiofrequency ablation; TACE = transcatheter arterial chemoembolization; HAIC = hepatic arterial chemotherapy using implanted port system; PR = partial response; SD = stable disease; PD = progressive disease.

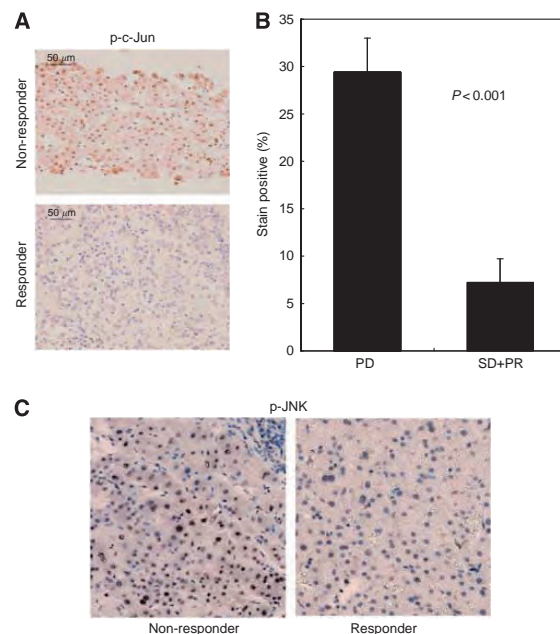**Figure 1** Association between JNK activation and poor therapeutic response in HCC. (**A**) Expression of phospho-c-Jun in HCC of patients with poor response (PD, $n = 18$) and favourable response to sorafenib (PR, SD, $n = 17$). Paraffin-embedded liver sections were immunostained with anti-phospho-c-Jun antibody. (**B**) Frequency of phospho-c-Jun-positive cells in HCCs. Data are the mean values ± s.e. (**C**) Expression of phospho-JNK in HCC of patients with poor response (PD) and favourable response to sorafenib (PR, SD). Paraffin-embedded liver sections were immunostained with anti-phospho-JNK antibody.
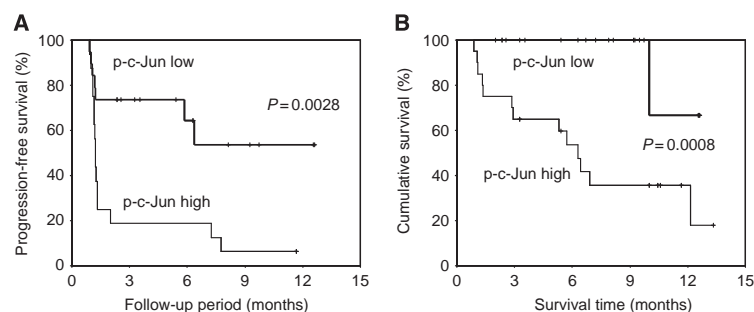
Molecular Diagnostics

Figure 2 Association between JNK activation, decreased time to progression and OS in patients treated with sorafenib. The Kaplan–Meier method was used to determine progression-free survival (**A**) and cumulative survival (**B**). The log-rank test was used to compare progression-free survival and cumulative survival between patients grouped according to phospho-c-Jun expression levels.
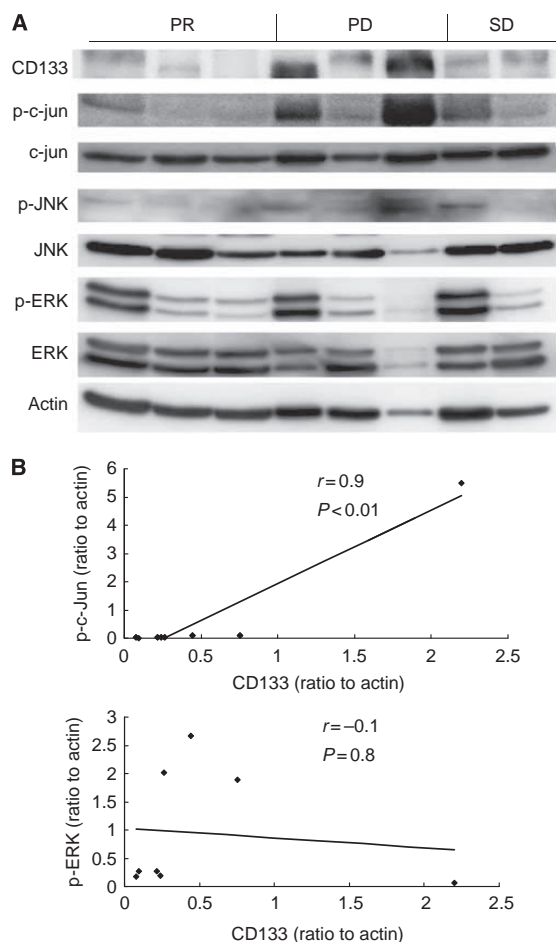
Figure 3 Relationship between CD133, p-c-Jun, p-JNK and p-ERK expression levels in HCCs. (**A**) Lysates of human HCCs were gel separated and analysed by immunoblotting with antibodies to the indicated proteins. (**B**) There was a significant positive correlation between CD133 and p-JNK/c-Jun expressions. There was no significant correlation between CD133 and p-ERK expressions.
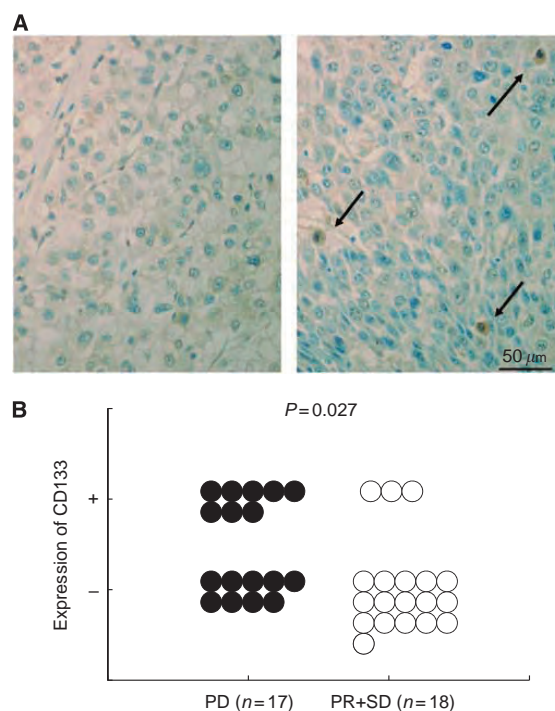
Figure 4 Correlation between CD133 expression and response to sorafenib. (**A**) Expression of CD133 in HCCs. Representative immunostaining of cases who exhibited PR (left) and PD (right). Paraffin-embedded liver sections were immunostained with anti-CD133 antibody. (**B**) Among 17 non-responders (PD), 8 cases exhibited CD133-positive cells. Among 18 responders (PR or SD), only three cases exhibited CD133-positive cells.

Association between JNK activation and CD133 expression in human HCCs

In patients treated with sorafenib, expressions of CD133, phospho-c-Jun and phospho-ERK were examined. Hepatocellular carcinomas positive for CD133 was also positive for phospho-c-Jun and phospho-JNK (Figure 3A). There was a significant positive correlation between CD133 and phospho-c-Jun expressions ($r = 0.854$ and $P = 0.007$). In contrast, there was no correlation

between CD133 and phospho-ERK expressions ($r = 0.254$ and $P = 0.544$) (Figure 3B).

In patients treated with sorafenib, correlation between CD133 expression and efficiency of sorafenib treatment was examined. Among 17 objective non-responders (PD), 8 cases exhibited CD133-positive cells. In contrast, among 18 objective responders (PR or SD), only 3 cases exhibited CD133-positive cells. There was a significant correlation between CD133 expression and response to sorafenib ($P = 0.027$) (Figure 4B). According to the status of HCC at the initiation of sorafenib treatment, patients were classified as B (intermediate) or C (advanced) using Barcelona Clinic Liver Cancer (BCLC) staging system. There was no

significant difference in JNK activity or CD133 positivity between BCLC stage B and stage C HCCs (data not shown).

We utilised FACS sorting to isolate CD133-positive and CD133-negative cells from HepG2 cells. CD133$^+$ cells and CD133$^-$ cells were inoculated subcutaneously at 8×10^4 cells per body into nude mice. From 1 week after subcutaneous inoculation, TAT control peptide and D-JNKi were administered at 25 nmol per mouse once a week and the mice were autopsied 4 weeks later. After autopsy, the volume of tumours was measured. CD133$^+$ cells could efficiently initiate tumours in mude mice compared with CD133$^-$ cells (Figure 5A). CD133$^+$ HepG2 cells produced large tumours in 100% of mice whereas CD133$^-$ cell fractions produced only small
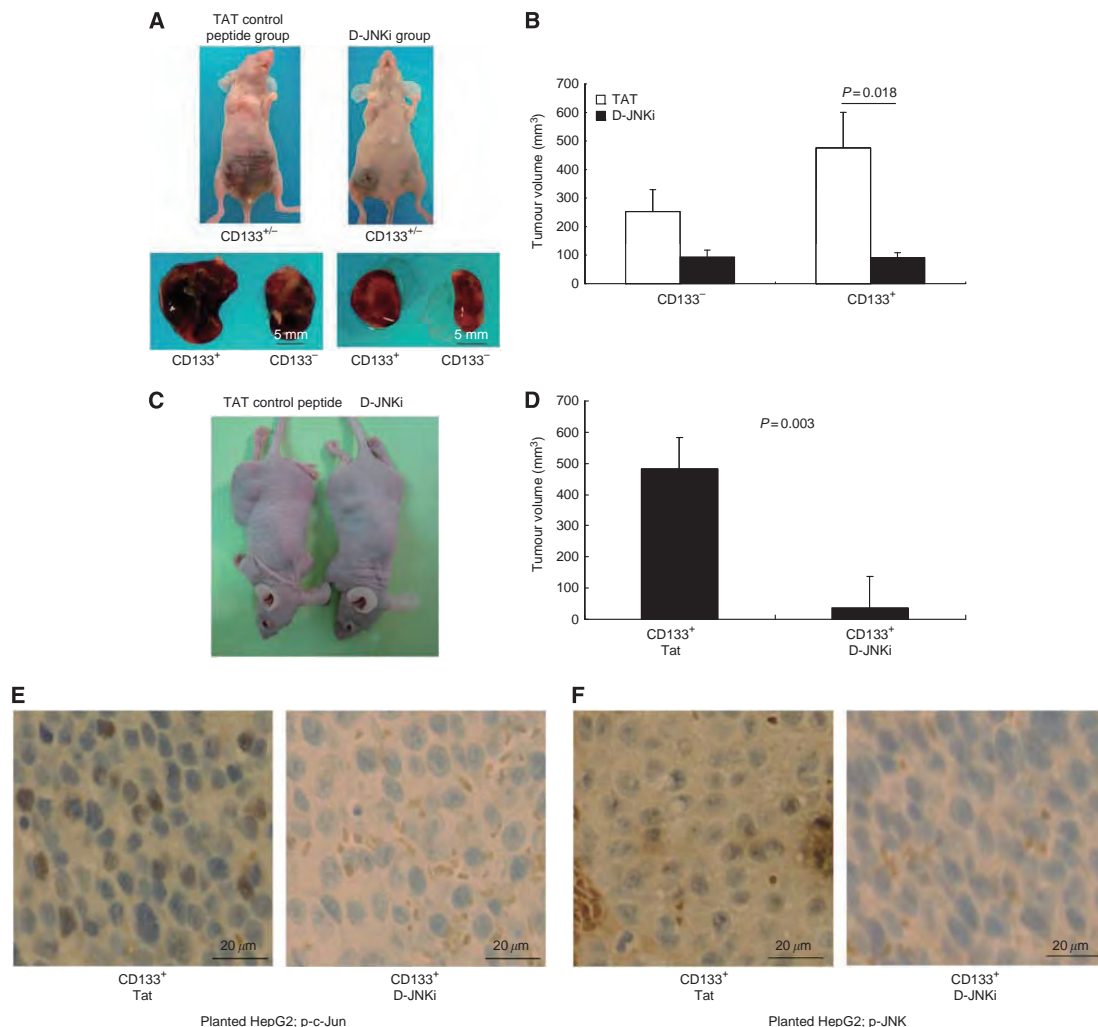
Figure 5 Effect of a JNK inhibitor on tumourigenic potential of CD133$^+$ HCC cells. (**A**) HepG2 cells positive or negative for CD133 were inoculated subcutaneously at 8×10^4 cells per body into nude mice ($n = 8$). From 1 week after subcutaneous inoculation, TAT control peptide and D-JNKi, a specific JNK inhibitor, were administered at 25 nmol per mouse once a week and the mice were autopsied 4 weeks later. Representative nude mice with subcutaneous tumours derived from CD133$^+$ (left) and CD133$^-$ (right) HepG2 cells. (**B**) Tumourigenicity of CD133$^+$ or CD133$^-$ HepG2 cells treated with D-JNKi or control Tat protein. (**C**) HuH7 cells positive for CD133 were inoculated subcutaneously at 1×10^6 cells per body into nude mice ($n = 6$). From 1 week after subcutaneous inoculation, TAT control peptide and D-JNKi were administered at 25 nmol per mouse once a week and the mice were autopsied 4 weeks later. Representative nude mice with subcutaneous tumours were shown. (**D**) Tumourigenicity of CD133$^+$ HuH7 cells treated with D-JNKi or control Tat protein. (**E**) Expression of phospho-c-Jun in xenografted tumours treated with D-JNKi or control protein. (**F**) Expression of phospho-JNK in xenografted tumours treated with D-JNKi or control protein.
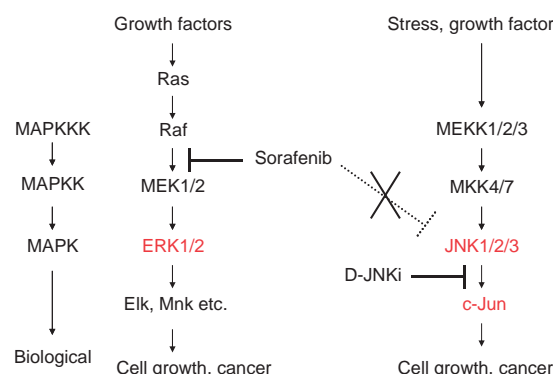
Figure 6 Association between sorafenib and the MAPK cascade. Sorafenib inhibits the Raf/ERK signalling pathway but not the JNK signalling pathway. The therapeutic efficacy of sorafenib would be limited when JNK is activated in HCCs. Treatment with sorafenib in combination with a JNK inhibitor might open promising therapeutic perspectives.

tumours in 50% of mice. On the other hand, mice treated with D-JNKi showed a marked reduction in tumour-initiating capacity of CD133$^+$ cells to the same level as in CD133$^-$ cells (Figure 5B). Similar results were obtained using another HCC cell line, a HuH7 cell (Figure 5C and D). Indeed, D-JNKi suppressed the expression of p-c-Jun and p-JNK in HCC (Figure 5E and F) and p-c-Jun in HepG2 cells (Supplementary Figure 1).

DISCUSSION

The therapeutic options for advanced-stage HCC are limited because HCC responds poorly to systemic treatments such as conventional chemotherapy and radiotherapy. Cancer stem cells may be more resistant to chemotherapeutic agents than differentiated tumour cells possibly owing to an increased expression of adenosine triphosphate-binding cassette transporters and anti-apoptotic proteins (Jordan *et al*, 2006). Thus, the development of an effective strategy to target cancer stem cell pools together with conventional chemotherapies is essential to eradicate a tumour mass (Dean *et al*, 2005). Recently, a CD133$^+$ subpopulation of multipotent cells with extensive proliferative and self-renewal abilities was identified as cancer stem cells and was proven to contribute to the initiation and growth of HCC (Ma *et al*, 2007). Here, we showed that CD133 expression level is correlated with JNK activity and predicts response to sorafenib in human HCC. In addition, pharmacologic inhibition of JNK has reduced tumour-initiating capacity of CD133$^+$ cells, suggesting that JNK activation in CD133$^+$ HCC cells enhances their tumourigenic capacity. Given that increased JNK activity contributes to proliferative advantage (Sakurai *et al*, 2006; Hui *et al*, 2008), the majority of HCC cells differentiated from CD133$^+$ HCC cells with increased JNK activity

would inherit the phenotype and exhibit the enhanced JNK activation.

Surrogate biomarkers that predict the biological and clinical efficacy of sorafenib will help tailor treatment on an individual patient basis. The predictive value of Raf/MEK/ERK signalling activity for the efficacy of sorafenib in HCC remains uncertain (Abou-Alfa *et al*, 2006; Calvisi *et al*, 2006; Newell *et al*, 2009). To date, a robust predictive biomarker has not been developed. In this study, we found a strong correlation between elevated JNK activity and poor therapeutic response to sorafenib. Evaluation of JNK activity in HCC can be useful to differentiate between responders and non-responders before starting sorafenib treatment and help to select patients who are likely to benefit from the treatment. In addition to ERK-mediated HCC cell growth, sorafenib also targets tumour angiogenesis by inhibiting the receptor tyrosine kinases of VEGF receptor (VEGFR)-1, VEGFR-2, VEGFR-3 and platelet-derived growth factor receptor α and β and stem cell factor receptor (KIT) (Wilhelm *et al*, 2004, 2006). Thus, the extent of angiogenesis might be a biomarker that can predict clinical efficacy of sorafenib. However, there was no significant relationship between tumour angiogenesis as assessed by CD31 staining and the therapeutic response to sorafenib (data not shown). c-Jun N-terminal kinase activity should be an independent predictive biomarker for sorafenib efficacy although this study is based on limited data of 39 patients from a single institution and further studies are needed to validate its value. Furthermore, we demonstrated that elevated JNK activity in HCC was associated with poor prognosis of patients treated with sorafenib. The ERK and JNK signalling pathways would activate mutually exclusive downstream molecules to contribute to HCC development. Consistently, JNK activation partially rescued sorafenib-induced cell toxicity, but was not sufficient to confer resistance to sorafenib (Supplementary Figure 2). These data suggest the possibility of using a JNK inhibitor as a second-line treatment of advanced HCC (Figure 6). In this study, we found that in human HCC, the activation of JNK and high expression level of CD133 are associated with resistance to sorafenib. CD133 expression level is linked to JNK activity whose inhibition significantly reduces tumourigenesis of human CD133$^+$ HCC cells after xenotransplantation. Our results demonstrate the importance of JNK in human HCC, and the potential application of JNK targeting for HCC therapy.

REFERENCES

Abou-Alfa GK, Schwartz L, Ricci S, Amadori D, Santoro A, Figer A, De Greve J, Douillard JY, Lathia C, Schwartz B, Taylor I, Moscovici M, Saltz LB (2006) Phase II study of sorafenib in patients with advanced hepatocellular carcinoma. *J Clin Oncol* **24:** 4293–4300

Calvisi DF, Ladu S, Gorden A, Farina M, Conner EA, Lee JS, Factor VM, Thorgeirsson SS (2006) Ubiquitous activation of Ras and Jak/Stat pathways in human HCC. *Gastroenterology* **130:** 1117–1128

Chang L, Karin M (2001) Mammalian MAP kinase signalling cascades. *Nature* **410:** 37–40

Dean M, Fojo T, Bates S (2005) Tumour stem cells and drug resistance. *Nat Rev Cancer* **5:** 275–284

Dhillon AS, Hagan S, Rath O, Kolch W (2007) MAP kinase signalling pathways in cancer. *Oncogene* **26:** 3279–3290

Eferl R, Ricci R, Kenner L, Zenz R, David JP, Rath M, Wagner EF (2003) Liver tumor development. c-Jun antagonizes the proapoptotic activity of p53. *Cell* **112:** 181–192

Hagiwara S, Kudo M, Chung H, Ueshima K, Inoue T, Haji S, Watanabe T, Park AM, Munakata H, Sakurai T (2011) Activation of JNK in the

non-cancerous tissue predicts a high risk of recurrence after hepatic resection. *Hepatol Res* **42**: 394–400

Hui L, Bakiri L, Mairhorfer A, Schweifer N, Haslinger C, Kenner L, Komnenovic V, Scheuch H, Beug H, Wagner EF (2007) p38alpha suppresses normal and cancer cell proliferation by antagonizing the JNK-c-Jun pathway. *Nat Genet* **39**: 741–749

Hui L, Zatloukal K, Scheuch H, Stepniak E, Wagner EF (2008) Proliferati on of human HCC cells and chemically induced mouse liver cancers requires JNK1-dependent p21 downregulation. *J Clin Invest* **118**: 3943–3953

Jordan CT, Guzman ML, Noble M (2006) Cancer stem cells. *N Engl J Med* **355**: 1253–1261

Llovet JM, Ricci S, Mazzaferro V, Hilgard P, Gane E, Blanc JF, de Oliveira AC, Santoro A, Raoul JL, Forner A, Schwartz M, Porta C, Zeuzem S, Bolondi L, Greten TF, Galle PR, Seitz JF, Borbath I, Häussinger D, Giannaris T, Shan M, Moscovici M, Voliotis D, Bruix J, SHARP Investigators Study Group (2008) Sorafenib in advanced hepatocellular carcinoma. *N Engl J Med* **359**: 378–390

Ma S, Chan KW, Hu L, Lee TK, Wo JY, Ng IO, Zheng BJ, Guan XY (2007) Identification and characterization of tumorigenic liver cancer stem/ progenitor cells. *Gastroenterology* **132**: 2542–2556

Newell P, Toffanin S, Villanueva A, Chiang DY, Minguez B, Cabellos L, Savic R, Hoshida Y, Lim KH, Melgar-Lesmes P, Yea S, Peix J, Deniz K, Fiel MI, Thung S, Alsinet C, Tovar V, Mazzaferro V, Bruix J, Roayaie S, Schwartz M, Friedman SL, Llovet JM (2009) Ras pathway activation in hepatocellular carcinoma and anti-tumoral effect of combined sorafenib and rapamycin *in vivo*. *J Hepatol* **51**: 725–733

Sakurai T, He G, Matsuzawa A, Yu GY, Maeda S, Hardiman G, Karin M (2008) Hepatocyte necrosis induced by oxidative stress and IL-1 alpha release mediate carcinogen-induced compensatory proliferation and liver tumorigenesis. *Cancer Cell* **14**: 156–165

Sakurai T, Kudo M (2011) Signaling pathways governing tumor angiogenesis. *Oncology* **81**(Suppl): 24–29

Sakurai T, Maeda S, Chang L, Karin M (2006) Loss of hepatic NF-kappa B activity enhances chemical hepatocarcinogenesis through sustained c-Jun N-terminal kinase 1 activation. *Proc Natl Acad Sci USA* **103**: 10544–10551

Schwabe RF, Bradham CA, Uehara T, Hatano E, Bennett BL, Schoonhoven R, Brenner DA (2003) c-Jun-N-terminal kinase drives cyclin D1 expression and proliferation during liver regeneration. *Hepatology* **37**: 824–832

Tang KH, Ma S, Lee TK, Chan YP, Kwan PS, Tong CM, Ng IO, Man K, To KF, Lai PB, Lo CM, Guan XY, Chan KW (2011) CD133(+) liver tumor-initiating cells promote tumor angiogenesis, growth and self-renewal through neurotensin/ IL-8/ CXCL1 signaling. *Hepatology* **55**: 807–820

Whittaker S, Marais R, Zhu AX (2010) The role of signaling pathways in the development and treatment of hepatocellular carcinoma. *Oncogene* **29**: 4989–5005

Wilhelm S, Carter C, Lynch M, Lowinger T, Dumas J, Smith RA, Schwartz B, Simantov R, Kelley S (2006) Discovery and development of sorafenib: a multikinase inhibitor for treating cancer. *Nat Rev Drug Discov* **5**: 835–844

Wilhelm SM, Carter C, Tang L, Wilkie D, McNabola A, Rong H, Chen C, Zhang X, Vincent P, McHugh M, Cao Y, Shujath J, Gawlak S, Eveleigh D, Rowley B, Liu L, Adnane L, Lynch M, Auclair D, Taylor I, Gedrich R, Voznesensky A, Riedl B, Post LE, Bollag G, Trail PA (2004) BAY 43-9006 exhibits broad spectrum oral antitumor activity and targets the RAF/ MEK/ERK pathway and receptor tyrosine kinases involved in tumour progression and angiogenesis. *Cancer Res* **64**: 7099–7109

Molecular Diagnostics

REGULAR PAPER

Mechanical Model Analysis for Quantitative Evaluation of Liver Fibrosis Based on Ultrasound Tissue Elasticity Imaging

Tsuyoshi Shiina, Tomonori Maki, Makoto Yamakawa, Tsuyoshi Mitake, Masatoshi Kudo, and Kenji Fujimoto

REGULAR PAPER

Mechanical Model Analysis for Quantitative Evaluation of Liver Fibrosis Based on Ultrasound Tissue Elasticity Imaging

Tsuyoshi Shiina, Tomonori Maki, Makoto Yamakawa[1], Tsuyoshi Mitake[2], Masatoshi Kudo[3], and Kenji Fujimoto[4]

Human Health Sciences, Graduate School of Medicine, Kyoto University, Kyoto 606-8507, Japan
[1] *Advanced Biomedical Engineering Research Unit, Kyoto University, Kyoto 606-8501, Japan*
[2] *Hitachi Aloka Medical Ltd., Kashiwa, Chiba 227-0804, Japan*
[3] *Department of Gastroenterology and Hepatology, Kinki University School of Medicine, Osakasayama, Osaka 589-8511, Japan*
[4] *Department of Internal Medicine, National Hospital Organization, Minami-Wakayama Medical Center, Tanabe, Wakayama 646-8558, Japan*

Precise evaluation of the stage of chronic hepatitis C with respect to fibrosis has become an important issue to prevent the occurrence of cirrhosis and to initiate appropriate therapeutic intervention such as viral eradication using interferon. Ultrasound tissue elasticity imaging, i.e., elastography can visualize tissue hardness/softness, and its clinical usefulness has been studied to detect and evaluate tumors. We have recently reported that the texture of elasticity image changes as fibrosis progresses. To evaluate fibrosis progression quantitatively on the basis of ultrasound tissue elasticity imaging, we introduced a mechanical model of fibrosis progression and simulated the process by which hepatic fibrosis affects elasticity images and compared the results with those clinical data analysis. As a result, it was confirmed that even in diffuse diseases like chronic hepatitis, the patterns of elasticity images are related to fibrous structural changes caused by hepatic disease and can be used to derive features for quantitative evaluation of fibrosis stage. © 2012 The Japan Society of Applied Physics

1. Introduction

Chronic liver damage attributable to hepatitis C virus (HCV) infection results in hepatic fibrosis, which progresses towards cirrhosis, leading to hepatocellular carcinoma, and more than 40,000 people every year die of cirrhosis and hepatic carcinoma in Japan.[1] Thus, a precise evaluation of the stage of chronic hepatitis C with respect to fibrosis is an important issue to prevent the occurrence of cirrhosis and to initiate appropriate therapeutic intervention such as viral eradication using interferon.[2]

At present, liver biopsy is still the gold standard for the assessment of liver fibrosis. However, it is an invasive method associated with patient discomfort and, in rare cases, with serious complications.[3,4] In addition, the accuracy of liver biopsy is limited because of significant intra- and interobserver variability and sampling errors.[5–7] Therefore, research has been focused on the development of non-invasive methods for the assessment of liver fibrosis.

Diagnostic imaging using B-mode images has been conventionally applied for the diagnosis of liver disease. However, it is not easy to diagnose at its early stage using conventional B-mode images because we have to read subtle changes of speckle patterns, which are not sensitive to the stage of fibrosis.

To overcome this problem, there has been considerable research on quantitative assessment of liver fibrosis based on ultrasonography, such as echo signal processing and texture analysis methods.[8,9] Yamaguchi and coworkers[10–12] have recently proposed a method of evaluating the stage of fibrosis using the deviation of echo amplitude distribution from the Rayleigh distribution of a normal liver.

From the viewpoint of directly measuring the stiffness of liver tissue, we investigated the application of tissue elasticity imaging to the evaluation of fibrosis stage. Ultrasonic tissue elasticity imaging can provide us novel diagnostic information based on tissue hardness.[13–15] Although the first practical system was developed by Shiina *et al.*[13] for tumor diagnosis, Fujimoto *et al.* have recently reported that the pattern of an elasticity image becomes patchy as fibrosis progresses in the case of diffuse diseases

such as chronic hepatitis.[16] We also proposed the index of liver fibrosis (LF index), which was derived from elasticity images and showed that there was a good correlation between the LF index and the degree of liver fibrosis.[16–18]

To evaluate fibrosis progression quantitatively on the basis of a strain image, it is important to clarify how fibrosis progression affects the mechanical properties of liver tissues and is consequently expressed in an elasticity image. In this study, we introduced a mechanical model of fibrosis progression and simulated the process by which hepatic fibrosis affects elasticity images and compared the results with clinical data analysis. As a result, it was confirmed that even in diffuse diseases like chronic hepatitis, the pattern of an elasticity image is related to the fibrous structure caused by hepatic disease and can be used to derive features for quantitative evaluation of fibrosis stage.

2. Experimental Methods

2.1 Evaluation of liver fibrosis by ultrasound tissue elasticity imaging

It is well known that chronic liver disease causes hepatic fibrosis, which is characterized by an unusual accumulation of extracellular matrix materials produced by fibroblast-like cells including stellate cells in the hepatic parenchyma. Diagnosing chronic liver disease in the early stage is necessary for the treatment of liver disease because hepatic cirrhosis often leads to other diseases such as liver cancer. In terms of the stage of chronic hepatitis, the new Inuyama scoring system was used, which was proposed by the Japanese Liver Study Group in 1994.[19] The new Inuyama scoring system classifies chronic hepatitis into five fibrosis stages (F0–F4) on the basis of the extent of the spreading fibrosis and four grades (A0–A3) on the basis of the degree of inflammation and necrosis using liver biopsy samples, as shown in Table I.

Recently, ultrasound systems for the measurement and imaging of tissue elasticity have been developed as noninvasive methods to evaluate the degree of liver fibrosis, providing alternatives to liver biopsy. FibroScan® (transient elastography) detects the propagation speed of a shear wave transmitted from a probe through the liver and calculates the

© 2012 The Japan Society of Applied Physics

Table I. New Inuyama scoring system.

|	Staging (fibrosis)		Grading (necrosis and inflammation)
F0	No fibrosis	A0	No
F1	Fibrous portal expansion	A1	Mild
F2	Bridging fibrosis	A2	Moderate
F3	Bridging fibrosis with lobular degeneration	A3	Severe
F4	Cirrhosis		

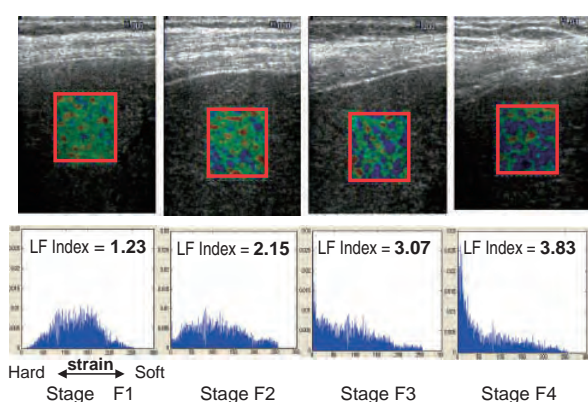Fig. 1. (Color) Display method of elasticity image.

Fig. 2. (Color) Elasticity images (strain) superimposed on B-mode (top) and histogram of the strain distribution within ROI (bottom) for each fibrosis stage of chronic hepatitis.

shear modulus of the liver to evaluate the degree of liver fibrosis.[20] Although FibroScan® is simple and easy to use and displays the results on a monitor immediately, it also has many limitations. It cannot be used in patients with narrow intercostal spaces, hepatic atrophy, and ascites since shear waves will not propagate through flues.[21,22] In addition, it is difficult to locally evaluate the degree of fibrosis since the result is based on one-dimensional information (1 line) only.

Ultrasound tissue elasticity imaging is developed for the visual assessment of tissue elasticity, especially for cancer diagnosis. The first practical system was developed by us and employs the algorithm referred to as the combined autocorrelation method proposed by Shiina.[23,24] The method can rapidly calculate a 2-dimensional distribution of tissue deformation, i.e., strain induced by external freehand compression with the probe or by internal heartbeats. In hard tissue, the amount of strain is low, whereas in soft tissue, the amount of strain is higher because soft tissue can be compressed more than hard tissue. However, the strain represents the relative hardness since it changes with compression level. For stable display of the strain distribution free of compression variation, the strain is normalized by the mean value within the region of interest (ROI), ε_0, and displayed with a translucent color superimposed on the B-mode image (soft: red/mean: green/hard: blue), as illustrated in Fig. 1. This method was commercialized in 2003, and referred to as the Real-Time Tissue Elastography® (RTE).[15] At present, several companies have released tissue elasticity imaging systems and different methods for imaging are adopted.

This technology has already been proved to be diagnostically valuable in detecting tumors of the breast, prostate, and other organs.[25] We found that the texture of the elasticity image (strain) of chronic hepatitis becomes a patchy pattern as liver fibrosis progresses and the images could be categorized into the four stages, as shown in Fig. 2.[16,17] The strain induced by heartbeats (diastole) is used to perform RTE. Hepatic fibrosis progresses towards cirrhosis, which causes the fine liver lobule structure to change to a coarse nodular structure stage by stage. The size of the nodules and the volume of the fibers changes with the progression of the disease. Considering this process of fibrosis, it is expected that fibrosis causes inhomogeneous distribution of tissue hardness, which produces a nonuniform texture pattern of strain images.

However, there are limitations to quantitative evaluation of the texture pattern by visual judgement. To increase objectivity, we extract nine image features, as shown in Fig. 3. First of all, the ROI was fixed to a rectangle of about $30 \times 20\,\text{mm}^2$. Pixel data in the colored strain image was
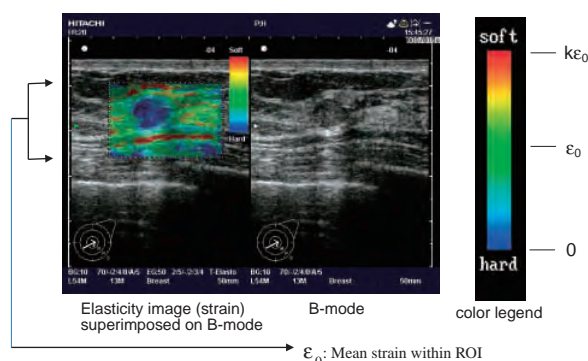
transformed into a histogram. Finally, we performed multiple regression analysis to derive the LF index in terms of four major features as follows:

$$\text{LF index} = a_1 \text{ MEAN} + a_2 \text{ SD} + a_3 \text{ \%AREA} + a_4 \text{ COMP.} \quad (1)$$

Four major features were defined as follows: MEAN is the mean of the relative (normalized by ε_0) strain value and SD is the standard deviation of the relative strain value, which are calculated from the strain histogram. The strain image is transformed into a binary image, then a blue (or low-strain) area, which indicates a hard area, is detected. %AREA indicates the percentage of the low-strain area or white region in Fig. 3(c) in the ROI. COMP is the complexity of the shape of an extracted low-strain area and is defined by eq. (1),

$$\text{COMP} = \frac{L^2}{S}, \quad (2)$$

where L and S are the boundary length and the area of the low-strain region, respectively.

Thus far, we have performed RTE on 310 cases including 295 patients with chronic hepatitis C and 15 healthy volunteers. As a result, the coefficients of the LF index, $a_1 = -0.00897$, $a_2 = -0.00502$, $a_3 = 0.0232$, and $a_4 =$
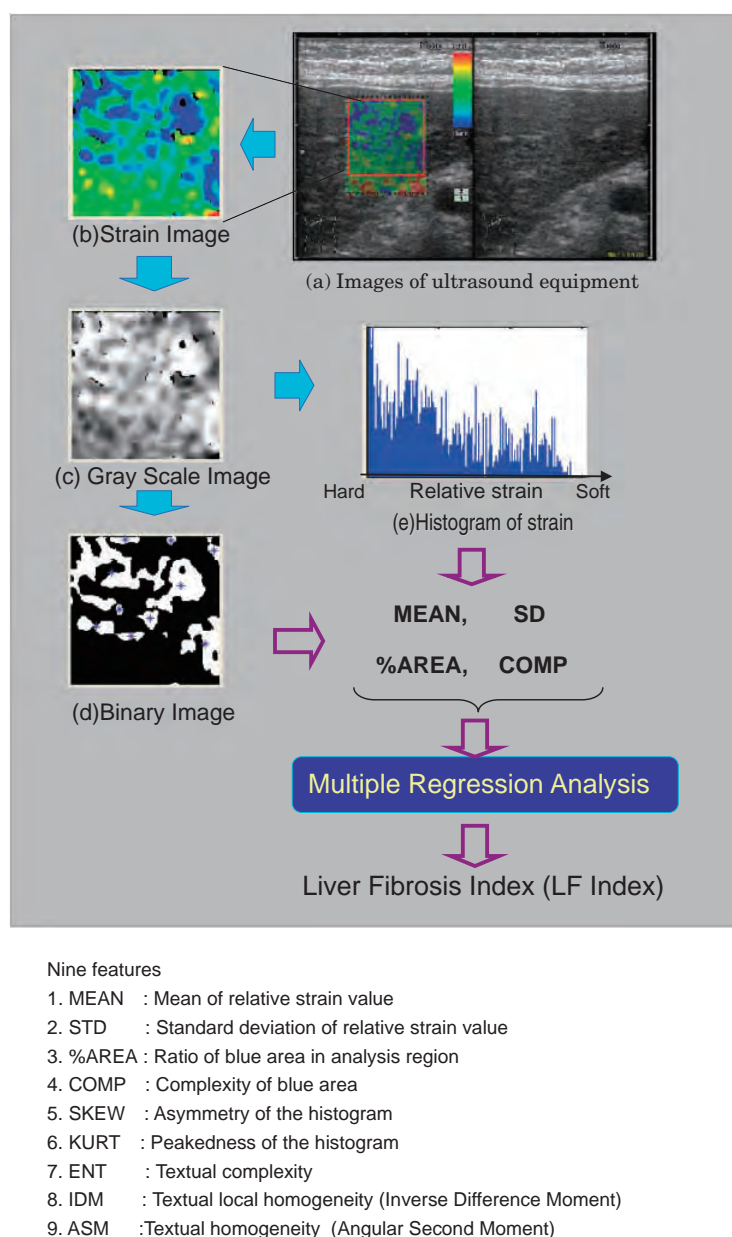
Nine features
1. MEAN   : Mean of relative strain value
2. STD   : Standard deviation of relative strain value
3. %AREA : Ratio of blue area in analysis region
4. COMP   : Complexity of blue area
5. SKEW   : Asymmetry of the histogram
6. KURT   : Peakedness of the histogram
7. ENT   : Textual complexity
8. IDM   : Textual local homogeneity (Inverse Difference Moment)
9. ASM   :Textual homogeneity (Angular Second Moment)

Fig. 3.   (Color) Extraction of image features from strain image and liver fibrosis index (LF index) for quantitative evaluation of fibrosis progression.

0.0253 were obtained. It was confirmed that the LF index highly correlated with the fibrous stage, as shown in Fig. 2.[16]

2.2   Mechanical model analysis of liver fibrosis
To clarify how fibrosis progression affects the elasticity image of chronic hepatitis, we analyzed the relation by simulating the process with a mechanical model of hepatic fibrosis. At first, the structural changes of liver tissue with fibrous progression are simulated, as shown in Fig. 4. Next, the changes in tissue stiffness and deformation by compression are simulated. Finally, the imaging process and feature extraction by RTE are conducted to compare the results with clinical data.

2.2.1   Modeling of tissue structure changes
The human liver is composed of many hexagonal structures termed liver lobules and containing a central vein. Fibrosis progression is accompanied by changes in tissue structure. When fibrosis progresses, the lobules are destroyed and replaced by regenerative nodules.

In terms of the modeling of the liver tissue structure changes caused by fibrous progression, Yamaguchi *et al.* have carried out much research and proposed a model using the potential distribution.[11] We referred to the potential distribution model as the initial part to simulate tissue structure changes. In this model, scatterers are distributed densely on the local minimum region of the monomodal potential function as expressed by eq. (3) and
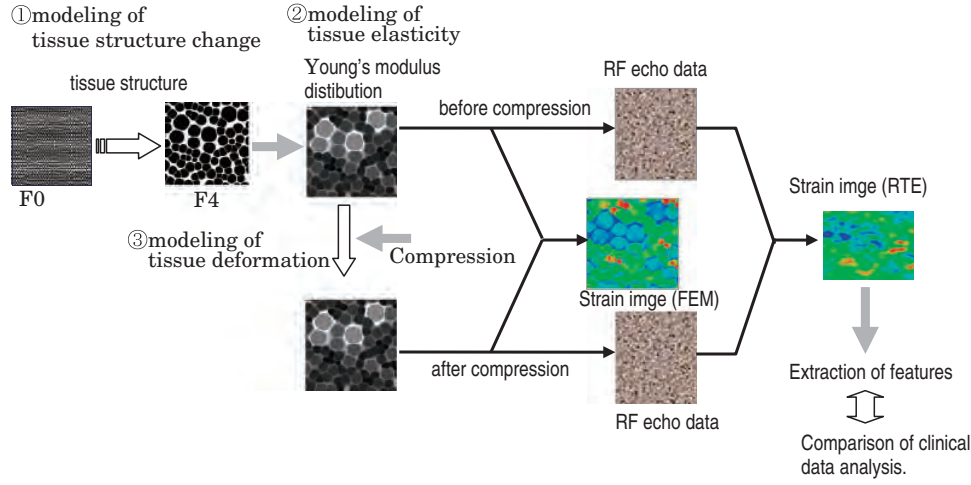
Fig. 4. (Color) Analysis of liver fibrosis progression and its influence on strain imaging using mechanical model.

the position of its peak corresponds to central points of the liver nodule:

$$p(r) = p_{max} \sin\left(\frac{\pi}{2} k^r\right), \qquad (3)$$

where r is the distance from the central point, p_{max} is the maximal value, and k is the form parameter that determines the distribution spread. The parameter p_{max} of all the potentials is randomly set to a value from 0.8 to 1.2 as an initial condition and k is set to $0.02 + 0.002 p_{max}$ as experimentally estimated values as discussed in ref. 11.

To simulate the process by which liver tissue changes from lobules to nodules, the randomly selected central point, r_m, conjugates with its nearest central point, r_n, generating a new central point, r'_m, and a new potential, $p_{max}(r'_m)$, as follows:

$$r'_m = \frac{\alpha r_n + \beta r_m}{\alpha + \beta}, \qquad (4)$$

$$p_{max}(r'_m) = \alpha + \beta, \qquad (5)$$

where $\alpha = p_{max}(r_m)$, $\beta = p_{max}(r_n)$.

As a result, fiber tissues generated by conjugation are represented as the minimum region of the potential distribution.

2.2.2 Modeling of tissue elasticity

To simulate tissue deformation, the finite element method (FEM) is applied to the tissue model. For FEM analysis, the ROI ($30 \times 30\,\mathrm{mm}^2$) is divided in a reticular pattern and 500×500 elements; consequently, the element size was $0.06 \times 0.06\,\mathrm{mm}^2$, which can attain the adequate spatial resolution for the strain image. First of all, values of Young's modulus are assigned to each grid point of the structural model in §2.2.1 as follows:

$$E_p(x, y) = \alpha(p_{max} - \bar{p}_{max,normal})^n + E_{normal}$$
$$\text{(for parenchyma)}, \qquad (6)$$
$$E_f(x, y) = \beta(p_{neighbor,max} - \bar{p}_{max,normal})^n + E_{normal}$$
$$\text{(for fibrous region)}, \qquad (7)$$

where the parenchyma represents the region of the lobule

Table II. Elastic modulus of liver tissues measured at each fibrous stage. Values in top, middle, and bottom rows are cited from refs. 26, 27, and 28, respectively (unit: kPa).

	F0	F1	F2	F3	F4
	<5	7	13	18	22
Young's modulus[a]	4.2	6.9	8.9	14.8	26.5
	5.5		6.4	10.0	30.0

a) Measured by FibroScan®.

and nodule except for the fibrous region. $\bar{p}_{max,normal}$ is the average of the maximal value of each potential for a normal liver model, and E_{normal} is the average of Young's modulus on the parenchyma of a normal liver model. $p_{neighbor,max}$ is defined as

$$p_{neighbor,max} = p_{max,k} \quad \text{for}$$
$$\left\{ k \mid \max\left(\frac{p_{max,i}}{d_i^2}\right), \ i = 1, 2, \dots, M \right\}$$

where $p_{max,i}$ $(i = 1, 2, \dots, M)$ are the maximal values of the potential neighbor to the grid point located within the fibrous region and d_i is the distance between the grid point and each central point of the potential.

Here, E_{normal} is set to 4 [kPa] using the values experimentally measured using FibroScan®, as shown in Table II.[26–28] The parameters α and β indicate the contribution ratio of the potential to Young's modulus. The parameter n regulates the rate of stiffness increase, that is, in the case of $n = 1$, E increases in proportion to the conjugated potential, and in the case of $n = 2$, E increases nonlinearly.

2.2.3 Modeling of tissue deformation

The Young's modulus distribution model is compressed from the top with a pressure, which causes a slight strain approximately equal to that of clinical examination (about 1%), and the Poisson ratio of the tissue model is set to 0.49. The tissue deformation, that is, the movement of each node of the element, is simulated by FEM assuming the two-dimensional stress state. Displacement of nodes along the axial direction is calculated by comparison of two frame
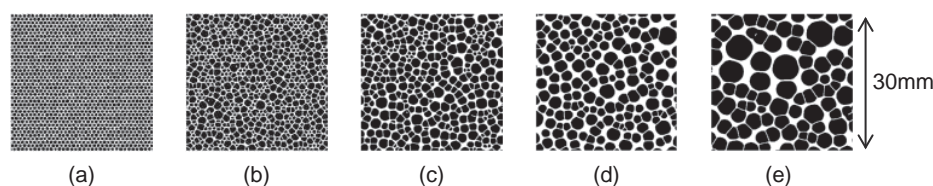
Fig. 5. Simulated tissue structure change caused by the fibrosis progression: (a) stage F0 (Normal): the number of central points is 2538 (the ratio of the number of the central points to that of initial central points is 1), (b) stage F1: 1269 (1/2), (c) stage F2: 635 (1/4), (d) stage F3: 317 (1/8), and (e) stage F4: 159 (1/16).
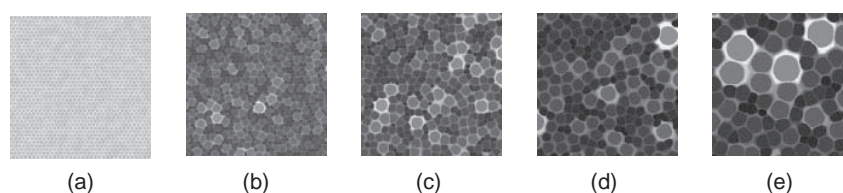

Fig. 6. Young's modulus distribution assigned to tissue structural model: (a) stage F0 (the range of the assigned values of Young's modulus: $E = 0$–5 kPa), (b) stage F1 ($E = 0$–18 kPa), (c) stage F2 ($E = 0$–30 kPa), (d) stage F3 ($E = 0$–72 kPa), and (e) stage F4 ($E = 0$–120 kPa).

data before and after compression. Then, the strain is calculated by differential processing of the displacement. The obtained strain distribution is color-coded and displayed as in RTE.

2.2.4 Feature extraction

For the purpose of evaluating how the tissue stiffness change caused by fibrosis progression is related to the strain distribution, the strain image is directly reconstructed from displacement by FEM analysis in §2.2.3. It is necessary to simulate the signal processing of ultrasound equipment (RTE), since in practice, the strain distribution must be estimated from echo signals.

The number of scatterers distributed within 30×30 mm^2 was set to 4500, that is, the density is 5 points/mm^2 and the scattering coefficient is set on the basis of the tissue structural model. The position of each scatterer after compression is obtained from the position of nodes by FEM analysis. RF echo signals are generated using the transmitted pulse with a Gaussian envelope, a center frequency of 5 MHz, and a duration of 0.4 mm. The beam width is set to 0.8 mm.

Then, the strain distribution is calculated by the combined autocorrelation method and the normalized strain is color-coded as RTE. Finally, four major features were extracted from the strain image and the LF index was calculated to compare the results with clinical cases.

3. Results and Discussion

Figure 5 illustrates the fibrous structures of a normal liver and a liver with chronic hepatitis obtained by modeling of tissue structure change. A two-dimensional model was applied and 2538 central points were distributed within an area $(40 \times 40$ mm$^2)$; in other words, liver lobules were located at a mean interval of 0.8 mm. Figure 5(a) presents a normal liver, and Figs. 5(b)–5(e) depict the liver tissue structural changes as fibrosis progresses. The number of iterations does not indicate the physical characteristic of the

Table III. Comparison of elastic modulus between model and measured values (unit: kPa).

	F0	F1	F2	F3	F4
Mean values of Young's modulus set to the model	4.0	6.2	10.0	17.1	35.7
Young's modulus[a]	4.9	6.5	9.4	14.3	26.2

a) Measured by FibroScan®. Averaged values from refs. 26–28.

liver directly, but is selected only to determine the size of nodules. Here, the conjugation process was repeated until the number of central points reduced to 1/2 (for stage F1), 1/4 (F2), 1/8 (F3), and 1/16 (F4) of the initial central points simply assuming that the average numbers of conjugations are 1, 2, 3, and 4, for each stage. We can observe that the sizes of the nodules and the widths of the fibers increase with the progression of liver fibrosis and inhomogeneous structures are also evident in serious cases.

Figure 6 illustrates the Young's modulus distribution assigned to the models in Fig. 5. The range of Young's modulus values for each image is indicated at the Fig. 6 legend. The parameters in eqs. (6) and (7) were set to $n = 1$ and $\alpha = \beta = 1.3$, so that the mean values of Young's modulus assigned for each stage were close to the values measured by FibroScan®, as shown in Table III.

As fibrosis progresses, the maximum potential p_{max} becomes higher, so the assigned values of Young's modulus $E(x, y)$ increase accordingly owing to eqs. (5) and (6). As a result, it can be seen that the region around a large nodule has large values of Young's modulus in Fig. 6, namely, it becomes hard.

The tissue model shown in Fig. 6 was compressed from the top by applying 50 Pa (1.25% of $E_{normal} = 4$ kPa) in the axial direction. Then, strain images were obtained, as shown in Fig. 7. The top images are strain images reconstructed directly from the displacement obtained by FEM analysis. The bottom images are estimated from the echo signals
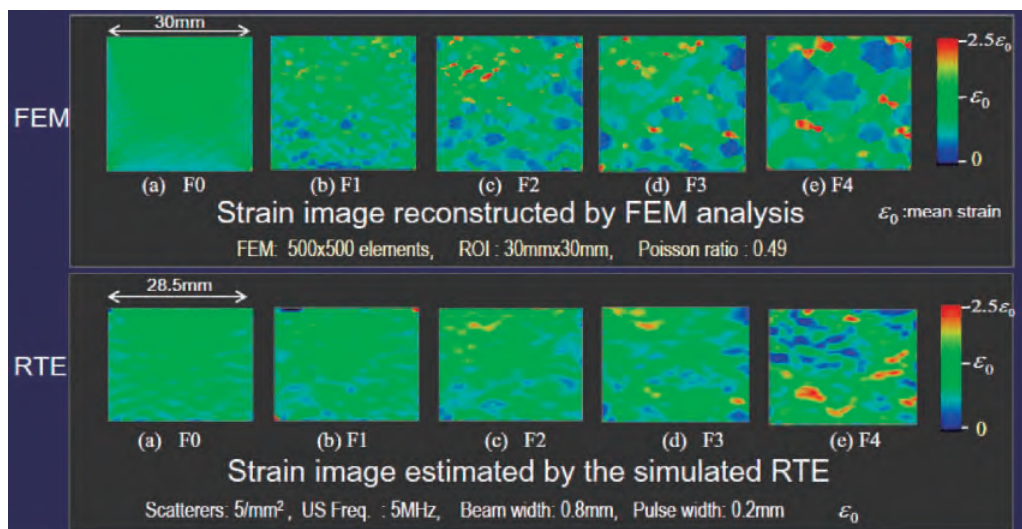
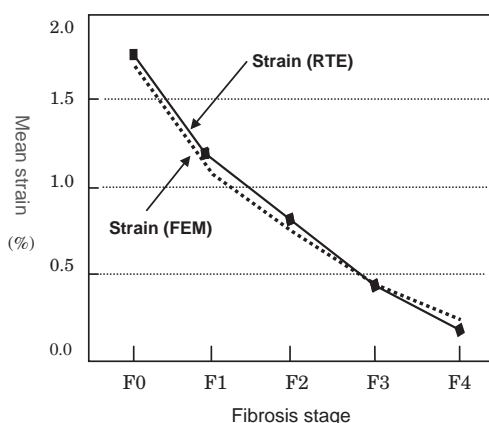**Fig. 7.** (Color) Strain images obtained by FEM analysis and simulated RTE.

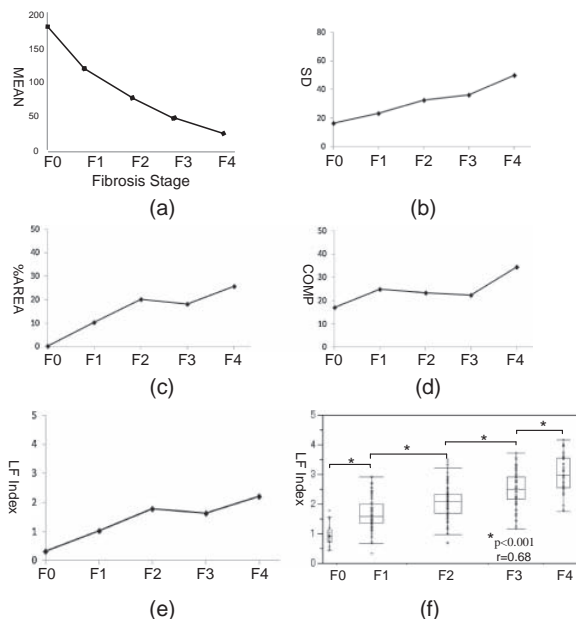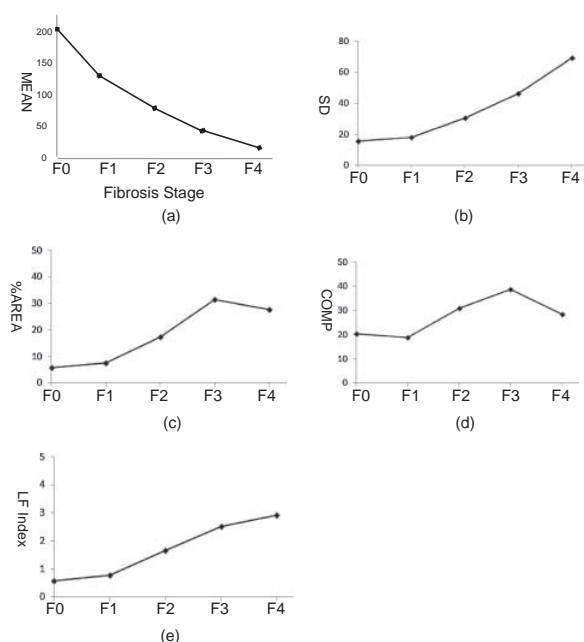

Fig. 8. Change in mean values of strain images.

Fig. 9. Features of strain image and LF index as a function of fibrosis stage in the case of $n = 1$, and $\alpha = \beta = 1.3$ [parameters in eqs. (6) and (7)]: (a) MEAN, (b) SD, (c) %AREA, (d) COMP, (e) LF index, and (f) the relationship of LF index and fibrosis stage obtained by clinical data analysis for 310 cases.

generated by simulating RTE. Compared with the strain image obtained by FEM, the display area of the strain image obtained by RTE is smaller ($28.5 \times 21.6 \, \mathrm{mm}^2$) since marginal parts are used for estimation. It can be seen that, as fibrosis progresses, the blue area increases, indicating that the area has become stiffer than the area around it. In addition, the strain distribution becomes increasingly complex.

Figure 8 represents the mean strain within the analyzed area for each stage. We can see that the mean strain decreases as the stage progresses. It should be noted that strain images obtained by FEM reflect the pattern of Young's modulus distribution in Fig. 6. In addition, there is naturally a good correlation between both strain images although strain images obtained by RTE are more blurred than those obtained by FEM since the former are estimated from echo signals.

Finally, four features extracted from the strain image (RTE) and LF index derived using eq. (1) as a function of

fibrosis stage are shown in Fig. 9. For the simulation in Figs. 9(a)–9(e), the parameter n in eq. (6) was set to 1 as well as in Figs. 6 and 7. It can be observed that MEAN decreases, while SD and %AREA increase as fibrosis progresses. COMP seems to become large in serious cases. As shown in Fig. 9(e), the LF index derived from these features also tends to increase. The relationship between the LF index and fibrosis stage obtained by clinical data analysis of the 310 cases is shown in Fig. 9(f). Although the result of

© 2012 The Japan Society of Applied Physics

Fig. 10. Features of strain image and LF index as a function of fibrosis stage in the case of $n = 2$, and $\alpha = \beta = 0.1$ [parameters in eqs. (6) and (7)]: (a) MEAN, (b) SD, (c) %AREA, (d) COMP, and (e) LF index.

Fig. 11. Change in %AREA as a function of fibrosis stage (clinical data analysis).

simulation analysis is for a single case, the LF index obtained using a mechanical model of fibrosis progression coincides with the result of the clinical data analysis.

These results indicate that even in diffuse diseases like chronic hepatitis, the pattern of strain images is related to the fibrous structure changes caused by hepatic disease and can be used to derive features for quantitative evaluation of fibrosis stage.

On the other hand, there remain several problems to be solved for the development of a clinically useful method. For example, the parameters of models described in §2.2.1 and §2.2.2 are defined only to determine the size of the nodules or the rate of stiffness increase. Therefore, they do not directly indicate the physical characteristic of the liver. In particular, the number of iterations is an important parameter, although there is no *a priori* information at present. In terms of the parameter n, representing the rate of stiffness increase, if parameters are set to $n = 2$ and $\alpha = \beta = 0.1$, the staging is accelerated, as shown in Fig. 10. To tune or optimize these parameters, it is indispensable to continue the simulation under several conditions and compare the results with a large number of clinical data.

As mentioned in §2.1, chronic hepatitis is scored by fibrosis staging and grading. Our clinical research validates that the LF index obtained by RTE stably reflects the fibrosis stage without being influenced by variables of inflammatory state or blood pressure. On the other hand, it is reported that the values measured by FibroScan® are influenced by variables such as hepatic steatosis and flares of transaminases.[21,22] This indicates that shear wave velocity is also changed by factors other than fibrosis stage. In terms of shear wave velocity measurement, some methods using
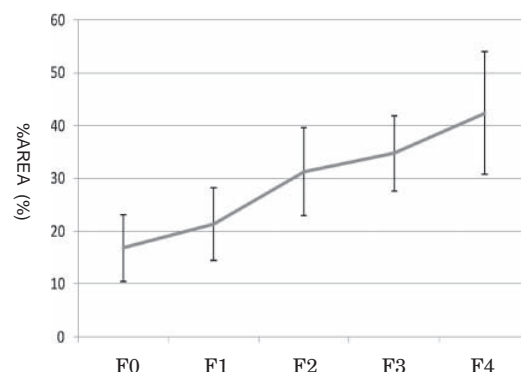
acoustic radiation force for shear wave generation within the body have been recently developed such as acoustic radiation force impulse (ARFI) imaging[29] and shear wave elastography (SWE).[30] These methods can also be used as noninvasive methods of assessing tissue stiffness. In addition, it is expected to utilize different diagnosis information by using both methods, that is, strain image and shear wave image.

4. Conclusions

In this study, we proposed a mechanical model of fibrosis progression. From the strain distribution, we could see that the area of low strain increases, and the strain distribution becomes increasingly complex as fibrosis progresses. The extracted features of strain and derived the LF liver index showed a definite correlation with fibrosis progression and coincided with the result of clinical data analysis. This indicates that even in diffuse diseases like chronic hepatitis, the pattern of strain images is related to the fibrous structure changes caused by hepatic disease and can be used to derive features for quantitative evaluation of fibrosis stage.

As mentioned above, to optimize the parameters used for simulation analysis, it is indispensable to continue the simulation under several conditions and compare the results with a large number of clinical data. For example, although the number of iterations for the conjugating process does not directly indicate the physical characteristic of the liver, the %AREA may be a useful reference to relate the number of iterations to the fibrosis stages. Figure 11 shows the %AREA obtained by clinical data analysis, which increases as a function of fibrosis stage and is similar to Fig. 9(c).

In addition, for future work, there remain some problems to be investigated. To extract reliable diagnosis information from a strain image, a stable data acquisition system that is robust against noise and artifacts must be developed. To improve the precision of simulation, we must investigate a way to obtain the precise values of Young's modulus for each component, such as the parenchyma and fibrous portion, for example, by microscopic measurement of tissues for each stage of hepatitis. Finally, in terms of the extraction of image features, it is one of the most important themes of this research to extract more appropriate features to be useful for the precise diagnosis of chronic hepatitis.

1) A. Ohshima: Proc. 123rd Symp. Japanese Association of Medical Sciences, 2003, p. 13 [in Japanese].
2) National Institutes of Health Consensus Development Conference Statement. Management of Hepatitis C: Hepatology **36** (2002) S3.
3) A. A. Bravo, S. G. Sheth, and S. Chopra: New Engl. J. Med. **344** (2001) 495.
4) I. Sporea, A. Popescu, and R. Sirli: World J. Gastroenterol. **14** (2008) 3396.
5) P. Bedossa, D. Dargère, and V. Paradis: Hepatology **38** (2003) 1449.
6) M. Ziol, A. Handra-Luca, A. Kettaneh, C. Christidis, F. Mal, F. Kazemi, V. de Ledinghen, V. P. Marcelin, D. Dhumeaux, J. C. Trinchet, and M. Beaugran: Hepatology **41** (2005) 48.
7) U. Arena, F. Vizzutti, G. Corti, S. Ambu, C. Stasi, S. Bresci, S. Moscarella, V. Boddi, A. Petrarca, G. Laffi, F. Marra, and M. Pinzani: Hepatology **47** (2008) 380.
8) Y. Fujii, N. Taniguchi, and K. Itho: Med. Imaging Technol. **21** (2003) 117.
9) T. Nishimura, H. Watanabe, M. Ito, Y. Matsuoka, K. Yano, M. Daikoku, H. Yaysuhasshi, K. Dohmen, and H. Ishibashi: Br. J. Radiol. **78** (2005) 189.
10) T. Yamaguchi, H. Hachiya, K. Kato, H. Fukuda, and M. Ebara: Jpn. J. Appl. Phys. **39** (2000) 3266.
11) T. Yamaguchi, K. Nakamura, and H. Hachiya: Jpn. J. Appl. Phys. **42** (2003) 3292.
12) Y. Igarashi, H. Ezuka, T. Yamaguchi, and H. Hachiya: Jpn. J. Appl. Phys. **49** (2010) 07HF06.
13) T. Shiina, N. Nitta, E. Ueno, and J. C. Bamber: J. Med. Ultrason. **29** (2002) 119.
14) M. Yamakawa, N. Nitta, T. Shiina, M. Matsumura, S. Tamano, T. Mitake, and E. Ueno: Jpn. J. Appl. Phys. **42** (2003) 3265.
15) A. Itoh, E. Ueno, E. Tohno, H. Kamma, H. Takahashi, T. Shiina, M. Yamakawa, and T. Matsumura: Radiology **231** (2006) 341.
16) K. Fujimoto, M. Kato, A. Tonomura, N. Yada, C. Tatsumi, M. Oshita, S. Wada, K. Ueshima, T. Ishida, T. Furuta, M. Yamasaki, M. Tsujimoto, M. Motoki, T. Mitake, S. Kim, K. Yamamoto, T. Shiina, M. Kudo, and N. Hayashi: Kanzo **51** (2010) 539 [in Japanese].
17) A. Tonomura, M. Motoki, T. Mitake, K. Fujimoto, M. Kato, C. Tatsumi, N. Yada, K. Ueshima, M. Kudo, and T. Shiina: Proc. 22nd Kanto-section Meet. JSUM, 2010, p. 36 [in Japanese].
18) C. Tatsumi, M. Kudo, K. Ueshima, S. Kitai, E. Ishikawa, N. Yada, S. Hagiwara, T. Inoue, Y. Minami, H. Chung, K. Maekawa, K. Fujimoto, M. Kato, A. Tonomura, T. Mitake, and T. Shiina: Intervirology **53** (2010) 76.
19) F. Ichida, T. Tsuji, M. Omata, T. Ichida, K. Inoue, T. Kaminuma, G. Yamada, K. Hino, O. Yokosuka, and H. Suzuki: Int. Hepatol. Commun. **36** (1996) 112.
20) L. Sandrin, B. Fourquet, J. M. Hasquenoph, S. Yon, C. Fournier, F. Mal, C. Christidis, M. Ziol, B. Poulet, F. Kazemi, M. Beaugrand, and R. Palau: Ultrasound Med. Biol. **29** (2003) 1705.
21) M. Friedrich-Rust, M. F. Ong, S. Martens, C. Sarrazin, J. Bojunga, S. Zeuzem, and E. Herrmann: Gastroenterology **134** (2008) 960.
22) U. Arena, F. Vizzutti, G. Corti, S. Ambu, C. Stasi, S. Bresci, S. Moscarella, V. Boddi, A. Petrarca, G. Laffi, F. Marra, and M. Ponzani: Hepatology **47** (2008) 380.
23) T. Shiina, M. M. Doyley, and J. C. Bamber: Proc. IEEE Ultrasonics Symp., 1996, 1331.
24) M. Yamakawa and T. Shiina: Jpn. J. Appl. Phys. **40** (2001) 3872.
25) E. Tohno and E. Ueno: Breast Cancer **15** (2008) 200.
26) National Center for Global Health and Medicine, Disease Control and Prevention Center (2008) [http://www.ncgm.go.jp/center/formedsp_cir.html] [in Japanese].
27) T. Yasuda, T. Takeda, Y. Nakayama, K. Uehata, H. Sakaguchi, M. Seki, A. Sawada, M. Yamashita, K. Abo, S. Takeda, and H. Asai: presented at 151st Osaka Abdomen Ultrasound, 2005 [in Japanese].
28) M. Ziol, A. Handra-Luca, A. Kettaneh, C. Christidis, F. Mal, F. Kazemi, V. de Lédinghen, P. Marcellin, D. Dhumeaux, J. C. Trinchet, and M. Beaugrand: Hepatology **41** (2005) 48.
29) M. L. Palmeri, M. H. Wang, J. J. Dahl, K. D. Frinkley, and K. R. Nightingale: Ultrasound Med. Biol. **34** (2008) 546.
30) J. Bercoff, M. Tanter, and M. Fink: IEEE Trans. Ultrason. Ferroelectr. Freq. Control **51** (2004) 396.

Sensing of Commensal Organisms by the Intracellular Sensor NOD1 Mediates Experimental Pancreatitis

Yoshihisa Tsuji,[1] Tomohiro Watanabe,[1,2,4,*] Masatoshi Kudo,[5] Hidenori Arai,[3] Warren Strober,[4] and Tsutomu Chiba[1]
[1]Department of Gastroenterology and Hepatology
[2]Center for Innovation in Immunoregulative Technology and Therapeutics
[3]Department of Human Health Sciences
Kyoto University Graduate School of Medicine, Kyoto 606-8507, Japan
[4]Mucosal Immunity Section, Laboratory of Host Defenses, National Institute of Allergy and Infectious Diseases, National Institutes of Health, Bethesda, MD 20852, USA
[5]Department of Gastroenterology and Hepatology, Kinki University School of Medicine, Osaka 589-8511, Japan
*Correspondence: tmhrwtnb@kuhp.kyoto-u.ac.jp
http://dx.doi.org/10.1016/j.immuni.2012.05.024

SUMMARY

The intracellular sensor NOD1 has important host-defense functions relating to a variety of pathogens. Here, we showed that this molecule also participates in the induction of a noninfectious pancreatitis via its response to commensal organisms. Pancreatitis induced by high-dose cerulein (a cholecystokinin receptor agonist) administration depends on NOD1 stimulation by gut microflora. To analyze this NOD1 activity, we induced pancreatitis by simultaneous administration of a low dose of cerulein (that does not itself induce pancreatitis) and FK156, an activator of NOD1 that mimics the effect of gut bacteria that have breached the mucosal barrier. The pancreatitis was dependent on acinar cell production of the chemokine MCP-1 and the intrapancreatic influx of CCR2^{+} inflammatory cells. Moreover, MCP-1 production involved activation of the transcription factors NF-κB and STAT3, each requiring complementary NOD1 and cerulein signaling. These studies indicate that gut commensals enable noninfectious pancreatic inflammation via NOD1 signaling in pancreatic acinar cells.

INTRODUCTION

Although most episodes of acute pancreatitis are mild, a subpopulation of patients with this condition develops a severe disease with local and extrapancreatic complications (Frossard et al., 2008). Bacterial colonization of the inflamed pancreas is involved in the latter cases and, in fact, infection of necrotic pancreatic tissue is one of the most important causes of mortality in acute pancreatitis (Frossard et al., 2008). It is now generally accepted that such colonization and associated inflammation result from failure of intestinal-barrier function and translocation of intestinal

microflora into the splanchnic vascular bed (Frossard et al., 2008; Rychter et al., 2009).

Microbe-associated molecular patterns (MAMPs) derived from the intestinal microflora activate the host innate immune system via pattern-recognition receptors such as Toll-like receptors (TLRs) and nucleotide-binding domain and leucine-rich repeat containing molecules (NLRs) (Akira and Takeda, 2004; Chen et al., 2009; Strober et al., 2006; Werts et al., 2011). Thus, it is probable that activation of TLRs and NLRs is involved in the mechanisms by which bacterial translocation accounts for the development of severe acute pancreatitis. Consistent with this idea, the severity of acute pancreatitis is ameliorated in mice lacking TLR4 (Sharif et al., 2009), and polymorphism in the TLR genes is associated with susceptibility to acute pancreatitis (Gao et al., 2007; Takagi et al., 2009). In addition, NF-κB, a downstream transcription factor of the TLR and NLR signaling pathways (Akira and Takeda, 2004; Strober et al., 2006), plays a critical role in the development of acute pancreatitis (Baumann et al., 2007; Rakonczay et al., 2008; Tando et al., 1999).

Studies have highlighted the role of the NLR family of proteins in the microbial-recognition system that functions in the intestinal milieu (Strober et al., 2006; Chen et al., 2009; Werts et al., 2011). NOD1, which belongs to this family, is of particular interest because it has been shown to play a protective role in infection of the mucosal surface (Strober et al., 2006). NOD1 contains a leucine-rich repeat region that serves as an intracellular sensor of small peptide components derived from bacterial peptidoglycan (PGN). Such recognition leads to NOD1 activation and the production of proinflammatory mediators, either through nuclear translocation of NF-κB or through interferon regulatory factors (IRFs) and type I interferon signaling (Chamaillard et al., 2003; Fritz et al., 2007; Watanabe et al., 2010).

The above properties of NOD1 suggest the possibility that this NLR family member could contribute to the development of noninfectious inflammatory states, particularly if it can be shown that NOD1 responds to gut commensal organisms as well as to pathogenic organisms (Girardin et al., 2003; Kim et al., 2004). Here, we addressed this possibility by defining the role of NOD1 in the development of cholecystokinin receptor (CCKR) agonist-induced acute pancreatitis (cerulein pancreatitis). In

a key initial finding, we showed that administration of high doses of cerulein, a well-established inducer of pancreatitis, requires the presence of gut commensal organisms acting through NOD1 for the development of pancreatic inflammation. This observation led us to develop a model of pancreatitis that would allow us to define the role of NOD1 signaling in pancreatitis. This consisted of the administration of low doses of cerulein that do not in themselves cause pancreatitis and of the administration of NOD1 ligand, which in this case could be shown to mimic the activity of gut commensal bacteria that enter circulation during pancreatitis. Using this model, we showed that NOD1 stimulation facilitates the migration of CCR2$^+$ myeloid cells to the pancreas in response to the robust acinar cell production of monocyte chemotactic protein-1 (MCP-1); the latter, in turn, results from cooperative NOD1-cerulein activation of NF-κB and STAT3. Overall, these findings reveal that NOD1 signaling plays a major role in the pathogenesis of cerulein-induced acute pancreatitis via its capacity to respond to commensal gut bacteria.

RESULTS

Bowel Sterilization by Broad-Spectrum Antibiotics Inhibits High-Dose Cerulein Pancreatitis

Repeated administration of high doses of cerulein (50–100 μg/kg), a CCKR agonist, is a well-established inducer of acute murine pancreatitis (Baumann et al., 2007; Sharif et al., 2009). To address the role of commensal organisms in the intestinal microflora in the development of high-dose cerulein pancreatitis, C57BL6 mice were administered a combination of antibiotics (ampicillin [AMP], vancomycin, neomycin, and metronidazole) in the drinking water for 3 weeks, a regimen previously used to achieve bowel sterilization (Fagarasan et al., 2002), and then challenged with repeated systemic intraperitoneal (i.p.) injections of high doses of cerulein (50 μg/kg). We found that mice administered normal drinking water and given seven hourly injections of cerulein developed severe pancreatitis associated with a marked increase in the serum concentrations of pancreatic enzymes, amylase, and lipase; in contrast, mice preadministered drinking water containing antibiotics developed barely detectable pancreatic inflammation and only marginal elevations in the serum concentrations of pancreatic enzymes (Figures 1A and 1B). In complementary studies addressing the effects of a single commensal organism, mice were first administered ampicillin and kanamycin (KM) in the drinking water for 3 weeks and then challenged with high doses of cerulein as before. We observed that, even with this less stringent bowel-sterilization regimen, the mice exhibited only a mild elevation in the serum concentrations of amylase associated with normal pancreatic architecture (Figures S1A and S1B available online). However, high serum amylase concentrations and severe pancreatic inflammation were again observed in mice that were administered AMP- and KM-containing drinking water and underwent periodic oral administration of AMP- and KM-resistant *E. coli* expressing LacZ (ECLACZ) (Yoshida et al., 2001) (Figures S1A and S1B). In contrast, periodic oral administration of ECLACZ alone did not induce a significant elevation of serum amylase levels (Figure S1C) and, in addition, did not enhance elevated serum amylase levels that were caused by administration of cerulein

in the absence of AMP and KM in the drinking water (Figure S1D). Thus, ECLACZ used in this study behaved like a commensal organism, with no capacity to induce pancreatitis on its own. Taken together, these data provide strong evidence that commensal organisms in the intestinal microflora are essential for the development of acute pancreatitis caused by high-dose cerulein.

NOD1 Activation Is Necessary for the Development of High-Dose Cerulein Acute Pancreatitis

The above results suggested that an intestinal microbial component recognized by a pattern-recognition receptor is important in the development of high-dose cerulein pancreatitis. To investigate this possibility, we compared serum concentrations of amylase after high-dose cerulein injections, as described above, in mice deficient in TLR2, TLR4, TLR9, or NOD1. Wild-type (WT) mice, TLR2-deficient (*Tlr2*$^{-/-}$) mice, and *Tlr9*$^{-/-}$ mice all developed similar increases in the serum concentration of amylase, suggesting that TLR2 and TLR9 are not required for pancreatitis induction (Figure 1C). In contrast, *Tlr4*$^{-/-}$ mice exhibited a significant decrease in serum amylase as compared to WT mice. This is consistent with a report that TLR4 activation is involved in pancreatitis induction (Sharif et al., 2009). More surprisingly, however, cerulein-induced elevations in serum amylase concentrations were almost completely abrogated in *Nod1*$^{-/-}$ mice (Figure 1C). These data suggest a critical role for NOD1, which senses a peptide derived from PGN of the intestinal bacteria in the induction of high-dose cerulein pancreatitis.

Low-Dose Cerulein Together with NOD1 Ligand Induces Pancreatitis

We sought an experimental model in which NOD1 ligand administration could be used as a substitute for MAMPs derived from gut bacterial flora so that the effects of NOD1 signaling could be easily isolated from those of cerulein. In searching for such a model we became aware that whereas repeated administration of high doses of cerulein (50–100 μg/kg) induces acute pancreatitis as indicated above, administration of low doses of cerulein does not have this effect, although such doses are still capable of acinar cell signaling (Baumann et al., 2007; Sharif et al., 2009). This suggested that low-dose cerulein does not induce pancreatitis because it does not by itself cause an influx of gut microorganisms sufficient to result in robust acinar cell NOD1 signaling, and thus low-dose cerulein would cause pancreatitis if administered with NOD1 ligand. To test this possibility, we administered FK156 (NOD1 ligand) or muramyl dipeptide (MDP, NOD2 ligand) (each at a dose of 200 μg i.p.) to C57BL6 mice, 2 hr prior to initiation of a low-dose cerulein regimen consisting of three hourly injections of a dose of cerulein (20 μg/kg i.p.) that does not induce pancreatitis when administered alone (Figures 2A and 2B). We found that serum concentrations of amylase and lipase were markedly elevated in mice treated with FK156 plus low-dose cerulein, but not in mice treated with MDP plus low-dose cerulein or in mice treated with either ligand or cerulein alone (Figure 2B). In addition, pancreatic edema, necrosis, and infiltration of immune cells were observed in mice treated with FK156 plus cerulein, but not under the other conditions (Figures 2C and 2D). Finally, we showed that comparable amounts of serum amylase were obtained when mice were
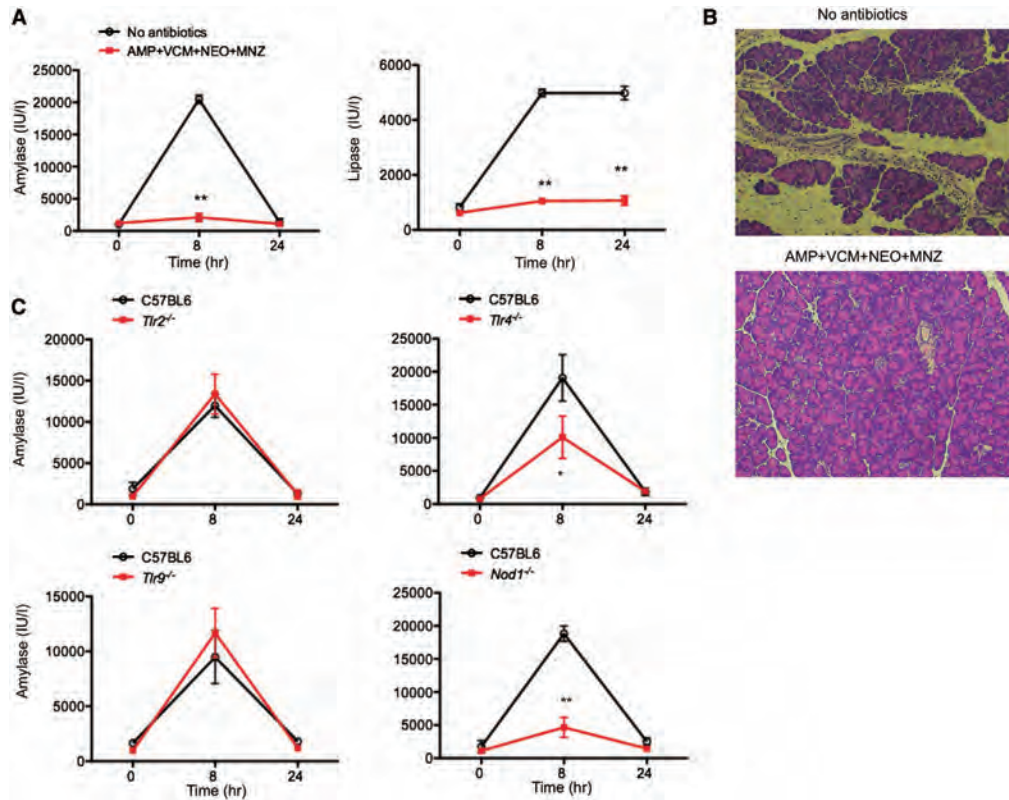
Figure 1. Bowel Sterilization by a Broad Range of Antibiotics Inhibits Development of Cerulein-Induced Pancreatitis

(A) Changes in serum levels of amylase and lipase in C57BL6 mice treated with or without antibiotics. Mice administered with AMP (1 g/l), neomycin (NEO, 1 g/l), vancomycin (VCM, 0.5 g/l) and metronidazole (MNZ, 1 g/l) in the drinking water for 3 weeks were challenged with a high dose of cerulein (50 μg/kg i.p.) for a total of seven times; results are expressed as means ± SD. **$p < 0.01$, as compared with group not administered antibiotics.

(B) Histopathology of mice treated with a broad range of antibiotics followed by systemic injection of a high dose of cerulein (50 μg/kg i.p.) for a total of seven times. Pancreatic tissue was obtained from mice at 8 hr after the first injection of cerulein. Lack of pancreatitis in mice treated with antibiotics, bottom panel. Magnification ×200.

(C) Changes in serum levels of amylase in $Tlr2^{-/-}$, $Tlr4^{-/-}$, $Tlr9^{-/-}$, or $Nod1^{-/-}$ mice without antibiotics. Mice were challenged with a high dose of cerulein (50 μg/kg i.p.) for a total of seven times. Results are expressed as means ± SD. *$p < 0.05$, **$p < 0.01$, as compared with C57BL6 WT mice.

administered FK156 before, at the same time, or after cerulein administration (Figure S2A). Thus, activation of NOD1 causes severe pancreatitis in mice treated with a low subinflammatory dose of cerulein, and thus combined low-dose cerulein and NOD1 ligand could be used as a model to test the role of NOD1 in cerulein-induced pancreatitis.

We sought to show that NOD1-ligand administration in the above-described low-dose cerulein model is acting in place of commensal bacteria. In these studies, C57BL6 mice administered drinking water containing AMP and KM were given three hourly injections of low doses of cerulein alone, an i.p. injection of ECLACZ alone, or an i.p. injection of ECLACZ and low doses of cerulein (Figure 2E). Treatment with i.p. injection of ECLACZ and low-dose cerulein resulted in acute pancreatitis as well as increased serum amounts of amylase, whereas treatment with ECLACZ or cerulein alone did not cause significant changes in these parameters. In additional studies, $Nod1^{-/-}$ mice were more resistant to pancreatitis induced by ECLACZ and low-

dose cerulein than were WT mice and $Tlr4^{-/-}$ mice (Figures 2E and 2F). Thus, intestinal bacteria evoke a NOD1 response similar to that obtained with NOD1 ligand, and therefore the latter is acting as a mimic of intestinal bacteria in this setting.

NOD1 Ligand and Low-Dose Cerulein Are Synergistic Inducers of MCP-1

Prior work has shown that MCP-1 and interleukin-6 (IL-6) are associated with the local inflammation of the pancreas (Grady et al., 1997). We therefore determined the involvement of these proinflammatory mediators in the development of pancreatitis induced by FK156 in combination with low-dose cerulein. Consistent with previous reports (Fritz et al., 2007; Watanabe et al., 2010), systemic injection of FK156, but not MDP, induced increased amounts of serum MCP-1 and IP-10 chemokines. Moreover, MCP-1 induction, but not IP-10 induction, was greatly enhanced by coadministration of cerulein, even though low-dose cerulein treatment alone did not induce MCP-1 (Figure 3A).
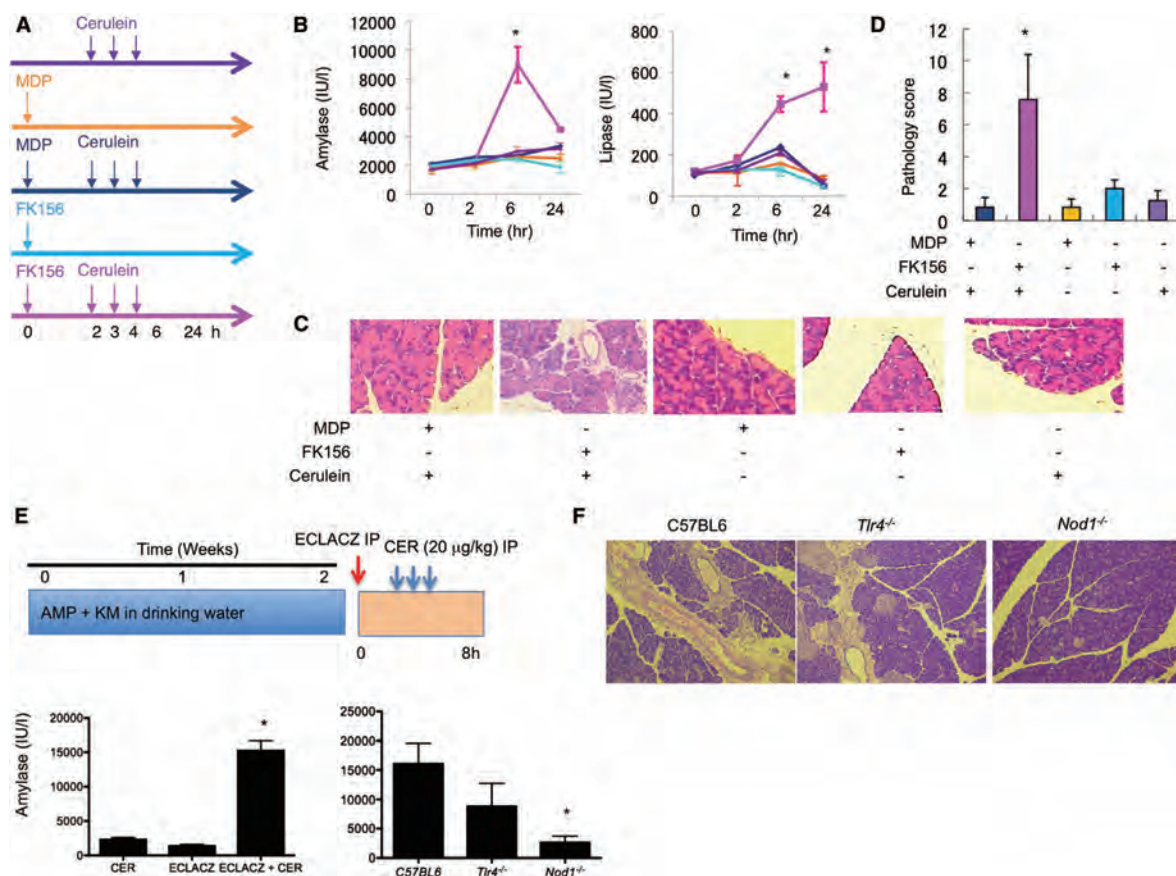
Figure 2. Induction of Acute Pancreatitis in Mice Treated with NOD1 Ligand or ECLACZ in Combination with Cerulein

(A–D) Induction of acute pancreatitis in mice treated with NOD1 ligand and cerulein.

(A) Experimental protocol: C57BL6 mice were administered FK156 (NOD1 ligand; 200 μg/mice i.p.) or MDP (NOD2 ligand; 200 μg/mice) followed by a low dose of cerulein (20 μg/kg i.p.) for a total of three times.

(B) Changes in serum levels of amylase and lipase in mice treated with NOD ligands and/or cerulein. Each color corresponds to group shown in Figure 2A. Results are expressed as means ± SD. *p < 0.01, as compared with other groups.

(C and D) Hematoxylin and eosin (H&E) staining (C) and histological scores (D) of pancreatic tissue harvested at 24 hr after the start of experiments; magnification ×200; each color corresponds to group shown in Figure 2A; scores are expressed as means ± SD. *p < 0.01, as compared with other groups.

(E and F) Induction of acute pancreatitis in mice treated with ECLACZ and cerulein.

(E) Experimental protocol. C57BL6 mice and $Tlr4^{-/-}$ or $Nod1^{-/-}$ mice exposed to AMP and KM in the drinking water were administered ECLACZ (1 × 10⁶ cfu, i.p.) followed by three hourly injections of low doses of cerulein (CER). Changes in serum levels of amylase in C57BL6 mice treated with ECLACZ and/or cerulein, (E), left panel. Changes in serum levels of amylase in C57BL6 mice and $Tlr4^{-/-}$ or $Nod1^{-/-}$ mice treated with ECLACZ and cerulein, (E), right panel. Results are expressed as means ± SD. *p < 0.01, as compared with other groups. Serum levels of amylase were determined 8 hr after the treatment with ECLACZ.

(F) Lack of pancreatitis in $Nod1^{-/-}$ mice treated with ECLACZ and cerulein. Magnification ×200.

FK156 treatment also led to increased serum IL-6 amounts that were again enhanced by low-dose cerulein, particularly at later time points. In contrast, induction of IL-12p40 was observed either with FK156 or MDP administration, and neither response was enhanced by low-dose cerulein. Comparable increases in serum amounts of MCP-1 were observed when FK156 was administered at the time of or after cerulein administration (Figure S2A). These data indicate that the severe pancreatitis induced by treatment with NOD1 ligand and low-dose cerulein is associated with the production of MCP-1 and IL-6. Finally, similar effects on MCP-1 could be elicited by administra-

tion of ECLACZ, in that i.p. administration of the latter followed by treatment with low doses of cerulein also led to a marked increase of the serum level of MCP-1 (Figure 3B). In contrast, $Nod1^{-/-}$ mice administered ECLACZ and low doses of cerulein exhibited little, if any, increase in the serum level of MCP-1 (Figure 3B).

Previous studies have shown that the interaction between MCP-1 and its receptor, CCR2, plays a role in macrophage recruitment and the macrophage-dependent inflammatory response in the development of pancreatitis (Grady et al., 1997; Bhatia et al., 2005; Zhao et al., 2005). One might therefore
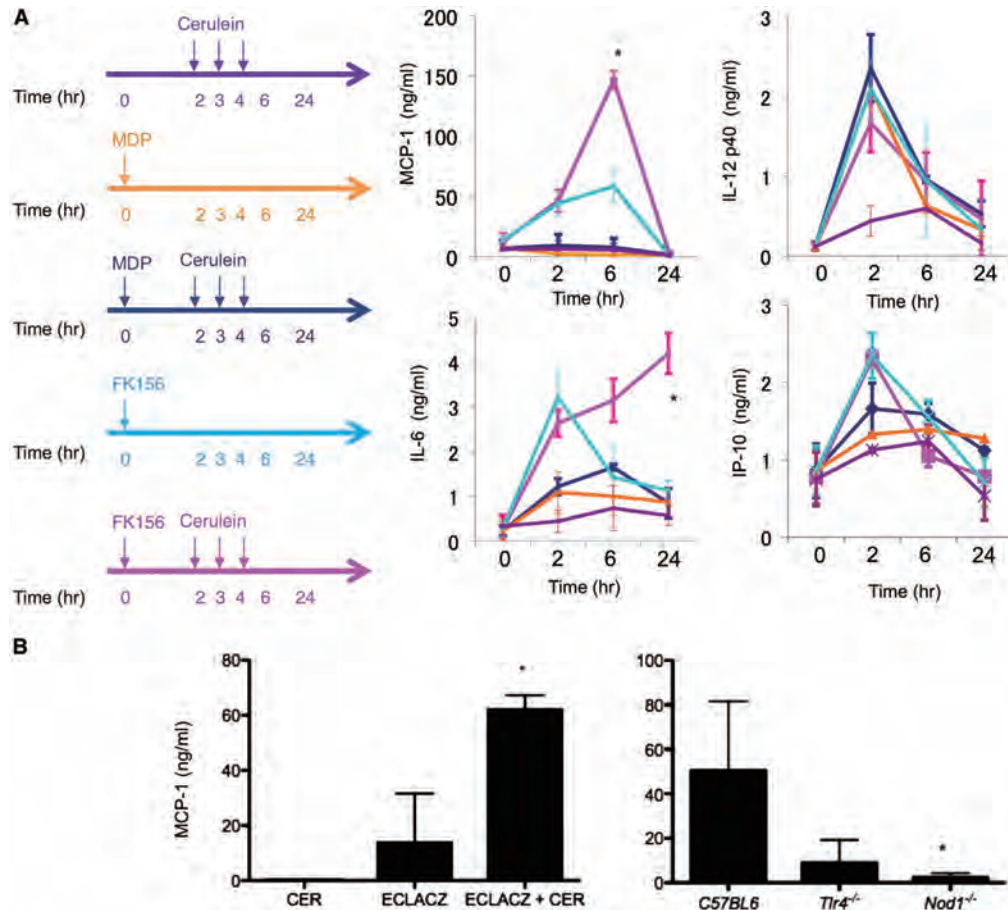
Figure 3. Concomitant Administration of NOD1 Ligand and Low-Dose Cerulein Induces Synergistic Production of MCP-1

(A) Changes in serum levels of proinflammatory cytokines and chemokines. C57BL6 mice received systemic administration of FK156 or MDP followed by i.p. injection of cerulein for a total of three times. Results are expressed as means ± SD. *p < 0.01, as compared with other groups. The results shown are representative of one of three experiments.

(B) Serum levels of MCP-1 in mice treated with ECLACZ and cerulein. Changes in serum levels of MCP-1 in C57BL6 mice treated with ECLACZ and/or cerulein, (B), left panel. Changes in serum levels of MCP-1 in C57BL6 mice and $Tlr4^{-/-}$ or $Nod1^{-/-}$ mice treated with ECLACZ and cerulein, (B), right panel. Results are expressed as means ± SD. *p < 0.01, as compared with other groups. C57BL6 mice and $Tlr4^{-/-}$ or $Nod1^{-/-}$ mice treated with AMP and KM in the drinking water were challenged with i.p. injection of ECLACZ followed by three hourly injections of low doses of cerulein. Serum levels of MCP-1 were determined 8 hr after the treatment with ECLACZ.

predict that low-dose cerulein pancreatitis is mediated by cells susceptible to MCP-1 chemoattraction. In tissue-staining studies (Figure 4A), combined administration of FK156 and low-dose cerulein was associated with massive infiltration of CD11b$^+$ myeloid cells and cells expressing CCR2. In contrast, these cells did not express CXCR3, the receptor of IP-10, indicating the induction of IP-10 by NOD1 probably has little or no role in this type of inflammation.

The relationship between MCP-1 induction and the infiltration of the pancreas by CCR2$^+$ cells was further explored through studies of induction of pancreatitis with FK156 and low-dose cerulein in CCR2-deficient ($Ccr2^{-/-}$) mice. Systemic administration of FK156 and low-dose cerulein to $Ccr2^{-/-}$ mice was associated with a marked reduction in the serum amylase level and

pathology score as compared with WT mice, even though CCR2-deficient mice were still capable of producing MCP-1 (Figure 4B). In addition, migration of both CD11b$^+$ cells and CCR2$^+$ cells into the pancreas was absent in $Ccr2^{-/-}$ mice (Figure 4C). These studies thus showed that induction of MCP-1 by FK156 and low-dose cerulein was associated with the infiltration of inflammatory CCR2$^+$ cells into the inflamed pancreas.

Low-Dose Cerulein Pancreatitis Does Not Depend on T Cells or B Cells

NOD1 is a component of the innate immune system that probably involves mainly non-T cells and non-B cells. To determine if this was in fact the case, we administered FK156 and low-dose cerulein to $Prkdc^{scid}$ mice with severe combined
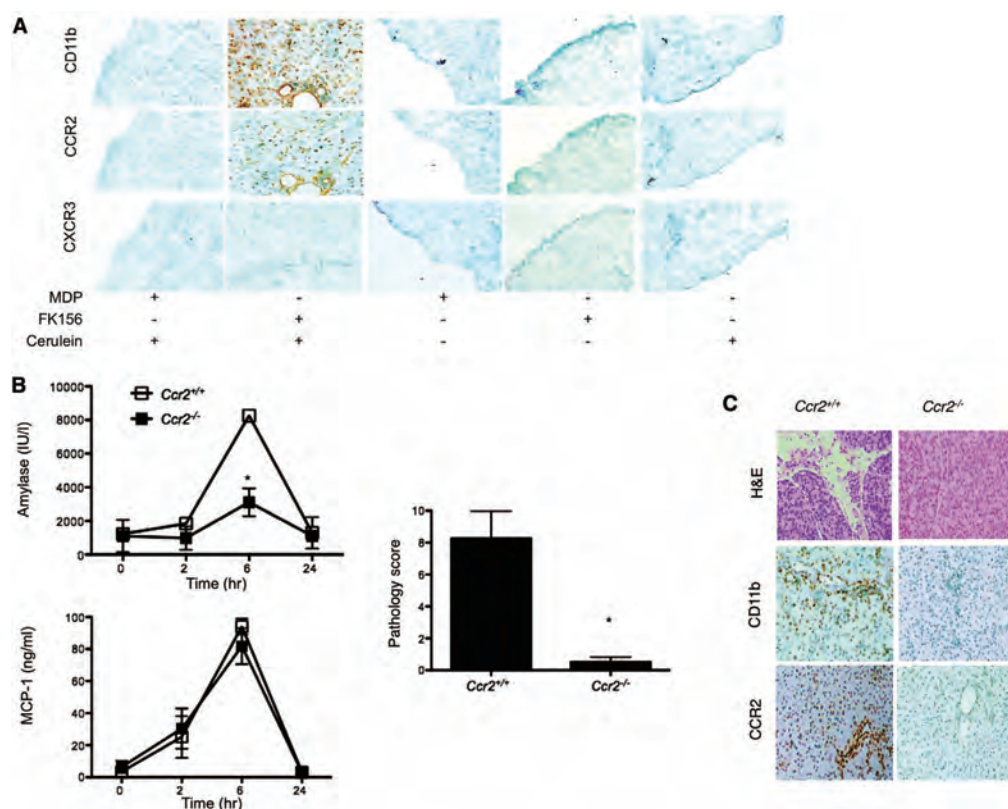
Figure 4. Migration of CCR2$^+$ Myeloid Cells Is Necessary for the Development of Pancreatitis

(A) At 6 hr after the injection of MDP or FK156, pancreatic tissue from C57BL6 mice was removed and subjected to immunohistochemical analysis for visualization of cells positive for CD11b, CCR2, and CXCR3.

(B and C) CCR2-intact (*Ccr2$^{+/+}$*) or CCR2-deficient (*Ccr2$^{-/-}$*) mice were administered FK156 followed by repeated administration of cerulein according to the protocol described in Figure 2A.

(B) Changes in serum levels of amylase and MCP-1 at the indicated time points and pathology scores of the pancreatic tissue at 24 hr; results are expressed as means ± SD. *p < 0.01, as compared with *Ccr2$^{+/+}$* mice; results shown are representative of one of three experiments.

(C) Pancreatic tissue was removed at 6 hr after the start of the experiments and subjected to immunohistochemical analysis for visualization of cells positive for CD11b and CCR2; magnification ×200.

immunodeficiency (SCID) that lacked both T cells and B cells. This treatment induced equally increased amounts of serum amylase and MCP-1 in WT and SCID mice (Figure S2B), suggesting that the acute pancreatitis induced by systemic injection of NOD1 ligand and low-dose cerulein does not depend on T cells or B cells.

Acute Pancreatitis Requires Activation of NOD1 in Nonhematopoietic Cells

We next turned our attention to the cellular location of the NOD1 involved in the acute pancreatitis model studied above. Our initial approach to this question was to conduct bone marrow (BM) chimera studies to determine if NOD1 was acting in hematopoietic cells or nonhematopoietic cells for the development of pancreatitis, but first we had to define the responses of *Nod1$^{-/-}$* cells to be used in such studies. To this end, we subjected *Nod1$^{-/-}$* mice and *Nod1$^{+/+}$* mice to treatment with FK156 or MDP and low-dose cerulein. *Nod1$^{+/+}$* mice, but not *Nod1$^{-/-}$*

mice, developed pancreatitis after such FK156 and cerulein administration, as evidenced by serum amylase and MCP-1 elevations and histology scores (Figure 5A). These studies indicated that NOD1 stimulation is essential for the induction of FK156 and low-dose cerulein pancreatitis.

We then performed the BM chimera studies mentioned above and showed that administration of FK156 and low-dose cerulein led to pancreatitis in *Nod1$^{+/+}$* green fluorescent protein (GFP)-transgenic mice reconstituted with *Nod1$^{-/-}$* BM cells (Figure 5B), but not in *Nod1$^{-/-}$* mice reconstituted with *Nod1$^{+/+}$* BM cells. Thus, the development of FK156 and cerulein acute pancreatitis involves NOD1 signaling in nonhematopoietic cells.

In a second approach to the identification of the site of NOD1 activity in this model, we conducted in vitro studies of isolated pancreatic acinar cells from untreated mice to determine whether these cells exhibited NOD1 activity following stimulation with FK156 and/or low-dose cerulein (Figure S3A). Although stimulation of acinar cells with FK156 alone induced a substantial
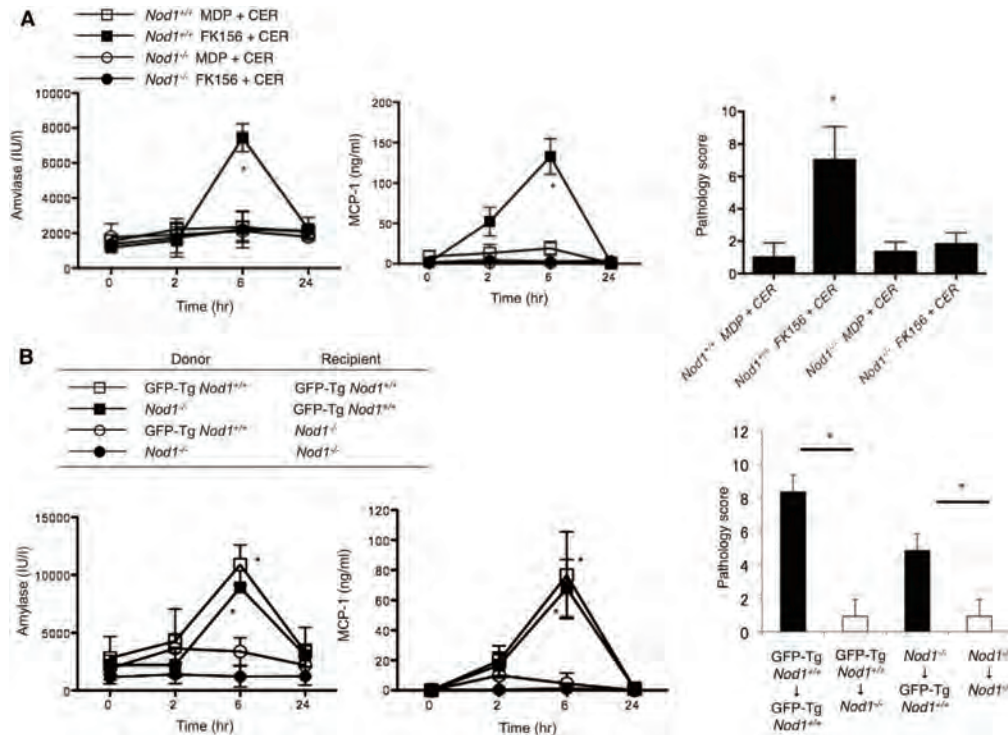
Figure 5. The Importance of NOD1 Signaling in Nonhematopoietic Cells for the Development of Severe Acute Pancreatitis

(A) $Nod1^{+/+}$ or $Nod1^{-/-}$ mice were treated with NOD ligands (FK156 or MDP) and/or cerulein (CER) as described in Figure 2A. Changes in serum levels of amylase and MCP-1 at the indicated time points, and pancreatitis histology score at 24 hr. *p < 0.01, as compared with the other groups.

(B) BM cells from GFP-transgenic (GFP-Tg) mice or $Nod1^{-/-}$ mice were transplanted into irradiated GFP-transgenic mice or $Nod1^{-/-}$ mice. These chimeric mice were treated with FK156 followed by repeated administration of CER. Changes in serum levels of amylase and MCP-1 at the indicated time points, and pancreatitis histology score at 24 hr. Results are expressed as means ± SD. *p < 0.01, as compared with the other groups. *p < 0.01 (pathology score). The results shown are representative of one of three experiments.

amount of MCP-1, synergistic production of MCP-1 was seen upon stimulation with FK156 plus low-dose cerulein in an FK156-dose-dependent fashion. In contrast, FK156 alone was sufficient for the induction of IP-10 production. Finally, the induction of MCP-1 under these conditions required the presence of NOD1 (Figure S3B). These studies established, first, that pancreatic acinar cells are the nonhematopoietic cellular site of NOD1 activation in the FK156 and low-dose cerulein model of acute pancreatitis. Second, they showed that MCP-1 induction requires dual NOD1 and low-dose cerulein signaling via NOD1 and CCKR, respectively.

As mentioned in Figure 3A, administration of FK156 and low-dose cerulein elicited elevations in circulating amounts of IL-6 as well as MCP-1. This finding correlates with the fact that acinar cells from $Nod1^{+/+}$ mice, but not cells from $Nod1^{-/-}$ mice, produced IL-6 upon stimulation with FK156 and low-dose cerulein and suggests that, as in the case of MCP-1, increased circulating amounts of IL-6 originate from acinar cells (Figure S3B). It seemed probable that the MCP-1 and IL-6 secretion might be interrelated, given that IL-6 participates in MCP-1 production via STAT3 activation (Deshmane et al., 2009). To address this possibility, we measured acinar cell production of MCP-1 in cells

isolated from $Nod1^{+/+}$ mice and then treated with FK156 and low-dose cerulein in the presence or absence of neutralizing IL-6 receptor (IL-6R) antibody (Ab). This blockade of IL-6 signaling inhibited the production of MCP-1, but only partially (Figure S3C); thus, IL-6 is not the only inducer of MCP-1 in this model.

NOD1 Plus Low-Dose Cerulein Signaling Induces Transactivation of STAT3 and NF-κB In Vivo

Because acinar cell MCP-1 production is a key factor in the development of FK156 and low-dose cerulein pancreatitis, we next turned our attention to the signaling pathways controlling such production. Previous studies have shown that MCP-1 production depends on STAT3 and NF-κB activation (Deshmane et al., 2009), and, indeed, we verified that these factors were necessary for the induction of FK156 and low-dose cerulein pancreatitis by measuring activation of both STAT3 and NF-κB in the pancreatic tissue of mice with pancreatitis. Nuclear expression of phospho-STAT3 (pSTAT3) and phospho-IκBα (pIκBα) was seen in the pancreatic acinar cells expressing amylase of $Nod1^{+/+}$ mice treated with low-dose cerulein and FK156, whereas little or no pSTAT3 or pIκBα was seen in acinar

cells of *Nod1*$^{-/-}$ mice (Figure S3D). Similar findings were obtained using conventional immunohistochemical analysis (Figure S3E).

To confirm the above findings, we performed staining studies of tissue obtained from BM-chimeric mice, consisting of irradiated *Nod1*$^{+/+}$ mice bearing a GFP-expressing transgene and irradiated *Nod1*$^{-/-}$ mice, reconstituted with *Nod1*$^{-/-}$ GFP-transgene-negative BM cells and *Nod1*$^{+/+}$ GFP-transgene-positive BM cells, respectively. Replacement of BM cells was confirmed by flow-cytometric analysis of GFP expression at 8 weeks after the transplantation (Figure S4A). We found that amylase-expressing acinar cells were GFP-positive in irradiated GFP-transgene-positive mice reconstituted with GFP-transgene-negative *Nod1*$^{-/-}$ BM cells, whereas they were GFP-negative in irradiated GFP-transgene-negative *Nod1*$^{-/-}$ mice reconstituted with GFP-transgene-positive *Nod1*$^{+/+}$ BM cells (Figure S4B). Thus, the GFP status of the acinar cells reflected the GFP status of the recipient, not the donor. In additional studies, we showed that expression of pIκBα and pSTAT3 was seen in acinar cell nuclei of irradiated GFP-transgene-positive *Nod1*$^{+/+}$ mice reconstituted with *Nod1*$^{-/-}$ BM cells (Figure S4B). In contrast, expression of these factors was barely detectable in acinar cell nuclei of irradiated GFP-transgene-negative *Nod1*$^{-/-}$ mice reconstituted with GFP-transgene positive *Nod1*$^{+/+}$ BM cells (Figure S4B). Similar findings were obtained using conventional immunohistochemical analysis (Figure S4C). These data thus provide additional evidence that activation of STAT3 and NF-κB in response to FK156 and low-dose cerulein administration is occurring in pancreatic acinar cells.

Administration of JSI-124, a specific STAT3 inhibitor, inhibited nuclear translocation of STAT3, and administration of IMD-0354, an NF-κB inhibitor, inhibited nuclear translocation of the NF-κB subunit p65 in the pancreas of mice administered FK156 and low-dose cerulein, as assayed in the Transfactor Binding Assay, establishing that these agents do in fact exert the expected inhibition of activation of STAT3 and NF-κB under these conditions (Figure S5A). In addition, administration of JSI-124 or IMD-0354 alone led to a partial reduction of serum levels of amylase and MCP-1, whereas administration of both agents led to complete reduction of serum levels of amylase and MCP-1 (Figure S5B). A similar result was obtained in respect to the inflammation score of the pancreas (Figure S5C). These studies, using pharmacological inhibitors for STAT3 and NF-κB, thus provide evidence that activation of both STAT3 and NF-κB in acinar cells acts in an additive fashion to bring about the development of pancreatitis induced by FK156 and low-dose cerulein.

Molecular Mechanisms Underlying the Activation of STAT3 and NF-κB in FK156 and Low-Dose Cerulein Pancreatitis

Having established that STAT3 and NF-κB are critical signaling components in the induction of FK156 and low-dose cerulein pancreatitis, we were interested in establishing how FK156 and low-dose cerulein act together to induce these components, whereas neither stimulant do so alone. In initial studies we focused on the signaling pathways leading to STAT3 activation and showed that treatment with FK156 alone induced expression of pSTAT3 in the pancreas of *Nod1*$^{+/+}$ mice, but not *Nod1*$^{-/-}$ mice (Figure 6A). This is consistent with our previous

report that NOD1 ligand induces type I IFN production (Watanabe et al., 2010) as well as with a study showing that type I IFN activates various STATs, including STAT3 (Yang et al., 1998). Similarly, treatment with cerulein alone induced pSTAT3 expression (in both *Nod1*$^{+/+}$ and *Nod1*$^{-/-}$ mice), presumably as a result of direct CCKR activation of JAK2 (Ferrand et al., 2005). However, treatment of *Nod1*$^{+/+}$ mice (but not *Nod1*$^{-/-}$ mice) with both FK156 and low-dose cerulein induced higher pSTAT3 expression as compared with either stimulus alone, and this was associated with similarly increased nuclear translocation (Figure 6B). Thus, FK156 and low-dose cerulein reinforce one another in STAT3 activation.

We also noted that expression of pSTAT1 was induced in the pancreas of *Nod1*$^{+/+}$ mice treated with FK156, but, in this case, such expression was not enhanced by combined treatment with FK156 and cerulein (Figure 6A). Moreover, expression of pSTAT1 was not induced in the pancreas of *Nod1*$^{-/-}$ mice, whether mice were treated with FK156 or cerulein. These results were corroborated by measurement of nuclear translocation (Figure 6B). Given the fact that STAT1 is a critical downstream signaling molecule for type I IFN, these data suggest that FK156 also activates a type I IFN pathway, as reported previously (Watanabe et al., 2010).

We next examined the signaling pathways leading to NF-κB activation. Although previous studies utilizing human embryonic kidney cells showed rapid activation of NF-κB upon stimulation with NOD1 ligands (Chamaillard et al., 2003; Fritz et al., 2007), the roles of NF-κB in NOD1-mediated signaling pathways have been poorly defined in primary pancreatic acinar cells. In initial studies, we found that neither NOD1 ligand nor low-dose cerulein administration alone resulted in expression of pIκBα or degradation of IκBα (Figure 6A). This is consistent with our previous report that NOD1 stimulation alone is a poor inducer of NF-κB in intestinal epithelial cells (Watanabe et al., 2010) as well as previous reports by other investigators that cerulein is also a poor inducer of NF-κB at low concentrations (Yu et al., 2005). Nevertheless, combined stimulation did result in such induction as shown by expression of pIκBα and nuclear translocation of p65 and p50 (Figures 6A and 6B). In explanation of this finding, we focused first on CCK signaling and noted that previous studies had shown that CCKR signaling induces protein kinase C (PKC) activation (Rakonczay et al., 2008; Tando et al., 1999). To verify that this pathway is in play in the low-dose cerulein model we treated mice with low-dose cerulein (in the presence or absence of FK156) and showed that such mice exhibited enhanced pancreatic cell expression of phospho-PKC (pPKC) (Figure 6A). Because both activated PKC generated by cerulein signaling and RICK (receptor-interacting protein-like interacting caspase-like apoptosis regulatory protein kinase) generated by NOD1 signaling are known to activate NF-κB via phosphorylation and/or ubiquitination of transforming growth factor β (TGF-β)-activated kinase 1 (TAK1) (Hasegawa et al., 2008; Shinohara et al., 2005), we next considered the possibility that TAK1 is a signaling molecule that serves as a nodal point in the low-dose cerulein and FK156 signaling pathways that facilitate NF-κB activation. In studies to explore this possibility, we performed immunoprecipitation studies of cell lysates isolated from the pancreas of *Nod1*$^{+/+}$ and *Nod1*$^{-/-}$ mice. We found that treatment with cerulein, but not FK156, induced physical interaction between
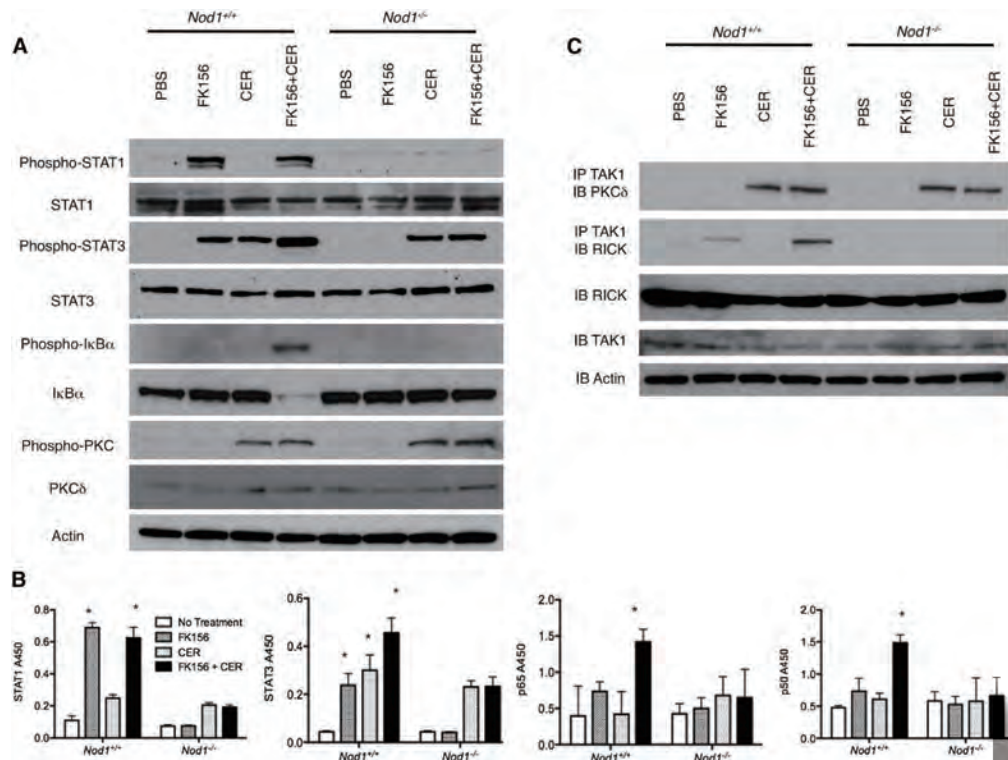
Figure 6. NOD1 Activation Followed by Cerulein Challenge Induces Transactivation of STAT3 and NF-κB In Vivo

Nod1^{+/+} or *Nod1*^{−/−} mice were treated with FK156 and/or cerulein (CER) as described in Figure 2A. Whole or nuclear extracts were prepared from the pancreas of mice at 5 hr after systemic challenge with FK156 and subjected to immunoblotting.

(A) The expression of pSTAT3, STAT3, pSTAT1, STAT1, pPKC, PKCδ, pIκBα, IκBα, and actin was shown with the use of whole-pancreatic extract.

(B) Activation of STAT1, STAT3, p65, and p50 with the use of nuclear extracts, as assessed by Transfactor assay. Results are expressed as means ± SD. *p < 0.01, as compared with the untreated group. The results shown are representative of one of three experiments.

(C) Physical interaction between RICK and TAK1 or between PKCδ and TAK1 in whole-pancreatic extracts. Pancreatic extracts were immunoprecipitated (IP) with TAK1 Ab, followed by immunoblotting (IB) with PKCδ or RICK Ab.

TAK1 and PKCδ in pancreatic cells of *Nod1*^{+/+} and *Nod1*^{−/−} mice (Figure 6C), suggesting induction of TAK1 activation through cerulein-mediated PKC activation. More importantly, as shown by immunoprecipitation with TAK1 Ab followed by immunoblotting with RICK Ab, interaction between RICK and TAK1 was markedly increased in the pancreas of mice treated with both FK156 and low-dose cerulein as compared to the marginal interaction observed with FK156 alone (Figure 6C). Taken together, these data are consistent with the hypothesis that synergistic NF-κB activation by low-dose cerulein and NOD1 is due to cerulein-induced PKC-TAK1 activation followed by opportunistic RICK utilization of the activated TAK1 to induce NF-κB.

NOD1-Induced Activation of STAT3 via Type I IFN

Finally, to more fully assess the role of NOD1 signaling in STAT3 activation via type I IFN, we investigated FK156 and low-dose cerulein induction of pancreatitis in IFN-αβ receptor (IFN-αβR)-deficient (*Ifnar1*^{−/−}) mice. In initial studies, we showed that *Ifnar1*^{−/−} mice exhibited an attenuated pancreatitis along with

a significant reduction of serum levels of amylase and MCP-1 as compared with those in *Ifnar1*^{+/+} mice (Figures 7A and 7B). In addition, upon challenge with FK156 and low-dose cerulein, pancreatic expression of pSTAT3 in *Ifnar1*^{−/−} mice was significantly reduced as compared to that in *Ifnar1*^{+/+} mice, suggesting that type I IFN signaling is necessary for maximal STAT3 activation in this model (Figure 7C).

As expected, pancreatic expression of pSTAT1 was completely absent in *Ifnar1*^{−/−} mice upon challenge with FK156 and low-dose cerulein, suggesting that pancreatic STAT1 activation is dependent upon NOD1-mediated type I IFN signaling in this model. In addition, consistent with the results of the signaling studies presented above, no significant difference in NF-κB activation was seen between *Ifnar1*^{−/−} and *Ifnar1*^{+/+} mice, as assessed by pancreatic expression of pIκBα and IκBα. Serum levels of IFN-β and IP-10, whose production requires activation of type I IFN signaling, were markedly reduced in *Ifnar1*^{−/−} mice treated with FK156 and low-dose cerulein as compared with those in *Ifnar1*^{+/+} mice. In contrast, no significant difference was seen in production of IL-6, whose production
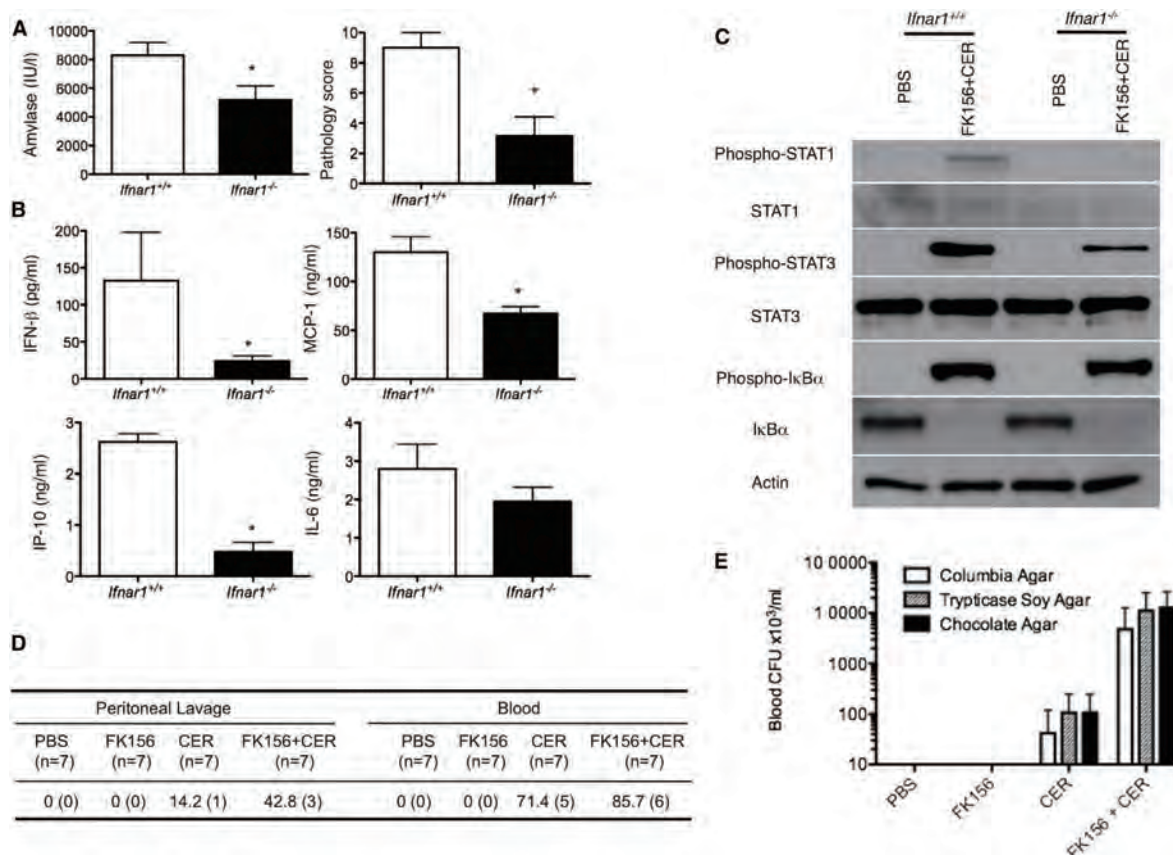
Figure 7. Involvement of Type I IFN Signaling in the Development of Pancreatitis

(A–C) IFNαβ receptor-intact (*Ifnar1*$^{+/+}$) or -deficient (*Ifnar1*$^{-/-}$) mice were subjected to induction of FK156 and low-dose cerulein pancreatitis, as indicated in Figure 2.

(A and B) Serum levels of amylase (A) and MCP-1, IL-6, IFN-β, and IP-10 (B) at 6 hr after systemic challenge with FK156 and pathology scores (A) of the pancreatic tissue at 24 hr after systemic challenge with FK156. Results are expressed as means ± SD. *p < 0.01, as compared with *Ifnar1*$^{+/+}$ mice.

(C) Whole-cell extracts were prepared from pancreatic tissue of mice at 5 hr after systemic challenge with FK156 and subjected to immunoblotting to determine expression of pSTAT3, STAT3, pSTAT1, STAT1, pIκBα, IκBα, and actin. The results shown are representative of one of two experiments.

(D and E) C57BL6 mice were subjected to induction of FK156 and low-dose cerulein pancreatitis; blood and peritoneal lavage fluid were collected 8 hr after the injection.

(D) Percentage and number (parentheses) of mice that were positive for bacterial culture in the blood and peritoneal lavage fluids.

(E) Bacterial loads in the blood determined by counting colonies in columbia agar, trypticase soy agar, and chocolate agar plates. Results are expressed as means ± SD and a summary of three independent experiments.

depends mainly upon activation of NF-κB. Taken together, these results indicate that type I IFN signaling induced by NOD1 activation is involved in the development of pancreatitis in this model.

Bacterial Translocation in Low-Dose Cerulein-Induced Pancreatitis

Intestinal barrier dysfunction and translocation of intestinal microflora into the systemic circulation play a critical role in the development of severe acute pancreatitis (Frossard et al., 2008; Rychter et al., 2009). We therefore addressed the role of bacterial translocation with studies of bacteremia in mice treated with low-dose cerulein alone or in combination with FK156. We

found that 5 of 7 mice treated with low-dose cerulein alone exhibited bacteremia, but that the level of bacteremia was relatively low in each case (Figures 7D and 7E). On the other hand, 6 of 7 mice subjected to combined treatment with FK156 and low-dose cerulein exhibited bacteremia, and in this case, the level of bacteria was much higher than that obtained by treatment with low-dose cerulein alone.

To more clearly identify the role of bacterial translocation from the gut into the circulation in low-dose cerulein pancreatitis, we treated mice with drinking water containing AMP and KM and administered oral ECLACZ prior to FK156 and low-dose cerulein administration. We again observed bacteremia, in this case at a level that increased in parallel with the oral ECLACZ dose

(Figure S6). As expected, the peak level of bacteremia was not as high as that obtained with normal "unperturbed" microflora in the initial study, probably due to the relative paucity of organisms present in the gut under these circumstances. However, it should be noted that serum amylase levels increased in proportion to the oral ECLACZ dose, indicating that even these relatively low levels of bacteremia supported the development of pancreatitis in mice that were administered FK156 and low-dose cerulein (Figure S6). These data are consistent with the view that low-dose cerulein administration alone does not induce pancreatitis in the absence of NOD1 ligand and, in addition, does not induce sufficient bacterial translocation to facilitate de novo NOD1 activation due to exposure to low levels of translocated organisms. In contrast, FK156 and low-dose cerulein administration not only initiated pancreatitis, but also caused bacterial translocation that can now sustain the pancreatitis.

DISCUSSION

We explored the mechanism by which commensal intestinal bacteria contribute to the development of pancreatitis induced by cerulein, a CCKR agonist. Our initial studies established that high-dose cerulein administration, capable of causing pancreatitis by itself, required the presence of a normal intestinal bacterial flora and, quite surprisingly, acted via stimulation of NOD1, an intracellular sensor of a peptide derived from the bacterial wall of both gram-positive and -negative bacteria. To further study this phenomenon, we developed a model of pancreatitis in which mice were administered a dose of cerulein that by itself was insufficient to cause pancreatitis but was nevertheless able to cause pancreatitis when coadministered with NOD1 ligand. This model thus allowed us to identify the specific roles of cerulein and NOD1 signaling in the induction of pancreatic inflammation.

Two key immunopathologic features of the pancreatitis in the low-dose cerulein model are that the inflammation is associated with acinar cells that produce large amounts of MCP-1, a chemoattractant of CCR2$^+$ cells, and that $Ccr2^{-/-}$ mice are almost completely resistant to the development of pancreatitis in this model. These findings strongly suggest that the pancreatitis is driven by MCP-1-mediated migration of CCR2$^+$ inflammatory cells into the pancreas. This conclusion is consistent with previous studies showing that abrogation of MCP-1:CCR2 interactions via administration of a plasmid expressing mutated MCP-1 or a blocker of MCP-1 synthesis protects animals from experimental pancreatitis (Bhatia et al., 2005; Zhao et al., 2005). In addition, in a clinical study, Regnér et al. (2008) showed that serum levels of MCP-1 at the time of a patient's admission to hospital are strongly associated with development of severe acute pancreatitis. Thus, it appears that acinar cell production of MCP-1 and MCP-1-dependent cell migration are essential to the development of acute pancreatitis, not only in this model, but also in other models, and in human pancreatitis as well.

The importance of MCP-1 to pancreatitis accounts for the need for NOD1 signaling in the induction and maintenance of this inflammation. Previous studies have shown that activation of both NF-κB and STAT3 is required for maximal production of MCP-1 (Deshmane et al., 2009; Ray et al., 2008). In the present studies, we corroborated this finding in the context of pancreatitis by showing that both the NF-κB and STAT3 signaling pathways are activated during MCP-1 induction and, indeed, pharmacological inhibition of both pathways is required for the suppression of pancreatitis. In addition, we found that although FK156 or cerulein could induce STAT3 alone, both were necessary for optimal induction and, perhaps more importantly, although neither stimulant could induce activation of the NF-κB signaling pathway alone, they could induce this pathway when acting in concert. It follows that NOD1 signaling is essential to pancreatitis induction because it is necessary for robust activation of the signaling pathways that lead to the production of MCP-1.

The poor NF-κB activation by NOD1 signaling alone in the present study is consistent with our previous studies of this signaling pathway. We showed in these studies that NOD1 activation of RICK (the adaptor protein immediately downstream of NOD1) leads to RICK binding to TRAF3, and thus to activation of TBK1 and IRF7; this, in turn, leads to induction of IFN-β and signaling via IFNαβR for inducing IFN-stimulated gene factor 3, a complex composed of STAT1, STAT2, and IRF9 that acts as a transcription factor for chemokines including IP-10 (Watanabe et al., 2010). Thus, in effect, NOD1 signaling bypasses NF-κB to induce chemokines via a type I IFN-dominated pathway. How, then, does NOD1 signaling cause NF-κB activation in association with low-dose cerulein? We believe the answer lies in the fact that even low doses of cerulein induce activation of TAK1 via PKC (Li et al., 2009; Shinohara et al., 2005) and that in the presence of such activation, RICK activated by NOD1 forms a complex with TAK1 to activate NF-κB. This idea is supported by an enhanced physical interaction between RICK and TAK1 in the mice treated with both FK156 and cerulein.

With respect to STAT3 activation in this model, previous studies have shown that cerulein can induce STAT3, at least at suboptimal levels (Yu et al., 2005). However, as shown in these studies, NOD1 signaling greatly augments such induction by at least two mechanisms. On the one hand, by facilitating NF-κB activation, NOD1 promotes the synthesis of IL-6, a cytokine capable of STAT3 activation. On the other hand, NOD1 signaling leads to production of type I IFN, a cytokine also capable of STAT3 activation (Yang et al., 1998).

Analysis of the level of bacteremia occurring after administration of a low dose of cerulein alone or in combination with NOD1 ligand provided insight into the role of bacterial entry into the circulation in the induction of low-dose cerulein pancreatitis. Low-level bacteremia was observed in mice treated with low doses of cerulein alone, indicating that the level of activation of CCKR with this dose leads to some degree of translocation of bacteria into the systemic circulation. Evidently, however, this level of translocation does not provide a sufficient NOD1 signal in acinar cells to initiate and sustain pancreatitis. In contrast, higher levels of bacteremia accompanied administration of NOD1 ligand and low-dose cerulein. It appears that such bacteremia, by providing a continued source of NOD1 signaling, is necessary to sustain the pancreatitis initiated by exogenous NOD1 ligand. Thus, low-dose cerulein-induced pancreatitis is equivalent to high-dose cerulein pancreatitis, except for the fact that the latter initiates a level of pancreatic inflammation

that causes sufficient bacterial translocation and NOD1 signaling on its own.

It has been generally assumed that NOD1 activation is induced exclusively by pathogenic organisms and that such activation elicits NOD1-mediated host defense responses (Girardin et al., 2003; Kim et al., 2004). However, it was recently shown that NOD1 signaling can also be initiated by commensal organisms in the neonatal gut, where it plays a role in lymphoid-tissue organogenesis via the induction of defensin and the production of a chemotactic factor (Bouskra et al., 2008). The present study extends this observation by showing that NOD1 activation by commensal organisms also occurs during an inflammatory response. These observations raise the question of why NOD1 activation by commensal organisms does not cause inflammation in the normal gut. We believe the answer to this question is that NOD1 does respond to commensal organisms in the normal uninflamed gut via type I IFN signaling rather than NF-κB signaling, and type I IFN signaling does not result in inflammation (Abe et al., 2007).

In conclusion, in the present study, we provide evidence that activation of NOD1 by commensal organisms can facilitate a severe form of acute pancreatitis by acting in synergy with low doses of a CCKR agonist, cerulein. In addition, we show that such synergy is necessary for the production of MCP-1, a chemokine that mediates migration and infiltration of CCR2+ pathogenic myeloid cells into the pancreas. Finally, we show that a critical feature of this model of pancreatitis, as well as high-dose cerulein pancreatitis, that does not require priming by NOD1 agonist, is that pancreatitis is driven by commensal organisms that stimulate NOD1 in acinar cells. Thus, although autodigestion of acinar cells mediated by activation of pancreatic enzymes such as trypsinogen is one necessary component of acute pancreatitis, bacterial translocation and the induction of acinar cell expression of inflammatory mediators are also necessary components (Dawra et al., 2011; Ji and Logsdon, 2011). It seems probable that therapeutic measures attacking these latter components, such as those directed at the inhibition of NOD1 signaling, offer a new approach to the treatment of acute pancreatitis.

EXPERIMENTAL PROCEDURES

Mice

C57BL6 mice, GFP-transgenic mice (Okabe et al., 1997), and *Prkdc*scid mice were purchased from CLEA. *Tlr2*−/−, *Tlr4*−/−, and *Tlr9*−/− mice were purchased from Oriental Bioservice. In some experiments, *Nod1*−/− (Watanabe et al., 2010) and *Ccr2*−/− mice (Boring et al., 1998) were used. Mice were reared under specific pathogen-free conditions. Animal use adhered to the Kyoto University animal-care guidelines, and protocols of animal experiments were approved by the review boards of Kyoto University.

Induction of Pancreatitis

Mice received i.p. injection of FK156 (200 μg) or MDP (200 μg) in combination with i.p. injection of cerulein (20 μg/kg) for a total of three times. Mice treated with AMP (1 g/l) and KM (1 g/l) in the drinking water for 2 weeks were challenged with i.p. injection of ECLACZ (Yoshida et al., 2001) (1 × 10^6 cfu) followed by i.p. injection of cerulein (20 μg/kg) for a total of three times. Mice treated with AMP (1 g/l), neomycin (1 g/l), KM (0.5 g/l), or metronidazole (1 g/l) in the drinking water for 3 weeks were challenged with i.p. injection of cerulein (50 μg/kg) for a total of seven times. Sera and pancreas tissue were obtained at the indicated time points.

Bone Marrow Transplantation

For the generation of BM-chimeric mice, recipient mice were irradiated with 10 Gy and were reconstituted with BM cells from the donor mice as previously described (Watanabe et al., 2010).

NF-κB and STAT3 Activation Assay

Whole extracts isolated from the pancreas were subjected to immunoblotting as previously described (Watanabe et al., 2010). pSTAT1, STAT3, pSTAT3, IκBα, pIκBα, pPKC, and PKCδ Abs were obtained from Cell Signaling. Actin, TAK1, and STAT1 Abs were obtained from Santa Cruz Biotechnology. Binding activity of nuclear extract to NF-κB subunits (p50 and p65), STAT1, and STAT3 was measured using a TransAM kit, obtained from Active Motif, as previously described (Watanabe et al., 2010). 7 or 15 μg of nuclear extracts were subjected to assay. Physical interaction between RICK and TAK1 or between PKCδ and TAK1 was analyzed via immunoprecipitation using whole-pancreatic extract. Pancreatic extracts were immunoprecipitated with TAK1 Ab followed by immunoblotting with PKCδ or RICK Ab (Cayman) as described previously (Watanabe et al., 2010).

Statistical Analysis

Student's t test was used to evaluate the significance of the differences. A value of $p < 0.05$ was regarded as statistically significant.

SUPPLEMENTAL INFORMATION

Supplemental Information includes six figures and Supplemental Experimental Procedures and can be found with this article online at http://dx.doi.org/10.1016/j.immuni.2012.05.024.

REFERENCES

Abe, K., Nguyen, K.P., Fine, S.D., Mo, J.H., Shen, C., Shenouda, S., Corr, M., Jung, S., Lee, J., Eckmann, L., and Raz, E. (2007). Conventional dendritic cells regulate the outcome of colonic inflammation independently of T cells. Proc. Natl. Acad. Sci. USA *104*, 17022–17027.

Akira, S., and Takeda, K. (2004). Toll-like receptor signalling. Nat. Rev. Immunol. *4*, 499–511.

Baumann, B., Wagner, M., Aleksic, T., von Wichert, G., Weber, C.K., Adler, G., and Wirth, T. (2007). Constitutive IKK2 activation in acinar cells is sufficient to induce pancreatitis in vivo. J. Clin. Invest. *117*, 1502–1513.

Bhatia, M., Ramnath, R.D., Chevali, L., and Guglielmotti, A. (2005). Treatment with bindarit, a blocker of MCP-1 synthesis, protects mice against acute pancreatitis. Am. J. Physiol. Gastrointest. Liver Physiol. *288*, G1259–G1265.

Boring, L., Gosling, J., Cleary, M., and Charo, I.F. (1998). Decreased lesion formation in CCR2-/- mice reveals a role for chemokines in the initiation of atherosclerosis. Nature *394*, 894–897.

Bouskra, D., Brézillon, C., Bérard, M., Werts, C., Varona, R., Boneca, I.G., and Eberl, G. (2008). Lymphoid tissue genesis induced by commensals through NOD1 regulates intestinal homeostasis. Nature *456*, 507–510.

Chamaillard, M., Hashimoto, M., Horie, Y., Masumoto, J., Qiu, S., Saab, L., Ogura, Y., Kawasaki, A., Fukase, K., Kusumoto, S., et al. (2003). An essential role for NOD1 in host recognition of bacterial peptidoglycan containing diaminopimelic acid. Nat. Immunol. *4*, 702–707.

Chen, G., Shaw, M.H., Kim, Y.G., and Nuñez, G. (2009). NOD-like receptors: role in innate immunity and inflammatory disease. Annu. Rev. Pathol. *4*, 365–398.

Dawra, R., Sah, R.P., Dudeja, V., Rishi, L., Talukdar, R., Garg, P., and Saluja, A.K. (2011). Intra-acinar trypsinogen activation mediates early stages of pancreatic injury but not inflammation in mice with acute pancreatitis. Gastroenterology *141*, 2210–2217, e2.

Deshmane, S.L., Kremlev, S., Amini, S., and Sawaya, B.E. (2009). Monocyte chemoattractant protein-1 (MCP-1): an overview. J. Interferon Cytokine Res. *29*, 313–326.

Fagarasan, S., Muramatsu, M., Suzuki, K., Nagaoka, H., Hiai, H., and Honjo, T. (2002). Critical roles of activation-induced cytidine deaminase in the homeostasis of gut flora. Science *298*, 1424–1427.

Ferrand, A., Kowalski-Chauvel, A., Bertrand, C., Escrieut, C., Mathieu, A., Portolan, G., Pradayrol, L., Fourmy, D., Dufresne, M., and Seva, C. (2005). A novel mechanism for JAK2 activation by a G protein-coupled receptor, the CCK2R: implication of this signaling pathway in pancreatic tumor models. J. Biol. Chem. *280*, 10710–10715.

Fritz, J.H., Le Bourhis, L., Sellge, G., Magalhaes, J.G., Fsihi, H., Kufer, T.A., Collins, C., Viala, J., Ferrero, R.L., Girardin, S.E., and Philpott, D.J. (2007). Nod1-mediated innate immune recognition of peptidoglycan contributes to the onset of adaptive immunity. Immunity *26*, 445–459.

Frossard, J.L., Steer, M.L., and Pastor, C.M. (2008). Acute pancreatitis. Lancet *371*, 143–152.

Gao, H.K., Zhou, Z.G., Li, Y., and Chen, Y.Q. (2007). Toll-like receptor 4 Asp299Gly polymorphism is associated with an increased risk of pancreatic necrotic infection in acute pancreatitis: a study in the Chinese population. Pancreas *34*, 295–298.

Girardin, S.E., Boneca, I.G., Carneiro, L.A., Antignac, A., Jéhanno, M., Viala, J., Tedin, K., Taha, M.K., Labigne, A., Zähringer, U., et al. (2003). Nod1 detects a unique muropeptide from gram-negative bacterial peptidoglycan. Science *300*, 1584–1587.

Grady, T., Liang, P., Ernst, S.A., and Logsdon, C.D. (1997). Chemokine gene expression in rat pancreatic acinar cells is an early event associated with acute pancreatitis. Gastroenterology *113*, 1966–1975.

Hasegawa, M., Fujimoto, Y., Lucas, P.C., Nakano, H., Fukase, K., Núñez, G., and Inohara, N. (2008). A critical role of RICK/RIP2 polyubiquitination in Nod-induced NF-kappaB activation. EMBO J. *27*, 373–383.

Ji, B., and Logsdon, C.D. (2011). Digesting new information about the role of trypsin in pancreatitis. Gastroenterology *141*, 1972–1975.

Kim, J.G., Lee, S.J., and Kagnoff, M.F. (2004). Nod1 is an essential signal transducer in intestinal epithelial cells infected with bacteria that avoid recognition by toll-like receptors. Infect. Immun. *72*, 1487–1495.

Li, S., Wang, L., and Dorf, M.E. (2009). PKC phosphorylation of TRAF2 mediates IKKalpha/beta recruitment and K63-linked polyubiquitination. Mol. Cell *33*, 30–42.

Okabe, M., Ikawa, M., Kominami, K., Nakanishi, T., and Nishimune, Y. (1997). 'Green mice' as a source of ubiquitous green cells. FEBS Lett. *407*, 313–319.

Rakonczay, Z., Jr., Hegyi, P., Takács, T., McCarroll, J., and Saluja, A.K. (2008). The role of NF-kappaB activation in the pathogenesis of acute pancreatitis. Gut *57*, 259–267.

Ray, S., Lee, C., Hou, T., Boldogh, I., and Brasier, A.R. (2008). Requirement of histone deacetylase1 (HDAC1) in signal transducer and activator of transcription 3 (STAT3) nucleocytoplasmic distribution. Nucleic Acids Res. *36*, 4510–4520.

Regnér, S., Appelros, S., Hjalmarsson, C., Manjer, J., Sadic, J., and Borgstrom, A. (2008). Monocyte chemoattractant protein 1, active carboxypeptidase B and CAPAP at hospital admission are predictive markers for severe acute pancreatitis. Pancreatology *8*, 42–49.

Rychter, J.W., van Minnen, L.P., Verheem, A., Timmerman, H.M., Rijkers, G.T., Schipper, M.E., Gooszen, H.G., Akkermans, L.M., and Kroese, A.B. (2009). Pretreatment but not treatment with probiotics abolishes mouse intestinal barrier dysfunction in acute pancreatitis. Surgery *145*, 157–167.

Sharif, R., Dawra, R., Wasiluk, K., Phillips, P., Dudeja, V., Kurt-Jones, E., Finberg, R., and Saluja, A. (2009). Impact of toll-like receptor 4 on the severity of acute pancreatitis and pancreatitis-associated lung injury in mice. Gut *58*, 813–819.

Shinohara, H., Yasuda, T., Aiba, Y., Sanjo, H., Hamadate, M., Watarai, H., Sakurai, H., and Kurosaki, T. (2005). PKC beta regulates BCR-mediated IKK activation by facilitating the interaction between TAK1 and CARMA1. J. Exp. Med. *202*, 1423–1431.

Strober, W., Murray, P.J., Kitani, A., and Watanabe, T. (2006). Signalling pathways and molecular interactions of NOD1 and NOD2. Nat. Rev. Immunol. *6*, 9–20.

Takagi, Y., Masamune, A., Kume, K., Satoh, A., Kikuta, K., Watanabe, T., Satoh, K., Hirota, M., and Shimosegawa, T. (2009). Microsatellite polymorphism in intron 2 of human Toll-like receptor 2 gene is associated with susceptibility to acute pancreatitis in Japan. Hum. Immunol. *70*, 200–204.

Tando, Y., Algül, H., Wagner, M., Weidenbach, H., Adler, G., and Schmid, R.M. (1999). Caerulein-induced NF-kappaB/Rel activation requires both Ca2+ and protein kinase C as messengers. Am. J. Physiol. *277*, G678–G686.

Watanabe, T., Asano, N., Fichtner-Feigl, S., Gorelick, P.L., Tsuji, Y., Matsumoto, Y., Chiba, T., Fuss, I.J., Kitani, A., and Strober, W. (2010). NOD1 contributes to mouse host defense against Helicobacter pylori via induction of type I IFN and activation of the ISGF3 signaling pathway. J. Clin. Invest. *120*, 1645–1662.

Werts, C., Rubino, S., Ling, A., Girardin, S.E., and Philpott, D.J. (2011). Nod-like receptors in intestinal homeostasis, inflammation, and cancer. J. Leukoc. Biol. *90*, 471–482.

Yang, C.H., Murti, A., and Pfeffer, L.M. (1998). STAT3 complements defects in an interferon-resistant cell line: evidence for an essential role for STAT3 in interferon signaling and biological activities. Proc. Natl. Acad. Sci. USA *95*, 5568–5572.

Yoshida, M., Watanabe, T., Usui, T., Matsunaga, Y., Shirai, Y., Yamori, M., Itoh, T., Habu, S., Chiba, T., Kita, T., and Wakatsuki, Y. (2001). CD4 T cells monospecific to ovalbumin produced by Escherichia coli can induce colitis upon transfer to BALB/c and SCID mice. Int. Immunol. *13*, 1561–1570.

Yu, J.H., Lim, J.W., Kim, H., and Kim, K.H. (2005). NADPH oxidase mediates interleukin-6 expression in cerulein-stimulated pancreatic acinar cells. Int. J. Biochem. Cell Biol. *37*, 1458–1469.

Zhao, H.F., Ito, T., Gibo, J., Kawabe, K., Oono, T., Kaku, T., Arita, Y., Zhao, Q.W., Usui, M., Egashira, K., and Nawata, H. (2005). Anti-monocyte chemoattractant protein 1 gene therapy attenuates experimental chronic pancreatitis induced by dibutyltin dichloride in rats. Gut *54*, 1759–1767.

Transcatheter endoscopy for pancreaticobiliary duct diseases (with videos)

Hiroki Sakamoto, MD, PhD,[1] Masayuki Kitano, MD, PhD,[1] Ken Kamata, MD,[1] Takeshi Miyata, MD,[1] Kunpei Kadosaka, MD,[1] Hajime Imai, MD,[1] Yoshifumi Takeyama, MD, PhD,[2] Masatoshi Kudo, MD, PhD[1]

Osaka-Sayama, Japan

To obtain an accurate diagnosis of bile and pancreatic duct diseases through biopsy, peroral cholangioscopy (POCS) was developed for imaging purposes. POCS is particularly useful for estimating the extent of tumor infiltration, which is difficult to determine by cholangiography.[1-9] However, although direct visualization of intraductal lesions by POCS offers definite theoretical advantages in establishing a diagnosis, it is a labor-intensive task because an endoscopic sphincterotomy (EST) is required and a papillary baby endoscope has to be inserted through the main endoscope. These procedures can cause POCS-related complications such as cholangitis and pancreatitis.[10-12] Moreover, it is difficult to insert the endoscope in the bile duct more peripherally than the hepatic portal region, and the observational range is limited because the stiffness of the mother endoscope used for POCS makes it difficult to maneuver. Recently, a peroral cholangiopancreatoscopy system (Spyglass, Microvasive Endoscopy; Boston Scientific, Natick, Mass) was developed. This system consists of a very thin optical glass-fiber probe that has an outer diameter of 0.77 mm and a disposable sheath that can be angled during maneuvers. The thin probe can also be removed from its sheath and inserted in an ordinary biliary catheter for delivering contrast agents during ERCP. We attempted to use the thin probe inserted in an ordinary catheter for cannulating the biliary and pancreatic ducts (Tandem XL; Boston Scientific), which allowed transcatheter endoscopy (TCE). Such transcatheter cholangiopancreatoscopy may be a safe, easy, and convenient way to observe the biliary and pancreatic ducts. Furthermore, it is not necessary to perform EST when using TCE in pancreaticobiliary tract diseases. This study evaluated the clinical feasibility and safety of TCE for observations of pancreaticobiliary tract diseases.

PATIENTS AND METHODS

In this study, the indications for TCE were indeterminate filling defects or strictures in the bile duct, biliary bleeding of unknown origin, and dilation of the pancreatic duct suggestive of intraductal papillary mucinous neoplasm (IPMN). If therapeutic ERCP was required beforehand, we conducted an endoscopic sphincterotomy without performing TCE. Between November and December 2011, a total of 17 patients underwent TCE at Kinki University Hospital according to these indications. All patients gave written informed consent, and the study was approved by the institutional review board of our institution.

TCE system

ERCP was performed with a duodenoscope (JF-260V; Olympus Optical Co, Ltd, Tokyo, Japan). A pancreaticobiliary catheter (Tandem XL; Boston Scientific) was used to inject contrast medium and for TCE. The catheter has 2 lumens: 1 lumen for contrast medium injection, and another lumen for inserting the guidewire. The width of the catheter tip is 5.5F (1.8 mm) and the maximum outer diameter of the catheter is 7F (2.3 mm), which can accommodate a guidewire up to 0.035 inch (0.89 mm) in size. The Spyglass optical probe of the Spyglass peroral cholangiopancreatoscopy system has an outer diameter of 0.77 mm and thus can pass through the catheter tube. After the bile duct or the pancreatic duct was cannulated with the tandem catheter in combination with the guidewire, contrast material was injected into the duct, and the guidewire was removed from the catheter. Sterile saline solution was continuously flushed through the contrast medium injection lumen by using a 20-mL syringe until clear bile or pancreatic juice appeared. When the contents in the duct were aspirated from the guidewire lumen, the fluid that
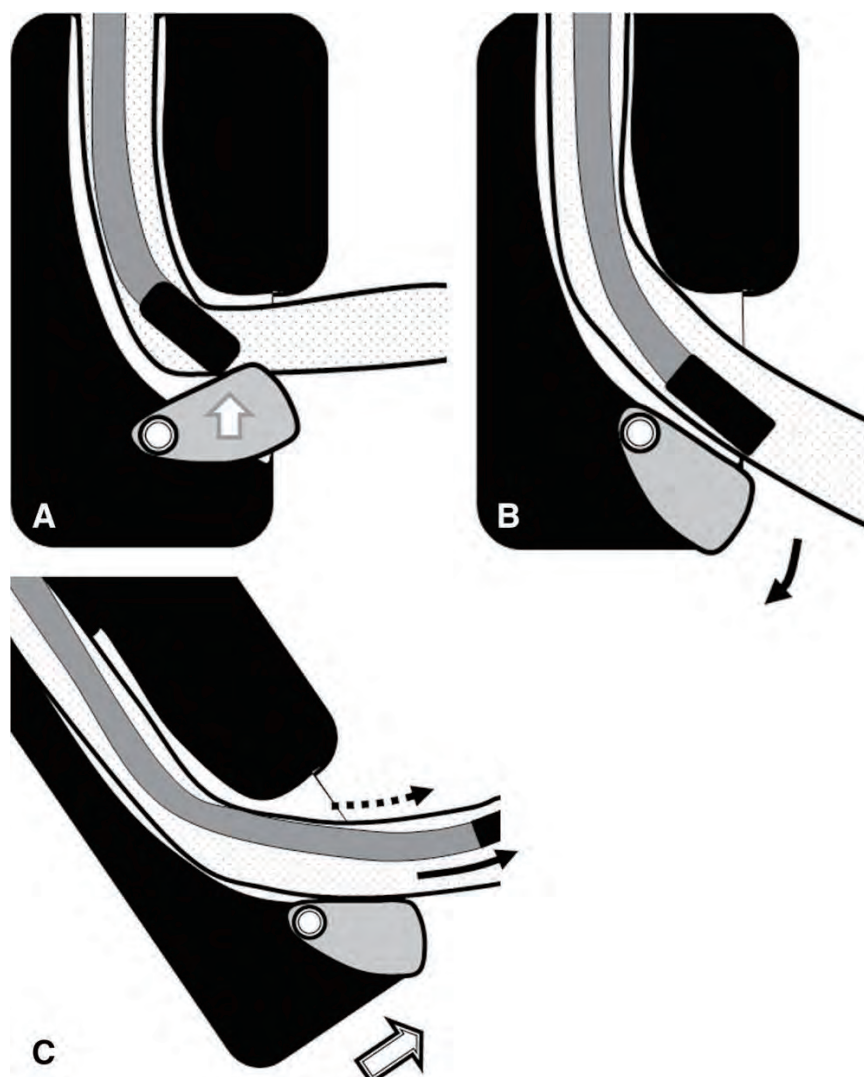
Figure 1. Procedures for insertion of the Spyglass probe into the tandem catheter. When the Spyglass probe is inserted in the tandem catheter, there is resistance at the forceps elevator (*arrow*) (**A**). The forceps elevator in the endoscope is deflexed downward (**B**). The tandem catheter is advanced while the endoscope is angled upward (**C**). Then, the tip of the Spyglass probe passes the portion of the elevator.

was aspirated was bile or pancreatic juice mixed with saline solution. The Spyglass probe was then advanced through the guidewire lumen to observe the pancreaticobiliary tract lesions. When the Spyglass probe was advanced through the tandem catheter guidewire lumen, there was resistance because of the bending of the catheter at the forceps elevator in the working channel (Fig. 1A). Then, the forceps elevator was deflexed downward (Fig. 1B), and thereafter the tandem catheter was advanced while the endoscope was angled upward (Fig. 1C). With these steps, the tip of Spyglass probe in the tandem catheter could be advanced into the bile duct without being damaged.

To observe the lesions, the tip of the Spyglass probe was advanced from the tip of tandem catheter into the bile duct. Visualization of the target lesions was achieved by moving the probe in and out through the tandem catheter (Fig. 2A). When the TCE catheter was advanced to pass a stricture or filling defect in the bile or pancreatic duct, the tip of the Spyglass was reinserted in the tandem catheter (Fig. 2B). The Spyglass in TCE was reused until it was broken in this study.

All endoscopies were performed in patients while they were sedated with intravenous midazolam and propofol under monitoring with an automated noninvasive blood pressure device, electrocardiogram tracing, and pulse oxi-
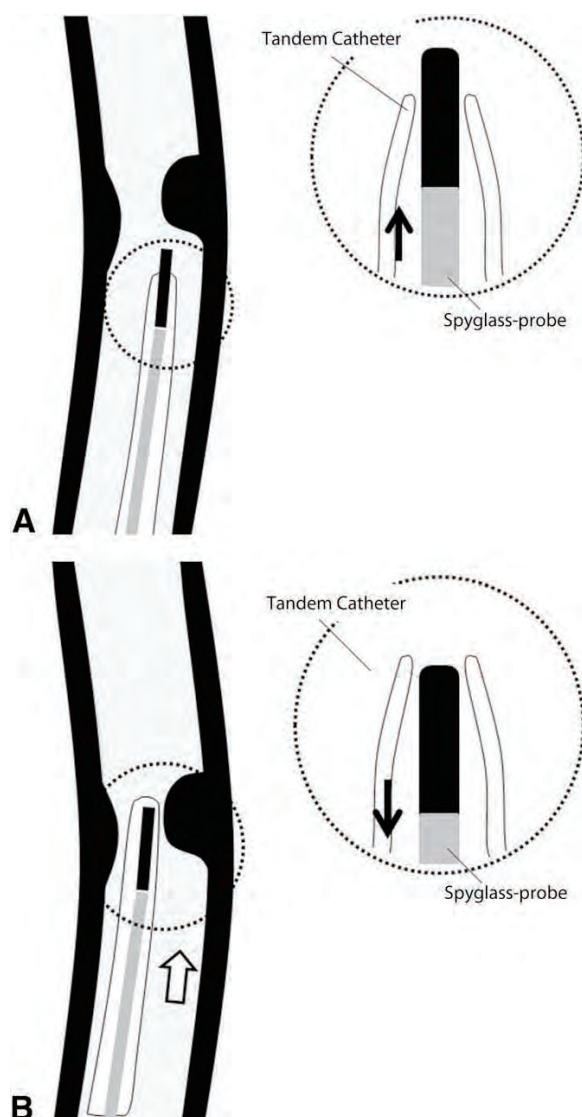
Figure 2. Procedures for observation of the lesions by transcatheter endoscopy (TCE). **A**, During observation of the lesions, the tip of the Spyglass probe is advanced from the tip of tandem catheter into the bile duct. By moving the probe forward and backward, proper position of the probe for observation can be adjusted. **B**, When TCE catheter is advanced into the narrow areas, the tip of the Spyglass probe is pulled back in the tandem catheter.

metry during the procedure. Two endoscopists (H.S. and M.K.), who have extensive experience in the diagnosis and management of pancreaticobiliary tract diseases, performed the procedures.

Evaluation of TCE observations

All endoscopic images were recorded by a digital video system. The procedure time from cannulation with the tandem catheter to the final evaluation of the TCE obser-

vation was measured. The blind reading was performed by 2 endoscopists (H.I. and K.K.) who were not present during TCE. They were not informed of the final diagnoses during evaluation of the videos. The 2 investigators reviewed images and assigned 1 of 3 evaluation scores to each lesion according to the quality of visualization: 1, poor; 2, fair; or 3, good. When the lesion was not identified by the TCE, it was categorized as poor. When the lesion was identified by the TCE but its structure was obscure, it was categorized as fair. When the lesion was identified and clearly characterized by the TCE, it was categorized as good. When the readings by the 2 independent reviewers differed, the saved images were reviewed together and reevaluated until agreement was reached.

Assessment of complications

In this study, the white blood cell count, serum lactate dehydrogenase, alkaline phosphatase, aspartate aminotransferase, alanine aminotransferase, total bilirubin, serum amylase, and C-reactive protein were measured 1 day after the procedure. Whether symptoms (abdominal pain, back pain, or fever) appeared up to 72 hours after the procedure was also recorded. Cholangitis and pancreatitis were classified according to the 1991 consensus guidelines reported by Cotton et al.[10] Cholangitis was defined as an increase in body temperature to more than 38°C resulting from a biliary cause (ie, without evidence of other concomitant infections). Pancreatitis was diagnosed when new-onset or worsened abdominal pain lasted for more than 24 hours and was associated with an increase in serum amylase level of at least 3 times the upper limit of normal 24 hours after the procedure.

RESULTS

Seventeen patients (7 men and 10 women) with a mean age of 68.8 years (range 59-80 years) with pancreatobiliary diseases (13 with biliary and 4 with pancreatic lesions) were enrolled (Table 1). Twelve patients had an indeterminate filling defect or stricture in the bile duct. One patient had biliary bleeding of unknown origin. Four patients had dilation of the pancreatic duct suggestive of IPMN. EST was not performed for cannulation with a tandem catheter before TCE in any of the patients. The mean time to perform TCE was 6 minutes, 15 seconds (range 2 minutes, 32 seconds to 12 minutes, 33 seconds). There was disagreement on the quality of visualization between the 2 investigators in a common bile duct polyp and an IPMN. For both lesions, independent evaluation of 1 investigator was good visualization, whereas it was fair by the other investigator. They reviewed the images of the 2 lesions together, reevaluated their findings, and concluded fair visualization for the common bile duct polyp and good visualization for the IPMN. TCE-related complications were not observed. Only 1 probe was used in 17 patients without being broken.

TABLE 1. Patient characteristics and outcomes

Patient	Age, y/sex	Location	ERCP findings	Final diagnosis	Procedure time	Visualization
1	68/F	Superior extrahepatic duct	Filling defect	IPNB (surgery)	12 min 33 s	Poor
2	70/M	Middle extrahepatic duct	Stricture	EBDC (surgery)	8 min 22 s	Poor
3	59/F	Bp	Filling defect	Common bile duct polyp (surgery)	3 min 8 s	Fair
4	66/F	Middle extrahepatic duct	Filling defect	Air (follow-up)	2 min 32 s	Good
5	64/M	Middle extrahepatic duct	Filling defect	EBDC (surgery)	4 min 53 s	Fair
6	70/M	Middle extrahepatic duct	Biliary bleeding	Biliary bleeding	6 min 19 s	Good
7	68/F	Middle extrahepatic duct	Stricture	EBDC (surgery)	5 min 43 s	Fair
8	74/M	Middle extrahepatic duct	Stricture	EBDC (surgery)	9 min 40 s	Poor
9	74/F	Bp	Stricture	EBDC (cytological diagnosis)	5 min 5 s	Good
10	67/F	Inferior extrahepatic duct	Filling defect	Common bile duct stone	2 min 48 s	Good
11	80/F	Middle extrahepatic duct	Filling defect	EBDC (surgery)	11 min 41 s	Poor
12	68/F	Middle extrahepatic duct	Filling defect	Common bile duct stone	3 min 18 s	Good
13	72/M	Middle extrahepatic duct	Filling defect	EBDC (cytological diagnosis)	9 min 22 s	Poor
14	70/F	Pancreatic body	MPD dilation, filling defect	IPMA (surgery)	4 min 55 s	Good
15	68/M	Pancreatic head	MPD dilation, filling defect	IPMC (surgery)	4 min 2 s	Good
16	73/F	Pancreatic body	MPD dilation, filling defect	IPMC (surgery)	8 min 18 s	Fair
17	75/M	Pancreatic body	MPD dilation	IPMA (surgery)	3 min 48 s	Fair

F, Female; *IPNB*, intraductal papillary neoplasm of the bile duct; *M*, male; *EBDC*, extrahepatic bile duct cancer; *Bp*, superior extrahepatic duct; *MPD*, main pancreatic duct; *IPMA*, intraductal papillary mucinous adenoma; *IPMC*, intraductal papillary mucinous adenoma.

For biliary lesions, the mean time to perform TCE was 6 minutes, 34 seconds (range 2 minutes, 32 seconds to 12 minutes, 33 seconds). The final diagnoses for the 13 biliary lesions after ERCP and TCE were as follows: bile duct cancer (n = 7), intraductal papillary neoplasm of the bile duct (n = 1), inflammatory polyp (n = 1), small incidental stone (n = 2), an air artifact in the bile duct (n = 1), and biliary bleeding (n = 1). Surgery was performed in 5 of the 7 patients with bile duct cancer, in the patient with intraductal papillary neoplasm of the bile duct, and in the patients with inflammatory polyps. The remaining 2 patients with advanced bile duct cancer with a diagnosis made by cytology of the bile juice received chemotherapy. The ERCP findings of the biliary lesions indicated that there were 4 strictures, 8 filling defects, and 1 biliary bleed.

TCE generated good, fair, and poor visualizations of 5 (38.5%), 3 (23.0%), and 5 (38.5%) biliary lesions, respectively. In particular, it clearly visualized the incidental small stones, whereas ERCP could not distinguish these lesions from air artifacts, and MRCP could not depict the small stones at all (Fig. 3). Both stones were removed by

basket catheter after EST. TCE also depicted the air artifact well. This artifact was detected during ERCP to evaluate an anomalous junction in the pancreatobiliary system. After it was identified by TCE as an artifact, the patient was followed as an outpatient. Similarly, in the patient with biliary bleeding, it was not possible to determine the source of the bleeding by interventional radiology or ERCP, but TCE could clearly identify it. This patient was treated by insertion of a metal stent in the bile duct after the source of the bleeding was identified by TCE (Fig. 4A and B; and Video 1, available at www.giejournal.org). For the 4 cases of bile duct cancer and the case of IPNB, TCE yielded poor visualization because the bile juice contained mucous clots or a mixture of necrotic tissue and blood. In addition, we could not maneuver the catheter correctly to observe some parts of the lesions by TCE. Eventually, 8 of the 13 patients underwent EST after TCE, whereas 5 did not.

For pancreatic lesions, the mean time to perform TCE was 5 minutes, 15 seconds (range 3 minutes, 48 seconds to 8 minutes, 18 seconds). The final diagnoses of the pancreatic lesions were as follows: intraductal papillary muci-
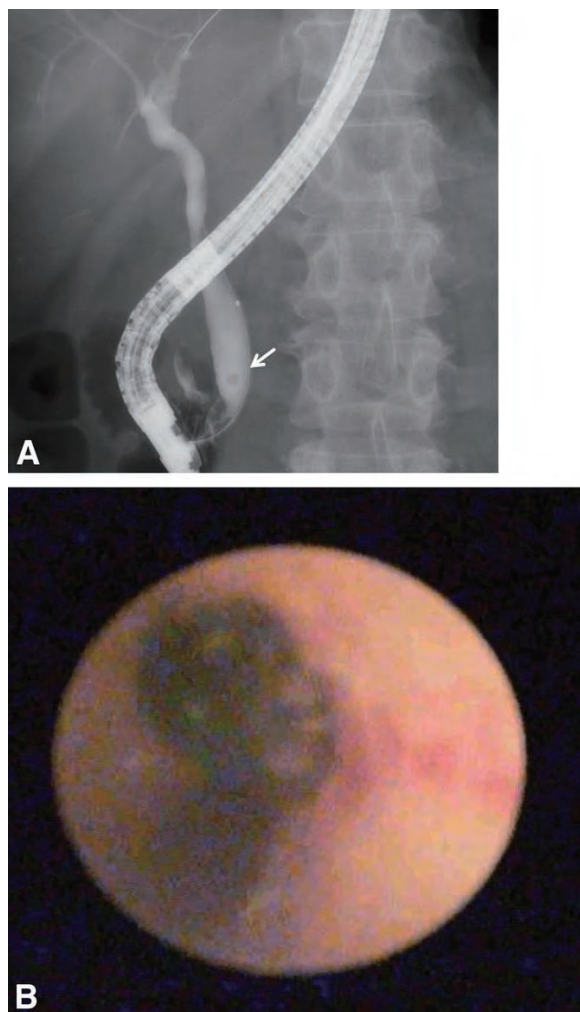
Figure 3. A, A 69-year-old woman was hospitalized for examination of a tumor in the gallbladder. When she underwent transpapillary cholangiography, a defect was found in the bile duct (*arrow*). However, it was unclear whether it was a stone or an air artifact. **B**, Transcatheter endoscopy revealed that it was an incidental stone in the bile duct, which was removed after performing endoscopic sphincterotomy.

nous adenocarcinoma (n = 2) and intraductal papillary mucinous adenoma (n = 2). All patients underwent total pancreatomy or pancreatoduodenectomy. ERCP revealed dilation of main pancreatic duct in all patients. The average diameter of the main pancreatic duct was 7.4 ± 2.9 mm (range 4.8-14.3 mm). TCE provided good and fair visualizations in 2 (50.0%) and 2 (50.0%) of the pancreatic lesions, respectively (Fig. 5; Video 2, available at www.giejournal.org). There were no poor visualizations. ERCP depicted filling defects in 3 of the 4 patients. Although 1 patient had highly mucinous secretions in the main pancreatic duct, they were aspirated and removed by a 7F catheter (Soehendra biliary dilation catheter; Cook Medi-

cal, Bloomington, Ind). The pancreatic lesion could then be observed by TCE after irrigation of the pancreatic duct. None of the 4 patients underwent EST after TCE.

DISCUSSION

POCS was developed over the past 3 decades as a diagnostic endoscopic modality that could be used to observe bile duct lesions that were difficult to evaluate by cholangiography and facilitate precise diagnostic biopsy.[6-9] Recently, 3 new POCS techniques have been reported. One was direct endoscopic cholangioscopy, in which an ultraslim upper endoscope is advanced over a balloon catheter that has been inserted in the pancreatobiliary duct of the patient; this allows direct visual examination of the biliary and pancreatic ducts.[11,12] Another technique is POCS with narrow-band imaging, which has been reported to be useful for identifying the surface structure and capillary vessels in the ducts.[13,14] The third technique is the Spyglass Spyscope system (Boston Scientific), in which a new single-operator endoscope is introduced into the endoscopic area.[15] This system involves a new intraductal endoscope that differs fundamentally from other existing mini endoscopes in terms of its structure, 4-way steering ability, separate irrigation channel, ease of use, and need for a single operator.[15] Although visualization by POCS offers an advantage in terms of establishing a diagnosis, an EST is necessary with these procedures, which can thus lead to several complications.

In TCE, the Spyglass probe is passed through the catheter for contrast injection into the papilla; in this way, the Spyglass probe can be used to observe the bile or pancreatic duct easily. In this study, TCE could discriminate between incidental stones and air artifacts in the bile duct in 3 patients. It also identified the source of bleeding in the bile duct in 1 patient. Furthermore, TCE was useful for diagnosing 4 cases of pancreatic lesions in which ERCP could not provide clear diagnoses. In 1 patient with a pancreatic lesion, TCE could detect a small tumor; in the remaining 4 patients, it could discriminate between mural nodules and mucous clots in the pancreatic duct lesions.

An advantage of the TCE system is that it can be performed without EST. It was unnecessary to perform EST for cannulation with the tandem catheter before TCE in all patients. Although 8 of 17 patients eventually underwent EST for biliary stenting and extraction of stones, the diagnoses of the lesions were made without endoscopic intervention including EST in the remaining 9 patients. TCE can also be performed in even patients who take anticoagulant medication. Another advantage is that it involves a thinner catheter than is usually used in POCS, which in turn reduces the chance of injury to the bile and pancreatic duct walls because only a catheter for contrast injection is used. Moreover, the TCE endoscope allows us to advance into and observe more peripheral thinner intrahepatic ducts than we can with POCS. Published case series have
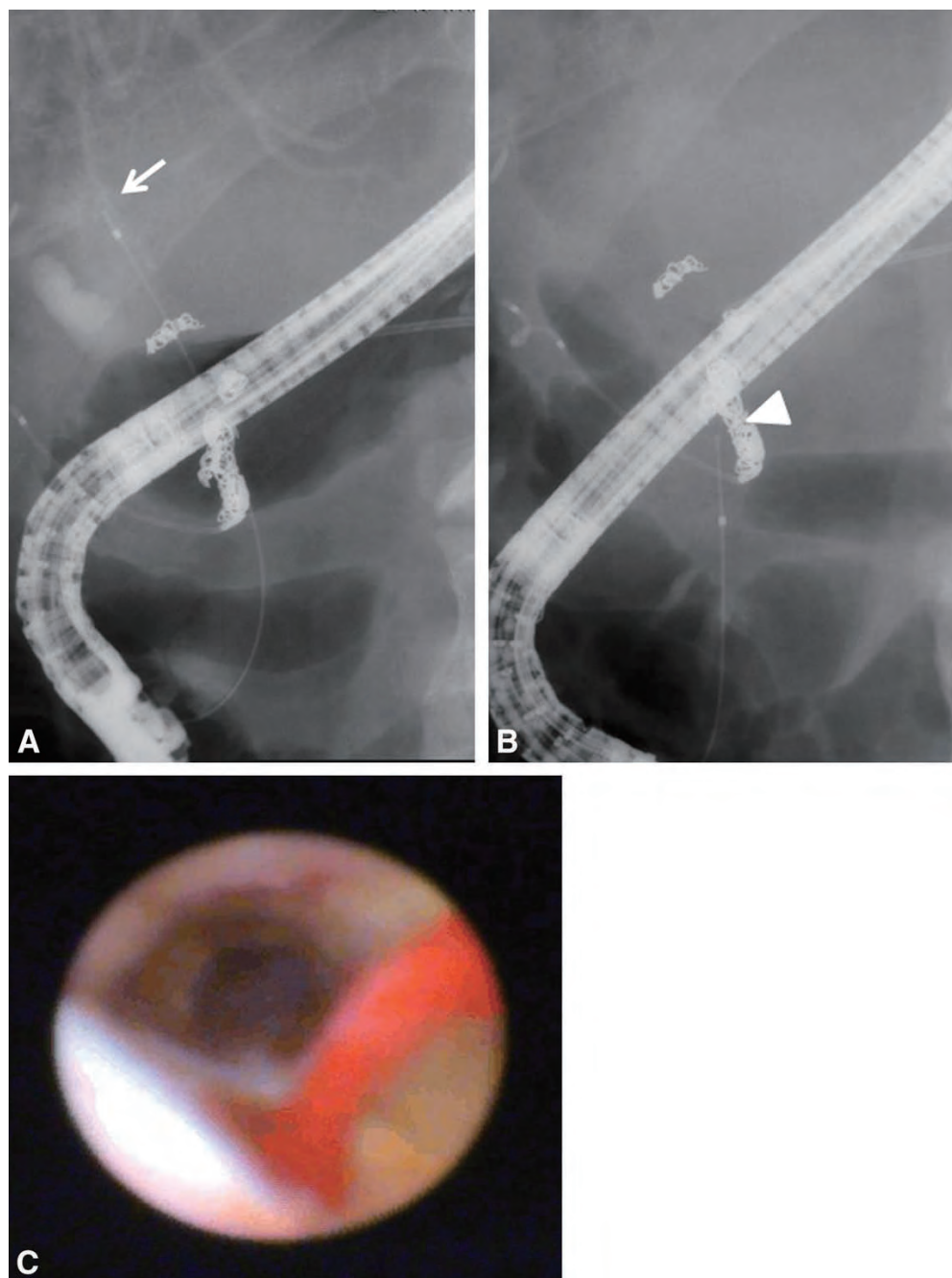
Figure 4. A 70-year-old man who received transcatheter arterial infusion to treat hepatocellular carcinoma was hospitalized for biliary bleeding. It was not possible to identify the source of the bleeding and thus to stop the bleeding by interventional radiology. Transcatheter endoscopy (TCE) of the bile duct could identify the source of the bleeding (**A–C**). A covered metal stent was then deployed to press on the bleeding point in the bile duct. **A**, Fluoroscopic image of the TCE probe inserted in the upper bile duct (*arrow* indicates the tip of TCE probe). **B**, Fluoroscopic image of the TCE endoscope inserted in the middle bile duct (*arrowhead* indicates the tip of TCE). **C**, TCE image of the source of the bleeding in the middle bile duct.

reported the rates of complications associated with POCS, including cholangitis (0-14%), hemobilia (0-3%), bile leakage (1%), and pancreatitis-related complications (0-6%).[16,17] Recently, Sethi et al[17] reported that ERCP with

cholangiopancreatoscopy may be associated with higher rates of complications than ERCP alone. In particular, POCS was associated with a significantly higher rate of cholangitis than was ERCP. Although there were no com-
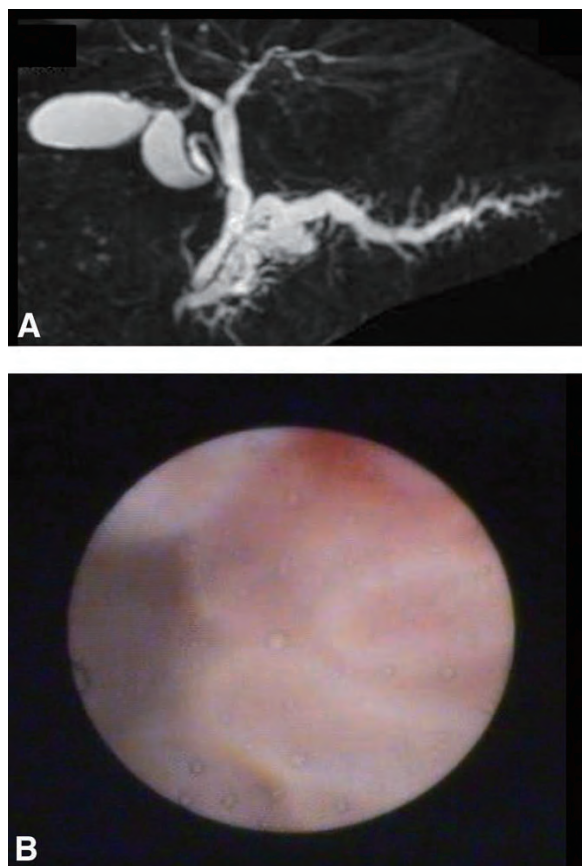
Figure 5. A, A 73-year-old woman was hospitalized for examination of the main pancreatic duct. She received oral anticoagulant medication for atrial fibrillation. She had a history of acute pancreatitis. MRCP did not identify any mural nodules, although it revealed dilation of the main pancreatic duct. **B**, Transcatheter endoscopy identified papillary lesions in the main pancreatic duct.

plications in this study, further study comparing TCE and conventional POCS with a larger number of patients is needed to evaluate the safety of TCE.

The TCE system may also be convenient in terms of cost and time savings. A disposable sheath for the ordinary Spyglass Spyscope system, which costs approximately $1000 (85,000 Japanese yen) is unnecessary for TCE. In addition, TCE required a short procedure time (mean procedure time 6 minutes, 15 seconds).

Compared with conventional POCS, the disadvantages of TCE are fragility; poor steerability; inability to perform simultaneous aspiration, flushing, and visualization; and inability to perform a biopsy under visualization. The glass-fiber probe is fragile, and without the sheath, it is even more fragile. To avoid breaking the Spyglass probe, we used special techniques while maneuvering the devices, by which the tip of Spyglass probe in the tandem catheter could be advanced into the bile duct without

being damaged. By using these techniques, only 1 probe was used in 17 patients without being broken. Ordinary POCS has 2- or 4-way deflected steering. In contrast, TCE does not have any steering system. Therefore, the intraductal maneuverability of the probe is limited without steerability of the sheath. One of the reasons why the 5 bile duct lesions (38.5%) could not be observed was because TCE was performed without steering the catheter. The poor visualization was also caused by a continuous overflow of contaminated bile juice even after irrigation of the bile duct. For TCE, aspiration and flushing were performed before insertion of the probe into the catheter. In the cases with sticky or contaminated bile juice in the bile duct, it may be necessary to perform simultaneous aspiration, flushing, and visualization by using a sheath such a Spyscope, which has 2 irrigation channels, for observation of the lesions in the bile duct. The fourth limitation is that TCE cannot be used for direct biopsies and electrohydraulic lithotripsy. Therefore, at the present time, TCE is used only for the diagnosis of indeterminate lesions.

In conclusion, TCE allowed direct observations of the bile and pancreatic ducts in a safe and convenient manner. Thus, it may play an important role in assessing biliary and pancreatic lesions that are difficult to diagnose by ERCP. Prospective large-scale clinical trials evaluating the clinical utility of TCE are currently under way.

REFERENCES

1. Nakajima M, Akasaka Y, FukumotoK, et al. Peroral cholangiopancreatoscopy (PCPS) under duodenoscopic guidance. Am J Gastroenterol 1976; 66:241-7.
2. Roesch W, Koch H. Peroral cholangioscopy in choledochoduodenostomy-patients using the pediatric fiberscope. Endoscopy 1978;10:195-8.
3. Kozarek R. Direct cholangioscopy and pancreatoscopy at time of endoscopic retrograde cholangiopancreatography. Am J Gastroenterol 1988;83:55-7.
4. Neuhaus H. Cholangioscopy. Endoscopy 1992;24:125-32.
5. Fukuda Y, Tsuyuguchi T, Sakai Y, et al. Diagnostic utility of peroral cholangioscopy for various bile-duct lesions. Gastrointest Endosc 2005; 62:374-82.
6. Itoi T, Sofuni A, fuminori M. Role of peroral cholangioscopy in the preoperative diagnosis of malignant middle and lower bile duct cancers: a preliminary study using 10 Fr plastic stent. Dig Endosc 2005;17:S57-9.
7. Sakai Y, Tsuyuguchi T, Tsuchiya S, et al. Value of peroral cholangioscopy for mucin-producing bile duct tumor. Hepatogastroenterology 2008; 55:58-61.
8. Nimura Y. Staging of biliary carcinoma: cholangiography and cholangioscopy. Endoscopy 1993;25:76-80.
9. Seo DW, Lee SL, Yoo KS, et al. Cholangioscopic finding in bile duct tumors. Gastrointest Endosc 2000;52:630-4.
10. Cotton PB, Lehman G, Vennes J, et al. Endoscopic sphincterotomy complications and their management: an attempt at consensus. Gastrointest Endosc 1991;37:383-93.
11. Larghi A, Waxman I. Endoscopic direct cholangioscopy by using an ultra-slim upper endoscope: a feasibility study. Gastrointest Endosc 2006;63:853-7.
12. Moon JH, Ko BM, Choi HJ, et al. Direct peroral cholangioscopy using an ultra-slim upper endoscope for the treatment of retained bile duct stones. Am J Gastroenterol 2009;104:2729-33.
13. Itoi T, Sofuni A, Itokawa F, et al. Initial experience of peroral pancreatoscopy combined with narrow-band imaging in the diagnosis of intra-

ductal papillary mucinous neoplasms of the pancreas (with video). Gastrointest Endosc 2007;66:793-7.

14. Itoi T, Sofuni A, Itokawa F, et al. Peroral cholangioscopic diagnosis of biliary-tract disease by using narrow-band imaging (with videos). Gastrointest Endosc 2007;66:730-6.

15. Chen YK, Pleskow DK. Spyglass single-operator peroral cholangiopancreatoscopy system for the diagnosis and therapy of bile-duct disor-ders: a clinical feasibility study (with videos). Gastrointest Endosc 2007;65:832-41.

16. ASGE Technology Committee, Shah RJ, Adler DG, Conway JD, et al. Cholangiopancreatoscopy. Gastrointest Endosc 2008;68:411-21.

17. Sethi A, Chen YK, Austin GL, et al. ERCP with cholangiopancreato-scopy may be associated with higher rates of complications than ERCP alone: a single-center experience Gastrointest Endosc 2011;73:251-6.

— 299 —

INTERNAL MEDICINE

Hepatic Nodules Associated with an Inferior Mesentric Arteriovenous Malformation

Ken Takahashi [1,2], Hiroshi Kashida [1,3] and Masatoshi Kudo [3]

Abstract

Splanchnic arteriovenous malformation (AVM) is a rare condition in which patients present with portal hypertension, which thus causes bleeding varices and ascites. However, to our knowledge, hepatic nodules associated with splanchnic AVM have not yet been described. We herein first report the case of a 78-year-old man with inferior mesenteric AVM presenting with portal hypertension and multiple hepatic nodules dominantly supplied by the portal vein. This unique case not only extends the spectrum of hepatic nodules resulting from abnormal hepatic circulation, but also provides clues for better understanding the etiology of hepatic nodules.

Key words: splanchnic arteriovenous malformation, portal hypertension, hepatic nodule

Introduction

With recent advances in imaging techniques, increasing numbers of benign hepatic nodules have been reported in non-cirrhotic patients. In such cases, abnormal hepatic circulation has been considered to be a possible etiological factor. Splanchnic arteriovenous malformation (AVM) is a rare but well-known cause of secondary portal hypertension (1). We herein report the first documented case of hepatic nodules associated with splanchnic AVM. The present case is quite unique in that the 'extrahepatic' abnormal circulation caused by splanchnic AVM induced 'intrahepatic' hemodynamic alterations that finally led to hepatic nodular formation. In this report, the imaging studies are presented and the possible etiology is discussed.

Case Report

A 78-year-old man with a recent history of progressive abdominal fullness was referred to our hospital for treatment of massive ascites and evaluation of multiple hepatic nodules demonstrated on ultrasound sonography (US). The pa-

tient was not a regular alcohol drinker. The liver function tests results as well as other routine laboratory data, including the serum glucose and lipid levels, were all within normal limits. Viral markers for hepatitis B and C and serological markers of autoimmune disease were also negative.

Abdominal US showed massive ascites and the presence of multiple hepatic nodules in Couinaud's segment V and VI with homogenous parenchyma. Neither atrophic nor fatty changes were observed. On contrast-enhanced US, the nodules were clearly enhanced in the portal phase (Fig. 1). Unenhanced computed tomography (CT) showed multiple low attenuating areas corresponding to the findings observed on US. The lesions were hypoattenuating in the arterial phase and enhanced in the portal phase on dynamic CT (not shown). Angiography demonstrated a dilated inferior mesentric artery (IMA) supplying an AVM (Fig. 2A) thus leading to the early filling of the large inferior mesentric vein (IMV) draining into the portal vein (Fig. 2B). CT hepatic arteriogram (CTHA) clearly showed the nodules demonstrated on US and CT to be hypoattenuating lesions (Fig. 3A), while CT during arterioportogram (CTAP) showed the nodules to be hyperattenuating lesions (Fig. 3B). Fourteen days after admission, the patient passed massive melena and an emer-
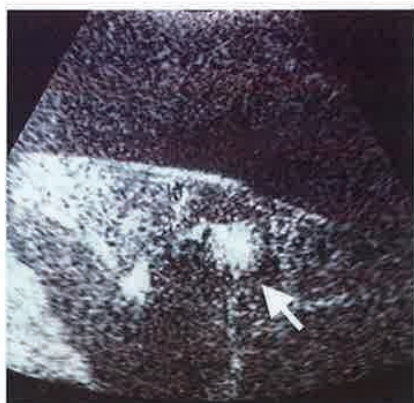
Figure 1. Portal-phase dynamic sonogram obtained 40 seconds after contrast medium injection revealing marked enhancement of the hepatic nodule in segment VI (arrow) on right intercostal scanning. Massive ascites is also demonstrated.

Figure 2. (A) Inferior mesentric arteriogram revealing an AVM (arrow head) supplied by a large IMA (arrow). (B) Inferior mesentric arteriogram obtained two seconds after panel A showing an early filling of IMV (arrow), indicating arterioportal shunting through the AVM.

gency upper gastrointestinal endoscopy revealed bleeding esophageal varices that were successfully treated with an endoscopic variceal ligation technique. Colonoscopy also revealed rectal varices.

Since the patient had no signs of liver cirrhosis, we speculated that the increased portal flow due to the inferior mesentric AVM was the cause of the portal hypertension. The patient underwent resection of the AVM. The intraoperative findings revealed a normal appearance of the liver. The pathological analysis of the resected AVM revealed dilated, thick-walled vascular channels (both arterial and venous) primarily occupying the serosal surface of the sigmoid colon; the findings were consistent with those of an AVM. Postoperatively, the ascites and hepatic nodular lesions disappeared rapidly, as confirmed on both CT and US performed one month after surgery. A follow-up gastrointestinal endoscopy showed marked regression of the esophageal and rectal varices. The patient was discharged 42 days after surgery and has since been free from any symptoms.

Discussion

Splanchnic AVMs are rare conditions. In most cases, these lesions develop between hepatic or splenic arteries and the portal vein (1). AVMs involving the inferior mesenteric vessels are very rare (2). AVMs usually develop following ruptured aneurysms or occur secondary to surgical procedures or trauma (1). On the other hand, congenital AVMs have been reported in only a few cases (2). Based on the pathological analysis of surgical specimens and the lack of any history of abdominal surgery or trauma, the present case was considered to be congenital.

Splanchnic AVMs can cause secondary portal hypertension in non-cirrhotic patients, often leading to ascites and
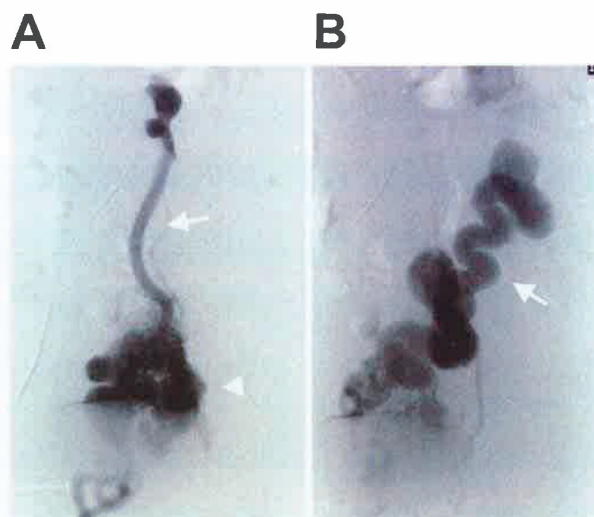
splanchnic AVM. Unfortunately, owing to massive ascites, we could not obtain any biopsy samples of the nodules before treatment. However, the fact that the nodular lesions disappeared soon after the surgical removal of the AVM is direct evidence of the AVM's contribution to the formation of the hepatic nodules.

In recent years, reports of benign hepatic nodules in non-cirrhotic livers have increased with advances in imaging techniques. In such cases, abnormal hepatic circulation has been considered as a possible etiological factor (3). Accordingly, hepatic nodules have been described in association with Budd-Chiari syndrome, a disorder resulting from the gross outflow blockage of hepatic veins with various causes, or congenital absence of the portal vein (4, 5). In addition, recently Ikeda et al. reported the presence of portal flow-dominant hepatic nodules in a patient with idiopathic portal hypertension (6). The present case is quite unique in that the 'extrahepatic' abnormal circulation caused by the splanchnic AVM induced 'intrahepatic' hemodynamic alterations that finally led to hepatic nodular formation. Although the exact pathogenesis of the hepatic nodules in our case remains obscure, one possible explanation might be that the increased and arterialized portal blood flow distributing heterogenously caused focal hepatic injury and the reactive regeneration occurred as a process of repair of the damaged hepatic tissue. Starzl et al. reported that hormonal factors such as insulin, glucagon and epidermal growth factor in the mesentric vein might be important for hepatocyte function and structure and may play vital roles in hepatic regeneration (7). Therefore, an influx imbalance of such substances combined
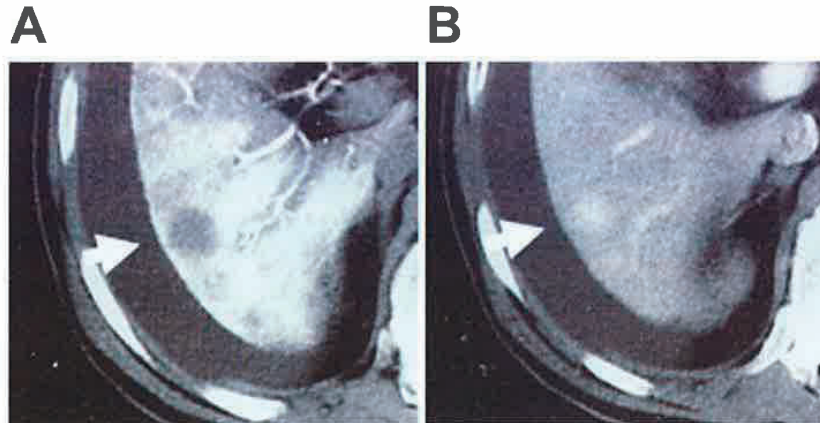
Figure 3. (A) CTHA revealing a hypoattenuating nodular lesion (arrow) in hepatic segment VI. (B) The same lesion is demonstrated as a hyperattenuating nodular lesion (arrow) on CTAP.

In conclusion, we herein presented a case of hepatic nodules associated with splanchnic AVM. This unique case not only extends the spectrum of hepatic nodules resulting from abnormal hepatic circulation, but also provides new insight for better understanding the etiology of hepatic nodules.

The authors state that they have no Conflict of Interest (COI).
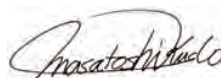
References

1. Van Way CW, Crane JM, Riddell DH, Foster JH. Arteriovenous fistula in the portal circulation. Surgery **70**: 876-890, 1971.
2. Baranda J, Pontes JM, Portela F, et al. Mesentric arteriovenous fistula causing portal hypertension and bleeding duodenal varices. Eur J Gastroenterol Hepatol **8**: 1223-1225, 1996.
3. Kondo F. Benign nodular hepatocellular lesions caused by abnormal hepatic circulation: etiological analysis and introduction of a new concept. J Gastroenterol Hepatol **16**: 1319-1328, 2001.
4. Maetani Y, Itoh K, Egawa H, et al. Benign hepatic nodules in Budd-Chiari Syndrome: radiologic-pathologic correlation with emphasis on the central scar. AJR **178**: 869-875, 2002.
5. Tsuji K, Naoki K, Tachiyama Y, et al. A case of congenital absence of the portal vein. Hepatol Research **31**: 43-47, 2005.
6. Ikeda A, Kita R, Nasu A, et al. Idiopathic portal hypertension with multiple hepatic hyperplastic nodules supplied by portal vein. Ann Hepatol **11**: 572-573, 2012.
7. Starzl TE, Francavilla A, Halgrimson CG, et al. The origin, hormonal nature, and action of hepatotrophic substances in portal venous blood. Surg Gynecol Obstet **137**: 179-199, 1973.

Liver Cancer

Editorial

Why Does Every Hepatocellular Carcinoma Clinical Trial Using Molecular Targeted Agents Fail?

Prof. M. Kudo

Editor Liver Cancer

   Sorafenib was approved for the treatment of unresectable hepatocellular carcinoma (HCC) in 2007 and is the first molecular targeted agent to be used for treating advanced HCC. It is also the only molecular targeted agent to have had a survival benefit demonstrated in two global phase III randomized controlled trials [1, 2], and it has since been approved for use worldwide.

   To date, more than 10 phase III global clinical trials of new molecular targeted agents have been undertaken or are currently ongoing. Of these, 8 have failed to meet their primary endpoint (as of August 2012).

   The trials are the adjuvant Vitamin K2 study [3], the Japanese/Korean post-Transarterial Chemoembolization (TACE) study [4], the sunitinib first-line study [5], the adjuvant pereti-noin (NIK333) study [6], the brivanib second-line study [7], the brivanib first-line study, the linifanib first-line study, and the SEARCH (Sorafenib and Erlotinib, a Randomized Trial Protocol for the Treatment of Patients with HCC) study, which is a phase III study of sorafenib plus erlotinib versus sorafenib plus placebo.

   The problems experienced in the Japanese/Korean post-TACE study may be related to the study design (sequential design), to the treatment lag after TACE (9.3 weeks), or to the high early discontinuation rate (low drug exposure rate) [4]. Problems with the sunitinib first-line trial may be due to high toxicity, low tolerability, or to the high dose reduction and drug discontinuation rates (low drug exposure rate) [5]. In the adjuvant Peretinoin study, where Peretinoin was administered after curative treatment, problems may have arisen because the 300 mg dose of Peretinoin failed to suppress HCC recurrence due to poor pharmacological activity. However, exploratory subset analysis revealed a positive signal for the 600 mg dose of Peretinoin, showing a significant decrease in recurrence compared with the placebo [6]. Stage migration may be a problem with the brivanib second-line study because sorafenib treatment was evaluated in more advanced stage cancer in the two initial phase III studies [1, 2]. In other words, sorafenib was administered for intermediate-stage HCC in those trials, and post-trial therapies such as TACE or systemic/arterial infusion chemotherapy might have been administered to patients for whom second-line therapy had failed, thereby affecting the findings. However, the study clearly demonstrated improved antican-

Liver
Cancer

cer efficacy, as evaluated by tumor response rate and time to tumor progression. The problems with the linifanib first-line study, the brivanib first-line study, and the SEARCH study remain unknown. Details are expected to be presented at a forthcoming scientific meeting.

In conclusion, clinical trials of new molecular targeted agents for the treatment of HCC in an adjuvant setting, first-line setting, second-line setting, or in combination with TACE, seem to be experiencing difficulty and yielding poor results. These failures may be attributed to any of the following reasons. First, HCC is usually associated with impaired liver function or liver cirrhosis; therefore, toxicity or intolerability may be enhanced relative to patients with normal liver function, resulting in early discontinuation or dose reduction. Second, aside from resection, there are many effective treatment options for HCC including ablation, TACE [8], and hepatic arterial infusion chemotherapy [9]. Therefore, post-trial treatment might have affected the results of the primary endpoints such as overall survival.

There is a need for new molecular targeted agents for treating HCC that suppress recurrence after curative treatment or TACE as well as for agents for treating advanced HCC in patients with sorafenib resistance or intolerance. We look forward to positive findings from current or future trials of agents that can overcome the difficulties associated with HCC of the cirrhotic liver.

References

1 Llovet JM, Ricci S, Mazzaferro V, Hilgard P, Gane E, Blanc JF, et al: Sorafenib in advanced hepatocellular carcinoma. N Engl J Med 2008;359:378–390.
2 Cheng AL, Kang YK, Chen Z, Tsao CJ, Qin S, Kim JS, et al: Efficacy and safety of sorafenib in patients in the Asia-Pacific region with advanced hepatocellular carcinoma: a phase III randomised, double-blind, placebo-controlled trial. Lancet Oncol 2009;10:25–34.
3 Yoshida H, Shiratori Y, Kudo M, Shiina S, Mizuta T, Kojiro M, et al: Effect of vitamin K2 on the recurrence of hepatocellular carcinoma. Hepatology 2011;54:532–540.
4 Kudo M, Imanaka K, Chida N, Nakachi K, Tak WY, Takayama T, et al: Phase III study of sorafenib after transarterial chemoembolisation in Japanese and Korean patients with unresectable hepatocellular carcinoma. Eur J Cancer 2011;47:2117–2127.
5 Cheng AL, Kang YK, Lin DY, Park JW, Kudo M, Qin S, et al: Phase 3 trial of sunitinib versus sorafenib in advanced hepatocellular carcinoma. ASCO, 2011.
6 Okita K, Matsui O, Kumada H, Tanaka K, Kaneko S, Moriwaki H, et al: Peretinoin reduces recurrence of hepatocellular carcinoma: results of a phase II/III randomized placebo-controleed trial. ASCO, 2012.
7 Llovet JM, Decaens T, Raoul JL, Boucher E, Kudo M, Chang C, et al: Brivanib versus placebo in patients with advanced hepatocellular carcinoma (HCC) who failed or were intolerant to sorafenib: results from the phase III Brisk-Ps Study. EASL, 2012.
8 Lencioni R: Chemoembolization in patients with hepatocellular carcinoma. Liver Cancer 2012;1:41–50.
9 Kudo M: Treatment of advanced hepatocellular carcinoma with emphasis on hepatic arterial infusion chemotherapy and molecular targeted therapy. Liver Cancer 2012;1:62–70.

Review

Treatment of Advanced Hepatocellular Carcinoma with Emphasis on Hepatic Arterial Infusion Chemotherapy and Molecular Targeted Therapy

Masatoshi Kudo

Department of Gastroenterology and Hepatology, Kinki University School of Medicine, Osaka, Japan

Key Words

Advanced liver cancer · HAIC combined with sorafenib · Hepatic arterial infusion chemotherapy · Molecular target therapy · Sorafenib

Abstract

Advanced hepatocellular carcinoma is defined as liver cancer with vascular invasion or extrahepatic metastasis that is untreatable by local therapy. In Japan, hepatic arterial infusion chemotherapy (HAIC) with interferon plus 5-fluorouracil (5-FU) or a combination of low-dose 5-FU and cisplatin, referred to as low-dose FP, is administered for treating advanced liver cancer and yields favorable outcomes. Outside Japan, the molecular targeted agent, sorafenib, is used as a first-line treatment for advanced liver cancer. New drug development for advanced liver cancer and clinical trials on combination therapy with sorafenib and HAIC are currently underway. The prognosis of advanced liver cancer will significantly improve if these clinical trials yield positive results.

Copyright © 2012 S. Karger AG, Basel

Introduction

Advanced liver cancer is defined as liver cancer at an advanced stage, which is unresponsive to local treatment and includes hepatocellular carcinoma (HCC) with vascular invasion and liver cancer with distant metastasis. Based on the treatment algorithm proposed by the Japan Society of Hepatology, advanced liver cancer is defined as one that is not eligible for

Masatoshi Kudo, MD, PhD

Department of Gastroenterology and Hepatology, Kinki University
School of Medicine
377-2 Ohno-Higashi, Osaka-Sayama city, Osaka 589-8511 (Japan)
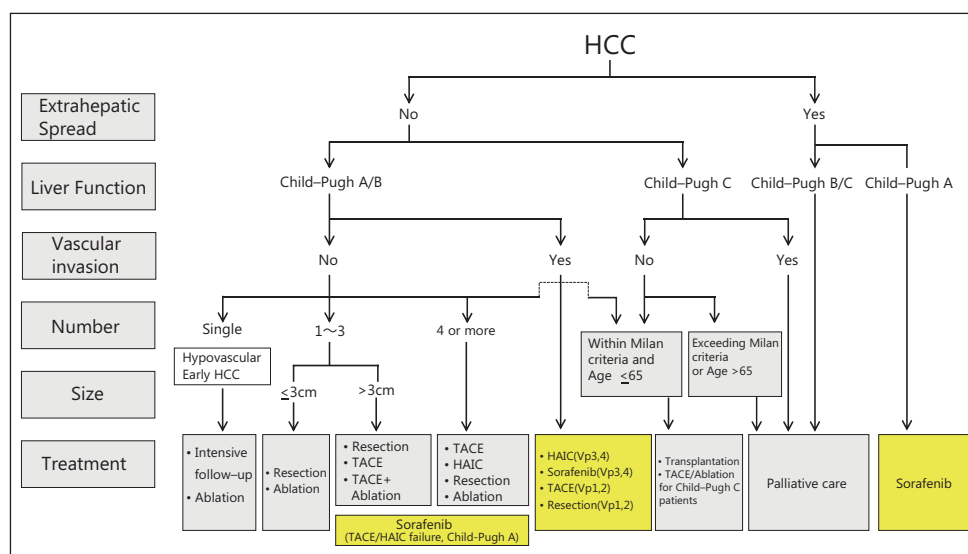E-mail: m-kudo@med.kindai.ac.jp

Kudo: Treatment of Advanced HCC

Fig. 1. Consensus-based treatment algorithm for HCC proposed by the Japan Society of Hepatology, revised in 2010. HAIC is recommended for treating multiple liver cancer and HCC with vascular invasion. Sorafenib is recommended for patients unresponsive to TACE and for those with liver cancer with vascular invasion or extrahepatic spread. Modified with permission from Kudo et al. [1].

curative treatment, transcatheter arterial chemoembolization (TACE), or equivalent treatment [1]. The Barcelona Clinic Liver Cancer (BCLC) classification system, used commonly in Western countries defines grade A as early HCC, grade B as intermediate stage, grade C as advanced stage, and grade D as terminal stage [2]. Terminal-stage disease corresponds to Child–Pugh grade C HCC. Therefore, advanced liver cancer corresponds to BCLC grade C cancer, which that is graded as Child–Pugh A or B with vascular invasion or distant metastasis. In Japan, cancers that are unlikely to respond to locoregional therapies such as resection, local ablation, or TACE are defined as advanced liver cancer. These include multiple liver cancer with 4 or more lesions and liver cancer with vascular invasion or distant metastasis.

Treatment

1. Systemic chemotherapy

As described in the American Association for the Study of Liver Diseases (AASLD) guidelines for liver cancer [2], systemic chemotherapy has not been shown to provide any survival benefit, and thus, is not recommended or used in practice. Therefore, this article does not discuss systemic chemotherapy.

2. Hepatic arterial infusion chemotherapy

In Japan, hepatic arterial infusion chemotherapy (HAIC) is primarily administered for treating HCC with vascular invasion. Based on the Japanese HCC management guideline [1, 3], HAIC is indicated and recommended for treating the following: multiple liver cancer with 4 or more lesions, HCC with major vascular invasion, and cancers with distant metastasis not considered a prognostic factor (fig. 1). According to the 18th nationwide survey of the Liver

Fig. 2. Treatment modality of initially diagnosed HCC in Japan. Only 5% patients received chemotherapy [19].
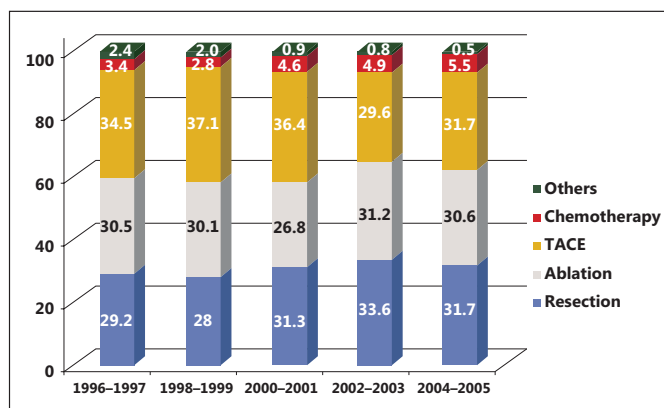

Fig. 3. Administration method of chemotherapeutic agent. Nearly 90% patients received HAIC [19].
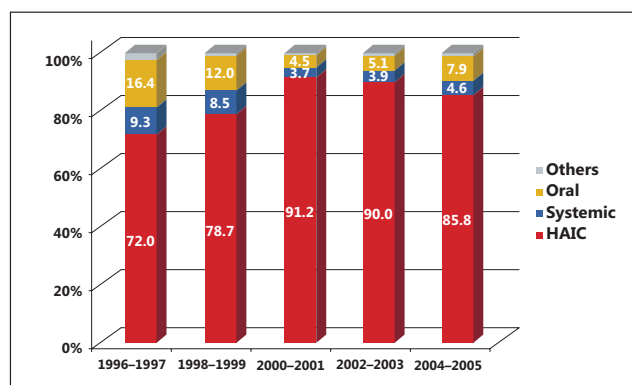
Cancer Study Group of Japan, chemotherapy is performed only in 5.5% patients with liver cancer (fig. 2), and approximately 90% of these patients undergo HAIC [4](Fig. 3). In addition, chemotherapy demonstrated an excellent outcome in a nationwide survey, with a response rate (complete response (CR) plus partial response (PR)) of 45.9% and a disease control rate of 76.5% (fig. 4). In Japan, the interferon (IFN) + 5-fluorouracil (5-FU), low-dose FP (low-dose 5-FU + cisplatin (CDDP)), and CDDP monotherapy regimens account for 49%, 30%, and 11% of all HAIC regimens, respectively (fig. 5). HAIC has also demonstrated a favorable outcome in our study, with a median survival time (MST) of 15.9 months and a time to progression (TTP) of 4.1 months [5](Figs. 6a and 6b). A subset of patients who responded to the therapy (CR + PR) exhibited MST of 40.7 months, while those who did not respond to the therapy (SD + PD) exhibited MST of 6.8 months, suggesting a better survival among responders than among nonresponders (fig. 6c). These results indicate that HAIC is superior to other treatments. Propensity analysis of the nationwide survey clearly revealed that HAIC is superior to the best supportive care based on a nationwide survey of Liver Cancer Study Group of Japan (fig. 7).

HAIC was developed in Japan but is not appreciated in Western countries because no randomized controlled trial (RCT) has been conducted and its use is based solely on empirical data. In fact, AASLD clinical practice guidelines for liver cancer strongly recommend that HAIC should not be used as the standard of care [6]. To overcome this obstacle, there is a strong need to conduct RCTs in Japan. However, since the effectiveness of empirically established

Fig. 4. Result of HAIC in Japan. The response rate is 45.9% and disease control rate is 76.5% [19].
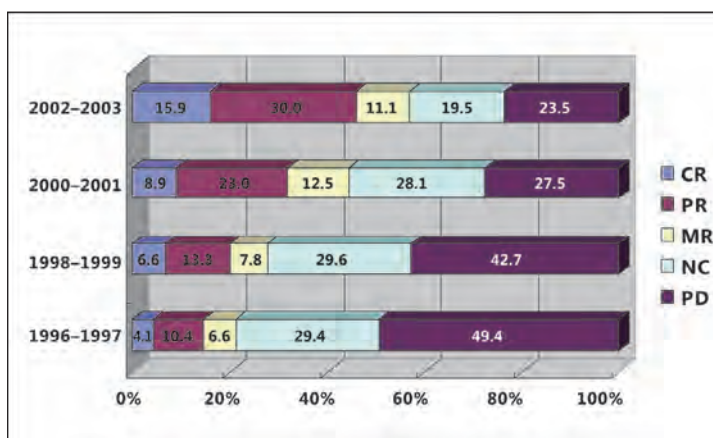
Fig. 5. Most commonly used HAIC regimens in Japan. IFN + 5-FU regimen followed by low-dose FP therapy is the most popular.
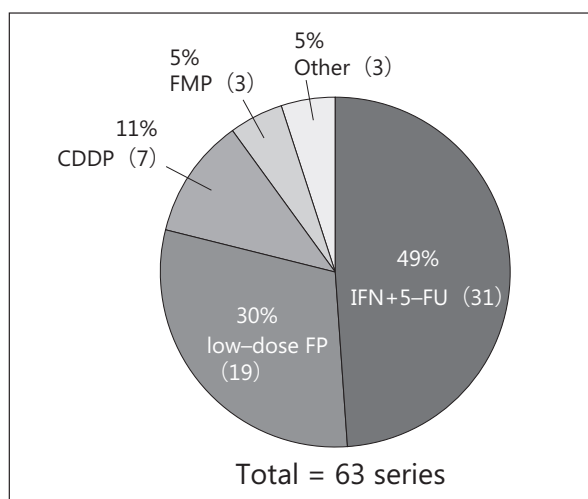
HAIC has been widely accepted by Japanese physicians and patients, the conduct of RCTs has been precluded by ethical concerns. This situation resembles that encountered in the history of TACE [7], which was also empirically developed in Japan but had not been approved until RCTs conducted in the West or East including Japan confirmed its efficacy and safety.

An advantage of HAIC is that the response can be estimated on the basis of tumor markers, imaging findings, or other parameters 2–4 weeks after therapy. Consequently, both responders and nonresponders can be distinguished from each other in less than 4 weeks. For nonresponders, treatment can be switched to a molecular targeted therapy such as sorafenib, a global standard of care for advanced HCC. There is a growing argument about whether HAIC or molecular targeted therapy should be selected as the first choice of treatment for liver cancers with vascular invasion, for patients not eligible for TACE therapy, and for those with multiple liver cancers unresponsive to TACE. HAIC generally provides good but variable outcomes, with a response rate of 8–71% and MST of 6–15.9 months. A finding that was similar to previous reports was that responders demonstrated better outcome than nonresponders. Considering this, HAIC will remain an essential treatment option for advanced liver cancer if used appropriately.

Liver Cancer

Liver Cancer 2012;1:62–70

DOI: 10.1159/000342402
Published online: September 28, 2012

© 2012 S. Karger AG, Basel
www.karger.com/lic

66

Kudo: Treatment of Advanced HCC

Fig. 6 a Kaplan–Meier analysis of overall survival of 52 patients treated by HAIC with low-dose FP therapy. **b** Kaplan–Meier analysis of time to progression in 52 patients treated by HAIC with low-dose FP therapy. The median time to progression was 4.1 months (95% CI 2.1–6.1). **c** The median survival for patients who underwent HAIC with low-dose FP therapy at Kinki University and who responded to the therapy (responders) w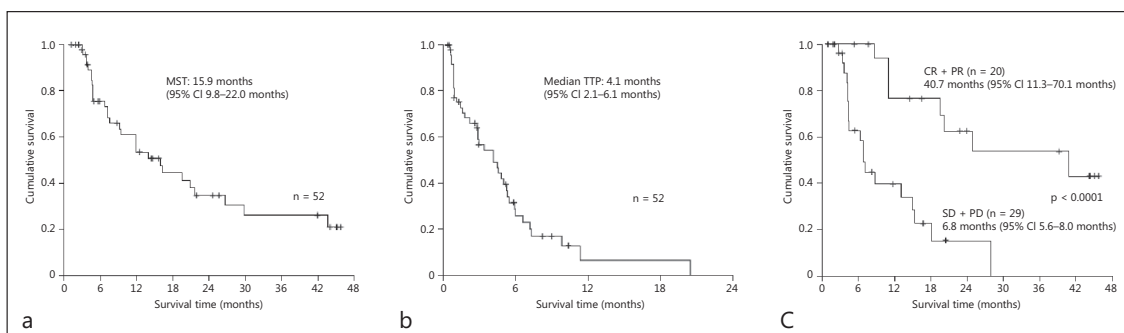as 40.7 months, which was significantly longer than nonresponders (6.8 months). Reproduced with permission from Ueshima, et al. [20]
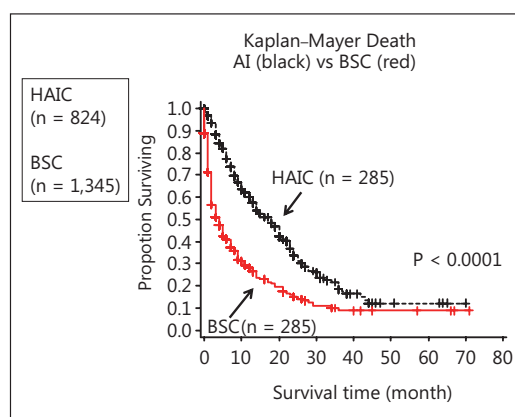
Fig. 7. Survival of patients with HCC with vascular invasion and/or extrahepatic spread and Child–Pugh A/B: transcatheter arterial chemoembolization and HAIC after case matching according to propensity score analysis. Number of patients before case matching in HAIC and BSC was 824 and 1,345, respectively.

3. Molecular targeted therapy

1) Mechanism of action and effects of sorafenib

Sorafenib is an oral molecular targeted agent that has been demonstrated to be effective for treating HCC for the first time and is currently the only insurance-covered drug. The Raf/MEK/ERK pathway, the so-called MAP kinase pathway, is a downstream pathway shared by VEGFR, PDGFR, and EGFR, and its activation has been demonstrated to be involved in the growth and survival of HCC. Sorafenib inhibits HCC growth by suppressing the serine/threonine kinase activity of the C-Raf and B-Raf components of the MAP kinase pathway and inhibiting FLT-3 and c-KIT activities. It also serves as a multikinase inhibitor that suppresses the tyrosine kinase activity of VEGFR and PDGFR, thereby inhibiting angiogenesis and the growth of endothelial cells and pericytes [8–10].

In a global phase III trial conducted in the West (SHARP study) [11], the median survival time was significantly improved in the sorafenib group compared with the placebo group (10.7 vs. 7.9 months, respectively; hazard ratio (HR): 0.69, P < 0.001), and the 1 year survival rate also improved from 33 to 44%. The median TTP significantly improved in the sorafenib group (5.5 months) compared with the placebo group (2.8 months, HR: 0.58, P < 0.001). In

an Asia-Pacific study [12] conducted in China, Taiwan, and North Korea, the median survival time significantly improved in the sorafenib group compared with the placebo group (6.5 vs. 4.2 months, respectively; HR: 0.68, P = 0.014) and TTP (2.8 vs. 1.4 months, respectively; HR: 0.57, P = 0.0005). In Japan, sorafenib was approved for insurance coverage in May 2009 after a phase I clinical trial confirmed its pharmacokinetics and safety [13].

2) Indications of sorafenib

The current indications of sorafenib are specified and described in the consensus-based treatment algorithm proposed by the Japan Society of Hepatology [1] (Fig. 1). These include patients with Child–Pugh grade A HCC with extrahepatic spread or vascular invasion and those not responding to TACE or HAIC. Sorafenib is not recommended for Child–Pugh grade B HCC because of the lack of safety data. It is important to identify unresponsiveness to TACE at the earliest and administer sorafenib before repeated courses of TACE cause impaired liver function or before the disease stage progresses beyond Child–Pugh A.

3) Future prospects

(1) Molecular targeted therapy combined with conventional therapy

a. Prevention of recurrence after curative treatment

Ongoing clinical trials aimed at preventing recurrence include the Sorafenib as Adjuvant Treatment in the Prevention of Recurrence of HCC (STORM) study of sorafenib and another study of peretinoin (NIK333), an acyclic retinoid. The STORM study is a global trial being conducted in Europe, North America, South America, and Asian countries, including Japan, to evaluate the preventive effect of sorafenib on recurrence in patients who have undergone radio frequency ablation or resection. Patient enrollment has been completed, and the study is currently in the follow-up period.

NIK333 (peretinoin) is an oral acyclic retinoid developed in Japan, which has a vitamin A-like structure and primarily targets the nuclear receptors of retinoid, namely retinoic acid receptor (RAR) and retinoid X receptor (RXR). This agent exerts transcriptional activation- and differentiation-inducing effects via RAR and RXR and is expected to prevent carcinogenesis through HCC precursor removal by apoptosis and differentiation induction [14]. A phase III clinical trial to establish the superiority of peretinoin 600 mg over placebo is currently underway.

b. Post-TACE adjuvant therapy

The majority of patients with HCC receive at least 1 cycle of TACE. In many cases TACE is repeated because it is not curative and is inevitably followed by recurrence. Although TACE has an antitumor effect, repeated use of this therapy causes gradual deterioration of liver function. Therefore, the adjuvant use of molecular targeted therapy is attracting attention. Although tumor shrinkage is observed following TACE, recurrence, including tumor regrowth and intrahepatic metastasis, can still occur [7]. A suggested mechanism of post-TACE recurrence is mediated by increased angiogenesis in response to increased VEGF levels caused by embolization-induced tumor hypoxia [15, 16]. Therefore, the suppression of angiogenesis following TACE is important to prevent post-TACE tumor recurrence. The combined use of TACE and angiogenesis inhibitors strongly suppresses post-TACE recurrence or regrowth of advanced HCC through the inhibitory effect of angiogenesis inhibitors on post-TACE increase in angiogenesis. Such a therapy is also expected to prolong the period during which tumor progression can be controlled by TACE and prevent deterioration of liver function by reducing the frequency of TACE. Although a study conducted in Japan and South Korea, the so-called post-TACE study, had various limitations [17], many clinical trials on molecular targeted therapy as a post-TACE–adjuvant or TACE-combination regimen are being conducted on the basis of these study results.

Kudo: Treatment of Advanced HCC

c. TACTICS study

The Transcatheter Arterial Chemoembolization Therapy in Combination with Sorafenib (TACTICS) study is a phase II clinical trial on TACE combined with sorafenib conducted in Japanese patients with unresectable HCC. The TACE regimen used in this study is based on actual clinical practice in Japan, which comprises Gelpart as an embolization agent and epirubicin hydrochloride or miriplatin as an anticancer agent. It is performed as on-demand TACE and administered after a certain degree of tumor growth has been observed. The study is designed to include patients with HCC untreatable by surgical resection or percutaneous ablation therapy. After undergoing TACE, patients will be randomized at a 1:1 ratio to receive or not receive oral sorafenib. The primary endpoint is time to untreatable progression, at which point TACE can no longer be performed. This study is currently enrolling patients.

d. BRISK-TA study (brivanib)

Brivanib is a kinase inhibitor that selectively inhibits VEGFR and FGFR. A phase III clinical trial that compares brivanib with placebo as an adjuvant therapy for TACE is underway.

e. ORIENTAL study (TSU68: orantinib)

TSU68 (orantinib) is a low-molecular weight oral angiogenesis inhibitor that inhibits VEGFR, PDGFR, and FGFR [18]. A phase III clinical trial that evaluates the superiority of combined use of TSU68 over placebo in terms of overall survival in patients with advanced HCC who have undergone TACE is currently underway.

f. Sorafenib combined with HAIC

In Japan, HAIC is initially performed for advanced HCC with major vascular invasion. Without established evidence, HAIC is accepted as a de facto standard and is rarely used outside Japan. Although technically complicated and invasive, this therapy provides excellent local control, and is thus considered effective. Several clinical trials that are evaluating the efficacy of combination therapy with HAIC and sorafenib for treating advanced HCC are currently underway. These include the SILIUS trial (NCT01214343), a randomized phase III study on sorafenib combined with HAIC and low-dose FP using a reservoir system aiming to demonstrate the additional benefits of HAIC. SILIUS is part of a multicenter cooperative study funded by the Ministry of Health, Labour and Welfare of Japan. The primary endpoint for this study is overall survival. Demonstration of additional benefits will be the first indirect demonstration of the survival benefit of low-dose FP therapy. The results of the phase I study were promising, demonstrating the additive effect of HAIC and sorafenib. The CDDP-Sor-rP2 study (UMIN000005703) is a randomized phase II study of sorafenib combined with a one-shot HAIC with CDDP. Similar to the SILIUS study, the CDDP-Sor-rP2 study aims to demonstrate additional benefits of HAIC without the use of a reservoir.

(2) Status of development of new drugs other than sorafenib

As summarized in fig. 8, various first-line and second-line therapies, combination therapies with HAIC/TACE and sorafenib, and adjuvant therapies after curative treatment are currently under investigation as potential new treatment strategies for patients with advanced liver cancer unresponsive or intolerable to sorafenib.

Conclusions

Since the effectiveness of sorafenib was confirmed, systemic chemotherapy with molecular targeted agents has established its position in the treatment of HCC, which otherwise had to rely on local therapy. This has finally allowed discussion of medication therapy for
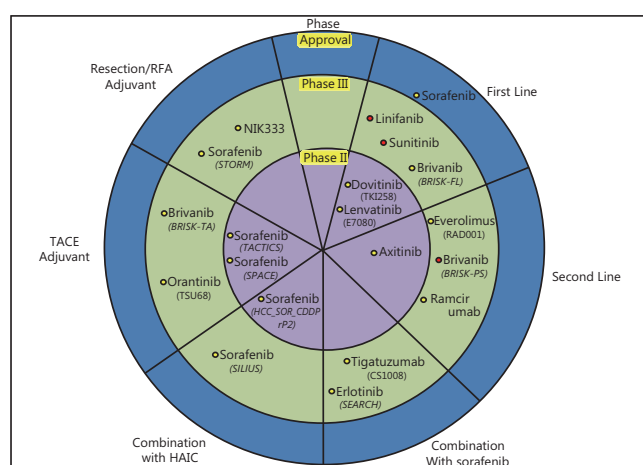
Kudo: Treatment of Advanced HCC

Fig. 8. Current development status of molecular targeted agents

HCC, similar to that for other types of carcinoma. At the same time, it must be remembered that HCC occurs in patients with underlying chronic liver diseases and is accompanied by concomitant conditions such as impaired liver function and pancytopenia. Drugs that cause severe adverse events or affect liver function cannot be used as therapeutic agents, even if they have a potent antitumor effect. The most important challenge for improving the survival outcome in HCC patients is determining ways to prevent deterioration of liver function due to underlying chronic liver disease. The development of less toxic drugs and treatment regimens is therefore desirable.

The prognosis of advanced liver cancer can significantly improve if positive results are obtained from new drug development and clinical studies on combination therapy with existing treatments.

References

1 Kudo M, Izumi N, Kokudo N, Matsui O, Sakamoto M, Nakashima O, et al: Management of hepatocellular carcinoma in Japan: Consensus-Based Clinical Practice Guidelines proposed by the Japan Society of Hepatology (JSH) 2010 updated version. Dig Dis 2011;29:339–364.
2 Bruix J, Sherman M: Management of hepatocellular carcinoma: An update. Hepatology 2011;53:1020–1022.
3 Ricke J, Seidensticker M, Mohnike K: Noninvasive diagnosis of hepatocellular carcinoma in cirrhotic liver: Current guidelines and future prospects for radiological imaging. Liver Cancer 2012;1:51–58.
4 Ikai I, Kudo M, Arii S, Omata M, Kojiro M, Sakamoto M, et al: Report of the 18th Follow-up Survey of Primary Liver Cancer in Japan. Hepatol Res 2010;40:1043–1059.
5 Ueshima K, Kudo M, Takita M, Nagai T, Tatsumi C, Ueda T, et al: Des-gamma-carboxyprothrombin may be a promising biomarker to determine the therapeutic efficacy of sorafenib for hepatocellular carcinoma. Dig Dis 2011;29:321–325.
6 Bruix J, Sherman M: Management of hepatocellular carcinoma. Hepatology 2005;42:1208–1236.
7 Lencioni R: Chemoembolization in patients with hepatocellular carcinoma. Liver Cancer 2012;1:41–50.
8 Wilhelm SM, Carter C, Tang L, Wilkie D, McNabola A, Rong H, et al: BAY 43–9006 exhibits broad spectrum oral antitumor activity and targets the RAF/MEK/ERK pathway and receptor tyrosine kinases involved in tumor progression and angiogenesis. Cancer Res 2004;64:7099–7109.
9 Liu L, Cao Y, Chen C, Zhang X, McNabola A, Wilkie D, et al: Sorafenib blocks the RAF/MEK/ERK pathway, inhibits tumor angiogenesis, and induces tumor cell apoptosis in hepatocellular carcinoma model PLC/PRF/5. Cancer Res 2006;66:11851–11858.
10 Chang YS, Adnane J, Trail PA, Levy J, Henderson A, Xue D, et al: Sorafenib (BAY 43–9006) inhibits tumor growth and vascularization and induces tumor apoptosis and hypoxia in RCC xenograft models. Cancer Chemother Pharmacol 2007;59:561–574.

Liver Cancer

Liver Cancer 2012;1:62–70

DOI: 10.1159/000342402
Published online: September 28, 2012

© 2012 S. Karger AG, Basel
www.karger.com/lic

70

Kudo: Treatment of Advanced HCC

11 Llovet JM, Ricci S, Mazzaferro V, Hilgard P, Gane E, Blanc JF, et al: Sorafenib in advanced hepatocellular carcinoma. N Engl J Med 2008;359:378–390.
12 Cheng AL, Kang YK, Chen Z, Tsao CJ, Qin S, Kim JS, et al: Efficacy and safety of sorafenib in patients in the Asia-Pacific region with advanced hepatocellular carcinoma: a phase III randomised, double-blind, placebo-controlled trial. Lancet Oncol 2009;10:25–34.
13 Furuse J, Ishii H, Nakachi K, Suzuki E, Shimizu S, Nakajima K: Phase I study of sorafenib in Japanese patients with hepatocellular carcinoma. Cancer Sci 2008;99:159–165.
14 Okita K, Matsui O, Kumada H, Tanaka K, Kaneko S, Moriwaki H, et al. Effect of peretinoin on recurrence of hepatocellular carcinoma (HCC): Results of a phse II/III randomized placebo-controlled trial. (Abstract #4024), ASCO, June, 2010.
15 Li X, Feng GS, Zheng CS, Zhuo CK, Liu X: Expression of plasma vascular endothelial growth factor in patients with hepatocellular carcinoma and effect of transcatheter arterial chemoembolization therapy on plasma vascular endothelial growth factor level. World J Gastroenterol 2004;10:2878–2882.
16 Sergio A, Cristofori C, Cardin R, Pivetta G, Ragazzi R, Baldan A, et al: Transcatheter arterial chemoembolization (TACE) in hepatocellular carcinoma (HCC): the role of angiogenesis and invasiveness. Am J Gastroenterol 2008;103:914–921.
17 Kudo M, Imanaka K, Chida N, Nakachi K, Tak WY, Takayama T, et al: Phase III study of sorafenib after transarterial chemoembolisation in Japanese and Korean patients with unresectable hepatocellular carcinoma. Eur J Cancer 2011;47:2117–2127.
18 Laird AD, Vajkoczy P, Shawver LK, Thurnher A, Liang C, Mohammadi M, et al: SU6668 is a potent antiangiogenic and antitumor agent that induces regression of established tumors. Cancer Res 2000;60:4152–4160.
19 Report of the 18th follow-up survey of primary liver cancer in Japan. The Liver Cancer Study Group of Japan, eds.,Media Planning Inc., Japan, 2009.
20 Ueshima K, Kudo M, Takita M, Nagai T, Tatsumi C, Ueda T, Kitai S, Ishikawa E, Yada N, Inoue T, Hagiwara S, Minami Y, Chug H: Hepatic arterial infusion chemotherapy using low-dose 5-fluorouracil and cisplatin for advanced hepatocellular carcinoma. Oncology 2010;78:S148–S153.

Original Contribution

p38MAPK suppresses chronic pancreatitis by regulating HSP27 and BAD expression

Ah-Mee Park [a], Masatoshi Kudo [b], Satoru Hagiwara [b], Masaki Tabuchi [c], Tomohiro Watanabe [d], Hiroshi Munakata [a], Toshiharu Sakurai [b],*

[a] Department of Biochemistry, Kinki University, Faculty of Medicine, Osaka 589-8511, Japan
[b] Department of Gastroenterology and Hepatology, Kinki University, Faculty of Medicine, Osaka 589-8511, Japan
[c] Department of Pharmacology, Kinki University, Faculty of Medicine, Osaka 589-8511, Japan
[d] Center for Innovation in Immunoregulative Technology and Therapeutics, Kyoto University Graduate School of Medicine, Kyoto, Japan

ARTICLE INFO

ABSTRACT

Mitogen-activated protein kinases (MAPKs) are ubiquitous proteins that function in both normal and stress-related pathophysiological states of the cell. This study aimed to analyze the importance of p38MAPK in pancreatic injury using WBN/Kob rats with spontaneous chronic pancreatitis. Male WBN/Kob rats were injected with the p38MAPK inhibitor SB203580, starting at the age of 4 weeks, and sacrificed 6 weeks later. Compared with vehicle-treated rats, p38 inhibitor-treated rats exhibited a significant increase in pancreatic cell death and inflammation as assessed by histologic examination and myeloperoxidase activity, respectively. p38 inhibition decreased the expression of heat shock protein 27 (HSP27), an antioxidant protein, and enhanced accumulation of reactive oxygen species (ROS). In addition, the proapoptotic protein BAD was increased in the pancreas of rats treated with p38 inhibitor. In a pancreatic cell line (PANC-1), HSP27 knockdown augmented reactive oxygen species accumulation and cell death induced by tumor necrosis factor-α plus actinomycin D. In conclusion, p38MAPK suppresses chronic pancreatitis by upregulating HSP27 expression and downregulating BAD expression.

© 2012 Elsevier Inc. All rights reserved.

Introduction

Chronic pancreatitis, defined as a progressive inflammatory disease of the pancreas, is a substantial risk factor for the development of pancreatic cancer, a highly lethal disease with the worst prognosis of all the major malignancies. The main histological features of chronic pancreatitis are chronic inflammation, progressive parenchymal atrophy, and extensive fibrosis of the exocrine pancreas. There are several etiologies for this disturbance. Chronic pancreatitis involves a complex cascade of events that begins with the development of acinar cell death, leading to an inflammatory response, thus provoking the release of inflammatory cytokines and the activation of stellate cells, the major cell type responsible for fibrosis. Cell death releases intracellular components, some of which serve as danger signals that damage neighboring cells and promote inflammation and cancer [1–3]. Although an important role for reactive oxygen species (ROS) [1] has been suggested in the pathogenesis of pancreatitis [4], little is known about the molecular mechanisms regulating ROS production and parenchymal cell death, a major pathologic response of pancreatitis.

The mitogen-activated protein kinase (MAPK) signaling pathways are ubiquitous cascades that regulate cellular growth, survival, and differentiation and the response to environmental stress [5,6]. In mammalian cells, at least three parallel pathways are differentially regulated by a number of extracellular signals that act via different cell-surface receptor types. Central to these signaling pathways are the MAPKs themselves: extracellular signal-regulated kinases, c-Jun N-terminal kinases (JNKs), and p38MAPKs. p38MAPK is a critical regulator of inflammation in several tissues. Activation of p38MAPK signaling has been implicated in cytokine production by macrophages [7] and cytokine-mediated pancreatic β-cell injury [8]. A recent study indicated that p38MAPK plays a critical role in parenchymal cell death in the liver. p38α, a major p38 isoform, controls the gene encoding heat shock protein 27 (HSP27), which acts as an antioxidant, to

prevent ROS accumulation and hepatocyte death [3]. Thus, in this study, we examined the effects of p38MAPK on parenchymal cell death in chronic pancreatitis. p38MAPK downregulates expression of BAD (Bcl-2 antagonist of cell death) and upregulates expression of HSP27, which prevents ROS accumulation and pancreatic acinar cell death. Tissue homeostasis in multicellular organisms requires a balance between cell death and proliferation. A rate of cell death exceeding the rate of proliferation leads to homeostatic imbalance in many pathological conditions. p38MAPK probably plays an important role in maintaining homeostasis of the pancreas and preventing chronic pancreatitis.

Materials and methods

Materials

WST-8 (2-(2-methoxy-4-nitrophenyl)-3-(4-nitrophenyl)-5-(2,4-disulfophenyl)-2H-tetrazolium, monosodium salt), available commercially as Cell Counting Kit-8, was purchased from Dojindo Laboratory (Kumamoto, Japan). Antibodies against HSP27, glyceraldehyde-3-phosphate dehydrogenase, and poly(ADP-ribose) polymerase (PARP) were obtained from Santa Cruz Biotechnology (Santa Cruz, CA, USA); 4-hydroxynonenal (4-HNE) was purchased from NOF Corp. (Tokyo, Japan); actin was from Sigma-Aldrich (St. Louis, MO, USA); HSP27 (for human) was from Signalway Antibody (Pearland, TX, USA); and BAD, phosphor-BAD, caspase-3, and p38MAPKs were from Cell Signaling Technology (Beverly, MA, USA).

Animal models

The WBN/Kob rat develops chronic pancreatitis and is used as a model for the human form of the disease. Four-week-old male WBN/Kob rats were purchased from SLC Japan (Hamamatsu, Japan). WBN/Kob rats were fed normal rat chow and were studied in accordance with institutional guidelines. Rats were injected with 2 mg/kg body wt of the p38 inhibitor SB203580, JNK inhibitor SP600125 (Calbiochem, La Jolla, CA, USA), or PPCES vehicle (30% PEG-400/20% polypropylene glycol/15% Cremophor EL/5% ethanol/30% saline) 11 times per week for 6 weeks. The rats were sacrificed at the 6th week and the pancreata were used for the study.

Histological scoring of chronic pancreatitis

Hematoxylin and eosin (H&E)-stained sections of the pancreas were used for histological examinations. Pancreatitis scores were determined based on the criteria reported by Schmidt et al. [9].

Myeloperoxidase activity

Myeloperoxidase (MPO) activity of pancreas homogenates was determined by using o-dianisidine dihydrochloride as a substrate as described previously [10]. Briefly, pancreatic tissue homogenates were mixed with 0.167 mg/ml o-dianisidine dihydrochloride and 0.003% hydrogen peroxide in 100 mM potassium phosphate buffer (pH 6.0), and the absorbance at 450 nm was monitored for 3 min. The maximum increase in optical density during 1 min was compared between control and SB203580-treated groups.

Western blotting and protein oxidation assay

Pancreatic tissue lysates were prepared with CelLytic MT (Sigma-Aldrich) containing Complete protease inhibitor (Roche

Diagnostics, Mannheim, Germany) and phosphatase inhibitor (Toyobo). The lysates were electrophoresed through a reducing SDS-polyacrylamide gel and electroblotted onto a polyvinylidene difluoride membrane. The membrane was blocked with 5% skim milk and probed with primary antibodies. The levels of each protein were detected with horseradish peroxidase-linked secondary antibodies and the ECL Plus System (GE Healthcare, Piscataway, NJ, USA). Protein carbonylation, a major form of protein oxidation, was determined using the Oxiselect protein carbonyl immunoblot kit (Cell Biolabs, San Diego, CA, USA), according to the manufacturer's instructions. To evaluate signal intensity, Western blot image data were quantified using ImageJ software (National Institutes of Health, Bethesda, MD, USA).

Cell culture and small interfering RNA (siRNA) knockdown of HSP27

Human pancreas carcinoma PANC-1 cells obtained from the Riken Cell Bank (Tsukuba, Japan) were seeded in RPMI 1640 medium (Gibco Invitrogen, Carlsbad, CA, USA) supplemented with 100 U/ml penicillin, 100 μg/ml streptomycin (Gibco), and 10% fetal bovine serum cultured at 37 °C under 5% CO_2/95% air.

HSP27 siRNA duplexes that target the sequences sense, 5′-UGAGAGACUGCCGCCAAGUAA-3′, and antisense, 5′-UUA-CUUGGCGGCAGUCUCAUU-3′, were synthesized by Genedesign (Osaka, Japan). siRNAs of four subtypes of p38MAPK (α, β, γ, δ) were purchased from Qiagen (Frederick, MD, USA). Transfection of siRNA was carried out using Lipofectamine 2000 (Invitrogen). Briefly, 1 day before transfection, cells were plated in 96- or 12-well plates at 2×10^5 cells/ml. On the day of transfection, the Lipofectamine 2000–siRNA complex was added to the cells. The final siRNA concentration in each well was 50 nM. A control (Lipofectamine 2000–control siRNA) was included in the experiments. In some experiments, the cells were treated with actinomycin D (ActD; Sigma-Aldrich) and tumor necrosis factor-α (TNF-α; Wako Pure Chemical, Osaka, Japan) to induce cell death 48 h after transfection [11]. Twenty-four hours after treatment, cell viability was determined using Cell Counting Kit-8 and the cell lysates were collected with CelLytic M containing Complete and phosphatase inhibitor. Cell lysates were used for Western blot analysis as described above.

To analyze the cell-protective effect of N-acetyl-L-cysteine (Wako Pure Chemical) against cell death induced by actinomycin D and TNF-α in combination, cell viability was determined by the trypan blue exclusion method 24 h after treatment.

Cloning and transfection of HSP27

Human wild-type HSP27 (HSPB1) was cloned by PCR using human lung complementary DNA obtained from Origene (Rockville, MD, USA). Primers for HSP27 were 5′-TTG*AATTC*ATGACC-GAGCGCCGCGTCCCC-3′ (forward) and 5′-TTT*AAGCTT*TTACTTGGCGG-CAGTCTCATCGGA-3′ (reverse). The primers encode restriction digest sites (in italic) for cloning into the pCMV-3Tag-1A expression vector (Sigma-Aldrich); the forward primer encodes an EcoRI site and the reverse primer encodes a HindIII site. PCRs were performed with KOD polymerase (Toyobo). PCR products were purified using the Gel, PCR-Product Purification Kit (Promega, Madison, WI, USA). Purified PCR fragments were digested for 1 h with EcoRI and HindIII (New England Biolabs, Beverly, MA, USA) at 37 °C. Digested DNA was run on an agarose gel, purified, and ligated into the pCMV-3Tag-1A expression vector by T4 DNA ligase (Epicenter, Madison, WI, USA). Vectors positive for inserts were screened by digestion and subjected to bidirectional sequencing. Transfection of PANC-1 cells with plasmid was performed using Lipofectamine 2000 (Invitrogen) following the manufacturer's instructions. Cells were cultured for 2 days and used for assays.

Statistical analysis

Data are presented as means ± SD. Differences were analyzed using Student's *t* test. *P* values of < 0.05 were considered significant.

Results

p38MAPK inhibits cell death and inflammation in the pancreas

To examine the effects of p38MAPK on the severity of chronic pancreatitis, WBN/Kob rats were subcutaneously injected with SB203580, a highly specific and cell-permeative inhibitor of p38 kinase, or vehicle 11 times per week for 6 weeks. Pancreata were harvested, fixed, stained with H&E, and examined morphologically. Treatment of WBN/Kob rats with vehicle resulted in mild chronic pancreatitis (Fig. 1A). In contrast, treatment of rats with SB203580 led to markedly augmented pancreatitis characterized by necrosis, hemorrhage, and inflammation (Fig. 1A). To assess these changes semiquantitatively, histologic slides of the pancreas were scored in a blinded manner. Treatment of rats with p38 inhibitor resulted in a significant increase in hemorrhage and inflammation (Fig. 1B). In SB203580-treated rats, caspase-3 cleavage was enhanced (Fig. 1C), showing that p38 inhibition augmented both necrosis and apoptosis in the pancreas. Rats treated with SB203580 exhibited elevated neutrophil infiltration as measured by MPO activity (Fig. 2), although it was not statistically significant. Thus, in agreement with its previously documented role in the liver [3], p38MAPK also plays a protective role in the pancreas. The part of the pancreas with endocrine function is made up of approximately 1 million endocrine cell clusters called islets. The cytotoxic effects of p38 inhibitor were less pronounced in endocrine cells than in acinar cells (Fig. 1A). Body weight and serum glucose levels were unaffected by p38 inhibitor (Supplementary Table 1).

JNK, another member of the MAPKs, plays an important role in a number of biological processes including cell proliferation, differentiation, apoptosis, cell survival, metabolism, and cytokine production [12]. JNK activation is the earliest direct contributor to the induction of secretagogue-induced pancreatitis in rats [13]. It has been reported that JNK is required for hepatocyte death in the diethylnitrosamine (DEN) model of hepatocellular carcinoma [14]. These studies suggest the possible involvement of JNK in the induction of pancreatic acinar cell death and pancreatitis. However, JNK inhibition did not affect cell death and inflammation in the pancreas (data not shown).

p38MAPK attenuates ROS accumulation in the pancreas

A causal link between oxidative stress and chronic pancreatitis has been proposed [15]. Ablation of hepatic p38α, the best characterized isoform of the p38MAPKs, enhances ROS accumulation after the injection of the chemical carcinogen DEN [3]. We assessed the effect of p38MAPK on the accumulation of ROS in the pancreas by measuring protein carbonylation levels. Inhibition of p38 significantly increased the levels of carbonylated proteins (Fig. 3A). 4-Hydroxynonenal is an unsaturated hydroxyalkenal, produced by cellular lipid peroxidation. A significant increase in
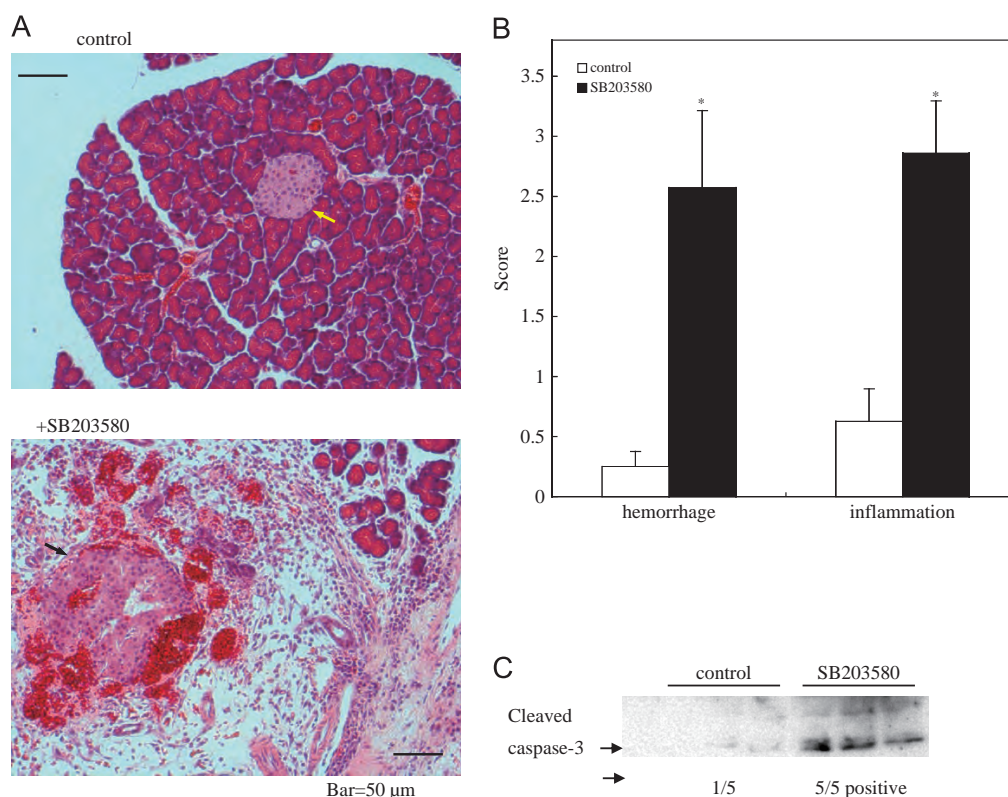
Fig. 1. p38MAPK inhibition aggravated chronic pancreatitis: (A) H&E staining of pancreatic tissue sections of WBN/Kob rats treated with vehicle (control) and SB203580, a p38MAPK inhibitor. Arrows indicate an islet. (B) The extent of hemorrhage and inflammation was quantified based on criteria reported by Schmidt et al. [9]. Data are expressed as the mean ± SEM (*n*=7). *P* < 0.05 vs. control. (C) The level of cleaved caspase-3 was determined by Western blot analysis.

the level of 4-HNE was seen upon administration of p38 inhibitor (Fig. 3B). Thus, p38MAPK attenuates ROS accumulation in the pancreas.

p38MAPK prevents pancreatic cell death by regulating expression of HSP27 and BAD

Overexpression of the small chaperone protein HSP27 protects against cerulean-induced pancreatitis [16]. Inhibition of p38 significantly decreased the level of HSP27 protein (Fig. 4A). In contrast, treatment with p38 inhibitor resulted in a marked increase in the expression of the proapoptotic protein BAD in the pancreas (Fig. 4B). The proapoptotic activity of BAD can be

inhibited by BAD phosphorylation [17]. Inhibition of p38 did not decrease BAD phosphorylation at Ser-112 (Fig. 4B). These results suggest that p38MAPK upregulates the expression of HSP27 and downregulates the expression of BAD, thereby maintaining pancreatic cell survival and suppressing pancreatic injury.

We next evaluated the contribution of HSP27 to ROS-mediated cell death in the pancreatic cell line PANC-1. Treatment of PANC-1 cells with p38 inhibitor resulted in decreased expression of HSP27 and increased expression of BAD. Inhibition of p38 did not have a significant effect on BAD phosphorylation (Fig. 5A). TNF-α produces other proinflammatory mediators that reinforce and amplify pancreatic injury and that play a central role in the progression of pancreatitis [18,19]. An in vitro study showed that TNF-α and ActD induced both ROS generation and cell death [11,20]. We assessed the effects of HSP27 on TNF-α plus ActD-mediated ROS accumulation and cell death. PANC-1 cells were transfected with HSP27 siRNA or nontargeting siRNA as a negative control. Forty-eight hours after transfection, the cells were treated with TNF-α plus ActD to induce cell death. HSP27 knockdown significantly increased ROS accumulation (Fig. 5B) and cell death (Fig. 5C). Proteolytic cleavage of PARP by caspases is a hallmark of apoptosis. HSP27 knockdown enhanced PARP cleavage (Fig. 5D). By contrast, overexpression of FLAG-tagged HSP27, which appeared around 31 kDa by Western blot analysis, attenuated protein oxidation (Fig. 6). Both endogenous and exogenous HSP27 protein levels were completely suppressed by SB203580 treatment (Fig. 6). Administration of the antioxidant N-acetyl-ʟ-cysteine (NAC) led to a marked reduction in TNF-α plus ActD-induced cell death (Fig. 7). Taken together, our results indicate that TNF-α plus ActD-induced cell death depends on the production of ROS in PANC-1 cells, which is regulated by HSP27, a downstream molecule of p38MAPK. Although expression of BAD was dependent on p38 activity, HSP27 knockdown did not affect BAD protein levels (Fig. 5D). Thus, BAD expression is regulated by p38MAPK independent of HSP27.
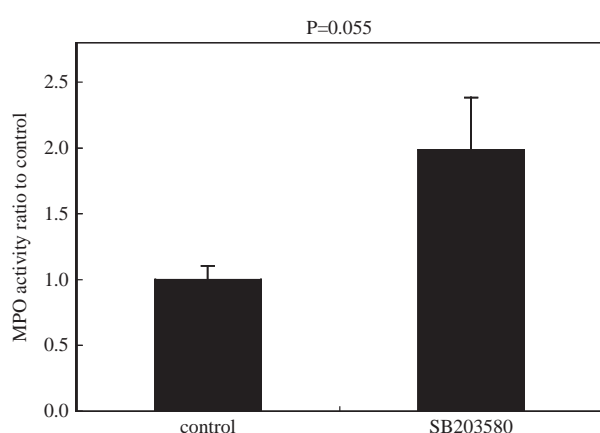
Fig. 2. p38MAPK inhibition increased MPO activity in the pancreas. MPO activity of pancreas homogenates was measured using o-dianisidine dihydrochloride. Data are expressed as the mean ± SEM ($n=7$).
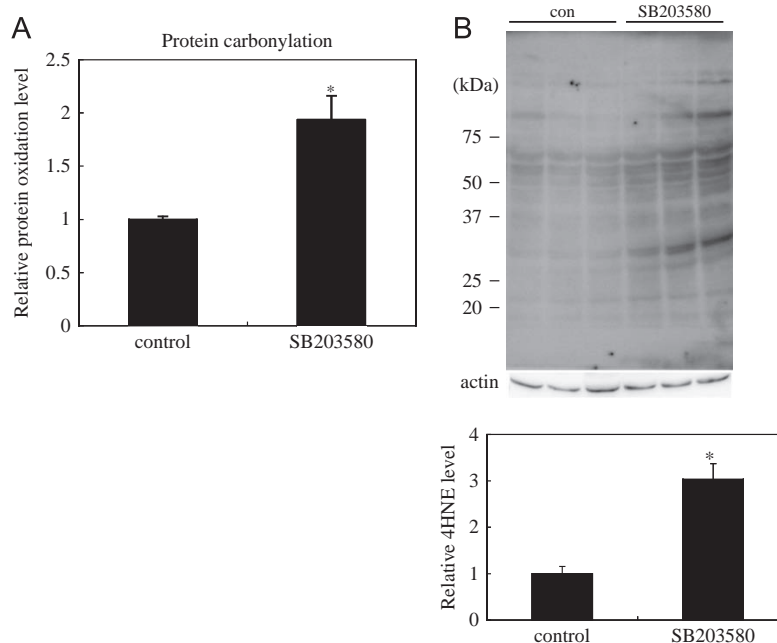
Fig. 3. p38MAPK inhibition enhances ROS accumulation in the pancreas: (A) Protein carbonylation of pancreas tissue lysate was detected using the Oxiselect kit. (B) 4-HNE was detected by Western blot analysis with specific monoclonal antibody. Data are expressed as the mean ± SEM ($n=5$ or 6). $^*P < 0.05$ vs. control.
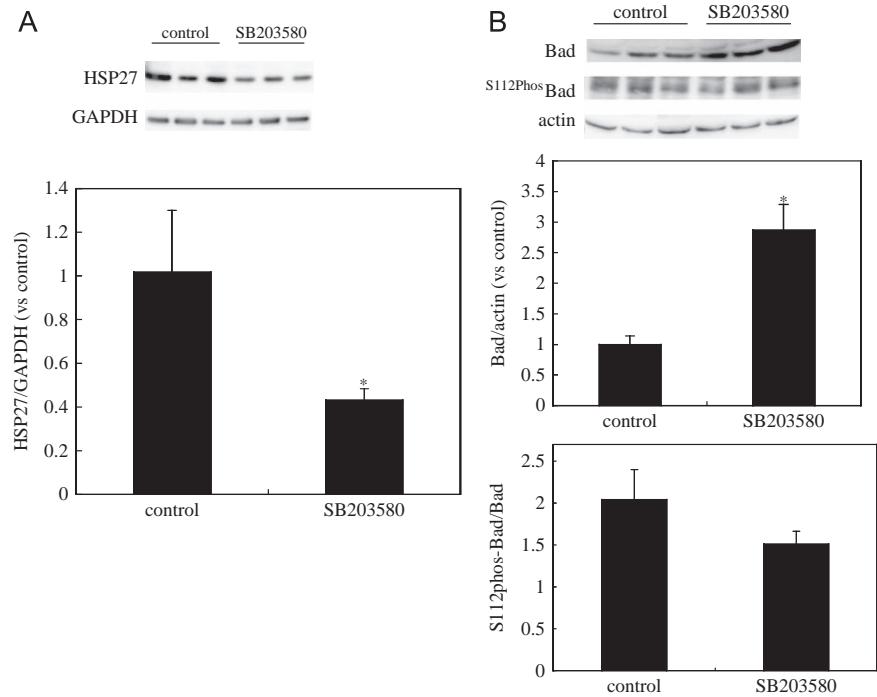
Fig. 4. p38MAPK inhibition upregulated HSP27 and downregulated BAD in the pancreas. The protein levels of (A) HSP27 and (B) BAD and phosphorylated BAD (S112) in the pancreas were determined by Western blot analysis. Data are expressed as the mean $\pm$ SEM (n=5 or 6). $^*P < 0.05$ vs. control.
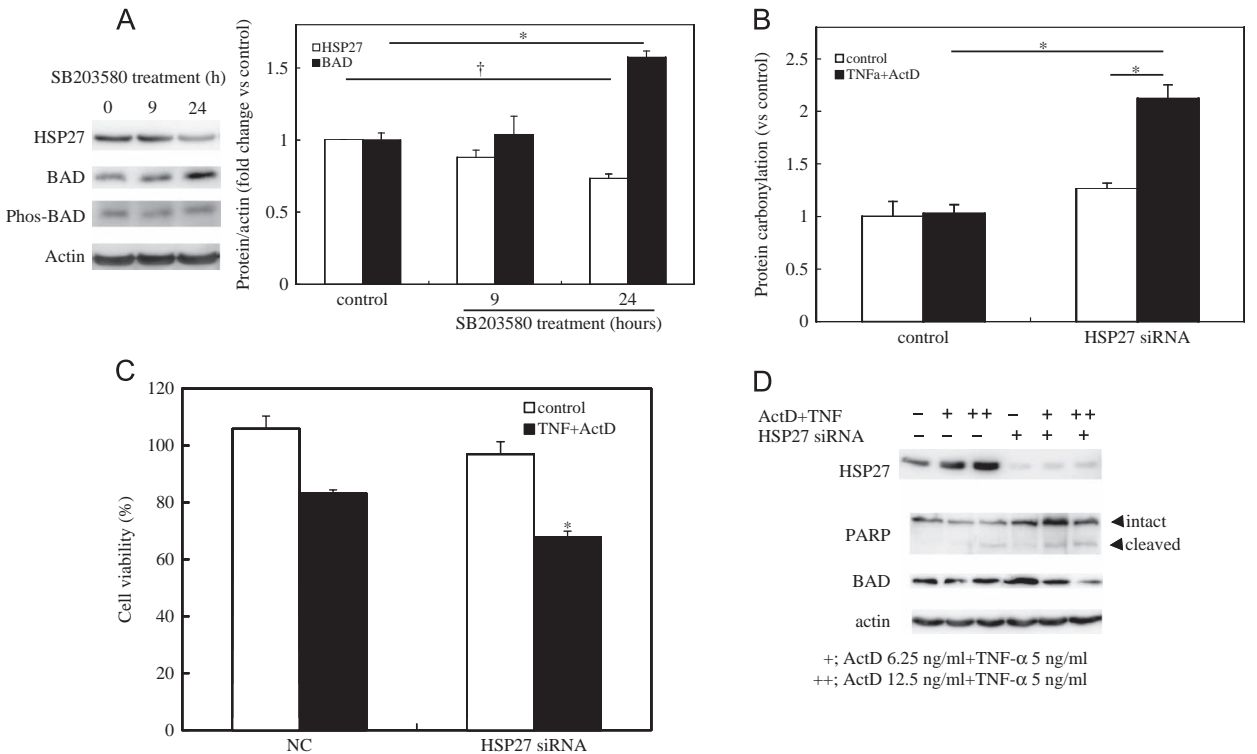
Fig. 5. HSP27 knockdown augmented ROS accumulation and cell death: (A) PANC-1 cells were cultured with or without 5 μM SB203580, a p38 inhibitor, for the indicated times. The protein levels of BAD, phosphorylated BAD (S112), and HSP27 were detected by Western blot analysis. $\dagger ^*P < 0.05$ vs. without SB203580 treatment. (B) HSP27 siRNA or control siRNA was transfected into PANC-1 cells. Cells were incubated with or without TNF-α and actinomycin D for 24 h. Protein carbonylation was determined using the Oxiselect kit. (C) PANC-1 cells were treated with or without TNF-α (5 ng/ml) and actinomycin D (6.25 ng/ml). After 24 h, cell viability was measured with the Cell Counting Kit-8. Data are expressed as the mean $\pm$ SEM (n=4). $^*P < 0.05$ vs. without HSP27 siRNA transfection. (D) Cells were incubated with or without TNF-α and actinomycin for 24 h. Lysates were in-gel separated and analyzed by immunoblotting with the indicated antibodies.
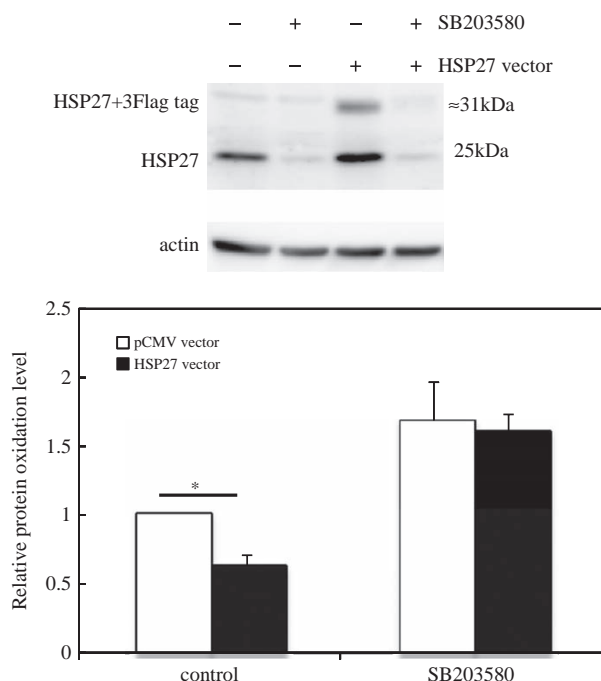
Fig. 6. HSP27 overexpression attenuates ROS accumulation in PANC-1 cells. HSP27 expression vector or control vector was transfected into PANC-1 cells. Cells were incubated with or without SB203580 for 24 h. The protein levels of HSP27 and actin were determined by Western blot analysis. Protein carbonylation was determined using the Oxiselect kit. Data are expressed as the mean ± SEM ($n=4$).
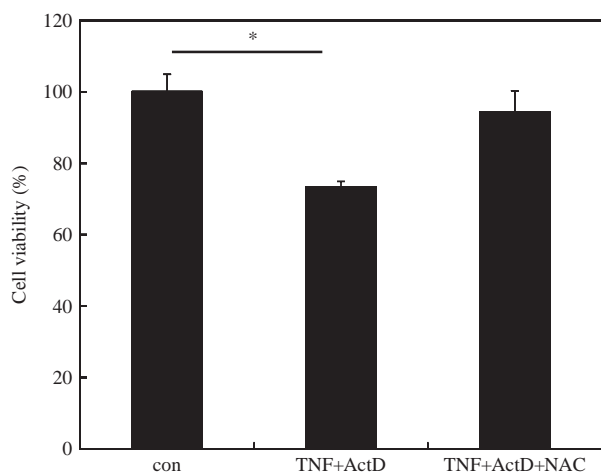
Fig. 7. TNF-α plus actinomycin D-induced cell death was prevented by administration of the antioxidant NAC. PANC-1 cells were cultured at 2×10^5 cells/well in 24-well plates. NAC (1 mM) was added 1 h before treatment with TNF-α (5 ng/ml) and actinomycin D (6.25 ng/ml). Cell viability was determined by the trypan blue exclusion method 24 h after the treatment with TNF-α and actinomycin D. Data are expressed as the mean ± SEM ($n=4$). $^*P < 0.01$ vs. control.

To clarify whether the effects of SB203580 are indeed due to the inhibition of p38MAPK or to other nonspecific effects of this small molecule, we transfected siRNAs of four subtypes of p38MAPK (α, β, γ, δ) into PANC-1 cells. Knockdown effect was detected by Western blot analysis with these subtype-specific antibodies (Fig. 8A). Knockdown of p38β decreased HSP27 protein

levels and strongly increased the TNF-α plus ActD-induced protein oxidation (Fig. 8B). Furthermore TNF-α plus ActD-induced cell death was also significantly increased in p38β-knockdown cells. On the other hand, knockdown of p38δ significantly increased cell proliferation (Fig. 8C). In TNF-α-treated PANC-1 cells, p38β inhibition mimicked the effect of SB203580 observed in the rat pancreas.

Discussion

Oxidative stress is implicated in the pathogenesis of pancreatitis [4,21], exerting many effects, including alteration of gene expression [22], enhanced cell death and proliferation, and induction of higher DNA-mutation rates [23]. However, the molecular mechanisms regulating ROS production in chronic pancreatitis are poorly understood. Herein, we found that ROS accumulation in the pancreas was enhanced by p38 inhibition by SB203580. ROS generated intracellularly or in close vicinity to acinar cells facilitate necrosis of acinar cells [18,24]. Correspondingly, our histological findings demonstrated that p38 inhibition dramatically enhanced the loss of acinar cells and infiltration of inflammatory cells. It is believed that necrotic cells release factors (danger signals or alarmins) that activate inflammatory cells; these in turn produce cytokines, such as TNF-α, interleukin 1 (IL-1), and IL-6, which promote ROS accumulation in parenchymal cells and ROS production in phagocytic leukocytes [3,25]. p38MAPK would therefore attenuate ROS-mediated pancreatic acinar cell death and subsequent recruitment of inflammatory cells. Four mammalian p38 isoforms have been characterized: p38α, β, γ, and δ. SB203580 mainly inhibits p38α and β [26]. The effect of SB203580 observed in the rat pancreas was similar to that of p38β inhibition in TNF-α plus ActD-treated PANC-1 cells.

p38MAPK functions in a cell-context-specific and cell-type-specific manner to integrate signals that affect proliferation, differentiation, and survival [27]. In the liver parenchymal cells, p38α ablation enhances ROS accumulation and hepatocyte necrosis, which are prevented by administration of an antioxidant [3], indicating the critical role of ROS in hepatocyte necrosis. Given that p38 is essential for ROS production in neutrophils [28] and proinflammatory cytokine production in macrophages [7], p38 inhibition in inflammatory cells would attenuate the inflammatory response. However, treatment with p38 inhibitor increased infiltration of inflammatory cells, including neutrophils, in the pancreas, as assessed by histological examination and MPO activity. Chronic pancreatitis is an irreversible progressive disease characterized by destruction of exocrine parenchyma and its replacement with fibrotic tissue. p38 inhibitor did not significantly affect proliferation of pancreatic stellate cells, a major cell type involved in fibrosis (Supplementary Fig. 1). A previous study reported that the p38MAPK signaling pathway is not involved in the regulation of islet cell death [8], which is consistent with our results. Taken together, these data suggest that p38MAPK in pancreatic acinar cells plays an important role in the pathogenesis of chronic pancreatitis, at least in the WBN/Kob rat model.

The functional significance of intracellular HSP27 accumulation and HSP27 phosphorylation in response to cell stress has been examined in multiple in vitro studies in which the overexpression of HSP27 reduced ROS accumulation and conferred resistance against oxidative stress [29]. In the present study, we showed that p38 inhibition reduced HSP27 protein levels in the pancreas. Furthermore, HSP27, a downstream target of p38MAPK, attenuated ROS accumulation and cell death in pancreatic cancer cells induced by TNF-α plus ActD. It is widely recognized that HSP27 is phosphorylated downstream of p38MAP kinase [30,31]. In addition to the expression level of HSP27, the cellular impact of
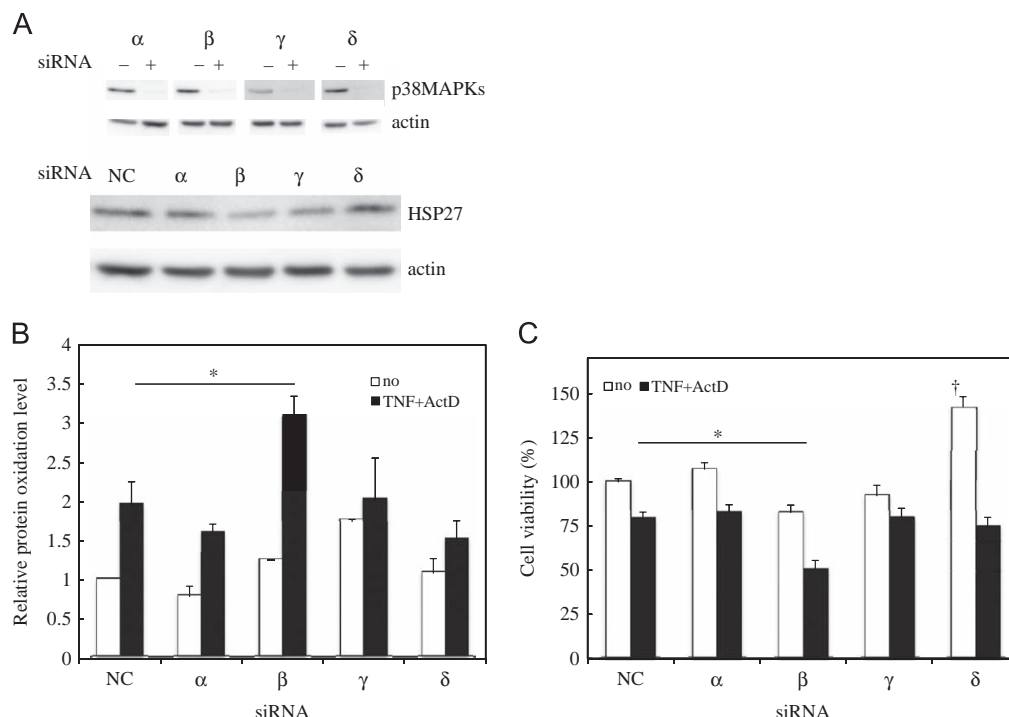
Fig. 8. p38β knockdown augmented ROS accumulation and cell death in PANC-1 cells. Each of four subtypes of p38MAPK (α, β, γ, δ) siRNA or control siRNA was transfected into PANC-1 cells. The cells were incubated with or without TNF-α and actinomycin D for 24 h: (A) The knockdown effect of each subtype of p38MAPK was detected by Western blot analysis using the subtype-specific antibodies. The protein levels of HSP27 and actin were determined by Western blot analysis. (B) Protein carbonylation of pancreas tissue lysate was detected using the Oxiselect kit. Data are expressed as the mean $\pm$ SEM ($n=3$). $^*P < 0.05$ vs. negative control. (C) Two days after siRNA transfection, cells were treated with or without TNF-α (5 ng/ml) and actinomycin D (6.25 ng/ml). After 24 h, cell viability was measured with the Cell Counting Kit-8. Data are expressed as the mean $\pm$ SEM ($n=4$). $^{\dagger *}P < 0.05$ vs. negative control. NC, negative control.

HSP27 is also influenced by its phosphorylation status. Overexpression of HSP27, but not HSP27 with the phosphorylatable residues Ser-15, -78, and -82 mutated to alanine (HSP27-AA), protects against cerulean-induced pancreatitis [16]. Consistently, overexpression of HSP27, but not HSP27-AA, ameliorated TNF-α-induced cell death and ROS accumulation in PANC-1 cells (data not shown).

The prosurvival proteins Bcl-xL and Bcl-2 protect acinar cells from not only apoptosis but also necrosis [32]. BAD, a proapoptotic member of the Bcl-2 family, heterodimerizes strongly with Bcl-xL and less strongly with Bcl-2, but does not bind to other members of the family. When BAD dimerizes with Bcl-xL, it displaces Bax and restores its apoptosis-inducing ability [33]. We demonstrated that treatment with p38 inhibitor enhanced cell death and increased expression of BAD in the pancreas. The decrease in the proapoptotic protein BAD might account for part of the protective effects of p38MAPK. Although HSP27 is a component of the p38MAPK signaling cascade, HSP27 knockdown did not affect the level of BAD protein, suggesting that p38MAPK regulates BAD expression independent of HSP27. The function of BAD is also regulated by its phosphorylation at serine residues. Unphosphorylated BAD binds and eventually inactivates antiapoptotic family members, primarily Bcl-xL, but also Bcl-2 [33]. Phosphorylation of BAD at Ser-112, Ser-136, and Ser-155 impairs its binding to Bcl-xL and promotes the sequestration of BAD from the surface of the mitochondria to the cytosol by the protein 14-3-3, which can prevent apoptosis [17]. We showed that p38MAPK did not affect the level of phosphorylated BAD in the pancreas.

In conclusion, this study demonstrated that p38MAPK inhibition augments tissue injury through downregulation of HSP27 and upregulation of BAD in chronic pancreatitis. Our results suggest that the roles of p38MAPK and HSP27 in patients suffering from different forms of persistent pancreatitis need to be evaluated. Targeting these molecules may provide an effective means of interfering with chronic pancreatitis and fibrosis.

Appendix A. Supplementary material

Supplementary data associated with this article can be found in the online version at http://dx.doi.org/10.1016/j.freeradbiomed.2012.03.010.

References

[1] Galluzzi, L.; Maiuri, M. C.; Vitale, I.; Zischka, H.; Castedo, M.; Zitvogel, L.; Kroemer, G. Cell death modalities: classification and pathophysiological implications. *Cell Death Differ* **14:**1237–1243; 2007.
[2] Kroemer, G.; Galluzzi, L.; Brenner, C. Mitochondrial membrane permeabilization in cell death. *Physiol Rev* **87:**99–163; 2007.
[3] Sakurai, T.; He, G.; Matsuzawa, A.; Yu, G. Y.; Maeda, S.; Hardiman, G.; Karin, M. Hepatocyte necrosis induced by oxidative stress and IL-1α release mediate

carcinogen-induced compensatory proliferation and liver tumorigenesis. *Cancer Cell* **14:**156–165; 2008.

[4] Schoenberg, M. H.; Birk, D.; Beger, H. G. Oxidative stress in acute and chronic pancreatitis. *Am J Clin Nutr* **62:**1306S–1314S; 1995.

[5] Chang, L.; Karin, M. Mammalian MAP kinase signalling cascades. *Nature* **410:**37–40; 2001.

[6] Dhillon, A. S.; Hagan, S.; Rath, O.; Kolch, W. MAP kinase signalling pathways in cancer. *Oncogene* **26:**3279–3290; 2007.

[7] Park, S. J.; Yoon, W. K.; Kim, H. J.; Son, H. Y.; Cho, S. W.; Jeong, K. S.; Kim, T. H.; Kim, S. H.; Kim, S. R.; Ryu, S. Y. 2,3,7,8-Tetrachlorodibenzo-*p*-dioxin activates ERK and p38 mitogen-activated protein kinases in RAW 264.7 cells. *Anticancer Res* **25:**2831–2836; 2005.

[8] Fukuda, K.; Tesch, G. H.; Yap, F. Y.; Forbes, J. M.; Flavell, R. A.; Davis, R. J.; Nikolic-Paterson, D. J. MKK3 signalling plays an essential role in leukocyte-mediated pancreatic injury in the multiple low-dose streptozotocin model. *Lab Invest* **88:**398–407; 2008.

[9] Schmidt, J.; Rattner, D. W.; Lewandrowski, K.; Compton, C. C.; Mandavilli, U.; Knoefel, W. T.; Warshaw, A. L. A better model of acute pancreatitis for evaluating therapy. *Ann Surg* **215:**44–56; 1992.

[10] Bradley, P. P.; Priebat, D. A.; Christensen, R. D.; Rothstein, G. Measurement of cutaneous inflammation: estimation of neutrophil content with an enzyme marker. *J Invest Dermatol* **78:**206–209; 1982.

[11] Kleeff, J.; Kornmann, M.; Sawhney, H.; Korc, M. Actinomycin D induces apoptosis and inhibits growth of pancreatic cancer cells. *Int J Cancer* **86:**399–407; 2000.

[12] Davis, R. J. Signal transduction by the JNK group of MAP kinases. *Cell* **103:**239–252; 2000.

[13] Grady, T.; Dabrowski, A.; Williams, J. A.; Logsdon, C. D. Stress-activated protein kinase activation is the earliest direct correlate to the induction of secretagogue-induced pancreatitis in rats. *Biochem Biophys Res Commun* **227:**1–7; 1996.

[14] Sakurai, T.; Maeda, S.; Chang, L.; Karin, M. Loss of hepatic NF-κB activity enhances chemical hepatocarcinogenesis through sustained c-Jun N-terminal kinase 1 activation. *Proc Natl Acad Sci USA* **103:**10544–10551; 2006.

[15] Shimizu, K. Mechanisms of pancreatic fibrosis and applications to the treatment of chronic pancreatitis. *J Gastroenterol* **43:**823–832; 2008.

[16] Kubisch, C.; Dimagno, M. J.; Tietz, A. B.; Welsh, M. J.; Ernst, S. A.; Brandt-Nedelev, B.; Diebold, J.; Wagner, A. C.; Goke, B.; Williams, J. A.; Schafer, C. Overexpression of heat shock protein Hsp27 protects against cerulein-induced pancreatitis. *Gastroenterology* **127:**275–286; 2004.

[17] Zha, J.; Harada, H.; Yang, E.; Jockel, J.; Korsmeyer, S. J. Serine phosphorylation of death agonist BAD in response to survival factor results in binding to 14-3-3 not BCL-X(L). *Cell* **87:**619–628; 1996.

[18] Gukovskaya, A. S.; Gukovsky, I.; Zaninovic, V.; Song, M.; Sandoval, D.; Gukovsky, S.; Pandol, S. J. Pancreatic acinar cells produce, release, and respond to tumor necrosis factor-α: role in regulating cell death and pancreatitis. *J Clin Invest* **100:**1853–1862; 1997.

[19] Leindler, L.; Morschl, E.; Laszlo, F.; Mandi, Y.; Takacs, T.; Jarmai, K.; Farkas, G. Importance of cytokines, nitric oxide, and apoptosis in the pathological process of necrotizing pancreatitis in rats. *Pancreas* **29:**157–161; 2004.

[20] Schlatter, R.; Schmich, K.; Lutz, A.; Trefzger, J.; Sawodny, O.; Ederer, M.; Merfort, I. Modeling the TNFα-induced apoptosis pathway in hepatocytes. *PLoS One* **6:**e18646; 2011.

[21] Sakurai, T.; Kudo, M.; Fukuta, N.; Nakatani, T.; Kimura, M.; Park, A. M.; Munakata, H. Involvement of angiotensin II and reactive oxygen species in pancreatic fibrosis. *Pancreatology* **11(Suppl. 2):**7–13; 2011.

[22] Allen, R. G.; Tresini, M. Oxidative stress and gene regulation. *Free Radic Biol Med* **28:**463–499; 2000.

[23] Toyokuni, S. Novel aspects of oxidative stress-associated carcinogenesis. *Antioxid Redox Signaling* **8:**1373–1377; 2006.

[24] Sandoval, D.; Gukovskaya, A.; Reavey, P.; Gukovsky, S.; Sisk, A.; Braquet, P.; Pandol, S. J.; Poucell-Hatton, S. The role of neutrophils and platelet-activating factor in mediating experimental pancreatitis. *Gastroenterology* **111:**1081–1091; 1996.

[25] Weiss, S. J. Tissue destruction by neutrophils. *N Engl J Med* **320:**365–376; 1989.

[26] Zarubin, T.; Han, J. Activation and signaling of the p38 MAP kinase pathway. *Cell Res* **15:**11–18; 2005.

[27] Wagner, E. F.; Nebreda, A. R. Signal integration by JNK and p38 MAPK pathways in cancer development. *Nat Rev Cancer* **9:**537–549; 2009.

[28] Chaves, M. M.; Costa, D. C.; de Oliveira, B. F.; Rocha, M. I.; Nogueira-Machado, J. A. Role PKA and p38 MAPK on ROS production in neutrophil age-related: lack of IL-10 effect in older subjects. *Mech Ageing Dev* **130:**588–591; 2009.

[29] Mehlen, P.; Hickey, E.; Weber, L. A.; Arrigo, A. P. Large unphosphorylated aggregates as the active form of hsp27 which controls intracellular reactive oxygen species and glutathione levels and generates a protection against TNFα in NIH-3T3-ras cells. *Biochem Biophys Res Commun* **241:**187–192; 1997.

[30] Stokoe, D.; Campbell, D. G.; Nakielny, S.; Hidaka, H.; Leevers, S. J.; Marshall, C.; Cohen, P. MAPKAP kinase-2; a novel protein kinase activated by mitogen-activated protein kinase. *EMBO J* **11:**3985–3994; 1992.

[31] Krump, E.; Sanghera, J. S.; Pelech, S. L.; Furuya, W.; Grinstein, S. Chemotactic peptide *N*-formyl-met-leu-phe activation of p38 mitogen-activated protein kinase (MAPK) and MAPK-activated protein kinase-2 in human neutrophils. *J Biol Chem* **272:**937–944; 1997.

[32] Sung, K. F.; Odinokova, I. V.; Mareninova, O. A.; Rakonczay Jr Z.; Hegyi, P.; Pandol, S. J.; Gukovsky, I.; Gukovskaya, A. S. Prosurvival Bcl-2 proteins stabilize pancreatic mitochondria and protect against necrosis in experimental pancreatitis. *Exp Cell Res* **315:**1975–1989; 2009.

[33] Yang, E.; Zha, J.; Jockel, J.; Boise, L. H.; Thompson, C. B.; Korsmeyer, S. J. Bad, a heterodimeric partner for Bcl-XL and Bcl-2, displaces Bax and promotes cell death. *Cell* **80:**285–291; 1995.

LETTERS, TECHNIQUES AND IMAGES

Case of Peutz-Jeghers syndrome with depressed-type early duodenal carcinoma

A 45-year-old man with Peutz-Jeghers syndrome (PJS) underwent endoscopy. A slightly elevated lesion with a depression (IIa+IIc) associated with converging folds was found at the distal duodenum (Fig. 1 and Fig. S1). Partial duodenectomy was carried out and histopathological examination confirmed submucosally invasive moderately differentiated adenocarcinoma without vessel permeation (Fig. 2 and Fig. S2). He was diagnosed as having PJS at 7 years of age and had undergone endoscopy and polypectomy two to three times a year. His physical examination, as well as family history, was non-contributory. After the duodenectomy, the patient has been followed up for 2 years and remains asymptomatic and recurrence free. Hamartomatous polyps surrounding and hiding the depressed-type duodenal cancer had been removed by polypectomy, which led to early detection of the cancer.

In PJS, the most challenging clinical aspect is identification of cancer. Two possible modes of cancer development have been proposed in PJS: de novo carcinogenesis and a hamartoma-carcinoma sequence. In our case, no dysplasia foci were pathologically found in polyps that had endoscopically been resected. The duodenal cancer was a depressed type, which looked totally different from surrounding hamartomas. These findings suggest that the duodenal cancer might have developed de novo.

Hemminki *et al*. described a mutation in the *LKB-1* gene.[1] A target of LKB in growth control is the tumor suppressor p53.[2] The expression of COX-2 is induced by p53 activation of the Ras/Raf/MAPK pathway. COX-2 inhibits DNA damage- or p53-induced apoptosis.[3] Gankyrin, a critical oncoprotein overexpressed in human cancers, binds to Mdm2, facilitating p53-Mdm2 binding, and increases degradation of p53.[4] On immunostaining, the cancer was positive for p53, COX2 and Gankyrin, whereas none of these proteins was expressed in the surrounding normal epithelium and hamartoma (Fig. S3 and data not shown), suggesting that these proteins might be involved in carcinogenesis in PJS.

Toshiharu Sakurai, Hiroshi Kashida and Masatoshi Kudo
Department of Gastroenterology and Hepatology, Kinki University, Osaka, Japan
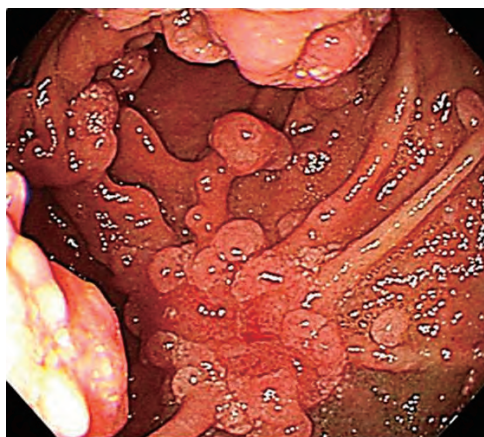
Fig. 1. Endoscopy revealed a superficial and slightly depressed lesion with converging folds in the duodenum.
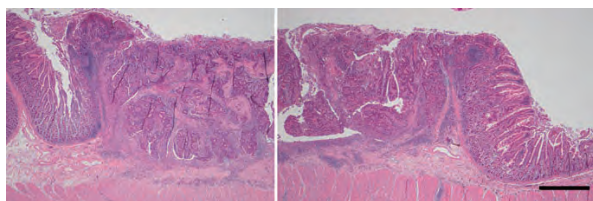
Fig. 2. Microscopic appearance of the cancer showing moderately differentiated adenocarcinoma. Scale bar, 1 mm.

REFERENCES

1. Hemminki A, Tomlinson I, Markie D *et al*. Localization of a susceptibility locus for Peutz-Jeghers syndrome to 19p using comparative genomic hybridization and targeted linkage analysis. *Nat. Genet.* 1997; **15**: 87–90.
2. Mihaylova MM, Shaw RJ. The AMPK signalling pathway coordinates cell growth, autophagy and metabolism. *Nat. Cell Biol.* 2011; **13**: 1016–23.
3. Han JA, Kim JI, Ongusaha PP *et al*. p53-mediated induction of Cox-2 counteracts p53- or genotoxic stress-induced apoptosis. *EMBO J.* 2002; **21**: 5635–44.
4. Higashitsuji H, Higashitsuji H, Itoh K *et al*. The oncoprotein gankyrin binds to MDM2/HDM2, enhancing ubiquitylation and degradation of p53. *Cancer Cell* 2005; **8**: 75–87.

SUPPORTING INFORMATION

Additional Supporting Information may be found in the online version of this article:

Fig. S1. Indigocarmine spraying and narrow band imaging of the duodenal cancer.
Fig. S2. Macroscopic view of the duodenal cancer. Scale bar, 1 cm.
Fig. S3. Expression of gankyrin, p53 and COX2 in normal epithelium and cancer. Scale bar, 50 µm.

Please note: Wiley-Blackwell are not responsible for the content or functionality of any supporting materials supplied by the authors. Any queries (other than missing material) should be directed to the corresponding author for the article.

Digestive Diseases

Viral Hepatitis and Hepatocellular Carcinoma: Update in 2012

Masatoshi Kudo

Department of Gastroenterology and Hepatology, Kinki University School of Medicine, Osaka, Japan

The 9th Korea-Japan Liver Symposium in Conjunction with the International Symposium of the Asan Liver Center was held on July 15–16, 2012, in Seoul, Korea.

Hagiwara et al. [1] reported two cases of hepatitis B reactivation receiving chemotherapy for solid cancer in terms of patterns and characteristics of reactivation. Accumulation of such cases will help in clarifying the clinical importance of hepatitis B reactivation during treatment of solid malignancies. Ueda et al. [2] reported that retreatment with peginterferon α-2a + ribavirin should be considered for relapsers and partial responders to previous peginterferon α-2b + ribavirin combination therapy. Their results suggest that prolonged administration is also favorable for early viral response cases to attain a higher sustained viral response. Hagiwara et al. [3] reported that maintenance therapy with the use of long-term, low-dose peginterferon α-2a is effective for preventing hepatocellular carcinoma (HCC) occurrence irrespective of the IL28B SNP, at least for a subset of chronic hepatitis C (CHC) patients. An initial response of serum ALT levels and body mass index provides a prognostic value for determining the risk for developing HCC later in life.

Nishida et al. [4] reported that male patients with CHC develop HCC more frequently when they have a non-cirrhotic liver than do female patients. This gender difference could be, at least partially, attributed to a different degree of iron deposition, which contributes to the development of HCC in the absence of liver cirrhosis in men with CHC. Lee et al. [5] reported that a biochemical but not virologic response to interferon-α therapy reduces independently the occurrence of HCC in patients with chronic hepatitis B. Kobayashi et al. [6] reported that Victoria blue and CK7 staining are very useful in the diagnosis of early HCC through biopsy tissue. Makino et al. [7] reported that the multimodality fusion imaging system has become quite an important tool for locoregional treatment of HCC because of its usefulness for both the guidance during the radiofrequency ablation procedure and the evaluation of its treatment effects. Tsuchida et al. [8] reported on a novel insertion method, a non-trocar technique, for laparoscopic radiofrequency ablation with the use of a convex scanning probe, whereby an ablation needle accurately and easily punctures the target tumor in the liver.

Minami and Kudo [9] reported that endoscopic retrograde biliary drainage (ERBD) and percutaneous transhepatic biliary drainage (PTBD) are the two main nonsurgical treatment options for obstructive jaundiced patients with HCC. ERBD is usually the first-line treatment because of low hemorrhage risk, while PTBD is an important second-line treatment when ERBD is impossible. The dominant effect of biliary drainage suggests that successful jaundice therapy could enhance anti-cancer treatment by increasing life expectancy, decreasing mortality,

Masatoshi Kudo, MD, PhD
Department of Gastroenterology and Hepatology
Kinki University School of Medicine
377-2, Ohno-Higashi, Osaka-Sayama, Osaka 589-8511 (Japan)
E-Mail m-kudo@med.kindai.ac.jp

or both. In addition, recent developments in interventional endoscopic ultrasound allow a transgastric approach to the left biliary system when the bile duct is inaccessible by conventional ERCP in patients with hilar block due to HCC.

Kim and Han [10] reported that progressive improvement has been made in the outcomes of HCC in the intermediate or advanced stage. Apart from development of novel treatment modalities including interventional techniques or targeted therapy, proper combination of the currently available therapies according to tumor characteristics might be necessary to further improve therapeutic outcomes of HCC.

Shim et al. [11] reported that tumoral overexpression of arrest-defective protein-1 may be useful for predicting the presence of microvascular invasion, which is a well-accepted indicator of poor prognosis after HCC resection. However, it did not appear to correlate significantly with tumor recurrence or patient survival post-surgery. This study provides a decisive base for further studies examining whether arrest-defective protein-1 expression can serve as an unfavorable prognostic factor in patients with HCC.

Kudo et al. [12] reported on real-life clinical practice with sorafenib in advanced HCC in a single-center experience. Patients in the long-term treatment group, who received sorafenib for ≥90 days, showed a favorable outcome compared with those in the short-term treatment group in which the administration period was <90 days. Multivariate analysis revealed treatment duration as a significant prognostic factor. Furthermore, patients who received post-sorafenib treatment had a better outcome than those who did not.

Bae et al. [13] reported that assessment of hepatic function with Gd-EOB-DTPA-enhanced liver MRI [14, 15] is a relatively new technique with great potential for clinical applications. It allows us to obtain both hepatic anatomical and functional information in a single imaging acquisition setting. In particular, for a patient with locally varying hepatic parenchymal abnormalities, a regional assessment of hepatic function mapped onto hepatic anatomy may be clinically more meaningful than conventional global metrics of hepatic function.

I firmly believe this issue will benefit all of the readers of *Digestive Diseases*, especially those who are interested in viral hepatitis and HCC.

References

1 Hagiwara S, Sakurai T, Nishina S, Tanaka K, Ikeda M, Ueshima K, Minami Y, Inoue T, Yada N, Kitai S, et al: Characteristic pattern of reactivation of hepatitis B virus during chemotherapy for solid cancers. Dig Dis 2012;30:541–546.

2 Ueda T, Tsuchiya K, Hashimoto S, Inoue T, Inao M, Tanaka A, Kaito M, Imazaki F, Nishiguchi S, Mochida S, et al: Retreatment with peginterferon alfa-2a plus ribavirin in patients who failed previous peginterferon alfa-2b plus ribavirin combination therapy. Dig Dis 2012;30:554–560.

3 Hagiwara S, Sakurai T, Takita M, Ueshima K, Minami Y, Inoue T, Yada N, Kitai S, Nagai T, Hayaishi S, et al: Risk of HCC development in cases of hepatitis C treated by long-term, low-dose PEG-IFNα2a. Dig Dis 2012; 30:561–567.

4 Nishida N, Arizumi T, Hayaishi S, Takita M, Kitai S, Yada N, Hagiwara S, Inoue T, Minami Y, Ueshima K, et al: Gender differences in the livers of patients with hepatocellular carcinoma and chronic hepatitis C infection. Dig Dis 2012;30:547–553.

5 Lee D, Chung YH, Lee SH, Kim SE, Lee Y, Kim KM, Lim YS, Lee HC, Lee YS, Yu E: Effect of response to interferon α therapy on the occurrence of hepatocellular carcinoma in patients with chronic hepatitis B. Dig Dis 2012;30:568–573.

6 Kobayashi S, Kim SR, Imoto S, Ando K, Hirakawa M, Saito J, Fukuda K, Otono Y, Sasaki M, Tsuchida S, et al: Histopathological diagnosis of early HCC through biopsy – Efficacy of Victoria blue and cytokeratin 7 staining. Dig Dis 2012;30:574–579.

7 Makino Y, Imai Y, Igura T, Ohama H, Kogita S, Sawai Y, Fukuda K, Ohashi H, Murakami T: Usefulness of the multimodality fusion imaging for the diagnosis and treatment of hepatocellular carcinoma. Dig Dis 2012; 30:580–587.

8 Tsuchida S, Fukumoto T, Toyokawa A, Awazu M, Kusunoki N, Kido M, Takahashi M, Tanaka M, Kuramitsu K, Kim SR, et al: Novel non-trocar technique for laparoscopic radiofrequency ablation. Dig Dis 2012;30:588–591.

9 Minami Y, Kudo M: Hepatocellular carcinoma with obstructive jaundice: endoscopic and percutaneous biliary drainage. Dig Dis 2012;30:592–597.

10 Kim DY, Han KH: How to improve treatment outcomes for hepatocellular carcinoma of intermediate and advanced stage. Dig Dis 2012;30:598–602.

11 Shim JH, Chung YH, Kim JA, Lee D, Kim KM, Lim YS, Lee HC, Lee YS, Yu E, Lee YJ: Clinical implications of arrest-defective protein 1 expression in hepatocellular carcinoma: a novel predictor of microvascular invasion. Dig Dis 2012;30:603–608.

12 Kudo M, Ueshima K, Arizumi T: Real-life clinical practice with sorafenib in advanced hepatocellular carcinoma: a single-center experience. Dig Dis 2012;30:609–616.

13 Bae KE, Kim SY, Lee SS, Kim KW, Won HJ, Shin YM, Kim PN, Lee MG: Assessment of hepatic function with Gd-EOB-DTPA-enhanced hepatic MRI. Dig Dis 2012;30:617–622.

14 Lee JM, Yoon JH, Joo I, Woo HS: Recent advances in CT and MR imaging for evaluation of hepatocellular carcinoma. Liver Cancer 2012;1:22–40.

15 Ricke J, Seidensticker M, Mohnike K: Non-invasive diagnosis of hepatocellular carcinoma in cirrhotic liver: current guidelines and future prospects for radiological imaging. Liver Cancer 2012;1:51–58.

Characteristic Pattern of Reactivation of Hepatitis B Virus during Chemotherapy for Solid Cancers

Satoru Hagiwara[a]   Toshiharu Sakurai[a]   Shinichi Nishina[b]   Kaoru Tanaka[b]

Masafumi Ikeda[d]   Kazuomi Ueshima[a]   Yasunori Minami[a]   Tatsuo Inoue[a]

Norihisa Yada[a]   Satoshi Kitai[a]   Masahiro Takita[a]   Tomoyuki Nagai[a]

Sousuke Hayaishi[a]   Tadaaki Arizumi[a]   Ah-Mee Park[c]   Hiroshi Munakata[c]

Naoshi Nishida[a]   Masatoshi Kudo[a]

Departments of [a]Gastroenterology and Hepatology, [b]Medical Oncology, and [c]Biochemistry, Kinki University School of Medicine, Osaka, and [d]Division of Hepatobiliary and Pancreatic Oncology, National Cancer Hospital East, Chiba, Japan

Abstract

Objective: A number of studies have reported reactivation of hepatitis B during intensive immunosuppressive therapy such as cases of hematological malignancy, whereas little has been reported for characteristics of reactivation triggered by chemotherapy for solid cancer. *Methods:* A total of 130 patients underwent chemotherapy for treatments of common solid cancer between May 2011 and May 2012 at Kinki University Hospital. Among them, 27 patients were suspected for a past infection of hepatitis B virus (HBV), showing positive for hepatitis B core antibody or surface antibody but negative for hepatitis B surface antigen, and were eligible for this study. *Results:* Hepatitis B reactivation was observed in 2 of 27 cases (7.4%). The duration between the start of chemotherapy and increase of serum HBV load was 30 days in both cases. *Conclusions:* We reported the 2 cases of hepatitis B reactivation receiving chemotherapy for solid cancer in terms of patterns and characteristics of reactivation. Accumulation of such cases will help in clarifying the clinical importance of hepatitis B reactivation during treatment of solid malignancies.

Copyright © 2012 S. Karger AG, Basel

Introduction

Recently, reactivation of hepatitis B virus (HBV) has widely attracted attention among physicians of several specialties, such as hepatologists, clinical oncologists, etc. Because several novel anticancer drugs have come into being recently, effective immunosuppression is potentially attributed to an increase of the reactivation rate of hepatitis B as a consequence of accelerated viral replication [1–3]. Generally, reactivation of hepatitis B can be observed in two populations: asymptomatic hepatitis surface antigen (HBsAg)-positive carriers and HBsAg-negative subjects with a past history of HBV infection.

About 85% of HBV carriers become asymptomatic with stable clinical manifestations due to spontaneously reduced viral replication. However, it is well known that

Naoshi Nishida, MD, PhD
Department of Gastroenterology and Hepatology
Kinki University School of Medicine, 377-2 Ohno-Higashi
Osaka-Sayama, Osaka 589-8511 (Japan)
E-Mail naoshi@med.kindai.ac.jp

Table 1. Characteristics of patients treated with chemotherapy

Characteristics	Patients, n
Total number of patients	27
Gender	
Male	20
Female	7
Age, years	
Median	66
Range	47–80
Viral markers	
Positive for both HBcAb and HBsAb	23
Positive only for HBcAb	4
Positive only for HBsAb	0
Combination with CDDP	
Yes	17
No	10

the virus remains even in asymptomatic carriers, which causes an increase of replication during or even after systemic chemotherapy as well as immunosuppressive therapy [4]. If systemic chemotherapy or administration of immunosuppressants is stopped even in asymptomatic HBV carriers, severe hepatitis should emerge as a consequence of immune reactivation, which should be an underlying mechanism of reactivation of hepatitis B in asymptomatic carriers. According to recent reports, reactivation is observed in 20–50% of HBV carriers who received intensive cancer chemotherapy or immunotherapy and, importantly, it triggered a fulminant hepatitis in a considerable number of cases [5–7].

Previously it was thought that HBV was completely eliminated from the host with a past history of infection. However, it has been found that HBV is present as cccDNA in hepatocytes and HBV DNA persistently replicates even in those subjects with a past history of acute hepatitis B showing positive for hepatitis B core antibody (HBcAb) as well as hepatitis B surface antibody (HBsAb) [8]. This type of reactivation triggered by chemotherapy and immunosuppressant in subjects with a past infection is called 'de novo hepatitis B'.

Hui et al. [1] examined de novo hepatitis B in 244 HBsAg-negative cases with malignant lymphoma in a cohort manner. They reported that the median period from the elevation of HBV DNA to the onset of hepatitis was 18.5 weeks. Therefore, administration of analogue agents soon after HBV DNA becomes positive would prevent the onset of hepatitis in patients with a past infection. On the basis of this knowledge, prophylactic administration of

nucleotide analogue was recommended for asymptomatic carriers in Japan, while HBV DNA should be measured once a month in subjects with a past infection and analogue agents should be administered when HBV DNA becomes positive.

So far, a number of studies have reported the characteristics of reactivation in cases who received intensive chemotherapy and immunosuppressive therapy, such as cases of hematological malignancy. On the contrary, little has been known as to the frequency and characteristics of reactivation during chemotherapy for common solid cancer. We speculate that a unique character of reactivation might exist during the therapy of a common solid tumor because the immunosuppressive effect should be different from those of hematological malignancy. This is an intensive report of reactivation of hepatitis B in cases of de novo hepatitis B who received systemic chemotherapy for common solid cancer.

Materials and Methods

Patient Characteristics and Study Design

A total of 27 cancer patients with a median age of 66 (47–66) years were enrolled in this study, which was approved by the ethical committee of Kinki University Hospital. The inclusion criteria were: (1) patients with a solid malignant tumor undergoing chemotherapy for the first time; (2) HBsAg-negative patients positive for either HBcAb or HBsAb, and (3) patients who gave written informed consent. The exclusion criteria were: (1) patients who underwent or were scheduled to undergo hemodialysis; (2) patients with hepatitis C virus (HCV) antibody-positive; (3) patients positive only for HBsAb with a history of HBV vaccination, and (4) patients who were judged by a physician as ineligible for enrolling in this clinical study. Serum HBsAg, HBsAb, HBeAg, and HBeAb were measured by CLIA with the Architect kit (Abbott Japan). Serum HBV-DNA level was quantified by real-time fluorescent probe PCR (Accugene; Abbott Japan) with a lower limit of quantification at 1.5 log copies/ml. Negative for serum HBV-DNA was confirmed before chemotherapy, and serum HBV-DNA was measured periodically once a month during chemotherapy to monitor HBV reactivation. Monitoring was continued for 12 months after the end of chemotherapy. In cases with HBV reactivation, a nucleotide analogue of entecavir (ETV) was administered. HBV reactivation was defined as a positive signal for amplification of HBV-DNA.

Results

Patient Characteristics

Tables 1 and 2 show the characteristics of the patients treated with chemotherapy. Among a total of 27 patients, 20 were males and 7 were females with a median age of

Table 2. Detailed characteristics and outcomes of patients treated with chemotherapy

Case No.	Age	Gender	Cancer origin	HBsAg	HBcAb S/CO	HBsAb mIU/ml	Regimen	Reactivation	Period until reactivation days	Combination with radiation	Follow-up days
1	60	M	Lung	–	908 (+)	4.1 (+)	CBDCA+PTX	–		+	390
2	71	M	Lung	–	0 (–)	1.9 (+)	CDDP+ETOP	–		–	372
3	47	F	Breast	–	170 (+)	3.2 (+)	AC	–		–	376
4	65	M	Pharynx, esophagus	–	0 (–)	11.8 (+)	CDDP+5-FU	+	30	+	361
5	66	M	Lung	–	45 (+)	4.8 (+)	CDDP+VNR	–		–	361
6	69	M	Lung	–	26 (+)	4.2 (+)	CBDCA+PTX	–		+	354
7	61	F	Esophagus, stomach	–	25 (+)	7.9 (+)	CDDP+5-FU	–		+	361
8	65	M	Pharynx	–	>1,000 (+)	2.6 (+)	CDDP	–		+	345
9	47	F	Breast	–	>1,000 (+)	9.1 (+)	TXT+CPA	–		–	298
10	71	M	Pharynx	–	>1,000 (+)	9.2 (+)	CDDP	–		+	302
11	80	F	Lung	–	44 (+)	4.7 (+)	CBDCA+PTX	–		+	265
12	70	F	Esophagus	–	317 (+)	11.0 (+)	CDGP+5-FU	–		+	202
13	64	F	Breast	–	402 (+)	9.7 (+)	PTX+trastuzumab	–		–	201
14	69	M	Pharynx	–	117 (+)	3.9 (+)	CDDP	–		+	190
15	75	M	Esophagus	–	793 (+)	9.3 (+)	CDDP+5-FU	–		+	170
16	80	M	Esophagus	–	24 (+)	10.5 (+)	CDGP+5-FU	–		+	146
17	72	M	Esophagus	–	320 (+)	9.9 (+)	CDDP+5-FU	–		+	115
18	67	M	Esophagus	–	4 (–)	9.7 (+)	CDDP+capecitabine	–		–	126
19	60	M	Pharynx	–	>1,000 (+)	9.9 (+)	CDDP	–		+	113
20	63	M	Pharynx	–	315 (+)	9.6 (+)	CDDP	–		+	108
21	67	M	Lung	–	68 (+)	10.7 (+)	CDDP+TXT	+	30	–	107
22	65	M	Pharynx	–	81 (+)	10.6 (+)	CDDP+5-FU	–		–	92
23	71	M	Gallbladder	–	5 (–)	9.4 (+)	GEM+low-dose CDDP	–		–	91
24	75	M	Esophagus	–	78 (+)	2.7 (+)	CDDP+5-FU	–		+	74
25	63	M	Lung	–	82 (+)	5.5 (+)	CBDCA+PTX	–		–	77
26	62	F	Esophagus	–	93 (+)	9.6 (+)	CDDP+5-FU	–		–	71
27	61	M	Lung	–	78 (+)	11.2 (+)	CDDP+ETOP	–		+	38

66 years. The profile of serological markers of HBV was as follows: 23 cases were positive for both HBcAb and HBsAb and 4 were positive for only HBcAb, while no case was positive for HBsAb alone. 17 cases were treated using a combination with CDDP, while 10 were treated using a regimen without including CDDP. The origins of cancer were: 9 cases of esophageal cancers, 8 lung cancers, 7 pharyngeal cancers, 3 breast cancers, and 1 gastric and gallbladder cancer, respectively. The median follow-up period after chemotherapy was 190 days, ranging from 38 to 390 days. Among 27 cases, HBV reactivation was observed in 2 cases (7.4%) (cases 4 and 21; table 2). The period before HBV reactivation was 30 days in both cases.

Clinical Course in Cases with HBV Reactivation
Case 4 (fig. 1). A 65-year-old male had synchronous double cancers of the pharynx and esophagus. He received the combination therapy of 5-fluorouracil (5-FU) and cisplatin (CDDP) (CDDP 70 mg/m², 5-FU 700

mg/m²) and underwent radiation simultaneously for a total dose of 60 Gy. Viral markers before chemotherapy were: HBsAg (–), HBcAb 11.8 S/CO (+), and HBsAb (–). One month after the start of chemotherapy, blood tests showed positivity for HBV-DNA at 1.8 log copies/ml and reactivation of hepatitis B was diagnosed. After the administration of ETV, HBV-DNA became negative persistently. Flare-up of hepatitis with elevation of serum ALT in association with appearance of serum HBV-DNA was not observed. Chemotherapy and radiation therapy for cancers were completed without discontinuation or cessation.

Case 21 (fig. 2). A 67-year-old male was suffering from lung cancer and started receiving chemotherapy with CDDP at 80 mg/m² and docetaxel (DTX) at 80 mg/m² on March 13, 2012. Viral markers before chemotherapy were: HBsAg (–), HBcAb 10.7 S/CO (+), and HBsAb (–). One month after the beginning of chemotherapy, blood examinations revealed a serum HBV-DNA level of <1.5

Fig. 1. Clinical course (case 4). A combination of FP (CDDP at 70 mg/m^2 and 5-FU at 700 mg/m^2) and radiation was started. One month after the beginning of chemotherapy, blood tests showed positive HBV DNA at 1.8 log copies/ml.
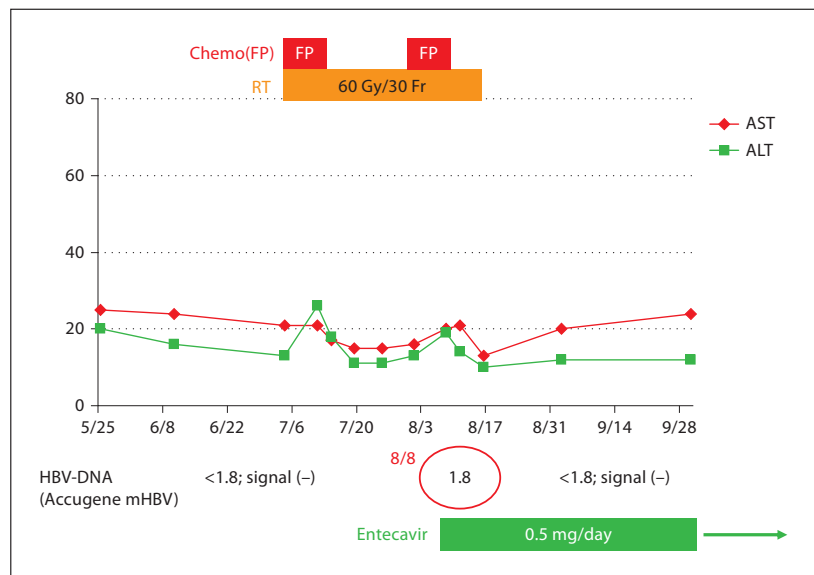
Fig. 2. Clinical course (case 21). CDDP at 80 mg/m^2 and DTX at 80 mg/m^2 were started. One month after the beginning of chemotherapy, blood tests showed HBV DNA at <1.5 log copies/ml but signals were detected.
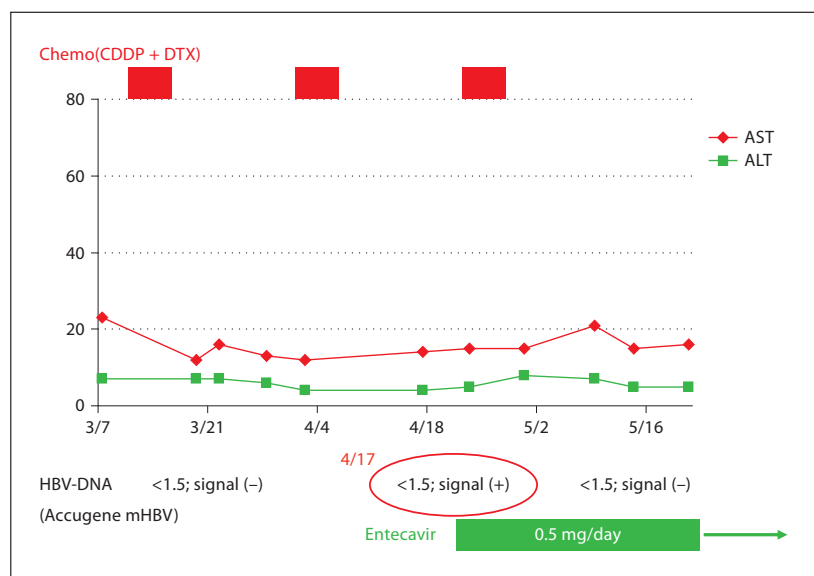
log copies/ml, but signals of amplification of HBV-DNA were detected which led to the diagnosis of HBV reactivation. ETV was administered and amplification signals have been persistently undetectable since then. No flare-up of ALT at the time of detection of HBV-DNA was observed. Chemotherapy for cancer was completed without discontinuation or cessation.

Discussion

Hui et al. [1] reported the frequency of de novo hepatitis B, or reappearance of HBV-DNA among the patients with a past history of hepatitis B positive for HBcAb and/or positive for HBsAb, in a cohort of 244 cases of HBsAg-negative malignant lymphoma. According to the report,

de novo hepatitis B appeared in 8 cases (3.3%). In particular, it appeared in 12.2% of the cases treated by combination chemotherapy of rituximab and steroid and 1.0% by chemotherapy without the combination, which suggested that receiving combination chemotherapy of rituximab and steroid was a remarkable risk for the onset of de novo hepatitis B.

In 2009, Yeo et al. [9] reported reactivation of hepatitis B in 5 (6.25%) of 80 HBsAg-negative cases with malignant lymphoma who received systemic chemotherapy. In all the 5 cases who showed reactivation, HBcAb was positive and HBsAb was negative before chemotherapy. Uemoto et al. [10] also examined de novo hepatitis B in cases who underwent a living donor liver transplant, and de novo hepatitis B was observed in 94% of the recipients after liver transplantation if the donors showed a past history of HBV infection. These reports indicate the importance of the presence of an undetectable level of HBV in hepatocytes on the pathogenesis of de novo hepatitis B under the immunosuppressant condition.

So far, a number of studies have reported de novo hepatitis B in the treatment of hematological disorders and transplant. On the other hand, this type of hepatitis has rarely been reported in cases receiving chemotherapy for common solid cancer. However, according to the increase of solid cancers and developing new agents for this type of tumor, it is of great importance to know the real frequencies and characteristics of de novo hepatitis B for this type of common disease. In the present study, HBV reactivation was observed in 2 cases (7.4%), which should be a considerable frequency and thus needs paying attention to.

According to the 2 cases we experienced, we noticed that both cases showed: (1) negative HBsAb (CLIA); (2) HBcAb (CLIA) at a high titer ≥10 (S/CO); (3) regimens containing CDDP, and (4) HBV reactivation in a relatively short term after the beginning of chemotherapy with a low HBV-DNA load after reactivation.

A decreased titer of neutralizing antibody (or HBsAb) was reported as a risk factor for de novo hepatitis B [9, 11, 12], and HBsAb was negative in the 2 cases of the present study. Furthermore, according to previous reports, HBV reactivation was more frequent in asymptomatic HBsAg-positive HBV carriers than HBsAg-negative carriers [13–15]. However, HBsAg was negative but HBcAb showed a high titer in the present cases, which suggested the possibility that HBsAg became negative due to a persistent viral decrease in asymptomatic HBV carriers.

A number of drugs have been reported to reactivate HBV-DNA [16, 17]. In addition to rituximab for malig-

nant lymphoma, it has been reported that TNF-α antagonists, such as infliximab, for rheumatoid arthritis and Crohn's disease and glucocorticoid monotherapy may also trigger the reactivation of HBV. On the contrary, although HBV reactivation by CDDP was reported previously, it was relatively rare compared to the other immunosuppressive agents [16]. In the 2 cases of the present study, both received CDDP for the treatment of a solid tumor. So far, it is believed that CDDP does not carry direct immunosuppressive activity and it is unclear how much of the induction of reactivation is a result of administrating CDDP. Actually, 15 of 25 cases without reactivation of hepatitis B also received CDDP. However, as both the de novo hepatitis B cases underwent a combination therapy including CDDP, the additive effect might exist for induction of HBV replication. This should be worth paying attention to because CDDP is a key agent for the treatment of common solid cancers. However, it seemed that low viral load at the time of reactivation might be another characteristic in the de novo hepatitis B of a common solid tumor compared to those among hematological malignancies. It could be possible that different immunosuppressive potentials of regimens for malignancies might attribute to the difference of viral load at the time of reactivation.

HBV reactivation is often observed in cases receiving chemotherapy and bone marrow transplant for hematological disorders, but the frequency in cases receiving chemotherapy for solid cancer and the characteristics of HBV reactivation have yet to be elucidated. In conclusion, although only in a few cases, we reported the characteristics of HBV reactivation in cases receiving chemotherapy for solid cancer. Further accumulation of such cases should be clinically important because a growing number of patients have received systemic anticancer therapy for a solid tumor along with the development of new agents and regimens.

Disclosure Statement

The authors have no conflicts of interest to disclose.

References

1 Hui CK, Cheung WW, Zhang HY, Au WY, Yueng YH, Leung AY, Leung N, Luk JM, Lie AK, Kwong YL, Liang R, Lau GK: Kinetics and risk of de novo hepatitis B infection in HBsAg-negative patients undergoing cytotoxic chemotherapy. Gastroenterology 2006; 131:59–68.

2 Calabrese LH, Zein NN, Vassilopoulos D: Hepatitis B virus reactivation with immunosuppressive therapy in rheumatic diseases: assessment and preventive strategies. Ann Rheum Dis 2006;65:983–989.

3 Esteve M, Saro C, González-Huix F, Suarez F, Forné M, Viver JM: Chronic hepatitis B reactivation following infliximab therapy in Crohn's disease patients: need for primary prophylaxis. Gut 2004;53:1363–1365.

4 Wursthorn K, Wedemeyer H, Manns MP: Managing HBV in patients with impaired immunity. Gut 2010;59:1430–1445.

5 Kusumoto S, Tanaka Y, Mizokami M, Ueda R: Reactivation of hepatitis B virus following systemic chemotherapy for malignant lymphoma. Int J Hematol 2009;90:13–23.

6 Lok AS, Liang RH, Chiu EK, Wong KL, Chan TK, Todd D: Reactivation of hepatitis B virus replication in patients receiving cytotoxic therapy. Report of a prospective study. Gastroenterology 1991;100:182–188.

7 Merican I, Guan R, Amarapuka D, Alexander MJ, Chutaputti A, Chien RN, Hasnian SS, Leung N, Lesmana L, Phiet PH, Sjalfoellah Noer HM, Sollano J, Sun HS, Xu DZ: Chronic hepatitis B virus infection in Asian countries. J Gastroenterol Hepatol 2000;15:1356–1361.

8 Mason AL, Xu L, Guo L, Kuhns M, Perrillo RP: Molecular basis for persistent hepatitis B virus infection in the liver after clearance of serum hepatitis B surface antigen. Hepatology 1998;27:1736–1742.

9 Yeo W, Chan TC, Leung NW, Lam WY, Mo FK, Chu MT, Chan HL, Hui EP, Lei KI, Mok TS, Chan PK: Hepatitis B virus reactivation in lymphoma patients with prior resolved hepatitis B undergoing anticancer therapy with or without rituximab. J Clin Oncol 2009;27:605–611.

10 Uemoto S, Sugiyama K, Marusawa H, Inomata Y, Asonuma K, Egawa H, Kiuchi T, Miyake Y, Tanaka K, Chiba T: Transmission of hepatitis B virus from hepatitis B core antibody-positive donors in living related liver transplants. Transplantation 1998;65:494–499.

11 Dervite I, Hober D, Morel P: Acute hepatitis B in a patient with antibodies to hepatitis B surface antigen who was receiving rituximab. N Engl J Med 2001;344:68–69.

12 Yoshida T, Kusumoto S, Inagaki A, Mori F, Ito A, Ri M, Ishida T, Komatsu H, Iida S, Sugauchi F, Tanaka Y, Mizokami M, Ueda R: Reactivation of hepatitis B virus in HBsAg-negative patients with multiple myeloma: two case reports. Int J Hematol 2010;91:844–849.

13 Lau GK: Hepatitis B reactivation after chemotherapy: two decades of clinical research. Hepatol Int 2008;2:152–162.

14 Hoofnagle JH: Reactivation of hepatitis B. Hepatology 2009;49:S156–S165.

15 Hsu C, Hsiung CA, Su IJ, Hwang WS, Wang MC, Lin SF, Lin TH, Hsiao HH, Young JH, Chang MC, Liao YM, Li CC, Wu HB, Tien HF, Chao TY, Liu TW, Cheng AL, Chen PJ: A revisit of prophylactic lamivudine for chemotherapy-associated hepatitis B reactivation in non-Hodgkin's lymphoma: a randomized trial. Hepatology 2008;47:844–853.

16 Yeo W, Johnson PJ: Diagnosis, prevention and management of hepatitis B virus reactivation during anticancer therapy. Hepatology 2006;43:209–220.

17 Lalazar G, Rund D, Shouval D: Screening, prevention and treatment of viral hepatitis B reactivation in patients with haematological malignancies. Br J Haematol 2007;136:699–712.

Gender Differences in the Livers of Patients with Hepatocellular Carcinoma and Chronic Hepatitis C Infection

Naoshi Nishida[a, b]   Tadaaki Arizumi[a]   Sosuke Hayaishi[a]   Masahiro Takita[a]

Satoshi Kitai[a]   Norihisa Yada[a]   Satoru Hagiwara[a]   Tatsuo Inoue[a]

Yasunori Minami[a]   Kazuomi Ueshima[a]   Toshiharu Sakurai[a]   Iwao Ikai[c]

Masatoshi Kudo[a]

[a]Department of Gastroenterology and Hepatology, Faculty of Medicine, Kinki University, Osaka, [b]Department of Gastroenterology and Hepatology, Kyoto University Graduate School of Medicine, Kyoto, and [c]Department of Surgery, National Hospital Organization Kyoto Medical Center, Kyoto, Japan

Abstract

Objectives: A unique causative aspect of hepatocellular carcinoma (HCC) is a gender difference in its incidence. To determine the specific factors that contribute to a male predominance, we analyzed the clinicopathological factors, and genetic and epigenetic alterations of HCCs in male and female patients. **Methods:** We retrospectively analyzed three cohorts of patients: the first cohort consisted of 547 patients identified with the first event of HCC, the second cohort included 176 HCC patients, and the third 127 patients with chronic hepatitis C (CHC). **Results:** Male patients were found to have HCC more frequently than female patients in cases of non-cirrhotic liver (p = 0.0030 by the χ^2 test), especially in hepatitis C-positive cases. However, there were no gender-specific differences in the genetic and epigenetic alterations of cancer-related genes. Deposition of iron was more severe in male CHC patients than in female patients. **Conclusions:** Male patients with CHC develop HCC more frequently when they have a non-cirrhotic liver than do female patients. This gender difference could be, at least partially, attributed to a different degree of iron deposition, which contributes to the development of HCC in the absence of liver cirrhosis in men with CHC.

Copyright © 2012 S. Karger AG, Basel

Introduction

Hepatocellular carcinoma (HCC) is a common malignancy worldwide and the overall prevalence of the at-risk population is expected to grow with time. HCC is causatively associated with several distinct risk factors, such as chronic infection with hepatitis B virus (HBV) or hepatitis C virus (HCV) [1]. Another unique causative aspect of this tumor is a gender-specific difference in its incidence. Men have a higher prevalence of HCC than women, and the ratio of affected men to affected women varies between 2:1 and 4:1 [1, 2]. Although the reasons for the difference in incidence between men and women are not

Naoshi Nishida, MD
Department of Gastroenterology and Hepatology
Kinki University School of Medicine, 377-2 Ohno-Higashi
Osaka-Sayama, Osaka 589-8511 (Japan)
E-Mail naoshi@med.kindai.ac.jp

fully understood, it is possible that they include several environmental factors such as a higher prevalence of viral hepatitis, alcohol intake, and smoking in men compared to women [3]. Recently, Naugler et al. [4] reported that hormonal factors might also play a role in the gender difference of the incidence of HCC development.

The male predominance of HCC is further supported by the clinical observation that chronic hepatitis progresses more rapidly to cirrhosis in men than in women. In fact, cirrhosis that leads to HCC development is considered to be more common in men and postmenopausal women, suggesting that sex hormones might play a role in the gender difference in the incidence of progression of liver fibrosis [5, 6]. In this study, we retrospectively analyzed three cohorts of patients to determine which factors contribute to the gender difference in the incidence of HCC. The first cohort consisted of 547 HCC patients who were diagnosed as the first event of HCC, and we tried to identify the background factors associated with the difference between male and female patients. The second cohort included 176 HCC patients in whom the genetic and epigenetic alterations in HCC tissues had been examined previously, and we analyzed the gender differences of genomic alterations in this group [7–9]. The third cohort consisted of 127 patients with chronic hepatitis C (CHC), and we analyzed the gender differences in liver tissue biopsies with special focus on iron deposition.

In this report, we show that male patients with chronic viral hepatitis, especially in HCV-positive cases, tend to develop HCC more frequently in a background of noncirrhotic liver with mild fibrosis than do female patients. This gender difference could be, at least partially, the result of a different degree of iron deposition, which contributes to the development of HCC in male CHC patients without severe fibrosis.

Materials and Methods

Patients

In the first stage of the study, 547 HCC patients consisting of 418 men and 129 women were examined retrospectively to determine the differences in their clinical backgrounds. These patients were identified with the first event of HCC at the Kyoto University Hospital between 1998 and 2006. The details of the profiles of the male and female patients are listed in table 1. The liver fibrosis stage (F-stage) of the background liver of the HCC patients was determined using the METAVIR scoring system [10]. Informed consent was obtained from patients, and the study was approved by the institutional review boards of the institutions involved.

Analysis of Genomic Alterations in HCC Tissues

Previously we analyzed 176 pairs of HCC and their corresponding non-cancerous liver for mutations in the p53 and β-catenin genes, promoter hypermethylation of tumor suppresser genes (TSGs), the methylation status of long interspersed nucleotide element (LINE-1), and the degree of chromosomal alteration [7–9]. Using the data of this HCC cohort (the second HCC cohort), we compared the profile of genetic alterations in HCCs from male and female patients to understand the difference in the molecular pathogenesis of HCC. Details of this patient cohort were described previously [7, 8].

Among them, mutation of the p53 and β-catenin genes were analyzed in 79 tumors by using direct sequencing of exon 3 of the β-catenin gene and exons 5 through 8 of the p53 gene in our previous study [7]. To determine the degree of hypermethylation of TSGs, we quantified methylation levels on the promoters of 8 TSGs (HIC1, GSTP1, SOCS1, RASSF1, CDKN2A, APC, RUNX3, and PRDM2), which should play an important role in the initial events of human hepatocarcinogenesis using combined bisulfite restriction analysis [9]. We analyzed the methylation status of interspersed nucleotide repeats, LINE-1, as a surrogate marker of global DNA methylation level using MethyLight [11]. A serial dilution of bisulfite-treated CpGenome™ Universal Methylated DNA (Chemicon International, Inc.) was used for a standard curve and as a reference. The methylation-independent consensus Alu sequence was used as an endogenous control [11]. In order to determine the number of chromosomal alterations, we analyzed allelic imbalance using 400 microsatellite markers (ABI PRISM® Linkage Mapping Set MD-10; Applied Biosystems). Fractional allelic loss (FAL) scores were calculated as the number of microsatellite loci with allelic imbalance divided by the number of total informative loci and expressed as a percentage, which broadly represents an index of the degree of chromosomal alteration in HCC [12].

In all, 22 and 13 of the 79 HCCs had a mutation of in p53 and β-catenin genes, respectively. The mean FAL (95% CI) was 22.6% (19.9–25.2). As the Z score was calculated as the difference between the methylation level of each tissue and the mean methylation level divided by the standard deviation, the mean methylation level expressed as a Z score should be zero. The mean methylation level (95% CI) on LINE-1 was 0.37 (0.34–0.40).

Evaluation of Iron Deposition in the Liver Tissues of CHC Patients

For the evaluation of iron deposition, we performed Prussian blue staining using liver biopsy samples from 127 CHC patients without a prior history of HCC. These patients consist of 84 men and 43 women with a median age of 57 years and interquartile range (IQR) of 46–64 years. The numbers of patients with F0, F1, F2, F3, and F4 were 7, 38, 36, 22, and 24, respectively. The degree of iron deposition in hepatocytes was classified as follows. If the proportion of hepatocytes with positive staining was ≥25% of the total hepatocytes population, this was regarded as a severe deposit, a positive staining rate of 24–6% was classified as a moderate deposit, and positive staining of ≤5% was classified as a weak deposit. Among 127 biopsies, 10 had a severe deposit, 41 had a moderate deposit, and 76 had a weak deposit.

Statistical Analyses

In order to compare the categorical variables for the detection of gender differences, we applied the Pearson's χ^2 test, whereas the

Table 1. Gender difference in characteristics of the patients with HCC

	Male (n = 418)	Female (n = 129)	p value*
Clinical factor			
Background factor			
Median age, years (25–75% IQR)	65 (56–71)	66 (60.5–73)	0.0208
Mean age, years (95% CI)	62.9 (61.9–63.9)	65.2 (63.4–67.0)	0.0282
Presence of hepatitis virus, HBV/HCV/B&C/negative	85/216/6/101	31/67/2/27	0.7835
Fibrosis of background liver, F0–F2/F3 or F4	179/151	36/61	0.0030
Tumor factor			
Mean maximal tumor size, cm (95% CI)	6.3 (5.8–6.9)	5.2 (4.2–6.2)	0.0579
Tumor differentiation			
Well/moderately or poorly	74/307	21/85	0.7486
Portal vein thrombosis, presence/absence	86/332	29/100	0.6423
Number of tumors, single/multiple	245/169	86/39	0.0582
	Male (n = 119)	**Female (n = 57)**	**p value***
Molecular factor of tumor			
Mutation of the p53, presence/absence	17/42	5/15	0.7423
Mutation of the β-catenin, presence/absence	11/48	2/18	0.3676
Fractional allele loss, >20%/≤20%	36/40	16/17	0.9146
Mean methylation level of TSGs, Z score (95% CI)	0.01 (–0.06 to 0.07)	0.02 (–0.07 to 0.115)	0.7722
Mean methylation level of LINE-1 (95% CI)	0.36 (0.32–0.40)	0.39 (0.34–0.44)	0.3548

For continuous variables of age, tumor size, methylation level of TSGs and LINE-1, the mean level and 95% CI or median (IQR) are shown. For the remaining factors of category variables, the number of cases with each category was listed. For a representative degree of chromosomal alteration, fractional allele loss was calculated using 400 microsatellite markers. For a representative of methylation level on TSG promoters, methylation levels on the promoters of eight TSGs *(APC, GSTP1, RASSF1, RUNX3, PRDM2, CDKN2A, HIC1* and *SOCS1)* were quantified using COBRA and the methylation levels were normalized using Z score. The methylation level of LINE-1 sequence was quantified using MethyLight.

* p values of the Wilcoxon rank-sum test and Student's t test for continuous variables and that of the χ^2 test for category variables.

Wilcoxon rank-sum test and Student's t test were used for comparisons of continuous variables. We applied the Z score for normalization when determining the methylation level on promoters of eight different TSGs. In order to discriminate between HCCs with different degrees of chromosomal alteration, we classified tumors into two groups: HCC samples with an FAL score >20% and tumors with FAL ≤20%. All p values were two-sided and $p < 0.05$ was considered statistically significant. All statistical analyses were calculated using the JMP version 9.0 software (SAS Institute, Inc., Cary, N.C., USA).

Results

Gender Differences in the Clinicopathological Parameters of HCC Patients

Initially, clinical background and status of tumor progression were compared between the 418 male and 129 female patients of the first cohort (table 1). The median age of the patients was significantly lower in the male group compared to the female group (median age and IQRs were 65 and 56–71 years for men and 66 and 60.5–73 years for women, p = 0.0208 by the Wilcoxon rank-sum test; table 1), suggesting that HCC emerges earlier in men than in women, as reported previously [1]. There was no gender difference with respect to the presence or absence of hepatitis virus, and the majority of patients were HCV-positive. There was, however, a marked difference in the distribution of F-stage values in background liver between male and female patients. The proportion of F0–F2 (mild fibrosis) was significantly higher in men compared to women (179 of 330 patients (60.0%) for men, and 36 of 97 (37.1%) for women; p = 0.0030 by the χ^2 test; table 1). The median tumor diameter was greater in male HCC patients compared to female HCC patients (median and IQRs were 4.5 and 3–7.5 cm for male patients, and 3.8 and 2.5–6.75 cm for female patients, p = 0.0314 by the Wilcoxon rank-sum test; table 1). However, there was no difference in tumor factors, indicating that the tumor stage was similar between the two groups.
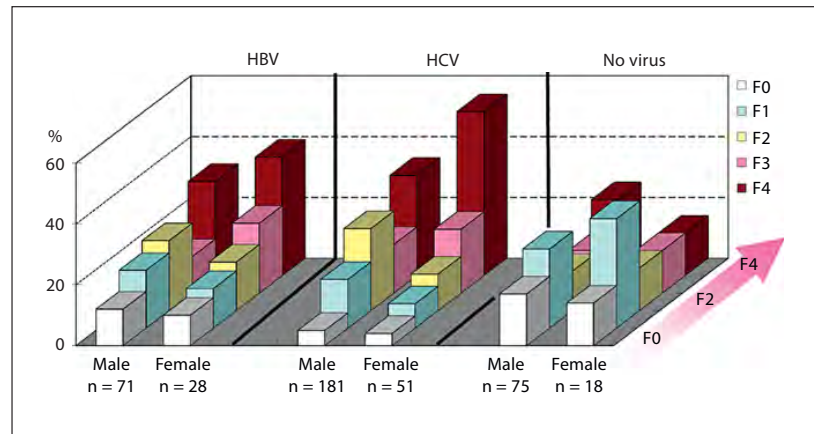
Fig. 1. Gender difference in fibrosis of background liver in newly diagnosed HCC patients. The distribution of fibrosis of background liver was compared between male and female patients with newly diagnosed HCC with HBV-positive, HCV-positive, and virus-negative cases. The vertical line shows the proportion of patients in each fibrosis stage. Among 99 HBV-positive cases where the F-stage was determined, the number of patients showing each fibrosis stage was as follows: 9 male patients were F0, 15 were F1, 18 were F2, 7 were F3, and 22 were F4. For the female patients, 3 were F0, 4 were F1, 5 were F2, 6 were F3, and 10 were F4. Similarly, among 232 HCV-positive cases the number of patients showing each fibrosis stage was as follows: 9 male patients were F0, 31 were F1, 50 were F2, 29 were F3, and 62 were F4. Among the female patients, 2 were F0, 4 were F1, 6 were F2, 12 were F3, and 27 were F4. For the 93 virus-negative cases, the number of patients showing each fibrosis stage was as follows: 13 male patients were F0, 24 were F1, 11 were F2, 8 were F3, and 19 were F4. Among female patients, 3 were F0, 8 were F1, 3 were F2, 2 were F3, and 2 were F4. The p values showing differences between male and female patients determined by the χ^2 test were p = 0.5209, p = 0.0224, and p = 0.7360 for HBV-positive, HCV-positive, and virus-negative cases, respectively. The p values showing gender difference using two categories of F0–F2 and F3 or F4 were: p = 0.1424, p = 0.0007, and p = 0.2256 for HBV-positive, HCV-positive, and virus-negative cases, respectively. Both HBsAg- and HCVAb-positive cases were included in the HBV-positive group as well as the HCV-positive group.

We also analyzed several genomic alterations in HCC tumors from male and female patients among the second cohort of 176 HCC patients. No significant difference was detected in the clinical features, such as tumor diameter, the proportion of cases with well-differentiated HCC, no portal vein thrombosis, and a solitary tumor between the male and female groups, suggesting that there is no difference in tumor stage between male and female HCC cohorts (data not shown). Therefore, we compared genetic and epigenetic alterations in male and female HCC patients in this cohort, because there was no bias arising from differences in tumor stages. The frequencies of mutation in the *p53* and *β-catenin* genes and the proportion of tumors with an FAL greater than 20% were 29% (17/59), 19% (11/59), and 47% (36/76), respectively, in male HCC patients, and 25% (5/20), 10% (2/20), and 48% (16/33), respectively, in female HCC patients. With respect to epigenetic alterations, the degree of hypermethylation in TSG promoters and hypomethylation of LINE-1 (a surrogate marker of global hypomethylation) in HCC tumors were similar in male and female patients. The mean methylation level of TSGs expressed as a Z score and 95% CI were 0.01 and –0.06 to 0.07 for HCC tumors in men, and 0.02 and –0.07 to 0.115 for tumors in women. The mean methylation level of LINE-1 and 95% CI were 0.36 and 0.32–0.40 for HCC tumors in men, and 0.39 and 0.34–0.44 for HCC tumors in women (table 1). Therefore, no gender difference was present with respect to genetic (mutation or chromosomal alteration) and epigenetic (methylation levels of gene promoter and repetitive DNA sequence) alterations, even between groups with similar tumor stages.

A Gender Difference in Background Liver Was Present Only in HCV-Positive Cases

Next, we analyzed the association between F-stage in the background liver of HCC patients and gender among HBV-positive, HCV-positive, and virus-negative cases (fig. 1).

There was no apparent gender difference with respect to F-stage in HBV-positive and virus-negative HCC cases (among the cases with F0–F4; p = 0.5209 and 0.7363 for HBV-positive and virus-negative HCC cases, respective-

ly, by χ^2 test; fig. 1). In contrast, the proportion of patients with 'mild' liver fibrosis of F0–F2 was significantly higher in male than in female HCV-positive HCC patients. Among 232 HCV-positive cases, the distribution of fibrosis scores was F0, 9; F1, 31; F2, 50; F3, 29, and F4, 62 in men and F0, 2; F1, 4; F2, 6; F3, 12, and F4, 27 in women (p = 0.0224 by χ^2 test; fig. 1). The p values showing gender difference using two categories of F0–F2 and F3 or F4 were p = 0.0007 in HCV-positive cases.

Gender Differences in Hepatocyte Iron Deposition among CHC Cases

The present analysis indicates that male CHC patients develop HCC more frequently when mild fibrosis is present in the liver. To clarify the factors that accelerate hepatocarcinogenesis in the absence of severe fibrosis, we examined the degree of iron deposition in the hepatocytes within CHC tumors by using 127 liver biopsies from the third cohort of CHC patients who had no prior history of HCC.

There was no difference in the F-stage between male and female patients in this CHC cohort (53 patients were regarded as F0–F2 and 29 were F3 or F4 among 84 male patients, and 28 were F0–F2 and 15 were F3–F4 among 43 female patients; p = 0.5936 by χ^2 test). However, iron deposition in hepatocytes was more prominent in CHC tumors from male patients than in those from female patients. Among the male patients, 10 of 84 biopsies (11.9%) showed severe deposits, 27 of 84 (32.1%) had moderate deposits, and 47 of 84 (60.0%) had weak deposits, whilst in females patients, 14/43 (32.6%) had moderate deposits and 29/43 (67.4%) had weak deposits, but there were no cases of severe deposits (p = 0.0565 by Pearson's χ^2 test and p = 0.0118 by the likelihood ratio χ^2 test). This trend of gender difference in the extent of iron deposition was present even among cases where mild fibrosis was present. 7 of 53 (13.2%) male CHC patients with F0–F2 showed severe iron deposits, 13 of 53 (34.0%) had moderate iron deposits and 28 of 53 (53.0%) had mild iron deposits. In the female patient group, however, 7 of 28 (25%) and 21 of 28 (75%) CHC cases with F0–F2 showed moderate and mild iron deposits, respectively, whereas there were no cases of severe iron deposits (p = 0.0589 by Pearson's χ^2 test and p = 0.0195 by the likelihood ratio χ^2 test).

Discussion

HCC is causatively associated with several distinct risk factors, and displays different types of genetic and epigenetic alterations [13, 14]. It is now well established that HCC is more prevalent in men worldwide, with the reported male:female ratios ranging from 2:1 to 4:1, although the reasons for this are still unclear [1]. In this retrospective study, we analyzed three cohorts of patients to determine the gender differences in HCC cases. We report that male patients with chronic viral hepatitis, especially in HCV-positive cases, tend to develop HCC more frequently in a non-cirrhotic background of mild liver fibrosis, compared to female patients.

Initially, we compared several clinical parameters between male and female patients with HCC by using the clinical records of a large number of HCC cases. Although we found no difference in tumor factors, male patients with HCC were on average significantly younger than female patients, and the fibrosis of background liver was significantly milder in male patients than in female patients. Previous reports have shown that epigenetic inactivation of TSGs as a result of promoter methylation is more prevalent in HCCs that develop in a cirrhotic liver of HCV-positive patients, and another pathway of hepatocarcinogenesis might exist where global DNA hypomethylation and profound chromosomal alteration took place [8, 9, 14, 15]. Therefore, we expected that molecular pathways underlying hepatocarcinogenesis might differ between male and female patients. However, we did not find a gender difference in the mutation of specific genes in HCC, nor in the degree of methylation of TSGs, the degree of global DNA hypomethylation, and the extent of chromosomal alteration. This suggests that the molecular pathways underlying the progression of HCC might be similar in both male and female patients with hepatocarcinogenesis.

To further study gender differences in HCC formation, we focused on the status of the background liver, because a considerable number of HCCs emerged in the liver with mild fibrosis (stage F0–F2) in male cases. Thus, an additional mechanism for the progression of fibrosis accompanied by inflammation and necrosis might exist and thus contribute to hepatocarcinogenesis in men [4, 6]. We analyzed the gender difference with respect to the progression of F-stage and infection with hepatitis virus. Interestingly, we found that gender differences in F-stage were present exclusively in HCV-related cases. However, although the fibrosis seemed to be milder in male than female patients in HBV-related HCC cases, this was not statistically significant. Recently, Naugler et al. [4] reported a protective effect of estrogen in hepatocarcinogenesis using a mouse model of HCC induced by diethylnitrosamine administration. Cellular damage induced by diethylnitrosamine led to the induction of interleukin-6

production in Kupffer cells via signaling of toll-like receptors, and estrogen was found to blunt this response [4]. As an inflammatory cytokine, interleukin-6 could induce hepatic apoptosis and hepatocyte proliferation, and it could be a potential risk factor for developing HCC, especially in men [4, 16]. It is also reported that an increased risk of HCC among men is associated with higher levels of androgen signaling leading to the induction of vascular endothelial growth factor or signal transducers and activator of transcription 3, especially in HBV-related HCC [16, 17]. Therefore, differences in the hormonal status between men and women may contribute to the higher incidence of HCC in men, even when the liver is non-cirrhotic. However, inflammation-mediated carcinogenesis may well be accompanied by severe fibrosis via the activation of hepatic stellate cells by inflammatory cytokines [4, 16]. Therefore, to clarify how HCC could emerge without severe fibrosis in men with CHC, we further analyzed the iron deposition in CHC patients because it could act as a carcinogen-promoting HCC development even in CHC patients. We studied a cohort of 127 CHC patients where there was no gender difference in F-stage. As expected, iron deposition was more severe in male CHC patients than in female patients, even when liver fibrosis was mild. It has been reported that iron could act as a mutagen because it can induce oxidative stress in several kinds of cells including hepatocytes through a Fenton reaction [18]. Iron deposition was also associated with an increased amount of 8-OHdG in DNA, which in turn leads to genetic and epigenetic alterations of cancer-related genes [18, 19]. We hypothesize that iron deposition contributes to the male predominance of HCC occurrence even among patients with mild fibrosis, especially in HCV-positive cases.

In this report, we have studied the gender difference in the background liver of HCC patients and concluded that HCC could develop from non-cirrhotic liver in the presence of mild fibrosis more often in male patients than in female patients, especially in HCV-positive cases. As we did not take the duration of chronic hepatitis into account [20], the data obtained here might, partially, be attributed to a bias of the retrospective analysis. Another limitation of the study was a lack of information regarding alcohol and tobacco consumption [1]. However, as we selected only the patients with a first-time HCC diagnosis for the analysis, and severe iron deposit could, at least partially, explain the male predominance of HCC in mild fibrosis; thus, it could be possible that HCC develops earlier in the clinical course of male CHC patients rather than female CHC patients, in the background of a mild F-stage. Further evidence is required to confirm the association between gender and HCC development in the context of hepatitis without severe fibrosis.

Acknowledgements

Disclosure Statement

The authors have no conflicts of interest to disclose.

References

1 Kim DY, Han KH: Epidemiology and surveillance of hepatocellular carcinoma. Liver Cancer 2012;1:2–14.

2 Wands J: Hepatocellular carcinoma and sex. N Engl J Med 2007;357:1974–1976.

3 Ohishi W, Fujiwara S, Cologne JB, Suzuki G, Akahoshi M, Nishi N, Takahashi I, Chayama K: Risk factors for hepatocellular carcinoma in a Japanese population: a nested case-control study. Cancer Epidemiol Biomarkers Prev 2008;17:846–854.

4 Naugler WE, Sakurai T, Kim S, Maeda S, Kim K, Elsharkawy AM, Karin M: Gender disparity in liver cancer due to sex differences in MyD88-dependent IL-6 production. Science 2007;317:121–124.

5 Poynard T, Ratziu V, Charlotte F, Goodman Z, McHutchison J, Albrecht J: Rates and risk factors of liver fibrosis progression in patients with chronic hepatitis C. J Hepatol 2001;34:730–739.

6 Rogers AB, Theve EJ, Feng Y, Fry RC, Taghizadeh K, Clapp KM, Boussahmain C, Cormier KS, Fox JG: Hepatocellular carcinoma associated with liver-gender disruption in male mice. Cancer Res 2007;67: 11536–11546.

7 Nishida N, Nishimura T, Nagasaka T, Ikai I, Goel A, Boland CR: Extensive methylation is associated with *β-catenin* mutations in hepatocellular carcinoma: evidence for two distinct pathways of human hepatocarcinogenesis. Cancer Res 2007;67:4586–4594.

8 Nishida N, Nagasaka T, Nishimura T, Ikai I, Boland CR, Goel A: Aberrant methylation of multiple tumor suppressor genes in aging liver, chronic hepatitis, and hepatocellular carcinoma. Hepatology 2008;47:908–918.

9 Nishida N, Kudo M, Nagasaka T, Ikai I, Goel A: Characteristic pattern of DNA methylation alterations predict emergence of human hepatocellular carcinoma. Hepatology 2012; 56:994–1003.

10 The French METAVIR Cooperative Study Group: Intraobserver and interobserver variations in liver biopsy interpretation in patients with chronic hepatitis C. Hepatology 1994;20:15–20.

11 Weisenberger DJ, Campan M, Long TI, Kim M, Woods C, Fiala E, Ehrlich M, Laird PW: Analysis of repetitive element DNA methylation by MethyLight. Nucleic Acids Res 2005; 33:6823–6836.

12 Nishimura T, Nishida N, Itoh T, Kuno M, Minata M, Komeda T, Fukuda Y, Ikai I, Yamaoka Y, Nakao K: Comprehensive allelotyping of well-differentiated human hepatocellular carcinoma with semiquantitative determination of chromosomal gain or loss. Genes Chromosomes Cancer 2002;35:329–339.

13 Nishida N, Goel A: Genetic and epigenetic signatures in human hepatocellular carcinoma: a systematic review. Curr Genomics 2011;12:130–137.

14 Nishida N: Impact of hepatitis virus and aging on DNA methylation in human hepatocarcinogenesis. Histol Histopathol 2010;25: 647–654.

15 Shen L, Ahuja N, Shen Y, Habib NA, Toyota M, Rashid A, Issa JP: DNA methylation and environmental exposures in human hepatocellular carcinoma. J Natl Cancer Inst 2002; 94:755–761.

16 Ruggieri A, Barbati C, Malorni W: Cellular and molecular mechanisms involved in hepatocellular carcinoma gender disparity. Int J Cancer 2010;127:499–504.

17 Kalra M, Mayes J, Assefa S, Kaul AK, Kaul R: Role of sex steroid receptors in pathobiology of hepatocellular carcinoma. World J Gastroenterol 2008;14:5945–5961.

18 Kato J, Kobune M, Nakamura T, Kuroiwa G, Takada K, Takimoto R, Sato Y, Fujikawa K, Takahashi M, Takayama T, et al: Normalization of elevated hepatic 8-hydroxy-2′-deoxyguanosine levels in chronic hepatitis C patients by phlebotomy and low iron diet. Cancer Res 2001;61:8697–8702.

19 Kato J, Miyanishi K, Kobune M, Nakamura T, Takada K, Takimoto R, Kawano Y, Takahashi S, Takahashi M, Sato Y, et al: Long-term phlebotomy with low-iron diet therapy lowers risk of development of hepatocellular carcinoma from chronic hepatitis C. J Gastroenterol 2007;42:830–836.

20 Ricke J, Seidensticker M, Mohnike K: Non-invasive diagnosis of hepatocellular carcinoma in cirrhotic liver: current guidelines and future prospects for radiological imaging. Liver Cancer 2012;1:51–58.

Retreatment with Peginterferon α-2a + Ribavirin in Patients Who Failed Previous Peginterferon α-2b + Ribavirin Combination Therapy

Taisuke Ueda[a]   Kaoru Tsuchiya[b]   Satoru Hashimoto[c]   Taisuke Inoue[d]   Nobuyuki Enomoto[d]
Mie Inao[e]   Atsushi Tanaka[f]   Masahiko Kaito[g]   Fumio Imazeki[h]   Shuhei Nishiguchi[i]
Satoshi Mochida[e]   Osamu Yokosuka[h]   Hiroshi Yatsuhashi[c]   Namiki Izumi[b]   Masatoshi Kudo[a]
for the RETRY Study Group

[a]Department of Gastroenterology and Hepatology, Kinki University School of Medicine, Osaka, [b]Department of Gastroenterology and Hepatology, Musashino Red Cross Hospital, Tokyo, [c]Clinical Research Center, National Hospital Organization, Nagasaki Medical Center, Nagasaki, [d]First Department of Internal Medicine, Faculty of Medicine, University of Yamanashi, Yamanashi, [e]Department of Gastroenterology and Hepatology, Faculty of Medicine, Saitama Medical University, Saitama, [f]Department of Medicine, Teikyo University School of Medicine, Tokyo, [g]Mie Gastroenterological Clinic, Mie, [h]Department of Medicine and Clinical Oncology, Graduate School of Medicine, Chiba University, Chiba, and [i]Division of Hepatobiliary and Pancreatic Disease, Department of Internal Medicine, Hyogo College of Medicine, Hyogo, Japan

Abstract

Background/Aims: Peginterferon (PEG-IFN) + ribavirin (RBV) combination therapy is the current standard of care for chronic hepatitis C. However, more than half of the patients cannot achieve sustained viral response (SVR). In Japan, the clinical benefit of retreatment with PEG-IFN + RBV combination retreatment is still unknown. ***Methods:*** We collected clinical data in 106 chronic hepatitis C patients who failed to achieve SVR with PEG-IFNα-2b + RBV combination therapy and were retreated with PEG-IFNα-2a + RBV. This retrospective study examined the efficacy of retreatment with PEG-IFNα-2a + RBV by evaluating the time to eradication of hepatitis C virus RNA, early virological response (EVR), and SVR. We compared the results of the previous therapy and retreatment in terms of efficacy and analyzed the factors influencing SVR. ***Results:*** The SVR rates in the non-responders and relapsers were 11 and 53%, respectively. EVR and prolonged treatment duration were associated with SVR. We also found that a prior response to PEG-IFN + RBV therapy was more important than the Interleukin-28B genotype for predicting the response to retreatment. ***Conclusions:*** Retreatment with PEG-IFNα-2a + RBV should be considered for relapsers and partial responders. Our results suggest that prolonged administration is also favorable for EVR cases to attain a higher SVR.

Copyright © 2012 S. Karger AG, Basel

Introduction

The development of a combination therapy consisting of peginterferon (PEG-IFN) and ribavirin (RBV) has increased the hepatitis C virus (HCV) RNA response rate to 65–69% at the end of therapy with a sustained HCV RNA response (sustained viral response, SVR) in 54–56% of chronic hepatitis C (CHC) patients. Conversely, this

Masatoshi Kudo
Department of Gastroenterology and Hepatology
Kinki University Faculty of Medicine, 377-2, Ohno-Higashi
Osaka-Sayama, Osaka 589-8511 (Japan)
E-Mail m-kudo@med.kindai.ac.jp

indicates that PEG-IFN + RBV therapy does not induce a response in 31–35% of such patients either because HCV RNA is not eliminated during therapy or the therapy is not completed. Furthermore, HCV RNA reappears in 11–13% of patients after the end of therapy [1, 2].

Retreatment with PEG-IFN + RBV for non-responding or relapse patients has been studied in Western countries [3, 4], but no large-scale studies have been performed in Japan. The AASLD guidelines [5] do not recommend retreatment with PEG-IFN + RBV. However, the Japanese guidelines [6] state that 'after examining cases with no effect in previous treatment, a treatment for SVR or for maintenance should be selected'; thus, retreatment with PEG-IFN + RBV is not completely excluded according to the Japanese guidelines.

A high SVR rate is observed after the addition of telaprevir to PEG-IFN + RBV [7–10]. However, some patients in Japan have not benefited from the launch of telaprevir, because CHC patients in Japan are older than those in Western countries [11, 12] and are often anemic. Thus, we retrospectively analyzed the results of retreatment with PEG-IFN + RBV in Japanese relapse and non-responding patients who previously received therapy with PEG-IFN + RBV. Core amino acid substitutions at position 70 [13] and host genome single-nucleotide polymorphism (SNP) genotyping of rs8099917, an interleukin-28B (IL28B) SNP [14, 15], are related to the efficacy of PEG-IFN + RBV therapy. Therefore, these factors were also examined in the study.

Materials and Methods

A total of 106 patients received combination therapy with PEG-IFNα-2a + RBV at 12 medical facilities in Japan from 2007 to 2009. We retrospectively evaluated the data of CHC patients who failed to achieve SVR (i.e. non-responders) or became HCV RNA negative on PEG-IFNα-2b + RBV therapy but relapsed again after the end of treatment (i.e. relapsers). The non-responders were divided into two groups according to the maximum decrease in HCV RNA titer during the initial treatment. Retreatment with PEG-IFNα-2a + RBV was performed to examine the relationships between SVR and patient background factors, timing of the HCV RNA response, and treatment duration.

For the previous treatment, PEG-IFNα-2b (PegIntron; MSD, Tokyo, Japan) at a dose of 1.5 μg kg^{-1} per week subcutaneously and RBV (Rebetol; MSD) were used. PEG-IFNα-2a (Pegasys; Chugai Pharmaceutical Co., Ltd, Tokyo, Japan) + RBV (Copegus; Chugai Pharmaceutical Co., Ltd) was started between 2007 and 2009. In principle, as a starting dose, PEG-IFN was given once weekly at 180 μg PEG-IFNα-2a while RBV was given at 600–1,000 mg/day based on body weight (body weight <60 kg, 600 mg; 60–80 kg, 800 mg; >80 kg, 1,000 mg), according to the standard treatment protocol in Japan.

Serum HCV RNA after PEG-IFNα-2b + RBV treatment was assessed by quantification using a Cobas Amplicor HCV monitor test (high range method: detection range, 5–5,000 KIU ml^{-1}, or version 2.0: limit of quantitation, 500 IU ml^{-1}; Roche Diagnostics Co. Ltd, Tokyo, Japan).

HCV RNA in retreatment was measured using a Cobas Taq-Man HCV test (Roche Diagnostics Co. Ltd) at 4-week intervals; the linear dynamic range was 1.2–7.8 log IU ml^{-1}. Samples with undetectable HCV RNA levels were reported as <1.2 log IU ml^{-1} (i.e. no detectable HCV RNA). Patients were judged to have attained SVR status if HCV RNA was not detected for 24 weeks after the end of treatment. Rapid viral response (RVR) was defined when HCV RNA was not detected at week 4; early virological response (EVR) was defined when HCV RNA was not detected at week 12 of treatment.

Univariate analysis was performed using a χ^2 test and Fisher's exact test. Multivariate analysis was performed using logistic regression using the stepwise method.

As a rule, dose modification followed the manufacturer's drug information on the intensity of potential adverse hematologic effects. The PEG-IFN doses were reduced to 50% of the original dose if the neutrophil count fell below 750/mm^3 and discontinued if the neutrophil count fell below 500/mm^3 or the platelet count (PLT) fell below 50,000/mm^3. RBV was also reduced from 1,000 to 600, 800 to 600, or 600 to 400 mg when hemoglobin (Hb) was below 10 g dl^{-1} and was discontinued when the Hb was below 8.5 g dl^{-1}. Both PEG-IFN and RBV were discontinued if there was a need to discontinue one of the drugs.

The baseline data of the patients are expressed as median values and ranges. In order to analyze the differences between baseline data and the factors associated with SVR, univariate analysis using the Mann-Whitney U test or a χ^2 test was performed; multivariate analysis was performed using stepwise and multiple logistic-regression models. p values <0.05 were considered significant.

This study was conducted in accordance with the ethical guidelines of the Declaration of Helsinki amended in 2008, and informed consent was obtained from each patient.

Results

Characteristics

The median age of the 106 subjects was 60 years. There were 63 non-responders and 43 relapsers who received previous treatment. Non-responders were divided into two groups according to their virological response to the previous treatment: partial responders, maximum HCV RNA decrease of >2 log; null responders, maximum HCV RNA decrease <2 log. HCV RNA genotypes 1 and 2 were detected in 101 and 5 subjects, respectively. The baseline characteristics of the study patients are shown in table 1.

Efficacy

Retreatment of the 106 subjects with PEG-IFNα-2a + RBV therapy resulted in an SVR rate of 28% (30/106). The

— 339 —

Table 1. Baseline patients' characteristics

	Relapser (n = 43)	Partial responder (n = 39)	Null responder (n = 24)
Age, years	64 (44–75)	58 (33–77)	60 (30–69)
Male/female	18/25	19/20	12/12
Body mass index	22.2 (16.6–31.0)	23.4 (18.2–32.3)	22.2 (17.8–29.8)
Genotype 1/2	42/1	36/3	23/1
Viral load, log IU/ml	6.3 (3.7–7.2)	5.7 (1.2–7.2)	6.4 (3.7–7.5)
ALT, IU/ml	39 (15–189)	41 (12–379)	43 (18–275)
γ-GTP, IU/ml	24 (9–175)	51 (17–326)	39 (19–366)
WBC count, /mm^3	4,500 (1,900–8,300)	4,100 (2,000–9,400)	3,495 (1,700–7,100)
Platelet count, ×10^4/mm^3	13.8 (7.6–24.9)	14.1 (4.5–28.6)	11.2 (4.5–29.3)
Hemoglobin, g/dl	13.8 (11.9–16.5)	13.3 (9.3–16.5)	12.4 (9.6–15.9)
LDL cholesterol, mg/dl	100 (42–167)	86 (32–128)	74 (15–122)
α-Fetoprotein, ng/ml	4 (1–48)	5.9 (1–30)	7.8 (2–108)
Core aa70, wild/non-wild	13/9	8/7	3/3
IL28B rs8099917 (TT/TG, GG)	21/5	12/7	3/7

Values are medians with ranges in parentheses or numbers.
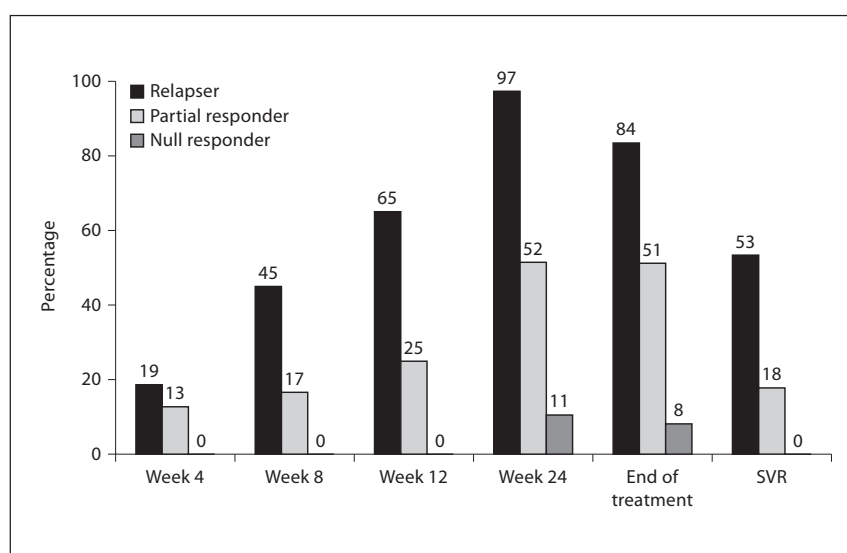
Fig. 1. Virological responses of PEG-IFNα-2a + RBV.

SVR rates in the relapsers, partial responders, and null responders were 53% (23/43), 18% (7/39), and 0% (0/24), respectively. The HCV RNA response rate in the relapsers was 65% at week 12 of the PEG-IFNα-2a + RBV therapy and 84% at the end of treatment (fig. 1). In contrast, the HCV RNA response rates in the non-responders were 15, 37, and 37% at week 12, week 24, and the end of retreatment, respectively. These rates were lower than those of the relapsers.

Examination of Previous Relapsers

The durations before an HCV RNA response was observed in the relapsers were ≤12 weeks in 65% (28/43) and 13–24 weeks in 26% (11/43) of the patients. In the 28 patients who achieved EVR, the SVR rates were 56% (9/16) and 92% (11/12) in the patients for whom retreatment commenced within 48 weeks and who received prolonged therapy, respectively; this difference was significant (p = 0.04).

Table 2. Factors associated to SVR

	Univariate analysis		Multivariate analysis	
	OR (95% CI)	p value	OR (95% CI)	p value
Response of previous treatment, relapsers/non-responders	9.20 (6.3–54)	<0.0001	–	n.s.
γ-GTP, <35/≥35 IU/l	2.92 (1.2–7.3)	0.0189	–	n.s.
Platelet counts, ≥12 × 10⁴/<12 × 10⁴/mm³	2.96 (1.1–7.7)	0.0232	–	n.s.
Hemoglobin, ≥13/<13 g/dl	3.24 (1.2–8.8)	0.0179	–	n.s.
LDL cholesterol, ≥100/<100 mg/dl	4.61 (1.5–14)	0.0046	–	n.s.
α-Fetoprotein, <6/≥6 ng/ml	4.16 (1.5–11)	0.0112	–	n.s.
Treatment duration, prolonged/standard	3.32 (1.4–8.0)	0.0063	5.16 (1.13–23.6)	0.0343
HCV RNA at week 12, negative/positive	18.5 (6.3–54)	<0.0001	10.3 (1.65–64.7)	0.0022
PEG-IFN adherence, ≥80/<80%	4.80 (1.6–14)	0.0025	–	n.s.
Ribavirin adherence, ≥60/<60%	3.69 (1.2–12)	0.0214	–	n.s.

We also compared the RVR and EVR rates between initial treatment and retreatment among the 41 patients whose timing of HCV negativity was available (fig. 2). The rates of RVR and EVR were higher in the retreatment patients (2 and 44% in initial treatment, and 20 and 66% in retreatment, respectively).

Examination of Previous Non-Responders

Among the non-responders, an HCV RNA response after retreatment was achieved only in partial responders. Of these patients, 23% (9/39) achieved EVR, 23% (9/39) within 13–24 weeks, and 8% (3/37) after 25 weeks. In the 9 subjects who achieved EVR among partial responders, the SVR rate was 25% (1/4) during the retreatment within 48 weeks but was 60% (3/5) when the retreatment period was prolonged. No SVR was achieved in retreatment subjects with an HCV RNA response that required ≥25 weeks.

Factors Associated with SVR

Analysis revealed that the SVR rate was significantly high in the following factors: relapsers; prolonged duration of retreatment; Hb level ≥13 g dl⁻¹; PLT ≥12 × 10⁴/mm³; α-fetoprotein (AFP) <6 ng ml⁻¹; low-density lipoprotein cholesterol (LDL-Chol) ≥100 mg dl⁻¹; γ-glutamyl transpeptidase (γ-GTP) ≥35 IU l⁻¹; adherence of PEG-IFN ≥80%; adherence of RBV ≥60%, and EVR. A multivariate analysis of SVR including the effect of initial treatment, duration of retreatment, Hb, PLT, AFP, LDL-Chol, γ-GTP, PEG-IFN adherence, RBV adherence, and EVR as variables showed that EVR and the period of retreatment were major factors contributing to SVR (table 2).
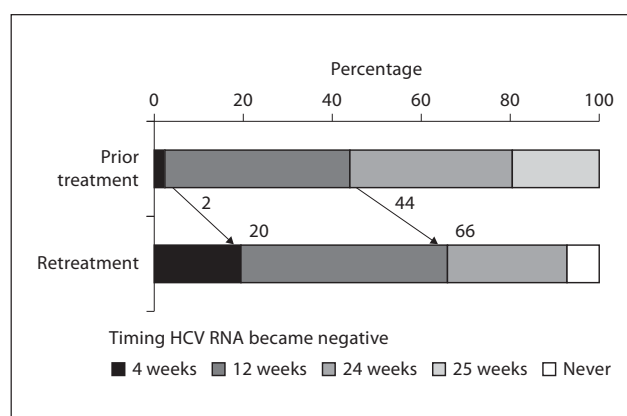
Fig. 2. Comparison of time to eradicate HCV RNA. Prior treatment: PEG-IFNα-2b + RBV combination treatment. Retreatment: PEG-IFNα-2a + RBV combination treatment.

IL28B SNP Genotype

55 patients agreed to undergo a test for IL28B SNP genotyping. Among them, 36, 18, and 1 had the TT, TG, and GG genotypes, respectively. The patients with TT had significantly lower γ-GTP and AFP levels; moreover, relapse patients were more frequently found to have TT. Among the patients with TT, 40% (14/35) showed an HCV RNA response at week 12, 70% (21/29) at week 24, and 56% (20/36) at the end of treatment. Among the non-TT patients, 16% (3/19) showed an HCV RNA response at week 12, 44% (6/16) at week 24, and 42% (7/19) at the end of treatment (fig. 3).
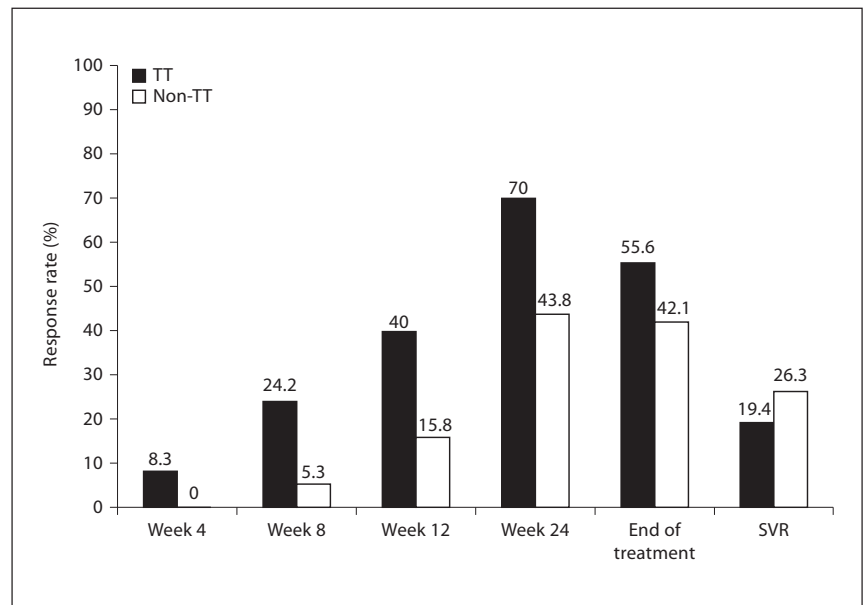
Fig. 3. Virological responses of PEG-IFNα-2a + RBV by IL28B genotype.
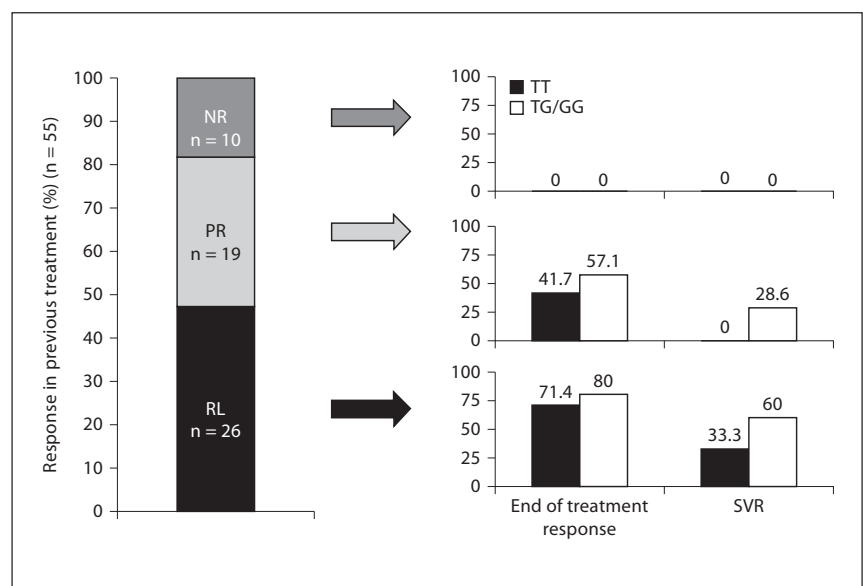
Fig. 4. Virological responses of PEG-IFNα-2a + RBV by IL28B genotype and response of prior treatment. NR = Null responders; PR = partial responders; RL = relapsers.

When we limited the analysis to relapsers, the EVR rates were 57% (12/21) and 40% (2/5) in the TT and non-TT patients, respectively. At week 24, the HCV RNA response rates were 90% (19/21) and 80% (4/5) in the TT and non-TT patients, respectively (fig. 3, 4).

Treatment Discontinuation

33 patients (31.1%) discontinued treatment during the study. 17 patients discontinued treatment due to lack of virological response, 5 due to personal reasons, 3 due to the incidence of hepatocellular carcinoma, and 8 (7.5%) due to adverse events. The reasons for the discontinuation of the 8 patients due to adverse events were anemia

(n = 2), fatigue (n = 2), depressed mental state (n = 1), unidentified fever (n = 1), heart failure (n = 1), and interstitial pneumonia (n = 1).

Discussion

We retrospectively examined the therapeutic efficacy and effective predictors after retreatment with PEG-IFNα-2a + RBV combination therapy in 106 CHC patients. These patients showed non-response or relapse after previous PEG-IFNα-2b + RBV combination therapy. SVR was achieved in 53% of the relapsers and 18% of the partial responders. In the relapsers, SVR was more likely to be achieved when HCV RNA became negative within 12 weeks after the commencement of therapy and the therapeutic effect was enhanced with prolonged administration. Among the non-responders, SVR was not achieved in cases without a ≥2 log decrease in HCV RNA during the previous therapy or in cases with an HCV RNA response after ≥25 weeks during the retreatment period. Similar to that observed in the relapsers, SVR in the non-responders was achieved after prolonged retreatment in patients who showed an HCV RNA response within 12 weeks.

Patients with genotype 1 who receive PEG-IFN + RBV therapy for the first time undergo response-guided therapy (RGT) [16], in which the therapeutic period is determined according to the timing of the HCV RNA response after the commencement of therapy. In RGT, PEG-IFN + RBV therapy is recommended for 48 weeks for patients who exhibit an HCV RNA response within 12 weeks after the commencement of therapy (i.e. complete early viral response, cEVR). However, the results of the present study suggest that prolonged administration is favorable for cEVR cases. Moreover, a different RGT is required in patients who receive retreatment and who have previously received PEG-IFN + RBV therapy.

We also examined the status of the IL28B genotype and found that the IL28B non-TT genotype is associated with factors that are unlikely to be related to the response including AFP levels, γ-GTP levels, and mutations in the core regions. However, when limiting the analysis to relapse patients, the rate of HCV RNA negativity did not differ among IL28B genotypes. This suggests that a prior response to PEG-IFN + RBV therapy is more important for predicting the response to retreatment than the IL28B genotype.

As stated earlier, some patients in Japan have not benefited from the launch of telaprevir, because CHC patients in Japan are older than those in Western countries [11, 12] and are often anemic. We believe that retreatment for elderly patients who cannot receive telaprevir-based therapy, especially relapsers and non-responders with a maximum virus decrease of ≥2 log during the previous therapy, should be considered after PEG-IFN + RBV therapy.

Disclosure Statement

The authors have no conflicts of interest to disclose.

References

1 Fried MW, Shiffman ML, Reddy KR, Smith C, Marinos G, Goncales FL Jr, Haussinger D, Diago M, Carosi G, Dhumeaux D, Craxi A, Lin A, Hoffman J, Yu J: Peginterferon alfa-2a plus ribavirin for chronic hepatitis C virus infection. N Engl J Med 2002;347:975–982.

2 Manns MP, McHutchison JG, Gordon SC, Rustgi VK, Shiffman M, Reindollar R, Goodman ZD, Koury K, Ling M, Albrecht JK: Peginterferon alfa-2b plus ribavirin compared with interferon alfa-2b plus ribavirin for initial treatment of chronic hepatitis C: a randomised trial. Lancet 2001;358:958–965.

3 Jensen DM, Marcellin P, Freilich B, Andreone P, Di Bisceglie A, Brandao-Mello CE, Reddy KR, Craxi A, Martin AO, Teuber G, Messinger D, Thommes JA, Tietz A: Retreatment of patients with chronic hepatitis C who do not respond to peginterferon-α2b: a randomized trial. Ann Intern Med 2009; 150:528–540.

4 Poynard T, Colombo M, Bruix J, Schiff E, Terg R, Flamm S, Moreno-Otero R, Carrilho F, Schmidt W, Berg T, McGarrity T, Heathcote EJ, Goncales F, Diago M, Craxi A, Silva M, Bedossa P, Mukhopadhyay P, Griffel L, Burroughs M, Brass C, Albrecht J: Peginterferon alfa-2b and ribavirin: effective in patients with hepatitis C who failed interferon alfa/ribavirin therapy. Gastroenterology 2009;136:1618–1628 e1612.

5 Ghany MG, Strader DB, Thomas DL, Seeff LB: Diagnosis, management, and treatment of hepatitis C: an update. Hepatology 2009; 49:1335–1374.

6 Kumada H, Okanoue T, Onji M, Moriwaki H, Izumi N, Tanaka E, Chayama K, Sakisaka S, Takehara T, Oketani M, Suzuki F, Toyota J, Nomura H, Yoshioka K, Seike M, Yotsu-yanagi H, Ueno Y: Guidelines for the treatment of chronic hepatitis and cirrhosis due to hepatitis C virus infection for the fiscal year 2008 in Japan. Hepatol Res 2010;40:8–13.

7 McHutchison JG, Manns MP, Muir AJ, Terrault NA, Jacobson IM, Afdhal NH, Heathcote EJ, Zeuzem S, Reesink HW, Garg J, Bsharat M, George S, Kauffman RS, Adda N, Di Bisceglie AM: Telaprevir for previously treated chronic HCV infection. N Engl J Med;362:1292–1303.

8 Zeuzem S, Andreone P, Pol S, Lawitz E, Diago M, Roberts S, Focaccia R, Younossi Z, Foster GR, Horban A, Ferenci P, Nevens F, Mullhaupt B, Pockros P, Terg R, Shouval D, van Hoek B, Weiland O, Van Heeswijk R, De Meyer S, Luo D, Boogaerts G, Polo R, Picchio G, Beumont M: Telaprevir for retreatment of HCV infection. N Engl J Med 2011;364:2417–2428.

9 Hayashi N, Okanoue T, Tsubouchi H, Toyota J, Chayama K, Kumada H: Efficacy and safety of telaprevir, a new protease inhibitor, for difficult-to-treat patients with genotype 1 chronic hepatitis C. J Viral Hepat 2012; 19:e134–e142.

10 Kumada H, Toyota J, Okanoue T, Chayama K, Tsubouchi H, Hayashi N: Telaprevir with peginterferon and ribavirin for treatment-naive patients chronically infected with HCV of genotype 1 in japan. J Hepatol 2012; 56:78–84.

11 Chung H, Ueda T, Kudo M: Changing trends in hepatitis c infection over the past 50 years in Japan. Intervirology 2010;53:39–43.

12 Tanaka Y, Kurbanov F, Mano S, Orito E, Vargas V, Esteban JI, Yuen MF, Lai CL, Kramvis A, Kew MC, Smuts HE, Netesov SV, Alter HJ, Mizokami M: Molecular tracing of the global hepatitis C virus epidemic predicts regional patterns of hepatocellular carcinoma mortality. Gastroenterology 2006;130:703–714.

13 Akuta N, Suzuki F, Sezaki H, Suzuki Y, Hosaka T, Someya T, Kobayashi M, Saitoh S, Watahiki S, Sato J, Matsuda M, Arase Y, Ikeda K, Kumada H: Association of amino acid substitution pattern in core protein of hepatitis C virus genotype 1b high viral load and non-virological response to interferon-ribavirin combination therapy. Intervirology 2005;48:372–380.

14 Ge D, Fellay J, Thompson AJ, Simon JS, Shianna KV, Urban TJ, Heinzen EL, Qiu P, Bertelsen AH, Muir AJ, Sulkowski M, McHutchison JG, Goldstein DB: Genetic variation in IL28B predicts hepatitis C treatment-induced viral clearance. Nature 2009;461:399–401.

15 Tanaka Y, Nishida N, Sugiyama M, Kurosaki M, Matsuura K, Sakamoto N, Nakagawa M, Korenaga M, Hino K, Hige S, Ito Y, Mita E, Tanaka E, Mochida S, Murawaki Y, Honda M, Sakai A, Hiasa Y, Nishiguchi S, Koike A, Sakaida I, Imamura M, Ito K, Yano K, Masaki N, Sugauchi F, Izumi N, Tokunaga K, Mizokami M: Genome-wide association of IL28B with response to pegylated interferon-α and ribavirin therapy for chronic hepatitis C. Nat Genet 2009;41:1105–1109.

16 Lee SS, Ferenci P: Optimizing outcomes in patients with hepatitis C virus genotype 1 or 4. Antivir Ther 2008;13(suppl 1):9–16.

Risk of Hepatocellular Carcinoma Development in Cases of Hepatitis C Treated by Long-Term, Low-Dose PEG-IFNα-2a

Satoru Hagiwara   Toshiharu Sakurai   Masahiro Takita   Kazuomi Ueshima

Yasunori Minami   Tatsuo Inoue   Norihisa Yada   Satoshi Kitai   Tomoyuki Nagai

Sousuke Hayaishi   Tadaaki Arizumi   Naoshi Nishida   Masatoshi Kudo

Department of Gastroenterology and Hepatology, Kinki University School of Medicine, Osaka, Japan

Abstract

Objective: Increasing evidence suggests the efficacy of maintenance therapy with interferon (IFN) for chronic hepatitis C (CHC) in reducing the risk of hepatocellular carcinoma (HCC). The aim of this study was to determine clinical characteristics on the risk of occurrence of HCC in CHC patients receiving maintenance IFN therapy. **Methods:** A total of 55 patients were treated in a single center with PEG-IFNα-2a monotherapy for CHC and evaluated for variables predictive of the occurrence of HCC. **Results:** The cumulative incidences of HCC were 0.092, 0.117 and 0.161 at 3, 5 and 7 years, respectively. Serum ALT level (>40 IU/l) in the 6th month after commencement of IFN therapy and BMI >25 were associated with shorter time-to-HCC emergence using multivariate analysis (relative risk 16.034, p = 0.01 for ALT >40 IU/l; relative risk 6.020, p = 0.026 for BMI >25, respectively). The IL28B SNP was extracted as a significant factor for the occurrence of HCC. **Conclusions:** Maintenance therapy with the use of long-term low-dose PEG-IFNα-2a is effective for preventing HCC occurrence irrespective of the IL28B SNP, at least for a subset of CHC patients. The initial response of serum ALT levels and BMI provides a prognostic value for determining the risk of developing HCC later in life.

Copyright © 2012 S. Karger AG, Basel

Introduction

Chronic infection of hepatitis C virus (HCV) is a leading cause of developing liver cirrhosis (LC) and hepatocellular carcinoma (HCC) in many countries, including Japan, the United Sates and some of Western Europe [1–5]. Preventing the development of HCC and liver failure due to advance of LC is a primal goal for treatment of chronic hepatitis C (CHC), and interferon (IFN) treatment has been applied to achieve it.

On the one hand, a number of studies have shown that IFN treatment reduces the risk of HCC emergence and improves the disease-free survival. In the randomized control study of type C LC, Nishiguchi et al. [6] reported that IFN treatment significantly suppressed the occurrence of HCC after a median follow-up of 4.9 years even in the case with advanced liver fibrosis. In addition, the Inhibition of Hepatocarcinogenesis by Interferon Therapy (IHIT) study, a multicenter collaborative cohort study,

Masatoshi Kudo, MD, PhD
Department of Gastroenterology and Hepatology
Kinki University School of Medicine, 377-2 Ohno-Higashi
Osaka-Sayama, Osaka 589-8511 (Japan)
E-Mail m-kudo@med.kindai.ac.jp

also revealed that IFN treatment significantly reduced the occurrence of HCC in CHC patients compared with those without any history of IFN therapy (odds ratio 0.516, p < 0.001), and sustained virological response (SVR) reduced the annual occurrence of HCC regardless of stage of liver fibrosis (F-stage) [7]. Taken together, it is conceivable to believe that achievement of SVR suppresses the occurrence of HCC dramatically.

On the other hand, a subset of CHC is known to be refractory to IFN therapy and hard to achieve SVR, such as the elderly and those with advanced liver fibrosis and background disease. In such cases, long-term low-dose IFN therapy appears to offer an option for treatment failures with advanced disease. It has been used in an attempt to prevent disease progression and HCC rather than viral eradication. Arase et al. [8] reported that long-term low-dose IFN therapy led to a reduction of serum AFP as well as ALT levels, even in the cases without sufficient viral response. In addition, the incidence of HCC reportedly decreased among the elderly patients of 60 years or older compared to those without treatment. The Hepatitis C Antiviral Long-Term Treatment against Cirrhosis (HALT-C) trial also revealed that administration of 90 μg of PEG-IFNα-2a once weekly significantly suppressed the emergence of HCC after a median follow-up of 6.1 years among non-responder cases on a previous combination therapy of PEG-IFNα-2a and ribavirin (RBV) (HR 0.45, p = 0.01) [9].

Given the results of several published reports, maintenance IFN therapy suppresses the occurrence of HCC to a certain extent, however the carcinogenic risk factor among the cases treated with low-dose IFN is still unknown. In this study, we clearly focus on this gap of knowledge. Long-term, low-dose PEG-IFNα-2a monotherapy was performed in 55 cases with CHC and risk factors for tumor development were assessed retrospectively. Here, we report that the initial response of serum ALT levels and BMI was a significant contributor for developing HCC among the cases who underwent maintenance IFN therapy, however IL28B single nucleotide polymorphism (SNP) did not affect the occurrence of HCC later in life.

Methods

Patients

Seventy patients with CHC were treated with PEG-IFNα-2a monotherapy between February 2005 and December 2010 at Kinki University Hospital. Among them, 55 were selected for this study based on the following criteria: (1) positive for anti-HCV and for HCV RNA using RT-PCR; (2) infected with HCV genotype 1; (3) naive to IFN therapy; (4) chronic hepatitis or cirrhosis confirmed by liver biopsy within 6 months prior to initiation of IFN therapy, and (5) leukocyte count >2,500/mm³, platelets >50,000/mm³ and serum bilirubin level <2.0 mg/ml. The exclusion criteria were: (1) prior history of HCC; (2) positive for hepatitis B surface antigen (HBsAg); (3) coinfection with human immunodeficiency virus, and (4) cases with hemochromatosis, Wilson's disease, alcoholic liver disease, autoimmune liver disease and primary biliary cirrhosis. HCV genotype was determined by polymerase chain reaction (PCR) amplification of the core region of the HCV genome using genotype-specific PCR primers. Serum HCV-RNA level was determined by TaqMan PCR assay (Cobas Amplicor HCV Monitor; Roche Molecular Systems, Pleasanton, Calif., USA). SNP near the IL28B gene was determined for all cases enrolled in this study. Samples for the genome-wide association survey were genotyped using the Illumina HumanHap610-Quad Genotyping BeadChip. Genotyping data were subjected to quality control before the data analysis. Genotyping for replication and fine mapping was performed using the Invader assay, TaqMan assay, or direct sequencing, as described previously [10, 11]. In this study, genetic variation near the IL28B gene (rs8099917), reported as a pretreatment predictor of treatment efficacy in Japanese patients, was investigated [12, 13].

Written informed consent was obtained from each patient for this study. The study protocol was approved by the Ethics Committee at Kinki University Hospital and performed in compliance with the Helsinki Declaration.

Treatment and Follow-Up Protocol

All cases received subcutaneous injections of PEG-IFNα-2a weekly with an initial dose of 90 μg/week. The duration of IFN therapy ranged from 48 to 267 weeks (median 70).

Follow-up of the patients began on the first day of IFN treatment with monthly evaluation of general condition, biochemical and hematological tests until death or the last hospital visit. For screening of emergence of HCC, ultrasonography, dynamic contrast-enhanced computed tomography (CT), dynamic contrast-enhanced magnetic resonance imaging (MRI), and/or measurement of tumor markers (AFP and DCP) were performed for all patients every 3–6 months. Serum AFP concentration was measured by chemiluminescent enzyme immunoassay (Lumipalse AFP-N; Fujirebio, Tokyo, Japan). Plasma DCP concentrations were measured by an electrochemiluminescent immunoassay (Picolumi PIVKA2; Eisai, Tokyo, Japan). The follow-up periods of all cases ranged from 1.8 to 7.4 years (median 4.6).

Liver Biopsy and Histopathological Examination

Liver biopsy specimens were obtained percutaneously, fixed in 10% formalin, digested with diastase and stained with hematoxylin. Histopathological diagnosis was made independently by an experienced liver pathologist who had no clinical information. All specimens for examination contained six or more portal areas. Baseline liver histology was diagnosed according to the scoring system of Desmet et al. [14].

Statistical Analysis

Among the 55 patients without HCC at the initiation of IFN, the prognostic factors involved in the development of HCC were compared by univariate analysis using the log-rank test between
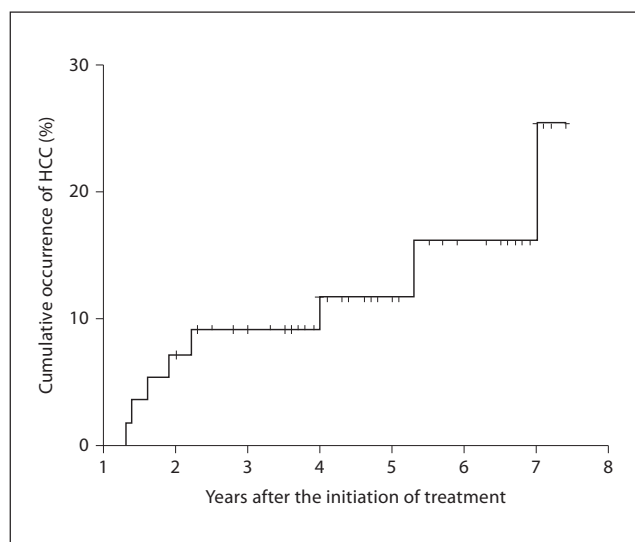
Fig. 1. Incidence of HCC. HCC was diagnosed in 8 (14.5%) patients during follow-up. The cumulative incidences of HCC were 0.092, 0.117 and 0.161 at 3, 5 and 7 years, respectively.

patients who developed HCC and those without emerging HCC during follow-up periods. Subsequently, multivariate analysis using a Cox regression model was performed and variables with significant differences determined. In addition, for the factors with significant differences determined by multivariate analysis, the hazard ratio (RR) for emergence of HCC was calculated. $p < 0.05$ was regarded as significant. All the analyses described above were performed using SPSS version 11.5 (SPSS, Inc., Chicago, Ill., USA).

Results

Baseline Characteristics of the Patients and Emergence of HCC

Table 1 shows the characteristics of the 55 patients who were enrolled and underwent PEG-IFNα-2a monotherapy. Median age was 65 years (range 44–78) and median BMI was 22.4 (range 16.2–29.8). 29 liver biopsies (53% of the total cases) revealed LC whereas, 26 were diagnosed as chronic hepatitis of F1–F3. The baseline level (before IFN therapy) of median serum AFP was 8 ng/ml (range 1–209). 40 cases carried the major allele (TT) of IL28B and 15 showed minor (TG or GG).

During the follow-up periods (median 4.6 years), HCC was diagnosed in 8 (14.5%) patients. The cumulative incidences of HCC were 0.092, 0.117 and 0.161 at 3, 5 and 7 years, respectively (fig. 1).

Table 1. Demographics of the enrolled patients (n = 55)

Age, years	65.0 (44–78)
Male/female	15/40
BMI	22.4 (16.2–29.8)
ALT, IU/l	42 (10–159)
Albumin, g/dl	4.1 (2.6–4.9)
PLT, $\times 10^{-4}$/mm^3	11.4 (4.1–28.8)
AFP, ng/ml	8 (1–209)
Liver fibrosis, F1–F3/F4	26/29
rs8099917, TT/TG or GG	40/15

Data are expressed as median value (range).

Table 2. Comparison between patients with and without developing HCC

Variables	HCC(–) (n = 47) n (%)	HCC(+) (n = 8) n (%)	p value
Age >65 years	23 (48.9)	4 (50.0)	0.73
Male	13 (27.7)	2 (25.0)	0.89
BMI >25	7 (14.9)	3 (37.5)	0.02*
ALT >40 IU/l[a]	24 (51.1)	5 (62.5)	0.05
Albumin >4 g/dl	25 (53.2)	3 (37.5)	0.30
PLT >10 $\times 10^{-4}$/mm^3	29 (61.7)	5 (62.5)	0.67
AFP >10 ng/ml[a]	16 (34.0)	7 (87.5)	0.04*
Liver cirrhosis	24 (51.1)	5 (62.5)	0.61
rs8099917, TT	34 (72.3)	6 (75.0)	0.91
AFP after IFN >10 ng/ml[b]	11 (23.4)	6 (75.0)	0.01*
ALT after IFN >40 IU/l[b]	11 (23.4)	7 (87.5)	0.0007*
HCV RNA after IFN undetectable[b]	21 (44.7)	2 (25.0)	0.32

* Statistically significant.
[a] Measurement at initiation of treatment. [b] Serum concentration 6 months after initiation of treatment.

Predictive Factors for the Occurrence of HCC

Predictive factors for the occurrence of HCC were analyzed in all 55 patients using the log-rank test (table 2). Univariate analysis showed that BMI >25 (p = 0.02) and baseline AFP level >10 ng/ml (p = 0.04) were associated with emergence of HCC during follow-up periods. In addition, regarding the AFP and ALT levels during the IFN therapy, higher serum AFP (>10 ng/ml) and serum ALT measured at 6 months after commencement of IFN therapy (>40 IU/l) showed a significant correlation with HCC occurrence (p = 0.01 for serum AFP of post-IFN and p = 0.0007 for serum ALT of post-IFN, respectively). However, interestingly, neither the IL28B SNP nor an unde-

— 347 —

a

b

c
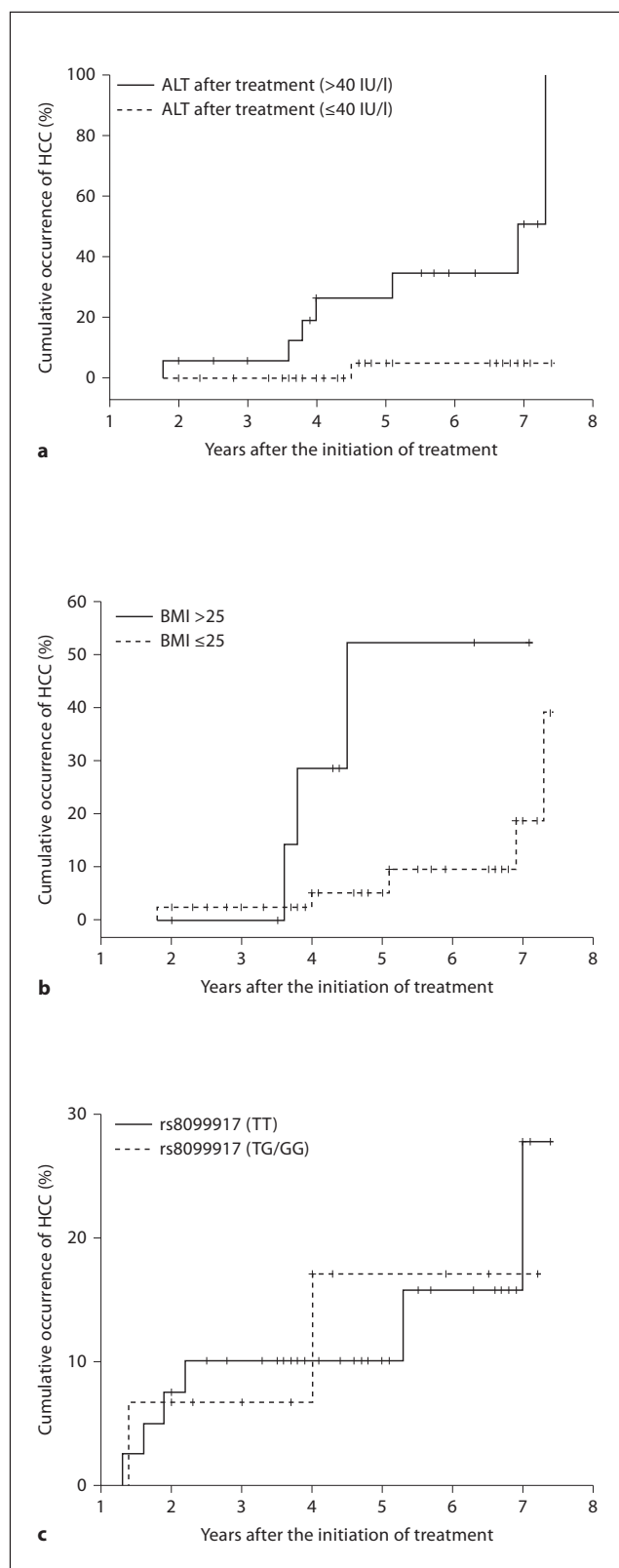
tectable level of HCV RNA at 6 months after commencement of IFN therapy was extracted as a significant factor.

To determine the independent variables and narrow down the risks for emergence of HCC after maintenance IFN therapy, we subsequently performed multivariate analysis using a Cox regression model, including the four variables detected as a significant by univariate analysis (table 3). Among them, ALT >40 IU/l at 6 months after commencement of IFN therapy (relative risk 16.034, p = 0.01) and BMI >25 (relative risk 6.020, p = 0.026) were significantly and independently associated with a higher risk of HCC emergence.

Cumulative Incidences of HCC in Patients Classified with Serological, Virological and Genetic Factors

Figure 2 shows Kaplan-Meier survival curves of patients classified based on the subgroups listed in table 3. The cumulative incidences of HCC in patients with ALT >40 IU/l at 6 months after commencement of IFN were much higher than those with ALT ≤40 IU/l throughout the follow-up periods (cumulative incidences of HCC in patients with ALT >40 IU/l were 0.056, 0.264 and 0.501 at 3, 5 and 7 years, and those in patients with ALT ≤40 IU/l were 0, 0.05 and 0.05 at 3, 5, and 7 years, respectively, p = 0.0007 by log-rank test; fig. 2a). Similarly, the cumulative incidences of HCC in patients with BMI >25 were 0, 0.524 and 0.524 at 3, 5 and 7 years, whereas those

Fig. 2. Incidence of HCC in relation to predictive factors. **a** The cumulative incidences of HCC in patients with ALT concentrations >40 IU/l at 6 months after commencement of IFN therapy were 0.056, 0.264 and 0.501 at 3, 5 and 7 years, respectively. On the other hand, the cumulative incidences of HCC in patients with ALT concentrations ≤40 IU/l at 6 months after commencement of IFN therapy were 0, 0.05 and 0.05 at 3, 5 and 7 years, respectively. The log-rank test gave a value of p = 0.0007, indicating that the incidence of HCC was significantly higher in the group with ALT concentrations >40 IU/l at 6 months after commencement of IFN therapy. **b** The cumulative incidences of HCC in patients with a BMI >25 were 0, 0.524 and 0.524 at 3, 5 and 7 years, respectively. On the other hand, the cumulative incidences of HCC in patients with a BMI ≤25 were 0.022, 0.052 and 0.187 at 3, 5 and 7 years, respectively. The log-rank test gave a value of p = 0.02, indicating that the incidence of HCC was significantly higher in the group with a BMI >25. **c** The cumulative incidences of HCC in IL28B SNP (TT) were 0.101, 0.101 and 0.157 at 3, 5 and 7 years, respectively. On the other hand, the cumulative incidences of HCC in patients with the IL28B SNP (TG or GG) were 0.067, 0.17 and 0.17 at 3, 5 and 7 years, respectively. The log-rank test gave a value of p = 0.91, indicating that the incidence of HCC did not differ significantly between TT and TG or G.

with BMI ≤25 were 0.022, 0.052 and 0.187 at 3, 5 and 7 years, respectively (p = 0.02 by log-rank test; fig. 2b).

On the contrary, the genetic variant of the IL28b gene, which was known as a predictive factor for effectiveness of IFN therapy, did not affect the incidence of HCC during follow-up periods of maintenance IFN therapy (the cumulative incidences of HCC in patients with the IL28B SNP (TT) were 0.101, 0.101 and 0.157 at 3, 5 and 7 years, and those with the IL28B SNP (TG or GG) were 0.067, 0.17 and 0.17 at 3, 5 and 7 years, respectively (p = 0.91; fig. 2c). Similarly, the HCV-RNA level at 6 months after commencement of IFN therapy did not show any effects on emergence of HCC.

Post-Treatment ALT Reduction Rates, Virological Response Rates and Rates of Occurrence of HCC in Relation to the IL28B SNP (table 4)

The median ALT reduction rate (= baseline ALT – ALT after IFN/baseline ALT) after treatment in cases with IL28B (TT) was 0.395 (range –1.00 to 0.925). On the other hand, in cases with IL28B (TG or GG), the median ALT reduction rate was 0.208 (range –0.405 to 0.813) and there was no significant difference from the TT cases (p = 0.15).

The virological response rate was 0.50 in cases with IL28B (TT) and 0.20 in cases with IL28B (TG or GG). Although there was no significant difference (p = 0.07), the rate tended to be lower in cases with IL28B (TG, GG).

The rate of HCC occurrence was 0.15 in cases with IL28B (TT) and comparable with 0.133 in cases with IL28B (TG or GG) (p = 1).

Discussion

Thanks to the recent advancement of treatment options including IFN, CHC is becoming a curative disease, at least in the majority of cases. However, there are still refractory cases in terms of elimination of HCV, such as the cases with advanced liver fibrosis, elderly cases, and with minor allele of the IL28B gene. These cases should be at higher risk of HCC because of a contentious inflammation due to ongoing HCV infection. From this point of view, reduction of HCC emergence is a top priority for these refractory patients. In this study, we intensively analyze the effect of long-term IFN monotherapy on refractory CHC cases in the context of emergence of HCC. Here, we clearly showed that IFN monotherapy suppressed the emergence of HCC, especially in cases with normal BMI and showing a decrease of ALT at the initial phase of IFN therapy regardless of the genetic background of IL28B.

Several findings of this study have direct implications for long-term PEG-IFNα-2a treatment of patients with chronic hepatitis or cirrhosis. In the present cohort, the cumulative rate of development of HCC in patients whose

Table 3. Summary of stepwise multiple Cox regression analysis of the occurrence of HCC

Variable	Relative risk	95% CI	p value
ALT after treatment >40 IU/l	16.034	1.952–131.673	0.010*
BMI >25	6.020	1.235–29.335	0.026*

* Statistically significant.

Table 4. Relationship of IL28B SNP with reduction in ALT after IFN therapy, virological response, and occurrence of HCC

	IL28B (TT) (n = 40)	IL28B (TG or GG) (n = 15)	p value
Median baseline ALT (range)	39.5 (10–159)	45 (17–115)	0.93
Median ALT after IFN (range)	22 (6–181)	28 (11–159)	0.25
Median ALT reduction rate, % (range)	39.5 (–100 to 92.5)	20.8 (–40.5 to 81.3)	0.15
Virological response rate, n (%)	20 (50)	3 (20)	0.07
Rate of occurrence of HCC, n (%)	6 (15)	2 (13.3)	1

ALT reduction rate (%) = baseline ALT – ALT after IFN/baseline ALT.

serum concentrations of ALT were within normal limits (≤40 IU/l) after initiation of PEG-IFNα-2a therapy was lower than that of patients with high concentrations of ALT of >40 IU/l (fig. 2a). This suggests that ALT could be a valuable indicator for predicting effectiveness of long-term PEG-IFNα-2a therapy in terms of HCC emergence. In other words, maintenance of low-dose IFN cannot be recommended if a sufficient decrease of ALT is not achieved within 6 months after the initiation of IFN. This is of importance for both clinical and financial viewpoints because the ineffective use of IFN should be avoided properly.

Previous reports have shown that a biological response suppresses the occurrence of HCC. Imai et al. [15] compared the rates of HCC occurrence in 419 cases with IFN treatment and 144 control cases and reported that the incidence of HCC decreased even among cases showing a biological response (p = 0.04) after an average follow-up period of 4 years. Okanoue et al. [16] also compared 1,370 cases treated with IFN and 54 untreated cases and reported that the rate of emergence of HCC was lower in biological response cases than in NR cases. On the other hand, long-term, low-dose therapy reportedly led to a decrease in ALT levels as well [8]. Therefore, it could be speculated that continuous inflammation, necrosis and regeneration of hepatocytes induced genetic injury in hepatocytes and clonal expansion of cells carrying a mutation in cancer-related genes. From this point of view, long-term low-dose IFN might control liver inflammation and suppress the occurrence of HCC.

In this study, BMI >25 was also extracted as a responsible factor for the occurrence of HCC. In all HCC cases with BMI >25, serum HCV-RNA decreased to an undetectable level. Under the condition of undetectable serum HCV-RNA, obesity rather than chronic HCV infection seemed to accelerate the development of HCC. Recently, a relationship between obesity and the development of HCC has been reported in a number of studies. According to the large-scale prospective study, the relative risk of development of HCC in obese cases (BMI >35) was 4.52 in males and 1.6 in females [17]. Muto et al. [18] investigated the risk of HCC occurrence in 622 cases with decompensated LC and concluded that obesity was associated with the development of HCC. It is well known that obesity is accompanied by insulin resistance. When adipose tissue is enlarged due to obesity, adiponectin secretion is reduced and secretion of adipokain, such as TNF-α and IL-6, increased, inducing insulin resistance [19–21]. Because insulin is known as a growth factor for hepatocytes, hyperinsulinemia due to insulin resistance

could be an important process for hepatocarcinogenesis [22, 23]. The results of this study suggested that, even in cases that achieved viral eradiation through IFN therapy, the risk of HCC was high in obese patients.

On the other hand, the IL28B SNP is a potent predictive factor for treatment response in combination therapy of PEG-IFN and RBV [12, 24, 25]. As the clinical response for elimination of HCV depends on the IL28B SNP, we speculated that this genetic variant might also influence serum ALT levels after treatment. Therefore, the relationships between the status of IL28B SNP and several serological markers, such as ALT, were also investigated in this study (table 4). However, the rate of reduction in ALT concentrations was 0.395 in TT cases and 0.208 in TG or GG cases, which yielded no significant difference (p = 0.15). The low-dose IFN therapy also showed no significant effect on the virological response rate, which was defined as an undetectable level of HCV RNA at 6 months after commencement of IFN therapy (0.50 in TT cases and 0.15 in TG and GG cases, respectively, p = 0.07). Similarly, the incidence of HCC during follow-up period did not show any difference (0.15 in TT cases and 0.133 in TG or GG cases, respectively). According to the data presented here, it might be attractive to speculate that a decrease of ALT is important to suppress HCC carcinogenesis regardless of SNP of IL28B, as both patients carrying TT allele and TG/GG allele show a similar degree of reduction of ALT and also a similar incidence of HCC.

In this study, we clearly demonstrated that the ALT level ≤40 IU/l and BMI <25 at 6 months after commencement of IFN therapy were extracted as favorite factors for HCC emergence in cases receiving long-term low-dose PEG-IFNα-2a therapy, regardless of SNP in IL28B. Therefore, cases with a decrease of ALT at the initial phase of IFN and normal BMI should be good candidates for an aggressive treatment of receiving low-dose PEG-IFNα-2a. On the other hand, if a decrease of ALT could not be achieved, especially in obese patients, other treatments, such as administration of SNMC and/or UDCA, should be considered. These are the unique and important points of this study because we can predict the emergence of HCC simply using ALT and BMI. Additional prospective studies with larger numbers of patients are required to validate the significance of these findings.

Disclosure Statement

The authors have no conflicts of interest to disclose.

References

1 Bruix J, Barrera JM, Calvet X, Ercilla G, Costa J, Sanchez-Tapias JM, Ventura M, Vall M, Bruguera M, Bru C, et al: Prevalence of antibodies to hepatitis C virus in Spanish patients with hepatocellular carcinoma and hepatic cirrhosis. Lancet 1989;2:1004–1006.

2 Colombo M, Kuo G, Choo QL, Donato MF, Del Ninno E, Tommasini MA, Dioguardi N, Houghton M: Prevalence of antibodies to hepatitis C virus in Italian patients with hepatocellular carcinoma. Lancet 1989;2:1006–1008.

3 Hasan F, Jeffers LJ, De Medina M, Reddy KR, Parker T, Schiff ER, Houghton M, Choo QL, Kuo G: Hepatitis C-associated hepatocellular carcinoma. Hepatology 1990;12:589–591.

4 Ikeda K, Saitoh S, Koida I, Arase Y, Tsubota A, Chayama K, Kumada H, Kawanishi M: A multivariate analysis of risk factors for hepatocellular carcinogenesis: a prospective observation of 795 patients with viral and alcoholic cirrhosis. Hepatology 1993;18:47–53.

5 Kim DY, Han KH: Epidemiology and surveillance of hepatocellular carcinoma. Liver Cancer 2012;1:2–14.

6 Nishiguchi S, Kuroki T, Nakatani S, Morimoto H, Takeda T, Nakajima S, Shiomi S, Seki S, Kobayashi K, Otani S: Randomised trial of effects of interferon-α on incidence of hepatocellular carcinoma in chronic active hepatitis C with cirrhosis. Lancet 1995;346:1051–1055.

7 Yoshida H, Shiratori Y, Moriyama M, Arakawa Y, Ide T, Sata M, Inoue O, Yano M, Tanaka M, Fujiyama S, Nishiguchi S, Kuroki T, Imazeki F, Yokosuka O, Kinoyama S, Yamada G, Omata M: Interferon therapy reduces the risk for hepatocellular carcinoma: national surveillance program of cirrhotic and noncirrhotic patients with chronic hepatitis C in Japan. IHIT Study Group. Inhibition of Hepatocarcinogenesis by Interferon Therapy. Ann Intern Med 1999;131:174–181.

8 Arase Y, Ikeda K, Suzuki F, Suzuki Y, Kobayashi M, Akuta N, Hosaka T, Sezaki H, Yatsuji H, Kawamura Y, Kobayashi M, Kumada H: Prolonged-interferon therapy reduces hepatocarcinogenesis in aged-patients with chronic hepatitis C. J Med Virol 2007; 79:1095–1102.

9 Lok AS, Everhart JE, Wright EC, Di Bisceglie AM, Kim HY, Sterling RK, Everson GT, Lindsay KL, Lee WM, Bonkovsky HL, Dienstag JL, Ghany MG, Morishima C, Morgan TR, HALT-C Trial Group: Maintenance peginterferon therapy and other factors associated with hepatocellular carcinoma in patients with advanced hepatitis C. Gastroenterology 2011;140:840–849.

10 Ohnishi Y, Tanaka T, Ozaki K, Yamada R, Suzuki H, Nakamura Y: A high-throughput SNP typing system for genome-wide association studies. J Hum Genet 2001;46:471–477.

11 Suzuki A, Yamada R, Chang X, Tokuhiro S, Sawada T, Suzuki M, Nagasaki M, Nakayama-Hamada M, Kawaida R, Ono M, Ohtsuki M, Furukawa H, Yoshino S, Yukioka M, Tohma S, Matsubara T, Wakitani S, Teshima R, Nishioka Y, Sekine A, Iida A, Takahashi A, Tsunoda T, Nakamura Y, Yamamoto K: Functional haplotypes of PADI4, encoding citrullinating enzyme peptidylarginine deiminase 4, are associated with rheumatoid arthritis. Nat Genet 2003;34:395–402.

12 Tanaka Y, Nishida N, Sugiyama M, Kurosaki M, Matsuura K, Sakamoto N, Nakagawa M, Korenaga M, Hino K, Hige S, Ito Y, Mita E, Tanaka E, Mochida S, Murawaki Y, Honda M, Sakai A, Hiasa Y, Nishiguchi S, Koike A, Sakaida I, Imamura M, Ito K, Yano K, Masaki N, Sugauchi F, Izumi N, Tokunaga K, Mizokami M: Genome-wide association of IL28B with response to pegylated interferon-α and ribavirin therapy for chronic hepatitis C. Nat Genet 2009;41:1105–1109.

13 Akuta N, Suzuki F, Hirakawa M, Kawamura Y, Yatsuji H, Sezaki H, Suzuki Y, Hosaka T, Kobayashi M, Kobayashi M, Saitoh S, Arase Y, Ikeda K, Chayama K, Nakamura Y, Kumada H: Amino acid substitution in hepatitis C virus core region and genetic variation near the interleukin-28B gene predict viral response to telaprevir with peginterferon and ribavirin. Hepatology 2010;52:421–429.

14 Desmet VJ, Gerber M, Hoofnagle JH, Manns M, Scheuer PJ: Classification of chronic hepatitis: diagnosis, grading and staging. Hepatology 1994;19:1513–1520.

15 Imai Y, Kawata S, Tamura S, Yabuuchi I, Noda S, Inada M, Maeda Y, Shirai Y, Fukuzaki T, Kaji I, Ishikawa H, Matsuda Y, Nishikawa M, Seki K, Matsuzawa Y: Relation of interferon therapy and hepatocellular carcinoma in patients with chronic hepatitis C. Osaka Hepatocellular Carcinoma Prevention Study Group. Ann Intern Med 1998;129: 94–99.

16 Okanoue T, Itoh Y, Kirishima T, Daimon Y, Toyama T, Morita A, Nakajima T, Minami M. Transient biochemical response in interferon therapy decreases the development of hepatocellular carcinoma for five years and improves the long-term survival of chronic hepatitis C patients. Hepatol Res 2002;23: 62–77.

17 Calle EE, Rodriguez C, Walker-Thurmond K, Thun MJ: Overweight, obesity, and mortality from cancer in a prospectively studied cohort of US adults. N Engl J Med 2003;348: 1625–1638.

18 Muto Y, Sato S, Watanabe A, Moriwaki H, Suzuki K, Kato A, Kato M, Nakamura T, Higuchi K, Nishiguchi S, Kumada H, Ohashi Y, for the Long-Term Survival Study (LOTUS) Group: Overweight and obesity increase the risk for liver cancer in patients with liver cirrhosis and long-term oral supplementation with branched-chain amino acid granules inhibits liver carcinogenesis in heavier patients with liver cirrhosis. Hepatol Res 2006; 35:204–214.

19 Hotamisligil GS, Peraldi P, Budavari A, Ellis R, White MF, Spiegelman BM: IRS-1-mediated inhibition of insulin receptor tyrosine kinase activity in TNF-α- and obesity-induced insulin resistance. Science 1996;271: 665–668.

20 Hotta K, Funahashi T, Arita Y, Takahashi M, Matsuda M, Okamoto Y, Iwahashi H, Kuriyama H, Ouchi N, Maeda K, Nishida M, Kihara S, Sakai N, Nakajima T, Hasegawa K, Muraguchi M, Ohmoto Y, Nakamura T, Yamashita S, Hanafusa T, Matsuzawa Y: Plasma concentrations of a novel, adipose-specific protein, adiponectin, in type 2 diabetic patients. Arterioscler Thromb Vasc Biol 2000;20:1595–1599.

21 Camera A, Hopps E, Caimi G: Metabolic syndrome: from insulin resistance to adipose tissue dysfunction. Minerva Med 2008; 99:307–321.

22 Calle EE, Kaaks R: Overweight, obesity and cancer: epidemiological evidence and proposed mechanisms. Nat Rev Cancer 2004;4: 579–591.

23 Kawaguchi T, Izumi N, Charlton MR, Sata M: Branched-chain amino acids as pharmacological nutrients in chronic liver disease. Hepatology 2011;54:1063–1070.

24 Suppiah V, Moldovan M, Ahlenstiel G, Berg T, Weltman M, Abate ML, Bassendine M, Spengler U, Dore GJ, Powell E, Riordan S, Sheridan D, Smedile A, Fragomeli V, Müller T, Bahlo M, Stewart GJ, Booth DR, George J: IL28B is associated with response to chronic hepatitis C interferon-α and ribavirin therapy. Nat Genet 2009;41:1100–1104.

25 Ge D, Fellay J, Thompson AJ, Simon JS, Shianna KV, Urban TJ, Heinzen EL, Qiu P, Bertelsen AH, Muir AJ, Sulkowski M, McHutchison JG, Goldstein DB: Genetic variation in IL28B predicts hepatitis C treatment-induced viral clearance. Nature 2009;461:399–401.

Histopathological Diagnosis of Early HCC through Biopsy: Efficacy of Victoria Blue and Cytokeratin 7 Staining

Sawako Kobayashi[a]　Soo Ryang Kim[b]　Susumu Imoto[b]　Kenji Ando[b]

Makoto Hirakawa[b]　Jun Saito[b]　Katsumi Fukuda[b]　Yumi Otono[b]

Madoka Sakaki[b]　Shinobu Tsuchida[c]　Soo Ki Kim[e]　Yoshitake Hayashi[d]

Masayuki Nakano[f]　Masatoshi Kudo[g]

[a]Department of Hepatology, Osaka City University Graduate School of Medicine, Osaka, [b]Department of Gastroenterology, Kobe Asahi Hospital, [c]Division of Hepato-Biliary-Pancreatic Surgery, Department of Surgery, and [d]Division for Infectious Disease Pathology, Center for Infectious Diseases, Kobe University Graduate School of Medicine, Kobe, [e]Department of Gastroenterology, Kyoto University, Kyoto, [f]Division of Pathology, Ohfuna Chuo Hospital, Kamakura, and [g]Department of Gastroenterology and Hepatology, Kinki University School of Medicine, Osaka-Sayama, Japan

Abstract

Objectives and Methods: Findings of histological analyses of 2 cases of liver biopsy revealing hypovascular nodules are described. *Results:* Ultrasound examination revealed hypovascular and hypoechoic nodules (8 mm in diameter) in segment 1 (case 1) and (8 mm) in segment 8 (case 2). The nodules were detected by only Gd-EOB-DTPA-enhanced MRI. Hematoxylin and eosin staining of ultrasound-guided biopsy of the nodules revealed slight hypercellularity without the features of early hepatocellular carcinoma (HCC) such as cell atypia, fatty change and pseudoglandular formation. Early HCC was suspected; however, Victoria blue staining disclosed terminal portal tract invasion, the most important finding of early HCC. Also, cytokeratin 7 staining revealed decreased ductular reaction compatible with early HCC. Taken together, these histological analyses confirmed the two nodules to be early HCC. *Conclusion:* Based on the criteria of the International Consensus Group, the two nodules were diagnosed as early HCC through biopsy.

Copyright © 2012 S. Karger AG, Basel

Introduction

In 2009, the International Consensus Group for Hepatocellular Neoplasia (ICGHN) published a consensus paper describing stromal invasion as most helpful in differentiating early hepatocellular carcinoma (HCC) from high-grade dysplastic nodules (HGDN) [1].

Here, we describe 2 cases of early HCC in chronic hepatitis C patients. Ultrasound (US)-guided biopsy of the nodules subjected to hematoxylin and eosin (HE) staining revealed slight hypercellularity without cell atypia, fatty change and pseudoglandular formation. Victoria

Soo Ryang Kim, MD
Department of Gastroenterology, Kobe Asahi Hospital
3-5-25 Bououji-cho, Nagata-ku
Kobe 653-0801 (Japan)
E-Mail asahi-hp@arion.ocn.ne.jp

blue staining and immunohistochemical staining with cytokeratin 7 (CK7) showed a stromal (portal tract) invasion and reduced ductular reaction compatible with early HCC.

Case Reports

Case 1: An 82-Year-Old Man with Chronic Hepatitis C
Laboratory data on admission disclosed α-fetoprotein (AFP) 4.4 ng/ml (normal 0–20) and protein induced by vitamin K absence II (PIVKA II) 31 mAU/ml (0–40). A routine abdominal ultrasonograph (US) revealed an 8-mm hypoechoic nodule in segment 1 (S1) (fig. 1a). Sonazoid-enhanced US revealed no hypervascular nodules in the early vascular phase and no defect in the Kupffer phase. Contrast-enhanced computed tomography (CT) revealed no enhanced lesion in the arterial phase and no washout lesion in the equilibrium phase. Gadolinium-ethoxybenzyl-diethylenetriamine pentaacetic acid (Gd-EOB-DTPA)-enhanced magnetic resonance imaging (MRI) revealed no hypervascular nodule in the arterial phase, but disclosed a defective nodule in the hepatobiliary phase (fig. 1b). Arterioportal angiography revealed no enhanced lesion in CT hepatic arteriography and no perfusion defect in CT arterial portography. Histological analysis of a US-guided biopsy of the nodule revealed slight hypercellularity without cell atypia, fatty change and pseudoglandular formation. Victoria blue staining showed stromal (portal tract) invasion compatible with early HCC (fig. 2a–c). Immunohistochemical staining with CK7 showed no ductular reaction in areas of stromal invasion (fig. 2d–f).

Case 2: A 62-Year-Old Man with Chronic Hepatitis C
Laboratory data on admission disclosed AFP 2.3 ng/ml and PIVKA II 158 mAU/ml. A routine abdominal US examination revealed an 8-mm hypoechoic nodule in S8 (fig. 3a). Sonazoid-enhanced US revealed no hypervascular nodule in the arterial phase and no defect in the Kupffer phase. Contrast-enhanced CT revealed no enhanced lesion in the early arterial phase and no washout lesion in the portal phase. Gd-EOB-DTPA-enhanced MRI revealed no enhanced nodule in the arterial phase, no washout lesion in the late phase, but revealed a defect in the hepatobiliary phase (fig. 3b). CT hepatic arteriography revealed no enhanced lesion, and CT arterial portography revealed no perfusion defect. Histological analysis of a US-guided biopsy revealed slight

hypercellularity without cell atypia, fatty change and pseudoglandular formation (fig. 4a). Victoria blue staining showed stromal invasion compatible with early HCC (fig. 4b). Immunohistochemical staining with CK7 showed a scanty ductular reaction between the lesion and the adjacent liver tissue (fig. 4c).

Discussion

The status of imaging studies in the diagnosis of HCC <2 cm has changed with the introduction of new contrast agents used in US and MRI. First, Sonazoid was exclusively approved in Japan in 2007 as a second-generation US contrast agent; second, Gd-EOB-DTPA, a new liver-specific contrast agent used in MRI [2, 3], was approved in 2008. Mita et al. [4] have compared the diagnostic sensitivity of contrast-enhanced CT, Sonazoid-enhanced US, Gd-EOB-DTPA-enhanced MRI, and CT arteriportal angiography in diagnosing HCC in nodules <2 cm. In the study of 34 nodules, 24 were moderately-differentiated and 10 well-differentiated HCC. Overall, the sensitivity was 53.9% by contrast-enhanced CT, 67.6% by Sonazoid-enhanced US, 76.5% by Gd-EOB-DTPA-enhanced MRI, and 88.2% by CT arteriportal angiography. A significant difference was observed in the sensitivity between contrast-enhanced CT and CT arteriportal angiography, but no difference among Sonazoid-enhanced US, Gd-EOB-DTPA-enhanced MRI and CT arteriportal angiography. The authors concluded that changing the main diagnostic modality for HCC <2 cm from CT arteriportal angiography to Sonazoid-enhanced US and Gd-EOB-DTPA-enhanced MRI was recommended.

Advances in these imaging techniques and the establishment of surveillance protocols for high-risk populations have led to the detection of small hepatic nodules in patients with chronic liver diseases, particularly those with cirrhosis or chronic hepatitis caused by B or C virus. Such nodules, comprising a broad range of diagnostic en-
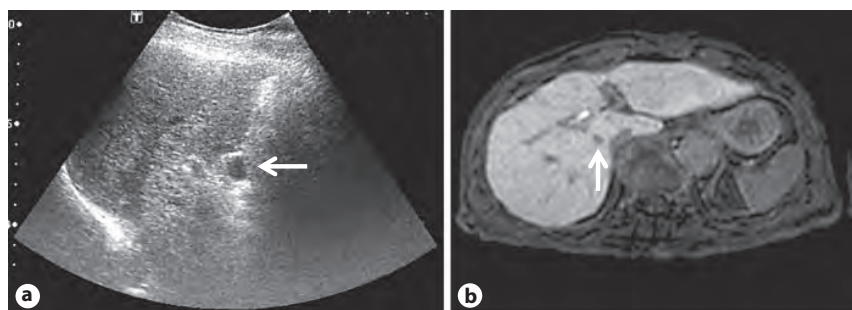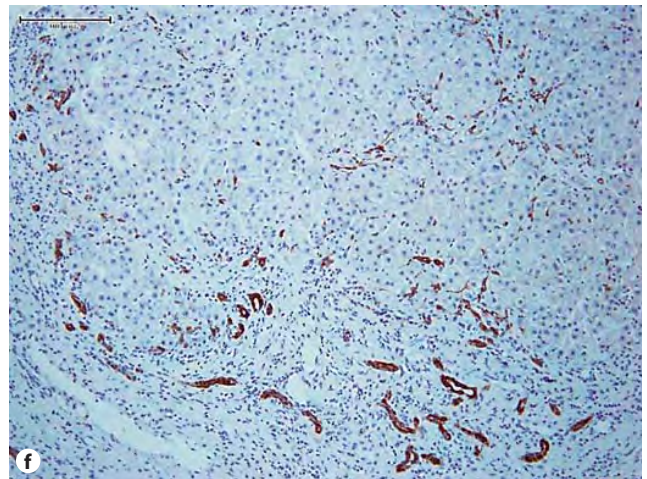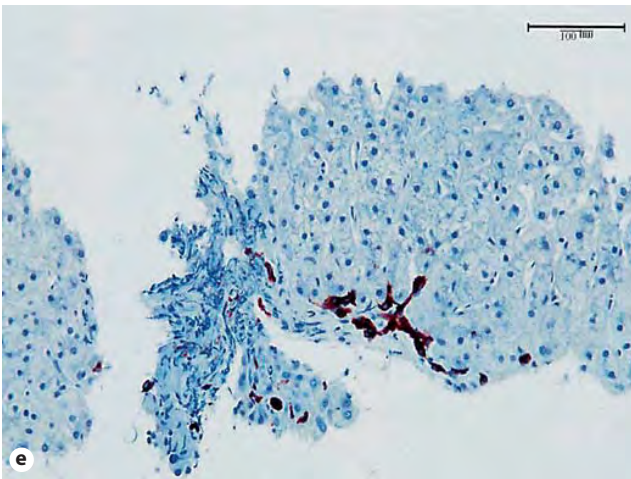

Fig. 1. B-mode US imaging; 8-mm hypoechoic nodule in S1 (**a**). Gd-EOB-DTPA-enhanced MRI revealed a defect in the hepatobiliary phase (**b**).

— 353 —

Kobayashi et al.
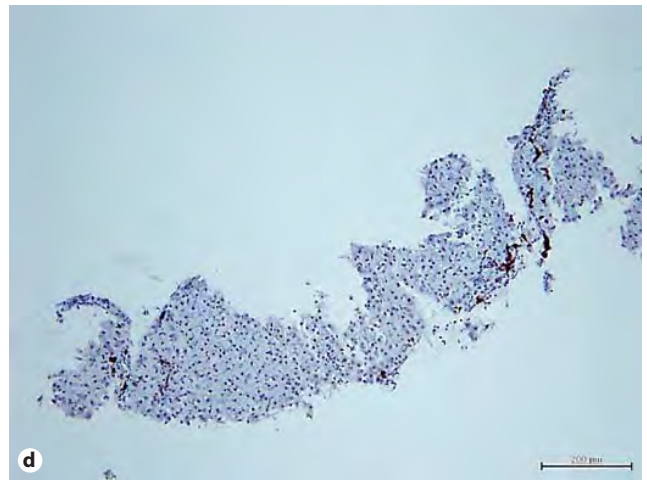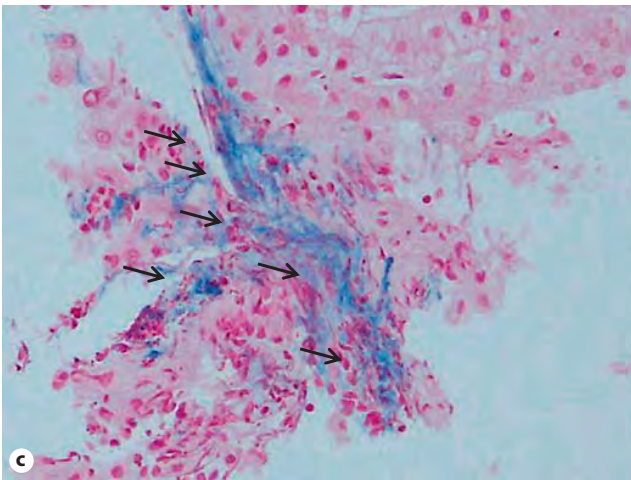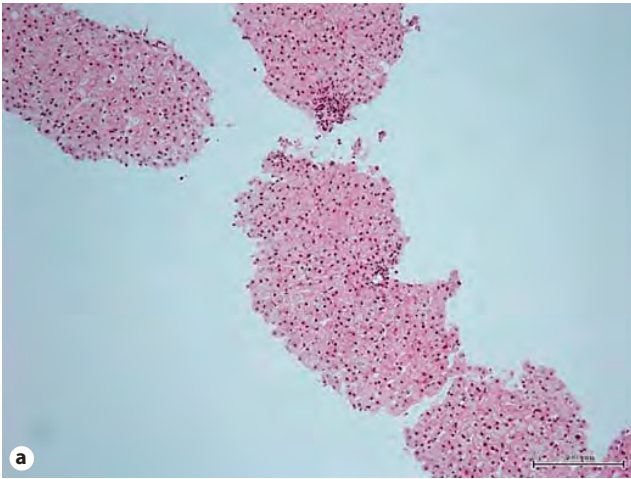
Fig. 3. B-mode US imaging. 8-mm hypoechoic nodule in S8 (**a**). Gd-EOB-DTPA-enhanced MRI revealed a defect in the hepatobiliary phase (**b**).
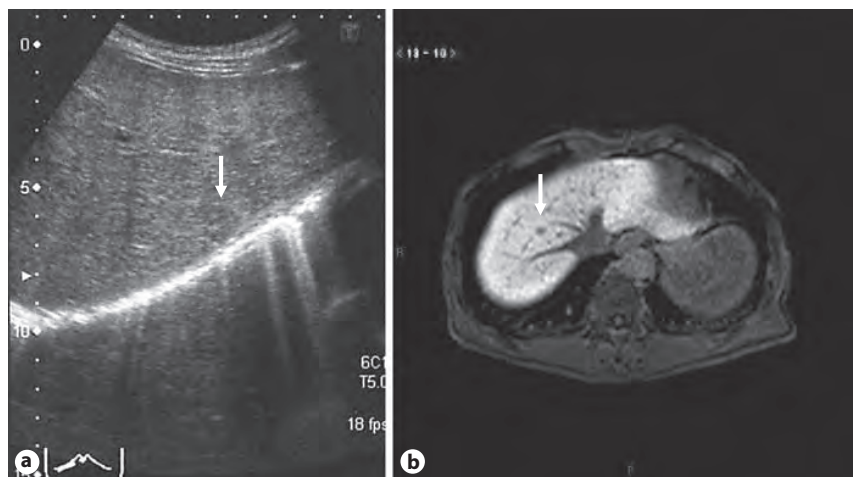
tities (some benign and some with malignant potential) are currently defined histologically, and their clinical management often depends on the ability to make a reliable histological diagnosis.

There has been considerable confusion regarding the nomenclature of and diagnostic approaches to these hepatic nodules. To clarify these issues, the International Working Party (IWP) of the World Congresses of Gastroenterology proposed a consensus – now widely adopted – and diagnostic criteria for hepatocellular nodular lesions in 1995 [5]. The IWP classified nodular lesions found in chronic liver disease into large regenerative nodules, low-grade dysplastic nodules, HGDN, and HCC. In addition, the IWP introduced the concept of dysplastic focus as a cluster of hepatocytes with features of early neoplasia (in particular small cell change of iron-free foci in a sideriotic background) measuring <0.1 cm, and defined small HCC as a tumor measuring <2 cm.

More recent studies support the division of small HCC into two clinicopathological groups termed early HCC and progressive HCC [6]. Early HCC has a vaguely nodular appearance and is well differentiated. Progressive

Fig. 2. Histological findings of the US-guided biopsy specimens. HE staining. Slight hypercellularity without cell atypia, fatty change and pseudoglandular formation (**a**). Victoria blue staining. Low magnification (**b**) and high magnification of oval enclosure: stromal invasion is observed (arrows) (**c**). Immunohistochemical staining with CK7. Low magnification (**d**), high magnification of tumor lesion (**e**), and high magnification of non-tumor lesion (**f**). Ductular reaction, absent in areas of stromal invasion (**e**) is florid around the cirrhotic nodules (non-tumor lesion) (**f**).

HCC has a distinctly nodular pattern and is mostly moderately differentiated, often with evidence of microvascular invasion. Early HCC takes longer to recur and has a higher 5-year survival rate compared with progressive HCC.

Small lesions with malignant potential are subtly different from the surrounding parenchyma, making them difficult to assess reproducibly. The ICGHN was convened to refine and make current the international consensus on the histopathological diagnosis of nodular lesions, such as dysplastic nodules and early HCC. Early HCC tumors are vaguely nodular and characterized by various combinations of the following major histologic features [7–9]: (1) increased cell density (more than twice that of the surrounding tissue) with an increased nuclear/cytoplasm ratio and an irregular thin trabecular pattern; (2) varying numbers of portal tracts within the nodule (intratumoral portal tract); (3) a pseudoglandular pattern; (4) diffuse fatty change, and (5) varying numbers of unpaired arteries. Nonetheless, all of these features may also be found in HGDN. Stromal invasion, described by ICGHN as helpful in differentiating early HCC from HGDN [1], is invasion into portal tracts of septal stroma within a hepatocellular nodule and is confirmed by Victoria blue staining.

Stromal invasion, which may be difficult to identify in early HCC because tumor cells show little or no cytologic atypia, is often focal; its identification is still more difficult when dealing with biopsied liver tissue in which only limited portions of nodules are sampled. Recently, Park et al. [10] have reported that CK7 immunostaining is useful in identifying stromal invasion. Ductular reac-

— 355 —

Fig. 4. Histological findings of US-guided biopsy. HE staining. Slight hypercellularity without cell atypia, fatty change and pseudoglandular formation are observed (**a**). Victoria blue staining. Stromal invasion is observed (**b**). Immunohistochemical staining with CK7. Ductular reaction is scanty between the lesion and the adjacent liver tissue (**c**).

tion, confirmed by CK7 staining, is frequently found in non-cancerous hepatocellular nodular lesions, whereas it is less frequently found in HCCs with true stromal invasion.

Here, the nodules of the 2 cases of early HCC were found hypovascular and were detected by only Gd-EOB-DTPA-enhanced MRI. HE staining of US-guided biopsy of the nodules revealed slight hypercellularity without the features of early HCC such as cell atypia, fatty change and pseudoglandular formation. Early HCC was suspected, however additional Victoria blue staining disclosed terminal portal tract invasion, which is the most important finding of early HCC. Also, CK7 staining revealed reduced ductular reaction compatible with early HCC. Thus, these histological analyses confirmed that these two nodules were early HCC. Victoria blue and CK7

staining are very useful in the diagnosis of early HCC through biopsy tissue. Further study is needed, however, to obtain consensus among pathologists regarding the efficacy of these two techniques in the diagnosis of early HCC.

Disclosure Statement

The authors declare that no financial or other conflict of interest exists in relation to the content of the article.

References

1 International Consensus Group for Hepatocellular Neoplasia: Pathologic diagnosis of early hepatocellular carcinoma: a report of ICGHN. Hepatology 2009;49:658–664.
2 Lee JM, Yoon JH, Joo I, Woo HS: Recent advances in CT and MR imaging for evaluation of hepatocellular carcinoma. Liver Cancer 2012;1:22–40.
3 Ricke J, Seidensticker M, Mohnike K: Noninvasive diagnosis of hepatocellular carcinoma in cirrhotic liver: current guidelines and future prospects for radiological imaging. Liver Cancer 2012;1:51–58.
4 Mita K, Kim SR, Kudo M, Imoto S, Nakajima T, Ando K, Fukuda K, Matsuoka T, Maekawa Y, Hayashi Y: Diagnostic sensitivity of imaging modalities for hepatocellular carcinoma smaller than 2 cm. World J Gastroenterol 2010;16:4187–4192.
5 International Working Party: Terminology of nodular hepatocellular lesion. Hepatology 1995;22:983–993.
6 Desmet VJ: East-West pathology agreement on precancerous liver lesions and early hepatocellular carcinoma. Hepatology 2009;49:335–357.
7 Hytiroglou P: Morphological changes of early human hepatocarcinogenesis. Semin Liver Dis 2004;24:65–75.
8 Kojiro M: Pathology of Hepatocellular Carcinoma. Oxford, Blackwell, 2006.
9 Hytiroglou P, Park YN, Krinsky G, Theise ND: Hepatic precancerous lesions and small hepatocellular carcinoma. Gastroenterol Clin North Am 2007;36:867–887.
10 Park YN, Kojiro M, Di Tommaso L, Dhillon AP, Kondo F, Nakano M, Sakamoto M, Theise ND, Roncalli M: Ductular reaction is helpful in defining early stromal invasion, small hepatocellular carcinoma, and dysplastic nodules. Cancer 2007;109:915–923.

Novel Non-Trocar Technique for Laparoscopic Radiofrequency Ablation

Shinobu Tsuchida[a, c]   Takumi Fukumoto[b]   Akihiro Toyokawa[a]   Masahide Awazu[a]
Nobuya Kusunoki[b]   Masahiro Kido[b]   Masanori Takahashi[b]   Motofumi Tanaka[b]
Kaori Kuramitsu[b]   Soo Ryang Kim[c]   Yonson Ku[b]   Masatoshi Kudo[d]

[a]Department of Surgery, Yodogawa Christian Hospital, Osaka, [b]Division of Hepato-Biliary-Pancreatic Surgery,
Department of Surgery, Kobe University Graduate School of Medicine, and [c]Department of Gastroenterology,
Kobe Asahi Hospital, Kobe, and [d]Department of Gastroenterology and Hepatology, Kinki University School of
Medicine, Osaka-Sayama, Japan

Abstract

We have developed a novel insertion method, a non-trocar technique (NTT), for laparoscopic radiofrequency ablation, whereby an ablation needle, guided by a 14.8-mm echo probe (PVM-787LA; Toshiba, Tokyo, Japan), accurately and easily punctures the target tumor in the liver. By existing methods, an ablation needle is inserted into the abdominal cavity through a puncture hole away from the echo probe because of the presence of a 15-mm trocar. Under such circumstances, fitting and sliding an ablation needle along the groove of the probe into the abdominal cavity is difficult because of the longitudinal dissociation between the needle and the probe. To avoid this dissociation, an echo probe is inserted directly through the small incision from which the 12-mm trocar is withdrawn and an ablation needle is introduced directly into the abdominal cavity through a puncture hole adjacent to and slid along the groove of the probe.

Copyright © 2012 S. Karger AG, Basel

Introduction

Percutaneous radiofrequency ablation (RFA) is an effective method for the treatment of small hepatocellular carcinoma (HCC) [1, 2]. When the lesions are located near gastrointestinal organs, however, or the nodules are difficult to identify by ultrasonography (US), laparoscopic RFA or laparotomic RFA is chosen. The former is superior to the latter because of its minimally invasive surgical procedure and the cosmetically more esthetic surgical scar [3]. When a laparoscopic ultrasound probe is inserted through a trocar, it is difficult to use the insertion point made by the probe or to attach and slide an ablation needle along the groove of the probe into the abdominal cavity because of the longitudinal dissociation between the needle and the probe [4, 5]. We have developed a novel insertion method, a non-trocar technique (NTT), for laparoscopic RFA with the use of a convex scanning probe, whereby an ablation needle accurately and easily punctures the target tumor in the liver.

Shinobu Tsuchida
Department of Surgery, Yodogawa Christian Hospital
1-7-50 Shibajima, Higashiyodogawa-ku
Osaka 533-0024 (Japan)
E-Mail fwin3348@nifty.com

Fig. 1. In the trocar group, a needle is inserted into the abdominal cavity through a puncture hole away from the probe because of the presence of a 15-mm trocar (virtual scheme).

Fig. 2. Insertion of the needle with the use of a trocar (existing method). It is difficult to lead the needle to and slide it along the groove of the probe because of the longitudinal dissociation between the needle and the probe.

Patients and Methods

Between March and September 2011, ten nodules considered difficult to treat with a percutaneous approach in 9 patients (5 men, 4 women; age 32–86 years, average 70.0) were subjected to laparoscopic RFA. The tumors ranged between 1.2 and 4.5 cm (average 2.0), and the nodules were located in segments 2–8. A convex scanning laparoscopic ultrasound probe (PVM-787LA; Toshiba Medicals, Tokyo, Japan) and an internally water-cooled RF electrode with an impedance-controlled generator (Cool-tip RF System; Radionics, Burlington, Mass., USA) were used. Of the 9 patients, 5 were treated with the use of a trocar as described by Ido et al. [6] (the trocar group). Briefly, after the insertion of a laparoscopic ultrasound probe through a 15-mm trocar, an ablation needle was introduced into the abdominal cavity through a puncture hole outside of the trocar, away from the probe because of the presence of the trocar (fig. 1). The other 4 patients were treated without the use of a trocar (non-trocar group). Briefly, a probe was inserted directly through the small incision from which the 12-mm trocar was withdrawn, and an ablation needle was inserted directly into the abdominal cavity through the insertion site adjacent to the guiding tract along the probe (fig. 3).

Results

In the trocar group, the insertion point was sited on the skin from the outside of the trocar, and a needle was inserted into the abdominal cavity through an incision inevitably at a distance from the probe because of the presence of the trocar (virtual scheme; fig. 1). The needle was then led into the guiding tract of the probe in the abdominal cavity. Leading the needle to and sliding it along

the groove of the probe was difficult because of the longitudinal dissociation between the needle and the probe. Because of the misalignment, the needle often slipped out of the groove after its introduction into the guiding tract of the probe (fig. 2), or the needle did not always slide along the guideline, as displayed on the monitoring screen of US. One patient underwent a laparotomy instead of a scheduled laparoscopic operation because of the inability of introducing the needle along the groove of the probe. Leakage of infused gas was not observed when the probe was inserted directly without a trocar. Without the trocar, the scanning efficiency of the probe in identifying nodules was not affected, and no complication was observed. In the non-trocar group, the probe was inserted directly through the insertion site from which the 12-mm trocar was withdrawn, and an ablation needle was inserted directly into the abdominal cavity through the insertion point adjacent to the probe (fig. 3). The needle was then easily and fittingly slid along the groove of the probe (fig. 4). The average duration of the operation was 153.5 min in the non-trocar group compared with 200.6 min in the trocar group.

Discussion

Although the treatment outcome of percutaneous RFA for small HCC is about the same as and even safer than that of hepatic resection [1, 2], complications have been reported in organs adjacent to the liver, such as the heart,

Fig. 3. Insertion of the needle without a trocar (our technique, or NTT). The echo probe is inserted directly through the opening through which the 12-mm trocar is withdrawn, and an ablation needle is inserted directly into the abdominal cavity through the insertion site adjacent to the probe.
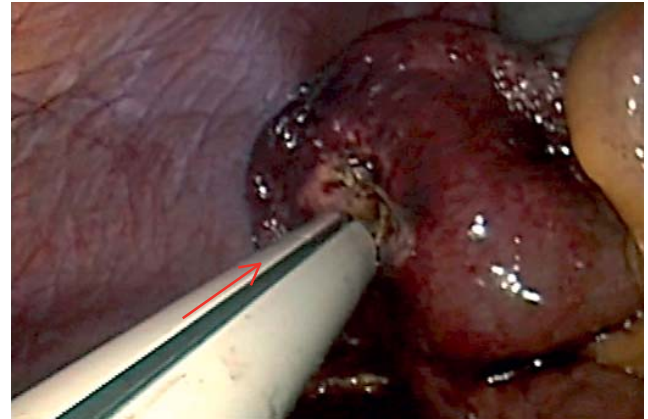
Fig. 4. Insertion of the needle along the groove of the probe without a trocar. An ablation needle can be more easily and fittingly slid along the groove of the probe than the existing method because of the small difference in the alignment between the probe and the needle.

the diaphragm and the intestines. To avoid such complications, the use of artificial ascites with percutaneous RFA is one alternative; nonetheless, laparoscopic RFA is reported to be safer and more efficient [7]. Moreover, the risk of hemorrhage and dissemination from protruding HCC on the surface of the liver is very high with percutaneous RFA [8, 9]. In such cases, laparoscopic RFA has been carried out safely [4]. Without US guidance, exact and safe insertion of needles is difficult into nodules indiscernible from the liver surface and into those located just below the diaphragm. Although a linear type probe provides good imaging of the liver and other vessels because of its wide view, it requires skill and experience to precisely target a nodule for ablation, especially that US imaging by the linear type probe and the direction of needle insertion are different. Laparoscopic treatment is difficult because of the inability of visualizing the tip of the needle.

Asahina et al. [4, 5] have developed a sector type ultrasonic probe (end-fire type), which is inserted through a 12-mm trocar, and although safe and accurate ablation is possible therewith, a 20-cm needle is difficult to handle. When a cool-tip type probe is used, a 25-cm long needle is requisite; however, such a needle may carry the risk of unnecessary overablation of small HCC, in that it can ablate only nodules 3 cm in diameter.

Ido et al. [6] have developed the convex array probe (PVM-787LA) equipped with a guiding tract on the shaft. Since the US image and the direction of the needle obtained by the convex array probe are the same, we adopt-

ed their method; however, an ablation needle needs to be inserted into the abdominal cavity through an insertion site away from the probe because of the presence of the 15-mm trocar (fig. 1). Under these circumstances, it is difficult to lead the ablation needle to and slide it along the groove of the probe in the abdominal cavity because of the longitudinal dissociation between the needle and the probe (fig. 2).

Since the presence of the trocar between the probe and the needle made insertion of the needle more difficult, we assayed our non-trocar method of insertion. Although leakage of the infused gas was a possibility, it was avoided when the probe was inserted directly through an opening smaller than the diameter of the trocar. The anticipated difficulty of scanning was overcome by the flexibility of the abdominal wall.

First, the echo probe was inserted directly through the opening from which the 12-mm trocar was withdrawn, and an ablation needle was inserted directly into the abdominal cavity through the insertion point adjacent to the probe (fig. 3). Insertion was very easily achieved and no leakage of infused gas was observed without ditch, etc. In the course of scanning, no resistance was perceived between the abdominal wall and the probe, and the handling of the probe was easy.

The difference in the alignment between the probe and the needle in the absence of the trocar was small enough for an ablation needle to easily slide along the groove of the probe.

Tolerability improved because of the reduced outer width of the trocar (from 15 to 12 mm), which allowed the safe insertion of the probe, even in the presence of a dilated vein in the abdominal wall.

In conclusion, our novel insertion method, a NTT for laparoscopic RFA, allows an ablation needle, guided by a 14.8-mm echo probe (PVM-787LA; Toshiba), to accurately and easily puncture the target tumor in the liver.

Disclosure Statement

The authors declare that no financial or other conflict of interest exists in relation to the content of the article.

References

1 Peng ZW, Lin XJ, Zhang YJ, Liang HH, Guo RP, Shi M, Chen MS: Radiofrequency ablation versus hepatic resection for the treatment of hepatocellular carcinomas 2 cm or smaller: a retrospective comparative study. Radiology 2012;262:1022–1033.

2 Minami Y, Kudo M: Radiofrequency ablation of hepatocellular carcinoma: a literature review. Int J Hepatol 2011;2011:104685.

3 Tanaka S, Shimada M, Shirabe K, Taketomi A, Maehara S, Tsujita E, Ito S, Kitagawa D, Maehara Y: Surgical radiofrequency ablation for treatment of hepatocellular carcinoma: an endoscopic or open approach. Hepatogastroenterology 2009;56:1169–1173.

4 Asahina Y, Nakanishi H, Izumi N: Laparoscopic radiofrequency ablation for hepatocellular carcinoma. Dig Endosc 2009;21:67–72.

5 Noguchi O, Izumi N, Inoue K, Nishimura Y, Ueda K, Tsuchiya K, Hamano K, Itakura J, Asahina Y, Uchihara M: Laparoscopic ablation therapy for hepatocellular carcinoma: clinical significance of a newly developed laparoscopic sector ultrasonic probe. Dig Endosc 2003;15:179–184.

6 Hozumi M, Ido K, Hiki S, Isoda N, Nagamine N, Ono K, Sato Y, Onobuchi Y, Kobayashi Y, Hirayama Y, Yanagawa T, Sugano K: Easy and accurate targeting of deep-seated hepatic tumors under laparoscopy with a forward-viewing convex-array transducer. Surg Endosc 2003;17:1256–1260.

7 Hirooka M, Kisaka Y, Uehara T, Ishida K: Efficacy of laparoscopic radiofrequency ablation for hepatocellular carcinoma compared to percutaneous radiofrequency ablation with artificial ascites. Gastroenterol Endosc 2010;52:278–285.

8 Santambrogio R, Opocher E, Costa M, Montorsi V: Survival and intra-hepatic recurrences after laparoscopic radiofrequency of hepatocellular carcinoma in patients with liver cirrhosis. Surg Oncol 2005;89:218–225.

9 Okabayashi T, Kobayashi M, Akimori T, Akisawa N, Iwasaki S, Onishi S, Araki K: Usefulness of laparoscopy ablation of hepatocellular carcinoma. Surg Technol Int 2005;14:177–181.

Hepatocellular Carcinoma with Obstructive Jaundice: Endoscopic and Percutaneous Biliary Drainage

Yasunori Minami   Masatoshi Kudo

Department of Gastroenterology and Hepatology, Kinki University Faculty of Medicine, Osaka, Japan

Abstract

Among patients with later stage hepatocellular carcinoma (HCC), only 1–12% manifest obstructive jaundice as the initial complaint. Endoscopic retrograde biliary drainage (ERBD) and percutaneous transhepatic biliary drainage (PTBD) are the two main non-surgical treatment options for obstructive jaundice in patients with HCC. ERBD is usually the first-line treatment because of its low hemorrhage risk. Some have reported that the successful drainage rate ranges from 72 to 100%. Mean stent patency time and mean survival range from 1.0 to 15.9 and 2.8 to 12.3 months, respectively. PTBD is often an important second-line treatment when ERBD is impossible. With regard to materials, metallic stents offer the benefit of longer patency than plastic stents. The dominant effect of biliary drainage suggests that successful jaundice therapy could enhance anti-cancer treatment by increasing life expectancy, decreasing mortality, or both. We present an overview of the efficacy of endoscopic and percutaneous drainage for obstructive jaundice in patients with HCC who are not candidates for surgical resection and summarize the current indications and outcomes of reported clinical use.

Copyright © 2012 S. Karger AG, Basel

Introduction

Obstructive jaundice as the main clinical feature is uncommon in patients with hepatocellular carcinoma (HCC) [1]. HCC may involve the biliary tract in several different ways: tumor compression, tumor thrombosis, hemobilia, and diffuse tumor infiltration. To avoid jaundice impairment and hepatic failure, biliary drainage has been proposed as a means of reversing the pathophysiologic disturbances seen in jaundiced patients. Generally there are two main non-surgical treatment options for obstructive jaundiced patients: endoscopic retrograde biliary drainage (ERBD) and percutaneous transhepatic biliary drainage (PTBD). ERBD is usually the first-line treatment in patients considered for drainage because of its low hemorrhage risk. PTBD is often an important second-line treatment when ERBD is impossible. However, as HCC tumors may extensively infiltrate intrahepatic or hilar bile ducts, it is often difficult to drain the bile duct

Masatoshi Kudo, MD, PhD
Department of Gastroenterology and Hepatology
Kinki University Faculty of Medicine, 377-2, Ohno-Higashi
Osaka-Sayama, Osaka 589-8511 (Japan)
E-Mail m-kudo@med.kindai.ac.jp

	Type 1	**Type 2**	**Type 3**
	Intraluminal obstruction	Hemobilia	Extraluminal obstruction
Intrahepatic biliary obstruction			
	Tumor thrombus	Blood clot	Multiple tumors

Fig. 1. Classification of intrahepatic biliary obstruction of HCC.

effectively and resolve the obstructive jaundice. Recent developments in interventional endoscopic ultrasonography (EUS) allow a transgastric approach to the left biliary system.

In this review, we focus our discussion on the efficacy of endoscopic and percutaneous drainage for obstructive jaundice in patients with HCC who are not candidates for surgical resection.

Obstructive Jaundice Caused by HCC

Jaundice presents in 19–40% of patients with HCC at the time of diagnosis and usually occurs in later stages [1–4]. However, only 1–12% of HCC patients manifest obstructive jaundice as the initial complaint. HCC invasion into a bile duct may be due to one of the three mechanisms (fig. 1) [1, 5, 6]. Type 1 obstruction is due to intraluminal biliary obstruction caused by either a biliary tumor thrombus or a free-floating tumor fragment. The biliary tumor thrombus gives a cholangiographic intraluminal filling defect that resembles a cork in the neck of a bottle. Lau et al. [7] termed this radiologic sign the 'cork sign'. In patients with intraluminal tumor fragments, the cholangiographic features are similar to those seen in choledocholithiasis but the edges of the filling defects secondary to the tumor fragments are irregular and less well defined than those of stones. Type 2 obstruction is due to hemobilia. The hemobilia gives rise to cholangiographic features of fluffy intraluminal filling defects, which obscure the underlying intraluminal tumor. Another cholangiogram should be carried out after the hemobilia has settled to clarify the actual extent of the intraluminal tumor. Type 3 obstruction is due to extraluminal biliary obstruction. Tumor invasion and/or encasement of the intrahepatic branches of the hepatic ducts gives rise to localized strictures with proximal ductal dilatation intrahepatically. The presence of malignant porta hepatis lymph nodes can compress the common hepatic or bile duct leading to extrahepatic biliary obstruction.

Percutaneous tumor ablation, such as ethanol injection and radiofrequency ablation, is now recognized as the primary treatment for HCC. Although percutaneous tumor ablation is a relatively safe procedure, it can cause biliary injury as a rare complication (0.3–0.7% per treatment) [8, 9].

Drainage

Endoscopic Retrograde Biliary Drainage
We investigated papers about hilar obstruction due to malignant biliary stricture including HCC and cholangiocarcinoma (table 1) [10–24]. The successful drainage rate ranges from 72 to 100%. Mean stent patency time and mean survival range from 1.0 to 15.9 and 2.8 to 12.3 months, respectively. However, several factors seem to correlate with survival and the dominant effect of biliary drainage suggests that successful jaundice therapy could enhance anti-cancer treatment by increasing life expectancy, decreasing mortality, or both. Stent patency is related to the need for repeated biliary drainage. Some researchers have reported that endoscopic drainage may be feasible and effective for malignant hilar biliary obstruction, and endoscopic reintervention is relatively simple.

Table 1. Successful drainage rates and stent patency times after ERBD for malignant biliary stricture

Reference (first author)	n	Mean follow-up period months	Successful drainage rate, %	Mean stent patency time months	Mean survival months
Banerjee, 1995 [10]	12	–	97.5	–	8.2
Matsueda, 2001 [11]	18	–	72	–	2.8
Higashizawa, 2002 [12]	61	–	85	–	–
Rerknimitr, 2002 [13]	50	–	97.5	–	–
Ahmad, 2002 [14]	32	–	–	8.4	–
Al-Mofleh, 2003 [15]	72	–	93	–	6.9
Freeman, 2003 [16]	45	–	77	8.9	–
Rerknimitr, 2004 [17]	63	–	96.8	2.9	–
Singh, 2007 [18]	18	–	–	1.0	7.5
Naitoh, 2009 [19]	36	–	91.7	15.9	8.6
Chahal, 2010 [20]	21	6.14	100	6.3	–
Gerhardt, 2010 [21]	29	11.4	100	5.8	12.3
Kogure, 2011 [22]	12	–	100	6.7	–
Kanno, 2011 [23]	20	7.3	100	8.3	–
Hwang, 2011 [24]	30	5.9	86.7	4.7	5.9

Metallic Stent versus Plastic Stent

With regard to materials used to manufacture stents, the biliary endoprostheses currently used in clinics fall into two broad categories, plastic (teflon, polyethylene or polyurethane) and metallic (stainless steel or nickel-titanium alloy) stents. A prospective randomized controlled trial compared the patency of conventional endoscopically-inserted plastic stents (PS) with that of self-expanding metal stents (SEMS) [25]. Median patency times were 1.8 and 3.6 months in the PS and SEMS groups, respectively (p = 0.002). Median survival was 4.5 months (5.3 and 3.9 months in the SEMS and PS groups, respectively; p = 0.28). Although metallic stents (MS) remain patent longer than PS, the optimal palliation of inoperable malignant biliary strictures remains controversial because of the high cost of MS and short patient survival. Prat et al. [26] randomized their patients to receive either an 11.5-Fr polyethylene stent to be exchanged in case of dysfunction, an 11.5-Fr stent to be exchanged every 3 months, or a self-expanding metallic Wallstent®. The authors recommended that MS were advantageous for patients surviving more than 6 months, whereas a PS was advantageous in patients surviving 6 months or less, it terms of cost analysis. However, Soderlund and Linder [25] mentioned that the total cost of MS or PS was about the same, irrespective of survival time, in their study.

Percutaneous Transhepatic Biliary Drainage

The use of a percutaneous approach allows drainage if ERBD is impossible. PTBD is often performed in patients who have received total gastrectomy with Roux-Y reconstruction. Long-term PTBD is a valid alternative to surgery in patients with malignant bile duct strictures in whom endoscopic drainage has failed. Born et al. [27] reported that there are frequently minor problems, mostly catheter-related, which require premature exchange of the drain in almost a half of the cases although PTBD was highly effective in relieving jaundice. Of the 157 PTBD exchanges, 73 (47%) had to be carried out earlier than scheduled. Premature exchange was needed for clinical reasons, such as fever indicating PTBD dysfunction, in only 19% of these cases. The other reasons were related to the PTBD catheter and consisted of bile leakage alongside the drain (33%), PTBD disconnection or complete dislocation (30%), or occlusion suspected during regular flushing of the drain (15%). Reducing the PTBD exchange interval from 3 to 2 months would have decreased the number of premature stent exchanges by 26%.

Percutaneous transhepatic metal or plastic biliary stent implantation for palliative treatment of malignant biliary obstruction has also become widely accepted [28]. The 30-day mortality rate was lower in the MS group (6/61, 9.8%) than in the PS group (9/34, 26.5%, p < 0.05). The 30-day reobstruction rate and complication rate were 15.0 and 16.4% in the MS group and 32.4 and 29.4% in the PS group, respectively (p < 0.01). The median patency period of stents and median survival period of the patients were 230 and 224 days in the MS group and 90 and 94 days in the PS group, respectively (p < 0.01). Therefore, MS is clinically confirmed to be superior to PS in the treatment of malignant biliary obstruction according to the percutaneous approach.

ERBD versus PTBD

At present, no prospective randomized trials exist regarding ERBD versus PTBD for obstructive jaundice caused by HCC. However, in patients with malignant bile strictures, there are two randomized controlled reports comparing ERBD with PTBD. Speer et al. [29] reported that the endoscopic method had a significantly higher success rate for relief of jaundice (81 vs. 61%, p = 0.017) and a significantly lower 30-day mortality (15 vs. 33%, p = 0.016) from 75 patients entered into their analysis. On the other hand, Piñol et al. [30] compared percutaneous SEMS with conventional endoscopic PS. The therapeutic success was higher in the percutaneous
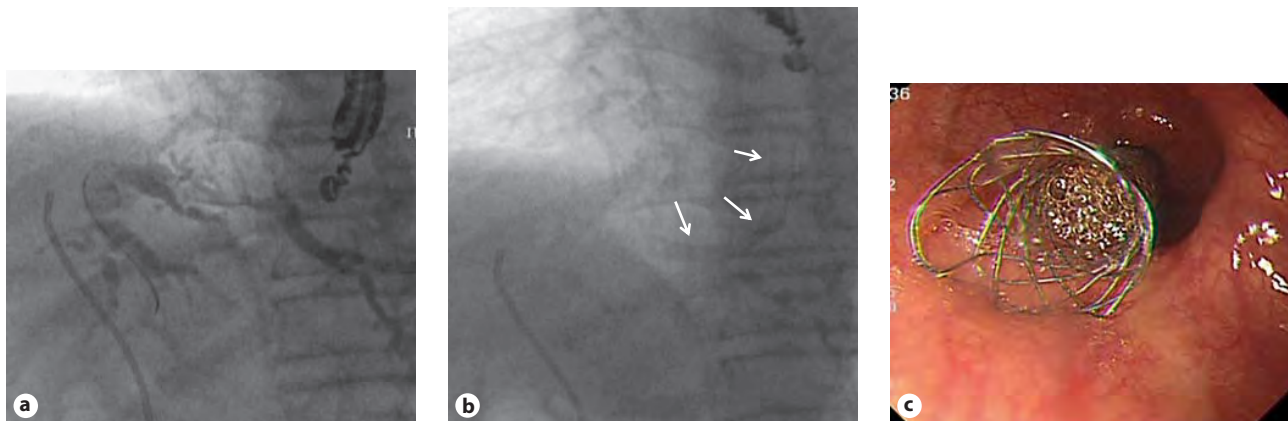
Fig. 2. Hilar obstruction in a HCC patient with an ineffective biliary PS. **a** EUS-guided cholangiographic image of dilated irregular left intrahepatic bile ducts. **b** Fluoroscopic image of self-expanding metal biliary stent (arrows) through the stomach into a left intrahepatic bile duct. **c**. Endoscopic image of self-expanding metal biliary stent in the stomach.

group (71% (20 of 28 patients) versus 42% (11 of 26 patients); p = 0.03). Overall median survival was significantly higher in the percutaneous group than in the endoscopic group (3.7 vs. 2.0 months; p = 0.02). Cox regression analysis identified placement of the percutaneous SEMS as the only independent predictor of survival (relative risk 2.19; 95% CI 1.11, 4.31; p = 0.02). We consider that stent characteristics seem to play an important role in long-term outcome.

Complications and Risk Factors

Major complication rates for ERBD and PTBD were 0.85–12.1 and 4.1–10.3%, respectively [31–34]. Mortality for ERBD and PTBD were 0.5–1.5 and 0.7–5.3%, respectively [31–34]. Major complications of ERBD included acute pancreatitis, acute cholangitis, acute cholecystitis, hemobilia, and stent dislocation, while minor complications included pain and fever. Major complications of PTBD included hemobilia, acute panperitonitis due to leaking bile, pneumothorax and stent dislocation, and minor complications included pain and fever.

The independent risk factors for ineffective biliary drainage were total bilirubin >13 mg/dl and Child-Turcotte-Pugh class C, and the mean survival times of patients who received effective or ineffective biliary drainage were 247 and 44 days, respectively [35]. When effective biliary drainage was achieved after an appropriate biliary drainage procedure in patients with obstructive jaundice caused by HCC, survival improved.

New Strategy: Endoscopic Ultrasound-Guided Biliary Drainage

Interventional EUS-guided biliary drainage (EUS-BD) is a new technique that allows drainage of the biliary system in benign and malignant diseases when the bile duct is inaccessible by conventional ERCP (fig. 2).

EUS-guided diagnostic cholangiography was first reported [36] in 1996 and the first EUS-BD was reported in 2001 [37]. These initial reports were followed by a description of technique modifications and expanding indications including EUS-guided hepaticogastrostomy with stent placement [38], transduodenal EUS-rendezvous biliary access [39, 40] and EUS-guided biliary therapy of choledocholithiasis with the creation of a neopapilla [41]. Traditionally, patients who had ultimately failed ERCP had been offered PTBD or surgical biliary decompression. EUS-guided decompression is not only minimally invasive but is a single-step procedure that provides more physiological internal bile drainage with improved patient comfort and decreased risk of fluid and electrolyte disturbances [42]. Furthermore, EUS-BD using transgastric puncture of the intrahepatic duct can be feasible in patients with hilar block due to HCC.

Conclusion

ERBD and PTBD are the two main non-surgical treatment options for obstructive jaundiced patients with HCC. ERBD is usually the first-line treatment because of

low hemorrhage risk. PTBD is an important second-line treatment when ERBD is impossible. At present, there exist no prospective randomized trials regarding ERBD versus PTBD for obstructive jaundice caused by HCC. However, the dominant effect of biliary drainage suggests that successful jaundice therapy could enhance anti-cancer treatment by increasing life expectancy, decreasing mortality, or both. In addition, recent developments in interventional EUS allow a transgastric approach to the left biliary system when the bile duct is inaccessible by conventional ERCP in patients with hilar block due to HCC.

Disclosure Statement

The authors declare that no financial or other conflict of interest exists in relation to the content of the article.

References

1 Qin LX, Tang ZY: Hepatocellular carcinoma with obstructive jaundice: diagnosis, treatment and prognosis. World J Gastroenterol 2003;9:385–391.

2 Lee NW, Wong KP, Siu KF, Wong J: Cholangiography in hepatocellular carcinoma with obstructive jaundice. Clin Radiol 1984;35:119–123.

3 Huang JF, Wang LY, Lin ZY, et al: Incidence and clinical outcome of icteric type hepatocellular carcinoma. J Gastroenterol Hepatol 2002;17:190–195.

4 Kim DY, Han KH: Epidemiology and surveillance of hepatocellular carcinoma. Liver Cancer 2012;1:2–14.

5 Lau WY, Leung JW, Li AKC: Management of hepatocellular carcinoma presenting as obstructive jaundice. Am J Surg 1990;160:280–282.

6 Lai EC, Lau WY: Hepatocellular carcinoma presenting with obstructive jaundice. ANZ J Surg 2006;76:631–636.

7 Lau WY, Leow CK, Leung KL, Leung TW, Chan M, Yu SC: Cholangiographic features in the diagnosis and management of obstructive icteric type hepatocellular carcinoma. HPB Surg 2000;11:299–306.

8 Giorgio A, Tarantino L, de Stefano G, Coppola C, Ferraioli G: Complications after percutaneous saline-enhanced radiofrequency ablation of liver tumors: 3-year experience with 336 patients at a single center. AJR Am J Roentgenol 2005;184:207–211.

9 Tateishi R, Shiina S, Teratani T, Obi S, Sato S, Koike Y, Fujishima T, Yoshida H, Kawabe T, Omata M: Percutaneous radiofrequency ablation for hepatocellular carcinoma. An analysis of 1,000 cases. Cancer 2005;103:1201–1209.

10 Banerjee B, Teplick SK: Nonsurgical management of primary cholangiocarcinoma. Retrospective analysis of 40 cases. Dig Dis Sci 1995;40:701–705.

11 Matsueda K, Yamamoto H, Umeoka F, Ueki T, Matsumura T, Tezen T, Doi I: Effectiveness of endoscopic biliary drainage for unresectable hepatocellular carcinoma associated with obstructive jaundice. J Gastroenterol 2001;36:173–180.

12 Higashizawa T, Tamada K, Tomiyama T, Wada S, Ohashi A, Satoh Y, Gotoh Y, Miyata T, Ido K, Sugano K: Biliary guidewire facilitates bile duct biopsy and endoscopic drainage. J Gastroenterol Hepatol 2002;17:332–336.

13 Rerknimitr R, Attasaranya S, Kladchareon N, Mahachai V, Kullavanijaya P: Feasibility and complications of endoscopic biliary drainage in patients with malignant biliary obstruction at King Chulalongkorn Memorial Hospital. J Med Assoc Thai 2002;85(suppl 1):S48–S53.

14 Ahmad J, Siqueira E, Martin J, Slivka A: Effectiveness of the Ultraflex Diamond stent for the palliation of malignant biliary obstruction. Endoscopy 2002;34:793–796.

15 Al-Mofleh IA, Al-Rashed RS, Al-Amri SM, Al-Ghamdi AS, Al-Faleh FZ, Al-Freihi HM, Isnani AC: Malignant biliary strictures. Diagnosis and management. Saudi Med J 2003;24:1360–1363.

16 Freeman ML, Overby C: Selective MRCP and CT-targeted drainage of malignant hilar biliary obstruction with self-expanding metallic stents. Gastrointest Endosc 2003;58:41–49.

17 Rerknimitr R, Kladcharoen N, Mahachai V, Kullavanijaya P: Result of endoscopic biliary drainage in hilar cholangiocarcinoma. J Clin Gastroenterol 2004;38:518–523.

18 Singh V, Kapoor R, Solanki KK, Singh G, Verma GR, Sharma SC: Endoscopic intraluminal brachytherapy and metal stent in malignant hilar biliary obstruction: a pilot study. Liver Int 2007;27:347–352.

19 Naitoh I, Ohara H, Nakazawa T, Ando T, Hayashi K, Okumura F, Okayama Y, Sano H, Kitajima Y, Hirai M, Ban T, Miyabe K, Ueno K, Yamashita H, Joh T: Unilateral versus bilateral endoscopic metal stenting for malignant hilar biliary obstruction. J Gastroenterol Hepatol 2009;24:552–557.

20 Chahal P, Baron TH: Expandable metal stents for endoscopic bilateral stent-within-stent placement for malignant hilar biliary obstruction. Gastrointest Endosc 2010;71:195–199.

21 Gerhardt T, Rings D, Höblinger A, Heller J, Sauerbruch T, Schepke M: Combination of bilateral metal stenting and trans-stent photodynamic therapy for palliative treatment of hilar cholangiocarcinoma. Z Gastroenterol 2010;48:28–32.

22 Kogure H, Isayama H, Nakai Y, Tsujino T, Ito Y, Yamamoto K, Mizuno S, Yagioka H, Kawakubo K, Sasaki T, Hirano K, Sasahira N, Tada M, Omata M, Koike K: Newly designed large cell Niti-S stent for malignant hilar biliary obstruction: a pilot study. Surg Endosc 2011;25:463–467.

23 Kanno Y, Ito K, Fujita N, Noda Y, Kobayashi G, Obana T, Horaguchi J, Takasawa O, Kato Y, Koshita S, Yamashita Y, Ogawa T: Single-session endoscopic bilaterally-configured placement of metal stents for hilar malignant biliary obstruction. Dig Endosc 2011;23:91–96.

24 Hwang JC, Kim JH, Lim SG, Kim SS, Yoo BM, Cho SW: Y-shaped endoscopic bilateral metal stent placement for malignant hilar biliary obstruction: prospective long-term study. Scand J Gastroenterol 2011;46:326–332.

25 Soderlund C, Linder S: Covered metal versus plastic stents for malignant common bile duct stenosis: a prospective, randomized, controlled trial. Gastrointest Endosc 2006;63:986–995.

26 Prat F, Chapat O, Ducot B, Ponchon T, Pelletier G, Fritsch J, Choury AD, Buffet C: A randomized trial of endoscopic drainage methods for inoperable malignant strictures of the common bile duct. Gastrointest Endosc 1998;47:1–7.

27 Born P, Rösch T, Triptrap A, Frimberger E, Allescher HD, Ott R, Weigert N, Lorenz R, Classen M: Long-term results of percutaneous transhepatic biliary drainage for benign and malignant bile duct strictures. Scand J Gastroenterol 1998;33:544–549.

28 Guo YX, Li YH, Chen Y, Chen PY, Luo PF, Li Y, Shan H, Jiang ZB: Percutaneous transhepatic metal versus plastic biliary stent in treating malignant biliary obstruction: a multiple center investigation. Hepatobiliary Pancreat Dis Int 2003;2:594–597.

— 366 —

29 Speer AG, Cotton PB, Russell RC, Mason RR, Hatfield AR, Leung JW, MacRae KD, Houghton J, Lennon CA: Randomised trial of endoscopic versus percutaneous stent insertion in malignant obstructive jaundice. Lancet 1987; 2:57–62.

30 Piñol V, Castells A, Bordas JM, Real MI, Llach J, Montañà X, Feu F, Navarro S: Percutaneous self-expanding metal stents versus endoscopic polyethylene endoprostheses for treating malignant biliary obstruction: randomized clinical trial. Radiology 2002;225: 27–34.

31 Voegeli DR, Crummy AB, Weese JL: Percutaneous transhepatic cholangiography, drainage, and biopsy in patients with malignant biliary obstruction. An alternative to surgery. Am J Surg 1985;150:243–247.

32 Hii MW, Gibson RN, Speer AG, Collier NA, Sherson N, Jardine C: Role of radiology in the treatment of malignant hilar biliary strictures. 2. Ten years of single-institution experience with percutaneous treatment. Australas Radiol 2003;47:393–403.

33 Weber A, Gaa J, Rosca B, Born P, Neu B, Schmid RM, Prinz C: Complications of percutaneous transhepatic biliary drainage in patients with dilated and nondilated intrahepatic bile ducts. Eur J Radiol 2009;72:412–417.

34 Tsuyuguchi T, Takada T, Kawarada Y, Nimura Y, Wada K, Nagino M, Mayumi T, Yoshida M, Miura F, Tanaka A, Yamashita Y, Hirota M, Hirata K, Yasuda H, Kimura Y, Strasberg S, Pitt H, Büchler MW, Neuhaus H, Belghiti J, de Santibanes E, Fan ST, Liau KH, Sachakul V: Techniques of biliary drainage for acute cholangitis: Tokyo Guidelines. J Hepatobiliary Pancreat Surg 2007;14:35–45.

35 Cho HC, Lee JK, Lee KH, Lee KT, Paik S, Choo SW, Do YS, Choo IW: Are endoscopic or percutaneous biliary drainage effective for obstructive jaundice caused by hepatocellular carcinoma? Eur J Gastroenterol Hepatol 2011;23:224–231.

36 Wiersema MJ, Sandusky D, Carr R, Wiersema LM, Erdel WC, Frederick PK: Endosonography-guided cholangiopancreatography. Gastrointest Endosc 1996;43:102–106.

37 Giovannini M, Moutardier V, Pesenti C, Bories E, Lelong B, Delpero JR: Endoscopic ultrasound-guided bilioduodenal anastomosis: a new technique for biliary drainage. Endoscopy 2001;33:898–900.

38 Giovannini M, Dotti M, Bories E, Moutardier V, Pesenti C, Danisi C, Delpero JR: Hepaticogastrostomy by echo-endoscopy as a palliative treatment in a patient with metastatic biliary obstruction. Endoscopy 2003; 35:1076–1078.

39 Mallery S, Matlock J, Freeman ML: EUS-guided rendezvous drainage of obstructed biliary and pancreatic ducts: report of 6 cases. Gastrointest Endosc 2004;59:100–107.

40 Kahaleh M, Wang P, Shami VM, Tokar J, Yeaton P: EUS-guided transhepatic cholangiography: report of 6 cases. Gastrointest Endosc 2005;61:307–313.

41 Püspök A, Lomoschitz F, Dejaco C, Hejna M, Sautner T, Gangl A: Endoscopic ultrasound-guided therapy of benign and malignant biliary obstruction: a case series. Am J Gastroenterol 2005;100:1743–1747.

42 Tarantino I, Barresi L, Fabbri C, Traina M: Endoscopic ultrasound-guided biliary drainage. World J Gastrointest Endosc 2012; 4:306–311.

Real-Life Clinical Practice with Sorafenib in Advanced Hepatocellular Carcinoma: A Single-Center Experience

Masatoshi Kudo   Kazuomi Ueshima   Tadaaki Arizumi

Department of Gastroenterology and Hepatology, Kinki University School of Medicine, Osaka, Japan

Abstract

To evaluate the efficacy of sorafenib monotherapy, we enrolled 188 patients with hepatocellular carcinoma (HCC) who had undergone sorafenib monotherapy during a 3-year period from May 2009 to June 2012. Median overall survival was 15.6 months, and the 1- and 2-year survival rate was 54.4 and 32.2%, respectively, showing a relatively favorable treatment outcome. In addition, outcome was more favorable in earlier TNM stages. HCC patients with stage IVB had a better outcome than those with stage IVA, indicating the involvement of vascular invasion had poor prognosis. Outcome was more favorable in patients with Child-Pugh class A than in those with Child-Pugh class B. Patients in the long-term treatment group, who received sorafenib for ≥90 days, also showed a favorable outcome compared with those in the short-term treatment group, in which the administration period was <90 days. Multivariate analysis revealed treatment duration as a significant prognostic factor. Furthermore, patients who received post-sorafenib treatment had a better outcome than those who did not.

Copyright © 2012 S. Karger AG, Basel

Introduction

Sorafenib is an oral molecular targeted agent which is currently the only approved targeted agent worldwide [1, 2]. The Raf/MEK/ERK pathway, also known as the MAP kinase pathway, is a downstream pathway shared by VEGFR, PDGFR, and EGFR, and its activation has been shown to mediate the growth and survival of hepatocellular carcinoma (HCC). Sorafenib inhibits the growth of HCC by suppressing the serine/threonine kinase activity of the C-Raf and B-Raf components of the MAP kinase pathway and by inhibiting FLT-3 and c-KIT activities. It also serves as a multikinase inhibitor that suppresses the tyrosine kinase activity of VEGFR and PDGFR, thereby inhibiting the growth of endothelial cells and pericytes, as well as angiogenesis [3–7]. The present study investigated the efficacy and situations associated with sorafenib in real-life clinical practice.

Aim

In Japan, sorafenib has been administered in accordance with the consensus-based treatment algorithm for hepatocellular carcinoma proposed by the Japan Society of Hepatology [8–10] (fig. 1). According to this algorithm,

Masatoshi Kudo, MD, PhD
Department of Gastroenterology and Hepatology
Kinki University School of Medicine, 377-2, Ohno-Higashi
Osaka-Sayama, Osaka 589-8511 (Japan)
E-Mail m-kudo@med.kindai.ac.jp

Fig. 1. Consensus-based treatment algorithm for HCC proposed by the Japan Society of Hepatology updated in 2010. Sorafenib is recommended for Child-Pugh A patients with extrahepatic spread, vascular invasion and TACE/HAIC failure patients.

Within the figure:

HCC

Extrahepatic spread: No / Yes

Liver function: Child-Pugh A/B / Child-Pugh C / Child-Pugh B/C / Child-Pugh A

Vascular invasion: No / Yes / No / Yes

Number: Single / 1–3 / 4 or more / Within Milan[7] criteria and age ≤65 / Exceeding Milan criteria or age >65

Size: Hypovascular early HCC[3] / ≤3 cm / >3 cm

Treatment:
- Intensive follow-up
- Ablation

- Resection
- Ablation

- Resection
- TACE
- TACE + ablation[4]

- TACE[5]
- HAIC[5]
- Resection[6]
- Ablation[6]

Sorafenib[5] (TACE or HAIC refractory, Child-Pugh A)

- HAIC (Vp3,4)[8]
- Sorafenib (Vp3,4)[8]
- TACE (Vp1,2)[9]
- Resection (Vp1,2)[9]

- Transplantation
- TACE/Ablation for Child-Pugh C patients[10]

Palliative care

Sorafenib

1, 2

[1] Treatment should be performed as if extrahepatic spread is negative, when extrahepatic spread is not regarded as a prognostic factor.

[2] Sorafenib is the first choice of treatment in this setting as a standard of care.

[3] Intensive follow-up observation is recommended for hypovascular nodules by the Japanese Evidence-Based Clinical Practice Guidelines. However, local ablation therapy is frequently performed in the following cases: (1) when the nodule is diagnosed pathologically as early HCC, (2) when the nodules show decreased uptake on Gd-EOB-MRI, or (3) when the nodules show decreased portal flow by CTAP, since these nodules are known to frequently progress to the typical advanced HCC.

[4] Even for HCC nodules exceeding 3 cm in diameter, combination therapy of TACE and ablation is frequently performed when resection is not indicated.

[5] TACE is the first choice of treatment in this setting. HAIC using an implanted port is also recommended for TACE refractory patients. The regimen for this treatment is usually low-dose FP (5-FU+CDDP) or intra-arterial 5-FU infusion combined with systemic interferon therapy. Sorafenib is also a treatment of choice for TACE refractory patients with Child-Pugh A liver function.

[6] Resection is sometimes performed even when number of nodules is >4. Furthermore, ablation is sometimes performed in combination with TACE.

[7] Milan criteria: tumor size ≤3 cm and tumor number ≤3; or solitary tumor ≤5 cm. Even when liver function is good (Child-Pugh A/B), transplantation is sometimes considered for frequently recurring HCC patients.

[8] Sorafenib and HAIC are recommended for HCC patients with Vp3 (portal invasion at the 1st portal branch) or Vp4 (portal invasion at the main portal branch).

[9] Resection and TACE are frequently performed when portal invasion is minimal such as with Vp1 (portal invasion at the 3rd or higher peripheral portal branch) or Vp2 (portal invasion at the 2nd portal branch).

[10] Local ablation therapy or subsegmental TACE is performed even for Child-Pugh C patients when transplantation is not indicated and in the absence of hepatic encephalopathy, uncontrollable ascites, and low bilirubin level (<3.0 mg/dl). However, it is regarded as an experimental treatment since no evidence of its survival benefit in Child-Pugh C patients has been observed. A prospective study is necessary to clarify this issue. Even in Child-Pugh A/B patients, transplantation is sometimes performed for relatively young patients with frequently or early recurring HCC after curative treatments.

Table 1. Patient background

Age (range), years	72.5 (31–90)
Male/female	141/47
HBV/HCV/NBNC	35/99/54
Child-Pugh A/B	149/39
Stage II/III/IVA/IVB	21/65/44/58
ALB (range), g/dl	3.6 (1.5–4.9)
BIL (range), mg/dl	0.7 (0.2–3.0)
PT (range), %	80.4 47.0–120.0)
WBC (range), /μl	4,750 (1,700–16,800)
Neutrophils (range), /μl	2,741.7 (397.8–13,524)
Hb (range), g/dl	12.3 (6.8–16.7)
PLT (range), /μl	13.9 (4.2–76.8)

Table 2. Response rate and disease control rate (n = 188)

	CR	PR	SD	PD	RR	DCR
RECIST 1.1	2	14	106	66	8.5	64.8
mRECIST	5	29	91	63	18.0	66.5
RECICL	5	30	88	65	18.6	65.4

Fig. 2. Flow chart of patient selection in this study. A total of 188 patients who were treated only with sorafenib were selected.

sorafenib is indicated for Child-Pugh A stage HCC cases with extrahepatic spread, or vascular invasion. Sorafenib is also recommended in Child-Pugh A cases where transcatheter arterial chemoembolization (TACE) and hepatic arterial infusion chemotherapy (HAIC) are not indicated. Here we investigated 236 HCC patients treated with sorafenib at Kinki University Hospital, Osaka, Japan, to elucidate the efficacy of sorafenib treatment and the characteristics of the clinical outcome.

Patients and Methods

We investigated 236 patients with HCC who started sorafenib therapy between May 20, 2009 and June 15, 2012. We excluded 43 patients who had received combination therapy with HAIC or TACE in a clinical trial; this left 193 patients who had received sorafenib monotherapy. After excluding a further 5 patients whose treatment period from the start of sorafenib to the initiation of this study was less than 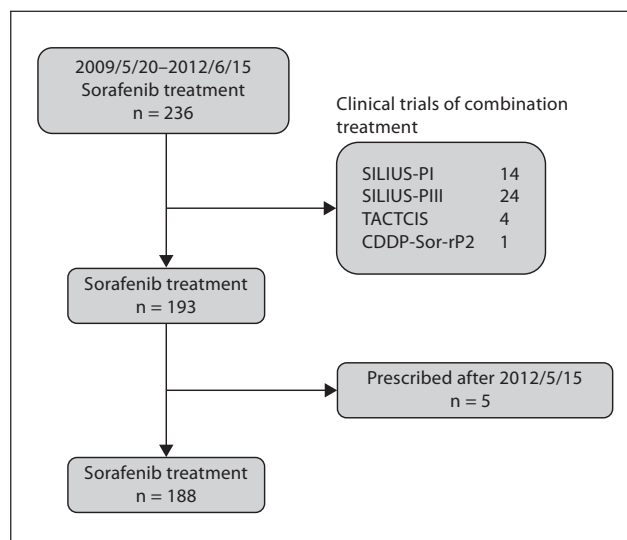1 month, 188 patients were enrolled (fig. 2). Study issues were prior treatment history, overall survival (OS) rate, and survival rate by TNM stage, Child-Pugh stage, etiology, and sorafenib treatment period. We also investigated survival-related factors and the effect of post-sorafenib treatment on the survival of patients. The log-rank test was used for statistical analysis.

Result

Patient Background

Patient background is shown in table 1. Patients, predominantly men, had a median age of 72.5 years. HCC was derived mostly from hepatitis C, followed by non-B, non-C HCC and hepatitis B (HBV)-related HCC. There were 149 Child-Pugh A cases, compared with the 39 cases of Child-Pugh B. Many patients were classified as TNM stage IVA/IVB. Levels of albumin and bilirubin, prothrombin time, white blood cell count, and platelet count were within the normal range.

Prior Treatment

Prior treatment in the 188 cases included 48 resections, 84 local ablations, 129 cases of TACE [11], and 22 cases of HAIC (fig. 3). Patients underwent TACE a median of 4.5 times, with 1 patient undergoing TACE 17 times (fig. 4).

Objective Response Rate and Disease Control Rate

The objective response rate was 8.5, 18.0, and 18.6% according to RECIST 1.1, modified RECIST [12] and Response Criteria in Cancer of the Liver (RECICL) [13]. The disease control rate was 64.8, 66.5, and 65.4% according to RECIST 1.1, modified RECIST and RECICL (table 2), respectively. Two cases of complete response were already reported [8].
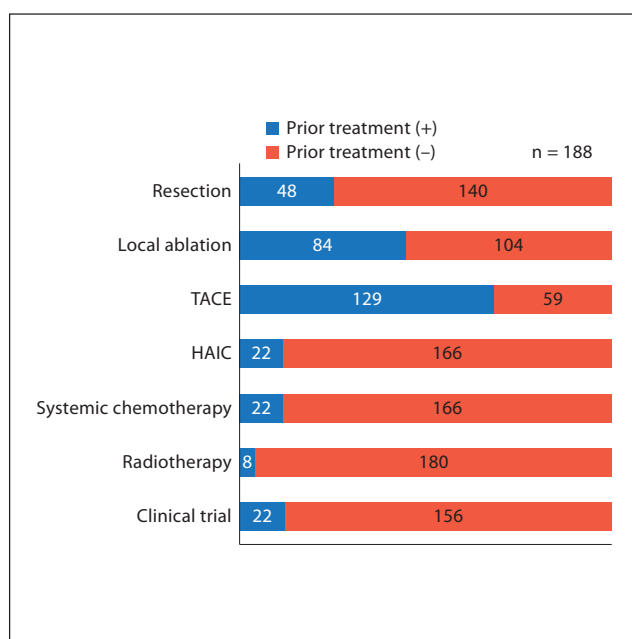
Fig. 3. Prior treatment history before sorafenib treatment. There are several overlapping cases.
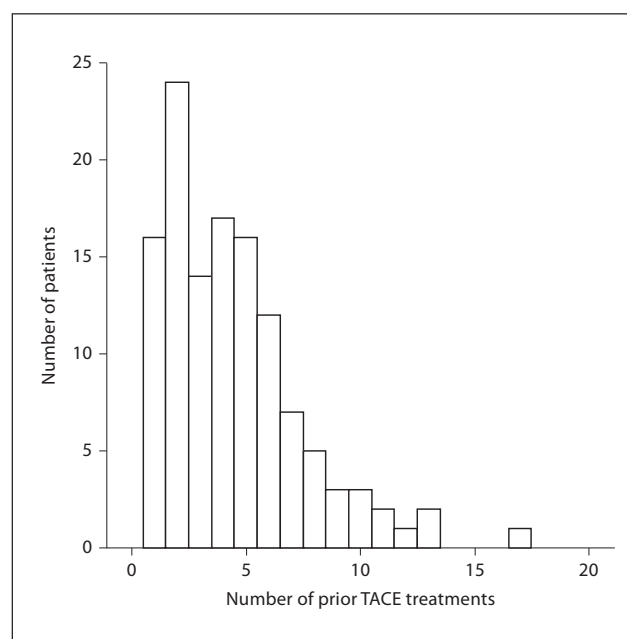

Fig. 4. Number of prior TACE treatments. Median number of TACE treatments was 4.5 (range 1–17).
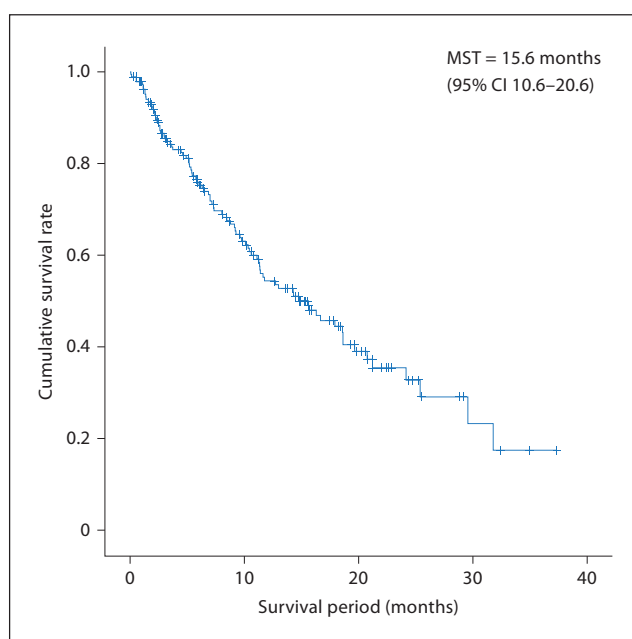

Fig. 5. OS of the 188 patients who underwent treatment with sorafenib alone. Median survival time was 15.6 months (95% CI 10.6–20.6), and the 1- and 2-year survival rate was 54.4 and 32.7%, respectively.
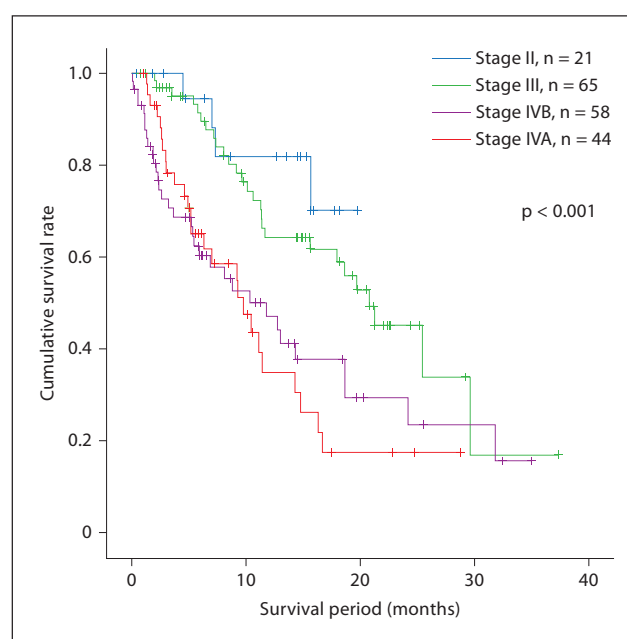
Fig. 6. OS according to TNM stage.
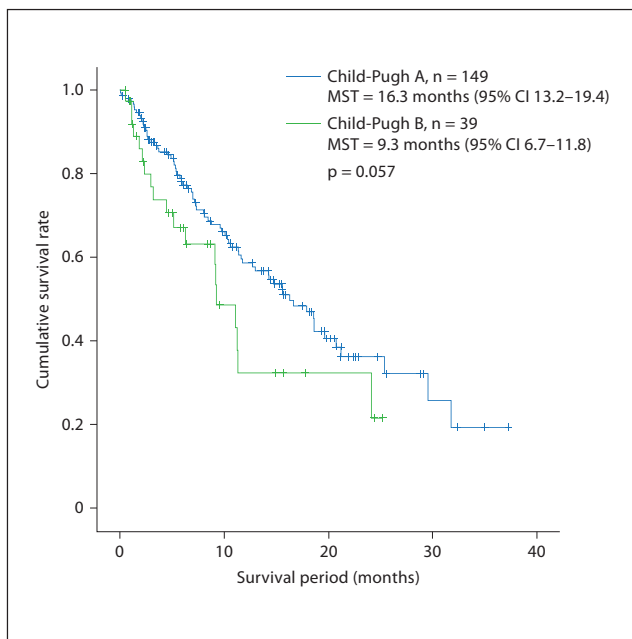
Fig. 7. OS according to Child-Pugh stage.
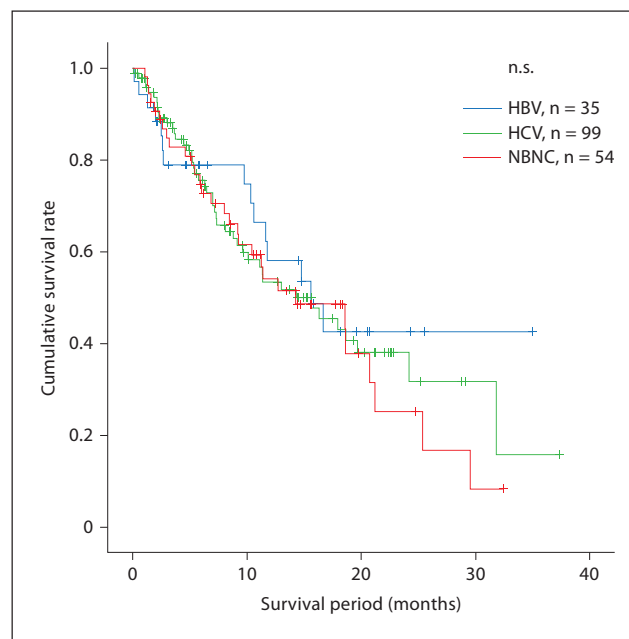
Fig. 8. OS according to background liver diseases.

Overall Survival

Median OS was 15.6 months, which was fairly favorable compared with the SHARP study [1] and the Asian-Pacific Study [2]. The 1- and 2-year survival rate was 54.4 and 32.7%, respectively (fig. 5).

OS according to TNM Stage

Analysis of OS according to TNM stage revealed that stage II patients had a significantly favorable outcome, followed by stage III and IV patients, with significant differences noted between stages (fig. 6). The most likely reason for the better outcome in stage IVB patients, compared with those in stage IVA, is that the stage IVA patients had vascular invasion, meaning that they started out as a group of patients with poor prognosis and resistance to sorafenib.

OS according to Child-Pugh Stage

Child-Pugh A HCC patients had a median OS of 16.3 months, which was longer, although insignificantly, than the OS of 9.3 months in Child-Pugh B patients (fig. 7).

OS according to Etiology

No significant differences in clinical outcome were observed between HCC caused by hepatitis B, C, non-B, and non-C, thus showing no etiology-related differences [14] (fig. 8).

OS according to Treatment Duration

Patients who had received sorafenib for ≥90 days had a significantly longer median OS of 20.8 months compared with those who received sorafenib for <90 days (5.9 months) (fig. 9). This indicates that a better clinical outcome was achieved at higher sorafenib doses.

OS-Related Factors

In univariate analysis, factors associated with OS were sorafenib treatment duration, portal venous invasion, extrahepatic metastasis, albumin, bilirubin, white blood cell count, AFP, AFP-L3, and PIVKA-II (table 3). Multivariate analysis showed that the duration of sorafenib treatment had the highest hazard ratio and significantly contributed to patient survival. Hepatic functional reserve indicators, such as bilirubin and the tumor markers AFP and DCP, were also factors contributing to OS (table 4).

Post-Sorafenib Treatment

Patients with post-sorafenib therapy had a significantly longer median OS of 17.7 months compared with 2.6 months in patients without post-sorafenib therapy
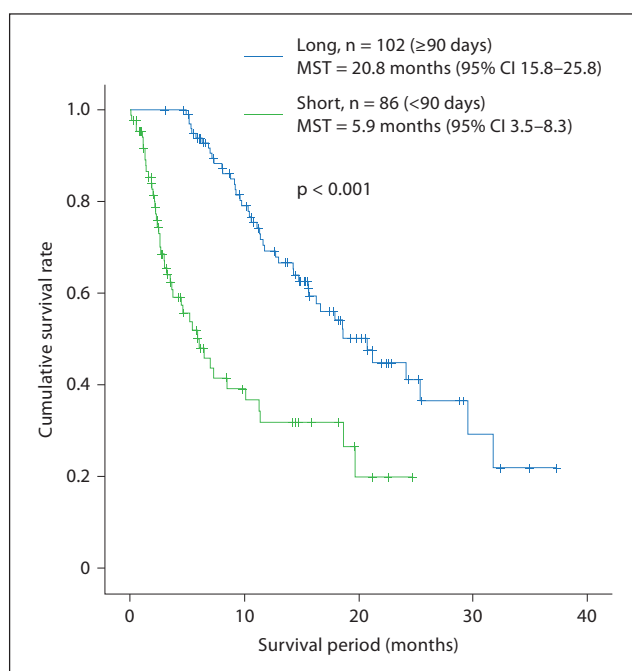
Fig. 9. OS according to treatment duration with sorafenib.
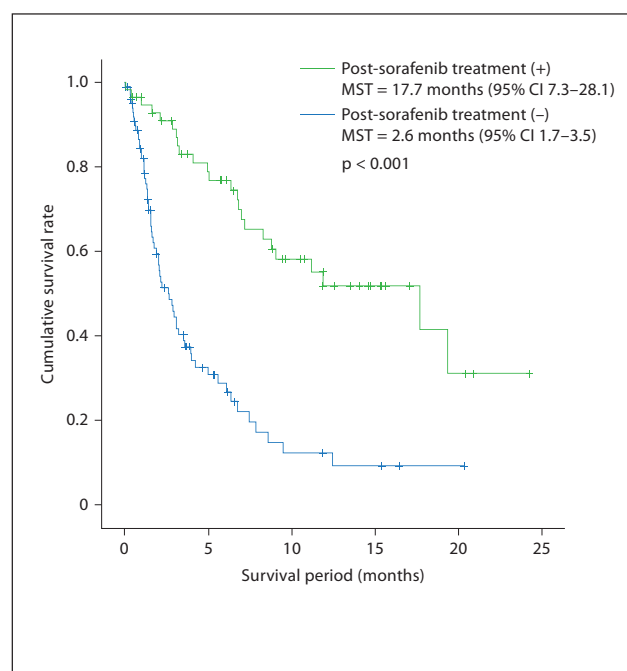
Fig. 10. OS according to whether or not post-sorafenib treatment was performed.

Table 3. Univariate analysis of factors affecting OS

Factor	Category	p value	Hazard ratio	95% CI lower limit	upper limit
Treatment duration	<90 days ≥90 days	<0.001	1 0.302	0.196	0.465
Portal invasion	no yes	0.002	1 1.420	1.130	1.783
Extrahepatic spread	no yes	0.017	1 1.736	1.098	2.745
ALB	≥3.6 <3.6	0.026	1 1.597	1.053	2.421
BIL	<1.0 ≥1.0	<0.001	1 2.315	1.514	3.541
WBC	>5,000 ≤5,000	0.029	1 0.795	0.646	0.978
AFP	<400 ≥400	<0.001	1 1.606	1.301	1.982
DCP (PIVKA-II)	<1,000 ≥1,000	<0.001	1 1.685	1.092	2.601
AFP-L3	<10 ≥10	0.012	1 1.888	1.232	2.892

Table 4. Multivariate analysis of factors affecting OS

Factor	Category	p value	Hazard ratio	95% CI lower limit	upper limit
Treatment duration	<90 days ≥90 days	<0.001	1 0.349	0.222	0.550
BIL	<1.0 ≥1.0	0.016	1 1.738	1.110	2.721
AFP	<400 ≥400	0.025	1 1.705	1.068	2.721
DCP (PIVKA-II)	<1,000 ≥1,000	0.001	1 2.300	1.437	3.683

Fig. 11. Post-sorafenib treatment was performed in 57 of the 188 patients.

(fig. 10). Post-sorafenib therapy included 26 cases of second-line targeted therapy in clinical trials, 20 cases of TACE, 7 cases of HAIC, 3 cases of systemic chemotherapy, and 1 resection (fig. 11).

Discussion

Here we investigated the clinical outcome of sorafenib therapy. Many patients were already on other treatment regimens such as TACE or had undergone resection prior to sorafenib therapy. Despite undergoing sorafenib therapy after adequately receiving another treatment, OS was 15.6 months, which is relatively favorable. This suggests that starting treatment with sorafenib at the early stage and continuing therapy for as long as possible improves survival. In fact, 102 of the 188 patients were able to continue sorafenib for over 3 months. It became apparent that sorafenib needs to be administered for a long time, with termination and dose reduction when necessary, to prolong OS. Of course, Child-Pugh A patients with a better hepatic functional capability and those with better TNM stages were expected to have a better outcome. However, multivariate analysis suggested the necessity of performing sorafenib therapy for >90 days, and if necessary, post-sorafenib therapy such as second-line targeted therapy, TACE, or HAIC to prolong survival time. It is possible to assume that the present patients stayed on sorafenib for a long duration and had a favorable outcome simply because they were in a good condition as far as tumor status and liver function status were concerned. Nonetheless, to improve clinical outcome, it is necessary to recognize patients with favorable prognostic factors, but without applicable locoregional therapy, and to start long-term administration of sorafenib.

Conclusion

To improve the survival rate of HCC patients, when locoregional therapy is not indicated, patients should be placed immediately on sorafenib therapy and continue the drug for as long as possible, even with dose reduction and interruption.
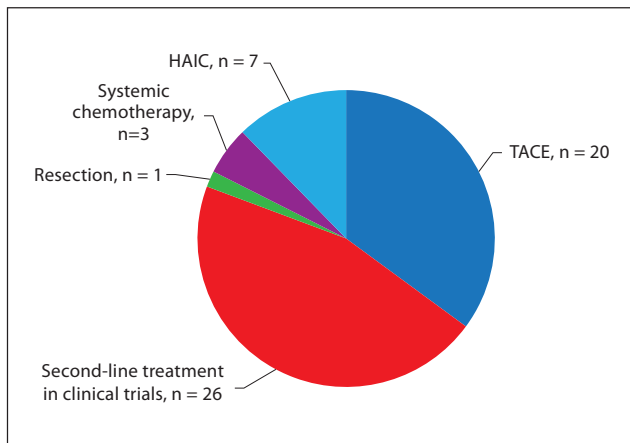
Disclosure Statement

The authors have no conflicts of interest to disclose.

References

1 Llovet JM, Ricci S, Mazzaferro V, Hilgard P, Gane E, Blanc JF, de Oliveira AC, Santoro A, Raoul JL, Forner A, et al: Sorafenib in advanced hepatocellular carcinoma. N Engl J Med 2008;359:378–390.
2 Cheng AL, Kang YK, Chen Z, Tsao CJ, Qin S, Kim JS, Luo R, Feng J, Ye S, Yang TS, et al: Efficacy and safety of sorafenib in patients in the Asia-Pacific region with advanced hepatocellular carcinoma: a phase III randomised, double-blind, placebo-controlled trial. Lancet Oncol 2009;10:25–34.
3 Wilhelm SM, Carter C, Tang L, Wilkie D, McNabola A, Rong H, Chen C, Zhang X, Vincent P, McHugh M, et al: BAY 43-9006 exhibits broad spectrum oral antitumor activity and targets the RAF/MEK/ERK pathway and receptor tyrosine kinases involved in tumor progression and angiogenesis. Cancer Res 2004;64:7099–7109.
4 Liu L, Cao Y, Chen C, Zhang X, McNabola A, Wilkie D, Wilhelm S, Lynch M, Carter C: Sorafenib blocks the RAF/MEK/ERK pathway, inhibits tumor angiogenesis, and induces tumor cell apoptosis in hepatocellular carcinoma model PLC/PRF/5. Cancer Res 2006;66:11851–11858.
5 Chang YS, Adnane J, Trail PA, Levy J, Henderson A, Xue D, Bortolon E, Ichetovkin M, Chen C, McNabola A, et al: Sorafenib (BAY 43-9006) inhibits tumor growth and vascularization and induces tumor apoptosis and hypoxia in RCC xenograft models. Cancer Chemother Pharmacol 2007;59:561–574.
6 Kudo M: Current status of molecularly targeted therapy for hepatocellular carcinoma: clinical practice. Int J Clin Oncol 2010;15:242–255.

7 Kudo M: Signaling pathway and molecular-targeted therapy for hepatocellular carcinoma. Dig Dis 2011;29:289–302.

8 Kudo M, Ueshima K: Positioning of a molecular-targeted agent, sorafenib, in the treatment algorithm for hepatocellular carcinoma and implication of many complete remission cases in Japan. Oncology 2010;78(suppl 1):154–166.

9 Kudo M, Izumi N, Kokudo N, Matsui O, Sakamoto M, Nakashima O, Kojiro M, Makuuchi M: Management of hepatocellular carcinoma in Japan: consensus-based clinical practice guidelines proposed by the Japan Society of Hepatology (JSH) 2010 updated version. Dig Dis 2011;29:339–364.

10 Kudo M: Treatment of advanced hepatocellular carcinoma with emphasis on hepatic arterial infusion chemotherapy and molecular targeted therapy. Liver Cancer 2012;1:62–70.

11 Lencioni R: Chemoembolization in patients with hepatocellular carcinoma. Liver Cancer 2012;1:41–50.

12 Lencioni R, Llovet JM: Modified RECIST (mRECIST) assessment for hepatocellular carcinoma. Semin Liver Dis 2010;30:52–60.

13 Kudo M, Kubo S, Takayasu K, Sakamoto M, Tanaka M, Ikai I, Furuse J, Nakamura K, Makuuchi M: Response Evaluation Criteria in Cancer of the Liver (RECICL) proposed by the Liver Cancer Study Group of Japan (2009 Revised Version). Hepatol Res 2010;40:686–692.

14 Kim DY, Han KH: Epidemiology and surveillance of hepatocellular carcinoma. Liver Cancer 2012;1:2–14.

Estimation of liver function using T2* mapping on gadolinium ethoxybenzyl diethylenetriamine pentaacetic acid enhanced magnetic resonance imaging

Takashi Katsube [a,1], Masahiro Okada [b,2], Seishi Kumano [b,2], Izumi Imaoka [b,2], Yuki Kagawa [b,2], Masatoshi Hori [c,3], Kazunari Ishii [b,2], Noboru Tanigawa [d,4], Yasuharu Imai [e,5], Masatoshi Kudo [f,2], Takamichi Murakami [b,*]

[a] Department of Radiology, Shimane University School of Medicine, 89-1 Enya-cho, Izumo, Shimane 693-8501, Japan
[b] Department of Radiology, Kinki University School of Medicine, 377-2 Ohno-Higashi, Osaka-Sayama, Osaka 589-8511, Japan
[c] Department of Radiology, Osaka University Graduate School of Medicine, 2-15 Yamadaoka, Suita, Osaka 565-0871, Japan
[d] Department of Radiology, Kansai Medical University Hirakata Hospital, 2-3-1 Shinmachi, Hirakata, Osaka 573-1191, Japan
[e] Department of Gastroenterology, Ikeda Municipal Hospital, 3-1-18 Johnan, Ikeda, Osaka 563-8510, Japan
[f] Department of Gastroenterology and Hepatology, Kinki University School of Medicine, 377-2 Ohno-Higashi, Osaka-Sayama, Osaka 589-8511, Japan

A R T I C L E   I N F O

A B S T R A C T

Purpose: To investigate the usefulness of T2* mapping of liver on gadolinium ethoxybenzyl diethylene-triamine pentaacetic acid (Gd-EOB-DTPA)-enhanced MRI for estimating liver function.
Materials and methods: 33 patients were classified into 3 groups as follows: normal liver function (NLF) ($n = 7$); mild liver damage (MLD) ($n = 16$) with Child-Pugh A; severe liver damage (SLD) ($n = 10$) with Child-Pugh B. T2*-weighted gradient-echo (T2*W-GRE) and T1-weighted gradient-echo (T1W-GRE) images were obtained before and after Gd-EOB-DTPA administration (3, 8, 13, and 18 min; 5, 10,15, and 20 min; respectively). T2* mapping of liver was calculated from T2*W-GRE, then T2* values of liver and T2* reduction rates of T2* value between pre- and post-contrast enhancement were measured. The increase rates of liver-to-muscle signal intensity (LMS) ratio on T1W-GRE between pre- and post-contrast enhancement were calculated.
Results: T2* values on pre- and post-contrast showed no significant differences among three groups. Significant differences in T2* reduction rates were found among groups, and those of LCB were lower than those of other groups (NLF:MLD:SLD, 3.8:6.0:0.6% at 3 min, 8.2:10.3:1.0% at 8 min, 10.7:11.5:1.2% at 13 min, and 16.1:13.2:3.5% at 18 min, respectively) ($P < 0.05$). Significant differences in increase rates of LMS ratio on T1W-GRE were identified (NLF:MLD:SLD, 1.53:1.46:1.35 at 5 min, 1.68:1.64:1.37 at 10 min, 1.79:1.76:1.44 at 15 min, and 1.89:1.78:1.49 at 20 min, respectively).
Conclusion: T2* reduction rate and increase rate of LMS ratio on T1W-GRE may allow us estimation of liver function according to Child-Pugh score.

1. Introduction

Estimation of liver function is essential for preventing postoperative hepatic failure and for the clinical management of patients with hepatic dysfunction. Scintigraphy with Tc[99m] iminodiacetic acid (IDA) [1] and Tc[99m] galactosyl human serum albumin (GSA) [2] are currently available for estimation of liver function, but the spatial resolution of those imaging modalities remains unsatisfactory and radioactive agents must be used. As a more recent development, T2*-weighted gradient-echo (GRE) images of superparamagnetic iron oxide (SPIO)-enhanced magnetic resonance imaging (MRI), which is mediated by phagocytic activity of Kupffer cells, is reportedly useful for evaluating Kupffer cell function with or without liver cirrhosis [3–5].

Recently, gadolinium ethoxybenzyl diethylenetriamine pentaacetic acid (Gd-EOB-DTPA) has come into use in routine clinical practice in many countries. After intravenous injection, Gd-EOB-DTPA is cleared from the body by two routes of elimination: receptor-specific uptake in hepatocytes with subsequent biliary excretion, and glomerular filtration in the kidney with subsequent

urinary excretion. The percentage of hepatobiliary elimination is 63–80% in rats and 32–34% in monkeys [6]. In human, the compound was completely eliminated in urine and feces in almost equal amounts (43.1–53.2% and 41.6–51.2%, respectively) [7]. In the hepatobiliary elimination route, Gd-EOB-DTPA is gradually taken up by hepatocytes and eventually excreted via the biliary pathway without any change to the chemical structure. In daily clinical use, Gd-EOB-DTPA is used to evaluate focal liver lesions, such as hepatocellular carcinoma (HCC) or liver metastasis, on T1-weighted imaging [8,9]. As signal intensity of the liver after Gd-EOB-DTPA administration depends on uptake by hepatocytes and bile excretion, Gd-EOB-DTPA is regarded as a useful imaging technique to evaluate liver functions [10–13], as well as to evaluate focal liver lesions.

In the area of MRI, T2* relaxometry has recently received increased attention as a quantitative analysis tool. Gd-EOB-DTPA not only has a T1 value-shortening effect, but also effects on T2 and T2* values. The utility of MRI analysis using T2* values thus motivated us to investigate correlations between liver function and T2* value change in the liver using Gd-EOB-DTPA.

The present study investigated the ability of T2* value mapping of liver parenchyma on Gd-EOB-DTPA-enhanced MRI for the estimation of liver function.

2. Materials and methods

2.1. Patients

This study was followed the principles of the Declaration of Helsinki. Informed consent was obtained from all patients who underwent contrast-enhanced MRI with Gd-EOB-DTPA. As Gd-EOB-DTPA enhanced MRI of the liver was performed as a routine abdominal scan to evaluate the presence of HCC, approval by the institutional ethics committee was obtained for this study.

Subjects comprised 33 adult patients (21 men, 12 women; mean age, 67.8 years) with suspicious liver tumor who underwent Gd-EOB-DTPA-enhanced MRI in our university hospital. Chronic hepatitis or hepatic cirrhosis was presented in 26 patients. Causes of chronic hepatitis or hepatic cirrhosis were hepatitis C ($n = 18$), hepatitis B ($n = 4$), alcohol abuse ($n = 2$), and cryptogenic ($n = 2$). Chronic hepatitis and hepatic cirrhosis of patients were confirmed by clinical manifestation, blood examination (albumin, total bilirubin, aspartate aminotransferaes, alanine aminotransferase, prothrombin time, and platelet count), and imaging findings. The remaining 7 patients had suspected liver metastatic lesion in normal liver parenchyma. They had no or a few metastases (mean tumor numbers 1.0, range 0–3) on Gd-EOB-DTPA enhanced MRI. Metastatic lesions those were thought not to influence liver function were included in this study. This means that these lesions were not located in hepatic hilum nor obstruct main bile ducts and blood vessels, neither that the patient of suspected liver metastasis had abnormal hepatobiliary data on blood examination. Finally, all the patients of suspected liver metastatic lesion were included in our study.

No patients of our study had previously undergone hepatic or biliary surgery, or had undergone transarterial chemoembolization, radiofrequency ablation, or percutaneous ethanol injections within 1 month before MRI.

All patients were classified into three groups according to Child-Pugh classification: normal liver function (NLF) group ($n = 7$); mild liver damage (MLD) group ($n = 16$), with chronic hepatitis and Child-Pugh A; and severe liver damage (SLD) group ($n = 10$), with Child-Pugh B or C. Blood examination for Child-Pugh classification was performed within 1 week of MRI.

2.2. Contrast material

Gd-EOB-DTPA (Primovist®; Bayer Schering Pharma AG, Berlin, Germany) was used as a hepatocytic contrast agent. All patients received 0.025 mmol/kg body weight of 0.25 mol/l gadoxetic acid solution administered at a speed of 2 ml/s though an intravenous line placed in a cubital or cephalic vein and flushed with 35 ml of 0.9% saline at the same speed.

2.3. MRI

MRI of the liver was performed using a clinically available 1.5-T system (Gyroscan NOVA; Philips Healthcare). For signal reception in all examinations, an 8-channel phased-array surface coil was used and covered the whole liver. For all patients, T2*-weighted gradient-echo (GRE) sequences (multi-echo 2D fast field echo: repetition time (TR)/echo time (TE), 246/△2.3 ms; flip angle, 30°; field of view (FOV), 296 mm × 370 mm; matrix, 256 × 256; thickness, 10 mm; acquisition time, 16.5 s) were obtained before and at 3, 8, 13, and 18 min after Gd-EOB-DTPA administration. Fat-suppressed T1-weighted GRE sequences (3D turbo field echo: TR/TE, 2.13/4.31 ms; flip angle, 15°; FOV, 306 mm × 380 mm; matrix, 512 × 512; thickness, 5 mm; acquisition time, 20 s) were obtained before and at 5, 10, 15, and 20 min after Gd-EOB-DTPA administration.

2.4. Image analysis

T2* relaxation time was calculated from multi-echo T2*-GRE by using the Philips Research Integrated Development Environment (PRIDE) T2* fitting tool (Philips Healthcare, Best, Netherlands) [14]. Assuming a mono-exponential decay and a liner field variation ΔB_0, the signal intensity is related to the TE according to the following equation:

$$S_{\Delta B_0}(\text{TE}) = S_0 \cdot \exp\left(\frac{-\text{TE}}{\text{T2*}}\right) \cdot \left[\frac{\sin(\gamma \cdot \Delta B_0/2 \cdot \text{TE})}{\gamma \cdot \Delta B_0/2 \cdot \text{TE}}\right]$$

TE is the gradient echo time and S_0 is the signal intensity at TE = 0. Based on this equation, PRIDE software can depict T2* values on a pixel-by-pixel basis in a color distribution map (T2* mapping image).

For T2* value assessment of the liver, regions of interest (ROIs) were drawn manually in the liver on a T2* mapping image from PRIDE obtained before and at 3, 8, 13, and 18 min after Gd-EOB-DTPA administration. Evaluation of representative liver T2* values was performed by fitting an appropriate model to the signal decay within the ROIs. Global liver T2* value was evaluated using a pixel-wise technique and optimized signal decay model.

Five ROIs (range, 50–100 pixels) were placed in liver parenchyma without focal hepatic lesions, major branches of the portal or hepatic veins, or imaging artifacts. For reproducible ROIs before and after Gd-EOB-DTPA administration, every effort was made to place ROIs at the same positions in the liver. Mean T2* value for the 5 ROIs was considered as the representative T2* value for the liver. In addition, reduction rate in T2* value between pre- and post-Gd-EOB-DTPA enhancement was calculated using the following definition:

$$\text{Reduction rate of T2* value} = \left[\frac{\text{T2*pre} - \text{T2*post}}{\text{T2*pre}}\right] \times 100 \quad (\%)$$

To evaluate signal intensity changes in liver parenchyma on T1-weighted GRE images, the liver-to-muscle signal intensity (LMS) ratio between signal intensities of liver parenchyma and erector spine muscle was calculated before and at 5, 10, 15, and 20 min after injection of Gd-EOB-DTPA. Signal intensity of liver parenchyma was

Table 1
T2* values of liver.

Group	Precontrast	Postcontrast phase			
		3 min	8 min	13 min	18 min
NLF	48.5 ± 6.7	46.4 ± 5.7	44.3 ± 7.1	43.2 ± 6.1	40.7 ± 7.3
MLD	46.6 ± 4.5	43.7 ± 3.8	41.1 ± 4.2	41.1 ± 3.8	40.4 ± 4.1
SLD	46.1 ± 7.2	45.7 ± 7.2	45.6 ± 7.6	46.6 ± 6.1	44.4 ± 7.2

Numbers represent mean ± standard deviation (ms).
In comparing the three groups, no significant differences were seen at any time including pre and post contrast ($P > 0.05$).

Table 2
Reduction rates of T2* value of liver.

Group	3 min	8 min	13 min	18 min
NLF	3.9 ± 5.4	8.2 ± 4.4[*]	10.7 ± 5.2[**]	16.1 ± 8.9[**]
MLD	6.0 ± 3.1[**]	10.3 ± 3.9[*,**]	.5 ± 3.4[**]	3.2 ± 4.2[**]
SLD	0.6 ± 4.1[**]	1.0 ± 5.6[*,**]	1.2 ± 4.3[**]	3.5 ± 5.4[**]

Numbers represent mean ± standard deviation (%).
At 3 min, a significant difference was found only between MLD and SLD groups ($P < 0.01$). At 8 min, significant differences were found between NLF and SLD groups ($P < 0.05$), and between MLD and SLD groups ($P < 0.01$). At 13 and 18 min, significant differences were found between NLF and SLD groups ($P < 0.01$). In comparing NLF and MLD groups, no significant differences were seen at any times.

[*] $P < 0.05$.
[**] $P < 0.01$.

taken as the mean value of 5 ROIs placed in liver parenchyma free of focal lesions, major branches of the portal or hepatic veins, or artifacts. Signal intensity of muscle was taken as the mean value of 4 ROIs comprising two ROIs in the right erector spine muscle and two ROIs in the left, with exclusion of ambient fat and artifacts. LMS ratio was calculated using the following equation:

$$\frac{\text{signal intensity of liver parenchyma}}{\text{signal intensity of muscle}}.$$

Increase rates of LMS ratio after GD-EOB-DTPA administration were calculated using the following definition:

$$\text{Increase rate of LMS ratio} = \frac{\text{post-contrast LMS ratio}}{\text{pre-contrast LMS ratio}}.$$

Values at each time point were compared among the 3 groups.

2.5. Statistical analysis

The Friedman test (SPSS; Statistical Package for the Social Sciences) was used to compare the T2* values at each time point in same group, also the same test was used to compare reduction rates of T2* value at each time point in same group. The Bonferroni/Dunn test (Statcel – The Usefull Addin Forms on Excel – 2nd ed.) was used to compare the T2* value at pre- and post-contrast enhancement, reduction rate of T2* value, and increase rate of LMS ratio on T1-weighted GRE imaging among the three groups. A P value less than 0.05 was considered to indicate a significant difference in all statistical tests.
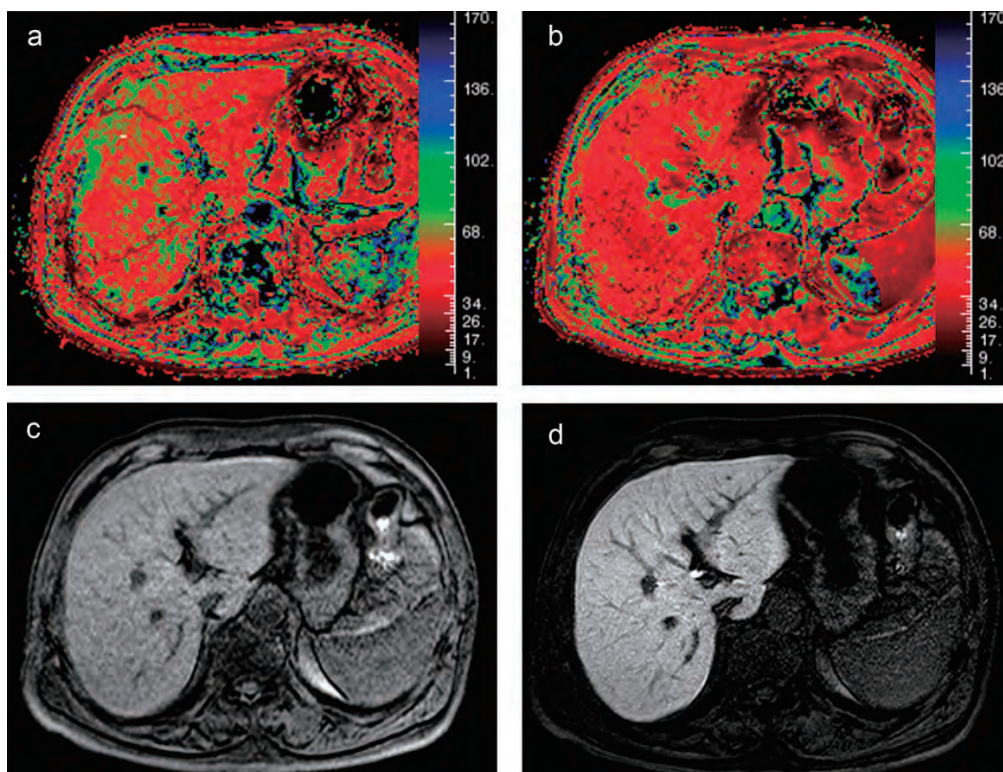
Fig. 1. Normal liver function in a 67-year-old man. Mean T2* values of the liver on pre- and post-contrast at 18 min were 49.7 ms and 39.8 ms, respectively. The reduction rate of T2* value was 19.9%. T2* value mapping of the liver on post-contrast T2* value mapping (b) showed darker red than that on pre-contrast mapping (a). This means that the T2* shortening effect after Gd-EOB-DTPA administration shows as darkening of liver parenchyma on T2* value mapping. On fat-suppressed T1-weighted GRE imaging (TR/TE, 2.13/4.31; flip angle, 15°) of pre- (c) and post-contrast (d) at 20 min, liver-to-muscle signal intensity ratios were 1.63 and 2.73, respectively. The increase rate was 1.67. We also noticed that the window level and width differed on each image (c, d) when paying attention to signal intensity differences in erector spine muscle.
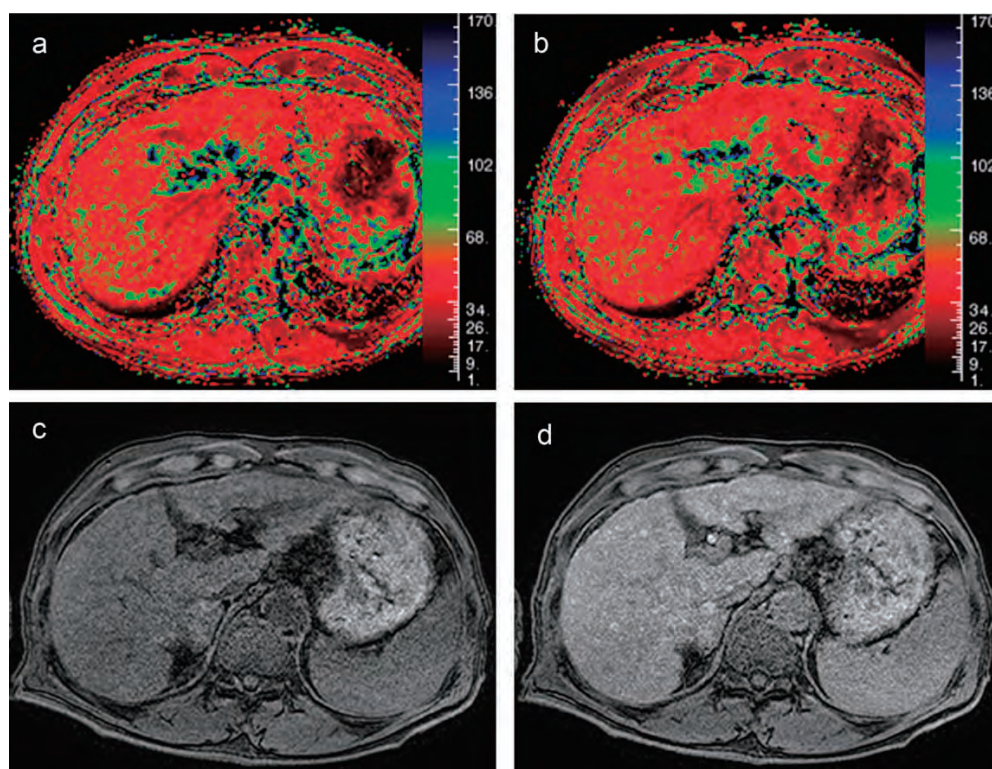
Fig. 2. Hepatic cirrhosis (Child-Pugh B) in a 69-year-old man. Mean T2* values of the liver on pre- and post-contrast imaging at 18 min were 49.8 ms and 49.1 ms, respectively. No signal change in the liver was apparent between pre- (a) and post-contrast (b) T2* value mapping images, as the T2* shortening effect of the liver was weaker than that for normal liver function. On pre- (c) and post-contrast (d) fat-suppressed T1-weighted GRE imaging (TR/TE, 2.13/4.31; flip angle, 15°) at 20 min, liver-to-muscle signal intensity ratios were 1.47 and 2.00, respectively. Increase rate was 1.36.

3. Results

T2* values of NLF and MLD were decreased significantly after Gd-EOB-DTPA administration compared with before ($P < 0.01$). However, T2* values of SLD did not change significantly after Gd-EOB-DTPA administration compared with before ($P > 0.05$). Among the NLF, MLD, and SLD groups, no significant differences in T2* values were seen for pre- and post-enhancement images of the liver ($P > 0.05$) (Table 1).

Means and standard deviations (SDs) of the reduction rate of T2* value are summarized in Table 2. Reduction rates of T2* value of NLF and MLD were increased significantly over time ($P < 0.01$). However, those of SLD did not show statistical significant changes over time ($P > 0.05$). For reduction rate of T2* value, significant differences were found between NLF and SLD groups at 8, 13, and 18 min after Gd-EOB-DTPA administration, and between MLD and SLD groups at 3, 8, 13, and 18 min ($P < 0.05$) (Table 2, Figs. 1 and 2). No significant differences were found between NLF and MLD groups.

Means and SDs of the increase rate of LMS ratio on T1-weighted GRE images are summarized in Table 3. No significant differences were seen among the 3 groups at 5 min ($P > 0.05$). However, at 10, 15 and 20 min, significant differences were found between NLF and SLD groups, and between MLD and SLD groups, although no significant differences were seen between NLF and MLD groups ($P < 0.05$) (Table 3).

4. Discussion

Gd-EOB-DTPA is a contrast medium for T1-weighted imaging, and some reports have described assessment of liver function using

Table 3
Increase rates of liver-to-muscle signal intensity ratio on T1-weighted GRE imaging.

Group	5 min	10 min	15 min	20 min
NLF	1.53 ± 0.16	$1.68 \pm 0.21^{*}$	$1.79 \pm 0.28^{*}$	$1.89 \pm 0.28^{*}$
MLD	1.46 ± 0.16	$1.64 \pm 0.20^{*,**}$	$1.76 \pm 0.24^{*,**}$	$1.78 \pm 0.28^{*}$
SLD	1.35 ± 0.21	$1.37 \pm 0.24^{*,**}$	$1.44 \pm 0.27^{*,**}$	$1.49 \pm 0.29^{*}$

Numbers represent mean ± standard deviation.
At 5 min, no significant difference was found among the three groups ($P > 0.05$). At 10 and 15 min, significant differences were found between NLF and SLD groups ($P < 0.05$), and between MLD and SLD groups ($P < 0.01$). At 20 min, significant differences were found between NLF and SLD groups ($P < 0.05$), and between MLD and NLF groups ($P < 0.05$). No significant differences were apparent between NLF and MLD groups at any time.

* $P < 0.05$.
** $P < 0.01$.

T1-weighted imaging with Gd-EOB-DTPA [10–13]. However, to the best of our knowledge, no reports have described evaluation of liver function on T2*-weighted GRE imaging with Gd-EOB-DTPA, although Gd-EOB-DTPA has the ability to shorten not only T1 values, but also T2* values. Our findings revealed that absolute T2* value of the liver parenchyma on Gd-EOB-DTPA-enhanced MRI can estimate liver function.

We observed significant differences in reduction rate of T2* value among the three groups with different degrees of liver function (NLF, MLD, and SLD). Pre-contrast T2* values of the liver showed no significant difference among the three groups in our study, suggesting that differences in reduction rates of T2*value were independent of the baseline signal intensity for the liver. At 3 min after Gd-EOB-DTPA administration, no significant difference in reduction rate of T2* value was seen between NLF and

SLD groups. This was thought to occur because contrast media was mainly in the vascular and interstitial compartments at 3 min after injection and uptake of Gd-EOB-DTPA in hepatocytes is insufficient even in the normal liver at 3 min after injection. So reduction rate of T2* value at 3 min after injection does not really reflect hepatic uptake, but those of T2* value between MLD and SLD showed significant difference. Therefore, hepatocyte phase images with adequate liver enhancement are recommended to be obtained about 15–20 min after contrast injection.

Reduction rates of T2* value showed no significant difference between NLF and MLD groups. This means normal and mild liver functional impairment is hard to distinguish using Gd-EOB-DTPA, given the relative absence of aberrations in levels of serum albumin, bilirubin, prothrombin activity, ascites, and encephalopathy relating to Child-Pugh classification.

Motosugi et al. reported that the liver–spleen contrast ratio during hepatocyte phase after Gd-EOB-DTPA administration on T1-weighted GRE was statistically correlation with indocyanine green clearance tests and Child-Pugh classification, and suggested the possibility of evaluating liver function by using Gd-EOB-DTPA enhanced MR imaging [15]. The present study also measured the increase rate of LMS ratio on T1-weighted GRE imaging as compared with T2* mapping, confirming that the increase rate of LMS on T1-weighted GRE imaging can estimate liver function similar to the reduction rate in T2* value.

However, quantitative comparison of signal intensity in each image of pre- and post-contrast enhancement did not show any straightforward relationship, as the window level and width of MRI differs with every image. This means that signal intensity on T1-weighted GRE imaging may change depending on the pulse sequence designed by different MRI system manufacturers. We therefore cannot directly compare signal intensities alone using ROIs of hepatic parenchyma. Conversely, T2* value is an absolute value, and is unaffected by these different factors.

Organic anion-transporting polypeptide 1 (OATP1) is known to mediate uptake of Gd-EOB-DTPA by hepatocytes and multidrug resistance protein 2 (MRP2) mediates biliary excretion of Gd-EOB-DTPA [16,17]. In addition, expression of OATP1 and MRP2 is reportedly decreased in hepatitis and cirrhosis [18,19]. The reduction rate in T2* value of the SLD group was very small compared to those of the NLF and MLD groups. Hypofunction of OATP1 and/or MRP2 may lead to decreased uptake of Gd-EOB-DTPA by hepatocytes in the SLD group.

The present study showed some limitations. Our group classification may not be precisely reflected histological hepatic damage, because of the lack of histological proof in all patients. However, our data of T2* mapping were highly correlated with Child-Pugh classification. So, our data suggest that we can evaluate segmental liver function correlated with Child-Pugh classification by the T2*mapping technique. We obtained images until 20 min after Gd-EOB-DTPA administration, so signal changes in MRI were not clear after 20 min. However, Reimer et al. mentioned that no further increase in liver enhancement was seen at 45 min after Gd-EOB-DTPA administration in comparison with that at 20 min [20]. With daily clinical use, the ability to evaluate imaging within around 20 min after Gd-EOB-DTPA administration appears desirable. The number of study population was not so many in this study. However, the significant difference could be seen in the number.

5. Conclusion

The reduction rate of T2* value after Gd-EOB-DTPA injection may allow estimation of the grade of liver function according to Child-Pugh score, as same with the increase rate of LMS ratio on T1-weighted GRE imaging.

Conflict of interest

The authors declare that they do not have any affiliation with or financial relationship/interest in a commercial organization that could pose a conflict of interest.

References

[1] Juni JE, Reichle R. Measurement of hepatocellular function with deconvolutional analysis: application in the differential diagnosis of acute jaundice. Radiology 1990;177(1):171–5.
[2] Kwon AH, Ha-Kawa SK, Uetsuji S, et al. Preoperative determination of the surgical procedure for hepatectomy using technetium-99m-galactosyl human serum albumin (99mTc-GSA) liver scintigraphy. Hepatology 1997;25(2):426–9.
[3] Tanimoto A, Yuasa Y, Shinmoto H, et al. Superparamagnetic iron oxide-mediated hepatic signal intensity change in patients with and without cirrhosis: pulse sequence effects and Kupffer cell function. Radiology 2002;222(3):661–6.
[4] Yamashita Y, Yamamoto H, Hirai A, Yoshimatsu S, Baba Y, Takahashi M. MR imaging enhancement with superparamagnetic iron oxide in chronic liver disease: influence of liver dysfunction and parenchymal pathology. Abdom Imaging 1996;21(4):318–23.
[5] Murakami T, Kim T, Takamura M, et al. Evaluation of regional liver damage by magnetic resonance imaging with superparamagnetic iron oxide in rat liver. Dig Dis Sci 2001;46(1):148–55.
[6] Schuhmann-Giampieri G, Schmitt-Willich H, Press WR, et al. Preclinical evaluation of Gd-EOB-DTPA as a contrast agent in MR imaging of the hepatobiliary system. Radiology 1992;183(1):59–64.
[7] Hamm B, Staks T, Mühler A, et al. Phase I clinical evaluation of Gd-EOB-DTPA as a hepatobiliary MR contrast agent: safety, pharmacokinetics, and MR imaging. Radiology 1995;195(3):785–92.
[8] Saito K, Shindo H, Ozuki T, et al. Gd-EOB-DTPA enhanced MRI for hepatocellular carcinoma: quantitative evaluation of tumor enhancement in hepatobiliary phase. Magn Reson Med Sci 2005;4(1):1–9.
[9] Fujita M, Yamamoto R, Fritz-Zieroth B, et al. Contrast enhancement with Gd-EOB-DTPA in MR imaging of hepatocellular carcinoma in mice: a comparison with superparamagnetic iron oxide. J Magn Reson Imaging 1996;6(3):472–7.
[10] Tsuda N, Okada M, Murakami T. Potential of gadolinium-ethoxybenzyl-diethylenetriamine pentaacetic acid (Gd-EOB-DTPA) for differential diagnosis of nonalcoholic steatohepatitis and fatty liver in rats using magnetic resonance imaging. Invest Radiol 2007;42(4):242–7.
[11] Shimizu J, Dono K, Gotoh M, et al. Evaluation of regional liver function by gadolinium-EOB-DTPA-enhanced MR imaging. Dig Dis Sci 1999;44(7):1330–7.
[12] Schmitz SA, Mühler A, Wagner S, Wolf KJ. Functional hepatobiliary imaging with gadolinium-EOB-DTPA. A comparison of magnetic resonance imaging and 153gadolinium-EOB-DTPA scintigraphy in rats. Invest Radiol 1996;31(3):154–60.
[13] Kim T, Murakami T, Hasuike Y, et al. Experimental hepatic dysfunction: evaluation by MRI with Gd-EOB-DTPA. J Magn Reson Imaging 1997;7(4):683–8.
[14] Dahnke H, Schaeffter T. Limits of detection of SPIO at 3.0 T using T2 relaxometry. Magn Reson Med 2005;53(5):1202–6.
[15] Motosugi U, Ichikawa T, Sou H, et al. Liver parenchymal enhancement of hepatocyte-phase images in Gd-EOB-DTPA-enhanced MR imaging: which biological markers of the liver function affect the enhancement? J Magn Reson Imaging 2009;30(5):1042–6.
[16] Pascolo L, Cupelli F, Anelli PL, et al. Molecular mechanisms for the hepatic uptake of magnetic resonance imaging contrast agents. Biochem Biophys Res Commun 1999;257(3):746–52.
[17] van Montfoort JE, Stieger B, Meijer DK, Weinmann HJ, Meier PJ, Fattinger KE. Hepatic uptake of the magnetic resonance imaging contrast agent gadoxetate by the organic anion transporting polypeptide Oatp1. J Pharmacol Exp Ther 1999;290(1):153–7.
[18] Geier A, Kim SK, Gerloff T, et al. Hepatobiliary organic anion transporters are differentially regulated in acute toxic liver injury induced by carbon tetrachloride. J Hepatol 2002;37(2):198–205.
[19] Planchamp C, Montet X, Frossard JL, et al. Magnetic resonance imaging with hepatospecific contrast agents in cirrhotic rat livers. Invest Radiol 2005;40(4):187–94.
[20] Reimer P, Rummeny EJ, Shamsi K, et al. Phase II clinical evaluation of Gd-EOB-DTPA: dose, safety aspects, and pulse sequence. Radiology 1996;199(1):177–83.

Characteristic Patterns of Altered DNA Methylation Predict Emergence of Human Hepatocellular Carcinoma

Naoshi Nishida,[1,2] Masatoshi Kudo,[2] Takeshi Nagasaka,[3] Iwao Ikai,[4] and Ajay Goel[5]

We aimed to identify the specific subset of tumor suppressor genes (TSGs) that are methylation-silenced during the earliest steps of hepatocarcinogenesis, and to further evaluate whether these genes can serve as predictive biomarkers of hepatocellular carcinoma (HCC) emergence. A total of 482 liver tissues including 177 pairs of HCCs and matched nontumor livers and 128 liver biopsies from chronic hepatitis C (CHC) patients were analyzed for quantitative methylation analysis in 24 TSG promoters and three MINT loci. The tumors were classified as early, less-progressed, and highly progressed HCCs using histology and radiological approaches. A subset of TSGs that harbored distinctly high levels of methylation in early HCCs were selected. Based on the methylation profiles of these genes, Kaplan-Meier analyses were performed to determine time-to-HCC occurrence in CHC patients. Subsequently, multivariate analysis was performed using age, gender, fibrosis stage, and number of methylated TSGs as covariates. Among TSGs analyzed, a subset of eight TSGs (*HIC1, GSTP1, SOCS1, RASSF1, CDKN2A, APC, RUNX3*, and *PRDM2*) demonstrated a distinct cluster by hierarchical clustering and receiver operating characteristic analyses. This subset of TSGs showed significantly higher methylation levels in the early HCCs ($P < 0.0001$). In the CHC patients, methylation frequencies in these TSGs were associated with shorter time-to-HCC occurrence ($P < 0.0001$), and number of methylated genes was an independent risk factor for HCC (hazard ratio = 5.21, 95% confidence interval = 2.25-11.76, $P = 0.0002$). *Conclusion:* Epigenetic inactivation of a subset of TSGs plays a critical role in the earliest steps of hepatocarcinogenesis. Furthermore, epigenetic inactivation of these genes in CHC provides a prognostic value for determining the risk for developing HCC later in life. (HEPATOLOGY 2012;56:994-1003)

Hepatocellular carcinoma (HCC) is one of the most common malignancies worldwide; however, the molecular mechanisms contributing to hepatocarcinogenesis remain unclear. It is widely accepted that HCC exhibits numerous genetic abnormalities, including chromosomal alterations, gene amplifications and mutations, as well as epigenetic alterations.[1] Studies in the past have indicated that, although several chromosomal alterations are observed, frequent *genetic* alterations of individual cancer-related genes rarely occurs in HCC, and even when present, their role in the earliest steps of human hepatocarcinogenesis remains controversial.[1] For instance, mutations in the tumor suppressor *P53* have been observed in human HCC, but these alterations are exclusively detected in the advanced stages and are seldom present in the early stage neoplasms.[2]

In contrast to genetic defects, *epigenetic* alterations, such as hypermethylation of promoter CpG islands, occur far more frequently and are believed to

994

constitute an essential mechanism of tumor suppressor gene (TSG) inactivation in HCC.[3] Furthermore, aberrant methylation of genes is not only present in HCC but can also be found in patients with chronic hepatitis or cirrhosis, which suggests the notion that epigenetic signatures emerge at early stages in the development of this disease.[4] In spite of its importance, the biological impact of individual methylation events in HCC development is sometimes difficult to appreciate because some of these may not be the real "drivers" of malignancy, but simply reflect a global methylation defect that is triggered by unrelated events elsewhere in the genome.[5] Therefore, a better understanding of specific methylation alterations at different stages of HCC, particularly in the earliest steps of hepatocarcinogenesis, will provide important molecular insights into the stepwise accumulation of epigenetic alterations during HCC development.

To address this important gap in knowledge, we used a systematic and multipronged approach to identify the most important genes that are the targets of aberrant methylation in the earliest stages of hepatocarcinogenesis. First, we performed quantitative methylation analysis in a panel of putative HCC-related TSGs. Here we analyzed a large tissue cohort comprising different stages of HCC and the matched corresponding nontumor liver tissues. To ensure stringent classification of early stage HCC, using histological analysis and state-of-the-art imaging techniques, we carefully categorized all tumors into three subcategories as "early," "less-progressed," and "highly progressed" lesions. Second, after the initial screening of a large number of methylated genes, we narrowed down our focus to a subset of genes that harbored high levels of aberrant DNA methylation in the earliest stages of HCC and examined associations between aberrant methylation and the corresponding changes in the expression of these TSGs. The rationale for this approach was that if methylation-induced transcriptional inactivation of this subset of TSGs in early tumors would provide a definitive growth advantage, the established tumor tissues must carry considerable levels of methylation at these genes as a result of clonal expansion of the affected cells. Lastly, to further validate the specificity of the early tumor-related TSGs, we next examined their methylation status in tissues from patients with chronic hepatitis C (CHC). In this instance, we also determined the relationship between the methylation events at these genes in the CHC tissues and subsequent emergence of HCC in these patients. These investigations allowed us to confirm that aberrant methylation of these TSGs in CHC tissues served as an important risk factor for developing HCC, and further suggested that these genes may act as drivers during the initial steps of human hepatocarcinogenesis.

This study is the first attempt that not only determines the role of individual methylation changes at different stages of hepatocarcinogenesis, but also specifically identifies the methylation events that orchestrate the earliest steps in HCC development. The findings reported in this study are of tremendous clinical significance because clarification of the impact of these epigenetic alterations could serve as a basis for the development of predictive biomarkers of tumor emergence and prevention in HCC.

Patients and Methods

Patients. A total of 482 liver tissues, including 177 HCCs and their matched corresponding nontumor livers were analyzed in this study. Among these, 300 liver tissues (150 pairs of HCCs and noncancerous livers) represented fresh-frozen samples that were obtained from surgical resection or biopsy, whereas 27 pairs of HCCs and noncancerous livers and 128 biopsy samples of CHC were formalin-fixed paraffin-embedded (FFPE) samples. According to our previous study, differences in sample processing between fresh-frozen and FFPE specimens did not affect the DNA quality for methylation analysis.[6]

We classified all HCCs into three stages as early HCC (eHCC), less-progressed HCC (less-pHCC), and highly progressed HCC (highly pHCC) as recommended by the International Consensus Group for Hepatocellular Neoplasia,[7] particularly in the context of accurate categorization of early stage tumors. The reason for such careful subclassification was because larger tumors or tumors with hypervascular patterns at

arterial phase are generally represented as progressive dedifferentiating lesions even when the pathological studies indicate these to be of well-differentiated histology.[8] The details of the criteria of tumor stage and the clinical background of the patients of each stage of tumor are summarized in Table 1.

For the determination of aberrant methylation as a predictive marker for time-to-HCC occurrence, we analyzed an additional group of biopsy specimens from CHC cases without a prior history of HCC. These cases were randomly selected from an archival collection of 349 biopsy specimens using the inclusion and exclusion criteria listed in Supporting Table 1. Among these cases, we were able to extract usable DNA (both in terms of quantity and quality) from 128 biopsy specimens for quantitative MethyLight assays for all eight TSGs analyzed in this study. We specifically focused on CHC cases because hepatitis C virus (HCV)-related HCC had the propensity to carry high levels of methylation on CpG loci selected for this analysis.[6] Liver fibrosis stage (F-stage) of each biopsy specimen was expressed using the METAVIR scoring system.[9] All cases received antiviral interferon therapy during the clinical course after donating a liver biopsy. The endpoint was emergence of HCC and diagnosis was confirmed by histology. Patients were censored at the time of last clinical visit or death before developing HCC. The details of background of the patients, follow-up, and response to interferon therapy are shown in Supporting Table 1. Informed consent was obtained from each patient and the study was approved by the institutional review boards of all the involved institutions.

Methylation Analysis and Corresponding Gene Expression in Human HCC, Nontumor Liver, and HCC-Derived Cell Lines. We performed quantitative methylation analysis for the promoter CpG islands of 24 HCC-related tumor suppressor genes (*HIC1, CASP8, GSTP1, SOCS1, RASSF1, CDKN2A, APC, RUNX3, PRDM2, SFRP2, CDH1, PTGS2, CAC-NA1G, RASSF2, RPRM, DCC, DAPK1, DPYD, CDKN2B, SFN, WRN, BLM, RECQL, RECQL5*) and three methylated in tumor (MINT) loci (*MINT1, MINT2,* and *MINT31*) in both the tumor and the matched corresponding nontumor liver tissues. For the quantitative methylation analyses of various genes and MINT loci, we used combined bisulfite restriction assay (COBRA). The primer sequences, polymerase chain reaction (PCR) conditions, and restriction enzymes for 14 of 24 gene promoters (*HIC1, RASSF1, CASP8, GSTP1, SOCS1, APC, RUNX3, PRDM2, CDH1, DPYD, WRN, BLM, RECQL* and *RECQL5*)

Table 1. Clinicopathological Features of the Patients in Each Stage of HCC

Clinical Background	Early HCC (n = 26)	Less-Progressed HCC (n = 37)	Highly Progressed HCC (n = 114)
Age (y.o)*			
Mean (95% CI)	59.1	63.3	59.2
	(55.1-63.1)	(60.4-66.2)	(57.3-61.2)
Median (25%-75%)	60.5	63.0	60.0
	(55.8-64.5)	(56.0-70.0)	(54.0-66.0)
Gender			
Male (119)	17	26	76
Female (55)	9	11	35
Missing (3)	0	0	3
Hepatitis virus			
HBV (39)	6	6	27
HCV (112)	19	29	64
HBV & HCV (3)	0	0	3
Negative (22)	1	2	19
Missing (1)	0	0	1
Background liver			
Without cirrhosis (55)	8	15	32
With cirrhosis (113)	18	21	74
Missing (9)	0	1	8

For the classification of tumor stages, we applied multiple criteria that combined histological tumor differentiation status, tumor size, and radiographic features obtained by the contrast-enhanced computed tomography (CE-CT). We classified tumors as early HCC (eHCC) if these lesions revealed well-differentiated HCC that were less than 2.0 cm in size and possessed a hypovascular pattern in arterial phase of CE-CT. Similarly, the HCCs were classified as less-progressed HCC (less-pHCC) if these were well differentiated, but measured greater than 2.0 cm or had hypervascular regions in the nodules in arterial phase of CE-CT. All HCCs that were moderately or poorly differentiated were categorized as highly progressed HCC (highly pHCC), regardless of their size or vascular pattern.

*Mean value (95% confidence interval) and median value (25%-75% percentile) are shown. In all, 97 pairs of HCCs and their nontumor liver were newly corrected and 80 pairs of HCCs and nontumor livers were previously studied.

are summarized in Supporting Table 2, whereas the details for the remaining assays have been described previously.[10,11] We also quantified methylation levels of all 27 TSGs/CpG loci in a panel of 11 HCC cell lines (HLE, HLF, HepG2, PLC/PRL/5, SNU398, SNU423, SNU449, SNU475, HuH7, Hep3B, and Li-7). The TSGs that demonstrated methylation in more than four cell lines were subsequently analyzed for the corresponding messenger RNA (mRNA) transcripts using the StepOne real-time detection system (Applied Biosystems, Foster City, CA).

Methylation Analysis of a Subset of Genes in CHC Patients. For the methylation status determination of a smaller subset of eight TSGs (*HIC1, GSTP1, SOCS1, RASSF1, CDKN2A, APC, RUNX3* and *PRDM2*) that were identified as important targets of epigenetic inactivation in the early tumors, we performed quantitative MethyLight assays using the StepOne real-time detection system (Applied Biosystems). The PCR primers and probes used in this assay were

described previously except for those of *PRDM2*.[12] The primers and probe sequences for *PRDM2* and conditions of MethyLight assays are described in Supporting Table 3.

   Statistical Analysis. To compare the differences in methylation levels in each tumor stage, one-way factorial analysis of variance (ANOVA) and post-hoc comparisons (Tukey-Kramer HSD multicomparison), or Dunnett's test were applied using *Z*-scores for normalization. For the discrimination of HCC from nontumor liver using methylation levels, we applied receiver operating curve (ROC) analysis and calculated the area under the curve (AUC) values. Hierarchical clustering analysis was also performed to identify a specific cluster of TSGs/CpG loci carrying the highest levels of methylation in tumor tissues. Correlation between methylation level and expression of the corresponding gene was evaluated using Spearman's rank correlation test. Time-to-HCC occurrence was estimated using Kaplan-Meier analysis, and univariate parameters were analyzed with a log-rank test. Variables with $P < 0.05$ on univariate analysis were further analyzed by Cox proportional-hazards regression to determine the independent determinants of outcome variables. All *P*-values were two-sided and $P < 0.05$ was considered statistically significant. All statistical analyses were performed using JMP v. 9.0 software (SAS Institute, Cary, NC).

Results

   Identification of Hypermethylated TSGs Responsible for the Earliest Events in HCC Pathogenesis. At first, we examined the differences in the methylation levels between tumor and nontumor liver tissues in 27 different CpG loci (24 TSGs and three MINT loci). Sixteen of 24 genes and all three MINT loci showed significant differences in methylation levels between tumor and the corresponding nontumor liver tissues. The eight genes that did not reveal any significant differences in the methylation levels included *DAPK1, DPYD, CDKN2B, SFN, WRN, BLM, RECQL, RECQL5,* and were excluded from further analysis (data not shown).

   We next studied the distribution of mean methylation levels of all CpG loci in different stages of HCC (early, less-progressed, and highly progressed) by comparing these with the matching nontumor liver tissues. The mean methylation levels and the 95% confidential intervals (CI) are listed in Supporting Table 4. Other than *DCC*, all TSGs showed significant differences in methylation levels among all stages of HCC ($P <$

0.0001 by ANOVA for 15 of 19 TSGs). Among these, a subset of eight gene promoters, *HIC1, GSTP1, SOCS1, RASSF1, CDKN2A, APC, RUNX3,* and *PRDM2,* revealed the most prominent differences in the methylation levels between nontumor liver and the eHCC ($P < 0.0001$ by Dunnett's test; Fig. 1). Interestingly, hierarchical clustering analysis using methylation levels of HCC on 19 TSGs/CpG loci further revealed that all eight eHCC-related TSGs were indeed classified as one distinct cluster and uniformly hypermethylated among eHCCs (Supporting Fig. 1). These data suggest that hypermethylation of this subset of genes, referred to as the "eHCC-related TSGs," perhaps is critical for the initial steps of human hepatocarcinogenesis.

   On the other hand, four TSGs (*CASP8, MINT31, PTGS2,* and *CACNA1G*) did not reveal any significant differences in the methylation between the nontumor liver and the eHCCs, but demonstrated significant hypermethylation in the less-pHCC (classified as less-pHCC-related TSGs; $P < 0.0001$ for *CASP8* and *CACNA1G,* $P = 0.0009$ for *MINT31* and $P = 0.0183$ for *PTGS2*). Furthermore, the methylation levels of these four genes continued to increase with the progression of the disease, indicating that these may play an important role in accelerating the progression of early stage HCCs to more advanced stages (Supporting Table 4 and Supporting Fig. 2A). At the remaining seven genes, the elevation in the methylation levels was specifically observed only in the highly pHCC in comparison to the nontumor liver tissues (classified as highly pHCC-related TSGs; *RASSF2, MINT1, MINT2, RPRM, SFRP2, CDH1* and *DCC;* Supporting Table 4 and Supporting Fig. 2B).

   Discrimination of HCC by ROC Analysis Using Methylation Levels of Various CpG Loci. We previously reported that methylation of certain TSGs in HCC is not exclusively detected in the tumor tissue but could also be found in the nontumor livers, as well as in normal aging livers.[6] These data question the specificity and the biological relevance of such methylation events as critical alterations underlying HCC pathogenesis. Therefore, in order to determine which methylation events specifically contribute to hepatocarcinogenesis most profoundly, we analyzed the quantitative methylation levels of various TSGs/CpG loci in their ability to successfully discriminate HCC from the nontumor livers using ROC analysis. It was intriguing to discover that six of eight eHCC-related TSGs represented AUC values higher than 0.80 (Table 2). In contrast, the AUC values of six of seven highly pHCC-related TSGs were below 0.60.
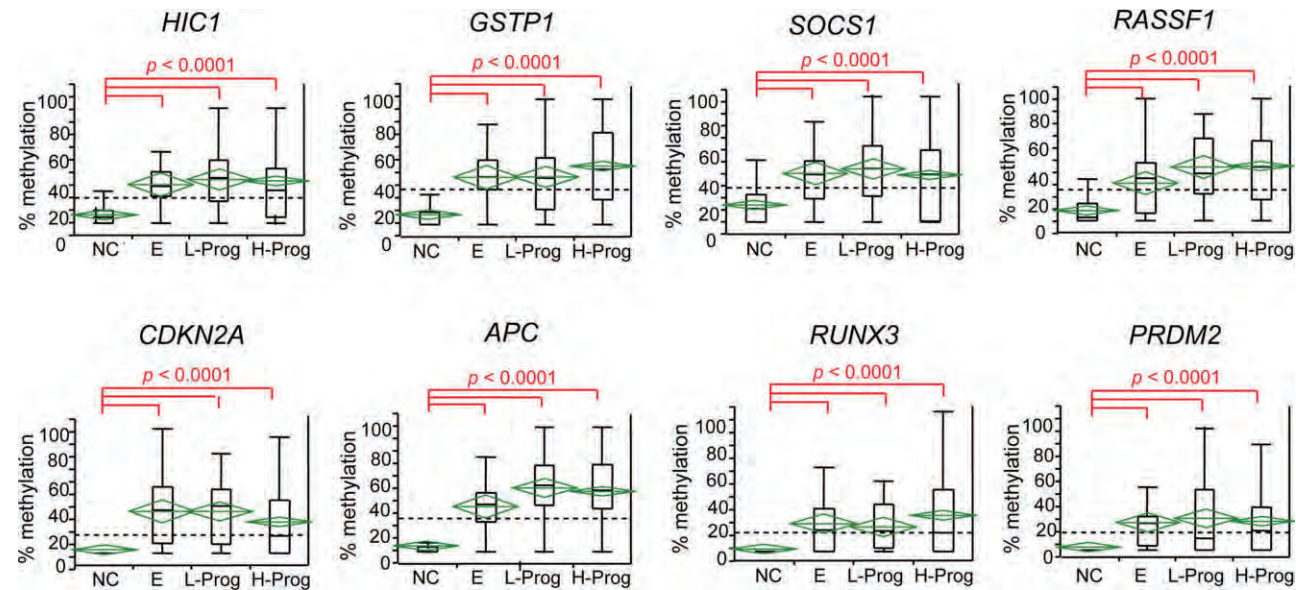
Fig. 1. Multiple comparisons of methylation levels at individual early HCC-related TSGs between noncancerous liver and different stages of HCC. This figure represents distribution of methylation levels in TSGs carrying prominent methylation in early HCCs (early HCC-related TSGs) in comparison to nontumor tissues. Methylation levels of each HCC stage are compared to that of noncancerous livers by Dunnett's multiple comparison tests. All comparisons depict significant differences with *P* < 0.0001 (highlighted in red). The green diamonds and the horizontal lines within the diamonds represent the mean values and the 95% CI. The box-and-whiskers plots denote 75% and 95% distributions, and the lines within the boxes denote median values. The horizontal dashed line indicates mean methylation levels of all tissues in each TSGs. NT, nontumor livers; E, early HCCs; L-Prog, less-progressed HCCs; H-Prog, highly progressed HCCs.

Methylation Levels in Early HCC-Related TSGs Inversely Correlate with Gene Expression in HCC Cell Lines. The high levels of methylation in the eHCC-related TSGs suggest that their epigenetic alteration is not a passive phenomenon, but might serve as a driver event in HCC. To further confirm that methylation events at these TSGs lead to their transcriptional inactivation, we quantified the methylation levels and the corresponding gene expression in 11 different HCC-derived cell lines. It was of interest to note that all eight eHCC-related TSGs specifically harbored considerable levels of methylation in HCC cell lines in comparison to other TSGs/CpG loci (Fig. 2A). In addition, the expression of these TSGs inversely correlated with their methylation status in the HCC cell lines (Fig. 2B). This evidence confirmed the functional significance of promoter hypermethylation of these TSGs because it affected their gene expression and highlighted their specific critical role in the emergence of HCC.

DNA Methylation in CHC Patients and Their Risk for Developing HCC. Our observations for the higher levels of methylation in the eHCC-related TSGs in the early stage tumors suggest that their epigenetic inactivation is not a passive phenomenon, but might serve as a driver event in HCC. Accordingly, we hypothesized that the presence of aberrant methylation

Table 2. ROC Curve Analysis for the Discrimination of HCC Tissues by Analyzing Methylation Levels of Each TSG/CpG Loci

TSG/CpG Locus	ROC Analysis			
	Best Threshold Limits (%)	Sensitivity	Specificity	AUC Value
APC	22.0	0.8409	0.9310	**0.90731**
GSTP1	20.3	0.7500	0.9194	**0.86620**
RASSF1	26.0	0.6875	0.9249	**0.84209**
RUNX3	5.5	0.6250	0.9355	**0.81019**
PRDM2	1.0	0.7216	0.8326	**0.80501**
CDKN2A	13.0	0.6257	0.9540	**0.80729**
HIC1	19.0	0.6477	0.9355	**0.79658**
SOCS1	35.4	0.5739	0.9355	**0.74789**
CACNA1G	1.0	0.4640	0.9839	**0.72616**
MINT31	7.0	0.4800	0.8871	0.69984
PTGS2	9.7	0.2800	1.0	0.63813
RASSF2	1.2	0.2640	0.9677	0.61823
MINT1	8.0	0.2258	1.0	0.61290
CASP8	17.0	0.3600	0.8790	0.59168
MINT2	1.7	0.1789	1.0	0.58943
RPRM	8.0	0.1067	0.9839	0.56406
SFRP2	8.3	0.1680	0.9435	0.55445
DCC	8.0	0.1440	0.9839	0.55187
CDH1	3.7	0.2823	0.8387	0.54855

Best threshold of methylation level (%) for the discrimination of HCC tissues from nontumor background liver, their sensitivity, specificity, and AUC values are shown.

AUC values of more than 0.80 are indicated in bold with an underline. AUC values of more than 0.70 are listed in bold. Methylation levels of six of eight TSGs, which carried significant hypermethylation in early HCC, showed AUC values of more than 0.80, suggesting that prominent increase of methylation level took place during a dedifferentiation process from noncancerous hepatocyte to early stage of tumors.
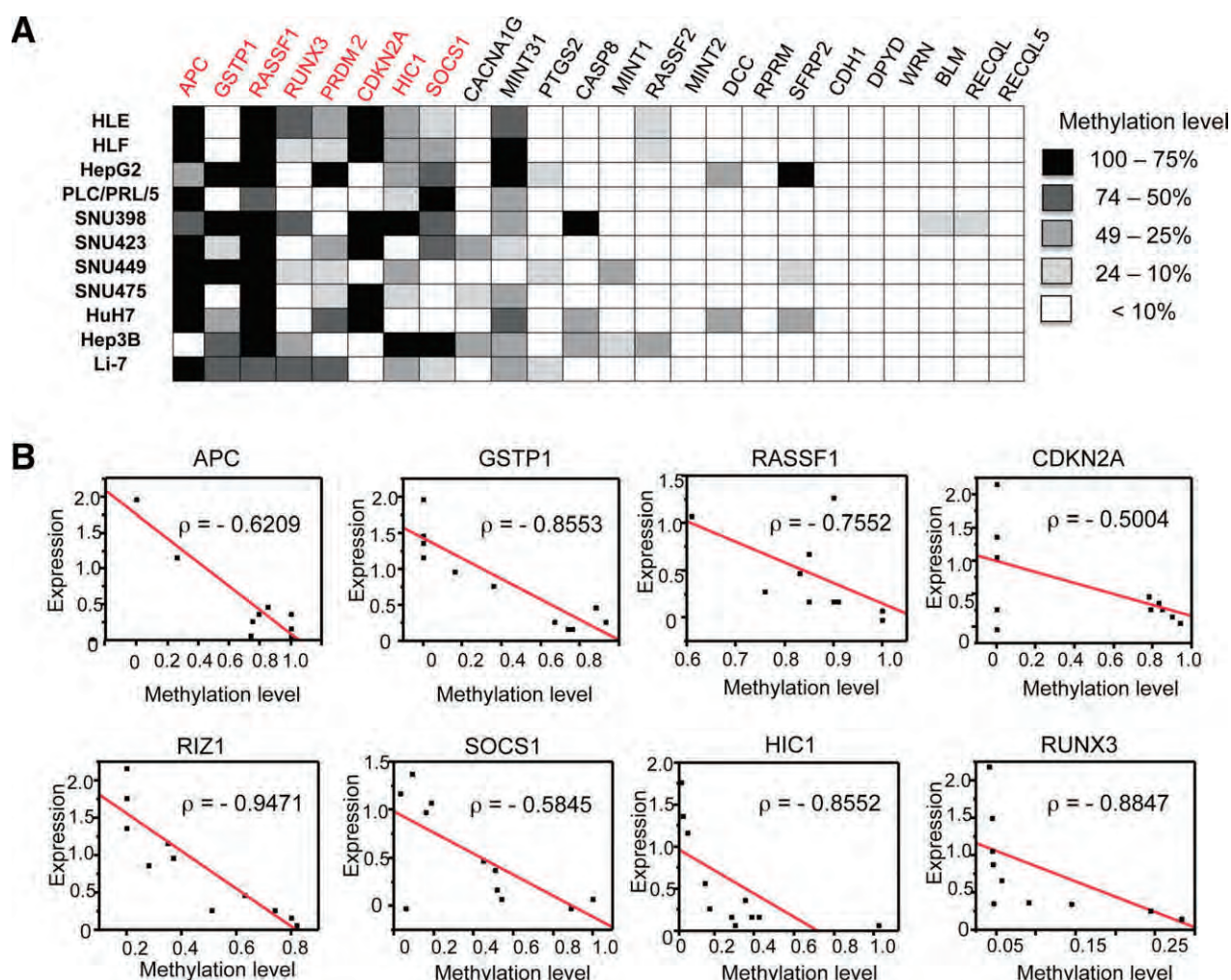
Fig. 2. Methylation profiles in HCC cell lines and the correlation between methylation levels and expression of various TSGs. (A) Eleven different HCC-derived cell lines were examined for quantitative methylation levels for 24 TSGs and three MINT loci using COBRA. Following the extraction of genomic DNA, 2 μg of DNA was subjected to bisulfite modification treatment. Eight early HCC-related TSGs are highlighted in red letters. This set of TSGs represents higher levels of methylation compared to other TSGs/CpG loci. (B) TSGs carrying methylation in more than four HCC cell lines were subsequently examined for the changes in the gene expression of the corresponding TSG. Gene expression levels in the cell lines were quantified by comparing them with normal livers, for which the total RNA was obtained commercially. Gene-specific primers and probes were obtained from TaqMan Gene Expression Assays and expression of the GAPDH gene was used as an internal control. For the relative quantification, total RNA from normal liver was used as an internal calibrator, and the quantity of RNA was determined as a ratio of the target to that of the calibrator using a standard curve. As shown in this figure, the methylation levels were inversely correlated with the mRNA expression of the methylated gene.

of these genes in CHC patients may serve as a risk factor for subsequent emergence of HCC. Therefore, we next analyzed the methylation status of these eight TSGs in 128 liver biopsy tissues from CHC patients and performed Kaplan-Meier analysis to determine the duration of time-to-HCC occurrence. As sustained viral response (SVR) would reduce cancer risk dramatically,[13] we not only specifically focused on non-SVR patients, but also analyzed the effect of response to interferon (nonresponse or relapse) on time-to-HCC occurrence in order to avoid an influence of antiviral interferon therapy. Standard risks of HCC in CHC such as age, gender, and F-stage were analyzed as well.

We noted that CHC cases with hypermethylation of ≥ 5 genes showed a significantly reduced time-to-HCC occurrence in comparison to the patients with either ≤ 1 gene or 2-4 genes exhibiting methylation ($P < 0.0001$, log-rank test; Fig. 3).

Older age (mean age ≥ 55 years), male gender, and progression of fibrosis (F3 or F4) were also significantly associated with shorter time-to-HCC occurrences. However, response to interferon therapy (nonresponse versus relapse) did not affect the time-to-HCC occurrence ($P = 0.0089$ for ≥ 55 years versus ≤ 54 years, $P = 0.0324$ for male versus female, $P = 0.0121$ for F4 or F3 versus F2-F0, and $P = 0.3946$
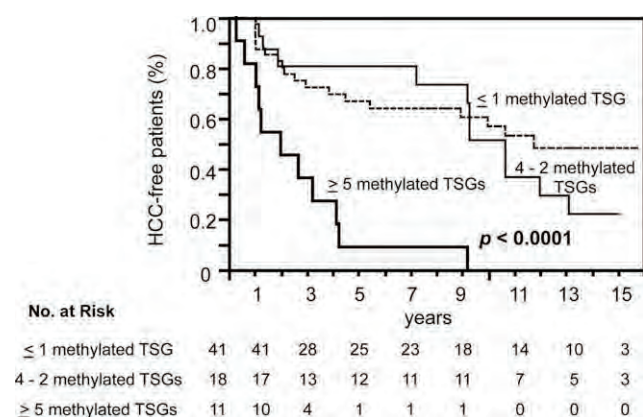
Fig. 3. Kaplan-Meier curves for time-to-HCC occurrence in the biopsies from CHC patients. Kaplan-Meier survival curves were generated based on the methylation status of early HCC-related TSGs in CHC patients. Survival analyses for non-SVR cases are illustrated. Number of cases analyzed and the number of the cases with positive events (occurrence of HCC) were as follows: CHC with methylated TSG ≥ 5, total cases = 11, cases with HCC occurrence = 11; CHC with methylated TSG 4-2, total cases = 18, cases with HCC occurrence = 11; CHC with methylated TSG ≤ 1, total cases = 41, cases with HCC occurrence = 18, respectively. The P values were calculated using a log-rank test.

for NR versus relapse by log-rank test; Table 3). We subsequently conducted a multivariate analysis using the Cox's proportional-hazards regression model

Table 3. Univariate Analysis for the Contribution of Each Variable on Time-to-HCC Occurrence in Biopsy Specimens from Non-SVR Chronic Hepatitis C (CHC) Cases

	No. of Non-SVR Cases		Univariate	
Variables	Total	With Event*	P value†	HR (95% CI)
Age				
$\geq$55 y.o	45	30	**0.0089**	**2.54 (1.27-5.50)**
$\leq$54 y.o	25	10		1
Gender				
Male	40	27	**0.0324**	**2.03 (1.06 - 4.08)**
Female	30	13		1
F stage				
F4 or F3	38	25	**0.0121**	**2.23 (1.19 - 4.36)**
F2-F0	32	15		1
Response to interferon‡				
NR	42	28	0.3946	1.34 (0.70 - 2.74)
Relapse	28	12		1
No. of methylated TSGs				
>5	11	11	**< 0.0001**	**5.98 (2.61 - 13.3)**
4-2	18	11		1.39 (0.64 - 2.91)
<1	41	18		1

A continuous variable of age was categorized into two groups with a mean age of $\geq$55 years, or $\leq$54 years. F-stage was also categorized as F0-F2 and F3/F4.

*No. of cases with HCC occurrence after biopsy.

†P-value by log-rank test. P values < 0.05 are shown in bold.

‡Nonresponse (NR), detectable for HCV-RNA during and after the treatment; relapse, no detectable HCV-RNA at the end of the treatment but detectable at 6 months after the end of the treatment.
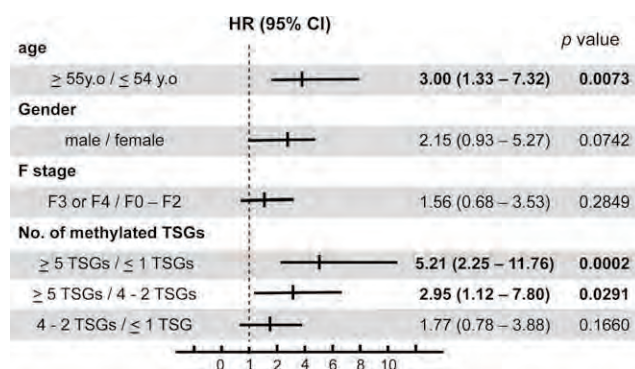
Fig. 4. Hazard ratios (HRs) and P-values obtained from the multivariate analysis for each variable in CHC patients for the emergence of HCC. The P-values were calculated using Cox's proportional hazards regression model. A continuous variable of age was categorized into two groups with a mean age of $\geq$55 years or $\leq$54 years. F-stage was also categorized as F0-F2 and F3/F4. The total number of cases and the number of patients with HCC occurrence in each group and the associated P-values of univariate analyses calculated using a log-rank test are shown in Table 3.

including age, gender, F-stage as variables, and compared these to the number of methylated TSGs. We noted that, whereas age and number of methylated TSGs were significant risk factors for shorter time-to-HCC occurrence, gender and F-stage were not associated with a significant risk for developing HCC ($P = 0.0073$ for age, $P = 0.0742$ for gender, $P = 0.2849$ for F-stage, and $P = 0.0002$ for the number of methylated TSGs of ≥ 5 versus ≤ 1, respectively; Fig. 4). In terms of the hazard ratios (HR) based on the number of methylated TSGs and the likelihood for the emergence of HCC in CHC patients, a dose-dependent effect was observed in which the HR of $\geq$5 methylated genes versus $1\leq$ methylated gene was the highest (HR = 5.21, 95% CI: 2.25-11.76), followed by that of $\geq$5 methylated genes versus 4-2 methylated genes (HR = 2.95, 95% CI: 1.12-7.80), and the lowest with that of 4-2 methylated genes versus $1\leq$ methylated gene (HR = 1.77, 95% CI: 0.78-3.88; Fig. 4).

Discussion

In this study we aimed to identify the contribution of DNA methylation changes as potential contributors in the earliest steps of human HCC. Inclusion of a reasonably large number of early stage tumors allowed us to carefully identify methylation patterns of genes that might be critical determinants during the initial phases of HCC development. We were able to successfully classify patterns of methylation progression of all the analyzed genes into three categories (as illustrated in the summarized model in Fig. 5), with eight genes being specifically hypermethylated in the eHCCs.
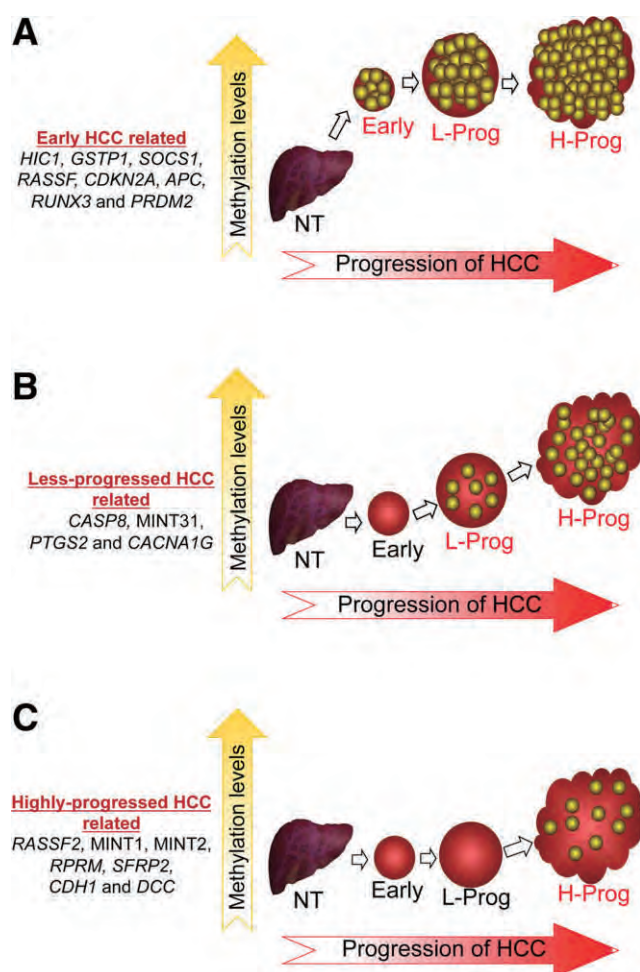
Fig. 5. A schematic representation of consolidated model for the pattern of methylation progression in various stages of HCC development. This figure illustrates the progression of methylation events in (A) eight early HCC-related TSGs; (B) four less-progressed HCC-related TSGs; and (C) seven highly progressed HCC-related TSGs. NT, nontumor livers; Early, early HCCs; L-Prog, less-progressed HCCs; H-Prog, highly progressed HCC. The yellow circles represent HCC cells carrying methylation on the corresponding TSGs/CpG loci. The methylation of early HCC-related TSGs leads to the clonal expansion and establishment of early tumors with high levels of methylation of the corresponding TSGs. In contrast, only a small number of scattered cells carry methylation in the highly progressed HCC-related TSGs even in the most advanced stages of HCC, indicating the possibility that these could be passive methylation events.

Interestingly, the subset of these eHCC-related TSGs not only revealed a methylation-induced transcriptional inactivation in HCC-cell lines, but also best discriminated HCC tissues from the normal livers by ROC analysis. In addition, Kaplan-Meier analysis demonstrated that increased methylation of these genes in CHC patients was associated with reduced time-to-HCC occurrence and served as an independent risk factor to predict the emergence of HCC in the CHC patients. Taken together, these data highlight that epigenetic inactivation of this subset of growth regulatory

genes is critical, and that these genes may act as "drivers" of neoplasia during the earliest steps of hepatocarcinogenesis.

DNA methylation has been considered an early event in hepatocarcinogenesis.[1] However, the identification of individual methylation events that are critical for an accelerated tumor growth during the earliest steps of HCC development has not been investigated previously. A logical approach to address this issue must include analysis of the early stage tumors, for the identification of genes that are not only methylated more frequently, but also carry high levels of methylation. Recently, the International Consensus Group for Hepatocellular Neoplasia revisited the concept of classifying eHCC.[7] In light of these recommendations, we were very stringent with our definition of early stage tumor (or eHCCs), and considered only the ones with well-differentiated histology with less than 2.0 cm in size, which was accompanied with a hypovascular imaging pattern. We reasoned that true critical methylation events must provide sufficient growth advantage in the affected cells to permit their subsequent clonal expansion as the tumor evolves. We feel that our stringent definition of "early HCCs," together with the quantitative methylation analysis of a large panel of HCC-related TSGs, was a unique strength of our study that allowed us to uncover a subset of critical genes that control the tumor cell growth in the earliest steps of hepatocarcinogenesis.

Among the TSGs or MINT loci analyzed, eight gene promoters carried very high levels of promoter hypermethylation in all stages of HCC. However, methylation of these loci was particularly higher in the eHCCs and formed a distinct cluster by hierarchical clustering analysis, implying that the epigenetic inactivation of these genes was potentially important during the earliest stage of tumor development. Furthermore, we were also able to identify two additional subsets of genes, whose methylation strongly correlated with the less-pHCCs and highly pHCCs, suggesting that their inactivation might play a more essential role in the later stages of HCC. We compared the methylation levels of individual TSGs by ROC analysis in an attempt to select methylated genes that could discriminate HCC from nontumor livers with a high degree of sensitivity and specificity.[14] Interestingly, six of eight eHCC-related TSGs possessed AUC values that were higher than 0.80, further lending credence to our other observations that these genes may trigger an aberrant methylation cascade during early hepatocarcinogenesis. In contrast, our observation for the lower AUC values obtained from two of four less-pHCC-

related TSGs is suggestive of their role in the dedifferentiation of early tumors to an intermediate stage. Likewise, even lower AUC values for the seven highly pHCC-related TSGs suggests that conceivably the methylation alterations present in these genes is simply a reflection of a passive change that occurs elsewhere in the genome due to ensuing tumorigenesis.

Recently, aberrant methylation of TSGs was reported in early HCC that had an HBV-positive genotype.[15] Interestingly, four of five methylated TSGs reported in that report also belong to the subset of our eight eHCC-related TSGs. In HCC cell lines a considerable degree of DNA methylation was observed in these TSGs regardless of HBV status, and their methylation levels were inversely correlated with expression of the corresponding genes (Fig. 2). Therefore, although the analysis of human HCC tissues indicate that methylation levels were higher in HCV-related than HBV-related tumors (Supporting Fig. 3), epigenetic inactivation of eHCC-related TSGs might play a role for both types of virus-related neoplasms. It was reported that cancer-specific promoter methylation mostly targeted genes, which normally had low baseline steady-state levels of expression.[16] Therefore, it is possible that unique profiles of methylated genes in HCC, which could be involved in multiple oncogenic pathways, attribute to the baseline expression in normal hepatocytes. However, our results also indicate that infection with different hepatitis-related viruses might cause a selective pressure for DNA methylation-induced transcriptional inactivation of certain TSGs. Genome-wide analyses of epigenetic alterations may help clarify the differences in the methylation profiles of HCC with various etiologies.

Another interesting feature of our study is that some of the eHCC-related TSGs are known to carry low levels of methylation even in the background liver of HCC patients, especially HCV-positive cases. Therefore, it is reasonable to speculate that some of these clones with methylation-silenced TSGs already exist in patients with chronic hepatitis, and may act as "seeds" for the development of early stage tumors.[5] As the number of methylated TSGs in hepatitis tissues is related to the risk of HCC, stepwise accumulation of methylation-inactivated genes must be required during the initial steps of hepatocarcinogenesis. The eight genes that showed high levels of methylation in eHCC in our study are involved in a variety of functions, suggesting that multiple pathways might be involved in emergence of eHCC.

A previous report indicated that DNA methylation alterations in HCC had an important prognostic and therapeutic implication for this malignancy.[17] In addition, a recent report suggested that aberrant DNA methylation of certain genes could predict recurrence-free survival of HCC patients who underwent hepatectomy.[18] However, the determination of recurrence-free survival of HCC is challenging because tumor recurrence typically has two components: true metastasis and metachronous tumors that arise *de novo*.[19] Therefore, analysis of hepatitis tissues without prior history of HCC provide a more logical and prudent substrate to evaluate the usefulness of methylation events at critical TSGs/CpG loci for assessing the risk of HCC development. To the best of our knowledge, none of the previous studies have investigated associations between epigenetic alterations in hepatitis tissues and determined the future risk of developing *de novo* HCC. This is another unique strength of our study in which we addressed this issue and discovered that an increased number of methylated TSGs was associated with shorter time-to-HCC occurrence. In addition, the increased number of methylated TSGs was an independent risk factor even when the analysis eliminated the effect of interferon therapy (Fig. 4). In contrast, multivariate analysis in our study revealed that F-stage, which was previously believed to a better predictor of HCC in CHC patients, failed to emerge as an independent risk factor when simultaneously analyzed with the number of methylated TSGs. This observation is in line with the report suggesting that CpG island methylator phenotype in HCC might also be associated with background liver in patients with cirrhosis.[10] Recently, it was reported that oxidative stress caused by HCV induced liver fibrosis,[20] and it also led to epigenetic inactivation of TSGs by way of DNA methylation.[21] From this viewpoint, it is conceivable to speculate that epigenetic inactivation of TSGs might be a more critical event that may take precedence over the effect of F-stage on the risk of HCC emergence. Interestingly, we also discovered a dose-dependent effect of the number of methylated TSGs on the HRs for the times-to-HCC occurrence, suggesting that sequential inactivation of these tumor suppressors may lead to the formation of *de novo* HCC in preneoplastic liver. However, our study cannot rule out the inadvertent bias in patient selection given the retrospective nature of our study, in which CHC cases with higher alanine aminotransferase or α-fetoprotein levels might have been prone to more frequent to liver biopsies. Therefore, we determined the rate of fibrosis progression using F-stages at the time of initial biopsies and HCC occurrence (Supporting Table 5). The mean progression of F-stage was 0.07 ± 0.10 unit/year for all

cases and 0.14 ± 0.10 unit/year for noncirrhotic cases, which was somewhat higher than that reported by Shiratori et al.[22] However, the mean age and proportion of advanced F-stage in our cohort is also higher than those reported by Shiratori et al., which might help explain the higher incidence of HCC observed in our study. Nonetheless, to address these important issues we are currently planning an independent validation of our results in which we will interrogate the significance of these methylation markers for the prediction of HCC emergence in a prospective multicenter patient cohort.

In summary, in this study we systematically characterized methylation patterns in a large panel of TSGs and identified a subset of genes that play a critical role in the earliest steps in hepatocarcinogenesis. Furthermore, we provide additional evidence that epigenetic inactivation of these genes in patients with CHC is an important and independent risk factor for predicting emergence of HCC late in life. Given the robustness of data presented in this article, we believe that these results are of significance, from both basic and clinical perspectives. From a basic research standpoint, these data provide a molecular understanding on the contribution of individual TSGs that are targets of transcriptional inactivation in the earliest steps of hepatocarcinogenesis. From a clinical viewpoint, in addition to the antiviral and antiinflammatory therapies, our data suggest that potential inclusion of epigenetic therapies in future might serve as effective adjuncts for CHC patients with refractory disease in reducing their risk for developing HCC.

References

1. Nishida N, Goel A. Genetic and epigenetic signatures in human hepatocellular carcinoma: a systematic review. Curr Genomics 2011;12: 130-137.
2. Nishida N, Fukuda Y, Kokuryu H, Toguchida J, Yandell DW, Ikenega M, et al. Role and mutational heterogeneity of the p53 gene in hepatocellular carcinoma. Cancer Res 1993;53:368-372.
3. Nishida N, Nishimura T, Nagasaka T, Ikai I, Goel A, Boland CR. Extensive methylation is associated with beta-catenin mutations in hepatocellular carcinoma: evidence for two distinct pathways of human hepatocarcinogenesis. Cancer Res 2007;67:4586-4594.
4. Kondo Y, Kanai Y, Sakamoto M, Mizokami M, Ueda R, Hirohashi S. Genetic instability and aberrant DNA methylation in chronic hepatitis and cirrhosis—a comprehensive study of loss of heterozygosity and microsatellite instability at 39 loci and DNA hypermethylation on 8

5. Ushijima T, Okochi-Takada E. Aberrant methylations in cancer cells: where do they come from? Cancer Sci 2005;96:206-211.
6. Nishida N, Nagasaka T, Nishimura T, Ikai I, Boland CR, Goel A. Aberrant methylation of multiple tumor suppressor genes in aging liver, chronic hepatitis, and hepatocellular carcinoma. HEPATOLOGY 2008;47: 908-918.
7. International Consensus Group for Hepatocellular Neoplasia. Pathologic diagnosis of early hepatocellular carcinoma: a report of the international consensus group for hepatocellular neoplasia. HEPATOLOGY 2009;49:658-664.
8. Takayasu K, Muramatsu Y, Mizuguchi Y, Moriyama N, Ojima H. Imaging of early hepatocellular carcinoma and adenomatous hyperplasia (dysplastic nodules) with dynamic CT and a combination of CT and angiography: experience with resected liver specimens. Intervirology 2004;47:199-208.
9. [No authors listed.] Intraobserver and interobserver variations in liver biopsy interpretation in patients with chronic hepatitis C. The French METAVIR Cooperative Study Group. HEPATOLOGY 1994;20:15-20.
10. Shen L, Ahuja N, Shen Y, Habib NA, Toyota M, Rashid A, et al. DNA methylation and environmental exposures in human hepatocellular carcinoma. J Natl Cancer Inst 2002;94:755-761.
11. Nagasaka T, Koi M, Kloor M, Gebert J, Vilkin A, Nishida N, et al. Mutations in both KRAS and BRAF may contribute to the methylator phenotype in colon cancer. Gastroenterology 2008;134: 1950-1960.
12. Weisenberger DJ, Siegmund KD, Campan M, Young J, Long TI, Faasse MA, et al. CpG island methylator phenotype underlies sporadic microsatellite instability and is tightly associated with BRAF mutation in colorectal cancer. Nat Genet 2006;38:787-793.
13. Shindo M, Di Bisceglie AM, Hoofnagle JH. Long-term follow-up of patients with chronic hepatitis C treated with alpha-interferon. HEPATOLOGY 1992;15:1013-1016.
14. Hua D, Hu Y, Wu YY, Cheng ZH, Yu J, Du X, et al. Quantitative methylation analysis of multiple genes using methylation-sensitive restriction enzyme-based quantitative PCR for the detection of hepatocellular carcinoma. Exp Mol Pathol 2011;91:455-460.
15. Um TH, Kim H, Oh BK, Kim MS, Kim KS, Jung G, et al. Aberrant CpG island hypermethylation in dysplastic nodules and early HCC of hepatitis B virus-related human multistep hepatocarcinogenesis. J Hepatol 2011;54:939-947.
16. Hahn MA, Hahn T, Lee DH, Esworthy RS, Kim BW, Riggs AD, et al. Methylation of polycomb target genes in intestinal cancer is mediated by inflammation. Cancer Res 2008;68:10280-10289.
17. Calvisi DF, Ladu S, Gorden A, Farina M, Lee JS, Conner EA, et al. Mechanistic and prognostic significance of aberrant methylation in the molecular pathogenesis of human hepatocellular carcinoma. J Clin Invest 2007;117:2713-2722.
18. Nagashio R, Arai E, Ojima H, Kosuge T, Kondo Y, Kanai Y. Carcinogenetic risk estimation based on quantification of DNA methylation levels in liver tissue at the precancerous stage. Int J Cancer 2011;129: 1170-1179.
19. Llovet JM, Di Bisceglie AM, Bruix J, Kramer BS, Lencioni R, Zhu AX, et al. Design and endpoints of clinical trials in hepatocellular carcinoma. J Natl Cancer Inst 2008;100:698-711.
20. Mormone E, Lu Y, Ge X, Fiel MI, Nieto N. Fibromodulin, an oxidative stress-sensitive proteoglycan, regulates the fibrogenic response to liver injury in mice. Gastroenterology 2012;142:612-621.
21. O'Hagan HM, Wang W, Sen S, Destefano Shields C, Lee SS, Zhang YW, et al., Oxidative damage targets complexes containing DNA methyltransferase, SIRT1, and polycomb members to promoter CpG islands. Cancer Cell 2011;20:606-619.
22. Shiratori Y, Imazeki F, Moriyama M, Yano M, Arakawa Y, Yokosuka O, et al., Histologic improvement of fibrosis in patients with chronic hepatitis C who have sustained response to interferon therapy. Ann Intern Med 2000;132:517-524.

Endoscopic Ultrasound: Contrast Enhancement

Masayuki Kitano, MD, PhD*, Hiroki Sakamoto, MD, PhD,
Masatoshi Kudo, MD, PhD

KEYWORDS

- Endoscopic ultrasonography • Contrast enhancement
- Contrast-enhanced harmonic EUS
- Ultrasound contrast agents • Sonazoid • SonoVue
- Definity • Microbubbles

ULTRASOUND CONTRAST AGENTS

Intra-arterial infusion of carbon dioxide (CO_2) gas was the first technology used for contrast-enhanced ultrasonography.[1–3] In this method, CO_2 is infused into the regional artery through a catheter during angiography. Fundamental B-mode ultrasonography sufficiently depicts signals from CO_2 microbubbles in a real-time manner.[1–3] Although intra-arterial CO_2 infusion combined with ultrasonography allows imaging with very high spatial and time resolutions, it has the limitation that ultrasonographic scanning must be performed during angiography.[1–3]

Intravenous ultrasound contrast agents are more convenient for contrast-enhanced ultrasonography because their use requires only a bolus infusion of the agent from a peripheral vein.[4,5] There are several ultrasound contrast agents commercially available.[4,5] Most of them are microbubbles consisting of gas covered with a lipid or phospholipid membrane. A certain range of acoustic power induces microbubble oscillation or breakage.[6,7] When microbubbles are oscillated or broken, signals are emitted that have different frequencies from the transmitted signals.[6,7] These signals can then be depicted by contrast-enhanced ultrasonography.[6,7]

The first-generation ultrasound contrast agents included Levovist (Schering AG, Berlin, Germany), which is composed of microbubbles of room air covered with a palmitic acid membrane.[4–7] Levovist required high acoustic power to oscillate or break its microbubbles. To overcome this disadvantage, second-generation ultrasound contrast agents, including SonoVue (Bracco Imaging, Milan, Italy), Sonazoid (Daiichi-Sankyo, Tokyo, Japan; GE Health care Milwaukee, WI, USA), and Definity (Lantheus Medical

Department of Gastroenterology and Hepatology, Kinki University School of Medicine, 377-2 Ohnohigashi, Osakasayama, 589-8511 Japan
* Corresponding author.
E-mail address: m-kitano@med.kindai.ac.jp

Imaging, North Billerica MA, USA), were created.[4–6] These agents are composed of gasses different from room air, and microbubbles of these agents can be oscillated or broken by lower acoustic powers.[4–6] These second-generation agents are more suitable for endoscopic ultrasonography (EUS) because the small transducer of EUS produces limited acoustic power.[8]

VASCULAR ASSESSMENT BY EUS

In the early days of EUS development, it was difficult to enhance vessels by mechanical radial EUS.[9] The first reports about contrast-enhanced EUS used fundamental B-mode EUS with an intravenous ultrasound contrast agent composed of sonicated albumin.[10,11] Although this method slightly enhanced the signals from lesions with rich vessels such as neuroendocrine tumors and cystic tumors in the pancreas, it did not enhance signals of other diseases and has a limitation in selective depiction of the contrast agent.[10,11] Electronic EUS equipped with color and power Doppler modes first enabled the identification of large vessels with colored images.[12] In particular, this method allowed the visualization of large vessels behind the gastrointestinal wall and improved the avoidance of intervening vessels during needle puncture. However, those modes only detect large vessels with fast flow because they depict the phase shift of signals from quickly moving substances.

Ultrasound contrast agents located in vessels emit phase shift (pseudo-Doppler) signals and enhance Doppler signals from vessels.[13] Contrast-enhanced Doppler EUS (CD-EUS) is used to evaluate not only large vessels but also tumor vascularity, by enhancing the intratumoral vessels (**Fig. 1**).[14–20] However, even the use of ultrasound contrast agents cannot depict fine vessels with slow flow because Doppler ultrasonography has low sensitivity to low flow.[7,8,15] Moreover, contrast-enhanced Doppler ultrasonography suffers from poor spatial resolution as well as motion and blooming artifacts, which can make it difficult to evaluate tumor vascularity.[7,8,15] Motion artifacts refer to the low signal intensity of flowing blood compared with that of tissue movement.[7] Blooming refers to the widened appearance of a blood vessel with power Doppler compared with the results with fundamental B-mode imaging (see **Fig. 1**).[7]

Contrast-enhanced harmonic imaging was developed to allow for more specific imaging of ultrasound contrast agents.[6–8] The main purpose of contrast-enhanced harmonic ultrasonography is the selective sensitive depiction of signals from
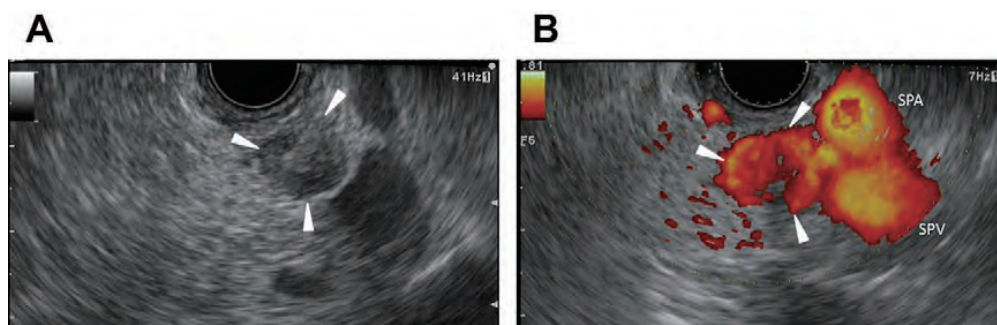
Fig. 1. Typical conventional EUS and contrast-enhanced power Doppler EUS images of a small endocrine tumor in the pancreas. (*A*) The conventional EUS image shows a small hypoechoic nodule (*arrowheads*) of 10 mm in diameter in the body of the pancreas. (*B*) The contrast-enhanced power Doppler EUS image shows abundant vessels in the nodule (*arrowheads*), although blooming artifact is observed at vessels in the nodule. Blooming artifact is also observed in the splenic artery (SPA) and splenic vein (SPV).

microbubbles in situ by filtrating signals from the tissue. The most important advantage of contrast-enhanced harmonic ultrasonography over contrast-enhanced Doppler ultrasonography is that it can depict microbubbles even though they do not flow.[6–8] By depicting microbubbles located in microvasculature, contrast-enhanced harmonic ultrasonography allowed imaging of parenchymal perfusion. In addition, it can depict vessels with very high resolution without Doppler-related artifacts.

Contrast-enhanced harmonic EUS (CH-EUS) was impossible with Levovist because the transducer of the echoendoscope was too small to oscillate and break the microbubbles, necessitating the use of CD-EUS.[9,15] Because second-generation ultrasound contrast agents can be oscillated or broken by lower acoustic powers,[4–6,9] CH-EUS can be used with these agents.

CONTRAST-ENHANCED DOPPLER EUS

Intravenous ultrasound contrast agents improve the Doppler detection of flow in vessels. CD-EUS is significantly more sensitive and accurate than power Doppler EUS in detecting the relatively hypovascular ductal adenocarcinomas of the pancreas.[14–16] Hypovascularity as a sign of ductal carcinomas in CD-EUS obtained a sensitivity of 85% to 94% and a specificity of 71% to 100%.[14–18] EUS is also a highly sensitive method for detection of pancreatic ductal carcinomas, particularly small ones.[9,21,22] In a study comparing the abilities of CD-EUS and contrast-enhanced multidetector-row computed tomography (MDCT) to diagnose small pancreatic tumors, the sensitivities for detecting pancreatic carcinomas sized 2 cm or less by EUS and MDCT were 94% and 50%, respectively, and CD-EUS diagnosed small pancreatic carcinomas sized 2 cm or less as tumors with hypoenhancement significantly better than MDCT.[15] EUS is also useful to detect small neuroendocrine tumors.[19,23,24] Detection rate of EUS for neuroendocrine tumors (92%–95%) is significantly higher than that of MDCT (63%–81%).[19,24] Ishikawa and colleagues[19] reported on the usefulness of EUS combined with contrast enhancement in the preoperative localization of pancreatic endocrine tumors. In their report, CD-EUS indicated that hyperenhancement was observed in 98% of neuroendocrine tumors.[19] In those previous reports about CD-EUS, ductal carcinomas and neuroendocrine tumors are characterized by CD-EUS as solid lesions with hypoenhancement and hyperenhancement, respectively. Taking into consideration the superiority of EUS in the detection rates, CD-EUS is a promising tool to characterize small pancreatic tumors that cannot be detected by other imaging methods.

In discrimination between benign and malignant mediastinal and abdominal lymph nodes, 2 groups reported the usefulness of CD-EUS.[20,25] Kanamori and colleagues[20] found that all malignant lymph nodes showed a defect of enhancement (sensitivity 100%), whereas diffuse enhancement was observed in 86% of benign lymph nodes (specificity 86%). Hocke and colleagues[25] used the following criteria for malignant lymph nodes: irregular appearance of the vessels and only arterial vessels visible. Using these criteria, the sensitivity and specificity in differentiating malignant from benign lymph nodes were 60% and 91%, respectively. If malignant lymphoma were excluded, the sensitivity of the CD-EUS for malignant lymph nodes increased to 73%.[25] Even though those reports differ in criteria and diagnostic accuracy for malignancy, CD-EUS is useful for characterization of enlarged lymph nodes.

PRINCIPLE OF CONTRAST HARMONIC IMAGING

When exposed to a certain range of ultrasonic beams, the microbubbles of ultrasound contrast agents are disrupted or resonated, which releases a large amount of

harmonic signals (**Fig. 2**).[6–8] When the tissues and microbubbles receive transmitted ultrasound waves, both produce harmonic components that are integer multiples of the fundamental frequency; however, the harmonic content from the microbubbles is higher than that from the tissues (see **Fig. 2**).[6–8] Selective depiction of the second harmonic component visualizes the signals from the microbubbles more strongly than those from the tissues.

When ultrasound pulses are transmitted multiple times in succession, the signals from the contrast agents vary greatly in phase (see **Fig. 2**), with no relation to its motion.[9,26,27] The signals in the part without contrast agents are hardly changed between multiple transmissions. This specific feature of the contrast agents (phase shifts) is also used for contrast-enhanced harmonic imaging.[9,26,27] Extended pure harmonic detection (ExPHD) is a mode for EUS systems that is specific for contrast harmonic imaging, which receives not only the second harmonic components but also signals with the relative phase shifts (see **Fig. 2**).[9,26,27] This processing enhances the imaging of signals from microbubbles in vessels with very slow flow without Doppler-related artifacts.

CONTRAST-ENHANCED HARMONIC EUS

Dietrich and colleagues[28] first reported the use of contrast-enhanced, low–mechanical index, real-time EUS using adapted dynamic-contrast harmonic wide-band pulsed inversion software. Using this method, they identified the celiac trunk, common hepatic artery, splenic artery, and portal vein and its branches and collaterals in patients with portal vein thrombosis.[28]

The development of another EUS system, equipped with an echoendoscope with a broadband transducer and ExPHD mode, enabled the authors to obtain images of the microcirculation and parenchymal perfusion in digestive organs (**Fig. 3**).[26,27] In contrast, CD-EUS cannot provide images of parenchymal perfusion or of branching vessels because blooming artifacts of large vessels are observed.[27,29]
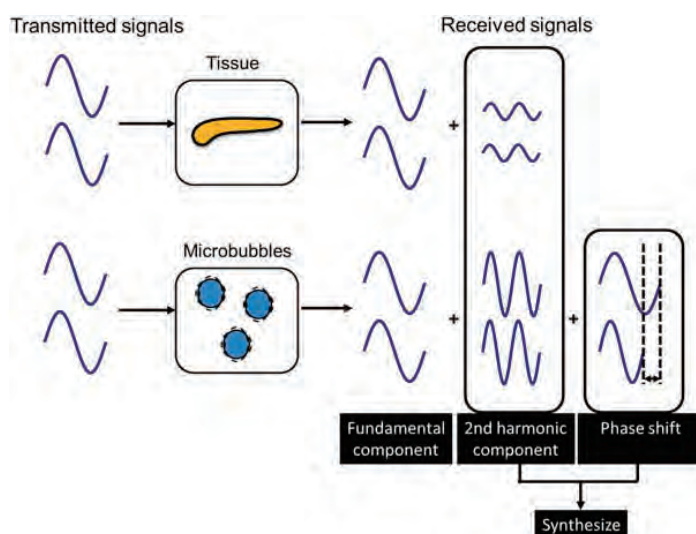
Fig. 2. Principle of extended pure harmonic detection (ExPHD) mode. The microbubbles produce stronger second harmonic signals as well as greater phase shifts than does the tissue. Contrast harmonic imaging based on the ExPHD mode selectively depicts signals from microbubbles by synthesizing the phase shift signals with the second harmonic components.
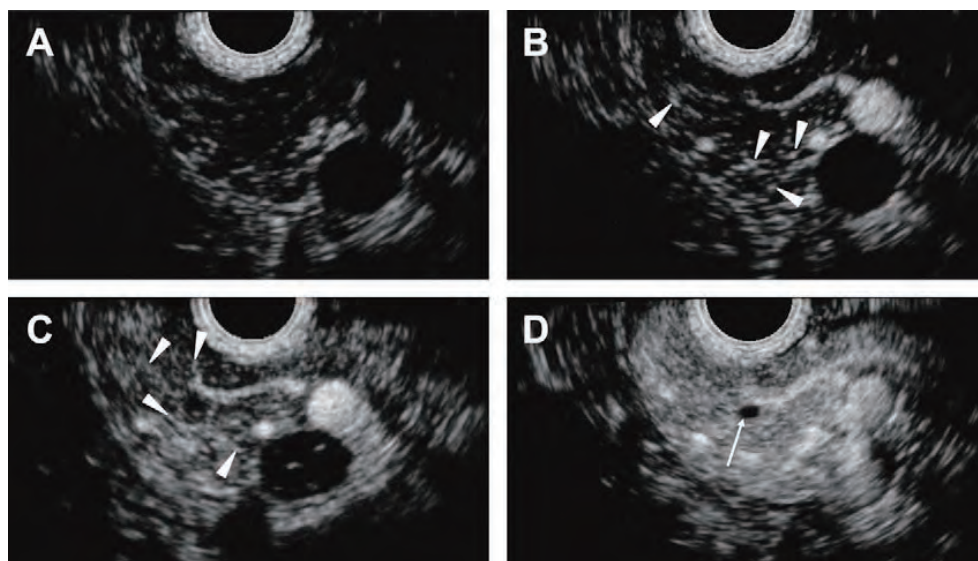
Fig. 3. Time course of CH-EUS images in a normal pancreas. (*A*) The CH-EUS image before infusion of the contrast agent. Neither signals from the tissue nor microbubbles can be observed. (*B*) The CH-EUS image 13 seconds after infusion of the contrast agent. Spotty signals from microbubbles (*arrowheads*) appear in the pancreas. (*C*) The CH-EUS image 15 seconds after infusion of the contrast agent. Fine branching vessels (*arrowheads*) are observed. (*D*) The CH-EUS image 22 seconds after infusion of the contrast agent. Diffuse parenchymal perfusion of microbubbles can be imaged. The pancreatic duct (*arrow*) is depicted as an avascular structure with strong contrast to the surrounding tissue.

The new EUS system depicts pancreatic ductal carcinomas as hypovascular nodules that mostly have irregular network-like vessels. In contrast, CH-EUS depicts most neuroendocrine tumors as a hypervascular pattern (**Fig. 4**).[27,29–31] This new CH-EUS system allowed diagnosis of pancreatic carcinomas with a high sensitivity (89%–96%) and specificity (64%–89%).[29–31] Particularly, CH-EUS was significantly more accurate than MDCT in diagnosing small ductal carcinomas (P = .034).[31]

Although EUS has a high spatial resolution, it misses some ductal carcinomas. Some factors, including chronic pancreatitis, a diffusely infiltrating and a recent episode of acute pancreatitis, increase the likelihood of a false-negative EUS examination.[32] CH-EUS improves the depiction of pancreatic tumors, compared with conventional EUS.[30,31] CH-EUS allowed detection of the outline of all ductal carcinomas with uncertain conventional EUS findings.[30,31] Similarly, when Imazu and colleagues[33] compared the abilities of conventional EUS and CH-EUS in terms of preoperative T staging of pancreatobiliary tumors, they found that CH-EUS correctly diagnosed T staging in 24 of 26 pancreatobiliary tumors, 6 of which were misdiagnosed by conventional EUS. In particular, CH-EUS depicted the wall of the portal vein more clearly, which means that it is superior in diagnosing portal invasion by pancreatic and bile duct cancers.[33]

CH-EUS is also used for evaluation of vascularity in organs other than the pancreas. In a study evaluating the microvasculature of benign and malignant intra-abdominal lesions of undetermined origin by CH-EUS, 96.3% of malignant lesions exhibited heterogeneous enhancement (**Fig. 5**), whereas benign lesions did not show heterogeneous enhancement.[34] This result suggests that heterogeneous enhancement on CH-EUS is a feature of malignant lesions. When CH-EUS was used for assessment of tumor vascularity of gastrointestinal stromal tumors (GISTs), CH-EUS identified
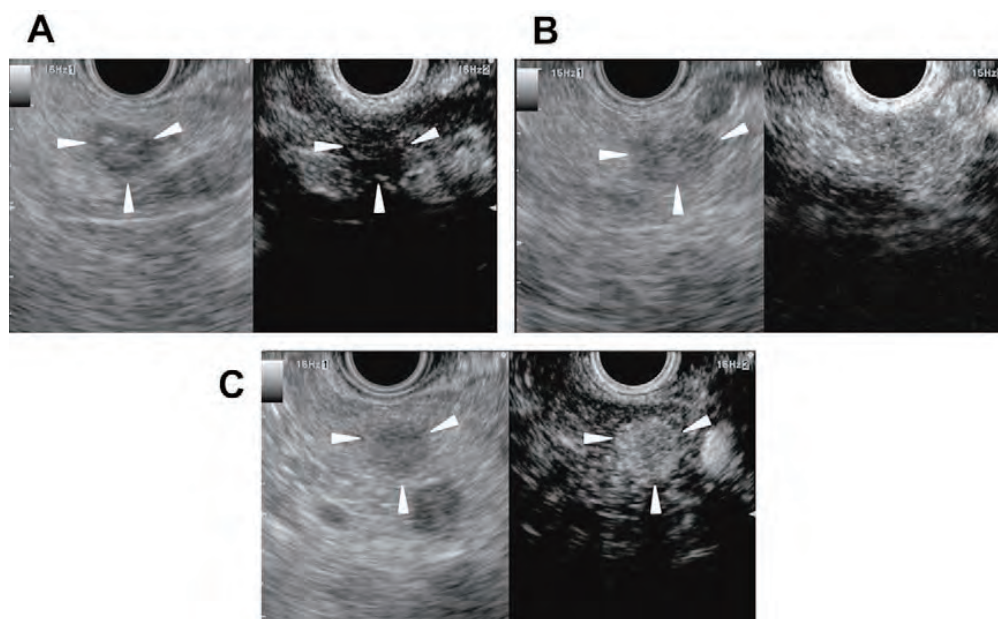
Fig. 4. Typical conventional EUS (*left*) and CH-EUS (*right*) images of small tumors in the pancreas. (*A*) A ductal carcinoma with hypoenhancement. Conventional EUS (*left*) shows a hypoechoic area (*arrowheads*) of 10 mm in diameter at the pancreas tail. CH-EUS (right) indicates that the area is hypovascular (*arrowheads*) compared with the surrounding tissue. (*B*) An inflammatory pseudotumor with isoenhancement. Conventional EUS (*left*) shows a hypoechoic area (*arrowheads*) of 11 mm at the pancreas tail. CH-EUS (*right*) indicates enhancement in this area similar to the surrounding tissue; a margin is not observed. (*C*) A neuroendocrine tumor with hyperenhancement. Conventional EUS (*left*) shows a hypoechoic mass (*arrowheads*) of 9 mm in diameter at the pancreas body. CH-EUS (*right*) indicates that enhancement (*arrowheads*) in the mass is higher than in the surrounding tissue.

irregular vessels in GISTs with high-grade malignancy (**Fig. 6**) with a sensitivity, specificity, and accuracy of 100%, 63%, and 83%, respectively, suggesting CH-EUS may play an important role in predicting the malignancy risk of GISTs.[35]

CONTRAST-ENHANCED EUS FOR EUS-GUIDED FINE-NEEDLE ASPIRATION

EUS-guided fine-needle aspiration (EUS-FNA) is a useful tool for characterizing a solid mass detected by conventional EUS.[36] If the EUS-FNA diagnosis is a malignant tumor,
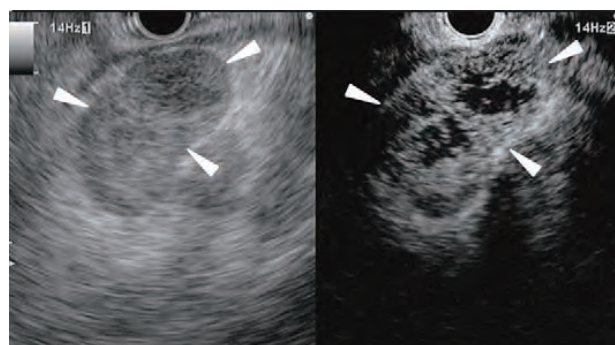
Fig. 5. Typical conventional EUS (*left*) and CH-EUS (*right*) images of a metastatic lymphadenopathy. Conventional EUS (*left*) shows a swollen lymph node (*arrowheads*) of 41 mm in diameter adjacent to the stomach. CH-EUS (*right*) indicates that enhancement in the lymph node is heterogeneous.
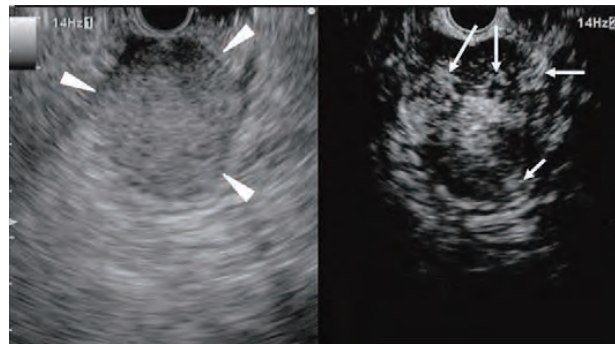
Fig. 6. Typical conventional EUS (*left*) and CH-EUS (*right*) images of a GIST with high-grade malignancy. Conventional EUS (*left*) shows a tumor (*arrowheads*) of 38 mm in diameter located in the fourth layer of the gastric wall. CH-EUS (*right*) depicts irregular vessels (*arrows*) in the tumor.

then patients should be recommended to undergo surgery, because EUS-FNA is highly specific for the identification of pancreatic carcinomas. However, deciding between surgery and follow-up in patients whose EUS-FNA findings are negative is sometimes difficult, because false-negative EUS-FNA results cannot be excluded. When Napoleon and colleagues[29] compared CH-EUS and EUS-FNA for the identification of pancreatic carcinomas, the sensitivity of CH-EUS for carcinoma identification was higher than that of EUS-FNA. Moreover, 4 of the 5 carcinomas with false-negative EUS-FNA findings had hypoenhancement. In the authors' recent study, CH-EUS was not superior to EUS-FNA for the identification of pancreatic carcinomas.[31] However, CH-EUS revealed that all ductal carcinomas with false-negative EUS-FNA findings had hypoenhancement. When the ductal carcinomas were regarded as tumors with a positive EUS-FNA finding and/or hypoenhancement on CH-EUS, combining CH-EUS with EUS-FNA improved the sensitivity of identifying ductal carcinomas from 92.2% to 100%.[31] Therefore, CH-EUS before EUS-FNA complements EUS-FNA in identifying ductal carcinomas and helps in making decisions about the next treatment approach. When CH-EUS reveals a hypovascular pattern in a pancreatic tumor, even if the EUS-FNA findings are negative, surgical resection or pathologic reevaluation by EUS-FNA of the tumor should be recommended.

As described earlier, CH-EUS is better than conventional EUS in clearly depicting the outline of some pancreatic carcinomas.[30,31] These results suggest that contrast harmonic imaging might be useful for the identification of some lesions that are not clearly defined by conventional EUS (**Fig. 7**). Consequently, it is likely that CH-EUS facilitates EUS-FNA of lesions by helping to identify the target for EUS-FNA (see **Fig. 7**). In addition, information from CH-EUS can potentially change the diagnosis and management of the lesions depicted by EUS. Romagnuolo and colleagues[37] reported 2 cases in which the management changed significantly after CH-EUS. EUS-FNA was avoided because CH-EUS revealed that a liver tumor was a hemangioma. EUS-FNA was performed in a mediastinal cystic lesion after CH-EUS confirmed it as solid.

FUTURE PERSPECTIVE OF CONTRAST-ENHANCED EUS

So far, the technique of contrast-enhanced EUS has largely been used for evaluation of vascularity. However, recent studies have revealed that this technique can also be applied for molecular imaging of vascular endothelial growth factor (VEGF) receptor.[38,39] Affinity of microbubbles for VEGF receptor may facilitate molecular profiling of angiogenesis and early assessment of antiangiogenic therapy effects.
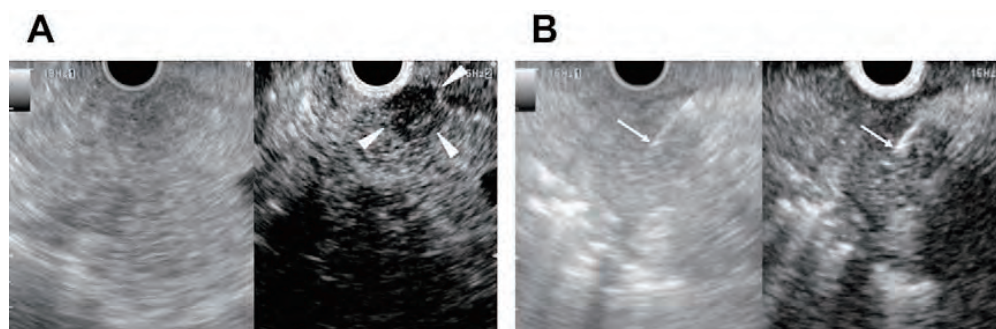
Fig. 7. Contrast-enhanced EUS-FNA. (*A*) Conventional EUS (*left*) and CH-EUS (*right*) images of a ductal carcinoma. Conventional EUS (*left*) shows a slightly hypoechoic area without a clear margin at the pancreas head. CH-EUS (*right*) depicts a tumor with hypoenhancement with a clear margin relative to the surrounding tissue. (*B*) Conventional EUS (*left*) and CH-EUS (*right*) images during needle puncture. The tumor with hypoenhancement is punctured by a needle (*arrow*) guided by CH-EUS (*right*). The targeted EUS-FNA of the hypovascular tumor detected malignant cells.

Recently, there has been a focus on EUS-guided ablation therapy for the treatment of focal pancreatic lesions. Experiments in pigs showed that contrast-enhanced EUS improved visualization of altered pancreatic vascular perfusion after local injection of ethanol, indicating that contrast-enhanced EUS can be used for follow-up of the ablated lesion.[40] Moreover, the development of contrast-enhanced EUS will be beneficial for targeted drug delivery applications in pancreatic tumors.[4,41] Drug substances, including plasmid DNA, can be delivered within the microbubbles. Strong ultrasound beams can potentially destroy microbubbles to release the drug "payload" only in the pancreas. Thus, the targeted drug delivery treatment should enhance drug action and reduce undesirable adverse effects. In the near future, the technology of contrast-enhanced EUS would expand to these promising applications.

REFERENCES

1. Matsuda Y, Yabuuchi I. Hepatic tumors: US contrast enhancement with CO_2 microbubbles. Radiology 1986;161:701–5.
2. Kudo M, Tomita S, Tochio H, et al. Small hepatocellular carcinoma: diagnosis with US angiography with intraarterial CO_2 micorbubbles. Radiology 1992;182:155–60.
3. Kato T, Tsukamoto Y, Naitoh Y, et al. Ultrasonographic and endoscopic ultrasonographic angiography in pancreatic mass lesions. Acta Radiol 1995;36:381–7.
4. Sanchez MV, Varadarajulu S, Napoleon B. EUS contrast agents: what is available, how do they work, and are they effective? Gastrointest Endosc 2009;69:571–7.
5. Reddy NK, Ioncică AM, Săftoiu A, et al. Contrast-enhanced endoscopic ultrasonography. World J Gastroenterol 2011;17:42–8.
6. Whittingham TA. Contrast-specific imaging techniques; technical perspective. In: Quaia E, editor. Contrast media in ultrasonography. Basic principles and clinical applications. Berlin: Springer; 2005. p. 43–84.
7. Kudo M. Various contrast-enhanced imaging modes after administration of Levovist. In: Kudo M, editor. Contrast harmonic imaging in the diagnosis and treatment of hepatic tumors. Tokyo: Springer; 2003. p. 22–30.
8. Kitano M, Kudo M, Maekawa K, et al. Dynamic imaging of pancreatic diseases by contrast enhanced coded phase inversion harmonic ultrasonography. Gut 2004; 53:854–9.

9. Kitano M, Kudo M, Sakamoto H, et al. Endoscopic ultrasonography and contrast-enhanced endoscopic ultrasonography. Pancreatology 2011;11(Suppl 2): 28–33.

10. Hirooka Y, Goto H, Ito A, et al. Contrast-enhanced endoscopic ultrasonography in pancreatic diseases: a preliminary study. Am J Gastroenterol 1998;93: 632–5.

11. Hirooka Y, Naitoh Y, Goto H, et al. Usefulness of contrast-enhanced endoscopic ultrasonography with intravenous injection of sonicated serum albumin. Gastrointest Endosc 1997;46:166–9.

12. Wiersema MJ, Chak A, Kopecky KK, et al. Duplex Doppler endosonography in the diagnosis of splenic vein, portal vein, and portosystemic shunt thrombosis. Gastrointest Endosc 1995;42:19–26.

13. Bhutani MS, Hoffman BJ, van Velse A, et al. Contrast-enhanced endoscopic ultrasonography with galactose microparticles: SHU508A (Levovist). Endoscopy 1997;29:635–9.

14. Hocke M, Schulze E, Gottschalk P, et al. Contrast-enhanced endoscopic ultrasound in discrimination between focal pancreatitis and pancreatic cancer. World J Gastroenterol 2006;12:246–50.

15. Sakamoto H, Kitano M, Suetomi Y, et al. Utility of contrast-enhanced endoscopic ultrasonography for diagnosis of small pancreatic carcinomas. Ultrasound Med Biol 2008;34:525–32.

16. Săftoiu A, Iordache SA, Gheonea DI, et al. Combined contrast-enhanced power Doppler and real-time sonoelastography performed during EUS, used in the differential diagnosis of focal pancreatic masses (with videos). Gastrointest Endosc 2010;72:739–47.

17. Becker D, Strobel D, Bernatik T, et al. Echo-enhanced color- and power-Doppler EUS for the discrimination between focal pancreatitis and pancreatic carcinoma. Gastrointest Endosc 2001;53:784–9.

18. Dietrich CF, Ignee A, Braden B, et al. Improved differentiation of pancreatic tumors using contrast-enhanced endoscopic ultrasound. Clin Gastroenterol Hepatol 2008;6:590–7.

19. Ishikawa T, Itoh A, Kawashima H, et al. Usefulness of EUS combined with contrast-enhancement in the differential diagnosis of malignant versus benign and preoperative localization of pancreatic endocrine tumors. Gastrointest Endosc 2010;71:951–9.

20. Kanamori A, Hirooka Y, Itoh A, et al. Usefulness of contrast-enhanced endoscopic ultrasonography in the differentiation between malignant and benign lymphadenopathy. Am J Gastroenterol 2006;101:45–51.

21. DeWitt J, Devereaux B, Chriswell M, et al. Comparison of endoscopic ultrasonography and multidetector computed tomography for detecting and staging pancreatic cancer. Ann Intern Med 2004;141:753–63.

22. Săftoiu A, Vilmann P. Role of endoscopic ultrasound in the diagnosis and staging of pancreatic cancer. J Clin Ultraound 2009;37:1–17.

23. Rösch T, Lightdale CJ, Botet JF, et al. Localization of pancreatic endocrine tumors by endoscopic ultrasonography. N Engl J Med 1992;326:1721–6.

24. Khashab MA, Yong E, Lennon AM, et al. EUS is still superior to multidetector computed tomography for detection of pancreatic neuroendocrine tumors. Gastrointest Endosc 2011;73:691–6.

25. Hocke M, Menges M, Topalidis T, et al. Contrast-enhanced endoscopic ultrasound in discrimination between benign and malignant mediastinal and abdominal lymph nodes. J Cancer Res Clin Oncol 2008;134:473–80.

26. Kitano M, Kudo M, Sakamoto H, et al. Preliminary study of contrast-enhanced harmonic endosonography with second-generation contrast agents. J Med Ultrasonics 2008;35:11–8.

27. Kitano M, Sakamoto H, Matsui U, et al. A novel perfusion imaging technique of the pancreas: contrast-enhanced harmonic EUS (with video). Gastrointest Endosc 2008;67:141–50.

28. Dietrich CF, Ignee A, Frey H. Contrast-enhanced endoscopic ultrasound with low mechanical index: a new technique. Z Gastroenterol 2005;43:1219–23.

29. Napoleon B, Alvarez-Sanchez MV, Gincoul R, et al. Contrast-enhanced harmonic endoscopic ultrasound in solid lesions of the pancreas: results of a pilot study. Endoscopy 2010;42:564–70.

30. Fusaroli P, Spada A, Mancino MG, et al. Contrast harmonic echo-endoscopic ultrasound improves accuracy in diagnosis of solid pancreatic masses. Clin Gastroenterol Hepatol 2010;8:629–34.

31. Kitano M, Kudo M, Yamao K, et al. Characterization of small solid tumors in the pancreas: contrast: the value of contrast-enhanced harmonic endoscopic ultrasonography. Am J Gastroenterol 2012;107:303–10.

32. Bhutani MS, Gress FG, Giovannini M, et al. The no endosonographic detection of tumor (NEST) study: a case series of pancreatic cancers missed on endoscopic ultrasonography. Endoscopy 2004;36:385–9.

33. Imazu H, Uchiyama Y, Matsunaga K, et al. Contrast-enhanced harmonic EUS with novel ultrasonographic contrast (Sonazoid) in the preoperative T-staging for pancreaticobiliary malignancies. Scand J Gastroenterol 2010;45:732–8.

34. Xia Y, Kitano M, Kudo M, et al. Characterization of intra-abdominal lesions of undetermined origin by contrast-enhanced harmonic EUS (with video). Gastrointest Endosc 2010;72:637–42.

35. Sakamoto H, Kitano M, Matsui S, et al. Estimation of malignant potential of GI stromal tumors by contrast-enhanced harmonic EUS (with videos). Gastrointest Endosc 2011;73:227–37.

36. DeWitt J. EUS in pancreatic neoplasms. In: Hawes RH, Fockens P, editors. Endosonography. Philadelphia: Saunders Elsevier; 2006. p. 177–203.

37. Romagnuolo J, Hoffman B, Vela S, et al. Accuracy of contrast-enhanced harmonic EUS with a second-generation perflutren lipid microsphere contrast agent (with video). Gastrointest Endosc 2011;73:52–63.

38. Willmann JK, Lutz AM, Paulmurugan R, et al. Dual-targeted contrast agent for US assessment of tumor angiogenesis in vivo. Radiology 2008;248:936–44.

39. Palmowski M, Huppert J, Ladewig G, et al. Molecular profiling of angiogenesis with targeted ultrasound imaging: early assessment of antiangiogenic therapy effects. Mol Cancer Ther 2008;7:101–9.

40. Giday SA, Magno P, Gabrielson KL, et al. The utility of contrast enhanced endoscopic ultrasound in monitoring ethanol-induced pancreatic tissue ablation: a pilot study in a porcine model. Endoscopy 2007;39:525–9.

41. Hermot S, Klibanov AL. Microbubbles in ultrasound-triggered drug and gene delivery. Adv Drug Deliv Rev 2008;60:1153–66.

Signaling pathway/molecular targets and new targeted agents under development in hepatocellular carcinoma

Masatoshi Kudo

Masatoshi Kudo, Department of Gastroenterology and Hepatology, Kinki University School of Medicine, Osaka-Sayama, Osaka 589-8511, Japan
Author contributions: Kudo M solely contributed to this paper.
Correspondence to: Masatoshi Kudo, MD, PhD, Department of Gastroenterology and Hepatology, Kinki University School of Medicine, 377-2, Ohno-Higashi, Osaka-Sayama, Osaka 589-8511, Japan. m-kudo@med.kindai.ac.jp
Telephone: +81-72-3660221 Fax: +81-72-3672880

Kudo M. Signaling pathway/molecular targets and new targeted agents under development in hepatocellular carcinoma. *World J Gastroenterol* 2012; 18(42): 6005-6017 Available from: URL: http://www.wjgnet.com/1007-9327/full/v18/i42/6005.htm DOI: http://dx.doi.org/10.3748/wjg.v18.i42.6005

Abstract

Advances in molecular cell biology over the last decade have clarified the mechanisms involved in cancer growth, invasion, and metastasis, and enabled the development of molecular-targeted agents. To date, sorafenib is the only molecular-targeted agent whose survival benefit has been demonstrated in two global phase Ⅲ randomized controlled trials, and has been approved worldwide. Phase Ⅲ clinical trials of other molecular targeted agents comparing them with sorafenib as first-line treatment agents are ongoing. Those agents target the vascular endothelial growth factor, platelet-derived growth factor receptors, as well as target the epidermal growth factor receptor, insulin-like growth factor receptor and mammalian target of rapamycin, in addition to other molecules targeting other components of the signal transduction pathways. In addition, the combination of sorafenib with standard treatment, such as resection, ablation, transarterial embolization, and hepatic arterial infusion chemotherapy are ongoing. This review outlines the main pathways involved in the development and progression of hepatocellular carcinoma and the new agents that target these pathways. Finally, the current statuses of clinical trials of new agents or combination therapy with sorafenib and standard treatment will also be discussed.

INTRODUCTION

Advances in molecular cell biology over the last decade have clarified the mechanisms involved in cancer growth, invasion and metastasis, and enabled the development of molecular-targeted agents, best represented by trastuzumab for breast cancer, imatinib and rituximab for hematopoietic tumors, and gefitinib and erlotinib for lung cancer. These molecular-targeted agents are broadly classified into two categories: drugs targeting cancer cell-specific molecules, and nonspecific molecular-targeted drugs for molecular biological abnormalities induced in the host stroma or blood vessels by the presence of cancer. Examples of the former approach include trastuzumab, which targets human epidermal growth factor receptor 2 (HER2), the expression of which is a poor prognostic factor for breast cancer; rituximab, which is used to treat B-cell lymphoma, targets CD20 expressed on normal and neoplastic mature B cells; while imatinib binds to the ATP-binding site of Bcr-abl, a protein that causes chronic myelogenous leukemia. However, no critical target molecules responsible for treatment response have been identified in hepatocellular carcinoma (HCC).

In recent years, clinical trials have been conducted for many agents that act on growth factor receptors, such as epidermal growth factor receptor (EGFR) and vascular endothelial growth factor receptor (VEGFR), and intracellular signaling pathways. In addition, multi-kinase inhibitors, including sorafenib, have emerged and been evaluated. Clinical trials are ongoing to compare drugs with the same mechanism of action and to test the combined efficacy and relative merits of these drugs with existing drugs for many cancers. Since the main treatment option for metastatic, advanced stage cancers, such as breast and colorectal cancer, is systemic chemotherapy, clinical trials are ongoing to investigate how to combine molecular-targeted agents with standard therapies based on the results of long-term, large-scale clinical trials, and to identify which molecular-targeted agents should be used as initial or second-line therapy.

However, for HCC, background liver damage limits the indication for systemic chemotherapy and no anti-cancer drugs were found to be effective in large-scale randomized controlled trials except sorafenib. Now that the usefulness of sorafenib has been demonstrated in two large scale randomized clinical trials, the development of new drugs that are effective for poor-prognosis advanced HCC, who are resistant to a standard of care agent, sorafenib.

In this review, the clinical impact of sorafenib and ongoing trials of new agents or combination trials with sorafenib will be described.

SIGNALING PATHWAYS AND MOLECULAR-TARGETED AGENTS IN HCC

As in other cancers, the molecular mechanisms involved in the development and progression of HCC are complex. After hepatitis B virus and hepatitis C virus infection and alcohol or aflatoxin B1 exposure, genetic and epigenetic changes occur, including oncogene activation and tumor-suppressor gene inactivation due to inflammation-induced increase in hepatocyte turnover and oxidative stress-induced DNA damage. Through apoptosis and cell proliferation, these changes lead to the multistep development and progression of a hyperplastic to dysplastic nodule, early HCC, and advanced HCC. A number of studies have reported changes in gene expression, chromosomal amplification, mutations, deletions and copy number alterations (gain/loss), somatic mutations, CpG hypermethylation, and DNA hypomethylation, as well as molecular abnormalities, which can constitute therapeutic targets[1-5].

The binding of growth factors to their receptor proteins activates protein-phosphorylating enzymes, thus activating a cascade of proliferative signaling pathways to transmit proliferative signals into the nucleus. Growth factors, such as EGF, transforming growth factor (TGF)-α/-β, insulin-like growth factor (IGF), and VEGF, also function in liver regeneration after injury, while fibroblast growth factor (FGF) and the platelet-derived growth factor (PDGF) family are involved in liver fibrosis and HCC growth[6-8]. The receptors for these growth factors are broadly classified into G protein-coupled receptors and protein kinases. On ligand binding, these receptors activate their downstream intracellular molecules in a cascade fashion. Many of the growth factor receptors and oncogenes have tyrosine kinase activity, and the tyrosine kinases are classified into transmembrane receptor tyrosine kinases, such as the EGFR and VEGFR, and cytoplasmic non-receptor tyrosine kinases, such as Abl and Src. On the other hand, Raf, mitogen-activated protein kinase (MAPK)/extracellular signaling-regulated kinase (ERK) kinase (MEK), and mammalian target of rapamycin (mTOR) are serine/threonine kinases.

In general, the MAPK, phosphoinositide 3-kinase (PI3K)/Akt/mTOR, c-MET, IGF, Wnt-β-catenin and Hedgehog signaling pathways, and the VEGFR and PDGF receptor (PDGFR) signaling cascades show altered activity in HCC, and agents targeting these pathways are under development (Figures 1-3; Table 1)[9-12]. Many molecular-targeted agents are now under development and the target signaling pathways and growth factors are outlined below.

MAPK pathway (Ras/Raf/MEK/ERK)

The MAPK intracellular signaling pathway, which is mainly involved in cell growth and survival, and regulates cell differentiation, is upregulated in cancer cells. Therefore, this pathway has been extensively studied as a therapeutic target. The MAPK pathway is a common downstream pathway for the EGFR, PDGFR and VEGFR, and is universally used for signal transduction downstream of cytokine receptors, integrin complexes, and G-protein receptors to Ras. The MAPK pathway also plays an important role in HCC, in that its activation is reportedly involved in HCC growth and survival. The downstream ERK is activated by two upstream protein kinases, which are coupled to growth factor receptors by Ras proteins. Ras, which is activated by ligand binding, activates Raf serine/threonine kinases and MEK (MAP kinase/ERK kinase), while MEK phosphorylates and activates ERK, which phosphorylates proteins involved in cell growth, apoptosis resistance, extracellular matrix production and angiogenesis[13-15].

Raf and Ras inhibitors: Raf and Ras are proto-oncogenes. In particular, K-Ras mutations are commonly observed in many cancers, including pancreatic and colorectal cancers. One study reported that 30% of HCCs have Ras mutations[16]. To our knowledge, no agents targeting Ras are planned to enter clinical trials at the present. However, because the binding of Ras protein to the cell membrane and its functional activation require farnesylation, several farnesyltransferase inhibitors are being tested for Ras-related tumors. In addition, vaccine therapy for mutant Ras proteins is currently being tested for solid cancers, including HCC.
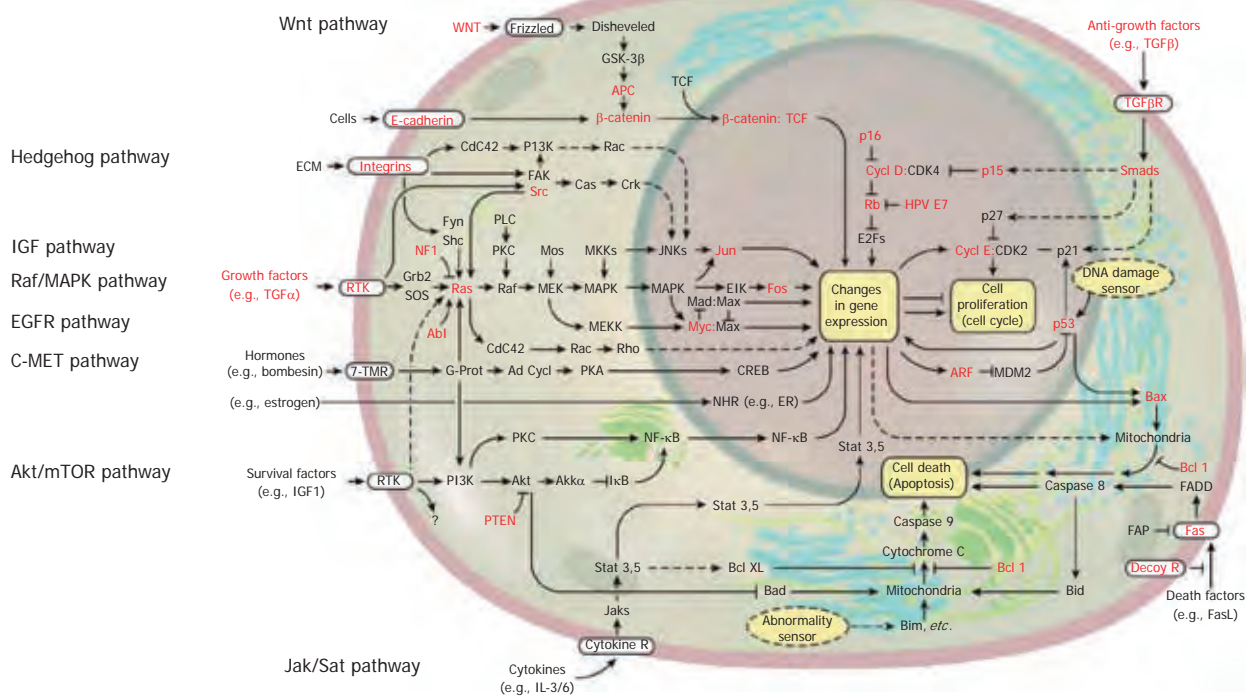
Figure 1 Signal transduction in solid cancer cells including hepatocellular carcinoma. Some of the genes known to be functionally altered are highlighted in red. These signaling pathways, including growth factor pathway, Wnt pathway, Hedgehog pathway, Akt/mammalian target of rapamycin (mTOR) pathway, and Jak/Stat pathway, can be a molecular targets for treatment of hepatocellular carcinoma. (Cited and modified from Hanahan *et al*[10] with permission.) EGFR: Epidermal growth factor receptor; TGF: Transforming growth factor; IGF: Insulin-like growth factor; MAPK: Mitogen-activated protein kinase; PI3K: Phosphoinositide 3-kinase; ERK: Extracellular signaling-regulated kinase; NF-κB: Nuclear factor-kappa B; IL: Interleukin.

Table 1 Molecular targeted agents for hepatocellular carcinoma: Targets and development status

Agents	Targets (angiogenesis)			Targets (proliferation)				Positioning	Development status
	VEGFR	PDGFR	FGF	EGFR	Raf	mTOR	TRAIL-R2 DR5		
Sorafenib	●	●			●			1st line	Approved
Sunitinib	●	●						1st line	PIII terminated
E7080	●	●	●					1st/2nd line	PII ongoing
Tigatuzumab (CS1008)							●	1st line (sorafenib combination)	PI / II ongoing
Linifanib (ABT-869)	●	●						1st line	PIII ongoing
Brivanib		●			●			1st line, 2nd line, TACE adjuvant	PIII ongoing
TSU-68		●	●					TACE combination	PIII ongoing
Ramucirumab		●						2nd line	PIII ongoing
Everolimus (RAD001)						●		2nd line	PIII ongoing
Axitinib		●	●					2nd line	PIII ongoing

VEGFR: Vascular endothelial growth factor receptor; PDGFR: Platelet-derived growth factor receptor; FGF: Fibroblast growth factor; EGFR: Epidermal growth factor receptor; mTOR: Mammalian target of rapamycin; TACE: Transarterial chemoembolization.

The Raf family consists of three isoforms, A-Raf, B-Raf and C-Raf/Raf-1. Genetic abnormalities, such as point mutations and gene rearrangements, have been reported in various cancers[17]; however, in HCC, *ras/raf* mutations are rare, and no *k-ras* or *b-raf* mutations have been detected[18]. On the other hand, wild-type Raf-1 was reported to be hyperactivated in many cancers, including HCC[19-21]. Sorafenib inhibits Raf, and has multiple characteristics in that it exhibits strong inhibitory activity against Raf-1 (C-Raf) kinase, B-Raf (wild-type B-Raf and mutant V600E B-Raf) serine/threonine kinase, the pro-angiogenic receptor tyrosine kinases VEGFR,

PDGFR and FGFR1, and tyrosine kinases, such as c-kit, Flt-3 and RET, which are involved in tumor progression and overall prognosis[22].

MEK: The MEK family consists of MEK1 and MEK2 proteins, which specifically phosphorylate tyrosine and threonine residues, and phosphorylates downstream Erk1 and Erk2[23].

In an immunohistochemical study, MEK1/2 overexpression, ERK1/2 overexpression, and ERK1/2 phosphorylation were observed in 100% (46/46), 91% (42/46), and 69% (32/46) of HCCs, respectively. In ad-
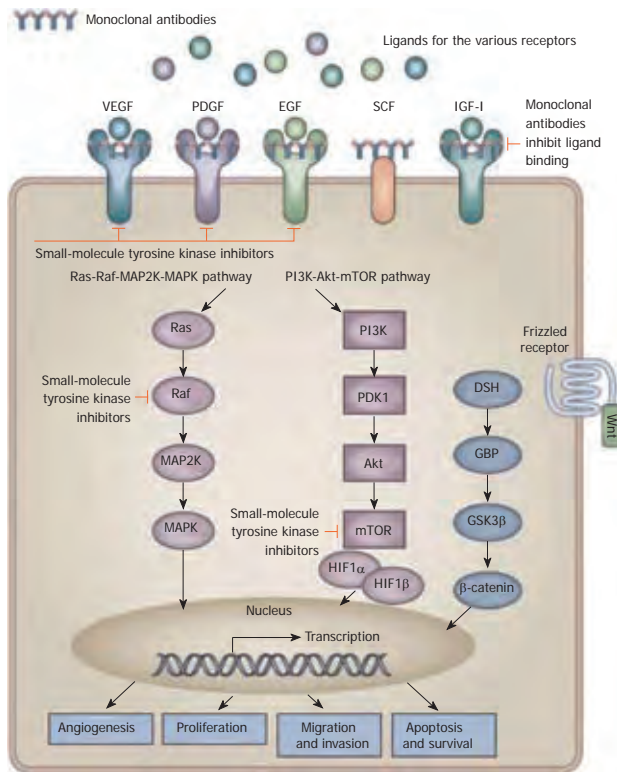
Figure 2 Signaling pathways and potential drug targets to inhibit hepatocarcinogenesis. Activation of receptor tyrosine kinases by their ligands activates downstream signaling pathways with effects on angiogenesis, proliferation, migration and invasion, and apoptosis or survival of cells. Monoclonal antibodies inhibit ligand binding to the receptor and small-molecule tyrosine kinase inhibitors inhibit propagation of the downstream signal. (Cited from Spangenberg et al[11] with permission.) IGF: Insulin-like growth factor; MAPK: Mitogen-activated protein kinase; PI3K: Phosphoinositide 3-kinase; EGF: Epidermal growth factor; VEGF: Vascular endothelial growth factor; PDGF: Platelet-derived growth factor; mTOR: Mammalian target of rapamycin; HIF: Hypoxia-inducible factor; SCF: Stem cell factor.

dition, the *in vitro* treatment of HepG2 and Hep3B cells with MEK1/2 inhibitors inhibited cell growth and up-regulated apoptosis[24].

The MEK inhibitors CI-1040, PD0325901, AZD6244, and RDEA119/BAY869766 have been tested in several cancers, including solid tumors such as HCC. Recently, the results of Phase I of AS703026 and E6201 studies against solid tumors were reported in ASCO2010. A phase Ⅱ study of AZD6244 (selumetinib, ARRY-142866) and a phase I / Ⅱ study of RDEA119/BAY869766 in combination with sorafenib are being conducted.

PI3K/Akt/mTOR pathway

The PI3K/Akt/mTORpathway also plays an important role in cell growth, survival regulation, metabolism, and anti-apoptosis. The membrane lipid phosphatidylinositol 4,5-bisphosphate (PIP2) is phosphorylated by PI3K into phosphatidylinositol 3,4,5-triphosphate (PIP3), which binds to and activates the serine/threonine kinase Akt. The tumor suppressor gene product phosphatase and tensin homolog (PTEN) deleted on chromosome is antagonistic to PI3K activity. PTEN is a lipid phosphatase that

dephosphorylates inositol phosphates, such as PIP3. The inactivation of PTEN through gene deletion increases PIP3 levels, and activates Akt, which inhibits apoptosis, leading to the development of tumors. The serine/threonine kinase mTOR is an important mediator in the PI3K/Akt pathway, which binds intracellularly to a protein called raptor or rictor, and exists as two different complexes, complex 1 and 2 (mTORC1 and mTORC2). mTORC2 (mTOR-rictor) activates Akt, while mTORC1 (mTOR-raptor) is activated downstream of Akt; thus, both molecules regulate protein synthesis (Figures 4 and 5)[25].

Inhibiting mTOR with molecules, such as RAD001, generates additive effects that accompany upstream and downstream target inhibition. Alternatively, upstream receptor inhibition is compensated for by inhibiting the downstream pathway, even if some resistance develops against receptor inhibition regardless of initial or acquired resistance. Therefore, RAD001 is a potential targeted agent for HCC.

Besides the finding that mTOR plays a key role in cell biology, it was also demonstrated that mTOR and S6K are overexpressed in 15%-41% of HCCs. mTOR inhibitors also have antitumor effects in various HCC cell lines and animal models[26-29]. Activation of mTOR is correlated with the development of HCC and recurrence after the excision of early HCC. Regulating this specific intracellular pathway (Ras-Raf pathway) with RAD001 is potentially more effective in suppressing sorafenib-resistant tumors.

A study of 528 HCC samples showed that the expression of pAkt, PTEN, p27 and S6 ribosomal protein (pS6) was a poor prognostic factor for survival[30]. A tissue microarray analysis of HCC samples revealed that the loss of PTEN and overexpression of pAkt and p-mTOR were correlated with tumor grade, intrahepatic metastasis, vascular invasion, TNM stage, Ki-67 labeling index, and matrix metalloproteinase (MMP)-2 and -9 upregulation. Meanwhile, PTEN mRNA expression in the cancerous tissue was downregulated compared with that in the non-cancerous tissue. The levels of PTEN, MMP-2, and MMP-9 mRNA expression were correlated with tumor stage and metastasis, and the levels of PTEN and MMP-9 mRNA expression were inversely correlated[31]. In an extensive analysis of 314 HCC samples in terms of mutation analysis, DNA copy number changes, mRNA levels and immunostaining, Villanueva et al[32] found that activation of the IGF pathway, upregulation of EGF, dysregulation of PTEN, and aberrant mTOR signaling were present in half of the samples, and that inhibiting mTOR activity with everolimus was effective in improved survival and suppression of recurrence.

The PI3K inhibitor RG7321 and the Akt inhibitor perifosine target the PI3K/Akt/mTOR pathway and are in early stages of clinical development, while the mTOR inhibitors everolimus (RAD001), sirolimus (Rapamune), and temsirolimus (CCI-779) are at more advanced stages of development. Everolimus is used to treat sorafenib-
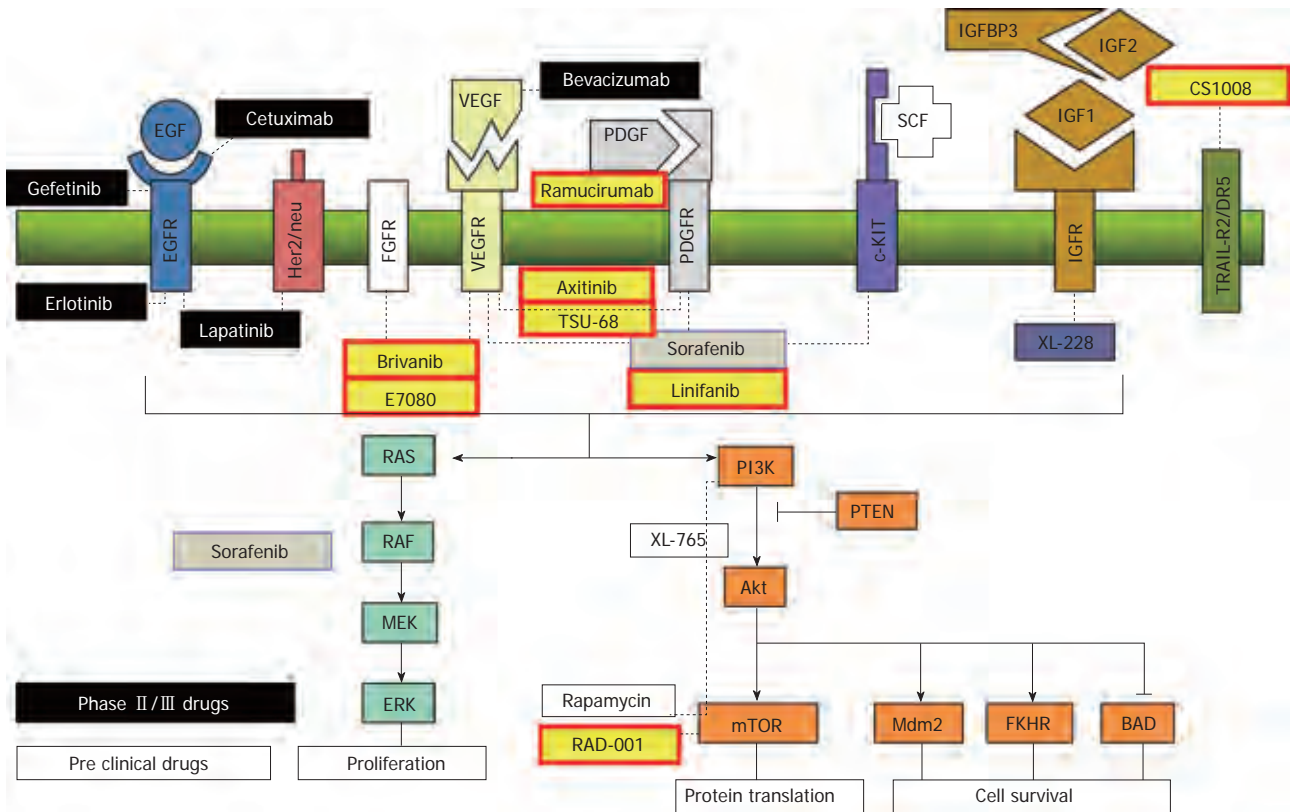
Figure 3 Target molecular and targeted agents under development. Monoclonal antibodies (VEGF: bevacizumab, EGFR: cetuxinab), tyrosine kinase inhibitors (VEGFR: sorafenib, brivanib, linifanib, axitinib, TSU-68; FGFR: E7080, brivanib), EGFR: erlotinib, lapatinib), serine/threonine kinase inhibitors (Raf: sorafenib, mTOR: rapamycin and everolimus) and agonistic ligand of TRAIL-R2/DR5 (CS1008). (Cited and modified from Villanueva *et al*[12] with permission.) IGF: Insulin-like growth factor; PI3K: Phosphoinositide 3-kinase; EGF: Epidermal growth factor; VEGF: Vascular endothelial growth factor; PDGF: Platelet-derived growth factor; mTOR: Mammalian target of rapamycin; PTEN: Phosphatase and tensin homolog; SCF: Stem cell factor; FGFR: Fibroblast growth factor receptor.
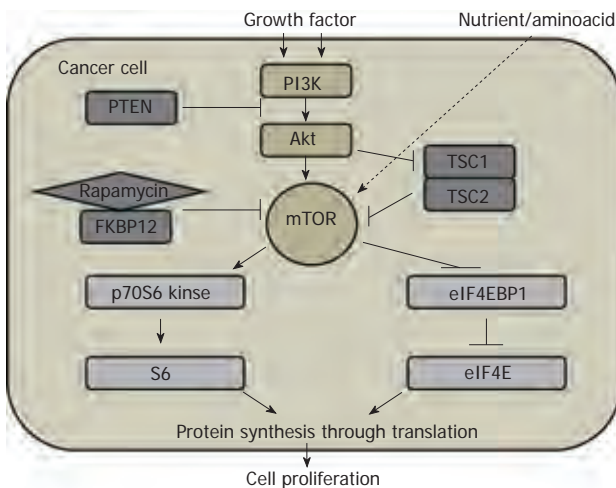
Figure 4 Phosphoinositide 3-kinase/Akt/mammalian target of rapamycin signaling pathway in cell proliferation in solid cancer. PI3K: Phosphoinositide 3-kinase; mTOR: Mammalian target of rapamycin; PTEN: Phosphatase and tensin homolog; TSC: Tuberous sclerosis; FKBP12: FK506-binding protein 12.
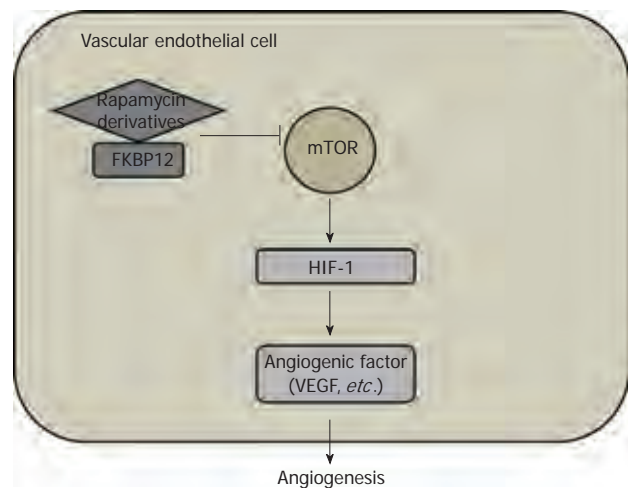
Figure 5 Mammalian target of rapamycin/hypoxia-inducible factor-1/vascular endothelial growth factor signaling pathway in angiogenesis in solid cancer. HIF: Hypoxia-inducible factor; VEGF: Vascular endothelial growth factor; mTOR: Mammalian target of rapamycin; FKBP12: FK506-binding protein 12.

intolerant patients, or for patients showing disease progression after sorafenib administration. A phase Ⅲ study to compare everolimus and a placebo (EVOLVE-1: Advanced Hepatocellular Carcinoma after Disease Progression or Intolerance to Sorafenib EverOlimus for Liver

cancer Evaluation) and a phase Ⅰ/randomized phase Ⅱ study (sorafenib + everolimus *vs* sorafenib alone) to test the efficacy and tolerance of sorafenib in combination with everolimus are underway. Since mTOR inhibitors exhibit cytostatic and antiangiogenic effects, they are

expected to be effective in combination with other angiogenesis inhibitors, such as bevacizumab, and may be appropriate for administration after transarterial chemoembolization (TACE). Furthermore, since the mTOR pathway is stimulated by factors such as EGFR, PDGFR, and TGFα, and is closely related to other signaling pathways, including the Ras/Raf/MEK/ERK pathway, they are likely to show promising efficacy when used in combination with other growth factor inhibitors[33].

VEGF/VEGFR, PDGFR, FGFR

Angiogenesis is an important event not only for HCC, but also for cancer growth and metastasis, and occurs because of complex alterations involving promoting factors such as VEGF, angiopoietin, and FGF, and inhibitory factors including thrombospondin and angiostatin, as well as the surrounding tissue. The VEGF family consists of VEGF-A, -B, -C, -D and –E, and placental growth factor (PIGF). The VEGFR family comprises VEGFR-1 (flt-1), VEGFR-2 (flk-1/KDR), and VEGFR-3 (flt-4). VEGF-A binds to VEGFR-1 and -2 and is involved in angiogenesis and the maintenance of mature blood vessels, while VEGF-C and -D mainly bind to VEGFR-3, are involved in lymphangiogenesis[34,35]. VEGF isoforms, such as $VFGF_{121}$ and $VEGF_{165}$, have been identified, and isoform subtypes also exist, such as $EGF_{166}b$. Thus, it is clear that these growth factors do not exhibit angiogenesis-promoting effects alone, and they have attracted attention as new therapeutic targets[36].

HCC typically exhibits active angiogenesis. During the progression from early to well- and moderately-differentiated HCC, angiogenesis increases and cancer cells acquire the ability to invade vessels and metastasize. Scientific and clinical studies have revealed that, during the progression from hepatitis to cirrhosis, angiogenesis and disruption of the vascular architecture are linked to the progression of HCC, and contribute to increased hepatic vascular resistance and portal hypertension, and decreased hepatocyte perfusion[37]. In addition, a meta-analysis has demonstrated that VEGF expression is a prognostic factor in HCC[38].

Phase Ⅱ studies have been started to test the usefulness of bevacizumab (Avastin®), which directly targets VEGF, in TACE-treated HCC, and the use of bevacizumab in combination with erlotinib (Tarceva®), an EGFR tyrosine kinase inhibitor.

Sunitinib (Sutent®) is a multi-kinase inhibitor that inhibits tyrosine kinases, such as VEGFR-1, -2, -3, PDGFR-α, -β and c-Kit. A phase Ⅱ study of sunitinib in 37 advanced HCC patients showed that the median progression-free survival (PFS) and median overall survival (OS) were 3.7 and 8 mo, respectively. In that study, adverse events included grade 3/4 thrombocytopenia in 37.8% of patients, neutropenia in 24.3%, asthenia in 13.5%, and hand-foot syndrome in 10.8%[39]. Since sunitinib has a lower IC_{50} for each target than sorafenib, it is expected to exhibit greater antitumor activity. However, this factor may be responsible

for the higher incidence of adverse events with sunitinib. The main evaluation item in the above phase Ⅱ trial was the response rate, which did not reach the expected value, leading to the conclusion that it was a negative study[40]. In that study, sunitinib was administered at 50 mg/d for four weeks followed by two weeks of rest per cycle[39], whereas Zhu et al[40] used a dosing schedule of 37.5 mg/d for four weeks followed by two weeks of rest per cycle, and reported that the median PFS and OS were 3.9 and 9.8 mo, respectively. An ongoing global cooperative phase Ⅲ controlled clinical trial to compare sorafenib and sunitinib head-to-head, and to seek approval for first-line indications for advanced HCC, adopted a sunitinib dosing schedule of 37.5 mg/d. However, in a "Reflection and Reaction" regarding the above trial results, Forner et al[41] cast doubt on whether the drugs at this dose could maintain tolerance and ensure efficacy. Consequently, the trial was terminated on March, 2010 because of the recommendation by data monitoring committee based on interim analysis, showing relatively high toxicity and no superior efficacy to sorafenib.

Brivanib is a kinase inhibitor that selectively inhibits VEGFR-1, -2 and -3, and FGFR-1, -2 and -3. Recent studies suggest that tumor progression following treatment with antiangiogenic agents that target the VEGF signaling pathway alone may result from either evasive or intrinsic resistance[42]. Furthermore, there is strong evidence to support the hypothesis that evasive resistance to anti-VEGF blockade is associated with reactivation of tumor angiogenesis by alternative signaling pathways. One such mechanism of resistance is the activation of the FGF signaling pathway[43,44]. Basic FGF (FGF2) is a potent angiogenic factor. Indeed, expression of FGF2 enhances growth, invasion, and angiogenesis of many tumor types[45,46]. Moreover, recent evidence has shown that FGF is overexpressed and activated in HCC, and that high FGF2 levels may predict a poor clinical outcome among patients with HCC[46].

Considering the proposed importance of FGF signaling in HCC angiogenesis, it is clear that novel antiangiogenic agents that combine inhibition of FGF receptor signaling with inhibition of VEGFR signaling might provide a potential mechanism to overcome anti-VEGF resistance in HCC (Figure 6). With this in mind, it is worthwhile considering the potential future impact of brivanib on the treatment of advanced HCC. Brivanib, a small-molecule tyrosine kinase inhibitor, is the first oral selective dual inhibitor of FGF and VEGF signaling. In multiple preclinical models of human xenograft tumors, including patient-derived HCC xenografts, brivanib has shown potent antitumor activity and no overt toxicity when dosed orally[47,48]. Furthermore, brivanib has demonstrated promising antitumor activity and acceptable tolerability in a phase Ⅱ, open-label study in patients with unresectable locally advanced or metastatic HCC[49,50]. Crucially, within this trial, brivanib showed activity both as first-line therapy (overall survival: 10 mo) or as second-
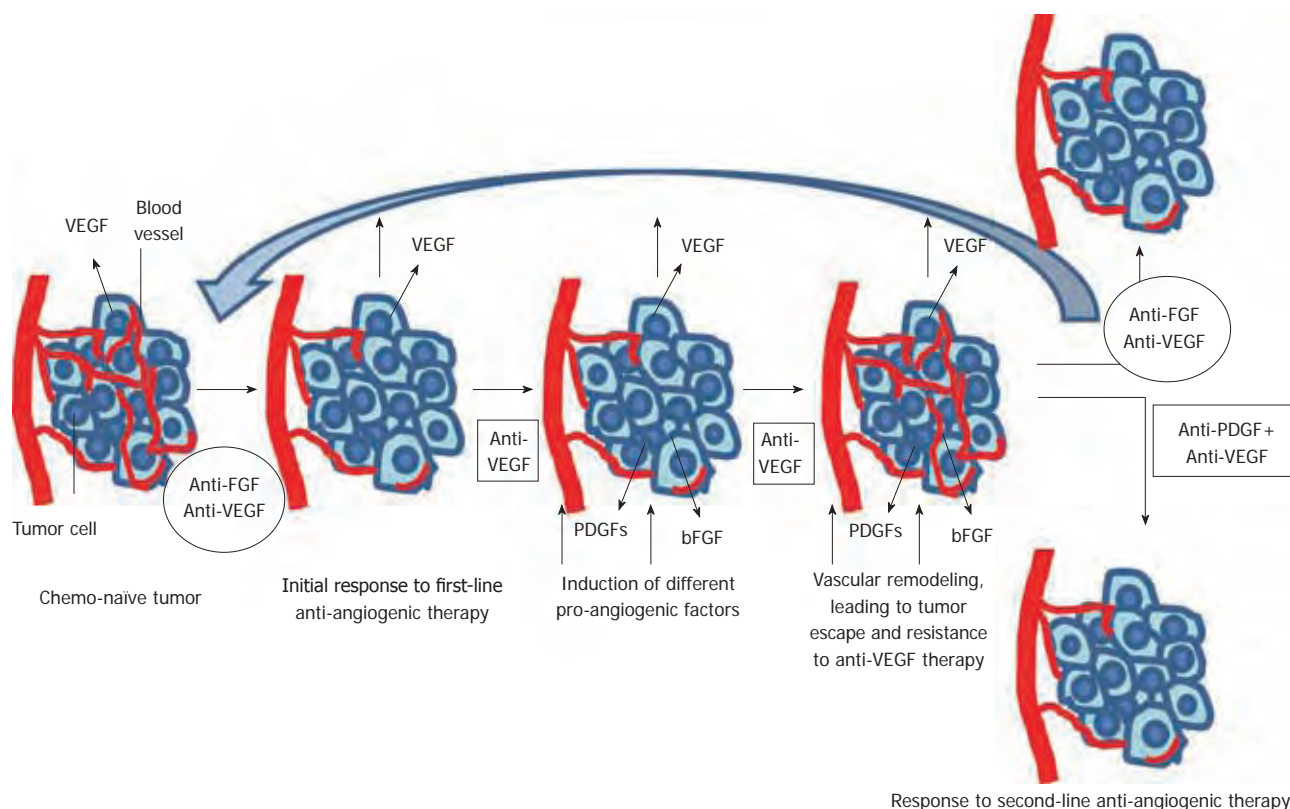
Figure 6 Brivanib may be effective for the failure or resistance of first line anti-angiogenic therapy for vascular endothelial growth factor. In addition, there is a possibility that anti-FGF agents can be first line anti-angiogenic agents. FGF: Fibroblast growth factor; VEGF: Vascular endothelial growth factor; PDGF: Platelet-derived growth factor.

line therapy in patients who had failed prior antiangiogenic treatment, primarily with sorafenib (overall survival: 9.5 mo)[50]. Of note, the incidence of all-grade hand-foot syndrome was only 8% in this study.

As for brivanib, an international global phase Ⅲ clinical trial to compare brivanib and sorafenib head-to-head and to seek approval for first-line therapy for advanced HCC has already been started, and the results are eagerly awaited. Since brivanib targets FGF and VEGF, and is associated with relatively mild adverse effects, a second-line study of brivanib in sorafenib-ineffective and -intolerant patients, and a trial to evaluate the use of brivanib in combination with TACE, are underway. Depending on the results of these trials, indications for use in HCC may be obtained; therefore, positive results are eagerly anticipated.

The results have been reported for a phase Ⅱ study of brivanib in 55 patients (cohort A) who had not received systemic therapy for curatively unresectable HCC and 46 patients (cohort B) previously treated with angiogenesis inhibitors, such as sorafenib or thalidomide[49]. The median TTP and OS were 2.8 mo and 10 mo, respectively, in cohort A versus 1.4 mo and 9.8 mo, respectively, in cohort B. Adverse events included fatigue (51.5%), diarrhea (41.6%), hypertension (42.6%), anorexia (41.6%), and nausea/vomiting (40.6%/30.7%) in total. Thus, these results demonstrated the efficacy of brivanib as a second-line treatment. The results of three phase Ⅲ clinical trials,

BRISK-PS (sorafenib failure or sorafenib-intolerant patients; brivanib + best supportive care (BSC) *vs* placebo + BSC), BRISK-FL (advanced HCC; brivanib *vs* sorafenib), and BRISK-TA (patients with unresectable HCC, brivanib *vs* placebo as post-TACE adjuvant therapy) are awaited (Table 2).

Linifanib (ABT-869), which strongly inhibits VEGFR and PDGFR, is also under global phase Ⅲ trial.

In a Japanese phase Ⅰ/Ⅱ trial of TSU-68, an oral molecular inhibitor of VEGFR, PDGFR, and FGFR, to test its safety and efficacy in 35 HCC patients, the response rate was 5.6% (CR, PR, SD, PD and NE in 1, 2, 15, 16 and 1 patients, respectively), and the disease control rate was 51.4%[51]. The global phase Ⅲ trial of TACE in combination with TSU-68 has just started on January 2011.

In addition, several phase Ⅰ/Ⅱ trials are being conducted to assess kinase inhibitors such as cediranib (AZD2171), which inhibit VEGFR, PDGFR, CSF-1R (cFms), Kit, and Flt3. Furthermore, a phase Ⅲ global study of axitinib, which is currently being tested in renal cell carcinoma, has also been started as a second line agents on 2011.

EGF/EGFR

EGFR is a member of the HER family, which includes EGFR (erbB1), HER2/neu (erbB3), and HER4 (erb4). All members of this family, except HER3, have an intracellular tyrosine kinase domain, and the binding of a ligand to its extracellular domain triggers signal transduc-

Table 2 Ongoing clinical trials (PⅢ)

First line
  Comparison study between sorafenib and single agent (head to head):
    Sunitinib → endpoint not met
    Brivanib
    Linifanib
  Combination with sorafenib and another agent:
    DXR, erlotinib (SEARCH), everolimus, CS-1008, *etc.*
Second line
  Sorafenib failure:
    Brivanib, everolimus (RAD001), ramucirumab, axitinib, S-1, *etc.*
Combination with standard therapy
  Adjuvant setting after surgery or RFA: STORM
  Combination with TACE: SPACE, BRISK-TA, TACTICS, ECOG1208
  Combination with HAIC: SILIUS

TACTICS: Phase Ⅱ study: Transcatheter arterial chemoembolization therapy in combination with sorafenib (ClinicalTrials.gov ID: NCT01217034), SILIUS: Randomized controlled trial comparing efficacy of sorafenib *vs* sorafenib in combination with low dose cisplatin/fluorouracil hepatic arterial InFUSion chemotherapy in patients with advanced hepatocellular carcinoma and exploratory study of biomarker predicting its efficacy (ClinicalTrials.gov ID: NCT01214343); HAIC: Hespatic arterial infusion chemotherapy; TACE: Transarterial chemoembolization.

tion through the above-described MAPK and PI3K/Akt/mTOR pathways. Thus, these receptors are involved in cell growth, differentiation, survival, and adhesion[52]. EGFR over expression has been reported in many cancers, and in HCC. For example, Buckley *et al*[53] reported that EGFR, detected by immunohistochemical analysis, was overexpressed in 50 (66%) of 76 HCCs, and that fluorescence *in situ* hybridization showed extra EGFR gene copies in 17 (45%) of 38 HCCs.

EGFR-targeting drugs include anti-EGFR antibodies, such as cetuximab and panitumumab, and small-molecule inhibitors of EGFR tyrosine kinases, such as gefitinib *etc*, and have been used widely for the treatment of several cancers other than HCC. Unfortunately, except for phase Ⅱ trial data, there are little clinical data on the efficacy of these drugs for the treatment of HCC.

Similar to gefitinib (Iressa®), erlotinib (Tarceva®) is an oral EGFR tyrosine kinase inhibitor. Philip *et al*[54] and Yau *et al*[55] have reported the results of phase Ⅱ studies of erlotinib in HCC; the median OSs in their studies were 13 and 10.7 mo, respectively. A phase Ⅲ clinical study (SEARCH study: Sorafenib and Erlotinib, a Randomized Trial Protocol for the Treatment of Patients with Hepatocellular Carcinoma) for sorafenib in combination with erlotinib *vs* sorafenib plus placebo is ongoing. Since erlotinib is associated with a high incidence of skin rash, dry skin and gastrointestinal toxicity, such as diarrhea, the results of the SEARCH study should be evaluated to assess whether this combination therapy can be used in clinical settings. Thomas *et al*[56] conducted a phase Ⅱ clinical study of erlotinib in combination with bevacizumab in 40 advanced HCC patients, and reported promising results; the median PFS and OS were 9 mo and 15.7 mo, respectively. However, they noted frequent treatment-related grade 3/4 toxicities, including fatigue

(20%), hypertension (15%), gastrointestinal bleeding (12.5%), wound infection (5%), diarrhea (10%), elevated transaminase levels (10%), and thrombocytopenia (10%), which necessitates further evaluation for drug tolerance. Although a clinical study of erlotinib in combination with bevacizumab (OPTIMOX-3 study) was also conducted in colorectal cancer patients, no tolerance was observed, which led to a change in the protocol[57,58].

After the introduction of a number of molecular-targeted drugs, strategies for the inhibition of similar or different signaling pathways (vertical or horizontal inhibition) with several drugs have been proposed. However, the combined use of molecular-targeted agents has remained largely unsuccessful, including panitumumab in combination with bevacizumab for the treatment of colorectal cancer[59]. Similarly, the results of sorafenib in combination with bevacizumab (vertical inhibition) have been reported[60]. Although some therapeutic responses were obtained, the combination therapy resulted in greater toxicity[60], suggesting the need for detailed evaluation of the dosing regimen.

Lapatinib (Tykerb®) is a dual inhibitor of EGFR and HER-2/neu, and inhibits tumor growth by downregulating MAPK, AKT, and p70S6 kinase[61]. In Japan, lapatinib is indicated for the treatment of breast cancer. In a phase Ⅱ clinical trial of lapatinib in 26 patients with unresectable advanced HCC, the median PFS and OS were 1.9 mo and 12.6 mo, respectively, and adverse events included diarrhea (73%), nausea (54%), and skin rash (42%)[62].

Cetuximab (Erbitux®) is a human/mouse chimeric monoclonal antibody consisting of the variable region of a mouse anti-human EGFR monoclonal antibody and the human immunoglobulin G1 constant region. Cetuximab inhibits the binding of endogenous EGFR ligands, such as EGF and TGFα, to EGFR. In a phase Ⅱ clinical trial of cetuximab in 30 patients with unresectable or metastatic HCC, the median PFS and OS were 1.4 mo and 9.6 mo, respectively, and treatment-related toxicities included grade 3 hypomagnesemia (3.3%) and grade 1/2 acne-like rash (83.3%), which was observed for the duration of anti-EGFR therapy in that study[63].

The EGFR offers a very interesting therapeutic target. As described above, the use of erlotinib in combination with sorafenib is still in the research stage. However, based on the results of phase Ⅱ studies, the efficacy of cetuximab or lapatinib as a monotherapy seems to be limited, and the results of further studies evaluating their efficacy in sorafenib-refractory or -intolerant patients are awaited with interest.

Hepatocyte growth factor/c-Met pathway
Since the hepatocyte growth factor (HGF)/Met pathway is involved in tumor growth, invasion, and angiogenesis in a wide range of neoplasms, HGF and Met have recently attracted attention as therapeutic targets. HGF is a heterodimer consisting of α and β chains bound together by a disulfate bond. The α-chain contains four
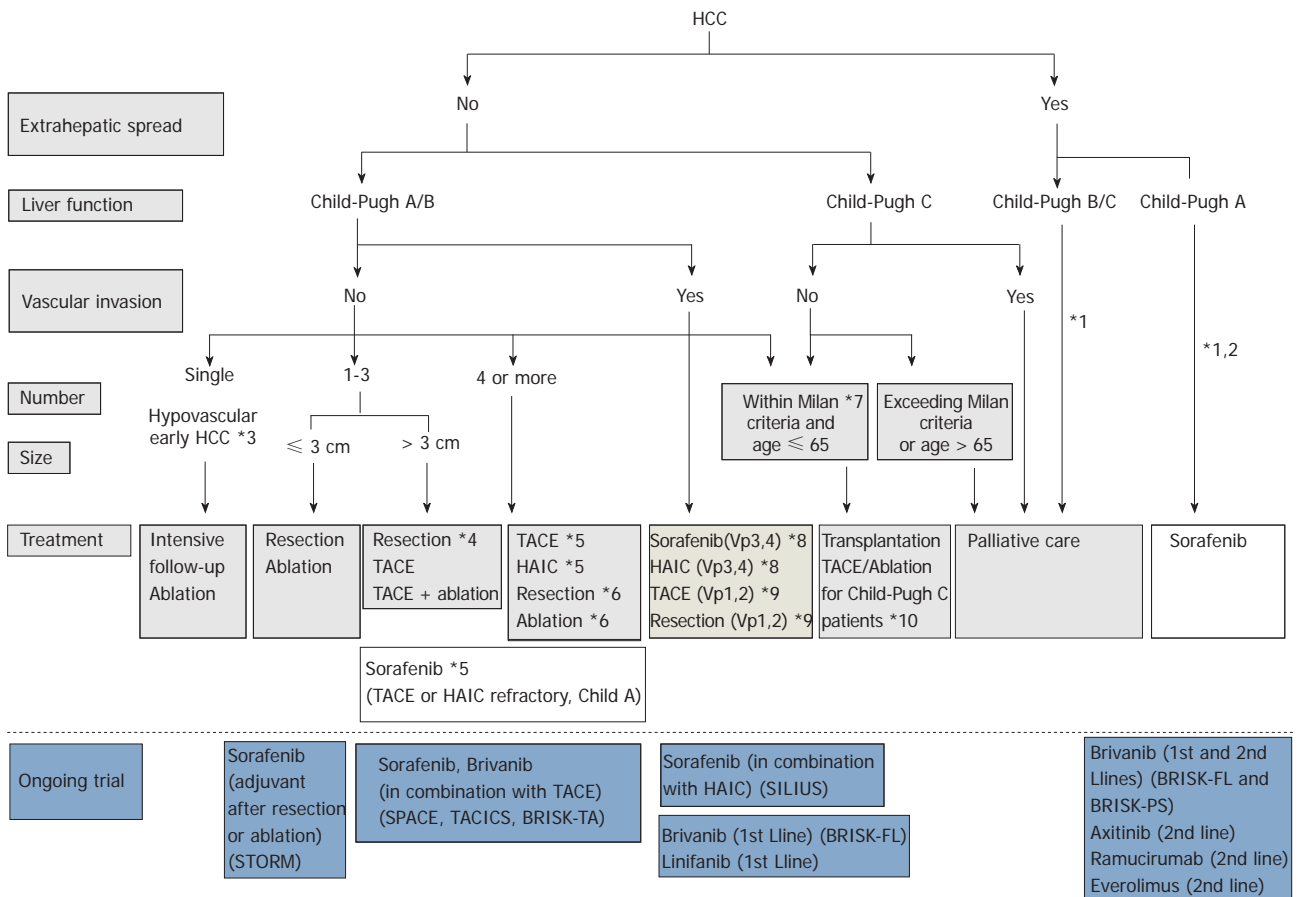
Figure 7 Consensus-based treatment algorithm for hepatocellular carcinoma proposed by Japan Society of Hepatology, revised in 2010. (Cited and modified from Kudo et al[67] with permission.) *1: Treatment should be performed as if extrahepatic spread is negative, when extrahepatic spread is not considered as a prognostic factor in Child-Pugh class A/B patients; *2: Sorafenib is the first choice of treatment in this setting as a standard of care; *3: Intensive follow-up observation is recommended for hypovascular nodules by the Japanese Evidence-Based Clinical Practice Guidelines. However, local ablation therapy is frequently performed in the following cases: (1) when the nodule is diagnosed pathologically as early hepatocellular carcinoma (HCC); (2) when the nodules show decreased uptake on Gd-EOB-MRI, or (3) when the nodules show decreased portal flow by CTAP, since these nodules frequently progress to advanced HCC; *4: Even for HCC nodules exceeding 3 cm in diameter, transcatheter arterial chemoembolization (TACE) in combination with ablation is frequently performed when resection is not indicated; *5: TACE is the first choice of treatment in this setting. Hepatic arterial infusion chemotherapy (HAIC) using an implanted port is also recommended for TACE-refractory patients. The regimen for this treatment is usually low-dose FP [5-fluorouracil (5-FU) + CDDP] or intra-arterial 5-FU infusion combined with systemic interferon therapy. Sorafenib is also recommended for TACE or HAIC-refractory patients with Child-Pugh class A liver function; *6: Resection is sometimes performed when more than 4 nodules are detected. Ablation is sometimes performed in combination with TACE; *7: Milan criteria: Tumor size $\leq$ 3 cm and tumor number $\leq$ 3, or solitary tumor $\leq$ 5 cm. Even when liver function is good (Child-Pugh A/B), transplantation is sometimes considered for frequently recurring HCC patients; *8: Sorafenib and HAIC are recommended for HCC patients with major portal invasion such as Vp3 (portal invasion in the 1st portal branch) or Vp4 (portal invasion in the main portal branch); *9: Resection and TACE are frequently performed when portal invasion is minor, such as Vp1 (portal invasion in the 3rd or more peripheral portal branch) or Vp2 (portal invasion in the 2nd portal branch); *10: Local ablation therapy or subsegmental TACE is performed even for Child-Pugh C patients when transplantation is not indicated when there is no hepatic encephalopathy, no uncontrollable ascites, and a low bilirubin level (< 3.0 mg/dL). However, it is regarded as an experimental treatment because there is no evidence of a survival benefit in Child-Pugh C patients. A prospective study is necessary to clarify this issue.

kringle domains, and the β-chain contains a serine protease-like domain. Met is a receptor tyrosine kinase for the HGF ligand, and contains a semaphorin-like domain. HGF or Met overexpression, and *Met* gene mutations and duplications, have been reported in various cancers, and abnormalities due to HGF/Met pathway activation have also been noted[64]. These abnormalities activate the downstream signaling cascade, leading to epithelial-mesenchymal transition and increased proliferative, migratory, invasive, and metastatic potentials of cancer cells[64].

HGF/c-MET-targeted drugs, including kinase inhibitors, HGF inhibitors and decoy c-Met receptor molecules are being developed. Of particular interest is ARQ-197, a

c-Met receptor tyrosine kinase inhibitor, which is a non-ATP-competitive molecule that binds near the ATP-binding site. A randomized phase Ⅱ study of ARQ-197 vs placebo is ongoing in patients with unresectable HCC after systemic therapy failure. In addition, the results of a phase Ⅰ study of ARQ-197 in combination with sorafenib was reported in ASCO 2010 (Abstract 3024).

IGF/IGFR

The IGF/IGFR system is involved in cell growth and the chemotherapeutic response. The ligands IGF-Ⅰ and -Ⅱ bind to their receptors IGF-1R and IGF-2R, and are involved in DNA synthesis and cell growth. Abnormali-
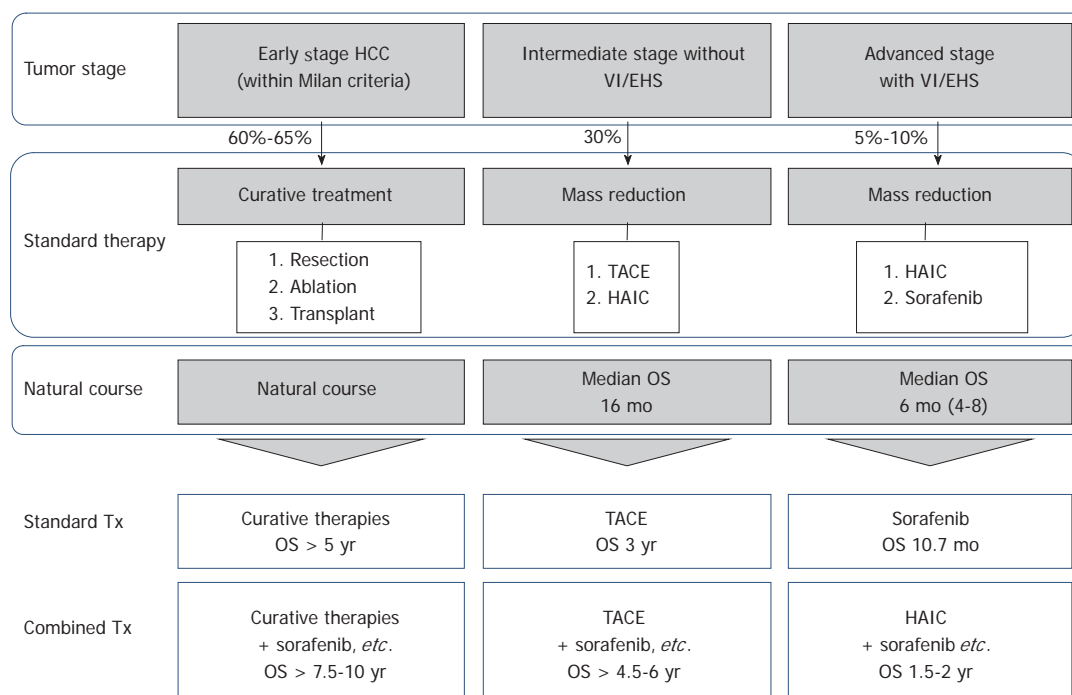
Figure 8 Outcomes of standard treatment modalities and expected future outcomes of combination therapy with molecular-targeted agents. By combining molecular targeted agents with resection or ablation, life expectancy [overall survival (OS)] is expected to be prolonged to 7.5-10 years. In addition, for intermediate stage hepatocellular carcinoma (HCC), the prognosis is expected to be improved to 4.5-6 years by combination with transarterial chemoembolization (TACE). For advanced stage HCC, the prognosis is expected to be improved to 1.5-2 years by combination with hepatic arterial infusion chemotherapy (HAIC).

Table 3 Subanalysis data of the SHARP study

		Advanced HCC with vascular invasion and/or extrahepatic spread	Advanced HCC without vascular invasion and/or extrahepatic spread
Hazard ratio		0.77 (95% CI: 0.60-0.99)	0.52 (95% CI: 0.32-0.85)
Median OS (MST) (mo)	Sorafenib	8.9 ($n = 209$) (95% CI: 7.6-10.3)	14.5 ($n = 90$) (95% CI: 14.0-N/E)
	Placebo	6.7 ($n = 212$) (95% CI: 5.2-8.0)	10.2 ($n = 91$) (95% CI: 8.6-15.5)

HCC: Hepatocellular carcinoma; OS: Overall survival; MST: Median survival time.

ties in IGF and IGF-1R, or their overexpression, have been reported in various cancers, including HCC. Their associations with disease stage, metastasis, survival[65], and the functions of IGF and IGFR in HCC[66] have been reported.

IGF-targeting drugs are currently being developed, and are mainly anti-IGF-1R antibodies, such as B ⅡB022, AVE1642, and cixutumumab (IMC-A12). A phase Ⅱ study of cixutumumab, a phase Ⅰb/Ⅱ study of sorafenib vs sorafenib plus BⅡB022, and phase Ⅰ/Ⅱ studies of AVE1642 as monotherapy or in combination with sorafenib or erlotinib are ongoing.

COMBINATION THERAPY OF STANDARD TREATMENT WITH SORAFENIB

In addition to the pharmaceutical-sponsored clinical trials of linifanib and brivanib as first- and second-line therapy in sorafenib-refractory patients, investigator initiated trials (IIT) of sorafenib in combination with hepatic arte-rial infusion chemotherapy (SILIUS trial: trial number NCT01214343), pharmaceutical and IIT trials of sorafenib in combination with TACE [SPACE, TACICS (trial number: NCT 01217034) and BRISK-TA trials], and a trial to test the inhibitory effect of sorafenibon tumor recurrence after curative treatment (STORM trial) are ongoing. The results of these trials are eagerly awaited (Figure 7)[67,68].

The working hypotheses in these studies can be deduced by extrapolating the median survival time (MST) and hazard ratios in overall survival (OS) calculated in a subanalysis of the SHARP study (Table 3). The results obtained suggest that starting treatment with molecular-targeted drugs at an earlier tumor stage in combination with standard treatment options such as resection, ablation, TACE, or hepatic arterial infusion chemotherapy can improve the prognosis of HCC. Thus, sorafenib has the potential to induce a paradigm shift in the treatment of HCC. For example, in a subanalysis of the SHARP trial, the hazard ratios for OS and MST ratio in intermediate stage HCC without vascular invasion or extrahepatic spread were 0.52 and 1.50, respectively (Table 3). This

suggests that survival of early stage HCC and intermediate stage HCC may be prolonged from 5 years to 7.5-10 years by using sorafenib in an adjuvant setting after curative treatment, and from 3 years to 4.5-6 years by using sorafenib in combination with TACE (Figure 8)[68].

CONCLUSION

Several clinical trials[39,40,49,54,63,69-74] of the molecular-targeted agents are ongoing. Angiogenesis-inhibiting drugs, particularly sorafenib, have been established for HCC, and drugs targeting several molecules are being developed.

Although sorafenib was recently approved, many issues remain to be addressed, including: (1) how to determine and define refractoriness; and (2) whether to continue TACE or hepatic arterial infusion chemotherapy (a de facto standard in Japan) in patients with TACE-refractory HCCs or portal tumor thrombi before starting sorafenib therapy. We strongly recommend that, based on the molecular-targeted agents currently under development, clinical studies (including IITs) should be conducted aggressively, and therapeutic strategies should be devised to resolve the limitations of currently used therapeutic approaches and to improve the therapeutic outcomes.

The introduction of sorafenib to treat HCC in 2007 in Western countries and in 2009 in Japan was undoubtedly the real beginning of a paradigm shift of HCC treatment, representing a significant breakthrough for HCC treatment not previously experienced for this unique tumor. Further development of survival benefit in HCC patients with new targeted agents are greatly expected.

REFERENCES

1   **Farazi PA**, DePinho RA. Hepatocellular carcinoma pathogenesis: from genes to environment. *Nat Rev Cancer* 2006; **6**: 674-687
2   **Mínguez B**, Tovar V, Chiang D, Villanueva A, Llovet JM. Pathogenesis of hepatocellular carcinoma and molecular therapies. *Curr Opin Gastroenterol* 2009; **25**: 186-194
3   **Villanueva A**, Newell P, Chiang DY, Friedman SL, Llovet JM. Genomics and signaling pathways in hepatocellular carcinoma. *Semin Liver Dis* 2007; **27**: 55-76
4   **Laurent-Puig P**, Zucman-Rossi J. Genetics of hepatocellular tumors. *Oncogene* 2006; **25**: 3778-3786
5   **Llovet JM**, Bruix J. Molecular targeted therapies in hepatocellular carcinoma. *Hepatology* 2008; **48**: 1312-1327
6   **Höpfner M**, Schuppan D, Scherübl H. Growth factor receptors and related signalling pathways as targets for novel treatment strategies of hepatocellular cancer. *World J Gastroenterol* 2008; **14**: 1-14
7   **Campbell JS**, Hughes SD, Gilbertson DG, Palmer TE, Holdren MS, Haran AC, Odell MM, Bauer RL, Ren HP, Haugen HS, Yeh MM, Fausto N. Platelet-derived growth factor C induces liver fibrosis, steatosis, and hepatocellular carcinoma. *Proc Natl Acad Sci USA* 2005; **102**: 3389-3394
8   **Ogasawara S**, Yano H, Iemura A, Hisaka T, Kojiro M. Expressions of basic fibroblast growth factor and its receptors and their relationship to proliferation of human hepatocellular carcinoma cell lines. *Hepatology* 1996; **24**: 198-205
9   **Kudo M**. Hepatocellular carcinoma 2009 and beyond: from the surveillance to molecular targeted therapy. *Oncology* 2008; **75** Suppl 1: 1-12
10   **Hanahan D**, Weinberg RA. The hallmarks of cancer. *Cell* 2000; **100**: 57-70
11   **Spangenberg HC**, Thimme R, Blum HE. Targeted therapy for hepatocellular carcinoma. *Nat Rev Gastroenterol Hepatol* 2009; **6**: 423-432
12   **Villanueva A**, Toffanin S, Llovet JM. Linking molecular classification of hepatocellular carcinoma and personalized medicine: preliminary steps. *Curr Opin Oncol* 2008; **20**: 444-453
13   **Roberts PJ**, Der CJ. Targeting the Raf-MEK-ERK mitogen-activated protein kinase cascade for the treatment of cancer. *Oncogene* 2007; **26**: 3291-3310
14   **Schmidt CM**, McKillop IH, Cahill PA, Sitzmann JV. Increased MAPK expression and activity in primary human hepatocellular carcinoma. *Biochem Biophys Res Commun* 1997; **236**: 54-58
15   **Calvisi DF**, Ladu S, Gorden A, Farina M, Conner EA, Lee JS, Factor VM, Thorgeirsson SS. Ubiquitous activation of Ras and Jak/Stat pathways in human HCC. *Gastroenterology* 2006; **130**: 1117-1128
16   **Bos JL**. ras oncogenes in human cancer: a review. *Cancer Res* 1989; **49**: 4682-4689
17   **Beeram M**, Patnaik A, Rowinsky EK. Raf: a strategic target for therapeutic development against cancer. *J Clin Oncol* 2005; **23**: 6771-6790
18   **Tannapfel A**, Sommerer F, Benicke M, Katalinic A, Uhlmann D, Witzigmann H, Hauss J, Wittekind C. Mutations of the BRAF gene in cholangiocarcinoma but not in hepatocellular carcinoma. *Gut* 2003; **52**: 706-712
19   **Jenke HS**, Deml E, Oesterle D. C-raf expression in early rat liver tumorigenesis after promotion with polychlorinated biphenyls or phenobarbital. *Xenobiotica* 1994; **24**: 569-580
20   **Beer DG**, Neveu MJ, Paul DL, Rapp UR, Pitot HC. Expression of the c-raf protooncogene, gamma-glutamyltranspeptidase, and gap junction protein in rat liver neoplasms. *Cancer Res* 1988; **48**: 1610-1617
21   **Hwang YH**, Choi JY, Kim S, Chung ES, Kim T, Koh SS, Lee B, Bae SH, Kim J, Park YM. Over-expression of c-raf-1 proto-oncogene in liver cirrhosis and hepatocellular carcinoma. *Hepatol Res* 2004; **29**: 113-121
22   **Wilhelm SM**, Adnane L, Newell P, Villanueva A, Llovet JM, Lynch M. Preclinical overview of sorafenib, a multikinase inhibitor that targets both Raf and VEGF and PDGF receptor tyrosine kinase signaling. *Mol Cancer Ther* 2008; **7**: 3129-3140
23   **Ohren JF**, Chen H, Pavlovsky A, Whitehead C, Zhang E, Kuffa P, Yan C, McConnell P, Spessard C, Banotai C, Mueller WT, Delaney A, Omer C, Sebolt-Leopold J, Dudley DT, Leung IK, Flamme C, Warmus J, Kaufman M, Barrett S, Tecle H, Hasemann CA. Structures of human MAP kinase kinase 1 (MEK1) and MEK2 describe novel noncompetitive kinase inhibition. *Nat Struct Mol Biol* 2004; **11**: 1192-1197
24   **Huynh H**, Nguyen TT, Chow KH, Tan PH, Soo KC, Tran E. Over-expression of the mitogen-activated protein kinase (MAPK) kinase (MEK)-MAPK in hepatocellular carcinoma: its role in tumor progression and apoptosis. *BMC Gastroenterol* 2003; **3**: 19
25   **Engelman JA**. Targeting PI3K signalling in cancer: opportunities, challenges and limitations. *Nat Rev Cancer* 2009; **9**: 550-562
26   **Sahin F**, Kannangai R, Adegbola O, Wang J, Su G, Torbenson M. mTOR and P70 S6 kinase expression in primary liver neoplasms. *Clin Cancer Res* 2004; **10**: 8421-8425
27   **Semela D**, Piguet AC, Kolev M, Schmitter K, Hlushchuk R, Djonov V, Stoupis C, Dufour JF. Vascular remodeling and antitumoral effects of mTOR inhibition in a rat model of hepatocellular carcinoma. *J Hepatol* 2007; **46**: 840-848
28   **Sieghart W**, Fuereder T, Schmid K, Cejka D, Werzowa J,

Wrba F, Wang X, Gruber D, Rasoul-Rockenschaub S, Peck-Radosavljevic M, Wacheck V. Mammalian target of rapamycin pathway activity in hepatocellular carcinomas of patients undergoing liver transplantation. *Transplantation* 2007; **83**: 425-432

29 **Zhou P**, Kudo M, Minami Y, Chung H, Inoue T, Fukunaga T, Maekawa K. What is the best time to evaluate treatment response after radiofrequency ablation of hepatocellular carcinoma using contrast-enhanced sonography? *Oncology* 2007; **72** Suppl 1: 92-97

30 **Zhou L**, Huang Y, Li J, Wang Z. The mTOR pathway is associated with the poor prognosis of human hepatocellular carcinoma. *Med Oncol* 2010; **27**: 255-261

31 **Chen JS**, Wang Q, Fu XH, Huang XH, Chen XL, Cao LQ, Chen LZ, Tan HX, Li W, Bi J, Zhang LJ. Involvement of PI3K/PTEN/AKT/mTOR pathway in invasion and metastasis in hepatocellular carcinoma: Association with MMP-9. *Hepatol Res* 2009; **39**: 177-186

32 **Villanueva A**, Chiang DY, Newell P, Peix J, Thung S, Alsinet C, Tovar V, Roayaie S, Minguez B, Sole M, Battiston C, Van Laarhoven S, Fiel MI, Di Feo A, Hoshida Y, Yea S, Toffanin S, Ramos A, Martignetti JA, Mazzaferro V, Bruix J, Waxman S, Schwartz M, Meyerson M, Friedman SL, Llovet JM. Pivotal role of mTOR signaling in hepatocellular carcinoma. *Gastroenterology* 2008; **135**: 1972-1983

33 **Treiber G**. mTOR inhibitors for hepatocellular cancer: a forward-moving target. *Expert Rev Anticancer Ther* 2009; **9**: 247-261

34 **Ferrara N**, Davis-Smyth T. The biology of vascular endothelial growth factor. *Endocr Rev* 1997; **18**: 4-25

35 **Griffioen AW**, Molema G. Angiogenesis: potentials for pharmacologic intervention in the treatment of cancer, cardiovascular diseases, and chronic inflammation. *Pharmacol Rev* 2000; **52**: 237-268

36 **Harper SJ**, Bates DO. VEGF-A splicing: the key to anti-angiogenic therapeutics? *Nat Rev Cancer* 2008; **8**: 880-887

37 **Fernández M**, Semela D, Bruix J, Colle I, Pinzani M, Bosch J. Angiogenesis in liver disease. *J Hepatol* 2009; **50**: 604-620

38 **Schoenleber SJ**, Kurtz DM, Talwalkar JA, Roberts LR, Gores GJ. Prognostic role of vascular endothelial growth factor in hepatocellular carcinoma: systematic review and meta-analysis. *Br J Cancer* 2009; **100**: 1385-1392

39 **Faivre S**, Raymond E, Boucher E, Douillard J, Lim HY, Kim JS, Zappa M, Lanzalone S, Lin X, Deprimo S, Harmon C, Ruiz-Garcia A, Lechuga MJ, Cheng AL. Safety and efficacy of sunitinib in patients with advanced hepatocellular carcinoma: an open-label, multicentre, phase II study. *Lancet Oncol* 2009; **10**: 794-800

40 **Zhu AX**, Sahani DV, Duda DG, di Tomaso E, Ancukiewicz M, Catalano OA, Sindhwani V, Blaszkowsky LS, Yoon SS, Lahdenranta J, Bhargava P, Meyerhardt J, Clark JW, Kwak EL, Hezel AF, Miksad R, Abrams TA, Enzinger PC, Fuchs CS, Ryan DP, Jain RK. Efficacy, safety, and potential biomarkers of sunitinib monotherapy in advanced hepatocellular carcinoma: a phase II study. *J Clin Oncol* 2009; **27**: 3027-3035

41 **Forner A**, Llovet JM, Bruix J. Sunitinib and the benefits of a negative study. *Lancet Oncol* 2009; **10**: 743-744

42 **Bergers G**, Hanahan D. Modes of resistance to anti-angiogenic therapy. *Nat Rev Cancer* 2008; **8**: 592-603

43 **Batchelor TT**, Sorensen AG, di Tomaso E, Zhang WT, Duda DG, Cohen KS, Kozak KR, Cahill DP, Chen PJ, Zhu M, Ancukiewicz M, Mrugala MM, Plotkin S, Drappatz J, Louis DN, Ivy P, Scadden DT, Benner T, Loeffler JS, Wen PY, Jain RK. AZD2171, a pan-VEGF receptor tyrosine kinase inhibitor, normalizes tumor vasculature and alleviates edema in glioblastoma patients. *Cancer Cell* 2007; **11**: 83-95

44 **Kopetz S**, Hoff PM, Eng MJ. Angiogenic cytokines are increased prior to disease progression in metastatic colorectal

cncer patients treated with bebacizumab. Proceedings of ASCO Gastrointestinal Cancers Symposium; 2009 Jan 15-17; San Francisco, USA. Abstract 292

45 **El-Assal ON**, Yamanoi A, Ono T, Kohno H, Nagasue N. The clinicopathological significance of heparanase and basic fibroblast growth factor expressions in hepatocellular carcinoma. *Clin Cancer Res* 2001; **7**: 1299-1305

46 **Poon RT**, Ng IO, Lau C, Yu WC, Fan ST, Wong J. Correlation of serum basic fibroblast growth factor levels with clinicopathologic features and postoperative recurrence in hepatocellular carcinoma. *Am J Surg* 2001; **182**: 298-304

47 **Huynh H**, Ngo VC, Fargnoli J, Ayers M, Soo KC, Koong HN, Thng CH, Ong HS, Chung A, Chow P, Pollock P, Byron S, Tran E. Brivanib alaninate, a dual inhibitor of vascular endothelial growth factor receptor and fibroblast growth factor receptor tyrosine kinases, induces growth inhibition in mouse models of human hepatocellular carcinoma. *Clin Cancer Res* 2008; **14**: 6146-6153

48 **Bhide RS**, Lombardo LJ, Hunt JT, Cai ZW, Barrish JC, Galbraith S, Jeyaseelan R, Mortillo S, Wautlet BS, Krishnan B, Kukral D, Malone H, Lewin AC, Henley BJ, Fargnoli J. The antiangiogenic activity in xenograft models of brivanib, a dual inhibitor of vascular endothelial growth factor receptor-2 and fibroblast growth factor receptor-1 kinases. *Mol Cancer Ther* 2010; **9**: 369-378

49 **Raoul JL**, Flinn RS, Kang YK, Park JW, Harris R, Coric V, Donic M, Walters I. An open-label phase II study of first- and second-line treatment with Brivanib in patients with hepatocellular carcinoma (HCC). *J Clin Oncol* 2009; **27**: Abstr 4577

50 **Raoul JL**, Finn RS, Kang WK, Park JW, Harris R, Coric V. Phase 2 study of first- and second-line treatment with brivanib in patients with hepatocellular carcinoma. *ILCA* 2009: Abstract P-0111

51 **Kanai F**, Yoshida H, Tateishi R, Shiina S, Ikeda M, Okusaka T, Kondo Y, Tagawa K, Omata M, TSU-68 HCC study group. Final results of a phse I/II trial of the oral anti-angiogenesis inhibitor TSU-68 in patients with advanced hepatocellular carcinoma. *J Clin Oncol* 2008; **26** (235 suppl): abstract 4589

52 **Ciardiello F**, Tortora G. EGFR antagonists in cancer treatment. *N Engl J Med* 2008; **358**: 1160-1174

53 **Buckley AF**, Burgart LJ, Sahai V, Kakar S. Epidermal growth factor receptor expression and gene copy number in conventional hepatocellular carcinoma. *Am J Clin Pathol* 2008; **129**: 245-251

54 **Philip PA**, Mahoney MR, Allmer C, Thomas J, Pitot HC, Kim G, Donehower RC, Fitch T, Picus J, Erlichman C. Phase II study of Erlotinib (OSI-774) in patients with advanced hepatocellular cancer. *J Clin Oncol* 2005; **23**: 6657-6663

55 **Yau T**, Chan P, Ng KK, Chok SH, Cheung TT, Fan ST, Poon RT. Phase 2 open-label study of single-agent sorafenib in treating advanced hepatocellular carcinoma in a hepatitis B-endemic Asian population: presence of lung metastasis predicts poor response. *Cancer* 2009; **115**: 428-436

56 **Thomas MB**, Morris JS, Chadha R, Iwasaki M, Kaur H, Lin E, et al. Phase II trial of the combination of bevacizumab and erlotinib in patients who have advanced hepatocellular carcinoma. *J Clin Oncol* 2009; **27**: 843-850

57 **Tournigand C**, Lledo G, Delord J, Andre T, Maindrault-Goebel F, Louvet C, W. Scheithauer, A. de Gramont. Modified folfox7/bevacizumab or modified Xelox/bevacizumab with or without erlotinib in first-line metastatic colorectal cancer (MCRC): Results of the feasibility phase of the DREAM-OPTIMOX3 study (GERCOR). *J Clinical Oncol* 2007; **25**: 4097

58 **Tournigand C**, Samson B, Scheithauer W, Louvet C, Andre T, Lledo G, Latreille J, Viret F, Chibaudel B, de Gramont A. mFOLFOX-bevacizumab or XELOX-bevacizumab then be-

vacizumab alone or with erlotinib in first-line treatment of patients with metastatic colorectal cancer (mCRC): Interim safety analysis of DREAM study. *J Clin Oncol* 2009; **27**: Abstract 4077

59   **Hecht JR**, Mitchell E, Chidiac T, Scroggin C, Hagenstad C, Spigel D, Marshall J, Cohn A, McCollum D, Stella P, Deeter R, Shahin S, Amado RG. A randomized phase IIIB trial of chemotherapy, bevacizumab, and panitumumab compared with chemotherapy and bevacizumab alone for metastatic colorectal cancer. *J Clin Oncol* 2009; **27**: 672-680

60   **Azad NS**, Posadas EM, Kwitkowski VE, Steinberg SM, Jain L, Annunziata CM, Minasian L, Sarosy G, Kotz HL, Premkumar A, Cao L, McNally D, Chow C, Chen HX, Wright JJ, Figg WD, Kohn EC. Combination targeted therapy with sorafenib and bevacizumab results in enhanced toxicity and antitumor activity. *J Clin Oncol* 2008; **26**: 3709-3714

61   **Burris HA**, Hurwitz HI, Dees EC, Dowlati A, Blackwell KL, O'Neil B, Marcom PK, Ellis MJ, Overmoyer B, Jones SF, Harris JL, Smith DA, Koch KM, Stead A, Mangum S, Spector NL. Phase I safety, pharmacokinetics, and clinical activity study of lapatinib (GW572016), a reversible dual inhibitor of epidermal growth factor receptor tyrosine kinases, in heavily pretreated patients with metastatic carcinomas. *J Clin Oncol* 2005; **23**: 5305-5313

62   **Bekaii-Saab T**, Markowitz J, Prescott N, Sadee W, Heerema N, Wei L, Dai Z, Papp A, Campbell A, Culler K, Balint C, O' Neil B, Lee RM, Zalupski M, Dancey J, Chen H, Grever M, Eng C, Villalona-Calero M. A multi-institutional phase II study of the efficacy and tolerability of lapatinib in patients with advanced hepatocellular carcinomas. *Clin Cancer Res* 2009; **15**: 5895-5901

63   **Zhu AX**, Stuart K, Blaszkowsky LS, Muzikansky A, Reitberg DP, Clark JW, Enzinger PC, Bhargava P, Meyerhardt JA, Horgan K, Fuchs CS, Ryan DP. Phase 2 study of cetuximab in patients with advanced hepatocellular carcinoma. *Cancer* 2007; **110**: 581-589

64   **Comoglio PM**, Giordano S, Trusolino L. Drug development of MET inhibitors: targeting oncogene addiction and expedience. *Nat Rev Drug Discov* 2008; **7**: 504-516

65   **Scharf JG**, Braulke T. The role of the IGF axis in hepatocarcinogenesis. *Horm Metab Res* 2003; **35**: 685-693

66   **Chen YW**, Boyartchuk V, Lewis BC. Differential roles of insulin-like growth factor receptor- and insulin receptor-mediated signaling in the phenotypes of hepatocellular carcinoma cells. *Neoplasia* 2009; **11**: 835-845

67   **Kudo M**, Izumi N, Kokudo N, Matsui O, Sakamoto M, Nakashima O, Kojiro M, Makuuchi M. Management of hepatocellular carcinoma in Japan: Consensus-Based Clinical Practice Guidelines proposed by the Japan Society of Hepatology (JSH) 2010 updated version. *Dig Dis* 2011; **29**: 339-364

68   **Kudo M**. The 2008 Okuda lecture: Management of hepatocellular carcinoma: from surveillance to molecular targeted therapy. *J Gastroenterol Hepatol* 2010; **25**: 439-452

69   **Thomas MB**, Chadha R, Glover K, Wang X, Morris J, Brown T, Rashid A, Dancey J, Abbruzzese JL. Phase 2 study of erlotinib in patients with unresectable hepatocellular carcinoma. *Cancer* 2007; **110**: 1059-1067

70   **Abou-Alfa GK**, Schwartz L, Ricci S, Amadori D, Santoro A, Figer A, De Greve J, Douillard JY, Lathia C, Schwartz B, Taylor I, Moscovici M, Saltz LB. Phase II study of sorafenib in patients with advanced hepatocellular carcinoma. *J Clin Oncol* 2006; **24**: 4293-4300

71   **Toh H**, Chen PJ, Carr BI, Knox JJ, Gill S, Steinberg J, Carlson DM, Qian J, Qin Q, Yong W. A phase II study of ABT-869 in hepatocellular carcinoma (HCC): Interim analysis. *J Clin Oncol* 2009; **27**: Abstr 4581

72   **Siegel AB**, Cohen EI, Ocean A, Lehrer D, Goldenberg A, Knox JJ, Chen H, Clark-Garvey S, Weinberg A, Mandeli J, Christos P, Mazumdar M, Popa E, Brown RS, Rafii S, Schwartz JD. Phase II trial evaluating the clinical and biologic effects of bevacizumab in unresectable hepatocellular carcinoma. *J Clin Oncol* 2008; **26**: 2992-2998

73   **O'Dwyer PJ**, Giantonio BJ, Levy DE, Kauh JS, Fitzgerald DB, Benson AB. Gefitinib in advanced unresectable hepatocellular carcinoma: Results from the Eastern Cooperative Oncology Group's Study E1203. *J Clin Oncol* 2006; **24**: Abstr 4143

74   **Ramanathan RK**, Belani CP, Singh DA, Tanaka M, Lenz HJ, Yen Y, Kindler HL, Iqbal S, Longmate J, Mack PC, Lurje G, Gandour-Edwards R, Dancey J, Gandara DR. A phase II study of lapatinib in patients with advanced biliary tree and hepatocellular cancer. *Cancer Chemother Pharmacol* 2009; **64**: 777-783

CASE REPORT

Septicemia due to *Vibrio cholerae* serogroup non-O1/non-O139 strain in a cirrhotic patient

Tatsuo Inoue · Satoshi Kitai · Sousuke Hayaishi · Masatoshi Kudo

Abstract We describe a case of non-O1/ non-O139 *Vibrio cholerae* septicemia in a 65-year-old male patient with alcoholic liver cirrhosis. He was admitted due to septic shock from non-O1/ non-O139 *V. cholerae*. An intravenous empiric antibiotic, ceftriaxone sodium hydrate, was administered together with amikacin sulfate, gamma globulin and dopamine. He was discharged feeling well 17 days after admission. Poor host defense mechanisms as seen in cirrhotic patients seem to be a determinant for systemic infection of non-O1/ non-O139 *V. cholerae*. Such patients should be warned and educated against eating raw or undercooked seafood to avoid the occurrence of non-O1/non-O139 *V. cholerae* septicemia.

Keywords Non-O1/ non-O139 *Vibrio cholerae* · Septicemia · Cirrhosis

Introduction

Patients with liver cirrhosis have impaired function of the reticuloendothelial system, leading to impairment of the host defense mechanism, which is the main cause of infectious complications. Previous studies reported that infection is a poor prognostic factor in cirrhotic patients [1, 2] and, therefore, the management of infections is needed to improve the prognosis of cirrhosis. When cirrhotic patients develop infections, they should be treated promptly and adequately to prevent exacerbation of infection and the progression of hepatic failure [3, 4].

T. Inoue · S. Kitai · S. Hayaishi · M. Kudo (✉)
Division of Gastroenterology and Hepatology, Kinki University
Faculty of Medicine, 377-2 Ohno-higashi, Osaka, Japan
e-mail: m-kudo@med.kindai.ac.jp

Vibrio cholerae O1 and O139 cause clinical disease by secreting a non-invasive enterotoxin that binds to receptors on the epithelial cell membrane of the small intestine, causing subsequent hypersecretion of fluid and electrolytes resulting in the characteristic 'rise water' diarrhea which leads to clinical dehydration [5]. In general, the toxin is non-invasive, and bacteremia does not occur. *V. cholerae* non-O1/ non-O139 may cause occasional outbreaks of diarrheal illness, but may also lead to invasive extraintestinal disease and bacteremia, almost invariably in patients with liver disease and in immunocompromised patients [6–8]. There are several case reports describing *V. cholerae* non-O1/ non-O139 infection in liver disease with septicemia [9–17]; however, to our knowledge, this is the first report describing *V. cholerae* non-O1/non-O139 bacteremia in a cirrhotic patient in Japan.

Case report

A 65-year old man with alcoholic liver cirrhosis, Child–Pugh class C, with refractory ascites and a history of hepatocellular carcinoma, was admitted with a 1-day history of high fever and low blood pressure. On the night preceding his initial symptoms, the patient consumed sea eel (hamo) in a restaurant. After admission, he complained of severe diarrhea 10–15 times a day. On examination, he was febrile with a temperature of 39 °C, a heart rate of 94 bpm and blood pressure of 70/46 mmHg. Laboratory data on admission are summarized in Table 1. Under the tentative diagnosis of septic shock, an intravenous empiric antibiotic, ceftriaxone sodium hydrate, was administered together with amikacin sulfate, gamma globulin and dopamine after two sets of blood cultures. After 24-h incubation, a curved Gram-negative bacillus developed in

🍎 Springer

Table 1 Laboratory data on admission

		Standard value			Standard value
WBC	12,800/μl	4,300–8,000	T-Bil	3.3 mg/dl	0–0.2
RBC		450–510	AST	54 IU/l	13–33
Hb	8.4 g/dl	12.4–17.2	ALT	20 IU/l	8–42
Ht	23.5 %	38.0–54.0	γGTP	115 IU/l	5–60
PLT	6.2×10^4/μl	13.0–34.0	ChE	75 IU/l	200–450
PT (INR)	1.27	0.90–1.10	GLU	139 mg/dl	70–105
PT (%)	60.8 %	80–120	CPK	88 IU/l	25–180
CRP	3.643 mg/dl	0–0.40	TP	7.7 g/dl	7.9
TP	7.7 g/dl	6.5–8.5	NH₃	43 μmol/l	7–35
Alb	2.5 g/dl	3.5–5.0	BNP	90.3 pg/ml	<20
BUN	11 mg/dl	7–18			
Cre	0.89 mg/dl	0.50–1.10			
Na	124 mEq/l	137–146			
K	5.2 mEq/l	3.8–5.1			
Cl	81 mEq/l	98–108			
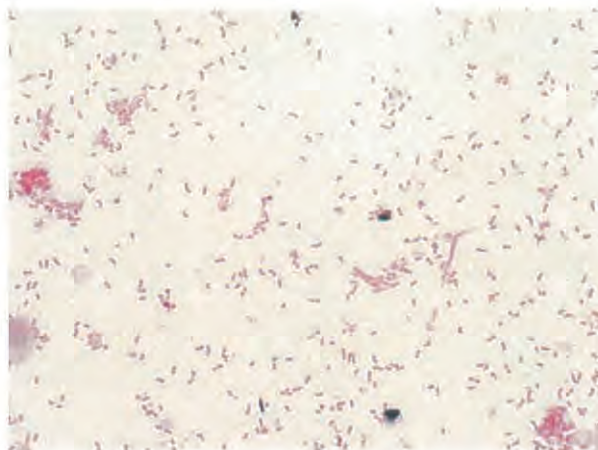
Fig. 1 A curved Gram-negative bacillus cultured in agar

Fig. 2 Clinical course

agar (Fig. 1). Final identification of the non-O1/non-O139 non-toxigenic *V. cholerae* strain was achieved at a public health center. Although we continued antibiotic therapy as mentioned above, severe diarrhea continued and his liver and renal function became worse. Therefore, we changed his medication to doripenem hydrate (DRPM) and pazu-floxacin mesilate (PZFX), after which his condition improved. He was discharged after 17-days having being prescribed sulbactam sodium for 7 days after DRPM and PZFX. The clinical course of the case is shown in Fig. 2.

Discussion

It is generally accepted that cirrhotic patients are predisposed to infectious diseases and may actually have a grave prognosis; a wide range of bacterial infections can decompensate hepatic status and lead to death in such patients. Cirrhosis of the liver is the terminal point of various multifactorial processes that lead to hepatic destruction and eventually death. Although the increased mortality in patients with cirrhosis is most often attributed to the development of hepatocellular carcinoma, a significant percentage of patients succumb to bacterial infection with infection-attributed mortality ranging from 7–40 % in various reviews [18].
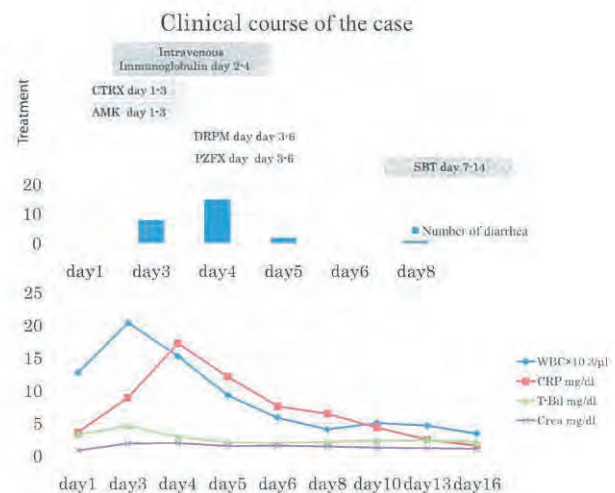
Vibrio species are highly abundant in aquatic environments worldwide, and appear at high densities in and on marine organisms [19]. *V. cholerae* are Gram-negative, comma-shaped, motile bacteria capable of producing serious infections. *V. cholerae* that agglutinate with antiserum

Table 2 Short literature review of of non-O1/non-O139 *Vibrio cholerae* septicemia reports

Place (year) serogroup reference (no.)	Age (years), sex	Risk factor	Presentation	Treatment and outcomes
Kuwait (1989) Non-O1 [13]	50, Female	Liver cirrhosis	Presented in comatose state	IV ampicillin-cloxacillin with gentamicin. Died
	31, male	Liver cirrhosis	Fever and jaundice	Treated at another hospital
TelAviv (1990) Non-O1, [28]	66, male	Liver cirrhosis	Fever, watery diarrhea, and diffuse abdominal pain	IV chloramphenicol. Recovered
Pensylvania, USA (2000) Non-O1, [21]	49, male	Gastrectomy	Severe profuse watery diarrhea, nausea and vomiting	IV ciprofloxacin. Recovered
Kuwait (2001) Non-O1, [14]	Neonates		Poor feeding cyanosis and generalized tonic–clonic convulsion. the baby developed brain abscess	Ampicillin and cefotaxime. Died
Bangkok (2001) Non-O1, [14]	41, male	Chronic liver diseases	Fever, chills and right leg pain. Develop cerebritis after admission	IV ciprofloxacin. Recovered
Brussels (2002) Non-O1, [23]	78, male	Rectal lung cancer	Abdominal cramp and constipation	IV ciprofloxacin for 10 days. patient died after 1 month at home and no cause identified
Durham (2004) Non-O1, [23]	53, male	Gastrointestinal surgeries for peptic ulcer disease	Fever, nausea and mild abdominal pain	IV ciprofloxacin. Recovered
Slovania (2005) Non-O1, non-O 139, [24]	20, male	Not stated	Vomiting, diarrhea and fever. Having complication on multiple liver and spleen abscesses.	Ampicillin, doxycycline and ciprofloxacin. Recovered
Poland (2006), Non-O1, non-O 139, [25]	49, male	Near drowning	High fever and diarrhea	Died suddenly
	79, male	Not stated	High fever and diarrhea and severe abdominal cramps	Amoxicillin with clavulanic acid and ciprofloxacin. Recovered
Doha (2006) Non-O1, non-O 139, [15]	47, male	Liver cirrhosis	Abdominal pain, high fever and diarrhea	IV piperacillin-tazobactams. Died 2 days after admission
New York (2006) Non-O1, [5]	59, male	End-stage liver disease	Fever, watery diarrhea and malaise	IV doxycycline after failed IV cefepime and ciprofloxacin. Recovered
Vientiane (2008) O21, [26]	20, male	Taking undercooked snails	Abdominal pain. fever, and watery diarrhea	IV ampicillin and gentamicin. Died
Arizone (2009) Non-O1, [29]	50, male	Liver cirrhosis	Myalgia and later unresponsiveness	Cefotaxime and doxycycline
Malaysia (2009) Non-O1, non-O 139, [16]	28, female	Thalassemia, hepatitis C infection, Splenectomy	High-grade fever, abdominal pain, malaise and prevaginal bleeding	Meropenem and doxycycline. Recovered
France (2010) Non-O1, non-O 139, [10]	63, male	Liver cirrhosis	Chills, fever, jaundice, ascites and encephalopathy	Ceftriaxone, metronidazole and oral ofloxacine. Recovered
Spain (2011) Non-O1, non-O 139, [27]	88, female	Diabetes mellitus Dialysis	Septic shock	Ceftazidime. Recovered
Canada (2012) Non-O1, non-O 139,	21, female	Biliary atresia Liver transplant	Fever, chills abdominal pain and tachycardia	Ceftriaxone and amoxicillin. Recovered.

O1 and O139 are responsible for the classic epidemic or pandemic cholera, a toxin-mediated acute diarrheal illness associated with watery, non-bloody, acute diarrhea.

As mentioned above, *V. cholerae* non-O1 and non-O139 cause occasional outbreaks of diarrheal illness, and sometimes lead to invasive extraintestinal disease and bacteremia, almost invariably in patients with liver disease and in immunocompromised patients. The majority of reported cases occur during the hot season and are associated with seafood consumption [19]. Our patient was not exposed to seawater or freshwater and the skin of his body was normal, but he had consumed a lot of sea eel and a food-borne mode of contamination seemed most likely.

Poor host defense mechanims as seen in cirrhotic patients seem to be a determinant for systemic infection of *V. cholerae* non-O1/ non-O139. Suggestive clues for transmission of *V. cholerae* infection include raw seafood consumption, seawater or freshwater exposure, and travel. Acute gastroenteritis is the most common clinical illness and is usually self-limited. Extraintestinal manifestations include wounds and septicemia. There have been several case reports of non-O1 *V. cholerae* invasive infection and bacteremia in Taiwan; however, *V. cholerae* bacteremia is uncommon in other places. Non-O1/non-O139 *V. cholerae* bacteremia is summarized in Table 2 [5, 10, 13–17, 20–29].

In addition, *V. cholerae* serogroups and many non-cholera *Vibrio* species such as *V. vulnificus* and *V. parahaemolyticus* are serious pathogens to humans, particularly cirrhotic patients [19, 29]. *V. vulnificus* infection, especially, has a poor prognosis and septic shock and necrotizing fasciitis often develop within a few days [30]. If *V. vulnificus* infection occurs, prompt and aggressive treatment at an early stage is extremely important [31]. There are no clear treatment recommendations; however, most isolates of non-O1 *V. cholerae*, *V. vulnificus*, and *V. parahaemolyticus* species are susceptible to third-generation cephalosporins, tetracyclines and fluoroquinolones [32]. Although spontaneous bacterial peritonitis has been acknowledged as a major factor in the morbidity and mortality of patients with cirrhosis, septicemia due to infection from non-O1/non-O139 *V. cholerae* has not been widely recognized, especially in Japan, even though it is associated with high mortality ranging from 23.8–61.5 % [15]. Nagao et al. [33] reported that only 14.5 % of patients with liver disease in Japan had general knowledge regarding *V. vulnificus* infections. Such patients should be warned and educated against eating raw or undercooked seafood to avoid septicemia from non-O1/non-O139 *V. cholerae* and *V. vulnificus*.

Conflict of interest The authors declare that they have no conflict of interest.

References
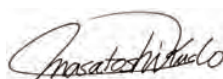
1. Caly WR, Strauss E. A prospectitve study of bacterial infections in patients with cirrhosis. J Hepatol. 1993;18:353–8.
2. Runyon BA. Bacterial infections in patients with cirrohosis. J Hepatol. 1993;18:271–2.
3. Yoneyama K, Miyagishi K, Kiuchi Y, Shibata M, Mitamura K. Risk factors for infections in cirrhotic patients with and without hepatocellular carcinoma. J Gastroenterol. 2002;37(12):1028–34.
4. Arvaniti V, D'Amico G, Fede G, Manousou P, Tsochatzis E, Pleguezuelo M, Burroughs AK. Infections in patients with cirrhosis increase mortality four-fold and should be used in determining prognosis. Gastroenterology. 2010;139(4):1246–56, 1256.e1–5 (Epub 2010 Jun 14).
5. Restrepo D, Huprikar SS, VanHorn K, Bottone EJ. O1 and non-O1 *Vibrio cholerae* bacteremia produced by hemolytic strains. Diagn Microbiol Infect Dis. 2006;54:145–8.
6. Hlady WG, Klontz KC. The epidemiology of *Vibrio* infections in Florida, 1981–1993. J Infect Dis. 1996;173:1176–83.
7. Ko W-C, Chuang Y-C, Huang G-C, Hsu S-Y. Infections due to non-O1 *Vibrio cholera* in southern Taiwan: predominance in cirrhotic patients. Clin Infect Dis. 1998;27:774–80.
8. Halabi M, Haditsch M, Renner F, Brinniger G, Mittermayer H. *Vibrio* cholerae non-O1 septicaemia in a patient with liver cirrhosis and Billroth-II-gastrectomy. J Infect. 1997;34(1):83–4.
9. Yang CJ, Wang CS, Lu PL, Chen TC, Chen YH, Huang MS, Lin CC, Hwang JJ. Bullous cellulitis in cirrhotic patients—a rare but life-threatening infection caused by non-O1, non-O139 *Vibrio cholerae* bacteraemia. J Med Microbiol. 2011;60(Pt 6):861–2 (Epub 2011 Feb 3).
10. Petsaris O, Nousbaum JB, Quilici ML, Le Coadou G, Payan C, Abalain ML. Non-O1, non-O139 *Vibrio cholerae* bacteraemia in a cirrhotic patient. J Med Microbiol. 2010;59(Pt 10):1260–2 (Epub 2010 Jul 8).
11. Lai CC, Liu WL, Chiu YH, Chao CM, Gau SJ, Hsueh PR. Liver abscess due to non-O1 *Vibrio cholerae* in a cirrhotic patient with hepatocellular carcinoma. J Infect. 2011;62(3):235–7 (Epub 2011 Jan 31).
12. Yang CC, Lee BJ, Yang SS, Lin YH, Lee YL. A case of non-O1 and non-O139 *Vibrio cholera* septicemia with endophthalmitis in a cirrhotic patient. Jpn Infect Dis. 2008;61(6):475–6.
13. Dhar R, Ghafoor MA, Nasralah AY. Unusual non-serogroup O1 *Vibrio cholerae* bacteremia associated with liver disease. J Clin Microbiol. 1989;27(12):2853–5.
14. Suankratay C, Phantumchinda K, Tachawiboonsak W, Wilde H. Non-serogroup O:1 *Vibrio cholerae* bacteremia and cerebritis. Clin Infect Dis. 2001;32(7):E117–9 (Epub 2001 Mar 20).
15. El-Hiday AH, Khan FY, Al Maslamani M, El Shafie S. Bacteremia and spontaneous bacterial peritonitis due to *Vibrio cholerae* (non-O1 non-O139) in liver cirrhosis. Indian J Gastroenterol. 2006;25(2):107.
16. Deris ZZ, Leow VM, Wan Hassan WM, Nik Lah NA, Lee SY, Siti Hawa H, Siti Asma H, Ravichandran M. Non-O1, non-O139 *Vibrio cholerae* bacteraemia in splenectomised thalassaemic patient from Malaysia. Trop Biomed. 2009;26(3):320–5.
17. Kadkhoda K, Adam H, Gilmour MW, Hammond GW. Non-toxigenic *Vibrio cholerae* septicemia in an immunocompromised patient. Case Rep Infect Dis. 2012;2012:698–746 (Epub 2012 Jul 10).
18. Bran OS. Infectious complications of cirrhosis. Curr Gastroenterol Rep. 2001;3:285–92.
19. Thompson FL, Iida T, Swings J. Biodiversity of vibrios. Microbiol Mol Biol Rev. 2004;68:403–31.
20. Namdari H, Klaips CR, Hughes JL. A cytotoxin-producing strain of *Vibrio cholerae* non-O1, non-O139 as a cause of cholera and

bacteremia after consumption of raw clams. J Clin Microbiol. 2000;38(9):3518–9.

21. Ismail EA, Shafik MH, Al-Mutairi G. A case of non-O:1 *Vibrio cholerae* septicemia with meningitis, cerebral abscess and unilateral hydrocephalus in a preterm baby. Eur J Clin Microbiol Infect Dis. 2001;20(8):598–600.

22. Berghmans T, Crokaert F, Sculier JP. *Vibrio cholerae* bacteremia in a neutropenic patient with non-small-cell lung carcinoma. Eur J Clin Microbiol Infect Dis. 2002;21(9):676–8 (Epub 2002 Sep 3).

23. Anderson AM, Varkey JB, Petti CA, Liddle RA, Frothingham R, Woods CW. Non-O1 *Vibrio cholerae* septicemia: case report, discussion of literature, and relevance to bioterrorism. Diagn Microbiol Infect Dis. 2004;49(4):295–7.

24. Strumbelj I, Prelog I, Kotar T, Dovecar D, Petras T, Socan M. A case of *Vibrio cholerae* non-O1, non-O139 septicaemia in Slovenia, imported from Tunisia, July 2005. Euro Surveill. 2005;10(10):E051020.6.

25. Stypulkowska-Misiurewicz H, Pancer K, Roszkowiak A. Two unrelated cases of septicaemia due to *Vibrio cholerae* non-O1, non-O139 in Poland, July and August 2006. Euro Surveill. 2006;11(11):E061130.2.

26. Phetsouvanh R, Nakatsu M, Arakawa E, Davong V, Vongsouvath M, Lattana O, Moore CE, Nakamura S, Newton PN. Fatal bacteremia due to immotile *Vibrio cholerae* serogroup O21 in Vientiane, Laos—a case report. Ann Clin Microbiol Antimicrob. 2008;25(7):10.

27. Zárate MS, Giannico M, Colombrero C, Smayevsky J. Non-O1, non-O139 *Vibrio cholerae* bacteremia in a chronic hemodialysis patient. Rev Argent Microbiol. 2011;43(2):81–3 (article in Spanish).

28. Toeg A, Berger SA, Battat A, Hoffman M, Yust I. *Vibrio cholerae* bacteremia associated with gastrectomy. J Clin Microbiol. 1990;28(3):603–4.

29. Patel NM, Wong M, Little E, Ramos AX, Kolli G. *Vibrio cholerae* non-O1 infection in cirrhotics: case report and literature review. Transpl Infect Dis. 2009;11:54–6.

30. Lee CH, Wang CC, Yue CT, Li KJ, Wu YK. Necrotising fasciitis caused by *Vibrio vulnificus* in a man with cirrhosis. Lancet Infect Dis. 2008;8(6):399.

31. Matsumoto K, Ohshige K, Fujita N, Tomita Y, Mitsumizo S. Clinical features of *Vibrio vulnificus* infections in the coastal areas of the Ariake Sea, Japan. J Infect Chemother. 2010; 16(4):272–9 (Epub 2010 Mar 13).

32. Su BA, Tang HJ, Wang YY, Liu YC, Ko WC. In vitro antimicrobial effect of cefazolin and cefotaxime combined with minocycline against *Vibrio cholerae* non-O1 non-O139. J Microbiol Immunol Infect. 2005;38:425–9.

33. Nagao Y, Matsuoka H, Seike M, Yamasaki K, Kato J, Nakajima T, Miyazaki Y, Ohno T. Knowledge of *Vibrio vulnificus* infection among Japanese patients with liver diseases: a prospective multicenter study. Med Sci Monit. 2009;15(10):PH115–120.

Editorial

Japan's Successful Model of Nationwide Hepatocellular Carcinoma Surveillance Highlighting the Urgent Need for Global Surveillance

Prof. M. Kudo

Editor *Liver Cancer*

Screening and surveillance for early detection of hepatocellular carcinoma (HCC) is currently being promoted in many clinical practice guidelines. These include guidelines issued by the American Association for the Study of Liver Diseases [1], the European Association for the Study of the Liver–the European Organization for Research and Treatment of Cancer (EASL–EORTC) [2], and the Asian Pacific Association for the Study of the Liver [3], as well as those established in Japan by the Japan Society of Hepatology [4, 5]. If HCC is detected at an early stage [e.g., Barcelona Clinic Liver Cancer (BCLC) classification stage 0 or A], curative treatments such as resection, ablation, or transplantation are indicated, with the aim of improving disease prognosis as well as minimizing overall medical costs. Moreover, the abovementioned three curative treatments are highly recommended in the EASL–EORTC guidelines because of substantial evidence supporting their value as therapeutic options. Furthermore, survival is improved if HCC is detected at a stage where these curative treatments are indicated.

However, nationwide surveillance for early detection of HCC has been established in Japan, and they have not yet been established in European, Asian, American, or African countries. In Japan, it has become common practice for not only tertiary referral centers, such as university hospitals, cancer centers, and main base hospitals, but also small hospitals and private practitioners to regularly conduct ultrasonography and tumor marker screening for the early detection of HCC in patients at high risk, such as those with cirrhosis and chronic hepatitis B or C. Physicians have lost a number of court cases because their high-risk patients who had been followed-up regularly with screening were diagnosed with HCC larger than 3 cm, for which curative treatments were not applicable. In part, because of such court cases, physicians who specialize in liver disease as well as general physicians nationwide are well aware that patients at high risk for HCC need to be screened regularly. Moreover, starting in the 1990s, the Japan Society of Hepatology designated a person in each of the 47 prefectures responsible for providing educational lectures several times a year to promote

Fig. 1. BCLC Classification. TACE = transcatheter chemoembolization.
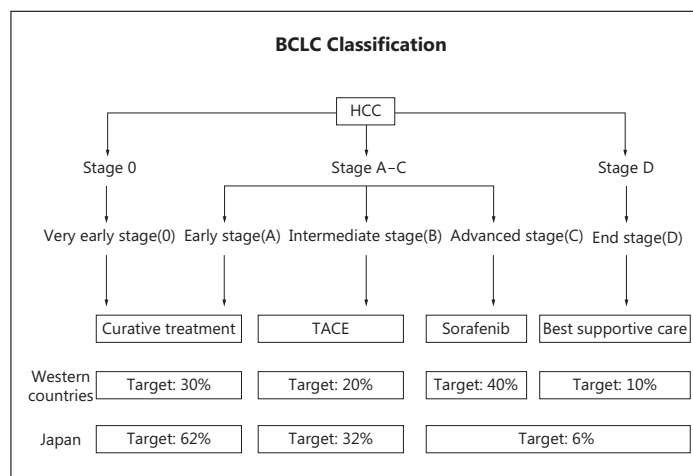
public awareness of the importance of early HCC detection by ultrasonography and tumor marker assessment. The Government actively engages in preventive measures against hepatitis and HCC, and offers free testing for hepatitis B and C virus at local public health centers and medical facilities nationwide to identify individuals at high risk. Furthermore, screening of individuals at high risk for HCC by ultrasonography and assessment of the tumor markers such as AFP, PIVKA-II, and AFP-L3 is covered by the national health insurance and the social insurance system.

As a result of these preventive measures, 62% HCC cases diagnosed in Japan are BCLC 0/A (early stage), 32% are BCLC B (intermediate stage), and only 6% are BCLC C/D (advanced/end stage). However, in Western countries, the figures are approximately 30% for BCLC A, 20% for BCLC B, 40% for BCLC C, and 10% for BCLC D (fig. 1). These figures indicate that HCC tends to be diagnosed after the onset of symptoms because of poor implementation of nationwide HCC surveillance in Western countries compared to Japan.

Another indicator of the effectiveness of nationwide surveillance is the 5-year survival rate of HCC patients. According to follow-up data from the Nationwide Registry implemented by the Liver Cancer Study Group of Japan, the nationwide 5-year survival rate of HCC patients in Japan was 43% for the last 5 years [6]. In contrast, the latest 5-year survival rate was 11–15% in the United States [7–10], suggesting that early detection of HCC is poorly practiced in this country despite the fact that it has the most advanced liver transplantation technology. However, many Asian countries have also not yet established nationwide surveillance systems, and even in Korea, which actively conducts screening of HCC high-risk patients at an institutional level. The latest nationwide 5-year survival rate in Korea was only 18.9% [11]. These findings clearly indicate that the prognoses of HCC patients could drastically improve by simply establishing a nationwide HCC surveillance system. Five-year survival rates are also influenced by lead time bias to a certain extent; nevertheless, there is no doubt that early detection of HCC, when curative treatment is indicated, will improve the prognoses of affected patients.

In conclusion, even though it is unquestionably important to continue developing new HCC treatment methods and remedies (e.g., extremely expensive molecularly-targeted drugs), from the Japanese experience, it is apparent that the most basic approach is lacking in the management of HCC in other countries. Japan's well-implemented nationwide HCC surveillance system is a successful model of national surveillance for early detection of the disease. The system is economical and drastically improves the prognosis of HCC patients.

143

We believe that other countries, including developing countries as well as countries in Europe and the United States, should follow Japan's lead and urgently establish their own nationwide surveillance systems.

Reference

1 Bruix J, Sherman M: Management of hepatocellular carcinoma: An update. Hepatology 2011;53:1020–1022.
2 European Association For The Study Of The Liver; European Organisation For Research And Treatment Of Cancer: EASL-EORTC clinical practice guidelines: management of hepatocellular carcinoma. J Hepatol 2012;56:908–943.
3 Omata M, Lesmana LA, Tateishi R, Chen PJ, Lin SM, Yoshida H, et al: Asian Pacific Association for the Study of the Liver consensus recommendations on hepatocellular carcinoma. Hepatol Int 2010;4:439–474.
4 Kokudo N, Makuuchi M: Evidence-based clinical practice guidelines for hepatocellular carcinoma in Japan: the J-HCC guidelines. J Gastroenterol 2009;44(Suppl 19):119–121.
5 Kudo M, Izumi N, Kokudo N, Matsui O, Sakamoto M, Nakashima O, et al: Management of hepatocellular carcinoma in Japan: Consensus-Based Clinical Practice Guidelines proposed by the Japan Society of Hepatology (JSH) 2010 updated version. Dig Dis 2011;29:339–364.
6 Kudo M, Izumi N, Sakamoto M, Matsuyama Y, Ichida T, Nakashima O, et al: Improved survival in patients with hepatocellular carcinoma over 30 years in Japan: Analysis of nationwide prospective registry of 148,161 patients. J Clin Oncol 2011;29:269 (Abstr. #4054).
7 Altekruse SF, McGlynn KA, Dickie LA, Kleiner DE: Hepatocellular carcinoma confirmation, treatment, and survival in surveillance, epidemiology, and end results registries, 1992–2008. Hepatology 2012;55:476–482.
8 Ries LAG, Melbert D, Krapcho M, et al (eds.). SEER Cancer Statistics Review, 1975–2005, National Cancer Institute, Bethesda, MD. Available at: seer.cancer.gov/csr/1975_2005/,2008. Accessed February 27, 2012.
9 American Cancer Society. Cancer facts and figures 2012.
10 El-Serag HB: Hepatocellular carcinoma. N Engl J Med 2011;365:1118–1127.
11 Park JW: Practice guideline for diagnosis and treatment of hepatocellular carcinoma. Korean J Hepatol 2004;10:88–98.

PHASE II STUDIES

A randomized phase II trial of intra-arterial chemotherapy using SM-11355 (Miriplatin) for hepatocellular carcinoma

**Takuji Okusaka · Hiroshi Kasugai · Hiroshi Ishii ·
Masatoshi Kudo · Michio Sata · Katsuaki Tanaka ·
Yasukazu Shioyama · Kazuaki Chayama ·
Hiromitsu Kumada · Masaharu Yoshikawa ·
Toshihito Seki · Hidetugu Saito · Naoaki Hayashi ·
Keiko Shiratori · Kiwamu Okita · Isao Sakaida ·
Masao Honda · Yukio Kusumoto · Takuya Tsutsumi ·
Kenji Sakata**

Abstract *Background* SM-11355 is a platinum complex developed to treat hepatocellular carcinoma (HCC) via administration into the hepatic artery as a sustained-release suspension in iodized oil. We conducted a multicenter phase II trial in patients with HCC to evaluate the efficacy and safety of SM-11355, using a Zinostatin stimalamer suspension in iodized oil as a reference. *Methods* Patients with unresectable HCC were randomized 2:1 to receive administration of the SM-11355 or Zinostatin stimalamer suspension into the hepatic artery. A second injection was given 4–12 weeks later. Efficacy was evaluated by CT 3 months after treatment and categorized as therapeutic

T. Okusaka (✉)
Hepatobiliary and Pancreatic Oncology Division, National Cancer
Center Hospital,
5-1-1 Tsukiji,
Chuo-ku, Tokyo 104-0045, Japan
e-mail: tokusaka@ncc.go.jp

H. Kasugai
Department of Gastrointestinal Oncology, Osaka Medical Center
for Cancer and Cardiovascular Diseases,
Osaka, Japan
e-mail: kasugai-clinic@lime.plala.or.jp

H. Ishii
Hepatobiliary and Pancreatic Section, Gastroenterological
Division, Cancer Institute Hospital,
Tokyo, Japan
e-mail: hiroshi.ishii@jfcr.or.jp

M. Kudo
Department of Gastroenterology and Hepatology, Kinki
University,
Osaka, Japan
e-mail: m-kudo@med.kindai.ac.jp

M. Sata
Division of Gastroenterology, Kurume University,
Fukuoka, Japan
e-mail: msata@med.kurume-u.ac.jp

K. Tanaka
Gastroenterological Center, Yokohama City University Hospital
Medical Center,
Kanagawa, Japan
e-mail: k_tanaka@yokohama-cu.ac.jp

Y. Shioyama
Department of Radiology, Dokkyo Medical University,
Tochigi, Japan
e-mail: shioyama@dokkyomed.ac.jp

K. Chayama
Department of Medicine and Molecular Science, Division of
Frontier Medical Science, Programs for Biomedical Research,
Graduate School of Biomedical Sciences, Hiroshima University,
Hiroshima, Japan
e-mail: chayama@hiroshima-u.ac.jp

H. Kumada
Department of Hepatology, Toranomon Hospital,
Tokyo, Japan
e-mail: kumahiro@toranomon.gr.jp

M. Yoshikawa
Department of Medicine and Clinical Oncology, Chiba University,
Chiba, Japan
e-mail: yoshikawa@faculty.chiba-u.jp

🐦 Springer

effect (TE) V to I, where TE V was defined as disappearance or 100% necrosis of all treated tumors. *Results* A total of 122 patients were evaluated for efficacy and toxicity (SM-11355, *n*=83; Zinostatin stimalamer, *n*=39). Baseline characteristics were similar in the two groups. The TE V rates were 26.5% (22/83) and 17.9% (7/39) in the SM-11355 and Zinostatin stimalamer groups, respectively. In the SM-11355 group, the most frequent drug-related adverse events (AEs) of≥grade 3 were elevated AST, elevated ALT, thrombocytopenia, and hyperbilirubinemia. The AEs with the largest difference between the two groups (SM-11355 vs. Zinostatin stimalamer) were hepatic vascular injury (0 vs.

T. Seki
Department of Gastroenterology and Hepatology, Kansai Medical University Takii Hospital,
Osaka, Japan
e-mail: sekit@takii.kmu.ac.jp

H. Saito
Department of Internal Medicine, School of Medicine, Keio University Hospital,
Tokyo, Japan
e-mail: hsaito@a2.keio.ac.jp

N. Hayashi · K. Shiratori
Department of Gastroenterology, Tokyo Women's Medical University Hospital,
Tokyo, Japan

K. Shiratori
e-mail: tskeiko@ige.twmu.ac.jp

K. Okita · I. Sakaida
Department of Gastroenterology and Hepatology, Yamaguchi University Graduate School of Medicine,
Yamaguchi, Japan

K. Okita
e-mail: icb68895@nifty.com

I. Sakaida
e-mail: sakaida@yamaguchi-u.ac.jp

M. Honda
Department of Gastroenterology, Kanazawa University Graduate School of Medicine,
Kanazawa, Japan
e-mail: mhonda@m-kanazawa.jp

Y. Kusumoto · T. Tsutsumi
Department of Internal Medicine, Nagasaki Municipal Hospital,
Nagasaki, Japan

Y. Kusumoto
e-mail: kusumoto@nmh.jp

T. Tsutsumi
e-mail: naika@nmh.jp

K. Sakata
Department of Gastroenterology, Omuta General Hospital,
Omuta, Japan

48.4%) and eosinophilia (84.3 vs. 41.0%). The 2-year and 3-year survival rates were 75.9% vs. 70.3% and 58.4% vs. 48.7%, respectively. *Conclusions* The results suggest that SM-11355 in iodized oil has similar efficacy to Zinostatin stimalamer and that repeated dosing of SM-11355 is possible without hepatic vascular injury in cases of relapse.

Keywords Iodized oil · MIRIPLA · Liver cancer · Suspension · Parallel study

Introduction

International cancer statistics from 2002 indicate that hepatocellular carcinoma (HCC) ranks third behind lung and gastric cancer in the number of deaths [1]. The impact of current standard treatments for advanced HCC, including conventional transcatheter arterial chemoembolization (TACE) using doxorubicin or cisplatin is limited and the prognosis is unsatisfactory [2]. Therefore, there is a clear need for new treatments in management of this disease.

SM-11355, (SP-4-2)-[(1*R*,2*R*)-cyclohexane-1,2-diamine-*N,N'*]bis (tetradecanoato-*O*) platinum monohydrate (Fig. 1) is a highly lipophilic platinum derivative that can be delivered suspended in iodized oil, an oily lymphographic agent, via injection into the hepatic artery [3]. Following injection into an HCC-feeding artery, iodized oil selectively accumulates in the tumor. Similarly, an iodized oil suspension of SM-11355 accumulates selectively within HCC nodules, allowing continuous release of active platinum compounds into tumor tissues. A phase I dose-finding study using different injection levels indicated a recommended dose of 20 mg/mL and an upper limit of the injection volume of 6 mL [4]. In an early phase II trial , SM-11355 showed a promising anticancer effect with a mild toxicity profile in patients with advanced HCC. Responses were evaluated by computed tomography (CT) three months after treatment, with complete response (CR) defined as disappearance or 100% necrosis of all tumors. Iodized oil accumulation in tumors was taken to indicate necrosis. Of 16 eligible patients, 9 (56%) showed CR [5]. This CR rate was superior to our expectation, because the CR rate in conventional TACE is 15–20% based on the same evaluation criteria [6, 7]. Therefore, the results of the early phase II study
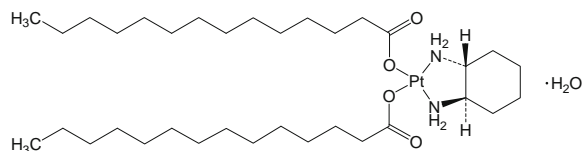
Fig. 1 Structural formula of SM-11355

indicated that SM-11355 has potential as an alternative to TACE in treatment of advanced HCC.

Based on these findings, we conducted a late phase II open-label trial of SM-11355. The aims of the study were to re-evaluate the efficacy, safety and pharmacokinetics of SM-11355 in a larger population, since only 16 eligible patients were included in the previous phase II study, and to confirm the candidacy of SM-11355 as an experimental treatment in a forthcoming clinical study in comparison with conventional TACE. To achieve regulatory approval of SM-11355 in Japan, it was necessary to undertake a parallel study. Therefore, we conducted a randomized phase II trial using Zinostatin stimalamer as a reference, because this agent is the only commercially available lipophilic drug for HCC in Japan and chemolipiodolization of Zinostatin stimalamer has been approved for treatment of advanced HCC in Japan [8, 9]. However, statistical comparisons between the two treatment groups were not planned since the goal of the study was re-evaluation of outcomes for SM-11355, and because the sample size required to conduct a statistical analysis was larger than expected.

Patients and methods

Inclusion criteria

Consecutive patients with HCC were eligible for the study if they had no indication for resection or local ablation therapy. The diagnosis was confirmed histologically and/or clinically using angiography and enhanced CT. Each patient was required to meet the following criteria: at least one measurable intrahepatic lesion that showed tumor staining by CT; tumor stage II or III in the staging system of the Liver Cancer Study Group of Japan [6, 7]; Child-Pugh classification A or B; adequate hematological function (WBC≥3000 /μL, blood platelets≥50000 /μL, hemoglobin≥9.5 g/dL), adequate hepatic function (AST and ALT≤ 5-fold the upper limit of normal, serum bilirubin <3 mg/dL, serum albumin≥3 g/dL), adequate renal function (serum creatinine≤the upper limit of normal); an Eastern Cooperative Oncology Group performance status of 0–2; age 20 to 74 years old; minimum life expectancy≥3 months, and provision of written informed consent. Patients who had undergone hepatic resection, local ablation therapy, and/or TACE were eligible if they showed no evidence of local tumor recurrence in the treated lesions. Patients who had undergone chemolipiodolization with anti-cancer agents other than Zinostatin stimalamer or a platinum-containing agent were also eligible if the treated lesions were resected. The previous anticancer treatment had to have been discontinued for at least 4 weeks before enrollment in this study.

Exclusion criteria

Patients were excluded if they met any of the following criteria: history of allergy to iodine-containing agents and/or contrast material; history of systemic chemotherapy; serious complication such as a cardiac disease or a thyroid disease ; concomitant malignancy; bile duct invasion; pregnant or lactating women and fertile patients who were not using effective contraception; and participation in another trial within 6 months before giving informed consent.

Study treatment

Patients who met the entry criteria were provisionally registered and randomly assigned to the SM-11355 or Zinostatin stimalamer group before undergoing angiography. Each investigator then confirmed registration after establishing that the patient met the following additional requirements based on angiographic findings: intrahepatic lesions that showed tumor staining and were fed by an artery with an appropriate structure for catheter insertion; no evidence of tumor thrombus in the portal or hepatic vein; no evidence of intrahepatic arteriovenous shunting; and no evidence of local tumor recurrence in previously treated lesions. The central random assignment by dynamic allocation to either a SM-11355 group or Zinostatin stimalamer group was stratified according to center and maximun tumor diameter.

A suspension of SM-11355 (MIRIPLA; Dainippon Sumitomo Pharma Co., Japan) or Zinostatin stimalamer (SMANCS; Astellas Pharma Inc., Japan) in iodized oil was injected into the hepatic artery using Seldinger's technique. Patients in the SM-11355 group received SM-11355 suspended in iodized oil (20 mg/mL) in a volume of up to 6 mL according to tumor size. Patients in the Zinostatin stimalamer group received Zinostatin stimalamer suspended in iodized oil (1 mg titer/mL) in a volume of up to 6 mL. When iodized oil accumulation in the treated tumor was insufficient and tumor staining was found in diagnostic imaging 5 weeks (±10 days) after the first injection, a second injection was given within 12 weeks after the first injection.

Efficacy and safety assessment

The antitumor effect was evaluated by CT or MRI 3 months after the last injection according to the response criteria proposed by the Liver Cancer Study Group of Japan [10], which are similar to the criteria proposed by the European Association for the Study of the Liver (EASL) Panel of Experts on HCC [11]. Tumor size was measured using the sum of the products of the perpendicular longest diameters of all measurable lesions. In the response evaluation criteria, iodized oil accumulation in a tumor is regarded as an indication of necrosis because significant positive correlations

have been reported between iodized oil accumulation observed on CT images and necrotic regions in resected tumors examined pathologically after TACE and after intra-arterial chemotherapy with iodized oil [5, 8, 12, 13]. Therapeutic effect (TE) was defined as follows: TE V, disappearance or 100% necrosis of all treated tumors; TE IV, more than 50% reduction in tumor size and/or more than 50% necrosis; TE III, more than 25% reduction in tumor size and/or more than 25% necrosis; and TE I, more than 25% increase in tumor size regardless of the necrotic effect. TE II was defined as a response not qualifying for classification as TE V, IV, III, or I. When a patient assigned to the SM-11355 group and judged to be TE V developed a tumor in a different region and requested SM-11355, the drug was given continuously after the study, provided that this was felt to be necessary by the investigator. The primary endpoint was the TE V rate. The secondary endpoints were the response rate based on the Response Evaluation Criteria in Solid Tumors (RECIST) and on the Japan Society for Cancer Therapy Criteria [14], which are similar to the World Health Organization (WHO) Criteria. The serum α-fetoprotein (AFP) level of each patient was measured before and 5 weeks after each treatment. Survival was evaluated using the Kaplan-Meier method. Toxicity was assessed according to the criteria of the Japan Society for Cancer Therapy [15], which are also fundamentally similar to WHO criteria.

Pharmacokinetics

Pharmacokinetic data were determined in patients in the SM-11355 group who gave written informed consent and were treated at institutions where a pharmacokinetic study could be conducted. Peripheral blood samples (5 ml) were collected 3 weeks after each treatment for determination of the total plasma platinum concentration and the platinum concentration in methanol extracts (SM-11355 metabolite concentration). The total platinum concentration in resected tissue was also determined in a patient who underwent surgery after evaluation of efficacy.

Statistical analysis

We anticipated enrollment of 120 patients at 17 participating hospitals over the study period of 3 years. A 2:1 ratio for SM-11355 to Zinostatin stimalamer randomization was chosen as a balance between the goals of the study, which were to re-evaluate the efficacy, safety and pharmacokinetics of SM-11355 in a larger population than that in the previous phase II study, and the current limited use of Zinostatin stimalamer. The number of subjects was determined based on the feasibility of the study because the sample size required to conduct a statistical analysis was larger than expected. Assuming a baseline 15% TE V rate for

conventional TACE [6], the SM-11355 arm would be considered 'favorable' if there was a 10% improvement in this endpoint (to 25%) with an acceptable toxicity profile. A total of 80 patients in the SM-11355 arm is needed to estimate the TE-V rate with an accuracy of ±10%.

This study was not powered to permit formal statistical comparison between the two treatment arms. However, it does allow an initial assessment of SM-11355 in terms of TE-V, response rate, overall survival and toxicity with a view to performance of a follow-on phase III study.

Results

Patient

From April 2002 to October 2004, 131 patients were enrolled in the study, and 126 were assigned randomly at a 2:1 ratio to receive SM-11355 (85 patients) or Zinostatin stimalamer (41 patients) (Fig. 2). Five patients were excluded from the randomization because tumor staining was not observed in angiography and/or an appropriate hepatic artery for selective catheter insertion was not found ($n=3$), multiple tumors were observed in angiography that required reconsideration of the treatment strategy ($n=1$), and withdrawal of consent ($n=1$). After administration, 4 patients were identified as ineligible due to a platelet count <50,000/μL ($n=1$), esophageal cancer ($n=1$) in the SM-11355 group, and deviation from correct use of the investigational products ($n=2$) in the Zinostatin stimalamer group. Therefore, 122 patients (SM-11355 group, $n=$ 83; Zinostatin stimalamer group, $n=39$) were analyzed for efficacy and safety. The baseline demographic and disease characteristics of the patients are listed in Table 1.

Of the 85 original patients in the SM-11355 group, 18 were withdrawn from the study before the planned evaluation of efficacy 3 months after the first injection because of marked progression of the primary disease ($n=5$), serious adverse events ($n=4$), use of prohibited concomitant therapeutic agents or a requirement for combination therapy ($n=3$), and other reasons (duplicated count). Treatment was terminated in 11 patients after evaluation of the first injection because complete necrosis of tumors (TE V) was obtained. The remaining 56 patients received a second injection.

Of the 41 patients in the Zinostatin stimalamer group, 9 were withdrawn before the planned evaluation of efficacy 3 months after the first injection, due to marked progression of the primary disease ($n=2$), serious adverse events ($n=1$), contravention of the protocol ($n=1$), appearance of hepatic injury ($n=1$), and other reasons (duplicated count). Treatment was terminated in 7 patients after evaluation of the first injection because complete necrosis of tumors (TE V) was obtained. The remaining 25 patients received a second injection.
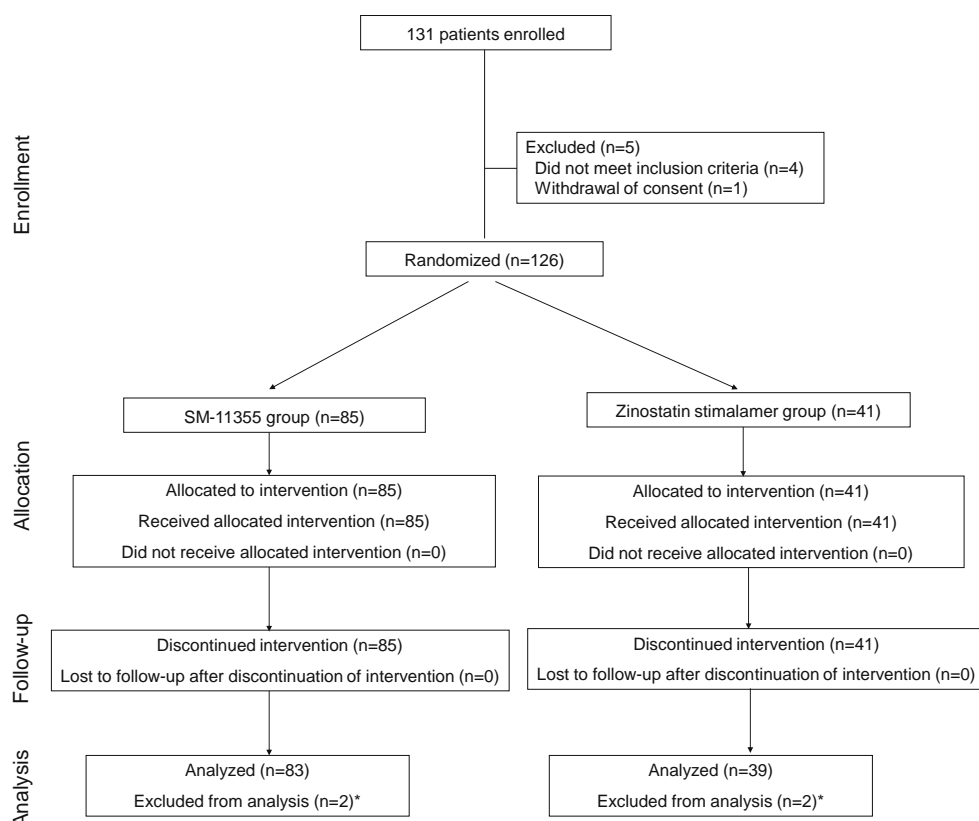
Fig. 2 Study flow diagram

Table 1 Patient background

	SM-11355	Zinostatin stimalamer
Number of patients	83	39
Sex (male:female)	70:13 (84.3%:15.7%)	30:9 (76.9%:23.1%)
Age (median)	67.0 (48–74)	68.0 (52–74)
PS (0:1:2:3:4)	80:3:0:0:0	35:4:0:0:0
HBs antigen positive	9 (13.6%)	1 (3.2%)
HCV antibody positive	55 (83.3%)	30 (96.8%)
HBs antigen · HCV antibody positive	2 (3.0%)	0 (0%)
Tumor stage (I:II:III:IV-A:IV-B)	0:43:40:0:0	0:19:20:0:0
Child-Pugh Classification (A:B:C)	61:22:0	32:7:0
Previously treated	25 (30.1%)	13 (33.3%)
Number of tumors 1	24 (28.9%)	9 (23.1%)
2	19 (22.9%)	11 (28.2%)
3	16 (19.3%)	7 (17.9%)
≥4	24 (28.9%)	12 (30.8%)
Maximum tumor diameter (mm) (Min-Max)	29.0 (10.0–80.0)	29.0 (10.0–94.0)

Table 2 Antitumor efficacy

Group	N	Antitumor efficacy						

"Criteria for Evaluation of Direct Effects on Hepatocellular Carcinoma" of the Liver Cancer Study Group of Japan

Group	N	V	IV	III	II	I	NE	Percentage of TE V (%) [95% CI]
SM-11355	83	22	21	12	7	17	4	26.5 [17.4–37.3]
Zinostatin stimalamer	39	7	14	4	10	1	3	17.9 [7.5–33.5]

Response Evaluation Criteria in Solid Tumors (RECIST)

Group	N	CR	PR	SD		PD	NE	Percentage of CR + PR
SM-11355	83	0	20	52		10	1	24.1 [15.4–34.7]
Zinostatin stimalamer	39	0	10	23		6	0	25.6 [13.0–42.1]

"Clinical Response Evaluation Criteria for Solid Tumor Chemotherapy" of the Japan Society for Cancer Therapy

Group	N	CR	PR	MR	NC	PD	NE	Percentage of CR + PR
SM-11355	83	0	17	10	36	19	1	20.5 [12.4-30.8]
Zinostatin stimalamer	39	0	9	5	19	6	0	23.1 [11.1–39.3]

Efficacy

The antitumor efficacy is shown in Table 2. The percentages of TE V patients were 26.5% (22/83) [95% confidence interval (CI): 17.4–37.3%] in the SM-11355 group and 17.9% (7/39) [95% CI: 7.5–33.5%] in the Zinostatin stimalamer group. In a RECIST assessment, response rates were 24.1% (20/83) [95% CI: 15.4–34.7%] and 25.6% (10/39) [95% CI: 13.0–42.1%] in the respective groups. Based on the Japan Society for Cancer Therapy Criteria, the tumor responses were 20.5% (17/83) [95% CI: 12.4–30.8%] and 23.1% (9/39) [95% CI: 11.1–39.3%] in the respective groups (Table 2).

Of 61 patients with a pre-treatment AFP level above the upper limit of normal in the SM-11355 group, 6 / 60 (10%) had an AFP level within the normal range 5 weeks after the

first injection. No data for the AFP level were available for 1 patient in the SM-11355 group at 5 weeks after the first injection. Among the 61 patients, 37 received a second injection and 6 (16%) had a normal AFP level 5 weeks after the second injection. Of the 26 patients in the Zinostatin stimalamer group with a pre-treatment AFP level above the upper limit of normal, none had an AFP level within the normal range 5 weeks after the first injection. Among the 26 patients, 18 received a second injection, but none had a normal AFP level 5 weeks after the second injection.

Cumulative survival rates are shown in Fig. 3. The follow-up period was approximately 3 years after the treatment period. The longest follow-up periods in the SM-11355 and Zinostatin stimalamer groups were both 5.6 years, and the median periods were 3.0 years and 2.8 years, respectively. The one-year survival rates in the SM-11355 and

Fig. 3 Cumulative survival rate
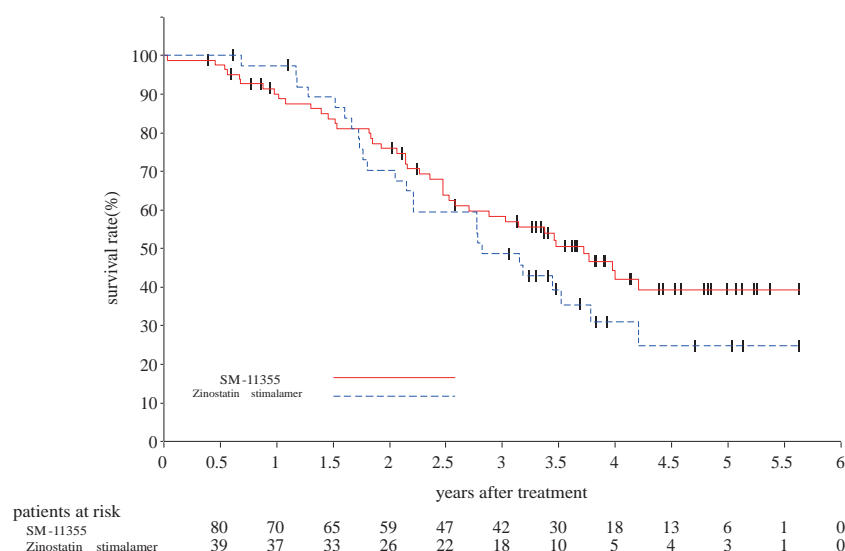
Table 3 Hematological and non-hematological adverse events

	SM-11355			Zinostatin stimalamer		
	No. of patients	All (%)	≥ Grade 3 (%)	No. of patients	All (%)	≥ Grade 3 (%)
Decrease in leukocytes	83	41.0	1.2	39	66.7	0
Decrease in lymphocytes	83	79.5	0	39	79.5	0
Decrease in neutrophils	83	53.0	8.4	39	43.6	2.6
Decrease in platelets	83	50.6	12.0	39	74.4	10.3
Decrease in hemoglobin	83	15.7	0	39	10.3	0
Increase in eosinophils	83	84.3	0	39	41.0	0
Increase in monocytes	83	57.8	0	39	76.9	0
Fatigue	83	39.8	0	39	46.2	0
Fever	83	96.4	3.6	39	97.4	0
Chills	83	39.8	0	39	51.3	0
Vomiting	83	55.4	1.2	39	51.3	0
Pain at injection site	83	43.4	0	39	41.0	2.6
Decrease in albumin	83	50.6	0	39	28.2	0
Increase in ALP	83	30.1	1.2	39	51.3	0
Increase in ALT	83	59.0	24.1	39	66.7	20.5
Increase in AST	83	62.7	26.5	39	79.5	38.5
Increase in bilirubin	83	57.8	12.0	39	71.8	5.1
Decrease in calcium	83	38.6	0	39	51.3	0
Increase in γ-GTP	83	49.4	0	39	61.5	0
Increase in glycemia	83	56.6	12.0	39	56.4	5.1
Increase in LDH	83	60.2	0	39	69.2	0
Increase in CRP	83	95.2	0	39	79.5	0
Prolonged PT time	83	42.2	1.2	39	28.2	0
Decrease in urinary creatinine	83	54.2	0	39	56.4	0
Increase in urinary creatinine	83	49.4	0	39	38.5	0
Increase in urinary NAG	83	89.2	0	39	87.2	0

Adverse events that occurred at a rate of >40% are shown

Zinostatin stimalamer groups were 90.1% and 97.4%, the 2-year survival rates were 75.9% and 70.3%, respectively, and the 3-year survival rates were 58.4% and 48.7%, respectively. The median survival time (MST) was 3.7 years in the SM-11355 group and 2.8 years in the Zinostatin stimalamer group.

Safety

Hematological adverse events were relatively mild and transient in both groups (Table 3). The incidences of neutropenia and decreased hemoglobin were similar in the two groups, but the incidence of eosinophilia was higher in the SM-11355 group, and the incidences of leukopenia and thrombocytopenia were higher in the Zinostatin stimalamer group. Most non-hematological adverse events (Table 3) were also mild and transient in both groups. Major events of grade 3 or higher involved liver dysfunction (including elevations in AST, ALT and hyperbilirubinemia) and

hyperglycemia, but these had similar incidences in both groups and most were reversible.

One patient in the SM-11355 group died of esophageal variceal rupture, which occurred 12 days after the first injection, and one patient in the Zinostatin stimalamer group died of hepatic failure 168 days after the second injection. Esophageal variceal rupture was considered not to be related to the treatment because the condition was recognized before initiation of treatment and the event was not classified as a toxicity. Other serious adverse events occurred in 8 patients in the SM-11355 group (increase in AST in 2 patients; and increase in ALT, sepsis, systemic inflammatory response syndrome (SIRS: a syndrome characterized by systemic inflammation and extensive tissue damage associated with serious infection), decrease in neutrophils, acute myocardial infarction (AMI), and hypotension in 1 case each) and in 2 patients in the Zinostatin stimalamer group (respiratory distress and arrhythmia, and abdominal pain in 1 case each). All the patients recovered with appropriate treatment. Most of these events

were considered to be probable or possible drug-related tox-icities, except for the cases of SIRS and AMI in the SM-11355 group. SIRS was judged to have no association with the investigational drug based on the results of blood culture and changes in test values. This patient was treated using a urinary catheter, and urinary tract infection is a cause of SIRS. A similar judgment was made for the case of AMI based on the chronological relationship between drug administration and the onset of disease.

In the subsequent angiographic examination before the second administration of SM-11355 or Zinostatin stima-lamer or in postprotocol treatment, hepatic artery damage that was probably due to intra-arterial drug administration was observed in 15/31 (48.4%) patients, shunt occurred in 5/31 (16.1%), and disorders of the hepatobiliary system were observed in 3/39 (7.7%) in the Zinostatin stimalamer group. None of these events were observed in patients in the SM-11355 group. Grade 3 hepatic artery damage and a grade 4 disorder of the hepatobiliary system were observed in 1 case each in the Zinostatin stimalamer group. Hepatobiliary dam-age that may have been caused by arterial damage was found in 3 patients in the Zinostatin stimalamer group (1 case each of liver atrophy and bile duct dilatation, bile duct necrosis, and liver failure and bile duct stricture), whereas there were no such findings in the SM-11355 group.

In the SM-11355 group, the percentages of patients with an increase in Child-Pugh score of one or more points compared to the pre-administration score were 27.7% (23/83) and 17.9% (10/56) in the 5 weeks after the 1st administration and the 5 weeks after the 2nd administration, respectively. In the Zinostatin stimalamer group, these percentages were 35.9% (14/39) and 50.0% (12/24), respectively (Fig. 4).

Pharmacokinetics

Total plasma platinum concentrations and platinum concen-trations in methanol extracts (Table 4) were determined in 30 and 24 patients in the SM-11355 group who were given one and two injections, respectively, and received median doses of 85 (Min-max: 24–120) and 120 (10–120) mg, respectively. The mean total platinum concentrations after the first and second injections were 9.6 and 12.9 ng/mL, respectively, and the mean percentages of the concentration in methanol extracts relative to the total plasma platinum concentration were 12.2% and 9.8% after the first and second injections, respectively. In one patient who underwent surgery 172 days after the second injection, the total platinum concentration was determined in the resected liver tissue. The total dose was 200 mg (first injection: 100 mg; second injection: 100 mg) and the concentration in the tumor region of sample S6, which had a 10% necrotic effect, was 62,000 ng/g tissue and that in the non-tumor region was 22,000 ng/g tissue. In contrast, the concentration in the tumor region of sample S8, which showed 50% necrosis, was 260,000 ng/g tissue and that in the non-tumor region was 67,000 ng/g tissue.

Discussion

Most anticancer agents used in TACE are water-soluble and inappropriate for suspension in iodized oil, and are usually administered as a water-in-oil emulsion. Consequently, these agents have reduced sustained release due to poorer retention in the tumor, leading to a limited antitumor effect and adverse effects caused by diffusion of the agents into the blood [16]. In contrast, lipophilic anticancer agents have a high affinity for iodized oil and those injected into the hepatic artery with iodized oil are retained selectively in tumors and exert contin-uous antitumor effects. SM-11355 is a structurally modified platinum complex with improved affinity for iodized oil due to increased lipophilicity [3]. In an AH109A-transplanted rat liver tumor model, the platinum concentration in the tumor was sustained for longer following administration of a iodized oil suspension of SM-11355 compared to a suspension of cisplatin, with SM-11355 distributed in tumor tissues more selectively than cisplatin [17]. Phase I and early phase II trials
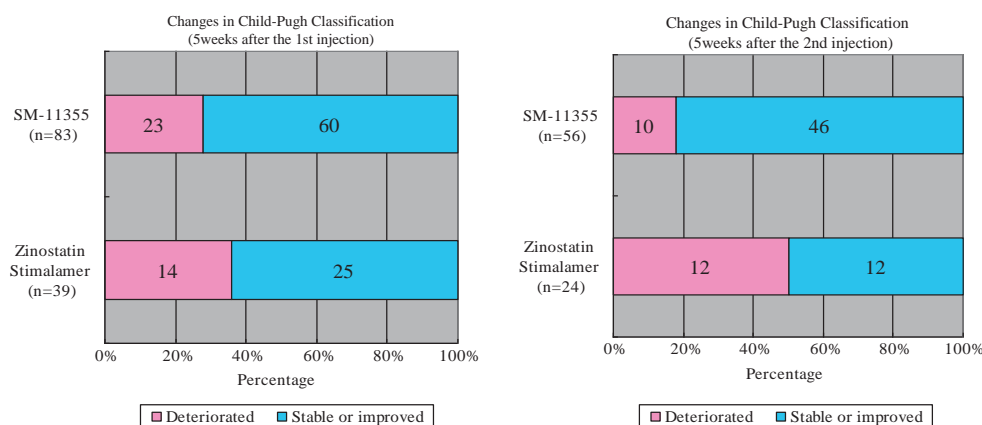

Fig. 4 Changes in Child-Pugh Classification

Table 4 Blood drug concentrations

Administration frequency		Once	Twice
Dose (mg)	Number of patients	30*	24*
	Median (Min-Max)	85.0 (24–120)	120.0 (10–120)
Total plasma platinum concentration (ng/mL)	Number of patients	30	24
	Mean	9.6	12.9
SM-11355 metabolite concentration in methanol extracts (ng/mL)	Number of patients	32	24
	Mean	1.17	1.19
[SM-11355 in methanol-extracted fraction*] / [total plasma platinum concentration] × 100 (%)	Number of patients	30	24
	Mean	12.2	9.8

Number of subjects in whom both the total plasma platinum concentration and SM-11355 metabolite concentration in methanol extracts were measured

* Methanol-extracted fraction: The fraction of SM-11355-derived substances includes components that may exert therapeutic activity as an anticancer agent and excludes components that are irreversibly bound to plasma protein

of SM-11355 have also shown that the total plasma platinum concentration is much lower than that with cisplatin [4, 5, 18]. Our pharmacokinetic data verify these results and suggest that SM-11355 is retained in liver tumors selectively and exerts a continuous effect on the tumor.

In patients in whom the total plasma platinum concentration and the platinum concentration in methanol extracts were determined after the first and second injections, the platinum concentration in methanol extracts 3 weeks after injection (estimated to be the peak of the total plasma platinum concentration) was approximately 10% of the total plasma platinum concentration. Of the platinum components released from the SM-11355 suspension and transferred into the systemic circulation, some are irreversibly bound to plasma proteins and are no longer bioactive. After exclusion of these components, the amount remaining in the plasma is estimated to be up to about 10% of the dose. The total platinum concentrations in several regions of the liver were also determined in one patient. The concentrations in tumors regions were significantly higher than those in non-tumor regions and several thousand-fold higher than the mean total plasma platinum concentration at 3 weeks ±3 days after the second injection (12.9 ng/mL). The total platinum concentration was also higher in tissues in which a higher antitumor effect was observed.

The results of the efficacy re-evaluation suggested that SM-11355 has a similar effect to that of Zinostatin stimalamer following injection of an iodized oil suspension of each drug into the hepatic artery. The primary endpoint (TE V rate based on the Criteria for Evaluation of Direct Effects on Hepatocellular Carcinoma) and the secondary endpoint (response rate based on the Japan Society for Cancer Therapy Criteria and RECIST) in the SM-11355 group were almost the same as those in the Zinostatin stimalamer group. However, the percentage of TE V cases in the SM-11355 group (26.5% [17.4–37.3%]) in this trial was lower than the value of 56% [30–80%] found in the early phase II trial. The discrepancy in the percentage of TE V cases may be due to differences in the

tumor burden in the two trials. Eleven (68.8%) of 16 patients in the early phase II study had 3 or less tumors and a longest tumor diameter of 3 cm or less, whereas only 38 (45.8%) of 83 patients in the late phase II study had these characteristics.

The major toxicities of grade 3 or higher involved liver dysfunction, including increases in AST, ALT and bilirubin, and a decrease in platelets in both groups. The incidences were similar in each group and most of the effects were reversible. An increase in eosinophils was found in 84.3% of patients in the SM-11355 group, and was considered to be a SM-11355-specific adverse event. The precise mechanism is unknown, but the finding was not thought to indicate anaphylaxis because the increase in eosinophils showed no marked correlation with an increase in IgE and/or allegic symptoms like wheezing. Renal disorder was transient in patients of the SM-11355 group, except for a patient with sepsis. The incidences and severity of increased blood creatinine and positive urine protein in the SM-11355 group were higher than the respective levels in the Zinostatin stimalamer group (9/83, 10.8% vs. 2/39, 5.1%; and 22/83, 26.5% vs. 2/39, 5.1%, respectively). Based on these data, we consider that the patients were thoroughly followed up.

Injection of SM-11355 did not lead to local vascular damage and had fewer irreversible effects on the hepatobiliary system compared with Zinostatin stimalamer. Zinostatin stimalamer has been reported to have major safety problems, including hepatic arterial damage and effects on the hepatobiliary system that are irreversible and prevent repeated treatment [5, 19, 20] Therefore, SM-11355 may be advantageous for frequent repeated treatment and maintenance of liver function. The changes in Child-Pugh Class indicated a low incidence of treatment-induced hepatic dysfunction in the SM-11355 group.

Based on the results of this trial, we conclude that SM-11355 in iodized oil has similar efficacy to that of Zinostatin stimalamer, which is the only drug currently approved for chemolipiodolization for HCC in Japan. The TE V rate of 26.5% in the SM-11355 group was considered 'favorable'

based on our assumption of a TE V rate of 15% for conventional TACE before the initiation of this study, and was equivalent or superior to the rate of about 20% found in patients receiving current standard TACE treatment in a recent report [7]. Our results also suggest that repeated dosing of SM-11355 in iodized oil is possible without development of hepatic vascular injury in a case of relapse. We are currently conducting a phase III study of intra-arterial treatment with SM-11355 in comparison with conventional TACE with epirubicin, which is designed to detect the superiority of intra-arterial treatment with SM-11355 in overall survival of TACE-naïve patients with advanced HCC (Appendix).

Appendix

Coordinating investigators
Members of the Committee for Efficacy and Safety
Members of the Committee for Efficacy Evaluation
Statistics Advisor
Investigators and Institutions

Coordinating investigators

Yasuhiko Kubo	Omuta City General Hospital
Kenichi Kobayashi	Kanazawa University Hospital
Shuichi Okada	National Cancer Center Hospital

Members of the Committee for Efficacy and Safety

Masaru Itakura	Surugadai Clinic, Medical Corporation Shun-ai-kai
Mariko Itsubo	Jikei University Hospital
Junji Shibata	Shibata Internal and Gastrointestinal Clinic
Shoji Fukushima	Faculty of Pharmaceutical Sciences, Kobe Gakuin University

Members of the Committee for Efficacy Evaluation

Shigetoshi Fujiyama	NTT West Kyushu Hospital
Yutaka Horie	Saiseikai Gotsu General Hospital
Fuminori Moriyasu	Tokyo Medical University Hospital
Hiroki Inoue	Foundation Jiaikai Imamura Hospital

Statistics Advisor

Tosiya Sato	Kyoto University School of Public Health

Investigators and institutions

Hiromasa Ishii	Keio University Hospital
Hidetugu Saito	Keio University Hospital
Shuichi Okada	National Cancer Center Hospital
Takuji Okusaka	National Cancer Center Hospital
Hiromitsu Kumada	Toranomon Hospital
Naoaki Hayashi	Tokyo Women's Medical University Hospital
Keiko Shiratori	Tokyo Women's Medical University Hospital
Masaharu Yoshikawa	Chiba University Hospital
Hiroshi Ishii	National Cancer Center Hospital East
Yasukazu Shioyama	Ibaraki Prefectural Central Hospital
Katsuaki Tanaka	Yokohama City University Hospital Medical Center
Masao Honda	Kanazawa University Hospital
Hiroshi Kasugai	Osaka Medical Center for Cancer and Cardiovascular Diseases
Masatoshi Kudo	Kinki University Hospital
Toshihito Seki	Kansai Medical University Takii Hospital
Kazuaki Chayama	Hiroshima University Hospital
Kiwamu Okita	Yamaguchi University Hospital
Isao Sakaida	Yamaguchi University Hospital
Yukio Kusumoto	Nagasaki Municipal Hospital
Takuya Tsutsumi	Nagasaki Municipal Hospital
Michio Sata	Kurume University Hospital
Kenji Sakata	Omuta City General Hospital

References

1. Parkin DM, Bray F, Ferlay J, Pisani P (2005) Global cancer statistics, 2002. CA Cancer J Clin 55(2):74–108

2. Lopez PM, Villanueva A, Llovet JM (2006) Systematic review: evidence-based management of hepatocellular carcinoma: an updated analysis of randomized controlled trials. Aliment Pharmacol Ther 23(11):1535–1547

3. Maeda M, Uchida NA, Sasaki T (1986) Liposoluble platinum(II) complexes with antitumore activity. Jpn J Cancer Res 77(6):523–525

4. Fujiyama S, Shibata J, Maeda S, Tanaka M, Noumaru S, Sato K et al (2003) Phase I clinical study of a novel lipophilic platinum complex (SM-11355) in patients with hepatocellular carcinoma refractory to cisplatin / lipiodol. Br J Cancer 89(9):1614–1619

5. Okusaka T, Okada S, Nakanishi T, Fujiyama S, Kubo Y (2004) Phase II trial of intra-arterial chemotherapy using a novel lipophilic platinum derivative (SM-11355) in patients with hepatocellular carcinoma. Invest New Drugs 22(2):169–176

6. Liver Cancer Study Group of Japan (1999) Survey and follow-up study of primary liver cancer in Japan. Report 13. Acta Hepatologica Japonica 40(5):288–300

7. Liver Cancer Study Group of Japan (2000) Survey and follow-up study of primary liver cancer in Japan. Report 14. Acta Hepatologica Japonica 41(12):799–811

8. Okusaka T, Okada S, Ishii H, Ikeda M, Nakasuka H, Nagahama H et al (1998) Transarterial chemotherapy with Zinostatin Stimalamer for hepatocellular carcinoma. Oncology 55(4):276–283

9. Okusaka T, Kasugai H, Shioyama Y, Tanaka K, Kudo M, Saisho H (2009) Transarterial chemotherapy alone versus transarterial chemoembolization for hepatocellular carcinoma: a randomized phase III trial. J Hepatol 51(6):1030–1036

10. Japanese Society of Liver Carcinoma (the Committee for Preparing Criteria for Evaluation of Multidisciplinary Treatment of Liver Carcinoma) (1994) Criteria for evaluation of direct effects of liver cancer treatment. Kanzo 35(2):193–205

11. Bruix J, Sherman M, Llovet JM, Beaugrand M, Lencioni R, Burroughs AK et al (2001) Clinical management of hepatocellular carcinoma. Conclusions of the Barcelona-2000 EASL conference. European Association for the Study of the Liver. J Hepatol 35 (3):421–430

12. Takayasu K, Arii S, Matsuo N, Yoshikawa M, Ryu M, Takasaki K et al (2000) Comparison of CT findings with resected specimens after chemoembolization with iodized oil for hepatocellular carcinoma. Am J Roentgenol 175(3):699–704

13. Okusaka T, Okada S, Ueno H, Ikeda M, Yoshimori M, Shimada K et al (2000) Evaluation of the therapeutic effect of transcatheter arterial embolization for hepatocellular carcinoma. Oncology 58 (4):293–299

14. Japan Society for Cancer Therapy (1986) The Japan Society for Cancer Therapy Criteria. J Jpn Soc Cancer Ther 21(5):929–942

15. Japan Society for Cancer Therapy (1997) Toxicity grading criteria of the Japan Society for Cancer Therapy. J Jpn Soc Cancer Ther 1 (32):61–65

16. Takayasu K, Shima Y, Muramatsu Y, Moriyama N, Yamada T, Makuuchi M et al (1987) Hepatocellular carcinoma: treatment with intraarterial iodized oil with and without chemotherapeutic agents. Radiology 163(2):345–351

17. Hanada M, Baba A, Tsutsumishita Y, Noguchi T, Yamaoka T, Chiba N et al (2009) Intra-hepatic arterial administration with miriplatin suspended in an oily lymphographic agent inhitibs the growth of tumors implanted in rat livers by inducing platinum-DNA adducts to form and massive apoptosis. Cancer Chemother Pharmacol 64(3):473–483

18. Shibata J, Fujiyama S, Sato T, Kishimoto S, Fukushima S, Nakano M (1989) Hepatic arterial injection chemotherapy with cisplatin suspended in an oily lymphographic agent for hepatocellular carcinoma. Cancer 64(8):1586–1594

19. Sakaguchi T, Yoshimatsu S, Sagara K, Yamashita Y, Takahashi M (1998) Intra-arterial infusion of SMANCS for treatment of patients with hepatocellular carcinoma–adverse reactions and complications. Gan To Kagaku Ryoho 25(Suppl 1):64–69

20. Ikeda K, Saitoh S, Kobayashi M, Suzuki Y, Suzuki F, Tsubota A et al (2000) Hepatic vascular side effects of styrene maleic acid neocarzinostatin in the treatment of hepatocellular carcinoma. J Gastroenterol 35(5):353–360

Original Article

Activation of c-Jun N-terminal kinase in non-cancerous liver tissue predicts a high risk of recurrence after hepatic resection for hepatocellular carcinoma

Satoru Hagiwara,[1] Masatoshi Kudo,[1] Hobyung Chung,[1] Kazuomi Ueshima,[1] Tatsuo Inoue,[1] Seiji Haji,[2] Tomohiro Watanabe,[4] Ah-Mee Park,[3] Hiroshi Munakata[3] and Toshiharu Sakurai[1]

Department of [1]Gastroenterology and Hepatology, [2]Surgery, and [3]Biochemistry, Kinki University School of Medicine, Osaka-Sayama, and [4]Center for Innovation in Immunoregulative Technology and Therapeutics, Kyoto University Graduate School of Medicine, Kyoto, Japan

Aim: Hepatocellular carcinoma (HCC) ranks as the third leading cause of cancer deaths worldwide. Hepatic resection is the mainstay of curative treatment for early stage HCC. Although c-Jun N-terminal kinase (JNK) activation contributes to hepatocyte proliferation and HCC development in mice, the extent of involvement of JNK in human HCC development is unknown. The aim of this study is to assess the predictive value of JNK for postoperative recurrence in HCC.

Methods: From April 2005 to March 2008, 159 patients underwent curative resection for HCC. From the 159 patients, 20 patients each matched for age, gender and etiology were registered as three groups: (i) without recurrence (no recurrence group), (ii) with recurrence within one year after surgery (early recurrence group), and (iii) with recurrence at one year or more after surgery (late recurrence group) (a

cross-sectional control study). We investigated factors contributing to postoperative early and late phase recurrence.

Results: Multivariate analysis using a Logistic regression model showed that JNK activity in non-cancerous liver tissue was correlated with postoperative late recurrence. ($P = 0.02$, odds ratio; 5.79, 95% confidence interval [CI]; 1.33–25.36).

Conclusions: JNK activity in non-cancerous liver tissue is considered as a reliable predictive biomarker for postoperative recurrence in HCC.

Key words: c-Jun, c-Jun N-terminal kinase, hepatocellular carcinoma, mitogen-activated protein kinases, postoperative recurrence

INTRODUCTION

HEPATOCELLULAR CARCINOMA (HCC) is one of the most common cancers worldwide, and its incidence is increasing.[1] Epidemiological studies suggest that the major risk factors for HCC are persistent infection with hepatitis B and C virus (HBV and HCV), hepatosteatosis and chronic exposure to toxic chemicals,[2–4] all of which cause chronic liver injury and inflammation.[2] Persistent inflammation can lead to progressive liver fibrosis and eventually cirrhosis. Indeed, the

majority of HCCs occur on a background of liver fibrosis. HCV-related HCC develops only after one or more decades of chronic HCV infection, and the increased risk is restricted predominantly to patients with cirrhosis or advanced fibrosis.[5] Although HCV-infected individuals with mild or non-hepatic fibrosis are unlikely to develop HCC, once severe fibrosis is established, HCC develops at an annual rate of 1–4% per year.[5] There is a strong correlation between liver fibrosis and HCC development.[6] Thus, the risk of hepatocarcinogenesis depends on the background liver factors.

Mitogen-activated protein kinases (MAPKs), serine/threonine-specific protein kinases, respond to extracellular stimuli and have a pivotal role in various cellular processes, such as gene expression, mitosis, differentiation, proliferation, and cell survival.[7,8] MAPK comprises the extracellular signal-regulated protein kinase (ERK), c-Jun N-terminal kinase (JNK) and p38. Accumulating

© 2012 The Japan Society of Hepatology

evidence suggests that activation or inactivation of MAPK regulates inflammatory responses and provides a growth advantage to hepatocytes during malignant transformation and liver tumorigenesis.[9–12] Mouse cancer models have shown that the JNK pathway is implicated in regulating liver carcinogenesis. c-Jun, a downstream target of JNK, promotes chemically induced liver cancer development through suppression of the p53 pathway.[13] JNK activation contributes to hepatocyte proliferation and HCC development by regulating cyclin D and vascular endothelial growth factor (VEGF), a potent proangiogenic substance responsible for tumor neovascularization.[10,14] However, the extent of involvement of JNK in the development of human liver cancers is unknown.

In this study, we demonstrated that in human HCC, JNK activation in non-cancerous liver tissue increases the risk of late phase recurrence after hepatic resection.

METHODS

Patients

FROM APRIL 2005 to March 2008, 159 patients underwent curative resection for HCC at Kinki University School of Medicine. We investigated the factors contributing to early and late phase recurrence. Several studies have used two years as the cut-off between the early and late phases.[15,16] Because there were only a few patients with recurrence at two years or more after hepatectomy in our study, we set one year as the cut-off between early and late recurrence as reported previously.[17] From the 159 patients, 20 patients each matched for age, gender and etiology were registered as three groups: (i) without recurrence (no recurrence group), (ii) with recurrence within one year after surgery (early recurrence group), and (iii) with recurrence at one year or more after surgery (late recurrence group) (a cross-sectional control study). Disease recurrence after surgical resection was monitored by serial measurement of tumor markers and ultrasonography every 3 months and computed tomography scans every 6 months.

Cancerous and non-cancerous tissues were separately obtained by surgery and non-cancerous tissues were more than 5 cm away from tumors. With regard to cause of disease, hepatitis C accounted for 55% of all patients enrolled in this study, followed by non-B non-C hepatitis and hepatitis B (Table 1).

The study protocols conformed to the ethical guidelines of the 1975 Declaration of Helsinki and were approved by the institutional review boards. Written informed consent was obtained from all patients for subsequent use of their collected tissues.

Western blot analysis

To prepare tissue lysates, cancer tissue and non-cancerous liver tissue was homogenized with CelLytic-MT Mammalian Tissue Lysis/Extraction reagent (Sigma-Aldrich, St. Louis, MO, USA) containing protease inhibitor, Complete (Roche Diagnostics, Mannheim, Germany), and phosphatase inhibitor cocktail (Nacalai Tesque, Kyoto, Japan). Equal protein amounts of tissue lysates were electrophoresed through a reducing sodium dodecyl sulfate (SDS) polyacrylamide gel and electroblotted onto a polyvinylidene fluoride (PVDF) membrane. The membrane was blocked with 5% skim milk and incubated with anti-phospho-JNK, anti-JNK, anti-phospho-AKT, anti-AKT, anti-phospho-ERK1/2, anti-ERK1/2 (Cell Signaling) and anti β-actin (Sigma-Aldrich) antibodies. Protein levels were detected using horse radish peroxidase (HRP)-linked secondary antibodies and the ECL-plus System (GE Healthcare, Buckinghamshire, UK). To evaluate signal intensity, western blot image data were quantified using Image J software. Activation of the JNK signaling pathway was assessed by measuring the amount of phospho-JNK.

Immunohistochemistry

Immunohistochemical analysis was performed on paraffin-embedded liver tissue. Immunohistochemical staining was carried out with antibodies raised against anti-phospho-c-Jun (1:100) from Cell Signaling technology (Beverly, MA, USA) and visualized using Dako LSAB System-HRP (Dako, Carpintaria, CA, USA).

Statistical analysis

We investigated factors contributing to postoperative recurrence by univariate analysis using the log-rank test and multivariate analysis using a Logistic regression model. All analyses were performed using the SPSS software (version 11.5; SPSS Inc., Chicago, IL, USA).

RESULTS

Association between the risk of late recurrence and background liver factors

NO RECURRENCES WERE observed in a follow-up period of 1003 ± 329 (range 620–1490) days. The period until recurrence was 153 ± 96 (range 40–360)

© 2012 The Japan Society of Hepatology

Table 1 Comparison of patient characteristics according to post-operative recurrence

Variable	No recurrence (*n* = 20)	Early recurrence (<1 year) (*n* = 20)	Late recurrence (≥1 year) (*n* = 20)	*P*-value (no recurrence vs early recurrence)	*P*-value (no recurrence vs late recurrence)
Age, years	66 (51–80)	67 (35–81)	70 (58–80)	Matched	Matched
Sex, no. (%)				Matched	Matched
Male	16 (80)	16 (80)	16 (80)		
Female	4 (20)	4 (20)	4 (20)		
Cause of disease, no. (%)				Matched	Matched
Hepatitis B	4 (20)	3 (15)	4 (20)		
Hepatitis C	11 (55)	11 (55)	11 (55)		
Non-B, Non-C	5 (25)	6 (30)	5 (25)		
Tumor size, no. (%)				0.41	0.48
<3 cm	5 (25)	3 (15)	3 (15)		
≧3 cm	15 (75)	17 (85)	17 (85)		
Tumor number, no. (%)				0.11	0.43
Single	15 (75)	19 (95)	18 (90)		
Multiple	5 (25)	1 (5)	2 (10)		
Tumor grade, no. (%)				**0.009**	0.34
Well	6 (30)	1 (15)	3 (5)		
Moderate	13 (65)	13 (65)	13 (65)		
Poor	1 (5)	6 (30)	4 (30)		
Portal vein invasion, no. (%)				**0.0007**	0.57
Negative	18 (90)	11 (55)	16 (80)		
Positive	2 (10)	9 (45)	4 (20)		
Non-cancerous liver tissue, no. (%)				0.64	**0.06**
No cirrhosis	11 (55)	10 (50)	5 (25)		
Cirrhosis	9 (45)	10 (50)	15 (75)		
ALT (IU/mL), no. (%)				0.29	0.13
<40	11 (45)	13 (75)	7 (35)		
≧40	9 (55)	7 (35)	13 (75)		
AFP (ng/mL), no. (%)				0.26	0.9
<40	14 (70)	10 (50)	15 (75)		
≧40	6 (30)	10 (50)	5 (25)		
DCP (mAU / mL) -no. (%)				0.62	0.73
<100	9 (45)	11 (55)	8 (40)		
≧100	11 (55)	9 (45)	12 (60)		
p-ERK in non-cancerous liver tissue (ratio to actin), no. (%)				0.29	0.92
Low (<0.3)	12 (60)	9 (45)	12 (60)		
High (≧0.3)	8 (40)	11 (55)	8 (40)		
p-JNK in non-cancerous liver tissue (ratio to actin), no. (%)				0.12	**0.02**
Low (<0.6)	16 (80)	12 (60)	8 (40)		
High (≧0.6)	4 (20)	8 (40)	12 (60)		
p-AKT in non-cancerous liver tissue (ratio to actin), no. (%)				0.30	0.97
Low (<0.3)	11 (55)	14 (70)	11 (55)		
High (≧0.3)	9 (45)	6 (30)	9 (45)		

Values in bold are statistically significant.
ALT, alanine aminotransferase; AFP, α-fetoprotein; DCP, des-gamma-carboxyprothrombin; ERK, extracellular signal-regulated protein kinase; JNK, c-Jun N-terminal kinase.

Table 2 Multivariate analysis using a logistic regression model of the risk factor associated with post-operative early (<1 year) recurrence

Variable	Odds ratio	95% CI	*P*-value
Tumor grade	4.32	0.92–20.31	0.06
Portal vein invasion	4.43	0.74–26.60	0.11

CI, confidence interval.

days in the early recurrence group and 521 ± 202 (range 365–1145) days in the late recurrence group. As shown in Table 1, aggressive tumor pathological factors such as high tumor grade and portal vein invasion were risk factors for early (less than one year) phase recurrence. Multivariate analysis with a logistic regression model as to the tumor grade and portal vein, significant factors identified by univariate analysis, revealed that the tumor grade alone was identified as a significant factor (Table 2). We found a weak correlation between late (one year or more) phase recurrence and background liver factors, such as the presence of cirrhosis, although the result was not statistically significant (Table 1). These data are consistent with previous reports that the risk of early phase recurrence depends on the characteristics of resected HCC while the risk of late phase recurrence depends on the background liver factors.[15–17]

Association between the risk of late recurrence and JNK activation in non-cancerous liver tissue

Next, we assessed the association between HCC recurrence and JNK activation in resected HCCs and non-cancerous liver tissues. The expression level of phospho-JNK, as a read out of JNK activity, in non-cancerous liver tissue was correlated with the risk for late phase recurrence, but not the risk of early phase recurrence (Fig. 1 and Tables 1–3). There was no significant correlation between JNK activities of HCC tissues and non-cancerous liver tissues of the same patients (Fig. 1). In patients with liver cirrhosis, p-JNK levels in non-cancerous tissues were significantly higher in the late phase recurrence group than in the no recurrence group ($P < 0.01$), whereas p-JNK level had no significant difference between no recurrence and early phase recurrence groups ($P = 0.13$) (Fig. 2). These results indicate that p-JNK expression level is an independent risk factor for the late phase recurrence. During tumor initiation, JNK plays important roles in not only hepatocyte but also non-parenchymal cells in the liver. JNK is activated in hepatocytes to promote cell death which triggers signals in Kupffer cells that promote compensatory hepatocyte proliferation and hepatocarcinogenesis.[7,10,12] JNK activation of hepatocytes and non-parenchymal cells in non-cancerous liver tissue was assessed by

Table 3 Multivariate analysis using a logistic regression model of the risk factor associated with postoperative late (<1 year) recurrence

Variable	Odds ratio	95% CI	*P*-value
p-JNK in non-cancerous liver tissue (high, $\geqq$0.6)	5.79	1.33–25.36	0.02
Non-cancerous liver tissue (cirrhosis)	3.51	0.81–15.09	0.09

CI, confidence interval.

Figure 1 Association between the risk of late recurrence and c-Jun N-terminal kinase (JNK) activation in cancer and non-cancerous liver tissue. Homogenates of cancerous and non-cancerous tissues of the same patients with late (one year or more after hepatectomy) phase recurrence or without recurrence were electrophoresed and immunoblotted with the indicated antibodies.

© 2012 The Japan Society of Hepatology
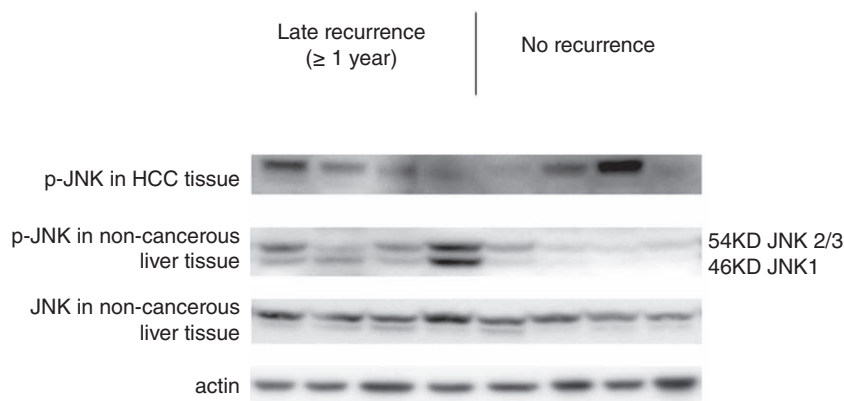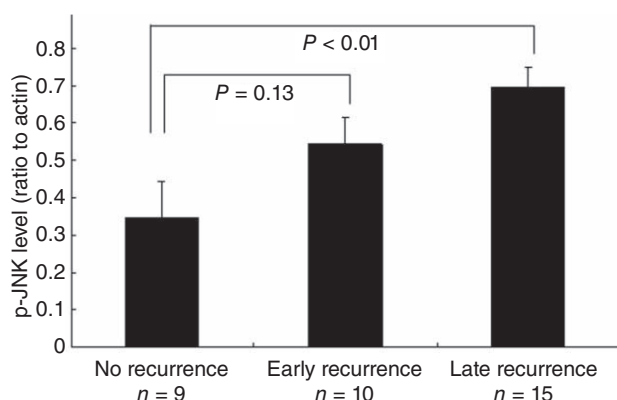
Figure 2 c-Jun N-terminal kinase (JNK) activities in non-cancerous liver tissues of cirrhotic patients with no recurrence, early recurrence or late recurrence. In the late phase recurrence group, p-JNK levels were significantly higher than in the no recurrence group ($P < 0.01$). Data are means ± standard error (SE).

immunohistochemistry. Since phospho-c-Jun is a well-known readout of JNK activity, we performed immuno-histochemistry using anti-phospho-c-Jun antibody. As shown in Figure 3, all hepatocytes were stained with anti-p-c-Jun antibody, while non-parenchymal cells were weakly stained.

c-Jun N-terminal kinase activation in resected HCCs, as assessed by western blot analysis and immunohis-tochemistry, was not correlated with the risk of either early or late phase recurrence (data not shown). Activation of ERK in HCCs indicates aggressive tumor behavior.[18] AKT phosphorylation in HCCs was also reported to be a risk factor for early recurrence.[17] These data suggest an association between early phase recurrence and the activation of ERK and AKT in HCCs. In contrast, we did not find an association between the risk of late

phase recurrence and phospho-ERK or -AKT expression in non-cancerous liver tissues (Fig. 4 and Table 1).

DISCUSSION

HEPATOCELLULAR CARCINOMA IS characterized by extremely frequent intrahepatic recurrence even after successful curative treatments.[15] Two modes of intrahepatic recurrence have been distinguished: de novo carcinogenesis and intrahepatic metastasis. Several studies have shown that early recurrence after resection of HCC is likely to be associated with aggressive tumor pathological factors such as high tumor grade, microvascular invasion, and microsatellite lesions, while late recurrence is more likely related to underlying liver conditions such as the presence of cirrhosis and inflammatory activity.[15–17] These findings suggested that early recurrence is most likely the consequence of occult metastasis from the initial tumor, whilst late recurrence more likely represents multicentric tumors attributable to de novo HCC development or rapid growth of small nodules. Here, we show that the risk of recurrence within one year is significantly related to high tumor grade most probably representing the potential of intrahepatic metastasis, while the risk of recurrence at one year or more after resection is correlated weakly with the non-cancerous liver condition, such as the presence of cirrhosis. This is consistent with previous reports.[15–17] Most importantly, the activation of JNK in the adjacent non-cancerous liver tissue is correlated with the risk of late (one year or more) phase recurrence. Elevated JNK activity contributes to reactive oxygen species (ROS) accumulation and hepatocyte death, resulting in IL-1α release and activation of IL-1R/MyD88 signaling in Kupffer cells. These responses induce IL-6 production, stimulation of compensatory proliferation, and subsequently HCC
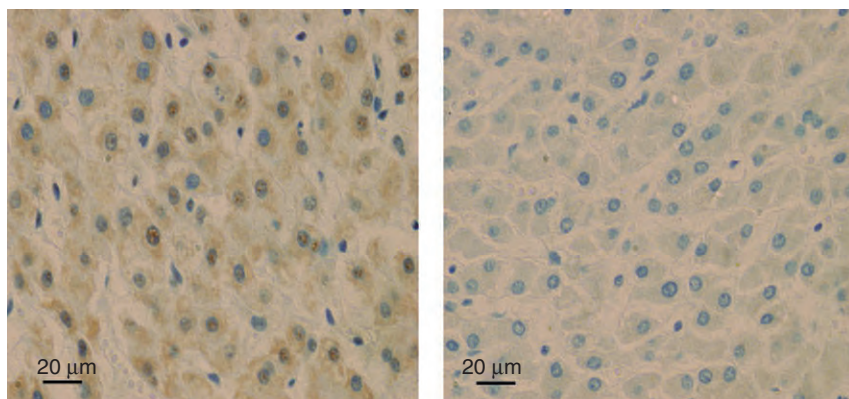
Figure 3 Expression of p-c-Jun in non-cancerous liver tissue. All hepatocytes were stained immunohistochemically with anti-p-c-Jun antibody, while non-parenchymal cells were weakly stained. Right is negative example.
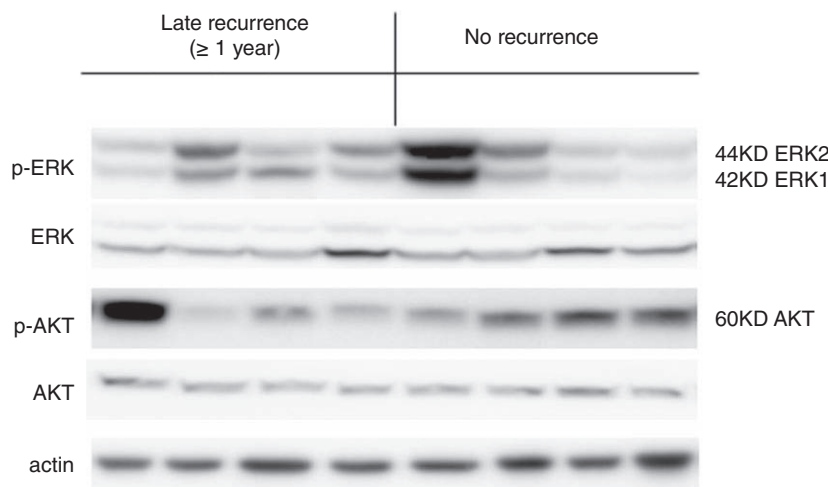
Figure 4 Association between the risk of late recurrence and extracellular signal-regulated protein kinase (ERK) and AKT activation in non-cancerous liver tissue. Homogenates of non-tumor liver tissues of patients with late (one year or more after hepatectomy) phase recurrence or without recurrence were electrophoresed and immunoblotted with the indicated antibodies.

development.[10–12] Activation of JNK in underlying liver tissue would play an important role in the development of multicentric tumors and late phase recurrence.

JNK activation in resected HCCs was not correlated with the risk of early phase recurrence (data not shown). In contrast, activation of ERK and AKT in HCCs was shown to be involved in early phase recurrence.[17,18] Intrahepatic metastasis from the initial tumor and early phase recurrence might be regulated in HCC mostly by the ERK and AKT signaling pathway, rather than the JNK signaling pathway. Surgical hepatectomy, curative treatment available for those who qualify, is a locoregional treatment in which the background liver disease with a high risk of de novo HCC development is left untreated. Therefore, it is important to control multicentric carcinogenesis as well as to treat HCC that is already established. Our results demonstrate the importance of JNK in human HCC, and the potential application of JNK targeting for HCC therapy.

REFERENCES

1 Thorgeirsson SS, Grisham JW. Molecular pathogenesis of human hepatocellular carcinoma. *Nat Genet* 2002; **31**: 339–46.

2 Bosch FX, Ribes J, Díaz M, Cléries R. Primary liver cancer: worldwide incidence and trends. *Gastroenterology* 2004; **127**: S5–S16.

3 Ascha MS, Hanouneh IA, Lopez R, Tamimi TA, Feldstein AF, Zein NN. The incidence and risk factors of hepatocellular carcinoma in patients with nonalcoholic steatohepatitis. *Hepatology* 2010; **51**: 1972–8.

4 Starley BQ, Calcagno CJ, Harrison SA. Nonalcoholic fatty liver disease and hepatocellular carcinoma: a weighty connection. *Hepatology* 2010; **51**: 1820–32.

5 Hoshida Y, Ikeda K, Kobayashi M *et al.* Chronic liver disease in the extremely elderly of 80 years or more: clinical characteristics, prognosis and patient survival analysis. *J Hepatol* 1999; **31**: 860–6.

6 Ikeda K, Saitoh S, Suzuki Y *et al.* Disease progression and hepatocellular carcinogenesis in patients with chronic viral hepatitis: a prospective observation of 2215 patients. *J Hepatol* 1998; **28**: 930–8.

7 Chang L, Karin M. Mammalian MAP kinase signalling cascades. *Nature* 2001; **410**: 37–40.

8 Dhillon AS, Hagan S, Rath O, Kolch W. MAP kinase signalling pathways in cancer. *Oncogene* 2007; **26**: 3279–90.

9 Whittaker S, Marais R, Zhu AX. The role of signaling pathways in the development and treatment of hepatocellular carcinoma. *Oncogene* 2010; **29**: 4989–5005.

10 Sakurai T, Maeda S, Chang L, Karin M. Loss of hepatic NF-kappa B activity enhances chemical hepatocarcinogenesis through sustained c-Jun N-terminal kinase 1 activation. *Proc Natl Acad Sci USA* 2006; **103**: 10544–51.

11 Hui L, Bakiri L, Mairhorfer A *et al.* p38alpha suppresses normal and cancer cell proliferation by antagonizing the JNK-c-Jun pathway. *Nat Genet* 2007; **39**: 741–9.

12 Sakurai T, He G, Matsuzawa A *et al.* Hepatocyte necrosis induced by oxidative stress and IL-1 alpha release mediate carcinogen-induced compensatory proliferation and liver tumorigenesis. *Cancer Cell* 2008; **14**: 156–65.

13 Eferl R, Ricci R, Kenner L *et al.* Liver tumor development. c-Jun antagonizes the proapoptotic activity of p53. *Cell* 2003; **112**: 181–92.

14 Schwabe RF, Bradham CA, Uehara T *et al.* c-Jun-N-terminal kinase drives cyclin D1 expression and proliferation during liver regeneration. *Hepatology* 2003; **37**: 824–32.

15 Imamura H, Matsuyama Y, Tanaka E *et al.* Risk factors contributing to early and late phase intrahepatic recurrence of hepatocellular carcinoma after hepatectomy. *J Hepatol* 2003; **38**: 200–7.

16 Portolani N, Coniglio A, Ghidoni S *et al.* Early and late recurrence after liver resection for hepatocellular

carcinoma: prognostic and therapeutic implications. *Ann Surg* 2006; **243**: 229–35.

17 Nakanishi K, Sakamoto M, Yamasaki S, Todo S, Hirohashi S. Akt phosphorylation is a risk factor for early disease recurrence and poor prognosis in hepatocellular carcinoma. *Cancer* 2005; **103**: 307–12.

18 Schmitz KJ, Wohlschlaeger J, Lang H *et al.* Activation of the ERK and AKT signalling pathway predicts poor prognosis in hepatocellular carcinoma and ERK activation in cancer tissue is associated with hepatitis C virus infection. *J Hepatol* 2008; **48**: 83–90.

Cancer Research

p38α Inhibits Liver Fibrogenesis and Consequent Hepatocarcinogenesis by Curtailing Accumulation of Reactive Oxygen Species

Toshiharu Sakurai, Masatoshi Kudo, Atsushi Umemura, et al.

Updated version	Access the most recent version of this article at: doi:10.1158/0008-5472.CAN-12-1602

Cited Articles	This article cites by 48 articles, 10 of which you can access for free at: http://cancerres.aacrjournals.org/content/73/1/215.full.html#ref-list-1
Citing articles	This article has been cited by 1 HighWire-hosted articles. Access the articles at: http://cancerres.aacrjournals.org/content/73/1/215.full.html#related-urls

E-mail alerts	Sign up to receive free email-alerts related to this article or journal.
Reprints and Subscriptions	To order reprints of this article or to subscribe to the journal, contact the AACR Publications Department at pubs@aacr.org.
Permissions	To request permission to re-use all or part of this article, contact the AACR Publications Department at permissions@aacr.org.

Molecular and Cellular Pathobiology

Cancer Research

p38α Inhibits Liver Fibrogenesis and Consequent Hepatocarcinogenesis by Curtailing Accumulation of Reactive Oxygen Species

Toshiharu Sakurai[1,2], Masatoshi Kudo[1], Atsushi Umemura[2], Guobin He[2], Ahmed M. Elsharkawy[2,4], Ekihiro Seki[3], and Michael Karin[2]

Abstract

Most hepatocellular carcinomas (HCC) develop in the context of severe liver fibrosis and cirrhosis caused by chronic liver inflammation, which also results in accumulation of reactive oxygen species (ROS). In this study, we examined whether the stress-activated protein kinase p38α (Mapk14) controls ROS metabolism and development of fibrosis and cancer in mice given thioacetamide to induce chronic liver injury. Liver-specific p38α ablation was found to enhance ROS accumulation, which appears to be exerted through the reduced expression of antioxidant protein HSP25 (Hspb1), a mouse homolog of HSP27. Its reexpression in p38α-deficient liver prevents ROS accumulation and thioacetamide-induced fibrosis. p38α deficiency increased expression of SOX2, a marker for cancer stem cells and the liver oncoproteins c-Jun (Jun) and Gankyrin (Psmd10) and led to enhanced thioacetamide-induced hepatocarcinogenesis. The upregulation of SOX2 and c-Jun was prevented by administration of the antioxidant butylated hydroxyanisole. Intriguingly, the risk of human HCC recurrence is positively correlated with ROS accumulation in liver. Thus, p38α and its target HSP25/HSP27 appear to play a conserved and critical hepatoprotective function by curtailing ROS accumulation in liver parenchymal cells engaged in oxidative metabolism of exogenous chemicals. Augmented oxidative stress of liver parenchymal cells may explain the close relationship between liver fibrosis and hepatocarcinogenesis. *Cancer Res; 73(1); 215–24. ©2012 AACR.*

Introduction

The liver plays an important role in oxidative metabolism and detoxification of endogenous and exogenous chemicals. The most common detoxification mechanism depends on cytochrome p450–mixed function oxidases (1). As a result, extensive and repetitive exposure to toxic chemicals can lead to accumulation of reactive oxygen species (ROS) in hepatocytes that are actively engaged in the detoxification of such chemicals. ROS accumulation can cause liver injury, which often progresses to liver fibrosis, cirrhosis, and cancer.

Hepatocellular carcinoma (HCC) is the most common form of liver cancer and the third leading cause of cancer deaths worldwide and is usually associated with a very poor prognosis (2). In addition to chronic exposure to toxic chemicals, chronic infections with hepatitis B virus (HBV) or hepatitis C virus (HCV) as well as hepatosteatosis are the major risk factors for both liver fibrosis and HCCs (3). In the case of HCV, a virus estimated to infect 4 to 5 million Americans (4), HCC develops only after one or more decades of chronic infection, and elevated risk of HCC progression is restricted largely to patients with cirrhosis or advanced fibrosis (5, 6). Although HCV-infected individuals with mild or nonhepatic fibrosis are unlikely to develop HCCs, once cirrhosis is established, HCC develops at a rate of 1% to 4% per year (6). Thus, the risk of hepatocarcinogenesis depends on background liver factors, of which fibrosis is a major one. Development and progression of liver fibrosis are associated with hepatocyte death and a subsequent inflammatory response (7), both of which involve ROS accumulation in injured hepatocytes (8). Hence, a better understanding of hepatoprotective mechanisms that prevent ROS accumulation and their impact on fibrogenesis and carcinogenesis is of great importance.

The chemical thioacetamide can induce liver cirrhosis and cancer of the bile ducts when given to rats over a period of several months (9). However, as described here, we found that

Authors' Affiliations: [1]Department of Gastroenterology and Hepatology, Faculty of Medicine, Kinki University, Ohnohigashi, Osaka-Sayama, Osaka, Japan; [2]Laboratory of Gene Regulation and Signal Transduction, Departments of Pharmacology and Pathology; [3]Department of Medicine, University of California, San Diego, School of Medicine, La Jolla, California; and [4]Liver Group, Institute of Cellular Medicine, Medical School, Newcastle University, Newcastle upon Tyne, United Kingdom

Corresponding Authors: Michael Karin, Laboratory of Gene Regulation and Signal Transduction, Departments of Pharmacology and Pathology, School of Medicine, University of California, San Diego, 9500 Gilman Drive MC 0723, La Jolla, CA 92093. Phone: 858-534-1361; Fax: 858-534-8158; E-mail: karinoffice@ucsd.edu; and Toshiharu Sakurai, Department of Gastroenterology and Hepatology, Faculty of Medicine, Kinki University, 377-2 Ohnohigashi, Osakasayama, Osaka, Japan. Phone: 8175-751-4302; Fax: 8175-751-4303; E-mail: sakurai@med.kindai.ac.jp

American Association for Cancer Research

— 441 —

mice given thioacetamide for 10 months develop HCCs rather than cholangiocellular carcinoma subsequent to appearance of severe liver fibrosis, thus providing a model that closely mimics the natural history of human HCV–related liver disease. In addition, the histology of the thioacetamide-exposed rat liver was reported to resemble human liver cirrhosis (10). Thus, the mouse thioacetamide model may be suitable for studying the relationship between ROS accumulation, liver fibrogenesis, and hepatocarcinogenesis and allows studies to be conducted that are of relevance to human HCV–related liver disease.

Mitogen- and stress-activated protein kinases (MAPK/ SAPK) play a pivotal role in the transduction of extracellular signals to the nucleus, thereby modulating numerous cellular responses, including cell survival, proliferation, differentiation, and metabolism (11, 12). One of the SAPKs, p38α, the major p38/MAPK isoform, is activated in response to inflammation and oxidative stress and, in turn, controls expression of cytokines, inflammatory mediators, survival genes, and antioxidants (13–16). As ubiquitous p38α ablation in all cells results in midgestational lethality, mainly due to placental insufficiency (17–20), we used a conditional $p38\alpha$ "floxed" ($p38\alpha^{F/F}$) strain (21) to generate $p38\alpha^{\Delta hep}$ mice, lacking p38α in liver parenchymal cells, to assess the role of this kinase in development of liver cancer (15). In the course of these studies, we found that p38α prevented the accumulation of ROS in liver parenchymal cells exposed to the hepatic carcinogen diethylnitrosamine. We now describe that p38α also prevents ROS accumulation, liver fibrogenesis, and subsequent hepatocarcinogenesis in mice exposed to thioacetamide. In both models, p38α prevents ROS accumulation by controlling the expression of HSP25, the mouse homolog of human HSP27. Restoration of HSP25 expression in the p38α-deficient liver prevents thioacetamide-induced ROS accumulation and fibrogenesis. We also show that the risk of HCC recurrence in post-hepatectomy patients is positively associated with ROS accumulation in the nontumor liver tissue.

Materials and Methods

Animals, tumor induction, and analysis

$p38\alpha^{F/F}$ mice (21) were crossed with Alb-Cre mice (Jackson Lab) to generate $p38\alpha^{\Delta hep}$ mice (15). All mice were maintained in the C57BL/6 background in filter-topped cages on autoclaved or nonautoclaved food at University of California, San Diego (La Jolla, CA) and Kinki University (Osaka, Japan), respectively. Mice were given 0.03% thioacetamide in drinking water. After 10 months on normal chow, mice were sacrificed and analyzed for presence of HCCs. Tumor-occupied areas were measured using ImageJ software.

Biochemical and immunochemical analyses

The c-jun-NH2 kinase (JNK) assays, real-time quantitative PCR (qPCR), immunoblotting, and immunohistochemistry were previously described (15). The primer sequences for TIMP-1, PDGF-b, SOX2 and Gankyrin were: forward primer 5′-CCAGAACCGCAGTGAAGAGT-3′, reverse primer 5′-AAGA-AGCTGCAGGCATTGAT-3′; and forward primer 5′-CCTCG-GCCTGTGACTAGAAG-3′, reverse primer 5′-AAGGCTCCTG-CACACTTGTT-3′; forward primer 5′-GAACGCCTTCATGGTA-

TGGT-3′, reverse primer 5′-TTGCTGATTCTCCGAGTTGTG-3′; respectively. Antibodies used were: anti-HSP27/25 and anti-α-fetoprotein (Santa Cruz Biotechnology); anti-actin (Sigma); anti-α-smooth muscle actin (α-SMA; Dako); anti-p38α, anti-MAPKAPK2, anti-phospho-MAPKAPK2, and anti-SOX2 (Cell Signaling); anti-PRMO1 (CD133, Abnova); anti-c-kit (R&D Systems); and anti-JNK1, (Pharmingen). Immunohistochemistry was conducted using ABC staining kit (Vector Laboratory) according to manufacturer's recommendations. Terminal deoxynucleotidyl transferase–mediated dUTP nick end labeling (TUNEL) staining was done on tissue sections using In Situ Apoptosis Detection Kit (Takara). To examine accumulation of superoxide anions or H_2O_2, freshly prepared frozen liver sections were incubated with 2 μmol/L dihydroethidine hydrochloride (Invitrogen) or 5 μmol/L 5-[and-6]-chloromethyl-2′,7′-dichlorodihydrofluorescein diacetate (CM-H_2DCFDA; Invitrogen), respectively for 30 minutes at 37°C, after which they were observed by fluorescent microscopy and quantified with Metamorph software. Protein oxidation was assessed by the OxyBlot Protein Oxidation Detection Kit (Millipore). Sirius Red staining was done to quantitate the amount of collagen present. To analyze the relative fibrotic area, the Sirius Red–positive areas were measured in 6 random fields (×100) on each slide and quantified using NIH imaging software. Myeloperoxidase (MPO) activity was measured using MPO Activity Assay Kit (Invitrogen). Livers were homogenized in myeloperoxidase buffer (0.5% hexadecyl trimethyl ammonium bromide, 10 mmol/L EDTA, 50 mmol/L Na_2HPO_4, pH 5.4). Hydroxyproline content was measured as described previously (22).

Adenoviral transduction

Adenovirus-expressing HSP25 was prepared as described previously (15). Adenovirus stocks were injected via the tail vein at 1×10^9 plaque-forming units (PFU) per mouse. Before infection, virus stocks were dialyzed against PBS containing 10% glycerol.

Patients and specimens

HCC tissues and noncancerous liver tissues were obtained from 43 patients, respectively, who had undergone curative hepatectomy for HCC at the Kinki University Hospital between 2004 and 2010. The specimens used were routinely processed, formalin-fixed, and paraffin-embedded. After hematoxylin and eosin (H&E) staining, all samples were diagnosed as HCC. Noncancerous tissue and HCC specimens were frozen and stocked at −80°C. The demographic profiles of the patients are summarized in the Supplementary Table. The study protocol conformed to the ethical guidelines of the 1975 Declaration of Helsinki and was approved by the Institutional Review Boards. Written informed consents were obtained from all patients for subsequent use of their resected tissues.

Statistical analysis

Data are presented as mean ± SEM. Differences were analyzed by Fisher exact test or Student t test. Recurrence-free survival curves were calculated by the Kaplan–Meier method and analyzed by the log-rank test. $P < 0.05$ was considered significant.

— 442 —

Results

Enhanced fibrogenesis in p38α[Δhep] mice

Hepatic stellate cells (HSC) which undergo a transition from a quiescent to an activated state after liver injury play an important part in the pathogenesis of liver fibrosis (23). HSC activation includes increased proliferation rate, a phenotypic transition to a myofibroblast-like α-SMA expression, and a dramatic increase in the synthesis of extracellular matrix proteins. After 8 weeks of thioacetamide treatment, we observed inflammation, HSC activation and formation of fibrotic septa as assessed histologically or by immunohistochemistry with a specific antibody against α-SMA (Fig. 1A). p38α[Δhep] mice exhibited more thioacetamide-induced liver damage

assessed by alanine aminotransferase (ALT) release and hepatocyte apoptosis measured by a TUNEL assay, relative to controls (Fig. 1A and B). Neutrophil infiltration was enhanced, based on measurement of myeloperoxidase activity (Fig. 1C). In addition, there were higher numbers of α-SMA–positive cells, higher levels of hydroxyproline, and larger fibrotic areas in p38α[Δhep] mice than in control mice (Fig. 1D–F). No significant difference in serum ALT levels or fibrotic areas was found between male and female p38α[Δhep] mice (data not shown).

We examined the consequences of p38α deletion in liver parenchymal cells on expression of fibrogenic markers. Loss of p38α significantly enhanced expression of the mRNAs for col1α1, TIMP1, TGF-β1, and PDGFb (Fig. 1G). No difference
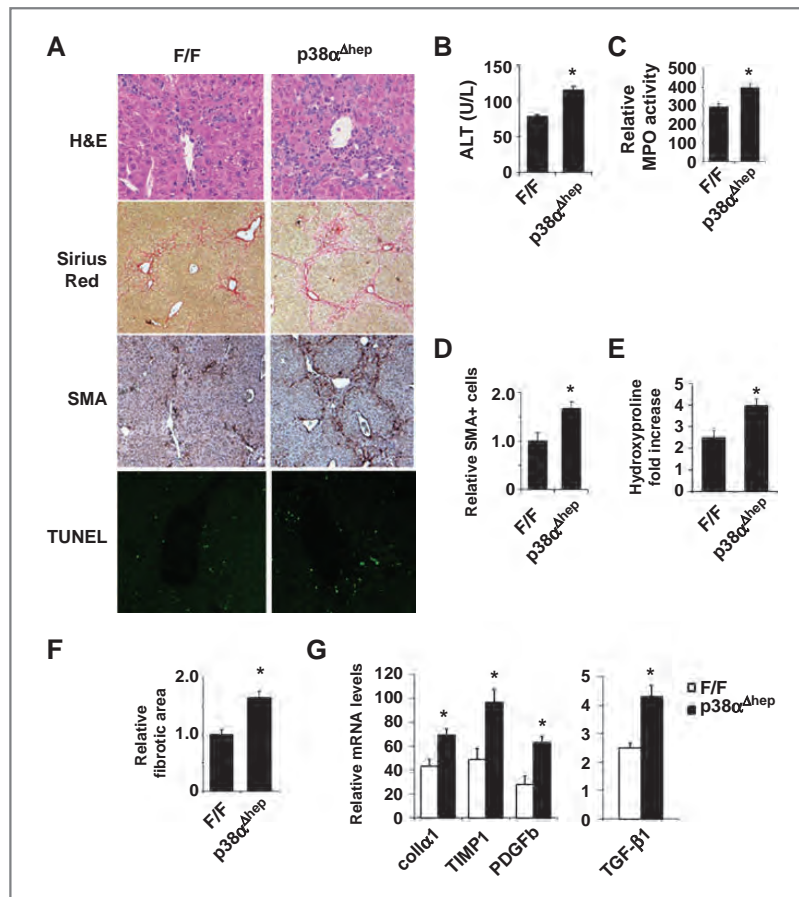
Figure 1. Enhanced fibrogenesis in p38α[Δhep] mice. A, histologic and immunohistologic analysis of livers from mice treated with thioacetamide for 8 weeks. Liver sections were examined using H&E and Sirius Red staining, immunohistochemistry with α-SMA–specific antibody, and TUNEL staining (original magnification, ×200). B, ALT levels in serum were determined after 8 weeks of thioacetamide treatment. Results are mean ± SEM ($n = 8$). *, $P < 0.05$ versus control (F/F) mice. C, extent of neutrophil infiltration was determined by myeloperoxidase assay. Myeloperoxidase activity in untreated liver was given an arbitrary value of 1.0. Results are mean ± SEM ($n = 8$). D–F, the surface area stained with Sirius Red or antibody against α-SMA was quantified. Hepatic hydroxyproline content was measured. Results are mean ± SEM ($n = 6$). G, mice were treated with thioacetamide for 8 weeks and liver RNA was extracted. Relative mRNA amounts of the indicated genes were determined by real-time qPCR and normalized to the amount of actin mRNA. The amount of each mRNA in untreated liver was given an arbitrary value of 1.0. Results are mean ± SEM ($n = 8$).

— 443 —

in the expression of these fibrogenic markers was found in uninjured livers taken from $p38\alpha^{F/F}$ and $p38\alpha^{\Delta hep}$ mice (data not shown).

Enhanced ROS accumulation in p38α$^{\Delta hep}$ mice accounts for increased liver injury and fibrogenesis

A causal link between oxidative stress and liver fibrosis was proposed (24). We assessed the accumulation of hepatocyte superoxides by staining freshly frozen liver sections with dihydroethidine, whose oxidation gives rise to the fluorescent derivative ethidine. More extensive fluorescence was seen in periportal areas (zone 1) after thioacetamide administration in $p38\alpha^{\Delta hep}$ mice than in control mice (Fig. 2A and B). Notably, the histologic location of thioacetamide-induced ROS accumulation differs from that of diethylnitrosamine-induced ROS, which are mainly detected in centrilobular (zone 3) hepatocytes (15, 25). This differential distribution of ROS-positive hepatocytes is likely to be due to a difference in the metabolism of the 2 compounds. Whereas diethylnitrosamine is metabolically activated by Cyp2E1, which is more abundant in zone 3 hepatocytes (26), thioacetamide can be converted to more toxic metabolites via a thioacetamide S-oxide intermediate by several enzymes including Cyp2B (27), whose spatial distribution in the liver is affected by exposure to different chemicals and growth factors (28). Increased H_2O_2 accumulation in livers of thioacetamide-treated $p38\alpha^{\Delta hep}$ mice was also detected

using the ROS indicator CM-H_2DCFDA (Fig. 2A). $p38\alpha^{\Delta hep}$ mice were found to have higher levels of oxidized protein than $p38\alpha^{F/F}$ mice (Fig. 2B).

To evaluate the contribution of oxidative stress to thioacetamide-induced liver damage and fibrosis, we placed a group of mice on chow diet supplemented with the antioxidant butylated hydroxyanisole (BHA). $p38\alpha^{\Delta hep}$ mice kept on this diet showed a significant reduction in thioacetamide-induced liver injury (Fig. 2C) and fibrosis (Fig. 2D). Thus, loss of p38α enhances thioacetamide-induced cell death and fibrogenesis through mechanisms that may depend on ROS accumulation.

The p38α-induced antioxidant gene HSP25 inhibits thioacetamide-induced fibrosis

As previously described for diethylnitrosamine-treated mice (15), HSP25 expression was also induced by thioacetamide administration, and the extent of induction was much lower in $p38\alpha^{\Delta hep}$ mice relative to $p38\alpha^{F/F}$ controls (Fig. 3A and B). HSP25 was reported to inhibit ROS accumulation (29, 30). Adenoviral transduction of HSP25 into $p38\alpha^{\Delta hep}$ liver (Supplementary Fig. S1) prevented thioacetamide-induced ROS accumulation, protein oxidation (Fig. 3C and D), liver damage (Fig. 3E), and fibrogenesis (Fig. 3F and G). These results provide further support for the notion that the enhanced accumulation of ROS in the p38α-deficient liver is responsible for the enhanced fibrogenic response of $p38\alpha^{\Delta hep}$ mice.
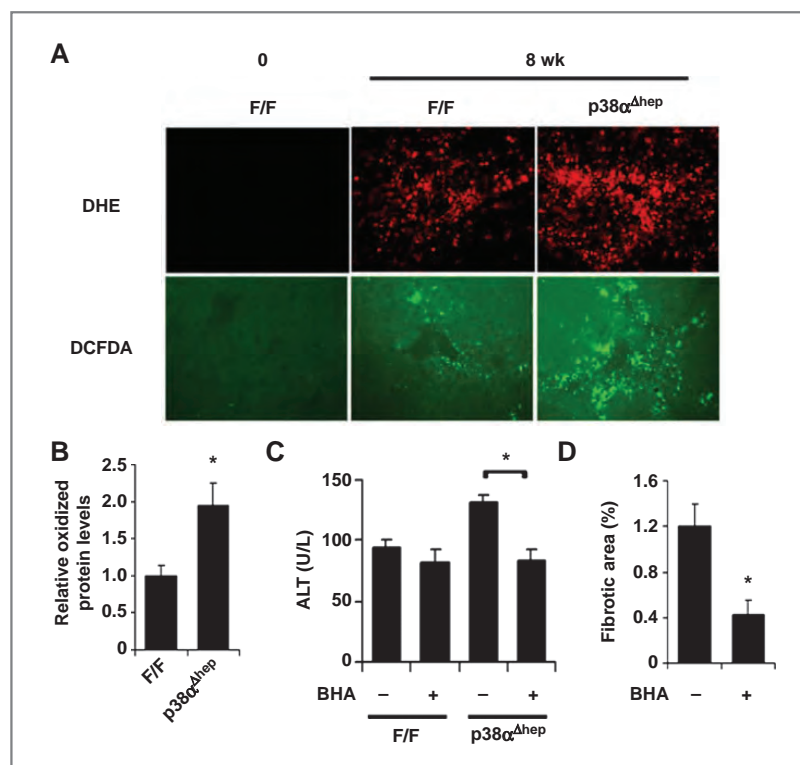
Figure 2. Enhanced ROS accumulation in $p38\alpha^{\Delta hep}$ mice accounts for increased liver injury and fibrogenesis. A, frozen liver sections prepared after 8 weeks of thioacetamide treatment were incubated with 2 μmol/L dihydroethidine hydrochloride (DHE) or 5 μmol/L 5-[and-6]-chloromethyl-2′,7′-dichlorodihydrofluorescein diacetate (DCFDA) for 30 minutes at 37°C. Cells staining positively for the oxidized dyes were identified by fluorescent microscopy (original magnification, ×100). B, protein oxidation was assessed by immunoblotting (OxyBlot) and quantified using NIH image analysis software. Results are mean ± SEM ($n = 6$). *, $P < 0.05$ versus control (F/F) mice. C and D, mice were fed either BHA-supplemented (0.7%) or regular chow. After 4 weeks of thioacetamide treatment, serum ALT was measured in $p38\alpha^{F/F}$ (F/F) and $p38\alpha^{\Delta hep}$ mice (C) and the surface area stained with Sirius Red was quantified in $p38\alpha^{\Delta hep}$ mice (D). Results are mean ± SEM ($n = 6$). *, $P < 0.05$.
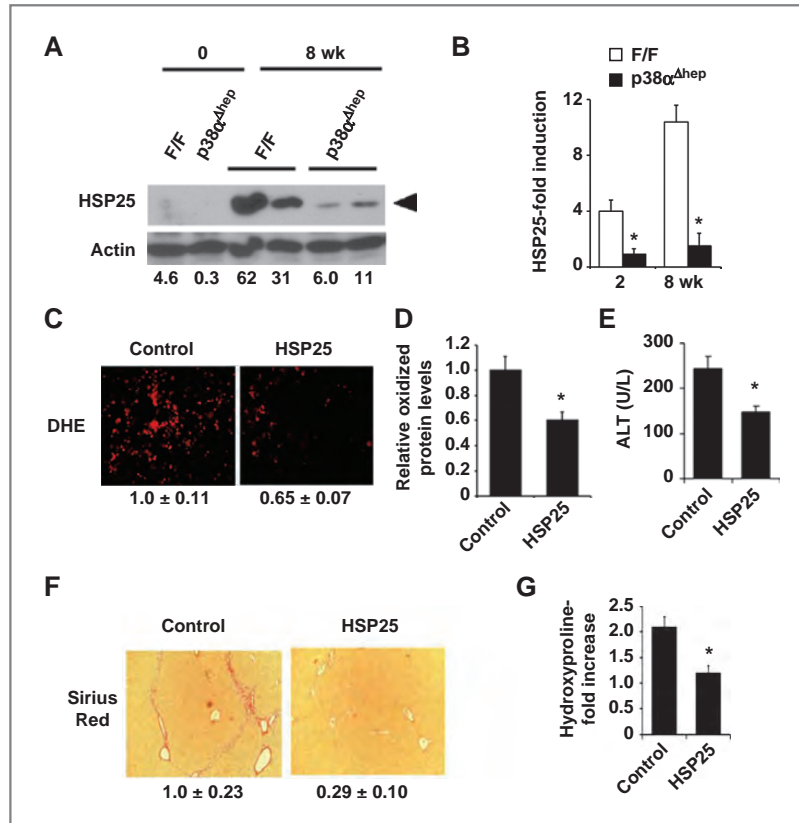
— 444 —

Figure 3. The p38α-induced antioxidant gene *HSP25* inhibits thioacetamide-induced fibrosis. A, mice were treated with thioacetamide for 8 weeks and their livers isolated and homogenized. Homogenates were gel-separated and immunoblotted with the indicated antibodies. The numbers below the panels indicate relative HSP25 expression levels. B, mice were treated as above, and total liver RNA was extracted at the indicated times. Amounts of mRNA relative to those in untreated $p38\alpha^{F/F}$ livers were determined by real-time qPCR. Results are mean ± SEM ($n = 6$). *, $P < 0.05$ versus control (F/F) mice. C–G, $p38\alpha^{\Delta hep}$ mice were infected with an adenovirus expressing HSP25 or a control adenovirus 20 hours before thioacetamide treatment. C, frozen liver sections prepared after 4 weeks of thioacetamide treatment were incubated with 2 μmol/L DHE for 30 minutes at 37°C and photographed. D, protein oxidation was assessed by immunoblotting (OxyBlot) and quantified using NIH image analysis software. E, ALT levels in serum were determined after 4 weeks of thioacetamide treatment. F, sections of livers prepared after 4 weeks of thioacetamide treatment were examined by Sirius Red staining. The numbers below the panels indicate relative fibrotic areas. G, hepatic hydroxyproline content was measured. Results are mean ± SEM ($n = 6$). *, $P < 0.05$.

Decreased expression of MAPKAP kinase-2 and increased expression of SOX2, c-Jun, and Gankyrin in thioacetamide-treated p38α^Δhep mice

Previous studies have described a critical role for c-Jun and JNKs in mediating HCC development (31, 32). In the thioaceta-mide model, p38α-deficient livers exhibited elevated c-Jun expression and increased JNK activity (Fig. 4A and B). Whereas cytokine-driven compensatory proliferation was suggested to promote diethylnitrosamine-induced hepatocarcinogenesis (15, 25, 33), there was no significant increase in interleukin (IL)-6 and TNF-α and IL-1β expression in thioacetamide-treated $p38\alpha^{\Delta hep}$ mice relative to $p38\alpha^{F/F}$ controls (Fig. 4B). An important downstream target for p38 is MAPKAP kinase-2 (MAPKAPK2) and MAPKAPK2-deficient cells are more sensitive to DNA damage-induced cell death (34). As shown in Fig. 4C, MAPKAPK2 expression and phosphorylation is downregulated in p38α-

deficient livers. Pluripotency-associated transcription factors such as SOX2 and Nanog are known as regulators of cellular identity in embryonic stem cells. More recently, SOX2 has been shown to participate in reprogramming of adult somatic cells to a pluripotent stem cell state and has been implicated in tumori-genesis in various organs (35). Loss of p38α significantly enhanced the expression of SOX2 mRNA and protein in thioa-cetamide-treated mice (Fig. 4D and F). Gankyrin, a liver onco-protein, was reported to mediate dedifferentiation and facilitate the tumorigenicity of rat hepatocytes (36). $p38\alpha^{\Delta hep}$ mice exhib-ited a significant increase in Gankyrin expression after thioace-tamide administration (Fig. 4E and F). No difference in the expression of Gankyrin was found in uninjured livers taken from $p38\alpha^{F/F}$ and $p38\alpha^{\Delta hep}$ mice (data not shown). To evaluate the contribution of oxidative stress to the increase in expression of these genes, we placed a group of mice on chow diet

— 445 —
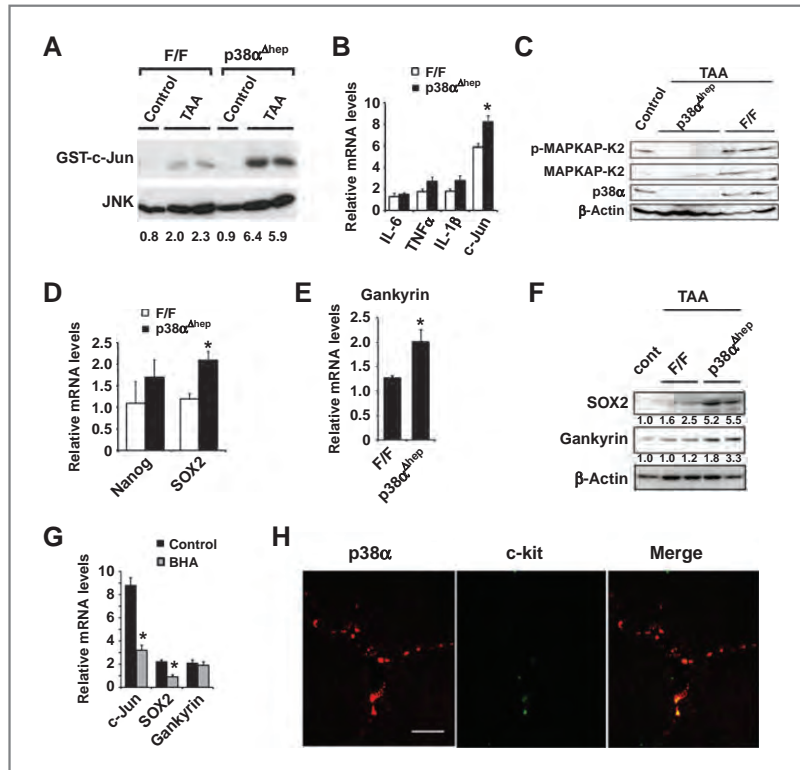
Figure 4. Decreased expression of MAPKAP kinase-2 and increased expression of SOX2, c-Jun, and Gankyrin in thioacetamide-treated p38α[Δhep] mice. Mice of the indicated genotypes were given thioacetamide for 8 weeks and their livers isolated and homogenized. A, JNK activity was determined by immune complex kinase assay. Protein recovery was determined by immunoblotting with JNK1 antibody. The numbers below the panels indicate relative JNK activities determined by densitometry. B, D, and E, liver RNA was extracted. Relative amounts of cytokine, Nanog, SOX2, and Gankyrin mRNAs were determined by real-time qPCR and normalized to the amount of actin mRNA. The amount of each mRNA in untreated liver was given an arbitrary value of 1.0. Results are mean ± SEM ($n = 6$). C and F, homogenates of liver tissues were gel-separated and immunoblotted with the indicated antibodies. Representative data are shown. The numbers below the panels indicate relative expression levels determined by densitometry. G, p38α[Δhep] mice were fed either BHA-containing (0.7%) or regular chow and treated with thioacetamide for 8 weeks. Relative amounts of mRNAs were determined by real-time qPCR and normalized to the amount of actin mRNA. The amount of each mRNA in untreated liver was given an arbitrary value of 1.0. Results are mean ± SEM ($n = 6$). H, immunohistochemistry was done on frozen liver sections of thioacetamide-treated p38α[Δhep] mice. Cells stained with indicated antibodies were identified by confocal microscopy. Scale bar, 50 μm.

supplemented with the antioxidant BHA. p38α[Δhep] mice kept on this diet showed a significant reduction in SOX2 and c-Jun expression but not in Gankyrin expression (Fig. 4G). Immunohistochemical analysis revealed that putative hematopoietic stem cells, c-kit–positive cells, were recruited to thioacetamide-treated livers (Fig. 4H) but not in nontreated livers (data not shown). We confirmed that c-kit–positive cells expressed p38α in p38α[Δhep] mice (Fig. 4H). Between p38α[F/F] and p38α[Δhep] livers, there was no significant difference in the number of c-kit–positive cells (data not shown), indicating that hepatic p38α deficiency does not increase hematopoietic stem cell recruitment.

Enhanced hepatocarcinogenesis in p38α[Δhep] mice

p38α[F/F] and p38α[Δhep] mice were given thioacetamide in their drinking water for 10 months. When sacrificed, all p38α[Δhep] mice given thioacetamide developed typical liver cirrhosis and 50% of p38α[Δhep] mice had ascites, a common clinical finding

indicative of portal hypertension. The liver surface was irregular, closely resembling human cirrhotic liver (Fig. 5A). All of the p38α[F/F] and p38α[Δhep] mice given thioacetamide for 10 months developed well-differentiated HCCs (Fig. 5B), whereas only a few and small number of cholangiocellular carcinomas were found. Many tumors were positive for α-fetoprotein (AFP) expression, a tumor marker specific for HCCs (Fig. 5C). Tumor sizes and areas were considerably larger in p38α[Δhep] mice relative to similarly treated p38α[F/F] controls (Fig. 5D). In contrast to mice, thioacetamide-treated rats develop cholangiocellular carcinoma (9). This may be because CD133-positive stem cells are induced by thioacetamide in mice but not in rats (Fig. 5E).

Association between risk of HCC recurrence and protein oxidation in human liver

Forty-two patients with HCCs were recruited in this study. Clinicopathologic profiles of the patients and their HCCs are
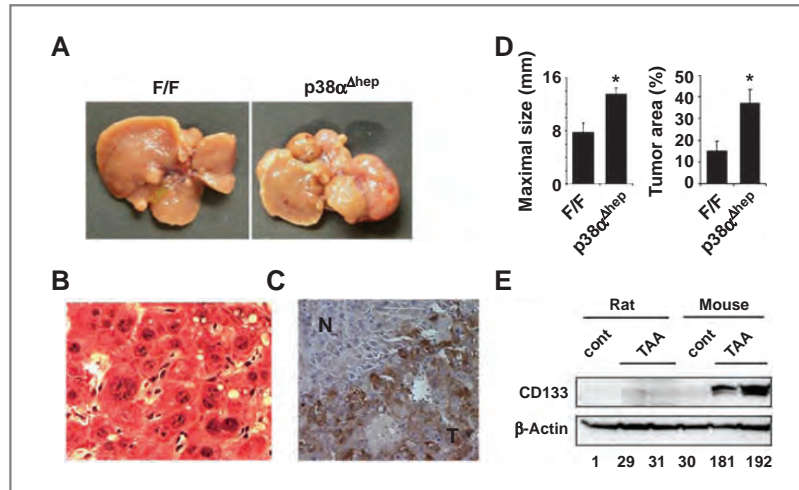
Figure 5. Enhanced hepatocarcinogenesis in $p38\alpha^{\Delta hep}$ mice. A, livers of $p38\alpha^{\Delta hep}$ and $p38\alpha^{F/F}$ mice after 10 months of thioacetamide treatment. B and C, sections of livers were examined using H&E staining (B) and by immunohistochemistry with AFP-specific antibody (C). Original magnification, ×200. N, noncancerous liver tissues; T, tumors. Distinction between tumor and noncancerous liver tissue was made by H&E staining. D, maximal tumor sizes (diameters) and percentages of liver area occupied by tumors in $p38\alpha^{F/F}$ (F/F, $n = 8$) and $p38\alpha^{\Delta hep}$ ($n = 8$) mice. *, $P < 0.05$ versus control mice (F/F). E, Sprague-Dawley rats and $p38\alpha^{F/F}$ control mice were given thioacetamide (0.03%) for 5 weeks and their livers isolated. Homogenates of rat and mouse liver tissues were gel-separated and immunoblotted with the indicated antibodies. The numbers below the panels indicate relative CD133 expression levels.

shown in the Supplementary Table. Intrahepatic HCC development after hepatectomy is caused by *de novo* HCC development and/or metastasis from the resected HCCs. The risk of the former depends on background liver factors such as liver fibrosis, whereas the risk of the latter mainly depends on the characteristics of the resected HCCs (37). In mouse models, HSP25-mediated inhibition of ROS accumulation is involved in control of liver fibrogenesis and can subsequently attenuate *de novo* HCC development. We examined whether this hypothesis is applicable to humans, focusing on noncancerous liver tissues rather than cancers to assess the potential for *de novo* HCC development or rapid progression of lesions that were undetectable or pre-neoplastic at the time of resection. In patients exhibiting HCC recurrence after hepatectomy, protein oxidation levels in the nontumor tissues, but not in tumors, were

significantly higher than in those without HCC recurrence (Fig. 6A). In addition, patients with low protein oxidation in noncancerous liver had a prolonged recurrence-free survival (Fig. 6B). In conclusion, elevated ROS accumulation in the liver is associated with increased risk of human HCC development or recurrence.

Discussion

Oxidative stress is thought to play a major role in the pathogenesis of hepatic fibrosis (8) and cancer development (38, 39), exerting many effects, including alteration of gene expression (40), enhanced cell death and proliferation as well as genomic instability (39). However, the exact impact of oxidative stress and antioxidant responses on hepatic fibrosis and subsequent HCC development need to be better understood. We previously found that the p38α/MAPK pathway prevents

Figure 6. Associations between the risk of HCC recurrence and protein oxidation in human liver. A, protein oxidation was assessed in tumors and nontumorous human liver tissues by immunoblotting (OxyBlot) and quantified using NIH image analysis software. *, $P < 0.05$ versus patients without HCC recurrence. B, recurrence-free survival versus protein oxidation. The Kaplan–Meier method was used to determine recurrence-free survival, and the log-rank test was used to compare recurrence-free survival between patients grouped according to amount of protein oxidation in liver. mo, month.

— 447 —
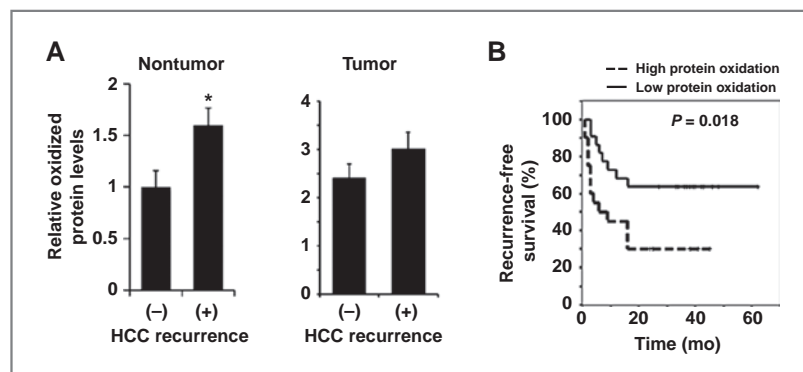
ROS accumulation in mice exposed to the non-fibrogenic hepatic carcinogen diethylnitrosamine (15). Here, we describe that p38α activity is also important for suppression of ROS accumulation upon thioacetamide administration, which leads to induction of fibrosis, cirrhosis, and HCCs. In the absence of the p38α target HSP25, the thioacetamide-exposed $p38\alpha^{\Delta hep}$ liver shows elevated ROS accumulation that correlates with augmented liver damage in these mice. Increased susceptibility to liver damage in $p38\alpha^{\Delta hep}$ mice is reversed by administration of the small-molecule antioxidant BHA or restoration of HSP25 expression. These results support the hypothesis that increased ROS accumulation may be the main cause of hepatocyte death in p38α-deficient mice regardless of the hepatotoxic chemical to which they were exposed. Expression levels of MAPKAPK2 and phospho-MAPKAPK2 were decreased in the p38α-depleted livers. Given the protective role of MAPKAPK2 in DNA damage-induced cell death (34), the downregulation of MAPKAPK2 expression and phosphorylation that takes place in the absence of p38α are likely to contribute, at least in part, to increased liver damage in $p38\alpha^{\Delta hep}$ mice. Hepatocyte death activates an inflammatory response, which promotes HSC activation via a paracrine mechanism (24), which we and others have suggested to involve IL-1α release (15, 41). This inflammatory response results in excessive synthesis of extracellular matrix proteins and fibrosis development (23). Correspondingly, BHA administration or restoration of HSP25 expression reverses enhanced thioacetamide-induced fibrogenesis caused by the p38α deficiency. A strong correlation between liver fibrogenesis and hepatocarcinogenesis has been reported in patients infected with HCV (6), and HCV infection has been shown to cause ROS accumulation and oxidative stress (42). We find that enhanced protein oxidation in the noncancerous portion of human liver is associated with a high risk of HCC recurrence after hepatectomy. These data support an important role of ROS accumulation within liver parenchymal cells in liver fibrogenesis and subsequent hepatocarcinogenesis.

HSP25/HSP27 has antioxidant properties (29, 30). Mice given thioacetamide showed an inverse correlation between HSP25 expression and ROS accumulation in the liver. In addition, we found that elevated ROS accumulation correlated with the presence of HCC recurrence after hepatectomy. However, we did not observe a statistically significant relationship between HSP27 expression and ROS accumulation in human livers (data not shown). While elevated HSP27 expression reduces ROS accumulation, HSP27 expression itself is upregulated following oxidative stress (43). Most probably, our findings may reflect complex mechanisms regulating ROS accumulation via several molecules in the human liver. The exact relationship between HSP27 and oxidative stress in human parenchymal cells remains to be elucidated. In the mouse liver, however, it is quite clear that p38α negatively regulates ROS accumulation through induction of HSP25, which maintains parenchymal cell viability and suppresses liver fibrogenesis. Enhanced cell death caused by the absence of p38α results in increased inflammation and hepatic fibrogenesis, which eventually augments HCC development, as seen before in diethylnitrosamine-treated mice (15, 32). Thus, the antitumorigenic activity of hepatocyte p38α is not model specific and may also apply to human liver.

Stem cell function is central for the maintenance of normal tissue homeostasis. SOX2 forms the core of the self-renewal transcription network in embryonic stem cells. Selective downregulation of SOX2 induces embryonic stem cell differentiation and exits from the pluripotent stem cell state. In contrast, combinatorial overexpression of SOX2, Nanog, and other transcription factors was shown to reprogram several types of adult somatic cells to a pluripotent stem cell–like state (44–46). In these experiments, cells were reprogrammed fully or only partially (47), possibly because of heterogeneous exposure to reprogramming factors. It is tempting to speculate that acquisition or overexpression of SOX2 can promote tumorigenesis by processes that resemble partial reprogramming (35, 44, 47). In our study, we showed that p38α deletion increased expression of SOX2 through enhanced ROS accumulation. Hepatocyte dedifferentiation has been reviewed as a key cellular event during hepatocarcinogenesis (48). Gankyrin, also named 26S proteasome non-ATPase regulatory subunit 10, is a critical oncoprotein overexpressed in human HCCs. A close association of Gankyrin expression with hepatocyte dedifferentiation was observed, and differentiation induced by Gankyrin interference reduced the population of cancer stem cells in hepatoma cell lines (36), suggesting that Gankyrin promotes HCC development by driving dedifferentiation of hepatocytes and facilitating HCC stem/progenitor cell generation. We found that the p38α deficiency enhances the induction of Gankyrin expression in livers of thioacetamide-treated mice. Recently, JNK activation was reported to be involved in stem cell expansion in human HCCs (49). JNK activity was significantly enhanced in p38α-deficient liver. The inactivation of p38α also leads to an immature and hyperproliferative lung epithelium that is highly sensitized to tumorigenesis (50). It has been shown that the Albumin-Cre driver does not only lead to deletion of genes in hepatocytes but also deletes genes in hepatic precursor cells. These data suggest an important role of p38α in regulating hepatic stem/precursor cell behavior.

In conclusion, p38α plays a critical role in liver fibrogenesis and hepatocarcinogenesis through the control of HSP27 expression and ROS accumulation in the mouse thioacetamide model, which may be suitable for studying the pathogenesis of HCV-related HCC development. Importantly, the risk of human HCC recurrence after hepatectomy is positively correlated with protein oxidation in liver. Deletion of p38α upregulates expression of SOX2 and Gankyrin, which may be involved in cancer stem cell maintenance.

Disclosure of Potential Conflicts of Interest

No potential conflicts of interest were disclosed.

Authors' Contributions

Conception and design: T. Sakurai, M. Kudo, M. Karin
Development of methodology: T. Sakurai, G. He, A.M. Elsharkawy, M. Karin
Acquisition of data (provided animals, acquired and managed patients, provided facilities, etc.): T. Sakurai, M. Kudo, G. He
Analysis and interpretation of data (e.g., statistical analysis, biostatistics, computational analysis): T. Sakurai, M. Kudo, G. He, M. Karin
Writing, review, and/or revision of the manuscript: T. Sakurai, M. Kudo, A. M. Elsharkawy, M. Karin

References

1. Rooney PH, Telfer C, McFadyen MC, Melvin WT, Murray GI. The role of cytochrome P450 in cytotoxic bioactivation: future therapeutic directions. Curr Cancer Drug Targets 2004;4:257–65.
2. Thorgeirsson SS, Grisham JW. Molecular pathogenesis of human hepatocellular carcinoma. Nat Genet 2002;31:339–46.
3. Bosch FX, Ribes J, Diaz M, Cleries R. Primary liver cancer: worldwide incidence and trends. Gastroenterology 2004;127:S5–16.
4. Ginick G. Hepatitis C: controversies, strategies and challenges. Eur J Surg 1998;65–70.
5. Ikeda K, Saitoh S, Suzuki Y, Kobayashi M, Tsubota A, Koida I, et al. Disease progression and hepatocellular carcinogenesis in patients with chronic viral hepatitis: a prospective observation of 2215 patients. J Hepatol 1998;28:930–8.
6. Hoshida Y, Ikeda K, Kobayashi M, Suzuki Y, Tsubota A, Saitoh S, et al. Chronic liver disease in the extremely elderly of 80 years or more: clinical characteristics, prognosis and patient survival analysis. J Hepatol 1999;31:860–6.
7. Ghany MG, Kleiner DE, Alter H, Doo E, Khokar F, Promrat K, et al. Progression of fibrosis in chronic hepatitis C. Gastroenterology 2003;124:97–104.
8. Parola M, Robino G. Oxidative stress-related molecules and liver fibrosis. J Hepatol 2001;35:297–306.
9. Gupta DN. Production of cancer of the bile ducts with thioacetamide. Nature 1955;175:257.
10. Zimmermann T, Müller A, Machnik G, Franke H, Schubert H, Dargel R. Biochemical and morphological studies on production and regression of experimental liver cirrhosis induced by thioacetamide in Uje: WIST rats. Z Versuchstierkd 1987;30:165–80.
11. Chang L, Karin M. Mammalian MAP kinase signalling cascades. Nature 2001;410:37–40.
12. Dhillon AS, Hagan S, Rath O, Kolch W. MAP kinase signalling pathways in cancer. Oncogene 2007;26:3279–90.
13. Cuenda A, Rousseau S. p38 MAP-kinases pathway regulation, function and role in human diseases. Biochim Biophys Acta 2007;1773:1358–75.
14. Park JM, Greten FR, Wong A, Westrick RJ, Arthur JS, Otsu K, et al. Signaling pathways and genes that inhibit pathogen-induced macrophage apoptosis–CREB and NF-kappaB as key regulators. Immunity 2005;23:319–29.
15. Sakurai T, He G, Matsuzawa A, Yu GY, Maeda S, Hardiman G, et al. Hepatocyte necrosis induced by oxidative stress and IL-1α release mediate carcinogen-induced compensatory proliferation and liver tumorigenesis. Cancer Cell 2008;14:156–65.
16. Wagner EF, Nebreda AR. Signal integration by JNK and p38 MAPK pathways in cancer development. Nat Rev Cancer 2009;9:537–49.
17. Tamura K, Sudo T, Senftleben U, Dadak AM, Johnson R, Karin M. Requirement for p38alpha in erythropoietin expression: a role for stress kinases in erythropoiesis. Cell 2000;102:221–31.
18. Adams RH, Porras A, Alonso G, Jones M, Vintersten K, Panelli S, et al. Essential role of p38alpha MAP kinase in placental but not embryonic cardiovascular development. Mol Cell 2000;6:109–16.
19. Mudgett JS, Ding J, Guh-Siesel L, Chartrain NA, Yang L, Gopal S, et al. Essential role for p38alpha mitogen-activated protein kinase in placental angiogenesis. Proc Natl Acad Sci U S A 2000;97:10454–9.
20. Allen M, Svensson L, Roach M, Hambor J, McNeish J, Gabel CA. Deficiency of the stress kinase p38alpha results in embryonic lethality: characterization of the kinase dependence of stress responses of enzyme-deficient embryonic stem cells. J Exp Med 2000;191:859–70.
21. Nishida K, Yamaguchi O, Hirotani S, Hikoso S, Higuchi Y, Watanabe T, et al. p38alpha mitogen-activated protein kinase plays a critical role in cardiomyocyte survival but not in cardiac hypertrophic growth in response to pressure overload. Mol Cell Biol 2004;24:10611–20.
22. Seki E, de Minicis S, Inokuchi S, Taura K, Miyai K, van Rooijen N, et al. CCR2 promotes hepatic fibrosis in mice. Hepatology 2009;50:185–97.
23. Bataller R, Brenner DA. Liver fibrosis. J Clin Invest 2005;115:209–18.
24. Casini A, Ceni E, Salzano R, Biondi P, Parola M, Galli A, et al. Neutrophil-derived superoxide anion induces lipid peroxidation and stimulates collagen synthesis in human hepatic stellate cells: role of nitric oxide. Hepatology 1997;25:361–7.
25. Maeda S, Kamata H, Luo JL, Leffert H, Karin M. IKKbeta couples hepatocyte death to cytokine-driven compensatory proliferation that promotes chemical hepatocarcinogenesis. Cell 2005;121:977–90.
26. Yang CS, Yoo JS, Ishizaki H, Hong JY. Cytochrome P450IIE1: roles in nitrosamine metabolism and mechanisms of regulation. Drug Metab Rev 1990;22:147–59.
27. Jeong TC, Gu HK, Park JI, Yun HI, Kim HC, Ha CS, et al. Pretreatment of male BALB/c mice with beta-ionone potentiates thioacetamide-induced hepatotoxicity. Toxicol Lett 1999;105:39–46.
28. Allen JW, Khetani SR, Bhatia SN. *In vitro* zonation and toxicity in a hepatocyte bioreactor. Toxicol Sci 2005;84:110–9.
29. Escobedo J, Pucci AM, Koh TJ. HSP25 protects skeletal muscle cells against oxidative stress. Free Radic Biol Med 2004;37:1455–62.
30. Garrido C, Brunet M, Didelot C, Zermati Y, Schmitt E, Kroemer G. Heat shock proteins 27 and 70: anti-apoptotic proteins with tumorigenic properties. Cell Cycle 2006;5:2592–01.
31. Sakurai T, Maeda S, Chang L, Karin M. Loss of hepatic NF-kappa B activity enhances chemical hepatocarcinogenesis through sustained c-Jun N-terminal kinase 1 activation. Proc Natl Acad Sci U S A 2006;103:10544–51.
32. Hui L, Bakiri L, Mairhorfer A, Schweifer N, Haslinger C, Kenner L, et al. p38alpha suppresses normal and cancer cell proliferation by antagonizing the JNK-c-Jun pathway. Nat Genet 2007;39:741–9.
33. Naugler WE, Sakurai T, Kim S, Maeda S, Kim K, Elsharkawy AM, et al. Gender disparity in liver cancer due to sex differences in MyD88-dependent IL-6 production. Science 2007;317:121–4.
34. Jackson RM, Garcia-Rojas R. Kinase activity, heat shock protein 27 phosphorylation, and lung epithelial cell glutathione. Exp Lung Res 2008;34:245–62.
35. Lengerke C, Fehm T, Kurth R, Neubauer H, Scheble V, Müller F, et al. Expression of the embryonic stem cell marker SOX2 in early-stage breast carcinoma. BMC Cancer 2011;11:42.
36. Sun W, Ding J, Wu K, Ning BF, Wen W, Sun HY, et al. Gankyrin-mediated dedifferentiation facilitates the tumorigenicity of rat hepatocytes and hepatoma cells. Hepatology 2011;54:1259–72.
37. Imamura H, Matsuyama Y, Tanaka E, Ohkubo T, Hasegawa K, Miyagawa S, et al. Risk factors contributing to early and late phase intrahepatic recurrence of hepatocellular carcinoma after hepatectomy. J Hepatol 2003;38:200–7.

— 449 —

38. Ames BN. Dietary carcinogens and anticarcinogens. Oxygen radicals and degenerative diseases. Science 1983;221:1256–64.

39. Woo RA, Poon RY. Activated oncogenes promote and cooperate with chromosomal instability for neoplastic transformation. Genes Dev 2004;18:1317–30.

40. Allen RG, Tresini M. Oxidative stress and gene regulation. Free Radic Biol Med 2000;28:463–99.

41. Chen CJ, Kono H, Golenbock D, Reed G, Akira S, Rock KL. Identification of a key pathway required for the sterile inflammatory response triggered by dying cells. Nat Med 2007;13:851–6.

42. Kato J, Kobune M, Nakamura T, Kuroiwa G, Takada K, Takimoto R, et al. Normalization of elevated hepatic 8-hydroxy-2′-deoxyguanosine levels in chronic hepatitis C patients by phlebotomy and low iron diet. Cancer Res 2001;61:8697–702.

43. Fulop T, Franceschi C, Hirokawa K, Pawelec G. Handbook on immunosenescence: basic understanding and clinical applications. Sweden: Springer; 2009. p. 519.

44. Park IH, Zhao R, West JA, Yabuuchi A, Huo H, Ince TA, et al. Reprogramming of human somatic cells to pluripotency with defined factors. Nature 2008;451:141–6.

45. Takahashi K, Tanabe K, Ohnuki M, Narita M, Ichisaka T, Tomoda K, et al. Induction of pluripotent stem cells from adult human fibroblasts by defined factors. Cell 2007;131:861–72.

46. Yu J, Vodyanik MA, Smuga-Otto K, Antosiewicz-Bourget J, Frane JL, Tian S, et al. Induced pluripotent stem cell lines derived from human somatic cells. Science 2007;318:1917–20.

47. Chan EM, Ratanasirintrawoot S, Park IH, Manos PD, Loh YH, Huo H, et al. Live cell imaging distinguishes bona fide human iPS cells from partially reprogrammed cells. Nat Biotechnol 2009;27:1033–7.

48. Lazarevich NL, Cheremnova OA, Varga EV, Ovchinnikov DA, Kudrjavtseva EI, Morozova OV, et al. Progression of HCC in mice is associated with a downregulation in the expression of hepatocyte nuclear factors. Hepatology 2004;39:1038–47.

49. Hagiwara S, Kudo M, Nagai T, Inoue T, Ueshima K, Nishida N, et al. Activation of JNK and high expression level of CD133 predict a poor response to sorafenib in hepatocellular carcinoma. Br J Cancer 2012;106:1997–2003.

50. Ventura JJ, Tenbaum S, Perdiguero E, Huth M, Guerra C, Barbacid M, et al. p38alpha MAP kinase is essential in lung stem and progenitor cell proliferation and differentiation. Nat Genet 2007;39:750–8.

— 450 —

Targeted Therapy for Liver Cancer: Updated Review in 2012

Masatoshi Kudo*

Department of Gastroenterology and Hepatology, Kinki University School of Medicine, Osaka 589-8511, Japan

Abstract: In May 2007, sorafenib (Nexavar®) was approved for "unresectable hepatocellular carcinoma (HCC)", and was the first molecular targeted agent for use in HCC. To date, sorafenib is the only molecular-targeted agent, whose survival benefit has been demonstrated in two global phase III randomized controlled trials, and has now been approved worldwide. Phase III clinical trials of other molecular targeted agents comparing them with sorafenib as first-line treatment agents are now ongoing. Phase III clinical trials of several targeted agents comparing them with placebo as second-line treatment agents for patients who failed or was intolerable to sorafenib are also ongoing. In addition, combination of sorafenib with standard treatment such as resection, ablation, transarterial chemoembolization, and hepatic arterial infusion chemotherapy are ongoing. This review outlines the clinical utility of sorafenib in the treatment algorithm of HCC. Furthermore, it also reviews the current status of clinical trials of new agents or combination therapy with sorafenib and standard treatment. Finally, further prospect of the paradigm shift of the HCC treatment is also discussed.

Keywords: Brivanib, complete remission, everolimus, hepatocellular carcinoma, molecular targeted agent, sorafenib.

INTRODUCTION

Sorafenib is a multi-kinase inhibitor of tumor growth and angiogenesis, and exhibits a strong inhibitory effect on C- and B-Raf serine/threonine kinases, vascular endothelial growth factor receptor (VEGFR) and platelet-derived growth factor receptor (PDGFR), tyrosine kinases, and FLT-3 and c-kit [1]. To date, sorafenib is the only molecular-targeted agent approved for the treatment of HCC with Child-Pugh A liver function based on the results of two large-scale clinical trials, i.e., the SHARP (Sorafenib HCC assessment Randomized Protocol) study [2] and the Asia-Pacific study [3]. As a result, sorafenib is recommended as the first line option in patients who cannot benefit from resection, transplantation, ablation or transarterial chemoembolization, and still have preserved liver function as recommended by the American Association for the Study of Liver Diseases (AASLD) guideline [4], Asian-Pacific Association of the Study of the Liver (APASL) guideline [5] and the Japan Society of Hepatology (JSH) guideline [6] for HCC management (Fig. **1**). This article focuses on the types of approaches currently under investigation or recently approved agents.

EXPERIENCE OF SORAFENIB USE AT OUR INSTITUTE

Since the approval of sorafenib on May 20, 2009, we have treated approximately 150 patients with sorafenib during 20 months, but few have discontinued therapy due to adverse effects or patient refusal to continue. Of these 113 patients were analyzed and two cases achieved complete response (CR) [7]. These two CR patients, in whom pulmonary, adrenal metastases and intrahepatic lesions all

disappeared, survived with free of recurrence for more than 3 years and 2 years, respectively at the time of writing (September, 2012), *i.e.*, they are still alive at the present time. In other patients group who apparently achieved stable disease (SD), the tumor marker levels reached a plateau after sorafenib administration, when their levels were rising rapidly before sorafenib administration. Even if hepatic lesions do not show a clear tendency to undergo necrosis or regression on CT images, three tumor markers, namely alpha-fetoprotein (AFP), protein induced by vitamin K absence or antagonist (PIVKA-II) and AFP-L3 fraction, are widely considered to serve as surrogate markers of tumor response to sorafenib. In fact, there is very little data on serum tumor markers, except for AFP, outside Japan. Only Japanese researchers have demonstrated the value of changes in these markers and the antitumor efficacy of sorafenib [7]. Interestingly, it is demonstrated that the levels of PIVKA-II or des-gamma-carboxyprothrombin (DCP) tend to be increased by inducing hypoxia [8, 9].

Of 113 patients, 85.8% was Child-Pugh A stage and 53.1 % of patients were HCV-related HCC. A total of 56% of patients were over 70 years old. Median survival time (MST) was 12.6 months and median treatment duration was 5.3 months [10]. Only 10% of the 113 patients showed progressive disease (PD) by RECIST. However, since the speed with which the patient develops PD may slow down due to tumor growth inhibition, it is very difficult to determine when to discontinue treatment because of resistance to sorafenib. Important issues for future studies include: 1) to identify biomarkers that can predict therapeutic responses, including CR or partial response (PR), in patient groups; 2) to evaluate the role of tumor markers in the determination of therapeutic responses; 3) to establish response evaluation criteria that can determine the therapeutic responses to molecular-targeted agents; and 4) to develop effective second-line therapies after sorafenib failure [11, 12].

*Address correspondence to this author at the Department of Gastroenterology and Hepatology, Kinki University School of Medicine, 377-2Ohno-Higashi, Osaka-Sayama, Osaka 589-8511, Japan;
Tel: +81-72-366-0221, ext.3149; Fax: +81-72-367-2880;
E-mail: m-kudo@med.kindai.ac.jp
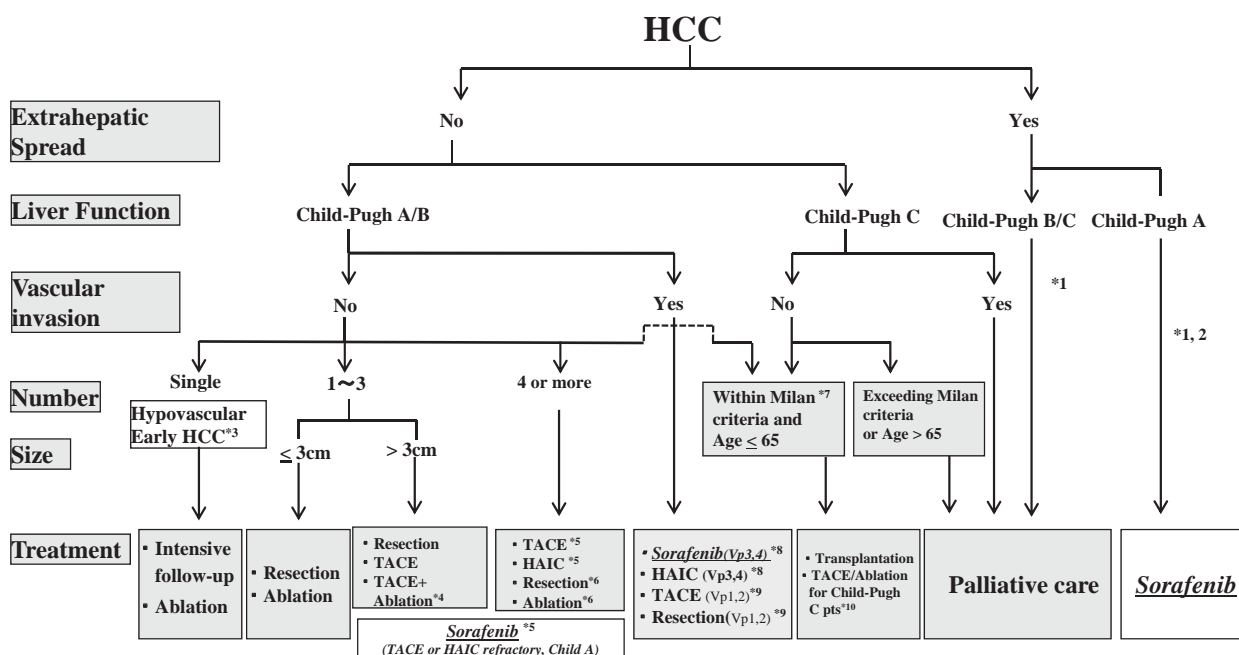
Fig. (1). Consensus-based treatment algorithm for HCC proposed by Japan Society of Hepatology revised in 2010 (cited and modified from ref. #6 with permission). *1: Treatment should be performed as if extrahepatic spread is negative, when extrahepatic spread is not considered as a prognostic factor in Child-Pugh class A/B patients. *2: Sorafenib is the first choice of treatment in this setting as a standard of care. *3:Intensive follow-up observation is recommended for hypovascular nodules by the Japanese Evidence-Based Clinical Practice Guidelines. However, local ablation therapy is frequently performed in the following cases: 1) when the nodule is diagnosed pathologically as early HCC, 2) when the nodules show decreased uptake on Gd-EOB-MRI, or 3) when the nodules show decreased portal flow by CTAP, since these nodules frequently progress to advanced HCC. *4: Even for HCC nodules exceeding 3 cm in diameter, TACE in combination with ablation is frequently performed when resection is not indicated. *5: Transcatheter arterial chemoembolization (TACE) is the first choice of treatment in this setting. Hepatic arterial infusion chemotherapy (HAIC) using an implanted port is also recommended for TACE-refractory patients. The regimen for this treatmentis usually low-dose FP (5FU+CDDP) or intra-arterial 5FU infusion combined with systemic interferon therapy. Sorafenib is also recommended for TACE or HAIC-refractory patients with Child-Pugh class A liver function. *6: Resection is sometimes performed when more than 4 nodules are detected. Ablation is sometimes performed in combination with TACE. *7: Milan criteria: Tumor size $\leq$3 cm and tumor number $\leq$ 3, or solitary tumor $\leq$5 cm. Even when liver function is good (Child-Pugh A/B), transplantation is sometimes considered for frequently recurring HCC patients. *8:Sorafenib and HAIC are recommended for HCC patients with major portal invasion such as Vp3 (portal invasion in the 1st portal branch) or Vp4 (portal invasion in the main portal branch). *9:Resection and TACE are frequently performed when portal invasion is minor, such as Vp1 (portal invasion in the 3rd or more peripheral portal branch) or Vp2 (portal invasion in the 2nd portal branch). *10: Local ablation therapy or subsegmental TACE is performed even for Child-Pugh C patients when transplantation is not indicated when there is no hepatic encephalopathy, no uncontrollable ascites, and a low bilirubin level (< 3.0 mg/dl). However, it is regarded as an experimental treatment because there is no evidence of a survival benefit in Child-Pugh C patients. A prospective study is necessary to clarify this issue.

According to the consensus based treatment algorithm by the JSH [13] updated in 2010 (Fig. **1**) [6], sorafenib is indicated for the treatment of patients with Child-Pugh A HCC with extrahepatic spread, vascular invasion or refractoriness to transarterial chemoembolization (TACE) or arterial infusion chemotherapy.The following situation should be regarded as TACE failure or refractory as per JSH guidelines:

1. Intrahepatic lesion

i   Two or more 2 consecutive incomplete deposition (<50%) of lipiodol is seen by response evaluation CT within the treated tumors at the 4 weeks after adequately performed TACE

ii   Two or more 2 consecutive appearance of new lesion (recurrence) is seen in the liver by response evaluation CT at the 4 weeks after adequately performed TACE

2. Appearance of vascular invasion

3. Appearance of extrahepatic spread

Continuous elevation of tumor markers even though right after TACE

4. Tumor marker

Continuous elevation of tumor markers even though right after TACE
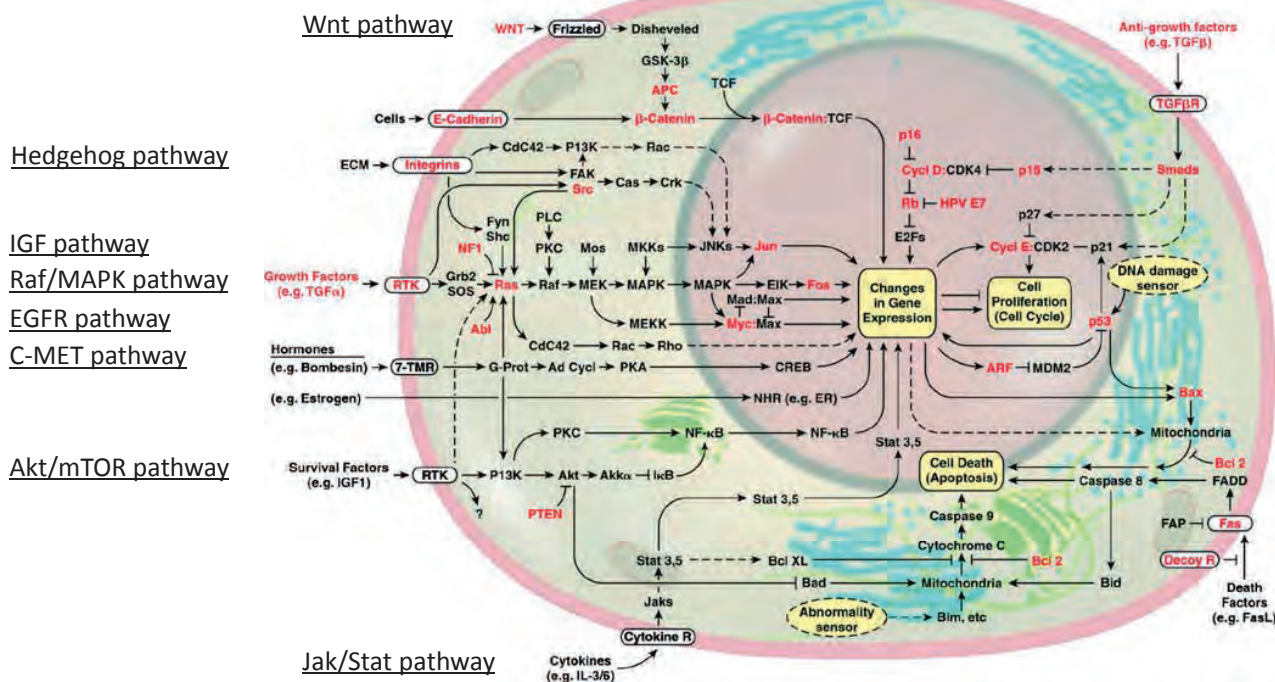
Fig. (2). Signal transduction in solid cancer cells including HCC. Some of the genes known to be functionally altered are highlighted in red. These signaling pathways including growth factor pathway, Wnt pathway, Hedgehog pathway, Akt/mTOR pathway, and Jak/Stat pathway can be a molecular target for treatment of HCC(cited and modified from ref. #14with permission).

In this setting, next treatment modality such as sorafenib should be considered.

NEW TARGETED AGENTS IN HCC

mTORinhibittor

The phosphatidylinositol 3-kinase (PI3K)/Akt/ mammalian target of rapamycine (mTOR) pathway also plays an important role in cell growth, survival regulation, metabolism and anti-apoptosis (Fig. **2**) [14]. Inhibiting mTOR with molecules, such as RAD001, generates additive effects that accompany upstream and downstream target inhibition; alternatively, upstream receptor inhibition is compensated for by inhibiting the downstream pathway, even if some resistance develops against receptor inhibition regardless of initial or acquired resistance. Therefore, RAD001 is a potential targeted agents for HCC (Table **1**, Fig. **3**) [15].

Besides the finding that mTOR plays a key role in cell biology, it was also demonstrated that mTOR and S6K are overexpressed in 15-41% of HCCs, and mTOR inhibitors have antitumor effects in various HCC cell lines and animal models [16-19]. Activation of mTOR is correlated with the development of HCC and recurrence after the excision of early HCC. Regulating this specific intracellular pathway (Ras-Raf pathway) with RAD001 is potentially more effective in suppressing sorafenib-resistant tumors.

A study of 528 HCC samples showed that the expression of pAkt, phosphatase and tensin homolog deleted on chromosome 10 (PTEN), p27 and S6 ribosomal protein (pS6) was a poor prognostic factor for survival [20]. A tissue microarray analysis of HCC samples revealed that the loss of PTEN and overexpression of pAkt and p-mTOR were correlated with tumor grade, intrahepatic metastasis, vascular invasion, tumor node metastasis (TNM) stage, Ki-67 labeling index and matrix metalloproteinase (MMP)-2 and -9 upregulation, Meanwhile, PTEN mRNA expression in the cancerous tissue was downregulated, compared with that in the non-cancerous tissue. The levels of PTEN, MMP-2, and MMP-9 mRNA expression were correlated with tumor stage and metastasis, and the levels of PTEN and MMP-9 mRNA expression were inversely correlated [21]. In an extensive analysis of 314 HCC samples in terms of mutation analysis, DNA copy number changes, mRNA levels and immuno-staining, Villanueva *et al.* [22] found that activation of the insulin growth factor (IGF) pathway, upregulation of epidermal growth factor (EGF), dysregulation of PTEN, and aberrant mTOR signaling were present in half of the samples, and that inhibiting mTORactivity with everolimus was effective in improved survival and suppression of recurrence.

The PI3K inhibitor RG7321 and the Akt inhibitor perifosine target the PI3K/Akt/mTOR pathway and are in early stages of clinical development, while the mTOR inhibitors everolimus (RAD001), sirolimus (Rapamune) and temsirolimus (CCI-779) are at more advancedstages of development. Everolimusis used to treat sorafenib-intolerant patients or for patients showing disease progression after

Table 1.   **Molecular targeted agents for HCC: targets and development status (as of september, 2012).**

Agents	Targets (Angiogenesis)			Targets (Proliferation)			TRAIL-R2	Positioning	Development Status
	VEGFR	PDGFR	FGFR	EGFR	Raf	mTOR	DR5		
Sorafenib*	●	●			●			*1ˢᵗ line*	*Approved*
E7080	●	●	●					1ˢᵗ / 2ⁿᵈ line	PII Ongoing
Tigatuzumab (CS1008)							●	1ˢᵗ line (Sorafenib combination)	PI/II Ongoing
Linifanib (ABT-869)	●	●						1ˢᵗ line	Terminated
Brivanib	●		●					1ˢᵗ line,	Terminated
								2ⁿᵈ line,	Terminated
								TACE adjuvant	Terminated
TSU-68	●	●						TACE combination	PIII Ongoing
Ramucirumab	●							2ⁿᵈ line	PIII Ongoing
Everolimus (RAD001)						●		2ⁿᵈ line	PIII Ongoing
Axitinib	●	●						2ⁿᵈ line	PIII Ongoing
Dovitinib (TKI-258)	●	●	●					1st line	PII Ongoing
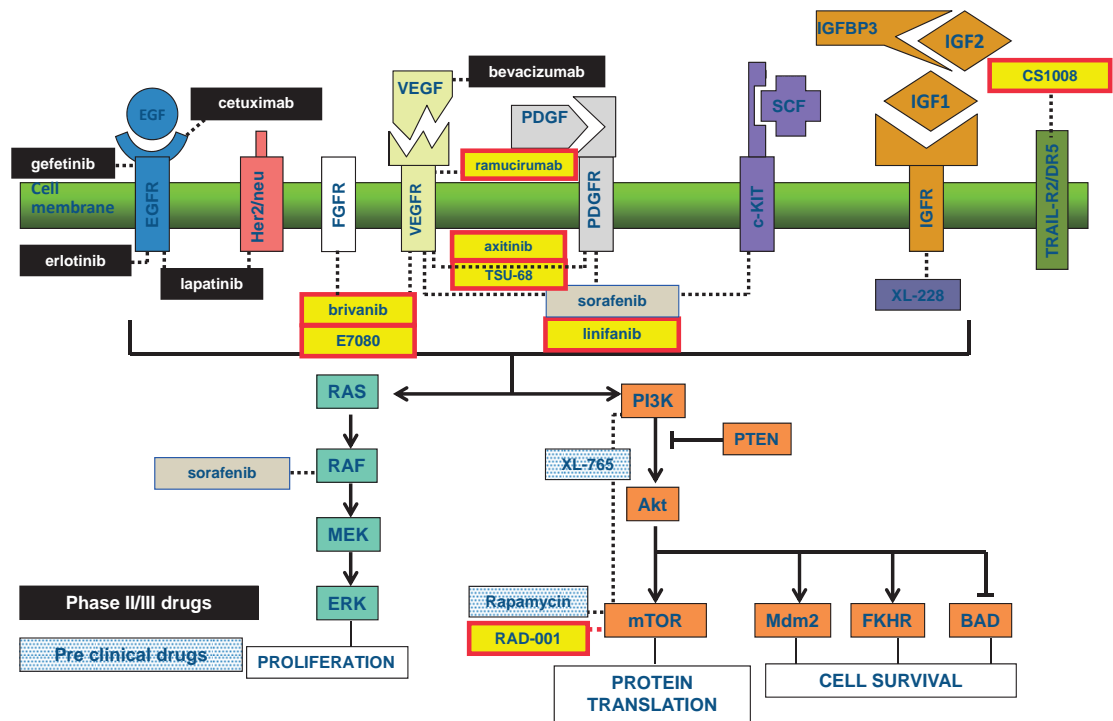
Fig. (3). Molecular targets in HCC and targeted agents under development. Monoclonal antibodies (VEGF: bevacizumab, EGFR: cetuxinab), tyrosine kinase inhibitors (VEGFR: sorafenib, brivanib, linifanib, axitinib, TSU-68; FGFR: E7080, brivanib), EGFR: erotinib, lapatinib), serine/threonine kinase inhibitors (Raf: sorafenib, mTOR: rapamycin and everolimus) and agonistic ligand of TRAIL-R2/DR5 (CS1008)(cited and modified from ref. #15with permission).

sorafenib administration. A phase III study to compare everolimus and a placebo (EVOLVE-1: Advanced Hepatocellular Carcinoma after Disease Progression or Intolerance to Sorafenib EverOlimus cancer Evaluation) and a phase I/randomized phase II study (sorafenib+everolimusvs. sorafenib alone) to test the efficacy and tolerance of sorafenibin combination with everolimusare underway. Since mTOR inhibitors exhibit cytostatic andantiangiogenic effects, they are expected to be effective in combination with other angiogenesis inhibitors such as bevacizumab, and may be appropriate for administration after TACE. Furthermore, since the mTOR pathway is stimulated by factors such as epidermal growth factor receptor (EGFR), PDGFR and transforming growth factor-α (TGFα), and is closely related to other signaling pathways including the Ras/Raf/MEK/ERK pathway, they are likely to show promising efficacy when used in combination with other growth factor inhibitors [23].

Brivanib

Angiogenesis is an important event not only for HCC but also for cancer growth and metastasis, and occurs due to complex alterations involving promoting factors such as VEGF, angiopoietinand fibroblast growth factor (FGF), and inhibitory factors including thrombospondin (TSP) and angiostatin, as well as the surrounding tissue. The VEGF family consists of VEGF-A, -B, -C, -D, and -E, and placental growth factor (PIGF).The VEGFR family comprises VEGFR-1 (flt-1), VEGFR-2 (flk-1/KDR) and VEGFR-3 (flt-4). VEGF-A binds to VEGFR-1 and -2 and is involved in angiogenesis and the maintenance of mature blood vessels, while VEGF-C and -D mainly bind to VEGFR-3, and are involved in lymphangiogenesis [24, 25]. VEGF isoforms such as $VEGF_{121}$and $VEGF_{165}$ have been identified, and isoform subtypes also exist, such as EGF_{166}b. Thus, it is clear that these growth factors do not exhibit angiogenesis-promoting effects alone, and they have attracted attention as new therapeutic targets [26].

HCC typically exhibits active angiogenesis. During the progression from early to well-, and to moderately-differentiated HCC, angiogenesis increases and cancer cells acquire the ability to invade vessels and metastasize. Scientific and clinical studies have revealed that, during the progression from hepatitis to cirrhosis, angiogenesis and disruption of the vascular architecture are linked to the progression of HCC, and contribute to increased hepatic vascular resistance and portal hypertension, and decreased hepatocyte perfusion [27]. In addition, a meta-analysis has demonstrated that VEGF expression is a prognostic factor in HCC [28].

Brivanib is a kinase inhibitor that selectively inhibits VEGFR-1, -2 and -3, and FGFR-1, -2 and -3. Recent studies suggest that tumor progression following treatment with antiangiogenic agents that target the VEGF signaling pathway alone may result from either evasive or intrinsic resistance [29]. Furthermore, there is strong evidence to support the hypothesis that evasive resistance to anti-VEGF blockade is associated with reactivation of tumor angiogenesis by alternative signaling pathways, one such

mechanism of resistance being activation of the FGF signaling pathway [30]. Basic FGF (FGF2) is a potent angiogenic factor. Indeed, expression of FGF2 enhances growth, invasion, and angiogenesis of many tumor types [31, 32]. Moreover, recent evidence has shown that FGF is overexpressed and activated in HCC and that high FGF2 levels may predict for a poor clinical outcome among patients with HCC [32].

Considering the proposed importance of FGF signaling in HCC angiogenesis, it is clear that novel antiangiogenic agents that combine inhibition of FGF receptor signaling with inhibition of VEGFR signaling might provide a potential mechanism to overcome anti-VEGF resistance in HCC. With this in mind, it is worthwhile to consider the potential future impact of brivanib on the treatment of advanced HCC. Brivanib, a small-molecule tyrosine kinase inhibitor, is the first oral selective dual inhibitor of FGF and VEGF signaling. In multiple preclinical models of human xenograft tumors, including patient-derived HCC xenografts, brivanib has shown potent antitumor activity and no overt toxicity when dosed orally [33, 34]. Furthermore, brivanib has demonstrated promising antitumor activity and acceptable tolerability in a phase 2, open-label study in patients with unresectable locally advanced or metastatic HCC [35]. Crucially, within this trial, brivanib showed activity both as first-line therapy (overall survival: 10 months) or as second-line therapy in patients who had failed prior antiangiogenic treatment, primarily with sorafenib (overall survival: 9.5 months). Of note, the incidence of all-grade hand-foot syndrome was only 8% in this study.

As for brivanib, an international global phase III clinical trial to compare brivanib and sorafenib head-to-head and to seek approval for first-line therapy for advanced HCC has been started, but this trial was terminated because it did not meet its primary endpoint. Since brivanib targets FGF and VEGF, and is associated with relatively mild adverse effects, a second-line study of brivanib in sorafenib-ineffective and -intolerant patients and a trial to evaluate the use of brivanib in combination with TACE are underway. However, second line study was also terminated because it did not meet its primary endpoint.

The results have been reported for a phase II study of brivanibin 55 patients (cohort A) who had not received systemic therapy for curatively unresectable HCC and 46 patients (cohort B) previously treated with angiogenesis inhibitors such as sorafenibor thalidomide [35]. The median TTP and OS were 2.8 and 10 months, respectively, in cohort A versus 1.4 and 9.8 months, respectively, in cohort B. Adverse events included fatigue (51.5%), diarrhea (41.6%), hypertension (42.6%), anorexia (41.6%), and nausea/vomiting (40.6%/30.7%) in total. Thus, these results demonstrated the efficacy of brivanib as a second-line treatment. The results of three phase III clinical trials, BRISK-PS (sorafenib failure or sorafenib-intolerant patients;brivanib + best supportive care (BSC) vs. placebo + BSC), BRISK-FL (advanced HCC;brivanib *vs*. sorafenib) and BRISK-TA (patients with unresectable HCC, brivanib vs. placebo as post-TACE adjuvant therapy) are awaited (Table **2**), but 2 of 3 trials were terminated as described above.

Table 2.　Ongoing clinical trials (PIII).

- First line
    - Comparison study between sorafenib and single agent (Head to head):
    TKI-258
    - Combination with sorafenib and another agent:
    DXR, Erlotinib (SEARCH), Everolimus, CS-1008, etc.
- Second line
    - Sorafenib failure: Everolimus (RAD001),
    Ramucirumab, Axitinib,S-1, etc.
- Combination with standard therapy
    - Adjuvant setting after surgery or RFA：*STORM*
    - Combination with TACE：*SPACE, ECOG1208, TACTICS,*
    ECOG1208, SORAMIC, SIRveNIB
    - Combination with HAIC*: SILIUS*

TACTICS: Phase II study: TranscatheterArterialChemoembolization Therapy In Combination with Sorafenib (ClinicalTrials.gov ID: NCT01217034), SILIUS: Randomized Controlled Trial Comparing Efficacy of Sorafenib versus SorafenibIn combination with Low dose cisplatin/fluorouracil hepatic arterial InfUSion chemotherapy in Patients with Advanced Hepatocellular Carcinoma And Exploratory Study of Biomarker Predicting Its Efficacy (ClinicalTrials.gov ID: NCT01214343), HAIC: hepatic arterial infusion chemotherapy.

Axitinib

Axitinib, a substituted indazole derivative, is an oral, potent, and selective inhibitor of VEGFR 1, 2, and 3. The molecular formula is $C_{22}H_{18}N_4OS$ with molecular weight of 386.47.

Retrospective analyses of five AG-013736 Phase 2 studies across multiple tumor types (RCC, melanoma, NSCLC, and thyroid cancer) demonstrated that patients who developed at least one in-clinic measurement of dBP>90 mmHg at any point during treatment had significantly better clinical outcomes for OS (30.1 vs 10.2 months; hazard ratio [HR]=0.546;P<0.01.

In the sorafenib-refractory RCC study (A4061023), most patients had the single-agent axitinib dose titrated to between 6-10 mg BID after tolerating the initial starting dose of 5 mg BID.

Except for an increase in hand-foot syndrome and slight increase in the incidence of hypertension, it appears that the patients dose titrated with axitinib to between 6-10 mg BID dose do not experience increased toxicities if they have previously tolerated an axitinib starting dose of 5 mg BID.

The effect of hepatic impairment on single-dose axitinib plasma pharmacokinetics was evaluated in a study (A4061036) that included subjects with mild hepatic impairment (Child-Pugh Class A; n=8), moderate hepatic impairment (Child-Pugh Class B; n=8), and healthy volunteers with normal hepatic function：(n=8).

Mild hepatic impairment did not alter axitinib plasma exposures ($AUC_{0-\infty}$ and Cmax) compared to normal hepatic function. However, there was a ~2-fold increase in axitinib $AUC_{0-\infty}$ and a 1.3-fold increase in axitinibCmax in subjects

with moderate hepatic impairment compared to subjects with normal hepatic function.

Phase II global clinical trials of axitinib for HCC patients who failed or intolerable to sorafenib are now ongoing.

E7080

Angiogenesis, the formation of new blood vessels from a pre-existing vascular network, is essential for growth and metastasis of tumors. The process begins with the local degeneration of the basal membranes that surround capillaries; then as endothelial cells infiltrate into the surrounding framework, angiogenesis in initiated. Migration of endothelial cells is accompanied by proliferation and formation of a 3-dimensional structure, and new blood vessels are then formed. VEGF, acidic fibroblast growth factor (aFGF), basic fibroblast growth factor (bFGF), hepatocyte growth factor (HGF), interleukin-8 (IL-8), and PDGF, etc. have been reported to promote angiogenesis.

Among these angiogenic factors, VEGF is thought to be important for both physiological and pathological angiogenesis, and enhanced expression of VEGF is reported to correlate with very poor prognosis in many cancers [36, 37]. VEGF, the most potent and cell-selective angiogenic factor, promotes growth of endothelial cells and tube formation mainly by affecting endothelial cells. VEGF exerts its activity *via* fms-like tyrosine kinase 1 (Flt-1) and kinase insert domain receptor (KDR), 2 types of receptors on the cell membrane. Between these 2 receptors, KDR appears to be the more important since signals derived from KDR are reported to be involved in the major processes of growth and survival of endothelial cells, tube formation, and microvascular permeability. KDR is dimerized by stimulation with ligand, tyrosine phosphorylation is intracellularly induced, and signals for promoting cell division, migration, and survival are generated.

E7080 inhibits phosphorlation of growth factor receptors such as the VEGF receptor, KDR, Flt-1, FGFR1, and PDGFRβ-receptors that are important for angiogenesis [38, 39]. FGF and PDGF are potent promoters of tumor cell proliferation. With this action, E7080 is expected to exert its potent inhibition on tumor proliferation led by anti-angiogenic effect with the inhibition of VEGF in addition to proliferation of tumor cells. In cell assays, E7080 inhibited VEGF-driven KDR phosphorylation and proliferation of human umbilical vein endothelial cells (HUVEC) in a concentration-dependent manner, with IC50 values of 0.25 and 3.4 nmol/L, respectively. Furthermore, E7080 inhibited VEGF-driven HUVEC tube formation with an IC_{50} value of 2.1 nmol/L in a sandwich tube formation (sTF) model. A significant inhibition of tumor proliferation was observed at 3 mg/kg or above doses when E7080 was orally administered at doses of 1, 3, 10, 30, and 100 mg/kg to subcutaneously transplanted mice. The above results suggest the possibility that E7080 could be useful as a novel anti-cancer drug that is based on an inhibitory effect on angiogenesis (Table **1**, Fig. **3**) [15].

The evidence-based Clinical Guideline for HCC [40] and criteria drafted by the Barcelona Clinic Liver Cancer Group

[41] stipulate that HCC be treated with hepatectomy, percutaneous therapy (local therapy; ethanol injection therapy, RFA, *etc*.), and transcatheter arterial embolization, depending on the number of tumors, size, and invasion into the vascular system. According to these guidelines and criteria, no radical therapy can be applied to advanced HCC, thus limiting available therapies for the treatment of advanced HCC [42, 43].

In addition, chronic hepatic diseases with reduced hepatic function underlie advanced HCC. Because reduced metabolism and excretion accompany reduced hepatic function, it is of concern that anticancer agents with cytotoxicity may affect background hepatic diseases and exacerbate adverse drug reactions. Therefore, administration methods such as arterial infusion chemotherapy tend to be utilized in advanced disease even though they may add to the hepatic burden or offer patients only limited efficacy [43].

HCC newly forms arterial vessels in the process of progression and shows high expression of VEGF [44, 45]. An angiogenesis inhibitor, therefore, which selectively inhibits VEGF receptors, could be a therapeutic agent that selectively treats HCC with little effect on background hepatic disease.

While E7080 is expected to induce tumor necrosis and suppression of progression by inhibiting angiogenesis and blocking blood flow into tumor foci in HCC with a high expression of VEGF, as an added benefit (compared with conventional anticancer agents), E7080 is expected to have low toxicity in patients with HCC who have chronic hepatic disease. Because it selectively affects blood vessels, E7080 should be less likely to induce resistance after long-term treatment since endothelial cells are unlikely to become resistant.

As with other VEGF inhibitors, hypertension and proteinuria have been observed as dose-limiting toxicities (DLTs) of E7080 and were treated with antihypertensive agents or dose reduction or withdrawal of E7080 [46-48]. Thrombocytopenia and increases in aspartate transaminase (AST) and alanine transaminase (ALT) have been reported as DLTs at dose higher than the maximum tolerated dose (MTD) in the Phase I study (bid 2 weeks-on/1 week-off in Japan) but were improved by suspended administration and dose reduction. Currently, the multicenter phase III study in treating advanced HCC is ongoing in Japan.

CS1008

CS1008 is an agonistic agent to death receptor (DR) 5 or TNF-related apoptosis inducing ligand (TRAIL). *In vitro* nonclinical studies have shown that CS-1008 exhibits anti-tumor activity in DR5 positive tumor cells treated with CS-1008 and cross-linking with anti-human IgG antibody. CS-1008 was shown to induce apoptosis in DR5 positive tumor cells resulting in cell death. This was shown *in vitro* by treating colorectal adenocarcinoma COLO 205 cells with CS-1008 and cross-linking with anti-human IgG antibody.

Since the liver is an organ known to express DR5, a nonclinical study was conducted to evaluate the safety of CS-1008 in comparison with that of TNF-related apoptosis inducing ligand (TRAIL) against primary human hepatocytes. In all experiments, CS-1008 was used under cross-linked conditions, with anti-human IgG antibody.

Primary human hepatocytes were treated with cross-lined CS-1008 or TRAIL, at concentrations from 1 to 1000 ng/mL (Lowry basis). After culturing human primary hepatocytes for 6 hours, cell viability was measured by ATPLite^{TM}-M assay kit. In 2 out of 3 lots of primary human hepatocytes used, TRAIL induced cell death in excess of 50% by cell count, and the IC_{50} values were 10.4 ng/mL and 9.9 ng/mL, respectively. On the other hand, IC50 values of cross-linked CS-1008 were both >1000 ng/mL, although CS-1008 demonstrated intense cytotoxic activity against COLO 205 cells under the same experimental conditions. Thus, the cytotoxicity of CS-1008 against primary human hepatocytes was considerably less than that of TRAIL (Table 1, Fig. **3**) [15].

The phase III study of CS-1008 in combination with sorafenib are now being conducted as a multinational global study as a first line setting. The results are eagerly awaited, but was terminated because it did not meet its primary endpoint.

Other Agents

Global phase III trial of linifanib (ABT-869), which strongly inhibits VEGFR and PDGFR, was also terminated in 2012.

In a Japanese phase I/II trial of TSU-68, an oral molecular inhibitor of VEGFR, PDGFR and FGFR, to test its safety and efficacy in 35 HCC patients, the response rate was 5.6% (CR, PR, SD, PD and NE in 1, 2, 15, 16 and 1 patients, respectively), and the disease control rate was 51.4%. The global phase III trial of TACE in combination with TSU-68 has just started on January 2011.

In addition, several phase I/II trialsare being conducted to assess kinase inhibitors such as cediranib (AZD2171), which inhibit VEGFR, PDGFR, CSF-1R (cFms), Kit and Flt3.

COMBINATION THERAPY OF STANDARD TREATMENT WITH SORAFENIB

In addition to the pharmaceutical institution-sponsored clinical trials of linifanib and brivanib as first- and second-line therapy in sorafenib-refractory patients, investigator initiated trials (IIT) of sorafenib in combination with hepatic arterial infusion chemotherapy (SILIUS trial: trial number NCT01214343), pharmaceutical and IITtrials of sorafenib in combination with TACE (SPACE, TACTICS [trial number: NCT 01217034], BRISK-TA trials, SORAMIC and SIRveNIB trials), and a trial to test the inhibitory effect of sorafenibon tumor recurrence after curative treatment (STORM trial) are ongoing, and the results of these trials are eagerly awaited [12].

The working hypotheses in these studies can be deduced by extrapolating the MST and hazard ratios in overall survival (OS) calculated in a subanalysis of the SHARP study (Table **2**). The results obtained suggest that starting treatment with molecular-targeted drugs at an earlier tumor stage in combination with standard treatment options such as resection, ablation, TACE or hepatic arterial infusion

Table 3.   **Hazard ratio and median OS from subanalysis data of the SHARP study.**

		Advanced HCC with vascularinvasion and extrahepatic spread	Advanced HCC withoutvascularinvasion or extrahepatic spread
Hazard Ratio		0.77 (95% CI: 0.60-0.99)	0.52 (95% CI: 0.32-0.85)
Median OS (MST)	Sorafenib	8.9M (n=209) (95% CI: 7.6-10.3M)	14.5M (n=90) (95%CI: 14.0M-N/E)
	Placebo	6.7M (n=212) (95% CI: 5.2-8.0M)	10.2M (n=91) 95% CI: 8.6-15.5M)

M: month
Sherman M, *et al.*, ASCO 2008 [49].
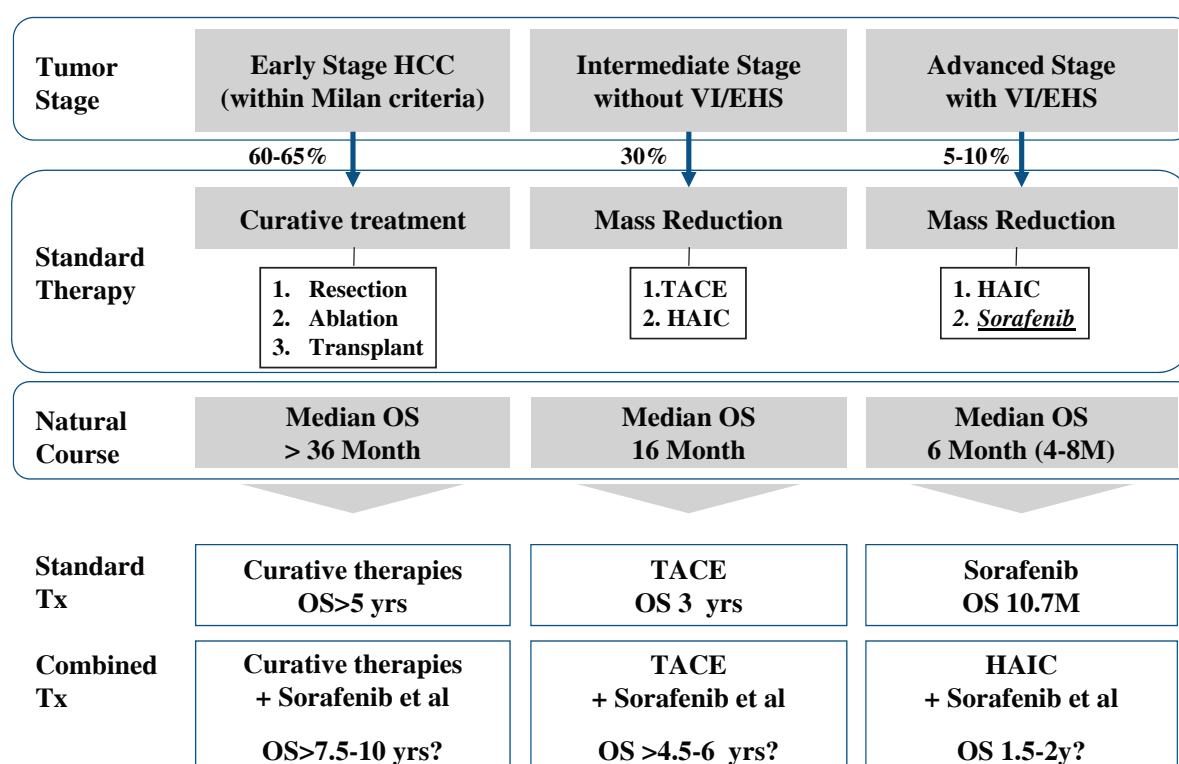
Fig. (4). Outcomes of standard treatment modalities and expected future outcomes of combination therapy with molecular-targeted agents. By combining molecular targeted agents with resection or ablation, life expectancy (overall survival) is expected to be prolonged to 7.5-10 years. In addition, for intermediate stage HCC, the prognosis is expected to be improved to 4.5-6 years by combination with transarterial chemoembolization (TACE). For advanced stage HCC, the prognosis is expected to be improved to 1.5-2 years by combination with hepatic arterial infusion chemotherapy (HAIC) (cited and modified from ref. #12 with permission).

chemotherapy can improve the prognosis of HCC.Thus, sorafenibhas the potential to induce a paradigm shift in the treatment of HCC. For example, in a subanalysis of the SHARP trial,the hazard ratiosfor OS and MST ratio in intermediate stage HCC without vascular invasion or extrahepatic spread were 0.52 and 1.50, respectively [49] (Table **3**). This suggests that survival of early stage HCC and intermediate stage HCC may be prolonged from 5 years to 7.5–10 years by using sorafenib in an adjuvant setting after curative treatment, and from 3 years to 4.5–6 years by using sorafenib in combination with TACE (Fig. **4**) [12].

CONCLUSION

Several clinical trials [35, 50-59] of the molecular-targeted agents are ongoing. Angiogenesis-inhibiting drugs, particularly sorafenib, have been established for HCC, and drugs targeting several molecules are being developed. Although sorafenib was recently approved, many issues remain to be addressed, including 1) how to determine and define refractoriness, and 2) whether to continue TACE or hepatic arterial infusion chemotherapy (a de facto standard in Japan) in patients with TACE-refractory HCCs or portal

tumor thrombi before starting sorafenib therapy. We strongly recommend that, based on the molecular-targeted agents currently under development, clinical studies (including IITs) should be conducted aggressively, and therapeutic strategies should be devised to resolve the limitations of currently used therapeutic approaches and to improve the therapeutic outcomes.

The introduction of sorafenibto treat HCC in 2007 in Western countries and in 2009 in Japan was undoubtedly the real begnning of a paradigm shift of HCC treatment, representing a significant breakthrough for HCC treatment not previously experienced for this unique tumor.

DISCLOSURE

CONFLICT OF INTEREST

The author confirms that this article content has no conflict of interest.

ACKNOWLEDGEMENTS

ABBREVIATIONS

AASLD	=	American Association for the Study of Liver Diseases
aFGF	=	acidic fibroblast growth factor
AFP	=	alpha-fetoprotein
ALT	=	alanine transaminase
APASL	=	Asian-Pacific Association of the Study of the Liver
AST	=	aspartate transaminase
bFGF	=	basic fibroblast growth factor
BSC	=	best supportive care
CR	=	complete response
DCP	=	des-gamma-carboxyprothrombin
DLTs	=	dose-limiting toxicities
DR	=	death receptor
EGF	=	epidermal growth factor
EGFR	=	epidermal growth factor receptor
FGF	=	fibroblast growth factor
Flt-1	=	fms-like tyrosine kinase 1
HCC	=	hepatocellular carcinoma
HGF	=	hepatocyte growth factor
HUVEC	=	human umbilical vein endothelial cells
IGF	=	insulin growth factor

IIT	=	investigator initiated trials
IL-8	=	interleukin-8
JSH	=	Japan Society of Hepatology
KDR	=	kinase insert domain receptor
MMP	=	matrix metalloproteinase
MST	=	median survival time
MTD	=	maximum tolerated dose
mTOR	=	mammalian target of rapamycine
NSCLC	=	non-small cell lung cancer
OS	=	overall survival
PD	=	progressive disease
PDGFR	=	platelet-derived growth factor receptor
PI3K	=	phosphatidylinositol 3-kinase
PIGF	=	placental growth factor
PIVKA-II	=	protein induced by vitamin K absence or antagonist
PR	=	partial response
pS6	=	S6 ribosomal protein
RCC	=	renal cell carcinoma
SD	=	stable disease
sTF	=	sandwich tube formation
TACE	=	transarterial chemoembolization
TGFα	=	transforming growth factor-α
TNM	=	tumor node metastasis
TRAIL	=	TNF-related apoptosis inducing ligand
TSP	=	thrombospondin
VEGFR	=	vascular endothelial growth factor receptor

REFERENCES

[1]   Wilhelm, S. M.; Adnane, L.; Newell, P.; Villanueva, A.; Llovet, J. M.; Lynch, M. Preclinical overview of sorafenib, a multikinase inhibitor that targets both Raf and VEGF and PDGF receptor tyrosine kinase signaling. *Mol. Cancer Ther.* **2008**, *7* (10), 3129-3140.

[2]   Llovet, J. M.; Ricci, S.; Mazzaferro, V.; Hilgard, P.; Gane, E.; Blanc, J. F.; de Oliveira, A. C.; Santoro, A.; Raoul, J. L.; Forner, A.; Schwartz, M.; Porta, C.; Zeuzem, S.; Bolondi, L.; Greten, T. F.; Galle, P. R.; Seitz, J. F.; Borbath, I.; Haussinger, D.; Giannaris, T.; Shan, M.; Moscovici, M.; Voliotis, D.; Bruix, J. Sorafenib in advanced hepatocellular carcinoma. *N. Engl. J. Med.* **2008**, *359* (4), 378-390.

[3]   Cheng, A. L.; Kang, Y. K.; Chen, Z.; Tsao, C. J.; Qin, S.; Kim, J. S.; Luo, R.; Feng, J.; Ye, S.; Yang, T. S.; Xu, J.; Sun, Y.; Liang, H.; Liu, J.; Wang, J.; Tak, W. Y.; Pan, H.; Burock, K.; Zou, J.; Voliotis, D.; Guan, Z. Efficacy and safety of sorafenib in patients in the Asia-Pacific region with advanced hepatocellular carcinoma: a phase III randomised, double-blind, placebo-controlled trial. *Lancet Oncol.* **2009**, *10* (1), 25-34.

[4]   Bruix, J.; Sherman, M. Management of hepatocellular carcinoma: An update. *Hepatology* **2011**, *53* (3), 1020-1022.

[5]   Omata, M.; Lesmana, L. A.; Tateishi, R.; Chen, P. J.; Lin, S. M.; Yoshida, H.; Kudo, M.; Lee, J. M.; Choi, B. I.; Poon, R. T.; Shiina,

S.; Cheng, A. L.; Jia, J. D.; Obi, S.; Han, K. H.; Jafri, W.; Chow, P.; Lim, S. G.; Chawla, Y. K.; Budihusodo, U.; Gani, R. A.; Lesmana, C. R.; Putranto, T. A.; Liaw, Y. F.; Sarin, S. K. Asian Pacific Association for the Study of the Liver consensus recommendations on hepatocellular carcinoma. *Hepatol. Int.* **2010**, *4* (2), 439-474.

[6] Kudo, M.; Izumi, N.; Kokudo, N.; Matsui, O.; Sakamoto, M.; Nakashima, O.; Kojiro, M.; Makuuchi, M. Management of hepatocellular carcinoma in Japan: Consensus-Based Clinical Practice Guidelines proposed by the Japan Society of Hepatology (JSH) 2010 updated version. *Dig. Dis.* **2011**, *29* (3), 339-364.

[7] Kudo, M.; Ueshima, K. Positioning of a molecular-targeted agent, sorafenib, in the treatment algorithm for hepatocellular carcinoma and implication of many complete remission cases in Japan. *Oncology* **2010**, *78(Suppl 1)*, 154-166.

[8] Murata, K.; Suzuki, H.; Okano, H.; Oyamada, T.; Yasuda, Y.; Sakamoto, A. Hypoxia-induced des-gamma-carboxy prothrombin production in hepatocellular carcinoma. *Int. J. Oncol.* **2010**, *36* (1), 161-170.

[9] Ueshima, K.; Kudo, M.; Takita, M.; Nagai, T.; Tatsumi, C.; Ueda, T.; Kitai, S.; Ishikawa, E.; Yada, N.; Inoue, T.; Hagiwara, S.; Minami, Y.; Chung, H.; Sakurai, T. Des-gamma-carboxyprothrombin may be a promising biomarker to determine the therapeutic efficacy of sorafenib for hepatocellular carcinoma. *Dig. Dis.* **2011**, *29* (3), 321-325.

[10] Kudo, M. Signaling pathway and molecular targeted therapy for hepatocellular carcinoma. *Dig. Dis.* **2011***, 29, 289-302.*

[11] Spangenberg, H. C.; Thimme, R.; Blum, H. E. Targeted therapy for hepatocellular carcinoma. *Nat. Rev. Gastroenterol. Hepatol.* **2009**, *6* (7), 423-432.

[12] Kudo, M. The 2008 Okuda lecture: Management of hepatocellular carcinoma: From surveillance to molecular targeted therapy. *J. Gastroenterol. Hepatol.* **2010**, *25*, 439-452.

[13] Kudo, M.; Okanoue, T. Management of hepatocellular carcinoma in Japan: consensus-based clinical practice manual proposed by the Japan Society of Hepatology. *Oncology* **2007**, *72*(Suppl 1), 2-15.

[14] Hanahan, D.; Weinberg, R. A. The hallmarks of cancer. *Cell* **2000**, *100* (1), 57-70.

[15] Villanueva, A.; Toffanin, S.; Llovet, J. M. Linking molecular classification of hepatocellular carcinoma and personalized medicine: preliminary steps. *Curr. Opin. Oncol.* **2008**, *20* (4), 444-453.

[16] Sahin, F.; Kannangai, R.; Adegbola, O.; Wang, J.; Su, G.; Torbenson, M. mTOR and P70 S6 kinase expression in primary liver neoplasms. *Clin. Cancer Res.* **2004**, *10* (24), 8421-8425.

[17] Schumacher, G.; Oidtmann, M.; Rueggeberg, A.; Jacob, D.; Jonas, S.; Langrehr, J. M.; Neuhaus, R.; Bahra, M.; Neuhaus, P. Sirolimus inhibits growth of human hepatoma cells alone or combined with tacrolimus, while tacrolimus promotes cell growth. *World J. Gastroenterol.* **2005**, *11* (10), 1420-1425.

[18] Semela, D.; Piguet, A. C.; Kolev, M.; Schmitter, K.; Hlushchuk, R.; Djonov, V.; Stoupis, C.; Dufour, J. F. Vascular remodeling and antitumoral effects of mTOR inhibition in a rat model of hepatocellular carcinoma. *J. Hepatol.* **2007**, *46* (5), 840-848.

[19] Sieghart, W.; Fuereder, T.; Schmid, K.; Cejka, D.; Werzowa, J.; Wrba, F.; Wang, X.; Gruber, D.; Rasoul-Rockenschaub, S.; Peck-Radosavljevic, M.; Wacheck, V. Mammalian target of rapamycin pathway activity in hepatocellular carcinomas of patients undergoing liver transplantation. *Transplantation* **2007**, *83* (4), 425-432.

[20] Zhou, L.; Huang, Y.; Li, J.; Wang, Z. The mTOR pathway is associated with the poor prognosis of human hepatocellular carcinoma. *Med. Oncol.* **2010**, *27* (2), 255-261.

[21] Chen, J. S.; Wang, Q.; Fu, X. H.; Huang, X. H.; Chen, X. L.; Cao, L. Q.; Chen, L. Z.; Tan, H. X.; Li, W.; Bi, J.; Zhang, L. J. Involvement of PI3K/PTEN/AKT/mTOR pathway in invasion and metastasis in hepatocellular carcinoma: Association with MMP-9. *Hepatol. Res.* **2009**, *39* (2), 177-186.

[22] Villanueva, A.; Chiang, D. Y.; Newell, P.; Peix, J.; Thung, S.; Alsinet, C.; Tovar, V.; Roayaie, S.; Minguez, B.; Sole, M.; Battiston, C.; Van Laarhoven, S.; Fiel, M. I.; Di Feo, A.; Hoshida, Y.; Yea, S.; Toffanin, S.; Ramos, A.; Martignetti, J. A.; Mazzaferro, V.; Bruix, J.; Waxman, S.; Schwartz, M.; Meyerson, M.; Friedman, S. L.; Llovet, J. M. Pivotal role of mTOR signaling in hepatocellular carcinoma. *Gastroenterology* **2008**, *135* (6), 1972-1983, 1983 e1971-1911.

[23] Treiber, G. mTOR inhibitors for hepatocellular cancer: a forward-moving target. *Expert Rev. Anticancer Ther.* **2009**, *9* (2), 247-261.

[24] Ferrara, N.; Davis-Smyth, T. The biology of vascular endothelial growth factor. *Endocr. Rev.* **1997**, *18* (1), 4-25.

[25] Griffioen, A. W.; Molema, G. Angiogenesis: potentials for pharmacologic intervention in the treatment of cancer, cardiovascular diseases, and chronic inflammation. *Pharmacol. Rev.* **2000**, *52* (2), 237-268.

[26] Harper, S. J.; Bates, D. O. VEGF-A splicing: the key to anti-angiogenic therapeutics? *Nat. Rev. Cancer* **2008**, *8* (11), 880-887.

[27] Fernandez, M.; Semela, D.; Bruix, J.; Colle, I.; Pinzani, M.; Bosch, J. Angiogenesis in liver disease. *J. Hepatol.* **2009**, *50* (3), 604-620.

[28] Schoenleber, S. J.; Kurtz, D. M.; Talwalkar, J. A.; Roberts, L. R.; Gores, G. J. Prognostic role of vascular endothelial growth factor in hepatocellular carcinoma: systematic review and meta-analysis. *Br. J. Cancer* **2009**, *100* (9), 1385-1392.

[29] Bergers, G.; Hanahan, D. Modes of resistance to anti-angiogenic therapy. *Nat. Rev. Cancer* **2008**, *8* (8), 592-603.

[30] Batchelor, T. T.; Sorensen, A. G.; di Tomaso, E.; Zhang, W. T.; Duda, D. G.; Cohen, K. S.; Kozak, K. R.; Cahill, D. P.; Chen, P. J.; Zhu, M.; Ancukiewicz, M.; Mrugala, M. M.; Plotkin, S.; Drappatz, J.; Louis, D. N.; Ivy, P.; Scadden, D. T.; Benner, T.; Loeffler, J. S.; Wen, P. Y.; Jain, R. K. AZD2171, a pan-VEGF receptor tyrosine kinase inhibitor, normalizes tumor vasculature and alleviates edema in glioblastoma patients. *Cancer Cell.* **2007**, *11* (1), 83-95.

[31] El-Assal, O. N.; Yamanoi, A.; Ono, T.; Kohno, H.; Nagasue, N. The clinicopathological significance of heparanase and basic fibroblast growth factor expressions in hepatocellular carcinoma. *Clin. Cancer Res.* **2001**, *7* (5), 1299-1305.

[32] Poon, R. T.; Ng, I. O.; Lau, C.; Yu, W. C.; Fan, S. T.; Wong, J. Correlation of serum basic fibroblast growth factor levels with clinicopathologic features and postoperative recurrence in hepatocellular carcinoma. *Am. J. Surg.* **2001**, *182* (3), 298-304.

[33] Huynh, H.; Ngo, V. C.; Fargnoli, J.; Ayers, M.; Soo, K. C.; Koong, H. N.; Thng, C. H.; Ong, H. S.; Chung, A.; Chow, P.; Pollock, P.; Byron, S.; Tran, E. Brivanib alaninate, a dual inhibitor of vascular endothelial growth factor receptor and fibroblast growth factor receptor tyrosine kinases, induces growth inhibition in mouse models of human hepatocellular carcinoma. *Clin. Cancer Res.* **2008**, *14* (19), 6146-6153.

[34] Bhide, R. S.; Lombardo, L. J.; Hunt, J. T.; Cai, Z. W.; Barrish, J. C.; Galbraith, S.; Jeyaseelan, R., Sr.; Mortillo, S.; Wautlet, B. S.; Krishnan, B.; Kukral, D.; Malone, H.; Lewin, A. C.; Henley, B. J.; Fargnoli, J. The antiangiogenic activity in xenograft models of brivanib, a dual inhibitor of vascular endothelial growth factor receptor-2 and fibroblast growth factor receptor-1 kinases. *Mol. Cancer Ther.* **2010**, *9* (2), 369-378.

[35] Raoul, J. L.; Finn, R. S.; Kang, Y. K.; Park, J. W.; Harris, R.; Coric, V.; Donica, M.; Walters, I. An open-label phase II study of first- and second-line treatment with Brivanib in patients with hepatocellular carcinoma (HCC). *J. Clin. Oncol.* **2009**, *26 (Suppl; Abstr 4577)*.

[36] Carmeliet, P.; Jain, R. K. Angiogenesis in cancer and other diseases. *Nature* **2000**, *407* (6801), 249-257.

[37] Ferrara, N. Vascular endothelial growth factor as a target for anticancer therapy. *Oncologist* **2004**, *9(Suppl 1)*, 2-10.

[38] Matsui, J.; Yamamoto, Y.; Funahashi, Y.; Tsuruoka, A.; Watanabe, T.; Wakabayashi, T.; Uenaka, T.; Asada, M. E7080, a novel inhibitor that targets multiple kinases, has potent antitumor activities against stem cell factor producing human small cell lung cancer H146, based on angiogenesis inhibition. *Int. J. Cancer* **2008**, *122*, 644-671.

[39] Matsui, J.; Funahashi, Y.; Uenaka, T.; Watanabe, T.; Tsuruoka, A.; Asada, M. Multi-kinase inhibitor E7080 suppresses lymph node and lung metastases of human mammary breast tumor MDA-MB-231 *via* inhibition of vascular endothelial growth factor-receptor (VEGF-R) 2 and VEGF-R3 kinase. *Clin. Cancer Res.* **2008**, *14* (17), 5459-5465.

[40] Summary of vital statistics annual report (round number). issued 2006, by the Ministry of health, Labour and Welfare, Available from: http://www.mhlw.go.jp/toukei/saikin/hw/jinkou/geppo/nengai06/index.html.

[41] Llovet, J. M.; Di Bisceglie, A. M.; Bruix, J.; Kramer, B. S.; Lencioni, R.; Zhu, A. X.; Sherman, M.; Schwartz, M.; Lotze, M.; Talwalkar, J.; Gores, G. J. Design and endpoints of clinical trials in

hepatocellular carcinoma. *J. Natl. Cancer Inst.* **2008**, *100* (10), 698-711.

[42]   Llovet, J. M.; Burroughs, A.; Bruix, J. Hepatocellular carcinoma. *Lancet* **2003**, *362* (9399), 1907-1917.

[43]   Makuuchi, M.; Kokudo, N.; Arii, S.; Futagawa, S.; Kaneko, S.; Kawasaki, S.; Matsuyama, Y.; Okazaki, M.; Okita, K.; Omata, M.; Saida, Y.; Takayama, T.; Yamaoka, Y. Development of evidence-based clinical guidelines for the diagnosis and treatment of hepatocellular carcinoma in Japan. *Hepatol Res.* **2008**, *38* (1), 37-51.

[44]   Yamaguchi, R.; Yano, H.; Iemura, A.; Ogasawara, S.; Haramaki, M.; Kojiro, M. Expression of vascular endothelial growth factor in human hepatocellular carcinoma. *Hepatology* **1998**, *28* (1), 68-77.

[45]   Poon, R. T.; Ho, J. W.; Tong, C. S.; Lau, C.; Ng, I. O.; Fan, S. T. Prognostic significance of serum vascular endothelial growth factor and endostatin in patients with hepatocellular carcinoma. *Br. J. Surg.* **2004**, *91* (10), 1354-1360.

[46]   Glen, H.; Boss, D.; Morrison, R.; Roelvink, M.; Wanders, J.; Mazur, A. A phase I study of E7080 in patients with advanced malignancies. *J. Clin. Oncol. 26* (Suppl May 20), abstr 3526.

[47]   Nemunaitis, J.; Senzer, N.; Kurzrock, R.; Ng, C.; Das, A.; Atienza, R. Phase I dose-escalation study of E7080, a multikinase inhibitor, in patients with advanced solid tumors. *J. Clin. Oncol.* **2008**, *26* (Suppl May 20), abstr 14583.

[48]   Yamada, K.; Hirata, T.; Fujiwara, Y.; Nokihara, H.; Yamamoto, N.; Yamada, Y. Phase I dose-escalation study and biomarker analysis of E7080 in patients with advanced solid tumors. *J. Clin. Oncol.* **2008**, *26* (Suppl May 20), abstr 3527.

[49]   Sherman, M.; Mazzaferro, V.; Amadori, D.; Seitz, J.; Moscovici, M.; Shan, M.; Nadel, A.; Llovet, J. M.; Bruix, J. Efficacy and safety of sorafenib in patients with advanced hepatocellular carcinoma and vascular invasion or extrahepatic spread: A subanalysis from the SHARP trial. *J. Clin. Oncol.* **2008**, *26*(Suppl), abstr 4584 (2008 ASCO Annual Meeting).

[50]   Faivre, S.; Raymond, E.; Boucher, E.; Douillard, J.; Lim, H. Y.; Kim, J. S.; Zappa, M.; Lanzalone, S.; Lin, X.; Deprimo, S.; Harmon, C.; Ruiz-Garcia, A.; Lechuga, M. J.; Cheng, A. L. Safety and efficacy of sunitinib in patients with advanced hepatocellular carcinoma: an open-label, multicentre, phase II study. *Lancet Oncol.* **2009**, *10* (8), 794-800.

[51]   Zhu, A. X.; Sahani, D. V.; Duda, D. G.; di Tomaso, E.; Ancukiewicz, M.; Catalano, O. A.; Sindhwani, V.; Blaszkowsky, L. S.; Yoon, S. S.; Lahdenranta, J.; Bhargava, P.; Meyerhardt, J.; Clark, J. W.; Kwak, E. L.; Hezel, A. F.; Miksad, R.; Abrams, T. A.;

Enzinger, P. C.; Fuchs, C. S.; Ryan, D. P.; Jain, R. K. Efficacy, safety, and potential biomarkers of sunitinib monotherapy in advanced hepatocellular carcinoma: a phase II study. *J. Clin. Oncol.* **2009**, *27* (18), 3027-3035.

[52]   Thomas, M. B.; Chadha, R.; Glover, K.; Wang, X.; Morris, J.; Brown, T.; Rashid, A.; Dancey, J.; Abbruzzese, J. L. Phase 2 study of erlotinib in patients with unresectable hepatocellular carcinoma. *Cancer* **2007**, *110* (5), 1059-1067.

[53]   Philip, P. A.; Mahoney, M. R.; Allmer, C.; Thomas, J.; Pitot, H. C.; Kim, G.; Donehower, R. C.; Fitch, T.; Picus, J.; Erlichman, C. Phase II study of Erlotinib (OSI-774) in patients with advanced hepatocellular cancer. *J. Clin. Oncol.* **2005**, *23* (27), 6657-6663.

[54]   Zhu, A. X.; Stuart, K.; Blaszkowsky, L. S.; Muzikansky, A.; Reitberg, D. P.; Clark, J. W.; Enzinger, P. C.; Bhargava, P.; Meyerhardt, J. A.; Horgan, K.; Fuchs, C. S.; Ryan, D. P. Phase 2 study of cetuximab in patients with advanced hepatocellular carcinoma. *Cancer* **2007**, *110* (3),581-589.

[55]   Abou-Alfa, G. K.; Schwartz, L.; Ricci, S.; Amadori, D.; Santoro, A.; Figer, A.; De Greve, J.; Douillard, J. Y.; Lathia, C.; Schwartz, B.; Taylor, I.; Moscovici, M.; Saltz, L. B. Phase II study of sorafenib in patients with advanced hepatocellular carcinoma. *J. Clin. Oncol.* **2006**, *24* (26), 4293-4300.

[56]   Toh, H.; Chen, P. J.; Carr, B. I.; Knox, J. J.; Gill, S.; Steinberg, J.; Carlson, D. M.; Qian, J.; Qin, Q.; Yong, W. A phase II study of ABT-869 in hepatocellular carcinoma (HCC): Interim analysis. *J. Clin. Oncol.* **2009**, *27*, 15s (suppl; Abstr 4581).

[57]   Siegel, A. B.; Cohen, E. I.; Ocean, A.; Lehrer, D.; Goldenberg, A.; Knox, J. J.; Chen, H.; Clark-Garvey, S.; Weinberg, A.; Mandeli, J.; Christos, P.; Mazumdar, M.; Popa, E.; Brown, R. S. Jr.; Rafii, S.; Schwartz, J. D. Phase II trial evaluating the clinical and biologic effects of bevacizumab in unresectable hepatocellular carcinoma. *J. Clin. Oncol.* **2008**, *26* (18), 2992-2998.

[58]   O'Dwyer, P. J.; Giantonio, B. J.; Levy, D. E.; Kauh, J. S.; Fitzgerald, D. B.; Benson, A. B. Gefitinib in advanced unresectable hepatocellular carcinoma: Results from the Eastern Cooperative Oncology Group's Study E1203. *J. Clin. Oncol.* **2006**, *24*, 18S (Suppl; Abstr 4143).

[59]   Ramanathan, R. K.; Belani, C. P.; Singh, D. A.; Tanaka, M.; Lenz, H. J.; Yen, Y.; Kindler, H. L.; Iqbal, S.; Longmate, J.; Mack, P. C.; Lurje, G.; Gandour-Edwards, R.; Dancey, J.; Gandara, D. R. A phase II study of lapatinib in patients with advanced biliary tree and hepatocellular cancer. *Cancer Chemother. Pharmacol.* **2009**, *64* (4), 777-783.

Special Report

Guideline on the use of new anticancer drugs for the treatment of Hepatocellular Carcinoma 2010 update

Shuichi Kaneko,[1,2,3] Junji Furuse,[1,2,4] Masatoshi Kudo,[1,2,5] Kenji Ikeda,[1,2,6] Masao Honda,[2,5] Yasunari Nakamoto,[2,7] Morikazu Onchi,[2,8] Goshi Shiota,[2,9] Osamu Yokosuka,[2,10] Isao Sakaida,[2,11] Tetsuo Takehara,[2,12] Yoshiyuki Ueno,[2,13] Kazumasa Hiroishi,[2,14] Shuhei Nishiguchi,[2,15] Hisataka Moriwaki,[2,16] Kazuhide Yamamoto,[2,17] Michio Sata,[2,18] Shuntaro Obi,[2,19] Shiro Miyayama[2,20] and Yukinori Imai[2,21]

[1]*Novel Anticancer Agent Guideline Drafting Committee,* [2]*Study Group on New Liver Cancer Therapies, Departments of* [3]*Gastroenterology, Graduate School of Medicine, Kanazawa University, Kanazawa,* [4]*Medical Oncology, Kyorin University School of Medicine, Mitaka,* [5]*Gastroenterology, Kinki University, Higashiosaka,* [6]*Hepatology, Toranomon Hospital, Tokyo,* [7]*Gastroenterology, Graduate School of Medicine, Fukui University, Fukui,* [8]*Gastroenterology and Metabology, Graduate School of Medicine, Ehime University, Matsuyama,* [9]*Division of Molecular and Genetic Medicine, Tottori University Graduate School of Medicine, Tottori, Departments of* [10]*Medicine and Clinical Oncology, Graduate School of Medicine, Chiba University, Chiba, Japan,* [11]*Gastroenterology and Hepatology, Yamaguchi University Graduate School of Medicine, Yamaguchi,* [12]*Gastroenterology and Hepatology, Osaka University Graduate School of Medicine, Osaka,* [13]*Gastroenterology, Tohoku University Graduate School of Medicine, Sendai,* [14]*Division of Gastroenterology, Department of Medicine, Showa University School of Medicine, Tokyo,* [15]*Division of Hepatobiliary and Pancreatic Diseases, Department of Internal Medicine, Hyogo College of Medicine, Kakogawa, Departments of* [16]*Gastroenterology, Gifu University Graduate School of Medicine, Gifu,* [17]*Gastroenterology and Hepatology, Okayama University Graduate School of Medicine, Okayama,* [18]*Division of Gastroenterology, Department of Medicine, Kurume University School of Medicine, Kurume, Departments of* [19]*Hepatology, Kyoundo Hospital, Tokyo,* [20]*Diagnostic Radiology, Fukuiken Saiseikai Hospital, Fukui, and* [21]*Gastroenterology and Hepatology, Faculty of Medicine, Saitama Medical University, Saitama, Japan*

The "*Guideline on the Use of New Anticancer Drugs for the Treatment of Hepatocellular Carcinoma*" was prepared by the Study Group on New Liver Cancer Therapies established by the "*Research Project on Emergency Measures to Overcome Hepatitis*" under the auspices of the Health and Labour Sciences Research Grant. The Guideline brings together data collected by the Study Group on the use and incidence of adverse events in 264 patients with advanced hepatocellular carcinoma (HCC) treated using sorafenib and in 535 patients with advanced HCC treated using miriplatin at 16 participating institutions up until 22 December 2010, as well as referring to the published studies, academic presentations, and reports from the private sector. The aim of this Guideline is to facilitate understanding and current thinking regarding the proper usage of new anticancer drugs towards actual use in therapy. In terms of the format, the Guideline presents "clinical questions" on issues pertaining to medical care, makes "recommendations" on diagnosis and treatment in response to each of these clinical questions, and provides a rationale for these recommendations in the form of "scientific statements".

Key words: hepatic arterial infusion, hepatocellular carcinoma, miriplatin, molecular targeting therapy, sorafenib

INTRODUCTION

THE MOLECULAR-TARGETED agent sorafenib has been found to significantly prolong survival in patients with hepatocellular carcinoma (HCC).[1,2] In May 2009, sorafenib was approved in Japan for unresectable

523

HCC. Furthermore, miriplatin was approved in Japan for the treatment of HCC in January 2010, and clinical trials are also currently underway on a number of other promising new anticancer agents. Treatment of HCC is thus undergoing a period of major transition, but the role of these anticancer drugs and conventional therapies remains unclear, leading to concerns about the risk of serious adverse events (SAEs).

The Study Group on New Liver Cancer Therapies (the Study Group) was formed as part of the "Research Project on Emergency Measures to Overcome Hepatitis" sponsored by the Health and Labour Sciences Research Grant, with the overall purpose of formulating a guideline to facilitate understanding on the practical usage of new anticancer drugs.

The Study Group collected information on the use of new anticancer drugs, sorafenib and miriplatin at 16 affiliated institutions and compiled current opinions regarding the proper use of these drugs based on published studies, academic conference papers and reports from the private sector. These results have now been compiled in the form of a guideline.

However, of note is that this guideline is provisional and has been prepared to expedite the provision of proper information because information on these new anticancer drugs is constantly being updated.

STUDY METHODS, SUBJECTS AND PARTICIPATING INSTITUTIONS

Basic statistics

THE STUDY GROUP'S "New Liver Cancer Therapies" (NLCT) study was based on data from patients with advanced HCC treated using sorafenib or miriplatin up until 22 December 2010 at the participating institutions. Clinical data were recorded by each institution in case report files (CRFs) created by the Study Group. Of the patients enrolled in this study, 264 were treated with sorafenib and 535 were treated with miriplatin. Any input variables that were unclear were excluded from the analyzed data. After analyzing collecting data on the use of these drugs, the Study Group compiled current opinions on proper use based on published papers, academic conference papers and reports from the private sector. The Study Group proposed a series of "clinical questions" (CQ) on issues pertaining to practical medical care and summarized the current evidence in response to each of these CQ in the form of "scientific statements", as well as making "recommendations".

Participating institutions

The 16 institutions that participated in this study were: Kinki University; Chiba University; Yamaguchi University; Kurume University; Kyorin University; Showa University; Ehime University; Okayama University; Kyoundo Hospital; Tohoku University; Osaka University; Gifu University; Hyogo College of Medicine; Toranomon Hospital; Saitama Medical University; and Kanazawa University.

RESULTS

Sorafenib therapy

Indications

CQ1-1   For which patients with HCC is sorafenib therapy indicated?

Recommendation   Sorafenib therapy is indicated in HCC patients with good performance status (PS) and Child–Pugh class A for whom surgical resection, local ablation therapy (LAT), and transcatheter arterial chemoembolization (TACE) are not possible or not indicated.

The safety and efficacy of sorafenib has not been established in Child–Pugh class B/C patients.

Furthermore, the usefulness of sorafenib as adjuvant chemotherapy after resection, LAT, or TACE of HCC has not been demonstrated.

Scientific statement   Two randomized, placebo-controlled trials demonstrating the usefulness of sorafenib were conducted on patients in whom surgical resection, LAT and TACE were not indicated or who were unresponsive to TACE.[1,2]

The Japan Society of Hepatology provides the following definitions for impossible and refractory cases to TACE.[3]

Definition of "Impossible cases to TACE"

1 Deterioration of treated vessel resulting in inability to select catheter for insertion into the nutrient vessel;
2 Deterioration in hepatic function to Child–Pugh class C due to repeated treatment;
3 Patients with tumor thrombus in main trunk or first branch of portal vein;
4 Patients with large arterio-portal shunts.

Definition of "Refractory cases to TACE"

(1) Intrahepatic lesion(s)
   (i) Poor Lipiodol deposits (≤50%) observed on at least two consecutive occasions in computed tomography (CT) assessment of therapeutic response immediately after (>1 month) correctly performing TACE;

   (ii) Multiple new lesions observed on at least two consecutive occasions in CT assessment of therapeutic response immediately after (>1 month) TACE;
(2) Appearance of vascular invasion;
(3) Appearance of distant metastasis;
(4) Tumor markers.
   (i) Continued increase in tumor markers with transient decrease only immediately after TACE procedure.

In the present NLCT study, as many as 91% of patients underwent prior treatment, in whom 29% received hepatic arterial infusion chemotherapy (HAIC). Comparison of the characteristics of the remaining NLCT study patients with those of previous clinical trials[1,2,4–6] is presented in Table 1.

An adverse event (AE) report on all-patient special drug use surveillance (SDUS) conducted in Japan[7] contains analysis and reporting of AEs for 777 patients for whom CRFs were collected up until 19 December 2009.

That report compared the clinical characteristics for 51 of these 777 patients who died within 30 days of treatment ("early death group") and the 382 patients who survived for ≥61 days ("control survival group"). The data indicate that the prevalence of Eastern Cooperative Oncology Group (ECOG) PS grades ≥2 tended to be high among patients in the "early death group" at 5.9% compared with those in the "control survival group" at 0.5%, suggesting the need to carefully follow the course of patients with poor PS. In the NLCT study, 98% of patients had a PS score of 0–1.

In terms of hepatic function, two randomized, placebo-controlled trials demonstrating the usefulness of sorafenib were conducted on Child–Pugh class A patients.[1,2]

Meanwhile, in the NLCT study, 81% of evaluable patients were Child–Pugh class A, and 94% had a Child–Pugh score of ≤7. Comparison of treatment results of Child–Pugh class A and B patients did not reveal any difference in tumor control rates (46% vs. 50%; $P = 0.52$), but overall survival (OS) was inferior in Child–Pugh class B patients (median OS: 11.5 months vs. 5.2 months; $P < 0.01$).

In a Phase I trial conducted in Japan, no clear increase in toxicity was observed in Child–Pugh class B patients compared with Child–Pugh class A patients.[8] On the other hand, the aforementioned SDUS found that hepatic functional reserve was poor in the "early death group" compared to the "control survival group".[4]

A Phase II study of sorafenib therapy in HCC patients including those with Child–Pugh class B is currently underway in Japan (UMIN [University Hospital Medical Information Network] 000002972). Another study currently being conducted worldwide is the Global Investigation of therapeutic decisions in HCC and of its treatment with sorafenib (GIDEON); a large-scale prospective study on actual sorafenib therapy of patients with unresectable HCC. The GIDEON study is recruiting 3000 patients from over 400 sites in more than 40 countries in the Asia-Pacific region, Europe, USA, Latin America, and Japan.[9] The study's first interim analysis has been released and the findings of 511 recruited patients including those in Child–Pugh class B have been examined. No significant difference in grade 3 or 4 AEs was found to exist between Child–Pugh class A and B patients, at 31% and 38%, respectively.[10] Future GIDEON study analyses are expected to provide crucial information concerning the safety of sorafenib for Child–Pugh class B patients.

A Phase III study of post-TACE adjuvant sorafenib chemotherapy versus placebo conducted in Japan and South Korea failed to demonstrate the usefulness of sorafenib administration.[11] In addition, a Phase III placebo-controlled trial of adjuvant sorafenib chemotherapy following radical treatment (either surgical resection or LAT) of HCC (STORM Trial) is currently underway.[12]

The NLCT study did not include any patients treated with sorafenib as adjuvant chemotherapy.

Method of administration

CQ1-2 What is the optimal dosage regimen for sorafenib therapy?

Recommendation The standard dosage regimen for sorafenib therapy is 400 mg administered twice daily (800 mg/day).

The safety and efficacy of sorafenib therapy in combination with other anti-neoplastic agents or TACE have not been established.

Scientific statement In the two aforementioned randomized, placebo-controlled trials demonstrating the usefulness of sorafenib, a single 400 mg dose of sorafenib was administered twice daily (800 mg/day),[1,2] and usefulness was not observed at a reduced dosage. A high-fat diet reportedly lowers the plasma concentration of sorafenib so administration should be avoided from 1 h before to 2 h after meals.

Reduced dose regimen due to AEs was conducted in the abovementioned studies as follows:
Step-down dose (step 1): 400 mg once a day
Step-down dose (step 2): 400 mg every another day

© 2012 The Japan Society of Hepatology

Table 1 Characteristics of patients receiving sorafenib therapy

	NLCT Study (*n* = 264) %	SDUS[4,6] (*n* = 777) %	SHARP Trial[1] (*n* = 299) %	Asia-Pacific Trial[2] (*n* = 150) %	Sorafenib phase II[5] (*n* = 137) %
Age (years)					
Median	70		64.9 ± 11.2	51	69
Range	33–87		(mean ± SD)	23–86	28–86
Gender					
Male	79		87	84.7	71
PS					
0	83	69.5	54	25.3	50
1	15	26.5	38	69.3	50
Child–Pugh class					
A	81	88.2	95	97.3	72
B	19	9.9	5	2.7	28
HBs antigen					
Positive	20	24.6	19	70.7	17
HCV antibody					
Positive	62	52.2	29	10.7	48
Prior treatment					
Yes	91	91.2	49		
Resection	31		19		
LAT	47		15		
TACE	78		29		
HAIC	29				
Advanced vascular invasion					
Yes	18		36	36.0	
Extrapulmonary lesion(s)					
Yes	51	54.4	53	68.7	–
Lymph node(s)	22	15.4	30	52	–
Lung(s)	26	30.6	22	30.7	–
Maximum tumor size (mm)	34				
Range	7–170				
≥30 mm	59				
Stage	†	‡	§	§	‡
I	1	1.2			0
II	9	4.8			3
III	30	20.7	B: 18	B: NE	31
IV A	17	23	C: 82	C: 95.3	66
IV B	43	47.6			
T-Bil (mg/dL)					
Median	0.8		0.7		
Range	0–7.7		0.1–16.4		
Alb (g/dL)					
Median	3.5		3.9		
Range	1.7–4.8		2.7–5.3		
AFP (ng/mL)					
Median	218		44.3		
Range	0.8–252150		0–2080000		
≥10	84			77.3	76

†Japanese Classification of Liver Cancer.
‡UICC classification.
§BCLC classification.
AFP, α fetoprotein; Alb, albumin; HAIC, hepatic arterial infusion chemotherapy; HBs, Hepatitis B surface antigen; HCV, hepatitis C virus; LAT, local ablation therapy; NLCT, New Liver Cancer Therapies; PS, performance status; SD, standard deviation; SDUS, special drug use surveillance; SHARP, sorafenib hepatocellular carcinoma assessment randomized protocol; TACE, transcatheter arterial chemoembolization; T-Bil, total bilirubin.

In the NLCT study, 77% of patients received the standard dosage regimen of 400 mg twice daily, while 21% were started on a reduced dose.

Comparison of the group started on the standard dose of 800 mg/day and the group started on a reduced dose did not reveal any significant differences in either duration of treatment (117 days vs. 81 days; $P = 0.05$) or number of dosing days (107 days vs. 78 days; $P = 0.10$). Furthermore, dosage was subsequently increased in 22% of the reduced initial dose group. Daily dosage intensity (DI) was 615 mg in the standard-dose group and 387 mg in the reduced-dose group.

It is conceivable to start sorafenib therapy at a reduced dose according to the condition of the patient or prevention of AEs. Because efficacy at reduced doses has not been demonstrated, as long as no AEs are encountered in the course of treatment, consideration should be given to increasing the dose to the standard dosage regimen.

With regard to sorafenib combination therapies, Phase I and Phase II studies on systemic chemotherapy in combination with sorafenib therapy have been published for radiotherapy,[13,14] doxorubicin,[15] tegafur/uracil,[16] and octreotide.[17] Several Japanese clinical trials are also being conducted on combination therapy, specifically low-dose cisplatin/fluorouracil HAIC (UMIN000004315), cisplatin HAIC (UMIN000001496), and S-1 chemotherapy (UMIN000002418, UMIN000002590). Therapies combining sorafenib with other anti-neoplastic agents are therefore still in the research stage, and their efficacy is yet to be demonstrated.

In terms of sorafenib combined with LAT, a Phase III placebo-controlled trial of adjuvant sorafenib chemotherapy following radical treatment (surgical resection or LAT) of HCC (STORM Trial) is presently underway.[12] Meanwhile, sorafenib combined with TACE has been investigated in a Phase III study of post-TACE adjuvant sorafenib chemotherapy versus placebo conducted in Japan and South Korea, but the study failed to demonstrate the usefulness of sorafenib administration.[11] Another Phase II trial on TACE in combination with sorafenib is presently being carried out in Japan (TACTICS; UMIN 000004316).

Discontinuation criteria

CQ1-3 How and when should sorafenib therapy be discontinued?

Recommendation Administration of sorafenib should be discontinued immediately in the event of SAEs.

Discontinuation should also be considered when disease progression is confirmed by radiological imaging or on the basis of patient symptoms.

Scientific statement In the two randomized, placebo-controlled trials demonstrating the usefulness of sorafenib therapy, administration was discontinued upon confirmation of radiologic or symptomatic progression or in the event of SAEs.[1,2]

In the NLCT study, sorafenib therapy was discontinued in 185 patients with 63% due to disease progression and 22% due to AEs. Moreover, 60% of discontinued patients did not undergo post-treatment.

No data are currently available on the efficacy/safety of continued administration of sorafenib after disease progression.

Adverse events

CQ1-4 What are the adverse events associated with sorafenib therapy?

Recommendation Some form of AE has appeared in almost all patients treated with sorafenib.

These AEs vary, and have even included serious adverse events (SAEs) resulting in death. Familiarity with these AEs is therefore essential, to carefully monitor patient progress while taking the necessary precautions, and to respond rapidly when an AE occurs.

The following AEs are known to occur frequently in patients treated with sorafenib.

1 Hand-foot skin reaction (HFSR);
2 Rash/desquamation;
3 Diarrhea;
4 Anorexia;
5 Hypertension;
6 Fatigue;
7 Alopecia;
8 Nausea.

While infrequent, life-threatening SAEs include hepatic failure, interstitial pneumonia, and gastrointestinal hemorrhage.

In addition, the following blood test abnormalities are known to occur frequently in patients treated with sorafenib.

1 Leukopenia;
2 Neutropenia;
3 Anemia;
4 Thrombocytopenia;
5 Hepatic impairment (elevated AST [aspartate aminotransferase], ALT [alanine aminotransferase], ALP [alkaline phosphatase], γ-GTP [γ-glutamyltransferase], T-Bil [total bilirubin]);

6 T-Bil elevation;
7 Amylase elevation;
8 Electrolyte abnormality (hyponatremia, hypokalemia, hypocalcemia, hypophosphatemia);
9 Hypoalbuminemia.

Scientific statement The incidence of sorafenib-related AEs was 80% in the Sorafenib Hepatocellular Carcinoma Assessment Randomized Protocol (SHARP) trial and 81.9% in the Asia-Pacific trial. Frequently occurring AEs were HFSR, rash/desquamation, diarrhea, anorexia, hypertension, fatigue, alopecia, and nausea.[1,2]

Sorafenib-related AE incidence in the NLCT study was 87%, of which 36% were ≥grade 3 AEs. While incidences of HFSR, diarrhea and alopecia in the NLCT study were similar to those of the Asia-Pacific trial[2] and SDUS,[6] incidences of rash/desquamation, anorexia, hypertension and fatigue were slightly higher in the present study (Table 2).

Evaluation of changes in clinical laboratory data was achieved by examining the CRFs to find the largest variations during sorafenib therapy, as well as the test date on which variations occurred. Consequently, the frequency of abnormal values in the NLCT study differed from those of the SHARP trial[1] and SDUS[6] (Table 3).

Changes in laboratory values were seen in 96% of the sorafenib group, with 64% showing an AE ≥ grade 3. Incidence of diminished blood cell counts was high compared with previous studies, with thrombocytopenia, leukopenia, neutropenia, and anemia seen in 56%, 43%, 37%, and 34% of the sorafenib group, respectively.

Hepatic impairment was also frequent, with elevated AST and ALT occurring in ≥50% of sorafenib-treated patients (70% and 55%, respectively), of whom a further 25% and 15% had AST and ALT readings ≥grade 3, indicating levels exceeding 200 IU/L after commencement of treatment. Similar results were observed for ALP and γ-GTP. Elevated T-Bil was seen in 53% of the sorafenib group, of whom 11% had readings that were ≥grade 3, which is more than three times the upper limit of normal (ULN).

Increased amylase was seen in 49% of the sorafenib group, of whom 12% had levels ≥grade 3, which is more than twice the ULN. In terms of electrolyte abnormalities, hyponatremia and hypokalemia were observed in 50% and 25% of the sorafenib group, respectively. Hypocalcemia and hypophosphatemia were also seen in ≥50% of the sorafenib group, but the valid response rate was low for these variables.

Hypoalbuminemia was seen in 48% of the sorafenib group, of whom only 5% had readings <2.0 g/dL.

No significant difference was seen in AE incidences for Child–Pugh class A and B patients, at 88% and 83%, respectively ($P = 0.53$). The incidence of AEs ≥grade 3 was also insignificant between Child–Pugh class A and B patients (35% vs. 39%, $P = 0.76$).

Similar comparisons for sorafenib group patients with Child–Pugh class A scoring 5 and 6 also did not reveal any significant differences in either total incidence of AEs at 89% and 88%, respectively ($P > 0.99$), or in the incidence of AEs ≥ grade 3, at 35% each ($P > 0.99$).

Incidence of abnormal laboratory data also did not vary significantly among Child–Pugh class A and B patients, at 96% and 95%, respectively ($P > 0.99$). Similarly, no significant difference was observed in the incidence of abnormal laboratory data ≥grade 3, at 63% and

Table 2 Incidence of drug-related adverse events with sorafenib therapy

AE	NLCT Study (n = 264)		SDUS[6] (n = 777)		SHARP Trial[1,6] (n = 267)		Asia-Pacific Trial[2] (n = 149)	
	Total (%)	G3/4 (%)	Total (%)	SAEs (%)	Total (%)	G3/4 (%)	Total (%)	G3/4 (%)
HFSR	44	10	47.9	2.8	21.2	7.7	45.0	10.7
Rash/desquamation	31	5	20.7	3.1	15.8	1.08	21.1	0.7
Diarrhea	32	5	21.9	1.4	39.1	8.4	25.5	6.0
Anorexia	27	4	13.8	1.9	13.8	0.3	12.8	0
Hypertension	26	8	19.2	0.6	5.1	1.7	18.8	2.0
Fatigue	24	2	4.6	0.6	–	–	20.1	3.4
Alopecia	15	0	11.4	–	13.8	–	24.8	–
Nausea	10	1	4.0	0.3	11.1	0.3	11.4	0.7

Common Terminology Criteria for Adverse Events (CTC-AE) v3.0
HFSR, hand-foot skin reaction; NLCT, New Liver Cancer Therapies; SDUS, special drug use surveillance; SHARP, sorafenib hepatocellular carcinoma assessment randomized protocol.

Table 3 Abnormal clinical laboratory values with sorafenib therapy

Clinical laboratory data	NLCT Study ($n = 264$)		SDUS[6] ($n = 777$)		SHARP Trial[1,6] ($n = 297$)	
			AE incidence			
	Total (%)	G3/4 (%)	Total (%)	SAEs (%)	Total (%)	G3/4 (%)
Leukopenia	43	8	1.9	0.3	0.3	0.3
Neutropenia	37	6	0.9	0.2	–	–
Anemia	34	11	0.8	0.2	4.4	1.3
Thrombocytopenia	56	12	8.5	0.9	1.7	0.7
PT-INR	25	2	–	–	–	–
Elevated AST	70	25	1.4	–	1.7	1.7
Elevated ALT	55	15	0.9	0.2	0.7	0.7
Elevated ALP	35	5	0.3	–	–	–
Elevated γ-GTP	36	19	0.2	–	–	–
Elevated T.Bil	53	11	2.6	0.2	0.7	–
Elevated amylase	49	12	4.2	–	–	–
Elevated lipase	78	37	3.7	–	1.3	–
Elevated Cre	23	2	–	–	–	–
Hyponatremia	50	14	–	–	–	–
Hypokalemia	25	6	–	–	–	–
Hypocalcemia	55	1	–	–	–	–
Hypophosphatemia	66	29	3.6	0.5	34.9	10.5
Hypoalbuminemia	48	5	1.1	–	–	–

Common Terminology Criteria for Adverse Events (CTC-AE) v3.0.
ALP, alkaline phosphatase; ALT, alanine aminotransferase; AST, aspartate aminotransferase; γ-GTP, γ-glutamyltransferase; NLCT, New Liver Cancer Therapies; SAEs, severe adverse events; SDUS, special drug use surveillance; SHARP, sorafenib hepatocellular carcinoma assessment randomized protocol; T-Bil, total bilirubin.

66% of class A and B patients, respectively. Performing the same comparisons for sorafenib group patients with Child–Pugh class A scoring 5 and 6 also failed to reveal any significant differences either in total incidence of abnormal laboratory values (97% and 95%, respectively; $P > 0.80$) or in the incidence of abnormal laboratory data ≥ grade 3 (58% and 68%, respectively; $P > 0.26$), despite a higher percentage for patients with Child–Pugh score 6.

AE management

CQ1-5   What measures should be taken in management to sorafenib-related AEs?

Recommendation   Preventative measures and careful monitoring of the patient are required for frequently occurring AEs such as HFSR, hypertension, and hepatic impairment.

Patients undergoing sorafenib therapy often experience AEs soon after beginning of treatment. Careful monitoring of the patient by carrying out blood test and medical examinations etc. at least once a week for 4 weeks after initiating therapy is therefore preferable.

Scientific statement   The NLCT study investigated measures taken in management to sorafenib-related AEs (Table 4). Management to HFSR was common, with topical application of emollients performed most frequently (69%), and followed by topical application of steroids (38%) and consultation to a dermatologist

Table 4 Incidence of drug-related adverse events with sorafenib therapy

Response to AE	Valid responses %	Prevention for AE %
Consultation to dermatologist	89	24
Steroid ointment	89	38
Emollient	91	69
Hypotensive drug dose increased	90	21
Intestinal drug	90	19
Anti-diarrheal drug	89	16
Antiemetic drug	89	5

AE, adverse event.

© 2012 The Japan Society of Hepatology

(24%). An increased dose of hypotensive drugs was prescribed in 21% of patients, while diarrhea was treated with antiflatulent and anti-diarrheal drugs in 19% and 16% of patients, respectively. Antiemetic agents were administered in 5% of patients.

Most AEs observed in the NLCT study, including abnormal laboratory values, occurred early at up to 8 weeks after initiating sorafenib therapy. For this reason, careful, early monitoring of the patient is essential. Bayer Yakuhin's "Nexavar Proper Use Guidelines"[7] recommends that a battery of tests be performed regularly or as required during sorafenib therapy (Table 5). Educating patients to withhold taking the drug and consult their doctors immediately if they begin to feel unwell early in the treatment is another important way to prevent AEs from becoming severe.

Serious adverse events (SAEs) should generally be handled by immediately withholding administration or reducing the dose, and reinstitution of treatment or dose increase can be considered if the patient recovers.

Provided below is a summary of management to prevent and respond to major sorafenib AEs.

• Hand-foot skin reaction (HFSR)

Prevention: HFSR occurs most frequently in areas affected by hyperkeratosis and induration. Risk factors for HSFR include physical stimulation of the skin such as compression, heat or friction, so the patient's hands and feet should always be inspected before treatment. Any thickening of the stratum corneum should be removed and the patient instructed to cover and bathe the affected areas to prevent physical stimulation. An emollient containing urea or salicylic acid should be applied to the hands from 1–2 weeks before commencing therapy.[7]

Management: Minor, painless skin changes such as erythema can be treated with steroid ointment without reducing or discontinuing sorafenib therapy. If further deterioration such as formation of blisters occurs, the dosage should be reduced. If the condition interferes with the patient's activities of daily living due to ulcers, cracking or pain etc., the therapy should be withheld and the patient consulted to a dermatologist as necessary. If the condition improves after withholding the sorafenib, therapy can be resumed at a reduced dose, and can subsequently be increased on the basis of the AE condition.

• Hepatic impairment, hepatic failure and hepatic encephalopathy

Prevention: Sorafenib therapy should be avoided in patients with severe liver impairment; particularly those with AST and ALT levels exceeding 200 IU/L.

Management: The patient should be carefully monitored by performing medical examinations and hepatic function tests once weekly for the first month of treatment, once fortnightly for the next 3 months, and once monthly thereafter. Reducing, withholding, or discontinuing sorafenib therapy should be considered if the patient exhibits symptoms of hepatic failure including hepatic encephalopathy and ascites or a sudden increase in AST and ALT levels. Immediate suspension of therapy and careful in- or outpatient monitoring is recommended if the patient's AST and ALT levels increase beyond 200 IU/L or if T-Bil exceeds 3.0 mg/dL.[7] Treatment can be resumed after the patient recovers and increased on the basis of the AE condition.

• Diarrhea

Prevention: Patients should refrain from eating foods and beverages that contain a lot of spices, fat, or caffeine. Laxatives and dietary fiber supplements should also be avoided.

Management: If frequency of defecation increases to 3 times/day, intestinal drugs such as bifidobacterium powders and albumin tannate, and anti-diarrheal drugs such as loperamide and cholestyramine should be administered.[18] In addition, the patient should be instructed to drink fluids to prevent dehydration. Reducing, withholding, or discontinuing sorafenib therapy should be considered if the frequency of defecation increases to ≥4 times/day and the patient exhibits symptoms of dehydration. Dehydration symptoms should be managed systemically with fluid replacement, etc. Treatment can be resumed after the patient recovers and subsequently increased on the basis of the AE conditions.

• **Hypertension**

Prevention: If hypertension is observed prior to sorafenib therapy, systolic blood pressure (SBP) and diastolic blood pressure (DBP) should be controlled to ≤140 mmHg and ≤90 mmHg, respectively.

Management: Patients should be instructed to measure home blood pressure during the early treatment period. If elevated blood pressure (BP) is observed, hypotensive drugs should be administered or the dosage increased. Calcium antagonists and angiotensin receptor blockers (ARBs) are commonly used as hypotensive agents. A single drug is typically administered to begin with, and other types of hypotensive drugs may be co-administered if the reduction in BP is insufficient. Regardless of therapy, administration of sorafenib should be withheld if SBP is ≥180 mmHg or DBP is ≥110 mmHg. Treatment can be resumed after the patient recovers and then increased on the basis of the AE conditions.

Table 5 Clinical laboratory tests recommended in proper use guidelines for sorafenib therapy[7]

Test/Test variable	Cautionary AEs etc.	Subjects	Baseline	1 week	2 weeks	3 weeks	4 weeks	6 weeks	8 weeks	10 weeks	12 weeks	16 weeks	20 weeks	–	Post-therapy
								Frequency/Duration							
Hepatic function	Hepatic impairment	All patients	○	○	○	○	○	○	○	○	○	○	○		○
Pancreatic function	Increased pancreatic function, pancreatitis	All patients	○		○		○	○	○		○	○	○		○
Blood count	Neutropenia, thrombocytopenia, etc.	All patients	○		○		○	○	○		○	○	○		○
Serum phosphate	Hypophosphatemia	All patients	○		○		○		○		○	○	○		○
Blood pressure	Hypertension, hypertensive crisis, reversible leukoencephalopathy	All patients	At hospital visit (simple HBP measurement once weekly [daily if possible])												
Abdominal imaging	GI perforation, pancreatitis	Patients complaining of abdominal pain	As appropriate												
Coagulation parameters	Hemorrhage	Patients on concomitant vitamin K antagonists	As appropriate												
Thyroid function (thyroid hormone, thyroid-stimulating hormone, etc.)	Reduced thyroid function	Patients with specific symptoms suggestive of reduced thyroid function	As appropriate												
Thoracic imaging (Chest x-ray, chest CT, KL-6)	Interstitial pneumonia	Patients with symptoms suggestive of interstitial pneumonia	As appropriate												

AEs, adverse events; CT, computed tomography; GI, gastrointestinal; HBP, home blood pressure.

© 2012 The Japan Society of Hepatology

- **Amylase elevation**

Management: Increases in amylase are usually transient and gradually subside even when sorafenib therapy is continued. However, some cases of pancreatitis has previously been reported in patients treated with sorafenib, so if the patient has abdominal pain or other symptoms suggestive of pancreatitis, or elevated amylase levels are sustained, sorafenib therapy should be withheld and imaging procedures such as dynamic CT performed to determine whether pancreatitis is present.[7]

- **Interstitial pneumonia**

Management: Interstitial pneumonia should be suspected and sorafenib therapy discontinued immediately in patients exhibiting clinical symptoms such as dyspnea, dry cough and fever, and lung crepitation or reduced SpO₂ (percutaneous oxygen saturation) on physical examination. In addition, diagnosis and proper treatment should be carried out based on prompt diagnostic imaging such as chest X-ray or high-resolution chest CT (HRCT) and blood tests such as KL-6 after consulting with a respiratory specialist.[7]

Evaluation of therapeutic response

CQ1-6   How and when should therapeutic response of sorafenib be evaluated?

Recommendation   The antitumor effects of sorafenib therapy are normally evaluated by diagnostic imaging with dynamic CT or dynamic magnetic resonance imaging (MRI) and subsequent measurement of tumor size based on a single cycle of 4–6 weeks of sorafenib administration.

Changes in intra-tumoral blood flow are often seen following sorafenib therapy, so evaluation can also be performed by measuring the area of tumor staining in addition to tumor size.

α-fetoprotein (AFP) and PIVKA-II (DCP) (protein induced by vitamin K absence or abnormality, des-γ-carboxyprothrombin) tumor markers are also typically evaluated in conjunction with tumor images at cycles of 4–6 weeks.

Elevated PIVKA-II (DCP) concentrations during sorafenib therapy may not always be due to disease progression. Consideration should also be given to evaluation of tumors in patients for whom treatment was interrupted due to AEs.

Scientific statement   In the two randomized, placebo-controlled trials demonstrating the usefulness of sorafenib therapy,[1,2] therapeutic response to sorafenib was evaluated every 6 weeks on the basis of diagnostic imaging.

In the NLCT study, median overall survival (OS) was 10.8 months, 6-month survival rate was 65%, 1-year survival rate was 45%, and median progression-free survival (PFS) was 2.1 months (Fig. 1). Comparison of efficacy evaluation findings with those of previous clinical trials[1,2,5] are presented in Table 6.

Reductions in intra-tumoral blood flow are often observed with sorafenib therapy, so instead of simply evaluating tumor size based on the conventional Response Evaluation Criteria in Solid Tumors (RECIST), the use of therapeutic response criteria for evaluating intra-tumoral necrotic regions such as modified RECIST[19] or the Response Evaluation Criteria in Cancer of the Liver (RECICL)[20] has recently been advocated.[21,22] Even if the size of the tumor has slightly increased, therapy may be deemed effective and subsequently continued if the area of reduced intra-tumoral blood flow has increased.

Previous studies have reported that PIVKA-II (DCP) expression is induced in hypoxic HCC cells following sorafenib therapy[23] and that elevated PIVKA-II (DCP) concentrations may act as surrogate markers for HCC tissue ischemia.[24] However, elevated PIVKA-II levels are also seen in disease progression, so care should be taken during assessment of therapeutic response.

According to the NLCT study data, therapeutic response was not evaluated in 20% of sorafenib group patients. However, short-term administration of sorafenib was found to inhibit tumors in some patients on whom therapy was interrupted due to AEs, suggesting that regular tumor assessment should also be considered for patients with interrupted treatment.

Continuation of therapy

CQ1-7   How long should sorafenib therapy be continued?

Recommendation   Sorafenib therapy should preferably be maintained until clear disease progression is determined on evaluation of therapeutic response.

If clear disease progression is not identified in diagnostic imaging, therapy may be continued after considering the risks and benefits.

No data are currently available on the efficacy/safety of continued sorafenib administration after disease progression has been confirmed.

Scientific statement   In the NLCT study, 31% of patients in the sorafenib group underwent some form of additional treatment after completion of the therapy. Specifically, 12% underwent TACE, 8% underwent systemic chemotherapy, 7% underwent HAIC, 4% underwent radiotherapy, and 2% underwent hepatectomy/LAT.
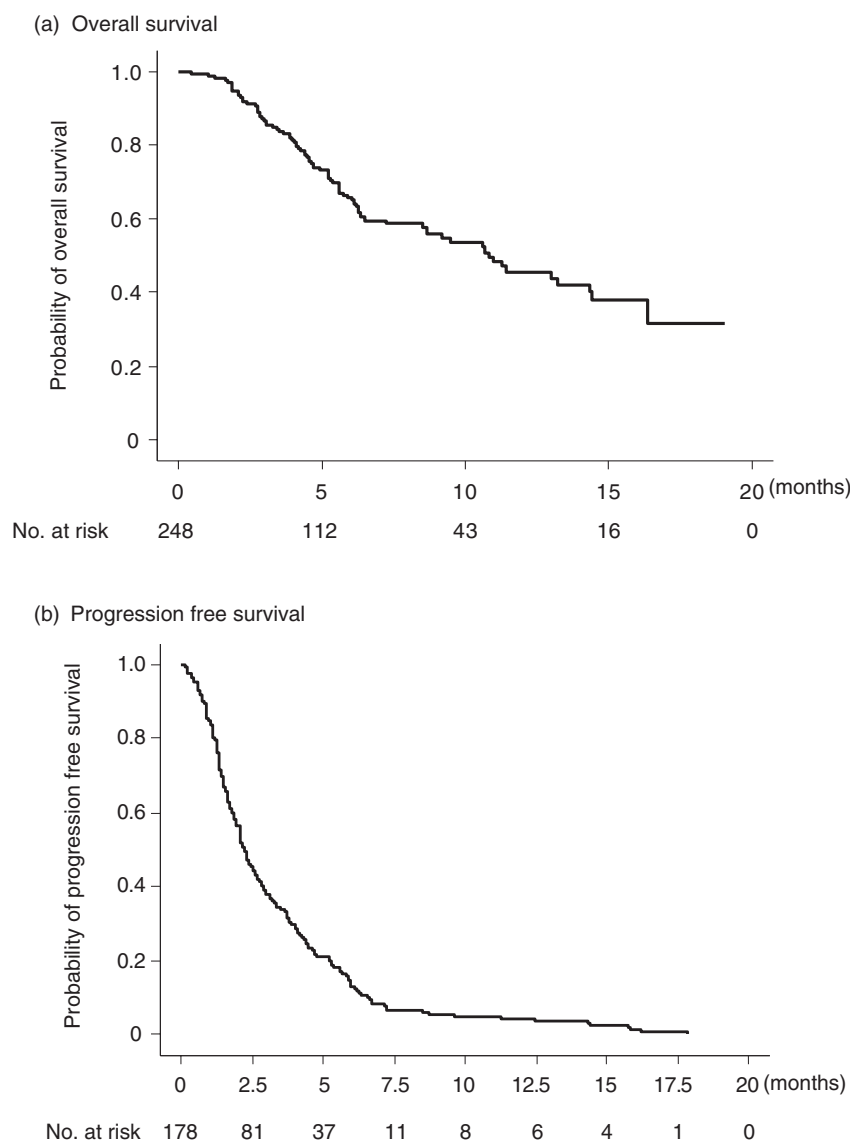
Figure 1 Therapeutic efficacy of sorafenib. (a) Overall survival. (b) Progression free survival.

Progressive disease (PD) was confirmed in 165 patients in the sorafenib group during the study's observation period, of whom a further 23 patients (14%) underwent continued oral administration of sorafenib for ≥1 month after PD confirmation. Comparison of these 23 patients with those in whom therapy was discontinued did not reveal any significant differences in OS, and no data are currently available regarding the efficacy/safety of continued sorafenib administration after confirmation of PD.

Predictors of therapeutic efficacy

CQ1-8 What are the predictors of therapeutic efficacy for sorafenib therapy?

Recommendation Clear predictors of therapeutic efficacy for sorafenib have yet to be established, but the number of intrahepatic lesions and pretreatment levels of tumor markers (AFP, PIVKA-II [DCP]) may be predictors of efficacy.

Scientific statement A study of biomarkers in patients treated with sorafenib has suggested the efficacy of sorafenib is associated with low serum HGF and high c-KIT levels at baseline.[25] Efficacy of sorafenib has also been linked to high levels of ERK expression in tumor tissue.[25,26] However, these reported associations cannot yet be described as established predictors of efficacy, and biomarkers are currently being sought in some prospective clinical trials using sorafenib.

© 2012 The Japan Society of Hepatology

Table 6 Summary of efficacy measures for sorafenib therapy

	NLCT Study ($n = 250$)	SHARP Trial[1] ($n = 299$)	Asia-Pacific Trial[2] ($n = 150$)	Sorafenib phase II[5] ($n = 137$)
OS (months)				
Median	11.0	10.7	6.5	9.2
1-year SR (%)	45	44	–	59
6-month SR (%)	65	–	53	–
PFS (months)	†			
Median	2.1	5.5	3.5	4.2/5.5
Antitumor effect (%)	‡			
Complete remission	0	0	0	0
Partial remission	4	2	5	2
Stable	45	71	46	34
Tumor control rate	49	43	53	–

†Patients who died without confirmation of disease progression were excluded.
‡Patients not evaluated for therapeutic response were excluded.
NLCT, New Liver Cancer Therapies; OS, overall survival; PFS, progression-free survival; SHARP, sorafenib hepatocellular carcinoma assessment randomized protocol.

The current results indicate that early AFP response is a useful surrogate marker to predict treatment response and prognosis in patients with advanced HCC who receive anti-angiogenic therapy.[27]

In an attempt to identify predictors of therapeutic efficacy for sorafenib, the NLCT study examined baseline patient characteristics (age, sex, BMI [body mass index], ECOG-PS [Eastern Cooperative Oncology Group – performance status], hepatic functional reserve, prior treatment, cause of hepatic impairment, clinical laboratory values) and tumor factors (presence or absence of intrahepatic/extrahepatic lesions, maximum tumor size, vascular invasion, stage), and consequently found that tumor control rates tended to be higher in patients with <5 intrahepatic lesions compared to those with ≥5 lesions (54% vs. 40%, respectively; $P = 0.058$). In addition, the tumor control rate was significantly higher in patients with a baseline AFP value <10 ng/mL compared with those with values ≥10 ng/mL (68% vs. 43%, respectively; $P = 0.021$). The tumor control rate also tended to be higher in patients with baseline PIVKA-II (DCP) value <40 mAU/mL than in those with a value of ≥40 mAU/mL (60% vs. 42%, respectively; $P = 0.051$) (Table 7).

Hepatic arterial infusion with miriplatin

Indications

CQ2-1 Is miriplatin a platinum preparation that can be used on renal disorder patients?

Recommendation Renal disorder patients can be treated using miriplatin as long as they are capable of undergoing angiography (serum Cre [creatinine] level <2.0 mg/dL) and as long as administration is performed carefully so as to avoid elevation in serum Cre levels after treatment.

Scientific statement Miriplatin remains in the tumor together with Lipiodol, where it slowly releases platinum compounds. This agent is thus believed to gradually increase serum platinum concentration with minimal adverse effect on renal function.

In a randomized phase II trial comparing miriplatin and zinostatin stimalamer (SMANCS) in patients with normal serum Cre levels, renal dysfunction indicated by serum Cre level >1.5 mg/dL was observed in only 2.4% of patients in the miriplatin treatment group (Table 8).[28]

In the NLCT study, median serum Cre prior to miriplatin therapy was 0.8 mg/dL (range, 0.4–10.5 mg/dL), of which patients with a serum Cre level >1.0 mg/dL accounted for 17.7%. Median serum Cre after treatment was 0.8 mg/dL (range, 0.1–12.6 mg/dL), which was unchanged from baseline, and 94.7% of patients experienced an increase of ≤0.5 mg/dL (Table 9). Only 1.8% of patients exhibited renal dysfunction ≥grade 3 as indicated by serum Cre level >3 mg/dL.

Analysis of patients with baseline serum Cre <2.0 mg/dL shows that just 2.5% of patients increased serum Cre >0.5 mg/dL, and no more than 0.6% of patients experienced renal dysfunction ≥grade 3 (Table 9).

In addition, no serious renal dysfunction was observed after miriplatin administration in patients with serum Cre levels around 2.0 mg/dL.

Table 7 Factor analysis of tumor control with sorafenib therapy

	n	Tumor control rate (%)	$P*$
Age (years)			
≥65	137	49	0.75
<65	56	46	
Gender			
Male	147	50	0.72
Female	43	47	
ECOG-PS			
0	163	50	0.24
1–3	29	38	
Child–Pugh score			
5	65	48	0.82
6	70	44	
7	23	48	
≥8	10	60	
Child–Pugh class			
A	135	46	0.52
B–C	33	56	
Prior treatment			
Yes	173	48	0.87
None	18	50	
HBs antigens			
Positive	36	50	0.91
Negative	149	49	
HCV antibodies			
Positive	112	50	0.66
Negative	77	47	
Intrahepatic lesions			
Yes	174	47	0.26
None	18	61	
Intrahepatic nodules			
≥5	95	40	0.058
<5	83	54	
Advanced vascular invasion			
Yes	36	50	0.68
None	141	46	
Extrapulmonary lesion(s)			
Yes	105	47	0.64
None	88	50	
Maximum tumor size (mm)			
≥30	108	47	0.79
<30	67	49	
Stage (Japanese Classification of Lung Cancer)			
I–II	15	53	0.41
III	53	57	
IV A	31	39	
IV B	84	46	
Initial dose			
Normal dose	153	48	0.91
Reduction	39	49	
Baseline AFP			
≥10	151	43	0.021
<10	25	68	
Baseline PIVKA-II			
≥40	132	42	0.051
<40	40	60	

*Fisher's exact test.
AFP, α fetoprotein; ECOG-PS, Eastern Cooperative Oncology Group Performance status; HBs, Hepatitis B surface antigen; HCV, hepatitis C virus.

Based on these findings, the Study Group considers that miriplatin therapy can be administered without instigating renal dysfunction in patients with serum Cre <2.0 mg/dL who are capable of undergoing angiography.

However, transcatheter arterial infusion (TAI)/TACE with miriplatin simultaneously uses an iodinated contrast medium with drugs that can cause renal dysfunction such as anti-inflammatory analgesics to treat postoperative fever. Sufficient consideration should therefore be given to the risk of drug-induced renal dysfunction, and monitoring of urine volume and fluid replacement should be implemented as necessary.

CQ2-2   Can miriplatin be used safely in patients with Child–Pugh class B?

Recommendation   Miriplatin can be used to treat these patients without causing serious complications.

Furthermore, no demonstrable difference in the antitumor effects of miriplatin has been observed between Child–Pugh class A and B patients.

Scientific statement   The NLCT study included 281 Child–Pugh class A and 144 Child–Pugh class B patients. In Child–Pugh class B patients, the only SAEs ≥grade 3 were fever and anorexia, at incidences of 0.7% each, with no cases of ascites or hepatic failure ≥grade 3 (Table 10). In a study of TAI with miriplatin, in 17 Child–Pugh class B patients, no significant differences were seen in pre- or posttreatment 15-min retention rates of indocyanine green (ICG_{15}), and no SAEs or increased ascites or hepatic failure necessitating additional therapy or prolonged hospitalization were observed.[30]

Although the retrospective analysis of the NLCT study coupled with differences in characteristics of Child–Pugh class A and B patient effectively precludes simple comparisons of these patients, no significant differences in respective AE incidences were seen, apart from a higher frequency of fever and thrombocytopenia ≥grade 3 among Child–Pugh class B patients (Tables 10 and 11).

In terms of evaluation of antitumor effects according to the RECICL proposed by the Liver Cancer Study Group of Japan, the present study did not reveal any significant differences in therapeutic responses of Child–Pugh class A and B patients (Table 12), while 50% of Child–Pugh class B patients in the aforementioned study of TACE with miriplatin achieved a treatment effect (TE) of "TE3" or "TE4", in which tumor was controlled.[30]

CQ2-3   Is miriplatin effective against cisplatin-resistant HCCs?

© 2012 The Japan Society of Hepatology

Table 8 Abnormal clinical laboratory values with miriplatin therapy

	NLCT Study (n = 535)		Phase III Trial[29] (n = 16)		Randomized Phase II Trial[28] (n = 83)	
	Total (%)	G3/4 (%)	Total (%)	G3/4 (%)	Total (%)	G3/4 (%)
Leukopenia	38.2	5.1	51	0	41.0	1.2
Neutropenia	20.1	5.1	63	19	53.0	8.4
Eosinophilia	14.6	–	100	0	84.3	0
Monocytosis	–	–	–	–	57.8	0
Lymphocytopoenia	–	–	51	0	79.5	0
Thrombocytopenia	32.1	9.3	44	0	50.6	1.2
Increased AST	49.9	12.4	56	44	62.7	26.5
Increased ALT	78.4	26.6	44	19	59	24.1
Increased bilirubin	31.6	3.2	31	19	57.8	12.0
Increased γGTP	16.1	2.0	–	–	49.4	0
Increased ALP	12.3	0.2	44	0	30.1	1.2
Elevated Cre	11.5	1.8	25	0	–	2.4†

CTC-AE v3.0 Japan Society of Clinical Oncology Adverse Drug Reaction Criteria.
†Increased Cre data includes G2 patients.
ALT, alanine aminotransferase; AST, aspartate aminotransferase; γ-GTP, γ-glutamyltransferase.

Table 9 Incidence of drug-related adverse events with miriplatin therapy (Renal dysfunction)

Elevated Cre	all (n = 513)	Baseline Cre <2.0 mg/dL	Baseline Cre ≥2.0 mg/dL
≤0.5 mg/dL	94.7%	97.5%	13.3%
0.6–1.0 mg/dL	2.4%	1.7%	20.0%
1.1–2.0 mg/dL	1.2%	0.2%	33.3%
2.1–3.0 mg/dL	0.6%	0.0%	20.0%
>3.0 mg/dL	1.0%	0.6%	13.3%

Recommendation   The clinical usefulness of miriplatin against cisplatin-resistant HCC is not currently known.

Scientific statement   Miriplatin is classified as a third-generation platinum drug and a basic research on the drug suggested potential activity in cisplatin-resistant HCCs because cisplatin-resistant HCC cell lines did not show cross-resistance to miriplatin.[31]

A Japanese Phase I trial combining miriplatin and TAI using Lipiodol (Lip-TAI) on HCC refractory to cisplatin/Lip-TAI has reported a treatment success rate of 18.2%.[32]

Table 10 Comparison of adverse events with miriplatin therapy according to Child–Pugh classification

	All (n = 535)		Child–Pugh class A (n = 281)		Child–Pugh class B (n = 144)	
	Total (%)	G3/4 (%)	Total (%)	G3/4 (%)	Total (%)	G3/4 (%)
Fever	81.3	0.2	75.5	0	86.1	0.7*
Biphasic fever	2.8	–	2.5	–	5.1	–
Anorexia	29.7	0.2	31.7	0	34.0	0.7
Administration site pain	21.2	0	25.6	0	15.3	0
Nausea	18.8	0	21.4	0	12.5	0*
Vomiting	13.5	0	11.6	0	6.1	0
Fatigue	9.3	0	12.2	0	10.3	0
Diarrhea	2.0	0	1.8	0	1.0	0
Ascites	1.2	0	0	0	3.0	0
Hepatic failure	0.3	0.3	0.3	0.3	0	0

CTC-AE v3.0.
*P < 0.05 (A vs. B).

Table 11 Comparison of clinical laboratory value anomalies with miriplatin therapy according to Child–Pugh classification

	All ($n = 535$)		Child–Pugh class A ($n = 281$)		Child–Pugh class B ($n = 144$)	
	Total (%)	G3/4 (%)	Total (%)	G3/4 (%)	Total (%)	G3/4 (%)
Leukopenia	38.2	5.1	18.2	3.3	25.2	5.8
Neutropenia	20.1	5.1	17.3	3.6	23.4	5.8
Eosinophilia	14.6	–	17.9	–	11.5	–
Thrombocytopenia	32.1	9.3	30.9	5.8	30.2	13.7*(G3)
Increased AST	49.9	12.4	45.2	13.5	50.7	19.4
Increased ALT	78.4	26.6	81.0	28.8	70.3	28.3*
Increased bilirubin	31.6	3.2	26.1	0	46.0	5.8*
Increased γGTP	16.1	2.0	15.8	2.6	14.5	0
Increased ALP	12.3	0.2	12.7	0	10.1	0.7
Elevated Cre	11.5	1.8	11.6	2.2	10.8	1.4

CTC-AE v3.0.
*$P < 0.05$ (A vs. B).
ALP, alkaline phosphatase; ALT, alanine aminotransferase; AST, aspartate aminotransferase; γ-GTP, γ-glutamyltransferase.

However, the study was conducted on a small patient population, so the usefulness of this therapy is yet to be established and future studies are awaited.

Furthermore, no data are currently available regarding the efficacy of miriplatin therapy in patients who are unresponsive to TAI/HAIC using cisplatin.

Method of administration

CQ2-4 What are the effects and AEs of combining embolic materials with miriplatin?

Recommendation Combination therapy of embolic materials and miriplatin is expected to improve antitumor effects compared with miriplatin alone, but there is currently insufficient evidence to support this.

Adverse events associated with combination therapy of embolic materials and miriplatin may not differ noticeably from those of conventional TACE therapy using epirubicin.

Scientific statement Compared with stand-alone therapy, the combination of embolic materials in the hepatic arterial catheterization treatment is generally considered to deliver enhanced antitumor effects based on its blood flow blockage effect,[33] so treatment combined with embolic materials are mostly selected for the treatment of HCC. However, Phase I and II trials using miriplatin have opted not to use embolic materials in combination with miriplatin.[29,32]

Meanwhile, two studies on miriplatin used in combination with embolic materials on a small number of patients have reported high rates of treatment success, with TE3 and TE4 scores obtained in 60.0–77.7% of patients.[30,34]

Table 12 Summary of efficacy measures with miriplatin therapy

	NLCT Study			Phase II Trial[29] ($n = 16$)	Randomized Phase II Trial[28] ($n = 83$)
	All ($n = 535$)	Child–Pugh class A ($n = 281$)	Child–Pugh class B ($n = 144$)		
Anti-neoplastic effect (%)					
TE4	22.8	25.3	23.6	56	26.5
TE3	24.3	26.7	20.8	6	25.3
TE2	26.0	26.0	29.9	19	22.9
TE1	16.6	12.5	17.4	19	20.5
Not evaluated	10.3	9.6	8.3	0	4.8
TE3 + TE4	47.1	52.0	44.4	61	51.8

Response Evaluation Criteria in Cancer of the Liver' (RECICL).

© 2012 The Japan Society of Hepatology

Table 13 Independent factors contributing to effective (TE3/4) achievement with miriplatin therapy

Factor	Category	Risk ratio	95% CI	*P*-value
Embolic material	None	1		<0.001
	Yes	3.66	2.13–6.29	
No. tumors	Single	1		0.017
	2–3	1.01		
	4–9	0.66		
	≥10	0.3	0.13–0.67	
Past history of TAE	None	1		0.018
	Yes	0.48	0.26–0.88	

Cox proportional hazards model.
CI, confidence interval; TAE, transcather arterial embolization.

In the NLCT study, embolic material was used in combination with miriplatin on 473 patients (88.4%). Simple comparison of patients undergoing miriplatin/embolic material combination therapy and those who underwent miriplatin alone therapy was not possible due to the retrospective nature of this study, as well as the different patient characteristics of the respective treatment groups. However, antitumor effects were higher in the miriplatin/embolic material therapy group than in the miriplatin therapy group, at 49% and 31%, respectively (Fig. 2). Analysis of independent factors contributing to the achievement of TE3/4 scores in TAI/TACE therapy using miriplatin showed that the use of embolic material had a higher risk ratio of 3.66 (*P* < 0.001) (Table 13).
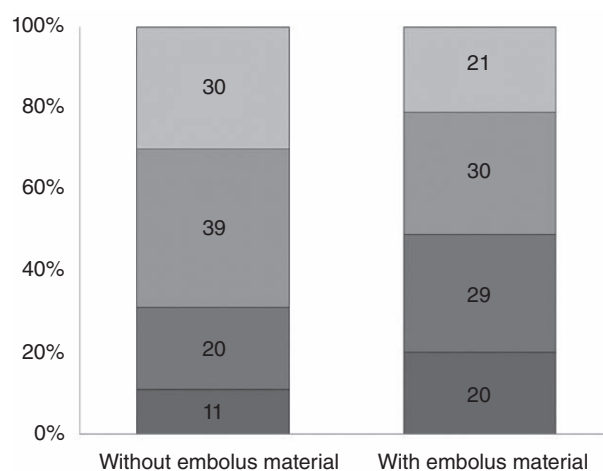
Figure 2 Therapeutic efficacy of miriplatin with or without embolus material.

A Phase III trial of TACE using miriplatin is currently underway, and the results will likely be useful in investigating the efficacy of using miriplatin in combination with embolic materials.

In the NLCT study, patients who underwent combination therapy with embolic material showed a high incidence of fever, suspected to be due to post-embolization syndrome. Although high incidences of hematological AEs neutropenia and elevated AST were seen, no significant differences were identified in the incidences of most AEs, and no serious complications such as hepatic failure or ascites were observed (Tables 14 and 15).

Table 14 Comparison of adverse events with or without embolic material during miriplatin therapy

	All (n = 535)		TACE patients (n = 425)		TAI patients (n = 54)	
	Total (%)	G3/4 (%)	Total (%)	G3/4 (%)	Total (%)	G3/4 (%)
Fever	81.3	0.2	84.4	0.2	56.1	0*
Biphasic fever	2.8	–	3.0	–	0	–
Anorexia	29.7	0.2	30.4	0.2	22.4	0
Administration site pain	21.2	0	22.2	0	13.8	0
Nausea	18.8	0	20.1	0	4.0	0
Vomiting	13.5	0	14.2	0	0	0
Fatigue	9.3	0	9.2	0	–	–
Diarrhea	2.0	0	2.1	0	0	0
Ascites	1.2	0	0.9	0	5.6	0
Hepatic failure	0.3	0.3	0.3	0.3	0	0

CTC-AE v3.0.
*P < 0.05 (TACE vs. TAI).
TACE, transcatheter arterial chemoembolization; TAI, transcatheter arterial infusion.

Table 15 Comparison of abnormal clinical laboratory values with or without embolic material during miriplatin therapy

	All (n = 535)		TACE patients (n = 425)		TAI patients (n = 54)	
	Total (%)	G3/4 (%)	Total (%)	G3/4 (%)	Total (%)	G3/4 (%)
Leukopenia	38.2	5.1	22.8	5.5	20.4	1.9
Neutropenia	20.1	5.1	21.4	5.5	3.7	0*
Eosinophilia	14.6	–	14.8	–	11.8	–
Thrombocytopenia	32.1	9.3	33.2	10.4	24.1	0
Increased AST	49.9	12.4	52.8	19.3	25.9	8.6*
Increased ALT	78.4	26.6	78	24.5	81.5	44.4*
Increased bilirubin	31.6	3.2	32.1	3.3	27.8	0
Increased γ-GTP	16.1	2.0	16.1	1.8	14.8	3.7
Increased ALP	12.3	0.2	12.6	0.2	9.3	0
Elevated Cre	11.5	1.8	10.7	1.8	18.5	1.9

CTC-AE v3.0.
*$P < 0.05$ (TACE vs. TAI).
ALP, alkaline phosphatase; ALT, alanine aminotransferase; AST, aspartate aminotransferase; γ-GTP, γ-glutamyltransferase; TACE, transcatheter arterial chemoembolization; TAI, transcatheter arterial infusion.

Similarly, a small pilot study (Phase II clinical trial) on miriplatin combined with an embolic material found some mild complications, but none of a serious nature.[34] Another study on the small number of patients did not reveal any serious complications.[30]

CQ2-5 Is standard hydration required prior to administration of miriplatin?

Recommendation Standard hydration is not required except in the case of renal failure.

Scientific statement Sufficient hydration before and after administration of cisplatin (IA-call, Nippon Kayaku, Tokyo, Japan) used in HAIC is necessary to prevent nephrotoxicity.

Miriplatin is highly soluble in Lipiodol and remains in tumor with Lipiodol, where it continuously releases platinum compounds.[35] So only a small amount enters systemic circulation expecting to reduce systemic AEs, including renal dysfunction.

As stated in CQ1, the effect of miriplatin on renal function is considered to be mild. Two of the aforementioned Phase II trials did not perform pretreatment hydration to prevent renal impairment.[28,30] In the NLCT study, patients with advanced renal insufficiency were excluded and no serious renal impairment occurred in patients treated with miriplatin without prior hydration.

Adverse events

CQ2-6 What are the adverse events associated with miriplatin therapy?

Recommendation Post-embolization syndrome characterized mainly by fever is often seen, and biphasic fever is relatively infrequent. Incidences of nausea and vomiting are also low compared with other platinum agents. Complications such as ascites, liver abscess, biloma, and dyspnea have incidences of about 1%.

Scientific statement In the NLCT study, post-embolization syndrome was observed in ≥90% of patients treated with miriplatin. However, the incidence of biphasic fever, which is said to be a characteristic AE associated with miriplatin, was low at 2.8% (Tables 16, 17).

Incidences of nausea and vomiting were low compared with other platinum agents, at 18.8% and 13.5%, respectively.

Hematological AEs were leukopenia at 38.2%, thrombocytopenia at 32.1%, and neutropenia at 20.1%. Incidence of eosinophilia, which is also reported as a characteristic AE of miriplatin, was relatively low at 14.6% (Table 8).[28,29]

Abnormal hepatic function was frequent, with elevated AST and ALT occurring in 49.9% and 78.4% of patients, respectively, of whom a further 12.4% and 26.6% had respective AST and ALT values ≥grade 3. Elevated T-Bil was seen in 31.6% of patients, of whom 3.2% had value ≥grade 3, more than three times the upper limits of normal (ULN).

CQ2-7 What is the extent of deterioration in hepatic function caused by TAI/TACE using miriplatin?

© 2012 The Japan Society of Hepatology

Table 16 Incidence of drug-related adverse events with miriplatin therapy (1)

	NLCT Study (n = 535)		Phase II Trial[29] (n = 16)		Randomized Phase II Trial[28] (n = 83)	
	Total (%)	G3/4 (%)	Total (%)	G3/4 (%)	Total (%)	G3/4 (%)
Fever	81.3	0.2	94	0	96.4	3.6
Biphasic fever	2.8	–	–	–	–	–
Anorexia	29.7	–	–	–	–	–
Abdominal pain	21.2	0	50	0	–	–
Nausea	18.8	0	25	0	–	–
Vomiting	13.5	0	–	–	55.4	1.2
Fatigue	9.3	0	–	–	39.8	0
Chills	–	0	–	–	39.8	0
Administration site pain	21.2	0	50	0	43.4	0
Diarrhea	2.0	0	31	0	–	–
Ascites	1.2	0	–	–	–	–
Hepatic failure	0.3	0.3	–	–	–	–
Vascular injury	–	–	–	–	0	0

CTC-AE v3.0 Japan Society of Clinical Oncology Adverse Drug Reaction Criteria

Recommendation Typically, no deterioration is seen in postoperative ICG_{15}, but prothrombin time (PT) ratio (%) may display a transient decline.

Scientific statement Hepatic impairment after miriplatin administration has been reported to peak within 2 weeks in 46% of patients, at 3–5 weeks in 23% of patients, and at 9–11 weeks in 31% of patients.[29]

The NLCT study also found that in evaluable patients, ICG_{15} values had not deteriorated at 1–2 weeks after therapy and that PT ratio (%) exhibited a transient decline, but subsequently recovered in the majority of patients.

Child–Pugh class B patients did not find any significant differences in pre- or post-treatment ICG_{15}, and did not find any SAEs or increased ascites or hepatic failure necessitating additional therapy and prolonged hospitalization.[32]

However, the safety of miriplatin used in combination with embolic materials has yet to be established, and a Phase III study on concomitant use of miriplatin and embolizing agents is currently underway.[34]

Table 17 Incidence of drug-related adverse events with miriplatin therapy (2)

	Incidence (%)
Ascites	1.2
Liver abscess	0.6
Biloma	0.3
Dyspnea	0.3

CQ2-8 Does vascular injury occur after intra-arterial administration of miriplatin?

Recommendation Vascular injuries such as hepatic artery occlusion, arterial stenosis and arterioportal shunts, and hepatic lobar atrophy caused by vascular damage are rare.

Scientific statement No reports have described vascular injuries from non-hematological toxicity in previous Japanese Phase I and II trials on miriplatin therapy.[29,32] Likewise, no vascular injuries have been reported in the NLCT study (Table 16). In TAI without the use of embolic materials, the aforementioned randomized phase II trial comparing miriplatin and zinostatin stimalamer (SMANCS) found that vascular injuries occurred in 48.4% of the SMANCS treatment group (n = 31), but that no vascular injuries occurred in the miriplatin treatment group (n = 73).[28] In a limiting study performing follow-up angiography on nine patients at 2–6 months after treatment, no arterial stenoses, arterial occlusions, or arterioportal shunts were observed.[30]

Evaluation of therapeutic response

CQ2-9 After how many weeks should therapeutic response to miriplatin be evaluated?

Recommendation Non-specific accumulation of Lipiodol appears on dynamic CT at 1 week after administration of miriplatin, so evaluation of therapeutic response should preferably be performed at 4–8 weeks after administration.

Scientific statement Evaluation of therapeutic response performed at 1 day or 1 week after starting miriplatin therapy may result in overestimation of response due to the appearance of non-specific Lipiodol deposits. Evaluation of therapeutic response using dynamic CT at 4–8 weeks after therapy is therefore preferable, to allow these non-specific deposits to disappear. In the above-mentioned Phase I clinical trial, therapeutic response to miriplatin was evaluated with dynamic CT at 1 week, 5 weeks, and 3 months after therapy,[32] while the Phase II trial evaluated the antitumor effects of miriplatin using dynamic CT every 3 months.[29]

REFERENCES

1 Llovet JM, Ricci S, Mazzaferro V *et al*. Sorafenib in advanced hepatocellular carcinoma. *N Engl J Med* 2008; **359**: 378–90.

2 Cheng AL, Kang YK, Chen Z *et al*. Efficacy and safety of sorafenib in patients in the Asia-Pacific region with advanced hepatocellular carcinoma: a phase III randomised, double-blind, placebo-controlled trial. *Lancet Oncol* 2009; **10**: 25–34.

3 Kudo M. *Chapter 3 Treatment Strategy for HCC Cases Refractory for TACE (Japanese) Hepatocelluar Carcinoma Practice Manual*, 2nd edn. Tokyo: Igaku-syoin, 2010; 118–21.

4 Nexavar® adverse reaction reports liver injury and interstitial pulmonary disease (Japanese). 2010. Bayer Heathcare May.

5 Abou-Alfa GK, Schwartz L, Ricci S *et al*. Phase II study of sorafenib in patients with advanced hepatocellular carcinoma. *J Clin Oncol* 2006; **24**: 4293–300.

6 Nexavar® special post marketing surveillance report for unresectable hepatocelluar carcinoma (Japanese). 2010. Bayer Heathcare September.

7 Akaza H, Okita K *et al*. Guideline for proper use of Nexavar® 2nd edition (Japanese). 2010. Bayer Heathcare May

8 Furuse J, Ishii H, Nakachi K *et al*. Phase I study of sorafenib in Japanese patients with hepatocellular carcinoma. *Cancer Sci* 2008; **99**: 159–65.

9 Lencioni R, Marrero J, Venook A *et al*. Design and rationale for the non-interventional Global Investigation of Therapeutic DEcisions in Hepatocellular Carcinoma and Of its Treatment with Sorafenib (GIDEON) study. *Int J Clin Pract* 2010; **64**: 1034–41.

10 Marrero J. Sorafenib treatment and safety profile in Child-Pugh B patients characterized in first interim results of Global Investigation of therapeutic DEcisions in hepatocellular carcinoma and Of its treatment with sorafeNib (GIDEON) study 61st Annual meeting of the American Association for the Study of Liver Diseases. 2010. 1721, poster presentation.

11 Okita K. Phase III study of sorafenib in patients in Japan and South Korea with advanced hepatocellular carcinoma

treated after transarterial chemoembolization. 2010. Gastrointestinal Cancers Symposium 2010.

12 Printz C. Clinical trials of note. Sorafenib as adjuvant treatment in the prevention of disease recurrence in patients with hepatocellular carcinoma (HCC) (STORM). *Cancer* 2009; **115**: 4646.

13 Zhao JD, Liu J, Ren ZG *et al*. Maintenance of Sorafenib following combined therapy of three-dimensional conformal radiation therapy/intensity-modulated radiation therapy and transcatheter arterial chemoembolization in patients with locally advanced hepatocellular carcinoma: a phase I/II study. *Radiat Oncol* 2010; **5**: 12.

14 Hsieh CH, Jeng KS, Lin CC *et al*. Combination of sorafenib and intensity modulated radiotherapy for unresectable hepatocellular carcinoma. *Clin Drug Investig* 2009; **29**: 65–71.

15 Abou-Alfa GK, Johnson P, Knox JJ *et al*. Doxorubicin plus sorafenib vs doxorubicin alone in patients with advanced hepatocellular carcinoma: a randomized trial. *JAMA* 2010; **304**: 2154–60.

16 Hsu CH, Shen YC, Lin ZZ *et al*. Phase II study of combining sorafenib with metronomic tegafur/uracil for advanced hepatocellular carcinoma. *J Hepatol* 2010; **53**: 126–31.

17 Prete SD, Montella L, Caraglia M *et al*. Sorafenib plus octreotide is an effective and safe treatment in advanced hepatocellular carcinoma: multicenter phase II So.LAR. study. *Cancer Chemother Pharmacol* 2010; **66**: 837–44.

18 Bhojani N, Jeldres C, Patard JJ *et al*. Toxicities associated with the administration of sorafenib, sunitinib, and temsirolimus and their management in patients with metastatic renal cell carcinoma. *Eur Urol* 2008; **53**: 917–30.

19 Lencioni R, Llovet JM. Modified RECIST (mRECIST) assessment for hepatocellular carcinoma. *Semin Liver Dis* 2010; **30**: 52–60.

20 Kudo M, Kubo S, Takayasu K *et al*. Response Evaluation Criteria in Cancer of the Liver (RECICL) proposed by the Liver Cancer Study Group of Japan (2009 Revised Version). *Hepatol Res* 2010; **40**: 686–92.

21 Spira D, Fenchel M, Lauer UM *et al*. Comparison of different tumor response criteria in patients with hepatocellular carcinoma after systemic therapy with the multikinase inhibitor sorafenib. *Acad Radiol* 2011; **18**: 89–96.

22 Horger M, Lauer UM, Schraml C *et al*. Early MRI response monitoring of patients with advanced hepatocellular carcinoma under treatment with the multikinase inhibitor sorafenib. *BMC Cancer* 2009; **9**: 208.

23 Murata K, Suzuki H, Okano H *et al*. Hypoxia-induced des-gamma-carboxy prothrombin production in hepatocellular carcinoma. *Int J Oncol* 2010; **36**: 161–70.

24 Ueshima K, Kudo M. PIVKA-II is a predictive marker in the treatment response of sorafenib to hepatocellular carcinom. *Kanzo* 2010; **51**: 681.

25 Llovet JM. Biomarkers predicting outcome of patients with hepatocellular carcinoma: results from the randomized

phase III SHARP trial Presidential Plennary Session. *Hepatology* 2008; **48**: 372A, Abstract no. 149.

26 Zhang Z, Zhou X, Shen H *et al*. Phosphorylated ERK is a potential predictor of sensitivity to sorafenib when treating hepatocellular carcinoma: evidence from an *in vitro* study. *BMC Med* 2009; **7**: 41.

27 Shao YY, Lin ZZ, Hsu C *et al*. Early alpha-fetoprotein response predicts treatment efficacy of antiangiogenic systemic therapy in patients with advanced hepatocellular carcinoma. *Cancer* 2010; **116**: 4590–6.

28 Okusaka T, Kasugai H, Ishii H. A randomized phase II trial of intra-arterial chemotherapy using a novel lipophilic platinum derivative (SM-11355) in comparison with zinostatin sitmalamer in patients with hepatocellular carcinoma ASCO Annual Meeting 2009. 2009. #4583 Poster session.

29 Okusaka T, Okada S, Nakanishi T *et al*. Phase II trial of intra-arterial chemotherapy using a novel lipophilic platinum derivative (SM-11355) in patients with hepatocellular carcinoma. *Invest New Drugs* 2004; **22**: 169–76.

30 Imai N, Ikeda K, Seko Y. Transcatheter arterial chemotherapy with miriplatin for patients with hepatocellular carcinoma and Child-Pugh B liver cirrhosis. *Kanzo* 2010; **51**: 758–60.

31 Hanada M, Takasu H, Kitaura M. Acquired resistance to miriplatin in rat hepatoma AH109A/MP10 is associated with increased Bcl-2 expression, leading to defects in inducing apoptosis. *Oncol Rep* 2010; **24**: 1011–8.

32 Fujiyama S, Shibata J, Maeda S *et al*. Phase I clinical study of a novel lipophilic platinum complex (SM-11355) in patients with hepatocellular carcinoma refractory to cisplatin/lipiodol. *Br J Cancer* 2003; **89**: 1614–9.

33 Yamashita Y, Takahashi M, Fujimura N *et al*. Clinical evaluation of hepatic artery embolization: comparison between Gelfoam and Lipiodol with anticancer agent. *Radiat Med* 1987; **5**: 61–7.

34 Ikeda K, Okusaka T, Ikeda M *et al*. [Transcatheter arterial chemoembolization with a lipophilic platinum complex SM-11355(miriplatin hydrate) – safety and efficacy in combination with embolizing agents]. *Gan to Kagaku Ryoho* 2010; **37**: 271–5.

35 Maeda M, Uchida N, Sasaki T. Liposoluble platinum(II) complexes with antitumor activity.(Japanese) Japanese Journal of. *Cancer Res* 1986; **77**: 523–5.

ORIGINAL ARTICLE—LIVER, PANCREAS, AND BILIARY TRACT

Assessment of Gd-EOB-DTPA-enhanced MRI for HCC and dysplastic nodules and comparison of detection sensitivity versus MDCT

Tatsuo Inoue · Masatoshi Kudo · Mina Komuta · Sosuke Hayaishi · Taisuke Ueda · Masahiro Takita · Satoshi Kitai · Kinuyo Hatanaka · Norihisa Yada · Satoru Hagiwara · Hobyung Chung · Toshiharu Sakurai · Kazuomi Ueshima · Michiie Sakamoto · Osamu Maenishi · Tomoko Hyodo · Masahiro Okada · Seishi Kumano · Takamichi Murakami

Abstract

Background We aimed to evaluate gadolinium ethoxybenzyl diethylenetriamine pentaacetic acid (Gd-EOB-DTPA)-enhanced magnetic resonance imaging (MRI) for the detection of hepatocellular carcinomas (HCCs) and dysplastic nodules (DNs) compared with dynamic multi-detector row computed tomography (MDCT), and to discriminate between HCCs and DNs.

Methods Eighty-six nodules diagnosed as HCC or DNs were retrospectively investigated. Gd-EOB-DTPA-enhanced MRI and dynamic MDCT were compared with respect to their diagnostic ability for hypervascular HCCs and detection sensitivity for hypovascular tumors. The ability of hepatobiliary images of Gd-EOB-DTPA-enhanced MRI to discriminate between these nodules was assessed. We also calculated the EOB enhancement ratio of the tumors.

Results For hypervascular HCCs, the diagnostic ability of Gd-EOB-DTPA-enhanced MRI was significantly higher than that of MDCT for tumors less than 2 cm ($p = 0.048$). There was no difference in the detection of hypervascular HCCs between hepatobiliary phase images of Gd-EOB-DTPA-enhanced MRI (43/45: 96%) and dynamic MDCT (40/45: 89%), whereas the detection sensitivity of hypovascular tumors by Gd-EOB-DTPA-enhanced MRI was significantly higher than that by dynamic MDCT (39/41: 95% vs. 25/41: 61%, $p = 0.001$). EOB enhancement ratios were decreased in parallel with the degree of differentiation in DNs and HCCs, although there was no difference between DNs and hypovascular well-differentiated HCCs.

Conclusion The diagnostic ability of Gd-EOB-DTPA-enhanced MRI for hypervascular HCCs less than 2 cm was significantly higher than that of MDCT. For hypovascular tumors, the detection sensitivity of hepatobiliary phase images of Gd-EOB-DTPA-enhanced MRI was significantly higher than that of dynamic Gd-EOB-DTPA-enhanced MRI and dynamic MDCT. It was difficult to distinguish between DNs and hypovascular well-differentiated HCCs based on the EOB enhancement ratio.

Keywords Gd-EOB-DTPA · Hepatocellular carcinoma · Dysplastic nodule

T. Inoue · M. Kudo (✉) · S. Hayaishi · T. Ueda · M. Takita ·
S. Kitai · K. Hatanaka · N. Yada · S. Hagiwara · H. Chung ·
T. Sakurai · K. Ueshima
Division of Gastroenterology and Hepatology,
Department of Internal Medicine, Kinki University Faculty
of Medicine, 377-2 Ohno-Higashi, Osaka-Sayama,
Osaka 589-8511, Japan
e-mail: m-kudo@med.kindai.ac.jp

M. Komuta · M. Sakamoto
Department of Pathology, Keio University Faculty of Medicine,
35 Shinanomachi, Shinjyuku-ku, Tokyo 160-8582, Japan

O. Maenishi
Department of Pathology, Kinki University Faculty of Medicine,
377-2 Ohno-Higashi, Osaka-Sayama, Osaka 589-8511, Japan

T. Hyodo · M. Okada · S. Kumano · T. Murakami
Department of Radiology, Kinki University Faculty of Medicine,
377-2 Ohno-Higashi, Osaka-Sayama, Osaka 589-8511, Japan

Introduction

Hepatocellular carcinoma (HCC) is one of the most common cancers worldwide and is a major cause of death in patients with cirrhosis. Therefore, it is important to detect and treat HCC at an early stage. The development of screening programs for high-risk HCC patients, involving periodic US, computed tomography (CT), and measurement of tumor markers [alpha-fetoprotein (AFP), protein induced by vitamin K absence or antagonist II, and

AFP-L3], has enabled small HCCs less than 2 cm in diameter to be easily detected and safely resected. As a result, we have encountered more early-stage HCCs, low-grade dysplastic nodules (LGDNs), and high-grade dysplastic nodules (HGDNs). Pathologically, almost all human HCCs develop in a multistep fashion in the following sequence: LGDN, HGDN, early HCC, well-differentiated HCC, nodule-in-nodule HCC, and, finally, moderately differentiated HCC.

The majority of early HCCs and DNs are hypo- or isovascular upon dynamic CT, angiography, and contrast-enhanced US [1–4]. Therefore, the enhancement pattern of such lesions when these imaging modalities are used is notably different from that of hypervascular HCC. However, it is difficult to differentiate DNs and hypovascular well-differentiated HCCs on the basis of intratumoral hemodynamics [1–4]. In the process of the multistep progression of hepatocarcinogenesis, Kupffer cells in the tumor gradually decrease as the tumor becomes less differentiated. Because Kupffer cells are absent in most classical HCCs, such tumors appear as high-intensity regions when analyzed by superparamagnetic iron oxide-enhanced magnetic resonance imaging (SPIO-MRI). Previous reports have suggested that SPIO-MRI is useful for the diagnosis of HCCs [5–7]. However, imaging findings of DNs and hypovascular well-differentiated HCCs show considerable overlap, making it difficult to differentiate between these lesions. Recently, a new liver-specific MR contrast agent, gadoxetic acid [gadolinium-ethoxybenzyl (Gd-EOB)-diethylenetriamine pentaacetic acid (DTPA)], has been introduced for clinical imaging.

Gd-EOB-DTPA-enhanced MRI enables the concurrent assessment of tumor vascularity and hepatocellular-specific properties within the tumor, and has had a significant impact on the imaging of HCC [8, 9]. However, little is known about the detection and diagnostic abilities of the hepatobiliary phase of Gd-EOB-DTPA-enhanced MRI for HCCs and borderline lesions, such as DNs and non-hypervascular well-differentiated HCCs.

The purpose of this study was to compare the ability of Gd-EOB-DTPA-enhanced MRI and multi-detector row CT (MDCT) to diagnose and detect HCC and borderline lesions, and to investigate whether hepatobiliary phase images can discriminate between hypovascular well-differentiated HCCs and DNs, which are difficult to distinguish based on tumor hemodynamics.

Methods

Patients

Between February 2008 and October 2009, 396 patients with 545 hepatic nodules underwent Gd-EOB-DTPA-

Table 1 Baseline patient characteristics

Characteristics	Value
Sex (male/female)	42/24
Median age, years	66 (range 54–84)
Child–Pugh classification (A/B/C)	53/13/0
Etiology and histology of underlying liver disease	
HCV-related chronic hepatitis	16
HCV-related cirrhosis	30
HBV-related chronic hepatitis	9
HBV-related cirrhosis	11

HCV hepatitis C virus

enhanced MRI. Of these patients, 66 patients with 86 nodules pathologically diagnosed as HCCs or DNs were retrospectively enrolled in this study. Baseline characteristics of the patients are shown in Table 1. Written informed consent was obtained from all patients. This study was approved by the institutional review board of the Kinki University Faculty of Medicine.

Diameter of tumors

Eighty-three of the 86 tumors were measured using hepatobiliary phase images of Gd-EOB-DTPA MRI, and the 3 remaining tumors, which showed iso-intensity on hepatobiliary phase images of Gd-EOB-DTPA MRI, were measured using B-mode US.

Diagnosis of HCC and DN

All 86 nodules were diagnosed pathologically as HCC (77 nodules) or DN (9 nodules).

Imaging

All imaging methods in each patient were performed within 1 month of each other.

CT during arterial portography (CTAP), and CT during hepatic arteriography (CTHA) examinations

For CTAP and CTHA, the femoral superficial artery was punctured under local anesthesia, using the Seldinger technique via an adapted fluoroscopic system and a 4-French angiographic catheter. CTAP imaging was started 43 s after the injection of 60 ml iopamidol (150 mg I/ml) at a rate of 2 ml/s via the catheter with its tip located in the superior mesenteric artery. After an interval of more than 10 min, early-phase CTHA imaging was started 10 s after the injection of 30 ml iopamidol (150 mg I/ml) at a rate of 1.5 ml/s via the catheter with its tip located in the common

hepatic artery. Late-phase scanning was started 15 s after the end of early-phase scanning. The CT unit used in this study was a 64-channel Light Speed VCT Vision unit (GE Healthcare, Milwaukee, WI, USA). CTAP, CTHA early-phase, and CTHA late-phase images were obtained during a single breath-hold with the entire liver imaged using a helical CT system (auto mA 120 kV, rotation time 0.4 s, image thickness/image interval 5.0 mm/5.0 mm, helical pitch 1.375).

Sonazoid-enhanced harmonic US

To minimize variation between operators, the Sonazoid-enhanced harmonic US studies were performed by either of two operators (K.H., M.K.). After the injection of Sonazoid (Daiichi-Sankyo, Tokyo, Japan; GE Health Care, Oslo, Norway), when the first microbubble signal appeared in the liver parenchyma, the patient was requested to hold his/her breath. The images of the ideal scanning plane were displayed in real-time mode for all phases. The vascular findings on phase-inversion harmonic US were shown as tumor vessel flow in the early vascular phase (about 15–40 s after the injection of Sonazoid). For imaging evaluation, two physicians (S.H., K.U.) reviewed the clips of contrast-enhanced harmonic US off-line in a consensus manner.

Evaluation of tumor vascularity

The evaluation of tumor vascularity was performed on the basis of CTHA–CTAP or contrast-enhanced US images. Hypervascular HCC was defined as follows: arterial blood flow into the tumor draining into surrounding hepatic sinusoids (corona enhancement) observed on CTHA, and portal blood flow absent on CTAP, or images showing hyperperfusion in the early vascular phase compared with the surrounding liver parenchyma and washout in the late vascular phase on contrast-enhanced (CE) US. Other tumors which did not have arterial blood flow on CTHA and hyperperfusion in the early vascular phase on CEUS were classified as hypovascular.

Dynamic multi-detector row CT examination

All patients underwent MDCT scanning using a 64-channel Light Speed VCT Vision unit (GE Healthcare; auto mA 120 kV, rotation time 0.4 s, image thickness and image interval 5.0 mm, helical pitch 1.375). Imaging was performed during suspended full inspiration by using a bolus trigger technique. A region of interest (ROI) was drawn for the abdominal aorta at the celiac artery. A total dose of 600 mg I/kg body weight of non-ionic contrast material containing 300–370 mg/ml iodine was administered

intravenously with a dual-head injector (Envision CT; Medrad, Warrendale, PA, USA) at a fixed duration of 30 s. The arterial phase scanning commenced manually 6 s after the attenuation value in the ROI reached a plateau and the aortic curve was decreasing. The portal venous phase scan was started 30 s after the end of the arterial phase scan. Each of the entire liver scans, performed in the cephalad-caudal orientation, was completed in 5 s.

In the assessment of the diagnostic ability of dynamic MDCT for hepatic nodules, when reviewers detected a lesion on dynamic MDCT showing arterial phase hypervascularity with portal venous phase washout, it was defined as typical HCC appearance. A tumor was defined as a non-typical lesion if it did not show enhancement in the arterial phase and the washout pattern on portal venous phase was vague, or the tumor showed enhancement in the arterial phase but no washout in the portal venous phase.

Dynamic MDCT studies were evaluated by blinded reviewers (MDCT; T.I., M.K., H.C.) who were unaware of the findings of the other imaging techniques and of the pathologic and clinical data. In cases of discrepancy, the reviewers assessed the saved images together and reevaluated their findings to reach an agreement.

MR examination

MRI was performed at 1.5 or 3 T using commercially available MRI systems; i.e., a Gyroscan Intera Nova (1.5 T) or an Achieva (3 T) series (Philips Medical System, Best, The Netherlands). All images were obtained in the axial plane. At first, MRIs were obtained using a T1-weighted gradient echo (GRE) sequence (dual echoes; in-phase and out-of-phase) and three-dimensional (3D) fat-suppressed T1-weighted GRE sequences. Gd-EOB-DTPA (Primovist®; Bayer Schering Pharma, Berlin, Germany) was used as a hepatocytic contrast agent. All patients received 0.025 mmol/kg body weight of Gd-EOB-DTPA administered at 2 ml/s though an intravenous line placed in a cubital or cephalic vein and flushed with 35 ml of 0.9% saline at the same rate. Unenhanced scans were obtained using a T1-weighted GRE sequence (dual echoes; in-phase and opposed-phase) and T1-weighted high-resolution sequence. After the injection of Gd-EOB-DTPA, imaging in the arterial (22–35 s post-injection), portal venous (70 s post-injection), and hepatobiliary phases (20 min after injection) was obtained using a T1-weighted high-resolution sequence in a single breath-hold (18–20 s).

Hepatobiliary phase images were obtained 20 min after injection using 3D fat-suppressed T1-weighted gradient echo sequences with the Gyroscan Intera Nova (TR/TE 4.5 m/2.2 ms, flip angle 10°, sensitivity encoding (SENSE) factor 1.8, slice thickness 5 mm, slice interval −2.5 mm, matrix 512 × 512 × 2.50 mm, reconstructed voxel size

0.73 × 0.73 × 2.50 mm, fat saturation +, field of view 375 mm, breath held for 17.7 s) and Achieva (TR/TE ms/ 1.4 ms, flip angle 10°, SENSE factor 1.9, slice thickness 3 mm, slice interval 1.5 mm, matrix 512 × 512 × 1.50 mm, reconstructed voxel size 0.68 × 0.68 × 1.50 mm, fat saturation +, field of view 350 mm, breath held for 19 s). MRI scans were interpreted by 3 experienced radiologists (M.O., S.K., T.M.) who were unaware of the findings of the other imaging techniques or of the pathologic and clinical data. In cases of discrepancy, the reviewers assessed the saved images together and reevaluated their findings to reach an agreement.

In the assessment of the diagnostic ability of Gd-EOB-DTPA-enhanced MRI for hypervascular HCC, when reviewers detected a lesion on Gd-EOB-DTPA-enhanced MRI showing arterial phase hypervascularity with portal phase washout or low-intensity areas in the hepatobiliary phase, it was defined as the typical appearance of HCC. A tumor was defined as a non-typical lesion if it did not show enhancement in the arterial phase and the washout pattern in the portal phase was vague or the tumor showed enhancement in the arterial phase but no washout in the portal phase and iso- to high intensity in the hepatobiliary phase. For qualitative analysis, we used the following 5-point scale to evaluate the lesion intensity relative to the surrounding liver parenchyma in the hepatobiliary phase of Gd-EOB-DTPA-enhanced MRI: 1 = definitely iso-intensity; 2 = slightly low intensity; 3 = definitely low intensity; 4 = slightly high intensity; 5 = definitely high intensity. When the lesion was rated as 2–5, it was defined as the presence of a tumor. In cases of discrepancy, the reviewers assessed the saved images together and reevaluated their findings to reach an agreement.

For the quantitative analysis of HCCs and DNs, the enhancement ratio (ER) of each lesion was calculated according to the method of Kogita et al. [10]. Briefly, relative signal intensity ratios of the lesion and adjacent liver parenchyma on unenhanced (pre-contrast EOB ratio) and hepatobiliary phase (post-contrast EOB ratio) images on 3D fat-suppressed T1-weighted gradient echo sequences were calculated by using an operator-defined ROI, which was specified as a round area up to 10 mm in diameter. We took ROI readings from 1 area of the tumorous lesion and from 3 areas of adjacent non-tumorous regions devoid of vascular structures. The mean value of the latter 3 points was used as the signal intensity of the non-tumorous liver.

To see the actual enhancement of the tumor by Gd-EOB-DTPA, we also calculated the ratio of these relative intensity ratios as the EOB ER, as follows: EOB ER = post-contrast EOB ratio/pre-contrast EOB ratio. Tumor enhancement was defined as high when the EOB ER was greater than 1(which signified that the tumor was enhanced more than the adjacent liver parenchyma) and as low when the EOB ER was less than 1.

Histological diagnosis of tumors

All nodules were histologically diagnosed in a blinded manner by 3 pathologists (O.M., M. Komuta, M.S.) according to the histological criteria of the International Working Party [11] and the International Consensus Group for Hepatocellular Neoplasia (ICGHN) meeting [12]. Liver specimens were obtained by 18-gauge needle core biopsy (Sonopsy-C1®; Hakko, Tokyo, Japan). In each case, at least 2 specimens were obtained from the nodular lesion and 1 specimen was obtained from the adjacent liver parenchyma. Additional specimens from tumors and non-tumorous tissue were obtained from patients during partial hepatectomy surgery. In cases of discrepancy, or if it was difficult to diagnose borderline lesions, such as DNs and hypovascular well-differentiated HCCs, including early HCCs, the pathologists used immunostaining methods such as heat shock protein (HSP)70 (dilution of 1:200; SC-24, Santa Cruz Biotechnology, Santa Cruz, CA, USA) and Glypican (GPC) 3 (dilution 1:20; Bio Mosaics, Burlington, VT, USA) and reevaluated their findings to reach an agreement [13, 14].

Statistical analysis

The Kruskal–Wallis test and Mann–Whitney U-test with Bonferroni's inequality were used to confirm differences between the groups classified by histology. McNemar's χ^2 test was used to analyze the data. The level of significance was set at $P < 0.05$ (Kruskal–Wallis test, McNemar's χ^2 test) and at $P < 0.05/4 = 0.0125$ (Mann–Whitney U-test). All analyses were performed with statistical software (SPSS, version 11; SPSS, Chicago, IL, USA) for Microsoft Windows.

Results

Histological diagnosis of tumors

The 86 nodules were grouped according to morphology: DNs, $n = 9$; well-differentiated HCCs (including 2 early HCCs), $n = 46$; moderately differentiated HCCs, $n = 21$; poorly differentiated (poorly) HCCs, $n = 7$; combined

Table 2 Histological diagnosis of hyper- and hypovascular tumors

Histological diagnosis	Hypervascular tumors	Hypovascular tumors
DNs	0	9
Well-differentiated HCC	14	32
Moderately differentiated HCC	21	0
Poorly differentiated HCC	7	0
Others	3 (combined HCC)	0

DN dysplastic nodule, *HCC* hepatocellular carcinoma

Table 3 Diagnostic sensitivity of gadolinium ethoxybenzyl diethylenetriamine pentaacetic acid (Gd-EOB)-enhanced magnetic resonance imaging (MRI) for hypervascular HCCs: comparison with multi-detector row computed tomography (MDCT)

HCCs : Comparison with MDCT

	Tumor size ≤ 2 cm		Tumor size > 2 cm	
	Typical HCC pattern	Non-typical HCC pattern	Typical HCC pattern	Non-typical HCC pattern
Gd-EOB-DTPA-enhanced MRI	21	3	20	1
Dynamic MDCT	14	10	20	1

P=0.048* (≤ 2 cm)   N.S. (> 2 cm)

HCC: Hepatocellular carcinoma
MDCT: Multi detector raw CT

* McNemar's chi-square test

HCCs, $n = 3$ (Table 2). Fifty-five cases of nodular lesions were diagnosed on the basis of needle biopsy specimens, and the other 31 cases were diagnosed based on resected specimens. The median diameter of the tumors was 2.1 cm (range 0.6–4.0 cm).

Vascularity of tumors

In the present study, 45 out of 86 nodules were diagnosed as hypervascular HCCs. Of these 45 nodules, 34 were diagnosed as hypervascular on the basis of CTHA, and the 11 remaining nodules were diagnosed based on contrast-enhanced US findings. Forty-one nodules were diagnosed as hypovascular tumors because they had no hypervascular area inside the tumor on CTHA.

Comparison of the diagnostic sensitivity of Gd-EOB-DTPA-enhanced MRI versus dynamic MDCT for hypervascular HCCs

For hypervascular HCCs, the diagnostic sensitivity of Gd-EOB-DTPA-enhanced MRI was 91% (41/45) versus 76% (34/45) with dynamic MDCT ($p = 0.0103$, McNemar's χ^2 test). When we evaluated both modalities based on the size of the tumors (2 or >2 cm), the diagnostic sensitivity of Gd-EOB-DTPA-enhanced MRI was significantly higher than that of MDCT for lesions of 2 cm or less ($p = 0.048$, McNemar's χ^2 test, Table 3).

Table 4 Detection sensitivity of hepatobiliary phase images of Gd-EOB-enhanced MRI for histologically proven hypervascular HCCs: comparison with MDCT

	Detectable	Not detectable
Hepatobiliary phase Image of Gd-EOB-DTPA-enhanced MRI	43	2
Dynamic MDCT	40	5

N.S.

HCC: Hepatocellular carcinoma
MDCT: Multi detector raw CT

* McNemar's chi-square test

Table 5 Detection sensitivity of Gd-EOB-enhanced MRI for hypovascular HCCs and DNs: comparison with MDCT

	Detectable	Not detectable
Dynamic MDCT	25	16
Dynamic study of Gd-EOB-DTPA-enhanced MRI	24	17
Hepatobiliary phase Image of Gd-EOB-DTPA-enhanced MRI	39	2

N.S.   p<0.001   P=0.0003

HCC: Hepatocellular carcinoma
MDCT: Multi detector raw CT

* McNemar's chi-square test

Table 6 Hepatobiliary phase images of Gd-EOB-DTPA-enhanced MRI

Hepatobiliary phase images of Gd-EOB-DTPA-enhanced MRI	DN	Hypovascular-well-differentiated HCC	Hypervascular well-differentiated HCC	Moderately differentiated HCC	Poorly differentiated HCC	Others (combined)
High intensity	2	0	3	0	1	0
Iso-intensity	1	0	2	0	0	0
Low intensity	6	32	9	21	6	3

DN dysplastic nodule, *HCC* hepatocellular carcinoma

Fig. 1 Case presentation of 60-year-old man with dysplastic nodules. **a** The tumor showed hypovascularity on CTHA (*arrow*). **b** The tumor showed isovascularity on CTAP (*arrow*). **c** Pre-contrast T1-weighted image showed iso intensity (*arrow*). **d** 20 min after Gd-EOB-DTPA bolus injection with dysplastic nodule displaying hyper intensity (*arrow*). The EOB enhancement ratio of this tumor was 1.76. **e** Routine staining with hematoxylin-eosin shows a mild increase in cell density with a clearer trabecular arrangement. **f** Immunostaining for GPC3 shows no expression in the cytoplasm of tumor cells
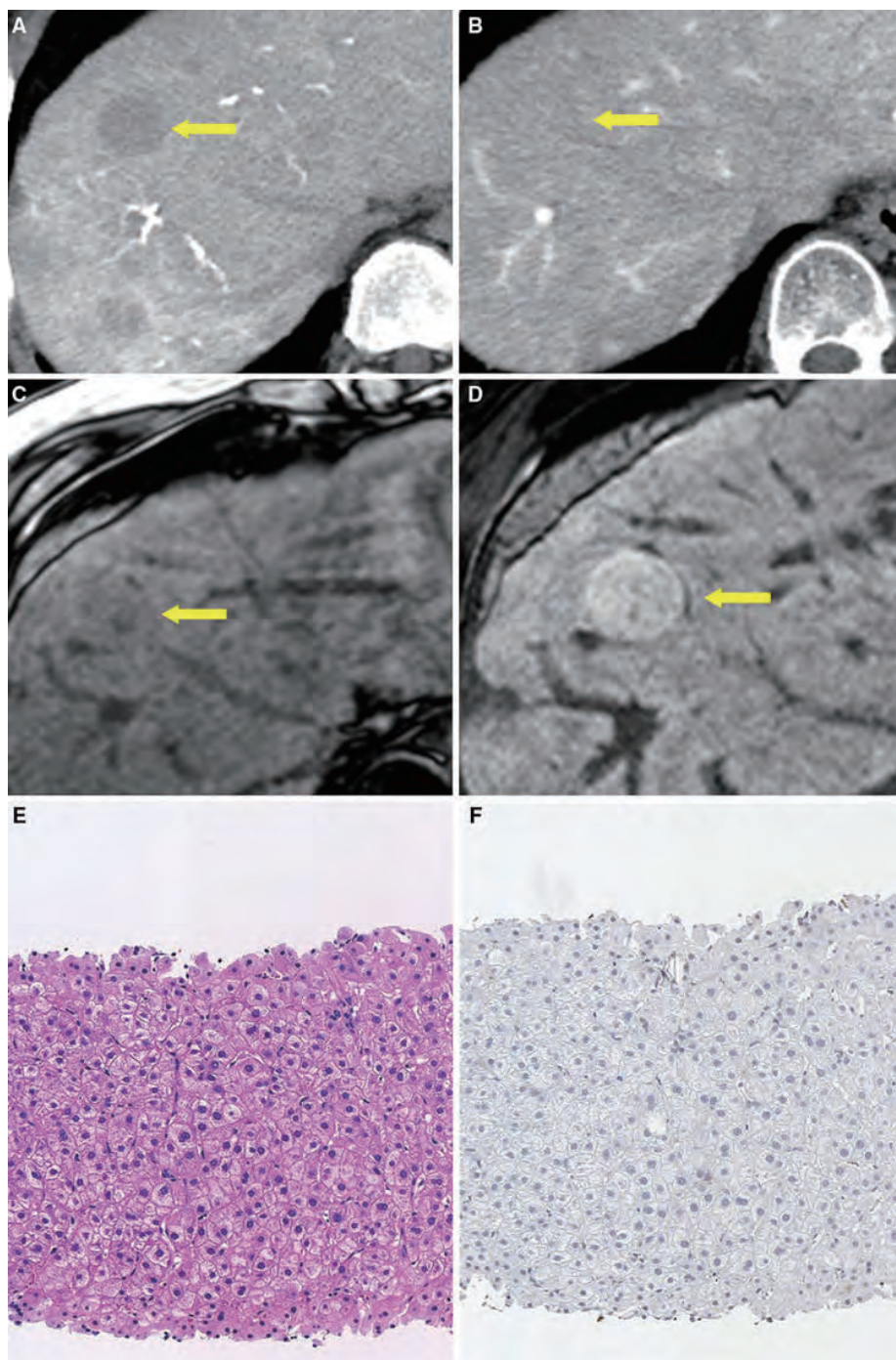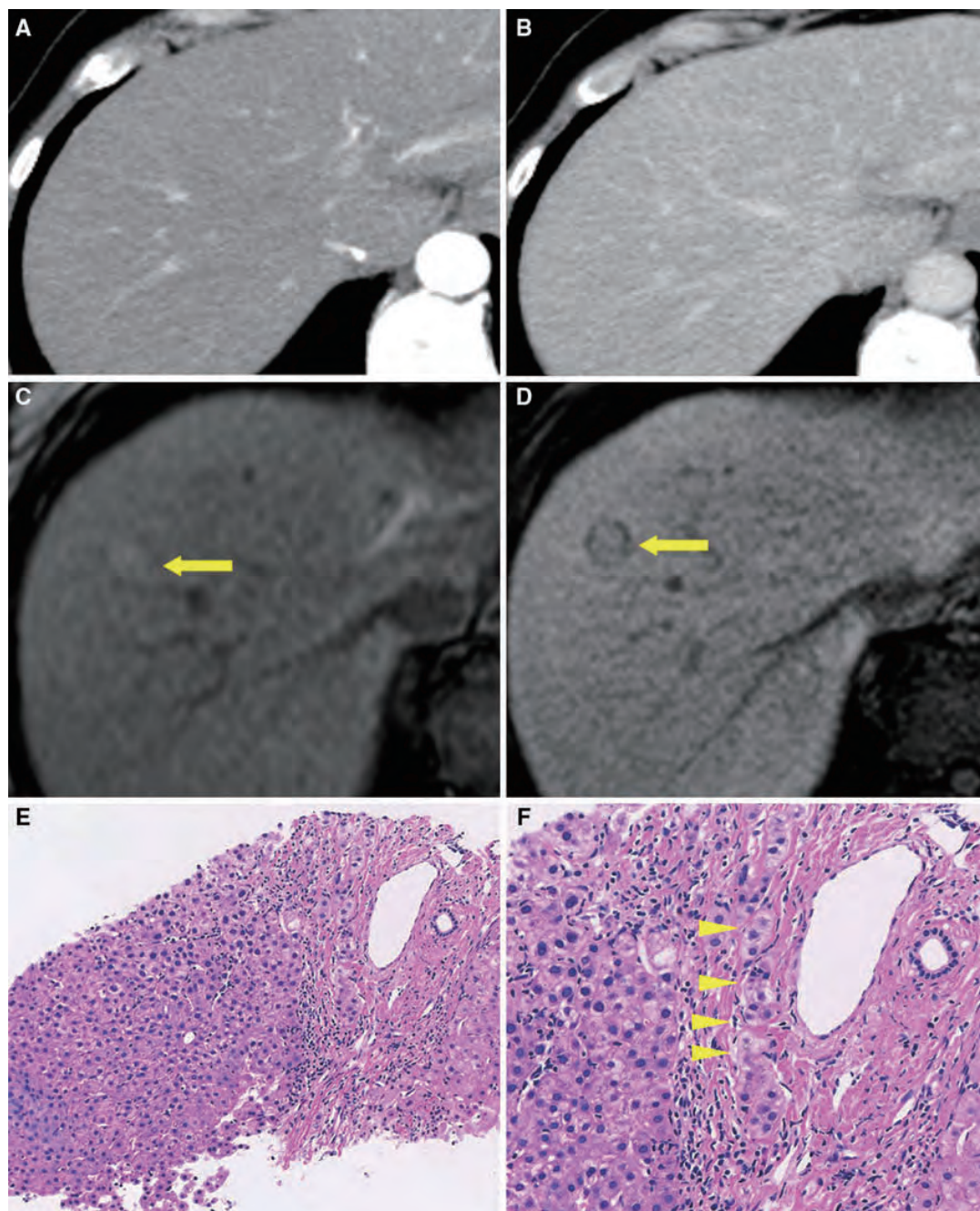
Fig. 2 Case presentation of 69-year-old woman with early HCC. **a**, **b** The tumor showed isovascularity on arterial- and portal-phase dynamic CT scans. **c** Pre-contrast T1-weighted image showed slight high intensity (*arrow*). **d** Image 20 min after Gd-EOB-DTPA bolus injection. The tumor showed low intensity (*arrow*). The EOB enhancement ratio of this tumor was 0.93. **e**, **f** The tumor cells show an irregular thin-trabecular pattern with occasional pseudoglands. The tumor cells are invading an intratumoral portal tract (stromal invasion in early HCC, *arrow heads*)

Fig. 3 Case presentation of 73-year-old man with early HCC. **a**, **b** The tumor showed slight hypovascularity on CTHA and CTAP (*arrow*). **c** No tumor was seen on pre-contrast T1-weighted image (*arrow*). **d** Image 20 min after Gd-EOB-DTPA bolus injection. The tumor showed low intensity (*arrow*). The EOB enhancement ratio of this tumor was 0.74. **e** Resected specimen of the tumor appeared as a vaguely nodular type (early HCC) (inside *dots*). **f** Varying numbers of portal tracts within the nodule (intratumoral portal tracts, *arrowheads*). **g** The tumor cell density increased to more than 2 times that of the surrounding tissue, with an increased nuclear/cytoplasm (N/C) ratio, irregular thin-trabecular pattern, and fatty change
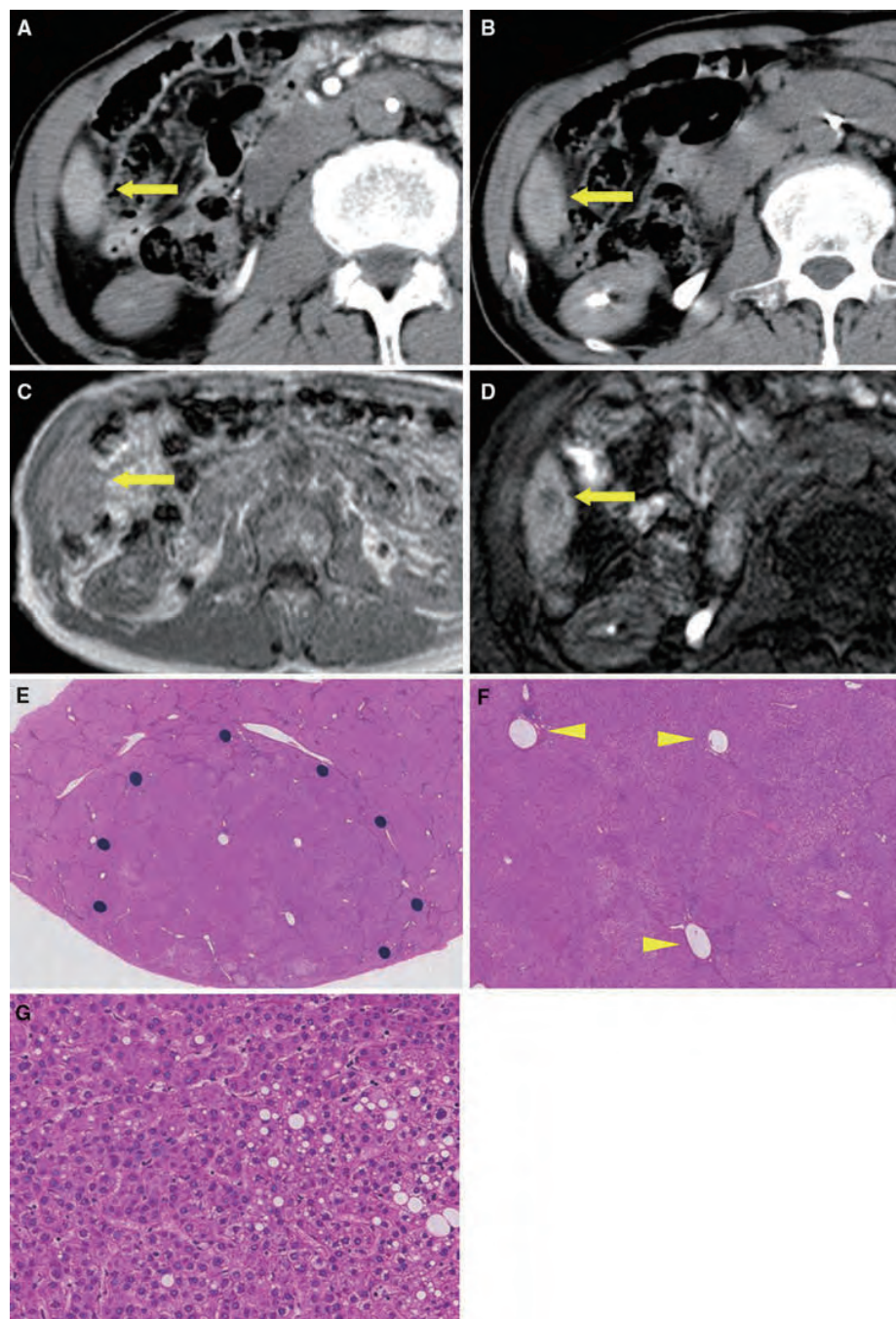
Comparison of the detection sensitivity of Gd-EOB-DTPA-enhanced MRI versus dynamic MDCT for HCCs and DNs

The detection sensitivity of hypervascular HCCs by hepatobiliary phase images of Gd-EOB-DTPA (43/45: 96%) did not differ from that of dynamic MDCT (40/45: 89%) (Table 4). Also, for hypovascular HCCs and DNs, there was no difference in the detection sensitivity between dynamic Gd-EOB-DTPA-enhanced MRI (24/41: 59%) and dynamic MDCT (25/41: 61%) (Table 5). The detection sensitivity of hepatobiliary phase images for hypovascular HCCs and DNs [32/32 for hypovascular HCCs and 7/9 for DNs, total 39/41 (95%)] was significantly higher than that achieved by dynamic MDCT [20/32 for hypovascular HCCs and 5/9 for DNs, total 25/41 (61%)] ($p = 0.003$, McNemar's χ^2 test, Table 5).
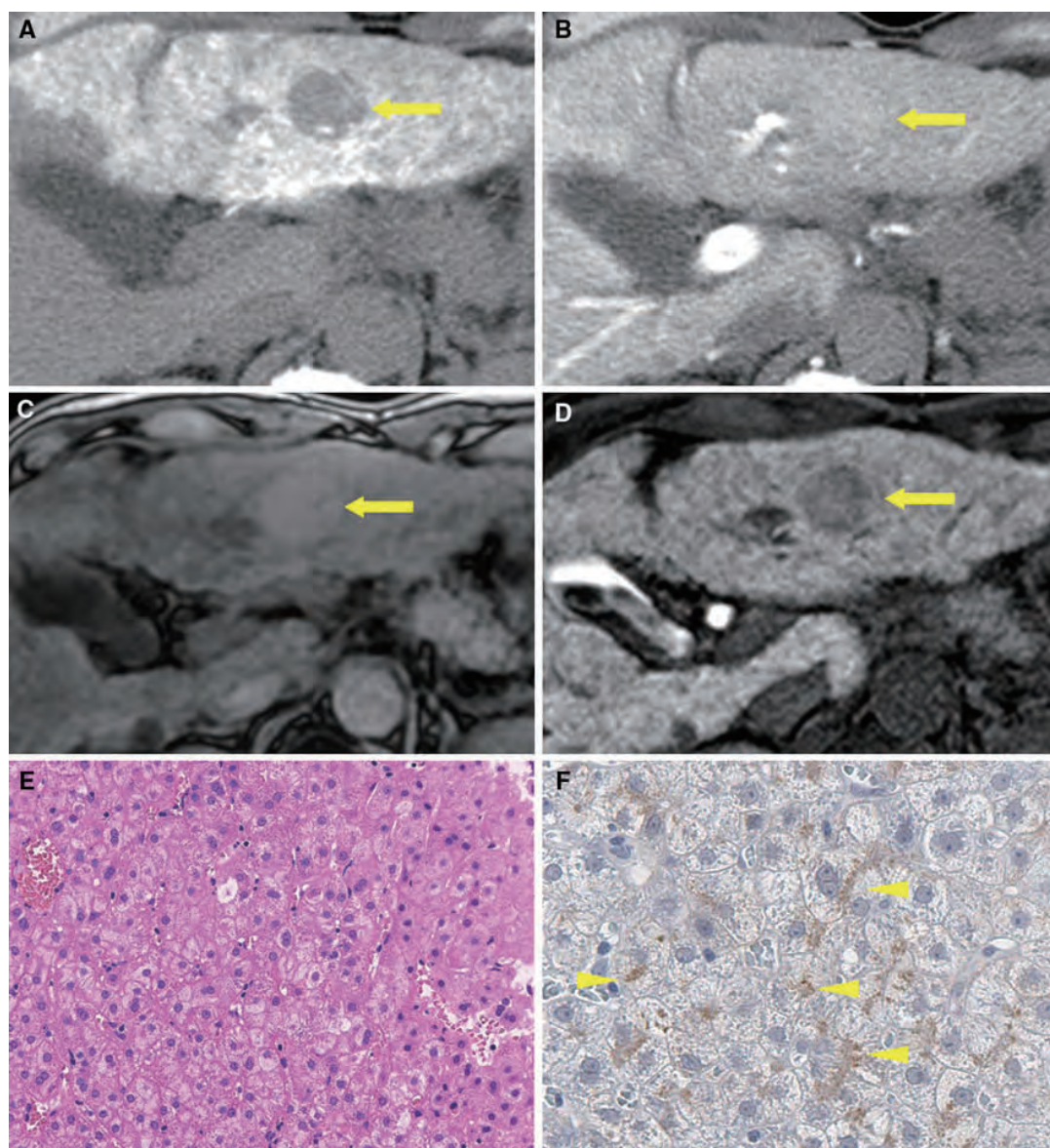
Fig. 4 Case presentation of a 59-year-old man with well-differentiated HCC. **a** The tumor showed hypovascularity on CTHA (*arrow*). **b** The tumor showed slight hypervascularity on CTAP (*arrow*). **c** Pre-contrast T1-weighted image showed slight high intensity (*arrow*). **d** Image 20 min after Gd-EOB-DTPA bolus injection. The tumor showed low intensity (*arrow*). The EOB enhancement ratio of this tumor was 0.65. **e** H&E staining shows a mild increase in cell density with a clearer trabecular arrangement, as well as a slightly increased N/C ratio. **f** Immunostaining for GPC3 shows expression in the cytoplasm of tumor cells (*arrowheads*)

Image findings of the hepatobiliary phase of Gd-EOB-DTPA-enhanced MRI

For qualitative analysis, 9 nodules (3 DNs, 5 well-differentiated HCCs, and 1 poorly differentiated HCC) appeared as regions of iso- to high intensity in the hepatobiliary phase of Gd-EOB-DTPA MRI (Table 6; Fig. 1). The other 77 nodules showed low intensity in the hepatobiliary phase of Gd-EOB-DTPA-enhanced MRI (Figs. 2, 3, 4).

EOB enhancement ratios (ERs) of histologically proven HCCs and DNs

To evaluate the uptake of Gd-EOB-DTPA by DNs and HCCs, we calculated EOB ERs. Moderately differentiated and poorly differentiated HCCs were merged to form 1 group (moderately plus poorly differentiated HCC group), yielding a total of 4 groups that were used in the subsequent analyses. The EOB ERs were 1.00 ± 0.12 for

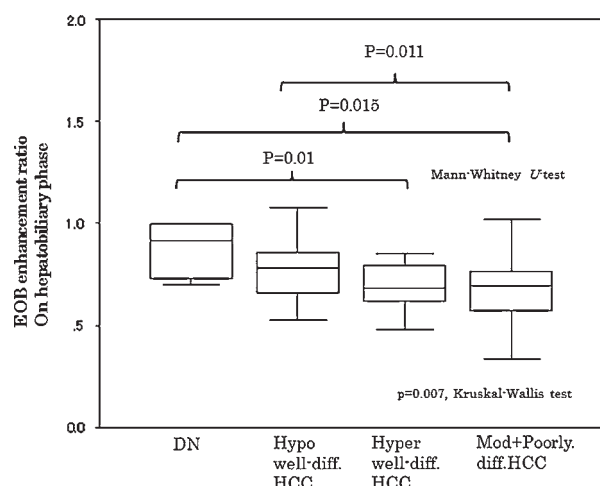**Fig. 5** *Box plots* illustrating EOB enhancement ratios (post-contrast EOB ratio/precontrast EOB ratio) excluding 5 hypervascular well and 1 poorly differentiated HCCs that showed high intensity on hepatobiliary phase images of Gd-EOB-DTPA MRI. The enhancement ratio significantly decreases from dysplastic nodules to moderately+poorly differentiated HCCs ($p = 0.007$; Kruskal–Wallis test). The EOB enhancement ratio of hypervascular well differentiated and moderately + poorly differentiated HCCs decreased to 0.67 ± 0.11 and 0.65 ± 0.19 respectively. There was no significant difference among EOB enhancement ratios of DNs and hypovascular well differentiated HCCs ($p = 0.113$, Mann–Whitney U test). The box extends from the 25th to the 75th percentile. The *lines in the middle of the boxes* represent the median and the *filled circle* indicates the mean. The *lines* extending vertically from either end of the *box* indicate the extent of the data beyond the 25th and 75th percentiles

DNs, 0.82 ± 0.21 for hypovascular well-differentiated HCCs, 0.75 ± 0.20 hypervascular well-differentiated HCCs, and 0.69 ± 0.06 for moderately + poorly differentiated HCCs ($p = 0.031$; Kruskal–Wallis test). When the 5 hypervascular well-differentiated HCCs and 1 poorly differentiated HCC that showed iso- to high intensity on hepatobiliary phase images of Gd-EOB-DTPA MRI were excluded, the ER significantly decreased from DNs to moderately + poorly differentiated HCCs [$p = 0.007$; Kruskal–Wallis test (Fig. 5)]. The EOB ERs of hypervascular well-differentiated and moderately + poorly differentiated HCCs decreased to 0.67 ± 0.11 and 0.65 ± 0.19, respectively (Fig. 5). There was a significant difference between DNs versus hypervascular well-differentiated HCCs ($p = 0.01$, Mann–Whitney U-test) and between hypovascular well-differentiated HCCs versus moderately + poorly differentiated HCCs ($p = 0.011$, Mann–Whitney U-test), but there were no significant differences between the other groups, although a trend for a difference between DNs and moderately + poorly differentiated HCCs was observed ($p = 0.015$, Mann–Whitney U-test).

Discussion

In the present study, we evaluated the ability of Gd-EOB-DTPA-enhanced MRI to diagnose and detect HCCs and DNs, and we found that the hepatobiliary phase of Gd-EOB-DTPA-enhanced MRI was more advantageous than dynamic MDCT for detecting tumors. Gd-EOB-DTPA-enhanced MRI plays a significant role in the diagnosis of HCC, and several reports comparing Gd-EOB-DTPA-enhanced MRI and dynamic MDCT have already been published [15–19]. These studies proved the superiority of Gd-EOB-DTPA-enhanced MRI over MDCT for the diagnosis of HCC. These studies, although focused mainly on the detection of classical HCCs, were corroborated by our data. In the present study, we also evaluated the detection ability of Gd-EOB-DTPA-enhanced MRI and MDCT for borderline lesions such as DNs and hypovascular well-differentiated HCCs, which are difficult to diagnose based on tumor hemodynamics. The detection sensitivity of hepatobiliary phase images of Gd-EOB-DTPA-MRI of these borderline lesions in the present study was significantly higher than that of MDCT (95% on Gd-EOB-DTPA-enhanced MRI, 61% on MDCT, $p = 0.003$, McNemar's χ^2 test).

These results suggest that alterations observed in the tumor images of the hepatobiliary phase of Gd-EOB-DTPA-enhanced MRI are detectable at an earlier stage of disease than are tumor hemodynamic changes, indicating that HCCs and borderline lesions can be detected earlier with this technique than with MDCT. Although these borderline lesions do not require expeditious treatment [20], their early detection by Gd-EOB-DTPA-enhanced MRI enables subsequent followup for progression based on hemodynamic changes that can be detected using other imaging modalities, such as CT angiography[3–5] and contrast-enhanced US with Sonazoid® [2], even though these techniques are less effective for the initial detection of such borderline cases. In the present study, we also evaluated whether hepatobiliary phase images of Gd-EOB-DTPA-enhanced MRI could discriminate between DNs and hypovascular well-differentiated HCCs. The image findings of some of these tumors overlapped on hepatobiliary phase images of Gd-EOB-enhanced MRI. Furthermore, Gd-EOB-DTPA uptake assessed by the EOB enhancement ratio (ER) was 1.00 ± 0.12 in DNs and 0.82 ± 0.21 in hypovascular well-differentiated HCCs (difference not significant; $p = $ NS). Although we evaluated only 9 cases of DNs, it was difficult to discriminate between DNs and hypovascular well-differentiated HCCs based on hepatobiliary phase images from Gd-EOB-DTPA-enhanced MRI. This result was similar to the findings reported by Kogita et al. [10].

This study had several limitations. The first concerns the diagnosis of HCCs and DNs. Diagnosis of most of the hypovascular well-differentiated HCCs and DNs was based on specimens obtained by US-guided needle core biopsy. To reduce sampling error to an acceptable minimum, at least 2 needle core biopsies were performed for each tumor, and all specimens in the present study were diagnosed by expert liver pathologists (M. Komuta, M.S.) and evaluated for HSP70 and GPC3 immunostaining, which are helpful indices for distinguishing early HCC from DNs [13, 14]. However, it is difficult to correctly diagnose the histological grade of partially differentiated nodules based on liver biopsy specimens in which there is no stromal invasion, which is a criterion for the diagnosis of early HCC [12, 21]. Therefore, to clarify the utility of hepatobiliary phase images for the diagnosis of borderline lesions, further case studies must be performed with a special focus on histopathological correlation with resected specimens. Second, we evaluated tumor vascularity by both CTHA and contrast-enhanced US. It is well known that the most sensitive modality capable of objectively depicting the early phase of carcinogenesis among currently available imaging systems is CTAP [20, 22]. The second earliest initial carcinogenic change is detected as an increase in intranodular arterial blood flow by CTHA or contrast-enhanced US [23]. Therefore, we evaluated the vascularity of tumors on CTHA and contrast-enhanced US images. Third, the overall number of cases included, especially DN cases, was small. Future research utilizing a larger number of subjects is recommended to confirm and extend our results. Finally, this study was conducted retrospectively, although we examined consecutive patients. A prospective study is needed to confirm our findings.

In conclusion, the diagnostic ability of Gd-EOB-DTPA-enhanced MRI for small hypervascular HCCs less than 2 cm was significantly higher than that of MDCT. For hypovascular HCCs and DNs, the detection sensitivity of hepatobiliary phase images of Gd-EOB-DTPA-enhanced MRI was significantly higher than that of dynamic MDCT. It was difficult to distinguish between DNs and hypovascular well-differentiated HCCs based on the EOB ER. Further study with additional resected specimens is needed to more accurately determine the diagnostic ability of Gd-EOB-DTPA-enhanced MRI for DNs and hypovascular well-differentiated HCCs.

**Conflict of interest** The authors declare that they have no conflict of interest.

References

1. Krinsky G. Imaging of dysplastic nodules and small hepatocellular carcinomas: experience with explanted livers. Intervirology. 2004;47:191–8.

2. Kudo M. Imaging diagnosis of hepatocellular carcinoma and premalignant/borderline lesions. Semin Liver Dis. 1999;19:297–309.

3. Matsui O, Kadoya M, Kameyama T, Yoshikawa J, Takashima T, Nakanuma Y, et al. Benign and malignant nodules in cirrhotic livers: distinction based on blood supply. Radiology. 1991;178:493–7.

4. Takayasu K, Muramatsu Y, Furukawa H, Wakao F, Moriyama N, Takayama T, et al. Early hepatocellular carcinoma: appearance at CT during arterial portography and CT arteriography with pathologic correlation. Radiology. 1995;194:101–5.

5. Asahina Y, Izumi N, Uchihara M, Noguchi O, Ueda K, Inoue K, et al. Assessment of Kupffer cells by ferumoxides-enhanced MR imaging is beneficial for diagnosis of hepatocellular carcinoma: comparison of pathological diagnosis and perfusion patterns assessed by CT hepatic arteriography and CT arterioportography. Hepatol Res. 2003;27:196–204.

6. Imai Y, Murakami T, Yoshida S, Nishikawa M, Ohsawa M, Tokunaga K, et al. Superparamagnetic iron oxide-enhanced magnetic resonance images of hepatocellular carcinoma: correlation with histological grading. Hepatology. 2000;32:205–12.

7. Inoue T, Kudo M, Watai R, Pei Z, Kawasaki T, Minami Y, et al. Differential diagnosis of nodular lesions in cirrhotic liver by postvascular phase contrast-enhanced US with Levovist: comparison with superparamagnetic iron oxide magnetic resonance images. J Gastroenterol. 2005;40:1139–47.

8. Hamm B, Staks T, Mühler A, Bollow M, Taupitz M, Frenzel T, et al. Phase I clinical evaluation of Gd-EOB-DTPA as a hepatobiliary MR contrast agent: safety, pharmacokinetics, and MR imaging. Radiology. 1995;195:785–92.

9. Halavaara J, Breuer J, Ayuso C, Balzer T, Bellin MF, Blomqvist L, et al. Liver tumor characterization: comparison between liver-specific gadoxetic acid disodium-enhanced MRI and biphasic CT—a multicenter trial. J Comput Assist Tomogr. 2006;30:345–54.

10. Kogita S, Imai Y, Okada M, Kim T, Onishi H, Takamura M, et al. Gd-EOB-DTPA-enhanced magnetic resonance images of hepatocellular carcinoma: correlation with histological grading and portal blood flow. Eur Radiol. 2010;20:2405–13.

11. [No authors listed]. Terminology of nodular hepatocellular lesions. International Working Party. Hepatology. 1995;22:983–993.

12. The International Consensus Group for Hepatocellular Neoplasia. Pathologic diagnosis of early hepatocellular carcinoma: a report of the International Consensus Group for Hepatocellular Neoplasia. Hepatology. 2009;49:658–64.

13. Sakamoto M, Mori T, Masugi Y, Effendi K, Rie I, Du W. Candidate molecular markers for histological diagnosis of early hepatocellular carcinoma. Intervirology. 2008;51(Suppl 1):42–5.

14. Di Tommaso L, Franchi G, Park YN, Fiamengo B, Destro A, Morenghi E, et al. Diagnostic value of HSP70, glypican 3, and glutamine synthetase in hepatocellular nodules in cirrhosis. Hepatology. 2007;45:725–34.

15. Kim YK, Kim CS, Han YM, Kwak HS, Jin GY, Hwang SB, et al. Detection of hepatocellular carcinoma: gadoxetic acid-enhanced 3-dimensional magnetic resonance imaging versus multi-detector row computed tomography. J Comput Assist Tomogr. 2009;33:844–50.

16. Kim SH, Kim SH, Lee J, Kim MJ, Jeon YH, Park Y, et al. Gadoxetic acid-enhanced MRI versus triple-phase MDCT for the preoperative detection of hepatocellular carcinoma. AJR Am J Roentgenol. 2009;192:1675–81.

17. Akai H, Kiryu S, Matsuda I, Satou J, Takao H, Tajima T, et al. Detection of hepatocellular carcinoma by Gd-EOB-DTPA-enhanced liver MRI: comparison with triple phase 64 detector row helical CT. Eur J Radiol. 2011;80:310–5.

18. Di Martino M, Marin D, Guerrisi A, Baski M, Galati F, Rossi M, et al. Intraindividual comparison of gadoxetate disodium-enhanced MR Imaging and 64-Section multidetector CT in the detection of hepatocellular carcinoma in patients with cirrhosis. Radiology. 2010;256:806–16.

19. Ahn SS, Kim MJ, Lim JS, Hong HS, Chung YE, Choi JY. Added value of gadoxetic acid-enhanced hepatobiliary phase MR imaging in the diagnosis of hepatocellular carcinoma. Radiology. 2010;255:459–66.

20. Hayashi M, Matsui O, Ueda K, Kawamori Y, Gabata T, Kadoya M. Progression to hypervascular hepatocellular carcinoma: correlation with intranodular blood supply evaluated with CT during intraarterial injection of contrast material. Radiology. 2002;225:143–9.

21. Kudo M, Japan Society of Hepatology. Management of hepatocellular carcinoma in Japan: consensus-based clinical practice manual proposed by the Japan Society of Hepatology. Oncology. 2007;72(suppl 1):2–15.

22. Tajima T, Honda H, Taguchi K, Asayama Y, Kuroiwa T, Yoshimitsu K, et al. Sequential hemodynamic change in hepatocellular carcinoma and dysplastic nodules: CT angiography and pathologic correlation. AJR Am J Roentgenol. 2002;178:885–97.

23. Kudo M. Multistep human hepatocarcinogenesis: correlation of imaging with pathology. 27. J Gastroenterol. 2009;44(Suppl 19): 112–8.
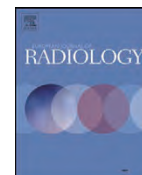
Pancreatic multicenter ultrasound study (PAMUS)

Mirko D'Onofrio [a,*], Emilio Barbi [b], Christoph F. Dietrich [c], Masayuki Kitano [d], Kazushi Numata [e], Atsushi Sofuni [f], Francesco Principe [a], Anna Gallotti [a], Giulia A. Zamboni [a], Roberto Pozzi Mucelli [a]

[a] Department of Radiology, University Hospital G.B. Rossi, University of Verona, Italy
[b] Department of Radiology, Hospital "Casa di Cura Pederzoli" – Peschiera, Verona, Italy
[c] Department of Internal Medicine, Chefarzt der Med. Klinik 2, Caritas-Krankenhaus, Bad Mergentheim, Germany
[d] Department of Gastroenterology and Hepatology, Kinki University School of Medicine, Ohno-Higashi, Osaka-Sayama, Japan
[e] Gastroenterolocical Center, Yokohama City University Medical Center, Minami-ku, Yokohama, Japan
[f] Department of Internal Medicine, Tokyo Medical University, Shinjyuku-ku, Tokyo, Japan

ARTICLE INFO

ABSTRACT

Aim: To describe the typical CEUS pattern of pancreatic lesions and to evaluate the diagnostic accuracy of Contrast-enhanced ultrasound (CEUS) in their characterization.

Materials and methods: All US and CEUS examinations of focal pancreatic masses performed in six centers during a period of five years were reviewed. Inclusion criteria were: focal pancreatic mass pathologically proved, visible at ultrasound (US) and studied with CEUS. All lesions were then evaluated for size, aspect and enhancement pattern. Sensitivity, specificity, positive and negative predictive values with 95% CIs were calculated to define diagnostic accuracy of CEUS in respect to pathology. Diagnostic confidence of US and CEUS, discerning between benign and malignant lesions, were represented by using ROC (receiver operating characteristics) curves. Agreement was evaluated by means of k statistics.

Results: 1439 pancreatic lesions were included. At CEUS the lesions were divided into solid (89%) and cystic (12%) masses and classified into six and eight categories, respectively. Among the solid lesions, adenocarcinomas were characterized with an accuracy of 87.8%. Among the cystic lesions, cystic tumors were diagnosed with an accuracy of 97.1%. ROC curve area increased from 0.637 for US to 0.877 for CEUS ($p < 0.0001$). Inter-observer agreement was slightly higher for solid ($k = 0.78$) than cystic ($k = 0.62$) lesions. In none of the centers side effects were reported.

Conclusion: CEUS is accurate in the characterization of pancreatic lesions. CEUS should be considered as a complementary imaging method for pancreatic lesions characterization.

© 2011 Elsevier Ireland Ltd. All rights reserved.

1. Introduction

Conventional B-mode ultrasonography (US) is a widely performed, relatively low cost and readily available examination for the pancreatic study [1].

The introduction of microbubble contrast agents has improved the diagnostic accuracy of US [2]. The real-time evaluation of the contrast-enhanced phases after the administration of a purely blood-pool second-generation contrast agent, allows accurate perfusional ultrasound studies, with a high temporal and spatial resolution [3].

Contrast-enhanced ultrasound (CEUS) is a well established imaging method for the detection and characterization of focal liver lesions [4], and its role has been recently better defined by multicenter studies and by the drawing up of guidelines [4–7].

The study of pancreatic tumors is a relatively new application of CEUS. This technique can improve the characterization of pancreatic lesions [8,9]. Currently, in the literature a number of papers describe the CEUS enhancement patterns of the most common benign and malignant solid and cystic pancreatic lesions [10–18]. Although increasing in number, all these studies are mono centric. It is not reported how useful the technique would be in the characterization of pancreatic masses with more general and widespread use.

Therefore a multicenter study has been performed to describe the typical CEUS enhancement pattern of pancreatic lesions and to evaluate its diagnostic accuracy in the characterization of the most common focal pancreatic lesions.

2. Materials and methods

All US and CEUS examinations of focal pancreatic masses performed in six centers during a period of five years were reviewed.

Table 1
Ultrasound scanner systems and contrast agents used.

Center	US scanners	Softwares		Contrast agents
I	Sequoia 512 (Acuson/Siemens, Germany)	Coherent Contrast Imaging	Cadence Contrast Pulse Sequencing	Sonovue (2.4 ml)
II	Aplio XG (Toshiba Medical Systems, Japan)	Contrast Harmonic Imaging		Sonovue (2.4 ml)
III	Sequoia 512 (Acuson/Siemens, Germany)	Cadence Contrast Pulse Sequencing		Sonovue (2.4 ml)
IV	Logiq 7 (General Electric Medical Systems, USA)	Coded Phase Inversion Harmonic Imaging		Levovist (6 ml)
V	Logiq 7 (General Electric Medical Systems, USA)	Coded Phase Inversion	Coded Harmonic Angio	Sonazoid (0.2 ml)
VI	Aplio XG (Toshiba Medical Systems, Japan)	Contrast Harmonic Imaging		Sonazoid (0.5 ml)

The centers involved in the study are identified as centers: I, II, III, IV, V, VI.

This is a retrospective study even though all the included lesions were prospectively judged on site during conventional and contrast-enhanced examinations.

This study was approved by institutional review board and conducted in accordance with the principles of Helsinki Declaration. All patients gave informed written consent.

2.1. Patients

Patients with a focal pancreatic mass visible at ultrasound and studied with contrast-enhanced ultrasonography were included. All lesions were also pathologically confirmed by fine needle aspiration/biopsy or after surgical resection. Other imaging modalities such as Computed Tomography and/or Magnetic Resonance and/or Endoscopic ultrasound were performed in all patients as part of the clinical work-up but arbitrarily not considered in the present study in which the only pathological results was considered as gold standard.

Inclusion criteria were: focal pancreatic mass pathologically proved, visible at ultrasound and studied with contrast-enhanced ultrasonography. Cases with incomplete data and lesions not of pancreatic origin were excluded.

2.2. Ultrasound study

2.2.1. Conventional ultrasound (US)

Conventional B-mode ultrasound (US) was performed using different scanners in the six centers involved (Table 1).

All pancreatic lesions were evaluated for: (a) size; (b) solid, cystic or mixed (indeterminate: not-solid not-cystic); (c) echogenicity of the solid lesions relative to the normal adjacent parenchyma (homogeneously or heterogeneously hypo-, iso- or hyper-echoic); (d) site (head, uncinate process, neck, body or tail or diffuse pancreatic involvement).

2.2.2. Contrast-enhanced ultrasound (CEUS)

All CEUS examinations were performed by physician operators with more than five years experience in CEUS and specialized in pancreatic pathology. The ultrasound imaging systems and the contrast agents are summarized in Table 1. Convex multifrequency abdominal probe and microbubble specific softwares were used (Table 1). All examinations were recorded on hard disk/magneto-optical disk/compact disk.

A bolus of contrast medium was hand-injected through a 22 Gauge i.v. catheter in an antecubital vein immediately followed by a 5 ml saline flush.

A standard "real-time" dynamic study, in the arterial phase (hyperechogenicity within the aorta, celiac and mesenteric arteries) about 15–20 s after contrast injection, and in the venous phase (hyperechogenicity of the spleno-mesenteric-portal tree) about 30–45 s after contrast injection, was performed in all cases. The maximum examination time was 5 min.

All pancreatic lesions were then evaluated for: (a) aspect (solid or cystic lesions, with or without septa and/or parietal nodules

and/or parietal vascularisation); (b) enhancement pattern, comparing to the baseline echogenicity of the tumor and the extra-lesional pancreatic parenchyma together with the adjacent vessels.

The solid pancreatic masses were classified into six categories of enhancement: homogeneously hypovascular/hypoechoic (lesions almost without enhancement or with homogeneous enhancement lower than the adjacent parenchyma and/or vessels); heterogeneously hypovascular/hypoechoic (heterogeneous lesions almost without enhancement or with non-uniform enhancement lower than the adjacent parenchyma and/or vessels); homogeneously isovascular/isoechoic (lesions with slight continuous enhancement or uniform enhancement similar to that of the adjacent parenchyma); heterogeneously isovascular/isoechoic (heterogeneous lesions with non-uniform enhancement similar to that of the adjacent parenchyma); homogeneously hypervascular/hyperechoic (lesions with uniform bright enhancement superior than the adjacent parenchyma or similar to that of the arteries); heterogeneously hypervascular/hyperechoic (heterogeneous lesions with non-uniform bright enhancement superior than the adjacent parenchyma or similar to that of the arteries).

The cystic pancreatic masses were classified into eight categories: simple cyst; cyst with septa; cyst with parietal nodules; cyst with septa and parietal nodules; cyst with structured measurable thick wall; cyst with structured measurable thick wall and septa; cyst with structured measurable thick wall and parietal nodules; cyst with structured measurable thick wall, septa and parietal nodules.

2.3. Safety evaluation

All operators were asked to annotate if and what type of adverse reactions to the contrast agents were observed.

2.4. Pathological evaluation

All pancreatic lesions included were pathologically confirmed.

2.5. Data analysis

All data supplied by the six centers were analyzed, independently and together, focusing on the typical CEUS enhancement pattern related to the pathological diagnosis. No data regarding ultrasound detection of focal pancreatic masses can be provided in the present study as a direct consequence of the inclusion criteria above reported.

All the lesions were prospectively judged at the time of conventional and contrast-enhanced examinations. The operators performing the examinations were blinded to the results of other imaging studies. In case of incomplete report the stored data were reviewed to complete the description by a different operator with the same experience blinded to the final diagnosis and to the results of other imaging studies. A different operator was chosen to ensure the blindness of the reader.

To describe the typical CEUS enhancement pattern, all pancreatic masses, mainly classified into solid and cystic lesions, were analyzed and sensitivity (SEN), specificity (SPE), positive (PPV) and

Table 2
List of all the pancreatic lesions included in the study, according to the pathological diagnosis.

Pathological diagnosis	Total
Ductal adenocarcinoma	1020/1439
Endocrine tumor	210/1439
Intraductal papillary-mucinous tumor	48/1439
Mucinous cystadenoma	39/1439
Pancreatitis	39/1439
Serous cystadenoma	26/1439
Pseudocyst	15/1439
Metastasis	13/1439
Solid-pseudopapillary tumor	13/1439
Cystadenocarcinoma	7/1439
Lymphoma	5/1439
Leiomyosarcoma	2/1439
Liposarcoma	1/1439
Pancreatoblastoma	1/1439

negative (NPV) predictive values with their respective 95% CIs were then calculated to define the diagnostic accuracy (ACC) of CEUS in lesion characterization.

2.5.1. Diagnostic confidence

To compare US and CEUS, each pancreatic mass was evaluated with three levels diagnostic score for solid and cystic lesions.

Solid lesions: 0 = absence of malignancy (isoechoic lesions at US; isovascular lesions at CEUS), 1 = indeterminate, and 2 = presence of malignancy (hypoechoic lesions at US; hypovascular or hypervascular lesions at CEUS).

Cystic lesions: 0 = absence of malignancy (simple cysts), 1 = indeterminate, and 2 = presence of malignancy (complex cysts).

Diagnostic confidence of US and CEUS in the characterization of pancreatic masses, discerning between benign and malignant lesions, were represented by means of the ROC (receiver operating characteristics) curves obtained by using a computer software package (Analise-it; Analise-it-software, Leeds, England).

2.5.2. Inter-observer variability

To verify the reproducibility of CEUS in the characterization of pancreatic lesions based on agreed-upon criteria, a subset of US and CEUS examinations, represented by all those performed in center "I" that has directed the study, were reviewed by a separate panel of two observers blinded both to the final diagnosis and the previous imaging results. Agreement was evaluated by means of *k* statistics.

3. Results

A total of 1439 patients (749 males and 690 females; mean age: 61.3 years; range: 16–90 years) were retrieved.

The six centers involved supplied the following data: 876/1439 (61%) lesions from the "I" center, 336/1439 (23%) lesions from the "II" center, 97/1439 (7%) lesions from the "III" center, 81/1439 (6%) lesions from the "IV" center, 29/1439 (2%) lesions from the "V" center and 20/1439 (1.4%) lesions from the "VI" center.

3.1. Total pancreatic lesions

According to the pathological diagnosis, the 1439 pancreatic lesions included are summarized in Table 2. All pancreatic lesions included were pathologically confirmed: 829 by FNA, 560 by resected specimen, and 50 by liver or lymph nodes metastases biopsy.

3.2. Conventional US

The mean diameter of the studied lesions was 39.8 mm (range: 5–160 mm) and they were classified into solid (1241/1439 = 86%), cystic (141/1439 = 10%) and mixed (57/1439 = 4%) groups.

In the solid group, 1172/1241 (94%) solid masses were homogeneously hypoechoic, 49/1241 (4%) heterogeneously hypoechoic, 9/1241 (0.7%) homogeneously isoechoic, 1/1241 (0.08%) heterogeneous isoechoic, 9/1241 (0.7%) homogeneously hyperechoic and 1/1241 (0.08%) heterogeneously hyperechoic.

Regarding the site, 767/1439 (53%) lesions were localized in the pancreatic head, 104/1439 (7%) in the uncinate process, 48/1439 (3%) in the isthmus, 262/1439 (18%) in the body and 251/1439
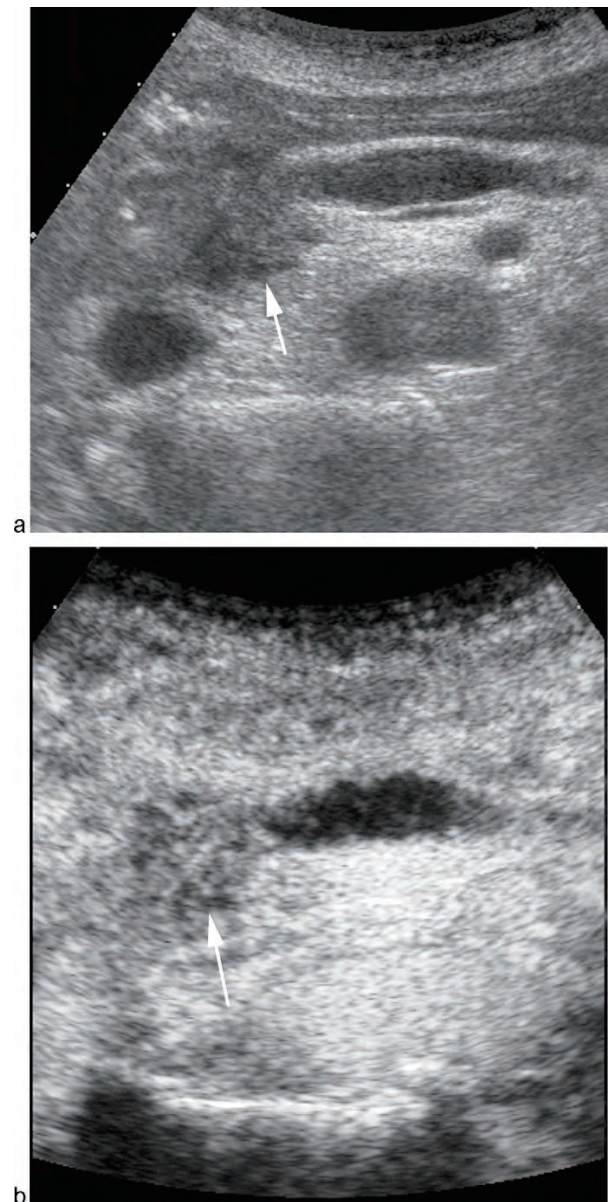

Fig. 1. Ductal adenocarcinoma. (a) Small mass (arrow) of the head of the pancreas solid and hypoechoic at US, with (b) homogeneous hypovascular pattern (arrow) at CEUS.

Table 3
Solid pancreatic lesions at CEUS: enhancement pattern correlated with pathology.

Pattern	n	Pathology	n
Homogeneous hypovascular	917/1273 (72%)	Adenocarcinoma	872/917 (95%)
		Neuroendocrine tumor	28/917 (3%)
		IPMN	5/917 (0.6%)
		Pancreatitis	5/917 (0.6%)
		Metastasis	3/917 (0.4%)
		Solid-pseudopapillary tumor	2/917 (0.2%)
		Cystadenocarcinoma	2/917 (0.2%)
Heterogeneous hypovascular	28/1273 (2%)	Adenocarcinoma	27/28 (96%)
		Lymphoma	1/28 (4%)
Homogeneous isovascular	60/1273 (5%)	Pancreatitis	26/60 (43%)
		Adenocarcinoma	18/60 (30%)
		Neuroendocrine tumor	9/60 (15%)
		Solid-pseudopapillary tumor	4/60 (7%)
		IPMN	2/60 (3%)
		Serous cystadenoma	1/60 (2%)
Heterogeneous isovascular	14/1273 (1%)	Adenocarcinoma	11/14 (79%)
		Pancreatitis	3/14 (21%)
Homogeneous hypervascular	226/1273 (18%)	Neuroendocrine tumor	140/226 (62%)
		Adenocarcinoma	61/226 (27%)
		Metastasis	9/226 (4%)
		Pancreatitis	5/226 (2%)
		Serous cystadenoma	3/226 (1%)
		Solid-pseudopapillary tumor	3/226 (1%)
		Lymphoma	3/226 (1%)
		IPMN	1/226 (0.5%)
		Leiomyosarcoma	1/226 (0.5%)
Heterogeneous hypervascular	28/1273 (2%)	Neuroendocrine tumor	13/28 (46.4%)
		Adenocarcinoma	9/28 (32%)
		Serous cystadenoma	1/28 (3.6%)
		Solid-pseudopapillary tumor	1/28 (3.6%)
		Metastasis	1/28 (3.6%)
		Lymphoma	1/28 (3.6%)
		Leiomyosarcoma	1/28 (3.6%)
		Pancreatoblastoma	1/28 (3.6%)

(17%) in the tail of the pancreas; 7/1439 (0.5%) diffusely involved the pancreatic gland.

3.3. CEUS enhancement patterns

All the pancreatic lesions were divided at CEUS into two main groups: solid (1273/1439 = 88%) and cystic (166/1439 = 12%) masses.

3.3.1. Solid lesions

All the pancreatic solid lesions were classified into six categories of CEUS enhancement pattern (Table 3). The solid homogeneously hypovascularized lesions were adenocarcinomas (Fig. 1) in 872/917 (95%) cases. The homogeneously isovascular pattern were due to 26/60 (43%) pancreatites (Fig. 2). The heterogeneous isovascular pattern was due to 11/14 (79%) adenocarcinomas. The homogeneously hypervascularized masses were endocrine tumors (Fig. 3) in 140/226 (62%). While the heterogeneously hypervascularized masses were endocrine tumors in 13/28 (46.4%).

3.3.2. Cystic lesions

All cystic pancreatic lesions were classified into eight categories after the administration of contrast agent (Table 4). The pancreatic lesions with a simple cystic pattern were pseudocysts in 14/27 (52%) cases (Fig. 4). The cystic lesions with septa were serous cystadenomas in 13/31 (42%) cases. The cystic lesions with parietal septa and nodules were intraductal papillary-mucinous neoplasms (IPMN) in 6/14 (43%) and mucinous cystadenomas in 6/14 (43%) cases. The cystic lesions with thick wall and septa were mucinous cystadenomas (Fig. 5) in 23/50 (46%). The cystic lesions with

thick wall, parietal nodules and septa were intraductal papillary-mucinous neoplasms in 4/9 (44%) cases (Fig. 6).

3.4. Pancreatic lesion characterization

CEUS enhancement patterns of the most frequent encountered and clinically relevant pancreatic focal masses are reported in Table 5. Two lesions (1 liposarcoma and 1 anaplastic adenocarcinoma) with cystic pattern at CEUS but solid at pathology have not been included in Table 5 resulting a total of 164 cystic lesions.

Sensitivity, specificity, positive and negative predictive values and accuracy of CEUS in lesion characterization related to final pathological diagnosis are reported in Table 6.

Among the solid lesions, at CEUS adenocarcinomas were correctly characterized with an accuracy of 87.8% while, among the cystic lesions, a cystic tumor was correctly diagnosed with an accuracy of 97.1% (Table 6).

3.4.1. Diagnostic confidence

The diagnostic confidence in the characterization of pancreatic masses, discerning between benign and malignant lesions, was significantly increased by the injection of contrast media with ROC curve areas (Fig. 7) from 0.637 for US to 0.877 for CEUS ($p < 0.0001$).

3.4.2. Inter-observer variability

In the separate panel review performed by two observers at center "I" the inter-observer agreement in the characterization of pancreatic masses was slightly higher for solid ($k = 0.78$) than cystic ($k = 0.62$) lesions.
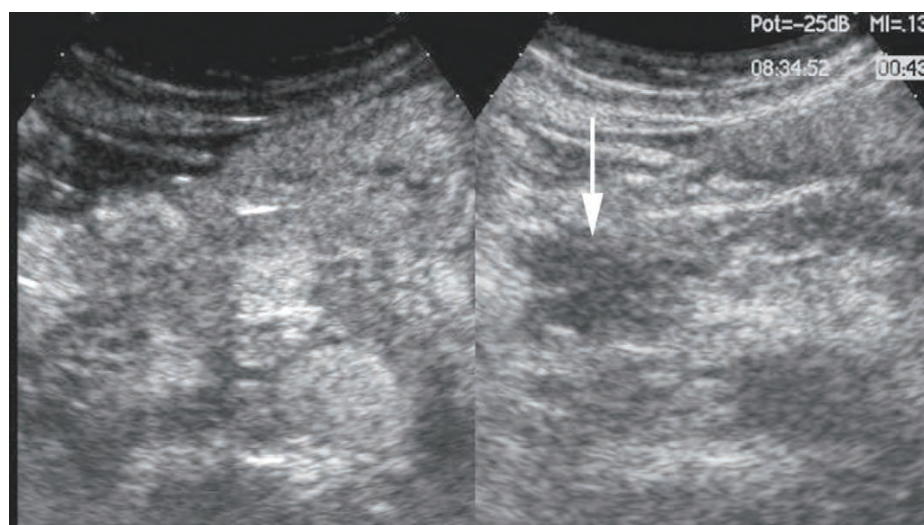
Fig. 2. Mass forming pancreatitis. Pancreatic head mass (arrow) hypoechoic at US and homogeneously isovascular at CEUS. Split-screen visualization of CEUS examination.

Table 4
Cystic pancreatic lesions at CEUS: enhancement pattern correlated with pathology.

Pattern	n	Pathology	n
Simple	27/166 (16%)	Pseudocyst	14/27 (52%)
		IPMN	5/27 (18.5%)
		Serous cystadenoma	5/27 (18.5%)
		Mucinous cystadenoma	3/27 (11%)
Septa	31/166 (19%)	Serous cystadenoma	13/31 (42%)
		Adenocarcinoma	7/31 (23%)
		IPMN	6/31 (19%)
		Neuroendocrine tumor	2/31 (6.5%)
		Solid-pseudopapillary tumor	2/31 (6.5%)
		Mucinous cystadenoma	1/31 (3%)
Nodules	2/166 (1%)	Cystadenocarcinoma	1/2 (50%)
		Mucinous cystadenoma	1/2 (50%)
Septa and nodules	14/166 (9%)	Mucinous cystadenoma	6/14 (43%)
		IPMN	6/14 (43%)
		Cystadenocarcinoma	1/14 (7%)
		Solid-pseudopapillary	1/14 (7%)
Thick wall	31/166 (19%)	Adenocarcinoma	13/31 (42%)
		Neuroendocrine tumor	9/31 (29%)
		Mucinous cystadenoma	4/31 (13%)
		IPMN	2/31 (7%)
		Pseudocyst	1/31 (3%)
		Serous cystadenoma	1/31 (3%)
		Liposarcoma	1/31 (3%)
Thick wall and septa	50/166 (30%)	Mucinous cystadenoma	23/50 (46%)
		IPMN	16/50 (32%)
		Neuroendocrine tumor	7/50 (14%)
		Serous cystadenoma	2/50 (4%)
		Cystadenocarcinoma	1/50 (2%)
		Adenocarcinoma	1/50 (2%)
Thick wall and nodules	2/166 (1%)	Mucinous cystadenoma	1/2 (50%)
		IPMN	1/2 (50%)
Thick wall, septa and nodules	9/166 (5%)	IPMN	4/9 (44%)
		Neuroendocrine tumor	2/9 (22.5%)
		Cystadenocarcinoma	2/9 (22.5%)
		Adenocarcinoma	1/9 (11%)

3.5. Safety evaluation

In none of the centers side effects were reported.

4. Discussion

Contrast-enhanced ultrasound (CEUS), performed with a blood-pool microbubble contrast agent that allows the visualization of

Table 5
Final pathological diagnosis and corresponding CEUS enhancement pattern of most frequent encountered and clinically relevant pancreatic focal masses.

Pathology	Ceus enhancement patterns						Total
Solid lesions	Homogeneously hypovascular	Heterogeneously hypovascular	Homogeneously isovascular	Heterogeneously isovascular	Homogeneously hypervascular	Heterogeneously hypervascular	
Adenocarcinoma	864	27	18	11	60	7	987
Endocrine tumor	28	–	9	–	140	13	190
Pancreatitis	5	–	26	3	5	–	39

| Cystic lesions	Simple	Septa	Nodules	Septa + nodules	Thick wall	Thick wall + septa	Thick wall + nodules	Thick wall + septa + nodules	Total
Tumor	13	31	2	14	28	50	2	9	149
Pseudocyst	14	–	–	–	1	–	–	–	15

Table 6
Data analysis of CEUS in lesion characterization related to final pathological diagnosis.

Pancreatic lesions	Sensitivity	Specificity	PPV	NPV	Accuracy
Solid					
Adenocarcinoma	0.875 [CI 95% (0.857, 0.892)]	0.883 [CI 95% (0.865, 0.899)]	0.942 [CI 95% (0.929, 0.953)]	0.764 [CI 95% (0.741, 0.786)]	87.8%
Endocrine tumor	0.737 [CI 95% (0.713, 0.759)]	0.931 [CI 95% (0.917, 0.943)]	0.619 [CI 95% (0.594, 0.645)]	0.959 [CI 95% (0.947, 0.968)]	90.5%
Pancreatitis	0.667 [CI 95% (0.642, 0.691)]	0.976 [CI 95% (0.966, 0.983)]	0.433 [CI 95% (0.408, 0.459)]	0.991 [CI 95% (0.984, 0.995)]	96.7%
Total	84.7%	94.4%	85.6%	94%	91.7%
Cystic					
Tumor	0.782 [CI 95% (0.759, 0.803)]	0.998 [CI 95% (0.994, 1.000)]	0.978 [CI 95% (0.969, 0.985)]	0.971 [CI 95% (0.960, 0.979)]	97.1%
Pseudocyst	0.933 [CI 95% (0.919, 0.945)]	0.991 [CI 95% (0.984, 0.995)]	0.519 [CI 95% (0.492, 0.545)]	0.999 [CI 95% (0.995, 1.000)]	99%
Total	79.4%	99.4%	90.4%	98.6%	98.1%
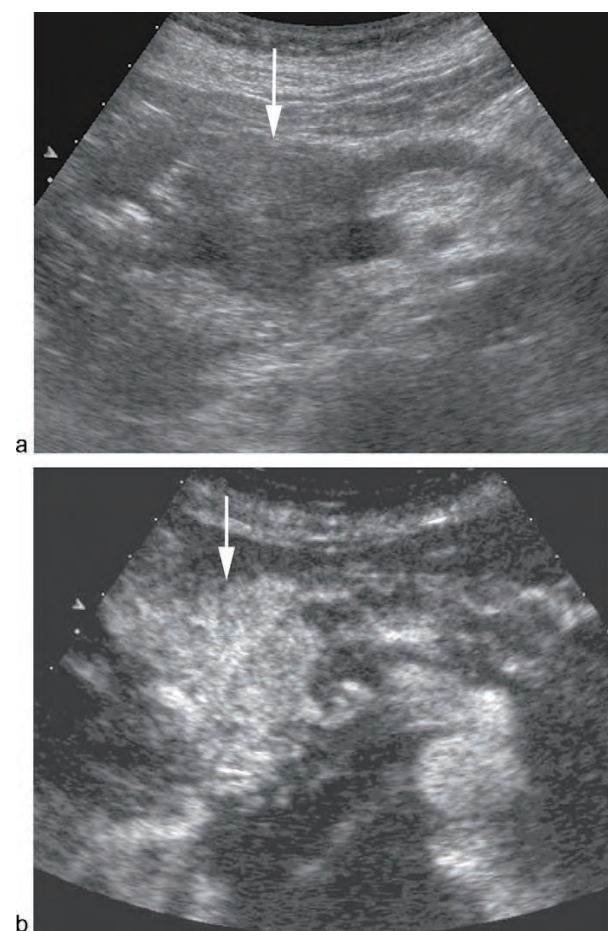
Fig. 3. Endocrine tumor. (a) Pancreatic head mass (arrow) solid and hypoechoic at US, with (b) homogeneous hypervascular pattern (arrow) at CEUS.

flow in small vessels during a real-time examination [4,19,20], is nowadays a well established liver imaging method [4–7]. Although the usefulness of CEUS has been widely evaluated in hepatic imaging [4,19–21], its applications in pancreatic imaging are relatively new even if increasingly reported in the literature [8–18].

The application of the purely intravascular contrast agent, the dynamic observation of the contrast-enhanced phases, and the high contrast and spatial resolution of current ultrasound harmonic imaging allow the visualization of the pancreatic tumor vascularisation [14]. CEUS requires specific software that subtract the background signal prior to the injection of contrast agent [2]. Following injection of contrast agent, a hyperechoic signal is produced only in regions where vessels are present with non-vascularized tissue remaining anechoic (non-enhancing). CEUS has been shown to be accurate in evaluation the vascularity of pancreatic lesions [2,8–10,22,23]. The vascular pattern of pancreatic tumors has been investigated in few studies with numerous population and pathologically proven data [10–18]. However the role of contrast-enhanced ultrasound in a large multicenter study has not been published so far. The multicenter nature of the present study may support more generalization of
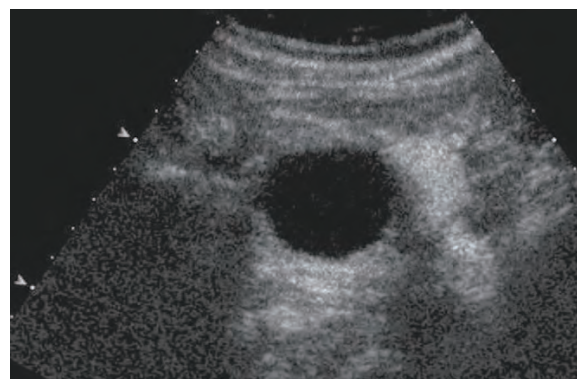
Fig. 4. Pseudocyst. Cystic lesion of the pancreatic head with a simple cystic pattern at CEUS.
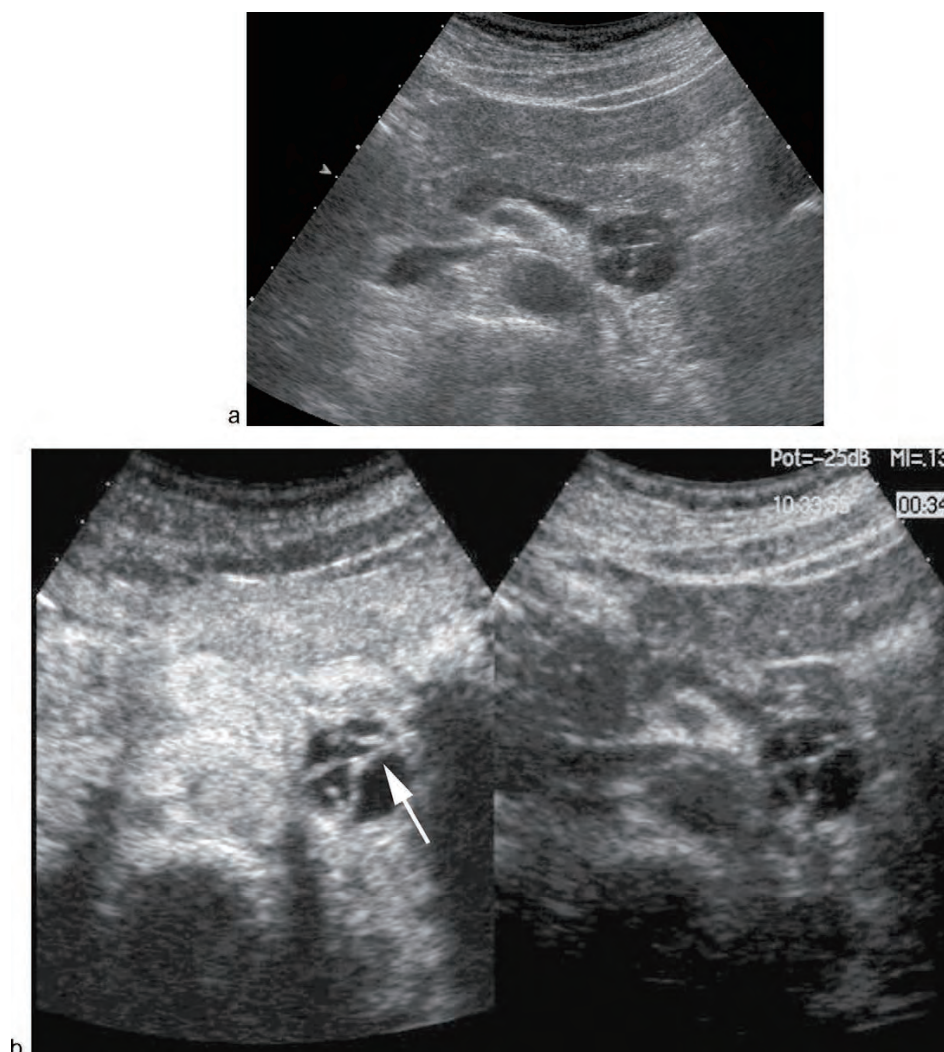
Fig. 5. Mucinous cystadenoma. (a) Small cystic lesion of the pancreatic body with (b) CEUS pattern characterized by thick wall and enhancing septa (arrow). Split-screen visualization of CEUS examination.

the results in the use of CEUS for pancreatic lesion characterization.

When a pancreatic tumor has been detected, its immediate and correct differential diagnosis is mandatory to direct appropriate management. Ultrasonography can be the non-invasive imaging modality chosen for the first evaluation of the pancreas, as it is widely performed, relatively low expensive and readily available examination [1]. Moreover the detection of an incidental pancreatic lesion at US is a relatively frequent clinical scenario. During ultrasound study, the administration of microbubble contrast media is reported to immediately improve the solid lesion characterization making possible a differential diagnosis [2,11–13,18]. As a result, a rapid diagnosis, very important dealing with pancreatic adenocarcinoma, and a better management of the studied pancreatic lesion could be expected.

Solid pancreatic lesions in our multicenter study were correctly characterized in respect to pathology with an accuracy of 91.7%. In particular, ductal adenocarcinoma was correctly characterized with an accuracy of 87.8% based on the hypovascular aspect at CEUS. This means that each single solid lesion detected at ultra-

sound and hypovascular at CEUS should be considered a ductal adenocarcinoma until otherwise proven. This result confirms previous reported data about the characterization of pancreatic ductal adenocarcinoma at CEUS: in five pathologically proved series with more than fifty cases, ductal adenocarcinoma is reported to be hypovascular in 73–93% of the cases [12,13,15,18,24].

CEUS seems also very accurate in demonstrating the endocrine tumor vascularisation [14,22,25]. The hypervascularity is the predominant imaging feature of neuroendocrine tumors independently of their functional status. In the present study the accuracy of CEUS in the characterization of endocrine tumors was 90.5%.

Contrast-enhanced ultrasonography favorably compares with MRI in displaying the anatomic features of the cystic pancreatic masses and is highly sensitive in the detection of the vascularisation of the cystic inclusions, both septa and nodules [16]. The demonstration at CEUS of a vascularised cystic inclusion suggests the diagnosis of a cystic tumor while the demonstration of a complete avascularisation supports the diagnosis of a pseudocyst. In a pancreatic cystic lesion, the presence of inclusions vascularized at CEUS excludes the diagnosis of pseudocyst while the diagnosis
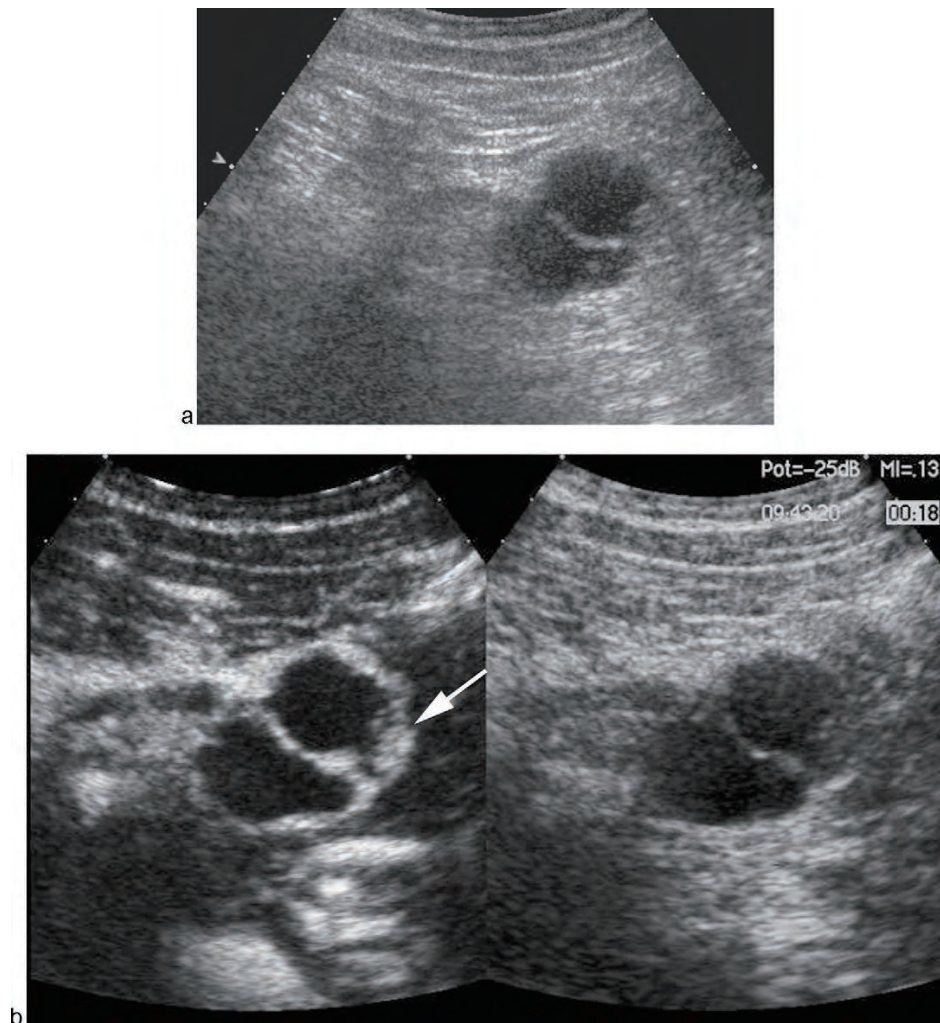
Fig. 6. Intraductal papillary-mucinous tumor. (a) Cystic lesion of the pancreatic body with (b) CEUS pattern characterized by thick wall, parietal nodules (arrow) and septa. Split-screen visualization of CEUS examination.

of cystic tumor has to be considered. Before analysing the imaging features of the cystic pancreatic masses, the clinical scenario has to be assessed. For example, the diagnosis of pseudocyst is not reliable in absence of any history of pancreatitis or without signs of chronic pancreatitis. In this multicenter study, cystic tumors and pseudocysts were correctly diagnosed at CEUS with an accuracy of 97.1% and 99%. A high diagnostic accuracy for CEUS in the characterization of pancreatic pseudocysts has already been reported [26,27].

CEUS can better characterize tissues than US in terms of correct identification of solid (vascularised) and cystic/necrotic (avascularised) parts of the pancreatic lesions, so improving their characterization. A primary more correct classification of the lesions as solid or cystic leads to better and faster define the further imaging work-up required to obtain a definite diagnosis. The better accuracy of CEUS in respect to US in characterizing pancreatic lesions resulted in the present study with a statistical significant difference ($p < 0.0001$) of the relative ROC curves.

This multicenter study has some intrinsic limitations derived from the retrospective data collection even if all the included lesions were prospectively judged on site during conventional

and contrast-enhanced examinations. Moreover a certain inhomogenicity of the data is also due to the different scanners, software and contrast media utilized, but this reflects the real difference among the institutes. At least, unfortunately, another intrinsic limitation is that no data about the ultrasound detection of focal pancreatic masses can be provided as a direct consequence of the study inclusion criteria.

To overcome subjectivity, the use of quantification software could be suggested for the characterization of pancreatic lesions during CEUS study, as recently reported in the literature [28].

Initially limited to the evaluation of liver lesions [4], EFSUMB – European Federation of Societies for Ultrasound in Medicine and Biology – new guidelines and good clinical practice recommendations for contrast-enhanced ultrasound, actually include pancreatic applications [19].

CEUS can improve the accuracy of the ultrasound study of pancreatic masses incidentally detected thus obtaining a faster diagnosis (i.e., immediate diagnosis of ductal adenocarcinoma). CEUS could also play two further roles that may represent proposals for additional investigations: first, better manage the lesions
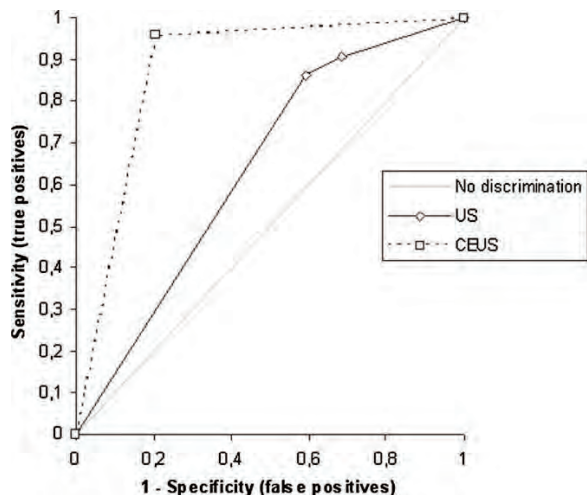
Fig. 7. Receiver operating characteristic curves of US and CEUS in the characterization of focal pancreatic masses.

during an ultrasound examination (i.e., moving to MRI or EUS directly for cystic tumors); second, act as a problem solving method (i.e., uncertain hypervascularity of a solid lesion or doubtful septa enhancement in a cystic lesion). Moreover, the interest in the use of microbubbles for the evaluation of chemotherapeutic effects and prognosis of pancreatic adenocarcinoma is documented in the literature [29–31].

Regarding the safety, no side effects have been reported in this multicenter study with more than one thousand cases.

5. Conclusion

Based on the results of this multicenter study CEUS is accurate in the characterization of pancreatic lesions. CEUS should be considered as a complementary imaging dynamic method for the pancreatic lesions characterization.

Conflict of interest

There is no conflict of interest.

References

[1] Martinez-Noguera A, D'Onofrio M. Ultrasonography of the pancreas. 1. Conventional imaging. Abdom Imaging 2007;32:136–49.
[2] D'Onofrio M, Zamboni G, Faccioli N, et al. Ultrasonography of the pancreas. 4. Contrast-enhanced imaging. Abdom imaging 2007;32:171–81.
[3] Cosgrove D. Advances in contrast agent imaging using Cadence contrast pulse sequencing technology (CPS) and SonoVue. Eur Radiol 2004;12.(Suppl. 8).
[4] EFSUMB Study Group. Guidelines for the use of contrast agents in ultrasound. Ultraschall Med 2004;25:249–56.
[5] Strobel D, Seitz K, Blank W, et al. Contrast-enhanced ultrasound for the characterization of focal liver lesions – diagnostic accuracy in clinical practice. Ultraschall Med 2008;29:499–505.
[6] Leen E, Ceccotti P, Kalogeropoulou C, et al. Prospective multicenter trial evaluating a novel method of characterizing focal liver lesions using contrast-enhanced sonography. Am J Roentgenol 2006;186:1551–9.
[7] Quaia E, Stacul F, Gaiani S, et al. Comparison of diagnostic performance of unenhanced vs SonoVue – enhanced ultrasonography in focal liver lesions characterization. The experience of three Italian centers. Radiol Med 2004;108:71–81.
[8] Takeda K, Goto H, Hirooka Y, et al. Contrast enhanced transabdominal ultrasonography in the diagnosis of pancreatic mass lesions. Acta Radiol 2003;44:103–6.
[9] Ozawa Y, Numata K, Tanaka K, et al. Contrast-enhanced sonography of small pancreatic lesions. J Ultrasound Med 2002;21:983–91.
[10] Numata K, Ozawa Y, Kobayashi N, et al. Contrast-enhanced sonography of pancreatic carcinoma: correlation with pathological findings. J Gastroenterol 2005;40:631–40.
[11] Dietrich CF, Braden B, Hocke M, et al. Improved characterization of solitary solid pancreatic tumors using contrast enhanced transabdominal ultrasound. J Cancer Res Clin Oncol 2008;134:635–43.
[12] Kitano M, Kudo M, Maekawa K, et al. Dynamic imaging of pancreatic diseases by contrast-enhanced coded phase inversion harmonic ultrasonography. Gut 2004;53(6):854–9.
[13] Sofuni A, Iijima H, Moriyasu F, et al. Differential diagnosis of pancreatic tumors using ultrasound contrast imaging. J Gastroenterol 2005;40(5):518–25.
[14] D'Onofrio M, Mansueto G, Falconi M, et al. Neuroendocrine pancreatic tumor: value of contrast enhanced ultrasonography. Abdom Imaging 2004;29:246–58.
[15] Nagase M, Furuse J, Ishii H, et al. Evaluation of contrast enhancement patterns in pancreatic tumors by coded harmonic sonographic imaging with a microbubble contrast agent. J Ultrasound Med 2003;22:789–95.
[16] D'Onofrio M, Megibow AJ, Faccioli N, et al. Comparison of contrast-enhanced sonography and MRI in displaying anatomic features of cystic pancreatic masses. AJR Am J Roentgenol 2007;189(6):1435–42.
[17] Itoh T, Hiroota Y, Htoh A, et al. Usefulness of contrast-enhanced transabdominal ultrasonography in the diagnosis of intraductal papillary mucinous tumors of the pancreas. Am J Gastroenterol 2005;100:144–52.
[18] D'Onofrio M, Zamboni G, Tognolini A, et al. Mass-forming pancreatitis: value of contrast-enhanced ultrasonography. World J Gastroenterol 2006;12(26):4181–4.
[19] EFSUMB Study Group. Guidelines and good clinical practice recommendations for contrast enhanced ultrasound (CEUS) – update 2008. Ultraschall Med 2008;29(1):28–44.
[20] Solbiati L, Tonolini M, Cova L, et al. The role of contrast-enhanced ultrasound in the detection of focal liver lesions. Eur Radiol 2001;11(Suppl. 3): E15.
[21] Quaia E, Calliada F, Bertolotto M, et al. Characterization of focal liver lesions with contrast-specific US modes and a sulfur hexafluoride-filled microbubble contrast agent: diagnostic performance and confidence. Radiology 2004;232(2):420–30.
[22] D'Onofrio M, Malagò R, Zamboni g, et al. Contrast-enhanced ultrasonography better identifies pancreatic tumor vascularization than helical CT. Pancreatology 2005;5(4–5):398–402.
[23] Rickes S, Rauh P, Uhle C, et al. Contrast-enhanced sonography in pancreatic diseases. Eur J Radiol 2007;64(2):183–8.
[24] Hocke M, Schulze E, Gottschalk P, et al. Contrast-enhanced endoscopic ultrasound in discrimination between focal pancreatitis and pancreatic cancer. World J Gastroenterol 2006;12(2):246–50.
[25] Malagò R, D'Onofrio M, Zamboni G, et al. Contrast-enhanced sonography of nonfunctioning pancreatic neuroendocrine tumors. AJR Am J Roentgenol 2009;192(2):424–30.
[26] Rickes S, Wermke W. Differentiation of cystic pancreatic neoplasms and pseudocysts by conventional and echo-enhanced ultrasound. J Gastroenterol Hepatol 2004;19(7):761–6.
[27] Rickes S, Monkemuller K, Malfertheiner P. Echo-enhanced ultrasound with pulse inversion imaging: a new imaging modality for the differentiation of cystic pancreatic tumours. World J Gastroenterol 2006;12(14): 2205–11.
[28] Kersting S, Konopke R, Kersting F, et al. Quantitative perfusion analysis of transabdominal contrast-enhanced ultrasound of pancreatic masses and carcinomas. Gastroenterology 2009 (Epub ahead of print).
[29] Tawada K, Yamaguchi T, Kobayashi A, et al. Changes in tumor vascularity depicted by contrast-enhanced ultrasonography as a predictor of chemotherapeutic effect in patients with unresectable pancreatic cancer. Pancreas 2009;38(1):30–5.
[30] Masaki T, Ohkawa S, Amano A, et al. Noninvasive assessment of tumor vascularity by contrast-enhanced ultrasonography and the prognosis with non-resectable pancreatic carcinoma. Cancer 2005;103(5):1026–1035.
[31] Kobayashi A, Yamaguchi T, Ishihara T, et al. Evaluation of vascular signal in pancreatic ductal carcinoma using contrast enhanced ultrasonography: effect of systemic chemotherapy. Gut 2005;54:1047.

HCC Expert Meeting – New Advances in HCC Management

Time / Date : 17:30 – 19:35, Mar 24th (SAT), 2012

Venue: **8F 綺麗廳 (Great)**, W Hotel Taipei (地址:台北市信義區忠孝東路五段 10 號, TEL: 02-7703-8877)

Time	Topic	Speaker	Moderator
17:30	Opening	陳培哲 教授 Prof. Pei-Jer Chen 臺大醫院 胃腸肝膽科	
Intermediate Stage HCC management			
17:35	From JSH Treatment Guideline to Combination Therapy	**Prof. Masatoshi Kudo** Chairman, Department of Hepatology and Gastroenterology, Kinki University School of Medicine, President, Kinki University Medical Center	高嘉宏 教授 Prof. Jia-Horng Kao 臺大醫院 胃腸肝膽科
18:05	Key Learning from TACE Combination Studies	許駿 副教授 臺大醫院 腫瘤醫學部	
18:25	Panel Discussion		
18:30	Bio-break		
Advance Stage HCC management			
18:45	Super Responder under Sorafenib Monotherapy: CGMH-KS Experience	洪肇宏 主任 Dr. Chao-Hung Hung 高雄長庚醫院 胃腸肝膽科	盧勝男 教授 Prof. Sheng-Nan Lu 高雄長庚醫院 胃腸肝膽科
19:00	Super Responder under Sorafenib Monotherapy: VGHTPE Experience	黃怡翔 教授 Prof. Yi-Hsiang Huang 台北榮民總醫院 胃腸肝膽科	趙毅 教授 Prof. Yee Chao 台北榮總 藥物放射治療科
19:10	Panel discussion		
19:20	Innovative approach to combine sorafenib with erlotinib: CGMH-LK Experience	林成俊 助理教授 Dr. Chen-Chun Lin 林口長庚醫院 胃腸肝膽科	林錫銘 教授 Prof. Shi-Ming Lin 林口長庚醫院 胃腸肝膽科
19:25	Discussion		
19:30	Closing Remark	陳培哲 教授 Prof. Pei-Jer Chen 臺大醫院 胃腸肝膽科	
Dinner @ 9F 商情會議室 3+4			

同門会　名簿

名前	施設	卒業年度	出身大学
工藤　正俊	近畿大学医学部	昭和53年	京都大学
樫田　博史	近畿大学医学部	昭和58年	京都大学
汐見　幹夫	近畿大学医学部	昭和55年	近畿大学
北野　雅之	近畿大学医学部	平成　2年	鳥取大学
西田　直生志	近畿大学医学部	昭和60年	大阪医科大学
松井　繁長	近畿大学医学部	平成　3年	近畿大学
上嶋　一臣	近畿大学医学部	平成　7年	神戸大学
櫻井　俊治	近畿大学医学部	平成　7年	京都大学
南　康範	近畿大学医学部	平成　9年	近畿大学
萩原　智	近畿大学医学部	平成 10年	近畿大学
井上　達夫	近畿大学医学部	平成 11年	近畿大学
矢田　典久	近畿大学医学部	平成 11年	滋賀医科大学
坂本　洋城	近畿大学医学部	平成 12年	近畿大学
朝隈　豊	近畿大学医学部	平成 14年	近畿大学
北井　聡	近畿大学医学部	平成 14年	近畿大学
川崎　正憲	近畿大学医学部	平成 15年	近畿大学
田北　雅弘	近畿大学医学部	平成 15年	近畿大学
永井　知行	近畿大学医学部	平成 16年	近畿大学
永田　嘉昭	近畿大学医学部	平成 16年	近畿大学
今井　元	近畿大学医学部	平成 17年	近畿大学
山雄　健太郎	近畿大学医学部	平成18年	東京医科大学
山田　光成	近畿大学医学部	平成18年	近畿大学
有住　忠晃	近畿大学医学部	平成 19年	近畿大学
鎌田　研	近畿大学医学部	平成 19年	近畿大学
峯　宏昌	近畿大学医学部	平成 19年	近畿大学
宮田　剛	近畿大学医学部	平成 19年	近畿大学
高山　政樹	近畿大学医学部	平成 19年	近畿大学
足立　哲平	近畿大学医学部	平成 21年	近畿大学
大本　俊介	近畿大学医学部	平成 21年	近畿大学
門阪　薫平	近畿大学医学部	平成 21年	近畿大学
田中　梨絵	近畿大学医学部	平成 22年	近畿大学
千品　寛和	近畿大学医学部	平成 22年	近畿大学
南　知宏	近畿大学医学部	平成 23年	近畿大学
岡元　寿樹	近畿大学医学部	平成 23年	近畿大学
黒木　恵美（旧姓 石川）		平成 11年	近畿大学
岡田　無文	山本病院	平成 13年	近畿大学
柴田　千栄（旧姓 辰巳）		平成 15年	近畿大学
上田　泰輔		平成 15年	近畿大学
上硲　俊法	近畿大学医学部臨床検査学	昭和60年	近畿大学
前川　清	近畿大学医学部超音波室		
辻　直子	近畿大学医学部堺病院	昭和60年	京都府立医科大学
谷池　聡子	近畿大学医学部堺病院	平成　7年	奈良県立医科大学
奥村　直己	近畿大学医学部堺病院		近畿大学
高場　雄久	近畿大学医学部堺病院		近畿大学

川崎　俊彦	近畿大学医学部奈良病院	昭和58年	京都大学
岸谷　譲	近畿大学医学部奈良病院	昭和62年	近畿大学
宮部　欽生	近畿大学医学部奈良病院	平成14年	近畿大学
清水　昌子	近畿大学医学部奈良病院	平成12年	近畿大学
茂山　朋広	近畿大学医学部奈良病院	平成17年	近畿大学
奥田　英之	近畿大学医学部奈良病院	平成19年	
木下　大輔	近畿大学医学部奈良病院	平成20年	
秦　康倫	近畿大学医学部奈良病院	平成21年	
水野　成人	近畿大学医学部奈良病院	昭和61年	京都府立医科大学
加藤　玲明	近畿大学医学部奈良病院	平成11年	近畿大学
宮本　容子（旧姓 北口）	近畿大学医学部奈良病院	平成12年	近畿大学
林　道友	林内科クリニック		
梅原　康湖	JR大阪鉄道病院	平成12年	近畿大学
山本　俊夫（ご逝去）		昭和26年	京都大学
山本　健二	岡本クリニック		神戸大学
亀山　千晴	しあわせクリニック	平成7年	近畿大学
南野　達夫	なんの医院	昭和55年	近畿大学
中里　勝	上ヶ原病院		
鍋島　紀滋	三菱京都病院	昭和61年	京都大学
由谷　逸朗	高石藤井病院	昭和62年	近畿大学
遠田　弘一	慈温堂遠田医院	平成7年	近畿大学
遠田　由紀			
川端　一史	川端内科クリニック	平成元年	近畿大学
米田　円	米田内科胃腸科	平成元年	近畿大学
小川　力	高松赤十字病院	平成11年	近畿大学
渡邉　和彦	結核予防会大阪府支部相談診療所	平成3年	近畿大学
森村　正嗣	森村医院	平成3年	帝京大学
中岡　良介	山本病院	平成8年	近畿大学
冨田　崇文	冨田病院	平成14年	近畿大学
西尾　健	南堺病院	平成14年	近畿大学
仲谷　達也	仲谷クリニック	平成3年	近畿大学
福永　豊和	北野病院	平成4年	京都大学
福田　信宏	朝日大学村上記念病院	平成10年	近畿大学
坂口　康浩	河崎内科病院	平成11年	近畿大学
永島　美樹	桃坂クリニック	平成12年	近畿大学
坂本　康明	坂本クリニック	平成15年	近畿大学
市川　勉	内海町いちかわ診療所	平成12年	近畿大学
齊藤　佳寿（旧姓 野田）	介護老人保健施設　徳田山	平成14年	近畿大学
高橋　俊介	市立堺病院	平成14年	近畿大学
末冨　洋一郎	末冨放射線科医院	平成8年	近畿大学
梅原　泰	辻腎太郎クリニック	平成11年	近畿大学
鄭　浩柄	神戸市立医療センター中央市民病院	平成8年	東京慈恵医科大学
小牧　孝充	富田林病院	平成7年	近畿大学
畑中　絹世		平成13年	川崎医科大学
早石　宗右	早石病院	平成18年	近畿大学
工藤　可苗	近畿大学医学部	平成12年	近畿大学
山本　典雄	医療法人山紀会	平成19年	近畿大学

鄭 扶美	近畿大学医学部 元秘書		
木村 由佳	近畿大学医学部 元秘書		
川辺 仁美	近畿大学医学部 元秘書		
西川 由佳	近畿大学医学部 元秘書		
二見 佳央里	近畿大学医学部 元秘書		
井上 真由美	近畿大学医学部 元秘書		
坂上 浩美	近畿大学医学部 元秘書		
小田 智裕子	近畿大学医学部 元秘書		
土井 由香利	近畿大学医学部 元秘書		
田中 真紀	近畿大学医学部 教授秘書		
村橋 亜季	近畿大学医学部 教授秘書		
上田 由未子	近畿大学医学部 教授秘書		
本廣 佳香	近畿大学医学部 教授秘書		
胡桃 由佳	近畿大学医学部 医局秘書		
朝隈 智	近畿大学医学部 医局秘書		
林 直子	近畿大学医学部 医局秘書		
田村 利恵	近畿大学医学部 肝癌研究会事務局		
前原 なつみ	近畿大学医学部 肝癌研究会事務局		
弓削 公子	近畿大学医学部 臨床研究補助員		
児玉 美由紀	近畿大学医学部 データマネージャー（CRC業務）		
鏡 郁子	近畿大学医学部 基礎研究補佐員（実験助手）		
垣井 麻莉	近畿大学医学部 基礎研究補佐員（実験助手）		

近畿大学消化器内科　同門会役員

会長　　　工藤正俊

副会長　　北野雅之

幹事　　　松井繁長

会計　　　上嶋一臣

庶務　　　西田直生志

同門会誌作製　秘書一同

近畿大学医学部消化器内科教室同門会会則

第一条　名称
　　　本会は近畿大学医学部消化器内科教室同門会と称する。
第二条　目的
　　　本会は会員相互の親睦及び教室の隆盛を図ることを目的とする。
第三条　会員
　　　会員は消化器内科教室出身者、教室員及び同教室の発展に寄与するものを
　　　もって構成される。
第四条　役員
１．　本会の運営を円滑にするために幹事会を設ける。幹事会は代表幹事を長
　　　とし、代表幹事が指名する教室員をもって構成する。尚、幹事会は代表
　　　幹事が随時召集するものとする。その他、会計をおく。
２．　会長
　①　会長は現職主任教授より選出される。
　②　会長退任後は名誉会長となる。また、名誉会長は主任教授経験者からも
　　　選出できる。
３．　顧問
　　　本会の発展に寄与したもので、幹事会が推戴する。
４．　役員の選出
　①　幹事は役員より選出する。
　②　代表幹事は医局長が兼任する。
５．　幹事の任期は２年とする。但し再任を妨げない。
第五条　会議
　　１．　総会は年１回の開催とする。
　　２．　幹事会において仮決議された条件の最終決定権は総会に委ねられる。
　　３．　決議は総会出席者の多数決により成立する。
第六条　会計
　　１．　本会の経費は会費をもって充てる。
　　２．　本会の会費は年額壱萬円とする。
　　３．　会計年度は４月１日から翌年３月 31 までとし、会計担当者は年１回
　　　　　会計報告を行う。

第七条
　　事務局は近畿大学医学部消化器内科教室内に置く。
第八条　会則の改正
　　会則の改正は幹事会の仮決議を経て総会で議決されるものとする。

附則　除名規定
　　本会の名誉を毀損したものや、その他本会に不適当と考えられるものは
　　幹事会の動議により総会にて除名が議決される。

編集後記

　2012 年版の annual report が完成しました。

　消化器内科の秘書は、現在、胡桃さん、田中さん、朝隈さん、田村さん、前原さん、林さん、村橋さん、弓削さん、鏡さん、上田さん、垣井さん、本廣さん、児玉さん（現在教授室 4 名、医局秘書 3 名、肝癌研究会事務局 2 名、データマネージャー（CRC 業務）1 名、臨床研究補助 1 名、実験助手 2 名）での 13 人体制となっております。

　2012 年版年報は遅めの発刊となってしまいましたが、2013 年版はもう少し早い機会に発刊したいと思います。

　年報業務に加えまして、その他業務におきましても、今後とも何卒宜しく御願い申し上げます。

平成 25 年 10 月 1 日

秘書一同